ADVANCES IN SPINAL FUSION

Molecular Science, Biomechanics, and Clinical Management

EDITED BY

KAI-UWE LEWANDROWSKI
Cleveland Clinic
Cleveland, Ohio, U.S.A.

DONALD L. WISE
Northeastern University
Boston, and
Cambridge Scientific, Inc.
Cambridge, Massachusetts, U.S.A.

DEBRA J. TRANTOLO
Cambridge Scientific, Inc.
Cambridge, Massachusetts, U.S.A.

MICHAEL J. YASZEMSKI
Mayo Clinic
Rochester, Minnesota, U.S.A.

AUGUSTUS A. WHITE III
Beth Israel Deaconess Medical Center
Boston, and
Harvard Medical School
Boston, Massachusetts, U.S.A.

MARCEL DEKKER, INC. NEW YORK • BASEL

Library of Congress Cataloging-in-Publication Data
A catalog record for this book is available from the Library of Congress.

ISBN: 0-8247-4310-5

This book is printed on acid-free paper.

Headquarters
Marcel Dekker, Inc., 270 Madison Avenue, New York, NY 10016, U.S.A.
tel: 212-696-9000; fax: 212-685-4540

Distribution and Customer Service
Marcel Dekker, Inc., Cimarron Road, Monticello, New York 12701, U.S.A.
tel: 800-228-1160; fax: 845-796-1772

Eastern Hemisphere Distribution
Marcel Dekker AG, Hutgasse 4, Postfach 812, CH-4001 Basel, Switzerland
tel: 41-61-260-6300; fax: 41-61-260-6333

World Wide Web
http://www.dekker.com

The publisher offers discounts on this book when ordered in bulk quantities. For more information, write to Special Sales/Professional Marketing at the headquarters address above.

Current printing (last digit):

10 9 8 7 6 5 4 3 2 1

PRINTED IN THE UNITED STATES OF AMERICA

Preface

Spinal fusion presents a challenge to all clinicians; the rate of failure can be high. Current approaches to the problem involve the mechanics and biology of spinal fusion. Extensive work is currently underway to improve healing and decrease the morbidity associated with conventional bone grafting using autologous material from the iliac crest. Less rigid implant systems, more bioactive and mechanically sound bone graft substitutes, and growth factor applications comprise some of the new approaches. Their clinical application has facilitated development of less invasive procedures, such as vertebroplasty. Experimental stimulation of spinal fusion has progressed to the DNA level, with the potential seen for gene therapy applications to overcome the problems with delivery vehicles for bone morphogenic protein (BMP)-based bone graft substitutes. Hence, alternative osteoinductive proteins and new delivery methods are currently under investigation and add to current concepts of local gene therapy for spine fusion. Cloned and sequenced complementary deoxyribonucleic acid (cDNA) of novel osteoinductive proteins are being developed that may foster expression of the genes needed to initiate the cascade of osteoinduction. In fact, transient local gene therapy may prove applicable to the induction of bone formation, thereby offering new clinical treatments for patients with a variety of spine disorders.

The illustrative description of the development of a new generation of materials and devices capable of specific biological interactions to enhance spinal fusion is the heart of this new reference. Improvement of these materials and devices is in a constant state of activity, with the challenge of replacing older technologies with those that allow better exploitation of advances in a number of technologies—e.g., biodegradable implants, drug delivery, recombinant DNA techniques, bioreactors, stem cell isolation and transfection, cell encapsulation and immobilization, and 2D and 3D scaffolds for cells. The book deals with issues in the selection of proper biomaterials that address biocompatibility, biostability, and structure–function relationships. Several chapters focus on the use of specific biomaterials, based on their physiochemical and mechanical characterizations. Integral to these chapters are discussions of standards in analytical methodology and quality control.

Readers will find this book to be derived from a broad base of backgrounds ranging from the basic sciences (e.g., polymer chemistry and biochemistry) to more applied disciplines (e.g., mechanical/chemical engineering, orthopedics, and pharmaceutics). To meet varied needs each chapter provides clear and fully detailed discussions. This in-depth, but practical, coverage should also assist recent inductees to the biomaterials circle. We trust that this reference book conveys the intensity of this fast-moving field in an enthusiastic presentation.

Kai-Uwe Lewandrowski
Donald L. Wise
Debra J. Trantolo
Michael J. Yaszemski
August A. White III

Contents

1

Reduction and Fixation of Sacroiliac Joint Dislocation by the Combined Use of S1 Pedicle Screws and an Iliac Rod

Kuniyoshi Abumi
Hokkaido University Health Administration Center
Sapporo, Japan

Manabu Ito and Yoshihisa Kotani
Hokkaido University Graduate School of Medicine
Sapporo, Japan

Michinori Saita
Hokushin Hospital
Sapporo, Japan

I. INTRODUCTION

Sacroiliac dislocation, which usually accompanies disruption of the symphysis pubis or fractures of the pelvic rami, is the most unstable type of pelvic ring injury. In sacroiliac dislocation, both the anterior and the posterior columns of the pelvic ring are disrupted, and the affected hemipelvis rotates internally or externally with vertical displacement (Fig. 1). Deformities of the pelvic ring remain with high frequency after nonoperative treatment of the sacroiliac dislocation [1]. According to published reports, the long-term functional prognosis of sacroiliac dislocation might be poor if reduction was not exact [1–3]. Tile described in a review article that patients with vertically unstable disruption of the pelvis had many problems, 60% of which were persistently painful. According to the investigator, the pain was usually present in the posterior sacroiliac area or the lower lumbar spine and was most frequently associated with unreduced sacroiliac dislocations [2]. Dujardin et al. showed in their report on sacroiliac dislocation that pure sacroiliac lesions were associated with poor functional results, especially if reduction was not exact [1].

External skeletal fixation has been popularly used for unstable pelvic injuries. This procedure provides enough stability for the pelvic injury without severe sacroiliac disruption in a way similar to that for Type B injury classified by Tile [4] (Table 1). However, anterior stabilization using an external fixator alone does not provide sufficient stability for Type C injury with severe disruption of the pelvic ring. Some reports have shown that optimum reduction of sacroiliac dislocation with large pelvic deformities comprises vertical displacement and that rotational deformity is sometimes difficult to treat with an external fixator alone [1,5–8]. Furthermore, long-term maintenance of nonanatomical position with an external fixator has been associated with difficulties in later posterior reduction [5]. An external fixator, which decreases blood loss

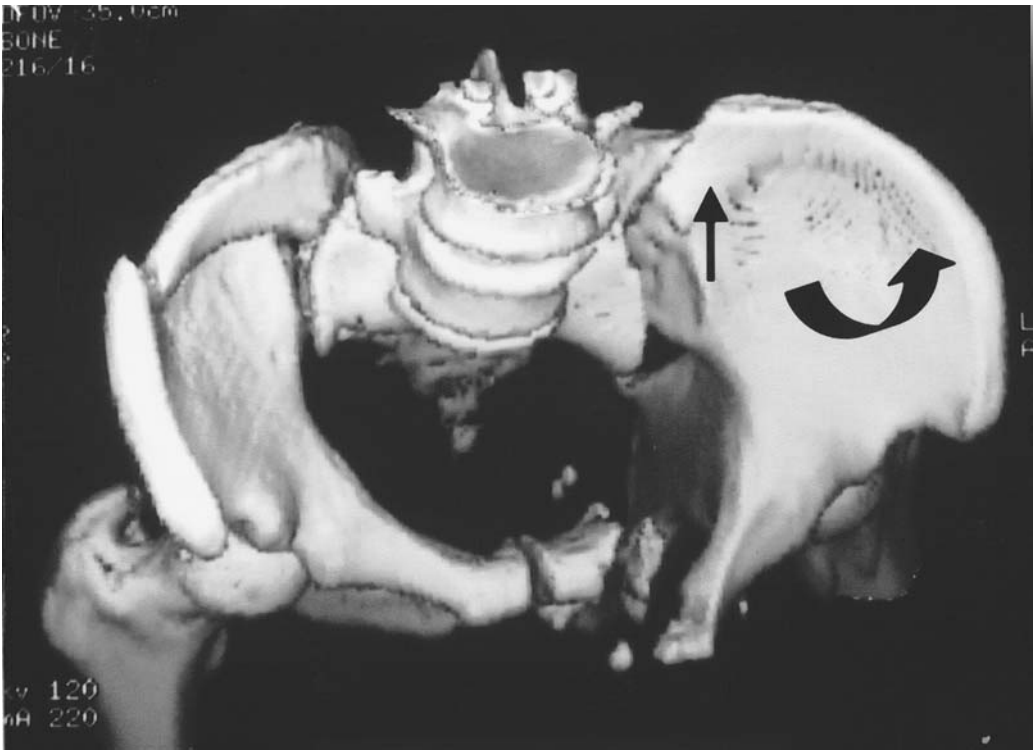

Figure 1 Pelvic deformity in sacroiliac dislocation. In sacroiliac dislocation, both the anterior and the posterior columns of the pelvic ring are disrupted, and the affected hemipelvis rotates internally or externally (curved arrow) with vertical displacement (arrow).

Table 1 Classification of Pelvic Ring Disruption by Tile

Type A	Stable injury
A1	Avulsion of the innominate bone
A2	Stable iliac wing fracture or stable minimally displaced ring fractures
A3	Transverse fractures of the sacrum
Type B	Partially stable injury: rotationally unstable, vertically stable
B1	Open-book injury
B2	Lateral compression injury
B3	Bilateral Type B injuries
Type C	Unstable injury: rotationally and vertically unstable
C1	Unilateral
C2	Bilateral, one side Type C, one side Type B
C3	Bilateral Type C lesions

Source: Ref. 4.

and allows patients to move, can be used for provisional fixation in the acute stage of the injury. On the other hand, open reduction and internal fixation procedures have been advocated by many investigators in terms of the management of sacroiliac dislocation and have been generally accepted [2,4,9,10]. However, the optimum reduction of sacroiliac dislocation with large vertical displacement sometimes becomes difficult even with a conventional internal fixator such as a screw, plate, or rod [18].

Some surgeons have reported the results of the management of sacroiliac dislocation using iliosacral screw fixation [6,11–14]. This simple internal fixation is useful for stabilization of sacroiliac dislocation, whereas the complicated anatomy of the sacral foramina causes a risk of nerve injury due to a screw [15–17] and the acquired stability may be not sufficient in the absence of support with an external fixator [5,14,18]. Sacral bars have been preferred by other surgeons [7,8,19]. Besides these procedures, Albert et al. utilized a reconstruction plate [20].

Among the anchors for lumbosacral fixation, a rod inserted between the inner and outer cortices of the ilium has been used for the most caudad anchor in reconstruction of the lumbosacral spine (Galveston technique) [21]. Van Savage utilized the Galveston technique for fixation of fracture-dislocation of the lumbosacral junction [22]. On the other hand, pedicle screw fixation has been developed as the procedure for posterior internal fixation of the thoracic, lumbar, and lumbosacral spines. Several reports have shown reduction and fixation of traumatic lumbosacral dislocation by lumbosacral pedicle screw fixation [23–25]. One article described results with seven patients with sacroiliac dislocation treated by combined use of pedicle screws of the sacrum and the Galveston technique [26]. Korovessis et al. published a similar work concerning the surgical treatment of sacral fractures in 12 patients and sacroiliac dislocation in 2 patients using iliac screws and S1 pedicle screws [27]. One major difference between the two techniques is the reduction capability of vertical translation with rotational deformity of the pelvic ring [28,29]. An iliac rod and two S1 pedicle screws converged medially in a triangular fashion, penetrating the anterior cortex of the sacrum in our series, provided sufficient reduction and immediate stability for the sacroiliac dislocation. However, as Korovessis et al. mentioned in their article, the displacement at the sacroiliac joint did not change significantly.

In this chapter we explain the surgical technique of reduction and fixation of sacroiliac dislocation by the combined use of pedicle screws of the sacrum and the Galveston technique, and present briefly the result in 15 patients.

II. SURGERY

A. Preoperative Management

If the general condition is unstable for injuries of the intra-abdominal or intrapelvic organs, including the major vessels, life-saving management should take precedence over internal fixation of sacroiliac dislocation. Internal stabilization should be performed after confirmation of the stability of the patient's general condition. In such cases external fixation can be used for provisional fixation in the acute stage of the injury, followed by rigid internal fixation after recovery of patient's general condition and adequate assessment of the stability of the pelvic ring. In addition, external fixation decreases blood loss and allows patients to move. Anteroposterior and inlet plain radiographs of the pelvis and computed tomographic (CT) scans are useful to evaluate the stability and deformities of the pelvic ring. Reconstructive CT is helpful to image the deformity three dimensionally (Fig. 1).

B. Surgical Techniques

The patient is placed in the prone position on longitudinal bolsters. Taking into consideration reduction of pelvic ring deformities, the use of a Relton-Hall frame, which applies lateral

compression force on the iliac wings, should be avoided. A straight transverse skin incision is made across the pedicle level of S1 (Fig. 2). Both sides of the paravertebral muscles are divided transversally at the same level as for the skin incision and are retracted craniad and caudad to expose the posterior cranial portion of the sacrum and the affected posterior iliac crest and to observe directly the disrupted sacroiliac joint during reduction. The superior portion of the origin of the musculus gluteus maximus is detached subperiosteally from the iliac crest, and the posterior portion of the iliac wing is exposed to control the direction of an iliac probe and the rod. The cartilaginous surface of the sacroiliac joint disrupted by fracture-dislocation is treated by debridement and extraction of the bony fragment, which may disturb the reduction.

Pedicle screws are inserted into the S1 pedicles bilaterally according to the ordinary pedicle screw insertion technique with the help of lateral x-ray image intensifier. The S1 pedicle screws are converged medially in a triangular fashion and penetrate the anterior cortex of the sacral vertebral body for the purpose of increasing the stability of screws. A block bone measuring approximately 2 $\times$ 2 cm is excised from the rod insertion point of the iliac crest to avoid skin irritation due to the rod (Fig. 3). Prior to the rod insertion, an iliac probe should be inserted between the inner and outer cortex of the ilium about 30° caudally to the coronal plane of the pelvis. A straight iliac rod is inserted tentatively to confirm the direction and the length under control of anteroposterior x-ray image intensifier. The position of the femoral head is the good landmark to determine the direction and the depth of the rod. The straight rod of the Isola spinal system is inserted once into the probing hole and then pulled out. The pulled-out rod is bent gently to be medially adapted to the prominence of the sacral lamina (open arrow) and bent sharply at the screw insertion point of the ilium (arrow head) at an anatomical angle of 45° between the iliac wing and the frontal plane of the sacrum. The rod is inserted into the probing hole between the inner and outer tables of the iliac wing. Two rod-screw connectors are attached to the inserted rod caudally placed in the rod connection portion to avoid irritation of the L5-S1 facet joint due to the connector (Fig. 4A). For reduction of vertical displacement and angular deformity of sacroiliac dislocation, compression force is applied between the inserted rod and each S1 pedicle screw using a rod holder and a compressor (Figure 4B). If the space of the sacroiliac joint is still widened, further compression force is applied between each S1 pedicle

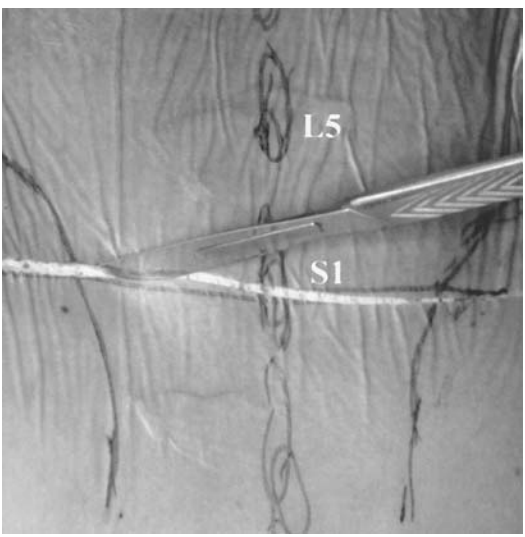

Figure 2 Skin incision. A straight transverse skin incision is made across the pedicle level of S1.

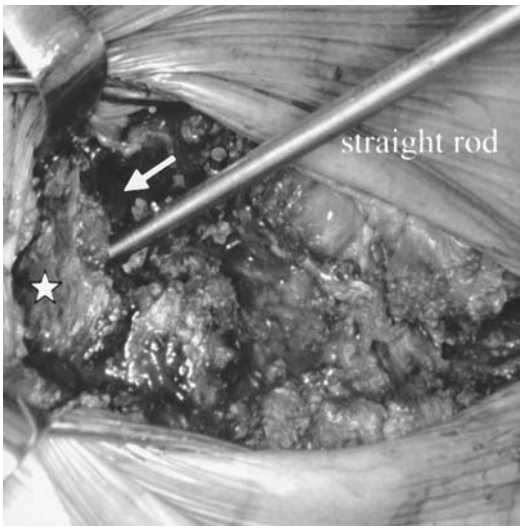

Figure 3 Iliac rod insertion. A block bone measuring approximately 2 × 2 cm is excised from the rod insertion point of the iliac crest to avoid skin irritation due to the rod. Prior to the rod insertion, an iliac probe should be inserted between inner and outer cortex of the ilium (asterisk) about 30 degrees caudally to the coronal plane of the pelvis. Straight iliac rod is inserted tentatively to confirm the direction and the length under control of anteroposterior x-ray image intensifier.

screw and the rod to close the opening (Fig. 5). After completion of internal fixation, divided paravertebral muscles are resutured, and ordinary skin closure is performed. No patients require bone grafting on the disrupted sacroiliac joint.

For patients with major disruption of the symphysis pubis with wide separation, additional fixation of the disrupted symphysis pubis in the supine position using a dynamic compression plate after the reconstruction of the posterior column of the pelvis is recommended (Fig. 6).

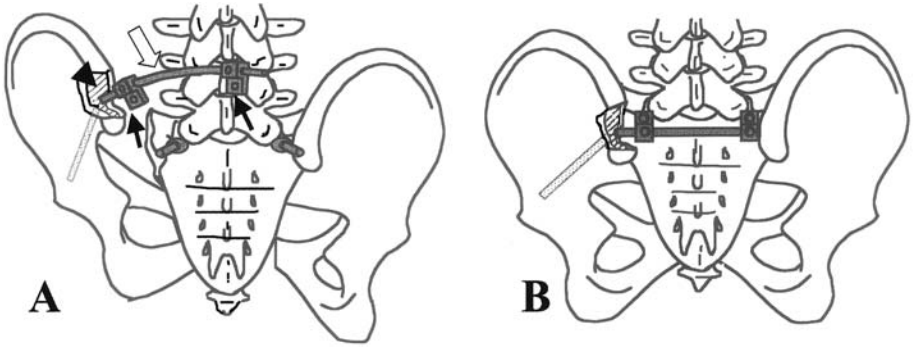

Figure 4 Reduction. (A) Two rod-screw connectors (arrow) are attached to the inserted rod caudally placed in the rod connection portion to avoid irritation of the L5-S1 facet joint due to the connector. (B) After introduction of the rod-screw connectors to the pedicle screws, nuts attached to the two screws are alternately tightened for further reduction.

Figure 5 Closing the opening gap. If the space of the sacroiliac joint was still widened, compression force would be applied between each S1 pedicle screw and the rod to close the opening using a rod holder and a compressor.

Patients with anterior injury as the form of fractured anterior rami and with minor disruption of the symphysis pubis can be treated by the posterior procedure alone (Fig. 7).

C. Postoperative Care

Postoperatively, all patients are encouraged to take a sitting position and to use wheelchairs for transfer within one week after surgery. Timing of the start of the gait with weight bearing varies mainly with the course of the treatment for associated injuries of the lower extremities. The weight-bearing gait is initiated 3 weeks postoperatively in the most of the patients without associated injury of their lower extremities.

D. Results

Between August 1993 and April 2001, 15 patients with dislocation of the sacroiliac joint underwent reduction and fixation by the combined use of pedicle screws for the sacrum and the Galveston technique at the authors' institutions. According to the classification system for pelvic ring disruption by Tile (Table 1) [4], all 15 patients had Type C pelvic injury associated with unilateral complete disruption of the sacroiliac joint. Nine of the 15 patients had Subtype C1 injury with unilateral sacroiliac dislocation, and 5 patients had Subtype C2 injuries associated with Type C on one side and Type B external rotational instability on the other side. The remaining patient had Subtype C3 injury associated with Type C on both sides. With regard to injury patterns of the anterior column, 5 of the 15 patients had disruption of the symphysis pubis, and the remaining 10 patients had fractures of the anterior rami. Four of 5 patients with major disruption of the symphysis pubis subsequently underwent additional plate fixation of the disrupted symphysis pubis.

1. Radiographical Evaluation

Postoperative alignment of the pelvic ring was evaluated using the published method [26]. Reduction of the vertical displacement was completed in 9 patients, and correction of the rota-

tional deformity was completed in 8 patients. In 2 patients, both reduction of vertical displacement and rotational deformity were incomplete. At the final follow-up, postoperative reduction was maintained in all patients except one, who underwent metal removal for skin irritation by screwhead prominence. A radiolucent zone around the rod inside the ilium in anteroposterior x-ray film, probably caused by physiological motion of the sacroiliac joint, was observed in all patients except one, who underwent removal of the implants for deep infection. However, no patients complained of problems associated with the lucency, and the implants were not removed.

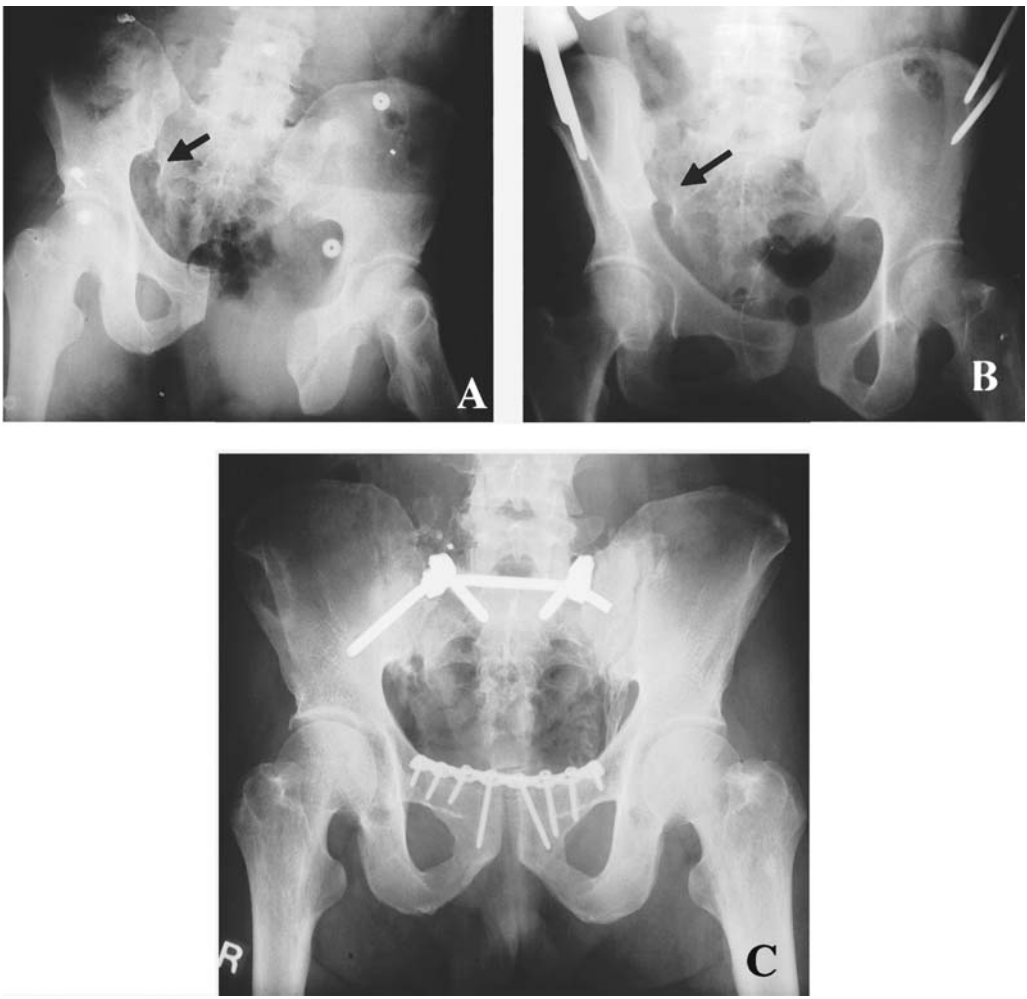

Figure 6 Type C patient with major disruption of the symphysis pubis. (A) The patient sustained Subtype C2 injury, Type C on right and Type B on left, with major disruption of the symphysis pubis. (B) External fixation was utilized for provisional fixation in the acute stage of the injury until the sufficient recovery of patient's general condition. Correction of both of the rotational deformity and vertical displacement was not sufficient. (C) Reduction and stabilization was performed using the iliac rod and S1 pedicle screws. For this patient with major disruption of the symphysis pubis with wide separation, additional fixation of the disrupted symphysis pubis using a was conducted after the reconstruction of the posterior column of the pelvis. (D,E) Pre- and postoperative CTs demonstrate reduction of the rotational deformity.

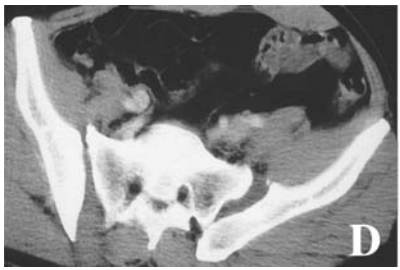

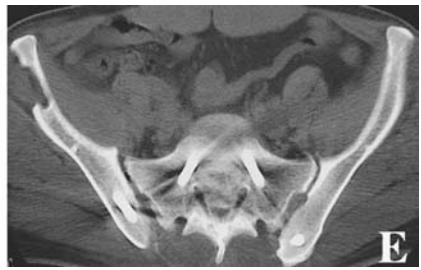

Figure 6 Continued.

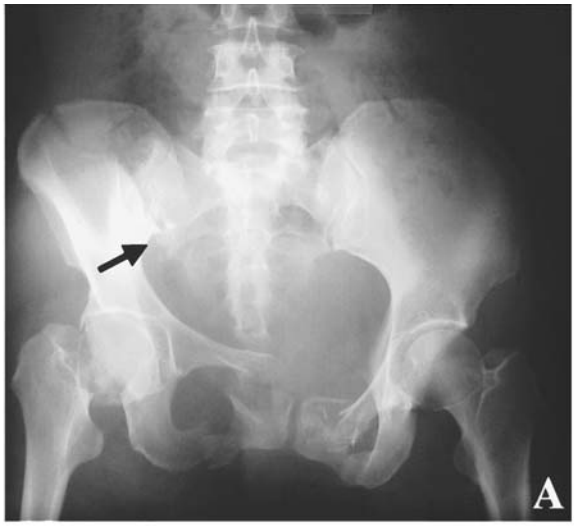

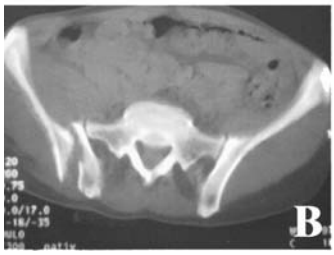

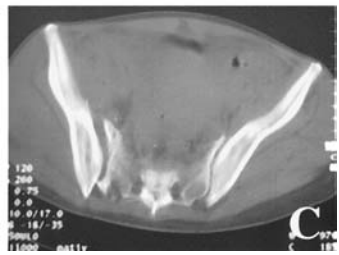

Figure 7 Type C patients with fractured anterior rami. (A) The patient sustained Subtype C1 injury with anterior injury as the form of fractured anterior rami. Plain anteroposterior x-ray film demonstrates rotational deformity and vertical translation of the right pelvis. (B,C). Preoperative CTs show internal rotation of the right pelvis. (D) Reduction and stabilization was performed using the iliac rod and S1 pedicle screws. Postoperative x-ray film demonstrates sufficient reduction of rotational and translational deformity. (E) Postoperative CT shows sufficient correction of rotational deformity.

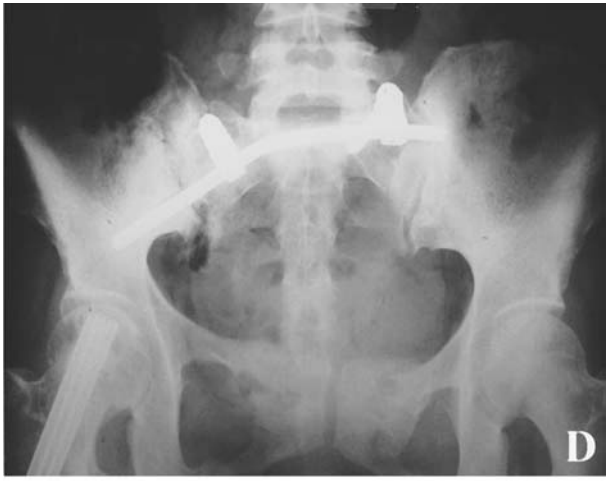

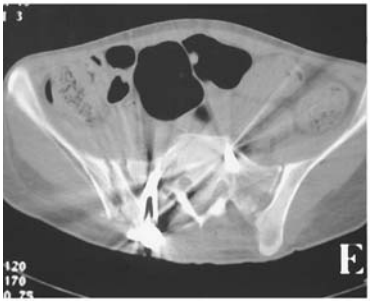

Figure 7 Continued.

2. Daily Activity

All patients showed normal walking capability at the final follow-up except one patient with associated femoral and sciatic nerve injury. Recovery of the nerve function was incomplete, and the patient required a cane and an orthosis to stabilize his frail lower extremity for ambulation. Three patients complained of mild pain on gait: one at the inguinal and gluteal region and two at the low back region, but they did not need pain medication. Regarding the working status at the final follow-up, a patient with femoral and sciatic nerve palsy was unemployed. A middle-aged female patient who postoperatively sustained deep infection was unemployed despite complete recovery of physical function. The remaining 13 patients had returned to their original jobs.

3. Complications

No patients experienced problems caused by transverse division of the paravertebral muscles, but one patient required secondary suture of the wound 2 weeks postoperatively. No patients sustained neurovascular complications of the inserted S1 pedicle screw. One patient had late deep infection around the iliac rod and the S1 screws 2 months postoperatively. The infection healed as a result of complete removal of the internal fixation devices and 2-week continuous irrigation, and progression of the pelvic ring deformity was not observed after removal of the

devices. Loss of correction was observed in one patient who required metal removal for skin irritation by screwhead prominence.

III. DISCUSSION

In sacroiliac dislocation, besides the posterior column disruption of the pelvis in the sacroiliac joint, the anterior column of the pelvis is usually disrupted as the forms of disruption of the symphysis pubis or the fractured anterior rami. Accordingly, sacroiliac dislocation is considered most unstable among the various types of traumatic pelvic ring disruption. In this type of injury, the vertically and rotationally unstable pelvis is associated with the loss of bilaterally symmetrical ring structure [2,4]. Several biomechanical studies have demonstrated that the use of an external fixator alone does not provide sufficient stability for a vertical shear injury of the sacroiliac joint and showed that the additional use of sacral bars substantially increases the strength and rigidity of fixation provided by external fixation alone [19,30,31]. Stocks et al. [31] also demonstrated that the combined use of sacral bars and symphysis plate for fixation provided the same stabilizing effect as that of external fixation with the additional use of sacral bars.

Pedicle screw fixation has been developed as a procedure for posterior internal fixation of the thoracic, lumbar, and lumbosacral spines. In our study the S1 pedicle screws were converged medially in a triangular fashion as the anchor of the sacrum. The triangulation has been presented in a biomechanical study to significantly enhance loads on pullouts of the pedicle screws [32]. In addition, the sacral pedicle screws penetrated the anterior cortex of the sacrum to increase the pullout resistance [33]. With regard to another fixation anchor for iliosacral fixation, we utilized a rod inserted between the inner and outer cortices of the ilium (Galveston technique). This fixation anchor has been demonstrated in biomechanical studies to be the most stable for lumbosacral fixation among the various fixation procedures [34,35]. The combined use of S1 pedicle screws and the Galveston technique, utilized in our series, provided sufficient reduction and good stabilization in the treatment of sacroiliac dislocation. With other posterior sacroiliac fixation techniques using sacral bars and iliosacral screws, reduction must be performed prior to internal fixation. On the other hand, the hybrid anchoring technique, which uses S1 pedicle screws and an iliac rod, provides sufficient reduction prior to fixation. From this point of view, the combined use of the S1 pedicle screw and the Galveston technique may be superior to other posterior internal fixation procedures for reduction and fixation of sacroiliac dislocation. However, further biomechanical studies are required for comparison of the stabilizing capability with those of other fixation procedures.

The iliac rod in the frontal plane was bent to 90° and inserted into the iliac wing in a horizontal direction, as reported by Allen and Ferguson [21]. Since then the Galveston technique has been performed by most surgeons with a more angled downward bent. The upward or horizontal direction, which allows one to introduce the rod into the thinner portion of the iliac wing, may enhance the stability of the rod. However, rod insertion into the thinner portion introduces the difficulty of rod setting and the risk of rod perforation from the iliac wing. The downward direction employed in most cases in our series provided immediate stability and sufficient reduction of the deformities, and the reduction was maintained without loss at the time of the final follow-up. Therefore we recommend the downward direction of the iliac rod considering the insertion facility.

Sacroiliac dislocation can be divided into two types according to the patterns of anterior injury: one for fractured anterior rami and the other for disruption of the symphysis pubis. With regard to internal stabilization of sacroiliac dislocation, posterior fixation using a sacral bar with additional anterior fixation using a symphysis plate has been revealed to be the most rigid

fixation procedure in biomechanical studies [19,36,37]. Kellam et al. advocated the combined use of external fixation of the pelvis and internal sacroiliac fixation for sacroiliac dislocation with this type of anterior pelvic fracture [7]. In our series we employed additional anterior stabilization in 4 patients with major disruption of the symphysis pubis. As a result, however, sufficient reduction and internal stabilization were achieved by posterior fixation alone in the remaining 10 patients with fractured anterior rami and one patient with disruption of the symphysis pubis. The 4 patients with sacroiliac dislocation with disruption of the symphysis pubis in our series, who were treated by the combined use of anterior and posterior internal fixation procedures, might have been managed by the posterior procedure alone without additional anterior fixation.

IV. CONCLUSION

The hybrid internal fixation procedure, combining the use of S1 pedicle screws and an iliac rod (Galveston technique), is useful for the reduction and fixation of sacroiliac dislocation associated with vertical and rotational instability of the pelvic ring.

REFERENCES

1. Dujardin FH, Hossenbaccus M, Duparc F, Biga N, Thomine JM. Long-term functional prognosis of posterior injuries in high-energy pelvic disruption. J. Orthop. Trauma 1998; 12:145–151.
2. Tile M. Pelvic ring fractures: Should they be fixed? J. Bone Joint Surg 1998; 70B:1–12.
3. Vanderschot P, Daenens K, Broos P. Surgical treatment of post-traumatic pelvic deformities. Injury 1998; 29:19–22.
4. Tile M. Classification. In: Tile M, ed. Fracture of the Pelvis and Acetabulum. 2d ed. Baltimore: Williams & Wilkins, 1995:66–101.
5. Browner BD, Cole JD, Graham JM, Bondurant FJ, Nunchuck-Burns SÇ, Colter HB. Delayed posterior internal fixation of unstable pelvic fractures. J. Trauma 1987; 27:998–1006.
6. Cole JD, Blum DA, Anset LJ. Outcome after fixation of unstable posterior pelvic ring injuries. Clin. Orthop 1996; 329:160–179.
7. Kellam JF, McMurtry RY, Paley D, Tile M. The unstable pelvic fracture: operative treatment. Orthop. Clin. North. Am 1987; 18:25–41.
8. Goldstein A, Phillips T, Sclafani SJA. Early open reduction and internal fixation of the disrupted pelvic ring. J. Trauma 1986; 26:325–333.
9. Duwelius PJ, Van Allen M, Bray TJ, Nelson D. Computed tomography-guided fixation of unstable posterior pelvic ring disruptions. J. Orthop. Trauma 1992; 6:420–426.
10. Failinger MS, McGanity PLJ. Current concept review: unstable fractures of the pelvic ring. J. Bone Joint Surg 1992; 74A:781–91.
11. Hirvensalo E, Lindahl J, Böstman O. A new approach to the internal fixation of unstable pelvic fractures. Clin. Orthop 1993; 297:28–32.
12. Routt ML, Simonian PT, Ballmer F. A rational approach to pelvic trauma. Clin. Orthop 1995; 318: 61–74.
13. Shuler TE, Boone DC, Gruen GS, Peitzman AB. Percutaneous iliosacral screw fixation: early treatment for unstable posterior pelvic ring disruptions. J. Trauma 1995; 38:453–458.
14. Ward EF, Tomasin J, Vander Griend RA. Open reduction and internal fixation of vertical shear pelvic fractures. J. Trauma 1987; 27:291–295.
15. Cecil ML, Rollins JR, Ebraheim NA, Yeasting RA. Projection of the S2 pedicle onto the posterolateral surface of the ilium: a technique for lag screw fixation of sacral fractures or sacroiliac joint dislocations. Spine 21:875–878.

16. Routt ML, Simonian PT, Mills WJ. Iliosacral screw fixation: early complications of the percutaneous technique. J. Orthop. Trauma 1997; 11:584–589.
17. Templeman D, Schmidt A, Freese J, Weisman I. Proximity of iliosacral screws to neurovascular structures after internal fixation. Clin. Orthop 1996; 329:194–198.
18. Pohlemann T, Bosch U, Gänsslen A, Tscherne H. The Hannover experience in management of pelvic fractures. Clin. Orthop 1994; 305:69–80.
19. Shaw JA, Mino DE, Werner FW, Murray DG. Posterior stabilization of pelvic fractures by use of threaded compression rods: case reports and mechanical testing. Clin. Orthop 1985; 192:240–254.
20. Albert MJ, Miller ME, MacNaughton M, Hutton WC. Posterior pelvic fixation using a transiliac 4.5-mm reconstruction plate: a clinical and biomechanical study. J. Orthop. Trauma 1993; 7:226–232.
21. Allen BL, Ferguson RL. The Galveston technique for L rod instrumentation of the scoliotic spine. Spine 1982; 7:276–284.
22. Van Savage JG, Dahners LE, Renner JB, Baker CC. Fracture-dislocation of the lumbosacral spine: case report and review of the literature. J. Trauma 1992; 33:779–784.
23. Bents RT, France JC, Glover JM, Kaylor KL. Traumatic spondylopelvic dissociation: a case report and literature review. Spine 1996; 21:1814–1819.
24. Cohn SL, Keppler L, Akbarnia BA. Traumatic retrolisthesis of the lumbosacral junction: a case report. Spine 1989; 14:132–134.
25. Hanley EN, Knox BD, Ramasastry S, Moossy JJ. Traumatic lumbopelvic spondyloptosis: a case report. J. Bone Joint Surg 1993; 75A:1695–1698.
26. Abumi K, Saita M, Iida T, Kaneda K. Reduction and fixation of sacroiliac joint dislocation by the combined use of S1 pedicle screw and the Galveston technique. Spine 2000; 25:1977–1983.
27. Korovessis P, Stamatakis M, Baikousis A. Posterior stabilization of unstable sacroiliac injuries with the Texas Scottish Rite Hospital spinal instrumentation. Orthopedics 2000; 23:323–327.
28. Korovessis P. Letter to the Editor RE: Reduction and fixation of sacroiliac joint dislocation by the combined use of S1 pedicle screw and the Galveston technique. Spine 2001; 26:1640–1641.
29. Abumi K. In Response to Letter to the Editor. RE: Reduction and fixation of sacroiliac joint dislocation by the combined use of S1 pedicle screws and the Galveston technique. Spine 2001; 26:1641.
30. Burgess A. External fixation. In: Tile M, ed. Fracture of the Pelvis and Acetabulum. 2nd ed. Baltimore: Williams & Wilkins, 1995:135–149.
31. Stocks GW, Gabel GT, Noble PC, Hanson GW, Tullos HS. Anterior and posterior internal fixation of vertical shear fractures of the pelvis. J. Orthop. Res 1991; 9:237–245.
32. Ruland CM, McAfee PC, Warden KE, Cunningham BW. Triangulation of pedicular instrumentation: a biomechanical study. Spine 1991; 16:S270–S276.
33. Zindrick MR, Wiltse LL, Widell EH. A biomechanical study of intrapeduncular screw fixation in the lumbosacral spine. Clin. Orthop 1986; 203:99–112.
34. Camp JF, Caudle R, Ashmun RD, Roach J. Immediate complications of Cotrel-Dubousset instrumentation to the sacro-pelvis: a clinical and biomechanical study. Spine 1990; 15:932–941.
35. McCord DH, Cunningham BW, Shono Y, Myers JJ, McAfee PC. Biomechanical analysis of lumbosacral fixation. Spine 1992; 17:S235–243.
36. Simonian PT, Routt ML. Biomechanics of pelvic fixation. Orthop. Clin. North Am 1997; 28:351–367.
37. Varga E, Hearn T, Powell J, Tile M. Effects of method of internal fixation of symphyseal disruptions on stability of the pelvic ring. Injury 1995; 26:75–80.

2

Percutaneous Vertebroplasty in the Treatment of Osteoporotic Fractures

Luis Alvarez and Antonio Pérez-Higueras
Fundación Jiménez Díaz
Madrid, Spain

I. INTRODUCTION

Vertebroplasty is a percutaneous technique used to treat vertebral body injuries that produce pain and/or risk of vertebral compression fractures due to weakening of bone structure. It consists of the injection of polymethylmethacrylate (PMMA) cement into the weak vertebral body in order to harden the vertebra to give it greater strength and stability, thus avoiding progression of collapse and pain. This technique was first used in 1987 by Galibert et al. [1] for the treatment of painful vertebral hemangiomas, myelomas, and metastatic lesions, with which they obtained magnificent results in pain management. Other small series subsequently stressed its efficacy in the treatment of these diseases [2,3].

The first results obtained with the use of this technique in the treatment of osteoporotic vertebral fractures were published in 1989 [4]. This study included a series of 5 patients with pain resistant to medical treatment who obtained immediate relief of their pain after a percutaneous vertebroplasty was carried out. Since then, different publications have demonstrated the good results obtained with this technique, with pain improvement in more than 80% of the cases [5–9].

II. INDICATIONS

The principal indication to perform a vertebroplasty is pain associated with a vertebral compression fracture in cases of osteolytic metastatic lesions, vertebral plasmocytomas, vertebral hemangiomas, and osteoporosis. The decision to use this technique is made by a multidisciplinary team that should assess the need for treatment, other than medical, either with radiotherapy, surgery, or a combination of several procedures. The final decision will depend on factors such as symptoms and signs, degree of dissemination of the disease, general health status, and foreseen survival.

III. OSTEOPOROSIS COMPRESSION FRACTURES

Osteoporosis is the most frequent bone metabolic disease. It affects more than 30% of the female population above 65 years of age, and it is expected that its incidence will quadruple in the world population during the next 50 years [10]. The spine is the most frequently affected region, with compression fractures of the vertebral bodies being produced.

Although most vertebral fractures are related to loss of bone density due to age, certain diseases, surgical procedures, and medications associated with the appearance of osteoporosis, such as steroid therapy, chronic pulmonary obstructive disease, and chronic alcoholism, are equally a cause of vertebral fracture due to microtraumatism.

Bone mineral density below 2 standard deviations and the existence of a previous vertebral fracture increase the risk of suffering a new vertebral fracture 7–20 times.

Fracture of the vertebral body by osteoporosis can be defined as reduction of more than 15% in height. The most frequent form is collapse at the expense of the superior plateau with or without anterior wedge deformity.

Vertebral compression fractures may occur spontaneously or after minimum trauma and are associated with some degree of pain in 84% of cases. They frequently cause acute and incapacitating pain, posing an important limitation of the person's daily activities [11]. In general, treatment with rest, analgesics, and use of external supports for a period of 2–12 weeks is effective in 85% of the cases [12]. However, in some cases the pain is persistent and very incapacitating, requiring the use of narcotics for its treatment.

In such cases, vertebroplasty has shown great efficacy, with decrease of pain in up to 90% of cases [7,8]. These effects are long-lasting; it has been demonstrated that there is no progression of the collapse in the cemented vertebrae and that a greater risk of fracture in the vertebrae adjacent to the cemented ones does not exist [13].

Although the candidate selection criteria for this procedure have not been clearly described in the literature, after a review of the first 250 cases of vertebral fractures due to osteoporosis treated in our center, we can recommend this technique in those patients who suffer vertebral compression fractures with severe and incapacitating vertebral pain, who do not respond to medical treatment, and in whom a spinal MRI confirms the presence of a loss of vertebral body volume, usually at the expense of the superior plateau, and with an alteration of the signal consisting in hyposignal in T1 and hypersignal in T2 and with a fat suppression technique (STIR). The presence of an intravertebral cyst of necrosis (Kümmel disease) is frequently observed, which supports the osteoporotic etiology of the lesion and does not contraindicate the procedure. When several vertebrae are affected, it is the location of the pain by clinical examination and the MRI image that indicates the pain-causing vertebra. Pain evolution time has little effect on the results, although it seems that better results are obtained in those cases of acute lesion having 6 weeks and worse ones in those that have more than one year of evolution.

Although the technique was initially developed to treat patients who did not respond to medical treatment [7,14,15], its use is indicated increasingly earlier because of the results obtained and the scarce number of complications observed [16–18]. However, we should continue to consider that this is a disease that is cured with medical treatment in more than 85% of cases and that there can be overtreatment of these lesions.

We have obtained worse results in those patients who have lost more than 70% in vertebral body height. In addition, the technique is not indicated in cases of vertebra plane with loss of 90% of its height. Furthermore, at present it is not considered to be indicated as a prophylactic treatment in patients with an important loss of bone mineral density in which there is no evidence of vertebral fracture.

IV. TECHNIQUE

A. Preprocedure Assessment

A presurgical study is performed with a chest x-ray, ECG, and blood biochemistry examination with hemorrhage and coagulation times. In our service, we perform a plain x-ray and MRI of

the spine in the days prior to the intervention to verify the present status of the process and the condition of the vertebra or vertebrae to be treated.

The patient and family are informed of the risks and benefits and treatment alternatives, and consent is obtained. If the patient is ambulatory, he or she is admitted to the hospital the afternoon before, and no premedication is administered normally.

B. Procedure

During recent years, different techniques to perform the percutaneous vertebroplasty have been developed in both Europe as well as the United States [7,16,17,19]. All have a similar base to that initially devised, there being, above all, differences in the cement injection method. This is a minimally invasive technique that basically consists of accessing the diseased vertebra body by posterior percutaneous route with a needle having sufficient caliber to make it possible to inject the cement into its interior.

Access is performed transpedicaularly in the dorsal and fifth lumbar vertebrae via a posterolateral approach in the rest of the lumbar vertebrae. In the cervical spine, the access is anterolateral with computed tomography and fluoroscopy arc control for the injection of the cement.

In the authors' experience, the procedure is performed with mild sedation and local anesthesia for the dorsal site and spinal, intradural anesthesia for the lumbar region. The patient is monitored cardiologically with oxymetric control, given that the patients are normally elderly and in prone decubitus situation, at least in the dorsal site.

Once the pedicles are located radiologically in posteroanterior projection, the skin and the pathway to the cortical wall are anesthetized and a small incision is made in the skin. Then the 14 gauge needle is introduced with diamond-tipped trocar until the upper third of the pedicular image is reached. A small blow with the hammer makes it possible to perforate the body cortical wall and, with lateral fluoroscopic guidance, to introduce the needle to the anterior third of the body, either with successive small blows or with mild pressure and rotation of the needle, depending on the consistency of the vertebra. Returning to the posteroanterior projection, the needle site is verified and puncture of another pedicle is performed.

In our experience, it is practically impossible or very dangerous to access the contralateral half of the body by transpedicular route, since we would need to perform a more external and oblique puncture with the risk of pedicular rupture. Therefore, we always perform a bilateral transpedicular puncture.

In the posterolateral route, the patient is placed in the left lateral decubitus position. The cutaneous puncture is performed 4 cm above the spinous line, and the vertebral body is accessed outside the transversal apophysis in the dihedral angle formed by the lateral and posterior sides of the body. Once the body cortical wall is perforated, the needle is advanced until it reaches the anterior third of the vertebral body, after the mean line of the anteroposterior projection.

In all cases, vertebrography with nonionic isoosmolar iodine contrast media was performed, with acquisition in digital subtraction and lateral projection. When there is lateral vein filling, it is also useful to perform a vertebrography in anteroposterior projection. The vertebrography results are very useful to orient the performance of the vertebroplasty. In most cases, the trabecula spongy bone is filled and, more or less rapidly, the basivertebral vein and posterior peridural venous plexus or a lateral segmental vertebral vein are filled with drainage towards the vena cava or azygous complex. Due to fracture of the superior or inferior plateau, contrast escape to the intervertebral disc is sometimes observed.

The immediate filling of one of these veins or the disc without trabecular filling makes it necessary to reposition the needle point, a maneuver that is sometimes not successful. In these cases, very slow injection of a drop of cement should be done with exhaustive fluoroscopic

control, visualizing the cement progress in the vein and stopping when the cement reaches the plexus.

The cement used is mixed with a small amount of tantalum or tungsten power to provide radio-opacity. The result is a semiliquid compound that should be very homogeneous, without lumps. When mixing in cold, we lengthen the hardening time of the cement, permitting a slower and more prolonged injection. Some cements with barium sulfate and appropriate viscosity have been manufactured especially for this procedure.

The mean amount of cement to be injected in a vertebra varied from 3 to 7 cc both in the transpedicular as well as posterolateral route. Injection of the cement should always be performed under direct and continuous fluoroscopic control. There are several mechanisms to perform the cement injection: direct manual injection with 1 and 2 cc syringes, injection by a pistol system, or injection by screw system. The authors prefer to use the screw systems because they allow slower and more controlled cement injection. With the manual or pistol systems it is difficult to prevent massive leakage of cement into the venous system if a sudden communication with the basivertebral plexus occurs during the procedure and with this an abrupt decrease of resistance to the injection. In addition, with the screw systems, higher injection pressure is obtained than with the other systems, which makes it possible to use lower caliber needles (14G vs. 10 and 11G).

It is very important to have radiology equipment with high-quality features such as those used in vascular radiology, with very good radioscopy and the possibility of enlarging the image and performing digital subtraction and even road mapping, and to have a previously made reference image of the vertebrography in order to have possible leakage points controlled at all times (Fig. 1).

Once the vertebroplasty is completed, the patient is maintained at rest for several hours, allowing mobilization according to tolerance. A control study should be done by CT scan of the vertebra treated to verify the filling and the presence of extravasations. In general, the patients can be discharged the next day, with ambulation and with analgesics according to the degree of pain. Afterwards they can gradually take up their usual daily activities (Fig. 2).

V. CONTRAINDICATIONS

The only absolute contraindication to performing a vertebroplasty is the existence of a serious coagulation alteration. Patients who are under dicumarinic treatment should discontinue the treatment 2 days before and use preventive doses of low molecular weight heparin. The technique should be avoided in patients with known infection. Existence of a practically flat vertebra makes it impossible to inject the cement. Furthermore, presence of a longitudinal fracture that produces a complete division of the anterior wall contraindicates the technique.

VI. COMPLICATIONS

The number of complications described in the literature using this technique is very low. On some occasions an increase in pain has been described during the procedure, probably due to the increase in pressure in a painful vertebra and during the first hours after the cement injections [2,20]. However, the most serious complications are related to cement leakage outside the vertebral body margins, both directly as well as through the venous plexus.

Cotten et al. [2] demonstrated the presence of both cortical wall as well as venous cement leakage in 29 of 40 patients treated for metastasis or myeloma in whom a CT scan was performed after the procedure. Most of these leakages were asymptomatic, but two that were in the intraver-

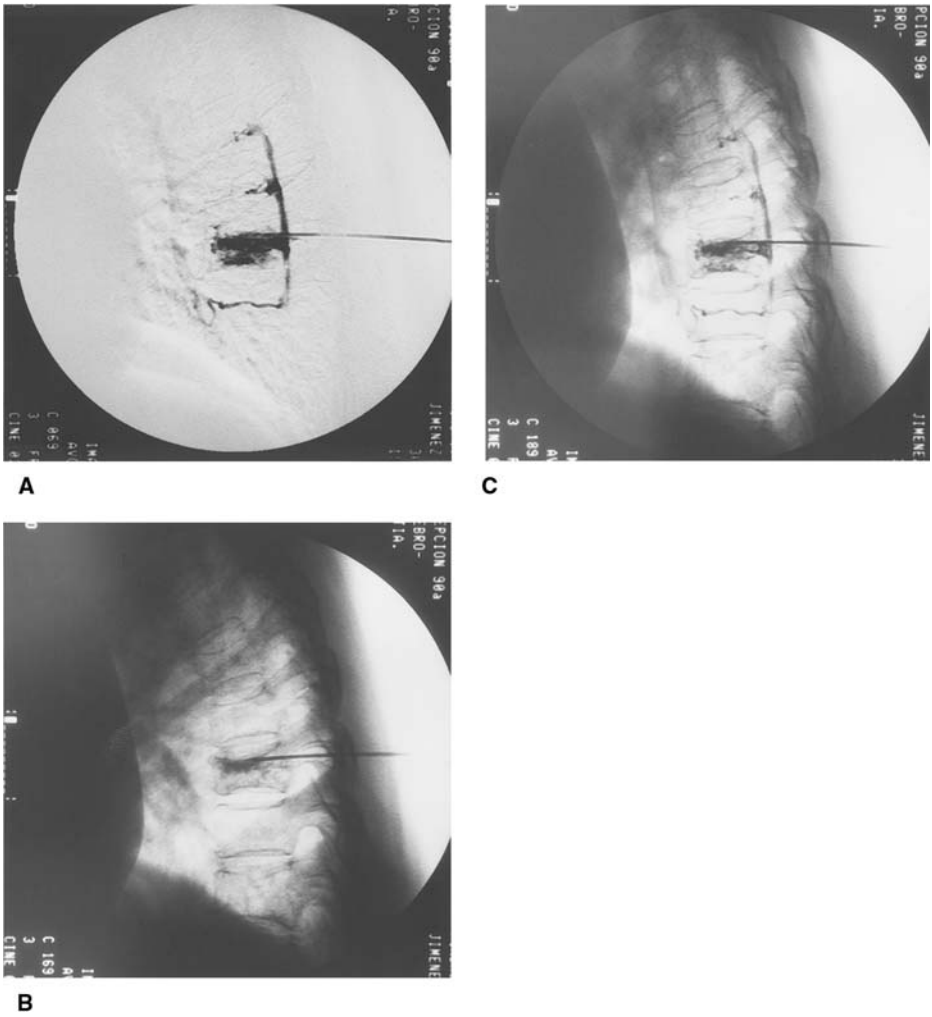

Figure 1 (A) Vertebrograph with a digital substraction showing complete trabecula filling and drainage to the posterior epidural venous plexus and an anterior azygous vein. (B) The image is retained and the cement is injected very slowly, stopping when it reaches the drainage points. (C) The result is the filling of the vertebral body.

tebral foramen needed surgical decompression. In a review, a larger series of patients [21] described one case of radicular compression out of 258 patients treated and 13 cases of radicular pain, 3 of whom needed surgical decompression of the root; the remaining cases abated with anti-inflammatory treatment. Most of the authors describe a low incidence of transitory neuritis (0–6%) [2,14,16,21–23], although there are cases of massive cement leakages that require emergency decompressive surgery [24]. In every case, the cause of the appearance of the complication was due to a defect in the technique, either in the preparation of the cement, its scarce visualization, or its uncontrolled injection.

The presence of leakage of the cement into the vertebral venous plexus does not interfere in the technique success. The heat released by the cement in its polymerization process could injure the nearby nervous structures, but as Wang et al. [25] demonstrated in an experimental

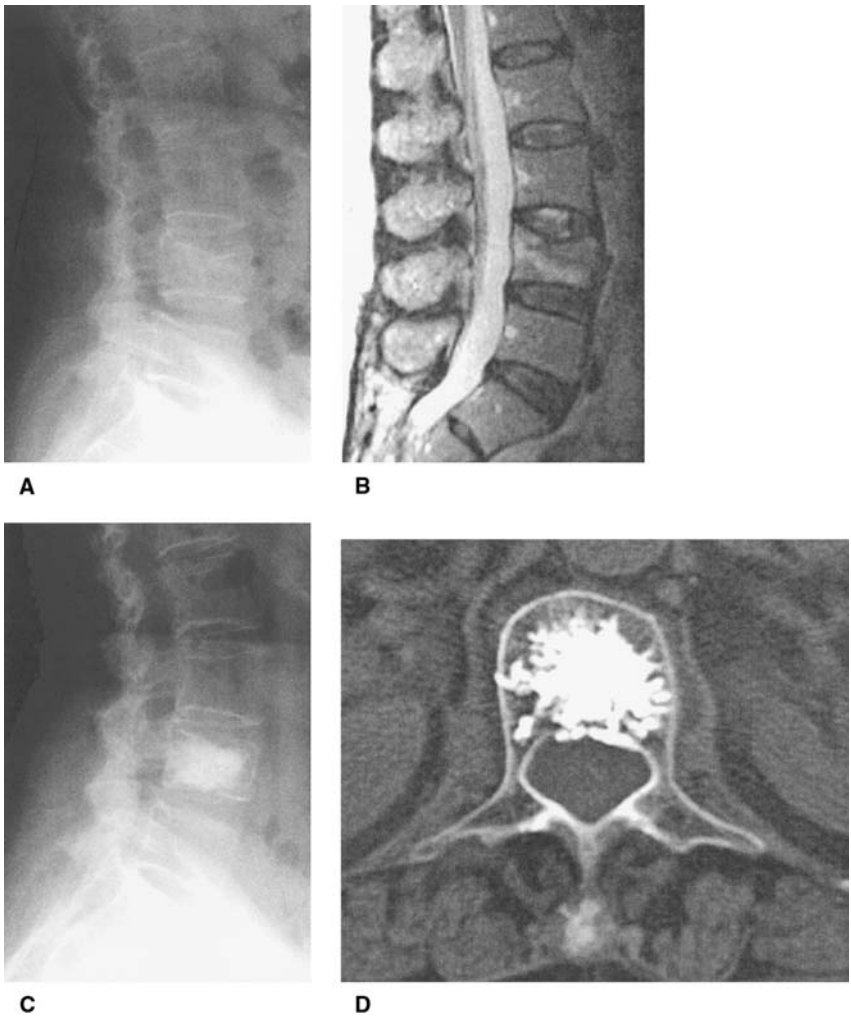

Figure 2 (A) Osteoporotic vertebral compression fracture of L4 in a patient with pain refractory to medication. (B) MRI shows a hyperintense T_2-weighted signal. (C) Vertebroplasty is performed with good filling of the vertebral body and an excellent result. (D) A postprocedural CT scan shows a small leakage of cement into the epidural venous plexus.

study in dogs, it seems that both the presence of the posterior vertebral common ligament, which would act as a barrier, as well as the continuous flow of cerebrospinal fluid that acts as a refrigerant prevent the locally reached temperature from being sufficient to cause this injury [26].

The presence of cement outside the vertebral frame was observed in 47% of 250 patients in whom postprocedure CT was performed. The functional results were similar in both the cases showing cement leakage as well as in the absolutely normal ones [9].

Other complications described in the literature include costal fractures, paravertebral hematomas, epidural abscesses, esophageal compression, and pulmonary embolism. The latter is due to massive leakage of cement into the central circulation [27].

VII. FUTURE DEVELOPMENTS

Percutaneous vertebroplasty has evolved very rapidly in recent years, and we have had the opportunity of seeing articles that retrospectively gather short series appear in the literature and prospective studies and longer series begin to arise [18]. It is expected that we will soon have better knowledge of the long-term results and that we will improve our inclusion criteria.

Two research fields are presently being developed: biocements and kyphoplasty.

Biocements are compounds of calcium phosphate that can be injected in liquid form and that harden at body temperature. They were initially developed for filling of the bone cavities and are totally reabsorbable products. In vitro experiments have demonstrated that the product, once hardened, is capable of strengthening the bone structure in the same way as PMMA cements [28–31]. However, its application in persons and its clinical indications must still be defined. We have found many difficulties in its use in experimental animals. When the mixture obtained has the viscosity characteristics recommended by the manufacturers, the pressure exerted for the injection of the product causes the separation of the solid and liquid phases within the puncture needle, producing its taponade. However, when the mixture obtained is more liquid and the injection is performed, the product is ''washed'' from the vertebral body by the blood flow so that the desired effect of strengthening the bone structure is not obtained. In addition, considering the magnificent results obtained with the use of the present PMMA cements, the advantages of absorbable cements, which may not prevent progression of the collapse of the treated vertebra, must still be defined [29]. However, it is possible that the development of these products will have great utility in the future as a prophylactic treatment more than as a treatment of symptoms.

Kyphoplasty is a technique by which an attempt is made to treat the pain caused by an osteoporotic vertebral fracture but that also aims to recover the vertebral body height and restore the sagittal plane lost by the wedging suffered. The technique consists in the placement of a balloon inside the affected vertebral body which, on being inflated at high pressure, restores the vertebral body height, posteriorly performing a filling of the rest of the remaining space with cement. The results obtained initially seem to be similar to those of the vertebroplasty regarding the improvement of the functional situation, with a 48% restoration of vertebral height, especially in patients treated within 6 weeks after fracture [32,33].

REFERENCES

1. Galibert P, Deramond H, Rosat P, Le Gars D. Preliminary note on the treatment of vertebral angioma as well as painful and debilitating diseases. Neurochirurgie 1987; 33:166–168.
2. Cotten A, Dewatre F, Cortet B. Percutaneous vertebroplasty for osteolytic metastases and myeloma: effects of percentage of lesion filling and the leakage of methyl methacrylate at clinical follow-up. Radiology 1996; 200:525–530.
3. Kaemmerlen P, Thiesse P, Bouvard H, Biron P, Mornex F, Jonas P. Percutaneous vertebroplasty in the treatment of metastases. Technic and results. J. Radiol 1989; 70:557–562.
4. Lapras C, Mottolese C, Deruty R, Lapras Ch, Remond J, Duquesnel J. Percutaneous injection of methyl-methacrylate in the treatment of severe vertebral osteoporosis and osteolysis. Ann. Chir 1989; 43:371–376.
5. Cortet B, Cotten A, Boutry N. Percutaneous vertebroplasty in the treatment of osteoporotic vertebral compression fractures: an open prospective study. J. Rheumatol 1999; 26:2222–2228.
6. Gangi A, Dietemann JL, Guth S, Steb JP, Roy C. Computed tomography (CT) and fluoroscopy-guided vertebroplasty: results and complications in 187 patients. Sem. Intervent. Radiol 1999; 16: 137–142.

7. Jensen ME, Evan AJ, Mathis JM, Kallmes DF, Cloft HJ, Dion JE. Percutanous polymethylmethacrylate vertebroplasty in the treatment of osteoporotic vertebral body compression fractures: technical aspects. Am. J. Neuroradiol 1997; 18:1897–1904.
8. Levine SA, Perin LA, Hayes D, Hayes WS. An evidence-based evaluation of percutaneous vertebroplasty. Manag. Care 2000; 9:56–60.
9. Alvarez L, Perez-Higueras A, Rossi RE, Calvo E. Vertebroplasty in osteoporotic fractures: clinical and radiological results after 5 years. Eur. Spine. J 2001; 10(suppl 1):S8.
10. Riggs BL, Melton LJ. The worldwide problem of osteoporosis: insights afforded by epidemiology. Bone 1995; 17(suppl):505–511.
11. Lyles KW, Gold DT, Shipp KM, Pieper CF, Martinez S, Mulhausen PL. Association of osteoporotic vertebral compression fractures with impaired functional status. Am. J. Med 1993; 94:595–601.
12. Rapado A. General management of vertebral fractures. Bone 1996; 18(suppl):191–196.
13. Pérez-Higueras A, Alvarez L, Rossi RE, Quiñones D, Al-Assir I. Percutaneous vertebroplasty: long-term clinical and radiological outcome. Neuroradiology 2002; 44:750–954.
14. Chiras J, Depriester C, Weill A, Sola-Martinez MT, Deramond H. Percutaneous vertebral surgery: techniques and indications. J. Neuroradiol 1997; 24:45–59.
15. Mathis JM, Petri M, Naff N. Percutaneous vertebroplasty treatment of steroid induced osteoporotic compression fractures. Arthritis. Rheum 1998; 41:171–175.
16. Deramond H, Depriester C, Galibert P, Le Gars D. Percutaneous vertebroplasty with polymethylmethacylate. Technique, indications and results. Radiol. Clin. North. Am 1998; 36:533–546.
17. Gangi A, Kastler BA, Dietemann JJ. Percutaneous vertebroplasty guided by a combination of CT and fluoroscopy. Am. J. Neuroradiol 1994; 15:83–86.
18. Zoarski GH, Snow P, Olan WJ, Stallmeyer MJB, Dick BW, Hebel R, De Deyne M. Percutaneous vertebroplasty for osteoporotic compression fractures: quantitative prospective evaluation of long-term outcomes. J. Vasc. Interv. Radiol 2002; 13:139–148.
19. Al-Assir I, Perez-Higueras A, Florensa J, Munoz A, Cuesta E. Percutaneous vertebroplasty: a special syringe for cement injection. Am. J. Neuroradiol 2000; 21:159–61.
20. Weill A, Chiras J, Simon JM, Rose M, Sola-Martinez T, Enkaoua E. Spinal metastases: indications for and results of percutaneous injection of acrylic surgical cement. Radiology 1999; 199:241–247.
21. Cotten A, Boutry N, Cortet B. Percutaneous vertebroplasty: state of the art. Radiographics 1998; 18: 311–320.
22. Barr JD, Barr MS, Lemley TJ, McCann RM. Percutaneous vertebroplasty for pain relief and spinal stabilization. Spine 2000; 25:923–8.
23. Heini PF, Walchli B, Berlemann U. Percutaneous transpedicular vertebroplasty with PMMA: operative technique and early results. A prospective study for the treatment of osteoporotic compression fractures. Eur. Spine J 2000; 9:445–50.
24. Wenger M, Markwalder TM. Surgically controlled, transpedicular methyl methacrylate vertebroplasty with fluoroscopic guidance. Acta. Neurochir. (Wien) 1999; 141:625–631.
25. Wang GJ, Wilson CS, Hubbard SL, Sweet DE, Reger SI, Stamp WG. Safety of anterior cement fixation in the cervical spine: in vivo study of dog spine. South Med. J 1984; 77:178–179.
26. Deramond H, Wright NT, Belkoff SM. Temperature elevation caused by bone cement polymerization during vertebroplasty. Bone 1999; 25(suppl):17–25.
27. Padovani B, Kasriel O, Brunner P, Peretti-Viton P. Pulmonary embolism caused by acrylic cement: a rare complication of percutaneous vertebroplasty. Am. J. Neuroradiol 1999; 20:375–377.
28. Belkoff SM, Mathis JM, Erbe EM, Fenton DC. Biomechanical evaluation of a new bone cement for use in vertebroplasty. Spine 2000; 25:1061–1064.
29. Belkoff SM, Mathis JM, Jasper LE, Deramond H. An ex vivo biomechanical evaluation of a hydroxyapatite cement for use with vertebroplasty. Spine 2001; 26:1542–1546.
30. Bo B, Laith MJ, Frederick JK, Spivak JM. The use of an injectable, biodegradable calcium phosphate substitute for the prophylactic augmentation of osteoporotic vertebrae and the management of vertebral compression fractures. Spine 1999; 24:1521–1526.
31. Lim TH, Brebach GT, Renner SM, Kim WJ, Kim JG, Lee RE, Andersson GB, An HS. Biomechanical evaluation of an injectable calcium phosphate cement for vertebroplasty. Spine 2002; 27:1297–1302.

32. Lieberman IH, Dudeney S, Reinhardt M. Initial outcome and efficacy of kyphoplasty in the treatment of painful osteoporotic vertebral compression fractures. Spine 2001; 26:1631–1638.
33. Lane JM, Girardi F, Parvaianen H, Cammisa FP, Jr. Preliminary outcomes of the first 226 consecutive kyphoplasties for the fixation of painful osteoporotic vertebral compression fractures. Osteoporosis. Int 2000; 11(suppl):S206.

3
Biomechanics of Vertebroplasty

Stephen M. Belkoff
The Johns Hopkins University/Johns Hopkins Bayview Medical Center
Baltimore, Maryland, U.S.A

I. INTRODUCTION

For almost four decades, vertebroplasty has been used to augment the purchase of pedicle screws for spinal instrumentation [1] and to fill voids resulting from tumor resection as a means of reducing the risk of fracture subsequent to the weakening caused by resection [2–5]. Vertebroplasty, initially an open procedure, introduced bone graft or some biomaterial, typically polymethylmethacrylate (PMMA) cement, into vertebral bodies (VBs) [2–4,6–12]. Percutaneous vertebroplasty (PV), a relatively new variant, is performed by injecting acrylic cement into VBs via cannulae. This procedure was reportedly first performed in 1984 to stabilize a C2 vertebra invaded by an aggressive hemangioma [13]. The successful mechanical stabilization of the VB and the resulting pain relief experienced by the patient led investigators to adapt the procedure for patients with painful osteoporotic vertebral compression fractures [14]. In recent years, the procedure has gained acceptance by many clinicians [15] and is being performed with increasing frequency, partly because of the often dramatic pain relief that reportedly occurs after the procedure [16–18] and partly because of the need for an alternative procedure to nonoperative therapy (bed rest and pain medication) for the growing numbers of elderly patients with osteoporotic compression fractures. Osteoporosis is a daunting public health concern and is the most common cause of vertebral compression fractures (VCFs) in the United States [19]. The incidence of VCF exceeds that of hip fractures [20]. Furthermore, as treatments for primary tumors become more effective, resulting in longer periods of patient survival, the incidence of metastatic lesions increases. The spine is the most common site for metastases, and osteolytic metastases and myeloma are the most frequent malignant lesions occurring in the spine [3]. PV is being used more frequently to augment mechanically VBs compromised by lytic lesions.

Accompanying the increase in the practice of PV are increases in the number of clinical investigations into the efficacy of the procedure and of basic science investigations into evaluating materials, instruments, and techniques. This chapter focuses on those biomechanical investigations.

II. MECHANISMS OF PAIN RELIEF

According to the literature, pain relief after PV treatment is experienced by approximately 90% of patients with osteoporotic VCFs [18,21] and approximately 60–70% of patients with various tumors [22,23]. Although the definitive mechanism of pain relief remains unidentified, proposed

mechanisms include mechanical stabilization [24,25] and thermal or chemical interaction with vertebral periosteal [26,27] or intraosseous pain receptors [28].

A. Thermal Effects

When PMMA polymerizes, it does so exothermically. Some hypothesize that the heat generated in the exothermic reaction of PMMA is sufficient to cause thermal necrosis of neural tissue and is therefore the mechanism responsible for pain relief [24]. Most investigations regarding thermal injury and PMMA polymerization stem from the use of PMMA cement in arthroplasty procedures, for which the volumes of cement used are substantially greater than those used in PV [29–31]. In those investigations, temperatures as high as 122°C have been measured [29]. However, at least one ex vivo study suggests that temperature is not a mechanism of pain relief [32]. In that study, temperature was measured at three locations (inside the anterior cortex, in the center of the VB, and in the spinal canal) after concurrent bipedicular injection of 10 mL of PMMA cement. Although temperatures exceeded 50°C for more than 1 minute at the center of the VB, the authors concluded that temperature was an unlikely mechanism of pain relief for several reasons. First, because the experiments were conducted on ex vivo VBs, the effect of active heat transfer due to blood profusion, as would be the case in vivo, was not included. Profusion would be expected to remove much of the heat generated during cement polymerization. Second, the volume of cement injected was greater than that typically used for PV [33]. And third, the cement was injected concurrently via both pedicles to maximize the thermal effect for experimental measurement. Clinically, PV would be performed in a staged procedure in which half of the cement would be injected through one cannula placed in a pedicle [25], and then the second half would be injected through the other cannula in the contralateral pedicle. Thus, the heat of polymerization from the initial injection would likely have dissipated to negligible levels before the second injection began polymerizing. However, in that same study, the experimental protocol departed from clinical practice in that the cannulae remained in the VBs during cement polymerization and may have served as cooling fins, reducing the intravertebral body temperature. That study was recently repeated except that the cannula were removed immediately after the cement injection [33a]. Temperatures were substantially higher in VBs from which the cannulae were removed than in those in the previous study, which retained the cannulae during polymerization. Thus, the issue of thermal injury during cement polymerization remains unresolved. To the author's knowledge there are no reported animal model histological investigations into any thermal effect on neural tissue of cement polymerization during PV, and in vivo measurements of intravertebral temperatures during VP are not currently available.

The threshold above which thermal necrosis of osteoblasts occurs is typically 50°C if that temperature is sustained for more than 1 minute [34,35]. Neural tissue may be more sensitive to temperature than osteoblasts [36]. Thermal necrosis follows an Arrhenius relationship in which temperature and exposure time are factors. Thus, tissue exposed to lower temperatures, but for longer periods of time, may also become necrotic. Conversely, tissue exposed to higher temperatures would require less exposure time to become injured. For example, a recent study reports that apoptosis occurred in osteoblasts exposed to 48°C for 10 minutes [37].

It should be noted that in both those ex vivo studies, temperatures recorded in the spinal canal did not reach 50°C [32,33a]. The spinal cord appears to be at little risk of thermal injury as long as the cement is properly injected and contained within the VB. If cement were to leak into the spinal canal and come into direct contact with the cord, it is not unrealistic to expect that thermal injury might occur.

B. Cytotoxicity

The methylmethacrylate (MMA) monomer component of PMMA cement is cytotoxic and therefore has been implicated as a mechanism of pain relief [24]. Cell cultures show that MMA monomer is toxic to leukocytes and endothelial cells when concentrations exceed 10 mg/mL [38], but its effect on neural tissue remains unknown. During knee arthroplasty, blood serum levels immediately after cementation and tourniquet release have been measured as high as 120 μg/mL but are typically much lower (<2 μg/mL) and drop precipitously minutes after implantation [39]. MMA monomer is highly volatile and, as such, is mostly expelled through the lungs during respiration. Thus, after the blood has circulated once through the body, the MMA concentration in the blood drops to negligible levels. Other investigators have reported blood serum concentration between 0.02 and 59 μg/mL during total hip replacement [40]. Considering that the volumes of cement used for total hip replacements and knee arthroplasty are two to three times greater than those typically used with PV, and that monomer concentrations measured for those procedures are 10–100 times less than MMA concentrations reported to be cytotoxic to tissue cultures [38], it seems unlikely that MMA toxicity is responsible for pain relief experienced with PV. Even so, local serum monomer concentrations measured immediately after PV are needed to determine definitively if MMA monomer cytotoxicity plays a role in pain relief.

MMA monomer toxicity has also been implicated in the necrosis of tumor cells. In histological sections taken postmortem from a patient who had previously undergone PV, a zone of necrosis was noted in the tumor cells nearest the injected cement [41]. In one study, necrosis of breast cancer cells occurred at concentrations greater than 5 μg/mL for a 1-hour exposure time, whereas apoptosis occurred at concentrations greater than 1 μg/ml for a 1-hour exposure [42]. The exposure times and concentrations are much greater than what would be expected to occur in vivo; therefore, it seems unlikely that cytotoxicity plays a role in creating the zone of necrosis noted histologically.

C. Mechanical Stabilization

Despite the possible roles played by cytotoxicity and thermal injury, mechanical stabilization appears to be the most likely mechanism of pain relief [32,43]. Pain associated with osteoporotic VCF is thought to be caused by motion at the fracture, which stimulates nociceptors concentrated in the periosteal region [25]. PV stabilizes the fractured VB [43–47], minimizes micromotion, and likely prevents painful nerve aggravation. PV appears to satisfy the requirements of fracture stabilization consistent with those of other sites in the body; namely, to prevent painful micromotion and provide a mechanically stable and biologically conducive environment for fracture healing. Several factors contribute to the mechanical stabilization achieved by PV, including the density of the VB, the volume and location of the cement injected, and the material properties of the cement. The optimal cement volume and material properties have not yet been determined.

III. MECHANICAL CONSIDERATIONS

How much cement is needed to stabilize VCFs has been a clinical concern since the onset of PV practice. A recent ex vivo study reported that only 2 mL of PMMA were needed to restore strength in osteoporotic VBs, but that larger volumes (4–6 mL) were needed to restore stiffness [43]. These volumes are lower than what was typically used and previously thought necessary, both clinically and in biomechanical investigations [32,44,46]. The correlation between cement volume and restoration of strength and stiffness was very weak [43]. It is likely that other factors, such as bone density and the geometry of the injected cement, affects restoration values. Those

authors hypothesized that strength and stiffness restoration would more closely correlate to the percentage of the VB volume filled than just the cement volume injected, but the correlation was not stronger [47a]. Finite element modeling of PV has suggested that a fill of 14%, or about 3.5 mL for an L1 VB, would be sufficient to restore stiffness [48]. Although that study showed that fill volume may restore stiffness for the single specimen evaluated, the results of an experimental study did not support that conclusion for all L1 VBs [47a].

Restoring initial strength would be expected to prevent refracture of the treated vertebra. If the spine were subjected to a load of the magnitude required to cause the original fracture, other vertebral levels would be expected to fracture before the repaired level refractured. Stiffness, not strength, is the mechanical parameter likely most closely linked with pain relief. Although fixation stiffness plays a large role in fracture healing [49], restoring or increasing VB stiffness relative to prefracture levels may not be necessary or even preferable [49]. As with other fractures, avoiding the extremes of mechanical stability is desirable. Repairs that are too stiff may result in stress shielding, remove mechanical feed back to osteoblasts, and impede fracture healing. Conversely, repairs that are not stiff enough allow too much motion and may result in nonunion.

Concerns have been raised that PV hypothetically creates a stress concentration, alters spine kinematics, and places adjacent levels at risk of fracture. This concern seems unfounded for several reasons. First, PV appears to restore, or nearly restores, stiffness and does not increase stiffness relative to prefracture levels [43–47]. Thus, adjacent levels should be at no greater risk than they were in the prefracture state. Even if the VB stiffness were increased relative the prefracture state, the stiffness of an individual level is unlikely to affect spinal kinematics. Most spinal motion occurs at the level of the disc, which is much more compliant than the VB. Therefore, only if cement were injected into the disc space would one expect disc mechanics to be altered and subsequently alter spine kinematics. Clinically, a preliminary report has suggested that the incidence of fractures in adjacent levels is no higher than that in remote levels [50].

In one study, pain relief was experienced in 90% of patients ($n = 29$) whose VBs were injected with an average volume of 7.1 mL (2.2–11.0 mL) of PMMA [18]. A recent clinical report showed that injection of 2–3 mL into the thoracic and 3–5 mL into the lumbar regions resulted in 97% moderate to complete pain relief [51]. These results suggest that pain relief may be achieved with volumes consistent with those needed to restore mechanical integrity ex vivo [43]; however, no correlation of level treated, volume injected, and clinical outcome has been explicitly reported. The volume of cement needed to produce a desired outcome still needs to be determined by carefully controlled, prospective, randomized clinical studies.

A. Unipedicular versus Bipedicular Injection

The ability to stabilize VBs through unipedicular injections may result in reduced procedure time and risk associated with bilateral cannulae. Tohmeh et al. [44] found that VB strength may be restored via a unipedicular cement injection without risk of VB collapse on the uninjected side. The amount of cement injected unipedicularly in that study, however, was 6 mL. It is unknown if the restoration was related to the volume of cement or to how and where it was injected. On the other hand, in a study using a finite element model, Liebschner et al. [48] suggested that unipedicular injections may place the VB at risk for collapse on the uninjected side. Clinically, the unipedicular procedure has been performed on a limited number of patients, and the clinical outcomes have been encouraging [51]. Even so, a prospective clinical trial needs to be conducted to determine the long-term benefits of unipedicular PV relative to bipedicular PV.

B. Height Restoration

Restoring height to collapsed VBs is of interest clinically because it has the potential benefit of reducing postfracture kyphosis and its associated sequelae [26,52–55]. A new device, the inflatable bone tamp, has been developed as a means of restoring height [56,57]. This tamp is placed inside the VB under fluoroscopic guidance via a percutaneously introduced cannula and inflated to create a void into which bone cement may be injected to stabilize the VB. In the process of inflating the tamp, the endplates are separated from each other, thereby reducing the fracture. The procedure has been termed kyphoplasty. Ex vivo tests have suggested that the tamp treatment restores significantly more height than does standard PV treatment and achieves similar mechanical restoration [56–59]. Ex vivo studies of osteoporotic VBs that were compressed to create simulated fractures and repaired with PV suggested that half of the compressed height recovers elastically [56,58]. A similar phenomenon has been reported in vivo [60]. When the ex vivo specimens were repaired using PV, about 30% of the permanent height loss was recovered [56]. There are no reports of height restoration subsequent to PV in vivo. The first results from a clinical trial indicated that height was restored in 70% of the patients treated using the tamp [61]; in 30% of those patients, however, no height restoration was achieved. The indications for the procedure need to be investigated more fully to determine which patients would benefit from the tamp. Additionally, there is an anecdotal report of height restoration being achieved by use of mild extension and traction [51]. The efficacy of such manual techniques remains unknown and needs evaluation. Furthermore, the clinical value of height restoration needs to be evaluated, not as an end in itself, but in terms of what effect it has on kyphosis reduction and, ultimately, on length and quality of life for the patient. An additional hypothetical benefit of the kyphoplasty procedure is that cement may be injected into the void under lower pressure than that needed for PV. This would allow more viscous cements such as hydroxyapatite cements to be injected. Such cements have been injected in ex vivo evaluations [58], but the issue of reducing injection pressure has yet to be verified.

IV. CEMENT CONSIDERATIONS

There is currently no commercially available cement specifically designed for PV in the United States, but some have received approval for use and are now available in Europe. When cements specifically manufactured for PV are not commercially available, the composition of the cements that are available are routinely altered by clinicians to make them amenable to PV [18,62,63]. This is typically accomplished by increasing the monomer-to-copolymer ratio to increase working time and decrease viscosity [18,63,64] and by adding radiopacifiers to increase cement visualization under fluoroscopy [18,63,64].

A. Cement Modifications

1. Monomer-to-Powder Ratio

Increasing the monomer-to-copolymer ratio decreases the compressive material properties of the cement [65,66]. Most PMMA cements are prepackaged for mixing 0.5 mL of monomer with 1 g of powder, or with a monomer-to-powder ratio of 0.5 mL/g. This mixture typically results in a cement with maximum compressive properties. The ratio of monomer to copolymer is about 0.56 mL/g, because $BaSO_4$ used to opacify the cement accounts for some of the weight (usually 10% w/w) of the powder. When agents are added to increase opacity of the cement for use in PV, typically the opacifying agent needs to constitute 30% of the mass of the powdered contents.

Such a concentration provides for proper fluoroscopic visualization, but it also increases the nonreactive component of the powder and increases the monomer-to-copolymer ratio to approximately 0.72 mL/g [62,66]. This increased monomer volume is needed to wet the powder, but because not all of the extra monomer is involved in the polymerization process, there is an increased amount of unbound monomer available to enter the circulatory system. Although the monomer-to-polymer ratio is larger, the quantity of cement injected (<10 mL) is smaller than that for hip arthrodesis (>40 mL) [39,40,67]. For this reason, the actual blood serum concentration of monomer during PV may be lower than that measured during total hip arthrodesis.

2. Radiopacification

Altering the concentration of radiopacifiers affects the cement's material properties, as does the combined alteration of monomer-to-powder ratio and opacification [62,66,68]. Although these modifications significantly alter the material properties of the cement [62,66,68], there have been no reported clinical problems associated with the cement's material properties. The composition that has been used clinically during the past decade in the United States with no complications associated with mechanical failure of the cement [18] is the weakest and least stiff of the cements used for vertebroplasty [62,66,68].

Although there are no reports of complications associated with the material properties of the cement, extravasation of the cement is a not infrequent occurrence of the procedure and may result in clinical complications [18,69–71]. Proper flouroscopic visualization during cement injection is essential for the safe practice of PV. As a general guide, approximately 30% of the dry cement component weight should be an opacifying agent so that the cement can be visualized under fluoroscopy and extravasation can be prevented [62]. Therefore, using a cement that can be injected easily and with proper opacification appears to take precedence over maintaining the ultimate material properties of the cement.

B. Alternative Cements

Recent attention has focused on using cements that are bioactive or bioresorbable [72–74], are naturally radiopaque [62,74], and have a lower or nonexistent exothermic reaction [32,72,74] than PMMA cements. Some of the calcium phosphate and hydroxyapatite cements have been difficult to inject, putting their application to PV in question [72], but recent advances suggest a more promising future for these cements [47,58,74]. One study reported the successful injection of calcium carbonate (coral) into osteoporotic VBs. Details of the injection process were not given and the mechanical effects of that augmentation were not measured [75]. Such more ''biocompatible'' cements may eliminate concerns about thermal necrosis and cytotoxicity and appear to result in mechanical stabilization of fractured VBs similar to that of PMMA [47,58,74]. Yet, if thermal and toxicity mechanisms are determined to play a role in pain relief, then the non-PMMA cements may not be as effective. The bioresorbable cements are appealing for use in prophylactic augmentation and in younger patients [76] because injected VBs would be mechanically augmented immediately and theoretically provide an osteoconductive material for subsequent bone repair and remodeling [75]. In the presence of osteoporosis, it is unknown whether the VB would once again be at risk of fracture after the cement is remodeled or resorbed.

V. CONCLUSIONS

PV appears to provide pain relief for 90% of patients with osteoporotic VCFs and approximately 60% of patients with metastatic lesions. Although pain relief may result from thermal or chemical

mechanisms, it is most likely the result of mechanical fracture stabilization. Restoration of VB stiffness is weakly correlated with the volume of cement injected, yet there seems little reason to completely fill the VB with cement. The PV procedure is accompanied by a risk of extravasation of the cement. To reduce this risk, smaller volumes of cement are now being injected than were injected previously. The risk of extravasation can also be reduced by using a properly opacified cement and monitoring the injection fluoroscopically. The role of non-PMMA cements for use in PV needs to be investigated clinically, as do the hypothetical benefits of height restoration and kyphosis reduction.

REFERENCES

1. Kostuik JP, Errico TJ, Gleason TF. Techniques of internal fixation for degenerative conditions of the lumbar spine. Clin. Orthop 1986; 203:219–231.
2. Cybulski GR. Methods of surgical stabilization for metastatic disease of the spine. Neurosurgery 1989; 25:240–252.
3. Alleyne Jr. CH, Rodts Jr. GE, Haid RW. Corpectomy and stabilization with methylmethacrylate in patients with metastatic disease of the spine: a technical note. J. Spinal Disord 1995; 8:439–443.
4. Sundaresan N, Galicich JH, Lane JM, Bains MS, McCormack P. Treatment of neoplastic epidural cord compression by vertebral body resection and stabilization. J. Neurosurg 1985; 63:676–684.
5. Scoville WB, Palmer AH, Samra K, Chong G. The use of acrylic plastic for vertebral replacement or fixation in metastatic disease of the spine. Technical note. J. Neurosurg 1967; 27:274–279.
6. Cortet B, Cotten A, Deprez X, Deramond H, Lejeune JP, Leclerc X, Chastanet P, Duquesnoy B, Delcambre B. [Value of vertebroplasty combined with surgical decompression in the treatment of aggressive spinal angioma. Apropos of 3 cases]. Rev. Rhum. Ed. Fr 1994; 61:16–22.
7. Harrington KD. Anterior decompression and stabilization of the spine as a treatment for vertebral collapse and spinal cord compression from metastatic malignancy. Clin. Orthop 1988; 233:177–197.
8. Harrington KD, Sim FH, Enis JE, Johnston JO, Diok HM, Gristina AG. Methylmethacrylate as an adjunct in internal fixation of pathological fractures. Experience with three hundred and seventy-five cases. J. Bone Joint Surg 1976; 58A:1047–1055.
9. Mavian GZ, Okulski CJ. Double fixation of metastatic lesions of the lumbar and cervical vertebral bodies utilizing methylmethacrylate compound: report of a case and review of a series of cases. J. Am. Osteopath. Assoc 1986; 86:153–157.
10. O'Donnell RJ, Springfield DS, Motwani HK, Ready JE, Gebhardt MC, Mankin HJ. Recurrence of giant-cell tumors of the long bones after curettage and packing with cement. J. Bone Joint Surg 1994; 76A:1827–1833.
11. Persson BM, Ekelund L, Lovdahl R, Gunterberg B. Favourable results of acrylic cementation for giant cell tumors. Acta Orthop. Scand 1984; 55:209–214.
12. Knight G. Paraspinal acrylic inlays in the treatment of cervical and lumbar spondylosis and other conditions. Lancet 1959; 2:147–149.
13. Galibert P, Deramond H, Rosat P, Le Gars D. [Preliminary note on the treatment of vertebral angioma by percutaneous acrylic vertebroplasty]. Neurochirurgie 1987; 33:166–168.
14. Lapras C, Mottolese C, Deruty R, Lapras Jr. C, Remond J, Duquesnel J. [Percutaneous injection of methyl-methacrylate in osteoporosis and severe vertebral osteolysis (Galibert's technic)]. Ann. Chir 1989; 43:371–376.
15. Mathis JM, Eckel TS, Belkoff SM, Deramond H. Percutaneous vertebroplasty: a therapeutic option for pain associated with vertebral compression fracture. J. Back Musculoskel. Rehab 1999; 13:11–17.
16. Zoarski GH, Snow P, Olan WJ, Stallmeyer MJB, Dick BW, Hebel JR, De Deyne M. Percutaneous vertebroplasty for osteoporotic compression fractures: quantitative prospective evaluation of long-term outcomes. J. Vasc. Interv. Radiol 2002; 13:139–148.

17. Grados F, Depriester C, Cayrolle G, Hardy N, Deramond H, Fardellone P. Long-term observations of vertebral osteoporotic fractures treated by percutaneous vertebroplasty. Rheumatology 2000; 39: 1410–1414.
18. Jensen ME, Evans AJ, Mathis JM, Kallmes DF, Cloft HJ, Dion JE. Percutaneous polymethylmethacrylate vertebroplasty in the treatment of osteoporotic vertebral body compression fractures: technical aspects. Am. J. Neuroradiol 1997; 18:1897–1904.
19. Riggs BL, Melton LJIII. The worldwide problem of osteoporosis: insights afforded by epidemiology. Bone 1995; 17:505S–511S.
20. Cooper C, Atkinson EJ, O'Fallon WM, Melton LJIII. Incidence of clinically diagnosed vertebral fractures: a population-based study in Rochester, Minnesota, 1985–1989. J. Bone Miner. Res 1992; 7:221–227.
21. Cyteval C, Sarrabere MPB, Roux JO, Thomas E, Jorgensen C, Blotman F, Sany J, Taourel P. Acute osteoporotic vertebral collapse: open study on percutaneous injection of acrylic surgical cement in 20 patients. AJR Am. J. Roentgenol 1999; 173:1685–1690.
22. Weill A, Chiras J, Simon JM, Rose M, Sola-Martinez T, Enkaoua E. Spinal metastases: indications for and results of percutaneous injection of acrylic surgical cement. Radiology 1996; 199:241–247.
23. Cotten A, Duquesnoy B. Vertebroplasty: current data and future potential. Rev. Rhum. Engl. Ed 1997; 64:645–649.
24. Bostrom MPG, Lane JM. Future directions. Augmentation of osteoporotic vertebral bodies. Spine 1997; 22:38S–42S.
25. Deramond H, Depriester C, Galibert P, Le Gars D. Percutaneous vertebroplasty with polymethylmethacrylate. Technique, indications, and results. Radiol. Clin. North Am 1998; 36:533–546.
26. Silverman SL. The clinical consequences of vertebral compression fracture. Bone 1992; 13:S27–S31.
27. Gennari C, Agnusdei D, Camporeale A. Use of calcitonin in the treatment of bone pain associated with osteoporosis. Calcif. Tissue Int 1991; 49:S9–S13.
28. Antonacci MD, Mody DR, Heggeness MH. Innervation of the human vertebral body: a histologic study. J. Spinal Disord 1998; 11:526–531.
29. Jefferiss CD, Lee AJC, Ling RSM. Thermal aspects of self-curing polymethylmethacrylate. J. Bone Joint Surg 1975; 57B:511–518.
30. Leeson MC, Lippitt SB. Thermal aspects of the use of polymethylmethacrylate in large metaphyseal defects in bone. A clinical review and laboratory study. Clin. Orthop 1993; 295:239–245.
31. Mjoberg B, Pettersson H, Rosenqvist R, Rydholm A. Bone cement, thermal injury and the radiolucent zone. Acta Orthop. Scand 1984; 55:597–600.
32. Deramond H, Wright NT, Belkoff SM. Temperature elevation caused by bone cement polymerization during vertebroplasty. Bone 1999; 25:17S–21S.
33. Cotten A, Dewatre F, Cortet B, Assaker R, Leblond D, Duquesnoy B, Chastanet P, Clarisse J. Percutaneous vertebroplasty for osteolytic metastases and myeloma: effects of the percentage of lesion filling and the leakage of methyl methacrylate at clinical follow-up. Radiology 1996; 200: 525–530.
33a. Belkoff SM, Molloy S. Temperature measurement during polymerization of polymethacrylate cement used for vertebroplasty. Spine, In press.
34. Eriksson RA, Albrektsson T, Magnusson B. Assessment of bone viability after heat trauma. A histological, histochemical and vital microscopic study in the rabbit. Scand. J. Plast. Reconstr. Surg 1984; 18:261–268.
35. Rouiller C, Majno G. Morphologische und chemische Untersuchung an Knochen nach Hitzeeinwirkung. Beitr. Pathol. Anat. Allg. Pathol 1953; 113:100–120.
36. De Vrind HH, Wondergem J, Haveman J. Hyperthermia-induced damage to rat sciatic nerve assessed in vivo with functional methods and with electrophysiology. J. Neurosci. Methods 1992; 45:165–174.
37. Li S, Chien S, Branemark PI. Heat shock-induced necrosis and apoptosis in osteoblasts. J. Orthop. Res 1999; 17:891–899.
38. Dahl OE, Garvik LJ, Lyberg T. Toxic effects of methylmethacrylate monomer on leukocytes and endothelial cells in vitro [published erratum appears in Acta Orthop Scand 1995 Aug;66(4):387]. Acta Orthop. Scand 1994; 65:147–153.

39. Svartling N, Pfaffli P, Tarkkanen L. Blood levels and half-life of methylmethacrylate after tourniquet release during knee arthroplasty. Arch. Orthop. Trauma Surg 1986; 105:36–39.
40. Wenda K, Scheuermann H, Weitzel E, Rudigier J. Pharmacokinetics of methylmethacrylate monomer during total hip replacement in man. Arch. Orthop. Trauma Surg 1988; 107:316–321.
41. San Millan Ruiz D, Burkhardt K, Jean B, Muster M, Martin JB, Bouvier J, Fasel JH, Rufenacht DA, Kurt AM. Pathology findings with acrylic implants. Bone 1999; 25:85S–90S.
42. Belkoff SM, Deramond H, Mathis JM. The effect of monomer on MCF-7 breast cancer cell viability. Poster presented at the 11th Interdisciplinary Research Conference on Biomaterials (Groupe de Recherches Interdisciplinaire sur les Biomateriaux Osteo-articulaires Injectables, GRIBOI), March 8–9, 2001.
43. Belkoff SM, Mathis JM, Jasper LE, Deramond H. The biomechanics of vertebroplasty: the effect of cement volume on mechanical behavior. Spine 2001; 26:1537–1541.
44. Tohmeh AG, Mathis JM, Fenton DC, Levine AM, Belkoff SM. Biomechanical efficacy of unipedicular *versus* bipedicular vertebroplasty for the management of osteoporotic compression fractures. Spine 1999; 24:1772–1776.
45. Belkoff SM, Maroney M, Fenton DC, Mathis JM. An in vitro biomechanical evaluation of bone cements used in percutaneous vertebroplasty. Bone 1999; 25:23S–26S.
46. Belkoff SM, Mathis JM, Erbe EM, Fenton DC. Biomechanical evaluation of a new bone cement for use in vertebroplasty. Spine 2000; 25:1061–1064.
47. Belkoff SM, Mathis JM, Jasper LE, Deramond H. An ex vivo biomechanical evaluation of a hydroxyapatite cement for use with vertebroplasty. Spine, 2001; 26:1542–1546.
47a. Molloy S, Mathis JM, Belkoff SM. The effect of vertebral body percentage fill on mechanical behavior during percutaneous vertebroplasty. Spine In press.
48. Liebschner MAK, Rosenberg WS, Keaveny TM. Effects of bone cement volume and distribution on vertebral stiffness after vertebroplasty. Spine 2001; 26:1547–1554.
49. Terjesen T, Apalset K. The influence of different degrees of stiffness of fixation plates on experimental bone healing. J. Orthop. Res 1988; 6:293–299.
50. Jensen ME, Kallmes DF, Short JG, Schweikert PJ, Marx WF. Percutaneous vertebroplasty does not increase the risk of adjacent vertebral fracture—a retrospective study. Presented at the 38th Annual Meeting of the American Society of Neuroradiology, Atlanta, GA, April 3, 2000.
51. Barr JD, Barr MS, Lemley TJ, McCann RM. Percutaneous vertebroplasty for pain relief and spinal stabilization. Spine 2000; 25:923–928.
52. Lyles KW, Gold DT, Shipp KM, Pieper CF, Martinez S, Mulhausen PL. Association of osteoporotic vertebral compression fractures with impaired functional status. Am. J. Med 1993; 94:595–601.
53. Schlaich C, Minne HW, Bruckner T, Wagner G, Gebest HJ, Grunze M, Ziegler R, Leidig-Bruckner G. Reduced pulmonary function in patients with spinal osteoporotic fractures. Osteoporos. Int 1998; 8:261–267.
54. Leech JA, Dulberg C, Kellie S, Pattee L, Gay J. Relationship of lung function to severity of osteoporosis in women. Am. Rev. Respir. Dis 1990; 141:68–71.
55. Leidig-Bruckner G, Minne HW, Schlaich C, Wagner G, Scheidt-Nave C, Bruckner T, Gebest HJ, Ziegler R. Clinical grading of spinal osteoporosis: quality of life components and spinal deformity in women with chronic low back pain and women with vertebral osteoporosis. J. Bone Miner. Res 1997; 12:663–675.
56. Belkoff SM, Mathis JM, Fenton DC, Scribner RM, Reiley ME, Talmadge K. An ex vivo biomechanical evaluation of an inflatable bone tamp used in the treatment of compression fracture. Spine 2001; 26:151–156.
57. Wilson DR, Myers ER, Mathis JM, Scribner RM, Conta JA, Reiley MA, Talmadge KD, Hayes WC. Effect of augmentation on the mechanics of vertebral wedge fractures. Spine 2000; 25:158–165.
58. Belkoff SM, Mathis JM, Deramond H, Jasper LE. An ex vivo biomechanical evaluation of a hydroxyapatite cement for use with kyphoplasty. AJNR Am. J. Neuroradiol 2001; 22:1212–1216.
59. Belkoff SM, Jasper LE, Stevens SS. An ex vivo evaluation of an inflatable bone tamp used to reduce fractures within vertebral bodies under load. Spine 2002; 27:1640–1643.
60. Nelson DA, Kleerekoper M, Peterson EL. Reversal of vertebral deformities in osteoporosis: measurement error or ''rebound''? J. Bone Miner. Res 1994; 9:977–982.

61. Lieberman IH, Dudeney S, Reinhardt MK, Bell G. Initial outcome and efficacy of ''kyphoplasty'' in the treatment of painful osteoporotic vertebral compression fractures. Spine 2001; 26:1631–1638.
62. Jasper LE, Deramond H, Mathis JM, Belkoff SM. Material properties of various cements for use with vertebroplasty. J. Mater. Sci. Mater. Med 2002; 13:1–5.
63. Cotten A, Boutry N, Cortet B, Assaker R, Demondion X, Leblond D, Chastanet P, Duquesnoy B, Deramond H. Percutaneous vertebroplasty: state of the art. Radiographics 1998; 18:311–323.
64. Deramond H, Depriester C, Toussaint P, Galibert P. Percutaneous vertebroplasty. Semin. Musculoskelet. Radiol 1997; 1:285–295.
65. Jasper LE, Deramond H, Mathis JM, Belkoff SM. The effect of monomer-to-powder ratio on the material properties of Cranioplastic. Bone 1999; 25:27S–29S.
66. Belkoff SM, Sanders JC. The effect of the monomer-to-powder ratio on the material properties of acrylic bone cement. J. Biomed. Mater. Res 2002; 63:396–399.
67. Svartling N, Pfaffli P, Tarkkanen L. Methylmethacrylate blood levels in patients with femoral neck fracture. Arch. Orthop. Trauma Surg 1985; 104:242–246.
68. Jasper L, Deramond H, Mathis JM, Belkoff SM. Evaluation of PMMA cements altered for use in vertebroplasty. Presented at the 10th Interdisciplinary Research Conference on Injectible Biomaterials, Amiens, France, March 14–15, 2000.
69. Padovani B, Kasriel O, Brunner P, Peretti-Viton P. Pulmonary embolism caused by acrylic cement: a rare complication of percutaneous vertebroplasty. AJNR Am. J. Neuroradiol 1999; 20:375–377.
70. Wilkes RA, MacKinnon JG, Thomas WG. Neurological deterioration after cement injection into a vertebral body. J. Bone Joint Surg 1994; 76B:155.
71. Perrin C, Jullien V, Padovani B, Blaive B. Percutaneous vertebroplasty complicated by pulmonary embolus of acrylic cement. Rev. Mal Respir 1999; 16:215–217.
72. Schildhauer TA, Bennett AP, Wright TM, Lane JM, O'Leary PF. Intravertebral body reconstruction with an injectable in situ-setting carbonated apatite: biomechanical evaluation of a minimally invasive technique. J. Orthop. Res 1999; 17:67–72.
73. Fujita H, Nakamura T, Tamura J, Kobayashi M, Katsura Y, Kokubo T, Kikutani T. Bioactive bone cement: effect of the amount of glass-ceramic powder on bone-bonding strength. J. Biomed. Mater. Res 1998; 40:145–152.
74. Bai B, Jazrawi LM, Kummer FJ, Spivak JM. The use of an injectable, biodegradable calcium phosphate bone substitute for the prophylactic augmentation of osteoporotic vertebrae and the management of vertebral compression fractures. Spine 1999; 24:1521–1526.
75. Cunin G, Boissonnet H, Petite H, Blanchat C, Guillemin G. Experimental vertebroplasty using osteoconductive granular material. Spine 2000; 25:1070–1076.
76. Verlaan JJ, van Helden WH, Oner FC, Verbout AJ, Dhert WJ. Balloon vertebroplasty with calcium phosphate cement augmentation for direct restoration of traumatic thoracolumbar vertebral fractures. Spine 2002; 27:543–548.

4

Kyphoplasty and Vertebroplasty for the Treatment of Painful Osteoporotic Vertebral Compression Fractures

Christopher Bono
Boston Medical Center, Boston University School of Medicine
Boston, Massachusetts, U.S.A.

Steven Garfin
University of California
San Diego, California, U.S.A.

I. INTRODUCTION

Spine care is trending towards procedures that are less invasive and motion sparing. Among the most innovative are kyphoplasty and vertebroplasty for the treatment of osteoporotic vertebral compression fractures (VCFs). They are performed percutaneously and focus on restoring the mechanical properties of the injured vertebra without fusing motion segments. These techniques have filled a void between prolonged nonoperative care and open surgical procedures by offering a highly effective treatment for pain relief with minimal risks to patients who otherwise would have few, if any, alternatives.

Vertebroplasty involves high-pressure injection of a bone filler material (e.g., bone cement) into a compressed vertebral body. While an effective method of pain relief, it is associated with a high rate of cement extrusion and does not enable fracture reduction. Kyphoplasty was developed in response to these pitfalls. The technique consists of inserting an inflatable bone tamp into the vertebral body that can restore height to the compressed bone and create a void into which bone cement can be introduced under low pressure. The rate of pain relief is comparable to vertebroplasty, while 50–90% height restoration can be achieved if treatment is performed within three months of injury [1–4].

The effectiveness of kyphoplasty and vertebroplasty relies on proper patient selection, meticulous technical application, and the quality of the injected materials. While methacrylate bone cement is currently the most frequent augmentation material used, the development of injectable bioabsorbable substances could have profound effects on exanding the indications of this procedure.

II. OSTEOPOROSIS: A PERVASIVE PROBLEM

Advances in modern medicine have increased the average life expectancy. An increasing proportion of the population is elderly. With this increased longevity comes a corresponding emphasis

on quality of life. These issues have made geriatric care an increasingly important focus of medical practice.

Osteoporosis is a significant problem in aging and postmenopausal people and is an increasingly recognized cause of painful fractures in the spine [5–10]. Women are more commonly affected, as they are subject to both postmenopausal and senile osteoporosis [11]. However, aged men are also sensitive to the sequelae of progressive bone loss [12,13].

The histological appearance of osteoporotic bone is normal. It is a disorder of quantity, not quality, with a decreased amount of bone per volumetric unit. Osteoporosis is caused by an imbalance of bone production and resorption, in contrast to osteomalacia, in which mineralization is altered [14]. While advances in pharmacological management promise better treatment and prevention of osteoporosis, they will have minimal impact on the large number of individuals with already advanced disease [15]. Other disorders, including vitamin deficiencies, improper diet, systemic diseases, and corticosteroid use, can also cause progressive bone loss, but through different pathomechanisms. These disorders should be recognized when evaluating patients with osteoporosis, addressing the underlying problem, rather than just the ''symptom'' of bone loss.

The relationship between loss of bone mineral density and skeletal weakening has been well established. While the entire skeleton is affected, particular regions are at proportionately higher risk for fracture. The vertebral column is the most frequently injured, followed by the distal radius (wrist) and upper femur (hip) [11]. Within the spine, there is a predilection for osteoporotic vertebral compression fractures (VCFs) in the upper lumbar and lower thoracic spine [13,16].

VCFs present different clinical challenges than wrist or hip fractures. Some osteoporotic VCFs can be asymptomatic, while pain associated with many symptomatic fractures resolves with time. This makes them difficult to diagnose and localize, in contrast to fractures of the wrist and hip, which are almost always painful, easy to localize, and do not resolve if left untreated.

In many cases, however, VCFs can be a troubling source of back pain, potentiating medical morbidity and mortality. Multiple, consecutive VCFs, common in untreated individuals, can lead to progressive anterior column shortening that results in painful thoracic, lumbar or thoracolumbar kyphosis. Such deformities can limit ambulatory function and pulmonary capacity and lead to eating disorders, such as early satiety, in an elderly population that is likely to have many concomitant comorbidities [5,7–9].

III. MECHANICS OF VERTEBRAL OSTEOPOROSIS

Osteoporosis affects a bone's mechanical structural properties. While bone quality is unaffected, strength is diminished by an overall decrease in the amount of bone present. The histological appearance of the bone is unchanged. Microstructurally, there is increased porosity. This can be assessed by measuring bone mineral density (BMD) with the use of dual-energy x-ray absorptiometry (DEXA) or quantitative computerized tomography (QCT). Critically low BMD values are associated with a predisposition to VCF.

In the cancellous portion of a normal vertebral body (VB), there are horizontal and vertical trabeculations. Osteoporosis causes a loss primarily of the horizontal trabeculations, leaving the vertical components unsupported. This causes significant weakness in resisting axial loads. Vertebral bodies bear the majority of the axial compressive forces sustained by the spine. Flexion moments increase these forces and, if they exceed the bone's capacity to resist them, can result in fracture.

Fractures first involve the anterior aspect of the VB (i.e., anterior column), which can result in wedge-type fractures. With further load the fracture can propagate to the posterior

VB wall (i.e., middle column), creating a burst-type patterns. Some osteoporotic fractures lie somewhere between a wedge and burst type, resulting from pure axial loading. These more uniform compression deformities of the VB appear as a crush type, which involves a portion of the posterior aspect of the VB. However, because the plane of the fracture is basically transverse, there is typically no fragment retropulsion. These lesions should be considered VCFs and are amenable to vertebral augmentation with kyphoplasty or vertebroplasty.

Treatment can be directed at one or both of two essential features, which are the vertebra being weakened and compressed. Metabolic therapy can address weakness by influencing the balance of bone deposition and resorption. Alendronate, estrogen, and calcitonin have demonstrated clinical efficacy in slowing, arresting, or reversing this process [15]. While they should be initiated in osteoporotic patients, they have limited effects on fracture risk in advanced cases. Vertebroplasty and kyphoplasty address bone fragility in a much more direct way. In vitro studies have demonstrated that both stiffness and strength are increased with PMMA in osteoporotic bone [17–19].

Because the fractured osteoporotic bone is so weak, the vertebra's mechanical properties after augmentation are virtually that of the bone filler. Not all bone cements are equal. Different substances create different changes in strength and stiffness. In a cadaveric study, Orthocomp (Orthovita, Malvern, PA) resulted in significantly stronger and stiffer vertebrae than Simplex P (Howmedica, Rutherford, NJ) [19]. The former restored initial prefracture stiffness values. Cranioplastic cement (CMW, Blackpool, England) and Simplex P did not completely restore stiffness to intact values [18]. The long-term clinical implications of these variables on augmentation durability remains to be seen [20]. Additionally, it is not known how much strength is needed to support the osteoporotic bone and spinal column. The senior author has routinely used Simplex P in over 100 kyphoplasty procedures with excellent long-term reuslts [1]. This is also true for most physicians who perform kyphoplasty. The cement powder/monomer ratio and addition of radiopaque media (e.g., barium) may alter material properties and should be considered when testing new formulations of filler.

Cement volume influences the mechanical properties after vertebral augmentation. In general, a greater amount of cement can be inserted using a bilateral, as compared to a unilateral, approach. In most cases a bilateral approach is recommended with kyphoplasty, though in some only unilateral injection might be possible. With vertebroplasty, unilateral injection is considered accetable if more than 50% of the VB is filled [3]. In cadaveric spines, bipedicular injection of 10 mL (5 mL on each side) resulted in significantly greater strength versus unipedicular injection of 6 mL of cement [17]. Both methods, however, resulted in restoration of initial stiffness. From these data, delivery of at least 6 mL of cement affords adequate stabilization to a vertebra.

IV. KYPHOSIS REDUCTION AND SAGITTAL BALANCE

The normal thoracic spine's sagittal kyphosis is approximately 20–40 degrees, with an apex around T6 or T7. It is primarily produced by physiological anterior vertebral body wedging. This is in contrast to the lumbar spine, which is in approximately 50 degrees of lordosis, produced primarily by the discs, which are larger anteriorly than posteriorly. These curves must be considered in concert. Overall sagittal balance can be assessed using a long-plate lateral radiograph, taking into account both thoracic and lumbar curvatures. A vertical plumb line (weightbearing line) is drawn from the base of the occiput. Sagittal balance is realized if that line intersects the seventh cervical VB cranially and lies within 1 cm of the sacral promontory caudally, centered over the hips. Increased kyphosis in the thoracic spine moves the weight-bearing line anteriorly.

However, this can be compensated by exaggerated lordosis in the lumbar spine. This moves the weight-bearing line back to its balanced position over the sacral promontory.

Because it is generally less mobile and is subject to fractures in both regions, there is little compensatory capacity in the osteoporotic spine. Sagittal deformity is usually characterized by uncompensated thoracic and lumbar kyphosis. Eventually, these can progress to a point at which the weight-bearing line can no longer return to a balanced point, resulting in a self-propagating imbalance. This can be compared to the leaning tower of Pisa. The tower presently remains erect because the weight-bearing line, or center of mass, falls within its base. This functions to maintain its current position. If, however, it continues to lean over so much that the center of mass lies outside its base, the tower will no longer be balanced. Therefore, the weight of the tower will be contributing to its own fall.

Corrective measures attempt to restore the weight-bearing line, or center of mass of the body, to the anatomical base, which is the sacral promontory. By increasing VB height at one or more levels, kyphoplasty can achieve this goal. An average of 96% VB height restoration has been documented in in vitro investigations [21]. This is corroborated by clinical evidence, demonstrating 99% and 92% of predicted anterior and middle VB dimensions, respectively, when kyphoplasty is performed less than 3 months after fracture [1]. Some surgeons claim that vertebroplasty can restore some VB height, although this has not been demonstrated in a clinical trial [21].

V. INDICATIONS

A. Kyphoplasty

1. As a Pain-Relieving Procedure

A major complaint of patients with osteoporotic VCFs is pain. This pain can become progressive and intractable, affecting the patient's ability to perform his or her daily activities. As a vertebral augmentation procedure, kyphoplasty is indicated for progressive or intractable pain associated with an osteoporotic VCF. In recent clinical series, greater than 90% of patients reported long-standing pain relief after surgery [1,2,22]. The most likely mechanism of pain relief is fracture stabilization, provided by the injected polymethylmethacrylate bone cement. However, some believe that the exothermic reaction during cement curing can have a denervation effect within the VB, although this remains hypothetical and unlikely based on the long-term maintained clinical success.

2. For Deformity Correction

In the proper setting, kyphoplasty has the ability to correct kyphotic deformtiy associated with osteoporotic VCFs. The benefits of kyphosis reduction are multifold. By placing the spine in a more balanced position, realignment may help reduce the incidence of further fractures. In addition, pulmonary dysfunction has been correlated to the severity of kyphotic deformities in osteoporotic patients [5,23]. While it is not known if the converse relationship is true, i.e., if kyphosis correction reverses or minimizes these sequelae, it is reasonable to think that kyphoplasty of correctable osteoporotic kyphosis may have beneficial effects on pulmonary function. Additional study of the effects of kyphoplasty on postcorrection pulmonary function is warranted.

Better height restoration can be expected in acute fractures (<3 months old) than chronic ones [1,22]. While the authors have observed some correction in VCFs one year or more after fracture, it is difficult to predict. Severe, rigid deformities from multiple healed fractures that compromise function, or quality of life, are probably better treated by other surgical methods,

if indicated. Moderately painful progressive VB collapse, if detected radiographically, is a developing indication for kyphoplasty. Though current reports of the safety of kyphoplasty are encouraging, subsequent study is needed to more clearly demonstrate a positive balance between the potential benefits of kyphosis correction versus procedural complications.

B. Vertebroplasty

Vertebroplasty is indicated for the treatment of painful osteoporotic VCFs. The rates of pain relief are comparable to those with kyphoplasty [24–27]. While some physicians claim that vertebral height restoration can be obtained by prone positioning followed by vertebroplasty, this has not been substantiated in a clinical series. Fracture reduction or kyphosis reduction cannot not be considered an indication for this procedure. Though restoration of ambulation and mobility from significant pain relief may have positive effects on overall health, it can be presumed that vertebroplasty would have minimal, if any, effect on compromised pulmonary function related to osteoporotic kyphosis.

VI. CONTRAINDICATIONS

Kyphoplasty and vertebroplasty are contraindicated in stable, healed, nonpainful fractures and in the presence of infection. Concomitant medical problems can make surgery and anesthesia dangerous. In patients with clotting disorders, epidural hematoma may result from VB cannulation, particularly if the pedicle borders, or posterior VB, have been violated. Though some surgeons have performed kyphoplasty in patients with osteoporotic burst fractures, it is the authors' opinion that this is a relative contraindication to either procedure. Fractures with severe VB height loss, as occurs with severe vertebra plana, may not be amenable to vertebral augmentation because of the inability to cannulate the VB.

VII. PREOPERATIVE PLANNING

For successful vertebral augmentation, the practitioner must first be confident that the osteoporotic VCF(s) is the source of the pain. Other causes of back pain, such as sacral insufficiency fractures, must be ruled out by a complete history and physical examination. Once this has been established, the next challenge is determining the symptomatic level. By percussing the midline of the spine, the most tender level is determined. This can then be marked by a radiopaque marker, such as paper clip, prior to obtaining radiographs. Also, the examiner can attempt to identify the number of the spinous process. Plain radiographs are useful in assessing overall spinal balance. Cobb angles can be measured to better quantitate the degree of deformity. Vertebral compression can be measured by comparing respective anterior and posterior VB heights to the closest adjacent normal levels. While the presence and morphology of a VCF can be well appreciated on plain films, the acuity of the fracture cannot be determined. If the symptomatic level is unclear by physical examination, advanced imaging modalities should be pursued. The authors routinely obtain an MRI prior to performing kyphoplasty (Figure 1). Acute fractures demonstrate increased signal intensity on T2 images [28,29]. STIR images are particularly helpful in differentiating fracture from malignancy. For patients in whom MRI cannot be performed, a computerized tomogram (CT) is another option. These images give better bony detail and are

superior to MRI for characterizing the fracture, but they should be used in conjunction with a bone scan to determine fracture acuity [28].

VIII. SURGICAL TECHNIQUE: KYPHOPLASTY

A. Setup

Either general or local anesthesia with sedation can been used. General anesthesia may be more suitable for multilevel procedures, while local anesthesia may be sufficient for one- or two-segment augmentation. The patient is positioned supine on a radiolucent table. Transverse rolls across the chest and thighs/iliac crests maintain epidural decompression and help extend the spine. If available, two image intensifiers (C-arms) should be used so that simultaneous antero-posterior (AP) and lateral views can be obtained. Prior to prepping and draping, it should be ensured that the spine can be adequately imaged. The pedicle and VB should be seen clearly on all views. The pedicle can be viewed en face by angling the beam about 10 degrees towards the midline, giving it an end-on appearance. This is useful for judging containment of the cannulation instruments within the pedicle borders.

B. Approaches

1. Transpedicular Approach

This is the preferred approach for any level with a pedicle diameter of at least 4–5 mm. It may not be suitable for upper thoracic levels with small pediclular dimensions. Also, lumbar pedicles in small individuals may not be amenable to the transpedicular approach, which may necessitate

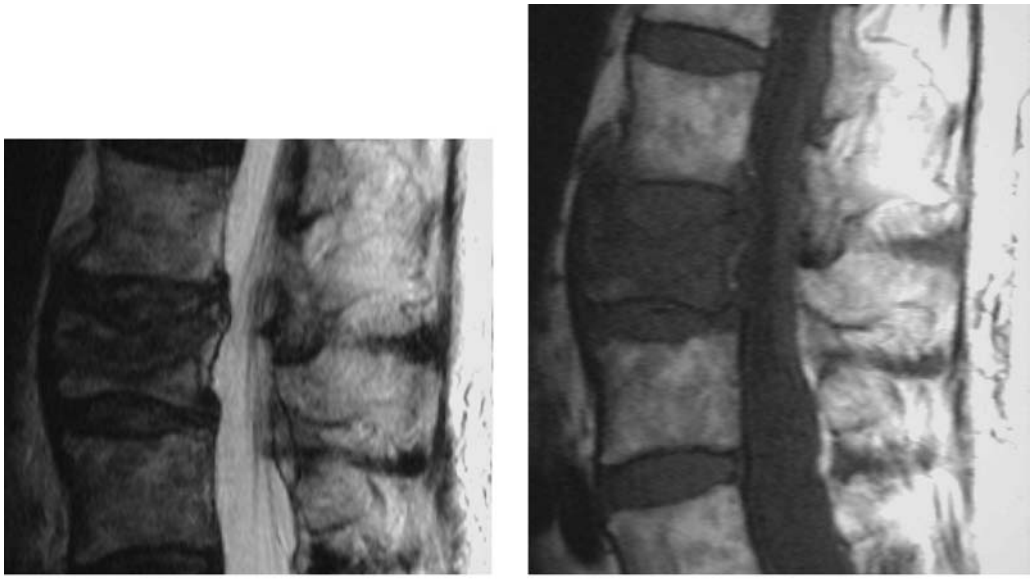

Figure 1 MR images (A, T_2-weighted; B, T_1-weighted) can demonstrate increased bone edema as well rule out fracture retropulsion into the canal.

a posterolateral technique (see below). This determination can be made using axial MRI or CT images. Bilateral VB cannulation can be performed using this approach. The endangered structures are the spinal cord medially and the nerve root superiorly and inferiorly if the pedicle is missed or its cortex violated. The pulmonary cavity is lateral, and large vessels are anterior to the vertebral body.

After the correct level of surgery is determined by orthogonal C-arm views, the midline is palpated and marked. Next, using the AP view, the skin is marked just lateral to the lateral border of the pedicle. Slight medial angulation of the instruments during pedicle cannulation is necessary. A 1 cm stab wound incision is created over this mark. The spinal, or Jamshidi, needle is then inserted. It should be angled approximately 10 degrees toward the midline in the thoracic and lumbar spine. In the lower lumbar spine, particularly at L5, more medial orientation may be needed. The needle should be advanced into the bone about 2–3 mm. The location is then checked on both radiographic views to confirm proper orientation. The Jamshidi needle is slowly advanced with a gentle twisting motion. Tactile feedback should help guide the instrument within bone. However, this may be difficult to discern because of decreased bone density. Sudden ''giving way'' can indicate that the pedicle borders have been violated. Radiographic appearance of optimal needle placement is the tip within the confines of the pedicle at all times. Gentle tapping of the needle into the bone with a light mallet can also be used.

The needle is advanced to the junction of the posterior cortex of the VB and the pedicle. As a general rule, the tip should not cross the midline on the AP view at any point during insertion, although the tip of a well-placed needle may appear slightly medial to the pedicle border once within the VB. If acceptable positioning is questionable, the en face view should be obtained. In this view, the needle should be entirely contained within the pedicle. If proper orientation cannot be confirmed, the needle should be repositioned.

In order to maximize the amount of cancellous bone between the bone tamp and the fractured endplate, the instruments can be directed towards the uninjured endplate. For example, if the superior endplate is depressed, the tools are directed towards the anterior lip of the inferior endplate. Importantly, the instruments should not be advanced through the intact endplate, as this can lead to cement extravasation into the disc space. Cranial/caudal orientation in the pedicle is best judged on the lateral view. If the vertebra is uniformly compressed, the tool is advanced towards the mid-body.

2. *Lateral Extrapedicular Approach*

This approach is appropriate for thoracic levels at which the pedicles are too small to cannulate, usually above T8. Bilateral cannulation can be performed using this approach. It is not appropriate for lumbar vertebrae, which are better instrumented through a posterolateral method, if the transpedicular approach is not achievable. The lateral extrapedicular approach relies on considering the rib head and the thoracic pedicle together as a larger ''effective pedicle.'' Through a similarly located incision as for the transpedicular method, the needle is inserted just lateral and superior to the pedicle. As it is advanced, the needle enters the lateral aspect of the pedicle near its junction with the rib lateral to it. In general, it is directed to the anteroinferior aspect of the vertebral body on the lateral view. More medial angulation of the needle, approximately 20 degrees, is usually necessary, as the starting position is more lateral. With a more lateral position, the spinal cord is at less risk than with the transpedicular method. However, lateral deviation endangers the lungs and risks pneumothorax. Penetration of the lateral vertebral body cortex can injure the segmental artery. The goal is to use the rib to protect the lungs, and the pedicle protects the cord.

3. Posterolateral Approach

For lumbar levels, in particular L2 to L4, at which the pedicles are too small to accept the kyphoplaty instruments, a posterolateral approach is recommended. The approach is similar to that for a discogram, except that it is directed at the VB. The needle is inserted about 8–10 cm lateral to the midline and directed at a 45 degree angle towards the midline. The needle path is anterior to the transverse processes, as the pedicle is not cannulated at any time. The lateral view is critical; the needle should lie anterior to the transverse process and neural foramen at all times. This avoids injury to the exiting nerve root. The en face view is not useful with this approach. The posterolateral approach enables unilateral cannulation only. Therefore, the needle must cross the midline to ensure adequate augmentation of the contralateral aspect of the VB.

C. Bone Tamp Insertion

The center sylet is removed from the Jamshidi needle and a flexible guidewire is inserted until it is just past the needle tip. The Jamshidi needle is removed with a slow, controlled twisting motion while holding the guidewire in place. The needle tract is dilated and a channel in the pedicle created by inserting a centering stylet over the guidewire. This dilator should be inserted just past the border of the pedicle and the VB. The guidewire is then removed and a larger diameter cannula is inserted over the centering stylet. The centering stylet can then be removed, leaving the working cannula in place. A hand-driven twist drill bit is inserted and advanced to, but not through, the anterior cortex of the VB (Figure 2). This must be performed carefully under radiographic guidance to avoid penetration of the cortex, as the osteoporotic bone is soft.

After the drill bit is removed, the inflatable balloon tamp is inserted (Figure 3). Tamps are available in large and small sizes. Most lumbar vertebra accept a large (20–25 mm) balloon, while smaller thoracic or lumbar vertebrae might accept only the small (15 mm) tamp. It should be inserted until the entire balloon tamp is contained within the VB. This can be judged by

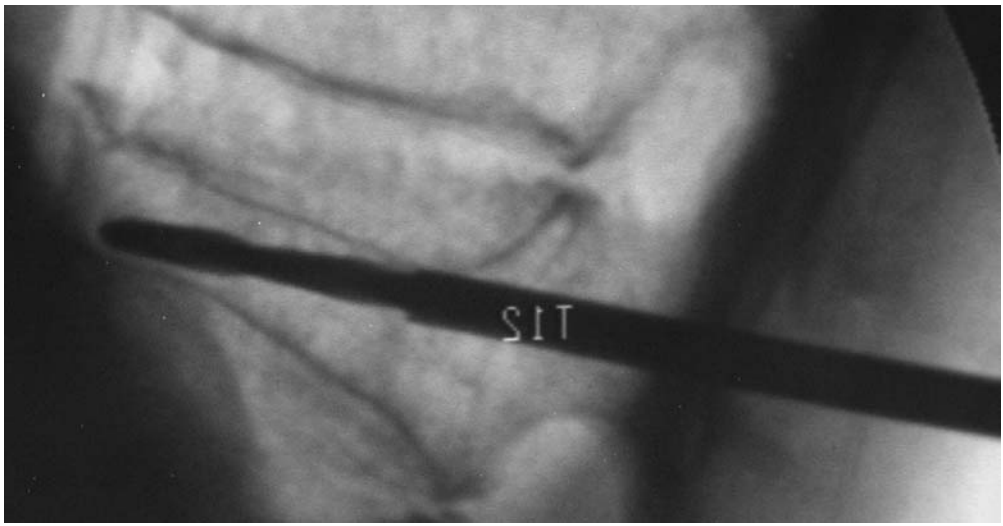

Figure 2 The drill bit is inserted into, but not through, the anterior vertebral body cortex. In this anterior wedge compression fracture, the instruments must be carefully directed so as not to penetrate the superior or inferior endplates.

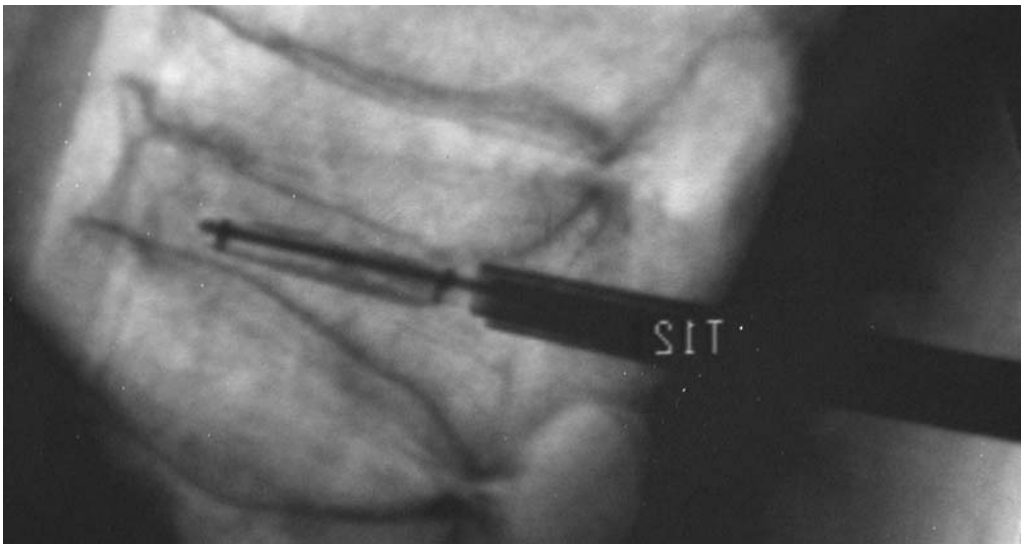

Figure 3 The balloon tamp is inserted into the vertebral body. The two radiopaque markers along the tamp should be within the bone, ensuring proper positioning of the device.

ensuring that the two radiographic markers, positioned at either end of the otherwise radiolucent balloon, are anterior to the posterior VB cortex. To provide more uniform compression within the cylindrically shaped bone, the balloon is ''cinched'' at its waist. This effectively creates anterior and posterior tamps instead of one large sphere that would have a tendency to expand maximally in the center. This facilitates en masse reduction of the fractured endplate.

The tamp is then inflated with radiopaque dye under manometrically controlled pressure using a screw-operated piston-like device (Figure 4). Inflation pressures are initially low as the balloon expands within the soft cancellous bone until it meets the resistance of the harder cortical endplates. Pressures can intermittently drop and rise again, representing ''giving'' of the endplates and, hopefully, reduction of the fracture. *Warning:* If pressure suddenly drops and remains low, the balloon should be removed and inspected. This is an indication that the balloon has ruptured. A replacement balloon should be inserted and the inflation process should be started again. During inflation, both volume and pressures should be noted. Volume measurements can be used to approximate the amount of cement needed to fill the bone void.

Fracture reduction is judged on the lateral fluoroscopic view. Importantly, there is a limit to the amount of reduction possible before the balloon ruptures or the cortical borders of the VB are violated. The most common area for this to occur are the endplates, which can appear as a small, well-defined protuberance of the balloon into the disc space noted best on the lateral view. If this occurs, inflation should not continue further. Care must be taken while injecting cement to avoid extravasation into the disc space. This complication is more common in older fractures.

D. Cement Composition

Currently, the major component of the bone filler material is polymethylmethacrylate (PMMA) cement. This material has been used for vertebral body replacement and augmentation with

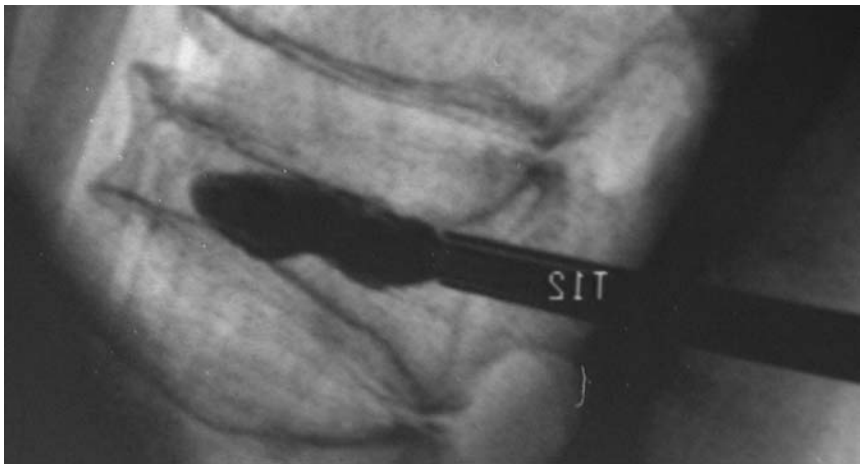

Figure 4 The tamp is inflated using a radiopaque dye to achieve and visualize fracture reduction.

open surgery for other pathological diagnoses and has demonstrated biocompatability. Though standard formulation of PMMA are somewhat radiopaque, the radiographic density is not enough for safe visualization of the small amounts injected into the VB during kyphoplasty. Therefore, a small amount of barium sulfate is added to the mixture to increase the cement radiopacity. To minimize the infection risk, antibiotic powder is also added. The following formula has been used successfully in the authors' clinical practice: PMMA powder 40 cc, liquid monomer 10 cc, barium sulfate 6 g, and one vial of antibiotic powder. Heat-stabile antibiotics, such as cefazolin (1 g), vancomycin (1 g), or tobramycin (1.2 g), are preferred.

E. Cement Delivery

The balloon tamps are kept inflated until the cement is ready for insertion. While it is still quite fluid, cement is injected into several 3 cc bone filler devices (BFD). The remaining cement is used to judge its readiness for injection. When a freshly expressed cement bead no longer has a glossy appearance and appears to be relatively viscous, the balloon tamps are deflated and removed. In particularly unstable fractures, a contralateral tamp can remain inflated to maintain reduction while cement is injected ipsilaterally. The BFDs are placed into the working cannula and advanced to within a few millimeters of the anterior cortex (Figure 5). A pusher stylet is used to inject the cement into the bone void. The tip of the next 3 cc BFD is located more towards the center of the VB, and the subsequent device closer to the posterior cortex. This enables uniform fill of the VB defect. *Warning*: The BFD tip should always be positioned within the confines of the VB. Injection should never proceed with the BFD tip within the pedicle.

Low-pressure cement injection proceeds until one of the following occurs: (1) cement has filled the anterior two thirds of the VB, (2) cement begins leaking through the cortical boundaries of the VB (including endplates), or (3) cement starts to fill the posterior aspect of the body or pedicle. Cement extravasation outside of the VB can occur if the mixture is too fluid. In this case, injection is temporarily stopped, allowing the peripheral cement to begin to cure. Optionally, the tamp can be reinserted and gently reinflated to distribute the cement peripherally. As the cement hardens, this acts to ''plug the holes,'' after which injection can be resumed. Injection is performed bilaterally. Between 2 and 6 mL of cement can usually be injected on each side.

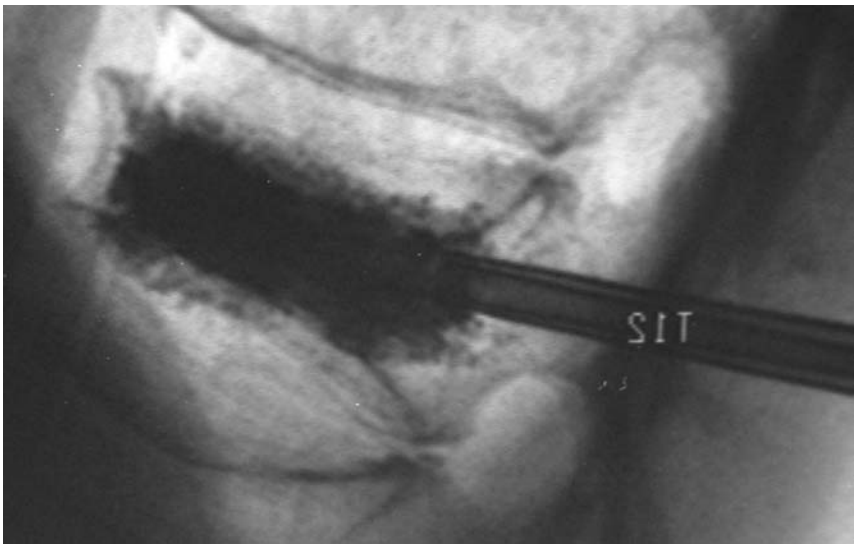

Figure 5 The cement is injected under low pressure into the vertebral body to fill the cavity/void created by the balloon tamp. Once cement has reached the posterior aspect of the vertebral body, injection is stopped.

The cement should be allowed to harden. This can taken from 5 to 10 minutes depending on the room temperature. The working cannulae are removed using a twisting action to dissociate it from the surrounding PMMA. Final intraoperative fluoroscopic views confirm fracture reduction and cement placement. The patient should remain prone for an additional 10 minutes to ensure final PMMA curing within the reduced fracture. In multilevel procedures, final cement curing should be allowed before proceeding to subsequent levels (Figure 6).

IX. SURGICAL TECHNIQUE: VERTEBROPLASTY

Set-up and approach are similar to those for kyphoplasty, with either general or local anesthesia suitable. Cannulation techniques are also similar. Mathis et al. [30] described three approaches: transpedicular, parapedicular (akin to extrapedicular), and posterolateral. Leakage appears to be more frequent with vertebroplasty than kyphoplasty. Vertebroplasty requires a lower cement viscosity to enable a higher pressure injection because there is no true bone void. The cement simply fills the interstices of the fractured vertebral body. The posterolateral approach has a higher propensity for extravasation than the other vertebroplasty approaches. In the current authors' experience, this has not been observed with kyphoplasty. Because of this higher risk, vertebrograms are routinely performed prior to vertebroplasty. This entails injection of radiopaque dye through the cannulation needle and estimates the most likely path of the cement. If a nearby vessel enhances, the needle is repositioned and retested.

Two to 3 mm of cement is injected though the cannulation needle with a syringe. Bone fill is monitored using the C-arm. As with kyphoplasty, injection is stopped when cement has reached the posterior aspect of the VB. The syringe is then removed, and the stylet is replaced into the needle to avoid leaving a ''tail'' of cement. Vertebroplasty can be performed unilaterally or bilaterally. While some routinely perform bilateral vertebroplasty when possible, Deramond

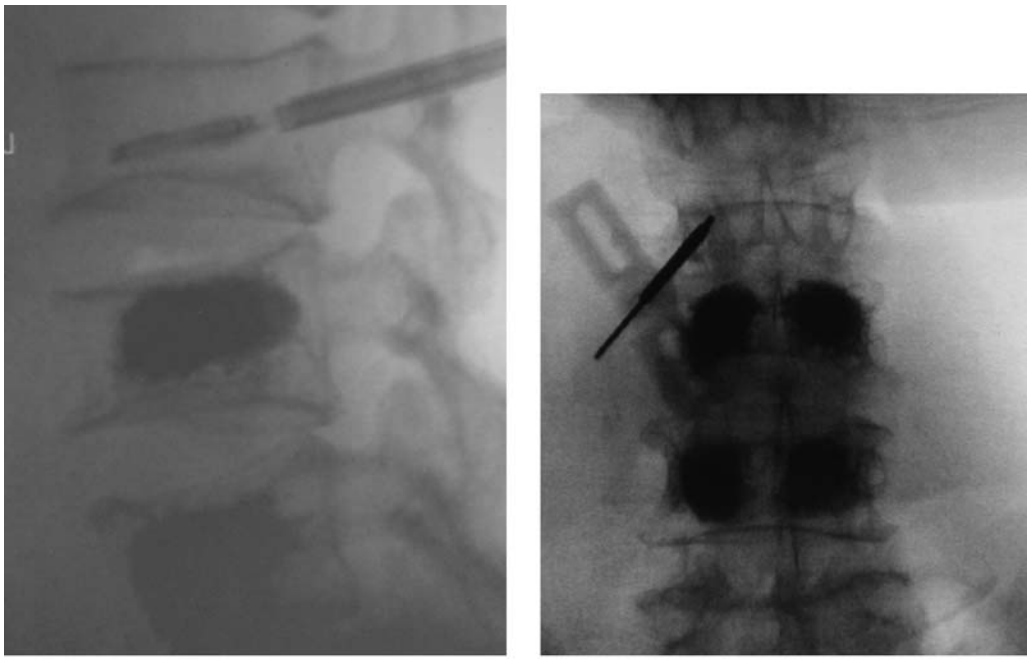

Figure 6 Multiple kyphoplasties may be performed. In the authors' practice, two to three levels can be augmented during a single procedure. If more levels are planned, staged procedures, with a 3- to 4-week interval delay, might be more prudent.

et al. [3] recommend a unilateral vertebroplasty first. More than 50% fill of the VB is considered adequate. If less than 50% fill is achieved, contralateral injection is recommended. Unilateral and bilateral cement injections have comparable restoration of strength and stiffness after vertebroplasty, with the cement volume being a more probable determinant of mechanical properties [17].

A. Postoperative Care

Both kyphoplasty or vertebroplasty can be performed on an outpatient basis. If general anesthesia was used, it is the authors' feeling that an overnight stay is more prudent particularly in an elderly, frail population. Minimal blood loss and reliable pain relief, usually within 24 hours, aid in a quick recovery. Narcotic pain medication is usually not necessary for more than 2 days after surgery. After this, pain can be typically managed with extra-strength acetaminophen or nonsteroidal anti-inflammatory drugs, if not contraindicated. Bracing is usually not of benefit unless the patient has multiple additional fractured levels which are planned to be addressed in a subsequent procedure(s). The patient is advised to avoid heavy lifting for a few weeks to minimize further fracture risk. Follow-up radiographs should be obtained one month postprocedure and repeated as indicated by clinical findings. Radiographic follow-up may be considered for one year because of the propensity for subsequent fractures.

B. Complications

While radiographic evidence of cement leakage occurs in up to 8.6% of cases, clinically significant complications have occurred in only 1.2% of patients and 0.7% of fractures [1,2,22]. Cement extravasation is usually clinically benign. However, neurological deficit secondary to cement in the spinal canal or neural foramina has been reported in both vertebroplasty and kyphoplasty [1,31].

Transient pyrexia is the most commonly reported clinical complication and is most likely from a mild systemic reaction to the cement [3]. This appears to be more frequent after vertebroplasty than kyphoplasty [1,3]. This may be related to the pressure of injection. Epidural hematomata can occur, particularly if the pedicle or VB borders have been violated. Anticoagulation, if used by the patient, should be delayed for at least 4 days to avoid this complication.

X. CLINICAL OUTCOMES

A. Kyphoplasty

The senior author (S.R.G.) has participated in an ongoing prospective evaluation of a collection of kyphoplasty cases performed for osteoporotic VCFs. Information from over 375 procedures has been analyzed, and the results are extremely encouraging. More than 90% of patients reported symptomatic relief and functional improvement at up to 18 months follow-up. Anterior and midline vertebral height was restored to within 99% and 92% of predicted dimensions, respectively. Pain relief and fracture reduction were highly consistent between centers and technicians.

Four important clinical complications were noted. Transient pyrexia, associated with a brief period of intraoperative hypoxia after cement injection, was documented in one patient. This was attributed to the cement being in too fluid a state. The patient's blood pressure quickly recovered with no apparent sequelae. An epidural hematoma developed in another patient after heparin anticoagulation had been initiated just 8 hours after the procedure. As with any other spinal or brain procedure, anticoagulant therapy should be delayed for 4 days. Two other patients had neurological complications. Anterior cord syndrome developed after a thoracic kyphoplasty performed through an extrapedicular approach. Reexamination of the preoperative MRI revealed an unrecognized fracture at the pediculo-body junction. The other neurological complication was a case of paraparesis from extrusion of cement into the spinal canal secondary to improper needle placement. The medial pedicle wall had been inadvertently violated by the Jamshidi needle. This complication was not related to use of the inflatable bone tamp itself. The paraparesis somewhat improved following emergent laminectomy and decompression. Neurological damage from cement most likely occured from mechanical compression; experimental data have demonstrated little chance of thermal damage during exothermic cement hardening. The major complications occurred within the first 100 fractures treated and have not occurred since then.

In a smaller prospective series, Lieberman and associates [22] reported similarly excellent results in 70 consecutive procedures in 30 patients. Outcomes were prospectively assessed with SF-36 scores for bodily pain, physical function, vitality, and mental health; statistically significant improvement was reported for these measurements. In contrast to the series by Garfin et al. [1], an average of only 35% of lost VB height was restored. It must be considered, however, that the average fracture age was almost 6 months, with a range of 0.5–24 months, so that the majority of fractures would not be considered acute. Similar rates of cement extravasation were reported. Other complications (pulmonary edema in one case and rib fractures in two cases) were not related to the kyphoplasty procedure itself.

B. Vertebroplasty

Numerous retrospective clinical reports of vertebroplasty for osteoporotic VCFs have been published since its conception, though few prospective series have been performed [4]. Barr et al. [25] retrospectively reviewed their results in 38 patients. Ninety-five percent of patients reported marked or moderate pain relief. One case of T3 radiculitis was documented, which resolved with oral steroids. Grados and associates [27] reported pain relief in 24 of 25 patients one month after the procedure in a similar retrospective series. Interestingly, the authors did not report immediate postprocedural pain values, limiting distinction between the treatment effect and eventual fracture healing. Two cases of transitory radiculitis were treated with nonsteroidals. Cement leakage into the disc space occurred in seven cases (28%), and asymptomatic pulmonary cement embolism occurred in one case. A substantially higher fracture risk adjacent to the augmented vertebrae was noted. Heini et al. [26] performed percutaneous vertebroplasty under local anaesthesia and sedation in 17 patients with 45 fractures. All patients reported significant pain relief at 1 day, 12 weeks, and 1 year after the procedure. Despite a high rate of cement extrusion (17%), with five cases of leakage into the paravertebral muscles, two cases into the spinal canal, and one case into a segmental spinal vein, no clinical sequelae were reported. Other reported complications from vertebroplasty are transitory fever, temporary worsening of fracture pain, infection, and rib fracture (probably from positioning) [4,32–35]. Spinal cord compression has been documented as well [31].

XI. FUTURE APPLICATIONS AND ADVANCEMENTS

Currently, kyphoplasty and vertebroplasty are primarily used for the treatment of painful osteoporotic compression fractures. The indications have been expanded by some for augmentation of neoplastic spinal lesions [32,36–38]. In selected cases these techniques have been employed with good results for metastatic and multiple myeloma lytic vertebral body lesions [32,37]. The principles of application are the same. Preoperative imaging should affirm that the tumor does not involve the pedicle or posterior vertebral body as to prevent inadvertent cement extrusion into the spinal canal. Of note, these techniques are best used for isolated, symptomatic lesions that are not associated with any neurological deficit. Specific guidelines are lacking as to its role among other modalities such as local beam radiation, bracing, and open surgical techniques [39].

A major concern with the current techniques is the implantation of PMMA into the VB. Because this is a nonresorbable (though biocompatible) material, it persists as a foreign substance. While this may be less of an issue in elderly patients, it may be more important if augmentation is considered in younger individuals. The development of bioactive, bioresorbable filler materials would help to expand the indications of these procedures for the treatment of acute, traumatic, nonosteoporotic VB fractures. Kyphoplasty, in particular, could be used to percutaneously reduce and stabilize an acute compression fracture with the potential of eventual native osseous replacement of the filler material. The optimal characteristics of such a material would be (1) sufficient immediate strength/stiffness, (2) adequate fatigue strength to endure repeated loads on the spine with activity, and (3) osteoconductivity/osteoinductivity. It is likely that the development of injectable bone morphogenic proteins in a bioresorbable carrier will have a place in future applications of kyphoplasty.

Cement extrusion is an inevitable sequela of PMMA/filler injection into the VB. This complication, however, would be obviated if the cement could be contained within an artificial, but resorbable device. At the present time, the inflatable balloon tamp is constructed of a nonresorbable, synthetic, silastic material. While it sustains the imparted mechanical stresses placed

on it by inflation within the bone, development of a tamp constructed of a resorbable material strong enough to endure these demands would be ideal. Injection of the bone filler directly into the tamp would eliminate material extravasation, while still providing the potential for complete osseointegration of the injected substance.

REFERENCES

1. Garfin SR, Yuan H, Lieberman IH. Early outcomes in the minimally-invasive reductions and fixation of compression fractures. Proceedings of the NASS. New Orleans, October, 2000:184–185.
2. Garfin SR, Yuan HA, Reiley MA. New technologies in spine: kyphoplasty and vertebroplasty for the treatment of painful ostoeporotic compression fractures. Spine 2001; 26:1511–1515.
3. Deramond H, Depriester C, Galibert P, Le Gars D. Percutaneous vertebroplasty with polymethylmethacrylate. Technique, indications, and results. Radiol Clin North Am 1998; 36:533–546.
4. Cortet B, Cotten A, Boutry N, Flipo RM, Duquesnoy B, Chastanet P, Delcambre B. Percutaneous vertebroplasty in the treatment of osteoporotic vertebral compression fractures: an open prospective study. J Rheumatol 1999; 26:2222–2228.
5. Schlaich C, Minne HW, Bruckner T, Wagner G, Gebest HJ, Grunze M, Ziegler R, Leidig-Bruckner G. Reduced pulmonary function in patients with spinal osteoporotic fractures. Ostoeoporos Int 1998; 8:261–267.
6. Robb-Nicholson C. By the way, doctor. I'm interested in having vertebroplasty, the treatment for vertebral fractures mentioned in your August issue. When I called Medicare to see if the procedure is covered, I was told ''Only if the FDA has approved it''; but when I checked with the FDA, I found that no one had applied for approval. Why is this? Is there some way to get vertebroplasty? Harv Womens Health Watch 1999; 7:8.
7. Leech JA, Dulberg C, Kellie S, Pattee L, Gay J. Relationship of lung function to severity of osteoporosis in women. Am Rev Respir Dis 1990; 141:68–71.
8. Lyles KW, Gold DT, Shipp KM, Pieper CF, Martinez S, Mulhausen PL. Association of osteoporotic vertebral compression fractures with impaired functional status. Am J Med 1993; 94:595–601.
9. Leidig-Bruckner G, Minne HW, Schlaich C, Wagner G, Scheidt-Nave C, Bruckner T, Gebest HJ, Ziegler R. Clinical grading of spinal osteoporosis: quality of life components and spinal deformity in women with chronic low back pain and women with vertebral osteoporosis. J Bone Miner Res 1997; 12:663–675.
10. Tamayo-Orozco J, Arzac-Palumbo P, Peon-Vidales H, Mota-Bolfeta R, Fuentes F. Vertebral fractures associated with osteoporosis: patient management. Am J Med 1997; 103:44S–48S; discussion 48S–50S.
11. Wasnich RD. Epidemiology of osteoporosis. In: Favus M, ed. Primer on the Metabolic Bone Diseases and Disorders of Mineral Metabolism. Philadelphia: Lippincott Williams and Wilkins, 1999:257–259.
12. Baillie SP, Davison CE, Johnson FJ, Francis RM. Pathogenesis of vertebral crush fractures in men. Age Ageing 1992; 21:139–141.
13. Biyani A, Ebraheim NA, Lu J. Thoracic spine fractures in patients older than 50 years. Clin Orthop 1996; 328:190–193.
14. Eastell R. Pathogenesis of postmenopausal osteoporosis. In: Favus M, ed. Primer on the Metabolic Bone Diseases and Disorders of Mineral Metabolism. Philadelphia: Lippincott Williams and Wilkins, 1999:260–262.
15. Watts NB. Pharmacology of agents to treat osteoporosis. In: Favus MJ, ed. Primer on the Metabolic Bone Diseases and Disorders of Mineral Metabolism. Philadelphia: Lippincott Williams and Wilkins, 1999:278–283.
16. Schneider PL, Dzenis PE, Kahanovitz N. Spinal trauma. In: Zuckerman JD, ed. Comprehensive Care of Orthopaedic Injuries in the Elderly. Baltimore: Urban and Schwarzenberg, 1990:213–267.

17. Tohmeh AG, Mathis JM, Fenton DC, Levine AM, Belkoff SM. Biomechanical efficacy of unipedicular versus bipedicular vertebroplasty for the management of osteoporotic compression fractures. Spine 1999; 24:1772–1776.
18. Belkoff SM, Maroney M, Fenton DC, Mathis JM. An in vitro biomechanical evaluation of bone cements used in percutaneous vertebroplasty. Bone 1999; 25:23S–26S.
19. Belkoff SM, Mathis JM, Erbe EM, Fenton DC. Biomechanical evaluation of a new bone cement for use in vertebroplasty. Spine 2000; 25:1061–1064.
20. Jasper LE, Deramond H, Mathis JM, Belkoff SM. The effect of monomer-to-powder ratio on the material properties of Cranioplastic. Bone 1999; 25:27S–29S.
21. Belkoff SM, Mathis JM, Fenton DC, Scribner RM, Reiley ME, Talmadge K. An ex vivo biomechanical evaluation of an inflatable bone tamp used in the treatment of compression fracture. Spine 2001; 26:151–156.
22. Lieberman IH, Dudeney S, Reinhardt MK, Bell G. Initial outcome and efficacy of ''kyphoplasty'' in the treatment of painful osteoporotic vertebral compression fractures. Spine 2001; 26:1631–1638.
23. Kado DM, Browner WS, Palermo L, Nevitt MC, Genant HK, Cummings SR. Vertebral fractures and mortality in older women: a prospective study. Study of Osteoporotic Fractures Research Group. Arch Intern Med 1999; 159:1215–1220.
24. Wenger M, Markwalder TM. Surgically controlled, transpedicular methyl methacrylate vertebroplasty with fluoroscopic guidance. Acta Neurochir 1999; 141:625–631.
25. Barr JD, Barr MS, Lemley TJ, McCann RM. Percutaneous vertebroplasty for pain relief and spinal stabilization. Spine 2000; 25:923–928.
26. Heini PF, Walchli B, Berlemann U. Percutaneous transpedicular vertebroplasty with PMMA: operative technique and early results. A prospective study for the treatment of osteoporotic compression fractures. Eur Spine J 2000; 9:445–450.
27. Grados F, Depriester C, Cayrolle G, Hardy N, Deramond H, Fardellone P. Long-term observations of vertebral osteoporotic fractures treated by percutaneous vertebroplasty. Rheumatology (Oxford) 2000; 39:1410–1414.
28. Maynard AS, Jensen ME, Schweickert PA, Marx WF, Short JG, Kallmes DF. Value of bone scan imaging in predicting pain relief from percutaneous vertebroplasty in osteoporotic vertebral fractures. Am J Neuroradiol 2000; 21:1807–1812.
29. Do HM. Magnetic resonance imaging in the evaluation of patients for percutaneous vertebroplasty. Top Magn Reson Imaging 2000; 11:235–244.
30. Mathis JM, Barr JD, Belkoff SM, Barr MS, Jensen ME, Deramond H. Percutaneous vertebroplasty: a developing standard of care for vertebral compression fractures. Am J Neuroradiol 2001; 22: 373–381.
31. Harrington KD. Major neurological complications following percutaneous vertebroplasty with polymethylmethacrylate: a case report. J Bone Joint Surg 2001; 83A:1070–1073.
32. Cortet B, Cotten A, Boutry N, Dewatre F, Flipo RM, Duquesnoy B, Chastanet P, Delcambre B. Percutaneous vertebroplasty in patients with osteolytic metastases or multiple myeloma. Rev Rhum Engl Ed 1997; 64:177–183.
33. Cyteval C, Sarrabere MP, Roux JO, Thomas E, Jorgensen C, Blotman F, Sany J, Taourel P. Acute osteoporotic vertebral collapse: open study on percutaneous injection of acrylic surgical cement in 20 patients. AJR Am J Roentgenol 1999; 173:1685–1690.
34. Chiras J, Sola-Martinez MT, Weill A, Rose M, Cognard C, Martin-Duverneuil N. Percutaneous vertebroplasty.. Rev Med Interne 1995; 16:854–859.
35. Jensen ME, Dion JE. Percutaneous vertebroplasty in the treatment of osteoporotic compression fractures. Neuroimaging Clin North Am 2000; 10:547–568.
36. Cardon T, Hachulla E, Flipo RM, Chastanet P, Rose C, Deprez X, Duquesnoy B, Delcambre B, Devulder B. Percutaneous vertebroplasty with acrylic cement in the treatment of a Langerhans cell vertebral histiocytosis. Clin Rheumatol 1994; 13:518–521.
37. Cotten A, Dewatre F, Cortet B, Assaker R, Leblond D, Duquesnoy B, Chastanet P, Clarisse J. Percutaneous vertebroplasty for osteolytic metastases and myeloma: effects of the percentage of lesion filling and the leakage of methyl methacrylate at clinical follow-up. Radiology 1996; 200: 525–530.

38. Ide C, Gangi A, Rimmelin A, Beaujeux R, Maitrot D, Buchheit F, Sellal F, Dietemann JL. Vertebral haemangiomas with spinal cord compression: the place of preoperative percutaneous vertebroplasty with methyl methacrylate. Neuroradiology 1996; 38:585–589.
39. Heary RF, Bono CM. Metastatic spine tumors. Neurosurg Focus 2001; 11:1–9.

5

Carbon Fiber–Reinforced Polymer Implants for Spinal Fusion: Biomechanical and Clinical Advantages of a New Material

John Brantigan
South Texas Orthopaedic and Spinal Surgery Associates
San Antonio, Texas, U.S.A.

I. INTRODUCTION

Treatment of painful degenerative disc disease has been dominated by several facts that have been well understood for more than half a century: excision of a herniated lumbar disc does not treat back pain, and the loads supported by a lumbar disc are very large. In a classic series of articles, Nachemson studied loading in vitro and in human volunteers [1–3] and determined that a normal individual leaning forward while holding a 10 kg weight carries of load between 2400 and 3300 N. Schultz measured intradiscal pressures at L3–4 in four human volunteers and reported loads as high as 2400 N with a subject in the upright position, flexed, and with arms out holding 8 kg [4].

Dr. Ralph Cloward defined the problem as the treatment of a broken intervertebral joint damaged by a disc rupture. Cloward felt that this broken joint was the most common cause of mechanical back pain, a problem that was not solved by removing more of the joint. In an effort to repair this broken joint, Cloward developed the posterior lumbar interbody fusion (PLIF) operation. Cloward noted that standard surgical procedures were successful in relieving sciatica, but many patients continued to have incapacitating low back pain. Standard posterior fusion procedures required long recovery times and usually did not allow patients to achieve a high functional capacity. In replacing the damaged disc with as many as five blocks of rectangular-shaped tricortical iliac crest allograft, Cloward's objective was to achieve immediate stability and prompt healing [5,6]. Although Cloward reported high rates of fusion and clinical success, he described the operation as ''a difficult operation requiring a high degree of technical skill'' [7].

Cloward's success was followed by other surgeons who made significant contributions, including Gabriel Ma, who developed mortising chisels that allowed more exact fit of the bone graft [8], and Paul Lin [9,10], who preferred tricortical iliac crest autograft. All of the surgeons who reported success with PLIF favored weight-bearing bone grafts that were rectangular in shape. As Ma stated frequently, square on round is unstable; square on square is stable.

Unfortunately, many other surgeons failed to duplicate the favorable results reported by Cloward, Lin, and Ma. In describing this operation, Wiltse [11] wrote ''when used alone, failure of fusion is the rule.'' Wetzel and LaRocca reviewed a series of patients with failed interbody

fusion and concluded ''we are unable to recommend any successful salvage for the failed PLIF'' [12]. Cloward's PLIF operation fell into disrepute for many years.

Anterior lumbar interbody fusion (ALIF) was pioneered in Hong Kong by Hodgson [13] in 1956 and further developed by Crock [14] in Melbourne and O'Brien [15] in London. ALIF achieved worldwide popularity, but was slow to be accepted in the United States after a cautionary study was reported by Stauffer [16] at the Mayo Clinic. Although the procedure appeared to work well in smaller Asian individuals, it did not appear to work satisfactorily in individuals of higher body mass. Denis et al. [17] reported that 100% of patients lost disc space height during the postoperative healing of traditional ALIF grafts. O'Brien et al. noted that combined posterior fixation was necessary to achieve reliable results in ALIF [15].

In the early 1980s Art Steffee [18] observed that in treatment of complex degenerative conditions of the lumbar spine, previous types of spinal instrumentation were not possible. Hooks, wires, and other attachments to the vertebral lamina could not be used if the lamina had already been surgically excised. Furthermore, distraction rods decreased lumbar lordosis and resulted in a painful flat-back condition. Steffee popularized the use of screw fixation in the vertebral pedicles and began a revolution in treatment of degenerative lumbar conditions. However, when other surgeons used the pedicle screw implants improperly, complications and poor results were followed by a frenzy of litigation.

Failures of these efforts to repair the broken intervertebral joint damaged by a disc rupture, whether PLIF or ALIF, have been largely due to the limitations of the allograft bone commonly used. The graft must bear substantially all of the patient's body weight while it achieves healing by the erosive process of ''creeping substitution.'' In a mechanical study of commercially available allograft for interbody fusion, it was determined that up to 35% of the allograft implants were of inadequate strength to support the required loads [19]. Clearly a new type of implant made of a new type of material was required to meet the mechanical and biological requirements that were already clearly defined.

Our group has worked since the mid-1980s with the support of the DePuy AcroMed Corporation in the development of a family of implants made of a carbon fiber–reinforced polymer (CFRP) material to separate the mechanical functions of interbody fusion from the biological requirements and replace them with improved elements. The CFRP implants provide a device designed to meet the mechanical requirements of interbody fusion, and they are filled with autologous cancellous bone graft, undoubtedly the best material for bony fusion success. These implants were described by Steffee as ''cages'' in the late 1980s, the first use of a title that has come to describe a generic class of implants. The Brantigan cage for PLIF shown in Figure 1 maintains Cloward's essential principles. The rectangular implants are seated precisely on flattened vertebral endplates. The entire disc is removed. And the disc space is filled with the greatest possible amount of autologous bone graft.

During the past 15 years we have described a number of cases in which we successfully reconstructed failed pedicle screw constructs with carbon fiber fusion cages and new screws of the exact same type that had previously failed when used alone [20]. We carried out laboratory validation of these principles with mechanical testing in cadaver spines [21] and with a 2-year animal study in the Spanish goat [22]. We have completed a 2-year investigational device study [23], which has resulted in FDA approval of these devices. Other surgeons have reported favorable clinical series [24,25]. This is the first approved and widely used application of carbon fiber–reinforced polymer as an implant material. Additional CFRP ''cage'' implants have been designed to meet the anatomical requirements of various spinal areas, including a large oval ALIF cage, a cervical cage, and stackable corpectomy cages for thoracolumbar tumors and fractures. The polymer material — currently PEEK-Optima (Invibio Inc., Greenville, SC) — is from the family of plastics known as polyaryletherketones. The purpose of this chapter is to

Figure 1 Photograph of the Brantigan CFRP cage for PLIF. (From Ref. 33.)

describe the mechanical, biological, radiographic, and clinical properties of the CFRP material that make it superior to titanium and other metals as an orthopedic implant material.

II. MECHANICAL REQUIREMENTS

The mechanical requirements of interbody fusion are summarized in Table 1. The static compressive strength of the CFRP cages is summarized in Figure 2, along with the static compressive strength of competing cages and tricortical allograft bone. The average vertebral body strength, about 8000 N, is shown by a horizontal line. The average compressive strength of tricortical allograft bone was determined by our group by compression tests of allograft bone that we purchased from commercial sources that sold this material for medical implant use [19]. It is immediately apparent that the average tricortical allograft is of insufficient strength to support the physiological loads of interbody fusion. The average CFRP cage, which is twice as strong as the average vertebral bone, has a significant strength margin over the physiological requirements. The competing cages, however, are excessively strong because the extra strength compromises the biological function of the implants. Once an adequate strength level is achieved, it is important to open the architecture of the cage to increase the bone graft surface area to facilitate bony union.

An important conclusion of our test of allograft bone strength is that even radiographically dense bone has inconsistent strength. Figure 3 shows a comparison between radiographic density of allograft bone specimens vs. static compressive strength. Although the specimens of greater density have a trend toward greater load to failure, there is no specific density that would assure adequate strength. It is well known that processing of bone by freeze-drying, ethylene oxide sterilization, or irradiation significantly decreases the mechanical strength of cortical allografts. Freeze-drying particularly creates microcracks in the bone that render mechanical properties unpredictable [26,27]. The unreliable compressive strength of cortical allograft should be kept in mind when considering use of allograft blocks machined into cage-like shapes for interbody fusion.

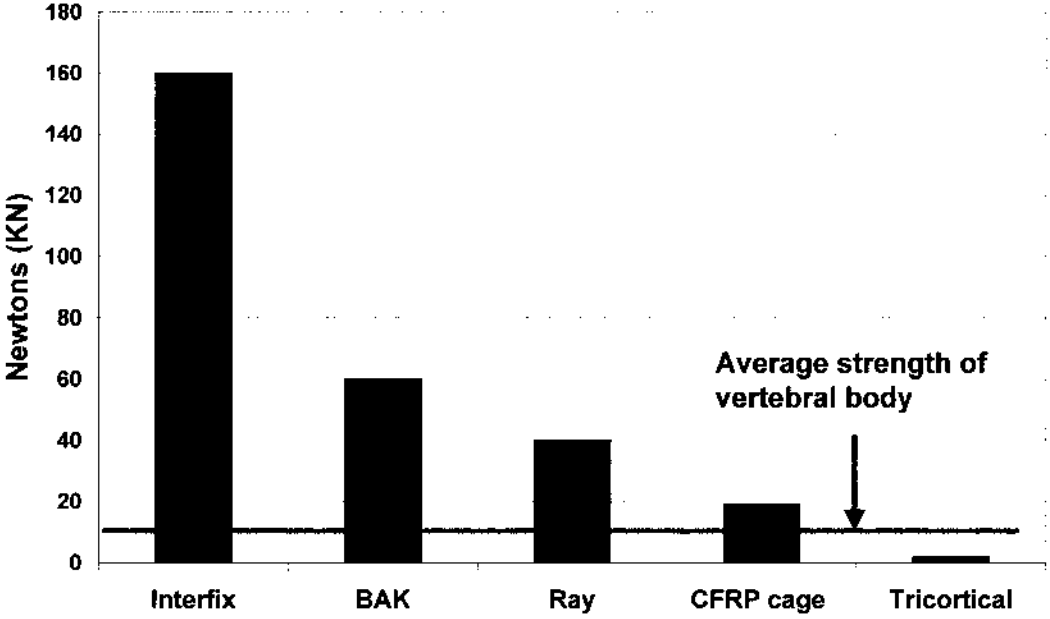

Figure 2 Static compressive strength of cages versus allograft. (Courtesy of H. Serhan, DePuy AcroMed Corp.)

Table 1 Required Properties of Interbody Fusion Devices

Adequate compressive strength
Adequate fatigue strength
Correct stiffness to match vertebral bodies
Correct stiffness to avoid stress shielding
Ability to resist retropulsion
Provide immediate stability during fusion
Provide adequate surface area to resist subsidence

Source: Courtesy of H. Serhan, DePuy AcroMed Corp.

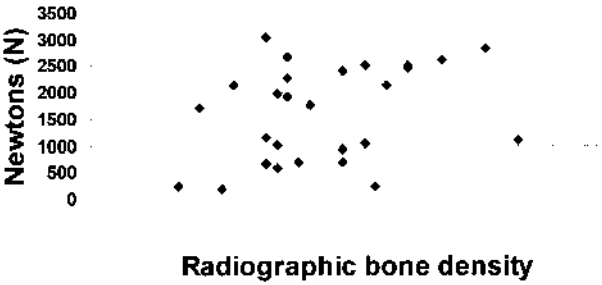

Figure 3 Allograft bone load to failure. (From Ref. 19.)

An implant should be evaluated to explore any known failure modes. For a posterior lumbar interbody fusion application, retropulsion of the graft historically has created neural impingement and foot drop in a percentage of cases, and subsidence of the graft with loss of disc space height has been a factor. For the traditional PLIF, Cloward used three to five blocks of tricortical allograft in order to increase the load-bearing capacity of the graft. Having more than two implants made it very difficult from a carpentry standpoint to equally compress all grafts. Consequently there were frequently one or more grafts relatively loose and subject to retropulsion. Supporting physiological loads with two side-by-side devices improves the probability of secure placement.

The CFRP cage has been tested mechanically in a series of fresh frozen cadaver spines [21] to assess these properties. When pulling against the broad posterior surface of the cage, an average force of 672 N was required to remove the CFRP cages from cadaver specimens, almost six times the 126 N measured for allograft. Motion segments were then prepared with bilateral CFRP cages and compressed to the point of mechanical failure (Figure 4). Unmodified motion segments failed at an average load of 6043 N compared with CFRP cage specimens that failed at an average load of 5288 N. The average compressive force, displacement, stiffness, and energy to failure for the CFRP cage specimen were statistically no different than the unmodified motion segments, indicating that subsidence is not a problem.

Mechanical properties of the bone/implant interface make important contributions to stability, load transfers, and bony healing. Figure 5 lists the Young's modulus of elasticity for various materials. The CFRP cage material is very close to the modulus of elasticity of human bone, whereas metal materials commonly used for implants are up to 10 times as stiff. Kanayama et al. [28] studied 11 different cage types in calf spines to determine construct stiffness and stress shielding. They found that no statistically significant differences existed in construct stiffness

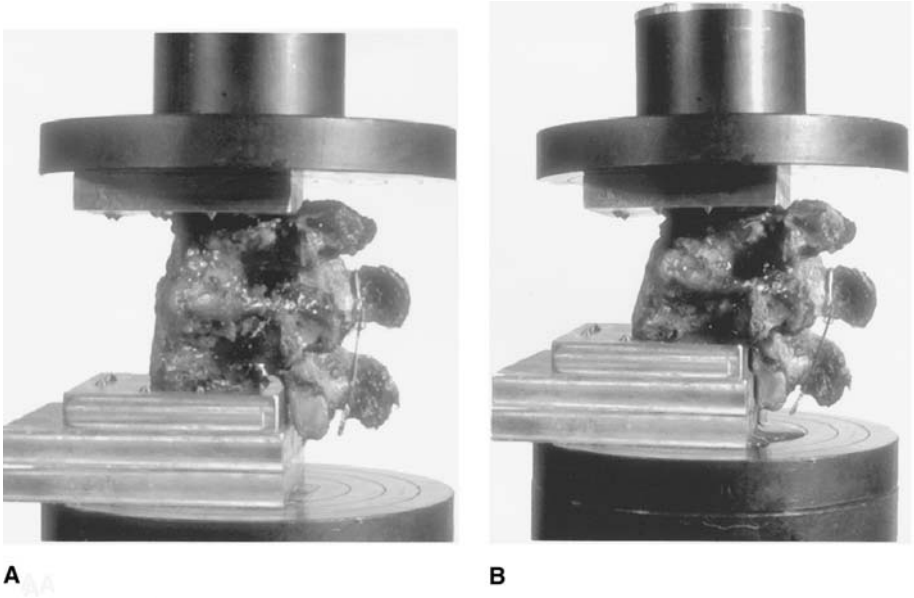

Figure 4 CFRP cage construct subject to compression testing: (A) before compression; (B) after compression failure. (From Ref. 21.)

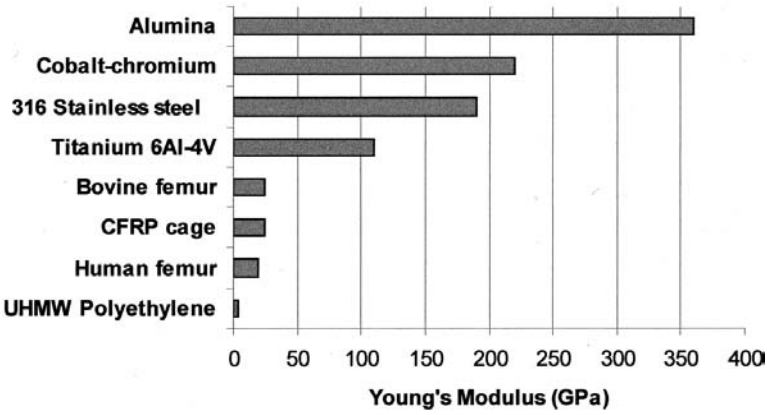

Figure 5 Modulus of elasticity of implant materials. (Courtesy of H. Serhan, DePuy AcroMed Corp.)

among the metal threaded cages and nonthreaded devices, concluding that the threaded devices did not achieve a greater stand-alone stability. However, the CFRP cage transmitted a significantly greater pressure to the elastomer inside the cage, higher by a factor of three, compared with the metal threaded cages. The reduced stress-shielding of the bone inside the CFRP cages would be expected to result in improved rate of bony healing.

Table 2 summarizes the mechanical properties of CFRP material compared with metal implants and allograft.

III. BIOLOGICAL REQUIREMENTS

Biocompatibility requirements for implant materials are defined by ASTM ISO-10-993 standards. These include chemical tests of sensitivity, toxicity, and carcinogenicity, summarized in Table 3. All of these tests were successfully completed for the CFRP cage material.

The most significant biological test was a 2-year implantation study in the Spanish goat [22] in which CFRP cages were compared with interbody fusion using allograft prepared from vertebral bodies of other goats and processed by a human bone bank in accordance with clinical standards. Because of the anatomical properties of goats, a lateral interbody fusion was done

Table 2 Comparison of CFRP, Metal, and Allograft

CFRP carbon	Metal	Allograft
Modulus of elasticity similar to bone	Modulus of elasticity 10× as stiff as bone	Modulus of elasticity same as surrounding bone
Mechanically compatible bone/implant interface	Greater stress shielding	Made brittle by processing; mechanically unreliable
Chemically inert	Subject to corrosion	Subject to "creeping substitution"
Radiolucent—allows visualization of bony healing	Radioopaque—blocks visualization of bony healing	Radiographically dense (cortical portion)—blocks visualization of changes in cancellous bone graft

Table 3 ISO-10-993 Tests for Material Biocompatability

Cytotoxicity—L929 mouse fibroblast
Pyrogenicity—rabbit
Acute systemic toxicity—mouse
Acute intracutaneous reactivity—rabbit
Genotoxicity—*Salmonella typhimurium*
Genotoxicity—DMSO extract
Muscle implantation—rabbit
Sensitization—guinea pig
Lymphoma mutagenesis—mouse
Carcinogenicity—2-year rat study

Source: Courtesy W. Christianson, DePuy AcroMed Corp.

using a single cage or allograft implant. No additional internal fixation was used. The specimens were studied with three-dimensionally reformatted CT scans and with histology. Figure 6 shows coronal, mid-coronal, and axial views of a 24-month cage specimen. Living bone clearly bridges the interspace with ossification of the anulus fibrosis. In comparison, Figure 7 shows the coronal and mid-coronal view of an allograft specimen at 24 months. The allograft has been apparently resorbed, there is loss of disc space height, and incomplete fusion has occurred by partial ossification of the anulus. Figure 8 shows histology of a 12-month specimen in which living bony trabeculae inside the cage are in continuity with the trabeculae above and below. There are no areas of pseudarthrosis. Ossification of the anulus is apparent outside the cage.

In this study, an independent radiologist and pathologist reported the result as 100% fusion success. There was minimal microscopic debris typical of that experienced around other implants. There was no inflammatory response, no osteolysis, no migration of carbon particles, and the cage levels healed quicker and more reliably than allograft.

In comparison, no animal study was done in support of the Ray cage. A study in the baboon was done for the BAK cage. The presentation of this study to the Food and Drug Administration indicated that the BAK cage did almost as well as allograft, and this study was never published. Weiner and Fraser [29] reported a study of metal cylindrical cages in sheep and reported that ''solid fusion through the cages did not occur — bony 'locking' with some growth through the holes but with intervening cartilaginous tissues remaining centrally, was the rule.'' It is likely that the higher stress shielding of the metal material is a primary cause of the lower fusion rate.

Obtaining a fusion using a cage implant requires understanding of more than just the mechanical and biological properties of materials. The cage must have a sufficiently open architecture and broad surface area of bone graft to allow a blood supply to grow from the adjacent bony surfaces. The orthopedic aphorism ''no blood, no bone'' applies equally to fracture healing and to interbody fusion. The Brantigan CFRP cage was designed to maintain this open design consistent with a broad enough surface area of support.

Obtaining a fusion biologically requires more than the simple implantation of a device, no matter how well designed. Cloward, Lin, Ma, and all the pioneers of PLIF have stated that a complete discectomy must be carried out with removal of all of the nucleus and all of the cartilaginous vertebral endplate. After the implants are placed, all crevices should be filled with as much cancellous bone graft as can be inserted. If additional bone graft is not placed, the segment has the possibility of obtaining bony healing beyond the cage because this area will

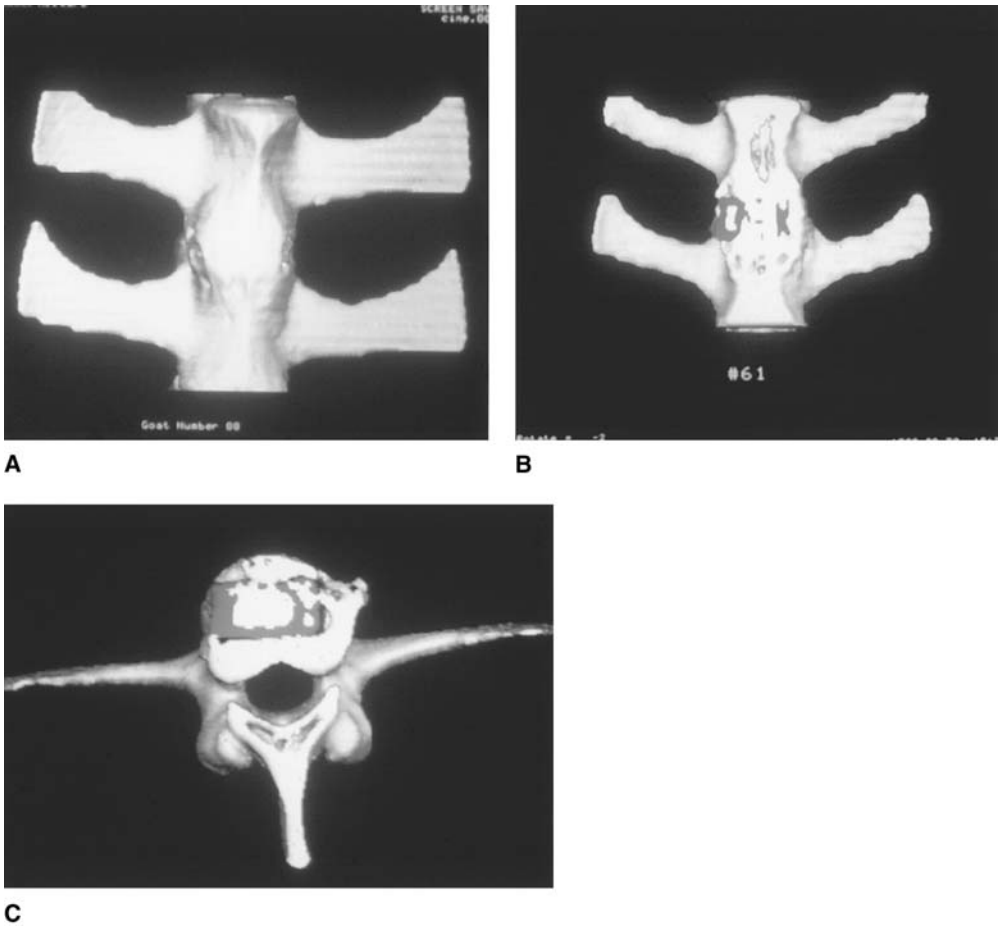

Figure 6 Reconstructed CT scans of CFRP cage after 2-year goat implantation: (A) coronal view; (B) mid-coronal sectional view; (C) axial view. (From Ref. 22.)

be filled with blood after surgery and become the equivalent of a fracture hematoma, but only if the vertebral endplate is curetted down to bleeding bone.

IV. CLINICAL TESTING OF THE CFRP CAGE

The Brantigan CFRP cage for PLIF was tested clinically in a investigational device exemption study under the supervision of the U.S. Food and Drug Administration. Inclusion criteria included degenerative disc disease in patients with prior failed discectomy surgery. The average patient had two prior failed decompression surgeries at two levels. Clinical success as evidenced by improvement in pain and function scores was achieved in 86%, and radiographic fusion success was achieved in 100% as evidenced by bone bridging the fusion area with no lucencies [23]. The Brantigan Cage for PLIF was approved by the FDA in February 1999.

Since then, successful clinical series have been reported by others [24,25]. Molinari reported a study of active-duty United States servicemen, in which 80% of CFRP cage patients

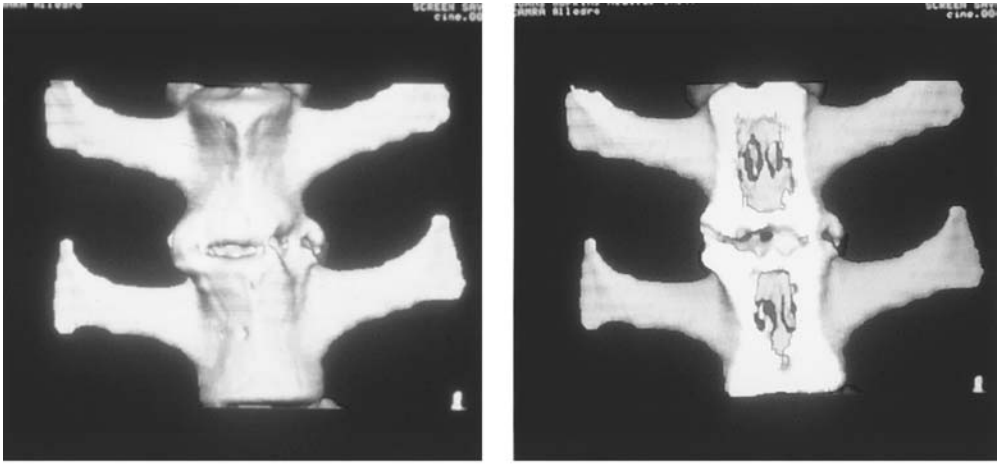

Figure 7 Reconstructed CT scans of allograft interbody fusion after 2-year goat implantation: (A) coronal view; (B) mid-coronal view. (From Ref. 22.)

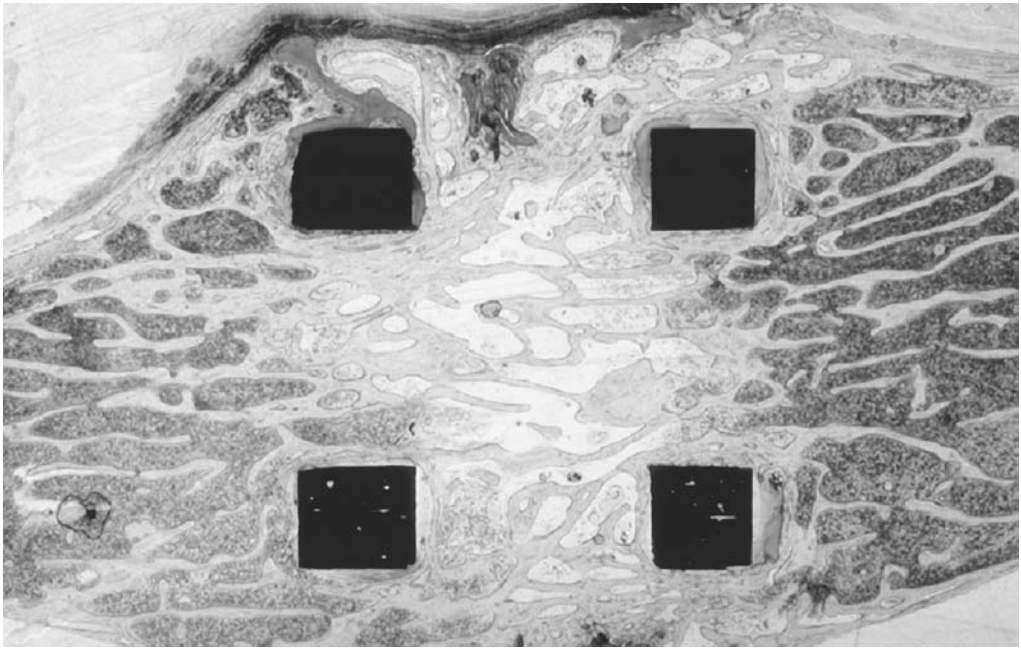

Figure 8 Histological appearance of cage fusion after 12-month goat implantation. (From Ref. 22.)

passed the rigorous army physical fitness test and retuned to full military duty, and 20% returned to military duty with some physical limitations. Additionally, Togawa et al. [30] studied a series of biopsy results in patients with radiographically successful CFRP cage fusions and reported histologically normal bone inside the cages.

Our group has shown that a wedged version of the CFRP cage achieves normal sagittal plane alignment in spondylolisthesis [31]. A 10-year study of the original IDE patients has revealed that although some patients develop adjacent segment degeneration, the rates of fusion and clinical success remain satisfactory at this time period [32].

V. RADIOGRAPHIC PROPERTIES OF CFRP MATERIAL

One of the greatest advantages of the CFRP material is radiolucency, allowing the biological changes of bony consolidation to be followed by normal plane radiographs. Because cages have the same density as cancellous bone, cage struts provide a constant density against which metabolic increases in bony density and maturation of the fusion can be compared. The carbon fiber–reinforced polymer material is compatible with all imaging methods, and MRI scans demonstrate normal bone after cage fusion. The radiolucency is best illustrated with a case report from the IDE study [33].

A 46-year-old male patient was evaluated in 1992 for the complaint of disabling back pain. He had injured his back in 1987 carrying a heavy load while working in a meatpacking plant. He had prior lumbar surgery, including discectomy at L5-S1 in 1988, but received no benefit from this surgery. His pain was described as unbearable. His walking was limited to two blocks. He was unable to participate in activities outside the home and he required assistance with dressing. He was receiving Medicaid and Medicare disability benefits. A lateral x-ray showed mild decrease in disc space height at L4-5 and L5-S1 (Figure 9). An MRI scan showed extensive degenerative change (Figure 10).

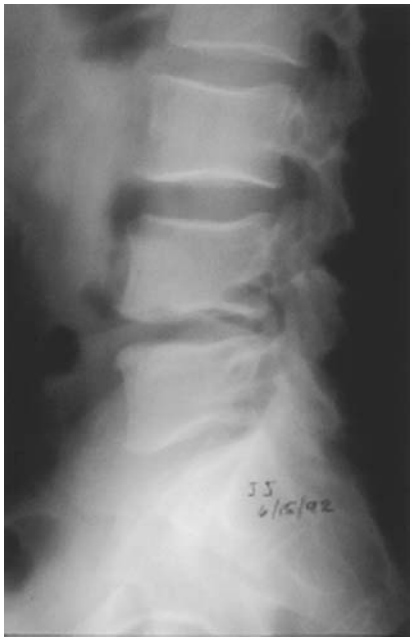

Figure 9 Preoperative lateral x-ray in case study. (From Ref. 33.)

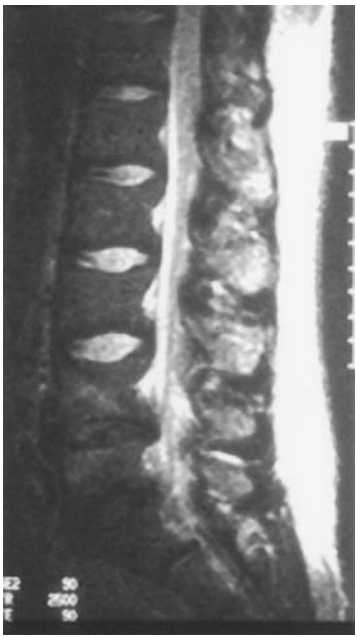

Figure 10 Preoperative MRI view in case study. (From Ref. 33.)

The patient had surgery on July 22, 1992, including CFRP cage PLIF at L4-5 and L5-S1 with VSP spinal fixation as part of the IDE study of these devices. Three months after surgery, routine x-rays documented bone inside the cages at both levels (Figures 11 and 12). Because the carbon cages are radiolucent, the bone density is clearly visible inside the cages. At this point, bone density is about the same as that of the carbon cages.

By 6 months after surgery, the patient reported that his pain was mild. He routinely walked 2–3 miles a day and had restriction of only strenuous activities. X-rays documented increased bone density in the fusion area (Figures 13 and 14). The cage struts are clearly visible on the up-angled AP x-ray, indicating that the bone density inside the cages has increased.

At one year postop, pain and function continued to improve slowly, and the patient returned to work in a light-duty capacity in a food processing plant. X-rays showed consolidation of bone inside the left-sided cage but some resorption of the bone inside the right-sided cage (Figures 15 and 16).

At 2 years postop the patient reported that he had no pain and no restriction of activities. He was working full-time in a heavy manual capacity in the food-processing company. X-rays showed increased bone density in all fusion areas.

At 4 years postop the patient continued to have no pain and no restriction of activity. He was taking no medication and continued to work full-time in a heavy capacity. X-rays showed solid bony fusion in all areas, including the bone inside the cage on the right (Figures 17 and 18).

The increased density and maturation of the bone graft and fusion is apparent in the sequence of films. The integrity of the fusion and any areas of fusion failure are fully visible on good-quality films.

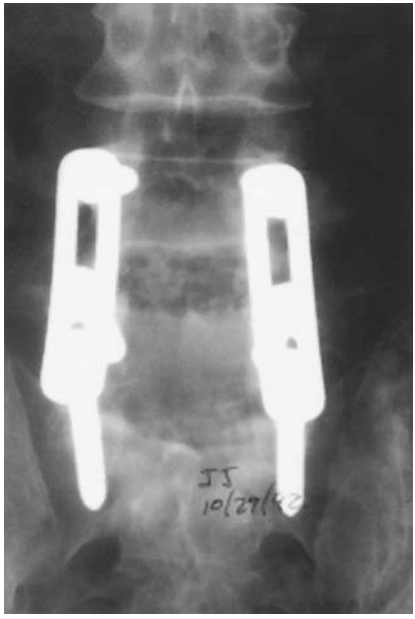

Figure 11 Three-month postoperative AP x-ray. The densities of cage and cancellous bone graft are approximately the same. (From Ref. 33.)

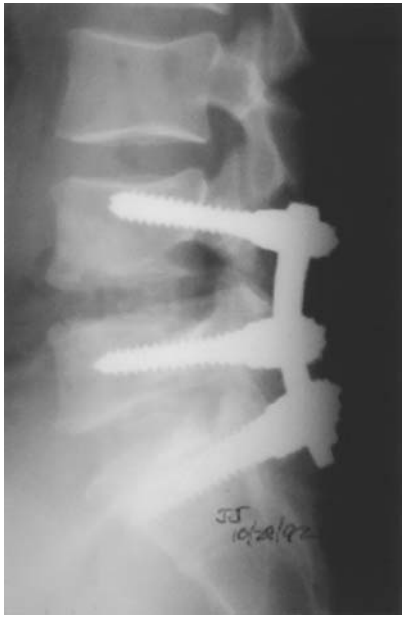

Figure 12 Three-month postoperative lateral x-ray. (From Ref. 33.)

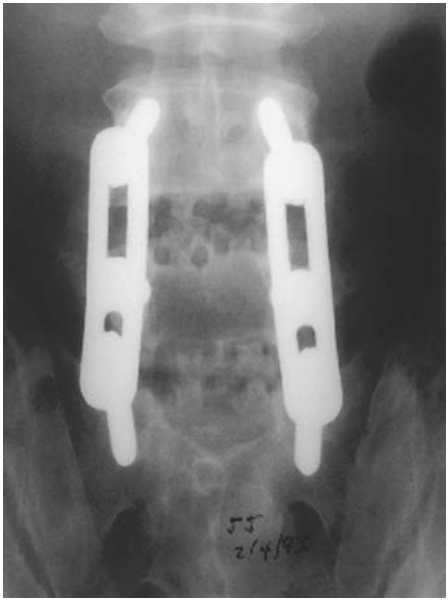

Figure 13 Six-month postoperative AP x-ray. The square cage struts are clearly visible, indicating that the bone density inside the cages has increased. (From Ref. 33.)

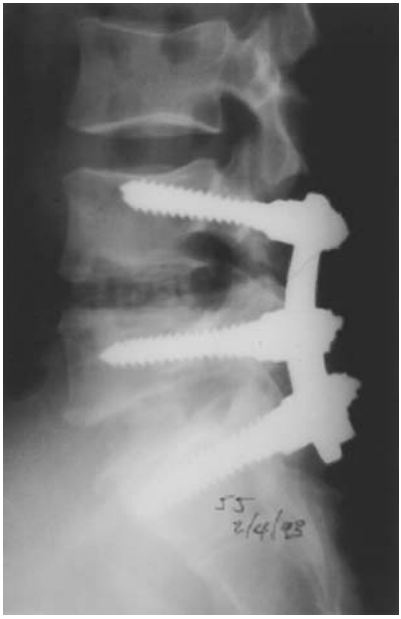

Figure 14 Six-month postoperative lateral x-ray. (From Ref. 33.)

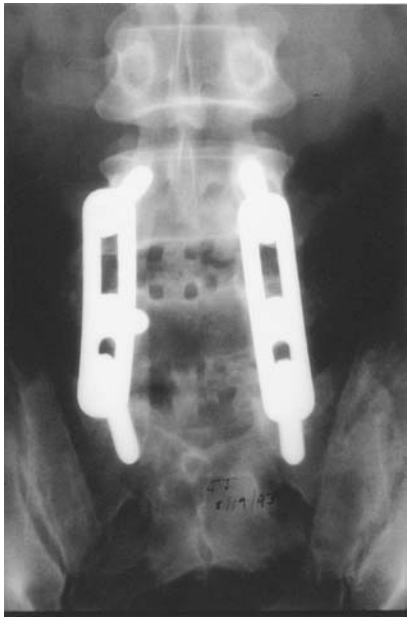

Figure 15 One-year postoperative AP x-ray. Bone inside the left-sided cage has consolidated; however, there is some resorption of bone inside the right-sided cage at L4–5. (From Ref. 33.)

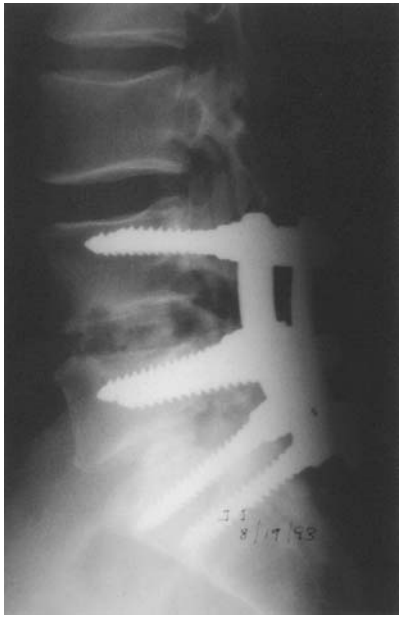

Figure 16 One-year postoperative lateral x-ray. (From Ref. 33.)

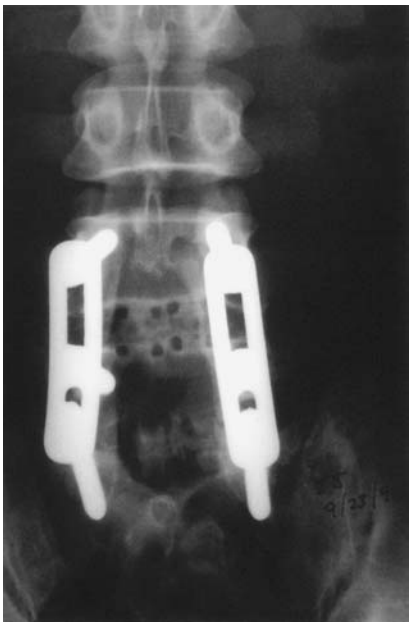

Figure 17 Four-year postoperative AP x-ray shows solid bony fusion in all areas, including the bone inside the cage on the right at L4–5. (From Ref. 33.)

Figure 18 Four-year postoperative lateral x-ray. (From Ref. 33.)

VI. CONCLUSION

The CFRP cage for PLIF has achieved the design objectives of meeting all mechanical requirements of the lumbar spine, meeting all requirements for long-term biocompatibility and allowing documented reliable fusion success when implanted according to established physiological principles. This is the first FDA-approved use of this type of implant material and the first in a family of implant devices designed to restore anterior column support and achieve fusion success in a variety of pathologies throughout the spine.

REFERENCES

1. Nachemson A. Lumbar intradiscal pressures—experimental studies on post-mortem material. Acta. Orthop. Scandinav. Suppl 1960; 43.
2. Nachemson A. The effect of forward leaning on lumbar intradiscal pressures. Acta. Orthop. Scand 1965; 35:314–328.
3. Nachemson A. The influences of spinal movements on the lumbar intradiscal pressure and on tensile stresses in the annulus fibrosus. Acta. Orthop. Scand 1963; 33:183–207.
4. Schultz A, Andersson G, Ortengren R, Haderspeck K, Nachemson A. Loads on the lumbar spine: validation of a biomechanical analysis of intradiscal pressures and myoelectric signals. J. Bone Joint Surg 1982; 64A:713–720.
5. Cloward RB. The treatment of ruptured lumbar intervertebral discs by vertebral body fusion. J. Neurosurg 1953; 10:154.
6. Cloward RB. Spondylolisthesis: treatment by laminectomy and posterior lumbar interbody fusion. Clin. Orthop 1981; 154:74–82.
7. Cloward RB. Posterior lumbar interbody fusion updated. Clin. Orthop 1985; 193:16–19.
8. Ma GW. Posterior lumbar interbody fusion with specialized instruments. Clin. Orthop 1985; 193: 57–63.
9. Lin PM, Cautilli RA, Joyce MF. Posterior lumbar interbody fusion. Clin. Orthop 1983; 180:154–168.
10. Lin PM. Posterior lumbar interbody fusion technique: complications and pitfalls. Clin. Orthop 193: 90–102.
11. Wiltse LL. Surgery for intervertebral disk disease of the lumbar spine. Clin. Orthop 1977; 129:22–45.
12. Wetzel FT, LaRocca H. The failed posterior lumbar interbody fusion. Spine 1991; 6:839–845.
13. Hodgson AR, Wong SK. A description of a technic and evaluation of results in anterior spinal fusion for deranged intervertebral disk and spondylolisthesis. Clin. Orthop 1968; 56:133–162.
14. Crock HV. Practice of Spinal Surgery. New York: Springer-Verlag, 1983:64–84.
15. O'Brien JP, Dawson MHO, Heard CW, Momberger G, Speck G, Weatherly CR. Simultaneous combined anterior and posterior fusion. Clin. Orthop 1986; 203:191–195.
16. Stauffer RN, Coventry MB. Anterior interbody lumbar spine fusion: analysis of Mayo Clinic series. J. Bone Joint Surg 1972; 54:230–237.
17. Denis S, Watkins R, Landaker S, Dillin W. Comparison of disc space heights after anterior lumbar interbody fusion. Spine 1989; 14:876–878.
18. Steffee AD, Brantigan JW. The VSP spinal fixation system—report of a prospective study of 250 patients enrolled in FDA clinical trials. Spine 1993; 18:1160–1172.
19. Brantigan JW, Cunningham BW, Warden K, McAfee PC, Steffee AD. Compression strength of donor bone for PLIF. Spine 1993; 18:1213–1221.
20. Brantigan JW. Reconstruction of failed pedicle screw fixation using a carbon PLIF cage and new pedicle screws of the same type: three cases. Techn. Neurosurg 1998; 4:216–225.
21. Brantigan JW, Steffee AD, Geiger JM. A carbon fiber implant to aid interbody lumbar fusion—mechanical studies. Spine 1991; 16:S277–282.
22. Brantigan JW, McAfee PC, Wang H, Orbegoso CM, Cunningham BC, Warden KE. Interbody lumbar fusion using a carbon fiber cage implant vs. allograft bone—an investigational study in the Spanish goat. Spine 1994; 19:1436–1444.

23. Brantigan JW, Steffee AD, Lewis ML, Quinn LM, Persenaire JM. Lumbar interbody fusion using the Brantigan I/F cage for PLIF and the VSP pedicle screw system: two year results of a Food and Drug Administration IDE clinical trial. Spine 2000; 25:1437–1446.
24. Hashimoto T, Shigenobu K, Kanayama M, Harada M, Oha F, Ohkoshi Y, Tada H, Yamamoto K, Yamane S. Clinical results of single-level posterior lumbar interbody fusion using the Brantigan I/F carbon cage filled with a mixture of local morselized bone and bioactive ceramic granules. Spine 2002; 27:258–262.
25. Molinari RW, Gerlinger T. Functional outcomes of instrumented posterior lumbar interbody fusion in active-duty US servicemen: a comparison with nonoperative management. Spine J 2001; 1:215–224.
26. Burchard H. The biology of bone repair. Clin. Orthop 1983; 174:28–42.
27. Friedlaender GE. Current concepts review: bone grafts. The basic science rationale for clinical applications. J. Bone Joint Surg 1987; 69A:786–789.
28. Kanayama M, Cunningham BW, Haggerty CJ, Abumi K, Kaneda K, McAfee PC. In vitro biomechanical investigation of the stability and stress-shielding effect of lumbar interbody fusion devices. J. Neurosur. (Spine 2) 2000; 93:259–265.
29. Weiner BK, Fraser RD. Spine update: lumbar interbody cages. Spine 1998; 23:634–640.
30. Togawa D, Bauer TW, Brantigan JW, Lowery GL. Bone graft incorporation in radiographically successful human intervertebral body fusion cages. Spine 2001; 26:2744–2750.
31. Brantigan JW, Neidre A. Achievement of normal sagittal plane alignment using a wedged carbon fiber reinforced polymer fusion cage in treatment of spondylolisthesis. NASS Spine Jrnl, in press.
32. Brantigan JW, Neidre A, Hall B. Lumbar interbody fusion using the Brantigan Cage for PLIF with pedicle screw fixation: ten year results of a Food and Drug Administration clinical trial, in press.
33. Brantigan JW. The Brantigan cage for PLIF, posterior lumbar interbody fusion, surgical technique. M.D JW Brantigan, ed, 2002.

6

Stand-Alone Anterior Lumbar Interbody Fusion Constructs: Effect of Interbody Design, Bone Graft, and Bone Morphogenetic Protein on Clinical and Radiographic Outcomes

Kenneth Burkus
The Hughston Clinic
Columbus, Georgia, U.S.A.

I. INTRODUCTION

Anterior lumbar interbody fusion (ALIF) is an effective treatment for patients with symptomatic lumbar spondylolisthesis, instability, and radiculopathy [1–4]. During the past decade, a variety of interbody constructs have been proposed for use in these indications, which have been reported to exhibit a wide range of clinical success [5–8]. Fusion success requires, in part, both mechanical stability and adequate graft material to provide a favorable biological environment in which fusion can occur. In clinical attempts to improve the rates of fusion, interbody construct design has evolved through the use of stand-alone interbody fusion devices, such as femoral ring allografts, to threaded cortical bone dowels, cylindrical metal fusion cages, and ultimately to tapered metal fusion cage devices.

Threaded interbody fusion devices such as threaded cortical bone dowels and interbody fusion cages are not intradiscal spacers that require additional segmental stabilization. These threaded devices are designed to withstand lumbar compressive loads while maximizing device porosity [9]. They also are designed to promote load sharing between the allograft and the host bone [10]. Threaded devices are seated within the central portion of the disc space through a controlled insertion technique. The threaded implants resist expulsion and stabilize the bone/implant interface.

The use of stand-alone impacted femoral ring allografts (Fig. 1) has been associated with high rates of pseudarthrosis, graft subsidence, and graft extrusion [11,12]. Threaded allograft bone dowels use precision-machined allograft to further enhance the stability of the spinal motion segment during interbody fusion (Fig. 2). The same surgical instruments that are used with similarly designed titanium cylindrical cages are used to place the allograft constructs (Fig. 3). Furthermore, threaded designs provide the ability to precisely control the depth during placement of the interbody devices as compared with impacted designs [10]. A tapered metal cage allows

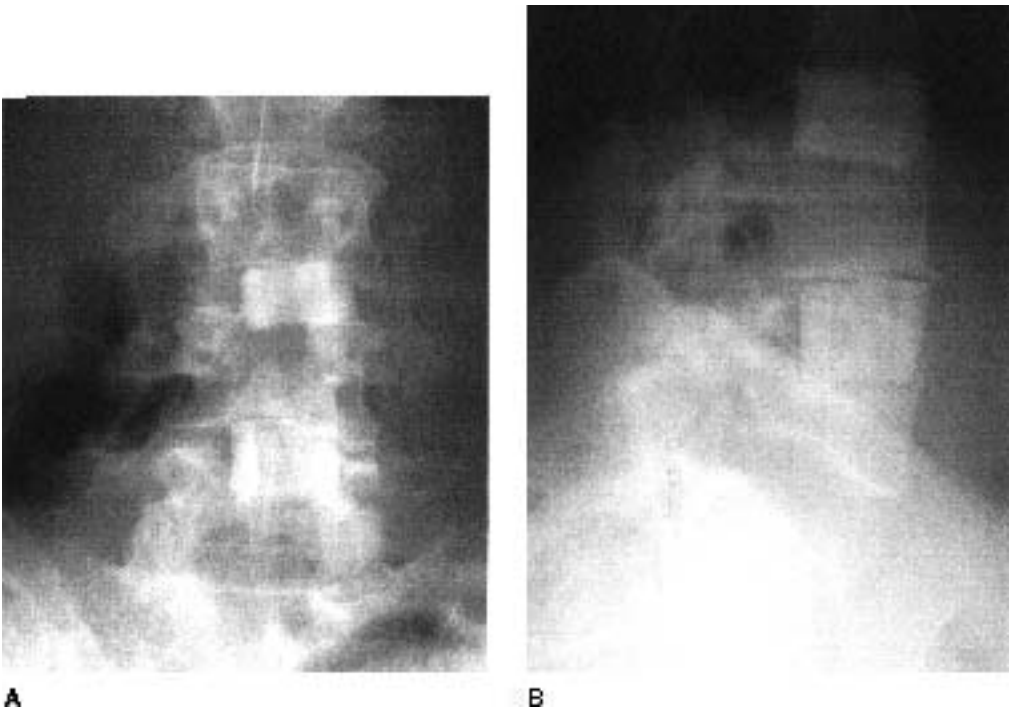

Figure 1 (A) Anteroposterior and (B) lateral radiographs of the lumbar spine show two femoral ring allografts placed centrally in the L3–4 and L4–5 disc spaces. The vertebral end plates have been prepared to uniformly contact the structural allografts. These impacted grafts act as spacers and require no supplemental fixation to stabilize the interface between the host bone and allograft. The grafts are recessed to prevent extrusion.

for a modified surgical technique that requires less aggressive reaming to preserve the end plates while maintaining lordosis (Fig. 4).

The gold standard for bone grafting in spinal fusion procedures has been autogenous cancellous bone harvested from the iliac crest [1–4]. However, this procedure has been associated with many complications [11–13]. The most frequently reported complication has been morbidity associated with the donor surgical site, which has been reported to persist for up to 10 years [14]. The long-term incidence of donor site pain has been reported to occur in 22–45% of patients [5,15,16].

Recombinant human bone morphogenetic protein-2 (rhBMP-2) is an osteoinductive protein that, when combined with the proper carrier at an appropriate concentration, has the potential to make autogenous bone grafting unnecessary. RhBMP-2 with an absorbable collagen sponge (ACS) carrier has been investigated in preclinical and clinical studies for its application in ALIF procedures with both metal interbody cages and allograft bone dowels [5,6,17–19].

A large, pivotal clinical study indicated that the use of rhBMP-2/ACS does provide equivalent clinical and radiographic outcomes to autogenous iliac crest while reducing time in the operating room and intraoperative blood loss [5]. The purpose of this study was twofold. First, FDA-approved prospective clinical and radiographic outcomes were compared at 24 months postoperatively for 405 patients who underwent a single-level, anterior lumbar discectomy and interbody fusion. The results were derived from different investigational device exemption (IDE)

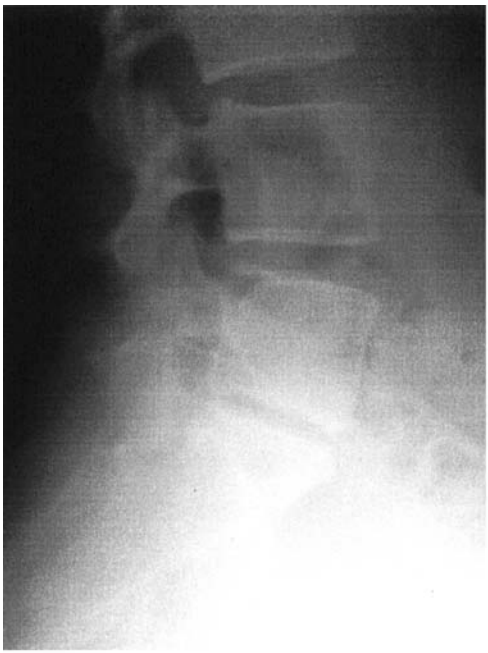

A

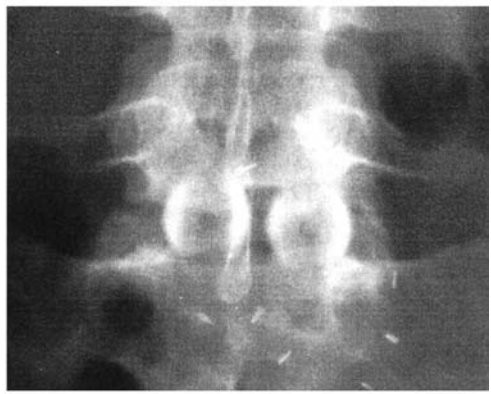

B

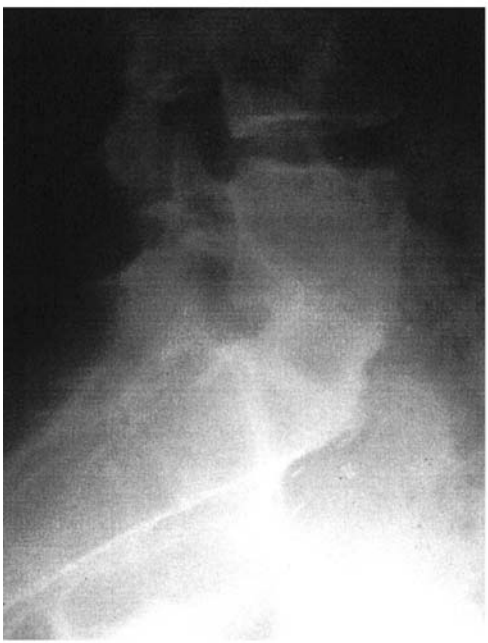

C

Figure 2 (A) Lateral radiograph of the lumbar spine shows significant disc space collapse and loss of segmental lordosis at the L5–S1 interspace. (B) Anteroposterior and (C) lateral radiographs after surgery show two threaded cortical bone dowels in place in the L5–S1 disc space. The threads engage the vertebral end plates and help to stabilize the intervertebral motion segment. At the operative level, normal disc space height and segmental lordosis has been restored.

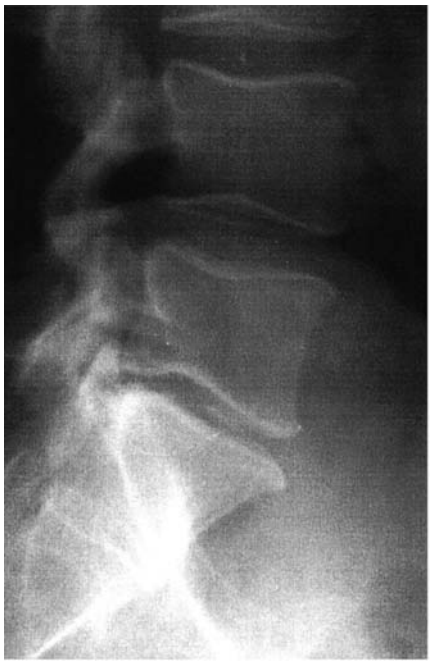

A

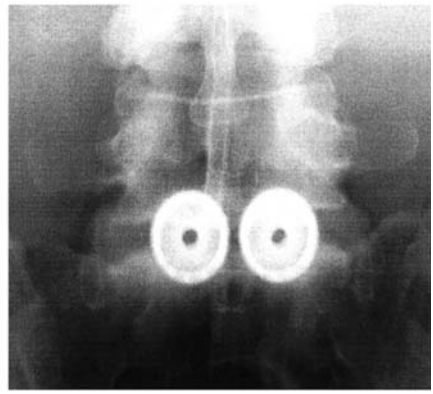

B

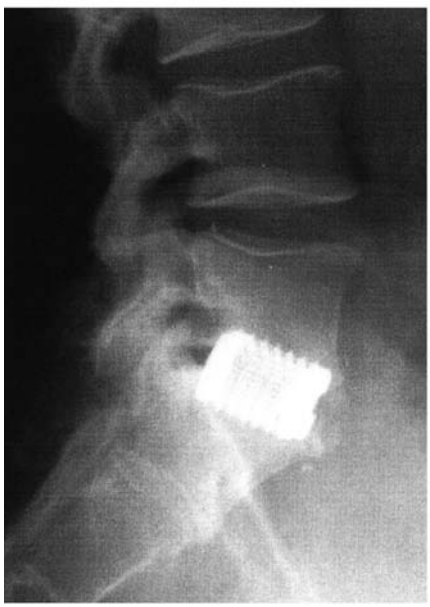

C

Figure 3 (A) Lateral radiograph shows disc space collapse at the L5–S1 interspace. (B) Anteroposterior and (C) lateral radiographs after surgery show the cylindrical titanium cages centrally placed in the L5–S1 disc space. Normal disc space height and lordosis have been restored. The implants have been reamed 3 mm into each vertebral end plate. The self-tapping threads of the implant form a secure interface with the host bone of the adjacent vertebra.

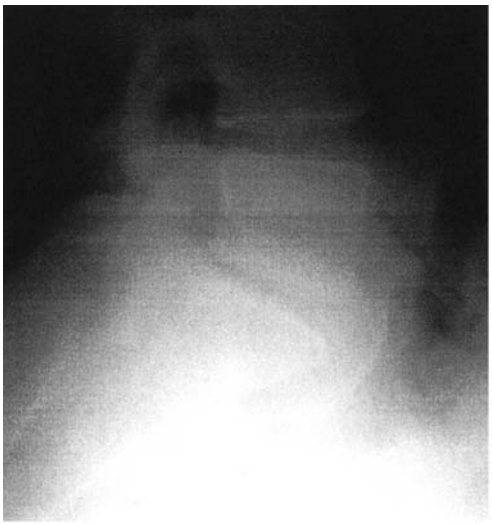

A

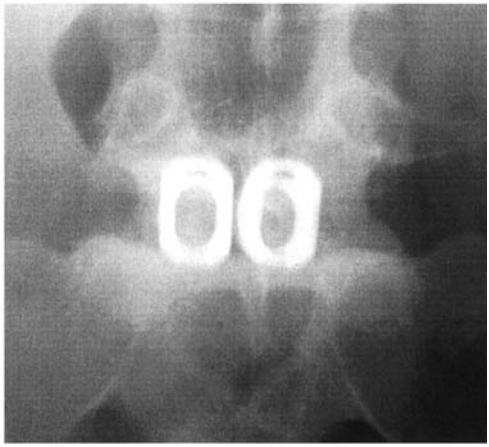

B

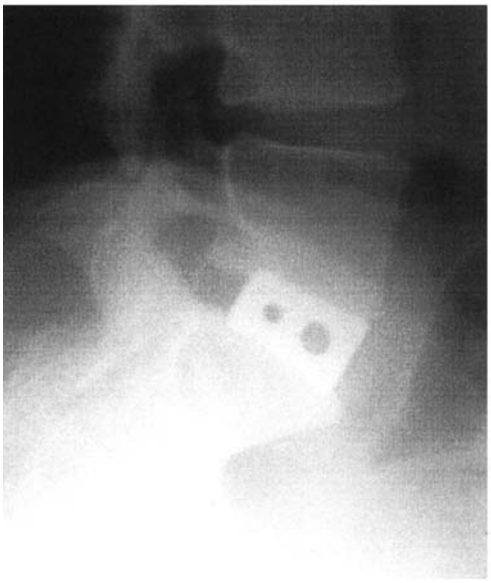

C

Figure 4 (A) Lateral radiograph shows significant L5–S1 disc space narrowing and loss of segmental lordosis. (B) Anteroposterior and (C) lateral radiographs after surgery show restoration of normal disc space height and segmental lordosis. The lordotic implant rests higher on vertebral end plates. The reamer opens on a 1.5-mm channel in each end plate. The lordotic shape of the implant also helps to maintain segmental lordosis across the disc space.

clinical studies [5,6,20]; however, each study utilized the same patient-selection criteria and adhered to comparable follow-up protocols. In addition, all procedures utilized autogenous iliac crest bone graft. Therefore, patients who were treated with impacted femoral ring allografts, threaded cortical allograft dowels, and cylindrical metal cages, as well as tapered titanium cages, could be compared directly. The second purpose of the study involved looking at the clinical and radiographic outcomes resulting from the implementation of rhBMP-2/ACS as a bone graft replacement when used in combination with the threaded cortical allograft dowels and tapered titanium cages.

II. STUDY DESIGN

Four sequential, prospective, multicenter, IDE clinical evaluations were conducted for the treatment of patients diagnosed with single-level degenerative disc disease from L4 to S1. Only patients with spondylolisthesis deemed grade 1 or lower were included. Discogenic pain may have been accompanied with radiculopathy. All patients had failed conservative treatment for at least 6 months before being enrolled in one of these studies.

All patients underwent a stand-alone, open anterior lumbar interbody fusion procedure. Several different interbody constructs were evaluated as part of this comparison: femoral ring allografts, threaded cortical bone dowels (MD-II™, Regenerative Technologies, Inc.), threaded cylindrical titanium cages (INTER FIX™ Threaded Fusion Device, Medtronic Sofamor Danek), and threaded tapered titanium cages (LT-CAGE™ Lumbar Tapered Fusion Device, Medtronic Sofamor Danek). In all procedures, autogenous iliac crest bone graft was used for all types of interbody constructs.

A total of 405 patients were treated with a stand-alone ALIF procedure and followed for 2 years in these prospective clinical studies. A total of 62 patients underwent an ALIF procedure using an impacted femoral ring allograft. A group of 207 patients received cylindrical threaded interbody constructs (22 allograft dowels and 185 metal constructs). Another 136 patients were treated by an ALIF procedure using a tapered metal interbody construct.

The combination of rhBMP-2/ACS (INFUSE™ Bone Graft, Medtronic Sofamor Danek) with either threaded cortical allograft dowels or tapered titanium cages was evaluated radiographically and clinically for 24 months following a stand-alone ALIF procedure. Twenty-four patients were randomized as part of a pilot clinical evaluation approved by the U.S. Food and Drug Administration (FDA) to receive rhBMP-2/ACS with threaded cortical bone dowels [6]. In a large pivotal FDA-approved clinical study, 143 patients received the rhBMP-2/ACS with tapered titanium interbody cages [5]. In both cases the rhBMP-2 was applied to the ACS at a concentration of 1.5 mg/mL. No autogenous graft was used. Instead, the rhBMP-2/ACS was used in 1:1 volume replacement for autogenous bone and placed within the interbody device. All other aspects of the surgical procedure and the subsequent clinical follow-up remained unchanged.

A. Surgical Procedure

All interbody implants were placed through an open surgical approach at either the L4–L5 or L5–S1 level. All implants were used as stand-alone devices without any additional anterior fixation. None of the patients received any supplemental posterior fixation. For each device, an incision was made in the annulus fibrosus and a complete discectomy was carried out. The vertebral end plates were similarly prepared in all patients. The cartilaginous portions of the end plates were removed, and the bony end plates were preserved.

The femoral ring allografts were sized and intraoperatively fashioned to match the disc space. The grafts were centrally packed with autogenous bone graft and impacted into the disc space. All grafts were recessed within the cortical margins of the disc space.

The same surgical instrumentation was used to position the threaded cortical bone dowels and the cylindrical metal cages. In preparation for implant placement, parallel reaming of the end plates was performed. The goal of parallel reaming was to prepare a 3 mm channel in the adjacent vertebral end plates and precisely expose cancellous bone of the vertebral bodies. Using the suggested templating techniques [10], the cages were recessed within each bony end plate at a depth of 3 mm. The same surgical instrumentation was used for the preparation of the disc space prior to placing these threaded cylindrical interbody devices; tapping was required before seating the threaded cortical bone dowels. This step could be eliminated with the use of cylindrical metal cages because they were designed with self-tapping threads. The surgical technique for the tapered metal cage differed in the distraction and reaming steps. When implanting a tapered cage, the vertebrae were distracted in parallel and reamed in parallel to symmetrically prepare the end plates. The reaming was less aggressive, resulting in tapered cages that were embedded 1 mm into the adjacent vertebral bodies. The tapered cages were better supported mechanically compared with the cylindrical constructs.

B. Clinical and Radiographic Assessment

Postoperatively, patients were clinically evaluated at 3,6,12, and 24 months. Functionality was determined using the Oswestry Disability Index questionnaire [21]. Two radiologists conducted radiographic evaluation independently at 6, 12, and 24 months [5,6,22]. Two different protocols were used during the course of these studies [20]. Two patient groups—receiving impacted femoral ring allograft spacers and cylindrical metal cages—were assessed using only plain radiographs. Flexion/extension films were assessed to determine if detectable motion existed, as defined by more than 3° angulation, more than 5° rotation, or radiolucent areas appearing on more than 50% of the implant interface. These patients were graded as a failure.

Two patient groups—receiving threaded cortical bone dowels and tapered metal cages—were also assessed using thin-slice computed tomography (CT) scans as part the study protocols. In addition to the criteria outlined above, these patients had to exhibit bridging bone in the intervertebral disc space to be considered radiographically fused. Furthermore, in accordance with the study protocols, patients who had undergone a second surgical intervention for back pain or suspected pseudarthrosis were deemed a fusion failure regardless of the radiographic assessment outlined above. This combination of radiographic and clinical criteria yielded a more critical assessment of fusion than typically used [22].

III. RESULTS

A. Patient Enrollment and Demographics

The percentage follow-up at 24 months and the demographics for each investigative group are shown in Table 1. Patient demographics demonstrate comparable patient populations for the patients who underwent ALIF utilizing the different interbody constructs with iliac crest bone grafting. All patients in these groups underwent an iliac crest harvesting procedure. Patient demographics are comparable across all patient groups and are representative of many practices

Table 1 Demographics for Patients Who Have Undergone an Iliac Crest Bone Graft Harvesting Procedure

	Femoral ring	Threaded cortical bone dowel	Cylindrical cage	Tapered cage
Follow-up at 24 months (%)	100	94	88	91
Age of patient (yr)	41.2	45.6	41.1	42.3
Weight of patient (lb)	172.8	175.9	172.4	181.1
Males (%)	53.2	45.5	45.1	50.0
Working (%)	37.1	40.9	40.7	36.8
Workers' compensation (%)	35.5	31.8	34.1	34.6
Litigation (%)	12.9	18.2	9.4	16.2
Tobacco use (%)	32.3	27.3	26.8	36.0
Previous back surgery (%)	43.5	31.8	39.6	40.4

with patients reporting tobacco use, workers' compensation, and spinal litigation. The percentage of follow-up at 24 months was high for each patient group as well, with the lowest being 88%.

The same data for the patient populations that were enrolled and followed in the rhBMP-2/ACS studies are provided in Table 2. Patient demographics demonstrate comparable populations for the patients that underwent a stand-alone ALIF procedure utilizing rhBMP-2/ACS as a bone graft replacement for autogenous iliac crest harvesting.

B. Clinical and Radiographic Outcomes Utilizing Autograft

The average improvements in Oswestry Disability Index scores relative to the patient's score preoperatively were calculated during each time period (Fig. 5). A notable increasing trend in clinical improvement was observed in all groups. All groups maintained the improvement in Oswestry Disability Index scores throughout the 24-month follow-up except for the threaded cortical bone dowel patients, in whom the improvement dropped slightly at 24 months. The use

Table 2 Demographics for Patients Who Have Undergone rhBMP-2/ACS Implantation as a Bone Graft Replacement

	TCBD + rhBMP-2/ACS	Tapered cage + rhBMP-2/ACS
Follow-up at 24 months (%)	100.0	92.5
Age of patient (yr)	41.5	43.3
Weight of patient (lb)	172.7	179.1
Males (%)	33.3	54.5
Working (%)	45.8	47.6
Workers' compensation (%)	20.8	32.9
Litigation (%)	16.7	12.6
Tobacco use (%)	33.3	32.9
Previous back surgery (%)	45.8	37.8

rhBMP-2/ACS, recombinant human bone morphogenetic protein-2/absorbable collagen sponge; TCBD, threaded cortical bone dowel.

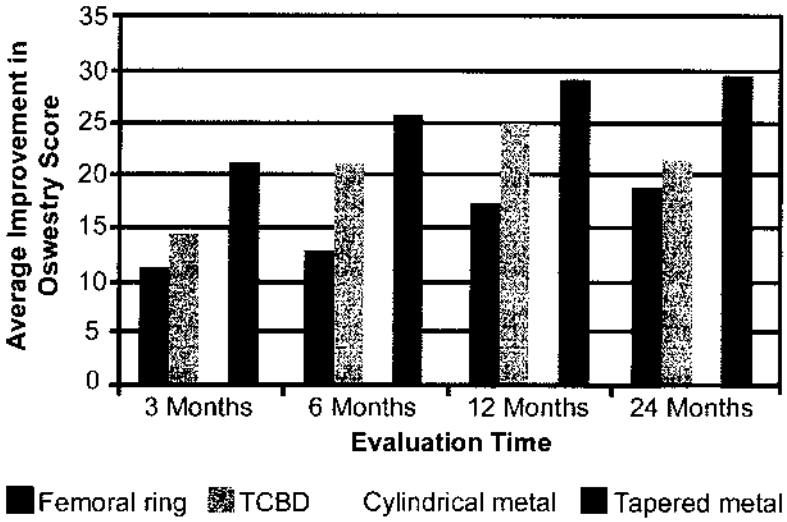

Figure 5 Average improvement in Oswestry Disability Index scores compared with the preoperative score as a baseline for each patient group. The tapered metal interbody cage device is shown to provide greater improvement, which is maintained through 24 months. TCBD = threaded cortical bone dowel.

of impacted femoral ring allografts as an interbody construct resulted in the least improvement among the four constructs [20].

The use of the tapered titanium cage in a stand-alone ALIF procedure generated and maintained the highest Oswestry Disability Index score improvement at all time points, ranging from an average improvement of 20.8 (at 3 months) to 29.5 (at 24 months). Furthermore, improvement in Oswestry Disability Index scores at 24 months averaged 46% compared with the preoperative assessment for the patients within this group [5,6]. The patients who received cylindrical constructs did not perform as well clinically as the patients who received tapered cages [5,6,20]. Although these patients exhibited steady improvement, their improvement in Oswestry Disability Index scores, when either the threaded allograft bone dowels or metal constructs were used, lagged at every time point relative to patients treated with the tapered cage. The tapered cage generated a 27% increase in improvement over the next best scoring option at 24 months.

Within each patient group, the clinical outcomes appeared to mirror the radiographic assessment results (Fig. 6). The impacted femoral ring allograft constructs exhibited the lowest fusion rates consistently at all time points [20]. The threaded cortical bone dowels performed better initially; however, the fusion rate was not maintained at 24 months. The titanium cages appeared to provide a more consistent outcome at all three time points with fusion rates approaching or surpassing 90%. Recalling that the radiographic assessment protocols differed for these two designs, the tapered titanium cage was evaluated using stricter criteria for success as compared with the cylindrical titanium cage. Thin-cut CT scans with reconstructions were not used in the fusion assessment of the cylindrical titanium cages.

C. Clinical and Radiographic Outcomes Utilizing rhBMP-2/ACS

The preoperative and postoperative average Oswestry Disability Index scores for the patients undergoing stand-alone ALIF utilizing threaded cortical bone dowels in conjunction with autoge-

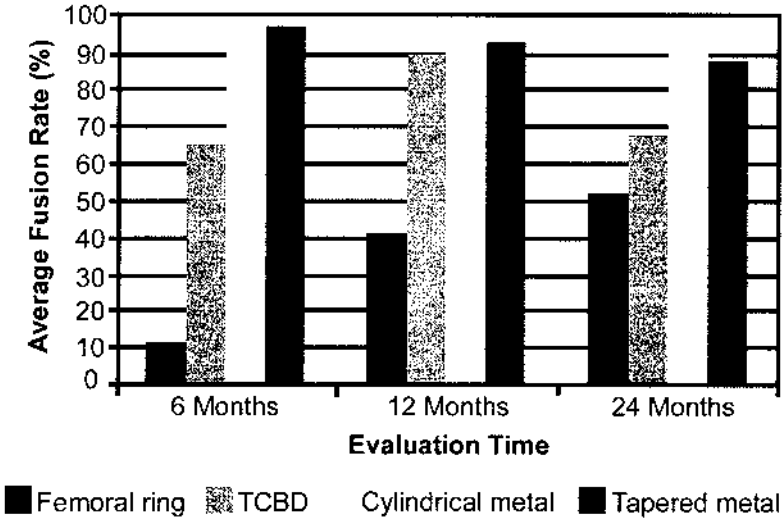

Figure 6 The rate of fusion success is provided for each of the study groups when autogenous iliac crest bone graft is used. TCBD = threaded cortical bone dowel.

nous iliac crest bone graft and rhBMP-2/ACS are shown in Figure 7. The patients receiving rhBMP-2/ACS as a bone graft replacement exhibited significantly improved scores compared with the autogenous bone graft group [5,6]. Furthermore, this appears to correlate well with the rate of fusion success shown in Figure 8.

The improvement noted with the use of rhBMP-2/ACS as a bone graft replacement was not seen when comparing the patients who underwent stand-alone ALIF procedures with a tapered metal cage (Figure 9). These patients exhibited statistically equivalent clinical outcomes at all follow-up time points compared with the autogenous iliac crest bone graft patients. In a similar fashion, the rates of fusion success were also equivalent between the two patient groups (Figure 10).

IV. DISCUSSION

For the first time, the clinical and radiographic results using four different interbody constructs in a single-level, stand-alone ALIF procedure have been directly compared using prospective multicenter IDE studies. Because the independent studies have similar patient inclusion criteria, demographics, and protocols, the results can be compared to examine the effect that interbody construct design can have on clinical outcomes. These results support the use of stand-alone interbody constructs filled with autogenous iliac crest bone graft in an ALIF procedure and have demonstrated continuous improvement through the 24-month evaluation period.

Improvement in the clinical outcomes following stand-alone ALIF procedures was monitored through the use of the Oswestry Disability Index questionnaire. The tapered interbody cage is associated with the best average improvement that peaked at 29.5 points after 24 months. Patients receiving the tapered titanium cages appear to be recovering consistently and more quickly compared with the patients in the other interbody fusion device groups. Even the patients receiving the cylindrical metal and allograft cages lag behind by as much as 10 points during their follow-up, despite their favorable radiographic results using plain radiographs [5,6,20].

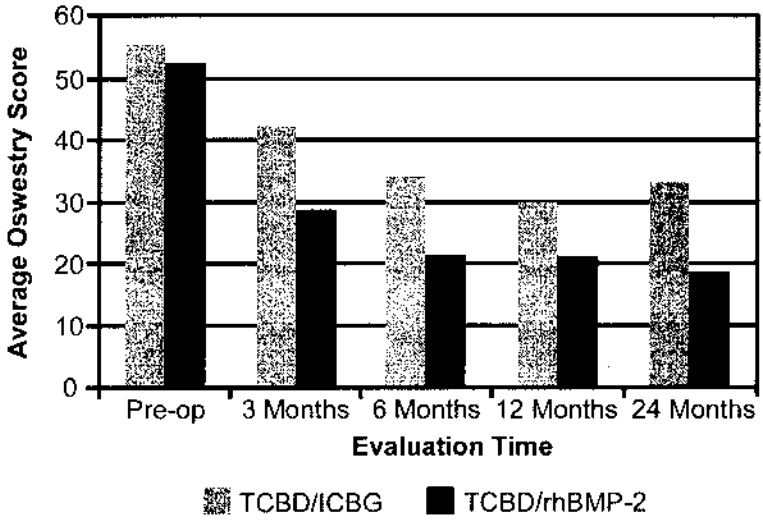

Figure 7 Patients receiving recombinant human bone morphogenetic protein-2/absorbable collagen sponge (rhBMP-2/ACS) as a bone graft replacement report improved average Oswestry Disability Index scores after surgery compared with autogenous iliac crest bone graft (ICBG) when used in conjunction with stand-alone anterior lumbar interbody fusion surgery using threaded cortical bone dowels (TCBD). (Decreasing scores indicate improvement.)

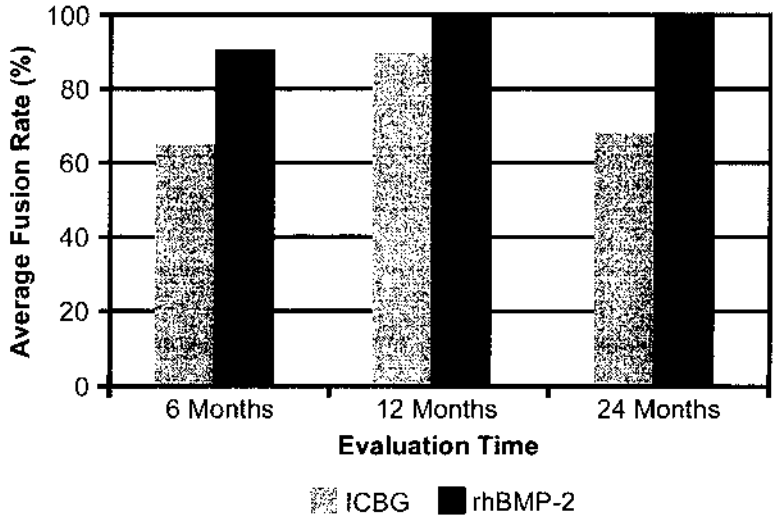

Figure 8 Fusion rates for threaded cortical bone dowels (TCBD). The use of recombinant human bone morphogenetic protein-2/absorbable collagen sponge (rhBMP-2/ACS) maintains a high fusion rate at longer follow-up times for patients receiving TCBD compared with those undergoing autogenous iliac crest bone grafting (ICBG) and threaded cortical bone dowels.

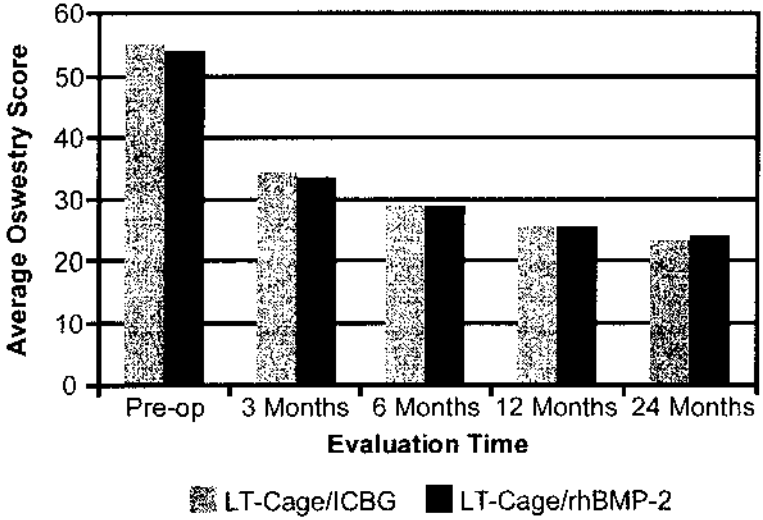

Figure 9 Patients undergoing stand-alone anterior lumbar interbody fusion surgery with a tapered metal interbody construct (LT-CAGE™) exhibited equivalent clinical outcomes regardless of whether recombinant human bone morphogenetic protein-2/absorbable collagen sponge (rhBMP-2/ACS) or autogenous iliac crest bone graft (ICBG) was used. (Decreasing scores indicate improvement.)

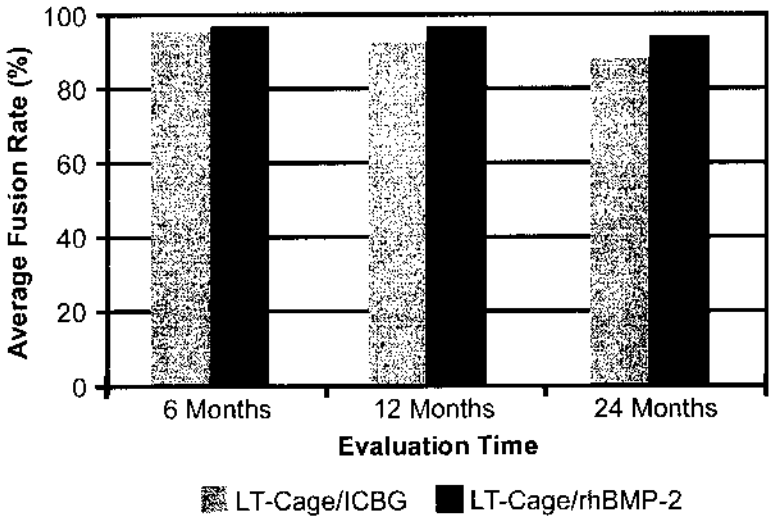

Figure 10 Patients undergoing stand-alone anterior lumbar interbody fusion procedures with tapered metal interbody constructs exhibit equivalent fusion rates at all follow-up times. Patients receiving recombinant human bone morphogenetic protein-2/absorbable collagen sponge (rhBMP-2/ACS) as an autograft replacement material do exhibit a slight trend toward improved fusion success rates compared with patients who received iliac crest bone graft (ICBG).

Radiographic interpretation of fusion, especially when titanium interbody cages are used, can be very difficult. The scatter from the metal results in producing a 3 mm zone of radiographic artifact surrounding the cage. Furthermore, it has been estimated that when loss of motion is the sole criterion, fusion success rates are approximately 20% higher than when bridging trabecular bone across the graftvertebrae interface is required [23,24]. For this reason, observation of the assessment protocol should be made before comparing published results.

Previous clinical reports convey comparable fusion success rates for the threaded cylindrical titanium cages and femoral ring allografts using the same radiographic criteria. In a 2-year clinical study, Kuslich and colleagues [7] reported a 93.0% fusion rate among the 591 patients undergoing one- and two-level ALIF procedures utilizing a cylindrical metallic fusion cage (BAK cage). These results compare well with 93.4% fusion rates reported here for cylindrical cages at the same follow-up time period. However, the protocols in the Kuslich study did not include the presence of bridging trabecular bone as a criterion for successful fusion [7]. Fusion was judged from plain and flexion/extension radiographs alone.

Likewise, similar results have been reported with femoral ring constructs in a smaller study. With an average follow-up of 33 months, the fusion rate among 16 patients (6 with two-level fusions) was only 54% [20]. For single-level procedures, the rate was slightly higher at 60%. This is comparable to the 51.9% fusion success rate at 24 months reported for single-level procedures in this study.

Differences in fusion assessment protocols are an issue for this study as well, because the fusion assessment following ALIF with cylindrical titanium cages was conducted using plain radiographs alone. Using the criteria for immobility alone may have contributed to the high fusion rates reported for the cylindrical cage. Both the cylindrical and tapered titanium cages were associated with high fusion rates; however, the patients who received the tapered cage exhibited higher improvements in Oswestry Disability Index scores at all time points [5]. This suggests that the fusion rates for the cylindrical titanium cage may have been slightly inflated, as suggested above.

The best method to assess the formation of bridging trabecular bone through an interbody fusion device is thin-slice CT scans, particularly with sagittal reconstructions [19,22]. The progressive development of the fusion mass through the interbody device can be directly assessed and followed in this manner. The use of CT scans has been validated in a rhesus monkey model by comparing CT assessment with histology from the same animal to confirm the absence of a soft tissue interface with the implant [25]. Even when using these more critical standards with the aid of sagittal reconstructions, and reporting second surgeries as failures, the tapered titanium cage provided excellent fusion rates at all time points. At 24 months, the use of tapered cages filled with autogenous iliac crest bone graft yielded an 88.7% fusion rate.

The favorable radiographic and clinical outcomes associated with the tapered interbody cage are likely attributable to its improved design and change in surgical technique compared with the other cylindrical constructs. The technique allows for minimal reaming, which helps to preserve the denser, stronger bone at the end plate and to position the cage with symmetrical engagement of the adjacent vertebrae. Preservation of the most dense bone in the vertebral body provides improved mechanical hold and improves initial stability. Furthermore, the cage is designed with self-tapping threads that improve the insertion torque.

However, despite the favorable result using tapered interbody cages, it has been previously reported that 32% of these same patients reported donor site pain associated with the iliac crest autograft harvest site at 24 months (Fig. 11) [5]. In this same report, it was documented that this morbidity could be avoided by replacing iliac crest autograft with INFUSE Bone Graft (Medtronic Sofamor Danek) while still preserving the excellent radiographic and clinical results documented here. The use of INFUSE Bone Graft resulted in statistically equivalent radiographic

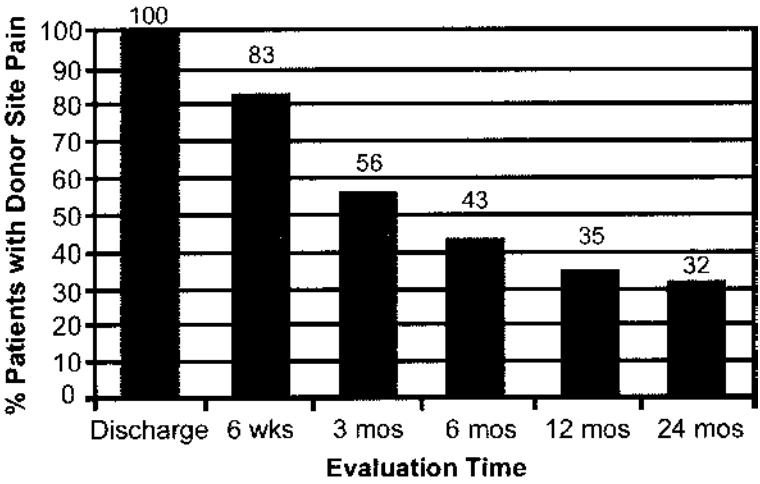

Figure 11 The incidence of donor site pain in patients undergoing single-level stand-alone anterior lumbar interbody fusion procedures with a tapered interbody cage.

and clinical outcomes in a large, prospective, randomized clinical study following 279 patients for 2 years after an open ALIF procedure for degenerative disc disease.

In two separate clinical studies, it was noted that using rhBMP-2/ACS as a bone graft replacement for autogenous iliac crest bone graft had different effects on the clinical outcomes depending on the interbody construct [5,6]. When threaded cortical bone dowels were used, the rhBMP-2/ACS provided a significant improvement in clinical outcomes as determined by Oswestry Disability Index scores compared with patients treated with iliac crest bone graft. However, when the tapered metal cage interbody construct was used, the outcomes were statistically equivalent [5].

One possible explanation for this observation may be related to poorer outcomes of threaded cortical bone dowels compared with the tapered metal interbody constructs when autograft is used. The tapered metal cage and the improved surgical technique might contribute to this difference. The rhBMP-2/ACS may provide a better outcome when threaded cortical bone dowels are used because there is more room for improvement over the standard of care, including the utilization of iliac crest bone graft in that procedure.

When a tapered metal interbody construct packed with autogenous bone graft was used, the average Oswestry Disability Index score at 24 months was 23.8. Previously, the average Oswestry Disability Index score for the normal population was reported as 10.2, with a standard deviation ranging from 2.2 to 12 based on six independent studies involving 461 patients [21]. With this in mind, it is conceivable that patients who have undergone a surgical procedure on the spine may not be able to improve significantly beyond that reported here for the tapered interbody device. The use of rhBMP-2/ACS in this instance does provide an increasing trend in fusion success, although not statistically significant, and does eliminate the need for the autograft harvesting procedure.

V. CONCLUSIONS

With the evolution of interbody fusion devices, stand-alone ALIF procedures are clinically viable surgical options to achieve high fusion rates and excellent clinical outcomes when iliac crest

bone graft is used. The tapered interbody metal cage is shown in this report to be an effective treatment for patients suffering from single-level degenerative lumbar disc disease with improved radiographic and clinical outcomes compared with early-generation fusion devices. The tapered design likely contributes to its high improvement in Oswestry Disability Index scores even early in the postoperative period because of improved initial stability. Furthermore, high fusion rates were observed at all time points even when using the strictest criteria for fusion assessment in which CT reconstructions were used to verify the presence of bridging trabecular bone. However, these excellent results coincide with a high incidence (32%) of donor site pain at 24 months follow-up. The utilization of rhBMP-2/ACS as a bone graft replacement provides a means of maintaining excellent clinical results while eliminating the need for the autograft harvesting procedure.

REFERENCES

1. Blumenthal SL, Baker J, Dossett A, Selby DK. The role of anterior lumbar fusion for internal disc disruption. Spine 1988; 13(5):566–569.
2. Chow SP, Leong JCY, Ma A, Yau AC. Anterior spinal fusion for deranged lumbar intervertebral disc. Spine 1980; 5(5):452–458.
3. Leong JCY, Chun SY, Grange WJ, Fang D. Long-term results of lumbar intervertebral disc prolapse. Spine 1983; 8(7):793–799.
4. Loguidice VA, Johnson RG, Guyer RD, Stith WJ, Ohnmeiss DD, Hochschuler SH, Rashbaum RF. Anterior lumbar interbody fusion. Spine 1988; 13(3):366–369.
5. Burkus JK, Gornet MF, Dickman C, Zdeblick TA. Anterior interbody fusion using rhBMP-2 with tapered interbody cages. J. Spinal Disord Tech 2002; 15(5):337–349.
6. Burkus JK, Transfeldt E, Kitchel SH, Watkins R, Balderston R. Clinical and radiographic outcomes of anterior lumbar interbody fusion using recombinant human bone morphogenetic protein-2. Spine 2002; 27(21):2396–2408.
7. Kuslich SD, Ulstrom CL, Griffith SL, Ahern JW, Dowdle JD. The Bagby and Kuslich method of lumbar interbody fusion: history, techniques, and 2-year follow-up results of a United States prospective, multicenter trial. Spine 1998; 23(11):1267–1278.
8. Newman MH, Grinstead GL. Anterior lumbar interbody fusion for internal disc disruption. Spine 1992; 17(7):831–833.
9. Burkus JK, Dorchak JD, Estes BT. Subsidence evaluation of reduced lateral profile threaded constructs. 7th International Meeting on Advanced Spine Techniques, Barcelona, Spain, July 5–8, 2000.
10. Boyd LM, Estes BT, Liu M. Biomechanics of lumbar interbody constructs: effect of design and materials. In: J.L. Husson, J.C. LeHuec, eds. Chirurgie Endoscopique et Mini-invasive du Rachis. Montpelier. France: Sauramps Médical, 1999:181–192.
11. Dennis S, Watkins R, Landaker S, Dillin W, Springer D. Comparison of disc space heights after anterior lumbar interbody fusion. Spine 1989; 14(8):876–878.
12. Kumar A, Kozak JA, Doherty BJ, Dickson JH. Interspace distraction and graft subsidence after anterior lumbar fusion with femoral strut allograft. Spine 1993; 18(16):2393–2400.
13. Watkins R. Anterior lumbar interbody fusion surgical complications. Clin. Orthop 1992; 284:47–53.
14. Frymoyer JW, Hanley E, Howe J, Kuhlmann D, Matteri R. Disc excision and spine fusion in the management of lumbar disc disease. A minimum ten-year follow-up. Spine 1978; 3(1):1–6.
15. Hacker RJ. A randomized prospective study of an anterior cervical interbody fusion device with a minimum of 2 years of follow-up results. J. Neurosurg 2000; 93(2 suppl):222–226.
16. Mirovsky Y, Neuwirth MG. Comparison between the outer table and intracortical methods of obtaining autogenous bone graft from the iliac crest. Spine 2000; 25(13):1722–1725.
17. Boden SD, Zdeblick TA, Sandhu HS, Heim SE. The use of rhBMP-2 in interbody fusion cages. Definitive evidence of osteoinduction in humans: a preliminary report. Spine 2000; 25(3):376–381.

18. Hecht BP, Fischgrund JS, Herkowitz HN, Penman L, Toth JM, Shirkhoda A. The use of recombinant human bone morphogenetic protein 2 (rhBMP-2) to promote spinal fusion in a nonhuman primate anterior interbody fusion model. Spine 1999; 24(7):629–636.
19. Sandhu HS, Toth JM, Diwan AD, Seim HB3rd, Kanim LE, Kabo JM, Turner AS. Histological evaluation of the efficacy of rhBMP-2 compared with autograft bone in sheep spinal anterior interbody fusion. Spine 2002; 27(6):567–575.
20. Timon S, Patel S, Dawson EG, Wang JC. Anterior lumbar discectomy and fusion using femoral ring allografts. 16th Annual Meeting of North American Spine Surgeons, Seattle, WA, October 31 – November 3, 2001.
21. Fairbank JCT, Pynsent PB. The Oswestry Disability Index. Spine 2000; 25(22):2940–2953.
22. Burkus JK, Foley K, Haid R, LeHuec JC. Surgical Interbody Research Group—radiographic assessment of interbody fusion devices: fusion criteria for anterior lumbar interbody surgery. Neurosurg. Focus 2001; 10(4):1–9.
23. McAfee PC. Interbody fusion cages in reconstructive operations on the spine. J. Bone Joint Surg. Am 1999; 81-A(6):859–880.
24. Santos ERG, Goss DG, Morcom RK, Fraser RD. Radiologic assessment of interbody fusions with cages. 29th Annual Meeting of International Society for the Study of the Lumbar Spine, Cleveland, OH, May 14–18, 2002.
25. Boden SD, Martin GJ, Horton WC, Truss TL, Sandhu HS. Laparoscopic anterior spinal arthrodesis with rhBMP-2 in a titanium interbody threaded cage. J. Spinal. Disord 1998; 11(2):95–101.

7
Overcoming Chemical Inhibition of Spine Fusion

Brian Claytor and Steven Theiss
University of Alabama at Birmingham
Birmingham, Alabama, U.S.A.

I. INTRODUCTION

Spine fusion is a commonly performed surgical procedure done for a variety of spinal pathologies. Yet the pseudarthosis or failure rate of the procedure is significant, approaching 40% in uninstrumented posterolateral fusions [1]. Numerous reasons for fusion failure have been established, including patient- and technique-related factors. Chief among patient-related factors is chemical inhibition of spine fusion formation. The two pharmacological agents most often responsible for fusion failure are nicotine and nonsteroidal anti-inflammatory drugs (NSAIDs). Both of these agents are widely used in the general population and influence significant numbers of patients undergoing spine fusion. Clearly, then, every clinician will have patients that are affected by these two agents. Fortunately, considerable work has been done to help the clinician understand both the clinical issues and basic pathophysiology affecting patients who utilize these agents. This chapter will outline the existing knowledge and developing strategies for improving the fusion outcome for patients affected by these potent chemical inhibitors.

II. NICOTINE

Nicotine is the major particulate component of tobacco smoke and is most likely the primary cause of addiction associated with smoking [2]. Nicotine acts primarily through activation of the sympathetic nervous system. It acts directly on peripheral vessels to cause increased arterial vasoconstriction, venoconstriction, and elevation of total vascular resistance [3]. Thus, it increases heart rate and blood pressure. Its primary systemic action appears to be through the association with specific nicotinic receptors that are found in a variety of species and tissues. These receptors have been found in neural tissue, muscle, and connective tissue [2]. Nicotine has been implicated in a variety of skeletal disorders. For instance, nicotine has been cited as a risk factor for postmenopausal osteoporosis, with significant tobacco use resulting in lower bone mineral density specifically in the spine [2,4]. Fracture healing and bone healing during tibial lengthening also are adversely affected by nicotine [5,6]. Thus, in general, nicotine has been noted to negatively affect bone metabolism.

Given this information, it is not surprising that much research has been devoted to the effects of cigarette smoking and nicotine on the healing of spinal fusions. All clinical studies

to date describe the affects of smoking in general and are inherently unable to implicate nicotine alone as the mediator of these effects. Yet empiric clinical observations indicate that smoking has a myriad of effects on spine fusion. Primary among these affects is a significantly higher rate of pseudarthrosis. In fact, the incidence of pseudarthrosis has been found to be as much as four times higher in smokers compared with nonsmokers [1]. This applies to virtually any type of spine fusion, from posterolateral lumbar fusions to anterior interbody fusions. This has been shown repeatedly in uncontrolled, nonrandomized clinical studies [7,8]. The effect on interbody fusions, though, does not seem to be as pronounced [7]. Despite these undisputed findings, relatively little is known about the specific clinical scenarios that affect outcomes the most. Yet, some clinical work has begun to offer some insight. For instance, investigators have attempted to differentiate between the effects of preoperative and postoperative smoking. Andersen et al. found preoperative smoking status to be weakly predictive of fusion failure [8]. Glassman et al. found that increased fusion rate could only be achieved by postoperative smoking cessation and not by stopping preoperatively [9]. Also, the effect of smoking may be dose dependent. Brown et al. indicated that only those patients who smoked 10 or more cigarettes daily had a statistically significant higher rate of nonunion [10]. Andersen et al. showed that smoking fewer than 10 cigarettes a day preoperatively was not as significantly associated with the development of nonunion compared with consumption of more that 10 cigarettes daily [8]. Also, irrespective of fusion success, a higher rate of cigarette consumption correlates with a worse outcome after lumbar pseudarthrosis repair [11].

Clinical research, therefore, has shown that smoking adversely affects lumbar fusion. As such, much basic science research has been dedicated to elucidating the mechanism responsible for the effect of smoking and specifically nicotine. First, a well-accepted rabbit model of lumbar posterolateral fusion has verified nicotine's impact alone on spine fusion. Silcox et al. [12] demonstrated a 100% pseudarthrosis rate in nicotine-exposed rabbits at 5 weeks as compared to a 44% pseudarthrosis rate in the control group not exposed to nicotine. In addition, the biomechanical strength of the fusion masses in the control group was superior to that of the nicotine group. Nicotine exposure was begun at the time of the fusion. Wing et al. [13] attempted to clarify the effects of nicotine in the rabbit model by changing the schedule of nicotine administration. Nicotine exposure was begun 2 months prior to surgery in two groups of animals, but discontinued in one group one week prior to fusion. The other group had nicotine administered continuously until euthanasia. The continuous nicotine group again had a 0% fusion rate, but the group in which nicotine administration was stopped had a fusion rate similar to that of the control group. This suggests, as do clinical studies, that the effects of nicotine can be reversed by abstinence. Whether cessation needs to begin preoperatively or at the time of fusion is still unclear.

The exact mechanism by which nicotine inhibits spinal fusion continues to be debated. The effects on the microvasculature and neovascularization likely are partly to blame. Work by numerous investigators has shown that exposure of animals to cigarette smoke reduces the blood flow to the vertebral column and disc space [7]. Daftari et al. [14] noted that nicotine administration delayed revascularization of bone grafts placed at an extraskeletal site, leading to an increased incidence of graft necrosis. Revascularization of bone graft is known to be an essential component in eventual successful fusion, and this is one way nicotine increases the pseudarthrosis rate. This effect on revascularization can be attributed to direct vasoconstriction by nicotine [14]. This, however, is not the only way in which nicotine affects the vascularity of developing bone. Recent work has also indicated that nicotine indirectly affects neovascularization by suppressing the release of growth factors responsible for angiogenesis. Particularly, gene expression of vascular endothelial growth factor (VEGF) and basic fibroblast growth factor (bFGF), two

growth factors responsible for angiogenesis, was inhibited by exposure to nicotine in the rabbit spine fusion model [1].

In addition to its effects on the vasculature, nicotine also has been shown to have a profound cellular effect on osteoblasts. Nicotine has been shown to suppress proliferation of osteoblasts harvested from an osteosarcoma cell line [15]. Several parameters of osteoblast function are affected by nicotine, including DNA synthesis, collagen synthesis, and oxygen consumption [7]. The exact mechanism by which this occurs is unknown. Recently, though, investigators have identified evidence of a nicotine receptor in osteoblasts. Specifically, Walker et al. [2], using reverse transcriptase-polymerase chain reaction(RT-PCR), demonstrated the presence of a subunit of the nicotinic receptor in human bone cells. Additionally, nicotine's effects on osteoblasts could be blocked by a nicotinic receptor antagonist. While this is the first conclusive evidence that nicotine receptors are present on ostoeblasts themselves, this was previously suggested by Romano et al., who found immunohistochemical evidence of these receptors in embryonic connective tissue [16].

It probably is not realistic though to think that a single mechanism is responsible for nicotine's inhibition of spine fusion. Even at the molecular level nicotine has a multifactorial effect on bone healing. Theiss et al. [1] demonstrated this in vivo in the rabbit model. Previous work with this model showed that there is an orderly expression of growth factors after spine fusion, which ultimately results in bone formation. The growth factors in general are first expressed adjacent to the transverse processes and then in the portion of the fusion between the transverse processes, termed the central zone. Administration of systemic nicotine, beginning at the time of spine fusion, did not alter the previously identified pattern of growth factor expression. But it did result in decreased expression of multiple growth factors, including bone morphogenetic protein (BMP) 2, 4, 6, and the angiogenesis factors bFGF and VEGF. This effect was most evident in the inner zone. The effect was seen as early as day 2 postfusion. The effect of nicotine on BMP expression in the central zone of the developing fusion is shown in Figure 1–3.

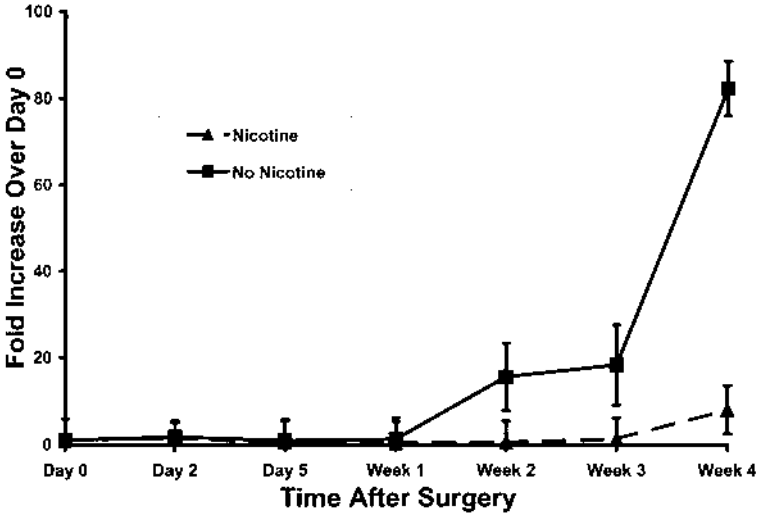

Figure 1 Gene expression of BMP 2 in the central zone, between the transverse processes, during spine fusion is inhibited by the presence of systemic nicotine, particularly at week 4. (From Ref. 1.)

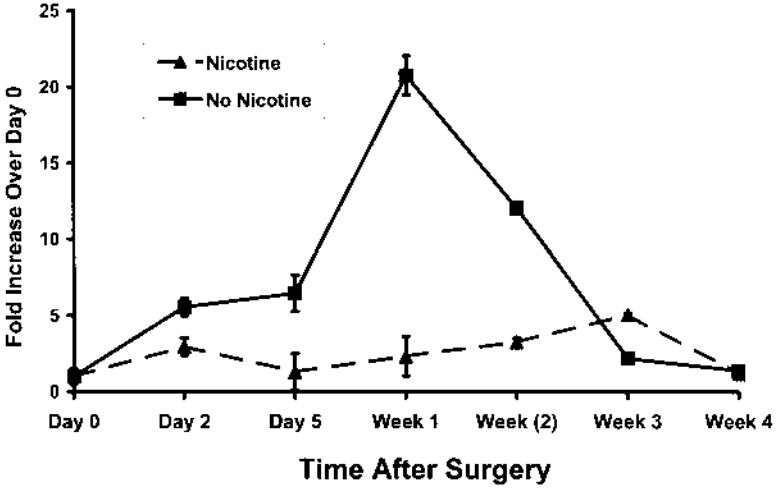

Figure 2 Nicotine inhibits the expression of BMP 4. (From Ref. 1.)

III. OVERCOMING NICOTINE INHIBITION

The evidence that nicotine and smoking inhibits spine fusion is conclusive. Thus, significant work has been done to develop strategies to overcome this inhibition. One solution is smoking cessation, as has been discussed above. It seems though that cessation postoperatively for at least 6 months is required for fusion rates to approach those of patients who abstain from smoking [8,9]. Cessation prior to surgery and amount smoked prior to surgery were not found by Glassman et al. to improve fusion rates, unless accompanied by postoperative cessation [9]. Wing et al.

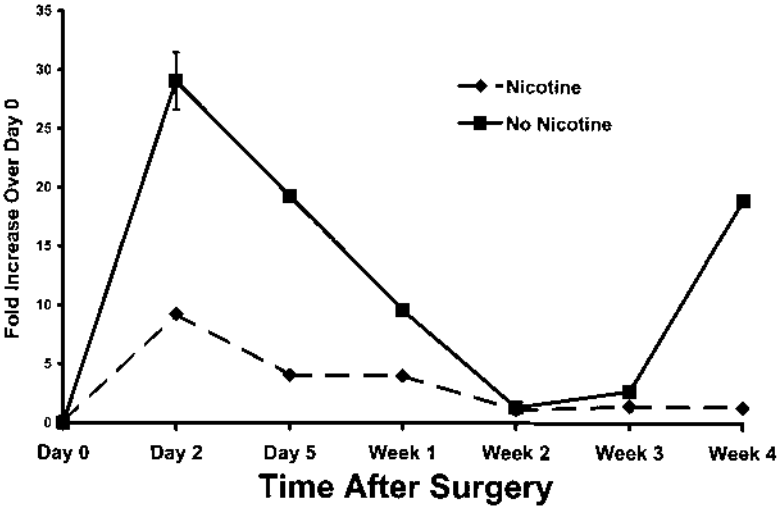

Figure 3 Expression of BMP 6 is significantly reduced in animals exposed to systemic nicotine. This effect is seen as early as day 2 postfusion. (From Ref. 1.)

showed that rabbits that had nicotine infusions stopped one week prior to fusion had a higher fusion rate, but he did not separately study postop nicotine cessation alone [13]. It is the patient population that cannot abstain from smoking where the greatest challenge lies. Perhaps the first solution that was proposed for this population was electrical stimulation of the developing fusion mass. Since 1974, many authors have shown that the use of postoperative implanted electrical spinal stimulation has improved fusion rates after spinal arthrodesis, especially in high-risk patients [17–19]. Meril [20], investigating direct current stimulation after interbody fusions, found significantly improved fusion rates in smokers receiving stimulation (92%) compared with smokers not receiving stimulation (71%). These results indicate that postoperative electrical stimulation may increase the rate of successful arthrodesis in smokers following spinal surgery.

Undoubtedly, the most exciting technology available to overcome smoking and nicotine inhibition is biological agents. Bone morphogenetic protein, (BMP) has been extensively studied and shown to result in reliable spine fusion in both in vivo models and clinical situations [21,22]. Its efficacy, though, has mostly been studied in rather ideal fusion scenarios. BMP has been used in vivo to overcome the inhibitory effect of systemic nicotine. The first to describe this was Silcox et al. [23], who used a bovine-derived osteoinductive bone protein extract (OBP) in the rabbit model of posterolateral fusion. They compared three groups of animals exposed to systemic nicotine: one fused with autograft alone, one fused with autograft combined with OBP, and one group fused with OBP alone. They found a 100% fusion rate in the group fused with autograft and OBP compared with a 64% fusion rate in the OBP alone and 0% in the autograft alone. Clearly, the OBP was able to overcome nicotine inhibition, both when used alone and in conjunction with autograft. Patel et al. [24] verified these findings using osteoinductive protein-1(OP-1), a genetically cloned BMP-7, in lieu of autograft in the rabbit model of posterolateral fusion in the presence of systemic nicotine. They achieved a 100% fusion rate with OP-1 compared with a 25% fusion rate with autograft. The mechanism by which this occurs is unknown, but BMP does increase gene expression of a variety of growth factors during fusion formation. This increase in growth factor expression likely offsets the expression inhibition shown by Theiss et al. [1]. Clinically, multiple trials, particularly involving recombinant BMP-2, are ongoing for a variety of spine fusion applications. These pilot and pivotal studies involve a significant number of smokers. Whether an increased fusion rate of the smokers in particular will be achieved remains to be seen [22]. One growth factor application, however, has demonstrated increased fusion rate in smokers. Platelet-derived growth factor, a slurry of growth factors derived from ultraconcentrated platelets, was shown clinically to lead to solid fusion in a small numbers of smokers included in a cohort study. While this study included multiple pathologies and types of spine fusions, the smokers in this population had a 100% fusion rate at 6 months postfusion [25].

IV. NSAIDs

Nonsteroidal anti-inflammatory drugs are some of the most widely used medications today, especially in patients with orthopedic conditions. However, there has been considerable debate regarding the potential deleterious effects of these drugs on bone healing. Thus, many surgeons have stopped using them in their fracture and fusion patients. NSAIDs are often the first-line agents used for many variations of acute and chronic musculoskeletal pain. These agents exert their anti-inflammatory action primarily through inhibiting the cyclooxygenase enzyme (COX), thereby blocking the production of prostaglandins. However, much research has indicated a deleterious effect on bone metabolism. A rat study by Ro et al. [26] first demonstrated that physiological doses of indomethacin significantly decreased fracture callous formation in femur

fractures, leading to weaker healing and increased rates of nonunion. Other studies revealed that NSAID administration after hip arthroplasty significantly reduced the amount of heterotopic ossification seen. This work also demonstrated that the decrease in bone formation occurred early in the healing process, within 2 weeks [27]. Because these early studies established that NSAIDS inhibit osteogenic activity, many physicians became reluctant to use them in their patients with fractures, but they are widely used to prevent heterotopic ossification

Although the evidence indicated that NSAIDS may inhibit bone healing, it remained unclear how this would apply to spinal fusion. A retrospective clinical study of adults with isthmic spondylolisthesis showed lower fusion rates (44% vs. 37%) after posterolateral fusion in those patients who continued to take NSAIDS for more than 3 months after surgery [28]. Even brief exposure to the injectable NSAID ketorolac in the acute postoperative period can increase the pseudarthrosis rate after spine fusion. Glassman et al. [29] showed that patients who received ketorolac postoperatively during their hospital stay (60 mg loading dose, followed by 30 mg every 6–8 hours as needed) were five times more likely to develop a nonunion. The nonunion rate appeared to increase in a linear manner with increasing number of doses received up to a threshold of 9–12 doses. These retrospective clinical observations have been verified by animal studies. Using a rat model of posterior spinal fusion, Dimar et al. [30] demonstrated that postoperative use of indomethacin significantly decreased the fusion rate to 10% after 12 weeks in the study group versus 45% in the control group. This study, though, has been criticized because the dose of indomentacin used was toxic to a significant number of animals. The most convincing study to date used the rabbit model of posterolateral fusion to study this issue. It showed that the fusion mass in rabbits that received postoperative ketorolac had smaller amounts of trabecular bone, more unremodeled iliac crest graft, and more gaps within the fusion mass compared with control animals. Animals received ketorolac for 7 days postfusion [31]. Thus, it appears that NSAID usage, even during the immediate postoperative period, can significantly impair fusion healing.

Recently, the development of drugs that selectively inhibit the cyclooxygenase-2 enzyme has significantly changed the way in which NSAIDS are prescribed. These COX-2 inhibitors have been shown to have significantly fewer side effects than the nonselective NSAIDS, especially in regards to gastrointestinal bleeding. Much interest has also arisen as to the possibility of using these COX-2 inhibitors after spinal fusion. It has been shown that perioperative use of celecoxib or rofecoxib can significantly reduce pain and opioid use in patients undergoing spinal fusion. This same study also demonstrated that these medicines do not have to be discontinued preoperatively and that their use did not increase the risk of intraoperative bleeding [32]. In addition, a study by Lewis et al. [33] indicated that postoperative use of COX-2 inhibitors did not lead to an increased number of pseudarthroses. They found that the fusion rate in rats at 8 weeks after posterolateral spinal fusion was not statistically different in those rats receiving celecoxib versus the control group. They did, however, find a statistically significantly higher rate of nonunion (50%) in those rats who received indomethacin postoperatively. Although these early results with COX-2 inhibitors after spinal fusion are encouraging, there needs to be more research with human studies before stating their definite safety.

Finally, attempts at overcoming NSAID's inhibitory effects have focused mainly on osteoinductive biological agents. Martin et al. [31] again used the rabbit model to study this issue. They demonstrated that the use of recombinant human bone morphogenetic protein-2 (BMP-2) when combined with autograft could successfully overcome the deleterious effects of ketorolac on fusion healing. Animals were divided into three experimental groups. One group received a posterolateral fusion with autograft only, without the administration of systemic ketorolac. The second group was fused with autograft only, but received a constant infusion of ketorolac, while the third group received ketorolac, but the autograft was soaked in rhBMP-2. The group that

received ketorolac and rhBMP-2 achieved a 100% fusion rate. This is contrasted with a 75% fusion rate in the autograft only group without ketorolac and a 35% fusion rate in autograft only group with ketorolac [31]. Thus, not only did this study verify the inhibitory effect of ketorolac, it also demonstrated the ability of rhBMP-2 to overcome this inhibition. Again, while these studies are encouraging and such osteogenic compounds warrant continued research.

V. CONCLUSIONS

Nicotine and NSAIDs have been shown both in animal models and clinically to inhibit spine fusion. The first step in overcoming this inhibition is to understand the basic mechanisms responsible for these actions. The cellular and molecular mechanisms responsible for this inhibition are beginning to be elucidated. Strategies to overcome these effects have primarily involved the use of various osteoinductive agents. These agents have shown great promise in animal models and pivotal clinical trials. As yet, no large controlled patient study has proven their superior efficacy. Other emerging technologies, though, including gene therapy, hold great promise in treating this difficult patient population.

REFERENCES

1. Theiss SM, Boden SD, Hair G, Titus L, Morone MA, Ugbo J. The effect of nicotine on gene expression during spine fusion. Spine 2000; 25:2588–2594.
2. Walker LM, Preston MR, Magnay JL, Thomas PBM, El Haj AJ. Nicotinic regulation of c-fos and osteopontin expression in human-derived osteoblast-like cells and human trabecular bone organ culture. Bone 2001; 28:603–608.
3. Benowitz N. Clinical pharmacology of nicotine. Ann. Rev. Med 1986; 37:21–31.
4. Kwiatkowski TC, Hanley EN, Ramp WK. Cigarette smoking and its orthopedic consequences. Am. J. Orthop 1996:590–597.
5. Ueng SW, Lee MY, Li AF, Lin SS, Tai CL, Shih CH. Effect of intermittent cigarette smoke inhalation on tibial lengthening: experimental study in rabbits. J Trauma-Injury Infect. Crit. Care 1997; 42: 231–238.
6. Hollinger JO, Schmitt JM, Hwang K, Buck D. Impact of nicotine on bone healing. J. Biom. Mater. Rese 1999; 45:294–301.
7. Hadley MN, Reddy SV. Smoking and the human vertebral column: a review of the impact of cigarette use vertebral bone metabolism and spinal fusion. Neurosurgery 1997; 41:116–124.
8. Andersen T, Christensen FB, Laursen M, Hoy K, Hansen ES, Bunger C. Smoking as a predictor of negative outcome in lumbar spinal fusion. Spine 2000; 26:2623–2628.
9. Glassman SD, Anagnost SC, Parker A, Burke D, Johnson JR, Dimar JR. The effect of cigarette smoking and smoking cessation on spinal fusion. Spine 2000; 25:2608–2615.
10. Brown CW, Orme TJ, Richardson HD. The rate of pseudarthrosis (surgical nonunion) in patients who are smokers and patients who are nonsmokers: a comparison study. Spine 1986; 11:942–943.
11. Carpenter CT, Dietz JW, Leung KYK, Hanscom DA, Wagner TA. Repair of a pseudarthrosis of the lumbar spine. A functional outcome study. J. Bone Jt. Surg 1996; 78:712–727.
12. Silcox DH, Daftari T, Boden SD, Schimandle JH, Hutton WC, Whitesides TE. The effect of nicotine on spinal fusion. Spine 1995; 20:1549–1553.
13. Wing KJ, Fisher CG, O'Connell JX, Wing PC. Stopping nicotine exposure before surgery. The effect on spinal fusion in a rabbit model. Spine 2000; 25:30–34.
14. Daftari TK, Whitesides TE, Heller JG, Goodrich AC, McCarey BE, Hutton WC. Nicotine on the revascularization of bone graft. An experimental study in rabbits. Spine 1994; 19:904–911.
15. Fang MA, Frost PJ, Iida-Klein A, Hahn TJ. Effects of nicotine on cellular function in UMR 106-01 osteoblast like cells. Bone 1991; 12:283–286.

16. Romano SJ, Corriveau RA, Schwarz RI, Berg DK. Expression of the nicotinic receptor α 7 gene in tendon and periosteum during early development. J. Neurochem 1997; 68:640–648.
17. Dwyer AF. Direct current stimulation in spinal fusion. Med. J. Aust 1974; 1:73–75.
18. Dwyer AF. The use of electrical current stimulation in spinal fusion. Orthop. Clin. North Am 1975; 6:265–273.
19. Kane WJ. Direct current electrical bone growth stimulation for spinal fusion. Spine 1988; 13:363–365.
20. Meril AJ. Direct current stimulation of allograft in anterior and posterior lumbar interbody fusions. Spine 1994; 19:2393–2398.
21. Boden SD, Schimandle JH. Biologic enhancement of spinal fusion. Spine 1995; 20:113S–123S.
22. McKay B, Sandhu HS. Use of recombinant human bone morphogenetic protein-2 in spinal fusion applications. Spine 2002; 27:S66–S85.
23. Silcox DH, Boden SD, Schimandle JH, Johnson P, Whitesides TE, Hutton WC. Reversing the inhibitory effect of nicotine on spinal fusion using an osteoinductive protein extract. Spine 1998; 23: 291–296.
24. Patel TC, Erulkar JS, Grauer JN, Troiano NW, Panjabi NM, Friedlaender GE. Osteogenic protein-1 overcomes the inhibitory effect of nicotine on posterolateral lumbar fusion. Spine 2001; 26: 1656–1661.
25. Lowery GL, Kulkaini S, Pennisi AE. Use of autologous growth factors in lumbar spinal fusion. Bone 1999; 25:47S–50S.
26. Ro J, Sudman E, Marton PF. Effect of indomethacin on fracture healing in rats. Acta. Orthop. Scand 1976; 47:588–599.
27. Ritter MA, Gioe TJ. The effect of indomethacin on paraarticular ectopic ossification following total hip arthroplasty. Clin. Orthop 1982; 167:113–117.
28. Deguchi M, Rapoff AJ, Zdeblick TA. Posterolateral fusion for isthmic spondylolisthesis in adults: analysis of fusion rate and clinical results. J. Spinal Disord 1998; 11:459–464.
29. Glassman SD, Rose SM, Dimar JR, Puno RM, Campbell MJ, Johnson JR. The effect of postoperative nonsteroidal anti-inflammatory drug administration on spinal fusion. Spine 1998; 23:834–838.
30. Dimar JR, Ante WA, Zhang YP, Glassman SD. The effects of nonsteroidal anti-inflammatory drugs on posterior spinal fusions in the rat. Spine 1996; 21:1870–1876.
31. Martin GJ, Boden SD, Titus L, Einhorn TA. Recombinant human bone morphogenetic protein-2 overcomes the inhibitory effect of ketorolac, a nonsteroidal anti-inflammatory drug (NSAID), on posterolateral lumbar intertransverse process spine fusion. Spine 1999; 24:2188–2193.
32. Reuben SS, Connelly NR. Postoperative analgesic effects of celecoxib or rofecoxib after spinal fusion surgery. Anesth. Analg 2000; 91:1221–1225.
33. Lewis SJ, Long J, Kuklo TR, Riew KD. The effect of COX-2 inhibitors on spinal fusion. Proceedings from the North American Spine Society 15th Annual Meeting, 2000.

8

Use of a Cloned Osteoprogenitor Cell in Spinal Fusion

Quanjun Cui, Zeng Ming Xiao, Gary Balian, and Gwo-Jaw Wang
University of Virginia School of Medicine
Charlottesville, Virginia, U.S.A.

I. INTRODUCTION

The recent progress in biomedical technologies including gene and cell therapy has the potential to transform orthopedic surgery. Surgeons have started to incorporate those innovations into their surgical practice. The application of the new technologies in spinal fusion is abundant, for example, more than 185,000 spinal arthrodesis procedures are performed each year in the United States, with reported failure rates ranging from 5 to 45% [6]. Therefore, procedures that may enhance bone repair and fusion need to be developed. Although autografts are the standard for stable spinal fusion, supply is limited and donor site complications exist [1,7,8]. Allografts are an alternative but not desirable, because of immunogenicity and the potential to transmit diseases [3,6,42,47]. Successful use of graft materials is based on their osteoinductive and/or osteoconductive properties that induce and provide a favorable environment for osteoprogenitor cells to grow and to differentiate into osteocytes. Different formulations of ceramics, collagen gels, demineralized bone matrix, and bone marrow have been studied to substitute for autogenous bone grafts [4,5,12,15,27,30,37,38,41,42,46]. However, the success rate of these studies has been limited due to the absence of either osteoinductive stimulants in these graft materials or their osteoconductive properties. These materials may be used as a bone graft extender but not as bone graft substitutes [4–9,11,16,36,41]. Growth factors delivered in the form of protein or cDNA constructs of their genes also have been tested to enhance bone repair [1,7,8,14,17,23,26,32–34,39,40,4]. It was demonstrated that growth factors such as bone morphogenetic proteins (BMPs) have the capability to heal critical-sized bone defects and induce bone formation ectopically [33,39,44]. However, these growth factors usually need to be combined with carriers, such as ceramics, including hydroxyapatite. Although several ceramic matrices currently are available for clinical use, the data supporting their efficacy are limited [32]. Moreover, substantially higher doses of protein have been required in limited human trials [7]. Thus, the need for developing novel grafting materials is evident. A number of studies have focused on the osteoprogenitor cells, particularly from marrow, to potentiate repair and thereby impact favorably on the process of fracture healing [9–13,15,28].

Several different cell-based tissue engineering approaches have been described for bone regeneration, including whole marrow, culture expanded mesenchymal stem cells, differentiated osteoblasts, and genetically modified cells expressing target gene products [9–13]. In this chap-

ter, the authors will review a serious study on an osteoprogenitor cell, D1-BAG [18–22], but will focus on its use in spinal fusion. D1-BAG cell was cloned from mouse bone marrow stroma and transfected with a traceable gene. D1 BAG cells possess characteristics of mesenchymal stem cells described by Bruder et al. [9–13], but the cell is cloned and originated from a single cell. The materials were previously published, and the following text is a summary from those publications [18–22].

II. MATERIALS AND METHODS

A. Cell Cloning and Analysis

Bone marrow cells were flushed out of the cut ends of the femora of 8-week-old Balb/c mice (Jackson Labs, Bar Harbor, ME). The stromal population was separated from hematopoietic elements by serial passaging of adherent cells. They were then separated from bone marrow macrophages by maintenance of the cultures without the addition of factors that sustain the proliferation of macrophages. A colony of fibroblast-like cells, which responded to parathyroid hormone and produced alkaline phosphatase and colony-stimulating factor 1, was isolated with the use of a cloning ring. From this cloned cell population, one subclone was obtained by serial dilution with the use of 24 chamber plates and designated as D1. Subcloned cells were maintained in α-minimum essential medium with vitamins (Gibco, Grand Inland, NY), pH 7.36, containing 15% fetal bovine serum at 37°C in 5% carbon dioxide, and passaged with standard trypsin-ethylene-diaminetetraacetic acid techniques for a total of more than 50 passages. The cells were stored in a cryobiological cell bank until used.

B. Transduction of D1 Cell with Traceable Genes

D1 cells were cultured in Dulbecco's Modified Essential Medium (Gibco, Grand Inland, NY), pH 7.6, containing 10% fetal bovine serum (Hyclone, Logan, UT), 50 μg of sodium ascorbate, 100 units of penicillin G, and 100 μg of streptomycin per mL of culture medium. Recombinant retroviruses were generated using the Ψ-CRE (CRE BAG2, ATCC, Manassas, VA) line producing replication-incompetent virus with an ecotropic host range, allowing transduction of mouse cells. The vector DNA encodes for β-gal and neomycin resistance, therefore the cell can be selected using neomycin in culture and identified using Xgal stain. Viral stock with 8 mg/mL polybrene was added to a subconfluent cell culture of D1 cells for 3 hours following established protocols. A replication-incompetent virus was used so that the transduced cells subsequently would be incapable of transducing neighboring cells. The transduced cells were analyzed and named as D1-BAG.

C. In Vitro and In Vivo Analysis of the Cell

The osteogenic properties were examined by staining with von Kossa, determination of alkaline phosphatase activity, cAMP production in response to stimulation with parathyroid hormone, and hybridization of total RNA in Northern blots with osteocalcin cDNA. A suspension containing 20×10^6 cells/mL phosphate-buffered solution was prepared for cell transplantation in vivo. 2×10^6 cells were injected into subcutaneous sites, the hindquarter muscles, and the renal capsule in 24 Balb/c mice. The fate of the transplanted cells was analyzed at different time points radiographically and histologically.

D. Cell Preparation for Spinal Fusion

D1-BAG cells, from a cryobiological cell bank, and primary marrow cells, which were prepared from the hindlimb long bones (femurs) of 6 week-old normal Sprague-Dawley rats by flushing the marrow cavity with Dulbecco's modified essential medium (DMEM) (Gibco BRL, Bethesda, MD), were used for spinal fusion. Marrow cells were collected from the marrow blowouts by centrifugation at $300 \times g_2$, resuspended in culture media, and transferred to 75 cm^2 flasks at a density of 4×10^4 cells/cm^2. Both D1-BAG and mixed marrow cells were cultured in DMEM containing 10% fetal bovine serum (Hyclone Laboratories, logan, VT), 50 μg sodium ascorbate, 100 units penicillin G, and 100 μg streptomycin per mL of culture media, in a humidified atmosphere of 5% carbon dioxide at 37°C for 10–16 days. Cells in culture were stained for alkaline phosphatase (Sigma) and with von Kossa to establish their osteogenic properties. Both the in vitro and in vivo experiments were carried out using the same source of cells.

E. Surgical Procedures

The investigation was approved by the University of Virginia Animal Research Committee. Fifty-two Harlan athymic nude rats (Hsd:RHrnu) were used for spinal surgery. Under general anesthesia with Ketamine (80 mg/kg) and Xylazine (7 mg/kg), animals were positioned prone, shaved, and covered with sterile drapes after the skin was washed with Betadine solution and 70% alcohol. A midline posterior longitudinal incision was made from L3 to L5. A small sharp elevator was used to elevate the periosteum along spinous processes and lamina to the lateral aspect of the facets. The facet joints were removed with a rongeur. The wound was then irrigated with normal saline and packed with gauze. After the fusion bed was prepared, 2×10^6 of either D1-BAG cells or mixed marrow stromal cells were suspended in Matrigel (Becton Dickinson Labware, Bedford, MA) in a total volume of 100 μL and implanted into the fusion bed of 32 animals in the experimental group. The same amount of matrigel without cells was used in 16 control animals. The deep fascia and skin was then closed after matrigel polymerized in the fusion bed; a pocket developed by dissection between lamina and paraspinal muscles. No postoperative immobilization devices were used. Postoperative analgesia with buprenorphine hydrochloride (0.1 mg/kg) was given.

F. Manual Palpation of Spine Fusions

L3 to L5 spine was excised en bloc from animals of the 6- and 9-week groups. The specimens were manually palpated by flexion and extension at levels L3–4 and L4–5 by two blinded observers. The arthrodesis sites were graded as solid when no motion was presented or not solid when any motion was detected. Only those graded as solid were considered fused. This method of evaluation was previously shown to be both more accurate than plain radiographs and to correlate with biomechanical testing data [7,8].

G. Radiographic Analysis

Posteroanterior and lateral radiographs of lumbosacral spine were obtained immediately after surgery and at 2, 3, 6, and 9 weeks when the animals were killed, with a HP43805-N x-ray system (Hewlett-Packard, McMinnville, OR). Computed tomographic (CT) scan was conducted for animals at 6 and 9 weeks, using a Picker PQ5000 CT Scanner (Picker International, Inc. Cleveland, Ohio).

H. Histologic Analysis

The excised specimen were fixed in 0.05% glutaraldehyde in phosphate-buffered saline (PBS) for 48 hours, decalcified in 0.25 M ethylene diamine tetraacetic acid (EDTA) in PBS (pH 7.4) for 2–3 weeks at 4°C, and then immersed in Xgal solution (1 mg/mL) overnight at 37°C. The specimens were embedded in paraffin; 5–7 μm sections were cut and counterstained with hematoxylin and eosin. To quantitate the fusion mass, 10 sections from each specimen were scanned using a Nikon Scanner (Nikon LS-3510AF, Melville, NY) and Adobe Photoshop (Adobe, Salinas, CA). The areas of bone formation were determined quantitatively using the software program Image-Pro (Media Cybernetics, Silverspring, MD). The average value of 10 sections from each specimen was taken as the bone area.

I. Statistical Methods

Statistical analysis was performed by James T. Patrie, Division of Biostatistics, Department of Health Evaluation Sciences, University of Virginia. Measurements of bone formation were transformed to the base 10 logarithmic scale prior to analysis in order to obtain equal residual variation among the treatment groups. The transformed data were analyzed by two-way ANOVA. Model specification was designed to estimate treatment effect, time effect, and treatment by time interaction, as well as subsampling error. Hypotheses related to comparisons of bone formation were assessed by a Bonferroni multiple comparison criterion [25] with an experimental type I error rate of 0.05. Statistical computations were carried out in SAS version 6.12 with the mixed model software of Proc Mixed (SAS/STAT^{R} Software, SAS Institute Inc., Cary, NC).

III. RESULTS

A. In Vitro and In Vivo Osteogenesis

D1 cell line has osteogenic, chondrogenic, and adipogenic properties. D1-BAG cells retained the pluripotent properties of their parental D1 cells, as demonstrated by the expression of osteocalcin mRNA, positive von Kossa staining, an increase in cyclic adenosine monophosphate in response to parathyroid hormone, and positive staining for alkaline phosphatase [18–21]. Two weeks after they were cultured in DMEM, both D1-BAG and mixed marrow cells stained positively for alkaline phophatase and with von Kossa. Only D1-BAG cells stained positively when incubated with Xgal. Radiopaque tissue appeared 2 weeks after D1-BAG cells were injected into muscle, subcutaneous site, and the renal capsule. Histological analysis demonstrated that these tissues consist of newly formed trabecular bone from transplanted cells which stained positively with Xgal (Fig. 1). There were no surgical or postoperative complications, and none of the animals were dropped from the study.

B. Radiographic Evaluation of Spine

Both anteroposterior and lateral views of the spine were taken. Two weeks after surgery, radiopaque tissue was seen at transplantation sites with D1-BAG cells and became evident after 6 weeks at sites with either D1-BAG cells or mixed marrow stromal cells plus Matrigel, but not at sites in which Matrigel alone had been placed. A larger bone mass was found along the fusion bed in animals that received D1-BAG, compared with mixed marrow cells. CT scan demonstrated that animals transplanted with D1-BAG or mixed marrow cells had achieved spinal fusion at 6 and 9 weeks after surgery. Three-dimensional reconstruction of CT images of rat spine showed that D1-BAG cells formed a larger fusion mass than mixed marrow cells (Fig. 2).

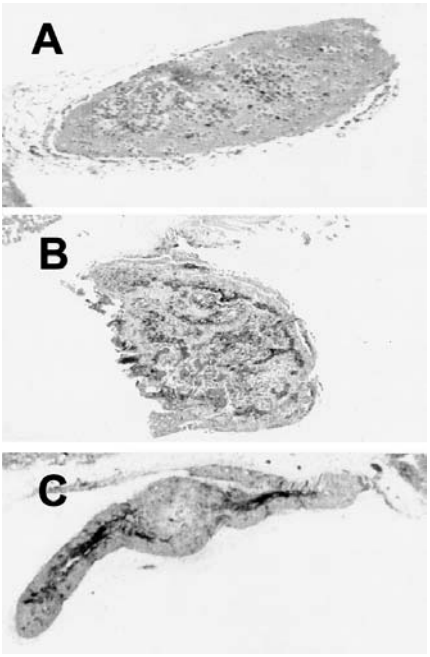

Figure 1 New bone formation by D1-BAG cells 2 weeks after injection into different sites: (A) subcutaneous, (B) intramuscular, and (C) renal capsule. The cells stained positively with Xgal (blue staining) are D1-BAG cells (X-gal and H & E stain, $\times 25$).

C. Manual Palpation of Specimens

Successful spine fusion at 6 and 9 weeks after surgery was obtained in 8 of 8 (100%) animals receiving D1-BAG cells, while only 4/8 (50%) in animals receiving mixed bone marrow cells. By contrast, 0 of 8 (0%) animals receiving Matrigel (carrier) achieved spinal fusion.

D. Histology and Histomorphometric Measurement

The fusion mass consisted of newly formed trabecular bone. Cells that stained positively with Xgal were detected in the spinal fusion mass of animals receiving D1-BAG cells by transplantation, indicating that newly formed bone originated from transplanted cells. Interestingly, no cartilaginous tissue could be detected at any time point during the study in animals transplanted with D1-BAG cells, indicating that the process of ossification was not endochrondral. However, endochrondral bone formation was observed in animals transplanted with mixed marrow stromal cells. Sections of all lumber spine specimens examined morphometrically using a computerized image analysis system showed that bone formation began at 2 weeks and reached the highest levels at 6 weeks and that transplantation of D1-BAG cells produced more bone and better spinal fusion (Fig. 3) than mixed marrow stromal cells. The difference in bone volume among the three groups is statistically significant ($p < 0.05$).

IV. DISCUSSION

Autografts are currently the preferred graft material, but supply is limited and complications abound. Bone graft substitutes are therefore being investigated extensively but still lag behind

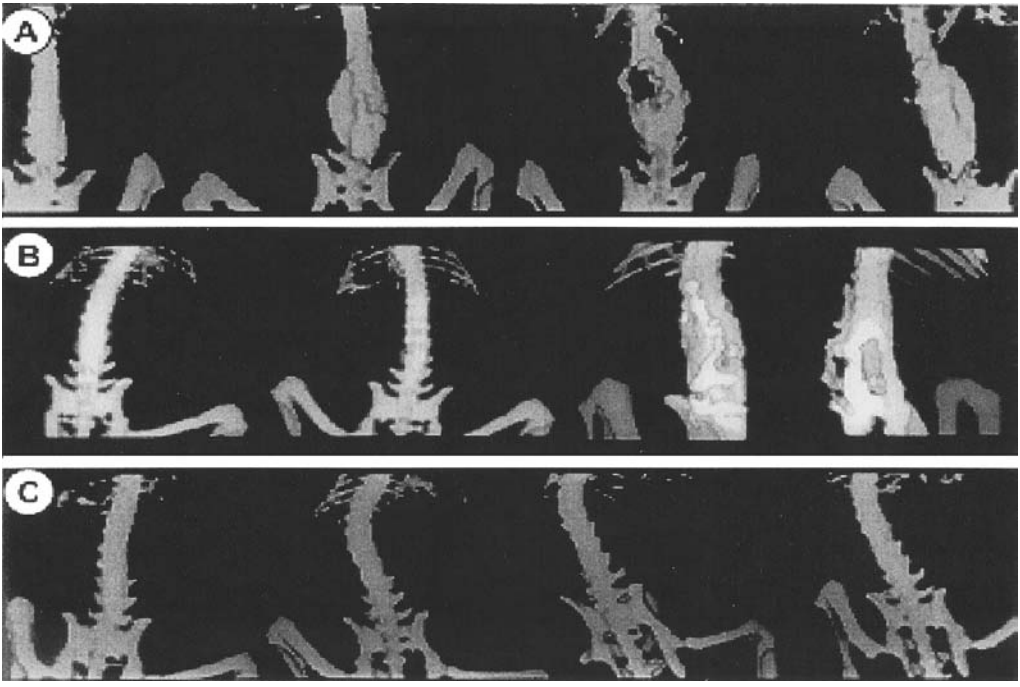

Figure 2 Three-dimensionally reconstructed CT images of rat spine at 9 weeks: (A) from animals transplanted with both Matrigel and D1-BAG cells showing marked bone formation within the spinal fusion mass, (B) from animals received mixed marrow cells showing 2 of 4 animals had paraspinal bone formation, and (C) from animals transplanted with Matrigel (carrier) only, which served as the control showing no new bone formation. (From Ref. 19).

the clinical needs. Techniques based on the singular or combined application of cells, growth factors, and extracellular matrix scaffolds have produced a limited number of clinically available therapeutic stratigies. In this study, an osteoprogenitor cell, D1-BAG [18–22], which was cloned from Balb/c mouse bone marrow stroma and transduced with a traceable gene encoding θ-galactosidase, and mixed marrow stromal cells from marrow blowouts were used in athymic rats to examine their effectiveness in eliciting posterior spinal fusion. The cloned osteoprogenitor cells demonstrated an earlier osteogenic process with a larger fusion mass than mixed stromal cells. Also, osteogenesis with D1-BAG cells occurred without a cartilaginous phase in contrast to the process of endochondral ossification that was seen with mixed marrow cells. The data indicate that cloned osteoprogenitor cells may serve as a substitute for bone autografts.

It is known that bone marrow contains a population of pluripotent progenitor cells, referred to as mesenchymal stem cells, capable of differentiation into bone, cartilage, tendon, and muscle [9–13,15,18–22,28,29]. However, the number of these cells in bone marrow is very low, approximately one per 100,000 nucleated cells [11]. Cell culture ex vivo can produce a significant increase in the number of progenitor cells and the cells can then be used as a graft material to treat bone defects in animals. Studies on culture-expanded animal and human bone marrow osteoprogenitor cells have demonstrated that this subpopulation of marrow cells contributes more effectively to the repair of segmental defects in cortical bone than freshly prepared marrow [9–11,15,19,33,43]. This study demonstrates that osteogenesis by the progeny of a cloned osteoprogenitor cell is more effective than ex vivo expanded, nonpurified marrow stromal cells,

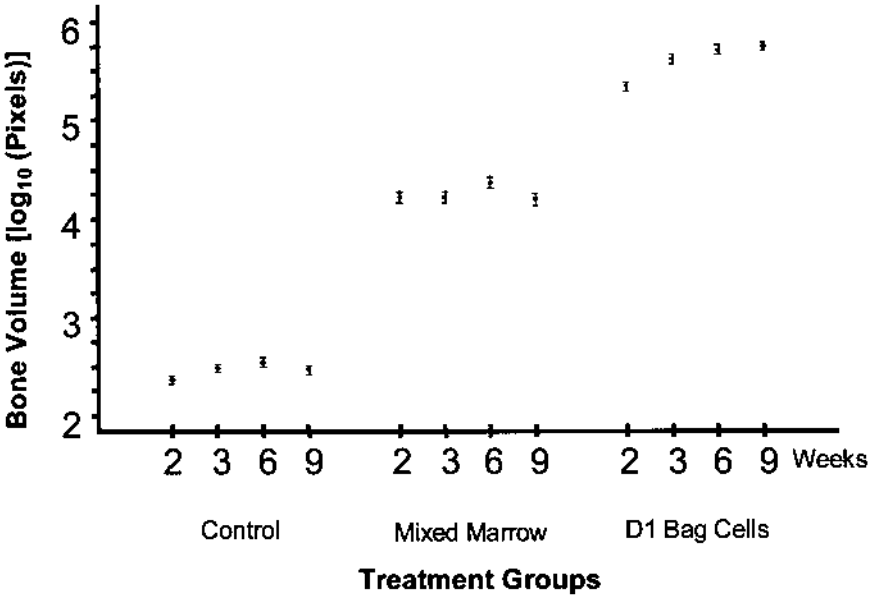

Figure 3 Areas of newly formed bone in the spinal fusion mass. Histomorphometry was performed on 10 sections taken from each specimen (4 animals from each group at each time point were analyzed). Mean area of trabecular bone was obtained by measuring total pixels. Data presented as mean ± standard deviation (error bar). (From Ref. 19.)

suggesting that cloned progenitor cells may be considered for further examination as a possible tool for therapeutic options.

Normally, there is a phase of endochondral ossification in the process of spinal fusion, which is similar to the osteogenic process induced by fresh marrow or culture-expanded stromal cells in bone defect repair [4–8,24,46]. However, there was no such chondrogenic phase with D1-BAG cells, as demonstrated in this study and in previous studies [19]. By contrast to the mixed marrow cells which contain chondrogenic and osteogenic cells that lead to endochondral ossification in spinal fusion, D1-BAG cells are predominately osteogenic [18–22], although it is chondrogenic under certain circumstances [21]. This may contribute to the lack of endochondral ossification by D1-BAG cells in the process of spinal fusion. This characteristic of the cloned osteoprogenitor cells can expedite the healing process and, therefore, may be useful clinically if further studies should prove that the absence of a chondral phase during spinal fusion is advantageous.

Many factors are involved in achieving a successful lumber spinal fusion. Both mechanical and biological factors play an important role in the fusion process [4]. The feasibility of biological enhancement of spinal fusion with different graft materials and growth factors has been shown in many animal studies. The ideal graft material, reviewed by Boden and Schimandle, should possess osteogenic, osteoinductive, and osteoconductive properties [4]. Osteoprogenitor cells, such as the D1-BAG cells used in the present study, are osteogenic and capable of forming bone directly without an intermediate cartilaginous stage. The advantage that this cell-based technique offers over other strategies for bone regeneration is the delivery of the cellular element that is required for bone formation. Osteoinduction is the process by which factors or substances, such as bone morphogenetic proteins (BMPs), stimulate progenitor cells to differentiate into an

osteogenic lineage, leading to bone formation. Autogenous bone, marrow, and allografts contain BMPs and transforming growth factor beta (TGF-θ), insulin-like growth factors (IGFs), fibroblast growth factors (FGFs), platelet-derived growth factors (PDGFs), and interleukins and, therefore, have osteoinductive properties [2–4,14,42]. Matrigel is a solubilized basement membrane preparation extracted from the Engelbreth-Holm-Swarm mouse sarcoma [31]. Its major components are laminin, collagen IV, proteoglycans. It also contains TGF-θ, FGF, and other growth factors. Matrigel itself is not tumorgenic but supports in vivo cell growth and differentiation [35]. Whether Matrigel is osteoinductive or not needs further study. Implantation of Matrigel only, when used without transplanted cells, did not induce bone formation. However, the unique property of Matrigel is that it is in liquid state at 4°C, so it can be easily mixed with cells and used as graft material and will polymerize at a temperature above 22°C, holding the graft material in situ. Therefore, it is useful as a vehicle for therapeutic agents such as growth factors or, in this instance, to deliver cells.

Local gene therapy is a new approach for spinal fusion [1,34,37]. Boden et al. [7] successfully delivered a therapeutic gene, LMP-1, which encodes a novel osteoinductive protein, using bone marrow cells. Solid spine fusion was obtained in 9 of 9 (100%) sites receiving marrow cells transduced with active LMP-1 gene. This new strategy may eliminate the need for local implantation of osteoinductive proteins since the natural protein may be scarce as adequate supply of recombinant protein requires elaborate genetic and proteomic technologies. The present study, using a cloned osteoprogenitor cell which carries a traceable reporter LacZ gene [21], showed that the gene-labeling technique is a useful tool for investigations of osteogenesis by marrow cells in vivo; meanwhile, the results demonstrated the feasibility of a cloned osteoprogenitor cell to deliver a therapeutic gene to enhance bone repair and spinal fusion.

While local gene therapy is successful experimentally in spinal fusion, therapeutic cells can serve as an alternative and should be broadly applicable [9–13,15,21,46], such as in the treatment of bone defects and osteoporosis. Autologous osteoprogenitor cells can be harvested from patients, allowed to proliferate in cultures in vitro, and transplanted subsequently into the host within a delivery system (carrier) appropriate for the clinical situation. The advantage of this approach is that it offers the direct delivery of cellular machinery required for bone formation. The technique is particularly useful when numbers of endogenous osteoprogenitor cells are limited.

In summary, the current study demonstrates that the cloned osteoprogenitor cells produce a larger bone mass and more rapid spinal fusion than mixed marrow stromal cells. The results suggest that the cloned osteogenic marrow cells may serve as a substitute for bone autografts and may be considered as a vehicle to deliver therapeutic genes.

REFERENCES

1. Alden TD, Hankins GR, Beres EJ, Kallmes DF, Helm GA. Bone morphogenetic protein gene therapy for the induction of spinal arthrodesis. Neurosurg. Focus 1998; 4(2):Article 12.
2. Balk ML, Bray J, Day C, Epperly M, Greenberger J, Evans CH, Niyibizi C. Effect of rhBMP-2 on the osteogenic potential of bone marrow stromal cells from an osteogenesis imperfecta mouse (oim). Bone 1997; 21:7–15.
3. Bauer TW, Muschler GF. Bone graft materials. Clin. Orthop. Rel. Res 2000; 371:7–15.
4. Boden SD, Schimandle JH. Biologic enhancement of spinal fusion. Spine 1995; 20:7–15.
5. Boden SD. The biology of posterolateral lumbar spinal fusion. Orthopaed. Clin. North Am 1998; 29:7–15.

6. Boden SD. Bone repair and enhancement clinical trial design: spine applications. Clin. Orthop. Rel. Res 1998; 355S:S336–S346.
7. Boden SD, Titus L, Hair G, Liu Y, Viggeswarapu M, Nanes MS, Baranowski C. Volvo award winner in basic science studies. Lumbar spine fusion by local gene therapy with a cDNA encoding a novel osteoinductive protein (LMP-1). Spine 1998; 23:7–15.
8. Boden SD, Martin GJ, Morone MA, Ugbo JL, Moskovitz PA. Posterolateral lumbar intertransverse process spine arthrodesis with recombinant human bone morphogenetic protein 2/hydroxyapatite-tricalcium phosphate after laminectomy in the nonhuman primate. Spine 1999; 24:7–15.
9. Bruder SP, Fink DJ, Caplan AL. Mesenchymal stem cells in bone development, bone repair, and skeletal regeneration therapy. J. Cell. Biochem 1994; 56:283–294.
10. Bruder SP, Jaiswal N, Haynesworth SE. Growth kinetics, self-renewal and the osteogenic potential of purified human mesenchymal stem cells during extensive subcultivation and following cryopreservation. J. Cell. Biochem 1997; 64:7–15.
11. Bruder SP, Jaiswal N, Ricalton NS, Mosca JD, Kraus KH, Kadiyala S. Mesenchymal stem cells in osteobiology and applied bone regeneration. Clin. Orthop. Rel. Res 1998–5; 355S:S247–S256.
12. Bruder SP, Kraus KH, Goldberg VM, Kadiyala S. The effect of implants loaded with autologous mesenchymal stem cells on the healing of canine segmental bone defects. J. Bone. Joint. Surg 1998; 80:7–15.
13. Bruder SP, Fox BS. Tissue engineering of bone: cell based strategies. Clin. Orthop. Rel. Res 1999; 367S:S68–83.
14. Canalis E, McCarthy T, Centrella M. Growth factors and the regulation of bone remodeling. J. Clin. Invest 1988; 81:7–15.
15. Connolly JF. Clinical use of marrow osteoprogenitor cells to stimulate osteogenesis. Clin. Orthop. Rel. Res 1998; 355S:S257–S266.
16. Cornell CN, Lane JM. Current understandings of osteoconduction in bone regeneration. Clin. Orthop. Rel. Res 1998; 355S:S267–S273.
17. Crystal RG. Transfer of genes to humans: early lessons and obstacles to success. Science 1995; 270: 7–15.
18. Cui Q, Wang GJ, Balian G. Steroid-induced adipogenesis in a pluripotential cell line from bone marrow. J. Bone. Joint. Surg 1997; 79:7–15.
19. Cui Q, Xiao Z, Balian G, Wang GJ. Comparison of lumbar spine fusion using mixed and cloned marrow cells. Spine 2001; 26(21):2305–2310.
20. Cui Q, Wang GJ, Balian G. Pluripotential marrow cells produce adipocytes when transplanted into steroid-treated mice. Connect. Tissue Res 2000; 41(1):45–56.
21. Dahir G, Cui Q, Anderson P, Simon C, Joyner C, Triffitt JT, Balian G. Pluripotential mesenchymal cells repopulate bone marrow and retain osteogenic properties. Clin. Orthop. Rel. Res 2000; 379S: S134–145.
22. Diduch DR, Coe MR, Joyner C, Owen ME, Balian G. Two cell lines from bone marrow stroma differ in collagen synthesis, osteogenic characteristics and matrix mineralization. J. Bone Joint Surg 1993; 75A(1):92–105.
23. Fang J, Zhu YY, Smiley E, Bonadio J, Rouleau JP, Goldstein SA, McCanley LK, Davidson BL, Roessler BJ. Stimulation of new bone formation by direct transfer of osteogenic plasmid genes. Proc. Natl. Acad. Sci. USA 1996; 93:7–15.
24. Feighan JE, Stevenson S, Emery S. Biologic and biomechanic evaluation of posterior lumbar fusion in the rabbit. Spine 1995; 20:7–15.
25. Fisher DL, van Belle G. Biostatistics: A Methodology for the Health Sciences. New York: John Wiley & Sons, 1993:pp. 611.
26. Goldstein SA. In vivo nonviral delivery factors to enhance bone repair. Clin. Orthop. Rel. Res 2000; 379S:S113–S119.
27. Guizzardi S, Silvestre M, Scandroglio R, Ruggeri A, Savini R. Implants of heterologous demineralized bone matrix for induction of posterior spinal fusion in rats. Spine 1992; 17:7–15.
28. Haynesworth SE, Baber MA, Caplan AI. Cell surface antigens on human marrow-derived mesenchymal cells are detected by monoclonal antibodies. Bone 1992; 13:7–15.

29. Haynesworth SE, Goshima J, Goldberg VM, Caplan AI. Characterization of cells with osteogenic potential from human marrow. Bone 1992; 13:7–15.
30. Holmes RE, Bucholz RW, Mooney V. Porous hydroxyapatite as a bone graft substitute in diaphyseal defects: a histometric study. J. Orthop. Res 1987; 5:7–15.
31. Kleinman HK, McGarvey ML, Liotta LA, Robey PG, Tryggvason K, Martin GR. Isolation and characterization of type IV procollagen, laminin, and heparan sulfate proteoglycan from the EHS sarcoma. Biochemistry 1982; 21:7–15.
32. Lane JM. Breakout Session 5: Biologic enhancement of fracture repair. Clin. Orthop. Rel. Res 1998; 355S:S359–S360.
33. Lane JM, Yasko AW, Tomin E, Cole BJ, Waller S, Browne M, Turek T, Gross J. Bone marrow and recombinant human bone morphogenetic protein-2 in osseous repair. Clin. Orthop. Rel. Res 1999; 361:7–15.
34. Lieberman JR, Daluiski A, Stevenson S, McAllister P, Lee Y, Wu L, Kabo JM, Finerman GAM, Witte ON. Regional gene therapy with BMP-producing bone marrow cells heals segmented femoral defects in rats. Orthop. Res. Soc. Trans 1998; 23:210.
35. Madison R, da Silva CF, Dikkes P, Chiu TH, Sidman RL. Increased rate of peripheral nerve regeneration using bioresorbable nerve guides and a laminin-containing gel. Exp. Neurol 1985; 88:767.
36. Muschler GF, Negami S, Hyodo A, Gaisser D, Easley K, Kambic H. Evaluation of collagen ceramic composite graft materials in a spinal fusion model. Clin. Orthop. Rel. Res 1996; 328:7–15.
37. Niyibizi C, Baltzer A, Lattermann C, Oyama M, Whalen JD, Robbins PD, Evans CH. Potential role for gene therapy in the enhancement of fracture healing. Clin. Orthop. Rel. Res 1998; 355S:S148–153.
38. Ohgushi H, Goldberg VM, Caplan AI. Heterotopic osteogenesis in porous ceramics induced by marrow cells. J. Orthop. Res 1989:568–79.
39. Reddi AH. Initiation of fracture repair by bone morphogenetic proteins. Clin. Orthop. Rel. Res 1998; 355S:S66.
40. Rosier RN. Breakout Session 6. 1998. Regional gene therapy. Clin. Ortho. Rel. Res 1998; 355S: S361–363.
41. Sempuku T, Ohgushi H, Okumura M, Tamai S. Osteogenic potential of allogeneic rat marrow cells in porous hydroxyapatite ceramics: a histological study. J. Orthop. Res 1996; 14:7–15.
42. Stevenson S. Enhancement of fracture healing with autogenous and allogeneic bone grafts. Clin. Orthop. Rel. Res 1998; 355S:S239–S246.
43. Takagi K, Urist MR. The role of bone marrow in bone morphogenetic protein induced repair of femoral massive diaphyseal defects. Clin. Orthop. Rel. Res 1982; 171:7–15.
44. Urist MR, DeLange RJ, Finerman GAM. Bone cell differentiation and growth factors. Science 1983; 220:7–15.
45. Virolainen P, Vuorio E, Aro HT. Different healing rates of bone autografts, syngeneic grafts, and allografts in an experimental rat model. Arch. Orthop. Trauma. Surg 1997; 116:7–15.
46. Werntz JR, Lane JM, Burstein AH, Justin R, Klein R, Tomin E. Qualitative and quantitative analysis of orthotopic bone regeneration by marrow. J. Orthop. Res 1996; 14:7–15.
47. Wolff D, Goldberg VM, Stevenson S. Histomorphometric analysis of the repair of a segmental diaphyseal defect with ceramic and titanium fibermetal implants: effects of bone marrow. J. Orthop. Res 1994; 12:7–15.

9

Axially Loaded Computed Tomography and Magnetic Resonance Imaging of the Lumbar Spine

Barbro Danielson and Jan Willén
Sahlgrenska University Hospital
Gothenburg, Sweden

Spondylogenic and neurogenic low back pain are among the most common health problems in the western world today, being the premiere cause of employee abseenteism in the United States. The total cost of low back pain to society is very high. In two European studies it has been reported as 1.7% of the gross national product [1,2] and in the United States as 0.5–2% [3].

About 80% of all human beings suffer from back pain during some time in their lives. In some patients the back problems remain and become chronic. The recovery rate is slow and uncertain. Chronic low back pain has been a subject of intense debate due to the fact that the etiology is often impossible to verify [4].

For the physician it is a challenge to diagnose a specific underlying pathology causing the pain leading to a specific treatment. Diagnostic efforts should include not only a serious clinical evaluation, with interview and physical investigation, but also a serious radiological investigation.

I. BASIC ANATOMY

The spine is flexible tube containing and protecting the cauda equina and at the same time provides a stable base for the locomotor system. Two adjacent vertebrae, the intervening disc, the upper and lower facet joints form a spinal motion segment called a functional spinal unit (FSU). The FSU is surrounded by ligaments, the joint capsule, and muscles. All these structures stabilize the spine. Every FSU provides flexibility but is also a weak point where trauma and degenerative processes can lead to changes impinging on the spinal canal and its neural content.

The relationship between the different parts of the FSU varies according to posture. This has been described in several reports using plain x-ray, computed tomography (CT), and magnetic resonance imaging (MRI). The posture influences the size of the dural cross-sectional area (DCSA), thickness of ligamenta flava, shape of the epidural fat pad, and size of recess and

foramen intervertebrale, especially in degenerative disorders. These postural changes imply a possibility to compromise the dural sac and the nerve roots in one position and not in another.

II. KINEMATIC STUDIES

Kinematic in vitro as well as in vivo studies of the spine have shown dynamic changes in the spinal canal. Studies on the interrelations between and within different FSU have been performed using plain x-ray, CT, and MRI.

A. Plain X-Ray

Knutsson [4] introduced the flexion and extension examination in plain x-ray as a tool for evaluation of movements in functional spinal units. Dupuis et al. [5] found dynamic roentgenograms in flexion-extension and in side bending to be a reliable and simple method to evaluate abnormal motion segments. Putto and Tallroth [6] argued that the flexion-extension studies should be performed in a sitting position to be able to diagnose abnormal movements in a more proper way. Flexion-extension radiography is still used to evaluate the stability of the spine pre- as well as postoperatively.

Experimental methods for evaluation of movements in the spine have been used. In an in vitro study of human lumbar spine specimens, Panjabi et al. [7] demonstrated the three-dimensional movements in the intervertebral foramina during physiological motions. They found changes in height, width, and area of the foramen as a function of major spinal movements.

The roentgen stereophotogrammetric method has been used to describe movements with great accuracy [8]. Tantalum ball implantation in the region of interest is a prerequisite for usage of this technique.

When myelography was introduced, the examination was initially performed in the supine position. Sortland and Schumacher found that the sagittal diameter of the dural sac increased in flexion and decreased in standing and extension of the lumbar spine [9–13].

B. CT Imaging

After the advent of CT technology the possibility to show ligaments, disc, and nerve roots within and outside the dural sac was improved. Coulier [14] studied the discrepancy between the supine CT myelogram and the upright flexion-extension myelography in patients with suspected spinal stenosis. He found a mean underestimation of 16% of the diameter of the dural sac when CT after myelography was compared with myelography in a standing position with extension of the spine. The conclusion was that upright flexion extension myelography should be used to exclude functional or dynamic position-dependent spinal stenosis when no other upright technology is available.

In a clinical study measurement of DCSA on axial CT images was found to be the most accurate method to define central spinal stenosis [15]. The borderline value for a relative (<100 mm^2) and an absolute (<75 mm^2) central spinal stenosis was defined from in vitro studies [16,17]. These values are often used as guidelines when radiological evaluation of the presence of central spinal stenosis is carried out.

Schönström [18] found in an experimental CT study of human spine specimens that the DCSA at the disc level decreases 40 and 50 mm^2 on average, respectively, between flexion and extension as well as between distension and compression. These results highlight the disparity in the dimension of the dural sac related to the position of the spine.

Diversity in size of other parts of the spinal canal has also been exposed. Inufusa et al. [19] studied the spinal canal and the foramina with CT and cryomicrotome. They found the cross-sectional area of the intervertebral foramina 12% greater in flexion and 15% smaller in extension compared to in the neutral position. Nowicki et al. [20] reported flexion and extension as well as axial rotation and side bending in human spine specimens to change the relationship between the ligamentum flavum and the intervertebral disc to the nerve roots contributing to a ''dynamic stenosis.''

In patients with neurogenic claudication and facet hypertrophy at disc levels L3–L5, compression of the nerve roots in the recess region when the spine was extended and relief of the nerve roots in flexion was demonstrated [21]. A considerable decrease in DCSA at the disc level in supine with extended knees was reported if the spine position was changed from 45 degrees of flexion to extension.

C. Magnetic Resonance Imaging

With the introduction of magnetic resonance imaging, excellent visualization of the different anatomical structures in the spinal canal in axial, sagittal, and oblique planes became available. The nerve root can be seen in and lateral to the foramen on parasagittal images and also well differentiated from the cerebral spinal fluid in the dural sac.

Harvey et al. [22] in an open-magnet system performed a kinematic MRI with the subjects in flexion and extension for range-of-motion measurements on the lumbar spine. Hamanishi et al. [23] measured the DCSA in patients examined with MRI in the supine position with flexed and extended knees. They found the DCSA value in the latter position was 93 $\pm$ 4% of those obtained in flexed position.

Chung et al. [24] reported on 20 normal volonteers examined by MRI in the supine position with their spine in neutral, flexed, extended, and rotated to the right and left. A decrease in the dural cross-sectional area and spinal canal in extension and rotation was found. There was also a decrease in the distance between the posterior margin of the disc and the facet and an increase in the thickness of the ligamentum flavum in extension and rotation. They concluded that these findings could serve as a basis for further studies on stenotic or borderline stenotic patients.

Wildermuth et al. [25] compared myelography to positional (upright in sitting with flexion and extension) MR imaging. The mid-sagittal diameter of the dural sac was measured, and the foraminal size was qualitatively scored. The mid-sagittal diameter of the dural sac was slightly larger in the upright flexion position. The conclusion was that the two techniques are comparable for quantitative measurements of the dural sac, but MRI had a higher patient acceptance.

Schmid et al. [26] compared MRI images of the spine in volonteers obtained in upright neutral, flexed, extended, and supine extended. They found the greatest difference in cross-sectional area of the spinal canal between upright flexed and upright extended. The maximum thickness of ligamentum flavum and the smallest cross-sectional area of the neural foramina were seen in the extended position.

Thirty subjects including 5 asymptomatic patients were examined in a sitting position in flexion and extension [27]. In extension an increase in disc bulge was seen especially in those with desiccation. Central canal size and foraminal size also decreased with extension.

Weishaupt et al. [28] in a recent study on patients with chronic low back pain found that the mean dural cross-sectional area significantly decreased between the supine neutral and the upright seated extended position as well as between the upright seated flexed and the upright seated extended position. They also found nerve root contact with the disc without deviation with increased frequency in the upright seated, flexed position compared to the supine position. Their conclusions were that positional MRI might reveal minor neural compromise not detectable

with conventional MRI and that position-dependent pain is related to changes in foraminal size with different postures.

III. SYMPTOMS RELATED TO POSITION

It is a well-known fact that symptoms in patients with neurogenic back pain depend of the position of the spine. In patients with spinal stenosis the symptoms are often elicited in a standing position and reduced in forward lumbar flexion or supine relaxed position, which is explained by the difference in space in the spinal canal between positions. Some patients experience pain in other positions such as in rotation.

CT examination is impossible to perform in a standing position. Stand-up MRI equipment is available, but there are still problems with its use due to increased motion artefacts related to pain in standing compared to in supine. In many patients examination in the position in which they experience their symptoms is not possible.

IV. RADIOLOGICAL EXAMINATION OF THE LUMBAR SPINE

Progress in radiological technique has been explosive during the last 20 years. Until recently the only possibility for radiological diagnostics involved ordinary x-ray examination. Computed tomography was then introduced, followed by magnetic resonance imaging. The evolution in radiological methods has meant a tremendous increase in the possibility to reveal pathology not earlier discovered.

Examinations by CT or MRI presuppose that the patient is positioned as comfortably as possible to avoid motion artefacts. The patient is placed supine with the hips and knees flexed with a pillow below their knees. This means that the spine is flexed and the space in the spinal canal increases. The load on the spine is minimized, which enables pathology to remain undetected. These facts contribute to a less accurate diagnosis. For this reason many spine surgeons still prefer preoperative myelography in some patients.

V. IMAGING IN THE SUPINE POSITION WITH AXIAL LOADING

The DynaWell L-spine™ (DynaWell International AB, Sweden) device makes it possible to perform CT and MRI of the lumbar spine with axial loading, which simulates the load existing in standing. The examination is performed in a position similar to that in which patients experience their symptoms. This results in a more precise diagnosis and thus a more accurate basis upon which the surgeon can choose the type of treatment.

A. CT and MRI in Axial Loading

The DynaWell L-spine device consists of two parts: a harness and a footplate. The footplate is made of plastic, the harness of neoprene and nylon. The harness is attached to the compression device by nylon straps. The straps are tightened to axially load the lumbar spine. The harness is constructed to ensure that the pressure is distributed across the lower part of the chest rather

than on the shoulders. To prevent flexion of the spine and preserve lumbar lordosis during the scanning, a pillow is positioned below the lumbar spine. The straps pass the dorsal part of the femoral major trochanter to maintain the lumbar lordosis. The axial load is adjustable and can be measured by scales on the footplate.

The applied load is chosen to be about half of the patient's body weight (one quarter on each leg). During in vivo disc pressure measurements, Nachemson [29] showed that the load on the L3–L4 disc when individuals were standing up was on average half of the body weight.

The load is applied at least for 5 minutes before scanning. The patients should be continuously asked about any pain in the spine or in the legs during the examination, especially during compression. If intractable pain appears, the pressure can be immediately released by telling the patient to flex his or her knees.

B. Studies After Axial Compression of the Lumbar Spine

A number of studies with CT and MRI in the psoas relaxed position (PRP) and the axially loaded position (ACE) using the DynaWell L-spine device have been published. Eight normal volunteers were examined with MRI of the lumbar spine in the PRP and ACE positions [30]. Intervertebral angles and disc height from L1 to S1 were measured before and during axial compression. Intervertebral angles changed significantly between the positions at L3–L4 and L5–S1. There was a significant decrease in disc height at L4–L5. A comparison of the results was performed with data collected in studies on persons examined in upright posture using plain radiographs. Kimura et al. [30] concluded that the axial loaded MRI examination of the lumbar spine using the compression device provides close simulation of the lumbar spine in a standing position with a stable compression force.

Examination with CT and MRI in asymptomatic subjects as well as in patients with discogenic or neurogenic back pain reveals pathological findings. Disc degeneration is a common finding even in asymptomatic individuals and with increasing frequency with age [31–35]. Disc protrusion, herniation, and spinal stenosis in normals have also been described [35–37]. Therefore, one would expect a decrease in DCSA in asymptomatic persons as well as in patients. Danielson and Willen [38] presented a study of 43 normal volunteers who had no history of low back pain. They were examined with MRI of the lumbar spine in PRP and ACE. The dural cross-sectional area in the two positions was compared. In 56% of the subjects there was a decrease in DCSA from PRP to ACE. The great difference compared to patients with neurogenic back pain is that a decrease from above to below the borderline value for an absolute central spinal stenosis (75 mm^2) was seen in only one person (2%) compared to in 22% among patients [39].

Several studies on patients with sciatica and/or neurogenic low back pain examined in ACE have also been presented. Studies on 84 patients with neurogenic claudication and/or sciatica using CT myelography or MRI have been published [39,40]. The patients were examined in a relaxed as well as in the axial loaded position. The examinations revealed a statistically significant decrease in the dural cross-sectional area in 76–80% of the patients in the axial loaded compared to the relaxed position. In 18 (22%) of the patients, the DCSA changed from above to below 75 mm^2, indicating that an absolute central spinal stenosis was detected in ACE but not in PRP. In patients with a DCSA of more than 130 mm^2, in PRP a decrease in relative central spinal stenosis (DCSA $<$ 100 mm^2) was never seen.

Axial loaded MRI of the lumbar spine is performed at our institution in selected cases with discogenic or neurogenic pain. This enhanced diagnostic method has been beneficial to many patients. In Figure 1 an increased recess stenosis in ACE compared to in PRP is shown in a patient with sciatica. In some cases the axial loaded images have contributed in resolving a

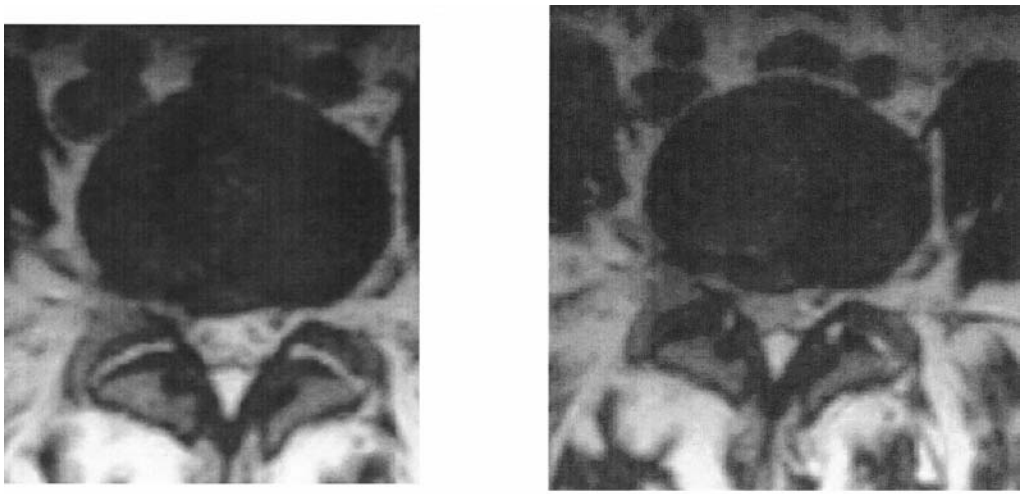

Figure 1 Female, 45 years old, with sciatica diagnosis of 3 years duration. At L4–L5, a paramedian right-sided disc herniation is shown. In ACE (b) there is a thickening of ligamentum flavum and increasing amount of fluid below the ligament with an increasing recess stenosis dx compared to in PRP (a).

differential diagnostic problem (Fig. 2). A diabetic patient with polyneuropathy and questionable neurogenic claudication showed an indubitable absolute central spinal stenosis in ACE but no stenosis in PRP.

The relevance of axially loaded MRI examination of the lumbar spine in patients with different clinical symptoms has been discussed. Willén and Danielson [41] evaluated the results from loaded CT and MRI in 172 patients divided into three groups according to preliminary clinical diagnosis: 55 patients had neurogenic claudication, 84 sciatica, and 33 low back pain. Criteria for additional valuable information (AVI) obtained by the axially loaded examination was defined as a significant reduction of DCSA (>15 mm^2) to areas below 75 mm^2 (the borderline value for canal stenosis) from PRP to ACE, or a suspected disc herniation, lateral recess or foraminal stenosis, or intraspinal synovial cyst at PRP becoming obvious with ACE.

AVI at ACE was found in 50 of all 172 patients (29%) in the study. Of the 55 patients with signs of neurogenic claudication, AVI was found in 36 (69%). In patients with sciatica AVI was found in 14%, if the inclusion criteria for performing the examination in ACE were not used. The inclusion criteria, described in the basic studies by Willén and Danielson [38,39] comprised a DCSA < 130 mm^2 on any disc level, a suspected narrow lateral canal, with or without deformation of the anterolateral part of the dural sac, or a suspected nerve root compression in PRP. If these indications for examination in ACE were added, the AVI was increased from 14 to 50% in the sciatica group, but from 69 to 72% in the neurogenic claudication group. No AVI was found in patients with low back pain. This study confirms the importance of proper selection of patients to undergo axial loaded CT or MRI examination.

Tallroth et al. [42] performed axial loaded CT in 100 patients with low back pain. In almost every patient and disc level they found a decrease in DCSA in axial compression compared to nonloaded examinations. For many patients the diagnosis of central spinal stenosis was established only with compression and thus in accordance with the patients' symptoms.

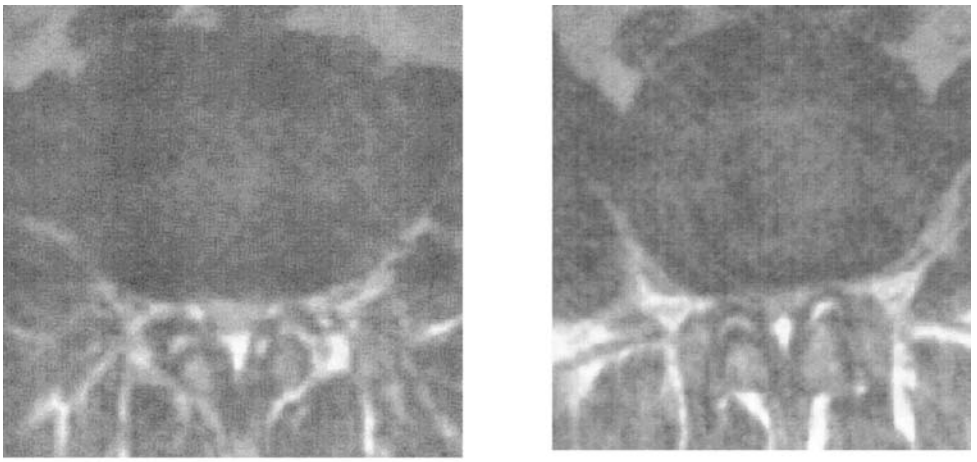

Figure 2 Male, 56 years old. History of diabetes, polyneuropathy, and possibly neurogenic claudication as well. L4–L5: An increased central spinal stenosis is revealed in ACE (B) compared to in PRP (A). DCSA is in PRP 90 mm^2 and in ACE 50 mm^2. An increased amount of fluid is shown below the ligamentum flavum in ACE (B) compared to in PRP (A).

Schöllhammer et al. [43] evaluated axially loaded MRI in 33 patients and found a significant decrease in DCSA in 67% of them. They found a less prominent decrease in disc height at L5–S1 compared to other disc levels. The authors confirmed that MRI in axial loading simulates standing position and could produce clinically relevant decrease in DCSA by an increase in disc protrusion.

Amendy et al. [44] presented a study on 10 patients with symptoms of spinal stenosis, normal Doppler examination, normal conventional CT/MRI, or symptoms disproportionate to findings, fit for surgery. Axial loading significantly contributed to the diagnosis in 6 out of 10 patients. In 4 patients narrowing of the spinal canal was enhanced, and in 2 patients a facet joint cyst was magnificently enlarged. An increase in lateral recess stenosis was found in one patient. They concluded that examination with axial loading of the lumbar spine could be a very useful supplement in selected patients with suspected spinal stenosis and equivocal MRI findings.

Kahn et al. [45] recently presented a study on 50 patients with clinical history of sciatica and neurogenic claudication. They underwent MRI examination in the supine position with flexed knee and in the axial loaded position using the device to simulate the upright position. Two hundred disc levels were evaluated, and sagittal scans revealed a reduction in the AP diameter of the dural sac in 50% of levels and axial scans a reduction in DCSA in 64% of levels. The decrease was in general caused by a thickening of ligamentum flavum, displacement of the epidural fat, an increase in disc bulging, and sometimes distension of epidural veins. Thirty-three percent of patients progressed from a value of DCSA above to a value below 75 mm^2 with axial loading, and 25% with a critical stenosis at one level developed a second critically stenotic level in the axial loaded position. Synovial cysts or diverticulae developed at 20 levels with axial loading. The authors concluded that simulated upright MRI might show causes of neurogenic claudication and sciatica not detectable by conventional MRI.

Experimental studies have revealed that double-level stenosis impairs local nerve blood flow and also nerve impulse propagation [46–49]. Porter and Ward [50] stated in a CT myelo-

graphic study on patients with neurogenic claudication that this disorder is often associated with a stenosis on at least two disc sites.

Axially loaded MRI could reveal another level of spinal stenosis in patients with spinal stenosis at only one level in supine nonloaded MRI, which may alter the surgical approach. These studies support the recommendation to locate all possible stenotic disc levels before deciding on the treatment strategy.

C. Synovial Cysts

Disc degeneration with reduction in disc height could cause segmental instability and osteoarthrosis in the intervertebral joints. The osteoarthrosis presents as a decrease in joint space, osteophyte formation, and eventually an increased amount of joint fluid. The location of the joint fluid changes with the position of the spine. Synovial cysts could cause entrapment of nerve roots in the recess [51].

In patients with sciatica or neurogenic claudication, synovial cysts not visible with supine MRI have been detected in axial loaded MRI. Impingement of the dural sac or compression of the recesses from synovial cysts has been found. The symptoms in these cases could be explained only with examinations in axial loading, (Fig. 3).

In some patients a protrusion of intervertebral joint fluid medially below the ligamentum flavum, decreasing the available space in the central spinal canal, has been shown from PRP to ACE (Figs. 1,2).

Findings of synovial cysts detectable with ACE only have been shown in other reports as well [44,45].

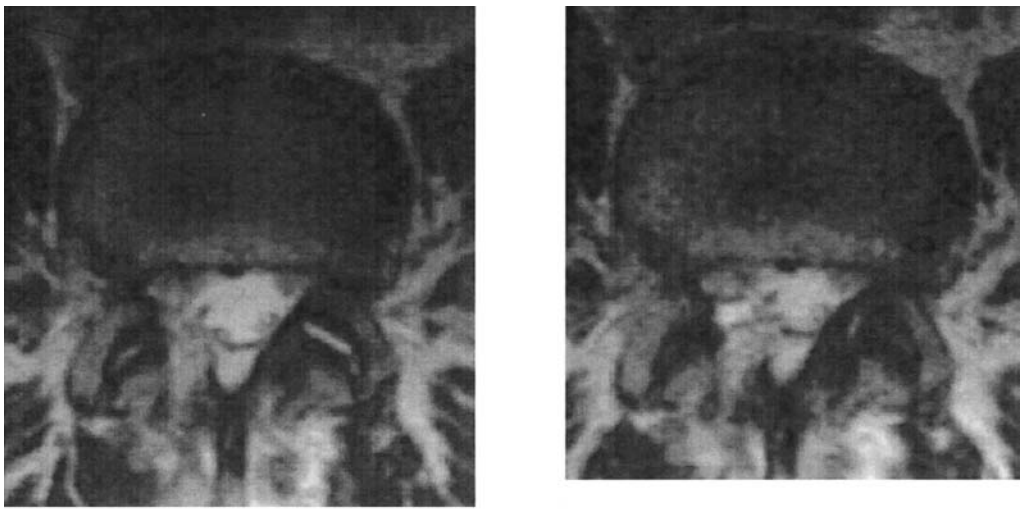

Figure 3 Male, 54 years old with sciatica diagnosis since a months of age. Patient was earlier operated due to a disc herniation L4–L5. L4–L5: In ACE (B) a synovial cyst and postoperative fat compress the L5 nerve root not detectable in PRP (A).

D. Instability

Mailleux et al. [52] presented two patients with degenerative spondylolisthesis of the lumbar spine causing canal stenosis not apparent on supine MRI examination due to reduction of the listhesis in that position. The patients showed an unusually large area of hypersignal at the facets on T2-weighted images. The authors concluded that their observation should raise the suspicion of spondylolisthesis in the standing position and an underestimation of the stenosis in the supine position. These results seem to encourage the use of axial loaded MRI in patients with suspected instability as well.

E. Epidural Lipomatosis

Spinal epidural lipomatosis is a rare condition found in the thoracic and lumbar spine. The reason for the overgrowth of fat could be general obesitas, steroid therapy, or endocrinopathies, or it might be idiopathic. Symptoms could be induced by the abnormal amount of fat contributing to impingement on the dural sac. Recently Lisai et al. [53] published a study on three patients with idiopathic epidural lipomatosis. MRI was recommended as the diagnostic method of choice, and the patients were operated on. After 2 years the patients were neurologically normal.

At our institution several young men were examined due to low back problems lasting for a long time period. They had no history of steroid therapy or endocrinopathy, but two of them showed obesitas. Examination by CT and MRI in the supine position had been performed with no pathological findings. Later the patients underwent MRI examination in PRP as well as ACE. An extensive compression of the dural sac in ACE due to a great amount of epidural fat compressing the dural sac was found, in some cases at more than one disc level, (Fig. 4).

F. Effect of MRI in Axial Loading on Choice of Treatment

An evaluation of the impact of MRI of the lumbar spine in PRP and ACE on the decision concerning treatment of patients with neurogenic claudication and/or sciatica has been carried out [54]. In 6 of 20 (30%) patients the surgeons changed their opinions from conservative to operative treatment when they were shown the ACE images. One of the neurosurgeons changed his treatment decision to operative in four additional patients when reading the ACE images. The presented results require further evaluation but suggest a clear indication for ACE examination in selected patients.

VI. CONCLUSION

According to the above-mentioned results, the axially loaded (ACE) CT or MRI examination should be performed after conventional study in patients with neurogenic claudication and sciatica. The selection of patients for extended examination in axial loading is crucial. Axially loaded CT and MRI increase the detectability of pathology in the lumbar spine, which optimizes the radiological diagnosis, providing the physician with a more reliable basis for the decision as to treatment.

An axially loaded CT and MR examination of the patient should start with a conventional investigation in PRP to avoid loading of an osteoporotic or fractured spine or a spine with a skeletal malignancy representing contraindications for loading. Examination in extension alone will improve the diagnostic specificity to a certain extent and might be used in elderly people or in patients with clinical signs of osteoporosis.

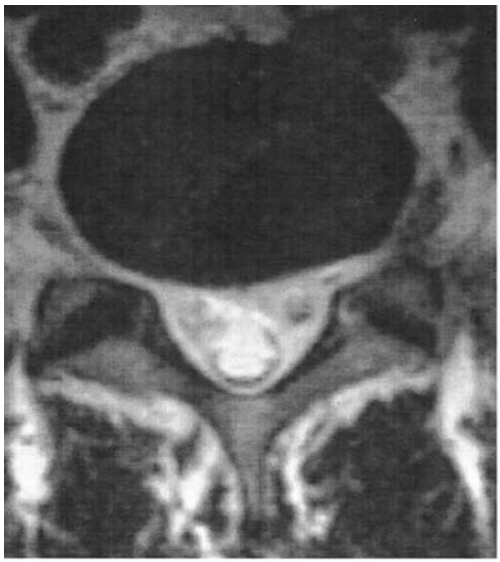

A

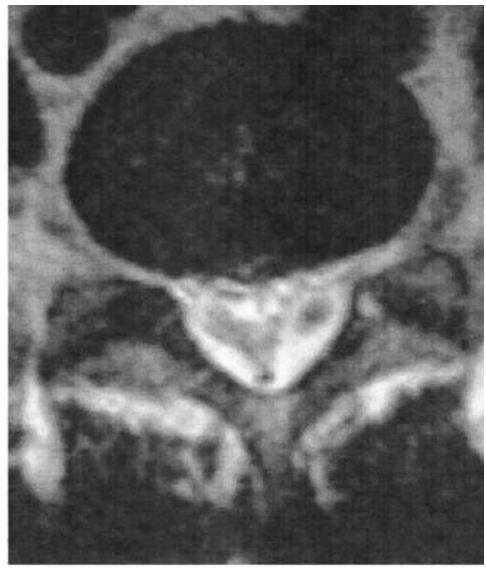

B

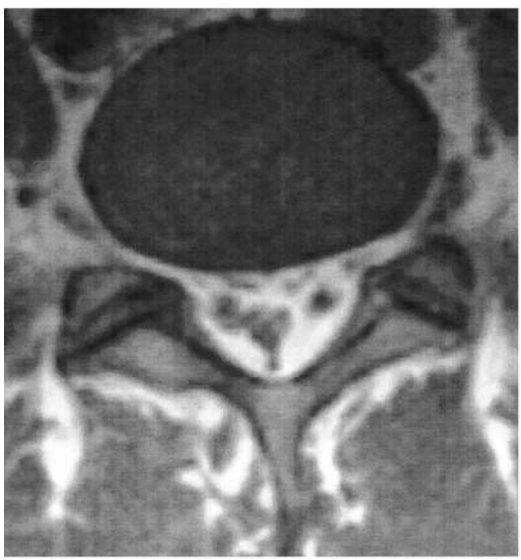

C

Figure 4 Male, 37 years of age, with neurogenic claudication of several years duration. L5–S1: A decrease in DCSA in ACE (B,C) compared to in PRP(A) due to epidural lipomatosis. (A,B) T_2-weighted; (C) T_1-weighted.

REFERENCES

1. Norlund AI, Wadell G. Cost of back pain in some OECD countries. In:. A.L. Nachemson, E. Jonsson, eds. Neck and Back Pain. The Scientific Evidence of Causes, Diagnosis, and Treatment. Philadelphia: Lippincott Williams & Wilkins, 2000:421–425.
2. Van Tulder MW, Koes BW, Bouter LM. A cost-of-illness study of back pain in the Netherlands. Pain 1995; 2:233–240.
3. Cats-Baril WL, Frymoyer JW. The economics of spinal disorders. In: J.W. Frymoyer, ed. The Adult Spine: Principles and Practice. New York: Raven Press, 1991:85–105.
4. Knutsson F. The instability associated with disc degeneration in the lumbar spine. Acta. Radiol 1944; 25:593–609.
5. Dupuis P, Doria C, Crissantu L, Meloni GB, Conti M, Achene A. Cauda equina syndrome secondary to idiopathic spinal epidural lipomatosis. Spine 2001; 26:307–309.
6. Putto E, Tallroth K. Extension-flexion radiographs for motion studies of the lumbar spine. Spine 1990; 15:107–110.
7. Panjabi MM, Takata K, Goel VK. Kinematics of lumbar intervertebral foramen. Spine 1983; 8: 348–357.
8. Selvik G. A stereophotogrammetric method for the study of the kinematics of skeletal system. Thesis, Lund AV-centalen, 1974.
9. Sortland O, Magnaes B, Hauge T. Functional myelography with metrizamide in the diagnosis of lumbar spinal stenosis. Acta. Radiol. Suppl 1977; 355:42–54.
10. Schumacher M. Die Belastungsmyelographie. Fortschr. Röntgenstr 1986; 145:642–648.
11. Amundsen T, Weber H, Lilleås F. Lumbar spinal stenosis. Clinical and radiological features. Spine 1995; 20:1178–1186.
12. Knutsson F. Volum- und Formvariationen des Wirbelkanals bei Lordosierung und Kyphosierung und ihre Bedeutung für die myelographische Diagnostik. Acta. Radiol 1942; 23:431.
13. Penning L, Wilmink JT. Biomechanics of the lumbosacral dural sac. A study of flexion-extension myelography. Spine 1981; 6:398–408.
14. Coulier B. Evaluation of lumbar canal stenosis: decubitus imaging methods versus flexion-myelography and surface measurements versus the diameter of the dural sac. JBR – BTR 2000; 83(2):61–67.
15. Schönström NSR, Bolender NF, Spengler DM. The pathomorphology of spinal stenosis as seen on CT scans of the lumbar spine. Spine 1985; 10:806–811.
16. Schönström NSR, Bolender NF, Spengler DM, Hansson TH. Pressure changes within the cauda equina following constriction of the dural sac. An in vitro experimental study. Spine 1984; 9:604–607.
17. Schönström NSR, Hansson T. Pressure changes following constriction of the cauda equina: an experimental study in situ. Spine 1988; 13:385–388.
18. Schönström NSR, Lindahl S, Willén J. Dynamic changes in the dimensions of the lumbar spinal canal. An experimental study in vitro. J. Orthop. Res 1989; 7:115–121.
19. Inufusa A, An HS, Lim TH, Hasegawa T, Haughton VM, Nowicki BH. Anatomic changes of the spinal canal and intervertebral foramen associated with flexion-extension movement. Spine 1996; 21:2412–2420.
20. Nowicki BH, Haughton VM, Schmidt TA. Occult lumbar lateral spinal stenosis in neural foramina subjected to physiologic loading. Am. J. Neuroradiol 1996; 17:1605–14.
21. Penning L, Wilmink JT. Posture-dependent bilateral compression of L4 and L5 nerve roots in facet hypertrophy. A dynamic CT-myelographic study. Spine 1987; 12:488–500.
22. Harvey SB, Smith FW, Hukins DW. Measurement of lumbar spin flexion-extension using a low-field open-magnet resonance scanner. Invest. Radiol 1998; 33:439–443.
23. Hamanishi C, Matukura N, Fujita M, Tomihara M, Tanaka S. Cross-sectional area of the stenotic lumbar dural tube measured from the transverse views of magnetic resonance imaging. J. Spinal. Disord 1994; 7:388–393.
24. Chung SS, Lee CS, Kim SH, Ahn JM. Effect of low back posture on the morphology of the spinal canal. Skeletal. Radiol 2000; 29:217–223.

25. Wildermuth S, Zanetti M, Duewell S, Schmid MR, Romanowski B, Benini A, Böni T, Hodler J. Lumbar spine: quantitative and qualitative assessment of positional (upright flexion and extension) MR imaging and myelography. Radiology 1998; 207:391–398.
26. Schmid MR, Stucki G, Duewell S, Wildermuth S, Romanowski B, Hodler J. Changes in cross sectional measurements of the spinal canal and intervertebral foramina as a function of body position: in vivo studies on an open-configuration MR system. A.J.R 1999; 172:1095–1102.
27. Zamani AA, Moriarty T, Hsu L, Winalski CS, Schaffer JL, Ibister H, Schenck JF, Rohling KW, Jolesz F. Functional MRI of the lumbar spine in erect position in a superconducting open-configuration MR system: preliminary results. J. Magn. Reson. Imaging 1998; 8:1329–1333.
28. Weishaupt D, Schmid MR. Positional MR imaging of the lumbar spine: does it demonstrate nerve root compromise not visible at conventional MR imaging? Radiology 2000; 215:247–253.
29. Nachemson A, Elfström G. Intravital dynamic pressure measurements in lumbar discs. Scand. J. Rehabil. Med 1970; 1:1–40.
30. Kimura S, Steinbach GC, Watenpaugh DE, Hargens A. Lumbar spine disc height and curvature responses to an axial load generated by a compression device compatible with magnetic resonance imaging. Spine 2001; 26:2596–2600.
31. Jensen MC, Brant-Zawadzki MN, Obuchowski N, Modic MT, Malkasian D, Ross JS. Magnetic resonance imaging of the lumbar spine in people without back pain. N. Engl. J. Med 1994; 14(331): 69–73.
32. Symmons DP, van Hemert AM, Vandenbroucke JP, Valkenburg HA. A longitudinal study of back pain and radiological changes in the lumbar spines of middle aged women. II. Radiographic findings. Ann. Rheum. Dis 1991; 50:162–166.
33. Wiesel SW, Tsourmas N, Feffer HL, Citrin CM, Patronas N. A study of computer-assisted tomography. I. The incidence of positive CAT scans in an asymptomatic group of patients. Spine 1984; 9: 549–551.
34. Witt I, Vestergaard A, Rosenklint A. A comparative analysis of x-ray findings of the lumbar spine in patients with and without lumbar pain. Spine 1984; 9:298–300.
35. Healy JF, Healy BB, Wong WH, Olson EM. Cervical and lumbar MRI in asymptomatic older male lifelong athletes: frequency of degenerative findings. J. Comput. Assist. Tomogr 1996; 20:107–112.
36. Boden SD, Davis DO, Dina TS, Patronas NJ, Wiesel SW. Abnormal magnetic-resonance scans of the lumbar spine in asymptomatic subjects. A prospective investigation. J. Bone Joint Surg. [Am.] 1990; 72:403–408.
37. Greenberg JO, Schnell RG. Magnetic resonance imaging of the lumbar spine in asymptomatic adults. Co-operative study=MAmerican Society of Neuroimaging. J. Neuroimaging 1991; 1:2–7.
38. Danielson BI, Willén J. Axially loaded magnetic resonance image of the lumbar spine in asymptomatic individuals. Spine 2001; 26:2601–2606.
39. Danielson BI, Willén J, Gaulitz A, Niklason T, Hansson TH. Axial loading of the spine during CT and MR in patients with suspected lumbar spinal stenosis. Acta. Radiol 1998; 39:604–611.
40. Willén J, Danielson B, Gaulitz A, Niklason T, Schönström N, Hansson T. Dynamic effects on the lumbar spinal canal. Axially loaded CT-myelography and MRI in patients with sciatica and/or neurogenic claudication. Spine 1997; 22:2968–2976.
41. Willén J, Danielson BI. The diagnostic effect from axial loading of the lumbar spine during computed tomography and magnetic resonance imaging in patients with degenerative disorders. Spine 2001; 26:2607–2614.
42. Tallroth K, Lindgren KA, Willén J. Axial loading of the lumbar spine in CT scanning. A valuable complement in the diagnosis of central spinal stenosis. Poster at the Nordic Orthopaedic Federation, Tampere, Finland, 2000.
43. Schöllhammer M, Schmid GJ, Willburger R, Köster O, Jergas M. Poster at German Radiology meeting, Wiesbaden, Germany, 2002.
44. Amendy J, Watura R, Goddard P. Presentation at the British Radiology meeting, Birmingham, United Kingdom, 2002.
45. Kahn S, Hemmer JF, Erly WK, Seeger JF. MR scanning of the lumbosacral spine during simulated upright positioning. Presentation No. 14, Symposium and ASNR 40th meeting, Vancouver, Canada, 2002.

46. Hamanishi C, Matukura N, Fujita M, Tomihara M, Tanaka S. Cross-sectional area of the stenotic lumbar dural tube measured from the transverse views of magnetic resonance imaging. J. Spinal. Disord 1994; 7:388–393.
47. Jespersen S, Hansen E, Hoy K, Christensen K, Lindblad B, Ahrensberg J, Bunger C. Two-level spinal stenosis in minipigs. Hemodynamic effects of exercise. Spine 1995; 24:2765–2773.
48. Takahashi K, Olmarker K, Holm S. Double level cauda equina compression: an experimental study with continuous monitoring of intraneural blood flow in the porcine cauda equina. J. Orthop. Res 1993; 11:104–109.
49. Olmarker K. Spinal nerve root compression. Nutrition and function of the porcine cauda equina compressed in vivo. Acta. Orthop. Scand. Suppl 1991; 242:1–27.
50. Porter R, Ward D. Cauda equina dysfunction. The significance of two-level pathology. Spine 1992; 17:9–15.
51. Kurz LT, Garfin SR, Unger AS, Thorne RP, Rothman RH. Intraspinal synovial cyst causing sciatica. J. Bone Joint Surg. AM 1985; 67-A:865–871.
52. Mailleux P, Ghosez JP, Bosschaert P, Malbecq S, Coulier B. Distension of the inter-facet joints in MRI: and indirect sign of an existing underestimation of spondylolisthesis and canal stenosis. J. Belge. Radiol 1998; 8:283–285.
53. Lisai P, Doria C, Crissantu L, Meloni G, Maurisio C, Achene A. Cauda equina syndrome secondary to idiopathic spinal epidural lipomatosis. Spine 2001; 26:307–309.
54. Westesson PL, Hiwatashi A, Moritani T, Danielson B. Presentation at RSNA. Radiological Society of North America, 88th Annual Meeting. Chicago, 2002.

10

Experience with OP-1 in a Rabbit Model of Lumbar Fusions

Jonathan S. Erulkar, Jonathan N. Grauer, Tushar Ch. Patel, and Gary E. Friedlaender
Yale University School of Medicine
New Haven, Connecticut, U.S.A.

I. INTRODUCTION

Spinal fusion is a common surgical procedure with multiple indications. Regardless of the technique used, bone grafting is essential to achieve bony fusion. However, there are limitations and risks associated with the current gold standard—autogenous iliac crest bone. Approximately 25–30% of patients who have iliac crest bone graft removed report chronic pain [1]. Pseudarthrosis occurs in as many as 50% of patients undergoing posterolateral fusions [2] and up to 70% of patients having anterior interbody fusions [3]. Results achieved using allogeneic, xenogeneic, and other synthetic grafting materials are not comparable to iliac crest bone autograft.

In addition to limitations of various grafting materials, several factors have been observed to further inhibit fusion. Smoking, for example, has been shown to increase the rate of pseudarthrosis two- to fivefold [4,5]. Osteoinductive proteins may provide a useful alternative, or adjunctive, means of improving outcomes.

The human cDNA for OP-1 (BMP-7) was first cloned in the late 1980s by Özkaynak et al. [6]. With this milestone acheived, OP-1 could be produced and purified in relatively large quantities using recombinant technology. The ability of OP-1 to induce new bone was first demonstrated in a rat muscle pouch. The bone formed was characterized by a cortical shell with normal-appearing medullary elements [7,8].

Cook et al studied OP-1 in spinal application by looking at posterior fusions in a canine model [9]. In this study, posterior fusion segments were evaluated biomechanically and histologically in adult dogs at 6, 12, and 26 weeks after surgery. OP-1–treated animals were completely fused by 12 weeks, compared with the autograft sites, which achieved fusion at 26 weeks after implantation. These results suggest that OP-1 implant might be effective in inducing fusion more rapidly than autogenous bone graft.

Other preclinical work has focused on lumbar interbody fusions in a sheep model using a dorsolateral approach with transpedicular fixation [10]. Three groups of sheep were implanted with autograft from the iliac crest, deproteinized bovine hydroxyapatite, or OP-1 implant. Biomechanically, the greatest rigidity was seen in sheep treated with autograft and OP-1 implant. The histological and histomorphometric evaluations of the fusion attempted with hydroxyapatite were characterized by pseudoarthrosis. Bone mineral density analysis of the OP-1 implant–in-

duced fusions exceeded the fusions in the autograft group by 40%. The mean fusion score based on plain radiographs and computed tomography (CT) images for the OP-1 implant–treated animals was statistically superior to iliac crest bone.

In addition to the above-referenced canine and sheep studies, the New Zealand white rabbit has been established as a model for posterolateral lumbar fusion [11–14]. The surgical technique used in these rabbits is similar to that used clinically. The observed pseudarthrosis rate of 33% with autograft in this model also mirrors clinical experiences [11]. Since its introduction, this pattern of fusion success rates has been reproduced at multiple centers [15–18].

With the New Zealand white rabbit model, the clinical observation that smoking interferes with fusion has also been confirmed [19,20]. Nicotine exposure decreased the rate of autograft fusion from 53–56% to 0% in the two reported studies. These results were determined by manual palpation and pull-apart biomechanical testing.

The objectives of our work were to define the functional, radiographic, and histological outcomes of OP-1–induced intertransverse process fusion in the New Zealand white rabbit model and to assess the ability of OP-1 to overcome the inhibitory effects of nicotine. To better characterize fusion in the New Zealand white rabbit, biomechanical three-dimensional flexibility testing was performed on nonoperative rabbit spines as well as those that underwent fusion surgery. The results of all work presented here have been previously published and are now summarized as an overview of several individual studies [21–24].

II. STUDY DESIGN

While the New Zealand white rabbit had been used previously as model for posterolateral fusion, there had not been a biomechanical comparison of the rabbit and human lumbar spines accomplished for other animal models such as the calf [25,26] and sheep [27]. The first portion of our work compared physiological biomechanics of non-operative rabbit lumbar spines to previous data of cadaveric human spines. In addition, the biomechanics of autograft fused rabbit spines were compared to that of the nonoperative spines. This work served as a basis for evaluation of OP-1 as a substitute for autograft in posterolateral fusion. Finally, the inhibitory effect of nicotine on posterolateral fusions was confirmed, and the ability of OP-1 to overcome that inhibitory effect was assessed.

First, 10 skeletally mature rabbit cadaveric lumbar spines were evaluated using biomechanical flexibility testing. For the subsequent portions of the study, single-level intertransverse process fusions were performed at the L5-L6 level of 49 New Zealand white rabbits (these animals have seven lumbar vertebrae) [12,28]. The rabbits were divided into five groups, receiving either: (1) autograft, (2) OP-1 with its commercially prepared carrier, (3) carrier alone, (4) autograft in the presence of nicotine, or (5) OP-1 with its carrier in the presence of nicotine. Animals in the nicotine groups were exposed to systemic nicotine via subcutaneous mini-osmotic pumps. Animals were sacrificed 5 weeks following surgery, and the success of fusions was evaluated by multiple testing modalities. This protocol was reviewed and approved by our institution's animal care and use committee.

III. CADAVERIC SPECIMENS FOR BIOMECHANICAL TESTING

Ten skeletally mature New Zealand white rabbit cadaveric spines were obtained. As noted above, this species had seven lumbar vertebrae. Osteo-ligamentous L4-L7 specimens were harvested en bloc. Specimens were dissected free of all soft tissues except for ligaments and joint capsules and then stored at $-20°C$ wrapped in saline-moistened gauze and sealed in double plastic bags

until testing was performed. Such storage conditions have been shown not to affect the outcome of standard biomechanical testing [29]. Biomechanical flexibility testing is described later in this section.

IV. POSTEROLATERAL FUSION TECHNIQUE

Surgical anesthesia was achieved with subcutaneous injection of acepromazine (0.75 mg/kg) followed by ketamine (15 mg/kg) and xylazine (2.5 mg/kg). The rabbits were then intubated, and isoflourane inhalation was used to maintain anesthesia. Enrofloxacin (5–10 mg/kg SC) was given subcutaneously immediately prior to surgery.

The rabbits were shaved, positioned, and prepped in a standard surgical fashion. A dorsal midline incision was made in the lumbar region. The L5 and L6 transverse processes were identified and exposed through two paramedian fascial incisions.

Autograft was recovered from all animals, regardless of the experimental group to which they would be assigned. This was done to expose all animals to the same operative stresses. Both iliac crests were exposed through separate fascial incisions, and approximately 2–3 cm^3 of corticocancellous graft was obtained. The crest sites were then irrigated, packed with gelfoam, and closed.

After irrigation, the transverse processes were decorticated with a power burr. The transverse process shavings produced by decortication were left in the lateral gutters in all cases.

One of the three graft materials had been selected preoperatively for each rabbit. The grafting materials were: (1) approximately 1–1.5 cm^3 of the recovered autograft per side, (2) 0.3 g of bovine collagen I matrix and 77 mg of carboxymethylcellulose per side (the commercially developed carrier for OP-1), or (3) the above carrier with 1.2 mg of OP-1 per side. This quantity of OP-1 was based upon previous studies [13,30] and was considered to be an appropriate volume for the fusion bed. The OP-1 /carrier grafting material has a putty-like consistency.

For those rabbits in the nicotine portion of the study, nicotine pumps were then implanted subcutaneously in the interscapular region. These miniosmotic pumps (Alzet, Palo Alto, CA) delivered 4.5 μg/kg/min of nicotine at a rate of 2.5 μL/hr. This dosing was based on earlier rabbit studies, which were able to achieve serum nicotine levels in the range of 10–70 mg/mL. [19,31,32] This range is comparable to those of a human smoking 20–30 cigarettes per day. [33–35]

Once the grafting material was placed and the incisions were closed, the rabbits were extubated. Postoperative radiographs were taken to confirm the level of fusion. Buprenex (0.04 mg/kg bid) and enrofloxacin (5 mg/kg qd) were given subcutaneously for 2 days following the procedure.

V. POSTOPERATIVE ANIMAL CARE

The rabbits were individually housed and monitored for 5 weeks. Serum levels of nicotine and nicotine's metabolite, cotinine, were monitored with initial and subsequent weekly blood sampling of all animals with nicotine pumps. Serum samples were collected, stored at −20°C, and later analyzed at an independent commercial laboratory.

A follow-up period of 5 weeks was chosen because fusions have been shown to be distinguishable from nonunions by this time. [12,28] Rabbits were given calcein (10 mg/kg sq) 1 and 11 days prior to sacrifice as a fluorescent marker of new bone mineralization for later histomorphometric examination. Rabbits were sacrificed with a sedating dose of subcutaneous ketamine followed by a lethal dose of intravenous pentobarbitol.

VI. EVALUATION OF SPECIMENS

The fusion masses of postoperative specimens were characterized and compared with manual, radiographic, biomechanical, and histological evaluations. As stated previously, 10 nonoperated cadaveric specimens were tested using biomechanical flexibility testing.

VII. MANUAL PALPATION TESTING

Manual manipulation has been thought of as an accurate indicator of successful lumbar fusion [28]. In the clinical setting, direct manual inspection at the time of surgical exploration is routinely used to establish whether or not a pseudarthrosis exists. In an analogous manner, two independent observers manually evaluated the rabbit lumbar spines for gross intervertebral motion immediately after sacrifice. Care was taken to limit the amount of force used to evaluate the fusion mass so as not to create gross trauma. Specimens were determined to be fused when no significant motion was noted by either observer.

VIII. RADIOLOGICAL EVALUATION

PA and lateral radiographs were taken to evaluate the fusion masses. Films were reviewed in a blinded fashion with fusion defined as calcification bridging from one transverse process to the next.

IX. THREE-DIMENSIONAL FLEXIBILITY TESTING

The superior (L4) and inferior (L7) vertebrae of harvested specimens were potted in resin mounts with the L5-L6 intervertebral disc oriented in the horizontal position. Screws were placed into the border vertebrae for additional fixation in the resin mounts.

The upper and lower mounts (representing L4 and L7) were fitted with Plexiglas motion detection flags on the lateral aspect of the specimen. L5 and L6 were fitted with similar flags attached to the vertebral bodies via pairs of 0.062 inch k-wires. Each flag was equipped with three noncolinear infrared light – emitting diodes designed for detection by an optoelectronic motion measurement system (Fig. 1). Radiographs were taken of each specimen to ensure that no underlying abnormalities or injuries were present and to ensure adequate positioning of the specimens.

To determine the multidirectional flexibility of the specimens, six pure moments (flexion and extension, left and right lateral bending, and left and right torsion) were applied to the upper vertebrae via a headpiece. This method of testing has been established and previously published for human specimens [36–38].

Human specimens were loaded to a maximum of 10 Nm in the studies referred to above. It was determined appropriate to decrease the testing moment applied to the rabbit spines in a body mass proportional fashion. Thus, a maximum moment of 0.27 Nm was selected for testing. The idea of loading based on body mass has been used in prior experiments [39].

Further validation of the selected testing moment was obtained from preliminary reproducibility experiments. Range of motion was found to be reproducible to 0.81° (0.68°) (mean ± SD) with the maximum testing moment of 0.27 Nm. This was felt to be within the error of the system and to indicate that no significant injury was produced by the loading protocol. Conversely, gross injury was observed with loading to 0.40 Nm.

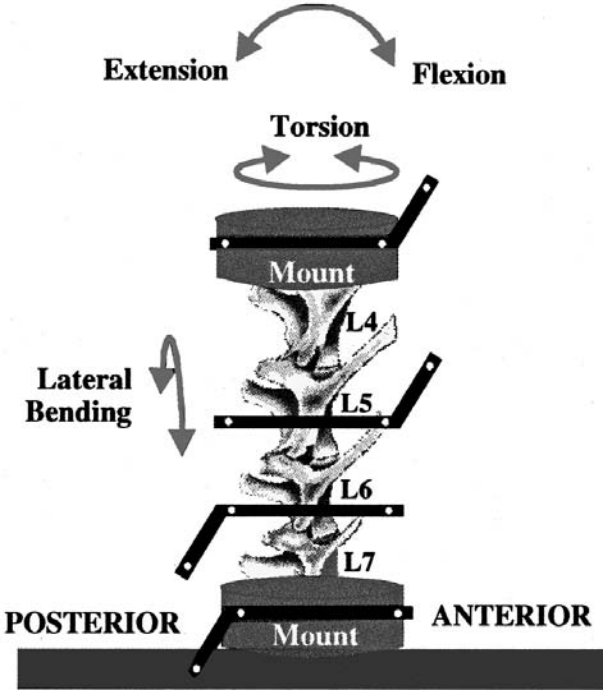

Figure 1 Biomechanical flexibility testing specimen preparation. Schematic of specimen as seen from the lateral perspective. Note the motion detection flags mounted on L5, L6, and both the upper and lower mounts. (From Ref. 22, courtesy of Lippincott, Williams and Wilkins.)

The testing protocol involved specimens loading in a stepwise fashion to the maximum load. Each step (0.00, 0.09, 0.18, and 0.27 Nm) was sequentially applied for 30 seconds to allow viscoelastic relaxation. A total of three load/unload cycles were performed for each motion studied, and data were gathered from the final loading cycle. This protocol had been established to minimize error due to the effects of creep.

X. HISTOLOGICAL ANALYSIS

Histological analysis was then performed to evaluate the regions of attempted fusion. This included an assessment of callus constituents: bone, cartilage, and fibrous tissue. Immediately after biomechanical testing, the L5-L6 spine segments were isolated and divided along the mid-sagittal plane. Each half specimen was prepared for either decalcified or undecalcified sectioning.

Specimens for decalcified sectioning were placed in buffered 10% formalin. After fixation, these specimens were decalcified in EDTA/HCL and embedded in paraffin. Six micrometer sections were stained with hematoxylin and eosin.

Specimens for undecalcified sectioning were dehydrated through graded ethanols, cleared in toluene under vacuum and pressure on a Tissue Tek VIP 2000 tissue processor. These specimens were then infiltrated with increasing concentrations of methylmethacrylate (MMA) and embedded in MMA. Five micrometer sections were stained with toluidine blue, pH 3.7. In addition, unstained 9 μm sections were obtained for analysis of fluorescent labeling.

XI. DATA ANALYSIS

In the nonoperative group, intervertebral rotations were calculated for each level. There were six main motions, corresponding to the six moments applied. For each direction of motion, range of motion (ROM) and neutral zone (NZ) were analyzed. ROM is defined as the displacement from initial neutral position of the specimen to that at the maximum load. NZ is defined as the motion from the initial neutral position to that at the unloaded position of the specimen at the beginning of the third load cycle. Results of all 10 specimens were averaged and standard deviations were calculated (mean $\pm$ SD).

For the autografted specimens, ROM and NZ were calculated. Changes in ROM and NZ were reported as percent changes from non-operative baseline specimens.

For the OP-1, autograft, and nicotine specimens, fusion rates as determined by manual palpation were compared using Fisher's exact test. Comparisons of biomechanical ROM data were made with unpaired Student's *t*-test. Comparisons of flexion ROM data of the three treatment groups (autograft, OP-1, and carrier alone) were made using one-way ANOVA analysis. The post hoc Scheffé test was performed on flexion ROM of individual groups to determine significant differences between groups. Significance for all tests was defined as $p < 0.05$.

XII. RESULTS

A. Baseline Cadaveric Spines

Figure 2 shows the motions of the L5-L6 intervertebral level as seen in the stepwise loading protocol. This is shown as representative of the three levels studied in this experiment. A signifi-

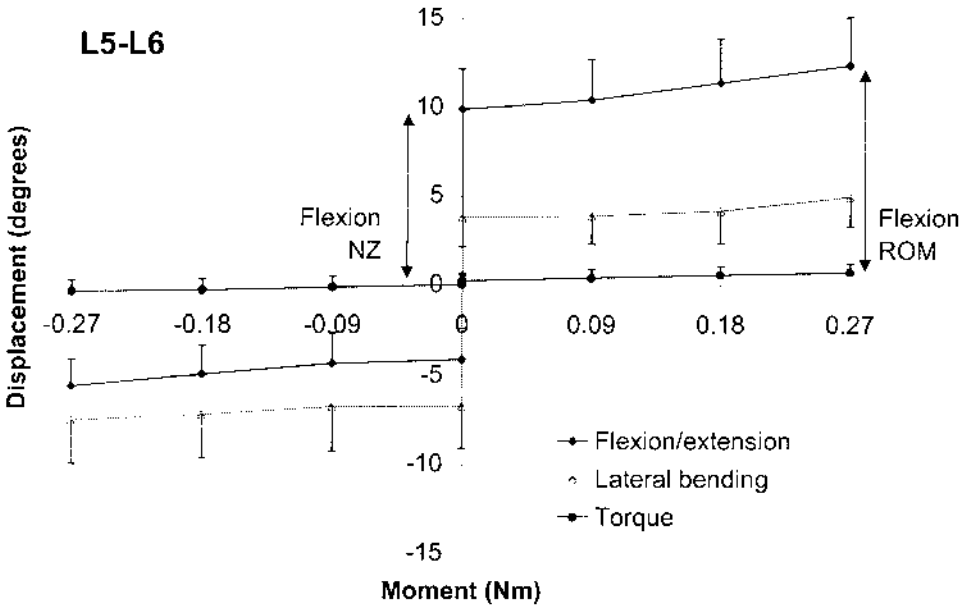

Figure 2 Biomechanical data of the normal rabbit spine. Mean (SD) measures of each main motion of the L5–L6 intervertebral level of the rabbit spine. Marked is the flexion NZ and ROM as examples of parameters drawn from testing protocol. (From Ref. 22, courtesy of Lippincott, Williams, and Wilkins.)

cant portion of the motion for each direction of applied moment was due to the NZ with a gradual increase in displacement with subsequent loading up to ROM with the application of 0.27 Nm.

Flexion and extension are independent study parameters. Lateral bending and torque are expected to be symmetrical due to the symmetry of the lumbar spine. The differences in these data are comparable to those in reported human data [38].

The three levels tested had roughly similar ROM and NZ parameters. There was a trend toward increased flexion and decreased lateral bending moving caudad through the levels tested. The greatest motion for each level tested was in flexion, with lesser motion in extension and lateral bending, and least motion with torque.

B. Surgical Complication Rates

Of the 49 rabbits receiving surgical fusion, 10 were excluded (20.4%): 5 due to sub-clinical deep infections discovered at the time of sacrifice, 4 due to anesthetic-related complications, and one due to sciatic nerve compression from the iliac crest harvest site. This complication rate is comparable to previous studies using this model (20%) [11]. Of the remaining 39 rabbits, 8 were in autograft, OP-1, carrier-alone, and nicotine-exposed autograft groups. Seven rabbits were in the nicotine-exposed OP-1 groups.

C. Autograft Spines

By manual palpation, five of the eight rabbits had solid fusions (63%). There were no differences in opinion between the two observers regarding the fusion status of the specimens.

Radiographically, fusion masses were visualized (Fig. 3). However, as all specimens were interpreted to have some bridging trabecular bone, all radiographs were read as fused. In other words, the method of determining fusion was very nonspecific.

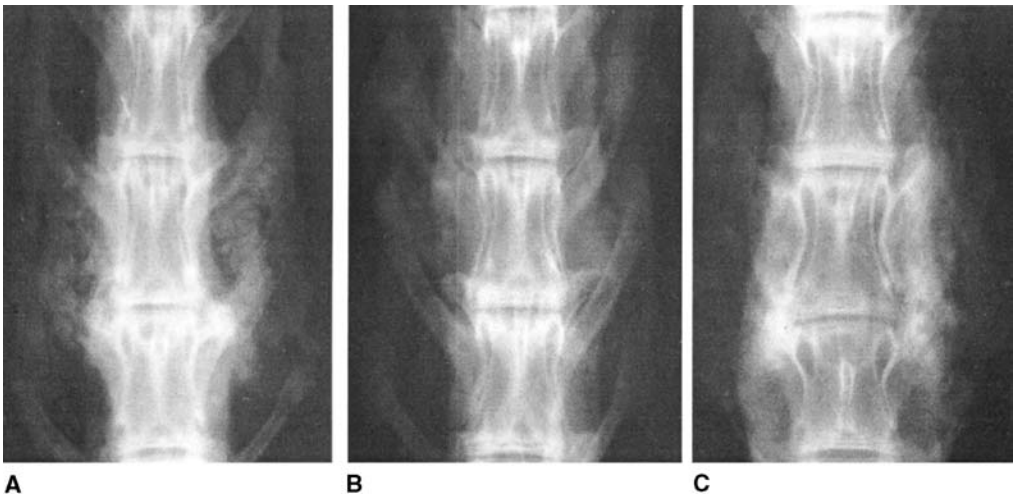

Figure 3 Autograft, carrier, and OP-1 spine radiographs. Representative PA radiographs of rabbit spines grafted with autograft (A), carrier alone (B), and OP-1 (C) 5 weeks postoperatively. (From Ref. 23, courtesy of Lippincott, Williams, and Wilkins.)

The ROM of the fused specimens was significantly decreased from that of baseline nonoperated specimens in flexion (81%), extension (61%), and right and left lateral bending (67% and 83%). Right and left axial rotations, which had significantly smaller baseline values than the other motions, were without significant change.

Those specimens determined to be unfused by manual palpation were similarly studied biomechanically. This group consisted of three specimens. In comparison to baseline non-operative flexibility data, the unfused specimens had a decrease in flexion ROM (51%). In flexion, the ROM of fused specimens had an additional decrease of 63% from the unfused specimens. Thus, the pseudarthrosis specimens represented a distinct intermediate stability between the baseline and fused specimens. Flexion ROM data for both fused and unfused specimens are shown in Figure 4.

Similar to ROM, the NZ of the fused specimens was significantly decreased from that of baseline nonoperated specimens in flexion (85%), extension (65%), and left lateral bending (88%). In comparison to baseline nonoperative flexibility data, the unfused specimens had a decrease in flexion NZ (50%). In flexion, the NZ of fused specimens had an additional decrease of 71% from the unfused specimens.

D. OP-1 and Carrier-Alone Spines

By manual palpation, none of the carrier-alone–treated rabbits fused (0%), and all rabbits receiving OP-1 fused (100%). Both autograft and OP-1 fusion rates, as determined by manual palpation, were significantly different from the carrier alone group, but were not significantly different from each other.

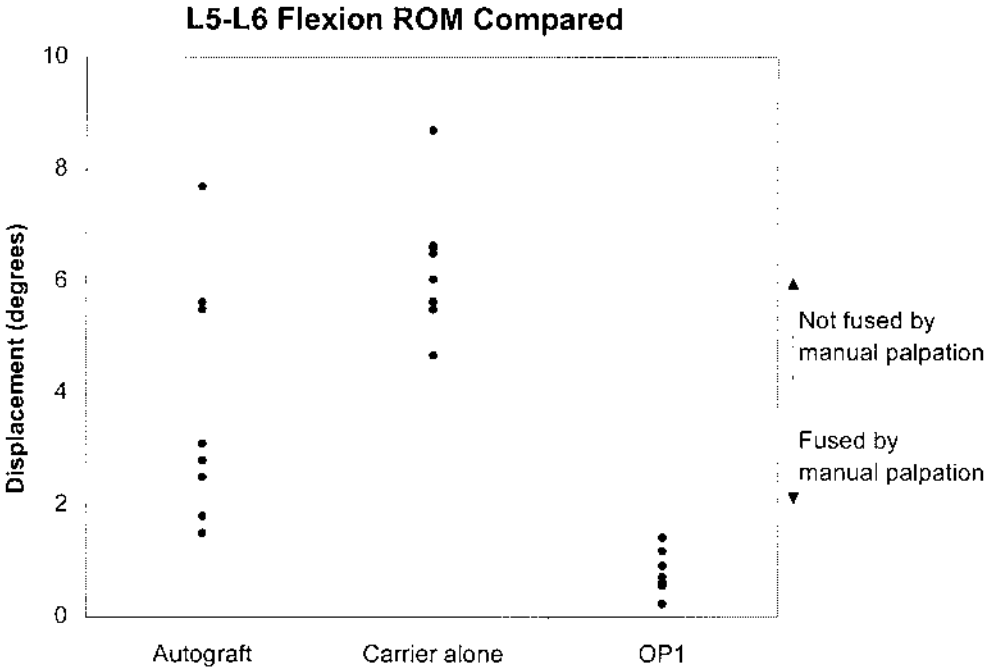

Figure 4 Flexion data of autograft, carrier, and OP-1 spines. L5–L6 flexion ROM for each specimen of the three study groups: autograft, carrier alone, and OP-1. The gray region represents fused versus unfused specimens as determined by manual palpation. (From Ref. 23, courtesy of Lippincott, Williams, and Wilkins.)

Radiographically, six of the eight carrier-alone specimens were correctly determined to be unfused, but two were incorrectly thought to be fused. Seven of the eight OP-1 specimens were correctly determined to be fused, but one was incorrectly thought to be unfused.

Overall, radiographs were 92% sensitive and 55% specific for determining fusion with a positive predictive value of 71% and negative predictive value of 86%.

The results of biomechanical testing further characterized the fusion masses. Based on findings from cadaveric rabbit spines (presented above), flexion was determined to be the best indicator for fusion as it was the direction of greatest motion for the rabbit lumbar spine. Fusion ROM is shown graphically for each specimen in Figure 4. Of the autograft specimens, the five that were fused by manual palpation had 2.3° (0.7°) of flexion. Conversely, those that were unfused by manual palpation had 6.3° (1.2°) of flexion. The OP-1–treated specimens, which were fused by manual palpation, had 0.8°(0.4°) of flexion. The carrier-alone specimens, which were unfused by manual palpation, had 6.3° (1.1°) of flexion. The differences in flexion ROM between the three groups were significant using one-way ANOVA analysis ($F = 28.6$). Furthermore, post hoc Scheffé tests revealed that flexion ROM data of autograft, OP-1, and carrier-alone groups were significantly different from each other. Not surprisingly, there was little difference between the flexion ROM of the unfused autograft specimens and the carrier-alone specimens. In addition, the OP-1 specimens had significantly less flexion than fused autograft specimens.

Similar to flexion ROM described above, multidirectional ROMs for OP-1 specimens were significantly less than those of autograft fused specimens in extension and lateral bending. Fewer statistically significant conclusions can be made from the nonflexion motions. Rotation, for example, has limited motion, even in the intact rabbit lumbar spine.

Histological sections were analyzed using several staining preparations. Toluidine blue staining highlighted the regions of calcification. Low magnification images are shown in Figure 5. Calcified islands were seen in the autograft fusion masses corresponding to the original grafting material. Essentially no calcified material was seen in the carrier-alone fusion masses. Conversely, bridging calcification was clearly seen in the OP-1 fusion masses.

Higher-magnification toluidine blue and hematoxylin and eosin staining further defined the fusion masses. Similar to a previous description [11,28], autograft fusion masses were characterized predominantly by cartilaginous tissue and small amounts of fibrous tissue between bone graft fragments. High magnification revealed multinucleated cells around the bone graft fragments.

The intertransverse region of the carrier-alone specimens demonstrated moderate fibrous tissue and remnants of the reabsorbing collagen-based carrier. Despite endochondral bone formation around the decorticated surfaces of the transverse processes, no intertransverse callus was seen. There was also no significant inflammatory reaction appreciated.

OP-1–induced fusion masses were characterized by a cortical rim of woven bone surrounding trabecular bone. While small amounts of cartilaginous material were present, the OP-1 fusion masses were predominantly maturing bone. High magnification revealed significant osteoblast activity.

Calcein fluorescent staining confirmed active mineralization fronts in the OP-1 specimens. This was present to a lesser extent in the autograft specimens and was negligible in the carrier-alone specimens.

E. Nicotine-Exposed Spines

Weekly nicotine and cotinine levels were determined by gas chromatography. As previously reported, the standard deviations of these values were substantial [27,28]. The average nicotine

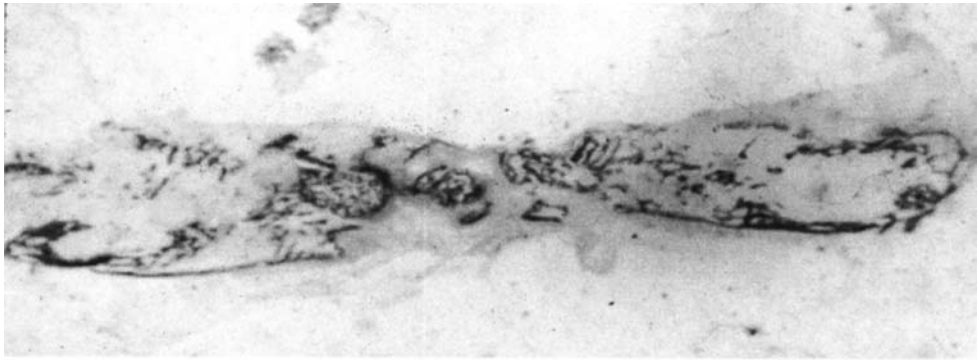

A. Autograft specimen

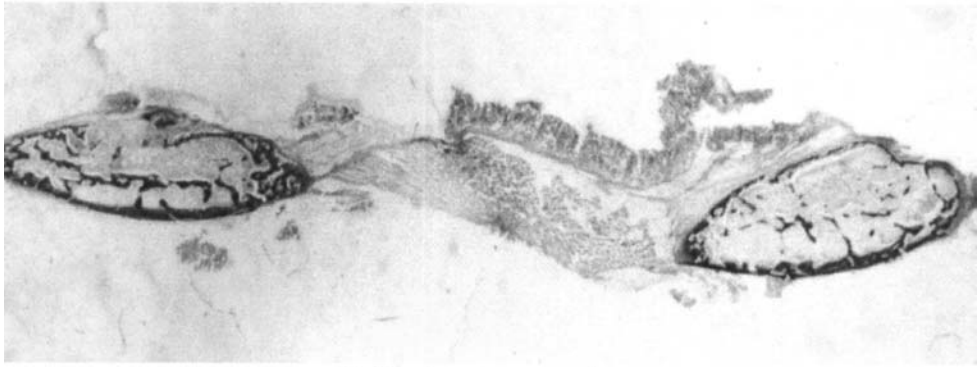

B. Carrier alone specimen

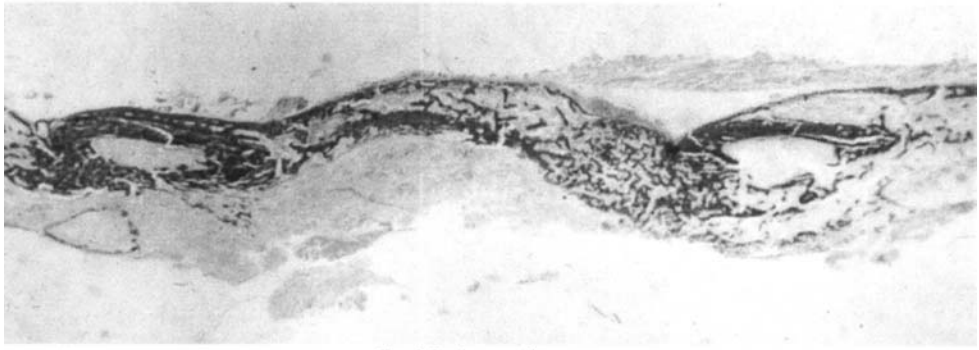

C. OP-1 specimen

Figure 5 Sagittal histology of autograft, carrier-alone, and OP-1 specimens. Toluidine blue–stained sagittal sections of L5 and L6 transverse processes and associated intertransverse regions. Autograft (A), carrier-alone (B), and OP-1 (C) specimens are shown (2.5 × magnification). (From Ref. 23, courtesy of Lippincott, Williams, and Wilkins.)

value for each time point studied was within the target range of 10–70 ng/mL. No clinical signs of nicotine toxicity were noted.

By manual palpation, two of the eight nicotine-exposed autograft rabbits fused (25%). This is less than the five of eight autograft fusions in rabbits not exposed to nicotine (63%) (presented above). These results are consistent with the inhibitory effect of nicotine on fusion, which has previously been reported [19,20]. Of note, the two nicotine-exposed autograft rabbits that were fused at 5 weeks had nicotine levels within the range of the other rabbits.

By manual palpation, all of the nicotine-exposed OP-1 rabbits fused (100%). This fusion rate is comparable to the 100% fusion rate of OP-1 rabbits not exposed to nicotine (presented above). In comparing fusion rates of the two nicotine-exposed groups, OP-1 specimens had a significantly higher fusion rate than autograft specimens (chi-squared analysis).

Radiographically, five of seven nicotine-exposed OP-1 rabbits were determined to be fused (Fig. 6). Thus, two of the fused nicotine-exposed OP-1 specimens were misinterpreted by radiographic assessment. Of the nicotine-exposed autograft rabbits, three of the six unfused specimens were interpreted to be unfused. One of the two nicotine-exposed autograft specimens that fused was interpreted to be fused. Overall, radiographs were 67% sensitive and 50% specific for determining fusion with a 67% positive predictive value and 50% negative predictive value.

Flexion ROM data of the nicotine exposed specimens are shown in Figure 7. Of the nicotine-exposed autograft specimens, the six that were unfused by manual palpation had 4.2° (0.8°) of flexion. Conversely, those that were fused by manual palpation had significantly less

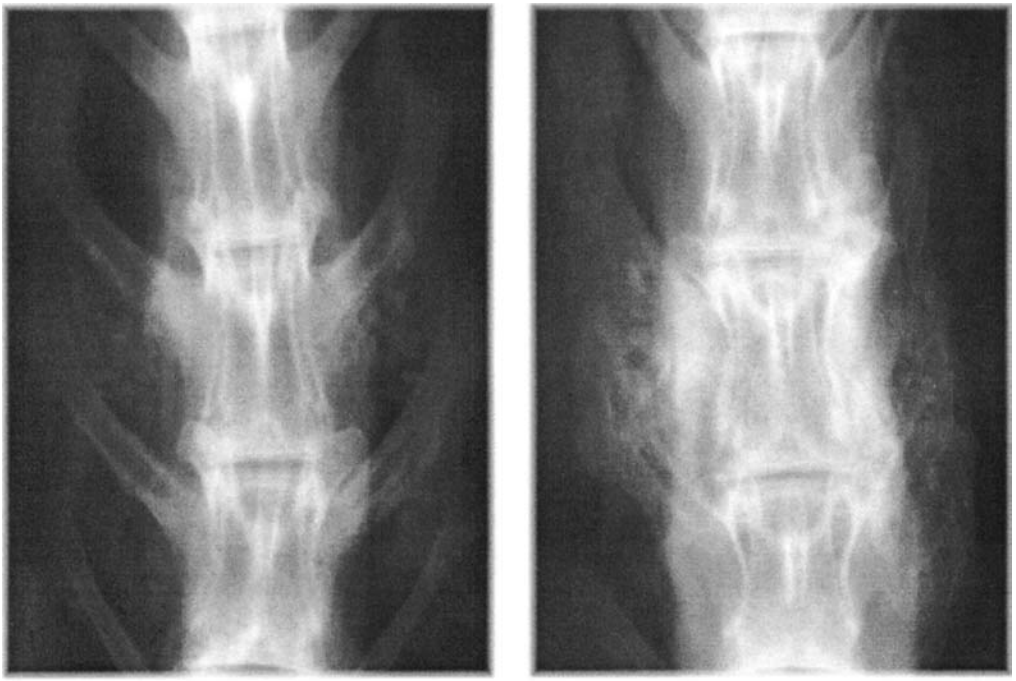

Figure 6 Nicotine-exposed autograft and OP-1 spine radiographs. Representative PA radiographs of nicotine-exposed specimens grafted with autograft (A) and OP-1 (B). (From Ref. 24, courtesy of Lippincott, Williams, and Wilkins.)

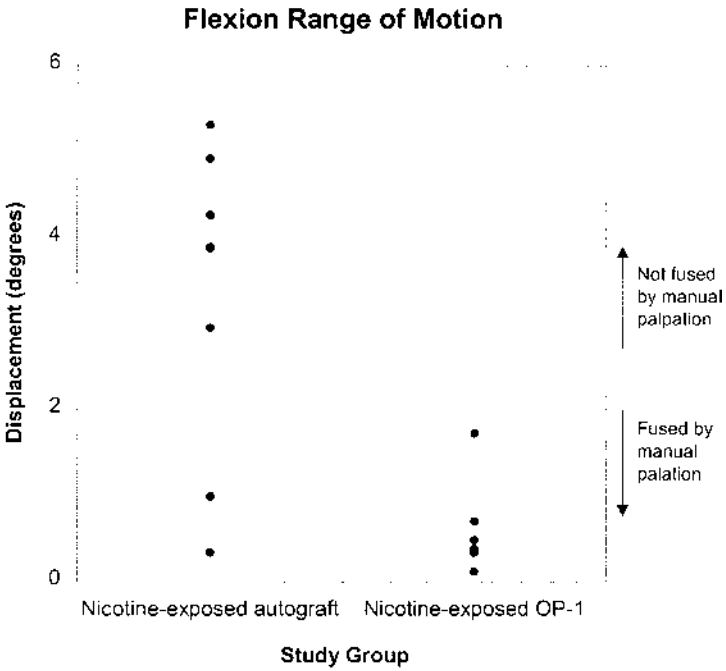

Figure 7 Flexion ROM data for nicotine-exposed autograft and OP-1 spines. Flexion ROM for each nicotine-exposed specimen from the autograft and OP-1 study groups. The labels on the right divide the specimens that were fused by manual palpation from those that were not fused by manual palpation. (From Ref. 24, courtesy of Lippincott, Williams, and Wilkins.)

flexion [0.7° (0.5°)] (students' *t*-test). The seven nicotine-exposed OP-1 specimens, which were all fused by manual palpation, had 0.6° (0.5°) of flexion.

The differences in flexion ROM between autograft and OP-1 groups with and without nicotine were significant using one-way ANOVA analysis ($F = 9.87$). Furthermore, post hoc Scheffé tests revealed that flexion data of autograft/nicotine and OP-1/nicotine groups were significantly different. In addition, there was little difference between flexion data of the OP-1 group with nicotine and the OP-1 group without nicotine.

Histological sections were analyzed using several staining preparations. Toluidine blue staining highlighted the regions of calcification. Low-magnification images are shown in Figure 8. Calcified islands corresponding to the original graft material characterized the nicotine-exposed autograft specimens. Calcified bridging was clearly seen in the nicotine-exposed OP-1 group. The fusion masses of this latter group were notable for a bony cortical rim with central trabecular bone.

Higher-magnification toluidine blue and hematoxylin and eosin staining further defined the fusion masses. Nicotine-exposed autograft fusion masses, particularly in the unfused specimens, were characterized by minimal amounts of cartilaginous and fibrous tissue between bone graft fragments. As seen on low magnification, the nicotine-exposed OP-1 fusion masses were characterized by a maturing bony callus. High magnification of the OP-1 fusion masses revealed significant osteoblast activity and substantial osteoid formation indicative of newly forming bone.

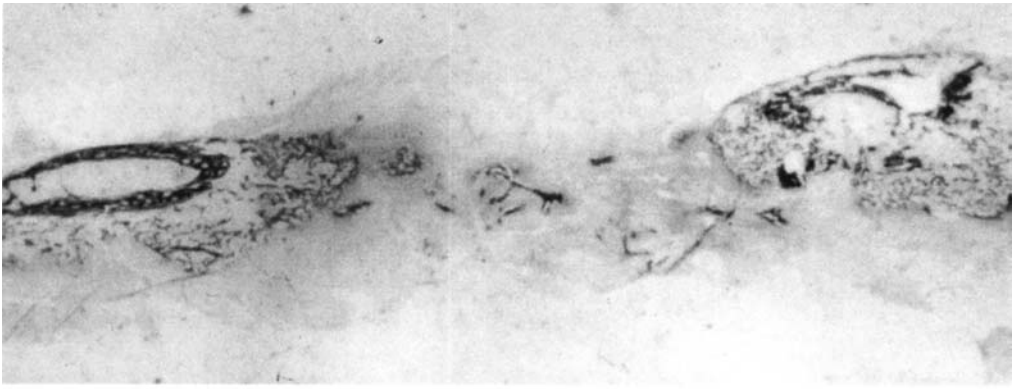

A. Nicotine-exposed autograft specimen

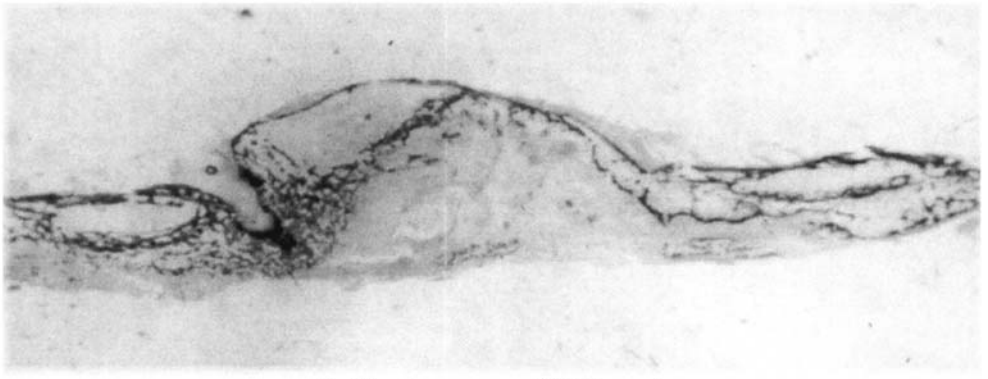

B. Nicotine-exposed OP-1 specimen

Figure 8 Sagittal histology specimens of nicotine-exposed specimens. Toluidine blue–stained sagittal sections of L5 and L6 transverse processes and associated intertransverse regions of nicotine-exposed autograft (A) and OP-1 specimens (B) (2.5 × magnification). (From Ref. 24, courtesy of Lippincott, Williams, and Wilkins.)

Calcein fluorescent staining confirmed active mineralization fronts in the OP-1 specimens. Fluorescent staining was negligible around the islands of bone graft found in the autograft group.

XIII. DISCUSSION

Our work used the New Zealand white rabbit model to perform in vitro characterizations of in vivo fusions using the techniques of manual palpation, radiography, biomechanical multidirectional flexibility testing, and histological analysis.

The autograft fusion rates reported in our work (62.5%) closely approximate previously reported fusion rates using the rabbit model (66%) [11].

While radiography was reasonably successful in identifying fusion masses, the technique was not useful in identifying pseudarthrosis. This is consistent with previous studies that have found a limited role for plane radiographs in defining fusion. Kant et al. found clinical radio-

graphs to be only 68% specific for detecting fusion as compared to manual palpation during surgical exploration [40].

Physiological biomechanical flexibility testing offers a precise method to characterize the changes in physiological motion that result from spinal fusion. In our study, posterolateral fusion led to significant stabilization of the L5–L6 motion segment with significant ROM decreases in flexion, extension, and lateral bending of 61–83%.

Overall, these findings suggest that successful fusion significantly limits, but does not eliminate, intervertebral motion at the time point studied. This may be due to small amounts of motion through the fusion masses or intervertebral motion despite solid posterolateral fusion. However, the findings of this study should remind the clinician that the primary goal of fusion surgery is spinal stabilization sufficient to eliminate pain and not necessarily to completely eliminate motion.

Unfortunately, the correlation between biomechanical stabilization and pain relief is a difficult one to study. As such, a limited number of studies have attempted to define this correlation. An in vivo study showed that external fixation relieved pain in 89% of patients with suspected cervical spine instability [41]. In addition, an in vitro study documented a marked reduction in motions of the cervical spine after external fixation [42]. While a direct correlation cannot be made, these two studies suggested that it was the reduction in motion caused by external fixation that reduced pain in a significant portion of the clinical study group. Undoubtedly, further information is needed regarding the minimum amount of stabilization necessary for relief of pain.

Bone morphogenetic proteins are being evaluated as potential substitutes for bone autograft in a wide variety of clinical circumstances. A primary goal of this study was to evaluate OP-1 as a bone graft substitute in posterolateral fusions using the New Zealand white rabbit model. Biomechanical flexibility testing revealed five of eight the autograft rabbits to be fused. This fusion rate was consistent with previous reports [11]. The histological appearance of these fusion masses showed an immature combination of bone and cartilage.

OP-1 induced fusion in all eight of the treated rabbits. This is higher than that seen with autograft, and is consistent with the fusion rate described for BMP-2 [14]. While fusion rates of OP-1 determined by manual testing were not significantly different from autograft fusion rates, biomechanical testing revealed that OP-1 fusions were more stable than the time-matched autograft fusions. Histologically, the OP-1 – induced fusion masses were characterized by predominantly remodeling bone that was more mature than that associated with autograft. This suggests that the fusion process was occurring more rapidly with OP-1 than with autograft.

Conversely, carrier alone did not induce fusion. The carrier is an important component of any potential bone graft alternative. This distributes the osteoinductive agent while keeping it in the desired location. In this case, the carrier was clearly not responsible for the osteogenic response. Of note, the bovine collagen I matrix/carboxymethylcellulose carrier was free of any significant inflammatory response.

OP-1 appears to be an effective bone graft alternative for intertransverse process spine fusion in the New Zealand white rabbit model. Our results are consistent the earlier findings of Cook et al. [43] and are more strongly encouraging than the results of Paramore et al. [44]. Nevertheless, clinical trials will be required to demonstrate to what degree these results can be replicated in humans.

Many questions remain. As noted, the carrier is an important component of any such implant. Not only does the carrier direct the BMP distribution, it also offers the potential for osteoconductive properties. Handling characteristics are also relevant. Additionally, the optimal dose of BMPs must be defined (this was beyond the scope of our previous studies).

Finally, we evaluated autograft- and OP-1 – induced posterolateral fusions that were exposed to systemic nicotine. It has previously been shown that nicotine inhibits posterolateral autograft lumbar fusion [19,20]. The present study similarly showed a decrease in autograft fusion rate from 63% to 25% with the introduction of systemic nicotine. As observed in prior studies [45] nicotine appeared to retard or preclude a successful bony healing process at the histological level.

OP-1 has been shown to induce 100% posterolateral lumbar fusions in the rabbit model in the absence of nicotine exposure. This rate of fusion is now shown to persist in the presence of systemic nicotine. The ability of OP-1 to induce fusion was demonstrated with manual and biomechanical testing. Histologically, maturing bony callus with a cortical rim was seen in the OP-1 study group despite the presence of nicotine.

As only one time point was evaluated in this study, no significant delay in bony repair could be determined for the nicotine-exposed OP-1 – induced fusion masses. However, there may have been an initial delay in healing which was not evident later in the healing process.

Further, it is possible that additional nicotine-exposed autograft specimens may have gone onto fusion with additional time. We are unable to differentiate, on the basis of this study, whether nicotine delays or prevents a proportion of posterolateral spine fusions. Nevertheless, it is clear that OP-1 is able to induce more mature fusion masses than autograft at the 5-week time point studied in this model. In addition, the success of OP-1 to achieve such fusions without the use of autograft implies the morbidity associated with autograft retrieval may be avoided in the future.

Overall, OP-1 appears able to overcome the inhibitory effects of nicotine on spinal fusion. While the role of OP-1 in the clinical setting remains to be defined, the final portion of the study suggests that OP-1 may be beneficial to the smoking patient in whom autograft may not provide reliable posterolateral lumbar fusion.

Since this initial validation of the osteoinductive capability of OP-1, extensive preclinical and clinical research has been done to examine the safety and efficacy of this protein in various animal and clinical studies [46–48]. Based upon this experience, OP-1 implant has been approved for some clinical uses by the regulatory authorities in the European Community, Canada, Australia, New Zealand, as well as the United States (under a Humanitarian Device Exemption).

REFERENCES

1. Summers BN, Eisenstein SM. Donor site pain from the ilium. A complication of lumbar spine fusion. J. Bone Joint Surg 1989; 71B:677–80.
2. Herkowitz HN, Kurz LT. Degenerative lumbar spondylolisthesis with spinal stenosis. J. Bone Joint Surg. (Am) 1991; 73:802–808.
3. Steinmann JC, Herkowitz HN. Pseudarthrosis of the spine. Clin. Orthop 1992; 284:80–90.
4. Blumenthal SL, Baker J, Dossett A, Selby DK. The role of anterior lumbar fusion for internal disc disruption. Spine 1986; 13:566–569.
5. Brown CW, Orme TJ, Richardson HD. The rate of pseudoarthrosis (surgical nonunion) in patients with are smokers and patients who are nonsmokers: a comparison study. Spine 1986; 11:942–943.
6. Özkaynak E, Rueger DC, Drier Ea. OP-1 cDNA encodes an osteogenic protein in the TGF-beta family. EMBO J 1990; 9:2085–2093.
7. Asahina I, Sampath TK, Hauschka PV. Human osteogenic protein-1 induces both chondroblastic and osteoblastic differentiation of osteoprogenitor cells derived from newborn rat calvaria. J. Cell. Biol 1994; 123:921–933.
8. Sampath TK, Maliakal JC, Hauschka PV. Recombinant human osteogenic protein-1 (HOP-1) induces new bone formation in vivo with a specific activity comparable with natural bovine osteogenic

protein and stimulates osteoblast proliferation and differentiation in vitro. J. Biol. Chem 1992; 267: 20352–20362.
9. Cook SD, Dalton JE, Tan EH. In vivo evaluation of recombinant human osteogenic protein (rhOP-1) implants as a bone graft substitute for spinal fusions. Spine 1994; 19:1655–1663.
10. Magin MN. Enhancement of lumbar vertebral interbody fusion by human recombinant osteogenic protein-1, OP-1, in a sheep model. Spine 2001; 26:469–478.
11. Boden SD, Schimandle H, Hutton WC. An experimental lumbar intertransverse process spinal fusion model: radiographic, histologic, and biomechanical healing characteristics. Spine 1995; 20:412–420.
12. Feiertag MA, Boden SD, Schimandle JH, Norman JT. A rabbit model for nonunion of lumbar intertransverse process spine arthrodesis. Spine 1996; 21:27–31.
13. Schimandle JH, Boden SD. Spine update: the use of animal models to study spinal fusion. Spine 1994; 19:1998–2006.
14. Schimandle JH, Boden SD, Hutton WC. Experimental spinal fusion with recombinant human bone morphogetic protein-2 (rhBMP-2). Spine 1995; 20:1326–1237.
15. Curylo LJ, Johnstone B, Petersilge CA, Janicki JA, Yoo JU. Augmentation of spinal arthrodesis with autologous bone marrow in a rabbit posterolateral spine fusion model. Spine 1999; 24:434–439.
16. Itoh H, Ebara S, Kamimura M, Tateiwa Y, Kinoshita T, Yuzawa Y, Takaoka K. Experimental spinal fusion with use of recombinant human bone morphogenetic protein 2. Spine 1999; 24:1402–1405.
17. Minamide A, Tamaki T, Kawami M, Hashizume H, Yoshida M, Sakata R. Experimental spinal fusion using sintered bovine bone coated with type I collagen and recombinant human bone morphogenetic protein-2. Spine 1999; 24:1863–1872.
18. Tay BK, Le AX, Heilman M, Lotz J, Branford DS. Use of collagen-hydroxyapatite matrix in spinal fusion: a rabbit model. Spine 1998; 23:2276–2281.
19. Silcox DH, Daftari T, Boden SD, Schimandle JH, Hutton WC, Whitesides TE. The effect of nicotine on spinal fusions. Spine 1995; 20:1549–1553.
20. Wing KJ, Fisher CG, O'Connell JX, and Wing PC. Stopping nicotine exposure before surgery: the effect on spinal fusion in a rabbit model. Spine 2000; 25:30–34.
21. Grauer JN, Erulkar JS, Patel TCh, Panjabi MM. Biomechanical evaluation of the New Zealand white rabbit lumbar model. Eur. Spine J 2000; 9:250–255.
22. Erulkar JS, Grauer JN, Patel TCh, Panjabi MM. Kinematic analysis of posterolateral fusions in a New Zealand white rabbit model. Spine 2001; 26:1125–1130.
23. Grauer JN, Patel TCh, Erulkar JS, Troiano NW, Panjabi MM, Friedlaender GE. Evaluation of OP-1 as a graft substitute for posterolateral lumbar fusion. Spine 2001; 26:127–133.
24. Patel TCh, Erulkar JS, Grauer JN, Troiano NW, Panjabi MM, Friedlaender GE. OP-1 overcomes the inhibitory effect of nicotine on posterolateral lumbar fusion. Spine 2001; 26:1656–1661.
25. Wilke HJ, Krischak S, Claes L. Biomechanical comparison of calf and human spines. J. Orthop. Res 1996; 14:500–503.
26. Wilke HJ, Krischak ST, Wenger KH, Claes LE. Load-displacement properties of the thoracolumbar calf spine: experiemtnal results and comparison to known human data. Eur. Spine J 1997; 6:129–137.
27. Wilke HJ, Kettler A, Claes LE. Are sheep spines a valid biomechanical model for human spines? Spine 1997; 22:2365–2374.
28. Boden SD, Schimandle JH, Hutton WC, Chen MI. The use of an osteoinductive growth factor for lumbar spine fusion: Part 1: biology of spinal fusion. Spine 1995; 20:2626–2632.
29. Panjabi MM, Krag M, Summers D, Videman T. Biomechanical time-tolerance of fresh cadaveric human spine specimens. J. Orthop. Res 1985; 3:292–300.
30. Cook SD, Salkeld SL, Brinker MR, Wolfe MW, Rueger DC. Use of osteoinductive biomaterial (rhOP-1) in healing large segmental bone defects. J. Orthop. Trauma 1998; 12:402–412.
31. Daftari TK, Whitesides TE, Heller JG, Goodrich AC, McCarey BE, Hutton WC. Nicotine in the revascularization of bone graft: an experimental study in rabbits. Spine 1994; 19:904–911.
32. Silcox DH, Boden SD, Schimandle JH, Johnson P, Whitesides TE, Hutton WC. Reversing the inhibitory effect of nicotine on spinal fusion using an osteoinductive protein extract. Spine 1998; 23: 291–297.
33. Benowitz NL, Jacob P. Daily intake of nicotine during cigarette smoking. Clin. Pharmacol 1984; 35:499–504.

34. Benowitz NL. Clinical pharmocology of nicotine. Ann. Rev. Med 1986; 37:21–32.
35. Isaac PF, Rand ML. Blood levels of nicotine and physiological effects after inhalation of tobacco smoke. Eur. J. Pharmacol 1969; 8:269–284.
36. Panjabi MM, Abumi K, Duranceau J, Crisco JJ. Biomechanical evaluation of spinal fixation devices: II. Stability provided by eight internal fixation devices. Spine 1988; 13:1135–1140.
37. Panjabi MM, Kifune M, Liu W, Arand M, Vasavada A, Oxland TR. Graded thoracolumbar spinal injuries: development of multidirectional instability. Eur. Spine J 1998; 7:332–339.
38. Yamamoto I, Panjabi MM, Crisco T, Oxland T. Three-dimensional movements of the whole lumbar spine and lumbosacral joint. Spine 1989; 11:1256–1260.
39. Wetzel FT, Panjabi MM, Pelker RR. Biomechanics of the rabbit cervical spine as a function of component transections. J. Orthop. Res 1989; 7:723–727.
40. Kant AP, Daum WJ, Dean SM. Evaluation of lumbar spine fusion: plain radiographs versus direct surgical exploration and observation. Spine 1996; 20:2313–2317.
41. Grob D, Dvorak J, Panjabi MM, Antinnes JA. Fixateur externe an der Halswirbelsaule, ein neues diagnostisches Mittel. Unfallchirurg 1993; 96:416–21.
42. Panjabi MM, Lydon C, Vasavada A, Grob D, Crisco JJ, Dvorak J. On the understanding of clinical instability. Spine 1994; 19:2642–50.
43. Cook SD, Dalton JE, an EH, Whitecloud TS, Rueger DC. In vivo evaluation of recombinant human osteogenin protein (rhOP-1) implants as a bone graft substitute for spinal fusions. Spine 1994; 19: 1655–1663.
44. Paramore CG, Lauryssen C, Rauzzino J, Waldlington VR, Palmer CA, Brix A, Hadley MN. The safety of OP-1 for lumbar fusion with decompression — a canine study. Neurosurgery 1999; 44: 1151–1165.
45. Reibel GD, Boden SD, Whitesides TE, Hutton WC. The effects of nicotine on incorporation of cancellous bone graft in an animal model. Spine 1995; 20:2198–2202.
46. Cunningham BW, Shimamoto N, Sefter JC, Dmitriev AE, Orbegoso CM, McCarthy EF, Fedder IL, McAfee PC. Osseointegration of autograft versus osteogenic protein-1 in posterolateral spinal arthrodesis. emphasis on the comparative mechanisms of bone induction. Spine J 2002; 2(1):11–24.
47. Patel TC, McColloch JA, Vaccaro AR, Truumees E, Fischgrund JS, Herkowitz HN, Albert TJ, Hillibrand A, Phillips FM, Wetzel T. A pilot safety and efficacy study of OP-1 (rhBMP-7) in postero-lateral lumbar fusion as a replacement for iliac crest autograft. North American Spine Society, 16th annual meeting, Seattle, WA, 2001.
48. Patel TC, Vaccaro AR, Trumees E, Fischgrund JS, Hilibrand AS, Herkowitz HN. Two-year follow up of a safety and efficacy study of OP-1 (rhBMP-7) as an ajunct to posterolateral lumbar fusion. North American Spine Society, 16th annual meeting, Seattle, WA, 2001.

11

Structure and Function of Normal, Degenerate, and Surgically Fixed Spinal Segments

Nicola Fazzalari
Institute of Medical and Veterinary Science
Adelaide, South Australia, Australia

John J. Costi and Trevor C. Hearn
Repatriation General Hospital and Flinders University
Daw Park, South Australia, Australia

I. INTRODUCTION

Spinal fusion is an important procedure in the management of patients with disorders of the spine. Spinal fusion is often undertaken by the spinal surgeon in the context of disc degeneration. Studies combining mechanical testing and morphometric analyses of tissue samples have shown that disc degeneration can influence the quality of bone in the vertebral bodies undergoing fusion. The quality of bone in the vertebral body is fundamental to the success of the surgical fusion procedure for the patient.

Vertebral deformity, intervertebral disc disorganization, and change in vertebral bone architecture are morphological features associated with degeneration of the spine [1]. This includes disc degeneration, facet joint osteoarthritis, compromised vertebral body bone quality, and muscle and ligament alterations. These changes result in increased or abnormal segmental spinal motion, modified load distribution across the spinal joint, and altered cancellous bone architecture with potentially adverse consequences. Degenerative disc disease is one of the major causes of back symptoms and is believed to be associated with segmental instability of the spine.

The rationale for spinal fusion is essentially to eliminate instability of the spine. Instability may be real or potential and can be due to many pathological causes, including trauma, with injury to bone and/or ligamentous structures of the spine; deformity, in either the sagittal or the coronal plane; vertebral body and disc destruction from tumor or infection; degenerative deterioration of the motion segment; and iatrogenic causes such as motion segment destruction or postlaminectomy loss of posterior elements [2,3]. The American Academy of Orthopedic Surgeons defined instability as an abnormal response to applied loads characterized by movement in the motion segment beyond normal constraints [4]. On the other hand, the engineering model is loss of stiffness of a functional spinal unit resulting in increased and/or abnormal motions in response to applied loads [5]. Others have attempted to translate these definitions into criteria that can reliably be applied to clinical diagnosis and treatment decisions [6,7]. Despite the

controversy about whether spinal fusion is helpful to the patient, currently accepted indications for spinal fusion in degenerative disorders of the spine can be broken down into a number of categories [8]:

1. Disc herniation
2. Disc degeneration
3. Spinal stenosis
4. Isthmic spondylolisthesis
5. Degenerative scoliosis

This chapter focuses on the pathway to instability associated with disc degeneration not accompanying deformity.

The mechanical stability of the intervertebral disc is critically dependent on the integrity of its two main components: the nucleus pulposus and the anulus fibrosus. The use of the term ''mechanical stability'' refers to the nondegenerate intervertebral disc's ability to effectively redistribute compressive stresses passing through the superior endplate. Degenerative changes in the disc influence the bone density distribution in the spine [9,10]. Furthermore, disc injury can cause significant changes in stiffness and other mechanical properties of the disc and vertebral body bone [11]. A small defect in the anulus is as deleterious as removing a large section of anular material [12,13]. The structural stiffness and mechanical strength of the bone in the vertebral body are critical for successful intervertebral fusion. Clinical observations have shown that the restored disc height immediately after surgery tends to return to the preoperative level or even below the preoperative level [14]. Hasegawa et al. [15] found that the maximum allowed load of the spine structure for intervertebral fusion was positively correlated with both whole vertebral bone mineral density (BMD) and local cancellous BMD. Their results on human cadaver spines suggested that local cancellous bone density beneath endplates was a more sensitive indicator for predicting the maximum allowed load than the whole vertebral BMD [15]. Other studies have found that the bone density of the adjacent vertebral bodies (from human cadaveric spines) had significant correlation with the stability provided by intervertebral fusion and that BMD had a significant effect on the mean force to failure (compressive strength) of the vertebrae [16,17]. Hence, the trabecular bone in the vertebral body is a significant factor for the stabilizing potential of intervertebral fusion.

II. THE SPINAL SEGMENT AND BONE QUALITY

The behaviour of the spine under load can be viewed as the aggregate of the responses of its individual structural components. A motion segment is the smallest functional unit that exhibits the generic characteristics of the spine. Although the disc is a major structural component of the spinal column, a spinal segment should be viewed as consisting of the disc and the two vertebral bodies. The biomechanical responses and pathological changes that occur in a spinal segment result from the interaction between the disc and facet joints. Failure or degeneration in any one element can significantly alter normal load sharing between the elements. It may also set in motion a chain reaction leading to degeneration of and pain at other elements.

A. The Intervertebral Disc

The intervertebral disc is a major component for segmental stability as well as a major load-bearing structure. Vertebrae are separated from each other by an intervertebral disc, which consists of two functionally different components: anulus fiberus and nucleus pulposus (Fig. 1).

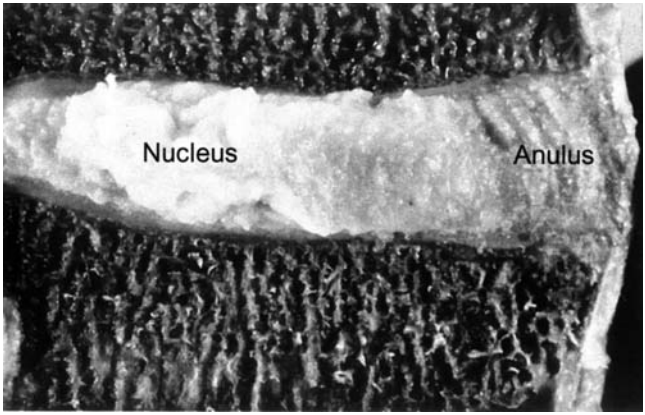

Figure 1 Vertebrae are separated from each other by an intervertebral disc, which consists of two functionally different components: anulus and nucleus pulposus.

In the middle of the disc is the nucleus pulposus, a gelatinous material that consists of 70–88% water and hydrophilic proteoglycans that progressively becomes less hydrated with age. The nucleus pulposus is surrounded by the anulus fibrosus. This consists of a series of concentric fiber layers; the fibers in neighboring layers cross each other at an angle of 20–30 degrees to the axial plane [18]. The normal disc acts as a fluid-filled cushion that distributes stress or load evenly across the vertebral endplate [19,20]. It has been found that with age there is increased disorganization of the intervertebral disc and decreased quality of vertebral cancellous bone [21]. Disc degeneration is usually observed earlier than vertebral deformity [22]. Intervertebral disc degeneration first appears in the second decade, and by 50 years of age 97% of lumbar discs show signs of degeneration [23].

The morphology of intervertebral disc degeneration is characterized by progressive fibrous change in the nucleus, loss of distinction from the anulus, loss of organization of the anular lamellae, and gradual disappearance of the cartilaginous vertebral endplate [24,25]. The presence of concentric (circumferential) and radiating tears and rim lesions is indicative of intervertebral disc degeneration. A standard method used for grading the gross morphology of intervertebral discs based on a sagittal section has been developed by Thompson et al. [26]. This consists of five levels, with grade I being a healthy normal, nondegenerate disc and grade V being severely degenerated. Due to the three-dimensional nature and lack of uniformity of tears and clefts, it was recently recommended that morphological classification and investigation of the extent of disc degeneration be conducted on multiple axial and/or sagittal slices through each intervertebral disc [27]. Radiological signs include disc space narrowing, disc bulging, endplate sclerosis, and the presence of osteophytes in the anterior and anterolateral regions [28–30]. However, radiological signs indicate degeneration in its advanced stage and cannot detect early degeneration.

The function of the intervertebral disc is complex and has various mechanical purposes. It serves as a strong but flexible bond between adjoining vertebral bodies and affects the transfer of the vertical loads passing down the spine. To achieve these purposes it is constructed of an outer fibrous anulus inserted into the rim of each vertebral body and a central nucleus which is gelatinous in infancy. Under normal circumstances, compression creates pressures in the nucleus, leading to compressive stresses at the center of the endplate and tension at the periphery where the anulus fibers attach, suggesting a relationship between the intervertebral disc and vertebral body bone [31]. The tendency for the nucleus to be extruded under the very substantial

loads sustained by the disc is resisted horizontally by the anulus and vertically by a layer of hyaline cartilage covering the face of each vertebral body endplate. The integrity of the anulus fibrosus is critically important for normal disc function. There are three common anular defects: concentric tears comprising crescentic separations of anulus lamellae; radial tears comprising irregular radial fissures extending from the nucleus toward, and sometimes through, the outer anulus; and rim lesions comprising defects in the anulus attachment close to the bone of the vertebral rim (Fig. 2). How the type and size of these disc lesions relate to the mechanics of the intervertebral joint complex has received limited investigation. One study investigating the mechanics of spinal motion segments in flexion, extension, and torsion and the stiffness and strength of the vertebral bone from cadaveric spines with varying severity of radial and concentric tears and rim lesions of the anulus has provided new insight into the interrelationships in the spinal segment [11].

The influence of tears on the joint torsional stiffness is very informative. It appears that increasing the severity of radial tears has little or no effect on the torsional stiffness. Increasing the severity of concentric tears reduces the torsional stiffness at the L2-L3 level, while increasing the severity of rim lesions has a greater effect in reducing the torsional stiffness at both the L2-L3 and L4-L5 levels. These results have logical explanations in terms of the nature of a torsional load and how it is transferred through the intervertebral disc during loading of the intact joint. The fibers in the lamellae of the disc and the zygapophysial joints carry this load. The center of rotation is located posteriorly to the nucleus of the disc, and a large proportion of the load is transferred as secondary shear. The interlamellar bonds in the anterior portion of the disc are required to oppose these shear forces. If the interlamellar bonds do not exist, as in the case of a concentric tear, the disc's ability to transfer the shear induced by the torsional load is compromised. Rim lesions involve a portion of the disc coming away from the vertebral body. In terms of torsional load transfer, this means that a whole section of the intervertebral disc is incapable of transferring a load from one vertebral body to another. Hence, the torsional load carrying ability of the disc is greatly affected [11]. This study has demonstrated that tears in the intervertebral disc are reflected in changes in the mechanics of both the vertebral bone and the intervertebral joint complex.

The major mechanical role played by the nucleus pulposus is that its hydrostatic pressure evenly transfers the vertebral spinal load to the adjacent vertebral body. The magnitude of this

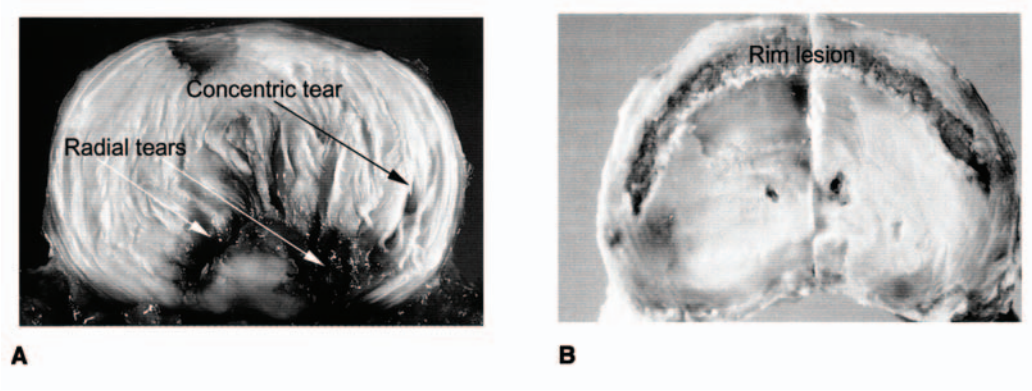

Figure 2 (A) Concentric tears comprising crescentic separations of anulus lamellae; radial tears comprising irregular radial fissures extending from the nucleus toward, and sometimes through, the outer anulus; (B) rim lesions comprising defects in the anulus attachment close to the bone of the vertebral rim

pressure is dependent on the amount of fluid within the nucleus and on the condition of the anulus. Nucleus stress drops as a result of reduced hydration with the stress in the posterior anulus increasing [32]. This drop in nucleus stress leads to a change in the distribution of stresses within the nucleus and anulus, and it has been shown that nucleus stress significantly decreases with degenerative grade [33]. If the nucleus is no longer able to obtain fluid from its environment, or if the anulus ''leaks'' due to tears, the hydrostatic pressure drops and the axial load on the anulus fibrosus increases. Studies have shown that partial or complete removal of the nucleus alters the response of the intervertebral disc to compressive stress with the inner anulus bulging inwards towards the nucleus [34,35]. The compression of this flexible ring then increases and is further amplified by the anulus bulging inwards. Nucleus pressure not only acts towards the vertebral endplates, but also towards the surrounding anulus, which is loaded under a radial tension. As the anulus is directly attached to the vertebral body, this leads to additional stresses near the vertebral endplate. It must be emphasized, however, that the radial tension of the anulus fibrosus does not decrease the axial load on the disc. The vertical compression on the vertebral body under the anulus is as large as under the nucleus [36].

The nucleus pulposus plays an important role in the function of the intervertebral disc and therefore in the external loading of the vertebra. Removal of the nucleus to represent the extreme case of disc degeneration or more particularly a complete surgical discectomy changes the stress field within the vertebral body [37]. Due to the removal/degeneration of the nucleus pulposus, the vertical load now is carried by the anulus fibrosus alone. The reversal of interior anular bulging after partial or complete nucleus removal has the effect of increasing the shear stresses in the anulus. This increase in shear stress is likely to tear the individual anulus layers apart [38]. Concentric tears are common in the early stages of disc degeneration [39,40].

The results of biomechanical analyses show an initial decrease of disc stiffness due to the inward bulging of the anulus, which had been prevented by the incompressible nucleus in the intact disc. Motion segment stiffness decreased with the initial stages of disc degeneration and then increased with further disc degeneration [30,42–47]. Nuclear herniation into the anular space causes loss of hydration and pressure in the nucleus, leading to the signs of advanced degeneration, as previously discussed. These effects have been demonstrated in animal models in which induced anular disruptions were created and their effects monitored longitudinally for morphological, biochemical, and biomechanical changes [48,49].

Stress profilometry involves the measurement of pressures within the intervertebral disc, typically by pulling a pressure transducer through a disc in the sagittal (antero-posterior) plane. Stresses in the intervertebral disc are not uniform over the cross section of the disc and vary with degree of degeneration [19,20,50,51]. The posterior anulus experiences high stresses during extension-compression loading. The stress in the nucleus was lower than in both the anterior and posterior anulus for axial compressive, combined flexion-compression and extension-compression loads and was relatively insensitive to these loading modes. This may be due to the central location of the nucleus in the coronal plane. Loads that are produced extend to the mid-sagittal plane in the coronal axis (flexion/extension) and can be expected to be symmetrical. The highest stresses were seen in the postero-lateral anulus under axial compression and extension-compression loads [52]. Sato et al., in an in vivo study measured the nucleus stress and found significant decreases in stress with increasing severity of degeneration [33].

B. Facet Joints

The facet joints are one of the main stabilizing structures of the spinal motion segment. Facet joints are true synovial articulations and undergo degenerative changes identical to those of

osteoarthritis [39]. The joints limit the range of motion of a spinal segment and therefore play an important role in the kinematics of the spine. The most notable influences of facet joints to the spinal segment are on the horizontal shear forces and axial torsion. The load-bearing role of the facet joints is altered by the progression of spinal degeneration [53]. The rotational flexibility of the spinal motion segment is also affected by osteoarthritis of the facet joints. The facet joints have no influence on spinal motions under axial compression, lateral bending, and flexion.

Invertebral loads that apply considerable forces to the facet joints are horizontal shear forces, extension, and axial torsion. These loads can result in large anterior compressive or bending stress near the base of the pedicles, which corresponds well with the main trabecular bone orientation at these sites. All of these loads contribute to the formation of the antero-medial bone orientation found at the pedicle base. In the pedicle, the load magnitudes vary considerably, corresponding with the high trabecular bone volume at this location. In addition, other loads must be applied to the vertebral body in order to compensate for bending and torsion moments. This often leads to contraction of contralateral muscles and consequently to extra axial compression. Further consideration of the influence of muscles on loading of the spine goes beyond the scope of this chapter.

C. The Vertebral Body

Adult human vertebrae are short bones, about 27 mm high, separated by an intervertebral disc, which is about 10 mm high anteriorly and 5 mm high posteriorly, and two facet joints. The form of the 24 vertebrae is basically the same; a lumbar vertebra is described below. The vertebral body consists of trabecular bone, 150–250μm thick [10], surrounded by a cortical shell with a highly variable thickness ranging between 100 and 750μm [54,55]. The upper and lower endplates are covered by a thin layer of cartilage with a thick bony ring at the border. The vertebral arch, a closed ring of bone with several processes, lies posteriorly. The foramina of all vertebrae together form the spinal canal. Superior and inferior vertebrae are connected via the facet joints. Other bony elements are the spinous process and the two transverse processes.

Changes in vertebral body shape are not necessarily the result of osteoporotic collapse [56]. The shape of the vertebral body may be influenced by many factors. Mild or even moderate vertebral deformity may arise from lifelong age-related changes in vertebral bone architecture [57], and vertebral wedging resulting from remodeling in osteoarthritis should not be confused with wedging due to osteoporotic fracture [58].

The principle that the form of bone is intimately coupled with its mechanical function is important for the study of spinal loading. Vertebral trabecular bone is a lattice of vertical and horizontal trabeculae. However, it is difficult to speak of a ‘‘normal’’ trabecular bone structure because of the influence of age and loading on the bone architecture. Age is universally associated with loss of bone mass, but bone adapts to its loading environment to maintain a physiologically sustainable level of bone deformation in normal living. Wolff’s law states that trabecular bone distributes and aligns itself according to the stress trajectories, that is, the orientations of two completely different entities, trabecular architectural geometry and stress, are quite similar. The principal stresses and trabecular bone architecture show some remarkable similarities with respect to their orientations [37]. This functional adaptation leads to an architecture in which all structural elements are equally deformed.

All vertebrae have bone structures that run in the vertical direction, which is also the orientation of the main principal stress under axial compression for all locations within the vertebral body. Axial compression is the most common load case of the spine and results in

vertical compression of the whole vertebral body. Axial compression is the main load to which vertebral trabecular bone is adapted. In a healthy disc, the nucleus and the anulus are equally loaded [59]. In addition, tension forces are experienced in the anulus fibers and hence the endplate. With degeneration of the nucleus, however, the hydrostatic pressure decreases, so that the anulus becomes more heavily loaded under axial compression and less under tension. This obviously leads to a different stress field within the vertebral body. In accordance with Wolff's law, this also must lead to an adaptation of the trabecular bone architecture.

The cellular processes responsible for functional adaptation of bone are bone modeling and remodeling. These processes primarily alter the amount and spatial distribution of bone to determine its form. The cells responsible are the osteoclasts and osteoblasts. Osteoclasts are multinucleated giant cells that resorb bone. Osteoblasts are bone-forming cells that produce osteoid. The activity of the bone-forming and resorbing cells is related to the strain at the bone surface. Mechanically induced bone modeling and remodeling is a dynamic process in which the load magnitude and frequency play an important role [60,61].

1. Trabecular Bone Architecture

In many cases where estimations of bone volume are presented, these figures represent average values of the whole vertebrae studied [62]. Research performed on vertebral bone trabeculae has found regional variations within vertebrae, such as the differences between endplate and central regions [31,63] and between anterior and posterior regions [63]. In addition, findings that overall bone volume may remain the same in the presence of differential responses of trabecular architecture to mechanical loading suggest that average values of bone volume for whole vertebral bodies may obscure regional variations in trabecular bone morphometry [64–66].

The relationship between disc degeneration and vertebral trabecular bone architecture has not been studied in detail. Both bone mineral density and structure vary considerably within the vertebral body and are significantly influenced by disc degeneration [10]. The characteristics of trabecular bone architecture at each location within the vertebral body are specific to their location [10,67,68]. Although all locations in the sagittal plane have the typical vertical orientation of trabeculae, it can be seen that the trabecular bone shows a much finer lattice near the endplates than in the center (Fig. 3). In the center, there are more plate-like structures and less interconnection in the horizontal directions. When viewed in the horizontal axial plane a dense array of trabecular bone is associated with the pediculi (Fig. 4). In addition, there is no preferred trabecular orientation in this horizontal plane. The range of bone volume fraction for the vertebral body is about 8–15%, while the bone volume fraction of the pedicle is about 25%.

2. Form and Function of Vertebral Trabecular Bone

Mechanical loading through the intervertebral disc alters as disc integrity deteriorates, resulting in nonuniform load distribution across the vertebral endplate [19,37,63]. The altered load distribution results in adaptive bone remodeling and osteophyte growth, which in turn alters vertebral body (Fig. 5) and endplate dimensions (Fig. 6) [39]. Furthermore, a finite element analysis of changes in bone and disc properties found that the effective stresses on a vertebral body moved to the peripheral area of the endplates, into the cortical wall and the vertebral rim [37]. Hence, unloaded trabeculae in the central region of the endplate undergo resorption. In addition, load transmission is directly influenced and leads to various failure modes of the vertebral body [57].

This is consistent with several histomorphological studies, which reported a decline of the horizontal strut thickness and the number of these transverse connections during aging [69]. Preteux et al. [70] found pronounced bone loss in the center of the vertebral body during aging, as well as a changed distribution of the trabeculae. Weight-bearing struts were twice as numerous

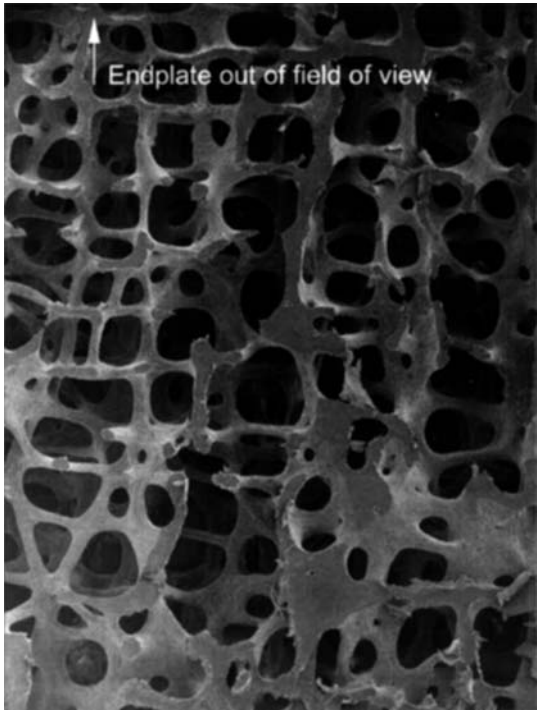

Figure 3 In the sagittal plane, trabeculae have vertical orientation; the trabecular bone shows a much finer lattice near the endplate.

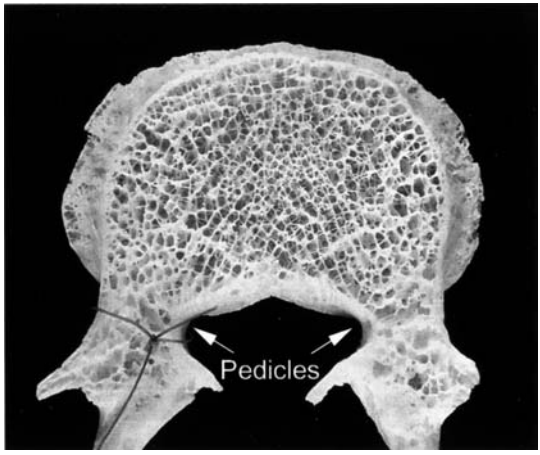

Figure 4 Viewed in the horizontal axial plane, a dense array of trabecular bone is associated with the pediculi.

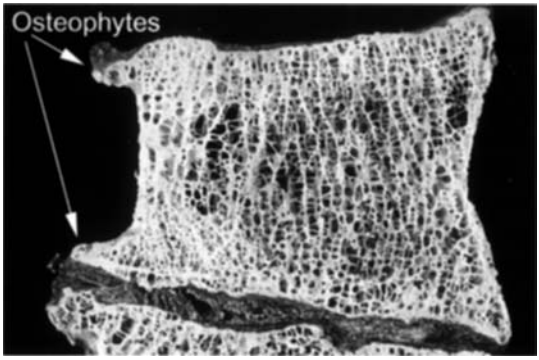

Figure 5 Altered load distribution results in adaptive bone remodeling and osteophyte growth, which in turn alters the vertebral body dimensions.

as transverse ones in people under 50 years of age, but six times as numerous in people older than 50 years of age. Keller et al. [31] found a negative correlation between the degree of disc degeneration and the bone strength under the disc nucleus. Disc degeneration leads to architectural changes within the vertebral body.

Age-related changes in vertebral trabecular architecture are seen as an alteration of trabeculae from plate-like, densely connected trabeculae to the rod-like structures seen in patients susceptible to vertebral crush fractures. Amling et al. [65] found that the osteoporotic group of their study had overall values of bone density within the range of normal subjects, but the selective loss of structural elements reduced the load-bearing capacities of these vertebrae. An important concept here is that even for a given bone mass, fracture risk increases with age [71], supporting the notion that there is a component of bone fragility that is independent of mass [72]. Cancellous bone of the same mass can have very different mechanical properties depending upon its structural integrity, which depends on cancellous bone architecture or material properties

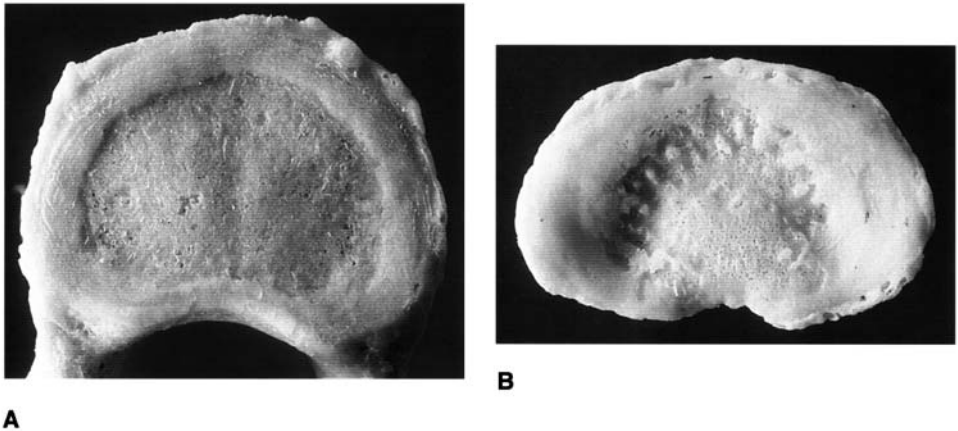

Figure 6 Altered load distribution results in adaptive bone remodeling, which alters endplate dimensions. Endplate associated with (A) normal disc and (B) degenerate disc.

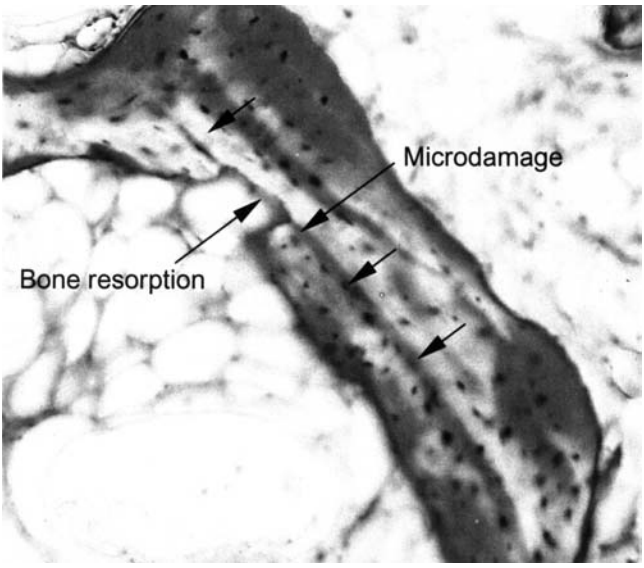

Figure 7 The targeted repair of microdamage is mechanistically similar to the process of continuous bone remodeling, which occurs normally throughout the body.

affected by accumulation of tissue microdamage as a result of fatigue. There is compelling evidence that microdamage is repaired by targeted bone remodeling [73,74] (Fig. 7). This repair process is distinct from trabecular microfracture healing that involves microcallus formation (Fig. 8). Microcallus formation in the vertebral body increases with advanced age in the absence of major spinal trauma [75]. The targeted repair of microdamage is mechanistically similar to the process of continuous bone remodeling, which occurs normally throughout the body. In some instances, microdamage may act as a positive feedback by increasing the resorption space associated with increased resorption [76]. This may put the cancellous bone structure at greater

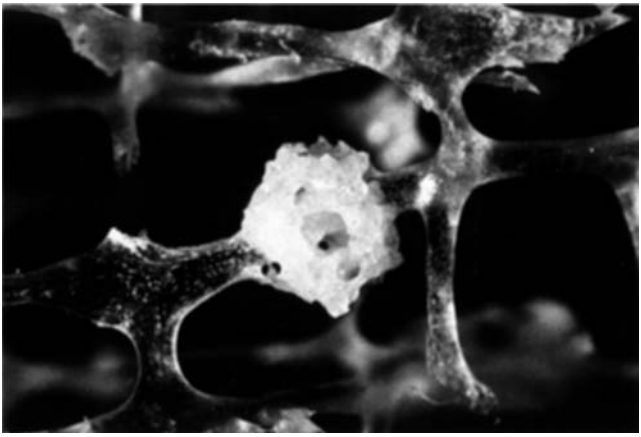

Figure 8 Trabecular microfracture healing involves microcallus formation.

risk of fracture due to the further accumulation of microdamage leading to increased resorption. Such a process may occur as a result of the altered load distribution through the vertebral body adjacent to a degenerated intervertebral disc or the creation of microdamage associated with the fusion surgery. Microdamage may accumulate because of increased susceptibility to fatigue due to altered vertebral body loading. Using a canine spine model, it has been shown that disc degeneration contributes to vertebral body fragility by causing microdamage accumulation, especially in vertebrae with low bone mass [77]. If these findings also hold for the human spine, there are significant implications particularly if patients are being treated with antiresorptive drugs such as bisphosphonates [78].

III. IMPLICATIONS OF BONE QUALITY IN THE BIOMECHANICS OF SURGICAL FIXATION

Biomechanical conditions following surgery provide the context for the biological process of fusion and are critical to the outcome of the procedure. Varying approaches can be assessed in accordance with two fundamental principles: (1) the fixation must have adequate *strength*, in all possible modes of failure, in response to various physiological loads; (2) the reconstruction must be *stable*. In practical terms, this requires that displacements under physiological loads fall within normal ranges, and that the amount of micromotion between bone and implant interfaces does not preclude fusion.

Bone graft or interbody fusion cages have been widely used to restore intervertebral disc height. With posterior instrumentation, vertebral pedicle screws have become one of the methods most widely used to increase stability. Although instrumentation has varied greatly in design, the strength and stability of spinal fusion constructs can be greatly affected by changes in bone quality in the vertebral body, cortical shell, or endplate.

A. Bone Quality and Fixation Strength

The potential for reconstruction failure under load exists in all parts of the construct. There has been extensive study of the strength of implants themselves and standardized procedures for their assessment [79]. In addition, reconstruction strength depends on the integrity of the interface between implant and bone. This includes bone graft and interbody fusion cages in contact with vertebral endplates and reamed trabecular bone. Where posterior augmentation is added, construct strength will also depend on the interface between vertebral bone and threaded pedicular anchors.

1. Interbody Cages and Bone Graft

A primary aim of using interbody fusion cages is to restore the degeneratively decreased disc height. This decompresses the neural structures in the intervertebral foramina. An immediate prerequisite for successful fusion therapy is adequate resistance to subsidence and reconstruction failure. Krammer et al. [80] tested three types of implants in eight single segment lumbar spine specimens. Each specimen underwent a cyclic loading test with the application of 40000 cycles at a rate of 5 Hz. A cyclic axial compression force ranging from 200 to 1000 N was applied while the axial translation was recorded as a measure of the subsidence. The specimens were then tested with increasing axial force until failure. There were only slight differences in subsidence for the various cage designs with the height reduction ranging between 0.9 and 1.4 mm. The median strength ranged from 5486 to 8413 N. No correlation was found between bone mineral density and failure load. Endplate preparation and cage design of the tested implants

did not influence the resistance of the segment to cyclic axial compression. Continuously increasing the compressive load revealed that implant-bone failure was not expected within physiological load ranges for any of the tested cage types.

Subsidence of the bone graft into the vertebral body can be a complication in anterior cervical fusion. The effects of endplate thickness, endplate holes, and the bone mineral density of the vertebral body on the biomechanical strength of the endplate/graft interface in an anterior interbody fusion of the cervical spine were investigated by Lim et al. [81]. Compression tests to failure and finite element analyses were conducted. Cervical vertebral bodies (C3–C7) isolated from seven cadaveric cervical spines (age at death 69–86 years, mean 79 years) were used for compression tests. The bone mineral density of each vertebral body was measured using dual energy x-ray absorptiometry. Endplate thickness was measured using three coronal computed tomography (CT) images of the middle portion of the vertebral body obtained using computer-assisted imaging analysis. Each vertebral body was then sectioned through the horizontal plane. Fifty-four specimens, consisting of one endplate and half of the vertebral body, were used. Specimens were assigned to one of three groups with different endplate conditions: intact, partial removal, and complete removal. Bone mineral density was similar in each group. Each endplate was compressed to failure using an 8-mm-diameter metal indentor while the maximum force was recorded. The study found no significant association between bone mineral density and endplate thickness. Load to failure was found to have a significant association with bone mineral density, but not with endplate thickness. However, load to failure tended to decrease with incremental removal of the endplate, and load to failure of the specimens with an intact endplate was significantly greater than that of the specimens with no endplate. Results of this study suggested that it is important to preserve the endplate as much as possible to prevent graft subsidence into the vertebral body, particularly in patients with poor bone quality.

2. *Pedicle Screws*

Vertebral pedicle screws have become one of the methods most widely used for spine stabilization. Despite overall clinical success, problems involving implant breakage at the thread-shaft junction and loss of thread purchase have occurred. A variety of loads can be expected to be applied to the implant postoperatively. These will generally include a component along the screw axis, and for this reason pullout tests have been performed to assess implant performance. Although screw length, diameter, and thread design all have an effect, bone quality is a primary determinant of the shear strength of the thread/bone interface.

A number of implant designs have been assessed in this way, using human, animal, and synthetic bone as a test medium. Insertion torque and pull-out strengths of conical and cylindrical pedicle screws were compared in human cadaveric vertebral bodies [82]. The objective was to compare the performance of conical and cylindrical designs and to determine whether insertion torque correlated with pull-out strength. Potentially, a tapered pedicle screw design may lessen the likelihood of implant failure, although its effect on thread purchase through interaction with trabecular bone is not known. Seventy-eight pedicles were assigned randomly to one of five designs of pedicle screws. Pedicle screws were inserted with a torque-measuring screwdriver. Each screw was extracted axially from the pedicle until failure while force data were recorded. The results showed that the conical design had the highest insertion torque. There were no significant differences in pull-out between any of the screw types (Fig. 9). Correlation between insertion torque and pull-out strength was statistically significant for only two of the designs in L4 and one design in L5. It was concluded that a conical screw profile increases insertion torque, although insertion torque is not a reliable predictor of pull-out strength in cadaveric bone from

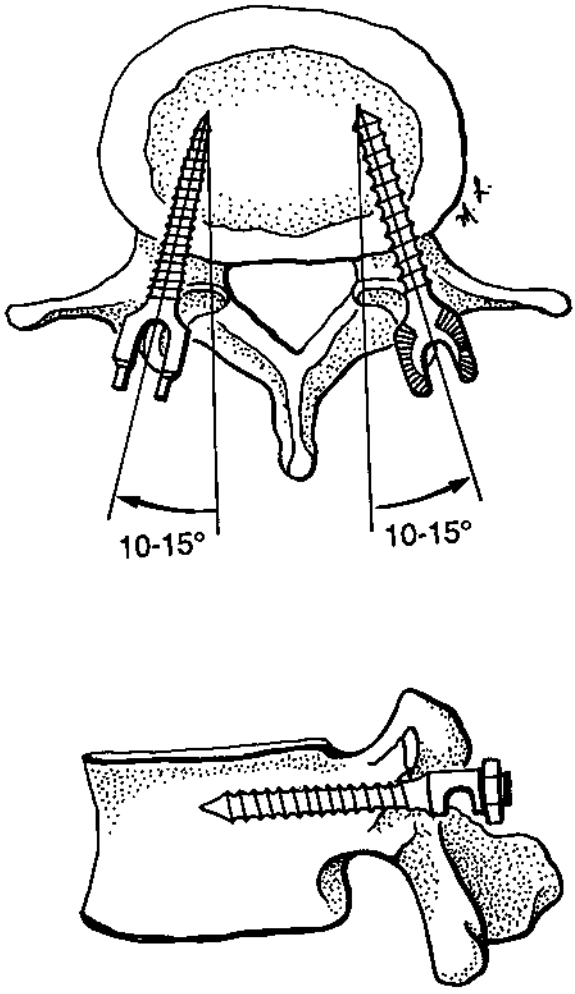

Figure 9 Examples of pedicle screw designs with thread purchase in the vertebral body. For all designs, the quality of the bone is a primary determinant of fixation strength and stability. (From Ref. 82.)

elderly donors. Screw profile (with similar dimensions) had little effect on straight axial pull-out strengths in this material.

B. Bone Quality and Fixation Stability

The clinical concept of stability generally corresponds to the biomechanical measure of stiffness. Physiologically, a stable spinal unit responds to applied loads within normal limits of displacement. The concept is more difficult to define following surgical reconstruction. In spinal fusion surgery, displacements in response to applied loads must not exceed amounts that could jeopardize the reconstructive effort. The biological processes are complex, and many details are yet to be determined. In the meantime, it is generally acknowledged that deformations of the overall construct and relative micromotion between implants and bone should be kept to a minimum.

1. *Interbody Cages*

Although there has been extensive study of implant design, there has been relatively little assessment of the role of bone properties in the stability of spinal fusion procedures using intervertebral body cages. In one investigation [83], the purpose was to compare the biomechanical properties of an interbody reconstruction using two standard threaded cages, a reconstruction using a single mega-cage, and a reconstruction using dual nested cages. This study also aimed to quantify the surface area of the cancellous bone bed exposed by reaming for the cages. Motion segments were tested in a nondestructive biomechanical loading sequence (compression, flexion, extension, lateral bending, and axial torsion). Load was first applied to the intact motion segment and again after the insertion of cages, and stiffness values determined at each step. After testing, each specimen was bisected through the disc and the surface area of the vascular bed was calculated. Comparison of the biomechanical properties of the three reconstructions showed that the dual nested cages produced the stiffest reconstruction. However, when the standard cages were compared with the nested cages, there was no significant difference, and, when compared with the mega-cage, the only difference was in flexion. The surface area of cancellous bone exposed by reaming for each of the three reconstructions showed the greatest value with the dual nested cages. Differences in contact area can also be expected to affect local stress distributions under load, with mechanical consequences mediated by bone quality.

Implant placement and orientation can also potentially interact differentially with vertebral bone in response to different loads. The lateral orientation has been increasingly used for intervertebral fusion. A direct biomechanical comparison between cages implanted either anteriorly or laterally in human cadaveric spines in order to determine which cage orientation resulted in greater immediate stability has been reported [84]. Human cadaveric lumbar spines underwent placement of threaded fusion cages in either an anterior or a lateral orientation. Spines underwent loading and angular rotation measurement in the intact state, after discectomy, after cage placement, and after cyclic loading. Angular rotations were compared between cage orientations and interventions. Fourteen spines were randomized into the anterior group (anterior discectomy and dual anterior cage placement) and the lateral group (lateral discectomy and single transverse cage placement). Pure bending moments were applied in flexion, extension, lateral bending, and axial rotation. Angular rotation was compared between anterior and lateral groups and, within each group, among the different interventions. The results showed that segmental ranges of motion were similar between spines undergoing either anterior or lateral cage implantation. It was concluded that there were few differences between angular rotation after either anterior or lateral implantation.

2. *Bone/Implant Micromotion*

Interface conditions are complex, and their interaction with biological processes is incompletely understood. The conclusion from the literature, over a wide range of joint replacement and fracture repair applications, suggests that excessive micromotion can prevent the biological establishment of a stable interface. Many details are yet to be determined, and optimal types and amounts of micromotion are not known. Based on limited information, micromotion of less than 50 μm has been suggested as a level conducive to a stable interface [85]. Loading conditions, mechanical properties of the materials, friction coefficients at the interfaces, and the geometry of spinal segments can potentially affect relative micromotion and spinal stability. In particular, relative micromotion is related closely to friction at bone–implant interfaces after arthroplasty, with bone properties being a primary determinant.

Finite element analysis has been used to address these complexities in the context of interbody fusion [86]. The effects of mechanical parameters at bone–implant interfaces of the

lumbar spine segments were investigated under various combined loads in order to investigate the mechanical behavior at bone–cage interfaces of lumbar spine segments with two interbody cages. A finite element model of human L3–L4 lumbar segments with two titanium interbody cages was constructed. This model was used to investigate mechanical behavior at the bonecage interface. Relative micromotion (slip distance on the contact surfaces), posterior axial displacement, and stresses were predicted for changes of friction coefficients, loading conditions, and age-related material and geometric properties of the spinal segments. It was found that relative micromotion at the interfaces was obvious at their edges under axial compression. The slip occurred primarily at the anterior edges under torsion with preload, while it occurred primarily at the edges of the one cage under lateral bending with preload. Relative micromotion at the interfaces increased significantly as the apparent density of cancellous bone or the friction coefficient of the interfaces decreased. A significant increase in slip distance at the anterior anulus occurred with the addition of torsion to the compressive preload. It was concluded that relative micromotion is sensitive to the friction coefficient of the interfaces, the bone density, and the loading conditions. On this basis, a reduction in bone density is less likely to allow bone growth into surface pores of the cage. However, it is likely that the larger the disc area or pedicle diameter, the more stable the interbody fusion construct.

3. Posterior Instrumentation

The use of interbody cages for lumbar fusion is well established, but complications such as cage subsidence and settling still occur. To address these complications, posterior instrumentation has been used to improve segmental stability. It is not well understood which patients require additional posterior instrumentation and the potential role of bone quality.

The influence of bone mineral density on the initial compressive stiffness of a segment that underwent posterior lumbar interbody fusion with two interbody cages, as well as the importance of additional posterior instrumentation for compressive stiffness with respect to bone mineral density, has been reported [87]. A validated finite element model including posterior decompression and stabilization with two cages was used to predict the initial compression stiffness with an axial load of 600 N. This model was used to predict the influence of various levels of bone mineral density on compression stiffness. A second model was generated in which additional posterior screw-rod instrumentation was simulated and this model was used to predict the influence of bone mineral density in axial loading. It was found that the responses of all models suggested that initial compressive stiffness will increase if there is an increase in bone density. The stiffness was always greater with posterior instrumentation. It was concluded that compression stiffness following posterior augmentation depends on bone mineral density. Additional posterior instrumentation resulted in an additional increase of compression stiffness. This effect was most pronounced in simulated bone of soft quality.

IV. CONCLUSIONS

While the relationship between disc degeneration and changes in vertebral bone is commonly invoked, the mechanisms of this relationship have largely been overlooked, with age changes given more attention. Quantitative studies of intervertebral discs and vertebral bodies are essential to elucidate the biomechanics and biology of spinal fusion in this context. Disc degeneration or injury changes the stress distribution across the anulus and alters motion segment stiffness. The interrelationships with changes in bone properties are complex (Fig. 10). Such changes in stress distribution and cancellous bone architecture are reflected in altered vertebral bone. When

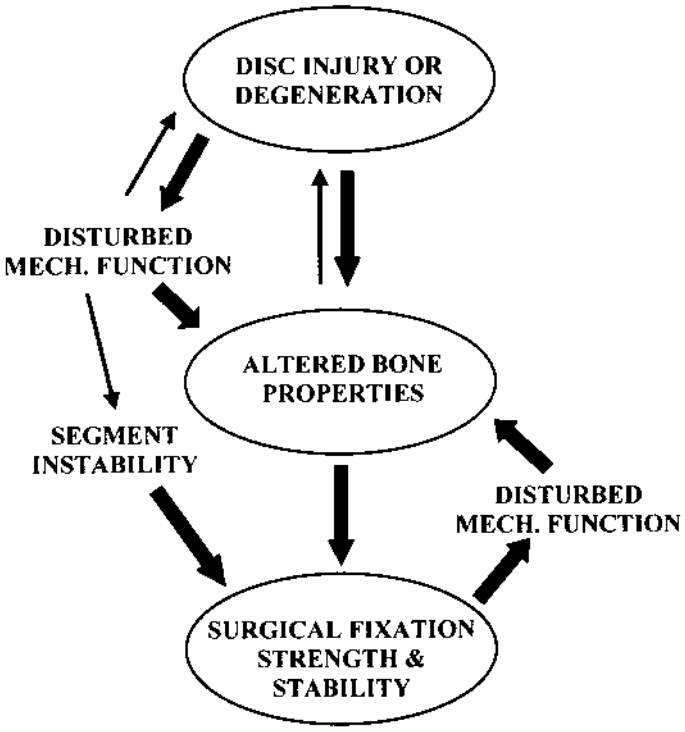

Figure 10 The interrelationships between disc degeneration, bone properties, and surgical fixation. Disc injury or degeneration leads to disturbed mechanical function and altered bone properties. Disturbed mechanical function may lead to segmental instability and require surgical fixation, which is affected by bone properties. Surgical fixation subsequently alters bone properties.

associated with segment instability, these changes can affect the strength and stability of surgical fixation aimed at intervertebral fusion.

ACKNOWLEDGMENT

The authors gratefully appreciate the editorial assistance of Dr. Wayne Rankin for proofreading the manuscript and making many helpful suggestions.

REFERENCES

1. Margulies JY, Payzer A, Nyska M, Neuwirth MG, Floman Y, Robin GC. The relationship between degenerative changes and osteoporosis in the lumbar spine. Clin. Orthop 1996; 324:145–152.
2. Pitkanen MT, Manninen HI, Lindgren KA, Sihvonen TA, Airaksinen O, Soimakallio S. Segmental lumbar spine instability at flexion-extension radiography can be predicted by conventional radiography. Clin. Radiol 2002; 57:632–639.

3. Bjarke CF, Stender HE, Laursen M, Thomsen K, Bunger CE. Long-term functional outcome of pedicle screw instrumentation as a support for posterolateral spinal fusion: randomized clinical study with a 5-year follow-up. Spine 2002; 27:1269–1277.
4. A Glossary on Spinal Terminology, American Academy of Orthopaedic Surgeons. 1985.
5. Pope MH, Panjabi M. Biomechanical definitions of spinal instability. Spine 1985; 10:255–256.
6. Frymoyer J, Krag MH. Spinal stability and instability: definitions, classifications and general principals of management. In: Dunsker SB, Schmidek HH, Frymoyer JW, Kahn A, eds. The Unstable Spine. Philadelphia: W.B. Saunders Co., 1986.
7. White AA, Punjabi MM. Kinematics of the spine. In: White AA, Punjabi MM, eds. Clinical Biomechanics of the Spine. Philadelphia: J. B. Lippincott, 1978.
8. Herkowowitz HN. Its current and future place in the degenerative lumbar spine. In:. Wiesel SW, Weinstein JN, Herkowitz H, Dvorak J, Bell G, eds. The Lumbar Spine. Philadelphia: W.B. Saunders Co, 1996.
9. Hansson TH, Keller TS, Panjabi MM. A study of the compressive properties of lumbar vertebral trabeculae: effects of tissue characteristics. Spine 1987; 12:56–62.
10. Simpson EK, Parkinson IH, Manthey B, Fazzalari NL. Invertebral disc disorganization is related to trabecular bone architecture in the lumbar spine. J. Bone Min. Res 2001; 16:681–687.
11. Thompson RE, Pearcy MJ, Downing KJW, Manthey BA, Parkinson IH, Fazzalari NL. Disc lesions and the mechanics of the invertebral joint complex. Spine 2000; 25:3026–3035.
12. Keller TS, Holm SH, Hansson TH, Spengler DM. Volvo Award in Experimental Studies. The dependence of intervertebral disc mechanical properties on physiologic conditions. Spine 1990; 15: 751–761.
13. Fazzalari NL, Costi JJ, Hearn TC, Fraser RD, Vernon-Roberts B, Hutchinson J, Manthey B, Parkinson IH, Sinclair C. Mechanical and pathological consequences of induced concentric anular tears in an ovine model. Spine 2001; 26:2575–2581.
14. Closkey RF, Parsons JR, Lee CK, Blacksin MF, Zimmerman MC. Mechanics of inter-body spinal fusion. Analysis of cortical bone graft area. Spine 1993; 18:1011–1015.
15. Hasegawa K, Abe M, Washio T, Hara T. An experimental study on the interface strength between titanium mesh cage and vertebra in reference to vertebral bone mineral density. Spine 2001; 26: 957–963.
16. Lund T, Oxland TR, Jost B, Cripton P, Grassmann S, Etter C, Nolte LP. Interbody cage stabilisation in the lumbar spine: biomechanical evaluation of cage design, posterior instrumentation and bone density. J. Bone Joint Surg. (Br) 1998; 80:351–359.
17. Hollowell JP, Vollmer DG, Wilson CR, Pintar FA, Yoganandan N. Biomechanical analysis of thoracolumbar interbody constructs. How important is the endplate. Spine 1996; 21:1032–1036.
18. Humzah MD, Soames RW. Human intervertebral disc: structure and function. Anat. Rec 1988; 220: 337–356.
19. McNally DS, Adams MA. Internal intervertebral disc mechanics as revealed by stress profilometry. Spine 1991; 17:66–73.
20. Adams MA, Freeman BJ, Morrison HP, Nelson IW, Dolan P. Mechanical initiation of intervertebral disc degeneration. Spine 2000; 25:1625–1636.
21. Hansson T, Roos B, Nachemson A. The bone mineral content and ultimate compressive strength of lumbar vertebrae. Spine 1980; 5:46–55.
22. Tertti M, Paajanen H, Laato M, Aho H, Komu M, Kormano M. Disc degeneration in magnetic resonance imaging. A comparative biochemical, histologic, and radiologic study in cadaver spines. Spine 1991; 16:629–634.
23. Miller JAA, Schmatz C, Schultz AB. Lumbar disc degeneration: correlation with age, sex, and spine level in 600 autopsy specimens. Spine 1988; 13:173–178.
24. Coventry MB, Ghormley RK, Kernohan JW. The intervertebral disc: its microscopic anatomy and pathology. Part III. Pathological changes in the intervertebral disc. J. Bone Joint Surg. (Am.) 1945; 27:460–464.
25. Eckert C, Decker A. Pathological studies of intervertebral discs. J. Bone Joint Surg. (Am.) 1947; 29: 447–454.

26. Thompson JP, Pearce RH, Schechter MT, Adams ME, Tsang IK, Bishop PB. Preliminary evaluation of a scheme for grading the gross morphology of the human intervertebral disc. Spine 1990; 15: 411–415.
27. Vernon-Roberts B, Fazzalari NL, Manthey BA. Pathogenesis of tears of the anulus investigated by multiple-level transaxial analysis of the T12-L1 disc. Spine 1997; 22:2641–2646.
28. Andersson GB. What are the age-related changes in the spine. Baillieres Clin. Rheumatol 1998; 12: 161–173.
29. Urban JP, Roberts S. Development and degeneration of the intervertebral discs. Mol. Med. Today 1995; 1:329–335.
30. Mimura M, Panjabi MM, Oxland TR, Crisco JJ, Yamamoto I, Vasavada A. Disc degeneration affects the multidirectional flexibility of the lumbar spine. Spine 1994; 19:1371–1380.
31. Keller TS, Hansson TH, Abram AC, Spengler DM, Panjabi MM. Regional variations in the compressive properties of lumbar vertebral trabeculae: effects of disc degeneration. Spine 1989; 14: 1012–1019.
32. McMillan DW, Garbutt G, Adams MA. Effect of sustained loading on the water content of intervertebral discs: implications for disc metabolism. Ann. Rheum. Dis 1996; 55:880–887.
33. Sato K, Kikuchi S, Yonezawa T. In vivo intradiscal pressure measurement in healthy individuals and in patients with ongoing back problems. Spine 1999; 24:2468–2474.
34. Meakin JR, Hukins DW. Effect of removing the nucleus pulposus on the deformation of the anulus fibrosus during compression of the intervertebral disc. J. Biomech 2000; 33:575–580.
35. Meakin JR, Redpath TW, Hukins DW. The effect of partial removal of the nucleus pulposus from the intervertebral disc on the response of the human anulus fibrosus to compression. Clin. Biomech 2001; 16:121–128.
36. van Dieen JH, Kingma I, Meijer R, Hansel L, Huiskes R. Stress distribution changes in bovine vertebrae just below the endplate after sustained loading. Clin. Biomech 2001; 16(suppl 1): S135–S142.
37. Kurowski P, Kubo A. The relationship of degeneration of the intervertebral disc to mechanical loading conditions on lumbar vertebrae. Spine 1986; 11:726–731.
38. Goel VK, Monroe BT, Gilbertson LG, Brinckmann P. Interlaminar shear stresses and laminae separation in a disc. Finite element analysis of the L3-L4 motion segment subjected to axial compressive loads. Spine 1995; 20:689–698.
39. Vernon-Roberts B, Pirie CJ. Degenerative changes in the intervertebral discs of the lumbar spine and their sequelae. Rheumatol. Rehabil 1977; 16:13–21.
40. Osti OL, Vernon-Roberts B, Moore R, Fraser RD. Anular tears and disc degeneration in the lumbar spine. A post-mortem study of 135 discs. J. Bone Joint Surg. (Br) 1992; 74:678–682.
41. Fazzalari NL, Costi JJ, Hearn TC. Mechanical and pathologic consequences of induced concentric anular tears in an ovine model. Spine 2001; 26:2575–2581.
42. Brown MD, Holmes DC, Heiner AD. Measurement of cadaver lumbar spine motion segment stiffness. Spine 2002; 27:918–22.
43. Goel VK, Goyal S, Clark C, Nishiyama K, Nye T. Kinematics of the whole lumbar spine. Effect of discectomy. Spine 1985; 6:543–54.
44. Panjabi MM, Krag MH, Chung TQ. Effects of disc injury on mechanical behavior of the human spine. Spine 1984; 7:707–13.
45. Fujiwara A, Lim TH, An HS, Tanaka N, Jeon CH, Andersson GB, Haughton VM. The effect of disc degeneration and facet joint osteoarthritis on the segmental flexibility of the lumbar spine. Spine 2000; 23:3036–44.
46. Haughton VM, Schmidt TA, Keele K, An HS, Lim TH. Flexibility of lumbar spinal motion segments correlated to type of tears in the anulus fibrosus. J. Neurosurg 2000; 92(suppl. 1):S81–S86.
47. Schulz KS, Waldron DR, Grant JW, Shell L, Smith G, Shires PK. Biomechanics of the thoracolumbar vertebral column of dogs during lateral bending. Am. J. Vet. Res 1996; 8:1228–1232.
48. Osti OL, Vernon-Roberts B, Fraser RD. Volvo Award in experimental studies. Anulus tears and intervertebral disc degeneration. An experimental study using an animal model. Spine 1990; 15: 762–767.

49. Latham JM, Pearcy MJ, Costi JJ, Moore R, Fraser RD, Vernon-Roberts B. Mechanical consequences of anular tears and subsequent intervertebral disc degeneration. Clin. Biomech 1994; 9:211–219.
50. Adams MA, McNally DS, Dolan P. 'Stress' distributions inside intervertebral discs. The effects of age and degeneration. J. Bone Joint Surg. (Br) 1996; 78:965–972.
51. Panjabi M, Brown M, Lindahl S, Irstam L, Hermens M. Intrinsic disc pressure as a measure of integrity of the lumbar spine. Spine 1988; 13:913–917.
52. Edwards WT, Ordway NR, Zheng Y, McCullen G, Han Z, Yuan HA. Peak stresses observed in the posterior lateral anulus. Spine 2001; 26:1753–1759.
53. Adams M, Hutton W. The mechanical function of the lumbar apophyseal joints. Spine 1983; 3: 327–330.
54. Ritzel H, Amling M, Posl M, Hahn M, Delling G. The thickness of human vertebral cortical bone and its changes in aging and osteoporosis: a histomorphometric analysis of the complete spinal column from thirty-seven autopsy specimens. J. Bone Min. Res 1997; 12:89–95.
55. Panjabi MM, Chen NC, Shin EK, Wang JL. The cortical shell architecture of human cervical vertebral bodies. Spine 2001; 26:2478–2484.
56. Kleerekoper M, Nelson DA. Vertebral fracture or vertebral deformity? Calcif. Tissue Int 1992; 50: 5–6.
57. Hansson T, Roos B. The relation between bone mineral content, experimental compression fractures, and disc degeneration in lumbar vertebrae. Spine 1981; 6:147–153.
58. Osman AAH, Bassiouni H, Koutri R, Nijs J, Geusens P, Dequeker J. Aging of the thoracic spine: distinction between wedging in osteoarthritis and fracture in osteoporosis—a cross-sectional and longitudinal study. Bone 1994; 15:437–442.
59. Horst M, Brinckmann P. Measurement of the distribution of axial stress on the endplate of the vertebral body. Spine 1981; 6:217–232.
60. Lanyon LE, Rubin CT. Static versus dynamic loads as an influence on bone remodeling. J. Biomech 1984; 17:897–905.
61. Rubin W, McLeod KJ. Biologic modulation of mechanical influences in bone remodeling. In:. Mow VC, Ratcliff A, Woo SLY, eds. Biomechanics of Diarthrodial Joints II. New York: Springer-Verlag: 97–118.
62. Fazzalari NL, Parkinson IH, Manthey B. Intervertebral disc disorganisation and its relationship to age adjusted vertebral body morphometry and vertebral bone architecture. Anat. Rec 2001; 262: 331–339.
63. Keller TS, Ziv I, Moeljanto E, Spengler DM. Interdependence of lumbar disc and subdiscal bone properties. A report of the normal and degenerated spine. J. Spinal Disord 1993; 6:106–113.
64. Cody DD, Goldstein SA, Flynn MJ, Brown EB. Correlations between vertebral regional bone mineral density (rBMD) and whole bone fracture load. Spine 1991; 16:146–54.
65. Amling M, Posl M, Ritzel H, Hahn M, Vogel M, Wening V, Delling G. Architecture and distribution of cancellous bone yield vertebral fracture clues. Arch. Orthop. Trauma Surg 1996; 115:262–269.
66. Kothari M, Keaveny T, Lin J, Newitt D, Majumdar S. Measurement of intraspecimen variations in vertebral cancellous bone architecture. Bone 1999; 25:245–250.
67. Flynn MJ, Cody DD. The assessment of vertebral bone macroarchitecture with x-ray computed tomography. Calcif. Tissue Int 1993; 53(suppl 1):S170–S175.
68. Keller TS, Moeljanto E, Main JA, Spengler DM. Distribution and orientation of bone in the lumbar spine. J. Spinal Disord 1992; 5:60–74.
69. Vogel M, Hahn M, Delling G. Relation between two- and three-dimensional architecture of trabecular bone in the human spine. Bone 1993; 14:199–203.
70. Preteux K, Bergot C, Laval-Jeantet AM. Automatic quantification of cancellous bone remodeling during age. Anat. Clin 1985; 7:203–208.
71. Hui SL, Slemenda CW, Johnston CC. Age and bone mass as predictors of fracture in a prospective study. J. Clin. Invest 1988; 81:1804–1809.
72. Caldwell CB, Willett K, Cuncins AV, Hearn TC. Characterization of vertebral strength using digital radiographic analysis of bone structure. Med Physics 1995; 22:611–615.
73. Mori S, Burr DB. Increased intracortical remodeling following fatigue damage. Bone 1993; 14: 103–109.

74. Bentolila V, Boyce TM, Fyhrie DP, Drumb R, Skerry TM, Schaffler MB. Intracortical remodeling in adult rat long bones after fatigue loading. Bone 1998; 23:275–281.
75. Hansson T, Roos B. Microcalluses of the trabeculae in lumbar vertebrae and their relation to the bone mineral content. Spine 1981; 6:375–380.
76. Garetto L, Chen J, Parr A, Roberts E. Remodeling dynamics of bone supporting rigidly fixed titanium implants: a histomorphometric comparison in four species including humans. Implant Denti 1995; 4:235–243.
77. Hasegawa K, Turner CH, Chen J, Burr DB. Effect of disc lesion on microdamage accumulation in lumbar vertebrae under cyclic compression loading. Clin. Orthop 1995; 311:190–198.
78. Hirano T, Turner CH, Forwood MR, Johnston CC, Burr DB. Does suppression of bone turnover impair mechanical properties by allowing microdamage accumulation. Bone 2000; 27:13–20.
79. Cunningham BW, Polly DW. The use of interbody cage devices for spinal deformity: a biomechanical perspective. Clin. Orthop 2002; 394:73–83.
80. Krammer M, Dietl R, Lumenta CB, Kettler A, Wilke HJ, Buttner A, Claes L. Resistance of the lumbar spine against axial compression forces after implantation of three different posterior lumbar interbody cages. Acta Neurochir (Wien) 2001; 143:1217–1222.
81. Lim TH, Kwon H, Jeon CH, Kim JG, Sokolowski M, Natarajan R, An HS, Andersson GB. Effect of endplate conditions and bone mineral density on the compressive strength of the graft-endplate interface in anterior cervical spine fusion. Spine 2001; 26:951–956.
82. Kwok AW, Finkelstein JA, Woodside T, Hearn TC, Hu RW. Insertional torque and pull-out strengths of conical and cylindrical pedicle screws in cadaveric bone. Spine 1996; 21:2429–2434.
83. Murakami H, Horton WC, Kawahara N, Tomita K, Hutton WC. Anterior lumbar interbody fusion using two standard cylindrical threaded cages, a single mega-cage, or dual nested cages: a biomechanical comparison. J. Orthop. Sci 2001; 6:343–348.
84. Heth JA, Hitchon PW, Goel VK, Rogge TN, Drake JS, Torner JC. A biomechanical comparison between anterior and transverse interbody fusion cages. Spine 2001; 26:E261–E267.
85. Chao EYS, Aro HT. Biomechanics of fracture fixation. In: Mow VC, Hayes WC, eds. 2d ed. Basic orthopaedic biomechanics. Philadelphia: Lippincott-Raven, 1997.
86. Kim Y. Prediction of mechanical behaviors at interfaces between bone and two interbody cages of lumbar spine segments. Spine 2001; 26:1437–1442.
87. Pitzen T, Matthis D, Steudel WI. The effect of posterior instrumentation following LIF with BAK cages is most pronounced in weak bone. Acta Neurochir (Wien) 2002; 144:121–128.

12

A Quantitatively Unstable Model to Evaluate the Biological Effects of Mechanical Forces on Spine Fusion

Mark R. Foster
Cherry Way Orthopaedics, P.C.
Pittsburgh, Pennsylvania, U.S.A.

I. INTRODUCTION

Spinal fusion has a long and complex history, with major differences by region. In the lumbar area, the posterior fusion is often attributed to Hibbs [1], who popularized this technique for deformity stabilization and correction, and thus for the thoracic area as well [2]. Lumbar posterior fusion is less commonly performed because of the risk of late overgrowth of the fusion mass causing iatrogenic spinal stenosis [3], having been replaced by a lateral approach (in the inter-transverse process space), or posterolateral, that is, also with fusion of the facet joints. The thoracic spine is intrinsically stabilized by the rib cage, and thus less commonly fused in the absence of deformity, but the posterior technique remains the primary technique. Fusion in the cervical spine is commonly performed anteriorly, following the description of an approach by Robinson and Smith [4], although posterior fusion remains useful and a component part of combined procedures, for example, after trauma or other anterior column deficiencies, such as tumor, infection, or failed prior fusion.

The most common indication currently for spinal fusion is degenerative disc disease, but unlike deformity surgery, where general guidelines for indications are commonly accepted as consensus [5], the indications remain clinical, requiring evaluation of the patient, their symptoms, such as pain, and the surgeons' judgment. The landmark description of a herniated nucleus pulposus by Mixtner and Barr [6] interestingly recommended fusion at that segment with local bone. Clearly, the herniated nucleus pulposus had documented pathology in that case; stabilization would perhaps be expected to reduce subsequent further problems. In retrospect, this was a severe underestimation of the difficulty in accomplishing a mechanically rigid fusion and, in a more contemporary context, failure of recognition of the limitations of a posterior fusion in completely stabilizing the functional segmental spinal unit.

Focus has turned to various structures as ''pain generators,'' but primarily to the disc as the pathology responsible for the pain, either by mechanical incompetence or by chemical means, where the leakage of nuclear material is accompanied by a severe inflammatory reaction with macrophages and other cells and pain-producing substances, for example, phospholipase A_2 [7]. These views of the mechanism of producing symptoms have led to interest in the lumbar area in specifically stabilizing the anterior column. Stabilization anteriorly may be considered as a

direct treatment by removal of the disc as the origin of inflammation and pain as well as mechanically eliminating micromotion that remains after satisfactory posterolateral fusion.

Assessment of outcome in patients who have spinal fusion for degenerative disc disease is much more complex than accomplishing and maintaining a fusion in deformity, not only addressing subjective issues primarily of pain, but also psychosocial factors, such as return to work and ability to function physically, including cases with litigation. Results with posterolateral fusion have been variable, but anterior (interbody) and combined (360°) fusions have been increasingly used, with promising early results [8]. Anterior lumbar fusion has undeniably increased following the popularization of cages, with associated technology and techniques to reliably achieve an arthrodesis, now supplemented with bioactive molecules, for example, BMP-2.

Considering the analogy of spinal fusions to fracture healing, immobilization of a fracture with a cast reduces pain, maintains adequate reduction, but is limited in the strictness of immobilization by the soft tissues across which forces are transmitted. The motion that is accepted results in healing by the mode of endochondral ossification or by a cartilaginous anlagen, which then ossifies and biologically resembles recapitulation of the growth plate, the origin of bone length development. Rigid fixation of long bone fractures has been described as primary bone healing or osteosynthesis, where a collagen model or intramembranous bone formation results from the lack of motion and intimate contact of bone fragments [9]. Cartilaginous matrix is seen when fragments are not in a proximity of 0.5 mm [10], although larger dimensions heal without endochondral ossification in unfractured lytic lesions after radiation therapy, unless a pathological fracture occurs. With fracture, the cartilaginous phase is entered with a subsequent high nonunion rate after radiation for the primary disease [11]. While the length of long bones is accomplished with the growth plate, the bulk of the bone volumetrically forms under the periosteum as an increase in the caliber of the bone and is actually the result of intramembranous or collagen model bone.

Spinal fusion, unlike fracture healing, is accomplished essentially by heterotopic ossification, where bone fragments are placed in an intended bed, which had been soft tissue, rather than restoring the structural integrity of a fractured bone. Various BMPs have been shown to be more effective in different settings, as BMP-6 has been shown to induce bone healing with the cartilage model [12] and BMP-2 has been show to induce healing in femoral segmental defects in sheep [13] and rats [14] and bony repair in a canine nonunion model [15] and a mandibular defects model [16]. Various physiological concentrations of a cascade of molecules at different times are present in normal healing, so specific applications of a knowledge of these biological processes would have direct bearing on optimal stimulus mixture designs.

II. MODELS

Boden et al. [17] characterized a rabbit model in response to the paucity of information in the literature regarding the biological process occurring in a lumbar arthrodesis. This model includes an intact disc and dimensions smaller than human or clinical cases, but documented histologically, that intramembranous bone formation was formed arising primarily from the transverse process, but also lateral intact host bone, and in most cases bridged the intertransverse process space, although in some cases cartilage was documented at the midsection. In a larger model using sheep, endochondral ossification has been demonstrated, which may be modified with bioactive molecules such as OP-1 to a direct intramembranous bone formation [18]. That change would represent an alteration of the biological process by osteoinduction, which would then lead to questions as to whether an arthrodesis could be achieved more rapidly [19] by essentially skipping a step and whether the eventual fusion mass would be superior. Biochemical analysis

of the consolidation of the fusion mass in a sheep spine has been presented [20] which suggests that the developing arthrodesis was calcifying within 6 weeks, as collagen content rose later to suggest the formation and remodeling of bone.

A serial study in an ovine model revealed that posterolateral fusion mass had an increased mechanical stiffness after the fourth week and mineralization which increased in a linear fashion after 8 weeks, with a significant discrepancy between biomechanical stability and histological maturation of the posterolateral fusion mass. The radiographic appearance of a solid fusion at 8 weeks was preceded by early substantial mechanical stiffness, from immature woven bone, which resulted in diminishing stress on spinal instrumentation prior to x-ray demonstration of the fusion [21].

Extrapolation from animal species is a very difficult and complex consideration ultimately requiring clinical or human confirmation of results; however, with regard to size, there are clearly some factors that scale while others do not. For example, the size of an erythrocyte does not vary in proportion to order of magnitude changes between species. Forces sustained by musculoskeletal structures or bony members of the skeletal system scale more with mass than linear dimension, but a complex relationship has been characterized [22], not a linear relationship with dimensions. Oxygen diffusion distance or other electrolyte transport mechanisms in biological body tissue fluids would be expected to have similar dimensions, as would the zone of influence around bioactive molecules, which are being studied particularly for their osteoinductive value.

As various species are considered for *in vivo* models to evaluate the process of developing a lumbar arthrodesis, the intertransverse dimension would be expected to scale with linear dimension, while disc pressures have been demonstrated to be proportional to body weight and hence mass, but all of these forces must be evaluated in the context of the mechanical rigidity of instrumentation systems which are customarily employed clinically following testing in various models. Initial testing in species of smaller size may direct subsequent experiments in species of larger size and assist subsequent experiments, but instrumentation testing would be limited to models of adequate size to allow realistic implantation.

Clinical relevance should also include disc insufficiency, as this common indication for performing a fusion, represents a modification of mechanical forces, otherwise accepted as improving the healing by instrumenting the fusion, which may subsequently modify the healing biological behavior of the fusion mass. An irreducible incidence of low back pain is seen following microdiscectomy [23], as after the herniation and the surgical intervention the disc is mechanically compromised. Experimentally removing the disc can model these factors, to provide a more realistic and challenging model as the complex and largely unknown effect on the disc of surgery, other than lacerations to initiate a simulation of the degenerative cascade [24–26] that has been documented as the natural history of human lumbar disc. Subsequent models have involved anterior, interbody fusions more often than posterolateral.

III. STRESS SHIELDING

Specific clinical indications for a lumbar arthrodesis remain controversial [27–29]. The objective of the spine fusion is to eliminate motion, thus altering the mechanics of the spine; forces transmitted through the fusion mass would thus represent a reduction of force through other normal structures. This has been referred to as stress shielding, because a form of disuse osteoporosis can occur in the anterior vertebral bodies after posterior fusion even without instrumentation.

Spinal instrumentation has revolutionized the treatment of deformities; for example, Harrington rods [30] eliminated months of bed rest and are easily evaluated in terms of success in

accomplishing a fusion, correction of deformity, and maintenance of that correction over time. The use of instrumentation for degenerative conditions has increased the success rate of accomplishing a fusion [31], but the introduction of cages for anterior, interbody fusion has complicated the analysis as another variable is added. Optimization of the mechanical construct would require far more information, specifically with regard to the underlying process of the healing of the fusion and its structural characterization, rather than merely whether or not continuous bone formation across a spinal segment is achieved.

Rigid spinal instrumentation provides a stiffer fusion mass [32,33], but the anterior vertebral body may lose bone as a result of device-related osteoporosis [34–36]. Instrumentation systems have compared various forms of instrumentation to evaluate their degree of rigidity, and some systems have been presented as maximally rigid or somewhat rigid to address these concerns with specific attention to the stress-shielding phenomenon and the subsequent arthrodesis after fusion was achieved [37,38]. While the differences between various available rigid instrumentation systems may be arguably small, several designs that sought maximum rigidity may be contrasted with others which attempt to provide a semi-rigid construct and which can also be compared to the absence of instrumentation [39]. Unfortunately, an optimal degree of rigidity has not been established.

IV. QUANTITATIVE INSTABILITY

A model has been presented [40] to characterize the biological process that occurs prior to the healing of a lumbar fusion, with a quantitative amount of instability. Sheep were selected due to their relative uniformity in bred stock and because they are of adequate size to test instrumentation with clinical realism. Custom pedicle screw instrumentation allow the opportunity to test the hypothesis that mechanical forces modify the biological processes, specifically with the introduction of a quantitative condition of segmental instability, which is provided by custom instrumentation.

Stereophotogrammetric studies have demonstrated that in human clinical cases with implanted tantalum balls in a healing spine fusion approximately 2 mm of motion occurs [41] but ceases upon healing of the lumbar arthrodesis. To allow anteroposterior motion of 2 mm, a bushing was designed to allow 2 mm of translation along the shaft of the pedicle screw, which would then be implanted in this model (Fig. 1). Five-millimeter-diameter customary pedicle screws were shortened to accommodate the dimensions of the sheep's vertebral body using Dorset sheep (female ewes, ~50 kg).

As an experimental design to test this quantitative level of instability, an annulectomy was performed anteriorly through a retroperitoneal approach as a challenging model, reported in a similar model [42] as healing in only 50% of cases. Anterior column deficiency essentially allowed the posterior instrumentation to translate the entire 2 mm mechanically of the mechanical constraint. Rather than test small differences, as is often presented between varying instrumentation systems, all of which provide significant mechanical stability, a rigid construct to stimulate a plated long bone or osteosynthesis was performed with an anterior interbody cage combined with posterior, crosslinked, rigid instrumentation as a control. This was contrasted with the experimental 2 mm anterior posterior translation to evaluate the effects of mechanical instability on the biological process, so the observation times of these experimental animals were selected prior to the development of a solid arthrodesis.

Lumbar fusion has been established with prior studies to have displayed some mechanical integrity within the first 2 months, and the time points to evaluate the biological process in the healing fusion mass were at 6 and 12 weeks. The surgical procedure was as described [40],

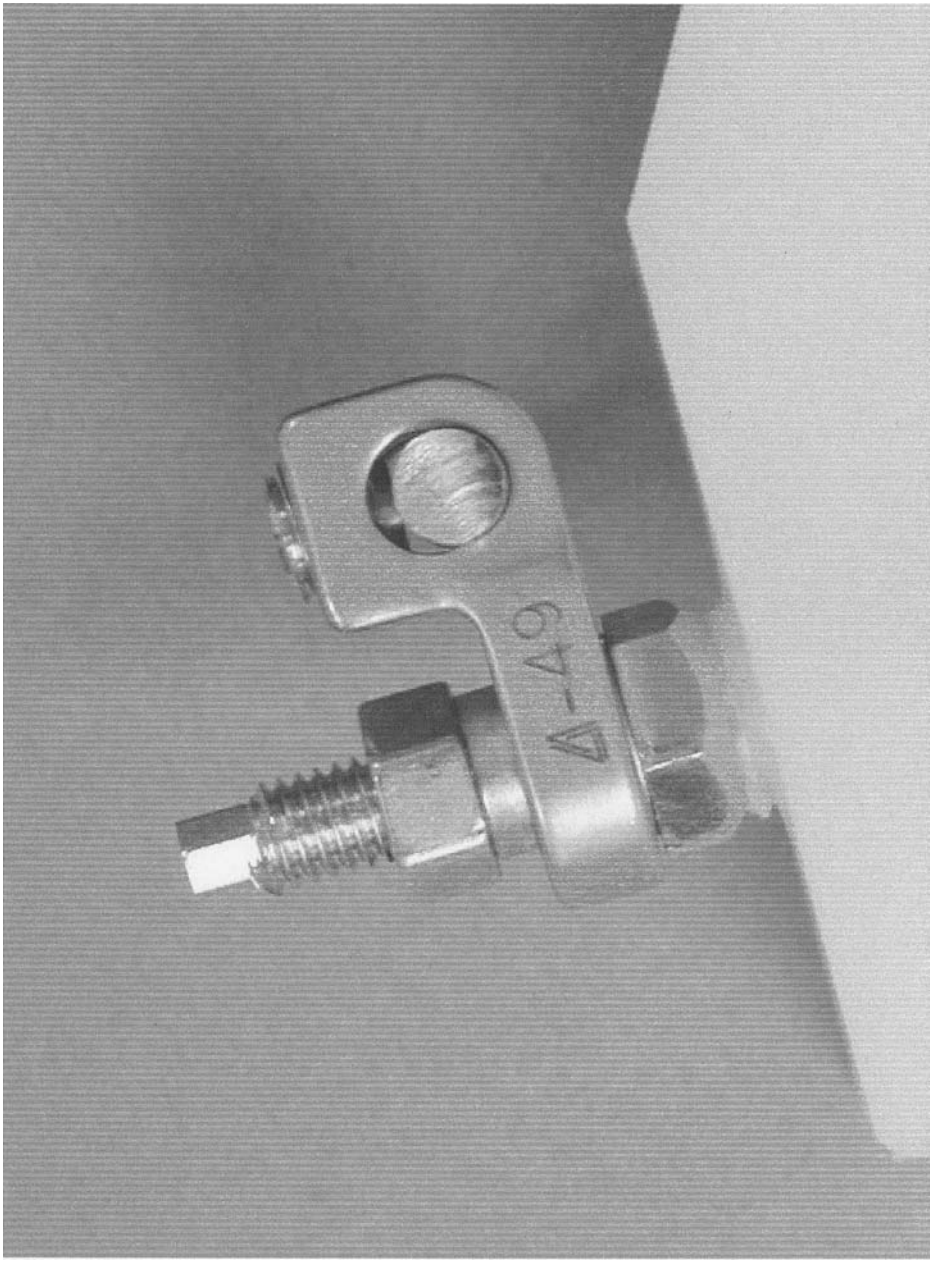

Figure 1 Custom instrumentation. A bushing machined to allow 2 mm of anterior-posterior motion along the shaft of the pedicle screw.

following which the sheep were euthanized and the spines were dissected free. Gross examination demonstrated that the 2 mm of allowed motion was not blocked by tissue and was achieved in every case. Radiographs were performed of the sheep at surgery, at 6 weeks, and at 12 weeks. Blinded evaluation of the radiographs demonstrated that fusion had not been achieved at these time points except in one sheep, an anterior fusion only, and in another, a posterior fusion only, but none had fused with both anterior and posterior arthrodeses.

Microradiographs of specimens were taken of the posterolateral regions between the intertransverse processes, which had been embedded for histological analysis. In this study, sequential sections through the fusion mass in the intertransverse process space compared a rigid control with an experimental quantitatively unstable construct. Both 6-week cases show residual bone graft, so the evaluation of new bone formation is not possible with the microradiographs alone. In contrast, at 12 weeks the bone graft has incorporated or resorbed, and hence observed bone would be expected to have acquired a circulation but the amount of bone present in terms of measured area is less with the rigid control case demonstrating clearly and confirming the concept of stress shielding. Stress shielding is evident in comparison of the experimental and control cases. Figure 2 demonstrates a section through the transverse processes in the control, or stable case. Bone formation is seen in proximity to the transverse process and noncontiguous ossification within the intertransverse space. In the experimental, or unstable case, Figure 3 demonstrates again reaction around the transverse process but also a connected fusion forming between the transverse processes. The accepted benefit of instrumentation to increase fusion rates favors stability, but maximal rigidity does not produce maximal bone formation, as quantitated by area measurements of bone formation from the microradiographs [40].

V. BIOLOGICAL PROCESS

After the instrumentation was removed, the spines were fixed in neutral buffered formalyn for at least 24 hours. The L4 segment, which had been instrumented, was then dissected free and transferred into 70% alcohol, and subsequently dehydrated through a graded series of alcohols to allow embedding in polymethylmethacrylate. Six sections from each side, right and left, were ground and stained to evaluate histologically and then quantitatively with histomorphometry. The amounts of cartilage and bone were measured to document the extent of bone formation and particularly the biological process of the healing arthrodesis, whether by cartilage or collagen mode.

Sanderson's rapid bone stain was used to stain the specimens. Histomorphometry was performed with point counting where the sections were divided into three regions: the area around the transverse processes, in the intertransverse process space where the fusion was developing, and the entire section. From one to three fields from each transverse process and one to five fields from each fusion site were captured and viewed under $5\times$ magnification with an Optronics CCD (charge coupled device) camera attached to a Nikon E-800 microscope. A grid containing 130 points was overlaid on the captured image and volume fraction of total bone, cartilage, and soft tissue determined with a point-counting technique.

Histological evaluation of developing fusion mass demonstrated endochondral ossification, including in the rigidly fixed control, and failing to demonstrate any analogy to osteosynthesis and long bone fractures. Clearly, the proximity requirement of osteosynthesis that the fixation or bone plate maintain fracture fragments within 0.5 mm is not achieved, although the graft fragments may be in proximity; they lack initially a blood supply. Intramembranous ossification collagen bone was observed in the vicinity of the transverse process, where proximity conditions are met, as opposed to the intertransverse process space, similar in both cases.

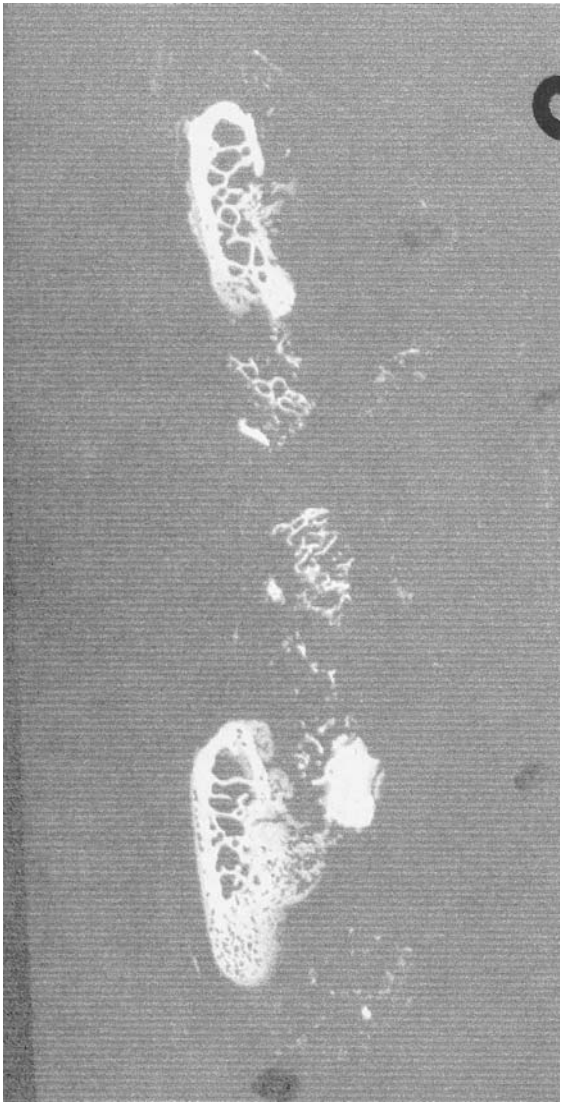

Figure 2 Microradiograph of fusion mass, saggital view from the 12-week control, rigid fixation case.

Consistent with the microradiographs, the histomorphometry demonstrated statistically more bone formation in the unstable case and more cartilage in the control, or rigidly fixed case [40]. These data suggest that the bone forms by a cartilage intermediate, which is modified by mechanical instability. Hence, an optimal rigidity exists and should be determined for design of spinal instrumentation.

The sheep has an intertransverse process space between 30 and 35 mm, so any mechanical forces relevant to that area would not be experienced by cells until at least the initial hematoma organized, and subsequently the development of healing in the area is primarily by metaplasia into cartilage cells and endochondral ossification. The cascade of bone morphogenic proteins,

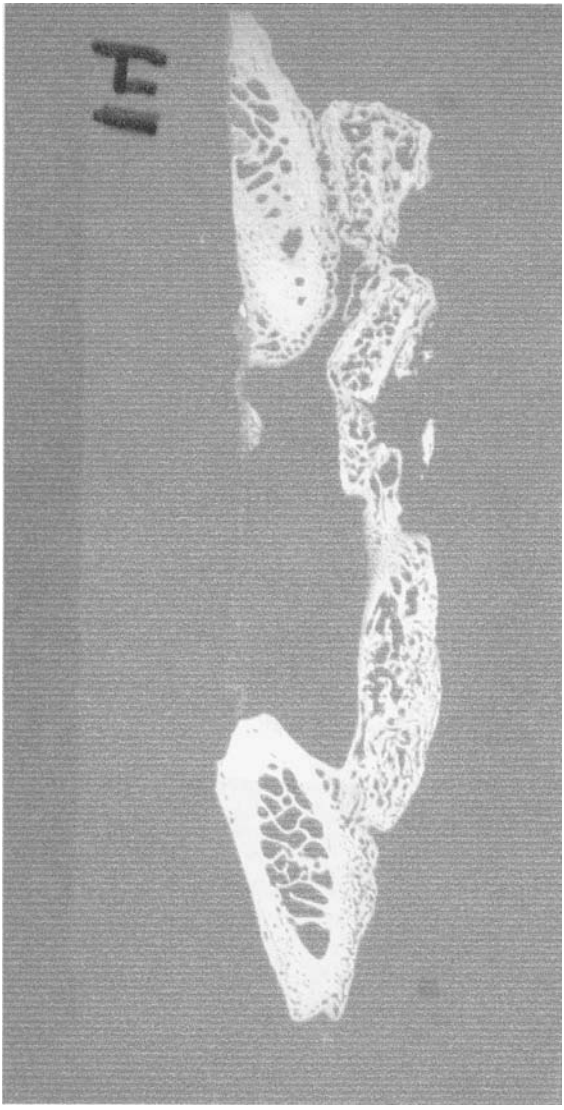

Figure 3 Microradiograph of fusion mass, saggital view from the 12-week experimental, quantitatively unstable fixation case.

which result in bone healing, are a family of molecules and various concentrations and timed at various intervals. BMP-2 is very effective in bone induction from fibrous tissues, but may not be optimal for cartilaginous tissues, so the optimum growth factor or BMP may differ with the size of the intertransverse process space, long bone healing the length of the gap to be filled, and may benefit from a combination of growth factors released at different times.

VI. FUTURE DIRECTIONS

Further characterization of this model is needed, particularly to evaluate the consequences of instability on the mechanical stiffness and strength of the fusion that results under varying

conditions. A mechanical solution to instability is the goal, and thus this model includes disc incompetence as a clinically realistic challenge to healing, so the question should evolve past whether or not the fusion heals to what degree of instrumentation rigidity results in the strongest eventual fusion.

The bone morphogenic proteins are in the TGF-β superfamily, which has an enormous array of functions. In heterotopic bone induced by cells from an osteosarcoma line, BMP 2, BMP 4, and BMP 6 were detected by immunohistochemistry, demonstrating promotion of differentiation and hence a role in bone repair [43]. Further, the differential effect of BMPs on osteoblastic differentiation has been considered [44] and remains an active area. As we understand the relative action of BMPs for tissues, and perhaps preferences [45], knowledge of the biological process involved in a healing lumbar fusion can be applied to optimize treatment. Use of bioactive proteins would require investigation of various carriers for delivery, dose, and timing. BMP 2 has been released for interbody use, but dose concerns remain for posterolateral fusion, including continuing iliac crest harvest in light of known complications.

Electrical stimulation of the healing of a lumbar fusion has been demonstrated with an implanted electrode. The environment of an electrode involves an increase in pH and decreases in oxygen tension, which have been demonstrated to enhance bone healing, including the fibrocartilaginous tissue of a failed attempt at healing or nonunion. While pulsed-electromagnetic fields have been demonstrated to be effective for long bone healing, they have not been effective in promoting the healing of a spinal arthrodesis [46]. However, noninvasive electrical stimulation with ''capacitive coupling'' has been demonstrated to promote the healing of a lumbar fusion even though the electrode effect would be absent as the technique is non-invasive. The relative effectiveness of these differing techniques may be a result of the underlying biology, which is not understood; nor is the preferred target for each of these methods of electrical stimulation known. Further, reports of the use of ultrasound as an adjunct to spinal fusion could benefit from delineation of the biological processes involved.

REFERENCES

1. Hibbs RA. An operation for progressive spinal deformities. NY Med J 1911; 93:1013–1019.
2. Hibbs RA, Rissner JC, Ferguson AB. Scoliosis treated by the fusion operation. An end result study of 360 cases. J Bone Joint Surg 1931; 13:91.
3. Rothman RH, Simeone F. Iatrogenic spinal stenosis. In: Rothman RH, Simeone F, eds. The Spine. Philadelphia: Saunders, 1982:613–614.
4. Robinson RA, Smith GW. Anterolateral cervical disc removal and interbody fusion for cervical disc syndrome. Bull Johns Hopkins Hosp 1955; 96:223–224.
5. Lenke LG, Betz RR, Haher TR, Lapp MA, Merola AA, Harms J, Shufflebarger HL. Multisurgeon assessment of surgical decision making in adolescent idiopathic scoliosis: curve classification, operative approach, and fusion levels. Spine 2001; 26(21):2347–2353.
6. Mixtner WJ, Barr JS. Rupture of the intervertebral disc with involvement of the spinal canal. N Engl J Med 1934; 211(5):210–215.
7. Saal JS, Franson RC, Dobrow R, Saal JA, White AH, Goldthwaite N. High levels of inflammatory phospholipase A2 activity in lumbar disc herniations. Spine 1990; 15(7):674–678.
8. Molinari RW, Gerlinger T. Functional outcome of instrumented posterior lumbar interbody fusion in active-duty U.S. serviceman: a comparison with nonoperative management. Spine J 2001; 1(3): 215–224.
9. Perren SM. Physical and biological aspects of fracture healing with special reference to internal fixation. Clin Orthop Rel Res 1979; 138:175–196.

10. Shapiro F. Cortical bone repair. The relationship of the lacunar-canalicular system and intercellular gap junctions to the repair process. J Bone Joint Surg 1988; 70A(7):1067–1081.
11. Brown RK, Pelker RR, Friedlaender GE, Eschel RE, Panjabi MM. Post-fracture irradiation effects on the biomechanical and histologic parameters of fracture healing. J Orthop Res 1991; 9:876–882.
12. Sekiya I, Colter DC, Prockop DJ. BMP-6 enhances chodrogenesis in a subpopulation of human marrow stromal cells. Biochem Biophys Res Commun 2001; 284(2):411–418.
13. Gerhart TN, Kirker-Heald CA, Kris MJ, et al. Healing segmental femoral defects in sheep using recombinant human bone morphogenic protein. Clin Orthop Rel Res 1993; 293:317–326.
14. Lee SE, Lee SC, Shea M, Battle MA. Healing of large segmental femurs in rat femurs is enhanced by rhBMP-2 in a PLGA matrix: a torsional and densitometric assessment. Transact Orthop Res Soc 1994; 19:206.
15. Heckman JD, Boyan BD, Aufdemorte TB, Abbott JT. The use of bone morphogenic protein in the treatment of non-union in a canine model. J Bone Joint Surg 1991; 73-A:750–764.
16. Toriumi DM, Kotler HS, Lux EN, Berg DP, Holtrop ME, Wang EA. Mandibular reconstruction with a recombinant bone-inducing factor: functional, histologic, and biomechanical evaluations. Arch Otolaryngol Head Neck Surg 1991; 117:1101–1112.
17. Boden SD, Schimandle JH, Hutton WC. An experimental lumbar intertransverse process spinal fusion model. Radiographic, histologic, and biomechanical healing characteristics. Spine 1995; 20:410–420.
18. Cunningham BW, Shimamato MD, Sefter J, Dmitrev A, Orbegoso C, McCarthy E, Fedder I, McAfee PC. Ossteintegration of autograft vs. osteogenic protein 1, North American Spine Society Transactions, 16th annual meeting p. 43, Oct 31–Nov 3, 2001.
19. Cunningham BW, Shimamoto N, Sefter JC, Dmitriev AE, McCarthy EF, Fedder IL, McAfee PC. Posterolateral spinal arthrodesis using osteogenic protein-1: an in vivo time course study using a canine model, Transaction p.577, ORS 47th Annual Meeting Feb 25–28, 2001.
20. Slater R, Nagel D, Smith RL. Biochemistry of fusion mass consolidation in the sheep spine. J Orthop Res 1988; 6:138–144.
21. Kanayama M, Dowson M, Cunningham BW, Weis JC, Parker LN, Kaneda K, McAfee PC. Maturation of the posterolateral spinal fusion and its effect on load-sharing of spinal instrumentation. An *in vivo* sheep model. J Bone Joint Surg 1997; 79-A:1710–1720.
22. Carter DR, Hayes WC. The compressive behavior of bone as a two-phase porous structure. J Bone Joint Surg 1977; 59A(7):954–962.
23. Hanley N, Shapiro DE. The development of low-back pain after excision of a lumbar disc. J Bone Joint Surg 1989; 71A:719–721.
24. Key JA;, Ford LT. Experimental vertebral-disc lesions. J Bone Joint Surg 1948.
25. Smith JW, Walmsley R. The experimental incision of the intervertebral disc. J Bone Joint Surg 1951; 33B:612–625.
26. Ostill R, Vernon Roberts B. Annular tears in intervertebral disc degeneration an experimental study using an animal model. 1990; 15:762–767.
27. Hanley EN, Phillips ED, Kostiuk JC. Who should be fused? In: Frymoyer JW, ed. The Adult Spine: Principles and Practices. New York: Raven Press, 1991:1893–1917.
28. Instructional Course Lecture #409, Low Back III Fusion Controversies, American Academy of Orthopaedic Surgeons. The Fifty-Eighth Annual Meeting, Anaheim, CA, Raven Press, March 12, 1991.
29. Deyo RA, Ciola MA, Cherkan BC, Loeser JD, Bigos SJ. Lumbar spine fusion: a cohort study of complications, reoperations, and resource use of the Medicare population. Spine 1993; 18:1463–1470.
30. Harrington PR. Correction and internal fixation by spine instrumentation. J Bone Joint Surg 1962; 44A:591.
31. Yuan HA, Garfin SR, Dickman CA, Merdjetko SM. A historical cohort study of pedicle screw fixation in thoracic lumbar and sacral spinal fusions. Spine 1994; 19(suppl):2279S–2296S.
32. Johnston CE, Ashman RB, Barrd AM, Allard RN. The effect of spinal construct stiffness on early fusion mass incorporation: experimental study. Spine 1990; 15:908–912.
33. Smith KR, Hunt TR, Asher MA, Anderson HA, Parsons WL, Robinson RG. The effect of stiff spinal implant on the bone-mineral content of the lumbar spine in dogs. J Bone Joint Surg 1991; 73A: 1115–1123.

34. McAfee TC, Farey ID, Sutterline CE, Gorr KR, Warden KE, Cunningham BW. Device related osteoporosis with spinal instrumentation. Spine 1999; 14:919–926.
35. Kliner JB, Odom JA, Moore MR, Wilson NA, Huffer WE. The effect of instrumentation on human spine fusion mass. Spine 1995; 20:90–97.
36. Dalenberg DD, Asher MA, Robinson RG, Jayaraman G. The effect of a stiff spinal implant and its loosening on bone mineral content in canines. Spine 1993; 18:1862–1866.
37. Craven TG, Carson WL, Asher MA, Robinson RG. The effects of implant stiffness on the bypassed bone mineral density and facet fusion stiffness of the canine spine. Spine 1994; 19:1664–16473.
38. Farrey ID, McAfee TC, Gurr KR, Randolph MA. Quantitative histologic studies on the influence of spinal instrumentation in a lumbar fusion: a canine model. J Orthop Res 1989; 7:709–722.
39. Cushner MA, Glaser JA. Case Report. Vertebral body osteopenia in an uninstrumented spine fusion. Orthopaedics 2000; 23(8):853–854.
40. Foster MR, Allen MJ, Shoonmaker JE, Yuan HA, Kanazawa A, Park SA, Liu B. Characterization of a developing lumbar arthrodesis in a sheep model with quantitative instability. Spine J 2002; 2(4): 244–250.
41. Johnsson R, Stromquvist B, Axelsson P, Selvik G. Influence of spinal immobilization on consolidation of posterolateral lumbosacral fusion. A roentgen stereophotogrammetric and radiographic analysis. Spine 1992; 17:16–21.
42. McAfee PC, Farey ID, Sutterlin CE, Gurr KR, Warden KE, Cunningham BW. The effect if spinal implant rigidity on vertebral bone density. A canine model. Spine 1991; 16(6S):S 190–197.
43. Waits C, Sipe J, Dhanyamraju R, Anderson HC. Distribution of bone morphogenic proteins (BMPs) during induced heterotopic bone formation, evaluated by immunohistochemistry, Transactions 48th annual ORS p. 518–, 2002.
44. Kraan van Der PM. Increased expression of BMP 2,4,6 during osteophyte formation in experimental osteoarthritis, Transactions 47th annual ORS p.673, San Francisco–, 2001.
45. Boskey A, Paschalia E, Stiner D, O'Shea O, Gokhale J, Binderman I, Doty S. BMP 6 accelerates both chondrogenesis and mineral maturation in differentiating chick limb bud mesenchymal cell cultures, Transactions ORS p. 97, 47th annual San Francisco Feb25–28, 2001.
46. Kahanovitz N, Arnoczky SP. The efficacy of direct current electrical stimulation to enhance canine spinal fusions. Clin Orthop Rel Res 1990; 251:295–391.

13

Ankylosing Spondylitis and Spinal Complications

Aaron M. From, Patrick W. Hitchon, Paul M. Peloso, and Matthew Brenton
University of Iowa College of Medicine and Veterans Administration Medical Centers Iowa City, Iowa, U.S.A.

I. THE SPONDYLOARTHROPATHIES IN RELATION TO COMMON JOINT DISORDERS

Ankylosing spondylitis (AS) is one of several spondyloarthropathies. The spondyloarthropathies involve the spine and peripheral joints. An algorithm for distinguishing these disorders from other common causes of joint pain is shown in Fig. 1. The diagnostic approach to joint pain requires first deciding whether it is inflammatory or not. Inflammation is suspected historically when there is pain at rest, prolonged morning stiffness, and generally greater than one hour of predictable relief with activity. The presence of swelling is readily discerned in peripheral joints, but cannot be seen or felt in the spine. Noninflammatory or mechanical joint pain, by contrast, is better with rest and worsened with activity. Inflammatory joint disorders can be further subdivided based upon the presence or absence of axial inflammation. Inflammatory joint disorders involving the spine can have prominent peripheral joint involvement, as occurs with psoriatic and reactive arthritis, to minimal to no peripheral joint involvement with prominent centralized back pain, as is more typical of ankylosing spondylitis [1–3]. The seronegative spondyloarthropathies (so named due to the absence of rheumatoid factor in the serum) are a clinically and pathologically distinct family of arthritides, with patterns of spinal involvement quite separate from rheumatoid arthritis and other inflammatory disorders. Thus, the following discussion is specific to the inflammatory spondyloarthropathies with spinal involvement, most typified by ankylosing spondylitis.

II. CLINICAL PRESENTATION AND DIAGNOSIS

Ankylosing spondylitis is predicted to affect nearly 1.5% of the U.S. Caucasian population, though a smaller percentage of those are formally recognized and diagnosed. Diagnostic features include onset typically under age 40 years and early morning low back stiffness that has persisted for longer than 3 months, which is predictably relieved with exercise. Examination reveals decreased spinal motion in all directions, although extension and lateral bending are most affected, with decreased chest wall motion evidence in advanced disease. Radiographs give evidence of sacroiliac joint erosions and sclerosis. Figure 2 shows a diagnostic approach to ankylosing spondylitis based on the Modified New York Criteria [4–6]. Up to 90% of patients with

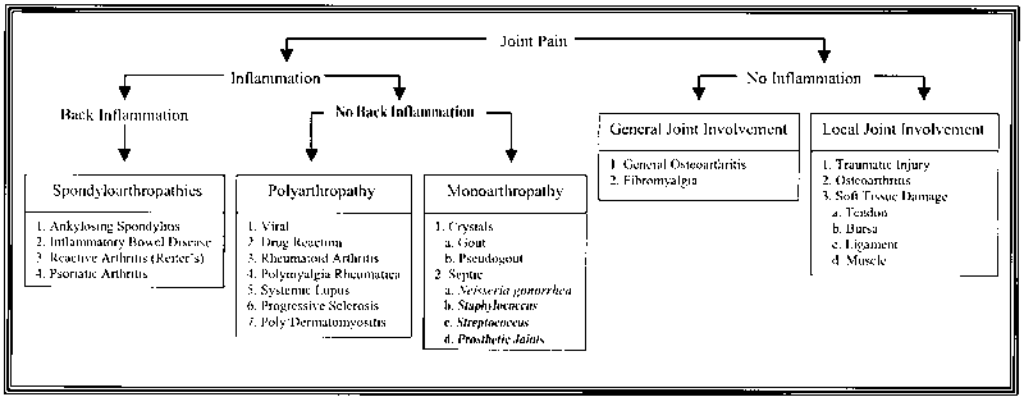

Figure 1 Algorithm for diagnosis of common joint disorders.

ankylosing spondylitis are positive for the HLA-B27 gene. HLA-B27 is thought to play an important role in disease pathogenesis, although the gene itself is not diagnostic of AS, occurring in up to 5–8% of the normal population [4].

A typical case presentation of ankylosing spondylitis would be as follows: A 26-year-old white male presents with complaints of severe early morning low back stiffness and pain that awakens him at 5 a.m. Historically the pain has persisted for about 4 months and at times is so severe that he must crawl or use a baseball bat as support to reach the bathroom. After a warm shower and moving around for an hour, the pain subsides and he functions more normally. He feels best playing basketball, and worse about 2 hours after quitting. The patient states that both his father and an uncle had ''back problems'' for most of their lives. His exam shows decreased lumbar flexion, extension, and side-to-side motion. A radiograph of his pelvis reveals bilateral erosions and sclerosis of the inferior portion of his sacroiliac joints (Fig. 3).

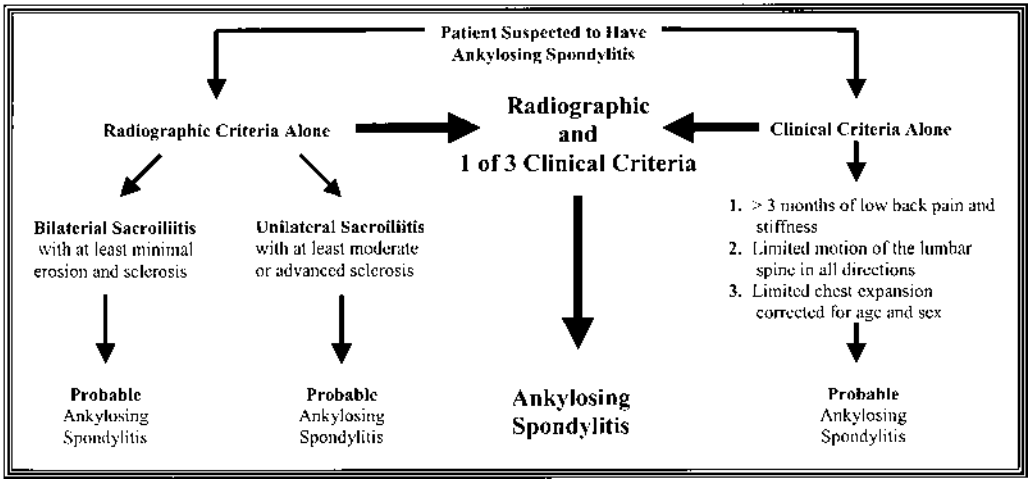

Figure 2 Algorithm for diagnosis of ankylosing spondylitis.

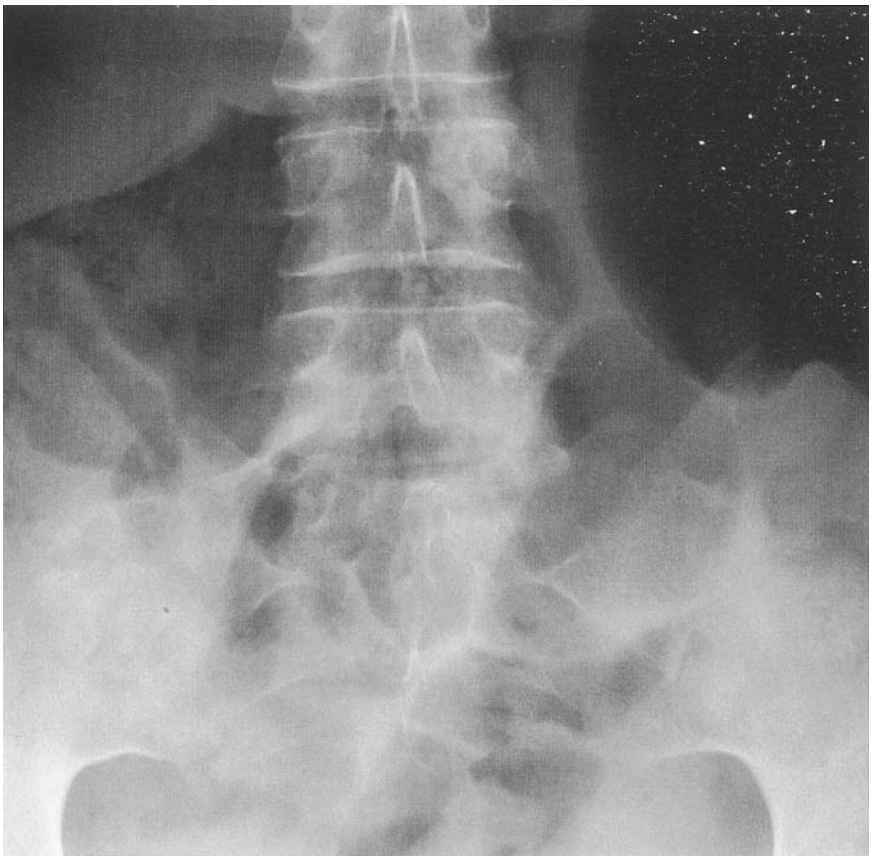

Figure 3 Plain film demonstrates early fusion and sclerosis of the sacroiliac joints.

III. ETIOLOGY AND PATHOGENESIS

Inflammation begins as HLA-B27 class I protein antigens interact with circulating cytotoxic T lymphocytes. This HLA-B27 presentation mechanism is known as the *arthritogenic peptide hypothesis* [7]. Furthermore, a second stimulatory factor has been hypothesized which includes microtrauma or chronic bacterial deposition in the bowel or joints, leading to an upregulation of cytokine production and subsequent increases in the inflammatory response [1,8–11]. The possible role of *Klebsiella aeruginosa* producing an inflammatory response by mimicking the HLA-B27 antigen has been suggested [1].

Clinical manifestation of the disease begins with enthesitis in the sacroiliac and lumbar vertebral joints [4,8,12]. Inflammation of the tendon and ligament attachment to bone, also known as enthesitis, is a unique identifier of all spondyloarthropathies [8,9]. Enthesitis is followed by fibrosis and ossification of the attached ligaments and intervertebral disk spaces (Fig. 3). Erosion of bone at the ligamentous attachment of the intervertebral disk to the vertebral body and calcification along the anterior longitudinal ligament leads to vertebral body squaring, evident on lateral lumbar spine films. In an attempt to repair inflamed and eroded vertebral bodies, bony growth ensues, resulting in syndesmophyte formation across the disk space. Eventually, the pattern of ossification progresses to the thoracic and cervical regions of the spine, resulting in

kyphotic deformity. This ossified spine, also known as the ''bamboo spine,'' suffers secondary osteoporosis due to chronic immobility, leaving the vertebral bodies brittle and easily susceptible to fracture [4,8,12].

IV. EXTRA SPINAL FEATURES OF ANKYLOSING SPONDYLITIS

A. Inflammatory Bowel Disease

Chronic bowel lesions of the colon and distal ileum, characterized by villous atrophy and blunting with increased cellularity and minimal neutrophil invasion, is seen in as many as 57% of ankylosing spondylitis patients [13]. The occurrence of inflammatory bowl disease (IBD) is more prevalent in patients lacking the HLA-B27 gene, but they nevertheless demonstrate characteristic inflammatory back pain [11]. On average, symptoms of IBD appear 6 years after onset of ankylosing spondylitis, but can also precede it [14]. It has been suggested that infectious organisms such as *Klebsiella* may enter through the gut in order to exacerbate the inflammatory process and lead to further enthesitis and bowel inflammation [1,11].

B. Heart

Aortitis and aortic valve incompetence are seen in 1% of patients who have had ankylosing spondylitis for 5–10 years [15], with increasing incidence with increased disease duration. Conversely, pericarditis and first-degree heart block are found most commonly in early disease [16].

C. Liver

Liver changes, as measured by serum gamma-glutamyl transpeptidase (GGT) and alkaline phosphatase (AP), appear to correlate with raised erythrocyte sedimentation rate (ESR) levels [14]. AP is raised in approximately 14–47.5% of all ankylosing spondylitis patients and can be a marker for both bone and liver involvement [17]. (GGT) elevation has been reported to occur in 26% of ankylosing spondylitis patients and appears to be a more specific identifier of liver involvement [17–21]. The clinical consequences of these changes are not certain.

D. Eye

Common eye symptoms reported in patients with ankylosing spondylitis include dryness, redness, and pain, which can be associated with conjunctivitis and iritis [1]. Inflammation of the iris is reported to occur in 12% of HLA-B27–positive patients [22]. Typically, symptoms of iritis usually present 10 years after the first signs of ankylosing spondylitis and are characterized by redness, pain, and photophobia. Iritis is more commonly found with other complications of ankylosing spondylitis, including psoriasis and IBD, and it can threaten the vision if not treated [14].

E. Kidney

Renal damage is measured indirectly through screening for microscopic hematuria, microalbuminuria, increased serum creatinine, increased levels of the tubular lysosomal enzyme *N*-acetyl-β-D-glucosaminidase (NAG), or proteinuria [23]. Abnormal renal function has been reported to occur in 10–35% of populations with ankylosing spondylitis. Possible sources of renal dys-

function include increased serum IgA levels, increased serum amyloid levels, and damaging effects of nonsteroidal anti-inflammatory drugs (NSAIDs) [23,24].

F. Lung

Total lung capacity and vital capacity of ankylosing spondylitis patients is significantly lower than in healthy control patients. This decrease in aerobic capacity does not appear to be related to axial enthesitis and bony fusion [25]. Furthermore, apical fibrosis of the lung due to tuberculosis, *Aspergillus* infection, or idiopathic pleural thickening is a recognized complication, reported to occur up to 30% of patients [26–29].

V. MEDICAL MANAGEMENT

Current medical management of ankylosing spondylitis focuses on symptom control as well as long-term disease modification. Four therapies form the mainstay of treatment: patient education, exercise, NSAIDs, and immune system–modifying agents [30]. Patients should be made aware of the possibility of disease progression and the risk of fractures related to fusion and secondary osteoporosis. Regular stretching and vigorous aerobic exercise appear to provide immediate gains in flexibility and may help decrease secondary osteoporosis of the spine by reducing immobility [31,32]. First-line drug therapy includes the use of NSAIDs for symptom control. Most NSAIDs have efficacy in pain management, with several having randomized trial proof of efficacy, including indomethacin, naproxen, and celecoxib [30]. NSAIDs reduce pain and morning stiffness but do not stop the course of the disease or the associated underlying inflammation of the spine [30,33]. In those patients with inflamed peripheral joints, the anti-inflammatory agent sulfasalazine and the immunosuppressant methotrexate and careful use of corticosteroids can be helpful, although none of these agents controls the spinal inflammation [30].

True changes in the natural history of ankylosing spondylitis will occur through novel approaches to immune modulation. Recent randomized trials published in 2002 suggest such a role for inhibitors of TNF-α (infliximab and etanercept) and use of the antiosteoporotic agent pamidronate [33–36]. Formal studies are underway for FDA approval of these agents in an attempt to inhibit and reverse the underlying spinal inflammation. It appears that the synovium is particularly susceptible to cytokines such as tumor (TNF-α) [9,37]. Inhibition of TNF-α with etanercept (an IgG molecule linked to a TNF-α receptor that blocks receptor action) or antibodies-directed TNF-α antibodies (infliximab) have shown significant and rapid reduction of active axial inflammation in ankylosing spondylitis [33,34,37], and preliminary studies suggest that they also have structural modification abilities.

VI. FRACTURES OF THE ANKYLOSED SPINE

Published reports suggest that extension fractures of the cervical spine are the most common fractures of the fused spine. However, the exact type of fracture is dependent upon the mechanism of the injury [38–40]. The heightened prevalence of cervical spine extension fracture reflects the common injury mechanism, wherein an individual falls forward, striking the head on the ground [38,41]. In the thoracic and lumbar spines, extension fractures occur as a result of falling backwards on the kyphotic spine [42].

The severity of fractures in ankylosing spondylitis is disproportionate to the trivial nature of the trauma. This reflects the extremely brittle nature of the cervical and thoracic spine, secondary to osteoporosis [4,12]. The fractures of the osteoporotic spine have been likened to the snapping of a stick or rock, resulting in two opposed solid pieces of bone meeting at a

fractured joint [43,44]. The fracture commonly involves both anterior and posterior structures of the spinal column. This in turn leads to a higher incidence of neurological deficit as well as delayed healing [41,43,45]

Transdiscal fractures appear to be common in either the cervical or thoracolumbar spine [12,39,46]. A proposed theory suggests that as the disk space ossifies, the normal bending force is no longer centered over the nucleus pulposus, but instead is displaced peripherally in the spinal column, resulting in unstable, shearing fractures [46].

VII. NONOPERATIVE MANAGEMENT OF FRACTURES

In stable fractures without neurological deficit or canal compromise, immobilization in a brace is generally sufficient. With cervical spine fractures without dislocation or spinal cord compression, use of a Miami or Philadelphia collar is necessary. Bed rest for up to one week may be necessary for pain control with thoracic and lumbar spines. Immobilization thereafter in a Jewett brace or clam shell is then necessary, with sequential radiographs to confirm healing. Orthotics are often recommended for up to 3 months to facilitate bony fusion [40,41]. Some accounts suggest that conservative, non-operative management of fractures result in better outcomes, fewer hospital days, and lower costs in ankylosing spondylitis [40,47].

VIII. SURGICAL MANAGEMENT OF FRACTURES

A. General Surgical Considerations

Spinal instability, often associated with neurological deficit, requires surgical intervention in the form of anterior or posterior instrumentation and fusion. In addition to stabilization, in the presence of neural compression, anterior or posterior decompression may also be necessary. Instability can be defined as disruption of all three columns of the spine, including the anterior vertebral body, anterior half of the disc, and anterior longitudinal ligament (anterior column), posterior vertebral body, posterior half of the disc, and posterior longitudinal ligament (middle column), as well as the neural arches and attached ligaments (posterior column) (Fig. 4) [48]. Figure 5 provides a summary treatment algorithm for fractures in ankylosing spondylitis.

B. Cervical Fractures

In case of fractures with dislocation, deformity, and cord compression, traction in the neutral position can assist in achieving reduction prior to surgery. Stabilization is generally achieved through a posterior approach by means of posterolateral screws with plates or rods (Fig. 6). Screw placement can be difficult in the fused cervical spine due to lack of distinct bony landmarks and the softness of osteoporotic bone [49,50]. The use of posterior bone grafts to achieve fusion is recommended [49]. When screw placement is impossible or impractical, spinous process wiring along with bone grafting can be used alone or in combination with placed plates and screws [41,50].

C. Thoracic and Lumbar Fractures

In the presence of three-column disruption involving the vertebral bodies or discs and neural arch and/or neural compression with deficit, stabilization is undertaken. Stabilization is achieved with pedicle screws, hooks and rods, and bony fusion. Hooks can be used to secure rods, but fusion of bone and calcification of the ligamentum flavum can make hook placement difficult [42].

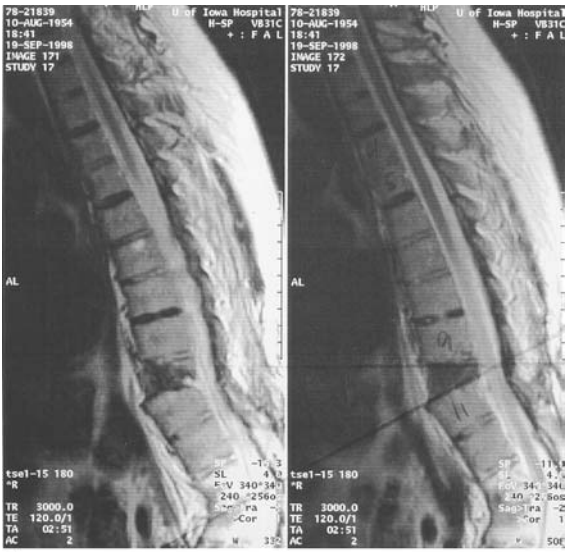

A

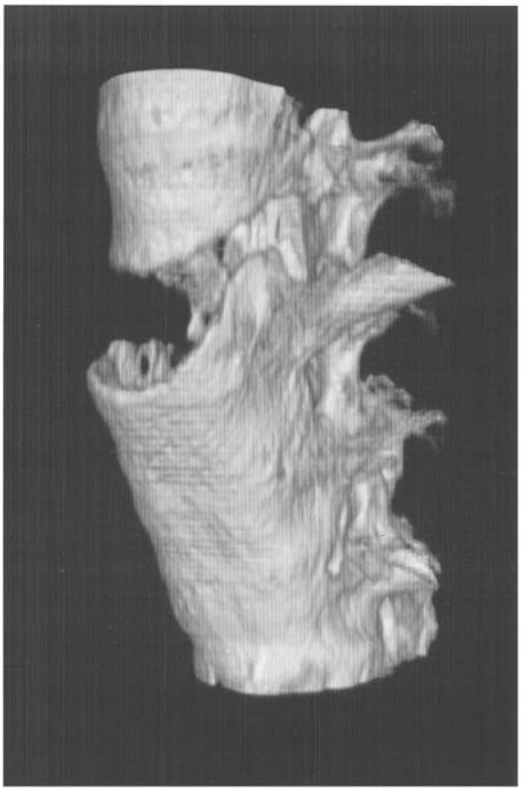

B

Figure 4 A 44-year-old male with ankylosing spondylitis. (A) T2-weighted magnetic resonance images demonstrates fracture of the T9–10 vertebral bodies and cord compression. (B) Three-dimensional computer tomography image of the same fracture demonstrates three column injury.

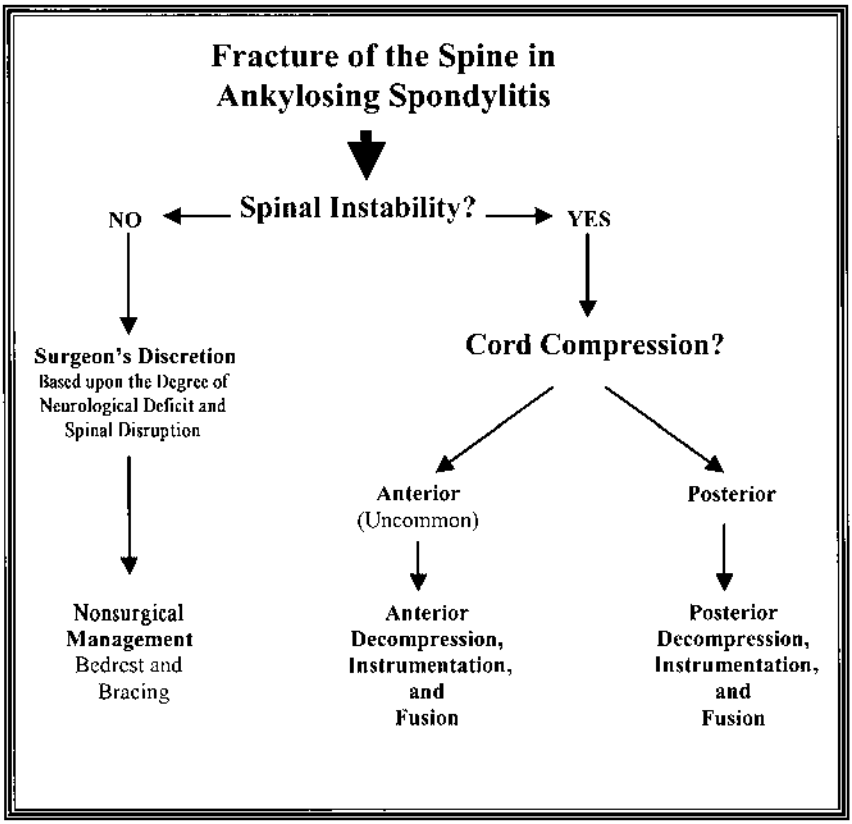

Figure 5 Algorithm for fracture treatment in ankylosing spondylitis.

In a retrospective review at the University of Iowa, 266 patients with a diagnosis of ankylosing spondylitis were identified. Six thoracic and five lumbar fractures were found in 8 men and 3 women, who ranged in age from 43 to 79 years [42]. Nine of 11 presented with negative spinal angulation or extension deformity, as demonstrated in Fig. 4. The predominance of extension fractures is a reflection of the kyphosis, brittleness, and osteoporosis that develops in the AS spine. The fragility of the ankylosed spine in our sample is highlighted by the fact that 8 patients had only minor trauma, such as falls from their own height or falls from transfers.

Nine of the 11 patients underwent surgery for spinal stabilization with hardware and bony fusion. Instrumentation included either hooks (in 3 patients) or pedicle screws (in 6 patients) to secure rods or plates. Two patients underwent both posterior and anterior fusion. Four patients diagnosed with posterior cord compression underwent laminectomy. The 2 patients who did not have surgery were treated with bed rest for up to one week, followed by gradual mobilization. Irrespective of operative or nonoperative management, thoracolumbar clam shell braces were worn for at least 3 months.

Based on Frankel scores at admission and subsequent follow-up, 5 of the 11 patients did not suffer motor or sensory damage as a result of the fracture. Of the 6 patients who had a postinjury neurological deficit, 3 demonstrated neurological improvement after treatment, whereas 3 showed no change in Frankel score. Spinal deformity was corrected as a result of surgery in 7 of the 9 operative patients by $12 \pm 10^{\circ}$ (mean $\pm$ SD) [42].

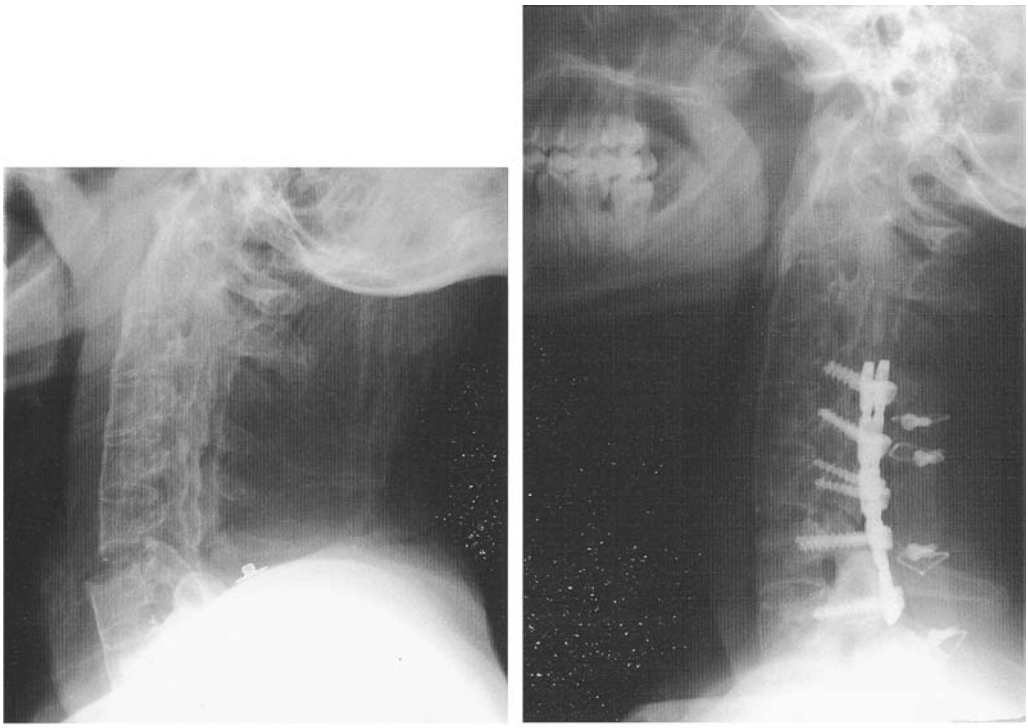

Figure 6 Lateral plain films of a 44-year-old male with ankylosing spondylitis demonstrates (A) C6–7 cervical fracture with obvious anterior vertebral body fusion and (B) cervical stabilization of the C6–7 bodies after fracture stabilization using lateral mass screws and spinous process wires.

D. Complications

Common complications following fractures and surgery include epidural hematoma and pulmonary infection. While spinal epidermal hematoma appears to be a complication of the fracture itself, pulmonary complications more likely arise due to nosocomial infection [39,40,44,51]. Increased rates of pulmonary infection could be due to the increased difficulty in ventilation of the patient due to factors including decreased lung capacity, kyphotic deformity, and apical fibrosis [12,25,26].

IX. SUMMARY POINTS

1. Ankylosing spondylitis has a protracted clinical course, which is generally managed by medications and lifestyle changes.
2. Cervical and thoracolumbar fractures occur following minimal trauma, which can result in serious neurological compromise.
3. Spinal fractures in ankylosing spondylitis require special surgical consideration due to their unstable nature in a brittle spine.
4. Surgical intervention of spinal fractures in ankylosing spondylitis depends on fracture stability, presence of cord compression, and fracture location.

REFERENCES

1. Keat A. Seronegative spondyloarthropathies: ankylosing spondylitis. In: Klippel JH, Crofford LJ, Stone JH, Weyand CM, eds. Primer on Rheumatic Diseases. 12th ed.. Atlanta: The Arthritis Foundation, 2001:250–255.
2. Boumpas DT, Illei GG, Tassiulas IO. Psoriatic arthritis Klippel JH, Crofford LJ, Stone JH, Weyand CM, eds. Primer on Rheumatic Diseases. 12th ed.. Atlanta: The Arthritis Foundation, 2001:233–237.
3. Arnett FC. Seronegative spondyloarthropathies: reactive arthritis and enteropathic arthritis Klippel JH, Crofford LJ, Stone JH, Weyand CM, eds. Primer on Rheumatic Diseases. 12th ed.. Atlanta: The Arthritis Foundation, 2001:245–250.
4. Fox M, Onofrio B. Ankylosing Spondylitis in Principles of Spinal Surgery Menezes AH, Sonntag VH, eds. New York: McGraw-Hill, 1996:735–750.
5. Van Der Linden S, Valkenburg HA, Cats A. Evaluation of diagnostic criteria for ankylosing spondylitis: a proposal for modification of the New York criteria. Arthr Rheumat 1984; 27(4):361–368.
6. Dougados M, van der Linden S, Juhlin R, Huitfeldt B, Amor B, Calin A, Cats A, Dijkmans B, Olivieri I, Pasero G. The European Spondylarthropathy Study Group preliminary criteria for the classification of spondylarthropathy. Arthr Rheumat 1991; 34(10):1218–1227.
7. Lopez de Castro JA. The pathogenetic role of HLA-B27 in chronic arthritis. Curr Opin Immunol 1998; 10(1):59–66.
8. Benjamin M, McGonagle D. The anatomical basis for disease localisation in seronegative spondyloarthropathy at entheses and related sites. J Anatomy 2001; 199(pt 5):503–26.
9. McGonagle D, Gibbon W, Emery P. Classification of inflammatory arthritis by enthesitis. Lancet 1998; 352(9134):1137–40.
10. McGonagle D, Emery P. Enthesitis, osteitis, microbes, biomechanics, and immune reactivity in ankylosing spondylitis. J Rheumatol 2000; 27(10):2302–2304.
11. Mielants H, Veys EM, Cuvelier C, De Vos M. Course of gut inflammation in spondylarthropathies and therapeutic consequences. Baill Clin Rheumatol 1996; 10(1):147–64.
12. Weinstein P, Karpman R, Gall E, Pitt M. Spinal cord injury, spinal fracture and spinal stenosis in ankylosing spondylitis. J Neurosurg 1982; 67:609–616.
13. Mielants H, Veys EM, Cuvelier C, de Vos M. Ileocolonoscopic findings in seronegative spondylarthropathies. Br J Rheumatol 1988; 27(suppl 2):95–105.
14. Brophy S, Pavy S, Lewis P, Taylor G, Bradbury L, Robertson D, Lovell C, Calin A. Inflammatory eye, skin, and bowel disease in spondyloarthritis: genetic, phenotypic, and environmental factors. J Rheumatol 2001; 28(12):2667–2673.
15. Ansell B, Bywaters G, Doniach I. The aortic lesion of ankylosing spondylitis. Br Heart J 1958; 20: 507.
16. Cosh JA. The heart and the rheumatic diseases. Rheumatol Phys Med 1972; 11(6):267–280.
17. Siede WH, Seiffert UB, Merle S, Goll HG, Oremek G. Alkaline phosphatase isoenzymes in rheumatic diseases. Clin Biochem 1989; 22(2):121–124.
18. Robinson AC, Teeling M, Casey EB. Hepatic function in ankylosing spondylitis. Ann Rheum Dis 1983; 42(5):550–552.
19. Sheehan NJ, Slavin BM, Kind PR, Mathews JA. Increased serum alkaline phosphatase activity in ankylosing spondylitis. Ann Rheum Dis 1983; 42(5):563–5.
20. Kendall MJ, Lawrence DS, Shuttleworth GR, Whitfield AG. Haematology and biochemistry of ankylosing spondylitis. Br Med J 1973; 2(5860):235–237.
21. Smith D, Spencer D, Allam B, Farish E, Borland W. Serum alkaline phosphatase in ankylosing spondylitis. J Clin Pathol 1979; 32:853–854.
22. Linssen A, Rothova A, Valkenburg HA, Dekker-Saeys AJ, Luyendijk L, Kijlstra A, Feltkamp TE. The lifetime cumulative incidence of acute anterior uveitis in a normal population and its relation to ankylosing spondylitis and histocompatibility antigen HLA-B27. Invest Ophthalmol Vis Sci 1991; 32(9):2568–2578.
23. Vilar MJ, Cury SE, Ferraz MB, Sesso R, Atra E. Renal abnormalities in ankylosing spondylitis. Scand J Rheumatol 1997; 26(1):19–23.

24. Jones DW, Mansell MA, Samuell CT, Isenberg DA. Renal abnormalities in ankylosing spondylitis. Br J Rheumatol 1987; 26(5):341–345.
25. Carter R, Riantawan P, Banham SW, Sturrock RD. An investigation of factors limiting aerobic capacity in patients with ankylosing spondylitis. Respirat Med 1999; 93(10):700–708.
26. Boushea DK, Sundstrom WR. The pleuropulmonary manifestations of ankylosing spondylitis. Semin Arthr Rheumat 1989; 18(4):277–281.
27. Chakera TM, Howarth FH, Kendall MJ, Lawrence DS, Whitfield AG. The chest radiograph in ankylosing spondylitis. Clin Radiol 1975; 26(4):455–459.
28. Lauritzen H, Medina J, Loken MD. Pulmonary disease in patients with ankylosing spondylitis (abstr). Am Rev Respir Dis 1968; 98:126.
29. Rosenow E, Strimlan CV, Muhm JR, Ferguson RH. Pleuropulmonary manifestations of ankylosing spondylitis. Mayo Clin Proc 1977; 52(10):641–649.
30. Koehler L, Kuipers JG, Zeidler H. Managing seronegative spondarthritides. Rheumatology 2000; 39(4):360–368.
31. Russel P, Unsworth A, Haslock I. The effect of exercise on ankylosing spondylitis: a preliminary study. Br J Rheumatol 1993; 32:498–506.
32. Inman R. Seronegative spondyloarthropathies: treatment. Klippel JH, Crofford LJ, Stone JH, Weyand CM, eds. Primer on Rheumatic Diseases. 12th ed.. Atlanta: The Arthritis Foundation, 2001:255–258.
33. Gorman JD, Sack KE, Davis JC. Treatment of ankylosing spondylitis by inhibition of tumor necrosis factor alpha. N Engl J Med 2002; 346(18):1349–1356.
34. Braun J, Brandt J, Listing J. Treatment of active ankylosing spondylitis with Infliximab: a randomized controlled multicenter trial. Lancet 2002; 359(9313):1187–1193.
35. Stone M, Lax M, Payne U, Lapp V, Inman R. Clinical and imaging correlates of response to treatment with Infliximab in patients with ankylosing spondylitis. J Rheumatol 2002; 28:1605–1614.
36. Maksymowich WP, Jhangri GS, Fitzgerald AA, LeClerq S, Chiu P, Yan A, Skeith KJ, Aaron SL, Homik J, Davis P, Sholter D, Russell AS. A six month randomized, controlled, double-blind, comparison of intravenous pamidronate (60 mg versus 10 mg) in the treatment of nonsteroidal antiinflammatory drug-refractory ankylosing spondylitis. Arthr Rheumat 2002; 46(3):766–773.
37. Keffer J, Probert L, Cazlaris H, Georgopoulos S, Kaslaris E, Kioussis D, Kollias G. Transgenic mice expressing human tumour necrosis factor: a predictive genetic model of arthritis. EMBO J 1991; 10(13):4025–4031.
38. Foo D, Bignami A, Rossier AB. Two spinal cord lesions in a patient with ankylosing spondylitis and cervical spine injury. Neurology 1983; 33(2):245–249.
39. Hunter T, Dubo HI. Spinal fractures complicating ankylosing spondylitis. A long-term follow-up study. Arthr Rheumat 1983; 26(6):751–759.
40. Apple DF, Anson C. Spinal cord injury occurring in patients with ankylosing spondylitis: a multicenter study. Orthopedics 1995; 18(10):1005–1011.
41. Fox MW, Onofrio BM, Kilgore JE. Neurological complications of ankylosing spondylitis. J Neurosurg 1993; 78(6):871–878.
42. Hitchon P, From A, Brenton M, Glaser J, Torner J. Fractures of the thoracolumbar spine complicating ankylosing spondylitis. J Neurosurg (Spine 2) 2002; 97:218–222.
43. Graham GP, Evans PD. Spinal fractures in patients with ankylosing spondylitis. Injury 1991; 22(5): 426–427.
44. Grisolia A, Bell RL, Peltier LF. Fractures and dislocations of the spine complicating ankylosing spondylitis. A report of six cases. J Bone Joint Surg 1967; 49(2):339–344.
45. Osgood CP, Abbasy M, Mathews T. Multiple spine fractures in ankylosing spondylitis. J Trauma-Injury Infect Crit Care 1975; 15(2):163–166.
46. Graham B, Van Peteghem PK. Fractures of the spine in ankylosing spondylitis. Diagnosis, treatment, and complications. Spine 1989; 14(8):803–807.
47. Rowed DW. Management of cervical spinal cord injury in ankylosing spondylitis: the intervertebral disc as a cause of cord compression. J Neurosurg 1992; 77(2):241–246.
48. Denis F. The three column spine and its significance in the classification of acute thoracolumbar spinal injuries. Spine 1983; 8(8):817–831.

49. Taggard DA, Traynelis VC. Management of cervical spinal fractures in ankylosing spondylitis with posterior fixation. Spine 2000; 25(16):2035–2039.
50. Cooper PR, Cohen A, Rosiello A, Koslow M. Posterior stabilization of cervical spine fractures and subluxations using plates and screws. Neurosurgery 1988; 23(3):300–306.
51. Foo D, Rossier AB. Post-traumatic spinal epidural hematoma. Neurosurgery 1982; 11(1 pt 1):25–32.

14

Atlantoaxial Transarticular Screw Fixation: Indication, Technique, Risks, and Pitfalls

Takeshi Fuji, Takenori Oda, and Yasuji Kato
Osaka Koseinenkin Hospital
Osaka, Japan

I. INTRODUCTION

Posterior atlantoaxial transarticular screw fixation was introduced by Magerl and Seemann [1] in 1986. Several in vitro studies [2–4] have shown that this technique is mechanically superior to posterior wiring techniques. Several authors [1,5–10] reported high fusion rates in the clinical series. However, this technique is potentially dangerous because the screw path is close to important structures, such as the vertebral artery and spinal cord. Some authors have pointed out the risk of vertebral artery injury [11–14].

The technique first described by Magerl included opening the lateral atlantoaxial joints and detecting screws in the joints [1]. Gebhard et al. [15] reported that the aiming device allowed safe instrumentation in patients with a normal anatomical situation. We have performed this technique under fluoroscopic monitoring without either opening the lateral atlantoaxial joints or using an aiming device. The purpose of this chapter is to describe the technique of this fixation method, to demonstrate the accuracy and safety of screw insertion by surgical record and by postoperative CT examination, and then to indicate the recommended points for safe screw insertion.

II. INDICATION

Indication for atlantoaxial transarticular screw fixation consists of reducible atlantoaxial instability associated with various diseases. For example, atlantoaxial instability associated with rheumatoid arthritis, os odontoideum, Down syndrome, athetoid cerebral palsy, or trauma is an indication for this type of fixation. Irreducible atlantoaxial instability is a contraindication for this method.

III. OPERATIVE TECHNIQUE

Our operative technique is as follows. Before the operation, a lateral radiogram in flexion, neutral, and extension positions and open-mouth antero-posterior radiogram are achieved to plan the correct screw trajectory. CT examination in the reduced position is also obtained. The screw

pathway should be simulated to avoid risky screw insertion. If the simulated screw pathway is into the vertebral artery foramen, atlantoaxial transarticular screw insertion should be avoided at this side (Fig. 1).

Our surgical procedures were almost the same as previously described by others [1,5–9,16]. Patients were laid in the prone position using a skull-fixation device or halo-vest apparatus. The positioning was important: reduction or adequate alignment of the atlas and the axis, defined as the position with an anterior atlantodental interval of 3 mm or less, was attempted. Lateral fluoroscopic monitoring with a C-arm was used in this procedure.

A midline longitudinal skin incision was made from the occiput to the cervical spine. With a conventional subperiosteal technique, dorsal aspects of the atlas, the axis, and the third cervical vertebra were exposed. Under fluoroscopy, further realignment of the atlas and the axis was gently tried by manual reduction for patients whose anterior atlantodental intervals were still more than 4 mm. The maneuver for manual reduction for anterior subluxation was as follows: the spinous process of the axis was gently pushed anteriorly and the posterior arch of the atlas was pulled posteriorly by a polyethylene suture placed around it. Under fluoroscopic monitoring, a guidewire was inserted. The insertion point was 2 or 3 mm cephalad to the C2/3 facet joint, and the width between the insertion points complied with the width measured by preoperative CT scan. The trajectory was usually straight ahead in a sagittal orientation and was aimed toward the dorsal cortex of the anterior arch of the atlas. After satisfactory trajectory of the guidewire was confirmed by fluoroscopy and manually confirmed by fixation between the atlas and the axis, measuring of the screw length, drilling, and tapping were performed. After guidewire insertion on both sides, a screw was inserted following by pulling out a guidewire. In early cases using cannulated screws, we performed drilling and screwing with the remaining guidewires. Screwing with the remaining guidewires risks breakage of the guidewire, as described later. The bone graft is performed by the Gallie's or Brooks' method.

IV. ACCURACY OF ATLANTOAXIAL TRANSARTICULAR SCREW INSERTION

We have evaluated the accuracy of atlantoaxial transarticular screw insertion in our clinical cases [17].

A. Patients and Methods

From 1989 to 1998, atlantoaxial transarticular screw fixation was performed in 56 consecutive cases with atlantoaxial instability. There were 19 males and 37 females. The age at operation ranged from 6 to 80 years, with an average age of 53.7 years. The causes of atlantoaxial instability were rheumatoid arthritis in 36, congenital anomaly (including os odontoideum) in 10, trauma in 4, Down syndrome in 3, athetoid cerebral palsy in 2, and metastatic cervical tumor in 1.

CT images were obtained in all cases preoperatively, and the position of the insertion point and the pathway of the screw were inspected on CT images. Screw length was measured and screw trajectory on sagittal plane was planned on lateral radiogram. During the same period, there was one case with high riding vertebral artery groove on both sides. We viewed the situation on preoperative CT image, and posterior atlantoaxial fusion using a hook and rod system was done for this case. Inserted were 76 4-mm-diameter cannulated screws, 1 3.5-mm-diameter AO screw, 6 4.5-mm-diameter AO screws, and 28 Olerud Cervical screws, 4.5-mm-diameter. We investigated complications during 112 screw insertions by surgical records. One screw could not be inserted and 111 screws were inserted for 112 sites (99.1%).

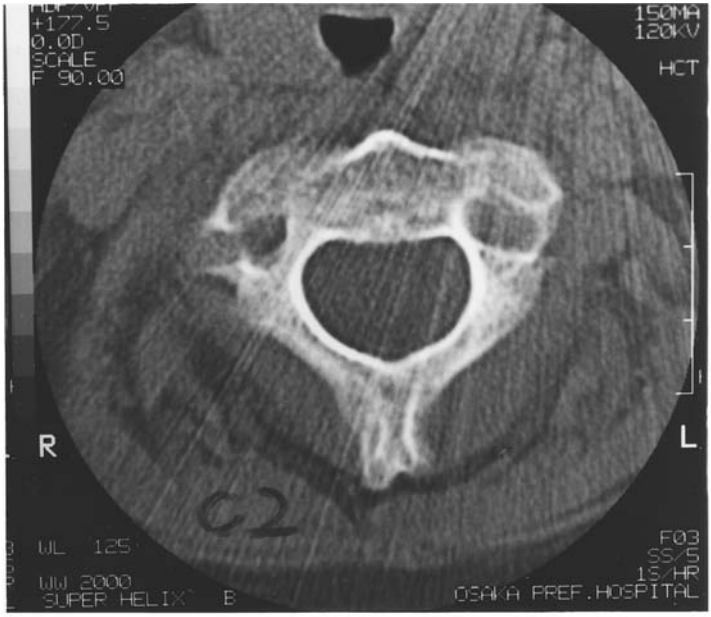

A

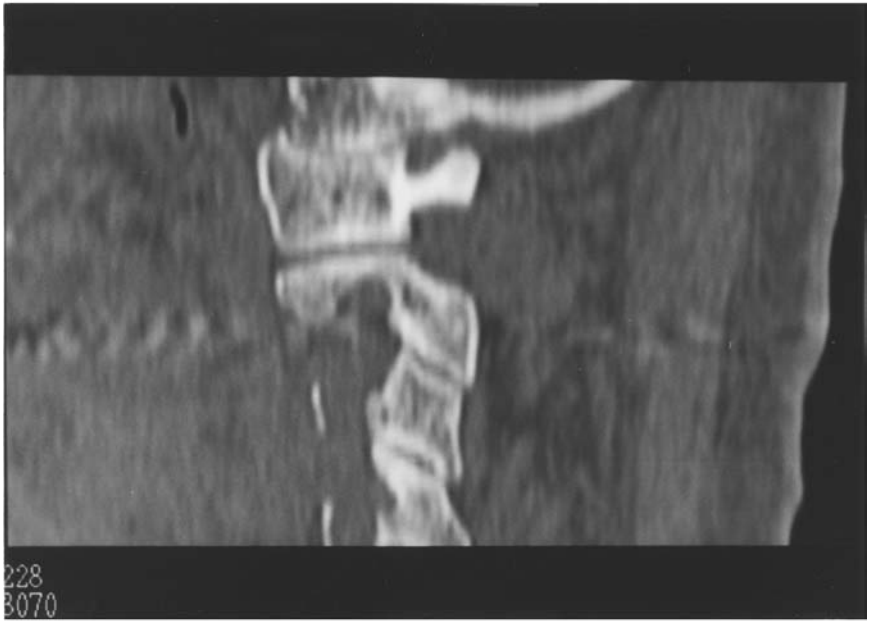

B

Figure 1 A case with abnormal route of left vertebral artery in the axis. (A) CT scan at the body level of the axis shows large vertebral artery foramen. (B) Reconstructive CT revealed the high riding vertebral artery. Atlantoaxial transarticular screw trajectory is cross with this foramen. In this case, atlantoaxial transarticular screw insertion should not be performed.

Radiologically 111 screws were assessed. We assessed perforation of the anterior cortex of the anterior arch of the atlas, perforation of the articular surface of the atlantoaxial joint and position of screw perforation at the atlantoaxial joint by CT scan as follows: screw perforation of anterior cortex of anterior arch of the atlas was defined when a screw was detected by recognizing the screw both in front of the anterior arch of the atlas on upper CT scan of the atlas (Fig. 2C) and within the anterior arch of the atlas on middle CT scan of the atlas (Fig. 2D). Screw perforation of the atlantoaxial joint was also defined by recognizing the screw with articular surface of the atlantoaxial facet joint of the atlas on the facet joint level CT scan (Fig. 2E). The screw position is detected on the same CT scan.

B. Results

There was no spinal cord injury or nerve root injury in this series. No episode of massive bleeding due to suspected vertebral artery injury during the operation or afterwards was experi-

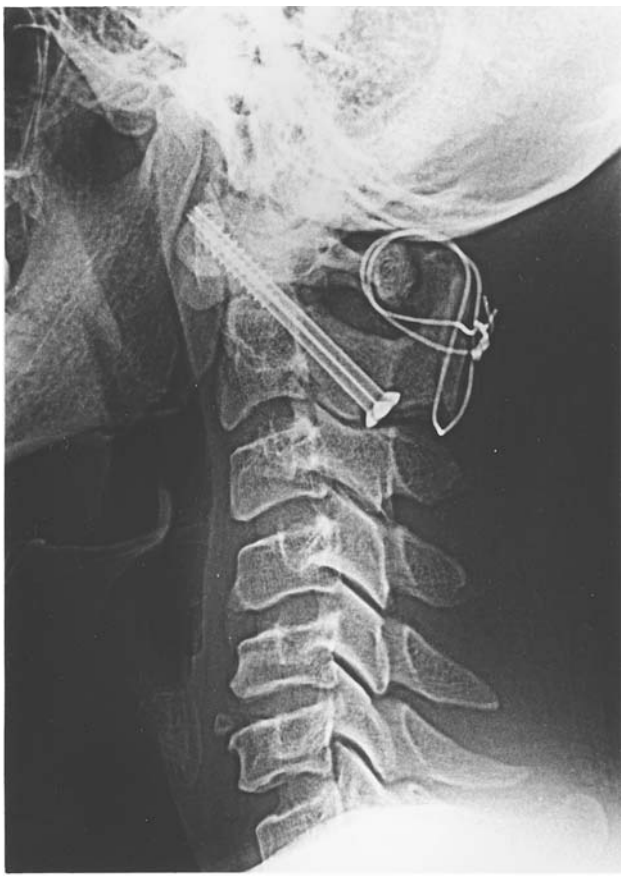

A

Figure 2 Case 10: A 30-year-old male, cervical myelopathy due to atlantoaxial instability. (A) Postoperative lateral radiogram shows suitable screw direction in the sagittal plane; (B) open mouth view; (C) CT scan at upper atlantal level (screw tips are found in front of the anterior arch of the atlas); (D) CT scan at middle atlantal level (screws are found within the anterior arch of the atlas); (E) CT at just atlantoaxial facet level (screw position at the joint level is visible). The penetrating position of the screw at the facet joint was recognized as within or out of the facet joint.

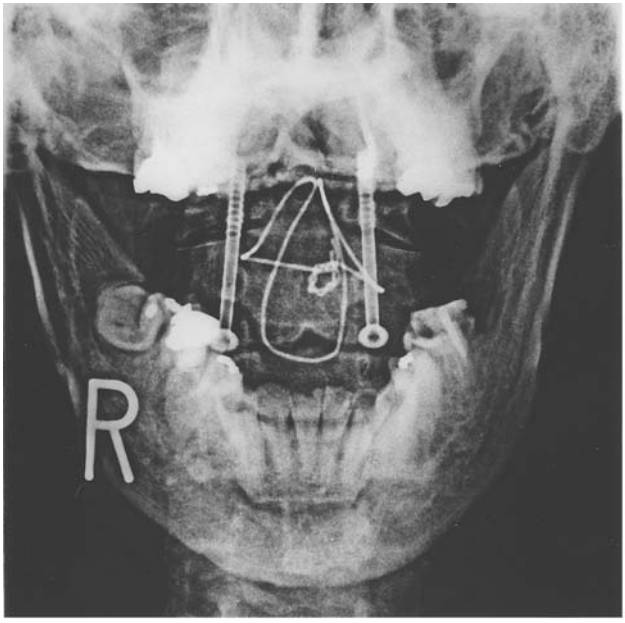

B

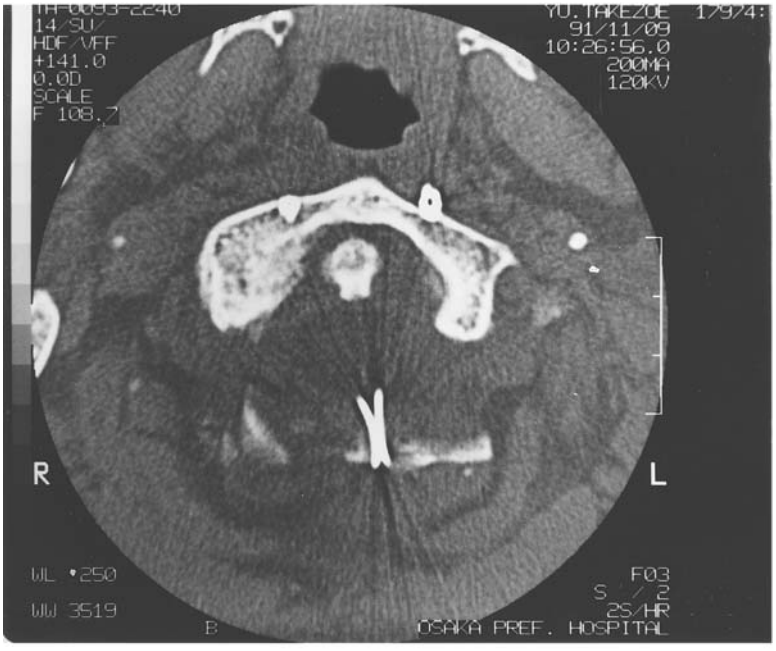

C

Figure 2 Continued.

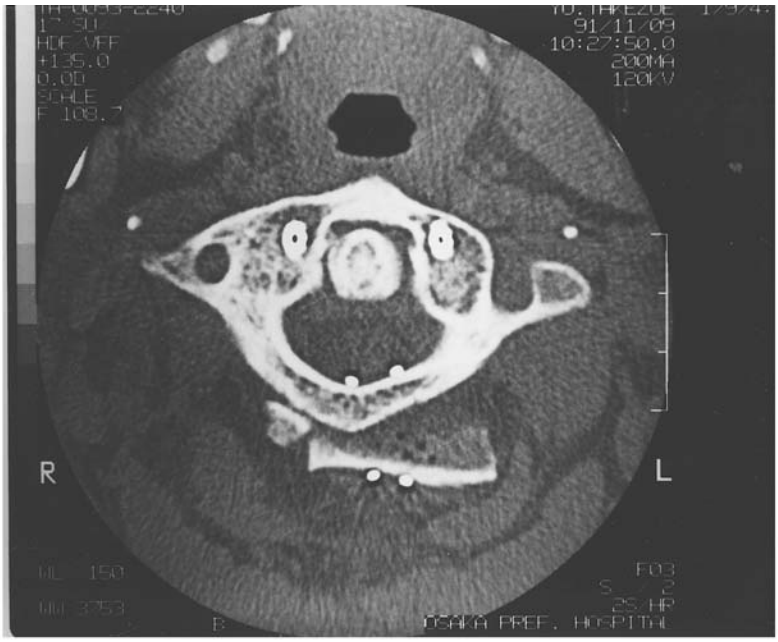

D

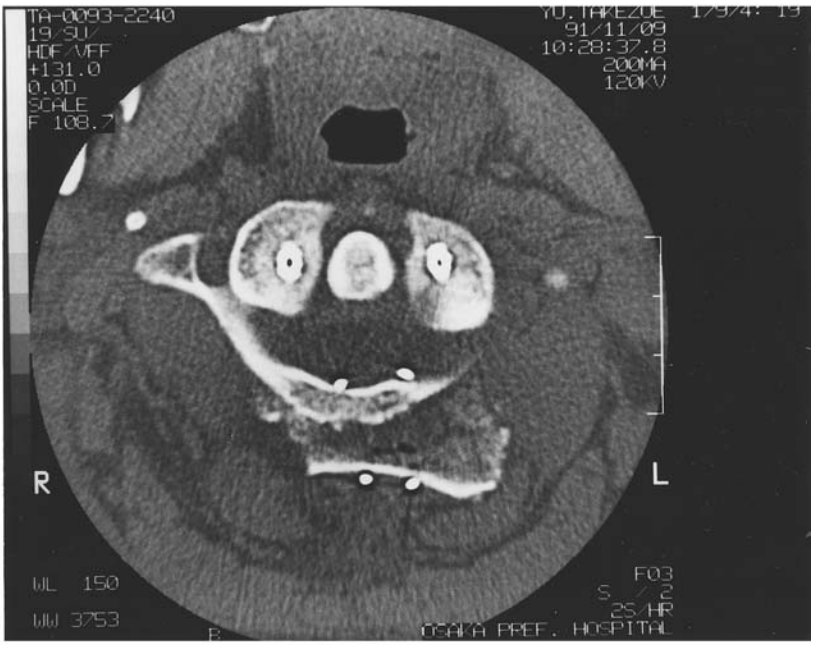

E

Figure 2 Continued.

enced. Breakage of a guidewire was experienced in one case, and one screw could not be inserted at the other side in the same case.

Out of 111 screws, 77 (69.4%), perforated the anterior cortex of anterior arch of the atlas. One hundred and six screws perforated the atlantoaxial joint. Therefore, the success of insertion of atlantoaxial transarticular screw fixation was 95.5%. Two screws were inserted outside the joint (Fig. 3), 2 at the medial (within the spinal canal) (Fig. 4), and 1 at the anteroinferior aspect of the joint (Fig. 5). There was no case in which a screw penetrated the occipitoatlantal joint.

V. DISCUSSION

There were several reports concerning the good clinical results of atlantoaxial transarticular screw fixation [1,5,7–10,16]. This procedure is comparatively safe, but several complications related to the screw insertion have been reported [1,3,6–8,10,11,18]. Madawi et al. [11] reported 5 out of 61 vertebral artery injuries with this operation. Coric et al. [18] reported a case with a vertebral artery to epidural venous fistula. Wright et al. [13] investigated the risk of vertebral artery injury during C1–2 transarticular screw placement by interviewing active members of the American Association of Neurological Surgeons/Congress of Neurological Surgeons (AANS/CNS). They reported that 31 out of 1318 patients (2.4%) had known vertebral artery injury and an additional 23 patients (1.7%) were suspected of having injuries. On the other hand, Grob et al. [5] reported on a series of atlantoaxial transarticular screw fixation cases and found no case

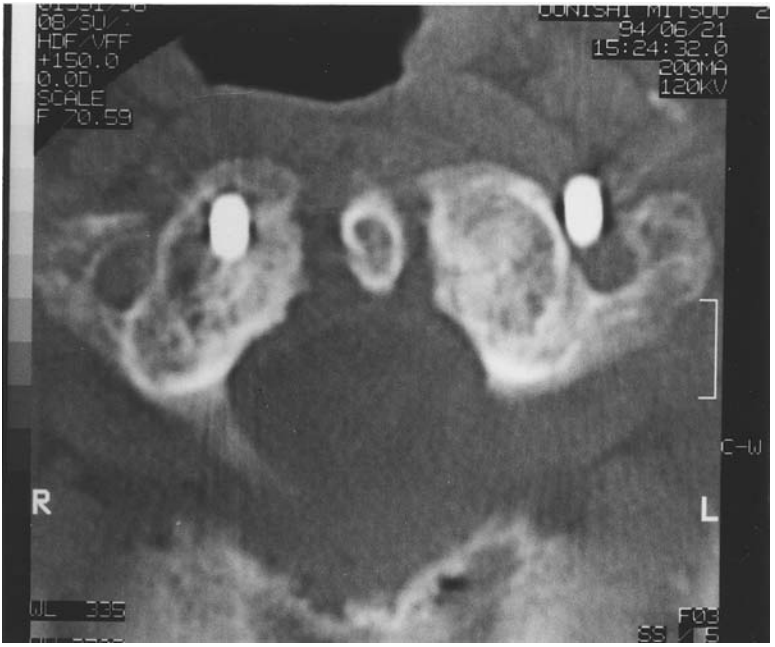

Figure 3 Case 23: A 70-year-old male, atlantoaxial subluxation with vertical subluxation associated with rheumatoid arthritis. Postoperative CT scan, demonstrating the left screw placed laterally to the lateral mass of the atlas within the transverse foramen. The cause of malposition of the screw seems to inadequate reduction related to the destruction of the lateral mass of the axis.

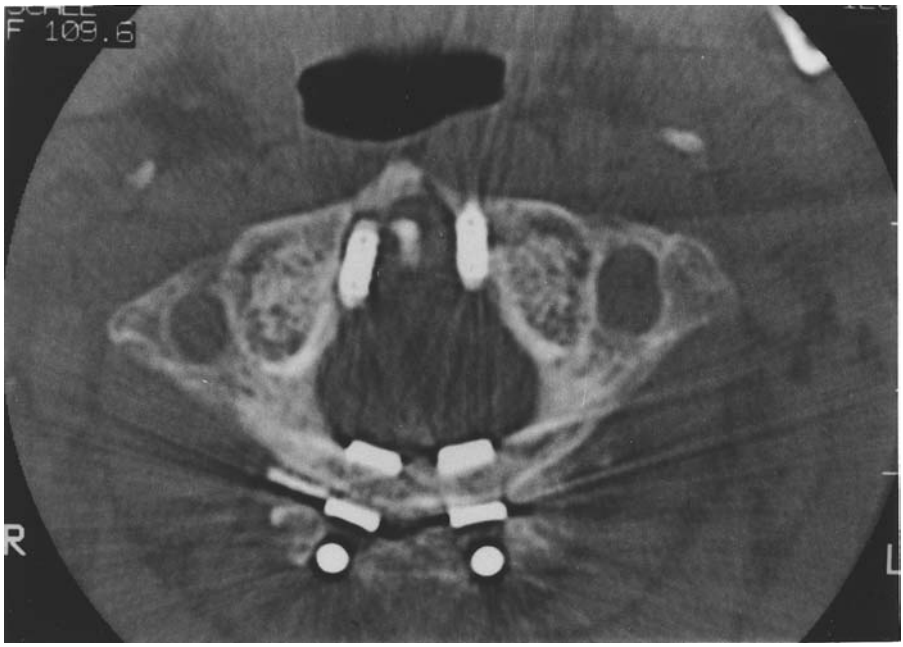

Figure 4 Case 35: A 69-year-old female, atlantoaxial subluxation associated with rheumatoid arthritis. The surgeon experienced massive venous bleeding during insertion of the left guidewire. He reinserted wires at medial direction. Postoperative CT scan, demonstrating the bilateral screws placed medially to the lateral mass of the atlas within the spinal canal.

of vertebral artery injury. Fortunately, we have not experienced the symptoms of these injuries. The incidence of such injuries seems to be very low, but it is important to recognize the risk of this technique. In our series, 6 of 112 screw insertions (5.4%) were done with some problems. Reports of malpositioned screws vary: 15% by Grob et al. [5], 4% by Jeanneret and Magerl [6], 6% by Marcotte et al. [7], 2% by Stillerman and Wilson [8], 14% by Madawi et al. [11], and 2.2% by Wright and Lauryssen [13]. This technique involves several problems related to screw insertion, such as guidewire breakage, vertebral artery injury, or spinal cord injury. In order to avoid such injuries, it is essential not only to master this technique well, but also to assess the morphology of this region precisely.

A. Guidewire Breakage

After the reduction of atlantoaxial subluxation, temporary fixation using bilateral guidewires is a safe method. In cases using cannulated screws, drilling and screwing can be done with the remaining guidewires. This technique offers accurate and safe screw insertion because it is possible to insert screws introduced by guidewires. We have inserted the screws using this technique in 38 cases. We experienced breakage of a guidewire in one screw insertion. This guidewire is 1.6 mm in diameter use with a 4-mm-diameter cannulated screw. The breakage of the guidewire in this series was caused by purely technical problems: the guidewire was broken during drilling using a cannulated drill. It was difficult to remove and remained in the atlas with anterior protrusion. In order to minimize this complication, it is necessary not to bend a guidewire and not to use power tools for drilling once the guidewire is positioned in the bone [9]. If the

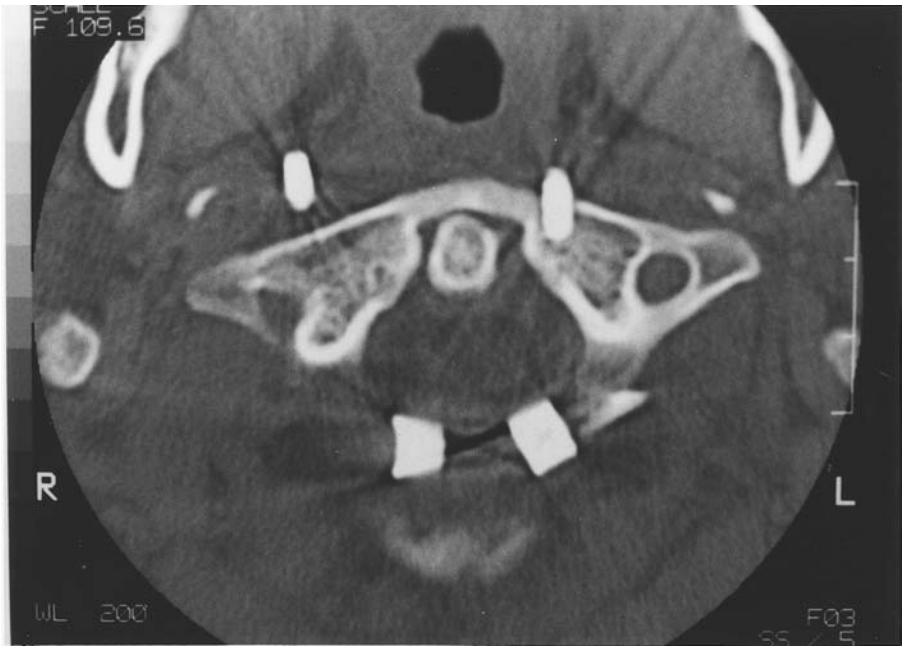

Figure 5 Case 41: A 74-year old male, atlantoaxial instability associated with os odontoideum. CT scan at atlantal level indicates that the right screw path was at anteroinferior of the joint. In os odontoideum, the reduced position is difficult to maintain during screw insertion due to posterior subluxation of the atlas.

guidewire is inserted with some curvature because of disturbance of the shoulder girdle due to upper thoracic kyphosis, breakage of the guidewire can easily occur. Therefore, drilling and screwing should be done after pulling out one guidewire following temporary fixation using two guidewires. In high thoracic kyphosis, an additional small skin incision should be made for the direct insertion of the guidewires or screws.

B. Malposition of Screw Insertion

Risky screw insertion of atlantoaxial transarticular screw fixation is caused by malposition. Lateral fluoroscopic monitoring and the use of a guidewire achieved secure placement in the cephalocaudal direction. However, the failure of placement in the medial or lateral direction still remains a problem. Screw direction in the horizontal plane is checked only by the surgeon's visualization. The surgeon usually stands at the one side of the patient, so it is difficult to determine the real direction of a screw or guidewire. A person can easily confirm the direction of guidewires from the cranial point outside the operation field. Therefore, careful checking by another person standing at the cephalad side of the patient can determine the screw trajectory on the horizontal plane more accurately. Anteroposterior fluoroscopic monitoring is one solution. An intraoperative real-time navigation system will be available in near future. In addition, it is important to set the neutral atlantoaxial rotation precisely and to expose the isthmus of the axis sufficiently.

When a guidewire or probe is inserted in the wrong direction, the penetrating point of the cortical bone of the atlas is at a different depth from the preoperative planned depth. Surgeons

should feel penetration of the cortical bone and check the depth by lateral image so as to confirm the correct screw pathway. In rheumatoid arthritis, because the cortical bone is not as hard as in noninflammatory disease, careful drilling or probing is necessary.

With inadequate reduction of atlantoaxial subluxation, especially remaining rotation, insertion of a guidewire is difficult and risky. Madawi et al. [11] reported incomplete reduction and destruction of lateral mass to be risk factors. In our series, misdirection of screw placement occurred because of rotational deformity between the atlas and the axis and massive destruction of lateral facets of the axis. In os odontoideum, a reduced position is hardly maintained during screw insertion due to posterior subluxation of the atlas. Careful checking of the lateral image should be performed often and both the atlas and the axis firmly stabilized during guidewire insertion. Computer-assisted navigation or an aiming device is useful for accurate screw insertion only in the axis. In cases of inadequate reduction or rotational deformity between the atlas and the axis, such techniques are less useful. For the present, careful checking of reduction and careful drilling with sensitive hand feeling is the way to avoid misdirection of screw insertion.

VI. CONCLUSION

Atlantoaxial transarticular screw fixation can be performed accurately and safely if surgeons know the causes of malpositioned screw insertion, plan the operative procedure precisely, and check the procedure often and carefully during the operation.

REFERENCES

1. Magerl F, Seemann PS. Stable posterior fusion of the atlas and axis by transarticular screw fixation. In: Kehr P, Weidner A, eds. Cervical Spine. Wien: Springer-Verlag, 1986:322–327.
2. Hanson P, Montesano P, Sharkey N, Rauschning W. Anatomic and biomechanical assessment of transarticular screw fixation for atlantoaxial instability. Spine 1991; 16:1141–1150.
3. Grob D, Crisco JJ, Panjabi M. Biomechanical evaluation of four different posterior atlantoaxial fixation techniques. Spine 1992; 17:480–490.
4. Hajek P, Lipka J, Hartline P, Saha S, Albright J. Biomechanical study of C1–C2 posterior arthrodesis techniques. Spine 1993; 18:173–177.
5. Grob D, Jeanneret B, Aebi M, Markwalder TM. Atlanto-axial fusion with transarticular screw fixation. J Bone Joint Surg [Br] 1991; 73-B:972–976.
6. Jeanneret B, Magerl F. Primary posterior fusion C1/2 in odontoid fractures: indications, technique, and results of transarticular screw fixation. J Spinal Disord 1992; 5:464–475.
7. Marcotte P, Dickman CA, Sonntag VKH. Posterior atlantoaxial facet screw fixation. J Neurosurg 1993; 79:234–237.
8. Stillerman CB, Wilson JA. Atlanto-axial stabilization with posterior transarticular screw fixation: technical description and report of 22 cases. Neurosurgery 1993; 2:948–955.
9. Dickman CA, Foley KT, Sonntag VK, Smith MM. Cannulated screws for odontoid screw fixation and atlantoaxial transarticular screw fixation. Technical note. J Neurosurg 1995; 83:1095–1100.
10. McGuire RA, Harkey HL. Focus on the spine: modification of technique and results of atlantoaxial transfacet stabilization. Orthopedics 1995; 18:1029–1032.
11. Madawi AA, Casey ATH, Solanki GA, Tutte G, Veres R, Crockard HA. Radiological and anatomical evaluation of the atlantoaxial transarticular screw fixation technique. J Neurosurg 1997; 86:961–968.
12. Jun B-Y. Anatomic study for ideal and safe posterior C1–C2 transarticular screw fixation. Spine 1998; 23:1703–1707.
13. Wright NM, Lauryssen C. Vertebral artery injury in C1–C2 transarticular screw fixation: results of a survey of the AANS/CNS section on disorders of the spine and peripheral nerves. J Neurosurg 1998; 88:634–640.

14. Xu R, Ebraheim NA, Misson JR, Yeasting RA. The reliability of the lateral radiograph in determination of the optimal transarticular C1–C2 screw length. Spine 1998; 23:2190–2194.
15. Gebhard JS, Schimmer RC, Jeanneret B. Safety and accuracy of transarticular screw fixation C1–C2 using an aiming device. An anatomic study. Spine 1998; 23:2185–2189.
16. Eleraky MA, Masferrer R, Sonntag VKH. Posterior atlantoaxial facet screw fixation in rheumatoid arthritis. J Neurosurg 1998; 89:8–12.
17. Fuji T, Oda T, Kato Y, Fujita S, Tanaka M. Accuracy of atlantoaxial transarticular screw insertion. Spine 2000; 25:1760–1764.
18. Coric D, Branch CL, Wilson JA, Robinson JC. Arteriovenous fistula as a complication of C1–2 transarticular screw fixation. Case report and review of the literature. J Neurosurg 1996; 85:340–343.

15
Biomechanics of Artificial Discs

Vijay K. Goel
Spine Research Center, University of Toledo, and Medical College of Ohio
Toledo, Ohio, U.S.A.

Andrew P. Dooris
DePuy AcroMed, Inc.
Raynham, Massachussets, U.S.A.

Dennis McGowan
Kearney Bone & Joint Clinic
Kearney, Nebraska, U.S.A.

S. Rengachary
University Health Center
Detroit, Michigan, U.S.A.

I. INTRODUCTION

Almost three quarters of the United States population has at one time experienced back pain, and approximately 4% of the population requires surgical intervention. Disability of patients with low back pain costs several billion dollars in the United States annually because of lost productivity and treatment costs [11], affecting millions of individuals [3,4,26–29, 37–39,41,42–44]. As the population ages, the problem will certainly grow [3,43].

The treatment of low back pain is predominantly conservative, and the majority of patients have resolution of symptoms within 2 months regardless of treatment prescribed. However, there is a small group of patients who continue to be disabled even after 6 months. For these, discogenic low back pain and segmental instability is often the etiology.

For these patients who remain disabled at a sedentary or lower level, spine fusion has been a treatment option. In the best of hands, a single level spine fusion may offer the patient a 60% probability or 60% improvement in pain, and activity tolerance often improves to a light-moderate level. The spine fusion never makes the back normal and frequently concentrates the stresses at adjacent levels, leading to premature adjacent degeneration. With time, adding on additional levels of surgical spine fusion becomes the usual natural history of a spine fusion [16,30,33]. Spine fusion is also significant surgery. Complications may also include infection, donor-site pain, nonunion, neurological deficit, and failure of fixation.

The practice of spine surgery is taking the same course as the orthopedic practice of treating degenerative joints in the extremities. Fusion was once considered the standard for significant degeneration of extremity joints, especially the hip and knee. Osteotomies for the very young and total joint arthroplasties for all others are now the standard. Exceptions to the

above are frequently dramatized by media coverage of the young professional athlete who, for example, has a total hip replacement and goes on to return to professional sport. In general, total joint replacements in the extremities work well. Such replacement surgery in the spine may give similar results and avoid the additional problems of fusion and should have complication rates no higher than spine fusion.

Traditional joint replacement technology has developed a variety of mechanical disc replacements for both the lumbar and cervical spine. New technology has developed materials to mechanically replace the disc nucleus. A few disc designs have undergone clinical trials with limited published results [20]. Likewise, some disc designs have been evaluated biomechanically [1,2,8,13,50]. This chapter provides a review of a few basic artificial disc designs and the relevant biomechanical studies. These designs vary greatly in their approach to restoring normal disc joint function.

II. ARTIFICIAL DISC DESIGNS

Bao et al. [5] have classified the designs of total disc replacements into four categories: (1) low-friction sliding surface; (2) spring-and-hinge systems; (3) contained fluid-filled chambers; and (4) discs of rubber and other elastomers. The first two designs seek to take advantage of the inherently high fatigue-resistant characteristics that all-metal designs afford. The latter two designs attempt to incorporate some of the viscoelastic and compliant properties that are exhibited by the normal, nondegenerated intervertebral disc. The materials incorporated into these designs vary considerably and are often mixed, such as a metal-polymer-metal layered design with metal interfacing the endplates and a deformable polymer between. A comprehensive review of these designs is not given here. Discussed here are only those designs for which a significant amount of testing has been reported.

A. The Ray Nucleus Replacement

In 1988 Ray presented a prosthetic nuclear replacement consisting of flexible woven filaments (Dacron^{TM}) surrounding an internal semi-permeable polyethylene membranous sac (Fig. 1) filled with hyaluronic acid and a thixotropic agent (i.e., a hydrogel) [30,46,47]. In the most recent design, Ray uses two woven sacs, a taller one anteriorly and a shorter one posteriorly, to create lordosis [30]. The implant can be inserted similar to a thoracolumbar interbody fusion device, either postero-lateral or transversely. Two are inserted per disc level in a partly collapsed and dehydrated state, but swell due to the strongly hygroscopic properties of the hyaluronic acid constituent. It is expected that the implant will swell enough to distract the segment while retaining enough flexibility to allow a normal range of motion. An option is to include therapeutic agents in the gel that would be released by water flow in and out of the prosthesis according to external pressures.

B. In Situ Curable Prosthetic Intervertebral Nucleus (PIN)

The device (Disc Dynamics, Inc., Minnetonka, MN) consists of a compliant balloon connected to a catheter (Fig. 2) [13,14]. This is inserted into the nucleus cavity through a small hole in the annulus and liquid polymer is injected into the balloon under controlled pressure, inflating the balloon, filling the cavity, and distracting the intervertebral disc. A compressive axial load of appropriate magnitude may be maintained during implantation. Within 5 minutes the polymer becomes cured.

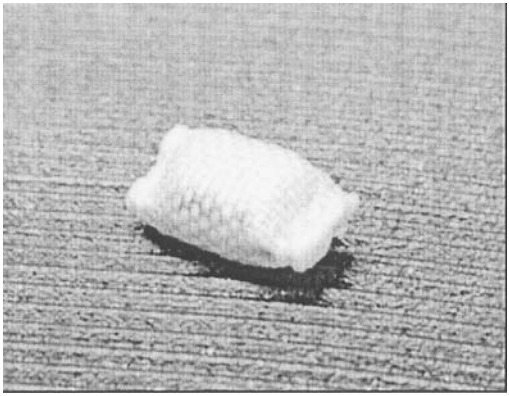

Figure 1 Prosthetic disc nucleus. (From Ref. 13.)

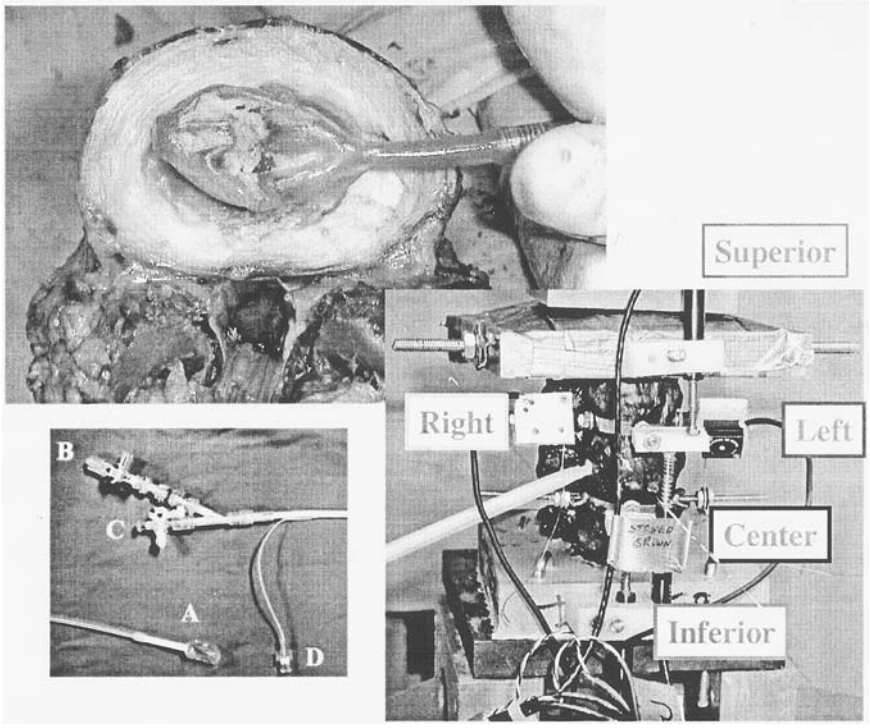

Figure 2 *In situ* curable prosthetic intervertebral nucleus (PIN) being developed by Disc Dynamics, Inc., Minnetonka, MN. (From Ref. 13.)

C. The Acromed AcroFlex Artificial Disc

Steffee presented the Acromed AcroFlex™ artificial disc in the late 1980s [52]. It consisted of a polyolefin rubber (Hexsyn™) fused between two titanium alloy plates (Fig. 3). The plates had four tapered posts each to provide an immediate fixation to the vertebral endplates, and a porous coating of sintered titanium beads (average 250 mm diameter) to provide long-term fixation. The implant geometry provided a large surface area for contact with the endplates to reduce stress concentration and subsidence. The Hexsyn core was vulcanized to each titanium plate separately, and then the halves were vulcanized together. Implantation required an anterior surgical approach with a very wide distraction in order to insert the endplate posts. Steffee listed three clinical conditions for use of the AcroFlex disc replacement: juxtafusion degeneration, patients under the age of 40 with disc degeneration, and isolated disc resorption [52].

D. Lee–Langrana Disc

Lee et al. [34] investigated incorporating three different polymers into their prosthetic intervertebral disc design and tried to represent the separate components (annulus fibrosis and nucleus) of the normal disc in varying proportion. They loaded their designs under 800 N axial compression and in compression-torsion out to 5 degrees. The results indicated that discs fabricated from homogeneous materials exhibited isotropy that could not replicate the anisotropic behavior of the normal human disc. Thus, 12 layers of fiber reinforcement were incorporated in an attempt to mimic the actual annulus fibrosis. This method resulted in more close approximation of the mechanical properties of the normal disc. Through this method of redesign and testing, authors claim that eventually ''a disc prosthesis that has mechanical properties comparable to the natural disc could be manufactured.''

E. Kaneda–Abumi Disc

An artificial intervertebral disc was developed, and its intrinsic biomechanical properties, bioactivity, and effectiveness as a total disc replacement were evaluated in vitro and in vivo [32]. The artificial intervertebral disc consisted of a triaxial three-dimensional fabric (3-DF) woven with an ultra-high molecular weight polyethylene fiber and spray-coated bioactive ceramics on the disc surface. The arrangement of weave properties was designed to produce mechanical behavior nearly equivalent to the natural intervertebral disc. Total intervertebral disc replacement

Figure 3 AcroFlex disc. (From Ref. 52.)

at L2-L3 and L4-L5 was performed using a 3-DF disc with or without internal fixation in a sheep lumbar spine model. The segmental biomechanics and interface histology were evaluated after surgery at 4 and 6 months. The tensile-compressive and torsional properties of prototype 3-DF were nearly equivalent to those of human lumbar disc. The lumbar segments replaced with 3-DF disc alone showed a significant decrease of flexion-extension range of motion to 28% of control values as well as partial bony fusion at 6 months. However, the use of temporary fixation provided a nearly physiological mobility of the spinal segment after implant removal as well as excellent bone-disc fusion at 6 months.

F. The Kostuik Artificial Disc

Hedman et al. described the Kostuik lumbar intervertebral disc replacement in 1991 [23,31]. This design (Fig. 4) was fairly complicated as the designers tried to mimic several natural ranges of motion in all directions. The bulk of the prosthesis was made of a cobalt chrome alloy, commonly known to be biocompatible, although with possible oncogenic potential in wear applications. A posteriorly located loose hinge provided between 15° and 20° of sagittal plane motion. A mismatch in hole-pin size at the lateral ends of the hinge provided lateral bending (~3°). Two anteriorly located mechanical (titanium alloy Ti-6Al-4V) springs provided stiffness in the sagittal plane. The authors experimentally found a 2.24 Nm/degree stiffness coefficient. The springs were seated into pockets in the implant to prevent spring dislodgement in extension and coil contact in flexion. The implant was rigidly fixed to the segment through four screws inserted laterally into the vertebral body (Fig. 4B). Long-term fixation was to be achieved by a porous coating on the anterior and posterior surfaces that also contained spikes.

G. Waldemar Link™ SB Charite III Artificial Disc

The SB Charite implant has a sliding design, including three parts (Fig. 5). Like the Acromed disc, two cobalt chrome plates engage the endplates through spikes [7]. The plates are concave in the center, matching the curvature of a high-density polyethylene core sliding between them.

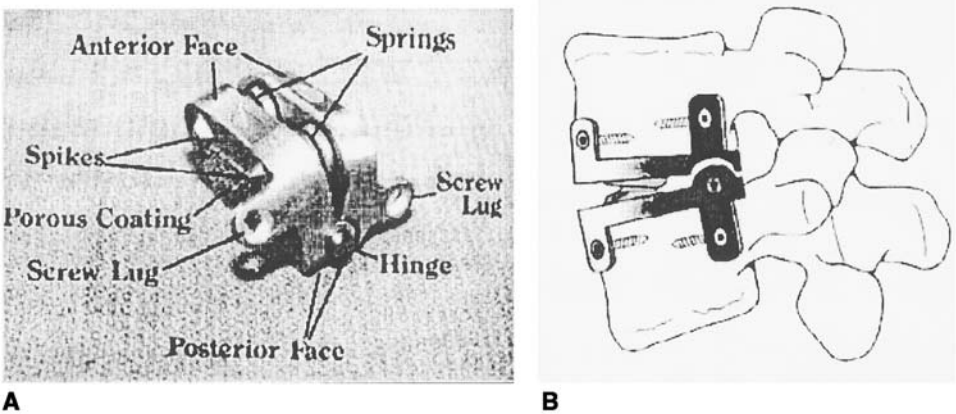

Figure 4 The Kostuik intervertebral disc replacement. The implanted Kostuik artificial disc with screws inserted.

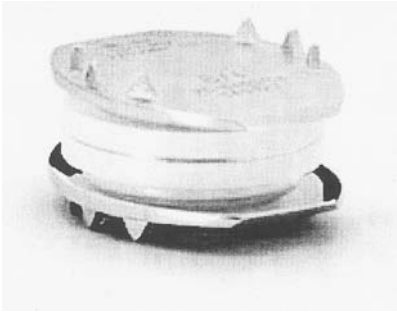

Figure 5 Waldemar Link^{TM} SB Charite III artificial disc.

Because the polyethylene core slides between the two surfaces, the design is sometimes referred to as a ''slip-core.'' A metal ring surrounds the polyethylene core at its horizontal mid-plane to assist in radiographic measurements. Several sizes and shapes allow for customization of the implant to the patient's size and segment level of interest. The implant is designed for 12–14° of rotation in the sagittal and transverse planes [7]. There is no inherent constraint for axial rotation. The disc is implanted from an anterior surgical approach. A window is cut in the anterior annulus by cutting horizontally along the superior and inferior endplates and peeling back the annulus. The nucleus is then removed. The joint is distracted and the implant inserted [53].

H. Medtronic Sofamor Danek^{TM} Artificial Disc

In 1996 Gilbertson et al. reported on in vitro biomechanical test results of a titanium ball-and-cup disc designed by Medtronic Sofamor Danek^{TM} (Fig. 6) [21]. This implant uses a tested tribologic design adapted from hip replacements, including two matching ceramic ball-and-cup components. Because the cup is shallow and its curvature decreases near its perimeter, the joint is slightly ''sloppy.'' The contacting surfaces are made of polycrystalline alumina and are surrounded by a titanium sleeve, which is grooved and beaded for bone in-growth.

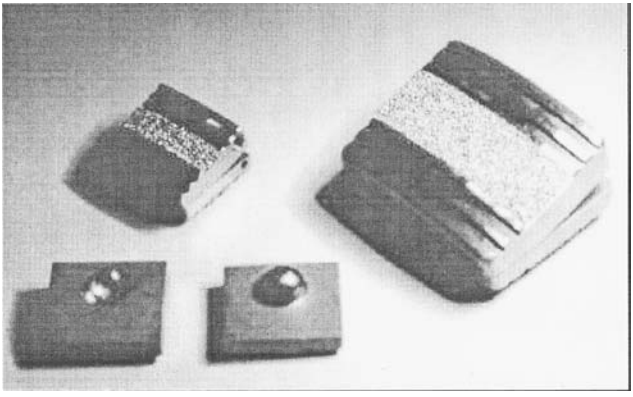

Figure 6 The Medtronic Sofamor Danek^{TM} artificial disc prototype, made of titanium alloy, with grooved and beaded surface for osseointegation. (From Ref. 13.)

III. DESIGN CHALLENGES AND BIOMECHANICS

There are many challenges involved in designing and implanting disc prostheses. The prosthesis must allow motion but still restrain motion beyond the range of the normal functional spinal unit. The prosthesis must restore disc space height to decompress the neural foramen and restore the normal sagittal plane alignment. The prosthesis must have adequate bone foundation to prevent subsidence into the adjacent vertebrae. It may be important for the prosthesis to act as a shock absorber. When the surgical implantation of the disc is being carried out, destruction of facets and ligaments must be avoided. Disc longevity is extremely important, especially based on prior statistics showing that the average patient who needs a disc replacement is 35 years of age. However, more likely than not, a disc replacement in a young patient will have to be revised at least once in the patient's life. Revision must be incorporated in the design. Extensive dissection through scar tissue can be very difficult and risky around the great vessels. Disc longevity of 50–60 years would be desirable. Biocompatibility is important so that the body does not warrant an inflammatory response against the prosthesis. Inflammation around the nerve roots and dorsal root ganglia may result in severe neuropathic pain similar to a disc herniation.

The chemical and mechanical properties of the materials used in manufacturing are crucial to future disc prosthesis. The fatigue strength must be strong (i.e., maintain its mechanical integrity to approximately 85 million cycles), and wear debris must be kept to a minimum (possibly even more than in total hip replacement designs) [23]. The artificial disc must provide immediate and long-term fixation to bone and, finally, provide *fail-safe* mechanisms such that if an individual component of the design fails, catastrophic failure is not immediately imminent and it does not lead to peri-implant soft tissue damage. Damage to the nerves may result in paralysis as well as nerve pain. Damage to the great vessels may result in exsanguinations. All of these are major contributing factors that have to be dealt with in attempting to design an artificial disc. This is certainly one of the greatest design challenges that bioengineers have encountered to date.

As with any new medical device, indications must be clearly defined. The indications for disc replacement will be intractable back pain refractory to all conservative care limited to one or two levels. Degeneration will be the etiology. The disc never degenerates by itself. The disc, facet joints, and ligaments always degenerate together, but frequently the disc degeneration will be more advanced than the others. Replacement of the disc with already markedly degenerated ligaments and facets would not be expected to significantly reduce the pain. Degeneration of the posterior elements, especially of the facet joints, has been found to be a source of low back pain by various clinical, biological, and biomechanical studies [19,25,33,35]. If it is true that degeneration of the posterior elements results from disc disease in most joint degeneration sequelae, then it appears reasonable that current protocols would contraindicate implantation with degenerated posterior elements [17,20]. Reports also suggest that in addition to preoperative degeneration, the posterior elements may be abnormally stressed by disc replacement, and therefore implantation should be avoided. The disc implant thus needs to be evaluated to assess the above-stated criterian. However, not all of the biomechanical parameters can be evaluated by using experimental protocols. Some parameters, such as bone stresses or joint forces, are difficult to analyze in cadaver studies. Cadaver studies involve an array of widely varying parameters, many of which are difficult to control, characterize, or even measure. For these reasons, biomechanical investigations, both experimental and theoretical, are needed, as described in the following sections.

A. Ray Nucleus

Recent reports on biomechanical tests of this device show that it can produce some degree of stabilization and distraction [56]. Loads of 7.5 Nm and 200 N axial were applied to six L4-L5 specimens. Nucleotomized spines increased rotations by 12–18% depending on load orientation, but implanted spines (implant placed transversely) showed a change of -12 to $+2$% from the intact with substantial reductions in neutral zone. Up to 2 mm of disc height was recovered by insertion. The device, however, was implanted and tested in its desiccated form. The biomechanics of the hydrated prosthesis may vary considerably from that of its desiccated form.

Clinical trials of the Ray nucleus replacement show a positive effect in patients with degenerative disc disease [30,45]. Osman reported a multinational follow-up of 150 patients implanted with the device who had chronic back pain [45]. Not all patients had sciatica or herniation. A posterior approach was used in 142 cases; 8 used a lateral approach. Of those implanted, 80% reported improvement of symptoms and returned to employment. Of the remaining 30 cases, however, 18 exhibited implant migration, and 6 experienced infection.

B. In Situ Curable Prosthetic Intervertebral Nucleus

Five fresh-frozen osteoligamentous three-segment human lumbar spines were prepared by putting the bottom vertebra in a stiff polymer mixture and the top in a steel loading frame [13,14]. Vertebral body rotations were tracked with an optoelectronic tracking system while specimens were loaded to 6 Nm in left and right torsion, left and right lateral bending, and flexion and extension. Displacement gauges monitored the changes in disc height of the top and bottom and the implanted middle discs (three gauges: front, left and right) when loading from 50 to 750 N in axial compression (Fig. 2). The specimens were radiographed and dissected to determine any structural damage inflicted during testing. The spines were tested in four configurations: intact, denucleated, implanted, and fatigued. Fatiguing was produced by cyclic loading from 250 to 750 N at 2 Hz for at least 100,000 cycles. Nuclectomy was performed through a 5.5 mm trephine hole in the right middle lateral side of the annulus. The device was placed in the nuclear cavity, as described earlier. The results revealed that the PIN device reversed the destabilizing effects of a nuclectomy and restored normal segment stiffness. Significant increases in disc height were also achieved. Adjacent motion segments had minimal kinematic changes after implantation of the nucleus prosthesis, suggesting a normal load-sharing relationship. After fatiguing, the implanted segment behaved similarly to intact adjacent segments—further evidence of a normal load-sharing condition. No implant extrusion or endplate fracture was observed in any of implanted disc levels after the fatigue test. Lastly, although implanting the majority of disc replacement systems requires significant annulus removal, this device requires minimal surgical compromise and has the potential to be a minimally invasive procedure.

C. Kaneda–Abumi Disc

Total intervertebral disc replacement at L2-L3 and L4-L5 was performed using 3-DF disc with or without internal fixation in a sheep lumbar spine model. The segmental biomechanics and interface histology were evaluated after surgery at 4 and 6 months. The tensile-compressive and torsional properties of prototype 3-DF were nearly equivalent to those of human lumbar disc. The lumbar segments replaced with 3-DF disc alone showed a significant decrease of flexion-extension range of motion to 28% of control values as well as partial bony fusion at 6 months. However, the use of temporary fixation provided a nearly physiological mobility of the spinal segment after implant removal as well as excellent bone-disc fusion at 6 months. An artificial

intervertebral disc using a three-dimensional fabric demonstrated excellent in vitro and in vivo performance in both biomechanics and interface histology.

D. The Acromed AcroFlex Disc

Reported mechanical tests of the implant have included fatigue testing and compression tests. The implant was tested in compression to 100 lb at a frequency of 2 Hz in a heated water bath to 11.5 million cycles. The disc was not noticeably worn, nor was wear debris found in the bath. A shear test was conducted with identical conditions except that the implant was oriented at 45° to the load. At 4 million cycles damage was seen at the point where the Hexsyn layers were fused together. By 11.5 million cycles a small tear had become a hole [52].

In vivo testing of the AcroFlex disc included implantation in three males and three females [15]. Mobilization began as early as one day after surgery, but a brace was worn for 6 weeks following surgery. Four of the six implantations were considered satisfactory. In one case no explanation could be made for failure. The patient continued to complain of pain despite normal radiographs. The patient was also receiving job disability and compensation. In another case the implant tore at the Hexsyn interface, resulting in an anterior translation. This patient had also undergone fusion at L3-S1 to correct scoliosis. The artificial disc was removed and an anterior interbody fusion performed. No inflammatory response was seen. In 1990 the FDA determined that a by-product of the vulcanization process may be toxic, and thus clinical trials of the AcroFlex disc were suspended. Two discs have been implanted since: one in the cervical spine of a female patient in 1991 and another in the lumbar spine of a male patient in 1992. Reports in 1994 described both of these patients as doing well, as were the four satisfactory cases in the first set of trials [40].

E. The Kostuik Artificial Disc

The multiple moving surfaces and spring deformations raised concerns about the implant's long term viability. Hellier et al. described an extended wear test of this implant to address this issue [24]. Two separate simulations were designed to test the two different moving part regions. A spring-in-pocket wear experiment included three forged and three hot isostatically pressed (HIPed) implant pairs to determine better implant wear resistance. The test stations simulated segment rotation via belt-driven cams such that the springs were compressed to 90% of their maximum (20° rotation). The test was run at 5 Hz for 3 million cycles. Implants were immersed in 150 mL of bovine serum. The second wear simulation tested the posterior hinge. Three forged, three HIPed, and two cast cobalt chrome alloy implant sets were tested. Again, the implants proceeded through 20° of rotation inside bovine serum. Tests were performed at 9 Hz for 6 million cycles initially. Hellier found better wear rates (smaller wear volume) in the HIPed component pockets, pins, and slots than with the forged or cast components, but better wear rates for the springs with the forged cobalt chrome components. This difference may be due to the higher carbon content in the HIPed components, and thus more carbides. Carbides are extremely stiff metal precipitates with excellent wear resistance. Average total wear rates for the HIPed total disc were estimated to be 3 mm^3/million cycles. Corrosion tests showed negligible response.

The Kostuik disc is one of the few designs that has undergone animal experimentation [31]. Six sheep were implanted with the prosthesis and allowed to move freely after surgery. Half the discs were removed after 3 months and the remainder at 6 months. No inflammatory response (gross or cellular) was seen in either group. No foreign body responses were seen in the lymph nodes, and only mild soft tissue in-growth was seen over the implant, with none at

the springs. Significant bone fixation was seen in two of the three implants recovered after 6 months. This type of animal study, however, is limited to evaluation of tissue response, including implant integration. In vivo testing in upright animal or human trials is necessary to examine the performance of the implant with respect to physiological load distribution, range of motion, and wear.

F. Waldemar Link™ SB Charite III Artificial Disc

Buttner-Janz et al. reported on biomechanical tests on the SB I and SB II in 1989 [8]. A servohydraulic machine applied compressive loads in either slow cyclic (quasi-static) or dynamic conditions. Hysteresis was found in the polyethylene with compressive loads to 4.2 kN. Cold flow in the plastic was seen in loads between 6 and 8 kN, and at 10.5 kN the height of the slip core was reduced by 10%. Dynamic testing included rotating the implant through $\pm 10^{\circ}$ about the neutral position at 5–10 Hz under a compressive load of 700 N. The compressive load was increased with one ''weekly maximum load of 8.0 kN'' and several intermediate load levels. Testing was carried out to 20 million cycles. The authors found no significant alteration in the implants after the dynamic tests other than ''slight track marks'' on the plates and core.

Ahrens et al. reported on in vitro tests performed with the Link SB III in 1996 [1]. Five fresh-frozen unconstrained cadaveric L4-L5 motion segments were tested by applying pure moments in extension, flexion, left and right lateral bending, and torsion. The intact and implanted discs were measured for rotation at the maximum applied moment. They found no significant difference between intact and implanted segment rotation in extension or lateral bending, but the implanted segments rotated more in flexion and torsion.

The Link SB Charite artificial intervertebral disc has gone through the most clinical trials. Development of the prosthesis began in 1984. Two significant design changes have resulted in the SB III used today in Europe. Although the first two designs experienced a number of failures, including metal plate failure (31%), anterior implant dislocation (22%), and subsidence (31%) [9], the Link SB III prosthesis has had considerably better success. In one study no metal endplate failure was found and subsidence was reduced to 3% and anterior dislocation to 9% [53]. Cinotti et al. reported on 46 patients implanted with the SB Charite III at an average follow-up time of 3.2 years [10]. Roughly half of these patients were previously diagnosed with disc degeneration and the other half with failed disc excision. In terms of overall satisfaction, 63% of patients had satisfactory results and 67% returned to preoperative work. Dislocation occurred in 2% and subsidence in 9% [10]. If grouped by operative condition, success occurred in 69% of patients with isolated disc replacement and 77% in patients with no previous back injuries. Average sagittal plane rotation range was 9° for the implanted level and 16° for the adjacent. Greater mobility was found in patients who started exercises 1 week after surgery in comparison to those who wore a brace. Placing the disc posteriorly as opposed to anteriorly also increased the range of motion. Cinotti et al. attributed a large portion of the unsatisfactory results to the surgical learning curve and misdiagnoses. Griffith et al. reported the clinical results of a larger population implanted with the Link SB III prosthesis: 43 women and 50 men with 139 total implantations from three surgeons [22]. The primary diagnosis for implantation was degenerative disc disease (65%). Failed nucleotomies accounted for 15%, internal disc derangement 11%, failed fusion 3%, and instability and herniated nucleus of 1% each. More than half had no prior surgical procedure and nearly a third just one. Almost all the implants were placed at the L4-L5 or L5-S1 level. The average follow-up length was nearly one year. The average number of patients unable to work after replacement was 42%, but 31% of those not working before the operation got employment post-surgery. One of the surgeons had a noticeably better success rate than the other two. Leg and back pain was significantly reduced (one surgeon not reporting).

Flexion range of motion increased for 82% of patients while extension range of motion increased for 74% of patients. It was also reported that 39% of the patients increased their maximum walking distance. More recent reports indicated good outcome despite age differences [48,56]. Another prospective study of 50 patients 2 year postimplantation reported a 70% success rate. The authors underscored the importance of patient selection. One revision required interbody fusion; four had complications due to the anterior approach. None had problems due to the prosthesis material.

The clinical results of the Link disc are promising but far from perfect. Overall satisfaction rates are generally lower than those for fusion. Some of the difficulties are surely related to the novelty of the procedure, making diagnosis and implantation difficult for an inexperienced surgeon. If these problems can be resolved, or if selective studies can be formed, then one may be able to isolate problems with design from problems with implantation. No significant problems appear to be related to the design other than dislodgement, which may also be due to implantation technique. Longer follow-up and more comprehensive and applicable biomechanical test reporting are warranted.

G. Sofamor Danek Disc

Seven fresh cadaver spines (L1 through S1) were cleaned of muscle and connective tissue and prepared for loading by fixing the sacrum and inserting rigid crossbeams through the L1 vertebra [21]. Three infrared light-emitting diodes (LEDs) were attached noncolinearly at each vertebral level and connected to an active optical tracking system (Selspot II System, Partille, Sweden). Pure bending moments, from 0 to 6 Nm, in increments of 1.5 Nm, were applied to L1 via a loading frame attached to the crossbeams. For each specimen, the intact spine was loaded in flexion and extension, and the three-dimensional displacements of each vertebral level at each loading increment were recorded simultaneously. Surgery was performed to excise the anterior longitudinal ligament at L4-L5, the anterior portion of the annulus, and the nucleus. The joint was distracted, and the ball- and- cup components of the artificial disc were inserted. The load-displacement characteristics then were recorded in flexion and extension to 6 Nm, as was done previously with the intact spine. The average and standard deviation of the motions were computed. The data for the implanted spine were compared with those of the intact spine to assess the ability of the artificial disc to restore normal motion.

Dooris investigated the wear characteristics of the Sofamor Danek disc [13] by simultaneously compressing and oscillating the implant ball component over the implant socket component in a saline bath. Periodic mass measurements of the components determined the mass changes. Three wear simulators built by EnduraTec (Stillwater, MN) were utilized to test three implant component pairs (Fig. 7). Given the substantially larger range of motion of the sagittal plane, the implants and system were arranged to provide motion in the sagittal plane. An offset cam on an electric motor was adjusted to rotate the socket component 14.5° ($\pm 0.3°$) flexion and 4.5° ($\pm 0.3°$) extension over the ball component. An adjustable pneumatic cylinder applied a static 700 N load ($\sim$37 psi) to the socket component in the vertical direction. The mass of each device was determined using a Mettler-Toledo AG 245 (Mettler-Toledo, Switzerland) analytic scale with a precision of ± 0.01 mg. Surface replicas from the 500,000 cycles measurement of Socket 5 were sputter-coated with a 100 nm layer of platinum-palladium particles. The sample was then viewed using a Hitachi S5000 scanning electron microscope. Three pairs of artificial disc components were tested to 10 million cycles. Measurements were made every 250,000 cycles to 1.5 million cycles. From 1.5 to 5 million cycles, measurements were made every 500,000 cycles. From 5 to 10 million cycles, measurements were made every 1 million cycles.

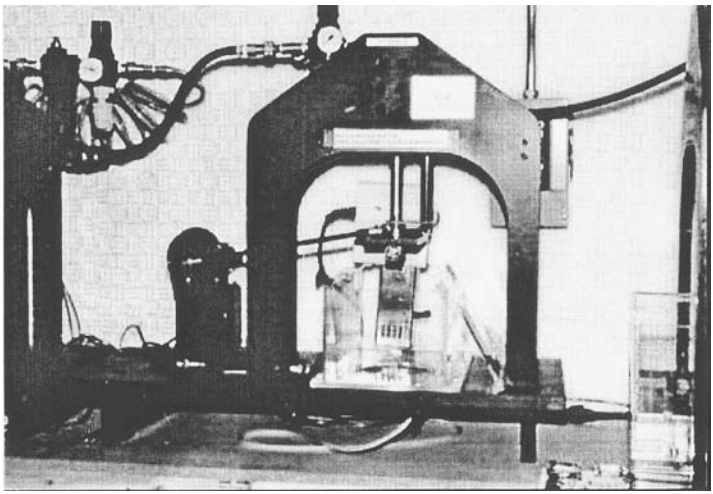

Figure 7 The EnduraTec wear simulator featuring pneumatic load actuator, saline bath with heater-circulator, and offset cam with electric motor. (From Ref. 13.)

Gravimetric wear results are shown in Figures 8 and 9 for all six implant components. Total mass change by 10 million cycles was less than 5 mg in any disc component. The results suggest a two-stage wear process. In the first stage (through 2 million cycles) the wear rate was relatively high, approximately 1.5 g per million cycles. In the second stage, the wear rate was considerably less, approximately 0.3 g per million cycles, and appears to stabilize by 6 million cycles. Figure 10 shows the change in the wear rate as a function of total accumulated cycles. Each point represents the quotient of the total mass lost since the last measurement divided by the total cycles experienced since the last measurement. This produced an exponentially declining

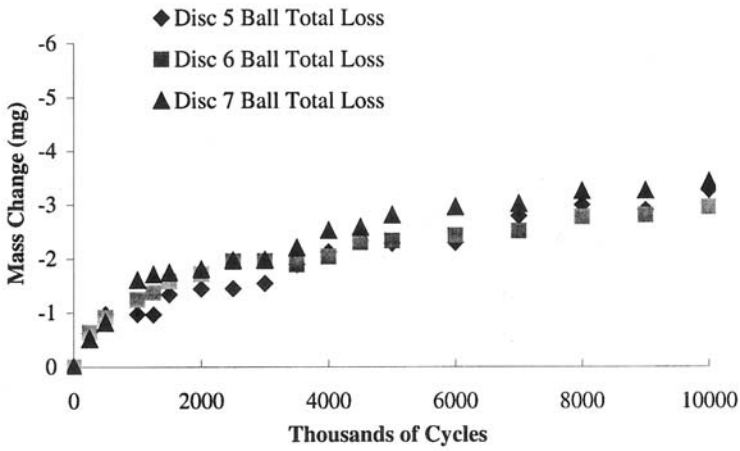

Figure 8 Mass change in ball components. Disc 7 ball component demonstrates the most wear. Variation between implant pairs is less than 1 mg. (From Ref. 13.)

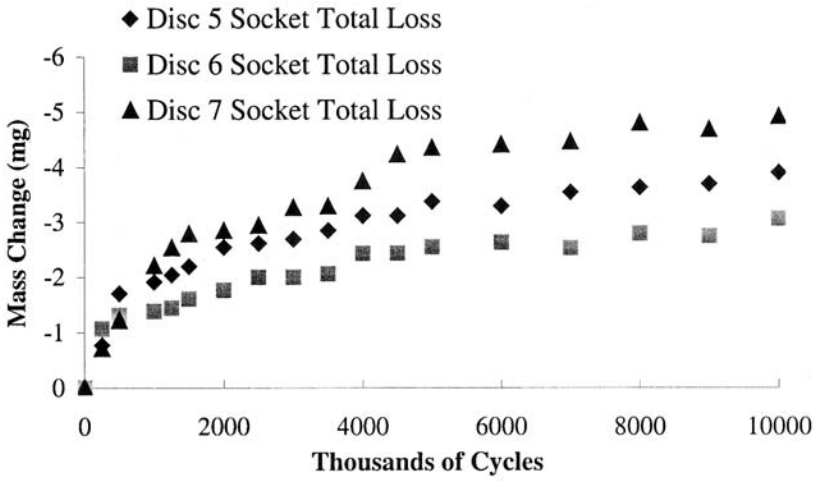

Figure 9 Mass change in socket components. (From Ref. 13.)

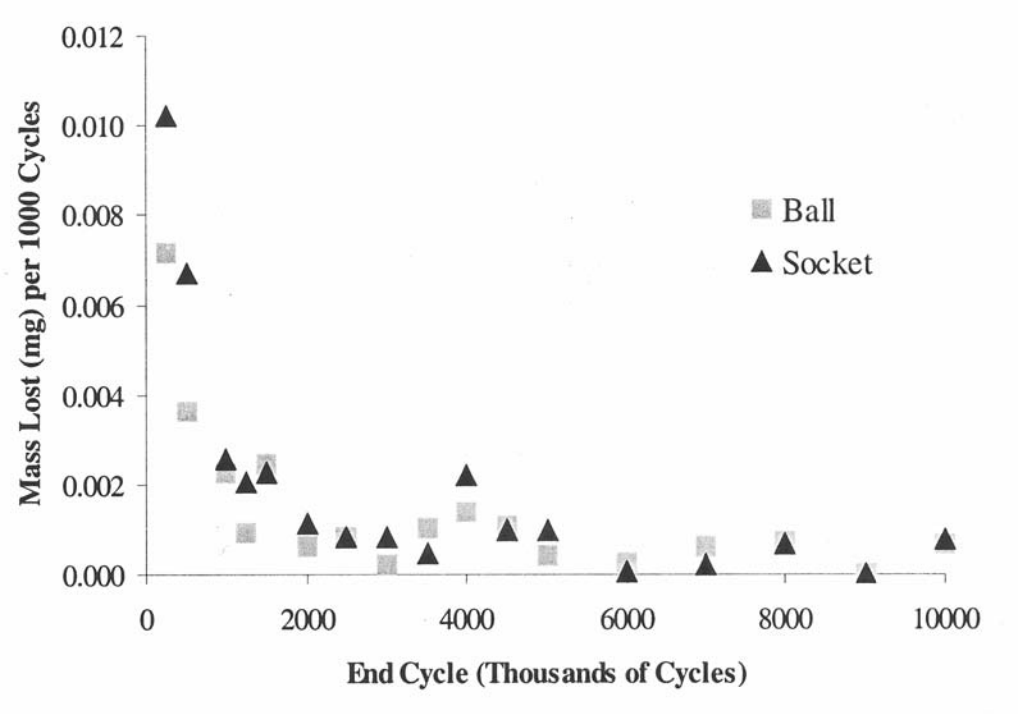

Figure 10 Average rate of mass change for ball-and-socket components. Mass lost in each testing period total cycles in testing period is plotted vs. end cycle count of the testing period. (From Ref. 13.)

graph. There was limited evidence of gross wear, including no evidence of chipping or severe cracking. Scanning election microscopic examination revealed a smooth surface with parallel tracks. Close inspection of the socket surface revealed a demarcation outlining the bottom. This region (approximately 30 mm^2, as measured by photographs analyzed with Scion Image software) correlated with the ball range of motion along the implant surface. Average total mass lost by the implant components was small in comparison to the total implant, averaging less than 4 mg in either component. This amount was distributed over an area of approximately 30 mm^2 on either component, resulting in very small radii changes, less than 0.1 mm, or less than 1% of the ball radius, as determined by the volume of material lost and the area of apparent wear described above. The implant's range of motion in the sagittal plane was unaffected as measured by the wear-testing system. It is expected that the implant range of motion or integrity will not be severely altered due to erosion of the sliding surfaces. Although this experiment was conducted to just 10 million cycles, just 1/10 the expected wear lifetime of a disc replacement [13], the asymptotic wear rate produced by this system predicts minimal wear beyond 10 million cycles, given the same testing methods utilized here. The quality and quantity of the wear debris determine biocompatibility. Total mass lost by 10 million cycles by any single implant in this test was less than 10 mg. This corresponds to less than 3×10^{-3} mL of wear particles over no less than 5 years by most estimates. The gravimetric changes produced by the wear simulation described above indicate that this prosthesis shows good resistance to wear. Functional changes (range of motion, integrity) observed in this study were negligible. The wear depth rate was found to be less than 0.1 mm/10 million cycles, resulting in very small changes in implant dimensions or kinematics. Previous biocompatibility studies suggest that the amount of wear debris produced by the implant components would be tolerated by the surrounding tissues. In vivo studies are necessary to determine this for certain.

The above-described studies provide valuable data on the biomechanics of the segment as effected by an artificial disc implantation. However, these studies fail to address the issue of load sharing between the disc and the posterior elements and related issues. Computational models are essential to gain an insight into these issues.

H. Computational Models

Finite element (FE) models of the intact motion segment (Fig. 11) and segments implanted with the Sofamor Danek disc (ball and socket design) (Fig. 12) and a Slip-Core Design disc (similar in principle to Waldemar Link™ SB Charite III artificial disc) (Fig. 13) were prepared [12,13]. In these models, softened, contact, unidirectional elements mimicked cartilaginous facet joints. The anulus consisted of layers of fiber-reinforced continuum elements, with fiber orientations at 30° and 120° to the horizontal, and fiber modulus changing from the center to the periphery of the disc space. Finite element model details are provided in Table 1. Specific assumptions and approximations facilitated model generation and analysis. For example, although the actual ball-socket implant has grooves and beads for osseointegration with the vertebral endplates, this complex surface was simulated as a flat plane, with implant nodes fixed to the endplate nodes, thereby assuming perfect bone in-growth. In addition, the implant was scaled to match the spine model's disc space height, resulting in the disc occupying 40% of the segment's cross-sectional area in the transverse plane. Distraction of the segment to restore disc height in a clinical restoration was not simulated, because the intact model had normal disc height initially. The alumina portion was assigned appropriate elastic material values ($E = 380$ GPa, $\mu = 0.26$) [13], as was the titanium portion ($E = 114$ GPa, $\mu = 0.32$) [13]. Friction was assigned a value

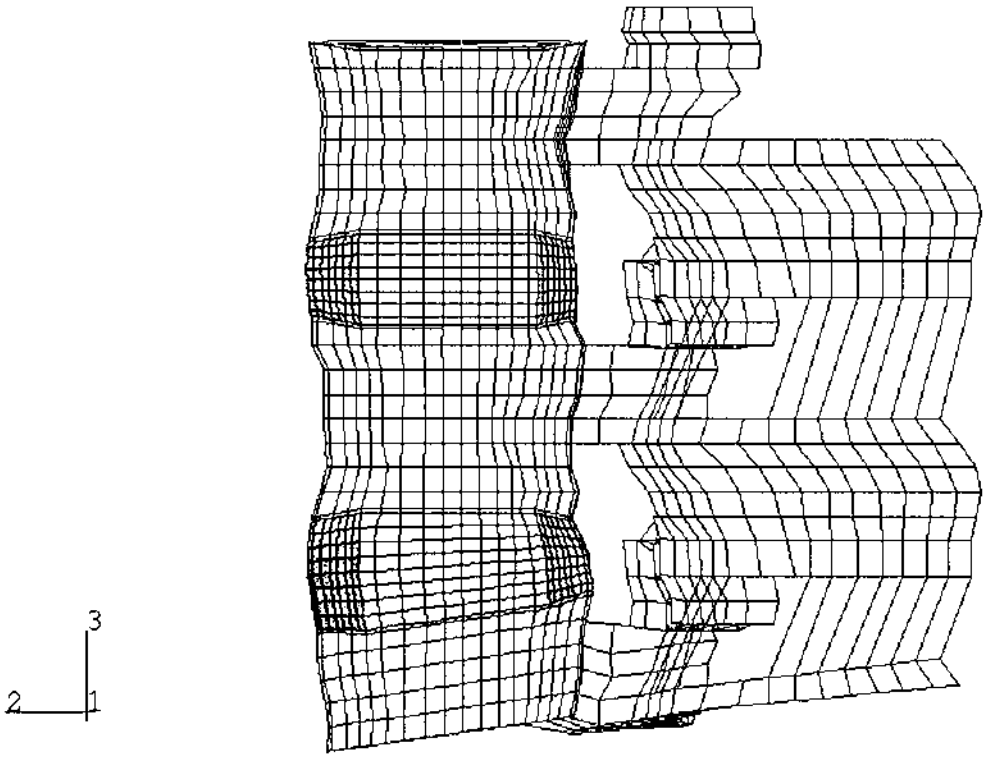

Figure 11 Three-dimensional nonlinear finite element model of the ligamentous L3–4–5 segment. Only the sagittal view is shown for the sake of clarity. (From Ref. 13.)

of 0.09, which is the value reported in literature for wet alumina-alumina sliding contact [13]. In a similar fashion, Slip-Core design was simulated.

Changing model parameters facilitated study of some segment biomechanics dependencies on surgical technique. For example, the ball-and-socket artificial disc was placed as posterior in the disc space as allowed by the remaining annulus (PD; Fig. 12B). This meant shifting the prosthesis 8 mm anterior, as far as it could be shifted without overhanging the endplate (AD; Fig. 12B). In another parameter, the smallest annular window possible was cut (A+; Fig. 12B), as dictated by the width of the implant for anterior insertion, whereas in a complementary case, fully one third of the annulus was removed (A−; Fig. 12B). After removal, the remaining annulus was 42% of the disc space in the A+ case and 35% in the A− case, the difference being entirely in the anterior third of the annulus. Last, the anterior longitudinal ligament was restored to its original form (not removed) to isolate the effects of annular and anterior longitudinal ligament resection. Similar changes were investigated for the Slip-Core design (Fig. 13).

This FE investigation included two loading schemes, corresponding first to model validation and then model investigation. Loading conditions for model validation included those used in in vitro experimental studies [1,21]. Model predictions from this set of conditions were compared to in vitro results. The second set of conditions included an axial compressive force of 400 N combined with flexion and extension moments up to 10 Nm. The effects of axial compression on the biomechanics were also studied by applying forces of up to 800 N.

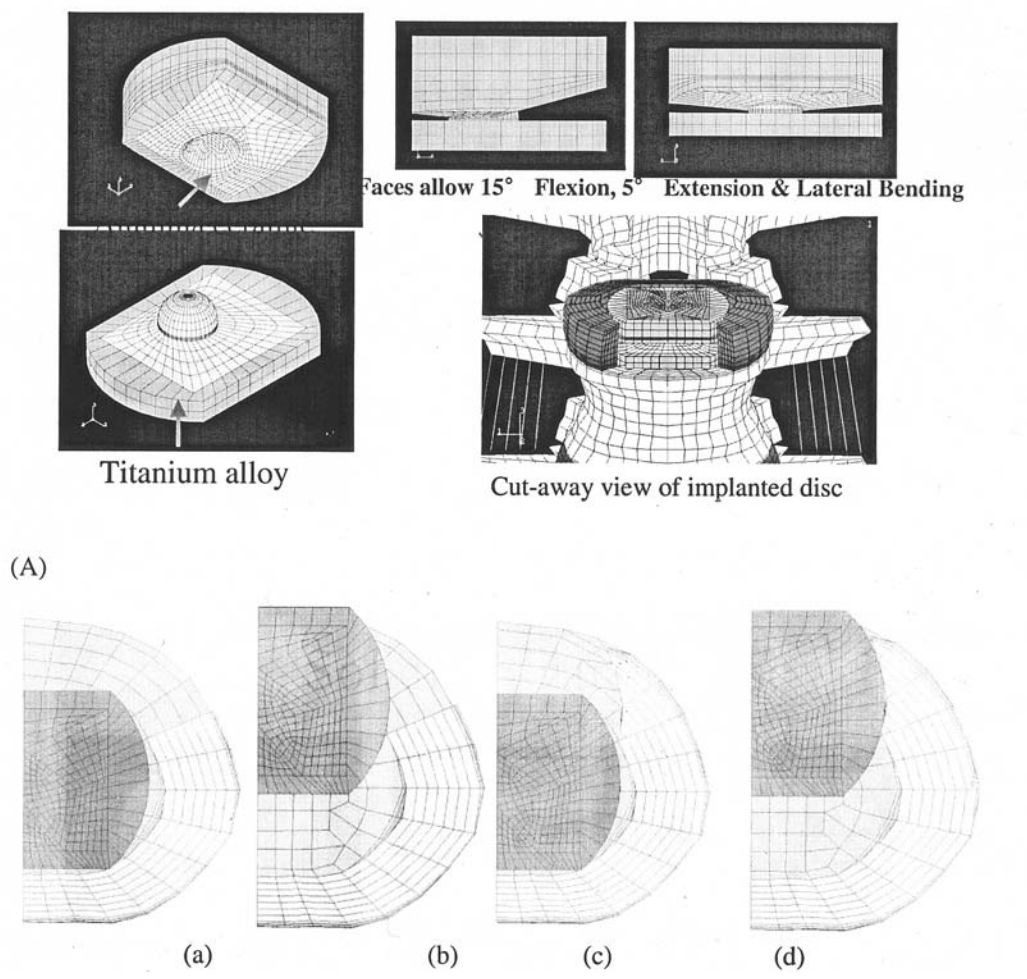

Figure 12 The intact finite element model was modified to simulate the ball-and-socket type of artificial disc. (A) The full model and (B) model variations – surgical variables as implemented in the finite element model. The artificial disc was placed anteriorly and posteriorly, and small and large amounts of anulus were removed. Posterior placement of the disc was limited by the annulus, and anterior placement was limited by the end plate. PD&A− = posterior disc with a large amount of annulus removed; PD&A+ = posterior disc with a small amount of anulus removed; AD&A− = anterior disc with a large amount of anulus removed; AD&A+ = anterior disc with a small amount of anulus removed. (From Ref. 13.)

The data shown in Tables 2 and 3 indicate that FE models are valid for further analyses. By accounting for both surgical variables in the in vitro procedures for ball-socket disc design, FE predicted rotations under applied moments either matched or straddled in vitro results (Table 2). In flexion, FE model predictions were either larger or smaller than in vitro results, depending on model parameters. In extension, the anteriorly placed disc results closely matched in vitro data. In general, predictions for segment rotations fell within one standard deviation of the in vitro data.

The Slip-Core design–implanted FE model was validated by comparing model predictions for motion segment rotations with results from a previous in vitro study by Ahrens et al., which

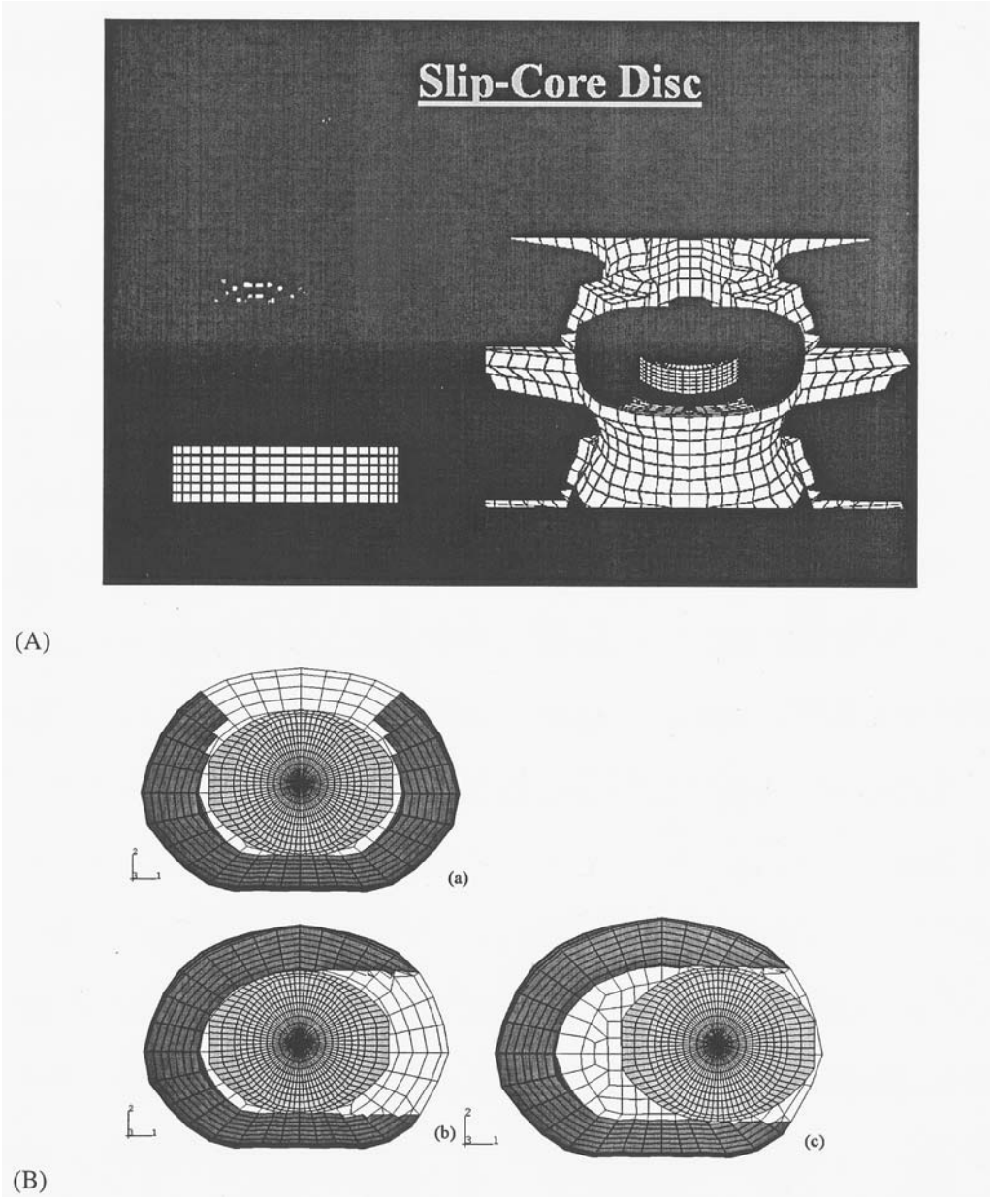

Figure 13 The intact finite element model was modified to simulate the slip core type artificial disc. (A) The full model and (B) model variations depicting different placements of the disc within the disc space. (From Ref. 13.)

Table 1 Material Property Designations and Element Types for the Intact L3–L5 Finite Element Model

Element set	Number of elements	ABAQUS element library type	Modulus of elasticity (MPa)	Poisson's ratio, ν	Cross sectional area (mm^2)
Bony regions					
Cortical bone	1872	C3D8	12000	0.30	
Cancellous bone	4368	C3D8	100	0.20	
Posterior bone	1256	C3D8	3500	0.25	
Intervertebral disc					
Annulus (ground substance)	3584	C3D8	1.2	0.45	
Annulus fibers		REBAR	357.5–550	0.30	0.00601–0.00884
Nucleus pulposus	1792	C3D8	1.0	0.4999	
Joints					
Apophyseal joints	80	GAPUNI	Softened, 3500		
Ligaments					
Anterior longitudinal	160	T2D2	15.6–20.0	0.30	74
Posterior longitudinal	96	T2D2	10.0–20.0	0.30	14.4
transverse	20	T2D2	12.0–59.0	0.30	1.8
Ligamentum flavum	16	T2D2	13.0–19.5	0.30	40
Interspinous	28	T2D2	9.8–12.0	0.30	40
Supraspinous	8	T2D2	8.8–15.0	0.30	30
Capsular	2	T2D2	8.48–32.9	0.30	34

For bilateral structures (apophyseal joints, capsular ligament), the total number of elements are listed.
Source: Ref. 13.

Table 2 Ball-and-Socket Disc Implanted Finite Element Model Predictions for Rotations in the Sagittal Plane[a]

Moment (Nm)	*In Vitro* average (SD)	AD&A−	AD&A+	PD&A−	PD&A+
−6	−4.4 (1.8)	−6.0	−4.2	−6.0	−4.1
−4.5	−3.1 (1.7)	−4.8	−3.4	−3.6	−3.3
−3	−2.1 (0.7)	−3.6	−2.5	−4.8	−2.3
−1.5	−0.8 (0.3)	−2.0	−1.3	−2.0	−1.2
0	0	0	0	0	0
1.5	1.5 (1.4)	1.6	1.6	3.0	2.6
3	2.8 (1.5)	2.5	2.5	4.9	4.5
4.5	3.7 (1.4)	3.4	3.3	4.9	4.5
6	5.1 (1.5)	4.0	4.0	5.8	5.2

[a] Four model variations were used to accommodate surgical variations.
Source: Ref. 13.

Table 3 Comparison of Reported *In vitro* Rotations and Finite Element Predictions for Lumbar Spines Implanted with the Slip-Core Intervertebral Disc Replacement[b]

Loading mode	Moment magnitude (Nm)	*In vitro* results ($n = 5$)[a,b]	FE predictions[b]
Flexion	12	1.27 (0.23)	1.24
Extension	12	0.94 (0.23)	1.30
Left lateral bending	8	0.85 (0.64)	1.36
Right lateral bending	8	1.41 (0.48)	1.36
Torsion	7	1.81 (0.44)	1.65

[a] From Ref. 1.
[b] Results are normalized by dividing the implanted spine rotation by the intact spine rotation. Agreement is obtained for all modes except extension in which the FE model predicts larger rotations.
Source: Ref. 13.

investigated the rotational stiffnesses of Waldemar Link™ SB Charite III IDR implanted lumbar spines (similar to Slip-Core design modeled here) [1]. Ahrens reported the rotations of five osteoligamentous specimens implanted with the Link IDR and loaded to 12 Nm in extension or flexion, 8 Nm in lateral bending, and 7 Nm in torsion (Table 3). The same load conditions were applied to the anteriorly inserted, centrally located implant model. Direct comparison failed to show agreement between the FE predictions and the in vitro results. However, when the implanted in vitro rotations were normalized by the intact in vitro rotations, agreement was achieved for all bending modes except extension. In extension, the FE model predicted an increase in motion from the intact, whereas the in vitro study predicted nearly the same. At this load (12 Nm) the implant components decoupled in the FE model. Thus, the maximum applied moment load in this FE study was restricted to 10 Nm.

I. Ball-and-Socket Versus Slíp-Core Design

In flexion and extension plus 400 N preload, the ball-socket design–implanted spine segment model exhibited less rotational stiffness than the intact model. In extension, segment rotations were sensitive primarily to the amount of remaining annulus. Segments with less annulus remaining (AD/PD, and A−) rotated approximately 40% more in extension (−5.12°, −5.23° vs. −3.7°), but segments with more annulus remaining (AD/PD, and A+) rotated approximately 30% more than the intact model (−4.78°, −4.79° vs. −3.7°). Under flexion moments, however, disc placement and amount of annulus affected rotation values. Placing the disc anteriorly decreased flexion by 19% (4.8° vs. 5.88), but placing it posteriorly increased flexion by 44% in the PD/A− and by 36% in the PD/A+ cases. Under axial compression, AD and A+/A− cases extended (−1.5° at 800 N), and PD and A+/A− cases flexed (2.4° and 4.4° for PD and A+/A−, respectively). In contrast, the intact segment's rotation was negligible under compression.

Forces across the facet joints increased with ball-and-socket artificial disc implantation (Fig. 14) under most loading conditions. Only with a posteriorly placed artificial disc at low loads (2 Nm or less) were facet loads lower in the implanted FSU. Placing the artificial disc anteriorly increased the load shift to the facets to more than that in the intact case and in the posteriorly placed case (at loads less than 10 Nm). The load shift also occurred earlier, such that facet loads were generated before any extension moment. Total facet unloading with the anteriorly placed artificial disc was not achieved until more than 2 Nm moment was applied in flexion. Under 800 N compression, the facet joint was unloaded completely with the posterior

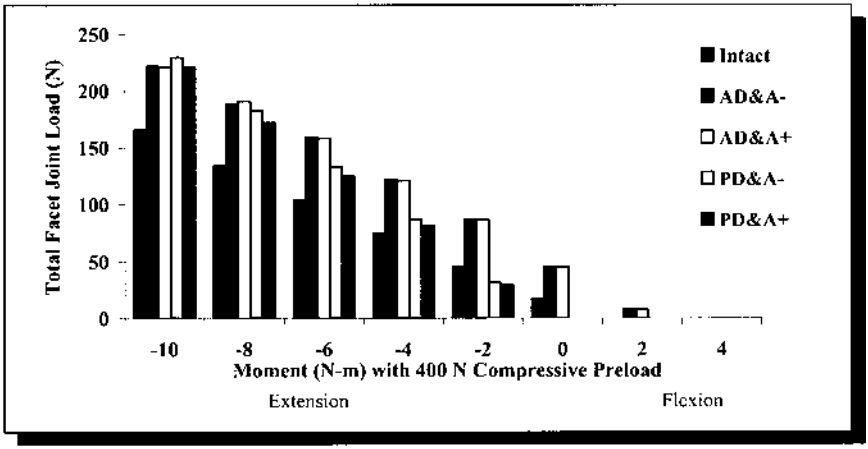

Figure 14 Facet contact forces as a function of applied moment, disc placement (AD and PD), and amount of remaining anulus (A+, A−). Disc placement affected posterior loads more than anulus resection. Facet contact forces in implanted cases were higher than those in intact conditions in segments with moments greater than 4 Nm; facet contact forces for moments less than 4 Nm were lowest in segments with posteriorly placed discs. (From Ref. 13.)

artificial disc placement. With anterior placement, however, loads across the facet joint increased to more than 150% of those in intact case (38 N vs. 98 N).

Restoring the anterior longitudinal ligament significantly affected segment mechanics in extension, as is shown in Table 4. The ligament had no effect on the segment under flexion because of its inability to transmit compressive loads. It did, however, marginally reduce rotation under compression for the AD/A± cases because of the segment's tendency to extend under compressive load. Rotation and facet contact forces all returned to nearly intact values under extension with posterior artificial disc placement. However, the main motion differed between the two disc designs and as compared to the intact as well (Fig. 15). Changes were also observed for the loads on the facets (Fig. 16).

Table 4 Effect of Restoring the Anterior Longitudinal Ligament

Condition	Facet Load (N)	Rotation (°)
Intact	166	−3.70
AD&A+/−	221/222	−4.8/−5.3
AD&A+/−& ALL	220/261	−3.9/−3.7
PD&A+/−	211/230	−4.8/−5.2
PD&A+/−& ALL	163/169	−3.8/−3.9

Restoration reduced segmental rotation in the AD&A+/− cases and reduced both facet loads and rotation in the PD&A+/− cases nearly back to intact levels for 10 Nm extension with 400 N compressive preload.

Table 5 Rotation Changes from Intact (degrees) at 6 Nm

Segment	LAR	RAR	RLB	LLB	FLX	EXT
Middle denucleated	+0.47	+0.80[a]	+1.35[b]	+1.68[b]	+1.22	+1.45[b]
Middle implanted	−0.33[c]	−0.09[c]	−0.32[c]	+0.43[c]	−0.42	−1.12[d]
Superior to implanted	+0.23	+0.30	−0.37	+0.92	−0.03	−0.53
Inferior to implanted	+0.13	+0.16	−0.30	+0.36[e]	+0.29	+0.77

Test repeatability was set at 0.25^{+}.
Significance at $p < 0.05$, trend at p 0.10 using paired t-test ($\delta - 0.25$).
[a] significance between intact and nuclectomize.
[b] trend between intact and nuclectomized.
[c] significance between nuclectomized and implanted.
[d] trend between nuclectomized and implanted.
[e] trend between intact and implanted.

Although an anterior surgical approach makes total preservation of the anterior longitudinal ligament unlikely with current artificial disc designs, synthetic replacement may provide a similar anterior restraint. The anterior longitudinal ligament provides a tensile resistance to rotation on the opposite side of the center of rotation from the facets (as does the anterior annulus), thus decreasing the facet load. An alternative method for preserving the anterior longitudinal ligament would be to implant the disc using a lateral approach. This would also preserve the entire anterior annulus, further stiffening the segment. However, a lateral approach may be deleterious to the lateral bending and torsional stiffness. Further studies are needed to investigate these issues.

Predicted loads in the spinal elements were found to be dependent on the implant design and the surgical variables. In a biomechanical study of related interest, Lemaire et al. observed that facet loads in torsion within a lumbar segment implanted with the SB Charité artificial disc can be as high as 2.5 times those of a healthy, intact segment [36]. In the current study, it was observed that a similar change could occur in compression with an anteriorly placed, fixed center of rotation disc implant. These results not only support the above observations but also underscore the importance of these variables through the quantification of changes in the loads/stresses in the posterior elements in flexion and extension modes. Such load shifts should be considered seriously when determining whether replacement surgery is the best option. Contraindications of malformed or degenerated posterior elements appear well justified by this analysis, although posterior load shifts can be moderated by surgical technique.

This study focused on the biomechanical effects of disc implantation in the sagittal plane of the L3-L4 disc space. By selecting this plane, the authors were able to isolate the effects of

Table 6 Average Disc Height Change Under Compression (50–750 N)

Condition	Left center	Front center	Right center	Above	Below
Intact	−0.19	0.24	0.10	0.38	−1.55
Denucleated	−0.56	−0.84	0.28	0.35	−0.80
Implanted	−0.40	0.53	0.07	0.21	−1.79

Compression < 0; distraction > 0 (all units in mm).

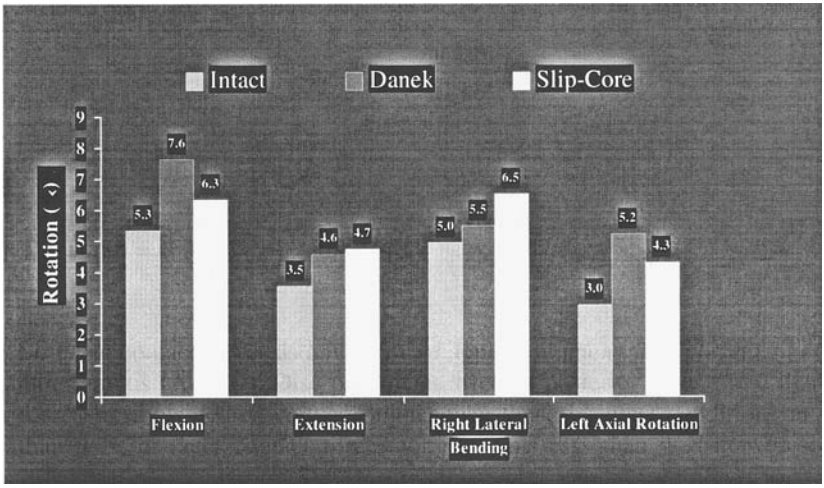

Figure 15 Predicted rotations for two disc designs as compared to the intact case. (From Ref. 13).

the selected surgical variables in the sagittal plane. However, the effects on axial rotation and lateral bending as well as the effects caused by eccentric placement in the lateral direction also need to be studied.

In summary, the experimentally validated finite element models of the intact and disc-implanted segments would suggest that both of the disc designs do not restore motion and facets loadings back to the control intact state. (These designs restore the intact biomechanics in a limited sense.) These differences are due not only to the size of the implants but also to the inherent design differences. Ball-and-socket design has a more ''fixed'' center of rotation as compared to the Slip-Core design in which the core undergoes a wider variation. A further

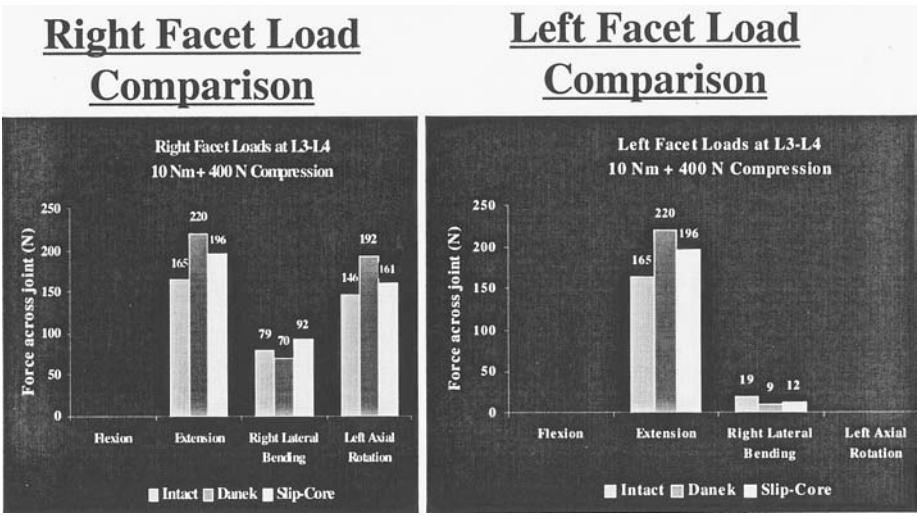

Figure 16 Predicted facet loads for two disc designs as compared to the intact case. (From Ref. 13.)

complicating factor is the location of the disc within the annular space itself, a parameter under the control of the surgeon. Thus, it will be difficult to restore the biomechanics of the segment back to normal using such designs. Only clinical follow-up studies will determine the effects of such variations on the changes in spinal structures as a function of time. The L5-S1 disc will most likely behave significantly differently than those at the mid-lumbar levels and also needs to be carefully evaluated by FE modeling.

IV. CONCLUSIONS

Disc joint replacement will soon be a clinically available option for the spine surgeon. The indications need to be clearly defined and will most likely be chronic severe low back pain refractory to all conservative care and limited to degeneration mainly at the disc and only at one or two levels. Regulations require that a disc or nucleus replacement meet certain guidelines before it can be considered for clinical trials, in particular it must meet biocompatibility and efficacy requirements. Rarely, however, has much consideration been given as to whether the device will fulfill the theoretical advantages of using an artificial disc over arthrodesis techniques, chief among these being the restoration of normal motion at the implanted motion segment as well as adjacent motion segments. Effects on adjacent motion segment mechanics and facet joint loads have not been reported. Load-sharing with the facets and neighboring segments, however, is crucial for long-term success. These aspects of the research are presented in this chapter. The dilemma of mechanical designs is that all devices made by humans eventually fail. This failure is the result of wear and fatigue. The new approach to joint replacement in the spine is tissue engineering. Tissue engineering would replace the disc with living tissue capable of repairing itself. Tissue engineering approaches include regeneration of the nucleus through introduction of growth factors or gene therapy, as well as cell transplantation and scaffolding. The spine is much more complicated than a hip or knee. The results of a disc arthroplasty may never equal the benefit of the TKR or the THR and are not fairly compared. The real success of disc replacement will be compared to the results of spine arthrodesis.

REFERENCES

1. Ahrens JE, Shelokov AP, L J. Normal joint mobility is maintained with an artificial disc prosthesis. Marseilles. France: Annual Proceedings of International Society for the Study of the Lumbar Spine, 1993.
2. Ambrosio L. Composite hydrogels for intervertebral disc prosthesis. J Mater Sci Mater Med 1996; 7:251–254.
3. Andersson GBJ. Epidemiology and cost. In: Occupational Low Back Pain: Assessment, Treatment and Prevention Pope MH, et al, ed. St. Louis: Mosby Year, 1991:95–113.
4. Arnoldi C, Brodsky AE, Cauchoix J. Lumbar spinal stenosis and nerve root entrapment syndromes: definition and classification. Clin Orthop 1976; 115:4.
5. Bao QB. The artificial disc: theory, design and materials. Biomaterials 1996; 17(12):1157–67.
6. Brodsky AE. Post laminectomy and post-fusion stenosis of the lumbar spine. Clin Orthop 1976; 115: 130–139.
7. Buttner-Janz K. Intervertebral disc endoprosthesis, 1988.
8. Buttner-Janz K, Schellnack K, Zippel H. Biomechanics of the SB Charite lumbar intervertebral disc endoprosthesis. Int Orthop 1989; 13(3):173–6.
9. Buttner-Janz K. The development of the Artificial Disc Charite SB. Dallas: Hudley & Associates, 1992.

10. Cinotti G, David T, Postacchini F. Results of disc prosthesis after a minimum follow-up period of 2 years. Spine 1996; 21(8):995–1000.
11. Cunningham LS, Kelsey JL. Epidemiology of musculoskeletal impairments and associated disability. Am J Public Health 1984; 74:574–579.
12. Dooris AP, Goel VK, Grosland NM, Gilbertson LG, Wilder DG. Load-sharing between anterior and posterior elements in a lumbar motion segment implanted with an artificial disc. Spine 2001; 26: E122–E129.
13. Dooris AP. Experimental and Theoretical Investigations into the effects of artificial disc implantation on the lumbar spine, PhD dissertation. Iowa City, IA: University of Iowa, 2001.
14. Dooris A, Hudgins G, Goel V, Bao C. Restoration of normal multisegement biomechanics with prosthetic intervertebral nucleus. 48th Annual Meeting of the Orthopaedic Research Society, 2002.
15. Enker P. Artificial disc replacement. Preliminary report with a 3-year minimum follow-up. Spine 1993; 18(8):1061–1070.
16. Esses SI. Kinematic evaluation of lumbar fusion techniques. Spine 1996; 21(6):676–684.
17. Eyre D. Basic science perspectives. In: New Perspectives on Low Back Pain Frymoyer JW, Gordon SL, eds. American Academy of Orthopaedic Surgeons. IL: Park Ridge, 1989:147–207.
18. Farfan HF. Mechanical Disorders of the Low Back. Philadelphia: Lea & Febiger, 1973.
19. Frymoyer JW. A comparison of radiographic findings in fusion and nonfusion patients ten or more years following lumbar disc surgery. Spine 1979; 4(5):435–440.
20. Frymoyer JW. Indications for consideration of the artificial dis. In: Clinical Efficacy and Outcome in the Diagnosis and Treatment of Low Back Pain. Weinstein JN, ed. New York: Raven Press, 1992: 227–236.
21. Gilbertson LG. Biomechanical evaluation of a new lumbar disc implant: in vitro-simulations of disc surgery, implantation, and post-op mobilization: International Society for the Study of the Lumbar Spine, 1996.
22. Griffith SL. A multicenter retrospective study of the clinical results of the LINK SB Charite intervertebral prosthesis. The initial European experience. Spine 1994; 19(16):1842–9.
23. Hedman TP. Design of an intervertebral disc prosthesis. Spine 1991; 16(6 suppl):S256–260.
24. Hellier WG, Hedman TP, Kostuik JP. Wear studies for development of an intervertebral disc prosthesis. Spine 1992; 17(6 suppl):S86–96.
25. Hsu KY. Deterioration of motion segments adjacent to lumbar spine fusion. In: North American Spine Society. CO: Colorado Springs, 1988.
26. Kahanovitz N. Osteoporosis. In: Wiesel SM, ed. The Lumbar Spine. Philadelphia: W B Saunders Co, 1990:760–769.
27. Kellgren JH, Lawrence JS. Osteo-arthritis and disk degeneration in an urban population. Ann Rheu Dis 1958; 17:388.
28. Kelsey JL, White AA. Epidemiology and impact on low back pain. Spine 1980; 5:133.
29. Kelsey JL, Pastides H, Bigbee GE. Musculoskeletal disorders: Their frequency of occurrence and their impact on the population of the United States. New York: Prodist, 1978.
30. Klara PM, Ray CD. Artificial nucleus replacement clinical experience. Spine 27(12):1374–1377.
31. Kostuik JP. Intervertebral disc replacement. Experimental study. Clin Orthop 1997(337):27–41.
32. Kotani Y, Abumi K, Shikinami Y, Takada T, Kadoya K, Shimamoto N, Ito M, Kadosawa T, Fujinaga T, Kaneda K. Artificial intervertebral disc replacement using bioactive three-dimensional fabric design, development, and preliminary animal study. Spine 27(9):929–935.
33. Lee CK. Accelerated degeneration of the segment adjacent to a lumbar fusion. Spine 1988; 13(3): 375–7.
34. Lee CK, Langrana NA, Parsons JR. Development of a prosthetic intevertebral disc. Spine 1991; 16(6):S253–S255.
35. Lehmann TR. Long-term follow-up of lower lumbar fusion patients. Spine 1987; 12:97–104.
36. Lemaire JP. Intervertebral disc prosthesis. Results and prospects for the year 2000. Clin Orthop 1997(337):64–76.
37. Lewin T. Osteoarthritis in lumbar synovial joints. Acta Orthop Scand 1964; 73(suppl):1–112.
38. Martz EO. Thesis: an artificial intervertebral disc exhibiting a negative poisson's ratio. Biomedical Engineering Department. Iowa City. IA: The University of Iowa, 1995.

39. McDevitt CA. Proteoglycans of the intervertebral disc. In:. Ghosh P, ed. The Biology of the Intervertebral Disc. Boca Raton, FL: CRC Press, 1988:151–170.
40. McMillin CR, D A. In 20th Annual Meeting of the Society for Biomaterials, Boston, 1994.
41. Miller JAA, Schmatz C, Schultz AB. Lumbar disc degeneration: correlation with age, sex, and spine level in 600 autopsy specimens. Spine 1988; 13:173.
42. Mooney V. Facet syndrome. In: Wiesel SM, ed. The Lumbar Spine. Philadelphia: W B Saunders co, 1992:422–441.
43. National Council on Compensation Insurance. Detailed claim information, lower back injuries, state of Massachusetts, breakdown by class code. Unpublished data, New York, 1983.
44. Naylor A. Enzymatic and immunological activity in the intervertebral disc. Orthop Clin North Am 1975; 6:51–58.
45. Osman M. Results of clinical studies for prosthetic disc nucleus. In: World Spine. Berlin. Germany, 2000.
46. Ray CD, P T. Prosthetic disc and method of implanting. U.S. Patent 4,772,287, 1990.
47. Ray CD, P T. Prosthetic disc containing therapeutic material. U.S. Patent 4,904,260, 1990.
48. Schellnack K. The intevertebral disc endoprosthesis SB Charite. In: First European Congress of Orthopaedics. Paris, 1993.
49. Schmorl G, Junghanns H. The Human Spine in Health and Disease. New York: Grune & Stratton, 1971.
50. Scott AH, Harrison DJ. Increasing age does not affect good outcome after lumbar disc replacement. Int Orthop 2000; 24(1):50–53.
51. Seroussi RE. Internal deformations of intact and denucleated human lumbar discs subjected to compression, flexion, and extension loads. J Orthop Res 1989; 7(122–131).
52. Steffee AD. The Steffee artificial disc. In: Weinstein JN, ed. Clinical Efficacy and Outcome in the Diagnosis and Treatment of Low Back Pain. New York: Raven Press, 1992:245–257.
53. Waldemar Link & Co, GmbH, LINK SB Charite Intervertebral Prosthesis, Product Brochure, Hamburg, Germany, 1989.
54. White AA, Panjabi MM. Clinical Biomechanics of the Spine. 2nd ed.. Philadelphia: >J B Lippincott Co., 1978.
55. Wilke H. Prosthetic disc nucleus can restore height and flexibility after a nuclectomy. In: World Spine. Berlin. Germany, 2000.
56. Zeegers WS. Artificial disc replacement with the modular type SB Charite III: 2-year results in 50 prospectively studied patients. Eur Spine J 1999; 8(3):210–7.

16

Comparison of the Leukotactic Properties of Nucleus Pulposus, Anulus Fibrosus, and Cartilage Following Subcutaneous Injection in Pigs

Mats Grönblad, Johanna Virri, and Aklilu Habtemariam
Institute of Surgery, University Central Hospital
Helsinki, Finland

Bertel Kommonen, Outi Laitinen, and Ilkka Alitalo
University of Helsinki
Helsinki, Finland

I. INTRODUCTION

Nucleus pulposus (NP) tissue has been shown to induce an inflammatory reaction [1–3]. Extruded disc tissue usually becomes infiltrated with inflammatory cells, macrophages in particular [4–8]. Similar to clinical disc herniations in humans, inflammatory cells were also observed in a porcine disc herniation animal model [9]. In a porcine animal model, subcutaneously implanted NP showed leukotactic properties when compared with an empty perforated titanium chamber or one loaded with fat tissue [2]. Disc herniation tissues store and secrete several cytokines and other proinflammatory substances [10–13] (Table 1). Some of this secretory activity originates in NP cells [12,14].

Several cytokines and other proinflammatory substances are also stored and secreted by articular chondrocytes [15–17] (Table 1). As can be seen from Table 1, most proinflammatory substances demonstrated are common to both intervertebral disc and cartilage tissues. They are observed in higher concentrations in pathological tissues, i.e., herniated or degenerated disc and osteoarthritic cartilage, respectively [10,11,13,17,18].

Even if most herniated disc tissues are mainly composed of NP, there may also be variably anulus fibrosus (AF) and endplate cartilage tissue components [27]. Since all of the three tissues mentioned may variably contribute to mechanisms of sciatica, it is of clinical interest to compare their leukotactic properties in an animal model. We used a wide-bore (1.5 mm) needle to inject approximately 110 mg of NP, AF, or cartilage tissues subcutaneously in pigs in an autologous manner. All tissues to be injected were suspended in a minimum volume (0.5 mL) of Ringer's solution, which was also used as an injection control.

II. MATERIAL AND METHODS

Altogether, 13 pigs weighing 20–30 kg were used. The experiment was approved by the local ethical committee for animal experimentation. Animals were premedicated with azaperon 5 mg/

Table 1 Cytokines and Other Proinflammatory Substances Demonstrated in Intervertebral Disc and Articular Cartilage Tissues

Proinflammatory substance	Disc	Cartilage
IL-1α	+ [10]	+ [24]
IL-1β	+ [4,10,12]	+ [15,17]
IL-6	+ [10–12,18]	+ [15]
IL-8	+ [18]	+ [15]
IL-10	+ [12]	+ [23]
TNFα	+ [10,14]	+ [17]
GM-CSF	+ [10,12]	?
NO	+ [11,22]	+ [25]
PGE_2	+ [11]	+ [26]
LTB_4	+ [13]	?
TxB_2	+ [13]	?
LIF	?	+ [15]
MCP-1	+ [19,20]	+ [16]
MIP-1α, MIP-1β	+ [21]	+ [16]
GRO-α	?	+ [16]
RANTES	?	+ [16]

IL: interleukin; TNF: tumor necrosis factor; GM-CSF: granulocyte-macrophage colony-stimulating factor; NO: nitric oxide; PGE_2: prostaglandin E_2; LTB_4: leukotriene B_4; TxB_2: thromboxane B_2; LIF: leukemia inhibitory factor; MCP-1: monocyte chemoattractant protein; MIP: macrophage inflammatory protein; GRO: growth-related gene product; RANTES: regulated upon activation normal T cells expressed and secreted. +: has been demonstrated, ?: not known if demonstrated.

kg i.m. (Stresnil 40 mg/mL vet. inject., Janssen Pharmaceutica, Beerse, Belgium), followed by ketamine hydrochloride 20 mg/kg i.m. (Ketalar inject. 10 mg/mL, Parke-Davis, UK) 20 minutes later. After preoxygenation with a face mask, anaesthesia was induced by thiopentone 8 mg/kg (Pentothal Natrium, Abbot, Queenborough, UK). Animals were endotracheally intubated and maintained by 1.5% halothane (Trothane, ISC Chemicals Ltd., UK) in oxygen. Immediately after intubation benzylpenicillin-sodium 40,000 I.U./kg (Novocillin vet. inject., Novo Nordisk Farma, Denmark) was administered i.v. During anesthesia and for 3 postoperative days buprenorphin hydrochloride 0.01 mg/kg (Temgesic inject. 0.3 mg/mL, Reckitt & Colman, Hull, UK) was administered i.m. twice per day for postoperative pain relief.

A ventral approach was used. The abdomen was opened at the linea alba, muscles were dissected bluntly left to the anterior longitudinal ligament, and then the AF of intervertebral discs L4-L5 and L5-L6 was fenestrated with a #11 scalpel blade. In 5 pigs NP (approximately 110 mg) from the L4-L5 and the L5-L6 levels, respectively, was sucked into a ball-pointed 1.5 mm inner diameter cannula attached to a 2 mL syringe. 0.5 mL sterile Ringer's solution was then drawn into each syringe. The two NP-Ringer's solution samples were then injected autologously and subcutaneously under the dorsal skin about 8 cm apart, on opposite sides of the back. As a control for the injection procedure, two injections of 0.5 mL Ringer's solution only were given as well, spaced at least 8 cm apart from the former NP injection sites.

In 4 separate pigs, the AF from L4-L5 and L5-L6 levels was taken out and sliced in Ringer's solution with small scissors. Approximately 110 mg of AF from each intervertebral level was mixed with 0.5 mL Ringer's solution and then injected autologously and subcutaneously in

an analogous manner with the NP, but in separate pigs. In each of the pigs there were two injection sites. No Ringer's solution control sites were injected in these animals.

From 4 additional pigs, small fragments of ear cartilage (CART) were dissected and sliced in a similar manner as the AF tissues. Then approximately 110 mg of CART was mixed with 0.5 mL Ringer's solution and injected analogously with the NP and AF tissues. Also for CART there were two injection sites in each pig, and in these pigs there were no control Ringer's solution injection sites.

Injection sites were always spaced at least 8 cm apart. The 2 × 50 mm injection needles were all wide-bore (inner diameter of 1.5 mm) (Phoenix, Kobayashi-Shoji K.K., Shiyoda-ku, Tokyo, Japan), and pilot trials were done to ensure free passage for all injected tissues. Immediately following each subcutaneous injection, there was a clearly discernible transient bulge at the tip of the needle, which allowed for marking the skin at the area of injection. Histological checking in pilot pigs showed the injection to be subcutaneous, and all subsequent injections were carried out in an identical manner.

At 1 and 2 weeks, respectively, skin biopsies of the injected sites were taken under sterile conditions and under general anaesthesia (Table 2). The skin biopsies were quick-frozen in liquid nitrogen following a rinse in Ringer's solution. All specimens were coded and later studied blindly. Cryostat sections of 8 μm thickness were placed on microscope slides precoated with Vecta-Bond (Vector Laboratories, Burlingame, CA) to increase section adhesion. Sections were then air-dried and fixed in cold acetone for 10 minutes. Monoclonal mouse anti-human antibodies to T cells (CD3) (DAKO, Glostrup, Denmark) or macrophages (CD68) (DAKO) were employed. The interspecies cross-reactivity table for DAKO antibodies shows a strong immunoreaction with inflammatory cells present in porcine tissues for these antibodies. The alkaline phosphatase anti-alkaline phosphatase (APAAP) method was employed. This method has been used in previous studies on inflammatory cells in pig intervertebral disc tissues [9], and results with the method have been compared in parallel with those obtained by the avidin-biotin-peroxidase complex (Vectastain Elite ABC kit, Burlingame, CA) method and found to be similar [28]. The APAAP method has also been used for studying inflammatory cells in human intervertebral disc herniation tissues [4,5,29].

Table 2 Description of Injection Sites Taken for Skin Biopsy at 1 and 2 Weeks

Pig no.	1 week	2 weeks
1	NP and Ringer	NP and Ringer
2	NP and Ringer	NP and Ringer
3	NP and Ringer	NP and Ringer
4	NP and Ringer	NP and Ringer
5	NP and Ringer	NP and Ringer
6	AF	AF
7	AF	AF
8	AF	AF
9	AF	AF
10	CART	CART
11	CART	CART
12	CART	CART
13	CART	CART

NP: nucleus pulposus; AF: anulus fibrosus; CART: cartilage; Ringer: Ringer's solution control site.

The presence of inflammatory cells was assessed by a semiquantitative grading system—− = no cells, (+) = only occasional cells, and + = abundant cells—which has been employed successfully in previous studies on pig disc tissues. From each skin biopsy two to three randomly cut frozen sections were stained with each of the two antibodies. When grading varied in frozen sections cut through a particular skin biopsy sample, the highest cell occurrence grade was always chosen. For example, if two sections cut through a particular skin biopsy sample showed gradings (+) and + for T cells, the cells were classified as being abundantly present [9]. Control sections for the immunostaining reaction were stained with Tris-buffered saline (TBS) only in the absence of the respective primary antibody [28].

III. RESULTS

When sections were treated in the absence of either primary antibody (to CD3 or CD68), respectively, no immunostained cells at all could be observed. At sites where only Ringer's solution had been injected, only scattered macrophages (CD68) at most could be observed. None of the sites showed either abundant macrophages or T cells at 1 or 2 weeks following injection.

One week following injection of NP, AF, or CART (Table 3), abundant T cells were present in 4 of 5 pigs following injection of NP and in 4 of 4 pigs following injection of CART. In contrast, they were only present in 1 of 4 pigs following injection of AF. Abundant macrophages were less often observed and in the highest number of pigs (2/4) following the injection of CART tissue.

Two weeks following injection of NP, AF, or CART (Table 3), Only NP showed a clear response for T cells (4/5 pigs) (Fig. 1), and this was also the case with respect to macrophages (3/5 pigs). With respect to both T cells and macrophages, the response had waned following the injection of either AF or CART (Fig. 2).

IV. DISCUSSION

The present study is the first to compare in an autologous subcutaneous injection animal model the leukotactic properties of all three tissue components that have been reported to be variably present in extruded disc tissue. Most commonly disc herniations (DH) contain nucleus pulposus tissue [27], but in some DH there is also anulus fibrosus and/or cartilaginous endplate tissue [27,30].

In an earlier study [2], where either NP tissue or retroperitoneally obtained fat tissue was placed subcutaneously into perforated titanium chambers in pigs, only NP showed leukotactic

Table 3 Comparison of Pigs Showing Inflammatory Response to Autologous Subcutaneously Injected Tissues

	CD3 (%)		*CD68* (%)	
	1 week	2 weeks	1 week	2 weeks
NP	80	80	20	60
CART	100	0	50	0
AF	25	25	25	0

NP: nucleus pulposus; AF: anulus fibrosus; CART: cartilage; CD3: T cells; CD68: macrophages.

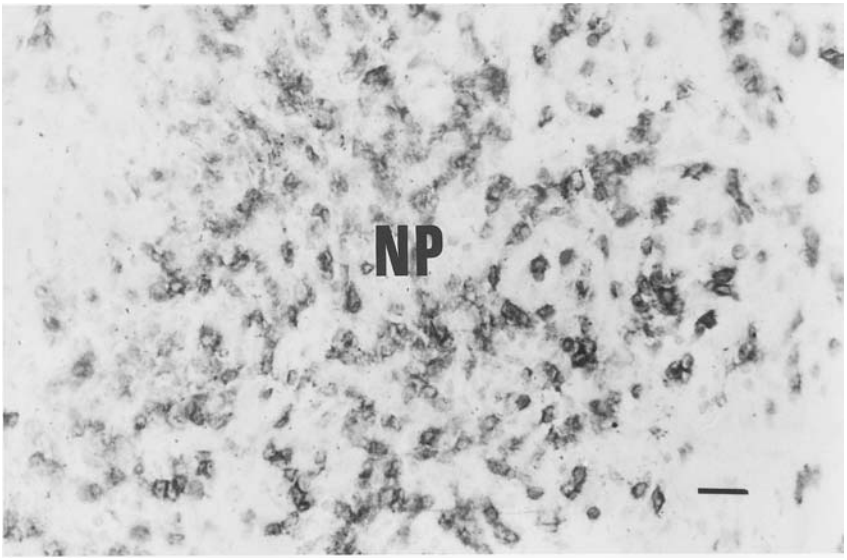

Figure 1 Abundant T cells seen at 2 weeks following autologous subcutaneous injection of nucleus pulposus (NP) in the pig. Alkaline phosphatase anti-alkaline phosphatase immunostaining, hematoxylin counterstaining. Scale bar = 30 μm.

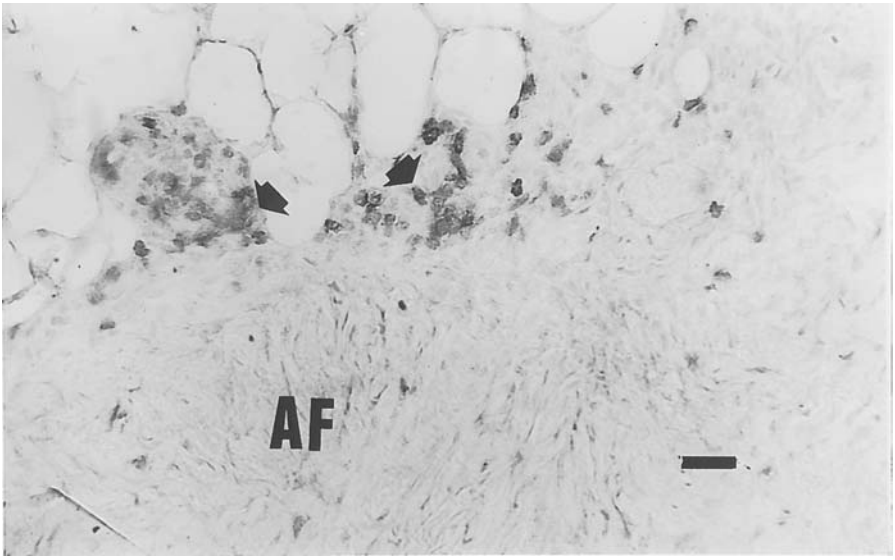

Figure 2 T cells (arrows) in the periphery of anulus fibrosus (AF) tissue 2 weeks following autologous subcutaneous injection in the pig. Alkaline phosphatase anti-alkaline phosphatase immunostaining, hematoxylin counterstaining. Scale bar = 30 μm.

properties. In another study [3], where subcutaneous vascular grafts in rabbits were loaded with NP or psoas muscle tissue alternatively, again only NP showed leukotactic properties, with an infiltration at 2 weeks of both macrophages and lymphocytes in most of the animals studied. These previous results accord well with those obtained in the present study, where alternatively NP, AF, and cartilage tissues were injected autologously and subcutaneously under the dorsal skin in pigs. As was previously observed in rabbits by Takino et al. [3], in the present study NP induced abundant T cells and macrophages in most of the animals studied at 2 weeks follow-up. Also in accord with the results of Takino et al. [3], macrophages were not yet abundantly present at 1 week. We did, however, observe abundant T cells in most animals studied at 1 week following NP injection. In the study on rabbits by Takino et al. [3], T cells were not yet abundantly present at 1 week, the difference in results possibly being explained by the use of different experimental animals or the different experimental setups (subcutaneously implanted vascular graft vs. subcutaneous injection in the present study). In their experiment on pigs, Olmarker et al. [2] observed leukotaxis at 1 week, but did not further characterize the types of infiltrating leukocytes.

In the present animal model, subcutaneously injected AF tissue did not show a leukotactic effect similar to that of NP. AF appears to be a more inert tissue than NP in this respect. Kawakami et al. [31] have compared pain-related behaviors in rats following the placement of either NP or AF on the nerve root. They reported *mechanical* hyperalgesia with NP and *thermal* hyperalgesia with AF [31]. They were able in their study to abolish the hypersensitivity to noxious mechanical stimuli induced by NP tissue, by epidural injection of a selective inhibitor of phospholipase A_2, whereas an inhibitor of nitric oxide synthase (NOS) abolished the thermal hyperalgesia induced by AF tissue [31]. Whether these results apply to human disc herniation patients is not yet known. Interestingly, however, Kawakami et al. [32] in a later study on their rat model observed the NP-induced mechanical hyperalgesia to depend on inflammatory cell infiltration. Thus, NP-induced leukotaxis as observed in the present study and also previously reported by Olmarker et al. in a pig model similar to ours [2], may be highly relevant clinically in mechanisms of sciatica.

Since effects of NP may be due to secretion from NP cells of cytokines and other proinflammatory mediators [11,14], we included cartilage tissue as a second comparison tissue, in addition to AF, to more completely elucidate leukotactic effects specific to NP tissue. For reasons of convenience, however, we used ear cartilage tissue as a substitute for endplate cartilage. Thus, our results may not be directly applicable to articular cartilage. As is the case with NP [11,14], articular chondrocytes have also been shown to store and secrete many proinflammatory mediators, e.g., cytokines [15]. Despite the very similar storage of proinflammatory substances, including cytokines, in NP and cartilage tissues (Table 1), our results suggested a more prolonged leukotactic effect for NP. Similar to our results, Rand et al. [33] observed macrophage recruitment following implantation of NP tissue into the peritoneal cavity of mice. Leukotaxis was observed for both NP and AF, with higher cell counts for NP. Viable disc cells were required to produce the inflammatory response [33].

NP tissue–induced leukotaxis appears to be involved in mechanisms of sciatica [32]. Macrophage recruitment, induced by both NP and AF tissues, respectively [33], is probably essential for spontaneous resorption of extruded disc tissue [20,21]. Thus, the observed leukotaxis may have wider implications with respect to the development of novel treatment protocols in the future.

REFERENCES

1. McCarron RF, Wimpee MW, Hudkins P, Laros GS. The inflammatory effect of nucleus pulposus. A possible element in the pathogenesis of low-back pain. Spine 1987; 12:760–764.

2. Olmarker K, Blomquist J, Strömberg J, Nannmark U, Thomsen P, Rydevik B. Inflammatogenic properties of nucleus pulposus. Spine 1995; 20:665–669.
3. Takino T, Takahashi K, Miyazaki T, Matsui T, Tomita K. Immunoreactivity of nucleus pulposus. Transactions of the International Society for the Study of the Lumbar Spine, annual meeting, Helsinki, Finland, June 18–22, 1995.
4. Grönblad M, Virri J, Tolonen J, Seitsalo S, Kääpä E, Kankare J, Myllynen P, Karaharju E. A controlled immunohistochemical study of inflammatory cells in disc herniation tissue. Spine 1994; 19:2744–2751.
5. Habtemariam A, Grönblad M, Virri J, Seitsalo S, Karaharju E. A comparative immunohistochemical study of inflammatory cells in acute-stage and chronic-stage disc herniations. Spine 1998; 23: 2159–2166.
6. Nohara Y, Tohmura T. An immuno-histological study of herniated nucleus pulposus of the lumbar spine. Transactions of the International Society for the Study of the Lumbar Spine, annual meeting, Marseilles, France, June 15–19, 1993.
7. Rothoerl R, Woertgen C, Holzschuh M, Brehme K, Ruschoff J, Brawanski A. Macrophage tissue infiltration, clinical symptoms, and signs in patients with lumbar disc herniation. A clinicopathological study on 179 patients. Acta Neurochir. (Wien) 1998; 140:1245–1248.
8. Matsui Y, Maeda M, Nakagami W, Iwata H. The involvement of matrix metalloproteinases and inflammation in lumbar disc herniation. Spine 1998; 23:863–868.
9. Habtemariam A, Virri J, Grönblad M, Holm S, Kaigle A, Karaharju E. Inflammatory cells in full-thickness anulus injury in pigs. An experimental disc herniation animal model. Spine 1998; 23: 524–529.
10. Takahashi H, Suguro T, Okazima Y, Motegi M, Okada Y, Kakiuchi T. Inflammatory cytokines in the herniated disc of the lumbar spine. Spine 1996; 21:218–224.
11. Kang JD, Georgescu HI, McIntyre-Larkin L, Stefanovic-Racic M, Donaldson WF, Evans CH. Herniated lumbar intervertebral discs spontaneously produce matrix metalloproteinases, nitric oxide, interleukin-6, and prostaglandin E2. Spine 1996; 21:271–277.
12. Rand N, Reichert F, Floman Y, Rotshenker S. Murine nucleus pulposus-derived cells secrete interleukins-1 $-\beta$, -6, and -10 and granulocyte-macrophage colony-stimulating factor in cell culture. Spine 1997; 22:2598–2602.
13. Nygaard ØP, Mellgren SI, Østerud B. The inflammatory properties of contained and noncontained lumbar disc herniation. Spine 1997; 22:2484–2488.
14. Olmarker K, Larsson K. Tumor necrosis factor alpha and nucleus-pulposus-induced nerve root injury. Spine 1998; 23:2538–2544.
15. Henrotin YE, DeGroote DD, Labasse AH, Gaspar SE, Zheng SX, Geenen VG, Reginster JY. Effects of exogenous IL-1 beta, TNF alpha, IL-6, IL-8 and LIF on cytokine production by human articular chondrocytes. Osteoarthritis Cartilage 1996; 4:163–173.
16. Pulsatelli L, Dolzani P, Piancentini A, Silvestri T, Ruggeri R, Gualtieri G, Meliconi R, Facchini A. Chemokine production by human chondrocytes. J. Rheumatol 1999; 26:1992–2001.
17. Tetlow LC, Adlam DJ, Woolley DE. Matrix metalloproteinase and proinflammatory cytokine production by chondrocytes of human osteoarthritic cartilage. Associations with degenerative changes. Arthritis Rheum 2001; 44:585–594.
18. Burke JG, Watson RWG, McCormack D, Dowling FE, Walsh MG, Fitzpatrick JM. Intervertebral discs which cause low back pain secrete high levels of proinflammatory mediators. J. Bone Joint Surg 2002; 84B:196–201.
19. Kikuchi T, Nakamura T, Ikeda T, Ogata H, Takagi K. Monocyte chemoattractant protein-1 in the intervertebral disc. A histologic experimental model. Spine 1998; 23:1091–1099.
20. Haro H, Shinomiya K, Komori H, Okawa A, Saito I, Miyasaka N. Upregulated expression of chemokines in herniated nucleus pulposus resorption. Spine 1996; 21:1647–1652.
21. Haro H, Komori H, Okagawa A, Murakami S, Muneta T, Shinomiya K. Sequential dynamics of monocyte chemotactic protein-1 expression in herniated nucleus pulposus resorption. J. Orthop. Res 1997; 15:734–741.
22. Fujita K, Nakagawa T, Hirabayashi K, Nagai Y. Neutral proteinases in human intervertebral disc. Role in degeneration and probable origin. Spine 1993; 18:1766–1773.

23. Tanabe BK, Abe LM, Kimura LH, Reinker KA, Yamaga KM. Cytokine mRNA repertoire of articular chondrocytes from arthritic patients, infants, and neonatal mice. Rheumatol. Int 1996; 16:67–76.
24. Shinmei M, Masuda K, Kikuchi T, Shinomura Y, Okada Y. Production of cytokines by chondrocytes and its role in proteoglycan degradation. J. Rheumatol 1991; 18(27 suppl):89–91.
25. Stadler J, Stefanovic-Racic M, Billiar TR. Articular chondrocytes synthesize nitric oxide in response to cytokines and lipopolysaccharide. J. Immunol 1991; 147:3915–3920.
26. Nietfeld JJ, Wilbrink B, Helle M. Interleukin-1 induced interleukin-6 is required for the inhibition of proteoglycan synthesis by interleukin-1 in human cartilage. Arthritis Rheum 1990; 33:1695–1701.
27. Moore RJ, Vernon-Roberts B, Fraser RD, Osti OL, Schembri M. The origin and fate of herniated lumbar intervertebral disc tissue. Spine 1996; 21:2149–2155.
28. Kanerva A, Kommonen B, Grönblad M, Tolonen J, Habtemariam A, Virri J, Karaharju E. Inflammatory cells in experimental intervertebral disc injury. Spine 1997; 22:2711–2715.
29. Virri J, Grönblad M, Seitsalo S, Habtemariam A, Kääpä E, Karaharju E. Comparison of the prevalence of inflammatory cells in subtypes of disc herniations and associations with straight leg raising. Spine 2001; 26:2311–2315.
30. Kokubun S, Sakurai M, Tanaka Y. Cartilaginous endplate in cervical disc herniation. Spine 1996; 21:190–195.
31. Kawakami M, Tamaki T, Hayashi N, Hashizume H, Nishi H. Possible mechanism of painful radiculopathy in lumbar disc herniation. Clin. Orthop 1998; 351:241–251.
32. Kawakami M, Tamaki T, Matsumoto T, Kuribayashi K, Takenaka T, Shinozaki M. Role of leukocytes in radicular pain secondary to herniated nucleus pulposus. Clin. Orthop 2000; 376:268–277.
33. Rand NS, Dawson JM, Juliao SF, Spengler DM, Floman Y. In vivo macrophage recruitment by murine intervertebral disc cells. J. Spinal Disord 2001; 14:339–342.

17

Advances in Bone Graft Substitutes in Spinal Fusion

Michael N. Tzermiadianos, Alexander G. Hadjipavlou, and John N. Gaitanis
University of Kriti Medical School
Iraklio Kriti, Greece

Bone grafting is essential for reconstruction of spinal defects and a prerequisite to obtaining solid arthrodesis imperative to spinal stability after reconstructive surgery [1]. Spinal fusion is commonly achieved by the adjunctive use of interbody or onlay cortical bone grafts (autograft or allograft). Success depends on factors such as the patient's age, sufficiency of local blood supply, degrees of postoperative movement, and, importantly, the physical and biological characteristics of the graft matrix.

Early attempts at bone grafting date back more than 500 years to the Arab, indigenous Peruvian, and Aztec cultures. In modern times, the first documented case of autogenous bone grafting was reported by Merem in 1810, and the first successful allografting case has been attributed to Macewn in 1881 [2].

Our present knowledge and scientific base for understanding the biology, banking, and widespread clinical applications of bone grafting is largely due to the work of Albee [3], Barth [4], Lexter [5], Phemister [6], and Seen [7] during the late nineteenth and early twentieth centuries. These substantive scientific contributions have made bone grafting techniques common and relatively effective clinical procedures.

There are three biological processes that impact the success or failure of bone graft: osteogenesis, osteoconduction, and osteoinduction [8].

Osteogenesis refers to the process whereby bone forms directly from living cells, such as the stem cells within autogenous bone. Osteoconduction describes the process in which bone grows into and along the surface of a biocompatible structure when placed in direct apposition to host bone through the process of intramembranous bone formation. The ability to osteoconduct is a passive characteristic of bone that allows it to act as a platform on which vascular invasion, resorption, and new bone formation can occur [1]. Osteoinduction is endochondral bone growth stimulated by specific growth factors (morphogens and/or mitogens) on pluripotential cells, such as mesenchymal stromal or stem cells. In particular, bone morphogenic proteins (BMPs), identified through the seminal work of Urist and colleagues [9], has demonstrated the capacity for inducing the differentiation of host perivascular mesenchymal cells into cartilage and bone [10].

In varying degrees, bone grafting source materials and techniques use these mechanisms of bioincorporation. Thus, the ideal bone graft should be capable of these processes and also

be free of immunological antigens and microbial pathogens. There are a variety of bone grafts to choose from, each presenting a unique set of advantages and disadvantages.

Autografts, because they are harvested from host bone stock from one body site for transfer to another location in the same individual, offer the maximum biological potential and histocompatibility. Immunological considerations and disease transmission are obviated through the use of autogenous bone.

The possibilities of meeting the needs of size, shape, and quantity of bone for any given procedure, however, are limited in autografting. The potential for morbidity by harvesting autologous iliac bone graft is ever- present [11] and can be caused by nerve injuries [12,15], vascular injuries [16,17], hernia through the iliac bone donor site [18,19], bowel obstructions [20], and other noteworthy drawbacks. Furthermore, harvesting fibular graft is related to a sense of instability or weakness in the lower extremity [21]. Operating room time is extended, as is the period during which the patient must remain under anesthesia. Any complications arising from these events, especially if compounded by the sequelae of donor site morbidity, may also increase the duration of hospitalization. Moreover, such a procedure often renders the bone donor site unacceptable for a subsequent operation.

Despite these disadvantages, what makes the autograft the gold standard for bone grafting is that it fulfills the three requirements necessary for bioincorporation: it is osteogenic, osteoconductive, and osteoinductive.

Available autologous bone grafts include cancellous, vascularized or nonvascularized cortical, and autologous bone marrow grafts. Bone formation from autologous grafts is believed to occur in two phases. The first phase lasts approximately 4 weeks, during which bone formation is mainly contributed from the cells of the graft. Cells from the host begin to contribute to the process during the second phase [22,23].

Autologous cancellous bone is easily revascularized and rapidly incorporated, leading to a high success rate. It does not provide substantial structural support but is a good space filler. Because only the osteoblasts and endosteal lining cells on the surface of the graft survive the transplant, a cancellous graft acts mainly as an osteoconductive substrate [24–27].

Osteoinductive factors released from the graft may also contribute to bone formation, but this is only a theory based on circumstantial evidence and has not yet been substantiated by scientific documentation [22,28,29]. Cancellous graft achieves strength equivalent to that of a cortical graft after 6–12 months [30].

Autologous cortical grafts include the fibula, ribs, and iliac crest. These grafts can be vascularized or nonvascularized. Autologous cortical grafts are mostly osteoconductive and have little or no osteoinductive properties, but the surviving osteoblasts provide some osteogenic properties [31,32].

Cortical grafts also provide excellent structural support, but nonvascularized cortical grafts become weaker than vascularized ones during the initial 6 weeks after transplantation as a result of resorption and revascularization [31,33]. Vascularized cortical grafts incorporate rapidly, and their remodeling is similar to that of normal bone. They do not undergo resorption and revascularization, thus providing superior strength during the first 6 weeks [31]. However, little difference in strength between vascularized and nonvascularized cortical grafts is evident by 6–12 months [31].

Allografts, usually obtained from cadaveric sources or incidental to operative procedures, offer satisfactory biological potential and eliminate the chance of donor site morbidity. Allografts provide an abundant supply of bone tissue, but their use for spinal fusion has been disappointing, especially for onlay intertransverse bone grafts [34–36]. Their use in scoliosis surgery has been flawed, with poor results in the 1960s [37]. In a recent study in humans, allografts in the form of fresh-frozen human femoral head were found to be at least as effective as autologous bone

in instrumented posterolateral spinal fusion surgery when the results were assessed in terms of clinical outcome [38].

Allografts, including fibular allografts, tricortical ilium allografts, and femoral shaft cortical ''rings,'' have been successfully utilized for anterior interbody fusions [39–41]. Structural femoral ring allografts have proved effective in salvaging failed lumbar fusions with a reported fusion rate of 79–98% [39,42]. Femoral ring allografts with the medullary canal packed with cancellous autograft have been found almost as effective as tricortical iliac autografts (6% vs. 0% pseudarthrosis rate) in anterior fusions in revision surgeries for pseudarthrosis or flatback deformity. Although long-term cortical allograft resorption has been observed in femoral rings packed with cancellous allograft chips that had been used for anterior lumbar intervertebral fusion, the center of the graft usually achieves solid arthrodesis [37].

The use of allografts poses biohazards arising from their potential to act as conduits for disease transmission from donor to recipient and the triggering of immunological reactions. Thus, strict adherence to bone banking methodology and sterilization procedures are essential to proper handling of allografts [43].

Xenograft, or cross-species bone tissue, although in abundant supply, has been found to be a less reliable graft material than autogenous and allogeneic bone. The emergence of such concerns as major histocompatibility difference leading to immune response provocation, the incompatibility of other species' anatomies with human anatomical parts, lessened biological activity, and the need for rigorous, meticulous processing and sterilization of bone derived from nonhuman species have largely reduced the opportunities for effective orthopedic reconstructive use of xenograft bone.

Bone cages have demonstrated great promise for spinal fusion, but they still require a substantial amount of bone graft material, especially for multiple-level fusion. It is therefore likely that the use of bone cages does not diminish the potential for serious complications associated with harvesting autologous iliac bone graft. For these reasons, researchers have directed their attention to the search for suitable substitutes for autograft and allograft bone. The endeavor to transcend the numerous drawbacks associated with natural sources of bone tissue has given rise to the development and manufacture of bone substitutes in various osteoinductive and osteoconductive forms (Table 1) [1,44].

Osteoconductive agents are collagen, tricalcium phosphate ceramics (TCP), hydroxyapatites (Ht), coral-derived biomaterials, mineralized collagen matrix (Healos), some osteoactive polymers, and calcium sulfate (plaster of Paris; POP). Materials with osteoinductive properties contain one or more factors such as bone morphogenetic proteins (BMPs). Whereas numerous growth factors may be involved in new bone formation, including platelet-derived growth factor (PDGF), transforming growth factor-β (TGF-β), and vascular endothelial growth factor (VEGF), there is evidence that only the BMPs are capable of initiating the entire process of new bone

Table 1 Osteoconductive and Osteoinductive Bone Substitutes

Osteoconductive agents	Materials with osteoinductive properties
Hydroxyapatites (Ht)	Demineralized bone matrix
Coral-derived biomaterials	Bovine osteogenic factors
Tricalcium phosphate ceramics (TCP)	Bone morphogenic proteins 2–8
Mineralized collagen matrix (Healos)	Osteogenin (BMP-3)
Osteoactive polymers	OP-1 (BMP-7)
Calcium sulfate (POP)	OP-2 (BMP-8)

formation [45–49]. BMPs can be found as recombinant proteins produced by genetic engineering or as purified extracts from bone. Demineralized bone matrix is a source of such growth factors but in much lower quantities.

A bone graft substitute material can be used as either a graft extender, a graft enhancer, or a graft substitute. A graft extender is a material that allows the use of less autogenous bone graft with the same end result or one that allows a given amount of autogenous bone to be stretched over a greater area with the same success rate [50]. A bone graft enhancer, when added to autogenous bone graft, increases its successful healing rate. A bone graft substitute is a material that may be used entirely in place of autogenous bone graft to achieve the same or better fusion success rate [50].

There is considerable variation in the type and speed of healing because of biological and biomechanical differences between anterior and posterior columns. The anterior or middle column of the spine is composed primarily of cancellous bone under compression loading, whereas the posterior column consists mostly of cortical bone and is frequently under tension. As a result, the dosage and the ideal bone graft substitute may differ by location, and results of healing for bone graft substitutes or augmentation devices in one region of the spine cannot necessarily be extrapolated for other regions.

For anterior column applications such as intervertebral fusions, biologically compatible materials are most suitable when they provide geometric spaces that invite the ingrowth and osteogenic differentiation of primitive mesenchymal cells. The ''industry'' has exploited this knowledge by providing porous calcium phosphate ceramics [51–53] and orthopedic implants with porous metallic coatings, which are now widely employed in hip and knee replacement surgeries. Suitable ''biological space'' was also found in coelenterate coral skeletons. Once it was discovered how to chemically convert $CaCO_3$ to bone-like hydroxyapatite, this material was marketed as a bone ingrowth system under a number of trademarks (e.g., Interpore 200/400, proOsteon Implant 500). There is now a sizable outcome literature reporting successful use of replamineform coral implants in the canine mandible and tibial plateau [54], in rabbit tibia [55,56], as well as in various human long bones [57]. To date, there are reports that plate-stabilized blocks of coralline material produce new bone within cervical disc spaces [58]. Good results have been reported with implants made of porous hydroxyapatite used to achieve cervical interbody fusion in humans [59]. However, osseous integration, which is usually promoted by hydroxyapatite coating, failed to occur in artificial intervertebral disc in dogs [60]. Studies using HA ceramic spacers to maintain the laminar spread in open door cervical laminoplasty have also reported good clinical results [61].

Although purely osteoconductive substitutes may be suitable in the anterior spine when it is rigidly immobilized, they are less effective in posterolateral spine fusions. In studies assessing posterolateral fusion, hydroxyapatite block alone has not functioned effectively as a complete graft substitute [62]. Osteoinductive substitutes are more likely to be successful as either extenders, enhancers, or substitutes for posterolateral spine fusion [50].

When freeze-dried human bone allograft is demineralized, the allograft is osteoinductive, since it causes bone to form heterotopically [63]. Current use of demineralized, freeze-dried bone allografts is based on this ability [64,65]. Additionally, they provide a space-filling osteoconductive matrix, facilitating bone formation. The osteoinductive ability of demineralized bone is believed to be due to its content of BMPs, other growth factors and cytocines. These factors interact with mesenchymal stem cells or osteogenic precursors in the host tissue [66–68], causing them to differentiate into bone-forming cells. However, the concentration of BMPs in demineralized bone matrix (DBM) is not thought to be sufficient for it to be a complete substitute for autogenous bone graft.

Clinical reports indicate that preparations of this material vary with respect to bone formation [63]. Also, the osteoinductive ability of commercial demineralized, freeze-dried human bone graft, when implanted heterotopically in mouse, varies widely among tissue banks [69].

Differences in procurement and processing methods might play a role, but donor characteristics have the major contribution. Donor age is the most important variable with respect to osteoinductive ability and was inversely correlated with the ability of demineralized, freeze-dried human bone graft to induce bone [63,70]. This age-dependent loss of osteoinductivity is due to a loss of bioactive factors [71]. Only demineralized, freeze-dried bone graft from patients younger than 42 years of age was osteoinductive in a study on humans [63].

The successful isolation and purification of BMPs and the synthesis of recombinant human BMP (rhBMP) was a major step in overcoming the problems with availability of growth factors in demineralized allografts. The BMPs are differentiation factors, causing mesenchymal cells to differentiate into bone-forming cells. In contrast, factors such as PDGF TGF-β and are growth factors, causing cells to divide, thus expanding their numbers. Such growth factors may also be used to enhance bone graft, but combining BMPs with growth factors not only lacks synergistic effect, but the factors may antagonize one another's activity [72,73].

Successful clinical application of rhBMP depends upon the design of appropriate delivery systems. These carriers may not only act as controlled- release delivery systems, maintaining a critical threshold concentration of BMP at the site of implantation for the desired period, but also as osteoconductive materials, serving as a scaffold for the ingrowth of capillaries and osteoprogenitor cells from the recipient host bed [74]. Carriers also contains the BMP at the site of application to prevent extraneous bone. Commonly used carriers include collagen sponges, calcium phosphate ceramics, and degradable synthetic and natural polymers. Ideally, a carrier is a resorbable material with a resorption rate that generally matches the rate of bone formation. If the carrier resorbs before adequate osteodeposition, the result may be misdirected bone formation and pseudarthrosis. If the carrier resorbs too slowly, it might impede bone formation and remodeling [75].

The osteogenic protein-1 (OP-1) is such a combination of human rhBMP-7 in bovine bone-derived type 1 collagen. OP-1 has been demonstrated to be effective as a bone graft substitute when performing posterior lumbar interbody fusion (PLIF) in a sheep model [74]. The amount of bone formation by OP-1 was statistically higher than either autograft or hydroxyapatite in sheep interbody fusion [76]. OP-1 has also demonstrated an ability to induce successful posterolateral spinal fusion in dogs without a need for autogenous bone graft. In humans, OP-1 achieved better results than autograft in posterolateral fusions, in both fusion rates and clinical outcome, when used either alone or in combination with autograft. Preliminary results of similar studies revealed equal or greater bone formation with OP-1 compared with autograft [77]. However, the use of OP-1 did not induce sufficient early structural bone support after intracorporal application on spinal fractures [78].

Hydroxyapatite-tricalcium phosphate has been used as a carrier for rhBMP-2 with good results in a posterolateral spinal fussion model in rhesus monkeys [45]. Tissue engineering using specific scaffold materials to support tissue growth and provide proper osteoinductive agents might make an ideal bone graft substitute in the future. New delivery systems being evaluated include depot delivery systems, viral vector systems, conjugated osteogenic factor delivery systems, and oral small molecule targets [75].

Promising results in recent investigations indicate that gene therapy may have a potential application in spinal fusion. Enhancement of spine fusion by gene transfer in animal models is evidence of the rapid progress that has been made [79]. BMP genes have mainly been used for this purpose. The local production of BMPs using gene therapy may have several advantages over the direct delivery of the recombinant protein. Direct BMP delivery leads to relatively short-term bioavailability. Although it may be adequate for inducing osteogenesis, the physiolog-

ical affects of BMPs may not be maximized using these techniques. The use of BMP gene therapy has the potential to induce long-term, high-level BMP production at sites requiring bone formation. The quality of bone formed using BMP gene therapy may be improved over that achieved with the recombinant protein [80]. Because endochondral bone formation requires angiogenesis within the newly formed tissue, it is possible that the upregulation of VEGF may also improve the efficacy of BMP gene therapy [81].

Percutaneous delivery of the cellular or viral BMP vector, permitting the application of minimally invasive techniques for spinal fusion, may be possible in the future. The incorporation of stereotaxic techniques should make these approaches safe in the clinical setting. However, significant advances need to be made in vector design, gene-regulation techniques, and tissue targeting before human clinical trials can be safely and successfully conducted [81].

Plaster of Paris is an inexpensive and readily available bone grafting material that has proved to be well tolerated by human tissue in nonvertebral settings. POP-filled defects in bone are gradually vascularized and replaced by bone tissue derived from the host [82–86]. To assess the effectiveness and safety of POP in spinal fusion and to compare it to autografts and other graft substances, we conducted three sets of experiments.

In the first set, 20 adult female sheep (30–40 kg body wt) were subjected to L1-L2, L3-L4, and L5-L6 discectomies. The intervertebral discs were excised, and the cartilaginous and bony endplates were cut away to expose the subchondral bone. Each space was then implanted with a 1.0 × 1.5 cm long tubular titanium cage, which had been filled with one of a variety of grafting materials (Table 2) or left empty as a control implant. Implant filling strategy was randomized.

At the time of sacrifice, 4 months postoperatively, host-derived trabecular bone had invested each interbody cage (Fig. 1). All individual segments, including a single interbody graft, were biomechanicaly tested to establish rotational stability and tensile load to failure. The tissues were recovered and sectioned. Sections of the recovered tissues were then microradiographed, and the total area of trabecular bone formed within each cage was quantitated by computer-driven software. Data were expressed in terms of percent trabecular bone volume.

The microradiographic analysis indicated that the different grafts and combinations of tissue types had produced volumes of new bone that were neither significantly different inter alia nor different from the outcome of the empty control implants. All bone present appeared to be of uniform and equal density on microradiographic investigation. Biomechanically, however, the behavior of the control fusion masses was inferior to that of the fusion masses formed under the influence of osteoconductive bony and apatitic substrates. The applied torque of ±2.5 Nm, which was insufficient to break the bony trabeculae, permitted a 1–2° displacement in the experimental groups versus a 3–4° displacement in the trabecular masses formed around the control cages. The POP grafts permitted, quantitatively at least, the smallest angular displacement, but no statistical difference occurred. The ‘‘pull-out’’ tensile test also affirmed that POP

Table 2 Cage-Filling Materials

1. Autogenous iliac crest cancellous bone (Auto)	
2. Frozen allogeneic cancellous iliac crest (Allo)	
3. Plaster of Paris (POP)	
4. Coralline hydroxyapatite (pro-Osteon 500)	
5. Demineralized bone (DBM)	
6. POP + Auto	(admixture 1 : 1)
7. pro-Osteon 500 + Auto	(admixture 1 : 1)
8. DBM + Auto	(admixture 1 : 1)
9. Empty control	

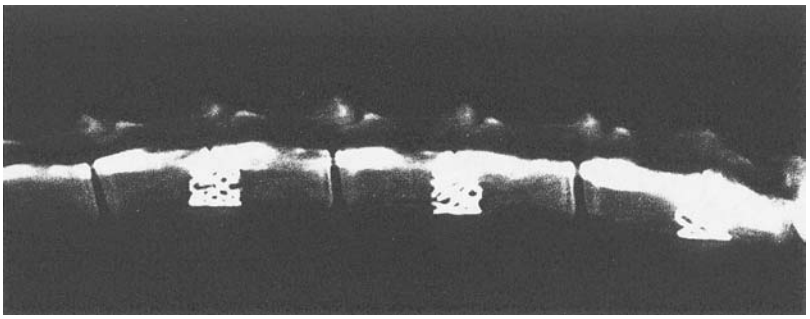

Figure 1 Roentgenograph showing the positioning of titanium cages within excavated disc spaces in the lumbar spine of a sheep 4 months postoperatively. The roentgenograph shows the interbody fusion masses within and around the titanium cages. (From Ref. 89c.)

and most of the other osteoconductive experimental graft types, alone or in combination with autologous bone, performed optimally, and that their fusion masses were biomechanically superior to those formed around the control (empty) cages. The tensile failure load of the sheep demineralized osteoinductive bone was equal to that of the control titanium cages that were implanted empty (Fig. 2). So, despite contrary expectations, the osteoinductive demineralized sheep bone preparations proved the least effective of the different substrates in achieving a solid interbody fusion. The addition of autogenous bone did little to improve DBM performance. The advanced age of the donor animals could have been a factor in its poor performance, since production of bone morphogenetic proteins declines with increasing maturity [87]. Yet it may be that mature sheep are poor BMP responders [70,88].

In that experiment, the small cages in intervertebral disc space provoked an exuberant bone reaction from the host tissues, thus compromising the results of bone graft testing. The mechanisms responsible for the new bone formation that enveloped the titanium-carrier mesh are likely to involve vascular ingrowth from the marrow of the vertebral bodies, with the intercession of the vertebral periosteum and psoas muscle pericytes (osteoprogenitor cells).

In order to prevent reactive exuberant bone formation when testing intervertebral bone cages in sheep, a large bone defect was required.

To address these concerns, a second set of experiments with two series of 15 sheep each was conducted. In a first series, the sheep were subjected to lumbar spine fusion after L4 corpectomy. The body of L4 was osteotomized with preservation of the pedicles and the more posterior components. The subchondral bone at L3 and L5 was removed to prepare a vascular bed into which a bridging titanium (Ti) cage (44 mm $\times$ 15 mm) was inserted to maintain the stability of the lumbar spine. Cages were implanted after they had been filled with either autologous iliac crest bone (five sheep) or POP (five sheep), or were left empty in a third group of five sheep.

At the time of sacrifice, 6 months postoperative, all cages appeared to be fully invested in bone (Fig. 3). Microradiography showed that identical volumes of bone were formed within the autograft and POP cages, but bone within the chambers that had been implanted empty was too little to permit quantitative morphometric evaluation. Furthermore, the quality of bone formed under the influence of POP and autogenous iliac crest graft was equal in terms of stiffness and strength at failure when tested in torsion.

To evaluate the sources of the bone investing the cages, the Ti implants were used in a somewhat different experimental setting, femoral segmental osteotomy, in which tissue geometry

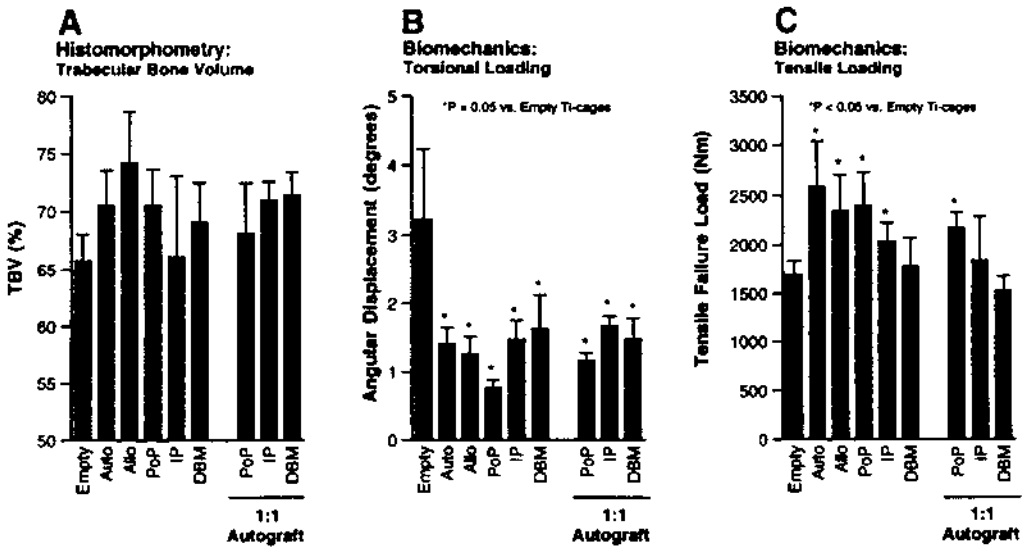

Figure 2 Graphs showing the quantitative histomorphometric and biomechanical evaluations of the bone formed under the influence of osteoconductive and osteoinductive substrates implanted within excavated lumbar spine spaces. (A) Histomorphometry; (B) biomechanics—angular displacements between -2.5 and $+2.5$ N m loads, (C) biomechanics—tensile failure load. Implants of empty titanium cages served as the control group. Data represented by bars marked with an asterisk (*) were statistically different from the empty control data at the $p < 0.05$ level of significance. *Auto*, autograft; *Allo*, frozen allografts; *PoP*, plaster of Paris; *IP*, replamineform coralline substrate; *BDM*, demineralized allogeneic sheep bone. (From Ref. 89c.)

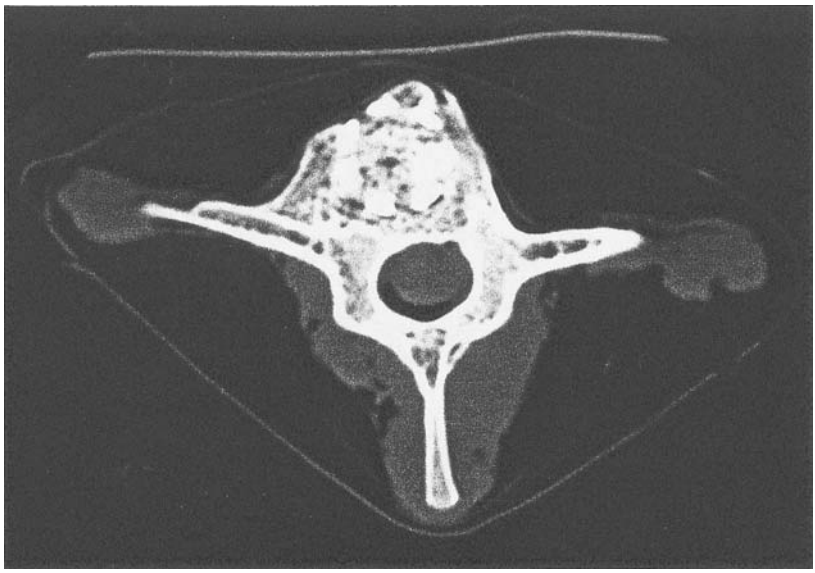

Figure 3 Computed Tomography scan of the L4 replacement titantium cage, showing fusion masses within and around the cage. (From Ref. 89b.)

improves the chance of isolating the contributions of cells made by investing soft tissues from those supplied by the marrow.

An 1 inch (2.5 cm) segmental midshaft defect was created after cortex cut away. The defect was filled with cages and stabilized with a compression plate. The Ti cages were Implanted unfilled (five sheep) or preloaded with either autogenous bone marrow (five sheep) or POP (five sheep).

In order to prevent, or at least retard, the ingrowth of vessels from surrounding tissues, Ti cages were lined with an oversized sheet of Millipore with pore size of 0.45 mm. The protruding ends of the Millipore sleeve were fitted closely over the stumps of the periosteum-free femoral cortex.

At autopsy, 6 months postoperative, the Ti cages had gradually been incorporated into the diaphyseal marrow (Fig. 4). There were no differences in the total volume of bone formed around the cages. Although equally stiff when evaluated in tension, chambers implanted empty remained incompletely filled and were the weakest when tested in torsion. There were no differences in the quantity and mechanical properties of the trabecular bone formed within the chambers by autogenous bone and POP (Fig. 5, Fig. 6).

These studies suggested that POP had an osteoconductivity equal to that of autogenous iliac crest marrow/bone. Both POP autologous bone induced the production of significant new bone with normal histology within and around the Ti cages [89b,c].

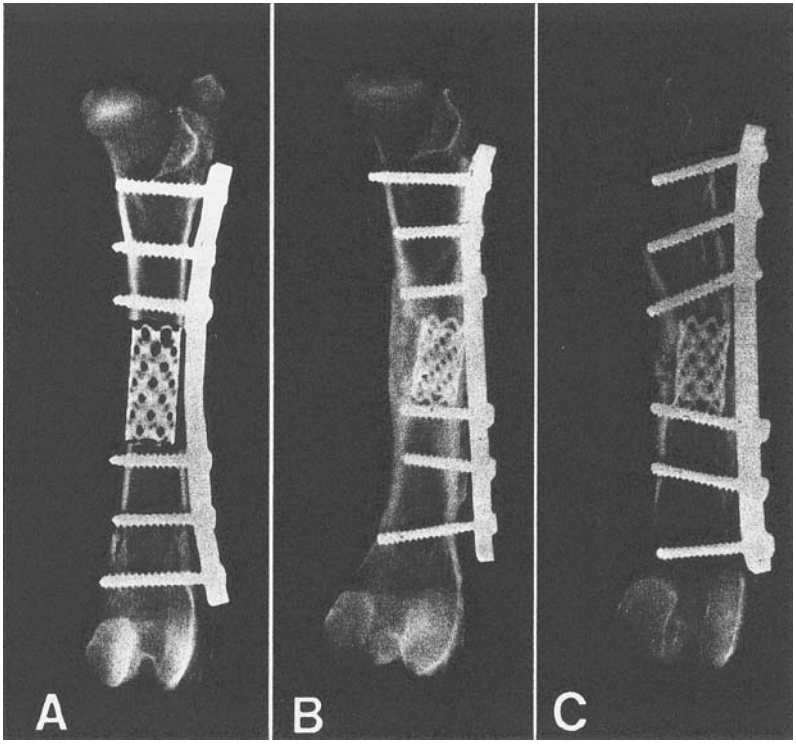

Figure 4 Roentgenographs showing postoperative appearances of a femoral midshaft titanium cage implant in a sheep: immediately after surgery (A), 6 months after iliac crest autograft procedure (B), and 6 months after POP implant (C). All graft sites were stabilized by lateral eight-hole compression plate. (From Ref. 89b.)

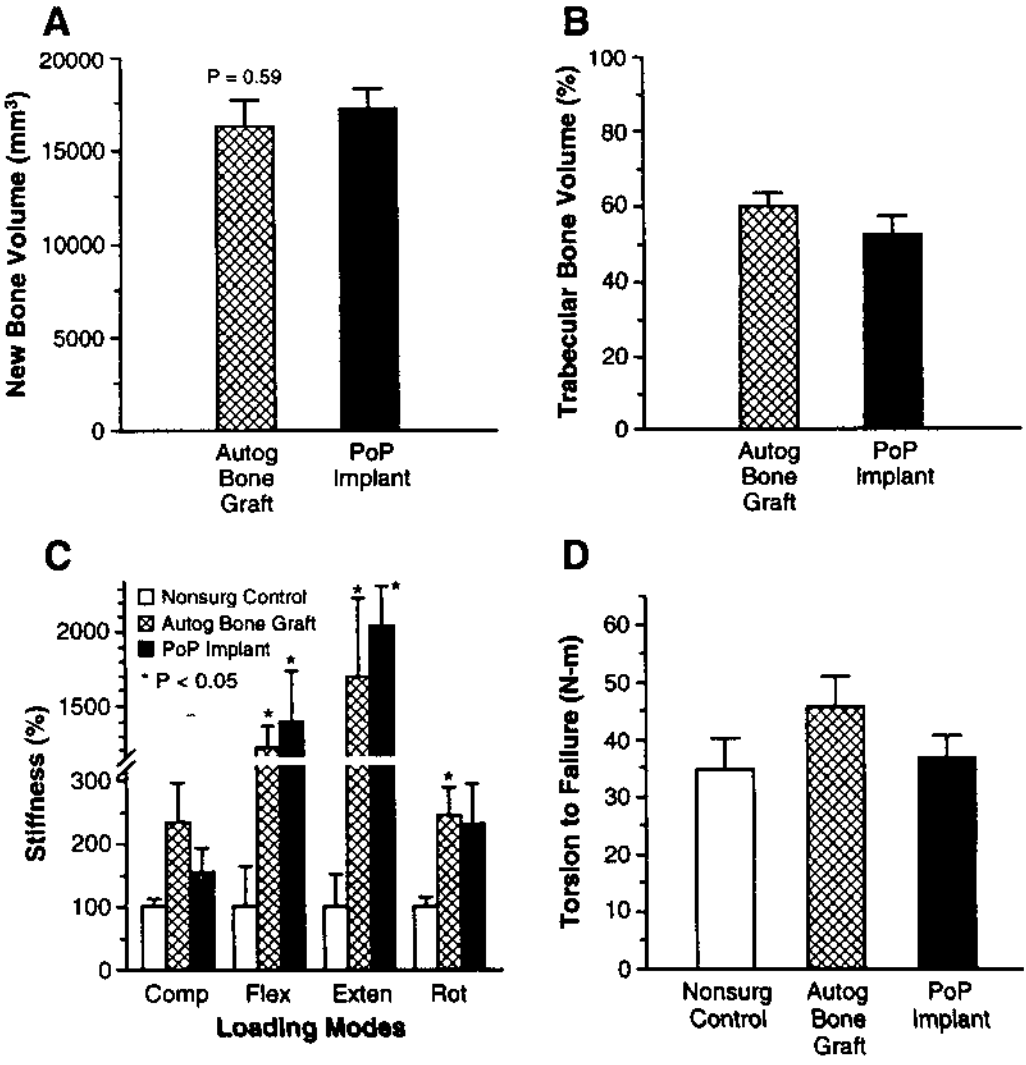

Figure 5 Histomorphometric and biomechanical measures of the stability of the postcorpectomy L4 lumbar interbody fusions in sheep 6 months after surgery. (A) Total volume of bone formed around and within the titanium cage; (B) trabecular bone volumes formed within the Ti cages; (C), flexural rigidity of fusion masses at 15° (Nm degrees); (D), tensile strength of the fusion masses (Nm). (From Ref. 89b.)

As shown by the experiments with femoral segmental osteotomy, we can conclude that bony core within the Ti cage largely derived from medullary osteoprogenitor elements, while bone that invested the Ti cages externally was the product of surrounding tissue cells. The millipore liner delimited the new bone that formed the central core within the Ti mesh from that which invested the cage externally. Significant displacement of the liner occurred only with the empty implants, whose crimping was caused by the more rapid formation of bone from the investing soft tissues. In those implants, the trabecular bone volumes attributable to a marrow stromal source were the lowest (Fig. 7). The original conformation of the Ti Millipore contact was well maintained, as showed by microradiography, in situations wherein osteoprogenitor

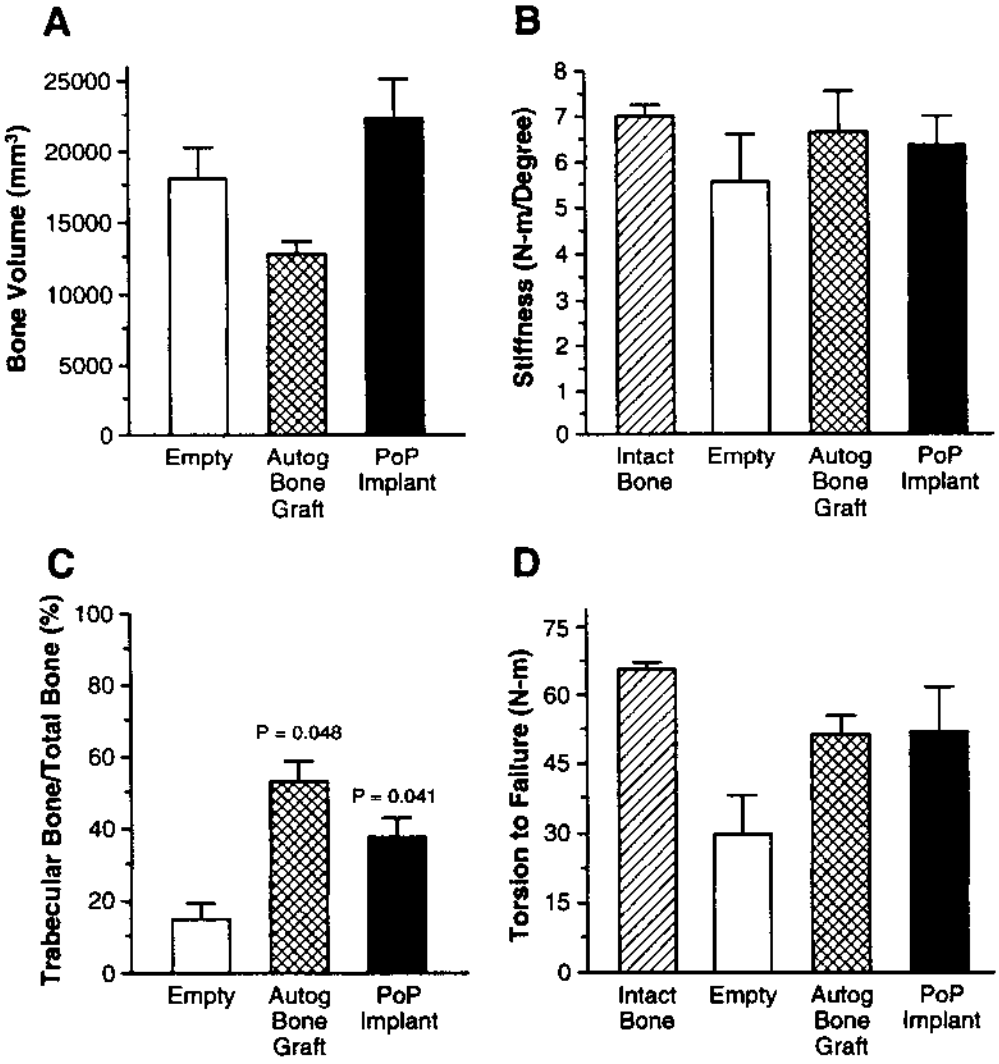

Figure 6 Histomorphometric and biomechanical measures of the stability of the midshaft femoral titanium cage implants. (A) Total volume of bone formed; (B) stiffness; (C) trabecular bone volumes formed within the Ti cages; (D) tensile strength of the fusion masses (Nm). (From Ref. 89b.)

cells were drawn from all sources. Accordingly, it seemed likely that the bony core had been derived largely from medullary osteoprogenitor elements, the stromal cells [89], whereas the bone that invested the Ti cage externally had been the product of periosteal osteoblasts and osteoprogenitor cells derived from muscle connective tissue elements [90].

The late results of plaster of Paris when used as a bone filler, to heal osseous defects, have been investigated. The early osteogenic effect on healing at the molecular level, however are not clear.

To study how implants of POP affect the time course during the first 3 months, we conducted a third set of experiments using a sheep lumbar vertebral defect model in 20 adult

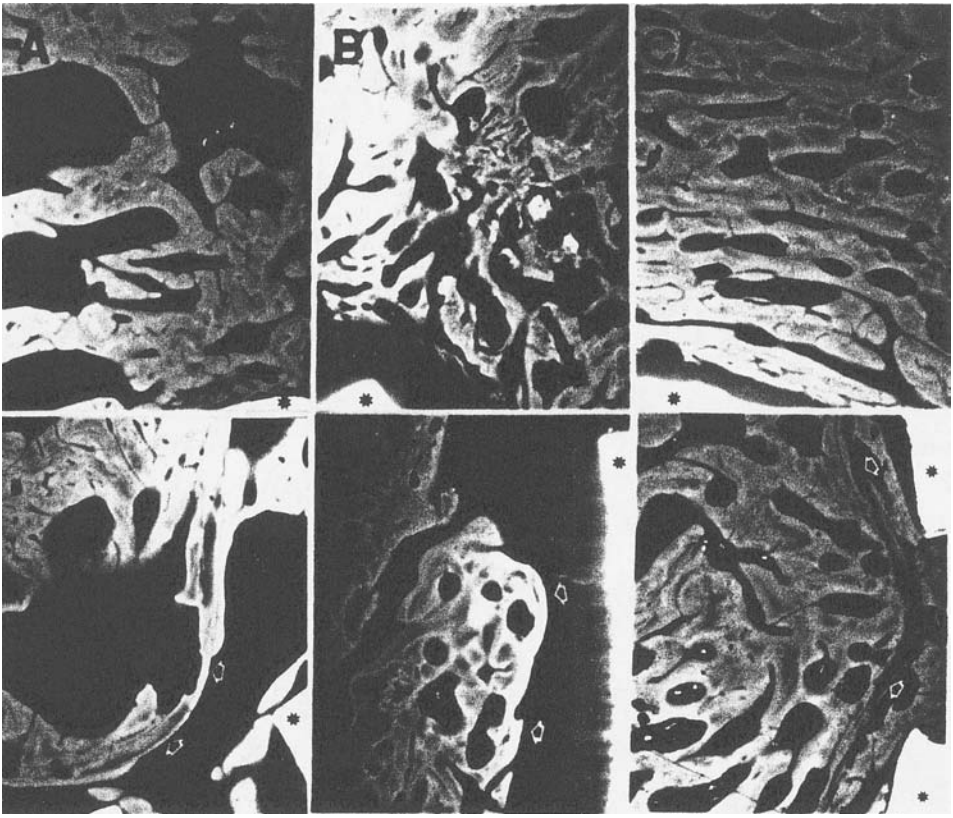

Figure 7 Microradiographs showing the relative amount and structure of the bone formed external to (*top*) and within (*bottom*) the titanium cage midshaft femoral implants in sheep 6 months after surgery. (A) Control/empty; (B) autogenous bone/marrow; and (C) POP. (From Ref. 89b.)

female sheep. In 15 sheep, defects 5.0 mm in diameter and >10 mm in depth were created in a ventral-dorsal direction, equally spaced from L1 to L5 (one hole per vertebral body) with a microscopic ring saw. In five sheep, the defects were 10 mm in diameter and >10 mm in depth, leaving a hole volume of ~740 mm^3. The 5 mm defects were packed with either POP or autogenous cancellous bone and marrow cored from the defects. The same procedure was followed in sheep bearing 10 mm defects, but a certain number of defects were left unfilled as controls.

The animals that received 5 mm defects were sacrificed at intervals of 1, 2, and 3 months postoperatively, while animals bearing 10 mm defects were sacrificed at 3 months.

The volume of the new bone filling the defect spaces was determined using 3D reconstructions of transverse images of the vertebrae. Implants of autogenous bone and POP afforded an equal stimulus to repair. In those cases ~96% of the original bone mass was restored after 3 months, while the defect left empty contained only half as much new bone (Fig. 8).

Histological sections were also analyzed to determine the percentage of the defect space occupied by mineralized bone and osteoid, the percentage of mineralized surface invested in osteoid, and the percentage of available trabecular surface covered by osteoblasts as well as the percentage of bone surface that had been eroded as index to remodeling. Tissue and cellular

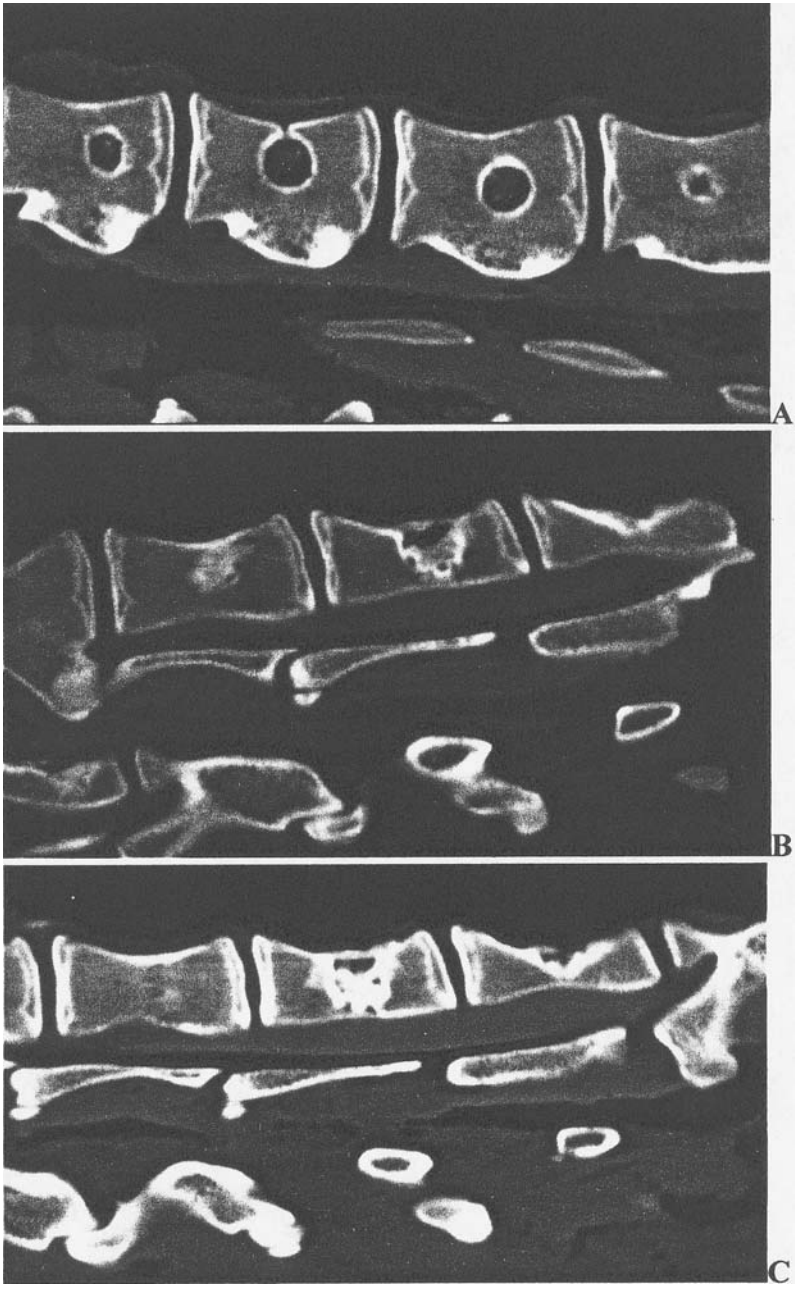

Figure 8 Computed tomography of lumbar spines with 10 mm defects at three months. (A) Defects initially left empty remained poorly filled. The implants of (B) autogenous bone and (C) POP showed a similar pattern of healing.

Table 3 Effects of Autogenous Bone Marrow Grafts and POP Implants on the Repair of Lumbar Yertebral Defects in Sheep

Defect size (mm)	Postop group	Treatment	*N*	Trabecular bone density (%)	Osteoblastic surface (% total)	Erroded bone surface (% total)
Baseline			1	30.07	3.27 (1)	22.27
5.0	1 month	Autograft	3	12.55 ± 3.20	16.62 ± 4.00	14.66 ± 3.81
		POP	3	20.67 ± 6.66	24.97 ± 4.51	20.64 ± 2.58
5.0	2 months	Autograft	3	29.91 ± 1.87	00.73 ± 0.63	08.03 ± 3.27
		POP	5	26.91 ± 2.75	05.81 ± 1.93	12.38 ± 2.31
5.0	3 months	Autograft	4	45.16 ± 7.32	1.71 ± 0.81	9.34 ± 2.49
		POP	6	39.70 ± 5.89	2.37 ± 1.26	7.85 ± 2.06
10.0	3 months	Empty	12	29.24 ± 3.86	16.31 ± 2.8	
		Autograft	4	46.47 ± 7.55	13.8 ± 4.09	
		POP	8	42.61 ± 6.30	12.93 ± 3.21	

Data expressed as the mean ± standard error of the mean (SEM).

profiles for the small 5.0 mm defects (Table 3) show that no matter nature of the graft, the trabecular bone volumes progressively increased with time from an average of ~17% at 1 month to ~42% at 3 months. However, POP improved repair processes at 2 months postop, increasing the remodeling as indicated by a 5-fold increase in fraction of trabecular bone surface involved in osteoblastic activity and 1.5-fold increase in bone surface involved in resorption (eroded bone surface).

The larger (10 mm) defects showed a similar pattern of healing. The implants of POP and autogenous bone were equally effective in promoting a 2-fold ingrowth of new bone with respect to defects left empty (Table 3). At 3 months the fractional cellular components involved in remodeling (osteoblasts and osteoclasts) and the levels of the osteoblasts activity (osteoid surface and bone mineralization rate) were similar (Table 4).

The principal finding from our studies was that POP has an osteoconductivity equal to that of autogenous iliac crest graft when used for filling bone cavities. This corroborated the findings of Peltier showing that the most important property of POP as a ''filler'' is its apparent natural rate of absorption—one that was equal to the rate at which new bone can grow into the

Table 4 Computer Analysis of Hematoxylin-Eosin Stained Slides Showing the Effects of Autograft and POP on Repair of Defects

Defect size (mm)	Postop group	Treatment	Osteoid surface (%)	No. osteoblasts/ unit trabecular perimeter	Bone minelalization rate (μm/day)	No. osteoclaststst/ unit trabecular perimeter
10.0	3 months	Control	35.31 + 6.63	11.40 ± 2.11	0.375 ± 0.034	0.53 ± 0.14
		Autograft	31.83 + 8.05	9.42 ± 2.90	0.415 ± 0.091	1.25 ± 0.87
		POP	29.04 + 7.31	9.22 ± 2.31	0.377 ± 0.021	0.99 ± 0.54

Data expressed as the mean + standard error of the mean. Bone mineralization rate was measured after labeling with tetracycline on the 20th and again on the 10th day prior to sacrifice.

defect [85]. This permits POP to provide structural support and prevent fibrous tissue ingrowth, while facilitating creeping substitution.

For promoting intertransverse posterior spinal fusion, POP should be used in combination with other grafts as graft enhancement material [91,92]. When used in combination with bone procured from the decompression sites, the results were equivalent to that of autogenous iliac bone crest bone for lumbar fusion [93]. POP is also a suitable vehicle through which osteoinductive materials may express optimal osteoactivity [94]. POP may also serve as an ideal carrier for osteoinductive agents as BMPs. Combination of POP with bovine osteogenic factors [95] or fibroblast growth factor (FGF) [96] can induce and increase the rate of bone formation.

Plaster of Paris can also be used as an effective carrier for local delivery of antibiotics. Antibiotic-loaded cylindrical pellets prepared from bone graft or demineralized bone matrix elute 70% and 45% of their antibiotic load by 24 hours, and negligible amounts are detected at 1 week. Plaster of Paris releases 17% of its load by 24 hours, with trace amounts detected at 3 weeks, while polymethylmethacyilate elutes 7% at 24 hours, with trace amounts detected for as long as 14 days [97]. Coating plaster of Paris pellets with a poly(lactide-co-glycolide) polymer decreases the burst effect of the elusion occurring on the first day and extends efficient release to more than 5 weeks [98].

REFERENCES

1. Friedlaender GE, Curting SL, Huo MH. Bone grafts and bone graft substitutes. In: Frymoyer JW, ed. The Adult Spine: Principles and Practices. 2nd ed.. Philadelphia: Lippincott-Raven, 1997:719–732.
2. Muscher GF, Lane JM. Clinical applications [of bone grafting] in orthopaedic surgery. In Habal MB, Reddi AH, eds. Bone Grafts and Bone Substitutes. Philadelphia: W.B. Saunders, 1992:375–407.
3. Albee FH. Fundamentals in bone transplantation: experience in three thousand bone graft operations. JAMA 1923; 81:1429–1432.
4. Barth A. Ueber histologische Befunde nach Knochenimplantationen. Arch. Klin 1893; 46:409–417.
5. Lexter E. Joint transplantation and arthroplasty. Surg Gynecol Obstet 1925; 40:782–809.
6. Phemister DB. The fate of transplanted bone and regenerative power of its various constituents. Surg Gynecol Obstet 1914; 19:303–333.
7. Seen N. On the healing of aseptic bone cavities by implantation of antiseptic bone. Am J Med Sci 1889; 98:219–243.
8. Burwell RG. The function of bone marrow in the incorporation of a bone graft. Clin. Orthop. Rel. Res 1985; 200:125–141.
9. Urist MR, Sato K, Brownell AG. Human bone morphogenetic protein (hBMP). Proc Soc Exper Biol Med 1983; 173:194–199.
10. Hsu K, Zucherman JF, White AH. Bone grafts and implants in spine surgery. In White AH, Rothman RH, Ray CD, eds. Lumbar spine Surgery: Techniques and Complications. Mosby: St. Louis, 1987: 434–458.
11. Younger EM, Chapman MW. Morbidity at bone graft donor sites. J. Orthop. Trauma 1989; 3:192–195.
12. Brown LT. The mechanics of the lumbosacral and sacro-iliac joints. J. Bone Joint Surg 1937; 19: 770–775.
13. Cocking J. Autologous bone grafting—complications at the donor site. J Bone Joint Surg Br 1971; 53:153.
14. Cooper JW. Cluneal nerve injury and chronic post surgical neuritis. J Bone Joint Surg 1967; 49:199.
15. Drury BJ. Clinical evaluation of back and leg pain due to irritation of the superior cluneal nerve. J Bone Joint Surg 1967; 49:199.
16. Escalas F, Dewald RL. Combined traumatic arteriovenous fistula and ureteral injury: a complication of iliac bone grafting, a case report. J. Bone Joint Surg 1977; 59:270–271.

17. Kahn B. Superior gluteal artery laceration: a complication of iliac bone graft surgery. Clin. Orthop 1979; 149:204.
18. Froimson AI, Gummings AG. Iliac hernia following hip arthrodesis. Clin. Orthop 1971; 30:89–91.
19. Lotem M, Maor P, Haimoff H, Woloch Y. Lumbar hernia at an iliac bone graft donor site: a case report. Clin. Orthop 1971; 80:130–132.
20. Challis JH, Lyttle JA, Stuart AE. Strangulated lumbar hernia and volvulus following removal of iliac crest bone graft. Acta. Orthop. Scand 1975; 46:230–233.
21. Tang CL, Mahoney JL, McKee MD, Richards RR, Waddell JP, Louie B. Donor site morbidity following vascularized fibular grafting. Microsurgery 1998; 18:383–386.
22. Axhausen W. The osteogenetic phases of regeneration of bone. A historical and experimental study. J. Bone Joint Surg. Am 1956; 38:593–600.
23. Axhausen W. Die Knochenregeneration—ein Zweiphasisches Geschehen. Zentralble Chir 1952; 77: 435–442.
24. Gray JC, Elves MW. Early osteogenesis in compact bone isografts: a quantitative study of contributions of the different graft cells. Calcif. Tissue Int 1979; 29:225–237.
25. Heslop BF, Zeiss IM, Nisbet NW. Studies on the transference of bone. I. A comparison of autologous and homologous bone implants with reference to osteocyte survival, osteogenesis and host reaction. Br. J. Exp. Pathol 1960; 41:269–287.
26. Burwell RG. Studies in the transplantation of bone. VII. The fresh composite homograft autograft of cancellous bone. An analysis of factors leading to osteogenesis in marrow transplants and in marrow-containing bone grafts. J. Bone Joint Surg. Br 1964; 46:110–140.
27. Williams R. Comparison of living autografts and homogeneous grafts of cancellous bone heterotopically placed in rabbits. Anat. Rec 1962; 143:93–105.
28. Vainio S. Observation on the regeneration of an autogenous transplant of the bone. Acta Chir. Scand 1950; 100:86–109.
29. Einhorn TA, Majeska RJ, Rush EB, Levine PM, Horowitz MC. The expression of cytokine activity by fracture callus. J. Bone Miner. Res 1995; 10:1272–1281.
30. Gazdag AR, Lane JM, Glaser D, Forster RA. Alternatives to autogenous bone graft: efficacy and indications. J Am Acad Orthop Surg 1995; 3:1–8.
31. Dell PC, Burchardt H, Glowczewskie FP. A roentgenographic, biomechanical, and histological evaluation of vascularized and non-vascularized segmental fibular canine autografts. J. Bone Joint Surg. Am 1985; 67:105–112.
32. Doi K, Tominaga S, Shibata T. Bone grafts with microvascular anastomosis of vascular pedicles: an experimental study in dogs. J. Bone Joint Surg Am 1977; 59:806–815.
33. Enneking WF, Burchardt H, Puhl JJ, Piotrowski G. Physical and biological aspects of repair in dog cortical-bone transplants. J. Bone Joint Surg. Am 1975; 57:237–252.
34. Hadjipavlou AG, Enker P, Dupuis P, Katzman S, Silver J. The causes of failure of lumbar transpedicular spinal instrumentation and fusion: a prospective study. Int. Orthop 1996; 20:35–42.
35. Heiple KG, Chase SW, Herndon CH. A comparative study of the healing process following different types of bone transplantation. J. Bone Joint Surg. Am 1963; 45:1593–1612.
36. Smith RT. The mechanism of graft rejection. Clin. Orthop 1972; 87:15–18.
37. Sarwat AM, O'Brien JP, Renton P, Sutcliffe JC. The use of allograft (and avoidance of autograft) in anterior lumbar interbody fusion: a critical analysis. Eur. Spine J 2001; 10:237–241.
38. Gibson S, McLeod I, Wardlaw D, Urbaniak S. Allograft versus autograft in instrumented posterolateral lumbar spinal fusion. A randomized control trial. Spine 2002; 27:1599–1603.
39. Buttermann GR, Glazer PA, Hu SS, Bradford DS. Revision of failed lumbar fusions. A comparison of anterior autograft and allograft. Spine 1997; 22(23):2748–2755.
40. Brown MD, Malinin TI, Davis PB. A roentgenographic evaluation of frozen allografts versus autografts in anterior cervical spine fusions. Clin. Orthop 1976; 119:231–236.
41. Kozak AJ, Heilman AE, O'Brien JP. Anterior lumbar fusion options: techniques and graft materials. Clin. Orthop 1994; 300:45–51.
42. Kumar A, Kozak JA, Doherty BJ, Dickson JH. Interspace distraction and graft subsidence after anterior lumbar fusion with femoral strut allograft. Spine 1993; 18:2393–3400.

43. Simmons JW. Bone banking. In White AH, Rothman RH, Ray CD, eds. Lumbar Spine Surgery: Techniques and Complications. Mosby: St Louis, 1987:459–470.
44. Burwell RG. The function of bone marrow in the incorporation of a bone graft. Clin. Orthop. Rel. Res 1985; 200:125–141.
45. Boden SD. Bioactive factors for bone tissue engineering. Clin. Orthop 1999; 367(suppl):84–94.
46. Boden SD. Clinical application of the BMPs. J. Bone Joint Surg. Am 2001; 83(suppl 1):161.
47. Boden SD, Schimandle JH. Biologic enhancement of spinal fusion. Spine 1995; 20:113–123.
48. Boden SD, Sumner DR. Biologic factors affecting spinal fusion and bone regeneration. Spine 1995; 20:102–112.
49. Ludwig SC, Boden SD. Osteoinductive bone graft substitutes for spinal fusion: a basic science summary. Orthop. Clin. North. Am 1999; 30:635–645.
50. Boden SD. Overview of the biology of lumbar spine fusion and principles for selecting a bone graft substitute. Spine 2002; 27:26–31.
51. Ducheyne P, Beight J, Cucler J, Evans B, Radin S. Effect of calcium phosphate coating characteristics on early bone operative bone ingrowth. Biomaterials 1990; 11:531–540.
52. Goshima J, Goldberg VM, Caplan AI. The origin of bone formed in composite grafts of porous calcium phosphate ceramic loaded with marrow cells. Clin Orthop 1991; 269:274–283.
53. Hong L, Hengshang X. Tensile strength of the interface between hydroxyapatite and bone. J. Biomed. Mater. Res 1992; 26:7–18.
54. Holms RE. Bone regeneration within a coralline hydroxyapatite implant. Plast. Reconstr. Surg 1979; 63:626–633.
55. Shimazaki K, Mooney V. Comparative study of porous hydroxyapatite and tricalcium phosphate as bone substitute. J. Orthop. Res 1985; 3:301–310.
56. Tencer AF, Woodard PL, Swenson J, Brown KL. Bone ingrowth into polymer coated synthetic coralline hydroxyapatite. J Orthop Res 1987; 5:275–282.
57. Holms RE, Mooney V, Bucholz RW, Tencer AF. A coralline replamineform hydroxyapatite implant for bone grafting. Clin. Orthop 1984; 188:282–292.
58. Thalgott JS, Fritts K, Giuffre JM, Timlin M. Anterior interbody fusion of the cervical spine With coralline hydroxyapatite. Spine 1999; 24:1295.
59. Kim P, Wakai S, Matsuo S, Moriyama T, Kirino T. Bisegmental cervical interbody fusion using hydroxyapatite implants: surgical results and long-term observation in 70 cases. J. Neurosurg 1998; 88:21–27.
60. Vuono-Hawkins M, Zimermman MC, Lee CK, Carter FM, Parsons JR, Langrana NA. Mechanical evaluation of canine intervertebral disk spacer: in situ and in vivo studies. J Orthop Res 1994; 12: 119–127.
61. Hirabayashi S, Kumano K. Contact of hydroxyapatite spacers with split spinous processes in double-door laminoplasty for cervical myelopathy. J. Orthop. Sci 1999; 4:264–268.
62. Totoribe K, Tajima N, Chosa E, Matsumoto M, Kataoka H, Koono M. Hydroxyapatite block for use in posterolateral lumbar fusion: a report of four cases. Clin. Orthop 2002; 399:146–151.
63. Lohmann CH, Andreacchio D, Köster G, Carnes DL, Cochran DL, Dean DD, Boyan BD, Schwartz Z. Tissue response and osteoinduction of human bone grafts in vivo. Arch. Orthop. Trauma. Surg 2001; 121:583–590.
64. Reddi AH, Huggins CB. Biochemical sequences in the transformation of normal fibroblasts in adolescent rats. Proc. Natl. Acad. Sci. USA 1972; 69:1601–1605.
65. Urist MR. Bone formation by autoinduction. Science 1965; 150:893–899.
66. Urist MR, Dawson E. Intertransverse process fusion with the aid of chemosterilized autolyzed antigen-extracted allogenic (AAA) bone. Clin. Orthop 1981; 165:97–113.
67. Urist MR. Bone morphogenetic protein, bone regeneration, heterotopic ossification and the bone-bone marrow consortium. In Peck WA, ed. Bone and Mineral Research. Amsterdam: Elsevier, 1989: 57–112.
68. Wozney JM, Rosen V, Celeste AJ, Mitsock LM, Whitters MJ, Kriz RW, Hewick RM, Wang EA. Novel regulators of bone formation: molecular clones and activities. Science 1988; 242:1528–1534.

69. Schwartz Z, Mellonig JT, Carnes DL, De La Fontaine J, Cochran DL, Dean DD, Boyan BD. Ability of commercial demineralized freeze-dried bone allograft to induce new bone formation. J. Periodontol 1996; 67:918–926.
70. Schwartz Z, Somers A, Mellonig JT, Carnes DL, Dean DD, Cochran DL, Boyan BD. Ability of commercial demineralised freeze-dried bone allograft to induce new bone formation is dependent on donor age but not gender. J. Periodontol 2001; 69:470–478.
71. Syftestad GT, Urist MR. Bone aging. Clin. Orthop 1982; 162:288–297.
72. Harris SE, Bonewald LF, Harris MA. Effects of transforming growth factor- on bone nodule formation and expression of bone morphogenetic protein 2, osteocalcin, osteopontin, alkaline phosphatase, and type I collagen mRNA in long-term cultures of fetal rat calvarial osteoblasts. J. Bone Miner. Res 1994; 9:855–863.
73. Marden LJ, Fan RS, Pierce GF. Platelet-derived growth factor inhibits bone regeneration induced by osteogenin, a bone morphogenetic protein, in rat craniotomy defects. J. Clin. Invest 1993; 92: 2897–2905.
74. Sampath TK, Rueger DC. Structure, function, and orthopedic applications of osteogenic protein-1 (OP-1). Complications Orthop 1994:101–107.
75. Seeherman H, Wozney J, Li R. Bone morphogenetic protein delivery systems. Spine 2002; 27:16–23.
76. Magin M, Delling G. Improved lumbar vertebral interbody fusion using rhOP-1. Spine 2001; 26: 469–478.
77. Vaccaro AR, Anderson DG, Toth CA. Recombinant human osteogenic protein-1 (bone morphogenetic protein-7) as an osteoinductive agent in spinal fusion. Spine 2002; 27:59–65.
78. Laursen M, Hoy K, Hansen ES, Gelineck J, Christensen FB, Bünger CE. Recombinant bone morphogenetic protein-7 as an intracorporal bone growth stimulator in unstable thoracolumbar burst fractures in humans: preliminary results. Eur. Spine J 1999; 8:485–490.
79. Nishida K, Gilbertson LG, Evans CH, Kang JD. Spine update. Potential applications of gene therapy to the treatment of spinal disorders. Spine 2000; 25(10):1308–1314.
80. Lieberman JR, Daluiski A, Stevenson S. The effect of regional gene therapy with bone morphogenetic protein-2-producing bone-marrow cells on the repair of segmental femoral defects in rats. J. Bone Joint Surg. (Am) 1999; 81:905–917.
81. Alden TD, Varady P, Kallmes DF, Jane JA, Helm GA. Bone morphogenetic protein gene therapy. Spine 2002; 27:87–93.
82. Edberg E. Some experiences of filling osseous cavities with plaster. Acta Chir Scand 1930; 67: 313–319.
83. Mackey D, Varlet A, Debeaumont D. Antibiotic loaded plaster of Paris pellets: an in vitro study of a possible method of local antibiotic therapy in bone infection. Clin. Orthop 1982; 167:263–268.
84. Nielsen A. Filling of sterile and infected bone cavities by means of plaster of Paris. Acta Chir. Scand 1944; 91:17–27.
85. Peltier LR. The use of plaster of paris to fill defects in bone. Clin. Orthop 1961; 21:1–31.
86. Peltier LR, Bickel EY, Lillo R, Thein MS. The use of plaster of Paris to fill defects in bone. Ann. Surg 1957; 146:61–69.
87. Bessho K, Izuka T. Changes in bone inducing activity of bone morphogenetic protein with aging. Ann. Chir. Gynaecol. Suppl 1993; 207:49–53.
88. Fleet JC, Cashman K, Cox K, Rosen V. The effects of aging on the bone inductive activity of recombinant human bone morphogenetic protein-2. Endocrinology 1996; 137:4606–4610.
89a. Yamaguchi A. Regulation of differentiation pathway of skeletal mesenchymal cells in cell lines by transforming growth factor-beta superfamily. J. Cell Biol 1995; 6:165–173.
89b. Hadjipavlou AG, Simmons JW, Yang J, Nicodemus CL, Esch O, Simmons DJ. Plaster of Paris as an Osteoconductive Material for Interbody Vertebral Fusion in Mature Sheep. Spine 2002; 25(1): 10–16.
89c. Hadjipavlou AG, Simmons JW, Tzermiadianos MN, Katonis PG, Simmons DJ. Plaster of Paris as bone substitute in spinal surgery. Eur Spine J 2001; 10:189–196.
90. Oni OO, Stafford H, Gregg PJ. An investigation of the contribution of the extraosseous tissues to the diaphyseal fracture callus using a rabbit tibial model. Injury 1992; 23:467–470.

91. Sato S, Koshino T, Saito T. Osteogenic response of rabbit tibia to hydroxyapatite particle-Plaster of Paris mixture. Biomaterials 1998; 20:1895–1900.
92. Al Ruhaimi KA. Effect of adding resorbable calcium sulfate to grafting materials on early bone regeneration in osseous defects in rabbits. Int. J. Oral Maxillofac. Implants 2000; 6:859–864.
93. Alexander DI, Manson NA, Mitchell MJ. Efficacy of calcium sulfate plus decompression bone in lumbar and lumbosacral spinal fusion: preliminary results in 40 patients. Can J Surg 2001; 44(4): 262–266.
94. Wilkins RM, Kelly CM, Giusti DE. Bioassayed demineralized bone matrix and calcium sulfate: use in bone-grafting procedures. Annal. Chir. Gynaecol 1999; 88(3):180.
95. Damien CJ, Parsons JR, Benedict JJ, Weisman DS. Investigation of a hydroxyapatite and calcium sulfate composite supplemented with an osteoinductive factor. J. Biomed. Mat. Res 1990; 24(6): 639–54.
96. Rosenblum SF, Frenkel S, Ricci JR. A. Diffusion of fibroblast growth factor from a plaster of Paris carrier. J. Appl. Biomater 1993; 4(1):67–72.
97. Miclau T, Dahners LE, Lindsey RW. In vitro pharmacokinetics of antibiotic release from locally implantable materials. J. Orthop. Res 1993; 11(5):627–632.
98. Benoit MA, Mousset B, Delloye C, Bouillet R, Gillard J. Antibiotic-loaded plaster of Paris implants coated with poly lactide-co-glycolide as a controlled release delivery system for the treatment of bone infections. Int. Orthop 1997; 21(6):403–408.

18

Titanium Mesh Cage in Spinal Reconstruction Surgery: Biomechanics and Clinical Application

Kazuhiro Hasegawa
Niigata Unifigversity Graduate School of Medical and Dental Sciences
Niigata, Japan

Toshiaki Hara
Niigata University
Niigata, Japan

I. INTRODUCTION

An ideal graft for lumbar interbody fusion should provide an osteogenic, immunologically equivalent matrix and immediate mechanical stability, while being technically easy to modify into an appropriate size and shape [1]. The stability of the graft site is the most important consideration during the immediate postoperative period. One obvious advantage of cortical bone is its stability, although one might hypothesize that the union rate associated with cortical bone is certainly less than that of cancellous bone. A titanium mesh cage has been developed as a substitute for bone graft. This cage provides interface compression strength that is superior to that of other graft materials, such as iliac crest, humerus, or rib [2]. The cage filled with cancellous bone has a significant advantage in bony union because it provides an adequate surface contact area to the vertebral endplate. It is technically easy to fill the defect resulting from surgery and provide immediate biomechanical support by using the cage [3,4].

Subsidence of the mesh cage into the vertebral body, however, may cause serious problems, such as collapse of the vertebral body, progression of kyphosis, or fusion failure. These problems may occur in an osteoporotic spine. Subsidence of the cage is generally brought about by loss of interface strength between the cage and the vertebral body. Since the contact area between the bone graft and the vertebral bone is predictive of graft stability [5], an end ring of the mesh cage system has been used to prevent the cage from sinking into the vertebra. Another predictive factor of the cage stability is the quality of the vertebral bone that is represented by bone mineral density (BMD), because BMD is an important determinant of vertebral strength [6–8]. However, a relationship between vertebral BMD and the interface strength of the cage, with or without an end ring system, has not been investigated.

In this chapter, we will clarify the effects of the size (diameter) of the cage and use of the end ring system on maximum load and stiffness of the cage/vertebral interface in compression loading and draw a relationship between vertebral BMD and the interface properties based on

our previous study [9]. We will also present clinical applications of the titanium mesh cage in cases of anterior column deficiency due to several pathologies.

II. BIOMECHANICS OF TITANIUM MESH CAGE: AN EXPERIMENTAL STUDY ON THE CAGE/VERTEBRAL INTERFACE PROPERTIES IN REFERENCE TO CAGE SIZE, END RING USE, AND VERTEBRAL BONE MINERAL DENSITY

A. Materials and Methods

Twenty-five lumbar vertebrae (16 L1 and 9 L5) were removed from 20 embalmed cadavers (8 male, 12 female; average age: 77.6 ± 6.8 years, 64–86 years, respectively). X-rays of all vertebrae showed them to be free of bony abnormalities. BMD of the whole vertebral body was measured by DXA (QDR-2000, Hologic, Inc., Waltham, MA) in a lateral position by placing the specimen in a water bath that was 15 cm deep [10]. Local BMD of subchondral cancellous bone, 5 mm below the endplate to which the mesh cage was compressed, was measured by pQCT (XCT 960, Stratec, Pforzheim, Germany) (Fig. 1). BMD measured by DXA is an apparent bone mineral density, while BMD measured by pQCT is a real volumetric density (mg/cm^3) obtained in 1 mm slice thickness. A bone area with a linear attenuation coefficient (LAC) lower than 0.5 was defined as cancellous bone. The threshold of BMD is used clinically to distinguish cancellous, subcortical, or cortical bone in human distal radius in vivo [11]. Each vertebra was separated, and the soft tissue was completely removed. The cartilaginous endplate was resected, preserving the bony endplate, and anteroposterior and lateral dimensions of each vertebra were measured with calipers. The area of the bony endplate was calculated by approximating the area as an ellipse.

The vertebrae were divided into four experimental groups according to the applied cage conditions:

L−: F25 mm, without internal end ring ($n = 6$)
S−: F19 mm, without internal end ring ($n = 6$)
L+: F25 mm, with internal end ring ($n = 8$)
S+: F19 mm, with internal end ring ($n = 5$)

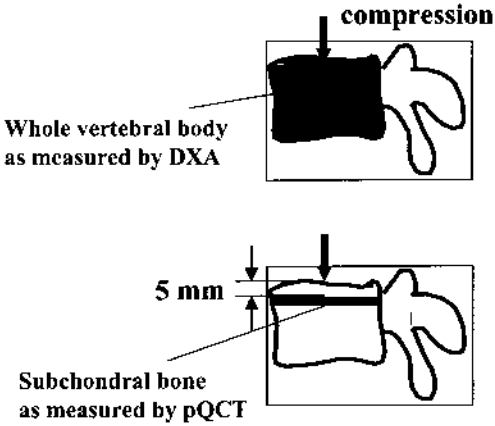

Figure 1 Bone mineral density measurement of whole vertebral body and subchondral bone.

The authors confirmed that there was no statistical difference between the whole vertebral BMD measured by DXA ($p = 0.915$, by one-way analysis of variance) and the endplate area ($p = 0.935$, by one-way analysis of variance) among the experimental groups.

B. Biomechanical Test

Each vertebra was set in a steel box using plaster with the endplate parallel to the horizontal plane. The box was set on an Instron-type testing machine (Shimadzu Autograph AGS-100A, Shimadzu Corp., Kyoto, Japan). A titanium mesh cage (PYRAMESH implant system, Medtronic Sofamor Danek, Inc., Memphis, TN) was compressed uniaxially onto the prepared superior end plate of the vertebra via a specially designed device with an interposing steel ball (Fig. 2). The titanium mesh cage is a cylinder made of a titanium fenestrated sheet and used as a vertebral spacer to support a defect of the spinal column (Fig. 3). There was no material packed inside the cage. The quasi-static compression load was applied with a crosshead speed of 0.5 mm/min, and the displacement of the upper steel plate relative to the steel box of the potted vertebra was recorded with a laser measurement system (Keyence laser feed monitor FC-2000, Keyence Corp., Osaka, Japan). Load-displacement data were collected with a personal computer (Versa 2535, Packard Bell NEC, Tokyo, Japan) via a data acquisition card (NR-110/150, Keyence Corp., Osaka, Japan).

In the load-deformation data, stiffness was defined as the slope of the elastic range and maximum load was defined as a peak load at which the compression load decreases for the first time. In the vertebrae compressed by a cage with an end ring (groups S+ and L+), the load-deformation curves were different from those of the vertebrae compressed by a cage without an end ring (groups S− and L−). The former showed a load-deformation curve with two peaks caused by encroachment of the cage spikes and an end ring (Fig. 4). Maximum load and stiffness were determined at the second peak of the load-deformation curve to represent the property between the vertebra and the end ring of the cage.

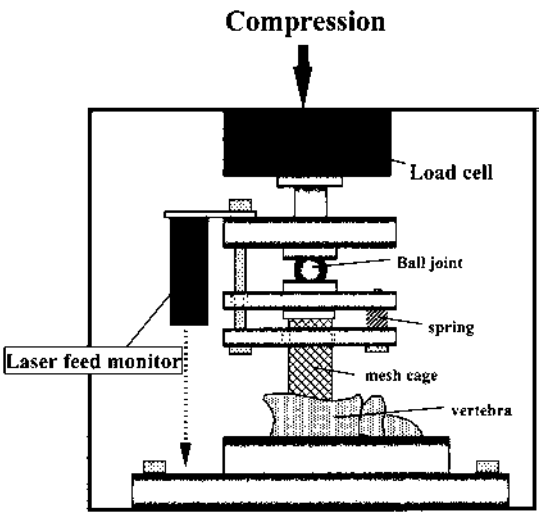

Figure 2 Experimental set-up. Each vertebra potted in a steel box is set on a testing machine. Uuniaxial compression loading onto the superior end plate is performed via a titanium mesh cage with a crosshead speed of 0.5 mm/min. The displacement of the upper steel box is recorded with laser measurement system.

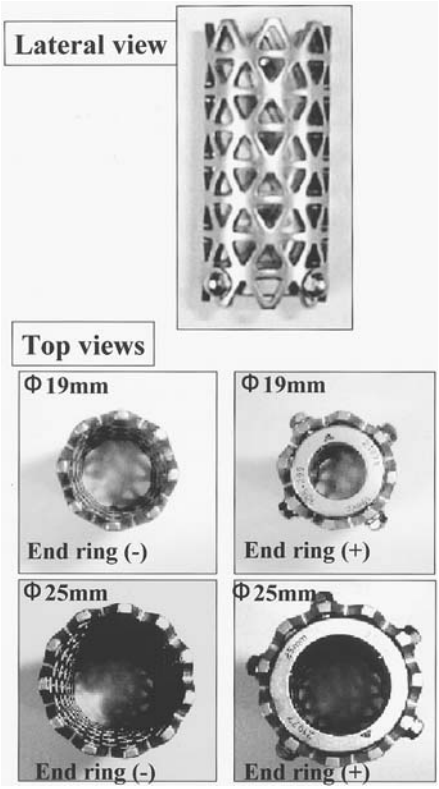

Figure 3 Titanium mesh cage (PYRAMESH Implant System). Mesh cages of 19 and 25 mm in diameter with or without an end ring system are shown.

Load-deformation data present macroscopic biomechanical phenomena of the interface between the mesh cage and the vertebra. The authors also used acoustic emission (AE) measurement to investigate microscopic failure characteristics of the interface. AE was measured during compression loading in 11 specimens by a resonance-type AE sensor of 140 kHz (AE-901S; NF Electronic Instruments, Yokohama, Japan) placed in the steel box with the vertebra. AE signals were measured by an AE measurement system (9501 AE tester; NF Electronic Instruments, Yokohama, Japan) and simultaneously recorded in load-deformation data. The details of the method were previously reported [10,12].

After mechanical testing, all vertebrae were dehydrated and embedded in methylmethacrylate. A 1 mm thick section was cut from the midsagittal plane of the vertebral body using a band saw (BS-3000; Exakt, Hamburg, Germany) (Fig. 5). Microradiographs were taken using a soft x-ray system (Softex-CMB, Nippon Softex Co., LTD., Tokyo, Japan) at a distance of 50 cm at 15 mA and 50 kV, and the failure patterns of the bony endplate and the trabecular bone beneath the cage were observed.

C. Statistical Analysis

Maximum load and stiffness were compared among the experimental groups using two-way analysis of variance (ANOVA) with a grouping factor of the size of the cage and the presence

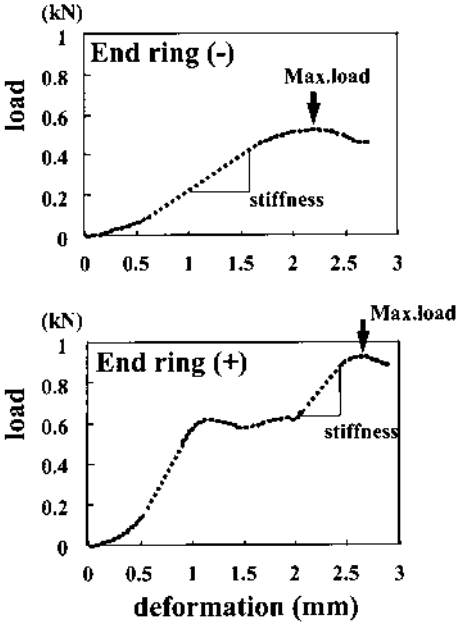

Figure 4 Representative load-deformation curves of the cage-vertebra complex without (top) or with (bottom) an end ring system.

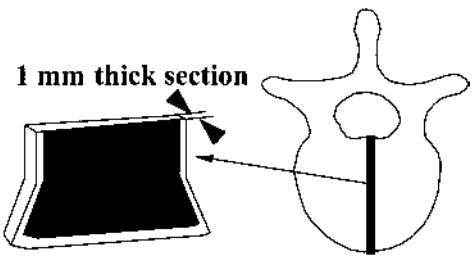

Figure 5 A 1 mm thick section for microradiography cut from mid-sagittal plane of the vertebra.

or absence of the end ring system, followed by Schèffe's analysis. Grouping factors were the cage size and the presence or absence of the end ring system. The Pearson correlation coefficient was calculated to examine the relationship between whole vertebral or subchondral cancellous BMD and mechanical parameters. StatView 4.11 (Abacus Concept, Berkeley, CA) was used for all statistical analyses.

D. Results

Vertebrae compressed with large cages (L− or L+) showed a greater maximum load than those compressed with smaller cages (S− or S+) ($p < 0.002$ by ANOVA followed by Schèffe's analysis). The end ring also contributed to the greater maximum load ($p < 0.005$ by ANOVA, followed by Schèffe's analysis) (Fig. 6). The size of the cage or the presence of the end ring,

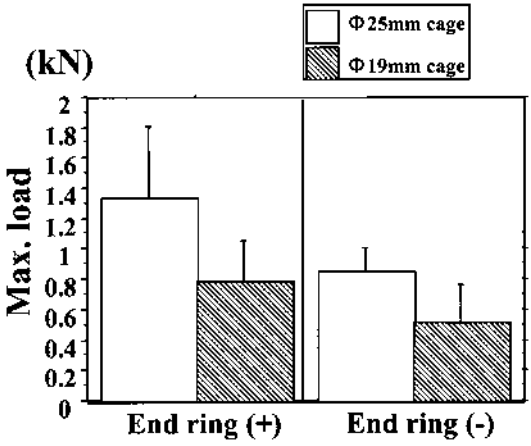

Figure 6 Results of maximum load. $p < 0.002$ on a factor of the cage size; $p < 0.005$ on a factor of the end ring augmentation

however, did not have any effect on stiffness ($p = 0.412$ for the size of the cage, $p = 0.395$ for the presence or absence of the internal end ring, by ANOVA) (Fig. 7). In an analysis of the pooled data, maximum load and stiffness were positively correlated with whole vertebral BMD as measured by DXA (Fig. 8A,B). The mechanical properties were also positively correlated with local cancellous BMD of subchondral bone as measured by pQCT (Fig. 8C,D). Correlation coefficient and *p*-value were more significant in the relationship of the mechanical properties and subchondral BMD as measured by pQCT than in the relationship of the parameters and whole vertebral BMD as measured by DXA.

A load-deformation curve with an AE event count rate for a cage-vertebra complex showed that significant AE signals were generated around maximum load in all 11 vertebrae. In vertebrae

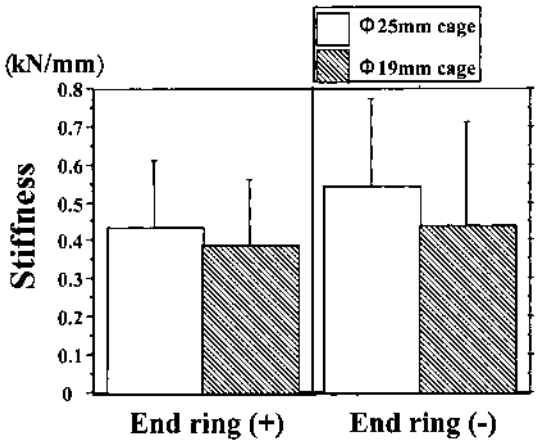

Figure 7 Results of stiffness. $p = 0.412$ on a factor of the cage size; $p = 0.395$ on a factor of the end ring augmentation.

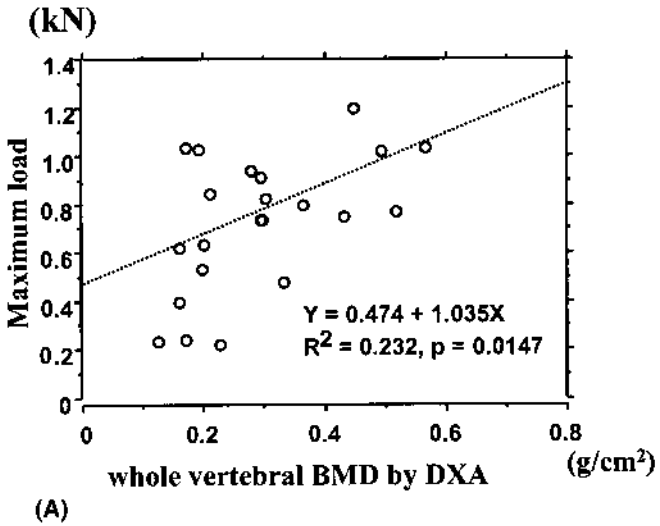

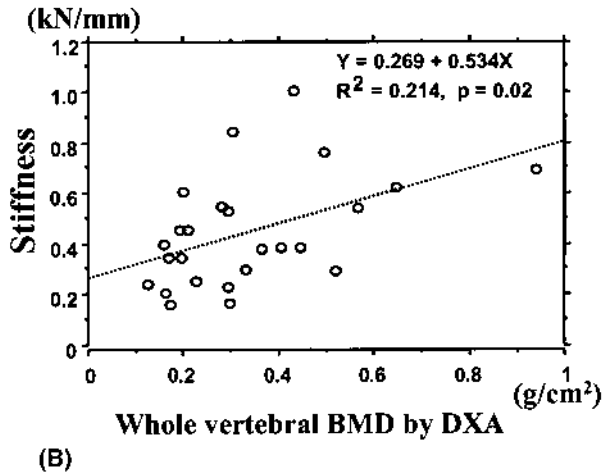

Figure 8 Relationships between mechanical properties and vertebral BMD: (A) maximum load vs. whole vertebral BMD measured by DXA; (B) stiffness vs. whole vertebral BMD measured by DXA; (C) maximum load vs. local subchondral BMD measured by pQCT; (D) stiffness vs. local subchondral BMD measured by pQCT.

compressed by the cage with the end ring (group S+, L+), however, significant AE signals were detected, even around the first peak of the load. The signals decreased after the first peak and increased again around the second peak (Fig. 9). The authors observed that there were significant AE signals around the first peak of the load-deformation curve during encroachment of the cage spikes into the endplate, leading to a decrease in stiffness at the interface.

On microradiography, most vertebrae compressed by the cage without the end ring showed encroachment of the cage spikes into the endplate or trabecular structure. On the other hand, those compressed by the cage with the end ring showed wider depressions of the endplates and

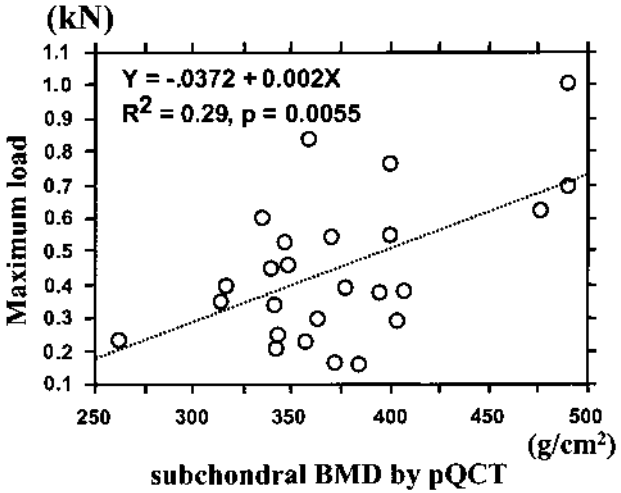

(C)

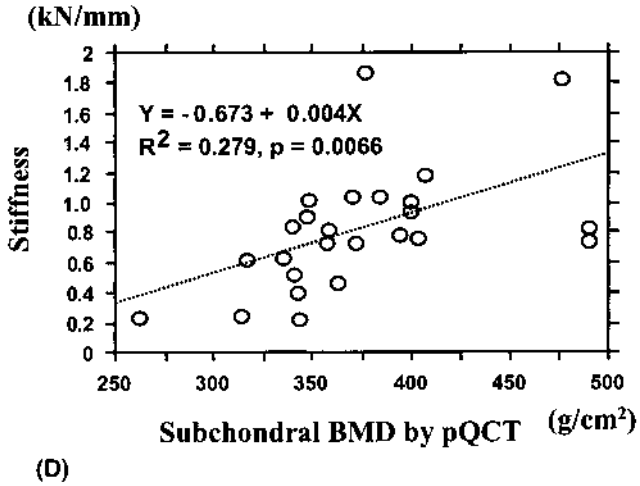

(D)

Figure 8 Continued.

trabeculae. In all vertebrae, however, most central portions of the vertebral structures were preserved (Fig. 10). Slices of four L5 vertebrae (16% of all vertebrae; one in group L−, two in group S−, and one in group S+) did not reveal any fractures.

III. CLINICAL APPLICATIONS OF THE TITANIUM MESH CAGE

Case 1

A 63-year-old man experienced progressive numbness of the right lower extremity and urinary disturbance of 14 months duration without any causative episode. The symptoms were aggravated

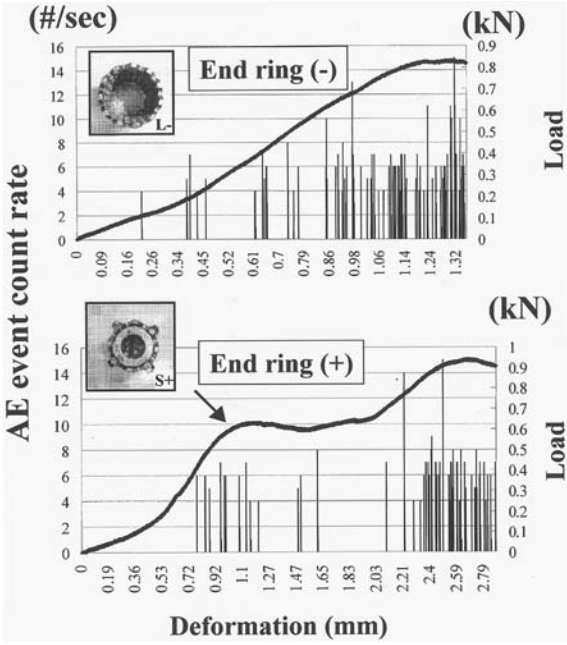

Figure 9 Load-deformation curve with an AE event count rate.

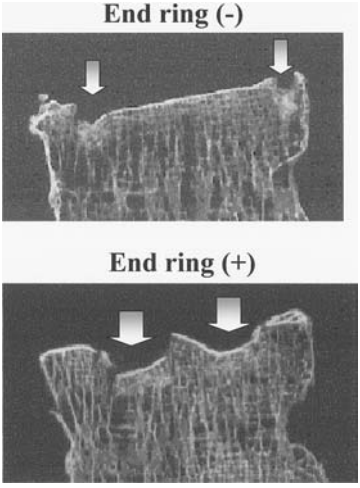

Figure 10 Representative microradiograms of mid-sagittal vertebral sections after load to failure (group L −), (A) or the internal end ring (group S +), (B). The cage spikes encroach into the vertebral end plate and trabeculae (arrows), preserving structures of most of the central portion of the vertebrae. Vertebra compressed by a cage with an internal end ring shows wider depression of the end plate (B) than those compressed by a cage without an end ring.

by walking. Lumbar radiographs revealed multilevel osteoarthritic changes without any osteoporotic finding. Magnetic resonance imaging (MRI) of the thoracolumbar region demonstrated canal stenosis due to hypertrophic posterior longitudinal ligament at the levels of T12 to L2 (Fig. 11A).

Anterior decompression and reconstruction using a titanium mesh cage (Titanium Surgical Mesh, DePuy AcroMed., Raynham, MA) and Kaneda-SR system (KANEDA-SR Spinal System, DePuy AcroMed., Raynham, MA) were performed through left extrapleural and retroperitoneal approach. Following L1 corpectomy and complete removal of the hypertrophic ligament, the anterior spinal column was then reconstructed with a 22 mm $\times$ 28 mm oval cage filled with cancellous bone. The surface of the bony endplate was minimally curettaged prior to application of the cage. Compression force was finally applied to the cage using the vertebral screws.

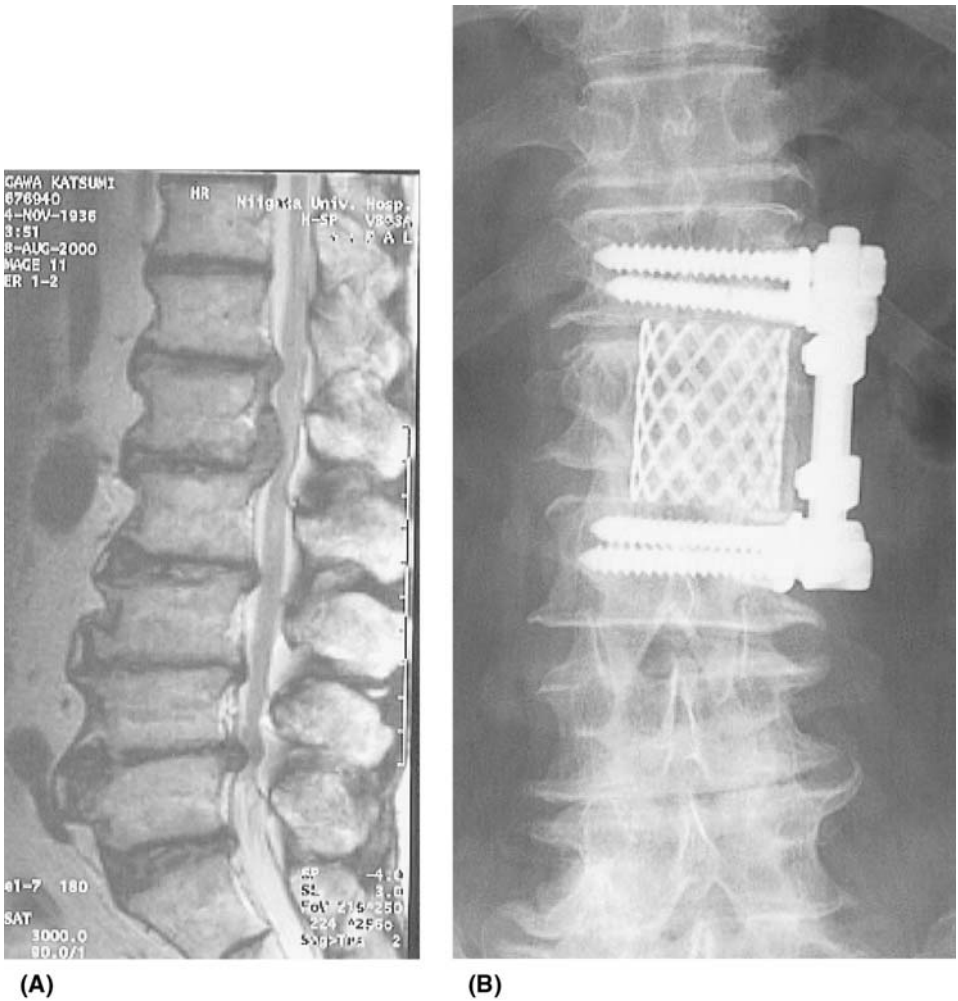

Figure 11 Case 1: a 63-year-old man with T12–L2 stenosis due to hypertrophic posterior longitudinal ligament. (A) Preoperative MRI; (B) radiograph 2 years after surgery.

Neurological disturbance was improved and postoperative course was uneventful. Radiographs taken 2 years after surgery revealed bony fusion without subsidence of the mesh cage into the adjacent vertebrae (Fig. 11B).

Case 2

A 78-year-old woman suffered from progressive paraparesis without any traumatic episode. The patient had been treated for rheumatoid arthritis with steroid medication for 20 years. On presentation she could not walk over 20 m because of the weakness of the lower extremities. She did not, however, complaint of any symptoms when she rested in bed. Radiographic examination confirmed L1 pseudarthrosis due to severe osteoporosis. MRI and computed tomography (CT) myelogram clearly demonstrated burst-type pseudarthrosis of L1 vertebra, resulting in compression of the cauda equina (Fig. 12A).

Anterior decompression and reconstruction through left extrapleural and retroperitoneal approach were performed using a titanium mesh cage (22 mm × 28 mm oval) and the Kaneda-SR

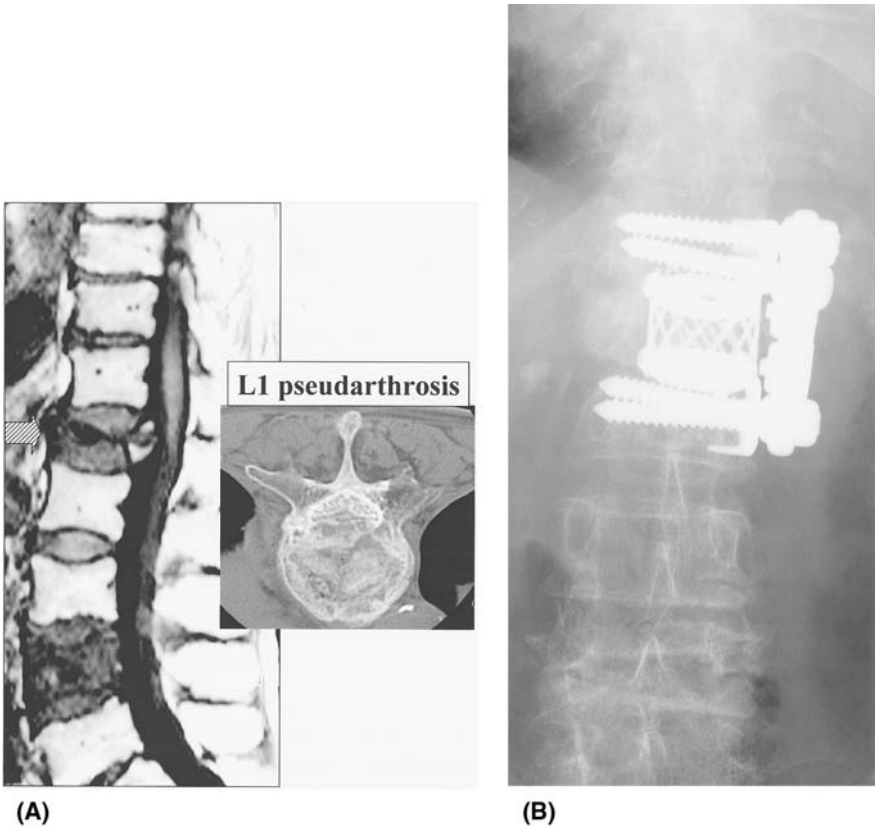

Figure 12 Case 2: a 78-year-old woman with osteoporotic L1 pseudarthrosis. (A) Preoperative MRI and CT myelogram; (B) radiograph one year after surgery.

system. Unlike in Case 1, insertion torque of the vertebral screws was quite low and application of compression to the cage via the screws was too dangerous to perform. After preparation of the surface of bony endplate, the cage, filled with resected T11th rib, was carefully place into the defect of the anterior spinal column without any compression force.

Postoperative course was uneventful and paraparesis was improved. Radiographs taken one year after surgery, however, show subsidence of the cage into the adjacent vertebrae, and fusion has not yet been confirmed (Fig. 12B).

Case 3

A 54-year-old man noticed left back pain with progressive weakness of the lower extremities. His symptoms gradually worsened and then rapidly became paraplegia within 2 months. Thoracolumbar radiographs were eventually taken, revealing a lytic lesion of T10 with erosion of the left pedicle. MRI and CT revealed a huge spinal tumor that extended from T9–T11 vertebrae and to the adjacent ribs and back muscles, causing severe compression of the spinal cord (Fig. 13A). A general examination confirmed left renal cell carcinoma, compatible with the spinal metastasis.

Following left nephrectomy, total en bloc spondylectomy including the three tumor vertebrae and adjacent ribs with muscles was performed through a combined anterior and posterior approach. The enormous defect of the spinal column was reconstructed using a titanium mesh cage (22 mm $\times$ 28 mm oval) and pedicle screw system (CD Horizon, Medtronic Sofamor Danek, Inc., Memphis, TN). The mesh cage, filled with iliac cancellous bone, was applied after curettage of the bony endplate of T8 and T12. Compression force was finally applied to the cage using the pedicle screws.

Although the patient complained of numbness of the lower extremities, his motor function was improved to the point that he was able to transfer from bed to a wheelchair. Radiograph one year after surgery demonstrated no local recurrence of the tumor and bony fusion of the anterior column (Fig. 13B,C).

IV. DISCUSSION

Among the aims of spinal reconstruction surgery are the potential for decompression, restoration of normal anatomical relations, immediate postoperative stability of the construct, and the resulting fusion. Titanium mesh cages are believed to satisfy the requirements for this type of surgery [4]. The area of decompression varies from the single disc level, e.g., in degenerative disc disease, to the multilevel level lesion, e.g., in a tumor of the spine (Fig. 13). The mesh cage can be trimmed and applied according to the size of the defect resulting from the decompression. The graft will usually be subject to compression, although it may be required to resist some shear force that tries to slide the graft across the surface of the host bone. The immediate postsurgical biomechanical aims are to carry reasonable loads that might correspond to moderate movement in the standing position and to be stiff under these loading conditions [13]. Hollowell et al. [2] reported on a comparative analysis of thoracolumbar interbody constructs in which thoracic vertebrae were loaded in compression. Several types of construct were tested: titanium mesh cage, humerus graft, tricorticated iliac graft, and triple rib strut graft, single rib graft on intact vertebrae or on cancellous trough of vertebrae. The titanium mesh cage construct provided the greatest resistance to axial load. According to earlier reports, maximum loads of lumbar vertebrae have ranged from around 1500 to 8000 N for static loads [14–16]. Most cages have a considerable margin of safety against failure. Furthermore, cancellous bone packed inside the cage and stress transmission through the bone provide an advantageous condition for bony union.

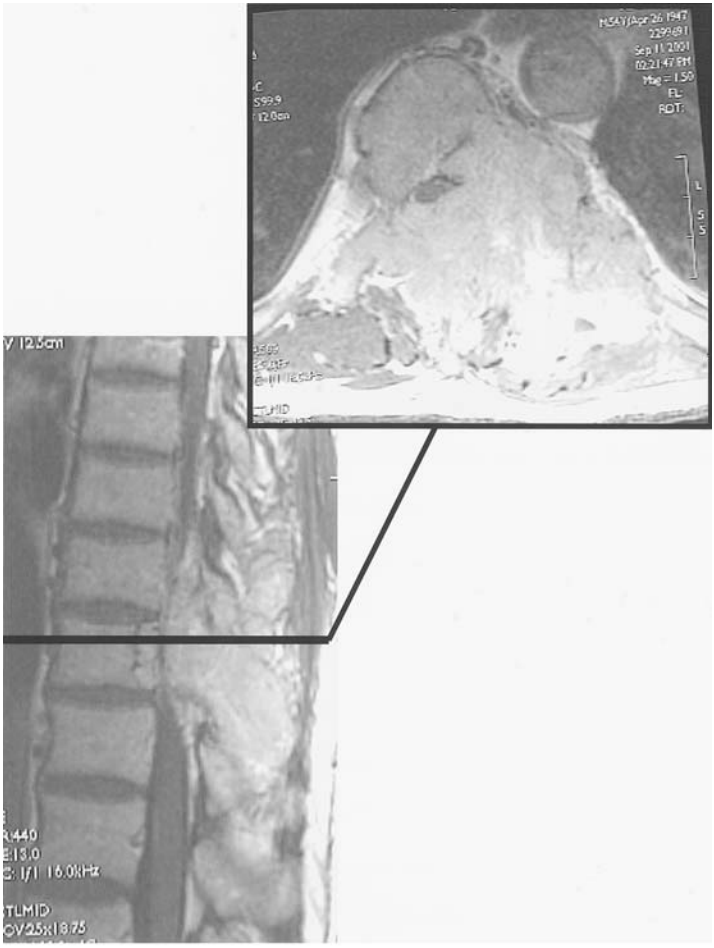

(A)

Figure 13 Case 3: a 54-year-old man, metastatic tumor of T9 to T11 (renal cell carcinoma). Total en bloc spondylectomy and reconstruction using a large titanium mesh cage and pedicle screw system were performed. (A) Preoperateive MRI; (B) radiograph (posteroanterior view) one year after surgery; (C) radiograph (lateral view) one year after surgery.

In an osteoporotic spine, however, one cannot expect the same stability from the mesh cage as would be expected in a normal spine. There is a correlation between bone mineral content (BMC) and ultimate compressive strength, and the strength has been found to increase linearly as bone mineral content increases [6,8]. Segment stiffness and fatigue strength also correlate to segment BMC [17]. These reports suggest that stability of the cage in reconstructive surgery is also affected by vertebral BMD. In reconstructive surgery with the mesh cage, subsidence of the mesh cage into the vertebral body may also cause serious problems, such as recurrence of the spinal deformity or fusion failure. Two important factors that are predictive of graft subsidence are vertebral bone strength and contact area between the cage and the vertebral bone. Closkey et al. [5] investigated a relationship between the contact area and compressive strength via a polymethylmethacrylate block (three different sizes). Eighty percent of the vertebral bodies

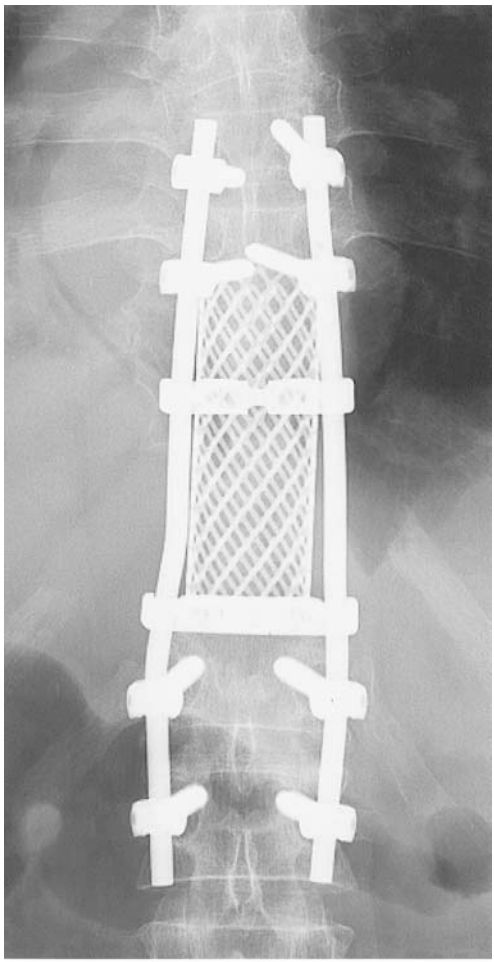

(B)

Figure 13 Continued.

with a graft covering 25% or less of the total endplate area failed at loads less than 600 N, while 88% of the vertebral bodies with 30% or greater coverage were able to carry a load greater than 600 N. In the present study, the authors investigated the immediate postoperative properties of the interface between the mesh cage and the vertebra. Vertebrae compressed by large cages (group L− or L+) had a greater maximum load than those with small cages (group S− or S+). The end ring contributed to the higher maximum load (Fig. 3). These results are compatible with the results of Closkey et al. [5], suggesting that increasing the contact area helps to avoid subsidence of the cage into the vertebral body. The average ratios between the cage size and the vertebral endplate area in each experimental group were: L(+) 0.32, L(−) 0.32, S(+) 0.20, S(−) 0.19. Thus, the smaller cage applied more load to the center of the endplate, which is structurally weaker than the periphery, where the cortical shell supports the compressive load. This may be one reason why the maximum load in the smaller cage group is lower than that in the larger cage group. Although augmentation by the end ring system increases maximum

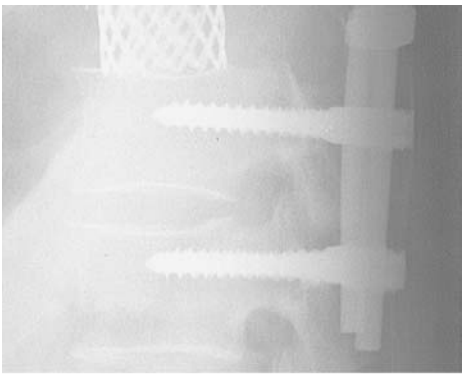

(C)

Figure 13 Continued.

load at the interface, the contact area between the bone graft inside the cage and the vertebral body decreases, which is an another disadvantage for fusion.

The relationship between the interface mechanical properties of the mesh cage and vertebral bone quality, represented by vertebral BMD, has not been fully investigated. In the present study, the relationships between maximum load or stiffness of the interface and whole or local subchondral vertebral BMD were analyzed. Maximum load and stiffness were positively correlated with whole vertebral BMD, measured by DXA, or with local cancellous BMD of subchondral bone, measured by pQCT (Fig. 8). Therefore, the stability of the cage may decline in a severely osteoporotic spine.The correlation coefficient and *p*-value were, however, more significant in the relationship between the mechanical properties and the local subchondral BMD measured by pQCT than in the whole vertebral BMD by DXA. These results suggest that the local trabecular structure beneath the endplate is an important component in the use of the mesh cage and that subchondral bone should be preserved as much as possible in anterior reconstructive surgery. Since removal of the vertebral bony endplate affects the trabecular structure and decreases local BMD, the authors disagree with a report by Hollowell et al. [2] stating that preservation of the vertebral endplate does not significantly increase resistance to graft subsidence.

On microradiography, the cage spikes encroached into the vertebral endplate or trabecular bone beneath the cage after loading to failure. Endplate failure occurred in the mode of depression 1–2 mm in depth with subchondral trabecular squeezing (Fig. 10). The squeezed trabecular structure sustained the cage. Therefore, subchondral trabeculae that were assessed by pQCT in this study have a significant role in the interface strength. From a clinical standpoint, excessive depression of the endplate beneath the cage should be avoided. Augmentation by other instrumentation, e.g., anterior plate system or pedicle screw system, is indispensable in reconstructive surgery with the mesh cage. The spinal column with normal bone density is successfully reconstructed by using these types of instrumentation (Fig. 11). If bone mineral density of the spine is normal and additional instrumentation is appropriate, the mesh cage is useful even in the reconstruction of an enormous spinal defect following three vertebral spondylectomy (Fig. 13). On the other hand, the surgeon should remember that it is very difficult to maintain the reconstructed spine using instrumentation in a case with extremely severe spinal osteoporosis (Fig. 12). Careful postoperative application of external support is mandatory in such a case.

V. CONCLUSION

A titanium mesh cage is useful in reconstructive surgery in the spine. The mesh cage with a large diameter and/or use of the end ring produces a significant increase in interface strength between the cage and the vertebra. A positive correlation between the interface strength and vertebral BMD, however, suggests that the stability of the cage may decline in a severely osteoporotic spine. Therefore, careful application of external support is mandatory even if reconstruction surgery is successful. On the other hand, should the spine have normal bone mineral density, large defect of the spinal column can be successfully reconstructed using an appropriate combination of the mesh cage and supplemental instrumentation.

ACKNOWLEDGMENT

The authors thank Medtronic Sofamor Danek, Inc., who donated the titanium mesh cage system (PYRAMESH implant system) used in this study.

REFERENCES

1. Kozak JA, Heilman AE, O'Brien JP. Anterior lumbar fusion options: operative technique and graft materials. Clin. Orthop 1994; 300:45–51.
2. Hollowell JP, Vollmer DG, Wilson CR, Pintar FA, Yoganandan N. Biomechanical analysis of thoracolumbar interbody constructs. How important is the endplate?. Spine ; 21:1032–1036.
3. Hertlein H, Mittlmeier T, Pitz S, Schurmann M, Kauschke T, Lob G. Spinal stabilization for patients with metastatic lesions of the spine using a titanium spacer. Eur. Spine J 1992; 1:131–136.
4. Lowery GL, Harms J. Titanium surgical mesh for vertebral defect replacement and intervertebral spacers. In Thatgott JS, Aebi H, eds. Manual of Internal Fixation of the Spine. Philadelphia: Lippincott-Raven Publishers, 1996:127–146.
5. Closkey RF, Parsons JR, Lee CK, Blacksin MF, Zimmerman MC. Mechanics of interbody spinal fusion: analysis of critical bone graft area. Spine 1993; 18:1011–1015.
6. Hansson TH, Roots B, Nachemson A. The bone mineral content and ultimate compressive strength of lumbar vertebrae. Spine 1980; 5:46–55.
7. Hansson TH, Keller TS, Panjabi MM. A study of the compressive properties of lumbar vertebral trabeculae: effects of tissue characteristics. Spine 1987; 11:56–62.
8. McBroom RJ, Hayes WC, Edwards WT, Goldberg RP, III AA. Prediction of vertebral body compressive fracture using quantitative computed tomography. J. Bone Joint Surg 1985; 67A:1206–12013.
9. Hasegawa K, Abe M, Washio T, Hara T. An experimental study on the interface strength between titanium mesh cage and vertebra in reference to vertebral bone mineral density. Spine 2001; 26: 957–963.
10. Hasegawa K, Takahashi H, Koga Y, Kawashima T, Hara T, Tanabe Y, Tanaka S. Mechanical properties of osteopaenic vertebral bodies monitored by acoustic emission. Bone 1993; 14:737–743.
11. Louis O, Boulpaep F, Van den Winkel P, Osteaux M. Cortical mineral content of the radius assessed by peripheral QCT predicts compressive strength on biomechanical testing. Bone 1995; 16:375–379.
12. Hasegawa K, Takahashi HE, Koga Y, Kawashima T, Hara T, Tanabe Y, Tanaka S. Failure characteristics of osteoporotic vertebral bodies monitored by acoustic emission. Spine 1993; 18:2314–2320.
13. Evans JH. Biomechanics of lumbar fusion. Clin. Orthop. Rel. Res 1985; 193:38–46.
14. Bartelink DL. The role of abdominal pressure in relieving the pressure on the lumbar intervertebral discs. J. Bone Joint Surg 1957; 39B:718–725.
15. Eie N. Load capacity of the low back. J. Oslo City Hosp 1966; 16:73–98.

16. Perey O. Fracture of the vertebral end plate in the lumbar spine. An experimental biomechanical investigation. Acta Orthop. Scand 1957; Suppl 25:1–100.
17. Hansson TH, Keller TS, Spengler DM. Mechanical behavior of the human lumbar spine. II. Fatigue strength during dynamic compressive loading. J. Orthop. Res 1987; 5:479–487.

19

Posterior Lumbar Interbody Fusion Using the Brantigan I/F Cage

Tomoyuki Hashimoto, Keichi Shigenobu, and Masahiro Kanayama
Hakodate Central General Hospital
Hokkaido, Japan

I. INTRODUCTION

Posterolateral fusion (PLF) is a standard surgical treatment of lumbar spinal instability [1–3]. With the use of spinal instrumentation, PLF has been widely used for lumbar degenerative pathology [2–9]. However, in the unstable spine, PLF may not restore disc space height or sagittal segmental alignment even with the use of spinal instrumentation. As an adverse effect of spinal fusion, accelerated degenerative change of motion segments above or below the spinal fusion site has been a concern of spine surgeons for many years [10–12]. Postoperative sagittal alignment might be a key to avoid adjacent segment deterioration after spinal fusion [13].

To reduce or eliminate these complications, interbody fusion implants have recently been gaining acceptance as a method for ensuring lumbar interbody arthordesis. Interbody fusion devices provide anterior structural support of the operative segment and eliminate the need for harvesting tricortical bone block from the iliac crest. Various types of interbody fusion devices have been developed.

Posterior lumbar interbody fusion (PLIF), pioneered by Cloward [14], has the potential mechanical advantage of allowing restoration of disc space height, sagittal plane alignment, and weight bearing through the anterior column. However, problems with donor bone have limited the clinical success of PLIF. Brantigan [15] questioned the adequacy of ethylene oxide sterilized allograft in meeting the mechanical and biological needs of PLIF. Wiltse [16] stated that failure of fusion results when PLIF is used alone. Steffee and Brantigan [17] recommended that pedicle screw fixation be combined with PLIF.

The mechanical environment is critical for successful bone healing and is closely related to the bone biology [18,19]. It has been of interest how different stress-shielded environments are created within the interbody fusion devices and how they may influence the bone quality of the developing interbody fusion mass. Cunningham et al. [20] examined, more than 8 years postsurgery, the histological composition of cervical interbody fusion in thoroughbred horses and found significantly decreased bone mineral density at the fusion site within the cage compared with the adjacent vertebral bodies. Kanayama et al. [21] investigated the mechanical environments within 11 different types of interbody fusion devices using an in vitro calf spine model. They found that threaded fusion cages provided more stress-shielding effect than the nonthreaded devices and structural allograft. Thus, threaded fusion cages had a biomechanical disadvantage for bone healing and remodeling.

More recently, interbody fusion cages have improved the clinical and fusion results of PLIF [22–27]. The Brantigan I/F Cage for PLIF was designed to separate the mechanical and biological functions of PLIF using autologous bone from the iliac crest [23,24]. Morbidity caused by harvest of bone from the iliac crest remains a concern [28].

Many variables are thought to influence the outcome of the fusion, including host site conditions (local blood supply, decortication procedure, level of fusion), graft materials (source, type, amount of bone), biomechanical environment (instability, instrumentation, bracing), and other factors (age, nutrition, smoking). The bone graft technique is the key to achieving a solid fusion in spinal arthrodesis, and a suitable graft material is required to induce and support the formation of new bone at the operative site. Autogenous iliac bone is the current gold standard for bone graft material. However, there are complications related to graft harvesting, including donor site morbidity, increased blood loss, and limited supplies of donor material. These donor site complications are reported in 40–50% of patients undergoing iliac crest harvesting [29,30]. To avoid these complications related to graft harvesting, various bone graft substitutes have been developed and investigated in basic animal research [31–37]. The goals for bone graft substitutes are to match fusion rate with autologous iliac bone graft while avoiding the morbidity of bone graft harvest and extending the quantity of available graft material. Bone graft substitutes are classified into osteoconductive or osteoinductive materials. To date, however, limited amounts of osteoinductive agents are available for clinical application. Osteoconductive materials include polylactic acid, collagens [33], biphasic calcium phosphate [33,36], hydroxyapatite (HA) [34,37], tricalcium phosphate (TCP) [34,37], and bioactive ceramics [35]. They have different biological properties. For example, it was postulated that HA is resorbed very slowly, whereas β-TCP is resorbed within 6 weeks after implantation. It remains unclear which types of ceramics are suitable for PLIF.

We will present here clinical and radiographic results of single-level PLIF using the Brantigan I/F Cage filled with a mixture of local morselized autologous bone and bioactive ceramic granules without iliac crest harvesting

II. MATERIALS AND METHODS

A. Demographics

Twenty-five patients underwent single-level PLIF using the Brantigan I/F Cage (DePuy AcroMed Corp., Raynham, MA) from July 1997 to October 1998 in our hospital. Spinal instrumentation was used in all cases including the Steffee Variable Screw Placement (VSP) pedicle screw system (DePuy AcroMed Corp.) in 20 patients and the Moss-Miami pedicle screw system (DePuy AcroMed Corp.) in 5. Fourteen male and 11 female patients were included, ranging in age at surgery from 17 to 23 years (mean 44 years). Mean postoperative follow-up was 2 years and 7 months (range 2 years to 3 years and 1 month). The spinal pathologies were isthmic spondylolisthesis in 15 patients, degenerative spondylolisthesis in 5, lumbar disc herniations in 3 (recurrent herniations in 2 and extraforaminal herniation in 1), foraminal stenosis in 1, and congenital spondylolisthesis in 1 patient. The involved level was L3-4 in 3 patients, L4-5 in 9, L5-S1 in 11, L6-S1 in 1, and L5-6 in 1.

B. Grafting Method

During surgical decompression, meticulously cleaned bone was taken from the laminectomy, medial facetectomy, or loose lamina and mixed with equal an approximately amount of bioactive ceramic granules [apatite–wollastonite containing glass ceramic (A-W GC)] as demonstrated

in Figure 1. During disc removal, the entire nucleus must be removed along with the cartilage from each vertebral endplate and any degenerative annulus. Before insertion of the cages into the posterior part of the disc space, a portion of the bone mixture was packed as tightly as possible into the anterior and lateral part of the disc space. Cages 21 mm in length were filled with this bone-ceramic mixture and placed in the posterior part of the disc space. The placement of graft and cages is shown in Figure 2.

C. Postoperative Care

At 4–7 days after the operation, the patient was allowed to ambulate with a polypropylene thoracolumbosacral orthosis, usually worn for 12–16 weeks. All patients were allowed to discharge within 6 weeks after the surgery.

D. Clinical Evaluation

Clinical outcomes were evaluated according to the scoring system of the Japanese Orthopaedic Association (JOA score) (Table 1). A full score is 29 points, based on three subjective symptoms

Figure 1 Preparation of bone graft mixture. (A) The left half is local bone taken from the decompression. The right half is bioactive ceramic granules. (B) The local bone and ceramic granules are mixed together. (C) The graft mixture is placed into a tube for packing into the disc space. (D) The carbon cage has been packed with the graft mixture.

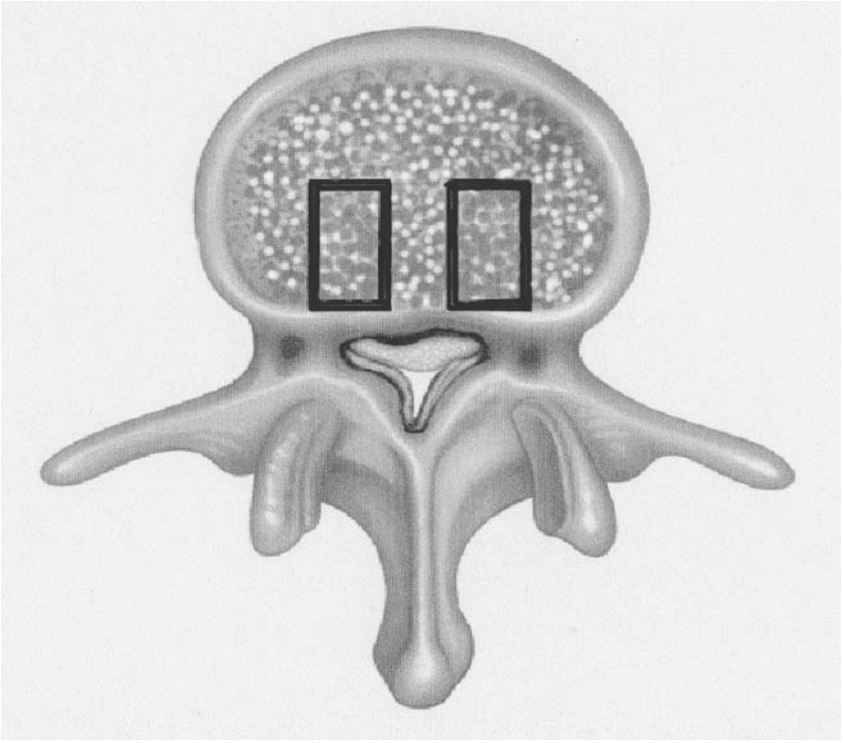

Figure 2 Position of carbon cage and graft mixture in the disc space.

(9 points), three clinical signs (6 points), and seven activities of daily living (14 points). Improvement rate was calculated by the following equation:

$$\text{Improvement rate} = \frac{\text{postoperative score} - \text{preoperative score}}{29 - \text{preoperative score}} \times 100 \quad (1)$$

The clinical scores were statistically analyzed by paired *t*-test between the evaluations before surgery and at final follow-up. A *p*-value of <0.05 was considered to be significant.

E. Radiographic Evaluation

The regional segmental lordosis was measured at the operated segment in the neutral position on standing lateral films. The regional lordosis was taken as the angle between the superior surfaces of the vertebral bodies of the unstable segment. The percentage of slip and percentage of posterior disc height was measured as shown in Figure 3. The regional lordosis was analyzed by paired *t*-test. The slip percentage and posterior disc height percentages were evaluated by statistical analysis with one-way measured ANOVA. A *p*-value of less than 0.05 was considered to be significant. Fusion status was recorded for each surgically treated segment at each follow-up. The operative segment was considered fused if there was radiographic evidence of bone bridging the disc space with no lucency and no motion during flexion and extension in lateral functional x-ray films.

Table 1 Japanese Orthopaedic Association Assessment of Treatment of Low Back Pain

I. Subjective symptoms (9 points)	**Points**
A. Low back pain	
a. None	3
b. Occasional mild pain	2
c. Frequent mind or occasional severe pain	1
d. Frequent or continuous severe pain	0
B. Leg pain and/or tingling	
a. None	3
b. Occasional mild symptoms	2
c. Frequent mild or occasional severe symptoms	1
d. Frequent or continuous severe symptoms	0
C. Gait	
a. Normal	3
b. Able to walk more than 500 m, even muscle weakness	2
c. Unable to walk more than 500 m due to leg pain, tingling, and/or muscle weakness	1
d. Unable to walk more than 100 m due to the symptoms above	0
II. Clinical signs (6 points)	
A. Straight leg raising test (including tight hamstrings)	
a. Normal	2
b. 30–70 degrees	1
c. Less than 30 degrees	0
B. Sensory disturbance	
a. None	2
b. Slight disturbance	1
c. Marked disturbance	0
C. Motor disturbance (manual muscle test)	
a. Normal (grade 5)	2
b. Slight weakness (grade 4)	1
c. Marked weakness (grade 0–3)	0

III. Restriction of activities of daily living (ADL) (14 points)

	normal	slightly restricted	severely restricted
a. Turn over while lying	2	1	0
b. Standing	2	1	0
c. Washing	2	1	0
d. Leaning forward	2	1	0
e. Sitting (about 1 hr)	2	1	0
f. Lifting heavy objects	2	1	0
g. Walking	2	1	0

IV. Urinary bladder function (−6–0 points)	
a. Normal	0
b. Mild dysuria	−3
c. Severe dysuria (incontinence, urinary retention)	−6
Total score	**29**

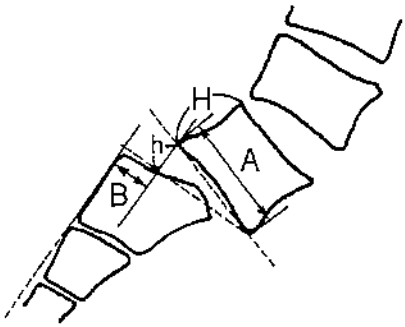

Figure 3 Calculations of percent slip and percent posterior disc height.

III. RESULTS

A. Surgical Parameters

Operative time averaged 193 ± SD 38 minutes with a range of 125–261 minutes. Blood loss averaged 215 ± SD 72 mL with a range of 35–675 mL. No patients needed blood transfusion. There were no neurological deficits, deep infections, instrumentation failures, or other major complications. There were two dural tears repaired at surgery without sequelae and two patients with thrombophlebitis of the lower extremities.

B. Clinical Outcomes

Patients were evaluated by the JOA score with a maximum possible score of 29 points. JOA scores averaged 11.8 ± SD 5.4 points preoperatively, 25.8 ± SD 3.5 points at discharge, and 26.1 ± 3.5 points at final follow-up. Finally, improvement rate was 83.1% on average. JOA scores were significantly better for the two postoperative ratings as compared with before surgery ($p < 0.02$), but there was no statistical difference between the two post-operative ratings.

C. Radiological Results

The sagittal alignment (regional lordosis) of the operative segments averaged 5.3 ± SD 6.1 degrees before surgery, 18.9 ± 5.8 SD degrees at discharge, and 18.1 ± 6.0 degrees at final follow-up.

In 21 patients with spondylolisthesis (15 isthmic, 5 degenerative, and 1 congenital), the preoperative percent slip was 28.5 ± SD 13.4%. This slip percent was decreased at follow-up to 4.7 ± 3.8%. Preoperative percentage posterior disc height was 25.9 ± SD 11.7%, increased at follow-up to 40.7 ± 7.2%. Both vertebral slip and disc height were significantly improved after the surgery ($p < 0.01$).

Fusion success was achieved in 25 of 25 patients. Two patients treated for L4-L5 degenerative spondylolisthesis with osteoporosis had collapsed fusion with loss of maintenance of disc height and correction of the slip. Two patients who had intervals of 10 and 11 months from surgery to fusion were considered to4 have delayed union.

IV. CASE PRESENTATION

A. Case 1

A 14-year-old girl had an L5 congenital spondylolisthesis with low back pain and bilateral L5 and S1 radiculopathy before admission. Preoperative myelograms (Fig. 4A–D) show a slippage of L5 with congenital spondylolysis and narrowing of the dural tube at L5-S1. Just after the surgery, mixture grafted bone was seen in the disc space of L5-S1 and the L5 vertebral body was able to be reduced with the increase of disc height (Fig. 4E,F). Ten months after the surgery she gained consolidation of fusion and maintained the regional lordosis with the restored disc space (Fig. 4G,H).

B. Case 2

A 70-year-old woman had a L4 degenerative spondylolisthesis with severe intermittent claudication and low back pain. Preoperative lateral myelogram at flexion position (Fig. 5A) shows moderate kyphotic deformity with slipping at L4-L5 level, and CT myelogram (Fig. 5B) shows lateral recess stenosis with hypertrophy of ligament flavum. Just after surgery the patient recovered normal lordosis with lucency of grafted bone between upper and lower endplates (Fig. 5C,D). Thirteen months after surgery she gained solid consolidation of L4-L5 level (Fig. 5E,F). Her complaints disappeared completely and she returned to normal daily activities.

C. Case 3

A 58-year-old woman had an L4-L5 degenerative spondylolisthesis. She complained of 3 years of low back pain and presented with progressive onset of neurogenic intermittent claudication of less than two blocks for 10 months. She had neurological deficits of bilateral L4 and L5 roots at admission. Myelograms before surgery (Fig. 6A,B) showed partial obstruction of the dural tube with kyphotic sagittal curvature and slippage at L3-L5 level. CT myelograms indicated moderate canal stenosis at L3-L4 and L4-L5 (Fig. 6C,D). A-P and lateral view of x-ray just after surgery clearly showed mixed grafted bone in both levels, and she gained good sagittal alignment (Fig. 6E,F). Two years and 3 months after surgery she maintained satisfactory sagittal alignment and good consolidation of fusion at both levels (Fig. 6G,H). She had no complaints of intermittent claudication and low back pain at the same period.

V. DISCUSSION

In the past, PLF has been widely used to treat degenerative lumbar conditions [1–6,38]; however, PLF is often unable to restore the normal lordotic curvature and disc space height even when used with spinal instrumentation. PLIF, as pioneered by Cloward [14], has had the potential to improve these parameters of fusion but has been limited by the mechanical and biological deficiencies of donor bone. More recently, various cages have become widely used to achieve a higher rate of success with PLIF.

The Brantigan I/F Cage for PLIF is made of a carbon fiber–reinforced polymer that has struts that support physiological loads. It has a hollow area to accept packing of autologous cancellous bone graft and a modulus of elasticity approximating that of cortical bone. The entire device is radiolucent so that bony healing can be assessed by normal radiographic methods. When the Brantigan I/F Cage is used with pedicle screw fixation, as recommended by Steffee [17], very reliable fusion success has been achieved [24]. The reliability of this fusion success

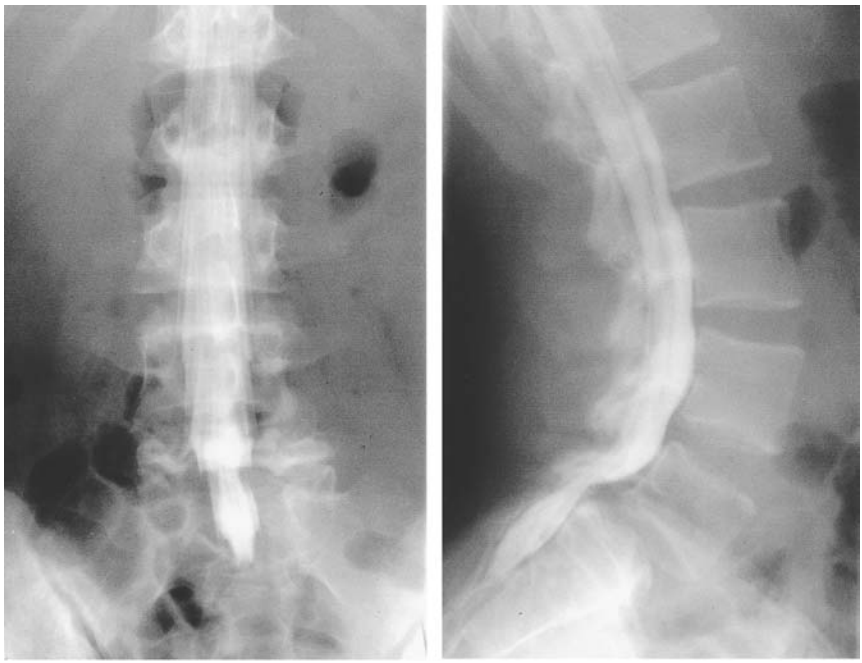

A

B

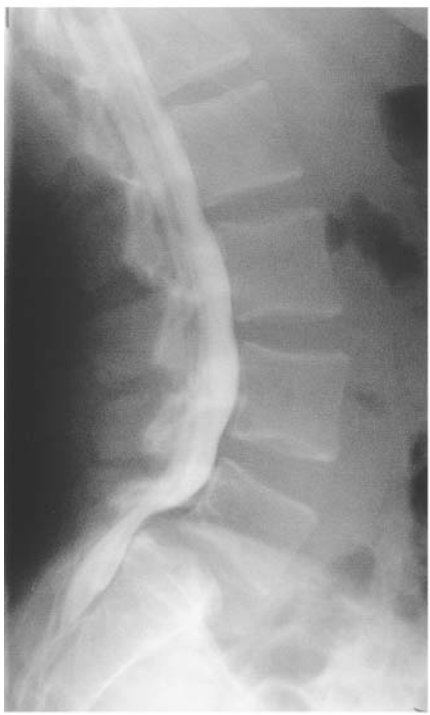

C

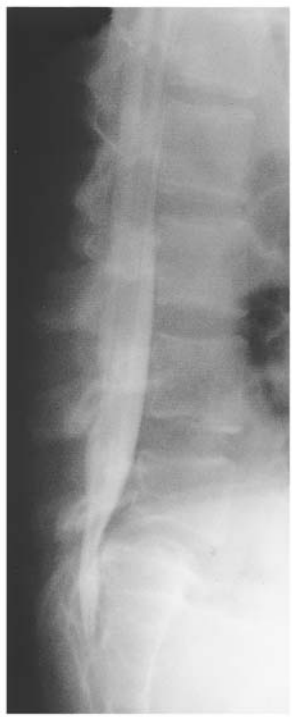

D

Figure 4 Case–1: 14-year-old female. (A) Preoperative myelogram at A-P view; (B) preoperative myelogram at extension position; (C) preoperative myelogram at neutral position; (D) preoperative myelogram at flexion position.

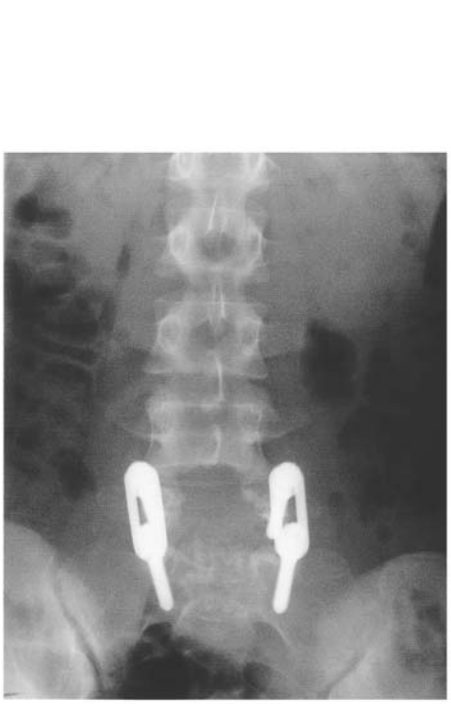

E

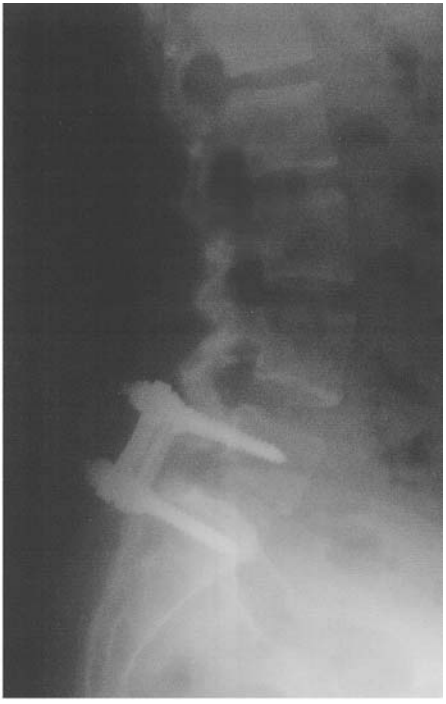

F

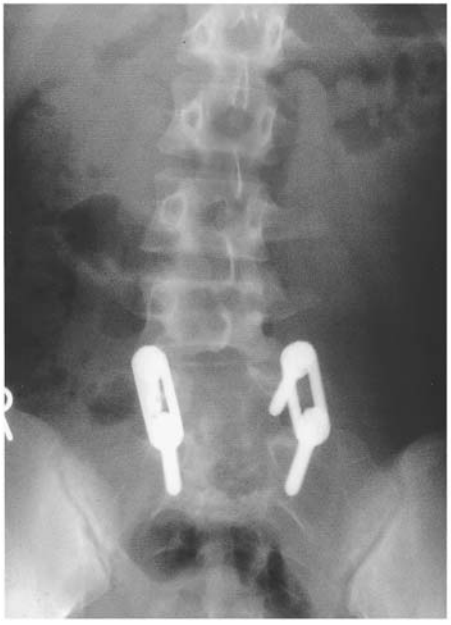

G

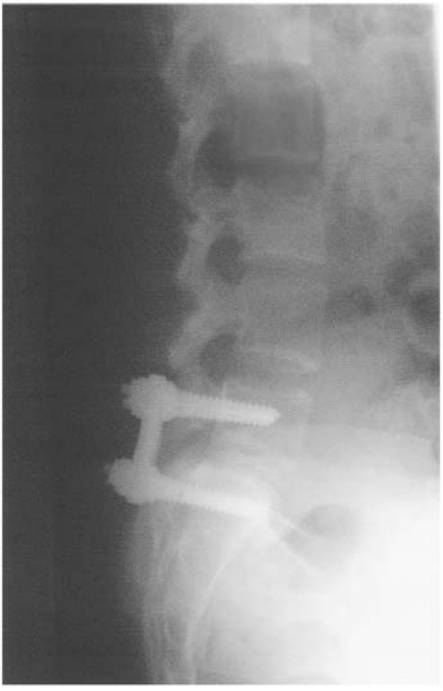

H

Figure 4 Continued. (E) A-P x-ray film just after surgery; (F) lateral x-ray film just after surgery; (G) A-P x-ray film 10 months after surgery; (H) lateral x-ray film 10 months after surgery.

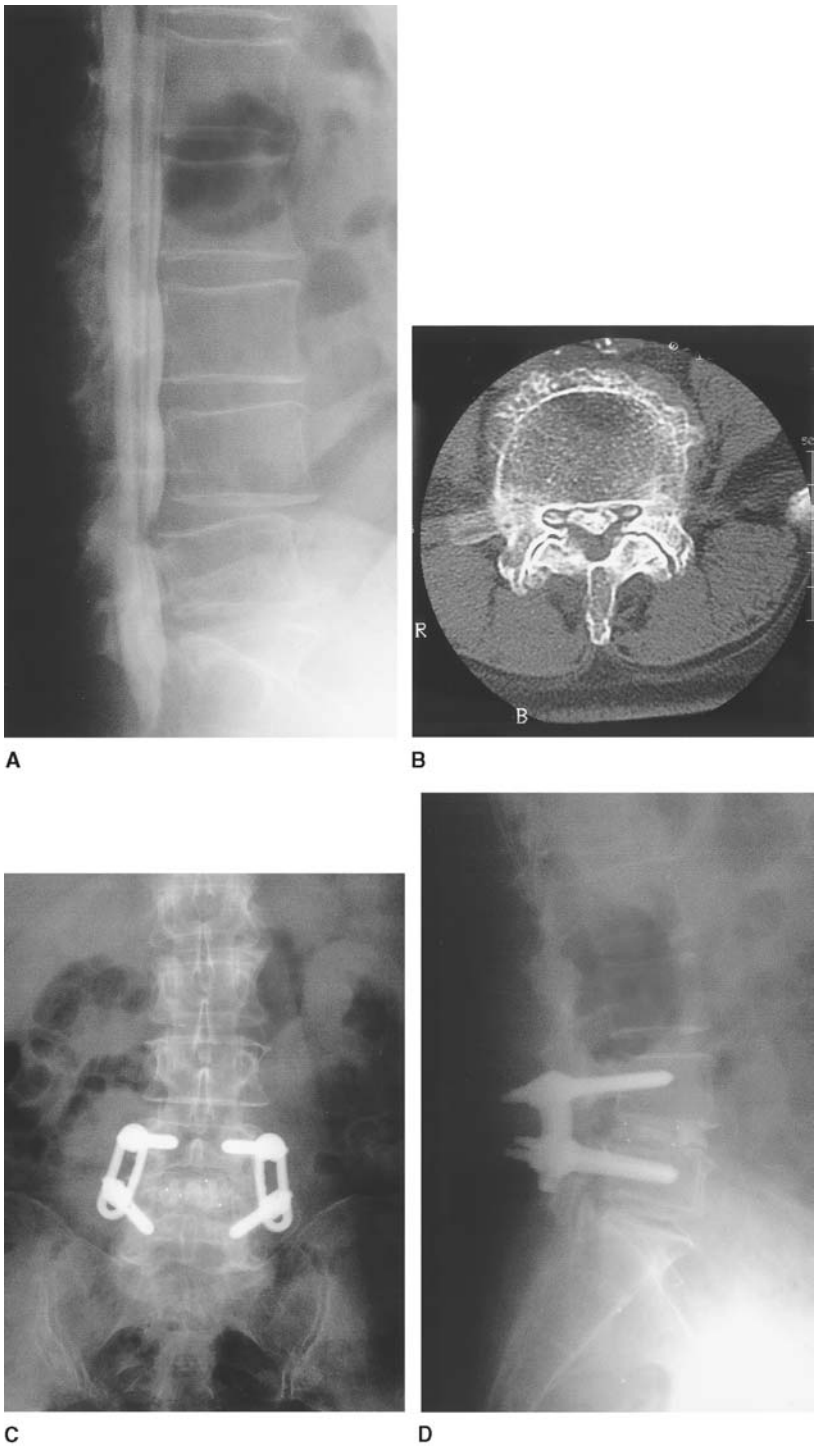

Figure 5 Case 2: 70-year-old female. (A) Preoperative lateral myelogram at flexion position; (B) preoperative CT myelogram at L4/5; (C) postoperative A-P x-ray film; (D) postoperative lateral x-ray film.

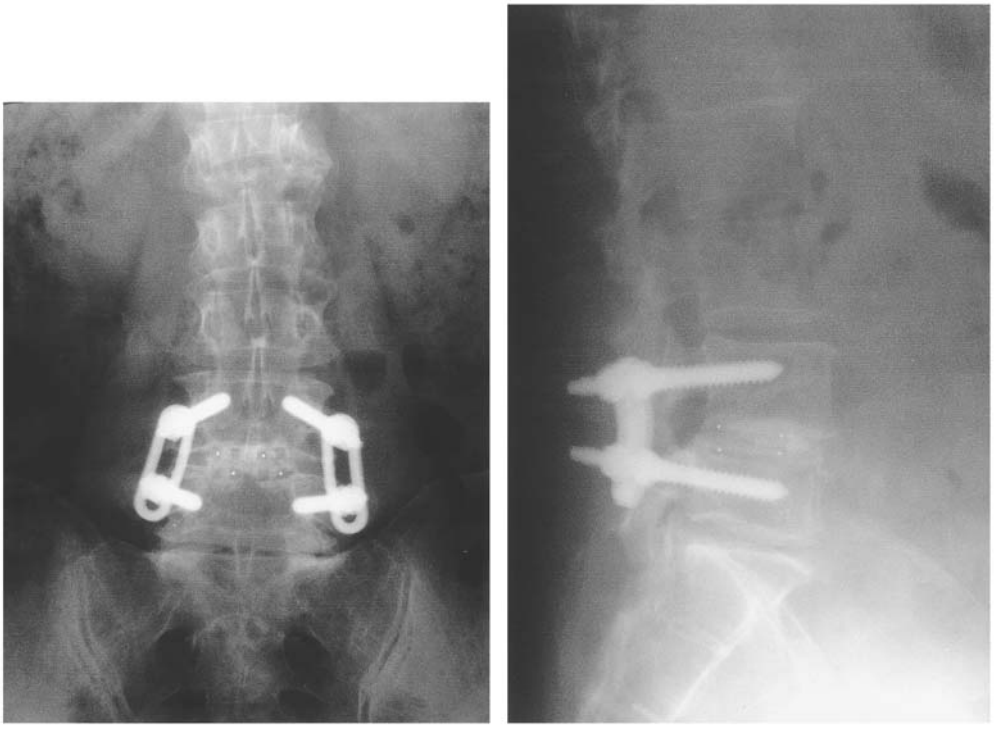

E F

Figure 5 Continued. (E) A-P x-ray film at 13 months after surgery; (F) lateral x-ray film at 13 months after surgery.

and accuracy of plane x-rays in determining fusion was documented in a group of patients having exploration of fusion during removal of posterior fixation [24].

Previous reports have recommended filling the cages with cancellous bone graft from the iliac crest. Nevertheless, problems with harvesting iliac bone have included donor site pain, pelvic instability, and fracture of the pelvis [28]. As a result, many orthopedic surgeons have investigated potential bone graft substitutes such as homologous bone, demineralized allograft, and synthetic organic and inorganic constituents of bone. In particular, synthetic materials may be very useful because they can be provided in infinite supply, they are easily sterilized and stored, and the significant risk of disease transmission by allograft bone is avoided.

The bioactive AW glass ceramics that we have been using for PLIF have demonstrated osteoconductive properties both experimentally and clinically [35,39,40,41]. Although the local bone taken from the decompression may have little volume, it adds osteoinductive properties and osteogenic cells. The careful grafting technique we describe follows the principles described for using impacted morselized bone graft to fill bony defects in total knee or hip arthroplasty cases [42]. The uniform fusion success achieved in this study confirms the hypothesis that a mixture of local bone with bioactive ceramic used with careful grafting technique achieves our goal of reliable fusion without harvest of bone from the iliac crest.

The PLIF procedure can be technically difficult, and some complications have been reported [23,43]. In particular, Elias et al. [43] reported that PLIF using a titanium threaded cage device had complications such as dural lacerations, blood transfusions, inadequate implant

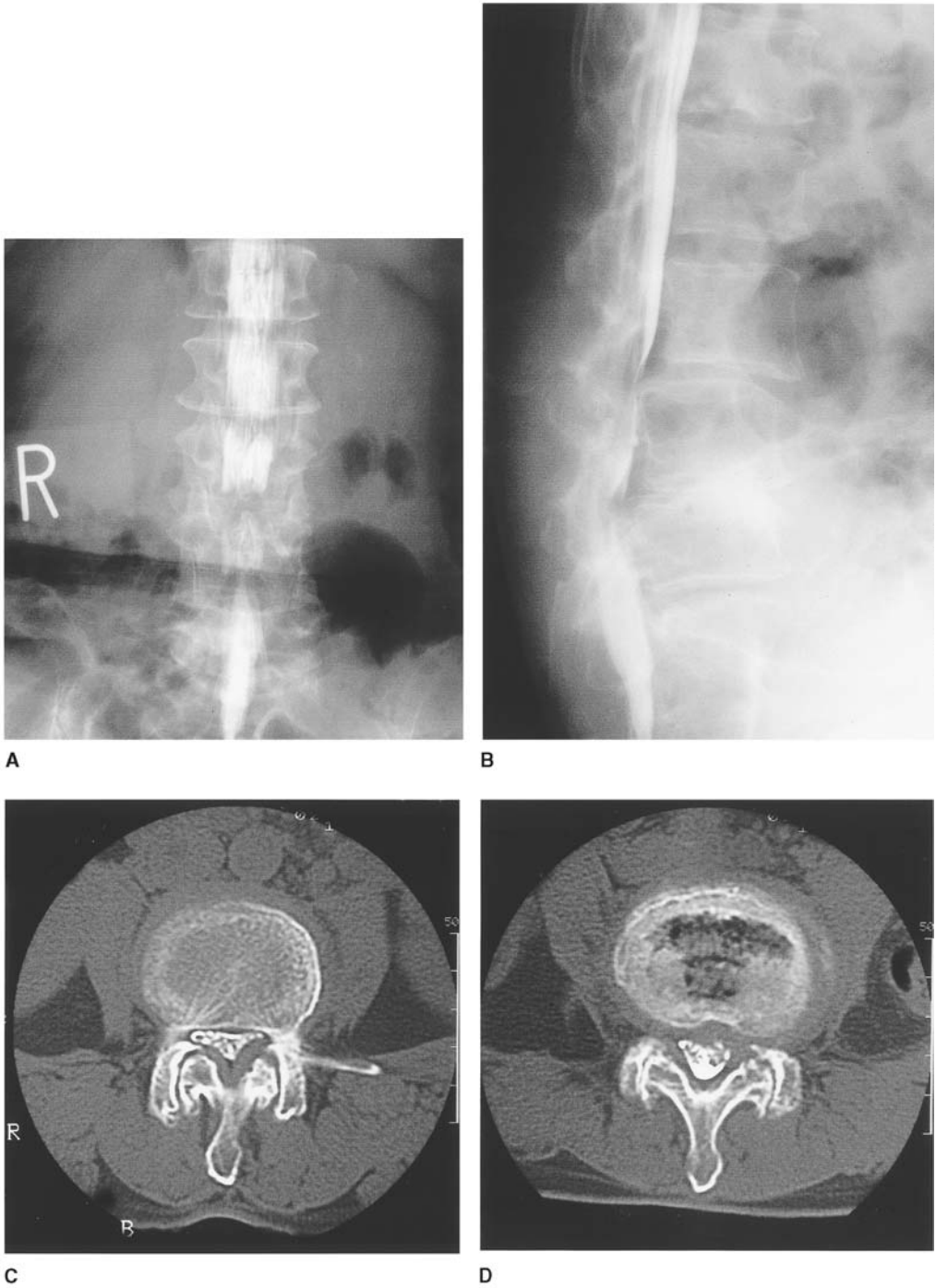

Figure 6 Case 3: 58-year-old female. (A) Preoperative A-P myelogram; (B) preoperative lateral myelogram at flexion position; (C) preoperative CT myelogram at L3/4; (D) preoperative CT myelogram at L4/5.

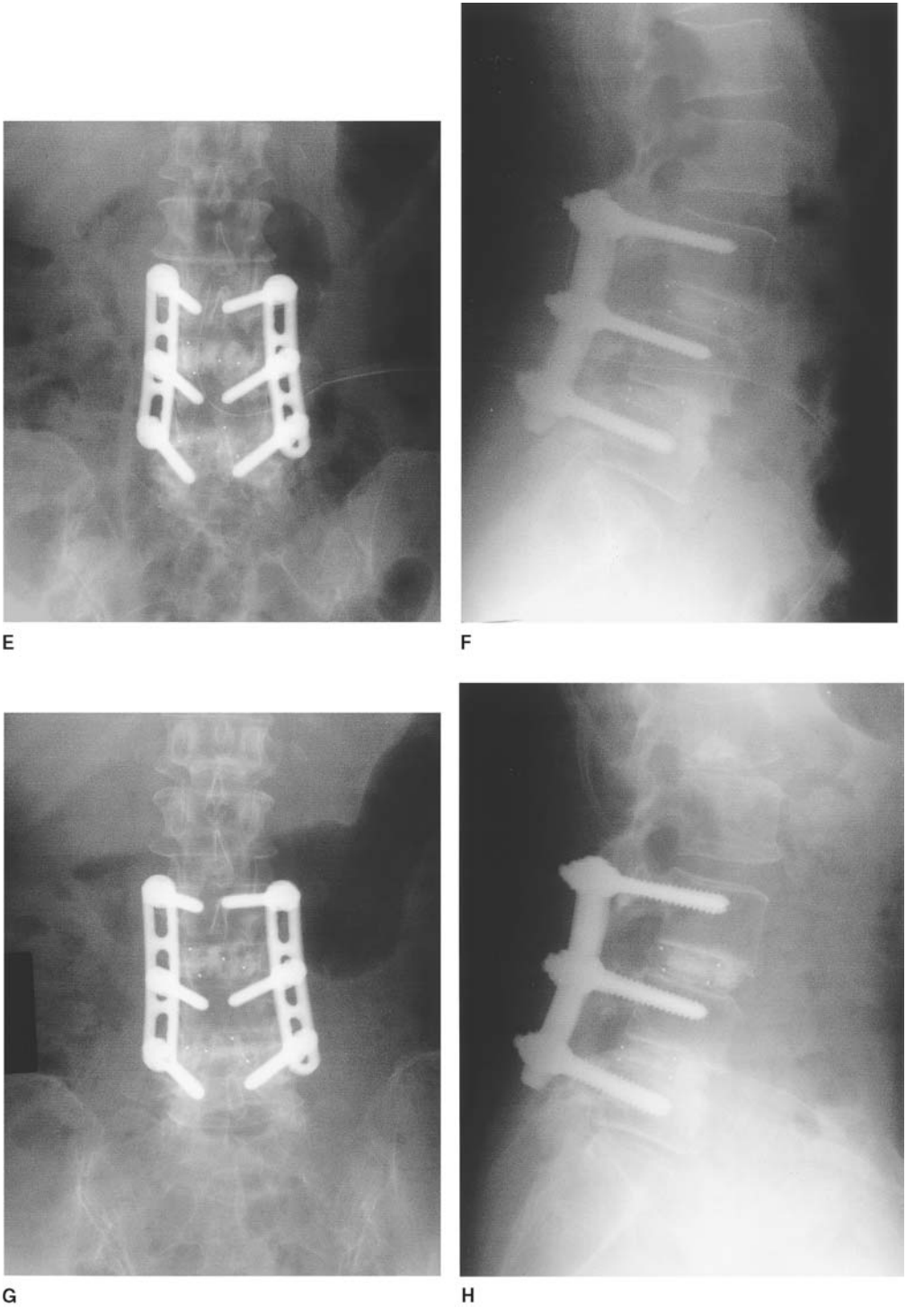

Figure 6 Continued. (E) postoperative A-P x-ray film; (F) postoperative Lateral x-ray film; (G) A-P x-ray film 2 years and 3 months after surgery; (H) lateral x-ray film 2 years and 3 months after surgery.

position, postoperative persistent low back pain, and occurrence of radiculopathy after surgery. They concluded that the findings were applicable to other cylindrical threaded titanium devices inserted via a posterior approach. Additionally it may be difficult to assess bony union in the cylindrical threaded cage. The rate of complications was greater than reported for the prospective clinical trials of these devices [25,26].

In comparison, the rectangular carbon cage is relatively smaller, and there is no need for extensive retraction of neural tissue and no need for total removal of facet joints for its insertion. Compared with the prospective clinical trial for the Brantigan I/F Cage [24], this study reports a lower blood loss, shorter operating times, lower complication rates, a higher clinical success, and the same uniform fusion success. These differences were most likely related to the different patient populations since the clinical trials included only patients who had prior failed surgery and the average patient had two prior failed surgeries at two levels.

PLIF using the Brantigan I/F Cage filled with a mixture of local morselized bone and bioactive ceramic granules yields satisfactory clinical results, maintains adequate regional lordosis and restored disc height, and can be a surgical option for treatment of degenerative lumbar conditions with instability, even if the iliac crest is not harvested for bone graft.

VI. SUMMARY

Twenty-five patients were treated for degenerative lumbar conditions using the Brantigan I/F Cage with pedicle screw fixation using a mixture of local bone and bioactive ceramic granules for grafting. All 25 patients achieved radiographic fusion. All 25 patients achieved significant improvements in JOA clinical scores. Patients treated for spondylolisthesis achieved significant improvements in sagittal plane alignment and disc space height. These patients experienced lower blood loss, operative time, and rates of complications than previously reported. Successful cage fusion can be reliably achieved using a mixture of local bone and bioactive ceramic granules without harvest of bone from the iliac crest.

REFERENCES

1. Herkowitz HN, Kurz LT. Degenerative lumbar spondylolisthesis with spinal stenosis: a prospective study comparing decompression with decompression and intertransverse process arthrodesis. J Bone Joint Surg 1991; 73A:802–808.
2. Mardjetko SM, Connoly PJ, Shott S. Degenerative lumbar spondylolisthesis: a meta-analysis of literature 1970–1993. Spine 1993; 19(suppl 20):2256S–2265S.
3. Stauffer AD, Coventry MB. Posterolateral lumbar spine fusion. J Bone Joint Surg 1972; 54A: 1195–1204.
4. Bridwell KH, Sedgenick TA, O'Brien MF, et al. The role of fusion and instrumentation in the treatment of degenerative spondylolisthesis with spinal stenosis. J Spinal Disord 1993; 6:461–472.
5. Kaneda K, Satoh S, Nohara Y, Oguma T. Distraction rod instrumentation with posterolateral fusion in isthmic spondylolisthesis—53 cases followed for 18–89 months. Spine 1985; 10:296–302.
6. Kaneda K, Kazama H, Satoh S, Fujiya M. Follow-up study of medial facetectomies and posterolateral fusion with instrumentation in unstable degenerative spondylolisthesis. Clin Orthop 1986:287–295.
7. Lorenz M, Zindrick M, Schwaegeler P. A comparison of single-level fusions with and without hardware. Spine 1991; 16(suppl 8):S455–S458.
8. Wood GW, Boyd RJ, et al. The effect of pedicle screw/plate fixation on lumbar/lumbosacral autogenous bone graft fusions in patients with degenerative disc disease. Spine 1995; 20:819–830.
9. Zdeblick TA. A prospective, randomized study of lumbar fusion: preliminary results. Spine 1993; 18:983–991.

10. Lehmann TR, Spratt KF, Tozzi JE. Long-term follow-up of lower lumbar fusion patients. Spine 1987; 12:97–104.
11. Leong JCY, Chun SY, Grange WJ, et al. Long-term follow-up of lumbar intervertebral disc prolapse. Spine 1983; 8:793–799.
12. Kanayama M, Hashimoto T, Shigenobu K. Adjacent-segment morbidity after Graf ligamentoplasty compared with posterolateral lumbar fusion. J Neurosurg (Spine 1) 2001; 95:5–10.
13. Oda I, Cunningham BW, Buckley RA, Goebel MJ, Haggerty CJ, Orbegoso CM, McAfee PC. Does spinal kyphotic deformity influence the biomechanical characteristics of the adjacent motion segments? An in vivo animal model. Spine 1999; 24:2139–46.
14. Cloward RB. The treatment of ruptured intervertebral discs by vertebral body fusion. Report of 750 cases. J Neurosurg 1953; 10:154–167.
15. Brantigan JW. Pseudarthrosis rate after allograft posterior lumbar interbody fusion with pedicle screw and plate fixation. Spine 1994; 19:1271–1279.
16. Wiltse LL. Surgery for intervertebral disk disease of the lumbar spine. Clin Orthop 1977; 129:22–45.
17. Steffee AD, Brantigan JW. The variable screw placement spinal fixation system. Report of a prospective study of 250 patients enrolled in Food and Drug Administration clinical trials. Spine 1993; 18: 1160–1172.
18. Kenwright J, Goodship AE. Controlled mechanical stimulation in the treatment of tibial fracture. Clin Orthop 1989; 241:36–47.
19. Oxland TR, Kohrs SW, Kuslich SD. Biomechanical rationale for the BAK lumbar interbody fusion system, 1993. Presented at the 8th Annual Meeting of NASS, San Diego, CA.
20. Cunningham BW, Ng JT, Haggerty CJ. A quantitative densitometric study investigating the stress-shielding effects of interbody spinal fusion devices. Emphasis on long term fusions in thoroughbred racehorses. Trans Orthop Res Soc 1998; 23:250.
21. Kanayama M, Cunningham BW, Haggerty CJ. In vitro biomechanical investigation of the stability and stress-shielding effect of lumbar interbody fusion devices. J Neurosurg (Spine 2) 2000; 93: 259–265.
22. Bagby GW. Arthrodesis by the distraction-compression method using a stainless steel implant. Orthopedics 1988; 11:931–934.
23. Wetzel FT, LaRocca H. The failed posterior lumbar interbody fusion. Spine 1991; 16:839–845.
24. Brantigan JW, Steffee AD. A carbon fiber implant to aid interbody fusion. Two-year clinical results in the first 26 patients. Spine 1993; 18:2106–2117.
25. Wood GW, Boyd RJ, Carothers TA. The effect of pedicle screw/plate fixation on lumbar/lumbosacral autogenous bone graft fusions in patients with degenerative disc disease. Spine 1995; 20:819–830.
26. Ray CD. Threaded fusion cages for interbody fusions. Spine 1997; 22:677–680.
27. Ray CD. Threaded fusion cages for lumbar interbody fusions. An economic comparison with 360 degree fusions. Spine 1997; 22:681–685.
28. Younger EM, Chapman MW. Morbidity at bone graft donor sites. J Orthop Trauma 1989; 3:192–195.
29. Kurz LT, Garfin SR, Booth RE. Harvesting autogenous iliac bone grafts. A review of complications and technique. Spine 1989; 14:1324–1331.
30. Summers BN, Einstein SM. Donor site pain from the ilium. A complication of lumbar spine fusion. J Bone Joint Surg 1989; 71-B:677–680.
31. Guini P, Plais PY, Flautre B, Viguier E, Blary MC, Chopin D, Lavaste F, Hardouin P. Experimental model of posterolateral spinal arthrodesis in sheep. Part 2. Application of the model: evaluation of vertebral fusion obtained with coral (Porites) or with a biphasic ceramic (Triosite). Spine 1994; 19: 2798–2803.
32. Holmes R, Mooney V, Bucholz R, Tencer A. A coralline hydroxyapatite bone graft substitute. Preliminary report. Clin Orthop 1984; 188:252–262.
33. Muschler GF, Negami S, Hyodo A, Gaisser D, Easley K, Kambic H. Evaluation of collagen ceramic composite graft materials in a spinal fusion model. Clin Orthop 1996; 328:250–260.
34. Shima T, Keller JT, Alvira MM, Mayfield FH, Dunsker SB. Anterior cervical discectomy and interbody fusion. An experimental study using a synthetic tricalcium phosphate. J Neurosurg 1979; 51:533–538.

35. Yamamuro T, Shikata J, Okumura H, Kitsugi T, Kakutani Y, Matsui T, Kokubo T. Replacement of the lumbar vertebrae of sheep with ceramic prosthesis. J Bone Joint Surg 1990; 72-B:889–893.
36. Zerwekh JE, Kourosh S, Scheinberg R, Kitano T, Edwards ML, Shin D, Selby DK. Fibrillar collagen-biphasic calcium phosphate composite as a bone graft substitute for spinal fusion. J Orthop Res 1992; 10:562–572.
37. Kanayama M, Oguma T, Hatayama A. A minimum three-year follow-up of posterolateral spinal fusion using hydroxyapatite/tricalcium phosphate (HA/TCP) granules and local bone: radiographic and histological evaluation (abstr). ISSLS 1999; 26.
38. Roy-Camille R, Saillant G, Mazel C. Internal fixation of the lumbar spine with pedicle screw plating. Clin Orthop 1986; 203:7–17.
39. Asano S, Kaneda K, Hashimoto T. Reconstruction of iliac crest defect with apatite and wollastonite containing glass ceramic prosthesis. Bioceramic 1992; 5:419–426.
40. Kaneda K, Asano S, Hashimoto T, Satoh S, Fujiya M. The treatment of osteoporotic-posttraumatic vertebral collapse using the Kaneda device and a bioactive vertebral prosthesis. Spine 1992; 17: 275–283.
41. Kitugi T, Yamamoto T, Kokubo T. Bonding behavior of a glass-ceramic containing apatite and wollastonite in segmental replacement of the rabbit tibia under load-bearing condition. J Bone Joint Surg 1989; 72A:264–272.
42. van Loon CJM, de Waal MC, Buma P, et al. Autologous morsellised bone grafting restores uncontained femoral bone defects in knee arthroplasty: an in vivo study in horses. J Bone Joint Surg 2000; 82:436–446.
43. Elias WJ, Simmons NE, Kaptain GJ, et al. Complications of posterior lumbar interbody fusion when using a titanium threaded cage device. J Neurosurg 2000; 93:45–52.

20

SF-36 Health Status and Oswestry Disability Index in Worker's Compensation Patients with Neck Pain

Hwan T. Hee, Thomas S. Whitecloud III, and Leann Myers
Tulane University Medical Center
New Orleans, Louisiana, U.S.A.

I. INTRODUCTION

Spinal disorders exert profound effects on the workforce and the health care resources available [1,2]. Back pain is recognized as a leading presentation of occupational injury in developed countries. Approximately 10% of the cases account for more than 80% of the health care costs for back pain due to their chronicity [3]. Studies have indicated that 80% of the population experiences back pain during their active lives [4]. Recovery from various spinal conditions depends not only on physical factors, but also on psychological factors [5]. Patients receiving compensation are more likely to be influenced by psychological factors [6], thus delaying recovery from back pain [7] and resulting in later return to work [6,8,9,10]. Individual factors are also hypothesized to be associated with chronic occupational back pain [11,12]. In another study, back injury, chronic stress, depression, and age 40–49 years were significantly associated with subsequent chronic back problems [13].

Worker's compensation and litigation negatively affect the postrehabilitation prognosis for chronic back pain [14]. As the ratio of compensation to preinjury wage increases, there is moderate evidence that the duration of the claim increases and that disability is more likely. Compensation status, particularly combined with higher pain intensities, is associated with poor prognosis after rehabilitation treatment programs [15]. Outcomes of posterolateral lumbar fusion among compensated patients are inconsistent, and the outcomes can be predicted by presurgical sociodemographic variables [16]. It has been reported that active worker's compensation and litigation issues are associated with poor operative management results for chronic back pain in adults with low-grade spondylolisthesis [17].

Because of the need to contain the costs of health care pertaining to managing chronic occupational back and neck pain, it is becoming more important than ever to demonstrate that the care being delivered is done in a cost-effective manner. Pain scales or scores are simple measures for assessing outcomes of treatment for spinal disorders. The presence and severity of pain alone is a poor definition of health outcome and physical function. Biomechanical measures, e.g., muscle strength and spinal mobility, may not have direct correlation with patients' symptoms [18]. Three components should be examined in order to better evaluate the severity of back pain: pain, physical impairment, and disability [19].

Various self-completed measures of back pain in current use have demonstrated reliability and validity, including the Oswestry Disability Index (ODI), Roland Morris Disability Scale, Waddell Disability Index, Aberdeen Low Back Pain Scale, Million Visual Analogue Scale, and Low Back Outcome Score. The ODI (Table 1) is a 10-question back pain–specific survey, which takes about 3–5 minutes to complete [20]. The index assesses general functional disability associated with back pain [20]. Scores range from 0 to 100: 0–20 (minimal disability), 20–40 (moderate disability), 40–60 (severe disability), and 60–100 (extremely severe to crippling disability).

The physical and mental health status of worker's compensation patients evaluated for spinal problems have historically received little attention [21]. The patients' perception of their health status is becoming increasingly important in outcomes research [22]. Assessment of the health status of patients receiving worker's compensation may allow identification of patients at higher risk for chronicity and absenteeism from work.

The Short Form Health Survey (SF-36) measures health-related qualities of life [23]. The SF-36 describes both the physical and mental components of health (Tables 2, 3). The 8 scales of the SF-36 are Physical Functioning (PF), role function as limited by physical problems, or Role Physical (RP), Bodily Pain (BP), General Health (GH), Vitality (VT), Social Functioning (SF), role function as limited by emotional problems, or Role Emotional (RE), and Mental Health (MH). Eight primary SF-36 scales form distinct physical and mental health domains [24]. For each of the 8 scales, scores range from 0 to 100, with greater scores reflecting better self-reported health profile. Two standardized summary scales, the Physical Component Summary Scale (PCS) and the Mental Component Summary Scale (MCS), were derived based on the 8 scores of the SF-36 in the general population in the United States [25]. In contrast to the 0–100 scoring used for the 8 individual SF-36 scores, a linear T score transformation was used such that both the PCS and MCS had a mean of 50 and a standard deviation of 10. Higher PCS or MCS scores also imply better self-reported health.

The SF-36 survey has been recommended for spine research because of its brevity, psychometric properties, and wide clinical use with patients who have other chronic medical conditions [26,27]. The ease of use and interpretability of the SF-36 questionnaire shows that it can be a useful adjunct in the assessment of patients with low back pain [27]. The SF-36 is acceptable to patients, internally consistent, and a valid measure of the health status of a wide range of patients [28].

The next section of this chapter will be devoted to the methodology in using these measures to compare two groups of patients with neck pain: patients who received worker's compensation versus those receiving other fomrs of payment.

II. METHODS, RESULTS, AND DISCUSSION

We conducted a cross-sectional study on 2356 patients with neck pain enrolled at first visit in the National Spine Network (NSN) database from January 1998 to April, 2000, inclusive [29]. The NSN, established in February 1995, is a nonprofit organization of 27 spine care centers located throughout the United States. These centers are professionally recognized as international leaders for high-quality patient care and for their commitment to appropriate treatment of spine-related condition. The NSN was formed as a mechanism to foster longitudinal research into the care of spine patients by spine specialists.

The data from our study were derived from the NSN's Initial Visit Health Survey questionnaire, which was completed by patients when first evaluated for neck pain. No criteria were applied to the initial patient selection. The patients answered questions regarding age, gender,

Table 1 Oswestry Disability Index

Section 1: Pain intensity in back and/or legs
- I have no pain
- The pain is very mild
- The pain is moderate
- The pain is fairly severe
- The pain is very severe
- The pain is the worst imaginable

Section 2: Personal care (e.g., washing, dressing)
- I can look after myself normally without causing extra pain
- I can look after myself normally, but it is very painful
- It is painful to look after myself, and I am slow and careful
- I need some help, but manage most of my personal care
- I need help every day in most aspects of self-care
- I do not get dressed, wash with difficulty, and stay in bed

Section 3: Lifting
- I can lift heavy weights without extra pain
- I can lift heavy weights, but it gives extra pain
- Pain prevents me from lifting heavy weights off the floor, but I can manage if they are conveniently positioned (e.g., on a table)
- Pain prevents me from lifting heavy weights, but I can manage light to medium weights if they are conveniently positioned
- I can lift only very light weights
- I cannot lift or carry anything at all

Section 4: Walking
- Pain does not prevent me walking any distance
- Pain prevents me walking more than 1 mile
- Pain prevents me walking more than 1/2 mile
- Pain prevents me walking more than 100 yards
- I can walk only by using a stick or crutches
- I am in bed most of the time and must crawl to the toilet

Section 5: Sitting
- I can sit in any chair as long as I like
- I can sit in my favorite chair as long as I like
- Pain prevents me from sitting more than 1 hour
- Pain prevents me from sitting more than 1/2 hour
- Pain prevents me from sitting more than 10 minutes
- Pain prevents me from sitting at all

Section 6: Standing
- I can stand as long as I want without extra pain
- I can stand as long as I want, but it gives me extra pain
- Pain prevents me from standing more than 1 hour
- Pain prevents me from standing more than 1/2 hour
- Pain prevents me from standing more than 10 minutes
- Pain prevents me from standing at all

Section 7: Sleeping
- My sleep is never disturbed by pain
- My sleep is occasionally disturbed by pain
- Because of pain I have less than 6 hours sleep
- Because of pain I have less than 4 hours sleep
- Because of pain I have less than 2 hours sleep
- Pain prevents me from sleeping at all

Section 8: Sex life (if applicable)
- My sex life is normal, and causes me no extra pain
- My sex life is normal, but causes me some extra pain
- My sex life is nearly normal, but it is very painful
- My sex life is severely restricted by pain
- My sex life is nearly absent because of pain
- Pain prevents any sex life at all

Section 9: Social life
- My social life is normal and causes me no extra pain
- My social life is normal but increases the degree of pain
- Pain has no significant effect on my social life apart from limiting my more energetic interests (e.g., sports)
- Pain has restricted my social life, and I do not go out as often
- Pain has restricted my social life to my home
- I have no social life because of pain

Section 10: Traveling
- I can travel anywhere without pain
- I can travel anywhere, but it gives extra pain
- Pain is bad, but I can manage journeys exceeding 2 hours
- Pain restricts me to journeys of less than 1 hour
- Pain restricts me to short necessary journeys shorter than 30 minutes
- Pain prevents me from traveling except to receive treatment

Section 11: Previous treatment: over the past 3 months, have you received treatment, tablets, or medicines of any kind for your pain?
- Yes
- No

The first 10 questions relate to symptoms. Question 11 does not contribute to the score. Each section is scored from 0 to 5. The final score equals total score for all sections completed/5 × number of sections answered × 100%.
Source: Ref. 20.

Table 2 Brief Description of the SF-36 Scale

SF-36 scale	No. of items	Description
Physical Functioning (PF)	10	Assesses limitations in performing physical activities
Role Physical (RP)	4	Assesses work problems or problems related to other activities of daily living due to physical health
Bodily Pain (BP)	2	Assesses frequency of pain and extent of role interference due due to pain
General Health (GH)	5	Assesses global evaluations of general health
Vitality (VT)	4	Assesses perceived energy level
Social Functioning (SF)	2	Assesses the extent to which mental or physical health interferes with normal social activities
Role Emotional (RE)	3	Assesses problems with work or other daily activities due to mental health
Mental Health (MH)	5	Assesses general mood or affect, including depression, anxiety, and positive well-being
Physical Component Summary (PCS)	35	Assesses the physical aspects of health-related quality of life[a]
Mental Component Summary (MCS)	35	Assesses the mental aspects of health-related quality of life[a]

[a] Each SF-36 item contributes differentially to these scales based on factor analyses of the 8 individual scales.
Source: Ref. 23.

ethnicity or race, marital status, highest education attained, smoking status, comorbidity, current working status, worker's compensation status, disability insurance status, litigation status, previous spinal surgery, presence and duration of symptoms related to the spine. They also completed the standardized, self-administered Medical Outcomes Trust's SF-36 health status questionnaire, and the ODI questionnaire. The treating physicians would then provide information about clinical signs (neurological signs, nonorganic signs, and dermatomal distribution of pain), diagnosis, and management strategies.

The patients were divided into two groups. One group consisted of patients not receiving worker's compensation. The other group included patients receiving worker's compensation. Baseline variables were obtained for all patients in the two groups (Table 4). The variables included age, gender, ethnicity or race, marital status, body mass index, highest education attained, smoking status, current working status, disability insurance status, legal action (none or considering/taken), medical co-morbidities, type of medical institution or hospital (public/private), radiculopathy (no/yes), duration of spine-related symptoms, duration of pain, neurological signs (no/yes), nonorganic or nonphysiological signs (no/yes), dermatomal distribution of pain (no/yes), previous spinal surgery (no/yes). Duration of spine-related symptoms refers to the length of time the patient has one or more of the following symptoms: pain in the spine or radiating pain in the extremities, numbness in the extremities, weakness in the extremities, and/or paresthesia in the extremities. Duration of pain refers to the length of time the patient has spinal pain or radicular symptoms. Dermatomal distribution of pain refers to pain in the extremities that follows particular dermatomal distributions. Radiculopathy refers to pain in the spine that radiates distal to the elbows.

Table 3 Questions and Responses from the 8 Individual Primary Scales of the SF-36

Scale	Questions	Response
PF	Vigorous activities, e.g., running, lifting heavy objects, doing strenuous sports	Yes, limited a lot/Yes, limited a little/No, not limited at all
	Moderate activities, e.g., moving table, pushing vacuum cleaner, bowling, or golfing	
	Lifting or carrying groceries	
	Climbing several flights of stairs	
	Climbing one flight of stairs	
	Bending, kneeling, or stooping	
	Walking more than one mile	
	Walking several blocks	
	Walking one block	
	Bathing or dressing yourself	
RP	Cut down the amount of time you spent on work or other activities	Yes/No
	Accomplished less than you would like	
	Were limited in the kind of work or other activities	
	Had difficulty performing the work or other activities	
BP	How much bodily pain have you had during the past 4 weeks	None/Very mild/Mild/Moderate/Severe/Very severe
	During the past 4 weeks, how much did the pain interfere with your normal work (including both work outside the home and housework)	Not at all/A little bit/ Moderately/Quite a bit/Extremely
GH	In general, would you say your health is:	Excellent/Very good/Good/Fair/Poor
	I seem to get sick a little easier than other people	Definitely true/Mostly true/Don't know/Mostly false/Definitely false
	I am as healthy as anybody I know	
	I expect my health to get worse	
	My health is excellent	
VT	Did you feel full of pep	All the time/Most of the time/A good bit of the time/Some of the time/A little of the time/None of the time
	Did you have a lot of energy	
	Did you feel worn out	
	Did you feel tired	
SF	During the past 4 weeks, to what extent have your physical health or emotional problems interfered with your normal social activities with family, friends, etc.	Not at all/Slightly/Moderately/Quite a bit/Extremely
	During the past 4 weeks, how much of the time have your physical health or emotional problems interfered with your social activities (visiting with friends, relatives, etc.)	All the time/Most of the time/Some of the time/A little of the time/None of the time
RE	Cut down the amount of time you spent on work or other activities	Yes/No
	Accomplished less than you would like	
	Didn't do work or other activities as carefully as usual	
MH	Have you been a very nervous person	All the time/Most of the time/A good bit of the time/Some of the time/A little of the time/None of the time
	Have you felt so down in the dumps that nothing could cheer you up	
	Have you felt calm and peaceful	
	Have you felt downhearted and blue	
	Have you been a happy person	

PF = physical functioning, RP = role physical, BP = bodily pain, GH = general health, VT = vitality, SF = social functioning, RE = role emotional, MH = mental health.

Source: Ref. 23.

Table 4 Demographic Variables and Worker's Compensation Status

	Not W Comp	W Comp	p(diff)[a]
Gender			
Females	1173 (54%)	68 (40%)	0.001
Males	1012 (46%)	103 (60%)	
Ethnicity			
White	1712 (87%)	142 (88%)	ns
Nonwhite	247 (13%)	20 (12%)	
Marital Status			
Married	1295 (66%)	97 (60%)	ns
Widowed	80 (4%)	3 (2%)	
Living with signif. other	96 (5%)	9 (6%)	
Never married	210 (11%)	26 (16%)	
Divorced/separated	279 (14%)	27 (17%)	
Education			
Less than high school	150 (8%)	23 (14%)	0.0001
High school graduate	505 (26%)	69 (43%)	
Some college	566 (29%)	48 (30%)	
College graduate	415 (21%)	14 (9%)	
Post graduate	335 (17%)	8 (5%)	
Smoking Status			
Never smoked	822 (41%)	47 (29%)	0.01
Smoke or quit	1178 (59%)	116 (71%)	
Current smoker	532	74	
Quit $>$ 1 year	576	35	
Quit $<$ 1 year	70	7	
Age			
Sample size	2178	171	0.0001[b]
$\bar{x} \pm$ SD	49.2 $\pm$ 13.4	44.1 $\pm$ 9.2	
Median	48	44	
Body Mass Index			
Sample size	2018	164	0.01[b]
$\bar{x} \pm$ SD	27.0 $\pm$ 5.3	28.3 $\pm$ 5.7	
Median	26.2	27.5	
Currently working			
No	996 (46%)	133 (78%)	0.0001
Yes	1189 (54%)	38 (22%)	
Disability insurance case			
No	2095 (96%)	157 (92%)	0.05
Yes	90 (4%)	14 (8%)	
Legal action			
None	1353 (81%)	62 (44%)	0.0001
Considering/taken	323 (19%)	78 (56%)	
Hospital			
Public	1704 (78%)	118 (69%)	0.01
Private	479 (22%)	53 (31%)	
Duration of symptoms			
$\leq$ 1 year	726 (38%)	84 (52%)	0.001
$>$ 1 year	1189 (62%)	77 (48%)	

(*Continued*)

Table 4 Continued

	Not W Comp	W Comp	p(diff)[a]
Neurological signs			
No	1288 (60%)	98 (58%)	ns
Yes	856 (40%)	72 (42%)	
Nonorganic signs			
No	2056 (96%)	156 (92%)	0.01
Yes	79 (4%)	14 (8%)	
Comorbidities			
No	601 (28%)	39 (23%)	ns
Yes	1584 (72%)	132 (77%)	
Duration of pain			
$<$ 7 weeks	320 (16%)	11 (7%)	0.05
7–12 weeks	200 (10%)	21 (13%)	
3–6 months	358 (17%)	36 (22%)	
$>$ 6 months	1173 (57%)	96 (59%)	
Dermatomal pain			
No	939 (45%)	66 (39%)	ns
Yes	1126 (55%)	104 (61%)	
Radiculopathy			
No	855 (39%)	46 (27%)	0.01
Yes	1330 (61%)	125 (73%)	
Previous surgery			
No	1868 (85%)	139 (81%)	ns
Yes	317 (15%)	32 (19%)	

W Comp = worker's compensation.
[a] Pearson's χ^2 test used to compare group distributions.
[b] ANOVA used to assess mean differences.
ns = not significant; $\bar{x} \pm SD$ = mean $\pm$ standard deviation.
The sum of some subgroups does not equal the total number of worker's or non–worker's compensation cases because not all patients in the NSN database filled up the survey forms completely, i.e., there are missing data for some patients.
Source: Ref. 29.

Group distributions of categorical variables were assessed using Pearson's χ^2 statistic. Differences in means of continuous variables (ODI scores, SF-36 scores, age and body mass index) were assessed using ANOVA methods (Table 4).

The ODI scores, 8 individual item SF-36 scores, as well as the component summary scores (PCS, MCS) were obtained for all study patients, placed in the two previously mentioned groups, and statistically analyzed (Table 5). The difference in means of the 11 scores between the two groups was assessed using F test (ANOVA). If there was evidence of nonnormality among any of the 11 scores, further statistical analyses would be performed using the nonparametric Kruskal-Wallis test.

Of the baseline variables (Table 4), race, marital status, presence of neurological signs, comorbidities, dermatomal pain, and previous surgery to the spine were not significantly different between worker's compensation and non–worker's compensation patients using the $p < 0.05$ criterion. The remaining variables and relevant interactions were used as potential predictors in stepwise linear regression models where the ODI and SF-36 scores were the outcomes and worker's compensation status was forced into the model as a predictor. Table 6 illustrates the

Table 5 SF-36 and ODI Scores (Bivariate Analysis)

	Not Worker's Compensation	Worker's Compensation	p(F)[a]
GH			
n	2135	170	
$\bar{x} \pm SD$	61.9 ± 22.7	59.1 ± 23.1	ns
Median	67	60	
PF			
n	2156	169	
$\bar{x} \pm SD$	58.9 ± 27.9	41.9 ± 25.6	0.0001
Median	65	4/0	
BP			
n	2150	166	
$\bar{x} \pm SD$	35.5 ± 22.2	23.9 ± 17.2	0.0001
Median	33	23	
MH			
n	2150	170	
$\bar{x} \pm SD$	65.0 ± 21.1	56.6 ± 22.6	0.0001
Median	68	60	
SF			
n	2155	170	
$\bar{x} \pm SD$	57.1 ± 29.3	41.0 ± 26.2	0.0001
Median	50	38	
VT			
n	2153	170	
$\bar{x} \pm SD$	42.2 ± 22.9	35.9 ± 22.1	0.001
Median	40	35	
RP			
n	2138	164	
$\bar{x} \pm SD$	24.8 ± 36.4	5.6 ± 21.1	0.0001[b]
Median	0	0	
RE			
n	2121	163	
$\bar{x} \pm SD$	62.1 ± 43.8	41.5 ± 43.2	0.0001[b]
Median	100	33	
PCS			
n	2040	158	
$\bar{x} \pm SD$	35.0 ± 10	30.0 ± 8.0	0.0001
Median	34	29	
MCS			
n	2040	158	
$\bar{x} \pm SD$	45.9 ± 12.3	41.1 ± 13.0	0.0001
Median	48	40	
ODI			
n	2117	169	
$\bar{x} \pm SD$	67.7 + 20.5	53.7 ± 18.8	0.0001
Median	71	53	

[a] Difference in means assessed using F test (ANOVA).

[b] Differences in distribution assessed by F test and nonparametric Wilcoxon test.

GH = General Health; PF = Physical Functioning; BP = Bodily Pain; MH = Mental Health; SF = Social Functioning; VT = Vitality; RP = Role Physical; RE = Role Emotional; PCS = Physical Component Summary; MCS = Mental Component Summary; ODI = Oswestry Disability Index; *n* = sample size; $\bar{x} \pm SD$ = mean ± standard deviation.

Source: Ref. 29.

ODI and SF-36 scores for the two groups after adjustment for the significant demographic covariates. The scores were a reflection of the regression analyses (least squares means).

Records were available for 2356 patients, of which 7% (171 patients) were receiving worker's compensation. The mean age of the 2356 patients was 48.8 (SD 13.2, range 18–91). The mean body mass index was 27.1 (SD = 5.3, range 13.2–57.9). Table 4 summarizes the demographics of the sample population by worker's compensation status. Compared to non–worker's compensation patients, patients receiving worker's compensation were more likely to have the following characteristics: male, education of high school or lower, current/previous smoker, younger age, higher body mass index, currently not working and disabled, currently considering or had taken legal action, initial evaluation at private hospital, presence of radicular symptoms and nonorganic signs, and 1 year or less of symptoms.

Table 5 shows the mean scores, based on worker's compensation status, derived for the ODI scores, 8 individual SF-36 scales, as well as the 2 summary scales (PCS, MCS). Analyses of differences in mean scores between the two groups using F test (ANOVA) revealed that worker's compensation patients scored significantly lower for ODI, all individual items (except General Health) and two component summary scales of the SF-36. The difference was highly significant ($p < 0.001$). Given the nonnormality of the Role Emotional (RE) and Role Physical (RP) scales of the SF-36, differences in these scores between worker's compensation and non–worker's compensation patients were also assessed using the nonparametric test as mentioned in the methodology section. The nonparametric test results were consistent with the ANOVA results (Table 5).

Multivariate analyses using stepwise linear regression methods (Table 6) revealed that, after controlling for confounding covariates, worker's compensation status was still a significant predictor of SF-36 score for Physical Functioning ($p < 0.05$).

The results of this study demonstrate that worker's compensation is associated with significantly lower SF-36 health status. This is the first report, to our knowledge, of the comparison of SF-36 health status scores at initial evaluation between worker's compensation and non–work-

Table 6 Adjusted SF-36 and ODI Scores

	Non–worker's compensation ($\bar{x} \pm SE$)	Worker's compensation ($\bar{x} \pm SE$)	p(F)[a]
GH	59.9 ± 0.6	63.0 ± 1.9	ns
PF	57.5 ± 0.7	52.1 ± 2.2	0.05
BP	34.6 ± 0.6	33.8 ± 1.9	ns
MH	63.2 ± 0.6	63.8 ± 1.8	ns
SF	56.1 ± 0.7	55.5 ± 2.4	ns
VT	40.6 ± 0.7	42.9 ± 2.0	ns
RP	23.9 ± 1.0	19.5 ± 3.1	ns
RE	58.5 ± 1.2	56.5 ± 3.7	ns
PCS	34.6 ± 0.3	33.3 ± 0.8	ns
MCS	44.8 ± 0.4	44.9 ± 1.1	ns
ODI	66.3 ± 0.5	63.3 ± 1.6	0.08

[a] Difference in adjusted means assessed using multiple regression.

ns = not significant, $\bar{x} \pm SE$ = mean ± standard error, GH = General Health, PF = Physical Functioning, BP = Bodily Pain, MH = Mental Health, SF = Social Functioning, VT = Vitality, RP = Role Physical, RE = Role Emotional, PCS = Physical Component Summary, MCS = Mental Component Summary, ODI = Oswestry Disability Index.

Source: Ref. 29.

er's compensation patients suffering from neck pain. The findings were derived from a large database, prospectively gathered from multiple centers specializing in the management of spine patients. As the NSN is a nonprofit organization, no funding arrangements or other considerations applied to the pre-selection of patients into this study. Thus, the worker's compensation population in this study is broadly equivalent to the total worker's compensation population.

Patients receiving worker's compensation had significantly lower Physical Functioning (PF) even after controlling for possible confounding covariates (Table 6). All available potential baseline variables that might confound the results were analyzed in our study. Patients receiving worker's compensation were significantly younger than their counterparts who were not receiving worker's compensation. Age is a significant risk factor for recovery from spinal problems. One study found that patients over the age of 50 returned to work with much less frequency after rehabilitation for chronic back pain [14]. Older age was also associated with increased time receiving benefits in patients with low back pain [30]. One may suggest that this is an indication of the size effect of the worker's compensation status. However, there were other significant baseline variables that were different, such as education and smoking status. Educational standard may be considered as a surrogate for socioeconomic status. There were significantly fewer subjects in the worker's compensation group of higher educational standard, and this is noted to be associated with poorer responses to outcome measurement. Similarly, more worker's compensation patients smoked. By the same argument, these variables were not significant in the multivariate analysis, as one SF-36 scale (PF) was still significantly different between the two groups of patients in our study.

Health-related quality-of-life assessment is gaining importance in the field of spinal research, especially in patient outcomes [31]. It is important to remember that SF-36 scores represent self-reported, and not objective data of the patients. The significant associations between lower SF-36 health status and worker's compensation may imply the need to assess the functional status of these patients when they are first evaluated for their cervical spinal disorders. The cause of poor treatment outcomes for worker's compensation patients with spinal disorders is debatable. One study focused on outmoded rehabilitation methods as a possible role [9]. In a worker's compensation venue, outmoded postoperative rehabilitation methods may be responsible for suboptimal outcomes after spinal surgery for degenerative conditions [9]. Another study found that in chronic low back pain, compensation involvement may adversely affect self-reported pain, depression, and disability before and after rehabilitation [32]. Psychological factors may have a profound influence on self-perceived general well-being and disability from back pain [33]. Poorer treatment outcomes in worker's compensation patients after surgery or rehabilitation, or both, may result from initial lower perceived health-related quality of life in these patients.

The relevance of these data has possible implications in clinical practice. First of all, using the initial visit SF-36 scores, we can identify which scores of the SF-36 are low in the worker's compensation patient before any treatment is instituted [34]. Most SF-36 scores, especially the physical domain scales, were associated with the variables of return to work, work retention, and use of health care resources [31]. One study demonstrated a relationship between preoperative SF-36 assessment of pain, social function, and mental health, and increased likelihood of a subsequent surgical procedure [35]. Further research may allow us to use first-visit SF-36 scores to predict which worker's compensation patient is at risk of chronicity, absenteeism, and poor treatment outcomes before any treatment is instituted. The criteria for successful outcome may have to be modified for this high-risk cohort group. A more realistic treatment goal may be required in managing these patients.

At the same time, active rehabilitation intervention strategies designed to improve physical and mental well-being should be promoted, as they could have an impact on enhancing positive

health outcomes [36]. Stress management, psychological counseling, and group therapy may help to improve the mental health of these patients. Interventions should be focused on psychosocial aspects such as health behavior and job satisfaction, and on the economic incentives for return-to-work [37]. Based on our study, perceived physical factors are just as important in the overall functional status and well-being of patients receiving worker's compensation. Treatment measures should include teaching skills to improve their overall quality of life, especially Physical Functioning (PF). Strategies to improve their Physical Functioning (PF) may involve work hardening and general physical fitness programs. Involvement of the immediate family members is helpful. Managing these patients usually involves a multidisciplinary approach [38]. A population-based strategy of providing positive messages about back pain improves population and general practitioner beliefs about it. This seems to influence medical management and reduce disability and worker's compensation costs related to back pain [39].

In spite of the common presumption that spine surgery patients fare poorly in a worker's compensation environment, one study showed that such patients can show remarkably successful objective outcomes if accompanied by effective rehabilitation [9]. Another large cohort study of outcomes in chronically disabled patients with work-related cervical spinal disorder produced results similar to those found in tertiary functional restoration rehabilitation in chronic lumbar spinal disorder [40]. Although measures to improve the physical and mental well-being of worker's compensation patients are beneficial, further studies may be needed to support our findings and treatment approaches.

The strengths of our study are several. First of all, this is the first report comparing the SF-36 health status scores between worker's compensation and non–worker's compensation patients with neck pain at initial evaluation. The study consists of a large prospectively gathered database of spinal patients evaluated at reputable centers that made up the National Spine Network. The establishment of the NSN has been a major step forward in spine research. The unique resource of the National Spine Network allowed us to gather data from various locations throughout the United States. The data are based on a large, diverse pool of 2356 patients. The size and spectrum of the data allowed us to analyze, with detail and by controlling for all available potential confounding covariates, the effect of worker's compensation status on the health status of these patients. Many possible covariates that might confound the study results were taken into account, e.g., smoking status, body mass index, educational level, litigation status, and presence of nonorganic signs. In our assessment study it appears that the primary focus is that the SF-36 scores can be used to objectively identify ''the patient at risk.'' Of course, further prospective studies need to be performed to confirm this finding.

One of the major findings of this study was that, although there were many differences in SF-36 scores between the worker's compensation and non–worker's compensation groups, only one scale (Physical Functioning) was significantly predicted following multivariate analysis. Our study demonstrated the significant impact of various confounding factors or variables on the measurement of disability and health status in patients with neck pain or other spine-related conditions. In the group analysis, worker's compensation patients were found to be significantly different in many of the baseline variables. These differences were subsequently found to be associated with many of the commonly recognized confounding factors. One of the principal difficulties in the assessment of effective treatment in these patients has been making a clear and accurate description of the patient group undergoing treatment. The value of this study, we believe, lies in the clear demonstration that confounding factors can have a major effect on the values (SF-36 scores) obtained on normal validated instruments. Our study also defines the requirements when describing a patient population for a prospective study.

One study revealed that there was substantial overlap between generic versus region-specific functional status measures on patients with cervical spine disorders [41]. Thus, it may appear that the use of both measures is probably not necessary.

The study also has several limitations. As a cross-sectional study, temporal relationships cannot be addressed, nor can causality. Although we controlled for all available potential confounders, there may be others for which data were not available. Finally, given the large sample size, very small differences may be statistically significant. As with any study, statistical significance should not be confused with clinical significance.

ACKNOWLEDGMENTS

We would like to acknowledge The National Spine Network (NSN) for allowing us access to the database. Our research would not be possible without the help of Brett Hanscom, MS of the National Spine Network.

Acknowledgments are also made to Elsevier Science for permitting us to use contents from The Spine Journal, Vol 1, Hee HT et al., SF-36 health status of workers compensation cases with spinal disorders, pages 176–182, 2001.

Acknowledgments are also made to Springer-Verlag for permitting us to use contents from European Spine Journal, Do worker's compensation patients with neck pain have lower SF-36 scores? Hee HT et al., Vol 11, pages 375–381, 2002.

REFERENCES

1. Bigos SJ, Battié MC. The impact of spinal disorders in industry. In: Frymoyer JW, ed. The Adult Spine: Principles and Practice. 2nd ed.. Philadelphia: Lippincott-Raven Publishers, 1997:151–162.
2. Frymoyer JW, Durett CL. The economics of spinal disorders. In: Frymoyer JW, ed. The Adult Spine: Principles and Practice. 2nd ed.. Philadelphia: Lippincott-Raven Publishers, 1997:143–150.
3. Murphy PL, Courtney TK. Low back pain disability: relative costs by antecedent and industry group. Am. J. Ind. Med 2000; 37:558–571.
4. Kelsey JL, White AA. Epidemiology and impact of low back pain. Spine 1980; 5:133–142.
5. Waddell G. A new clinical model for the treatment of low back pain. Spine 1987; 12:632–641.
6. Repko GR, Cooper R. A study of the average worker's compensation case. J. Clin. Psychol 1983; 39:287–295.
7. Greenough CG, Fraser RD. The effects of compensation on recovery from low back pain. Spine 1989; 14:947–955.
8. Guck T, Meilman P, Skultety F, Dowd E. Prediction of long-term outcome of multidisciplinary pain treatment. Arch. Phys. Med. Rehabil 1986; 67:293–296.
9. Mayer T, McMahon MJ, Gatchel RJ, Sparks B, Wright A, Pegues P. Socioeconomic outcomes of combined spine surgery and functional restoration in worker's compensation spinal disorders with matched controls. Spine 1998; 23:598–606.
10. Sander R, Meyers J. The relationship of disability to compensation status in railroad workers. Spine 1986; 11:141–143.
11. Fransen M, Woodward M, Norton R, Coggan C, Dawe M, Sheridan N. Risk factors associated with the transition from acute to chronic occupational back pain. Spine 2002; 27:92–98.
12. Volinn E, van Koevering D, Loeser JD. Back sprain in industry: the role of socioeconomic factors in chronicity. Spine 1991; 16:542–548.
13. Perez CE. Chronic back problems among workers. Health Rep 2000; 12:41–55.
14. Fredrickson BE, Trief PM, VanBeveren P, Yuan HA, Baum G. Rehabilitation of the patient with chronic back pain. A search for outcome predictors. Spine 1988; 13:351–353.
15. Teasell RW. Compensation and chronic pain. Clin. J. Pain 2001; 17:S46–S64.
16. DeBerard MS, Masters KS, Colledge AL, Schleusener RL, Schlegel JD. Outcomes of posterolateral lumbar fusion in Utah patients receiving workers' compensation: a retrospective cohort study. Spine 2001; 26:738–746.

17. Vaccaro AR, Ring D, Scuderi G, Cohen DS, Garfin SR. Predictors of outcome in patients with chronic back pain and low-grade spondylolisthesis. Spine 1997; 22:2030–2034.
18. Holt AE, Shaw NJ, Shetty A, Greenough CG. The reliability of the low back outcome score for back pain. Spine 2002; 27:206–210.
19. Waddell G, Main CJ. Assessment of severity in low back disorders. Spine 1984; 9:204–208.
20. Fairbank JC, Couper J, Davis JB. The Oswestry low back pain disability questionnaire. Physiotherapy 1980; 66:271–273.
21. Beaton DE, Bombardier C, Hogg-Johnson SA. Measuring health in injured workers: a cross-sectional comparison of five generic health status instruments in workers with musculoskeletal injuries. Am. J. Ind. Med 1996; 29:618–631.
22. Liang MH, Katz JN, Phillips C, Sledge C, Cats-Baril W. The American Academy of Orthopaedic Surgeons Task Force on outcome studies. J. Bone Joint Surg. (Am) 1991; 73:639–646.
23. Ware JE, Sherbourne CD. The MOS 36-item short-form health survey (SF-36). Conceptual framework and item selection. Med Care 1992; 30:473–483.
24. Ware JE, Snow KK, Kosinski M, Gandek B. SF-36 Health Survey: Manual and Interpretation Guide. Boston: The Health Institute, New England Medical Center, 1993.
25. Ware JE, Kosinski M, Keller SD. SF-36 Physical and Mental Health Summary Scales: A user's Manual. Boston: The Health Institute, New England Medical Center, 1994.
26. Flores S, Gatchel RJ, Polatin PB. Objectification of functional improvement after non-operative care. Spine 1997; 22:1622–1633.
27. Taylor SJ, Taylor AE, Foy MA, Fogg AJB. Responsiveness of common outcome measures for patients with low back pain. Spine 1999; 24:1805–1812.
28. Garratt AM, Ruta DA, Abdalla MI, Buckingham JK, Russell IT. The SF36 health survey questionnaire: an outcome measure suitable for routine use within the NHS? Br Med J 1993; 306:1440–1444.
29. Hee HT, Whitecloud TS, Myers L, Roesch W, Ricciardi JE. Do worker's compensation patients with neck pain have lower SF-36 scores? Eur. Spine J 2002; 11:375–381.
30. McIntosh G, Frank J, Hogg-Johnson S, Bombardier C, Hall H. Prognostic factors for time receiving worker's compensation benefits in a cohort of patients with low back pain. Spine 2000; 25:147–157.
31. Gatchel RJ, Mayer T, Dersh J, Robinson R, Polatin P. The association of the SF-36 health status survey with 1-year socioeconomic outcomes in a chronically disabled spinal disorder population. Spine 1999; 24:2162–2170.
32. Rainville J, Sobel JB, Hartigan C, Wright A. The effect of compensation involvement on the reporting of pain and disability by patients referred for rehabilitation of chronic low back pain. Spine 1997; 22:2016–2024.
33. Oleske DM, Andersson GBJ, Lavendar SA, Hahn JJ. Association between recovery outcomes for work-related low back disorders and personal, family, and work factors. Spine 2000; 25:1259–1265.
34. Hee HT, Whitecloud TS, Myers L, Gaynor J, Roesch W, Ricciardi JE. SF-36 health status of workers compensation cases with spinal disorders. Spine J 2001; 1:176–182.
35. Glassman SD, Dimar JR, Johnson JR, Minkow R. Preoperative SF-36 responses as a predictor of reoperation following lumbar fusion. Orthopaedics 1998; 21:1201–1203.
36. Oleske DM, Andersson GBJ, Lavendar SA, Hahn JJ. Association between recovery outcomes for work-related low back disorder and personal, family, and work factors. Spine 2000; 25:1259–1265.
37. Van der Giezen AM, Bouter LM, Nijhuis FJ. Prediction of return-to-work of low back pain patients sicklisted for 3 to 4 months. Pain 2000; 87:285–294.
38. Lanes TC, Gauron EF, Spratt KF, Wernimont TJ, Found EM, Weinstein JN. Long-term follow-up of patients with chronic back pain treatment in a multidisciplinary rehabilitation program. Spine 1995; 20:801–806.
39. Buchbinder R, Jolley D, Wyatt M. Population based intervention to change back pain reliefs and disability: three part evaluation. Br Med J 2001; 322:1516–1520.
40. Wright A, Mayer TG, Gatchel RJ. Outcomes of disabling cervical spine disorders in compensation injuries. A prospective comparison to tertiary rehabilitation response for chronic lumbar spinal disorder. Spine 1999; 24:178–183.
41. Riddle DL, Stratford PW. Use of generic versus region-specific functional status measures on patients with cervical spine disorders. Phys. Ther 1998; 78:951–963.

21
Interbody Fusion in the Elderly

Lee D. Hieb
Consultant
Yuma, Arizona, U.S.A.

I. INTRODUCTION

Spinal surgeons, and indeed all physicians in America, are confronting an aging population. Patients are not only living longer, they are expecting a higher quality of life. Indeed, people over 90 years of age constitute the fastest growing segment of society. Very athletic, healthy 80-year-olds may request surgery to resume activities such as swimming or tennis. Spinal fusion in an elderly population may be indicated for a variety of conditions but has often been avoided due to the intraoperative and postoperative complications. It has been my experience treating a large number of geriatric patients that interbody fusion has fewer complications and offers significant advantages in this population. In this chapter I will examine the various indications for spinal fusion in the elderly, the potential role of interbody stabilization in this population, as well as my experience with techniques, complications, and outcome.

II. GENERAL CONSIDERATIONS

Most fusion literature lumps all patients together or concentrates on younger patients. But surgery on the elderly is different in many ways from surgery on younger patients. Elderly spines behave differently than those of 30 year olds. Healing potential and bone growth potential are diminished. Intercurrent diseases (most importantly diabetes and the ravages of a lifetime of smoking) are often significant and make recovery times longer and more unpredictable. Many of the orthopedic techniques learned in training on 30-year-olds do not work when applied to 70-year-olds. Recent studies confirm the common wisdom that the elderly suffer more complications following classic posterolateral fusion surgery than younger patients [1]. Because of this, prophylactic fusion to prevent instability after decompression (or fusion for lumbar pain) has been avoided in older people, even when it would have been recommended in younger patients [2,3].

In some ways, surgery on elderly patients is much more straightforward. Most ''hidden agendas'' that influence outcomes in working-aged patients have been left behind in the process of maturation. The geriatric spinal surgeon spends less time sorting out worker's compensation claims or disability, alleviating fears of reinjury at work, detecting spousal manipulation, or other reasons for secondary psychosocial gain. Most elderly patients are highly motivated to get well and maximize their function to remain independent. This makes assessment of clinical outcomes much easier. There is no more grateful patient than the elderly person returned to the dance floor after years of progressive inability to walk.

There is, however, no more disappointed patient than the elderly stenosis patient who was relieved of pain for a time, only to have recurrent leg pain due to segmental collapse of the spine. It is this group of older ''failed-back'' patients that has sparked an interest in fusion techniques in the elderly. Every new spinal surgeon's waiting room first fills with surgical failures who flock to his or her doorstep for a ''miracle cure.'' In my retirement community, many of these patients were over 75 years old and displayed a variety of ''up-down'' stenosis, fixed or dynamic lateral recess stenosis or true spondylolisthesis. Clearly these patients were the tip of the surgical ''iceberg,'' since most patients are cured of their degenerative stenosis with the first operation. True instability after laminectomy does not exceed 2% according to the literature [4,5], but this may not consider the more subtle forms of instability and lateral recess compromise as described by Farfan et al. [6], Kirkaldy-Willis and Farfan [7], Burton et al. [8], and others (for review, see Ref. 9). It has been my experience, as well as others, that the true rates of deterioration require longer periods of observation than are generally reported [10].

Several authors have supported the notion that fusion at the time of decompression increases the likelihood of a good or excellent result [2,10–12]. Because most patients in these studies were treated with some variant of posterolateral fusion, the potential for morbidity excluded many patients from consideration. ''Prophylactic fusion'' becomes more acceptable if the morbidity from the fusion is minimal. The decision to fuse, ignoring for the moment cost, must take into account (1) the probability of failure occurring, (2) the magnitude of failure if it occurs (the significance to the patient), (3) the ability to treat the decompensated unfused spine, and (4) the added morbidity to the patient of prophylactically stabilizing the spine during decompression. Although an exact formula is not possible, it is clear that reducing the morbidity of the fusion allows us to accept less risk of failure (i.e., the threshold for fusion can be lowered) [13]. In 1980, when discussing the ''ideal'' fusion, Farfan, wrote that the fusion should be

> limited to the single injured joint. It would restore torque strength to near normal, correct any deformity at this joint, and fix the joint in the position of function, preferably without the aid of internal fixation. ⋯ The fusion should not extend the operating time substantially, nor should the morbidity be unduly prolonged. A mere additional half-hour of anaesthesia or a prolonged convalescence does not justify the difficulties the patient might experience if a fusion was not done when judged essential. There is no spinal fusion that meets all of these ideal conditions.

III. PROBLEMS OF POSTEROLATERAL FUSION IN THE ELDERLY

Classic posterolateral fusion, at one level, without internal fixation results in union approximately 80–85% of the time, and the rate can be improved 5–10% with pedicular instrumentation. Multiple level fusions benefit even more from segmental fixation. But screw rod constructs are not without problems. Because the pedicle of the upper end of the fusion lies in the vicinity of the unfused facet above, the screw head or the rod may lie within or abut the facet capsule of the superior unfused joint. Pedicle screws attach to bone that is often porotic in the elderly patient. The pullout strength of the device attached to the pedicle in osteoporotic bone is lessened [15,16]. Hook rod constructs are similarly affected, as laminar osteoporosis can lead to cutout of the end hooks. This can be particularly devastating in frail patients with little subcutaneous tissue—the metal can perforate the skin or at least create a prominent painful mass in the back.

Additionally, posterolateral fusions with internal fixation, even in very capable hands, necessitate significant retraction and dissection of soft tissues. Mean blood loss for one- and two-level fusions as reported in a recent large multicenter study was 665 mL (max = 1560 mL) in noninstrumented fusions and 1284 mL (max = 2409 mL) in pedicle screw fusions.

Operating times in this series ranged from 62 to 271 minutes. Prolonged operative times, blood loss, and concomitant fluid shifts are poorly tolerated in elderly patients. Tissue dissection also leads to postoperative pain, and narcotic pain medications in the elderly are difficult to titrate. Narcotic levels sufficient for pain control are more apt to lead to confusion in older patients due to the slower clearance of the drug's metabolites.

IV. THE CASE FOR INTERBODY FUSION IN THE ELDERLY

There are a number of theoretical advantages of interbody fusion in the elderly. The biomechanical advantages of fusion through the mechanical axis have long been appreciated. Although an interbody fusion is close to the center of rotation, physiological torsional stability with threaded devices is achieved. As Farfan desired, the fusion is limited to the affected levels. The facet joints above the fusion are not harmed by metal implants. Specifically important in the elderly, interbody devices attach to endplate bone, which has been shown to be preserved even in the face of severe osteoporosis [17,18], and so may result in fewer metal-related complications. Since the interbody technique does not require wide exposure to the transverse processes, tissue trauma, blood loss, and pain is lessened. Finally, in patients with previous surgery, stabilization and distraction of the neural foramina can sometimes be done from the front, thereby avoiding reexploration of a scarred dura.

V. EXPERIENCE WITH INTERBODY FUSION

Recently 237 personal cases of interbody fusions were reviewed. Seventy-one patients who were 2 years from the date of surgery and were 55 years old or older at the time of surgery were selected for special consideration. The ages in this cohort ranged from 55 to 85, with a mean age of 67.9 years. The age of 55 years was chosen for inclusion in the study because by this age many of the comorbidities of aging, such as osteoporosis, hypertension, coronary artery disease, and chronic obstructive pulmonary disease, have become established. Nineteen patients underwent anterior interbody fusion alone through a paramedian retroperitoneal approach. Thirty patients underwent anterior lumbar interbody fusion through a retroperitoneal approach followed by immediate posterior decompressive laminectomy. Twelve patients underwent decompression and posterior lumbar interbody fusion (PLIF). Neither low bone mineral density, calcification of the great vessels, nor previous posterior surgery were considered contraindications in patients who were symptomatic enough to warrant operative intervention. Morbidly obese patients were not excluded but were generally avoided. When surgical intervention could not be avoided, only posterior procedures were performed. All surgery was performed by the author. There were 36 one-level, 27 two-level, and 8 three-level stabilizations. Eleven percent of patients were diabetic and 17% were smokers.

Mean surgery time in this series in the anterior lumbar interbody fusion (ALIF) group was 2 hours and 40 minutes, in the PLIF group 3 hours and 23 minutes, and in the combined ALIF-decompressive laminectomy (DL) group 3 hours and 2 minutes. (Subsequently, however, with increased experience in the techniques, mean times have drastically decreased. A single-level lumbar decompressive laminectomy that would normally take 55 minutes, now adds only an additional 20 minutes for a total operating time of 1 hour and 15 minutes.)

The procedures were tolerated well in these patients. Only three patients had major complications. One patient developed aspiration pneumonia, from which she recovered. She and two other patients developed hernias at the site of their anterior retroperitoneal approaches, which required revision with mesh grafts. There were no cage migrations and no deaths in this series.

In spite of compression manipulation of the great vessels, no deep venous thrombosis or embolic complications occurred.

Mobilization was quite remarkable in this entire group of patients. As more and more patients were being stabilized at the time of surgery, the nursing staff on the surgical ward commented that patients were easier to mobilize and were feeling better sooner in their postoperative course. In many cases the combined anterior interbody fusion decompressive laminectomy patients were discharged sooner than the simple posterior laminectomy patients. All patients were mobilized on the first postoperative day. None were braced. Mean hospitalization was 3.9 days. Mean blood loss in the group was 274 cc, and in the combined ALIF-DL group 347 cc. Overall blood loss in the PLIF group was 579 cc, but with experience in the technique this blood loss has significantly decreased. Implementation of an ''outside-in'' facet take-down technique (as described later) led to the diminished blood loss. In the last 10 PLIF cases, mean blood loss was 265 cc. This includes both single and multilevel cases.

Sixty-five of the 71 patients were available for follow-up at 2 years. Preoperatively 4 patients were nonambulatory from weakness and leg pain. Postoperatively all these patients were ambulatory, with only one patient using an assistive device. Overall, patients improved both back and leg symptoms, although in most cases back pain was not the primary indication for surgery. In this series there were 4 patients whose symptoms were clearly not relieved by the surgery. One patient had stabilization of an L4-L5 spondylolisthesis and decompressive laminectomy at that level, but continued to have unilateral leg pain that subsequently responded to decompression of a far out extraforaminal stenosis at L5-S1. Another patient had unusual L4 dermatomal pain and was thought to have lateral recess stenosis which did not resolve after decompression. A third patient developed generalized fatigue and multifocal pain that overshadowed any stenotic sciatic symptoms. A fourth patient with classic stenosis and spondylolisthesis failed to resolve after decompression and stabilization. No clear reason for this failure was identified.

In this series I looked specifically at bowel and bladder complaints because it has been my impression that slowly developing cauda equina syndrome is very common in the elderly with stenosis. Seventeen (24%) of the patients had developed some sort of bowel or bladder complaints. In 15 patients this was retention of urine or incontinence of bowel or bladder. Two patients reported increasing constipation unrelated to pain medication. Postoperatively only 4 (6%) of the patients reported continued bowel or bladder complaints.

In sum, interbody fusion with titanium threaded cages is not only well tolerated physiologically, but leads to good patient outcomes.

VI. SUBSIDENCE

Subsidence, or settling of the disc endplates around the cages, is a topic of much current debate. There is, however, no generally accepted method for measuring subsidence after lumbar interbody fusion. The first difficulty is determining the baseline to which other measurements will be compared. Preoperative films are not adequate for measuring disc heights, because the goal of surgery is often to distract the disc space. Intraoperative films may not be acceptable for measuring disc height because gravity is eliminated with the patient prone. A certain amount of disc compression occurs immediately upon assumption of upright stance. Presumably, however, this would be the best baseline measurement, but it is not practical to have patients stand for x-rays on their first foray from bed. Additionally, when settling or subsidence does occur postoperatively, it may not occur uniformly across the disc space. Measuring the top of the entire construct (from the superior endplate of the top of the fusion level to the inferior endplate

of the bottom of the fusion level) may not realistically reflect what is happening at the disc space. Measuring the disc heights between the endplate above and endplate below immediately behind the cage, using the cage as an index to magnification, is one possible technique. However, as fusion progresses with time, the endplates become blurred and the disc space obliterated. In the above series subsidence was assessed as follows: the posterior rim of the cage was measured and became the index for magnification of the films. The disc height was measured directly behind this posterior aspect of the cage. All films preoperatively as well as postoperatively were done standing. Subsidence was able to be measured with some confidence at 61 levels in 44 patients.

Theoretically, subsidence should be lessened if endplate bone is preserved. In the past, the recommend technique for performing interbody fusion has involved placing sequentially larger distraction ''plugs'' until firm retention of the ''plug'' is reached. Because elderly spines have more lax ligamentous structure around them, the disc can easily be overdistracted without attaining this endpoint. (It had been my experience that soft tissues will allow distraction of the spine anteriorly to the point of breaking the pars posteriorly during an ALIF.) Additionally, placing too large a distraction plug results in overreaming the space. This removes the only good- quality bone left in the osteoporotic patient. Therefore, pullout strength is not the best endpoint to gauge cage size in the elderly. Rather, carefully templating and obtaining reasonable stability of the distraction plug is more prudent. Using this technique in over 200 patients I have had no cage migration. In the series noted above (examining 61 levels) mean subsidence was 2 mm. Finally, we should ask the question: Since a narrowed disc generally increases stability, why is subsidence important? Subsidence is really only important in maintaining the interpedicular distance to avoid pinching of the nerve roots as they exit the spinal canal and in restoring or maintaining sagittal contour. Depending on the geometry of the canal and the size of the foramen relative to the disc height, the importance of this may vary from patient to patient, but in general it seems reasonable to avoid settling of the disc space.

VII. CHOICE OF SURGICAL APPROACH

Interbody fusion may be performed anteriorly (laparoscopically or through a variety of open approaches) or posteriorly (either as a classic PLIF utilizing two cages on either side of the midline, or transforaminally, inserting a single cage obliquely through the lateral aspect of the disc space). At the present time the choice is made usually on the basis of surgeon experience and preference for technique. However, some generalizations may be made.

The limited paramedian retroperitoneal approach is very adaptable to older patients. Two major benefits of this technique are apparent. In patients with previous lumbar surgery for whom stabilization alone is required, this approach avoids the tedious dissection of scar from dura and surrounding structures. This approach will allow distraction of the disc space and thus the neural foramina and has been successfully used to salvage postdecompression lateral recess stenosis. Pain from an anterior approach is rarely prolonged and is not confused with the preoperative pain. Therefore, often an immediate symptomatic benefit of stabilization can be detected. Patients will remark that, although they may have some incisional pain, their longstanding back pain has been relieved. Bowel recovery and mobilization were quite good in patients treated via the anterior approach. Some patients were able to be discharged at 48 hours. Average hospitalization, however, in our series remains 3 days. Hernia at the surgical site was a problem in three of the 49 ALIF patients in our review.

Grade II spondylolisthesis and very mobile Grade I spondylolisthesis are best stabilized through an anterior approach. Even when decompression is required and is done through a

separate posterior approach, the facets can be preserved with a minimum of undercutting to provide a checkrein to further slippage. In personal communication, several surgeons have reported further slippage after posterior interbody fusion of a Grade I mobile spondylolisthesis.

VIII. SURGICAL TECHNIQUE

The patient is placed supine over a lumbar bolster to slightly hyperextend the spine. A paramedian approach is performed through a vertical incision two finger breadths to the left of midline. (Some surgeons prefer a transverse or oblique incision, but the vertical incision is truly extensile and can be used for multilevel procedures.) The length of the incision for one level-fusion need be only the width of the surgeon's hand. To approach the L5-S1 level, the incision is centered on a point halfway between the umbilicus and pubis. An L4-L5 disc is approached through an incision centered on a point below the umbilicus one fourth of the distance to the pubis. The anterior rectus sheath is incised vertically but slightly lateral to the line of the skin incision. The rectus muscle is then retracted medially. The inferior rectus sheath is then carefully incised vertically and separated from the underling peritoneum using metzenbaums and kitners. If the peritoneum is too thin or adhered to the sheath, it is sometimes helpful to begin the incision more laterally or inferiorly.

The peritoneum is then swept medially and held with a self-retaining retractor. We use a Thompson retractor attached to the table, placing long narrow reinforced blades medially, a thicker reinforced blade superiorly, and a short curved blade laterally retracting the skin and subcutaneous tissue. To approach the L4-L5 disc, the soft tissue is carefully dissected from the left common iliac. The ascending lumbar vein is identified as it descends into the pelvis from a point approximately 2–3 cm inferior to the bifurcation. Two vascular clips are applied distally and one proximally before dividing the vessel. The great vessels are then retracted medially with kitners, thereby placing the adventitial tissue adherent to the disc and anterior longitudinal ligament in tension. This tissue is then released with cutting cautery. Usually, the segmental vessels at L4 are clipped and divided.

To determine the true midline of the disc, the table is leveled until on fluoro image the pedicles appear equal and oval. A small vertical incision is made in the midline of the disc. A silk ligature is tied to a washer and placed over a short screw, which is then inserted into the rent in the annulus. After the fluoroscopic image or x-ray is obtained, the vessels are carefully retracted to avoid catching on the head of the screw. The midline is marked with cautery and the screw removed with a right angle clamp and traction on the ligature. This technique avoids the problem of obliquity of the beam when using a long k-wire to mark the midline.

Several points deserve emphasis. The great vessels in elderly patients may be quite friable. That, in combination with prevertebral adhesion of the anterior longitudinal ligament to the vessels, may make moving the great vessels, challenging. When adhesions are encountered, extreme caution must be taken not to sheer the posterior wall of the common iliac—an event that tends to raise the blood pressure of even the most fearless of surgeons. Having an assistant—preferably a vascular surgeon—gently retract the great vessels with kitners and inserting the cages through a single barrel drill tube will decrease the time these delicate great vessels are in compression. The ascending lumbar vein should be ligated in all cases of L4-L5 fusion. Occasionally a small accessory vein comes off the ventral surface of the left common iliac and, if not recognized, can tether and tear the iliac with retraction across the midline. Anterior laparoscopic surgery has been widely used, however, to date, no series in elderly patients has been reported. Given the delicacy of elderly vessels and the difficulty of stopping bleeding through a laparoscope, it is my inclination not to use the technique in the elderly.

The most obvious benefit of the posterior approach is that it allows decompression as well as fusion to be done through one incision. However, early in the series it seemed easier to perform an ALIF and secondary decompression at the same sitting rather than a PLIF. Techniques to avoid bleeding and to efficiently remove bone have greatly lessened operating time and trauma to both the patient and the surgeon such that I now do nearly all fusions from a posterior approach. Whether inserting two cages from a straight posterior approach or a single oblique cage, the major challenge of the approach is maintenance of hemostasis while gaining access to the lateral posterior disc space.

Most bleeding occurs from veins clustered under the facet. If a standard laminectomy is done from the midline out, bleeding from these vessels begins at a time when the surgeon does not have adequate access to cauterize them. I now routinely use an ''outside-in'' facet takedown technique: The dissection is begun in the midline, but the lateral lamina is retained (Fig. 1). Using a small round burr (Fig. 2) the facet is then drilled from the *outer* portion of the facet *into the midline* until the facet is a thin cup-shaped surface. The dura is protected by the medial facet and remnant lamina. At this point (Fig. 3) a Kerrison can be used to quickly remove the remaining lamina and medial facet. Because it only takes two or three bites of the kerrison at this point, pressure and bipolar cautery can be quickly applied to stop bleeding. The plexus of cauterized vessels is then divided with a 15 blade and packed away with cottonoids to expose the lateral disc space (Fig. 4).

A major benefit of this approach is the ability to stabilize the unexpectedly mobile spine. Large spinal fusions require large planning—blood donation, informed consent, scheduling more

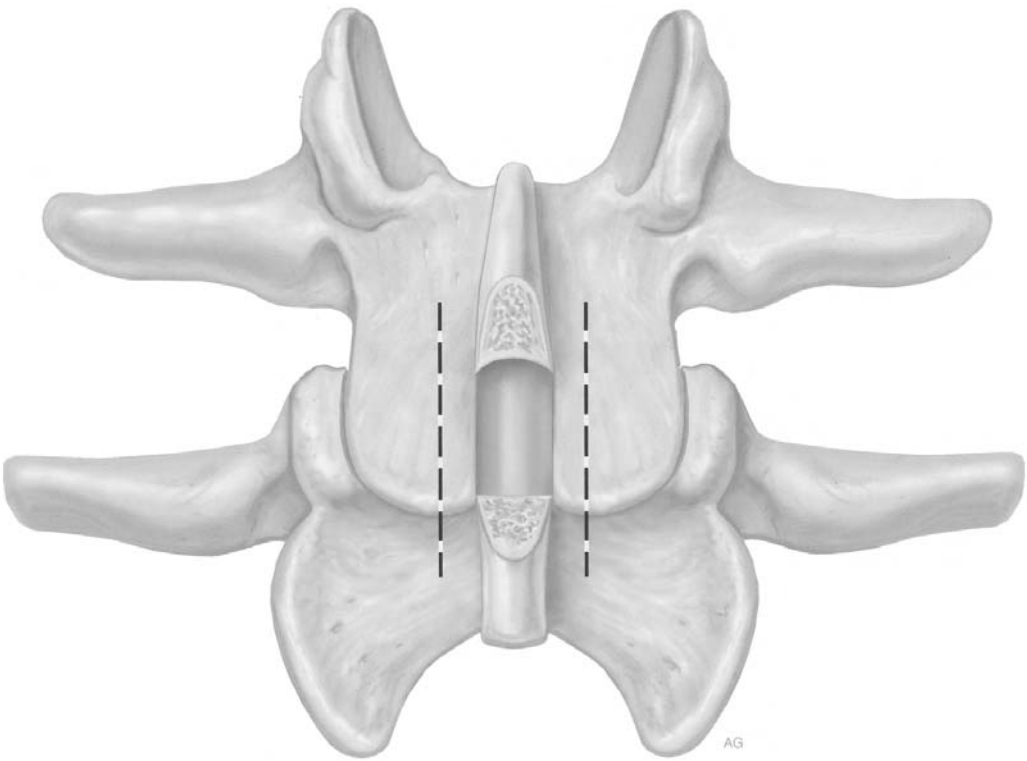

Figure 1 The dissection is begun in the midline, but the lateral lamina is retained.

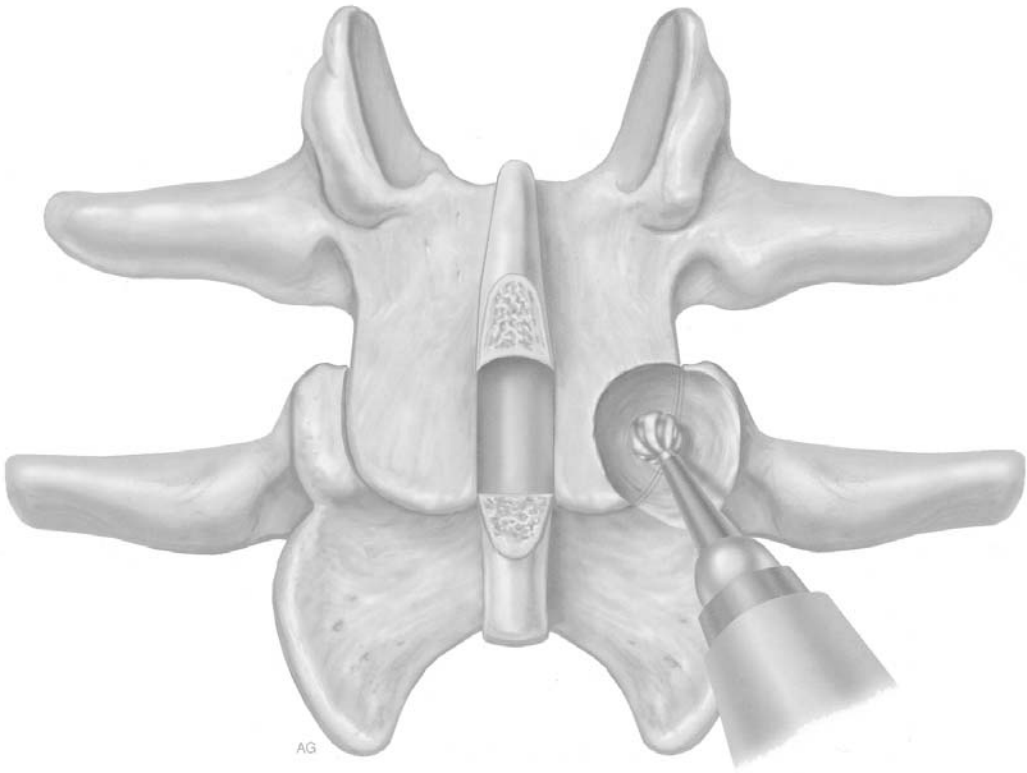

Figure 2 Using a small round burr, the facet is drilled from the *outer* portion of the facet *into the midline* until the facet is a thin cup-shaped surface.

operating room time, etc. When fusions involve pedicular instrumentation, or at the least a large iliac crest graft and expanded dissection, a decision to fuse can rarely be made during surgery should an unexpected spondylolysis or area of hypermobility be encountered. Using the interbody technique it is possible to stabilize a hypermobile segment with essentially no additional blood loss, adding approximately 15 minutes. to the procedure (if one transforaminal cage is inserted; or 30 minutes. additional time for a standard bilateral PLIF). I now inform patients preoperatively of the possibility of interbody stabilization almost routinely, although most decompressions are still done without fusion.

While stand-alone cages may not always be adequate in younger patients, older spines behave differently. In a personal series of over 200 cases, no cage migration has occurred. One increased translation of a mobile Grade I spondylolisthesis occurred which was stabilized posteriorly. This was successfully treated with bracing for several months, and did not require reoperation

IX. POSTOPERATIVE MANAGEMENT

Mobilization can usually be done on the first postoperative day. Sitting is limited to 30 minutes initially. Sequential compression devices are used to minimize the risk of deep venous thrombosis until the patient is fairly mobile.

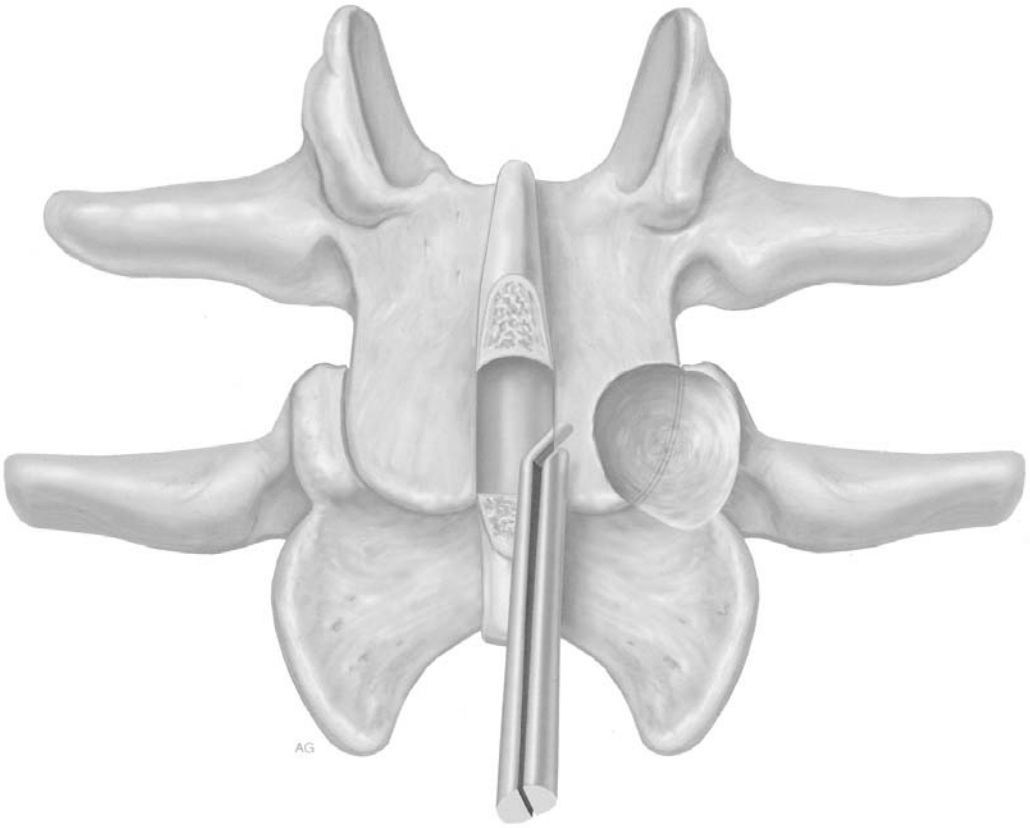

Figure 3 A Kerrison is used to quickly remove the remaining lamina and medial facet.

Pain management is begun at the time of surgery with ''preemptive analgesia,'' injecting Marcaine with epinephrine at the surgical incision site, in the paraspinous muscles, and to the lamina. At the end of the surgical procedure the area of decompression is routinely covered with Gelfoam soaked in Duramorph. Postoperatively a variety of pain-management techniques have been tried at our institution. It has been our experience that Demerol leads to confusion more frequently than other narcotic analgesics in the elderly population, presumably due to breakdown products. This effect is maximal at 72 hours after surgery when otherwise they would be ready to be discharged, and therefore presents a significant hindrance to progress. For this reason, Fentanyl PCA has been used for the past year and has proved quite satisfactory for both pain management and lack of confusion. It is usually discontinued at 48 hour, at which point oral long-acting analgesics supplemented with short-acting narcotic pain medications are instituted. If confusion is prominent, Propoxyphene with Tylenol has been found quite useful in pain management in this population.

''Old age'' is that phase of life when we turn our attention from our genitals to our bowels. It behooves the surgeon to pay close postoperative attention to bowel recovery. Routinely we put patients on stool softener immediately postoperatively. An often overlooked reason for constipation is disruption of normal caffeine intake, which should be normalized as soon as the patient is eating.

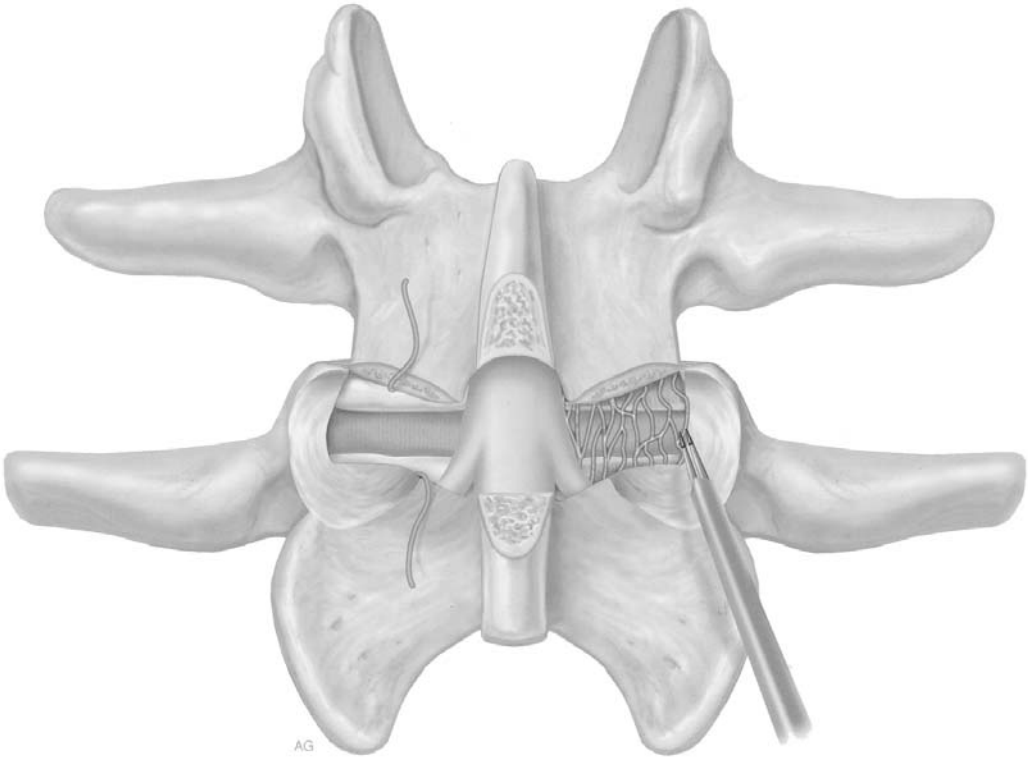

Figure 4 The plexus of cauterized vessels is divided with a 15-blade and packed away with cottonoids to expose the lateral disc space.

X. ILLUSTRATIVE CASES

A. Dynamic Lateral Recess Stenosis Following Decompression

A 74-year-old female had a long history of back pain with pain radiating into the right buttock and lower extremity. She received a series of epidural steroids, and then underwent decompression laminectomy at another facility in 1991 and again in 1992 with no relief. She reported right leg pain with any standing, lying, or walking, which was relieved by sitting. Physical examination revealed loss of lower extremity reflexes and inability to reach full lumbar extension while standing. Attempt at lumbar extension reproduced some of her leg symptoms. Radiographs revealed degenerative scoliosis and a wide decompression from L2 to L5 (Fig. 5). Asymmetrical disc narrowing was most notable on the right at L3-L4. A CT myelogram demonstrated continued compression of the nerve root on the right at L3-L4. For this reason, we performed reexploration with partial right pedicular excision L3 and foraminotomy L3-L4. Subsequent to that surgery she noted relief of her symptoms lying down, but continued symptoms with standing. Bending films showed narrowing of her L3-L4 space, mechanically pinching the nerve when standing—so-called up-down stenosis. In 1997 the patient underwent ALIF to distract the disc space on the right, using threaded titanium cages (BAK interbody fusion system) with left iliac crest morselized bone graft (Figs. 6, 7). Postoperatively she awoke without her hip and leg pain and has remained asymptomatic since that time. She stated the day after surgery that ''fifteen years of leg pain is gone.'' This relief was total at 2 years follow-up.

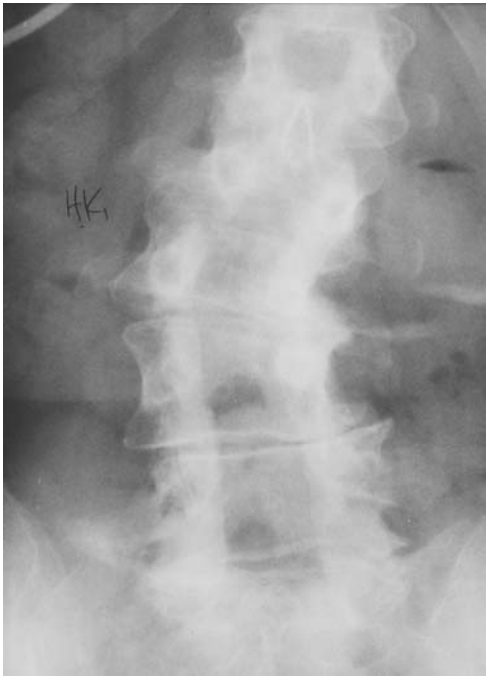

Figure 5 Radiographs revealed degenerative scoliosis and a wide decompression from L2 to L5.

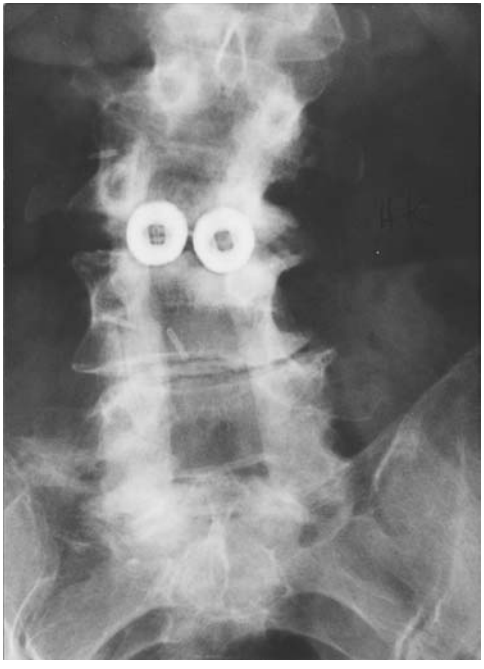

Figure 6 Bending films show the narrowing of the L3–4 space (mechanically pinching the nerve when standing), Bso-called Aup-down@ stenosis.

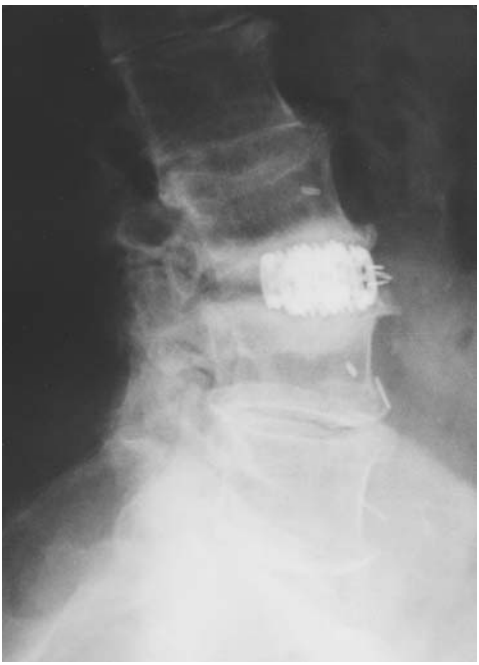

Figure 7 To distract the disc space on the right, threaded titanium cages (BAK interbody fusion system) were used with left iliac crest morselized bone graft.

B. Spondylolisthesis After Decompression

A 71-year-old female developed spinal stenosis at L4-L5 and L5-S1. She did well for 6 months and then developed leg and back pain. Radiographs demonstrated progressive post–decompressive spondylolisthesis at L4-L5. (Fig. 8). This was felt to be due to insufficiency fractures of the pars in an osteoporotic patient. This was treated very successfully with anterior lumbar interbody fusion (Fig. 9).

C. Chronic Back Pain and Lateral Recess Stenosis

A 74-year-old male had developed back pain and progressive pain in the left leg that was worse with lying flat or standing up. He also had developed some weakness in the left leg. His back pain, however, was his major complaint. A CT myelogram demonstrated dynamic lateral stenosis at L3-L4 and L4-L5 particularly. The MRI revealed bony endplate changes significantly around L2-L3, L3-L4, and L4-L5. Anterior lumbar interbody fusion at three levels was performed with a special attempt at distracting the disc spaces (Fig. 10). One month after surgery the patient wished to return to golf, and did so 2 months postop—somewhat to my consternation. He has needed no pain medications and has been fully functional since.

D. Stabilization of Transfer Lesions

A 68-year-old active male became paraparetic with severe weakness of both lower extremities and balance abnormalities. Ten years before, decompression and fusion at L3-L4 with pedicular

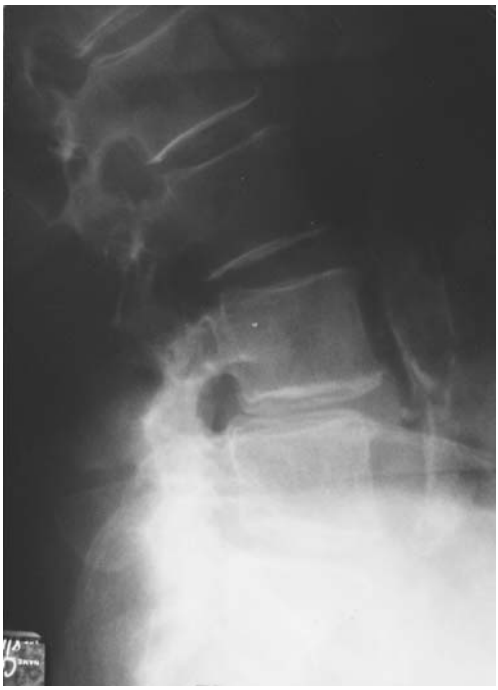

Figure 8 Radiographs demonstrate progressive post-decompressive spondylolisthesis at L4–5.

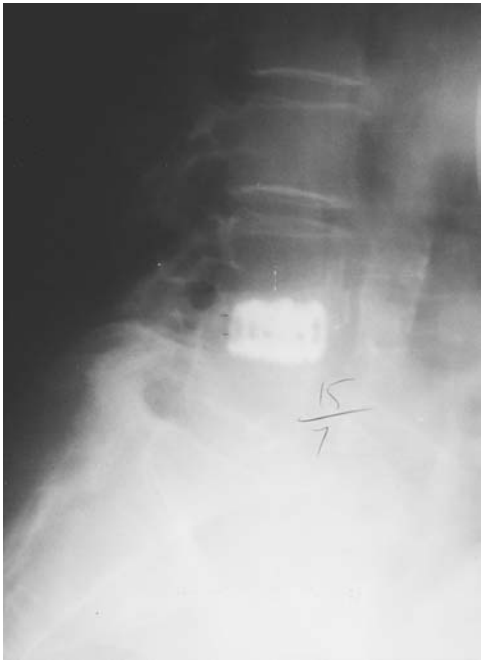

Figure 9 Insufficiency fractures of the pars in an osteoporotic patients were treated very successfully with anterior lumbar interbody fusion.

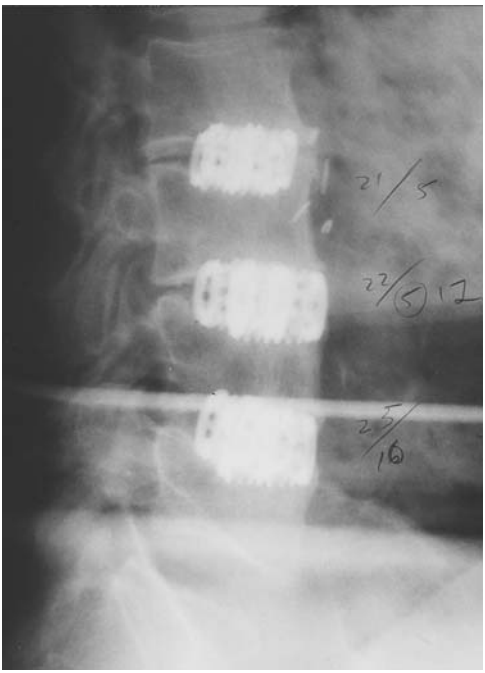

Figure 10 Anterior lumbar interbody fusion was performed at three levels with a special attempt at distracting the disc spaces.

stabilization had been performed elsewhere, and he had done well until 6 months prior to presentation. After being admitted emergently, studies revealed high-grade stenosis at L2-L3 from ligamentous hypertrophy, and facet overgrowth, but some continued motion at L2-L3. A PLIF was performed to decompress the area and stabilize the transfer lesion (Fig. 11). At 4 years follow-up he was without pain, has regained strength, and is ambulatory using only a cane due to some continued balance impairment.

E. Stenosis with Scoliosis

A 62-year-old female with longstanding developmental scoliosis (a double major curve) (Fig. 12) developed some incontinence of bowel and bladder, leg weakness, and left leg pain. A CT myelogram demonstrated L3-L4 stenosis, especially present with extension. The patient had no back pain, and her spine was very rigid on bending radiographs. The scoliosis put her at risk of instability following a decompression, but a long instrumented fusion to prevent this seemed overkill. For this reason, an anterior L3-L4 interbody fusion was performed with the intention of decompression at a secondary sitting. The stabilization alone gave the patient enough relief that she did not wish further surgery (Fig. 13). Three years later, however, she decided her leg symptoms were no longer improving, and wished to proceed. A posterior decompression relieved her leg symptoms completely. Again, the patient did extremely well for 4 years. At that time she complained of left low back pain. Radiographs revealed a transfer lesion at L4-L5 with lateral olisthesis (Fig. 14). This then required stabilization to the sacrum. Unilateral pedicular instrumentation supplementing transforaminal PLIF was performed (Figs. 15, 16). The patient was mobilized without bracing, and at age 69 she was able to return to her activities with only mild back pain.

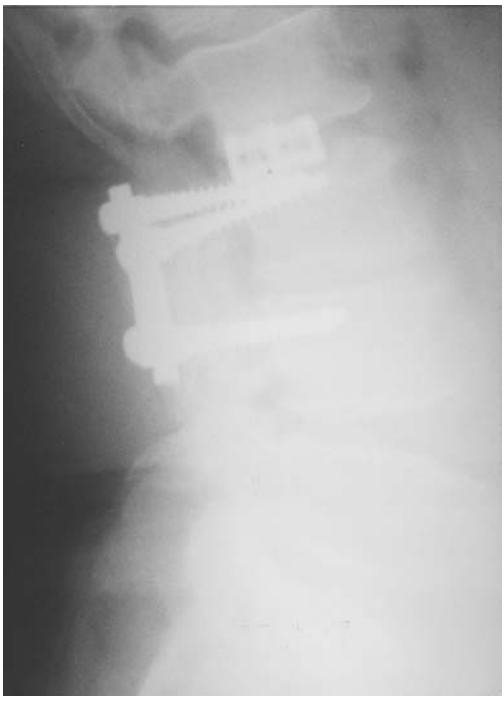

Figure 11 A PLIF was performed to decompress the area and stabilize the transfer lesion.

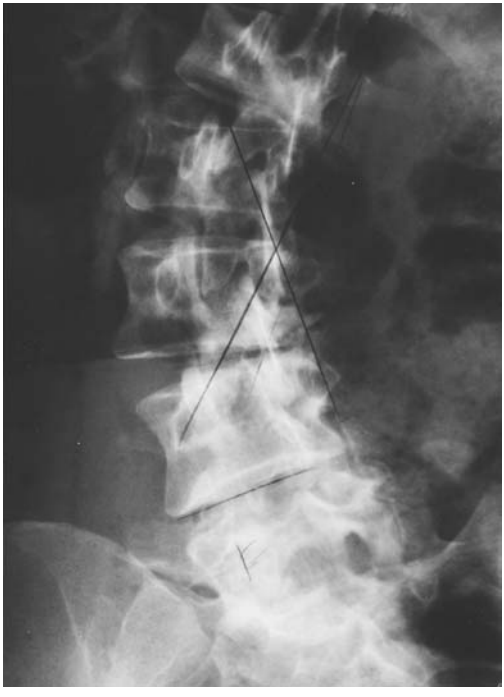

Figure 12 A 62 year-old female with longstanding developmental scoliosis (a double major curve).

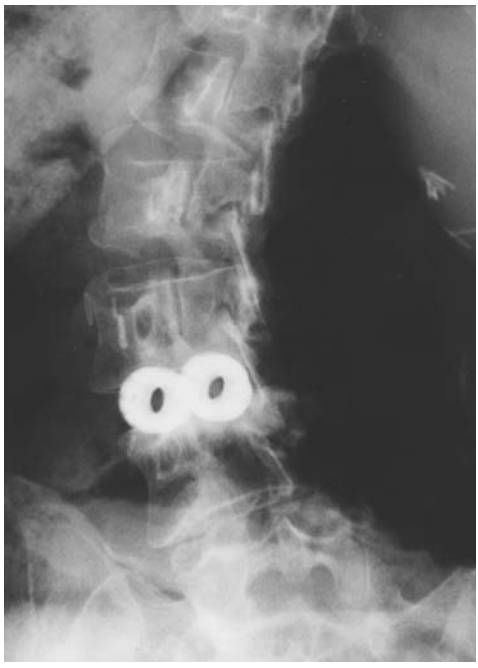

Figure 13 An anterior L3–4 interbody fusion was performed with the intention of decompression at a secondary sitting. The stabilization alone gave the patient enough relief that she did not wish further surgery.

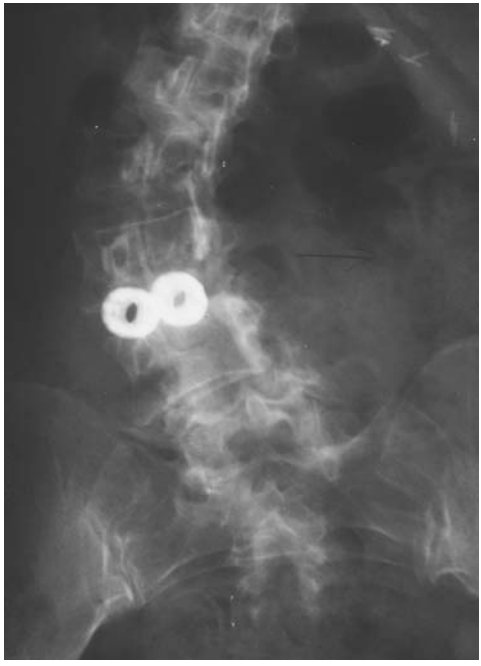

Figure 14 Radiographs reveal a transfer lesion at L4–5 with lateral olisthesis.

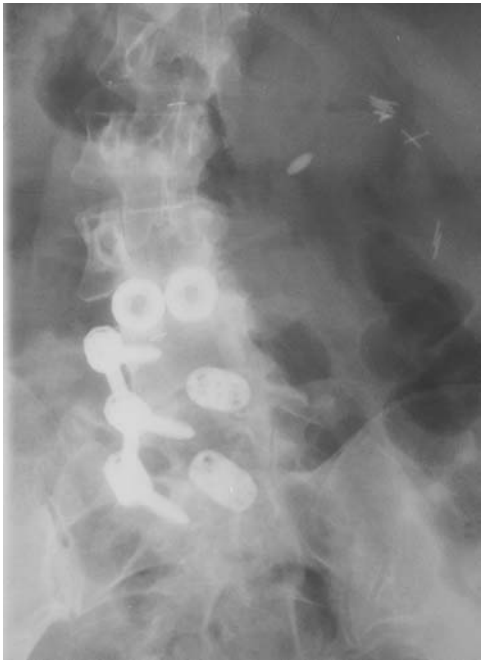

Figure 15 To stabilize to the sacrum, a unilateral pedicular instrumentation supplementing transforaminal PLIF was performed.

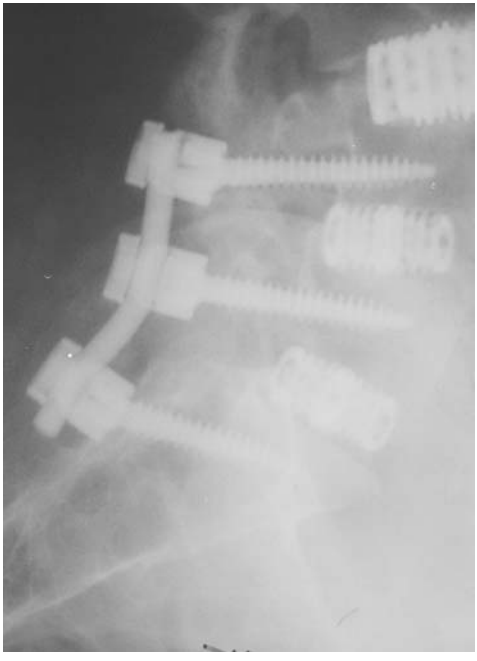

Figure 16 To stabilize to the sacrum, a unilateral pedicular instrumentation supplementing transforaminal PLIF was performed.

F. Degenerative Spondylolisthesis

A 56-year-old female had had a long history of ''atonic bladder'' and had been on a self-catheterization program. No explanation for this had been identified. Two years prior to surgery she developed low back pain. In the several months prior to surgery her back pain became worse and she developed left-sided pain radiating into the buttock, calf, and thigh. She then noted bilateral lower extremity weakness and falling. Radiographs of the lumbar spine showed progressive spondylolisthesis at L4-L5 with disc space narrowing. A CT myelogram showed high-grade stenosis at L4-L5 with a large arthritic facet on the right side and slightly open facet on the left. This was treated with decompression, sparing the right facet, and transforaminal left posterior lumbar interbody fusion. Her bowel sensation resolved, but the atonic bladder did not. Her buttock and leg symptoms completely resolved.

G. Unrecognized Spondylolysis

A 66-year-old male developed left leg pain and buttock pain treated elsewhere with laminotomy discectomy at L4-L5. His symptoms resolved completely for 6 months, but then he developed similar symptoms on the right side. Facet hypertrophy and foraminal stenosis were noted on the right. Bending films failed to show segmental instability or spondylolisthesis. At the time of surgery, however, an unrecognized degenerative spondylolysis was discovered at L4-L5. For this reason after complete laminectomy was performed, stabilization was done to avoid subsequent instability (Figs. 17, 18). Operative time was 75 minutes, and blood loss was 200 cc. The patient was mobilized on the first postoperative day and discharged on the second postoperative day with no buttock or leg pain. He had 3 months of unilateral low back pain on the side of the transforaminal opening into the disc, which subsequently resolved.

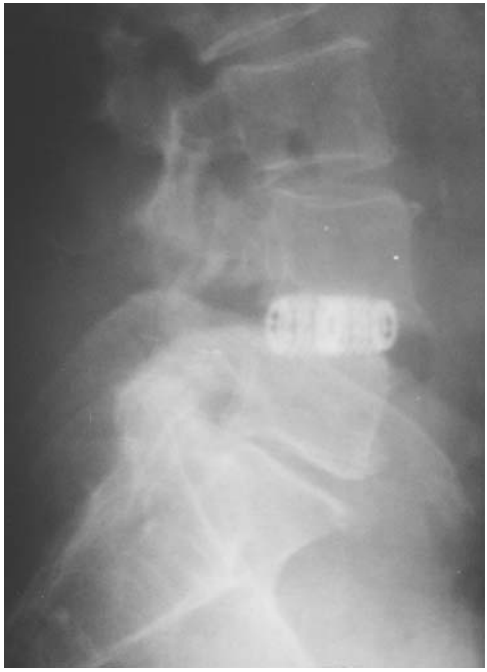

Figure 17 An unrecognized degenerative spondylolysis was discovered at L4–5.

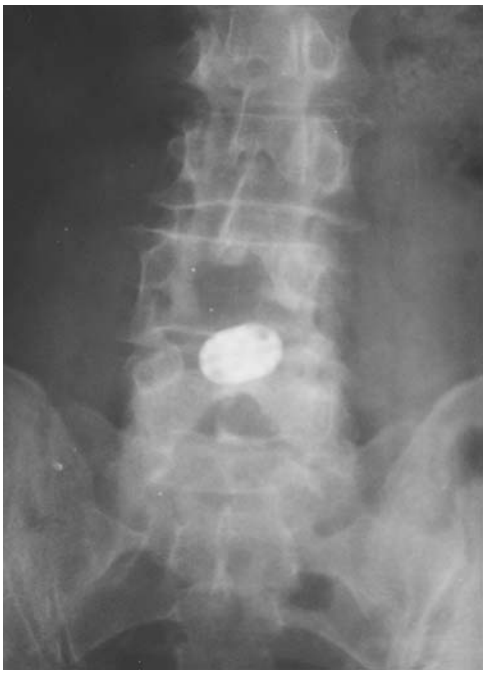

Figure 18 After a complete laminectomy was performed, stabilization was necessary to avoid subsequent instability.

REFERENCES

1. Zheng F. Revision with lumbar instrumentation fusion in patients above and below 60 years of age. Scientific Paper Presentation, Spine Across the Sea, July 23, 2000.
2. Frymoyer F, John W. Degenerative spondylolisthesis: diagnosis and treatment. J Am Acad Orthop Surg 1994; 2(1):9–15.
3. Kalbarczyk A, Lukes A, Seiler RW. Surgical treatment of lumbar spinal stenosis in the elderly. Acta Neurochir 1998; 140:637–641.
4. Grabius S. The treatment of spinal stenosis. J Bone Joint Surg Am 1980; 62 A:308–313.
5. Shenkin HA, Hash CJ. Spondylolisthesis after multiple bilateral laminectomies and facetectomies for lumbar spondylosis. J. Neurosurg 1979; 50:45–47.
6. Farfan HF, Osteria V, Lamy C. The mechanical etiology of spondylosis and spondylolisthesis. Clin Orthop Rel Res 1976; 117:40–54.
7. Kirkaldy-Willis WH, Farfan HF. Instability of the lumbar spine. Clin Orthop Rel Res 1982; 165: 110–123.
8. Burton CV, Kirkaldy-Willis WH, Hong-Hing K. Causes of failure of surgery on the lumbar spine. Clin Orthop Rel Res 1981; 157:191.
9. Genant H. Spine update. 1984. San Francisco: Radiology Research and Education Foundation, 1983.
10. Herkowitz HN, Kurz LT. Degenerative lumbar spondylolisthesis with spinal stenosis: a prospective study comparing decompression with decompression and intertransverse process arthrodesis. J Bone Joint Surg Am 1991; 73:802–808.
11. Katz JN, Lipson SJ, Larson MG. The outcome of decompressive laminectomy for degenerative lumbar stenosis. J Bone Joint Surg Am 1991; 73:809–816.

12. Herkowitz HN, Kurz LT. Degenerative lumbar spondylolisthesis with spinal stenosis: a prospective study comparing decompression with decompression and intertransverse process arthrodesis. J. Bone Joint Surg Am 1991; 73:802–808.
13. Conley FK, Cady CT, Lieberson RE. Decompression of lumbar spinal stenosis and stabilization with knodt rods in the elderly. Neurosurgery 26:758–763.
14. Farfan HF, Kirkaldy-Willis WH. The present status of spinal fusion in the treatment of lumbar intervertebral joint disorders. Vol. CORR: #158, 1981:198–214.
15. Hirano R, Kasegawa K, Takahashi HE. Structural characteristics of the pedicle and its role in screw stability. Spine 1997; 22:2504–2510.
16. Fritzell P, Hagg O, Wessberg P, Nordwall A. Chronic low back pain and fusion: a comparison of three surgical techniques. Spine 2002; 27(11):1131–1141.
17. Bullough PG, Boachie-Adjei O. Atlas of Spinal Diseases. Philadelphia, 1988:148–150.
18. Resnick DO, Niwayama G. Diagnosis of Bone and Joint Disorders. Philadelphia: W.B. Saunders Co., 1981:1661–1671.

22

Choice of Anterior and Posterior Thoracolumbar Spinal Implants

Patrick W. Hitchon, Mathew Brenton, Andrew G. Black, Aaron M. From, Jeremy Harrod, Kurt Eichholz, and James Torner
University of Iowa College of Medicine and Veterans Administration Medical Center Iowa City, Iowa, U.S.A.

I. ANTERIOR IMPLANTS

Anterior approaches allow greater access to the ventral aspect of the canal without sacrificing the spinous processes, laminae, facets, and intervening ligaments. By implanting a graft in place of the fractured body and applying a lateral implant, the anterior column is reconstructed. To optimize fusion, bone grafts should be maintained under compression, and this is better achieved through an anterior rather than posterior approach. Also, the anterior approach generally requires fixation to only one level above and one level below the fracture, whereas posterior instrumentation often extends two to three levels above and below the fracture. The posterior approach requires some sacrifice to the posterior elements, i.e., laminae and facets, if decompression from a burst fracture is to be achieved.

A host of titanium anterior devices have been approved for clinical use by the U.S. Food and Drug Administration. Some, such as the smooth rod Kaneda (SRK, AcroMed, Raynham, MA), consist of rods and four constrained bicortical screws that allow compression and distraction [10,29,30,34,35]. Others, like the ''Z'' plate (Sofamor-Danek, Memphis, TN), consist of a slotted plate that provides compression by means of two constrained bicortical bolts [16,43]. The Anterior Thoracolumbar Locking Plate (ATLP) (Synthes, Paoli, PA), on the other hand, affords limited compression by means of two temporary bone screws and fixation with four constrained screws [38,39].

Owing to the different biomechanical features of the above three devices, the following biomechanical testing was conducted. To simulate implantation in patients, this study was performed in human cadaveric spines subjected to a total L1 corpectomy, with excision of the attached anterior and posterior longitudinal ligaments and anterior strut grafting.

A. Methods

Human spines were potted rostrally at T9 and caudally at L3 with a potting mixture of 2/3 Bondo body filler and 1/3 fiberglass resin. The potted spine was thawed overnight and then attached to a solid, immovable base plate for load testing. Three infrared light-emitting diodes (LEDs) were attached to each neural arch of T11, T12, L1, and L2 (transverse processes, laminae,

and spinous process) as well as the base plate. The three-dimensional motion of the LEDs is tracked by two photosensitive cameras of the Selspot II system (Innovision Systems, Inc., Warren, MI) that sense the intensity of the infrared light from each LED. Processing of this position data generated the angular rotations of the spine in response to the applied loads.

Using a system of weights and pulleys, quasistatic loads were applied to the spine sequentially in opposite direction creating pure moments of 0, 1.5, 3.0, 4.5, and 6.0 Nm. These loads were applied in six directions in the following order: flexion (FLEX), extension (EXT), right (RLB) and left (LLB) lateral bending, and right (RAR) and left (LAR) axial rotation, as detailed by Goel et al. [17–19,24–26]. The spines were first load-tested in the intact state. Thereafter, an L1 corpectomy was performed, with grafting using a 1.25 in. (32 mm) diameter oak wooden dowel and stabilization with the ATLP device in 9 (Fig. 1), SRK in 10 (Fig. 2), and Z-plate in 10 (Fig. 3). Wooden dowels were used for the sake of convenience and to eliminate variations in graft material. All implants were applied on the left side in a manner similar to that used in the operating room and in accordance with the manufacturer's specifications. In the case of the ATLP, compression upon the graft was applied by means of two temporary 4 mm $\times$ 35 mm bone screws engaging the vertebrae and tapered holes in the plates. The plate is affixed to the spine by four unicortical constrained bone screws measuring 7.5 mm in diameter and 45 mm in length. In the SRK, 6.25 mm diameter bone screws were applied, with a length of 45–55 mm selected to achieve bicortical purchase. These bone screws are constrained to two 6.35 mm rods by means of set screws. In turn, the rods are spanned by two couplers for the prevention of translation and axial rotation. With the Z-plate bicortical constrained 7.0 mm diameter bolts are implanted posteriorly and nonconstrained 6.5 mm diameter screws 45–55 mm in length for bicortical purchase are implanted anteriorly.

Spines were then affixed to a Materials Testing System (Material Testing Systems, Minneapolis, MN) and fatigued for 5000 cycles of flexion/extension with a frequency of 0.5 Hz, using a load of ± 3 Nm as measured by the load cell. The specimen was returned to the testing cage and retested as described above.

Angular rotation in degrees of T12 relative to L2 is measured in each of the six directions. Thus, an increase in angular rotation of T12 relative to L2 (T12-L2) meant a decrease in stability or stiffness. In this study the authors present data with moments of 6.0 Nm. Manipulations within each device were compared using the general linear models procedure as well as the Tukey's studentized range test. Significance was determined at the alpha 0.05 $\leq$ level.

B. Results and Discussion

The donors were equally distributed between genders and ranged between 53 and 89 years for the entire group, with a mean $\pm$ SD of 69 $\pm$ 8 years for the ATLP, 75 $\pm$ 10 for the SRK, and 68 $\pm$ 9 for the Z-plate, respectively. There was no significant difference between groups in terms of age distribution ($p = 0.190$). The average bone mineral densities (BMDs) were 0.70 $\pm$ 0.10 g/cm^2 for the ATLP spines, 0.64 $\pm$ 0.09 g/cm^2 for the SRK spines, and 0.80 $\pm$ 0.21 g/cm^2 for the Z-plate spines. There were no significant differences in the BMDs of T12 ($p = 0.0531$), L1 ($p = 0.1704$), or L2 ($p = 0.1043$) between the three devices.

Postfatigue angular rotations (mean $\pm$ SD) of the intact and instrumented spines are shown in Table 1 and Figure 4. There were no differences between the SRK and Z-plate instrumented spines in any direction. Generally, the SRK and Z-plate implanted spines were as stiff or stiffer than the intact spines in flexion, extension, right and left lateral bending, but not axial rotation. In RLB, but not LLB, the SRK- and Z-plate–implanted spines were more rigid than the intact spines ($p \leq 0.05$). The ATLP-implanted spines were generally not as stiff as the SRK- or Z-

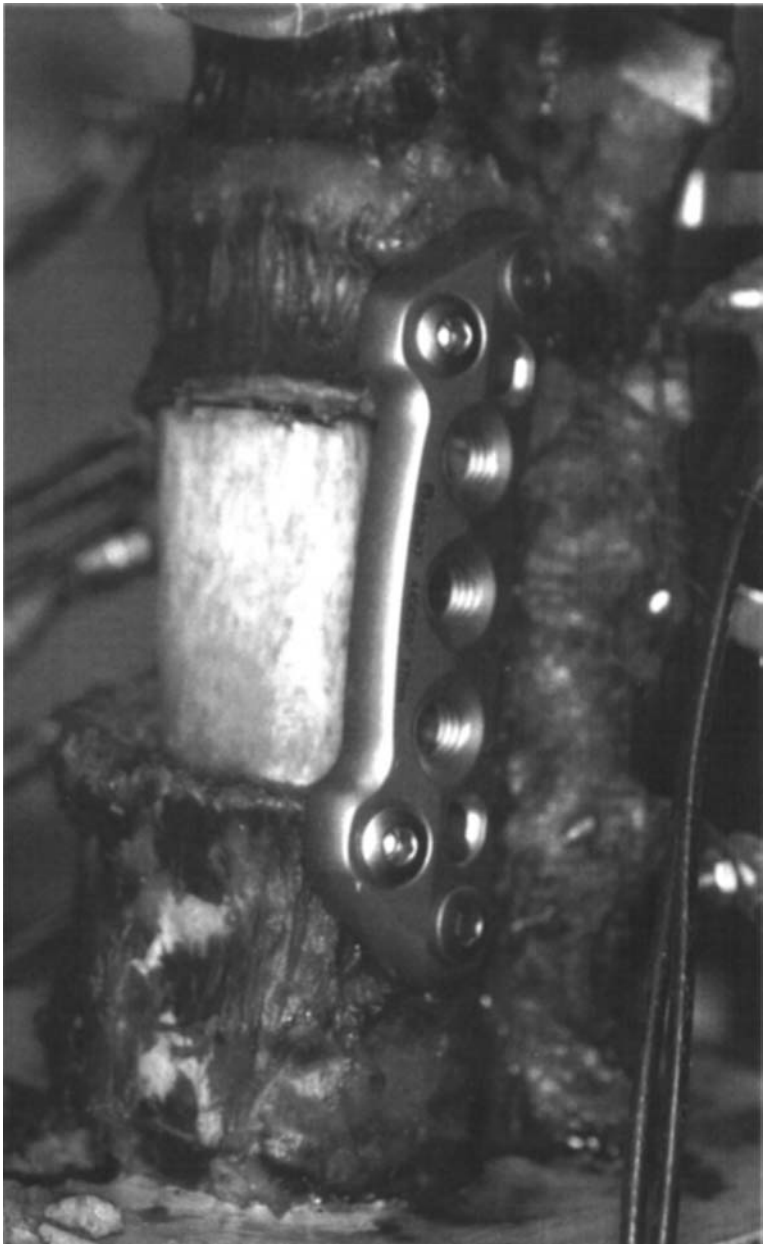

Figure 1 The ATLP device with four constrained unicortical screws applied between T12 and L2. This constraint prevents angular rotation or backing out.

Figure 2 The SRK device applied with four bicortical screws across T12 and L2. These bone screws are constrained to the rods.

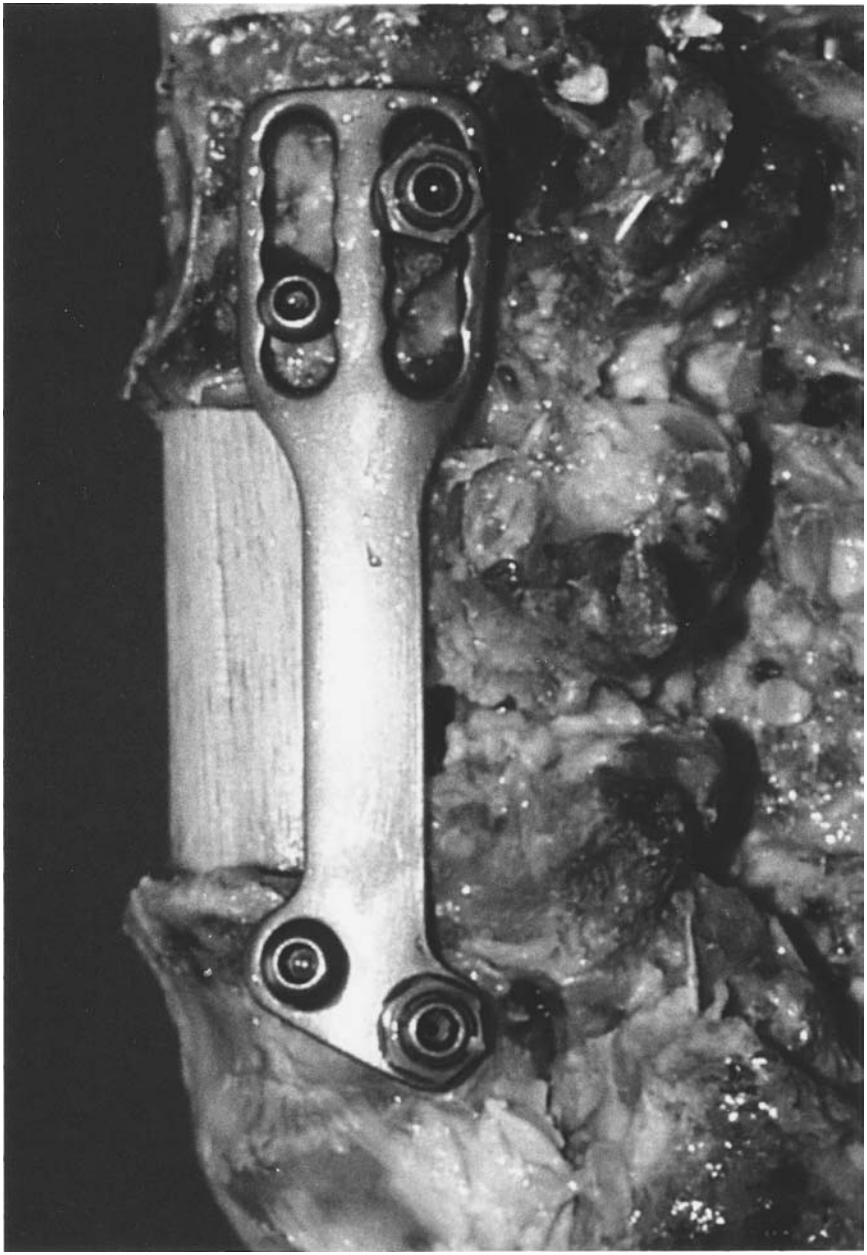

Figure 3 The Z-plate applied across T12 and L2 using two constrained bicortical bolts and two non-constrained bicortical screws.

Table 1 Mean Rotations (± Standard Deviation) Across t12–12 in the Intact and Fatigued States in Response to 6 Nm Bending Movement

		Flexion	Extension	R. lateral bending	L. lateral bending	R. axial rotation	L. axial rotation
Z-Plate	Intact	4.4 ± 1.6	4.1 ± 2.5	5.1 ± 1.8	5.4 ± 1.8	2.4 ± 1.4	2.6 ± 1.9
	Fatigue	4.9 ± 3.3	4.4 ± 2.7	1.3 ± 1.7*,+	4.4 ± 2.5 +	4.0 ± 2.1	3.3 ± 2.2
SRK	Intact	5.3 ± 4.2	6.2 ± 4.2	5.6 ± 2.4	5.6 ± 2.0	2.0 ± 1.3	2.3 ± 1.6
	Fatigue	4.2 ± 3.2	2.4 ± 3.4	1.1 ± 1.5*	1.2 ± 3.4	2.3 ± 1.3	2.6 ± 1.3
ATLP	Intact	5.5 ± 1.7	5.1 ± 1.1	5.0 ± 1.3	5.2 ± 1.5	1.7 ± 0.7	1.7 ± 0.7
	Fatigue	8.9 ± 4.9	6.4 ± 2.9	3.9 ± 3.6	4.4 ± 2.6	4.9 ± 3.3	4.3 ± 3.3

* Significantly different from the intact state ($p \leq 0.05$).
+ Significantly different from one another ($p \leq 0.05$).

plate–instrumented spines. In flexion and extension, the angular rotation of ATLP-implanted spines was significantly greater than the rotations of SRK spines ($p \leq 0.05$) (Fig. 4). Performance of all implants appeared to be poorest in axial rotation.

This performance by implants described in our results, as well as others [1,31,41], is related to design. Devices allowing maximal compression upon the graft, such as the Kaneda and TSRH, with screws constrained to the rods provide greater rigidity. The testing of devices for their inherent rigidity is important for many reasons. Not only does an implant correct and

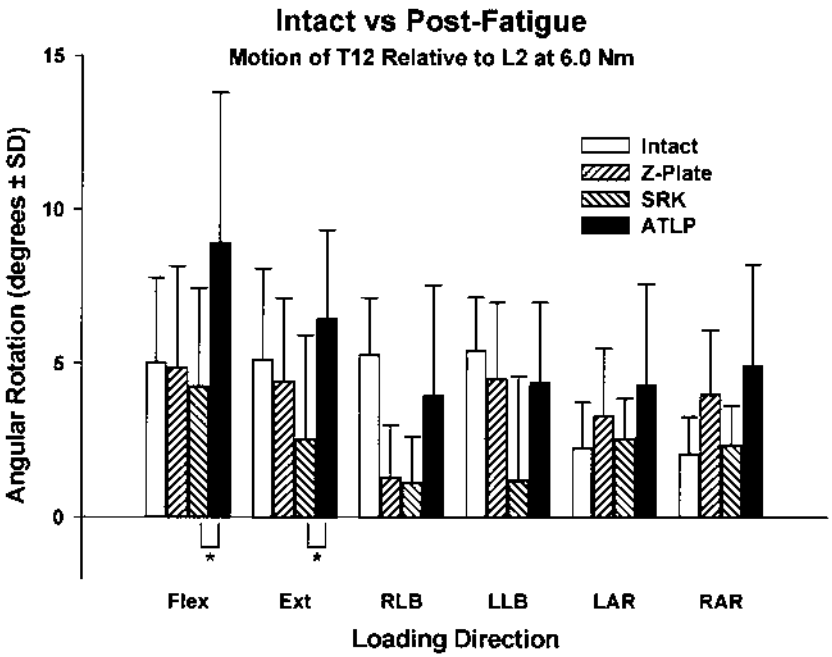

Figure 4 Comparative motion in six directions of the spines instrumented with the three devices following fatigue of 5000 cycles at ±3 Nm in the sagittal plane. The ATLP-stabilized spines were significantly ($p \leq 0.05$) less rigid than SRK instrumented spines in flexion and extension.

maintain proper alignment, but its stiffness enhances fusion. Fusion rates in the spine have been shown to be enhanced with instrumentation [12,15,28,37,40,42]. Thus, the more rigid implant is less likely to fail and is able to maintain correction and enhance fusion rates. The Z-plate– and SRK-stabilized spines after fatigue were more rigid than the intact (Table 1). Owing to the rigidity of the SRK construct, no differences were encountered between right and left lateral bending in the fatigued spines (Table 1). The Z-plate–stabilized spine, on the other hand, was significantly more rigid in right than left lateral bending in the fatigued state. This difference in the Z-plate between right and left lateral bending is attributed to its placement on the left side of the spine (Fig. 2). In right lateral bending the graft restricts bending to the right, and the Z-plate restricts distraction of the spine on the left. The ATLP was equally nonrestrictive in right or left lateral bending.

Though the SRK- and Z-plate–instrumented spines behaved similarly without significant difference between them, it was only the fatigued SRK (4.2 $\pm$ 3.2°, 2.4 $\pm$ 3.4°) that was more rigid than the fatigued ATLP in flexion and extension (8.9 $\pm$ 4.9°, 6.4 $\pm$ 2.9°) (Table 1, Fig. 4). This rigidity imparted to the spine by the SRK and Z-plate is in part attributed to the specified bicortical engagement of their bolts and screws and the ability of these devices to maximally compress the graft between the vertebral end plates. The ATLP provides only minimal compression by virtue of two 4 mm $\times$ 35 mm temporary screws. The additional rigidity provided by the SRK over the Z-plate is attributed in the former to the constraint of screws to the rods, whereas in the Z-plate it is the bolts only that are constrained to the plates but not the anterior screws. Thus, for maximal rigidity of an anterior spinal construct, the ideal device is one that provides graft compression by means of four bicortical, constrained screws.

II. POSTERIOR IMPLANTS

Three implants currently used in the thoracolumbar spine include sublaminar wires and cables, sublaminar hooks, and pedicle screws. Though they do require sublaminar dissection, cables offer simplicity without the need for intraoperative fluoroscopy. Sublaminar cables have been used solely with rods and rectangles [23] as well as as an adjunct to hooks [27]. Hooks are recommended where pedicles have been deemed too small to allow engagement by screws [2,4,6,14]. Compared to unilateral pedicle screws and sublaminar wires, unilateral hooks have been shown to have significantly higher pullout strength and have been recommended for fixation in osteoporotic spines [9].

Pedicle screws for the treatment of unstable spinal fractures have been demonstrated to be effective and touted for their engagement into all three columns of the spine: pedicles, anterior, and posterior halves of the vertebral bodies [11,22]. Unfortunately, failures with pedicle screws have been demonstrated and consist of screw bending or breakage, progressive spinal angulation, screw loosening, and in some cases screw pullout [5,7,13,36].

The following study compares the pullout strength of bilateral sublaminar cables, bilateral sublaminar claw hooks to that of bilateral pedicle screws in the human cadaveric thoracic spine.

A. METHODS

Twelve fresh frozen human cadaveric spines were used in this study. A total of 20 bilateral pedicle screws, 20 bilateral claw hooks, and 20 bilateral titanium cable constructs were randomly assigned to different levels so that the distribution per level was: T5(6), T6(6), T7(8), T8(10), T9(8), T10(8), T11(8), T12(6). Spinal instrumentation was implanted based on clinical practice, and manufacturer's specifications as follows. Titanium pedicle screws (40 $\times$ 5 mm, DePuy-Motech, catalogue #1755–37–140, Raynham, MA) were inserted after tapping. Owing to the small dimensions of the bodies in one T5 and one T6 vertebra, 35 mm screws (DePuy-Motech,

catalogue #1755–37–135) were used. Titanium rods (DePuy-Motech, catalogue #1755–74) 10 cm in length × 5.5 mm in diameter were secured to the polyaxial screws. Cross-links (DePuy-Motech, catalogue #1755–65) were secured to the rods rostrally and caudally in accordance with clinical practice. Upgoing pedicle hooks (DePuy-Motech, catalogue #1755–50) and downgoing ramped hooks (DePuy-Motech, catalogue #1755–51) were applied bilaterally and secured to the 10 cm titanium rods under compression [2,4,6,14]. Cross-links were added rostrally and caudally as described for the pedicle screws above. Titanium sublaminar cables (DePuy-Motech, model 7925–0115) were applied bilaterally around each lamina. Cables were tightened around the titanium rods to 200 Newtons, such that the rostral end of the cables exited medial to the rod and caudally exited laterally. Cross-links were added rostrally and caudally as in the case of screws and hooks.

The instrumented vertebrae were then potted in a 70:30 mixture of autobody filler and fiberglass resin. The neural arches were left exposed to allow for the application of the posterior implants. Pullout testing was performed using a Bionix 858 biaxial TestStar II servo-hydraulic Material Testing System (MTS system, Minneapolis, MN) (Fig. 5) [21]. Maximal pullout (MPO) was defined as the point at which the specimen was maximally loaded directly prior to a precipitous drop in the load displacement curve. The distance from the point of application of the distraction force to that of MPO was measured and referred to subsequently as displacement at maximal load. Beyond the point of MPO, the construct failed by one of four major mechanisms: screw pullout, pedicle fracture, laminar fracture, and middle column fracture.

B. Results and Discussion

Statistical analysis was performed on 60 specimen from T5 to T12: 20 screw constructs, 20 hook constructs, and 20 cable constructs. Specimen age and BMD values were evenly distributed across all groups (Table 2). There were no statistically significant differences between the screw, hook, and cable groups in age ($p > 0.05$) or BMD ($p = 0.0952$).

The measured values for MPO for screw, hook, and cable groups were: 972 ± 330, 802 ± 356, and 654 ± 248 Ns, respectively (Table 2). Looking strictly at construct type and no other variables, the above values for MPO were significantly different from one another ($p = 0.0090$), with pedicle screws showing the highest pullout, and cables the least. The Pearson correlation coefficient between BMD and MPO for screw, hook, and cable groups were: $p = 0.0507$, $p = 0.541$, and $p = 0.989$, respectively.

The measured values for displacement at maximum load for screws, hooks, and cables were: 4.42 ± 2.15 mm, 3.73 ± 1.42 mm, and 6.80 ± 3.95 mm, respectively (Table 2). The above values for displacement were significantly different from one another, with the cable displacement being significantly greater than that of the hooks and screws ($p < 0.05$).

A significant difference existed in the mechanism by which the implants tended to fail ($p < 0.0001$) (Table 3). The majority of screws tended to fail by backing out, whereas the majority hooks and cables failed by pedicle fracture.

The above results showed a significant difference in the pullout of the three posterior spinal implants, with the pedicle screws outperforming hooks and cables (Table 1). Bilateral implants when triangulated result in a large wedge of bone separating the pedicle screws in addition to the bone incorporated in the screw threads. Thus, cross-linked triangulated pedicle screws have greater tensile pullout strength than single [20] or parallel [3] pedicle screws.

The pullout of pedicle screws was shown to have the strongest correlation with bone mineral density ($p = 0.0507$). On the other hand, since hooks and cables engage the cortical laminae, which are less susceptible to osteoporosis, afflicting primarily cancellous bone, the MPO of hooks and cables are less affected by changes in BMD.

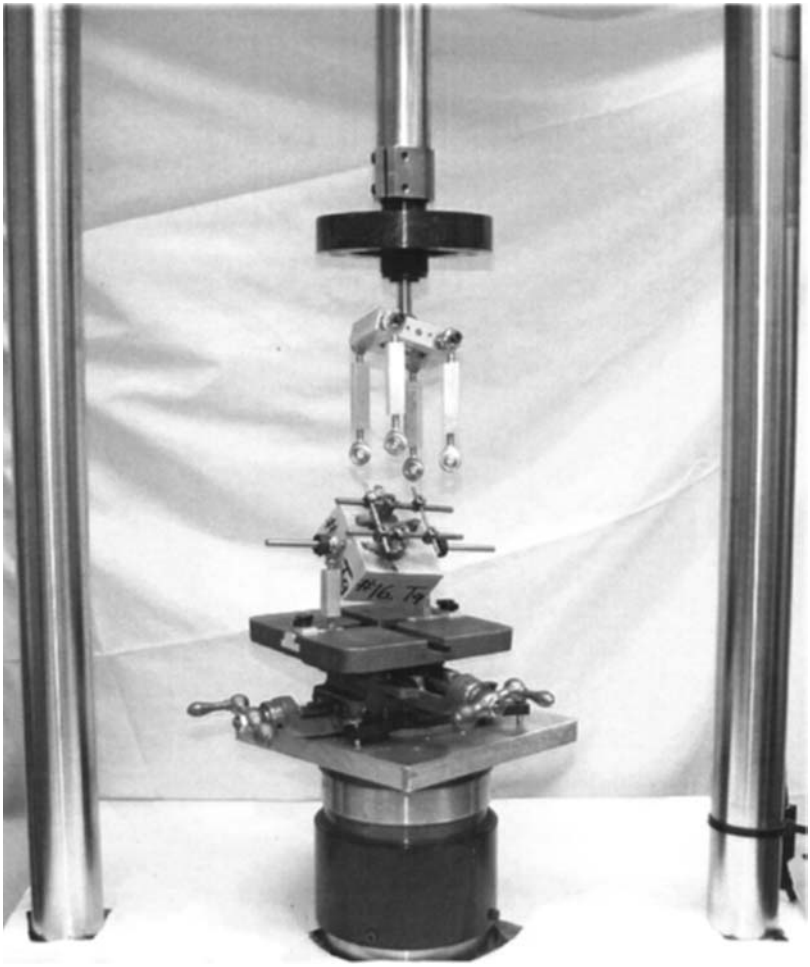

Figure 5 Photograph of the MTS setup. Custom-engineered jig attached to the MTS actuator to apply distraction upon the spinal construct. The jig consisted of a universal ball-and-socket joint connected to a plate with four adjustable shoulder bolts. The specimen itself is mounted on an XY platform, which sits upon the load cell, accurately measuring loads and displacements.

Table 2 Maximum Load to Construct Failure (Newtons), Displacement at Max Load (Millimeters), and Bone Mineral Density (Grams per cm^2), for the Three Experimental Groups

Construct	Max load	Displacement	BMD	Donor age
SCREWS	972.257 +/− 330.278*	4.416 +/− 2.148†	0.604 +/− 0.120	74.12 +/− 20.16
HOOKS	801.905 +/− 355.552	3.735 +/− 1.420	0.572 +/− 0.119	70.50 +/− 22.88
CABLES	653.873 +/− 248.043*	6.796 +/− 3.950†	0.528 +/− 0.084	82.64 +/− 9.34

* Significantly different from one another ($p \leq 0.05$)
† Significantly different from one another ($p \leq 0.05$)
(MEAN +/− STANDARD DEVIATION)

Table 3 Number and Type of Fracture/Construct Failure for Each of the Three Groups

Construct	Screw back-out	Laminar fracture	Pedicle fracture	Middle Column fracture	Number
Screws	11	0	3	6	n = 20
Hooks	0	2	16	2	n = 20
Cables	0	3	16	1	n = 20

Our results showed that sublaminar wires fell short of screws in maximal pullout and were associated with the greatest flexibility or displacement (Table 2). The large displacement at maximum load associated with the cables can be attributed to the slack in the cable that is present posttensioning and the narrow cable indenting the bone during testing. The high stresses at the bone/cable interface associated with the small cross-sectional area of the cable exceeds that for the hooks and screws.

The mechanism of failure was significantly different ($p < 0.001$) between the three implants (Table 3). Whereas 11 of the 20 screws backed out, pedicle fractures occurred in 16 each of the 20 hook and 20 cable constructs, but in only three pedicle screw–implanted spines. Thus, in spite of triangulation, when pedicle screws fail they often fail by backing out, and not with pedicle or middle column fractures. This mechanism of failure offers the advantage of ease of revision. In clinical practice, in case of construct failure as a result of screw backout, revision can be performed with larger and longer screws [32], screw augmentation with cement [44], or supplementation with hooks [8,33]. Failure with hooks or cables often requires major revision with most likely an extension of the instrumented segment.

ACKNOWLEDGMENTS

This project was made possible through the financial support of **AcroMed** (Raynham, MA) **Sofamor-Danek** (Memphis, TN), and **Synthes AO/ASIF** Foundation (Bern, Switzerland).

REFERENCES

1. An HS, Lim T, Hong JJ, Eck J, McGrady L. Biomechanical evaluation of anterior thoracolumbar spinal instrumentation. Spine 1995; 20(18):1979–1983.
2. Asher MA, Strippgen WE, Heinig CF, Carson WL. Isola spinal implant system: principles, design, and applications. In: HA, Cotler JM, eds. Spinal Instrumentation. Baltimore: Williams and Wilkins, 1992:325–351.
3. Barber JW, Boden SD, Ganey T, Hutton WC. Biomechanical study of lumbar pedicle screws: Does convergence affect axial pullout strength?. J Spinal Disord 1998; 11(3):215–220.
4. Bennett GJ. Cotrel-Dubousset instrumentation for thoracolumbar instability. In: Hitchon PW, Traynelis VC, Rengachary SS, eds. Techniques in Spinal Fusion and Stabilization. New York: Thieme Medical Publishers, Inc., 1995:209–217.
5. Benson DR, Burkus JK, Sutherland TB, McLain RF. Unstable thoracolumbar and lumbar burst fractures treated with the AO fixateur interne. J Spinal Disord 1992; 5(3):335–343.
6. Benzel EC, Baldwin NG, Ball PA. Texas Scottish rite Hospital hook-rod spinal fixation. In: Hitchon PW, Traynelis VC, Rengachary SS, eds. Techniques in Spinal Fusion and Stabilization. New York: Thieme Medical Publishers, Inc., 1995:229–239.

7. Carl Al, Tromanhauser SG, Roger DJ. Pedicle screw instrumentation for thoracolumbar burst fractures and fracture-dislocations. Spine 1992; 17(8S):S317–S323.
8. Chiba M, McLain RF, Yerby SA, Moseley TA, Smith TS, Benson DR. Short segment pedicle instrumentation. Biomechanical analysis of supplemental hook fixation. Spine 1996; 21(3):288–294.
9. Coe JD, Warden KE, Herzig MA, McAfee PC. Influence of bone mineral density on the fixation of thoracolumbar implants: a comparative study of transpedicular screws, laminar hooks, and spinous process wires. Spine 1990; 15(9):902–907.
10. Cohen M, McAfee P. Kaneda anterior spinal instrumentation. In Hitchon PW, Traynelis VC, Rengachary S, eds. Techniques in Spinal Fusion and Stabilization. New York: Thieme, 1995:264–278.
11. Denis F. The three column spine and its significance in the classification of acute thoracolumbar spinal injuries. Spine 1983; 8:817–831.
12. Dickman CA, Yahiro MA, Lu HTC, Melkerson MN. Surgical treatment alternatives for fixation of unstable fractures of the thoracic and lumbar spine: a meta-analysis. Spine 1994; 19(20S): 2266S–2273S.
13. Ebelke DK, Asher MA, Neff JR, Kraker DP. Survivorship analysis of VSP spine instrumentation in the treatment of thoracolumbar and lumbar burst fractures. Spine 1991; 16(8S):S428–S432.
14. Flores E, Rengachary SS, Hitchon PW. Isola Instrumentation. In: Hitchon PW, Traynelis VC, Rengachary SS, eds. Techniques in Spinal Fusion and Stabilization. New York: Isola Instrumentation Thieme Medical Publishers, Inc., 1995:Ch. 23 pp 218–228.
15. Garfin S. Summation. Spine 1994; 19(20S):2300S–2305S.
16. Ghanayem AJ, Zdeblick TA. Anterior instrumentation in the management of thoracolumbar burst fractures. Clin Orthop Related Res 1997; (335):89–100.
17. Goel VK, Weinstein JN. Biomechanics of the Spine: Clinical and Surgical Perspective. Boca Raton. FL: CRC Press, 1990:111–118.
18. Goel VK, Goyal S, Clark C, Nishiyama K, Nye T. Kinematics of the whole lumbar spine effect of discectomy. Spine 1985; 10:543–554.
19. Goel VK, Nye T, Clark C, Nishiyama K, Weinstein JN. A technique to evaluate an internal spinal device by use of the Selspot System: an application to Luque Closed Loop. Spine 1987; 12:150–159.
20. Hadjipavlou AG, Nicodemus CL, Al-Hamdan FA, Simmons JW, Pope MH. Correlation of bone equivalent mineral density to pull-out resistance of triangulated pedicle screw construct. J Spinal Disord 1997; 10(1):12–19.
21. Hitchon PW, Coppes JK, Brenton MD, From AM, James C, Torner JC. Factors affecting the relative pullout strength of two different designs of anterior cervical screws. Spine 2003; 28(1):9–13.
22. Hitchon PW, Follett KA. Transpedicular screw fixation of the thoracic and lumbar spine. In: Hitchon PW, Traynelis VC, Rengachary SS, eds. Techniques in Spinal Fusion and Stabilization. New York: Thieme Medical Publishers, Inc., 1995:240–247.
23. Hitchon PW, Follett KA. Luque instrumentation for the thoracic and lumbar spine. In: Hitchon PW, Traynelis VC, Rengachary SS, eds. Techniques in Spinal Fusion and Stabilization. New York: Thieme Medical Publishers, Inc., 1995:198–203.
24. Hitchon PW, Goel VK, Rogge T. Biomechanical studies of a dynamized anterior thoracolumbar implant. Spine 2000; 25(3):306–309.
25. Hitchon PW, Goel VK, Rogge T. In vitro biomechanical analysis of three anterior thoracolumbar implants. J Neurosurg (Spine 2) 2000; 93:252–258.
26. Hitchon PW, Goel VK, Grosland NM, Torner J. Biomechanical studies on two anterior thoracolumbar implants in cadaveric spines. Spine 1999; 24:213–218.
27. Hitchon PW. Harrington distraction rods for thoracic and lumbar fractures. In: Hitchon PW, Traynelis VC, Rengachary SS, eds. Techniques in Spinal Fusion and Stabilization. New York: Thieme Medical Publishers, Inc., 1995:204–208.
28. Johnston CE, Ashman RB, Baird AM, Allard RN. Effect of spinal construct stiffness on early fusion mass incorporation experimental study. Spine 1990; 15(9):908–912.
29. Kaneda K, Abumi K, Fujiya M. Burst fractures with neurologic deficits of the thoracolumbar-lumbar spine results of anterior decompression and stabilization with anterior instrumentation. Spine 1984; 9(8):788–795.

30. Kaneda K, Taneichi H, Hashimoto T, Satoh S, Fujiya M. Anterior decompression and stabilization with the Kaneda device for thoracolumbar burst fractures associated with neurological deficits. J Bone Joint Surg 1997; 79-A(1):69–83.
31. Kotani Y, Cunningham BW, Parker BW. Static and fatigue biomechanical properties of anterior thoracolumbar instrumentation systems. A synthetic testing model. Spine 1999; 24(14):1406–1413.
32. Krag MH, Beynnon BD, Pope MH, DeCoster TA. Depth of insertion of transpedicular vertebral screws into human vertebrae: effect upon screw-vertebra interface strength. J Spinal Disord 1989; 1(4):287–294.
33. Margulies JY, Casar RS, Neuwirth MG, Haher TR. The mechanical role of laminar hook protection of pedicle screws at the caudal end vertebra. Eur Spine J 1997; 6:245–248.
34. McAfee PC. Complications of anterior approaches to the thoracolumbar spine. Emphasis on Kaneda instrumentation. Clin Orthop Related Res 1994; 306:110–119.
35. McAfee P C, Bohlman H H, Yuan H A. Anterior decompression of traumatic thoracolumbar fractures with incomplete neurological deficit using a retroperitoneal approach. J Bone Joint Surg 1985; 67-A(1):89–104.
36. McLain RF, Sparling E, Benson DR. Early failure of short-segment pedicle instrumentation for thoracolumbar fractures. J Bone Joint Surg 1993; 75(2):162–167.
37. Steffee AD, Brantigan JW. The variable screw placement spinal fixation system report of a prospective study of 250 patients enrolled in Food and Drug Administration clinical trials. Spine 1993; 18(9): 1150–1172.
38. Thalgott J S, Kabins M B, Timlin M, Fritts K, Giuffre J M. Four year experience with the AO thoracolumbar locking plate. Spinal Cord 1997; 35(5):286–291.
39. Thalgott J S. Indications and techniques for the AO titanium anterior thoracolumbar locking plate. In: Thalgott JS, Aebi M, eds. Manual of Internal Fixation of the Spine: Principles of Techniques in Spine Surgery. Philadelphia: Lippincott-Raven Publishers, 1996:65–76.
40. Yuan H A, Garfin S R, Dickman C A, Mardjetko S M. A historical cohort study of pedicle screw fixation in thoracic, lumbar, and sacral spinal fusions. Spine 1994; 19(205):2279S–2296S.
41. Zdeblick T A, Warden K E, Zou D, McAfee P C, Abitbol J J. Anterior spinal fixators: a biomechanical in vitro study. Spine 1993; 18(4):513–517.
42. Zdeblick T A. A prospective, randomized study of lumbar fusion preliminary results. Spine 1993; 18(8):983–991.
43. Zdeblick TA. Z-plate anterior thoracolumbar instrumentation. In: Hitchon PW, Traynelis VC, Rengachary S, eds. Techniques in Spinal Fusion and Stabilization. New York: Thieme, 1995:279–289.
44. Zindrick MR, Leon LW, Thomas JC, Holland WR, Field BT, Spencer CW. A biomechanical study of interpeduncular screw fixation in the lumbosacral spine. Clin Orthopaed Related Res 1986; 203: 99–112.

23

Spondylotic Cervical Myelopathy: Clinical Aspects

Z. Kadanka and J. Bednarik
Masaryk University and University Hospital
Brno, Czech Republic

I. INTRODUCTION

Spondylotic cervical myelopathy (SCM) is the most frequent cause of cervical myelopathy in the population over 50 years of age [1–3] and even over 15 years of age (SCM 23.6%, spinal tumor 16.4%, multiple sclerosis 9.1%, after magnetic resonance imaging (MRI) 17.8%, motor neuron disease 4.1%) [4]. What makes SCM so clinically loaded is its potentially malignant natural history (including the deleterious effect of small injuries to the cervical spine or even prolonged hyperflexion or hyperextension [5] at the hairdresser, dentist, or during general anesthesia [6]) and the potentially calamitous results of surgery [7,8]. The treatment of SCM is a matter of controversy in the literature. Surgery is a logical response to the stenotic process, but no good evidence exists that decompressive surgery with anterior or posterior approach can improve the clinical outcome for the victims of this disease, particularly in the long term. Prospective studies of the surgical approach to this disease are generally lacking. The results of our randomized prospective study did not show any important difference between the outcome for patients with mild and moderate forms of SCM treated surgically or conservatively over a 36-month period [9,10]. Neither of these methods can prevent an unfavorable (but not necessarily disastrous) course for a proportion (20–30%) of patients. The possibility remains (alongside efforts to improve our therapeutic armamentarium) of analyzing a group of patients responding positively or negatively to conservative and surgical treatment and to assess the prediction factors for good or bad outcomes, i.e., to find measures enabling the choice of patients who may profit from the conservative or from the surgical approach.

In this chapter we will present the current state of knowledge about the pathogenesis, diagnostics, prediction, and treatment of this disease.

II. PATHOGENESIS

A narrowing of the spinal canal in a sagittal direction due to degeneration of the spine (particularly in individuals with congenitally narrow canal) is considered to be the most important pathogenic factor [11]. The degenerative process of the spine starts at the intervertebral disc. The aging and overloading of the spine results in tears in the annulus fibrosus that allow bulging or frank herniation of disc material into the spinal canal. With this change in architecture, the

ball-bearing movement at the intervertebral joint is lost and is replaced by a sliding motion and posterior longitudinal ligaments and vertebrae, resulting in osteophyte formation. As the degenerating cervical disc narrows, the resulting apposition of the vertebral bodies causes deformity of the uncovertebral joints, hypertrophy of face, narrowing of the intervertebral foramen, and formation of an osteophytic bar along the ventral spinal wall. An acquired anteroposterior diameter of $<$11–12 mm results in deformation of the cord [normal sagittal diameter of the spinal cord at C5 segment $x = 9.6$ mm (8.5–11) taken from myelogram and from cord preparations]. Although there is a correlation in population studies between a narrow sagittal diameter of the spinal canal and SCM, there is a considerable degree of overlap between the frequency histograms for the minimum anteroposterior diameter of the asymptomatic population and those with SCM [12].

A more appropriate measurement is, however, cross-sectional area of the cord. A reduction of 30% or 55% shows symptoms and signs of myelopathy [13,14], while a reduction of subarachnoid space is also worthwhile; <0.7 cm^2 has been accompanied by 90% probability and 83% specificity [15].

The spinal cord is reported to lose its functional tolerance if the transverse area measured by computed tomographic myelography and MRI is less than 55–75% of the normal value [13,14]. Prognosis of spinal surgery is unfavorable if the compression ratio is <0.4 and cross-sectional area is <0.4 cm^2 [16,17].

Most commonly, disc degeneration occurs at multiple levels with aging, but the lower cervical spine is the most vulnerable. This has been considered to be due to its extensive mobility.

Cord compression is found most frequently at the C5-6 interspace, followed by C4-5, C6-7, and C3-4 [18,9]. The C3-4 segment takes precedence in the elderly because of the greater angulation associated with age-related postural change and hypermobility compensating for decreased mobility at the lower segments [19].

In addition to small spinal canal size (congenital and at the level of stenosis), impairment of **blood supply** to the spinal cord and mechanical factors are held to be important causes of spondylotic myelopathy [12,20,21]. However, we do not possess strong clinical evidence for interference in the blood supply. It has been noted that the temporal profile of patients with SCM is unlike that of other ischemic disorders [22], and anterior spinal artery thrombosis has only rarely been verified pathologically [23]. Moreover, it is not possible to disclose and estimate the vascular factor in clinical practice.

The blood supply in SCM patients possesses yet another aspect. There is a risk of vertebrobasial insufficiency resulting in transitory or permanent loss of vision during or after spine surgery. Pretreatment atherosclerosis, incorrect position of the head, blood loss, and intraoperative hypotension, as well as smoking, high blood pressure, diabetes, and high blood viscosity, have all been cited as significant contributors [24–28]. Thrombosis of the atherosclerotic carotid artery during anterior surgery is another vascular risk for patients with SCM [29,30].

When the neck is flexed and extended, the spinal cord moves cranially and caudally in the spinal canal [31]. During hyperextension, the ligamenta flava bulge, thereby compressing the spinal cord dorsally [32]. Bulging ligamenta flava compress the posterior and lateral columns and the dorsal root entry zone. During extension, the cross-sectional area of the cervical spinal cord has been found to enlarge [33]. These findings may explain the occasional exacerbation of symptoms and the clinical improvement often observed when the neck is immobilized with a collar [34]. Symptoms and signs may also be exacerbated by neck flexion. The spinal cord is then injured as it is stretched over a ventral osteophytic wall. Quick or slow anteflexion (rarely extension) is a maneuver provoking Lhermitte's sign (a shock-like sensation in the trunk or limbs).

III. CLINICAL FEATURES

Symptoms most frequently begin between 50 and 70 years of age, but may occur much earlier or in more advanced years. Most patients visit their doctor at 50–55 years of age [35–38]. Men are affected more frequently (2–3:1) than women [36,38,35].

Symptoms may develop progressively or in stepwise fashion, with remissions between periods of deterioration. Symptoms and signs may arise for the first time or be aggravated following injuries such as a carrying a weight, a fall on a slippery surface, a motor vehicle accident, or forced hyperextension of the neck.

Most frequent and characteristic symptoms are gait disorders (82%), clumsy hands (84%), and neck and back pain (95%) (Table 1). Pain in the neck (67%), shoulder, and arms is a common presenting complaint [35,39]. Pain may radiate in a radicular distribution and is usually dermatomal. However, it may occasionally occur in the distribution of the affected myotome. Paresthesias (78%), fasciculations in upper extremities (32%), and muscle weakness in the distribution of the affected nerve roots (30%) are often encountered. Reduction in the reflexes may be observed in upper extremities, but in lower extremities may be associated with hyperactive reflexes (60%) [35]. Although the patient may complain of only unilateral lower extremity symptoms, neurological examination usually reveals signs of bilateral disturbance of long tract function. Spasticity (62%) is one typical sign, and suddenly stretching legs may be reported. Sensory complaints, especially pain in the lower extremities, could be misleading. Lhermitte's sign is very specific, though of low sensitivity (14–27%) [18,35]. Disturbances of sphincter function (24%) are late phenomena, are usually mild, and generally do not occur in the absence of advanced spinal cord dysfunction, which manifests itself earlier by dysfunction of other modalities [35].

The duration of signs and symptoms varies considerably according to personal history. It may last from several hours through many (25–35) years, but typically occurs over one or several years [35–38].

IV. IMAGING, ELECTROPHYSIOLOGICAL, AND LABORATORY STUDIES

A. Imaging of the Cervical Spine

Plain radiographs of the cervical spine most frequently show narrowing of the intervertebral disc spaces, with adjacent osteophytes narrowing the spinal canal and neuroforamina, deformation of

Table 1 Incidence of Signs and Symptoms of SCM

	Incidence (%)	
Sign symptom	Ref. 36	Ref. 35
Neck pain	10	67
Paresthesias in UL	42	78
Paresthesias in LL	3	70
Hypesthesia in LL	34	54
UL palsy	24	67
LL palsy	24	57
Loss of sphincter control	0	24
Limitation of neck movement	mostly normal mobility	40

the spinal bodies (platyspondylia), sclerosis of the vertebral endplates, degeneration and osteophyte formation on the facet and uncovertebral joints. On oblique projections, better visualization of the neuroforamina, of dynamic projections (in flexion and extension), of hypermobility (or instability in a segment), and hypomobility is achieved. Computer tomography (CT) may demonstrate the dimensions of the spinal canal and reveal the location of osteophytes better than MRI in relation to the intervertebral foramina and spinal cord. An optimal degree of diagnostic accuracy can be obtained by myelography followed by CT, but this technique is used only occasionally because of its invasiveness and radiation load. It is reserved especially for patients with metallic implants and extreme deformity of the spine.

MRI is an excellent means of visualization of a narrowed spinal canal associated with spinal cord compression due to degeneratively changed spine. New modalities such as multiarray coils provide high-resolution sagittal images of the entire cord in a single scan and fast spin-echo sequences produce high-resolution T2-weighted imaging (T2WI) within a short time [40].

In healthy subjects aged 18–72 years, degenerative changes, especially in the cervical region, are present on MRI in 64% and are associated with cord compression in 11% [40]. If only subjects aged 64 or more years are taken into account, disc protrusions are seen in 57% and cord compression in 26% [41]. These facts necessarily reflect on clinical interpretations of MRI findings; a frequent clinical pitfall lies in erroneously attributing neurological symptoms to common spondylotic degeneration, especially in older people (overestimation of imaging findings).

MRI can reveal cord signal abnormalities on T2WI at (or near) the site of compression, which may signal evidence of edema, demyelinization, gliosis, or myelomalacia.

The clinical value of **increased signal intensity on MR scans** is controversial. Some studies have found a negative correlation between the outcome of surgery or conservative treatment and increased signal intensity [42–45], but others have not [46], or even noted a positive correlation [47]. Some found this relation predictive only in cases with multilevel manifestation [48] or when a low-signal on T1WI and a high-signal on T2WI were combined [49]. In our study (unpublished), the appearance of increased signal intensity in the cervical spinal cord did not predict the outcome in either type of treatment. Postoperative MRI may demonstrate that the reason for poor clinical outcome is inadequate decompression or cord atrophy [50]. MRI findings could be challenged in patients in whom an operation is accompanied by metallic implants.

In summary, the combination of plain radiographs of the cervical spine with flexion-extension views read in conjunction with MRI has been found to be more sensitive and specific for the diagnosis of causes of spinal canal stenosis, herniated disc, and intradural lesions than results observed in most patients undergoing plain CT or CT-assisted myelography alone [51,52]. We used this combination technique in most patients, but in some it proved necessary to add a plain CT at the level of maximal compression for better visualization of osteophytes and CT after myelography in patients with metallic implants or with extreme spine deformation.

B. Electrophysiological Studies

Magnetic resonance imaging defines anatomical lesions of the spine and spinal cord well, but it can give no information about cervical cord dysfunction, whereas electrophysiological examinations (somatosensory and motor-evoked potentials) are very sensitive and objective in the detection of functional lesion of the spinal cord in patients with SCM. Their clinical benefit is based on a capacity to detect subclinical lesions of the spinal cord and roots [53,54] at the location of the level of significant cord compression [55] and as an objective tool for the evaluation of outcome of the treatment [56,57], as well as being an essential means of differential diagnosis.

In mild nonprogressing forms of SCM, it can help to identify patients with potentially progressive forms [58].

Cerebrospinal fluid examination is typically normal or shows a nonspecific elevation in protein concentration (0.6–0.8 g/L) [39]. Nowadays it does not form a part of diagnostic work-up in SCM but may exceptionally be employed for purposes of differential diagnostic. An important point is that patients with SCM may have IgG oligoclonal bands in CSF, which may introduce a puzzling element into diagnosis and misleadingly support a finding of multiple sclerosis [59].

C. Natural History

In order to be sure that a health intervention is effective, one has to have a sound epidemiological basis of the natural history of disease. However, valid information about the natural history of SCM is still lacking, in spite of its prerequisite role in developing a rational plan for treatment and for measurement of effectiveness [60]. Several retrospective studies, reaching sometimes controversial conclusions, are available. There is a tendency for SCM patients to progress to severe disability, but it is not known to what degree or how quickly, how many patients in the population might suffer, or what method is suitable for identifying these patients in advance. Reports of some series refer to a steady progression in all patients [3,37,61,62], while another study reported only 67% of patients as having steady, progressive deterioration [63]. Yet another retrospective study showed that the disability is mild in the majority of cases and that the prognosis for these mildly affected cases and even for the more severely disabled is good [12], confirming similar findings of a previous study by Lees and Turner in 1963 [64]. The only feature associated with deterioration was age. Retrospective studies, however, are prone to a significant bias. In summary, we can say that the natural history is not precisely known and that there is a tendency to deteriorate, to remain stable, or to improve with approximately the same degree of probability. No reliable prognostic factor is known that enables a determination of the outcome in the individual patient. Almost all studies are retrospective and lacking in standard and commonly accepted criteria; they merely yield some plausible hypotheses.

V. MANAGEMENT

Management of patients with SCM includes both nonsurgical and surgical means. Many investigators have employed treatment with a cervical collar or simple observation and have noted improvement in 29–55% of their patients [1,36,65,66]. Conservative treatment further consists of the use of anti-inflammatory medications and intermittent bed rest in patients with pain and the active discouragement of high-risk activities and avoidance of risky environments (physical overloading, getting too cold, movement on slippery surfaces, manipulation therapies, vigorous or prolonged flexion of the head) [9]. A conservative approach to the treatment of SCM is supported by a very long history of myelopathy in some patients, which can last 30 or more years without any major deterioration [67]. Particularly in myelopathy caused by cervical soft herniation in patients with median-type and diffuse-type herniation, conservative treatment is an effective treatment option in 63% of patients [68].

Operative treatment for SCM has been a popular form of therapy for nearly 40 years. Current surgical methods include an anterior (Cloward or Smith-Robinson technique) [69,70] or posterior approach (laminectomy, hemilaminectomy), both with good and probably equal results; recently open-door laminoplasty and vertebral corpectomy have been added [71–73]. Laminectomy is an very old treatment for cervical spine and cord problems. The Greek physician

Paul of Aegina (ca. 625–690 a.d.) was the first (recorded) to perform laminectomy on patients with injury of the cervical spine. The next record of successful laminectomy dates from 1829 (by Alban Smith of Danville, Kentucky), but William Rogers [74] and Robinson and Southwick [75] developed the basic principles of laminectomy for modern times.

The indication for surgery is usually severe and progressive course of the disease. To the best of our knowledge, no comparison of the effects of conservative and operative treatments has been made in a randomized controlled trial. The majority of published reports come from surgical departments, provide optimistic results, and are retrospective [12,17,48,76–86]. In many surgical and orthopedic departments, however, almost all cases of SCM referred by neurologists are operated upon without consideration of the grade of functional deficit [87]. Little is known about the operation in patients with a definite but mild or moderate form without or with very slow progression, who represent the large majority of patients with SCM and in whom surgery is more logical (to prevent unpredictable and severe deterioration). Some authors suggest early surgery in these cases, because irreversible changes may occur in the spinal cord and the best results could be obtained in patients who have decompression within 6 months to one year of the onset of symptoms and in those who have early, mild myelopathic findings [29,88,89]. However, evidence supporting this concept is lacking.

We have performed a prospective randomized study comparing surgical and conservative treatment of SCM in a group of mild and moderate forms without or with slow progression [9]. A comparison of the two groups showed no significant differences in changes over time in modified score of Japanese Orthopedic Association (mJOA) [90] or quantified gait, but there were significant differences in the score of daily activities recorded by video at 24 months, which was a little lower in the surgical group, and also in RR and subjective evaluation, which were both worse in the surgical group at months 12 and 24. However, at month 6 this last parameter was significantly better in the surgical than in the conservative group. We concluded that surgical treatment of mild and moderate forms of SCM in our study design, comprising patients with no progression or very slow, insidious progression and a relatively long duration of symptoms, did not show better results than conservative treatment over the 2-year follow-up. No difference in average does not mean that patients did not change at all over these 2 years. They improved and deteriorated in both groups (Table 2). In the **conservatively treated group** five patients improved in mJOA scale by 2 points, one by 3 points and one by 5 points, whereas one patient deteriorated by 5 points, one by 2, and one by 3 points. In the **surgery group** one patient improved by 4 points on the mJOA scale, two patients by 3 points, and two by 2 points. Two patients deteriorated by 2 points, two by 3 points, and one by 4 points. Three patients expired during the follow-up in the surgery group.

After 3 years of follow-up in a slightly larger group of patients, again we did not find, on average, a better effect of surgery in the treatment of mild and moderate forms of SCM [10].

Table 2 mJOA Scale Improvement or Deterioration at 2-year Follow-up

Improved by	Conservative treatment	Surgery	Deteriorated by	Conservative treatment	Surgery
5 points	1		5 points	1	
4 points		1	4 points		1
3 points	1	2	3 points	1	2
2 points	5	2	2 points	1	2
Points in sum	18	14	Points in sum	10	14

Nevertheless, there was a slight but significantly increased number of patients with a negative trend in the score of daily activities in the conservatively treated group (but no significant differences in other parameters such as mJOA score, timed 10 m walk, and patient satisfaction).

VI. FACTORS PREDICTIVE OF OUTCOME

The pretreatment functional status is an important predictive factor for surgery [89]. It has been indicated that in mild myelopathy a better outcome could be expected than in severe forms [29,91]. However, this has not been verified in prospective studies and has not been compared with conservative treatment.

The anteroposterior diameter and transverse area of the spinal cord are considered significant predictive factors [17,43]. It has been found that if the compression of the spinal cord is submaximal (i.e. (i.e., $\leq$30 mm^2), the effect of surgery is unsatisfactory [16,43], but this parameter did not show any significant prognostic value in one other study [89].

The prognostic value of **increased signal intensity areas** in the spinal cord on TW2 MR is mentioned above. Its predictive value remains tentative.

The **age** of patients is a controversial factor. Some studies consider old age a risk factor [12,43,92], others have found no correlation [93].

The **duration of symptoms** is frequently considered a significant factor with predictive value for long-term results [16,17,83]. However, it is necessary to approach the evaluation of this factor with care, because recognition of the precise onset of the disease could prove a difficult task.

The **number of compressed levels of compression** can affect the outcome of treatment or the natural history. A single compression level produces a mild functional deficit in comparison to multiple compression, as has been shown experimentally [94]. According to some studies, the results of surgery are better in single-level than in multilevel compressions [91,95].

The **congenital stenosis** of the spinal canal: a congenitally narrow canal per se has not proved a negative prognostic parameter in surgery for SCM [96]. In our study (unpublished), a higher Pavlov's index was predictive of good outcome in the conservatively treated group, but was not predictive in the surgery group.

Preliminary results from our study dealing with the predictive value for clinical outcome of conservative and surgical treatment show that a good outcome in conservatively treated patients is to be expected in elderly subjects with large spinal canal diameter. In surgically treated patients, a good prognosticator is a lower mJOA score (near 12 points on the mJOA scale).

All of these predictors are valid for mild and moderate forms of SCM (mJOA score $\geq$12 points) without progression or with slow insidious progression, constituting the majority of patients with this disease.

From all our studies dealing with the treatment of SCM and from the data in other reports, we can conclude that, over a 3-year period, both treatments (conservative and surgical) are equally successful in patients with mild and moderate forms of SCM without or with slow progression. With conservative treatment, the various risks of surgery can be avoided; with surgery, the potential progression of the disease in future years is prevented. Patients should rather be treated conservatively if they have congenitally normal size of the spinal canal, spinal transversal area $>$70 mm^2 and are of older age. Surgery is more suitable for patients with clinically worse status (expressed as lower mJOA score, i.e., near 12 points) and smaller transversal area of the spinal cord at the level of maximal compression. This is in concordance with authority-based recommendations to operate on patients with significant cord compression and

significant clinical problems, reserving conservative treatment for patients with nonprogressive forms with slight cord compression and slight signs and symptoms of the disease.

ACKNOWLEDGMENT

This study was supported by the Internal Grant Agency of the Ministry of Health of the Czech Republic, Grant No. NF 6521–3.

REFERENCES

1. Wilkinson M. The morbid anatomy of cervical spondylosis and myelopathy. Brain 1960; 83:589–616.
2. Simeone FA, Rothman RH. Cervical disc disease. In: The Spine. 2nd ed.. Philadeplhia: W.B. Saunders, 1982:440–476.
3. Montgomery DM, Brower RS. Cervical spondylotic myelopathy. Clinical syndrome and natural history. Orthop Clin North Am 1992; 23:487–493.
4. Moore AP, Blumhardt LD. A prospective survey of the causes of non-traumatic spastic paraparesis and tetraparesis in 585 patients. Spinal Cord 1997; 35:361–367.
5. Kaye KL, Ramsay D, Young GB. Cervical flexion myelopathy after valproic acid overdose. Spine 2001; 26:459–461.
6. Munoz Corsini L, Garcia del Valle A, Galindo S, Porras M. Anterior cervical myelopathy in the early postoperative period. Can J Anaesth 1997; 44:872–876.
7. Snow RB, Weiner H. Cervical laminectomy and foraminotomy as surgical treatment of cervical spondylosis: a follow-up study with analysis of failures. J Spin Disord 1993; 6:245–251.
8. Macdonald RL, Fehlings MG, Tator CH, Lozano A, Fleming JR, Gentili F, Bernstein M, Wallace MC, Tasker RR. Multilevel anterior cervical corpectomy and fibular allograft fusion for cervical myelopathy. J Neurosurg 1997; 86:990–997.
9. Kadanka Z, Bednarik J, Vohanka S, Vlach O, Stejskal L, Chaloupka R, Filipovičova D, Surelova D, Adamova B, Novotny O, Nemec M, Smrcka V. Conservative treatment versus surgery in spondylotic cervical myelopathy: a prospective randomised study. Eur Spine J 2000; 9:538–544.
10. Kadanka Z, Mares M, Bednarik J, Smrcka V, Krbec M, Stejskal L, Chaloupka R, Surelova D, Novotny O, Urbanek I, Dusek L. Approaches to spondylotic cervical myelopathy:conservative vs surgical results in a three-year follow-up study. Spine 2000; 27(20):2205–2211.
11. Epstein JA. The surgical management of cervical spine stenosis, spondylosis, and myeloradiculopathy by means of posterior approach. Spine 1988; 13:864–869.
12. Nurick S. The pathogenesis of the spinal cord disorder associated with cervical spondylosis. Brain 1972; 95:87–100.
13. Hukuda S, Wilson CB. Experimental cervical myelopathy: effect of compression and ischemia on the canine cervical cord. J Neurosurg 1972; 37:631–652.
14. Fujiwara K, Yonenobu K, Hiroshima K, Ebara S, Yamashita K, Ono K. Morphometry of the cervical spinal cord and its relation to pathology in cases with compression myelopathy. Spine 1988; 13: 1212–1216.
15. Muhle C, Brossmann J, Biesdere J, Grimm J, Mohr A, Heller M. Value of kinematic MRI in the evaluation of patients with exacerbated pain in cervical spine motion compared with static MRI. Rofo Fortschr Geb Rontgenstr Neuen Bildgeb Verfahr 2001; 173:126–132.
16. Fujiwara K, Yonenobu K, Ebara S, Yamashita K, Ono K, Fujiwara K, Yonenobu K, Ebara S, Yamashita K, Ono K. The prognosis of surgery for cervical compression myelopathy. An analysis of the factors involved. J. Bone Joint Surg., J Bone Joint Surg 1989; 71B:393–398.
17. Koyanagi T, Hirabayashi K, Satomi K, Toyama Y, Fujimura Y. Predictability of operative results of cervical compression myelopathy based on preoperative computed tomographic myelography. Spine 1993; 18:1958–1963.

18. Crandal PH, Batzdorf U. Cervical spondylotic myelopathy. J Neurosurg 1996; 24:57–66.
19. Mihara R, Ohnari K, Hachia M, Kondo S, Yamada K. Cervical myelopathy caused by C3-4 spondylosis in elderly patients: a radiographic analysis of pathogenesis. Spine 2000; 25:796–800.
20. Bohlman HH, Emery SE. The pathophysiology of cervical spondylosis and myelopathy. Spine 1988; 13:843–846.
21. Brain WR. Rupture of the intervertebral disc in the cervical region. Proc R Soc Med 1948; 49: 509–511.
22. Adams C. Cervical spondylotic radiculopathy and myelopathy. Handbook Clin Neurol 1976; 26: 97–112.
23. Taylor AR. Vascular factors in the myelopathy associated with cervical spondylosis. Neurology 1964; 14:62–68.
24. Brown RH, Schauble JF, Miller NR. Anemia and hypotension as contributors to perioperative loss of vision. Anesthesiology 1994; 80:222–226.
25. Williams EL, Hart WM, Templehoff R. Postoperative ischemic optic neuropathy. Anesth Analg 1995; 80:1018–1029.
26. Mayers MA, Hamilton SR, Bogosian AJ, Smith CH, Wagner TA. Visual loss as a complication of spine surgery. Spine 1997; 22:1325–1329.
27. Kawaguchi T, Fujita S, Hosoda K, Shibata Y, Iwakura M, Tamaki N. Rotational occlusion of the vertebral artery caused by transverse process hyperrotation and unilateral apophyseal joint subluxation. Case report. J Neurosurg 1997; 86:1031–1035.
28. Oga M, Yuge I, Terada K, Shimizu A, Sugioka Y. Tortuosity of the vertebral artery in patients with cervical spondylotic myelopathy. Risk factor for the vertebral artery injury during anterior cervical decompression. Spine 1996; 21:1085–1089.
29. Lesoin F, Boussakao N, Clarisse J, Rouseaux M, Jomin M. Results of surgical treatment of radiculomyelopathy caused by cervical arthrosis based on 1000 operations. Surg Neurol 1985; 23:350–355.
30. Chozick BS, Watson P, Greenblatt SH. Internal carotid artery thrombosis after cervical corpectomy. Spine 1994; 19:2230–2232.
31. Adams CBT, Logue V. Studies in cervical spondylotic myelopathy. I. Movement of the cervical roots, dura and cord and their relation to the course taken by extrathecal roots. Brain 1971:557–568.
32. Taylor AR. The mechanism of injury to the spinal cord in the neck without damage to the vertebral column. J Bone Joint Surg 1951; 33:543–547.
33. Waltz TA. Physical factors in the production of the myelopathy of cervical spodylosis. Brain 1967; 90:395–404.
34. Adams CBT, Logue V. Studies in cervical spondylotic myelopathy. I. Movement of the cervical roots, dura and cord and their relation to the course taken by extrathecal roots. Brain 1971; 94:557–568.
35. Kadanka Z, Bednarik J, Vohanka S, Vlach O. Spondylotic cervical myelopathy: a clinical update. Scripta Med 1996; 65:157–172.
36. Brain WR, Northfield DWC, Wilkinson M. The neurological manisfestations of cervical spondylosis. Brain 1952; 75:187–225.
37. Sadasivan KK, Reddy RP, Albright JA. The natural history of cervical spondylotic myelopathy. Yale J Biol 1993; 66:235–242.
38. Gregorius FK, Estrin T, Crandal PH. Cervical spondylotic radiculopathy and myelopathy. Arch Neurol 1976; 33:618–625.
39. Brain WR, Wilkinson M. Cervical spondylosis and other disorders of the cervical spine, 1967:232.
40. Thorpe JW, Kidd D, Kendall BE, Tofts PS, Barker GJ, Thompson AJ, MacManus DG, McDonald WI, Miller DH. Spinal cord MRI using multi-array coils and fast spin echo I. Technical aspects and findings in healthy adults. Neurology 1993; 43:2625–2631.
41. Teresi LM, Lufkin RB, Reicher MA, Moffit BJ, Vinuela FV, Wilson GM, Bentson RJ, Hanafee WN. Asymptomatic degenerative disk disease and spondylosis of the cervical spine: MR imaging. Radiology 1987; 164:83–88.
42. Okada Y, Ikata T, Hamada H, Sakamoto R, Katoh S. Magnetic resonance imaging study on the results of surgery for cervical compression myelopathy. Spine 1993; 18:2024–2029.
43. Kohno K, Kumon Y, Oka Y, Matsui S, Ohue S, Sasaki S. Evaluation of prognostic factors following expansive laminoplasty for cervical spinal stenotic myelopathy. Surg Neurol 1997; 48:237–245.

44. Bucciero A, Vizioloi L, Carangelo B, Tedeschi G. MR signal enhancement in cervical spondylotic myelopathy. Correlation with surgical results in 35 cases. J Neurosurg Sci 1993; 37:217–222.
45. Takahashi M, Yamashita Y, Sakamoto Y, Kojima R. Chronic cervical cord compression: clinical significance of increased signal intensity on MR images. Radiology 1989; 173:219–224.
46. Matsumoto M, Toyama Y, Ishikawa M, Chiba K, Suzuki N, Fujimura Y. Increased signal intensity of the spinal cord on magnetic resonance images in cervical compressive myelopathy. Does it predict the outcome of conservative treatment?. Spine 2000; 25:677–682.
47. Singh A, Crocard HA, Platts A, Stevens J. Clinical and radiological correlates of severity and surgery-related outcome in cervical spondylosis. J Neurosurg 2001; 94:189–198.
48. Wada E, Yonenobu K, Suzuki S. Can intramedullary signal changes on MRI predict surgical outcome in cervical spondylotic myelopathy?. Spine 1999; 24:455–461.
49. Morio Y, Teshima R, Nagashima H, Nawata K, Yamasaki D, Nanjo Y. Correlation between operative outcomes of cervical compression myelopathy and MRI of the spinal cord. Spine 2001; 26:1238–1245.
50. Clifton A, Stevens J, Whitear P. Identifiable causes for poor outcome in surgery for cervical spondylosis. Neuroradiology 1990; 32:450–455.
51. Braakman R. Management of cervical spondylotic myelopathy and radiculopathy. J Neurol Neurosurg Psychiatry 1994; 37:257–263.
52. Brown BM, Schwartz RH, Frank E. Preoperative evaluation of cervical radiculopathy and myelopathy by surface-coil MR imaging. Am J Neuroradiol 1988; 9:859–866.
53. Berthier E, Turjman F, Mauguiere F. Diagnostic utility of somatosensory evoked potentials (SEPs) in presurgical assessment of cervical spondylotic myelopathy. Neurophysiol Clin 2002; 26:300–310.
54. Brunholzl C, Claus D. Central motor conduction time to upper and lower limbs in cervical cord lesions. Arch Neurol 1994; 51:245–249.
55. Tani T, Yamamoto H, Kimura J. Cervical spondylotic myelopathy in elderly people: a high incidence of conduction block at C3-4 or C4-5. J Neurol Neurosurg Psychiatry 1999; 66:456–464.
56. Bednarik J, Kadanka Z, Vohanka S, Stejskal L, Vlach O, Schroder R. The value of somatosensory- and motor-evoked potentials in predicting and monitoring the effect of therapy in spondylotic cervical myelopathy. Spine 1999; 24:1593–1598.
57. Kotani H, Senzoku F, Hattori S, Moritake Z, Hara T, Omore K. Evaluation of cervical cord function using spinal evoked potentials from surface electrodes. Spine 1992; 17:339–344.
58. Bednarik J, Kadanka Z, Vohanka S, Novotny O, Surelova D, Filipovicova D, Prokes B. The value of smotatosensory and motor evoked potentials in pre-clinical cervical cord compression. Eur Spine J 1998; 7:493–500.
59. Cohen O, Biran I, Steiner I. Cerebrospinal fluid oligoclonal bands in patients with spinal arterovenous malformation and structural central nervous system lesions. Arch Neurol 2000; 57:553–557.
60. LaRocca H. Cervical spondylotic myelopathy: natural history. Spine 1988; 13:854–855.
61. Clarke E, Robinson PK. Cervical myelopathy: a complication of cervical spondylosis. Brain 1956; 79:483–510.
62. Epstein JA, Janin Y, Carras R, Lavine IS. A comparative study of the treatment of the cervical spondylotic myelopathy. Experience with 50 cases treated by means of extensive laminectomy, foraminotomy, and excision of osteophytes during the past 10 years. Acta Neurochir 1982; 61:89–104.
63. Symon L, Lavender P. The surgical treatment of cervical spondylotic myelopathy. Neurosurgery 1967; 17:117–127.
64. Lees F, Turner JWA. Natural history and prognosis of cervical spondylosis. Br Med J 1963; 2: 1607–1610.
65. Phillips DG. Surgical treatment of myelopathy with cervical spondylosis. J Neurol Neurosurg Psychiatry 1973; 36:879–884.
66. Roberts AH. Myelopathy due to cervical spondylosis treated by collar immobilization. Neurology 1966; 16:951–954.
67. Yamashita M, Yamamoto T. A case of very slowly progressive, high-cervical spondylotic myelopathy presenting with symmetric deep sensory deficits in the palms. No To Shinkei 1955; 47:893–897.
68. Matsumoto M, Chiba K, Ishikawa M, Maruiwa H, Fujimura Y, Toyama Y. Relationships between outcomes of conservative treatment nad magnetic resonance imaging findings in patients with mild cervical myelopathy caused by soft disc herniations. Spine 2001; 26:1592–1598.

69. Cloward RB. The anterior approach for removal of ruptured cervical disks. J Neurosurg 1958: 602–617.
70. Smith GW, Robinson RA. The treatment of certain cervical-spine disorders by anterior removal of the intervertebral disc and interbody fusion. J Bone Joint Surg 1958; 40:607–624.
71. Hanai K, Fujiyoshi F, Kamel K. Subtotal vertebrectomy and spinal fusion for cervical spondylotic myelopathy. Spine 1986; 11:310–315.
72. Bernard TN, Whitecloud TS. Cervical spondylotic myelopathy and myeloradiculopathy. Anterior decompression stabilization with autogenous fibula strut graft. Clin Orthop 1987; 221:149–160.
73. Hirabayashi K, Miyakawa J, Satomi K, Maruyama T, Wakano K. Operative results and postoperative progression of ossification among patients with ossification of cervical posterior longitudinal ligament. Spine 1981; 6:354–364.
74. Rogers WA. Treatment of fracture dislocation of the cervical spine. J Bone Joint Surg 1942; 24: 245–258.
75. Robinson RA, Southwick WO. Indications and techniques for early stabilization of the neck in some fracture dislocation of the cervical spine. South Med J 1960; 53:565–579.
76. Kato Y, Iwasaki M, Fuji T, Yonenobu K, Ochi T. Long-term follow-up results of laminectomy for cervical myelopathy caused by ossification of the posterior longitudinal ligament. J Neurosurg 1998; 89:217–223.
77. Goto S, Mochizuki M, Watanabe T, Hiramatu K, Tano T, Kitahara H, Moria H. Long-term follow-up study of anterior surgery for cervical spondylotic myelopathy with special reference to the magnetic resonance imaging findings in 52 cases. Clin Othop Rel Res 1993; 291:142–153.
78. Hirai O, Kondo A, Aoyama I, Nin K. Anterior decompression surgery of aged patients with cervical myelopathy. No Shinkei Geka 1991; 19:1017–1023.
79. Magnaes B, Hauge T. Surgery for myelopathy in cervical spondylosis: safety measures and preoperative factors related to outcome. Spine 1980; 5:211–213.
80. Seifert V, Stolke D. Multisegmental cervical spondylosis: treatment by spondylectomy, microsurgical decompression, and osteosynthesis. Neurosurgery 1991; 29:498–503.
81. Utley D, Monro P. Neurosurgery for cervical spondylosis. Br J Hosp Med 1989; 42:62–70.
82. Yangia OU, Jike L, Jite M, Cheng-li M, Jianghui Z, Yujun L, Ning Jiang S. Extensive anterior decompression for mixed cervical spondylosis. Resection of uncovertebral joints, neural and transverse foraminotomy, subtotal corpectomy, and fusion with strut graft. Spine 1994; 23:2651–2657.
83. Yonenobu K, Okada K, Fuji T, Fujiwara K. Causes of neurologic deterioration following surgical treatment of cervical myelopathy. Spine 1985; 11:818–823.
84. Naito M, Ogata K, Kurose S, Ozama M. Canal- expansive laminoplasty in 83 patients with cervical myelopathy. Int Orthop 1994; 18:347–351.
85. Onimus M, Destrumelle N, Gangloff S. Surgical treatment of cervical disk displacement. Anterior or posterior approach. Rev Chir Orthop Repar Appar Mot 1995; 81:296–301.
86. Tegos S, Rizos K, Papathanasiu A, Kyriakopulos K. Results of anterior discectomy without fusion for treatment of radiculopathy and myelopathy. Eur Spine J 1994; 3:62–65.
87. Kadanka Z, Bednarik J, Vohanka S, Vlach O. Operative management of spondylotic cervical myelopathy in Czech and Slovak Republic. Rozh Chir 1996; 75:535–540.
88. Epstein JA, Epstein NE. The surgical management of cervical spinal stenosis, spondylosis, and myeloradiculopathy by means of the posterior approach. In: Cervical Spine Research Society Editorial Committee (eds). The Cervical Spine. Philadelphia: J.B. Lippincott, 1989:625–643.
89. Hamburger C, Buttner A, Uhl E. The cross-sectional area of the cervical spinal canal in patients with cervical spondylotic myelopathy. Correlation of preoperative and postoperative area with clinical symptoms. Spine 1997; 22:1990–1994.
90. Benzel EC, Lancon J, Kesterson L, Haden T. Cervical laminectomy and dentate ligament section for cervical spondylotic myelopathy. J Spin Disord 1991; 4:286–295.
91. Hirabayashi K, Uzawa M. Multilevel anterior cervical interbody fusion: a new method of subcortical binding to prevent graft dislocation. Neuro-Orthoped 1995; 17/18:21–28.
92. Arnold H, Feldmann U, Missler U. Chronic spondylogenic cervical myelopathy. A critical evaluation of surgical treatment after early and long-term follow-up. Neurosurg Rev 1993; 16:105–109.

93. Irvine GB, Strachan WE. The long-term results of localized anterior cervical decompression and fusion in spondylotic myelopathy. Paraplegia 1987; 25:18–22.
94. Shinomiya K, Mutih N, Furuya K. Study of experimental cervical spondylotic myelopathy. Spine 1992; 17:383–387.
95. Emery SE. The pathophysiology of cervical spondylosis and myelopathy. Spine 1998; 13:843–846.
96. Wang YL, Tsau JC, Huang MH. The prognosis of patients with cervical spondylotic myelopathy. Kao Haiung I Hsueh Ko Hsueh Tsa Chih 1997; 13:425–431.

24

Autogenous Free Fat Grafts After Posterior Lumbar Surgery

Masahiko Kanamori
Toyama Medical and Pharmaceutical University
Toyama, Japan

I. INTRODUCTION

The exact relationship of postoperative scar tissue and symptoms remains controversial, although epidural and peridural fibrosis is considered to be the cause of pain in a number of patients [1–3]. In the first two decades of this century, the use of autogenous grafts of subcutaneous fat in an attempt to inhibit or prevent epidural and perineural fibrosis after lumbar laminectomy was reported by Rehn [4], Hilse [5], and Lexer [6]. The development of epidural and perineural fibrosis secondary to posterior lumbar surgery has been investigated in both experimental and clinical studies [1,2,7–10]. LaRocca and Macnab [8] reported postoperative peridural fibrosis after laminectomy in dogs. They called this peridural fibrosis the ''laminectomy membrane''; the extent of the membrane was proportional to the area of the laminectomy. Free fat graft has been found to be superior to gelfoam in the prevention of postoperative scarring [11]. It has been subsequently recommended by various authors [12–15]. Other investigators, however, who also based their comments on clinical experience with these grafts, questioned their usefulness in preventing epidural and perineural fibrosis [16] and even described complications attributable to the grafts [17–21] or at least recognize that their effectiveness had not been established. However, free fat graft is now generally accepted in order to avoid possible epidural fibrosis after surgical decompression of neural tissue [3,22–24].

II. IMAGE EVALUATION

Evaluations of changes in grafted fat have been reported on computed tomogram (CT) scans [25,27]. It has been shown both experimentally and clinically that although fat grafts shrink to about 30% to 50% of their original size with time, they remain viable, retaining the characteristic appearance of normal fat when evaluated on CT scan.

We evaluated the clinical serial magnetic resonance imaging (MRI) observations of grafted fat after posterior lumbar surgery [28]. We studied 22 patients with degenerative lumbar disease (16 men and 6 women; 17–79 years old; mean age: 44.5 years) who underwent posterior lumbar decompressive surgery. MRI manifestations of the grafted fat were determined by the size and the signal intensity of the T1 images. T1- and T2-weighted axial MRI of the lumbar spine were obtained at 3, 7, 21, 42 days and 1 year after surgery. The signal intensity of the fat was classified

as grade I (almost equal to the subcutaneous fat tissue), grade II (low signal intensity compared to the subcutaneous fat tissue), grade III (speckled intensity), and grade IV (signal void, suggesting the change to scar tissue). From the T2-weighted image, the time-related cross-sectional area of the subarachnoid space was measured at the same level of each T1-weighted image.

We present two representative cases (Figs. 1 and 2). The onlay-grafted fats were identified throughout the observation time. The postoperative serial MRI evaluation of autogenous fat grafts revealed survival of the transplant with reduction in size of approximately 57% at 42 days and to 33% at one year, compared with the condition at 3 days after surgery. The size of the grafted fat was reduced in accordance with the expansion of the subarachnoidal space (Fig. 3). On the 3-day postoperative MRI, grafted fats were revealed in various shapes and had a fairly vague outline because the dura was shrunken and the surrounding muscles were swollen and edematous. It appeared as if the grafted fat compressed the dura mater, but these findings disappeared with time. On day 42, these findings completely disappeared, and the shape of the

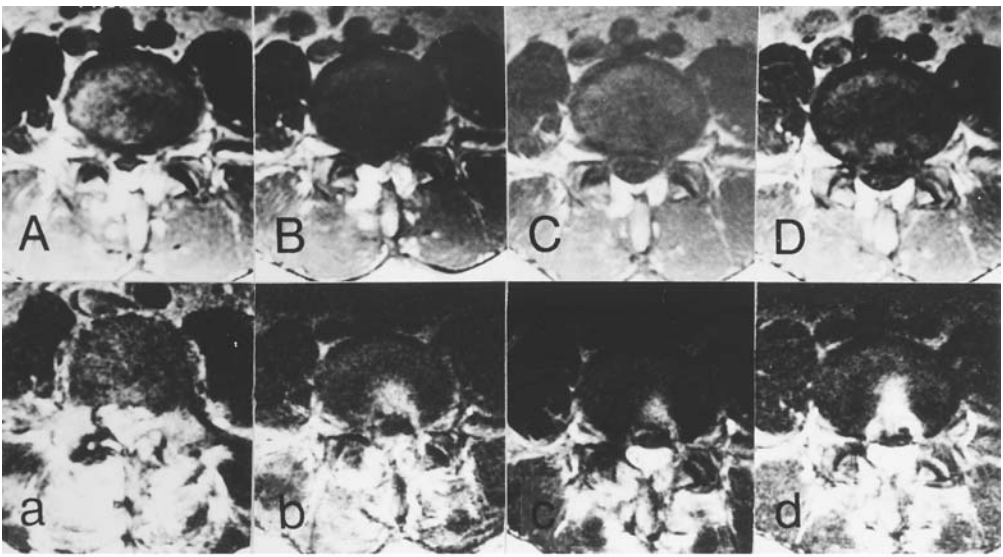

A

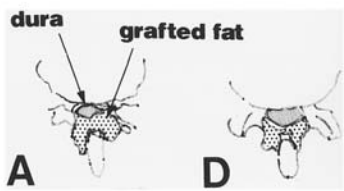

B

Figure 1 (Top) MRI evidence of the reduction and remodeling of the grafted fat at the L4–L5 level in a 56-year-old man who underwent L3–L5 laminectomy. He also underwent a discectomy at the L4–L5 level 9 years previously. The remodeling of the shape of the grafted fat (T1 images) occurred in relation to the postoperative reexpansion of the dura mater (T2 images). (A/a) Three days after surgery. It seems that grafted fat compressed the dura mater. (B/b) Seven days after surgery. (C/c) Twenty-one days after surgery. (D/d) Forty-two days after surgery. Capital letters indicate T1-weighted images. Small letters indicate T2-weighted images. (Bottom) Illustrations of A/a and D/d in above.

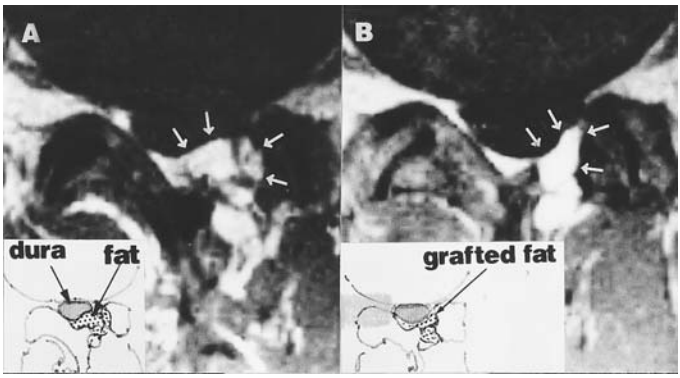

Figure 2 MRI and illustrations showing the change of grafted fat (T1 images). MRI evidence of the reduction and remodeling of the grafted fat with time at the L5–S1 level in a 22-year-old man who underwent unilateral left side interlaminar laminotomy and discectomy. The size of the grafted fat is reduced, and the shape is changed to conform the shape of the dura mater. White bars indicate the grafted fat. (A) Three days after surgery. It seems that grafted fat compressed the dura mater. (B) One year after surgery.

grafted fat was changed to approximate that of the dura mater. The remodeling of the shape of the grafted fat was recognized to have a relationship to the postoperative transient shrinkage and re-expansion of the dura mater. Signal intensity of the grafted fat was evaluated in comparison to normal subcutaneous fat tissue. In the early stage (within 6 weeks after surgery), the signal intensity of the grafted fat was lower compared to that of subcutaneous fat tissue. But its intensity was recovered to normal by one year after surgery (Fig. 4).

Our clinical postoperative serial MRI studies clarified that the size of grafted fat was reduced and the shape was changed along the shape of the dura mater. The remodeling of the shape of the grafted fat occurred in relation to the postoperative transient shrinkage and re-expansion of the dura mater. Matsui et al. [29] reported that posterior lumbar surgery produces

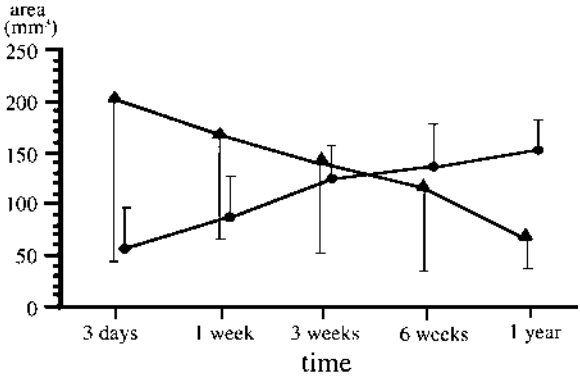

Figure 3 Correlation between the size of the grafted fat and the area of the subarachnoidal space in the transverse section on MRI. The size of the grafted fat is reduced in accordance with the expansion of the subarachnoidal space with time. (●), subarachnoidal space; (▲), grafted fat. Bars: standard deviation.

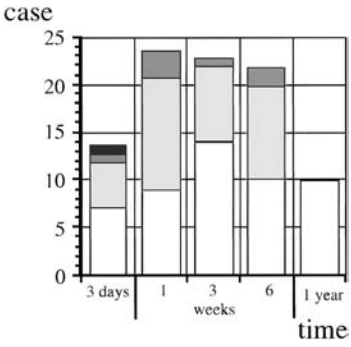

Figure 4 The change in grafted fat signal intensity. Almost half of the cases in this series showed low signal intensity of the grafted fat on MRI within 6 weeks after surgery, but it recovered by one year after surgery. Grade I: almost equal to the subcutaneous fat tissue (clear bar); grade II: low signal intensity compared to the subcutaneous fat tissue (shaded bar); grade III: speckled intensity (dark bar); grade IV: signal void suggesting change in scar tissue (black bar).

cauda equina adhesions and shrinkage of the subarachnoidal space; cauda equina adhesions at the level of the laminectomy were seen in the early postoperative stage. The cauda equina adhesions began to resolve spontaneously about 1 week after surgery and became normal at 6 weeks. We found that the reduction and remodeling of the grafted fat occur along the same time course of the dura shrinkage and reexpansion. In the early stage, when the dura mater was shrinking, it seemed as if the grafted fat compressed to the dura mater. We have studied the signal intensity of the grafted fat. Almost half of the cases showed low signal intensity of the grafted fat on MRI within 6 weeks after surgery. We consider this finding to indicate the depression of the viability of the grafted fat. We cannot confirm the histological evidence at this time, but it is natural to suppose that the grafted fat is still alive from the finding of reaquisition of high signal intensity on late-stage MRI.

III. HISTOLOGICAL EVALUATION

The histological analyses of the free-grafted fat were mainly investigated from the surgical specimen taken at the repeated lumbar surgery. We studied 18 patients with degenerative lumbar disease (13 men and 5 women; 22–70 years old; mean age: 53.6 years at first operation) who underwent repeated posterior lumbar surgery after posterior decompression and free fat graft [30]. We evaluated the fat globules using osmium-paraffin stain technique [31].

In 12 patients the free fat harvested from the left buttock was grafted onto the decompressive area at a first operation. In the other 6 patients, the free fat harvested from the local subcutaneous fat tissue in the operative field was used. The mean term between the first and the second operations was 65.8 months. Sections from surgically resected specimens were routinely and rapidly fixed in 10% buffered formalin and embedded in paraffin. The specimens were stained with hematoxylin-eosin (HE) or osmium. In the osmium-paraffin stain, the sections were fixed with 1% osmium tetraoxide (OsO_4) at room temperature for 24 hours and embedded in paraffin. Serial sections (5 μm thick) were cut.

HE staining revealed increased collagen fiber and hyperplasia of blood vessels entering the fat tissue that survived. These findings were common to all patients and consistent with previously reported findings [12,32]. A reduction in size of the grafted fat has been reported

on experimental study. Histological study in dogs showed an initial breakdown of fat cells and revascularization [12].

There have been no reports in the literature evaluating fat globules. In the HE-staining step, the lipid is soluble in the alcohol when the sections are dehydrated. The frozen section must be prepared in order to observe the change in fat globules. But this procedure is rather complicated. The osmium-paraffin staining method uses 1% osmium tetraoxide with fixation simultaneously. The procedure is simple, and fat globules can be observed with little artifact. We showed that grafted survival fat tissue was accompanied by various changes such as variation in fat globules size, polymorphism, and vacuolar degeneration. In the normal gluteal fat, relatively uniform and roundish fat globules were observed. In the fat tissue after grafting, fat globules were reduced in size, resulting in polygons of various sizes. From the repeated surgery sample, the mean area of the fat globules in the grafted fat from the buttock region was 422.9 $\pm$ 193.1 pixels, and that in the graft fat from the local subcutaneous site was 406.8 $\pm$ 91.9 pixels. The mean area of the normal gluteal fat was 663.0 $\pm$ 157.7 pixels. The globules of the grafted fat were reduced compared with the normal gluteal fat globules. They were reduced to about 63.7% in the case of buttock fat, and to about 61.4% for local subcutaneous fat ($p < 0.05$ for each). But there was no significance to the decreased rate in each group.

To analyze the shape and quality of the fat globules, we use our original grading system which is classified into three groups: stage I (almost equal to the gluteal fat tissue showing uniform and roundish fat globules), stage II (remarkably variable size of the fat globules), and stage III (vacuolar degeneration in the majority of the fat globules) (Fig. 5). Representative staining of samples from a patient who underwent reoperation is shown in Figure 6. In this evaluation, all patients were classified as stage II or III. Histologically, graft survival was observed in all patients, but accompanied by considerable changes such as various sizes, polymorphism, and vacuolar degeneration of the fat globules.

IV. SYMPTOM EVALUATION

We evaluated the clinical findings and follow-up results by the Japanese Orthopedic Association assessment scoring system (JOA score) [33]. The categories consist of subjective symptoms (9 points), clinical signs (6 points), impairment of activity of daily living (14 points), and urinary bladder function (0–6 points). A completely normal condition would rate 29 points—a total of the best score in each category. The postoperative improvement rate was determined by the following equation:

$$\frac{\text{Postoperative JOA score} - \text{preoperative JOA score}}{29 - \text{preoperative JOA score}} \times 100\% \tag{1}$$

The mean preoperative JOA score in our series was 11.3 $\pm$ 3.7 points. The mean score had improved to 20.1 $\pm$ 3.2 points 3 weeks after surgery. We evaluated the improvement rate of the JOA score between the fat size–unchanged group and the fat size–decreased group. The mean improvement rate of the JOA score of the former was 51.7 $\pm$ 29.6% and in the latter was 47.6 $\pm$ 18.9%. There was no significant difference between each group. There was also no significant difference between the fat intensity–suppressed group and the fat intensity–unchanged group. The mean improvement rate of the JOA score was 49.9 $\pm$ 17.7% and 46.4 $\pm$ 21.7%, respectively. Nothing definite can be stated concerning details of the intensity and size of the grafted fat.

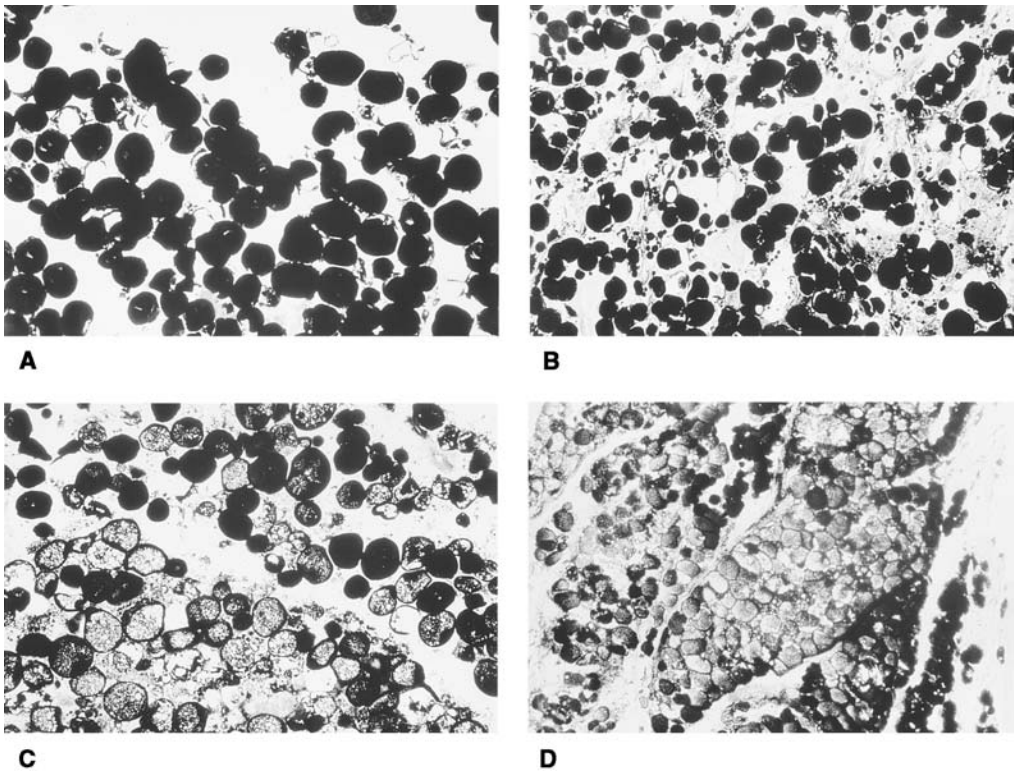

Figure 5 Histological stage of the grafted fat: (A) stage I—the uniform roundish fat globules; (B) stage II—remarkable variable size of the fat globules; (C) stage III—vacuolar degeneration in the half number of the fat globules; 2nd (D) stage IV—vacuolar degeneration in the majority of the fat globules.

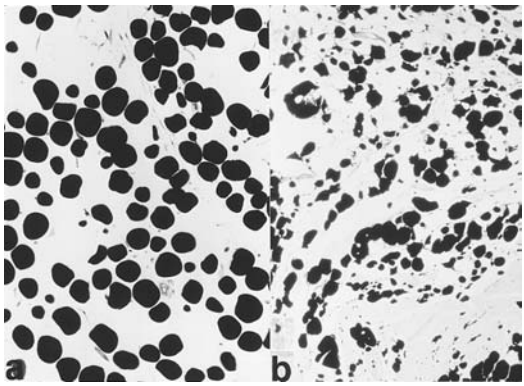

Figure 6 Histological evidence of grafted fat in 70-year-old male. (a) Fat globules in a normal buttock region; (b) fat globules in a grafted fat tissue.

Recently Bernsmann et al. [34] reported a prospective randomized trial performed with and without autologous fat graft in lumbar microdisc surgery. They found no significant differences between the fat graft group and the control group regarding either clinical outcome or social aspects. They stated that further investigations are needed to examine the relationship between epidural scar formation and postoperative clinical findings. There has been no study about prospective randomized trials in total laminectomy.

V. PERFORMING THE FAT GRAFT

The epidural fat pad is thought to be important in the spinal canal [35]. We prefer to use the free fat tissue harvested from the buttock rather than local subcutaneous fat from the operative field in order to avoid unsuitable fat materials (local subcutaneous fat is sometimes scarce and in a thin patient can be fibrotic). It may be possible to harvest enough quality fat tissue from the local subcutaneous fat in an obese patient. Gill et al. [36,37] reported on the usefulness of pedicle fat grafts, which were not generally used in surgery.

Fat tissue should be incised and molded at a thickness of about 5 mm, but not in small pieces. Full-thickness fat grafts seem to survive better than multiple particulate grafts [38]. Because of the danger of nerve compression, surgeons will avoid using fat grafts that are are too large. To our knowledge there are no guidelines as to what size fat grafts should be. Thin fat grafts have been thought to be ineffective because grafted fat diminishes postoperatively. We routinely use and recommend using 5 mm thick grafted fat. Grafted fat of this thickness protects the dura sufficiently and allows for some diminution of the graft without excessive formation of fibrous tissues. A suction drain should be routinely used.

VI. COMPLICATIONS

Although dural compression by a free autogenous fat graft is very rare, some cases have been reported [17–21]. We have experienced only 2 [20] in 1052 cases (0.2%) from 1983 to 1998. Possible mechanisms of the complication are formation of a hematoma anterior to the graft and direct compression by a large fat graft that is pushed by the paraspinal erector muscles.

VII CONCLUSIONS

The grafted fat used in posterior lumbar surgery is reduced in total amount, but it is alive and remodeled to the shape of the dura mater in relation to its shrinkage and reexpansion on MRI. This remodeling of the grafted fat is meaningful and effective in protecting the dura mater (Fig. 7). Histologically, the grafted fat globules are reduced in size and quality compared with the normal fat tissue. However, they have been confirmed to survive long term.

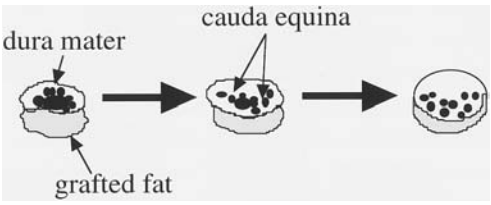

Figure 7 Illustration of the correlation between the area of grafted fat and the subarachnoidal space. Free fat graft is alive and remodeled to the shape of the dura mater in relation to its shrinkage and reexpansion.

REFERENCES

1. Benner B, Ehni G. Spinal arachnoiditis. The postoperative variety in particular. Spine 1978; 3:40–44.
2. Burton CV. Lumbosacral arachnoiditis. Spine 1978; 3::24–30.
3. Tsuji H. Comprehensive Atlas of Lumbar Spine Surgery. St. Louis: Mosby Year Book, 1991:58–61.
4. Rehn E. Die Fetttransplantation. Langenbecks Arch. Klin. Chir 1912; 98:1–37.
5. Hilse A. Experimenelle Untersuchungen über freie Fetttransplantation bei Blutungen parenchymatoser Bauchorgane. Langenbecks Arch. Klin. Chir 1914; 103:1042–1083.
6. Lexer E. Zwanzig Jahre Transplantations forschung in der Chirurgie. Langenbecks Arch. Klin. Chir 1925; 138:294–297.
7. Haughton VM, Eldevik OP, Ho KC, Larson SJ, Unger GF. Arachnoiditis from experimental myelography with aqueous contrast media. Spine 1978; 3:65–69.
8. LaRocca H, Macnab I. The laminectomy membrane. Studies in its evolution, characteristics, effects and prophylaxis in dogs. J. Bone Joint Surg 1974; 56-B:545–550.
9. Tsuji H, Yamada H. Clinical aspects of lumbar adhesive arachnoiditis. Evaluation of 28 cases and review of literature (in Japanese). Seikeigeka MOOK 1979; 11:286–297.
10. Yamagami T, Matusi H, Tsuji H, Ichimura K, Sano A. Effects of laminectomy and retained extradural foreign body on cauda equina adhesion. Spine 1993; 18:1774–1781.
11. Jacobs RR, McClain O, Neff JR. Control of postlaminectomy scar formation. An experimental and clinical study. Spine 1980; 5:223–229.
12. Saunders MC, Keller JT, Dunsker SB, Mayfield FH. Survival of autologous fat grafts in humans and in mice. Connect Tissue Res 1981; 8:85–91.
13. Keller JT, Dunsker SB, McWhorter JM, Ongkiko CM, Saunders MC, Mayfield FH. The fate of autogenous grafts to the spinal dura. An experimental study. J. Neurosurg 1978; 49:412–418.
14. Kiviluoto O. Use of free fat transplants to prevent epidural scar formation. Acta Orthop. Scand. (suppl) 1976; 164:66–69.
15. Yong-Hing K, Reilly J, Korompay V, Kirkaldy-Willis WH. Prevention of nerve root adhesions after laminectomy. Spine 1980; 5:59–64.
16. Barber J, Gonzalez J, Esquerdo J, Broseta J, Barcia-Salorio JL. Prophylaxis of the laminectomy membrane. An experimental study in dogs. J. Neurosurg 1978; 49:419–24.
17. Cabezudo JM, Lopez A, Bacci F. Symptomatic root compression by a free fat transplant after hemilaminectomy. J. Neurosurg 1985; 63:633–635.
18. Israel Z, Constantini S. Compressive autologous free fat graft in a patient with failed back syndrome: case report. J. Spinal Dis 1995; 5:240–242.
19. Mayer PJ, Jacobsen FS. Cauda equina syndrome after surgical treatment of lumbar spinal stenosis with application of free autogenous fat graft. J. Bone Joint Surg (Am) 1989; 71:1090–1093.
20. Ohmori K, Kanamori M, Ishihara H, Kawaguchi Y, Yasuda T, Kimura T. Cauda equina syndrome caused by a free grafted fat after decompressive surgery of the lumbar spine: report of two cases. Neuro-Orthopedics 2000; 27:1–5.
21. Prusick VR, Lint DS, Bruder WJ. Cauda equina syndrome as a complication of free epidural fat-grafting. J. Bone Joint Surg. (Am) 1988; 70:1256–1258.
22. Crenshaw AH. Campbell's Operative Orthopaedics. St. Louis: Mosby Year Book, 1992:3764–3765.
23. Bryant MS, Bremer AM, Nguyen TQ. Autogeneic fat transplants in the epidural space in routine lumbar spine surgery. Neurosurgery 1983; 13:367–370.
24. Langenskiöld A, Kiviluoto O. Prevention of epidural scar formation after operation on the lumbar spine by means of free fat transplantations. Clin. Orthop. Res 1976; 115:92–95.
25. Van Akkerveeken PF, Van De Kraan W, Muller JW. The fate of the free fat graft. A prospective clinical study using CT scanning. Spine 1986; 11:501–504.
26. Weisz GM. The value of CT in diagnosing postoperative lumbar conditions. Spine 1986; 11:164–166.
27. Langenskiöld A, Valle M. Epidurally placed free fat grafts visualized by CT scanning 15–18 years after discectomy. Spine 1985; 10:97–98.
28. Kanamori M, Kawaguchi Y, Ohmori K, Kimura T, Tsuji H, Matsui H. The fate of autogenous free-fat grafts after posterior lumbar surgery. Part 1, A postoperative serial magnetic resonance imaging study. Spine 2001; 26:2258–2263.

29. Matsui H, Tsuji H, Kanamori M, Kawaguchi Y, Yudoh K, Futatsuya R. Laminectomy-induced arachnoiditis: a postoperative serial MRI study. Neuroradiology 1995; 37:660–666.
30. Kanamori M, Kawaguchi Y, Ohmori K, Kimura T, Tsuji H, Matsui H. The fate of autogenous free-fat grafts after posterior lumbar surgery. Part 2, Magnetic resonance imaging and histologic studies in repeated surgery cases. Spine 2001; 26:2264–2270.
31. Chang LW, Lalich JJ, Dudley AW. The evidence of the lipid in the paraffin block (in Japanese). Histo-Logic 1975; 3:41–42.
32. Weisz GM, Gal A. Long-term survival of a free fat graft in the spinal canal. Clin. Orthop. Res 1986; 205:204–206.
33. Assessment of surgical treatment of low back pain (in Japanese). J. Jpn. Orthop. Assoc 1984; 58: 1183–1187.
34. Bernsmann K, Krämer J, Ziozios I, Wehmeier J, Wiese M. Lumbar micro disc surgery with and without autologous fat graft. Arch. Orthop. Trauma. Surg 2001; 121:476–480.
35. Herzog RJ, Kaiser JA, Saal JA, Saal JS. The importance of posterior epidural fat pad in lumbar central canal stenosis. Spine 1991; 16:S227–233.
36. Gill GG, Sakovich L, Thompson E. Pedicle fat grafts for the prevention of scar formation after laminectomy. An experimental study in dogs. Spine 1979; 4:176–186.
37. Gill GG, Schck M, Kelley ET, Rodrigo JJ. Pedicle fat grafts for the prevention of scar in low-back surgery. A preliminary report on the first 92 cases. Spine 1985; 7:662–667.
38. Martin-Ferrer S. Failure of autologous fat grafts to prevent postoperative epidural fibrosis in surgery of lumbar spine. Neurosurgery 1989; 24:718–721.

25
In Vitro Stability of Cervical Spine Cages

F. Kandziora, J. Schaefer, M. Scholz, R. Pflugmacher, K. Ludwig, T. Eindorf, and N. P. Haas
Universitätsklinikum Charité der Humboldt-Universität Berlin
Berlin, Germany

I. INTRODUCTION

For cervical spondylosis, anterior decompression and interbody fusion is a widely accepted surgical treatment. The tricortical iliac crest bone graft as the gold standard has been known to be associated with high donor site morbidity. Additional problems such as pseudarthrosis, graft collapse with kyphotic deformity, and graft extrusion have led to a rapid increase in the use of cervical spine interbody fusion cages (CSIFC) as an adjunct to spondylodesis [3,19,22,23,26,43]. Yet, biomechanical data is lacking.

In the quest for interspace structural stability during bony fusion, interbody fusion cages are being developed. They have been promoted with the aim to provide immediate strong anterior column support and appear in several different interbody construct designs. According to Weiner and Fraser [43], these construct designs can be subdivided into three groups: screw (horizontal cylinder), box, or cylinder (vertical ring) designs. Although several comparative biomechanical studies of lumbar interbody fusion cages are available [2,4,9,10,12,16,21,28,32–34,40,41,50], cervical spine constructs have not been addressed yet, and few biomechanical data concerning comparative evaluation of different cage designs are available.

II. MATERIALS AND METHODS

A. Spine Preparation

Eighty cervical spines (C2–C5) of 2-year-old female Merino sheep (average weight 67.2 $\pm$ 4.6 kg) were chosen for biomechanical testing.

En bloc specimens were stored at -20°C until they were thawed in a water bath at 25°C. The motion segment C3–C4 was isolated, and superficial musculature was removed. Care was taken to preserve all ligaments. Each specimen was screened radiographically to exclude abnormalities that might compromise the mechanical properties of the sheep cervical spine.

To simulate essential clinical features, a complete discectomy C3–C4 with resection of the anterior longitudinal ligament was performed. The endplates were shaved using a high-speed diamond burr. Cervical interbody fusion cages were implanted according to manufacturers' information.

B. Cervical Spine Interbody Fusion Cages

The height, width, and depth of the cervical spine interbody fusion cages used in this study (Fig. 1) are depicted in Table 1. To allow comparison between the different cage designs, cages of similar height, width, and depth were used.The volume of the cages was determined by water-displacement technique, according to Archimedes principle [11]. To measure endplate implant contact area, cages were cut in two horizontal parts. Standardized axial digital pictures were taken for upper and lower parts of each cage. Endplate implant contact area was measured using a digital picture analysis system (Kontron, Zeiss, Jena, Germany)

C. Test Setup

Testing was performed using a nondestructive flexibility method using a nonconstrained testing apparatus [14,15]. Pure bending moments were applied using a system of cables and pulleys to induce flexion, extension, left and right lateral bending, and left and right axial rotation, correspondingly. Tension was applied to the cables with a uniaxial testing machine (Zwick 1456, Zwick GmbH, Ulm, Germany). Applied forces were measured with an axial load cell (Z 12, HBM, Darmstadt, Germany) mounted on the testing frame. Moments were calculated by multiplying the applied force by the radius of the pulley on the spine-testing fixture. Three-dimensional displacement of each motion segment was measured using an optical measurement system (Qualysis Inc., Sävebalden, Sweden). Nonlinear diodes (Qualysis Inc., Sävebalden, Sweden) were attached to the corpora of C3 and C4. Marker positions were detected with two cameras and recorded with a computerized motion analysis system (PC-Reflex, Qualysis Inc., Sävebalden, Sweden). Angular displacement of the upper vertebra in relation to the lower vertebra was calculated from marker position using custom-made computer software. The experimental error associated with this method was ± 0.12 degrees.

D. Study Protocol

Groups of eight spines were randomly assigned to one of the following groups: (1) intact, (2) autologous *tricortical* iliac bone graft, (3) two titanium screws (Novus CTTi, Sofamor Danek), (4) two titanium screws (BAK-C 8 mm, Sulzer Orthopedics), (5) one titanium screw (BAK-C 12 mm, Sulzer Orthopedics), (6) carbon box (Novus CSRC, Sofamor Danek), (7) titanium box (Syncage, Synthes), (8) titanium mesh cylinder (Harms, DePuy Acromed), (9) titanium cylinder (MSD, Ulrich), (10) titanium cylinder (Kaden, BiometMerck). Specimens were kept moist during tests. C2 and C5 were mounted in pots using PMMA (Technovit 3040; Heraeus Kulzer GmbH, Wehrheim/Ts, Germany). The lower pot was rigidly attached to the basis of the testing apparatus. This test setup resulted in a compressive preload of 25 N due to the weight of the upper fixation pot, which represents the average weight of the head of the sheep. Moments were applied in a quasistatic manner in increments of 1 Nm to a maximum of 6 Nm. At each step, the specimen was allowed to relax for 60 seconds to minimize viscoelastic response before data were recorded. Test modes were flexion, extension, left and right axial rotation, and left and right lateral bending. Specimens were preconditioned with three cycles of 6 Nm load with a velocity of 1.2 mm/sec of the traverse bar. The fourth cycle was measured. The mean apparent stiffness values in the elastic zone were calculated from the corresponding load-displacement curves. Volume-related stiffness was determined by dividing stiffness results through cage volume.

E. Analysis

Statistical analysis was performed using the Mann-Whitney U-test and Wilcoxon rank sum test. Statistical significant differences were defined at a 95% confidence level. The values are

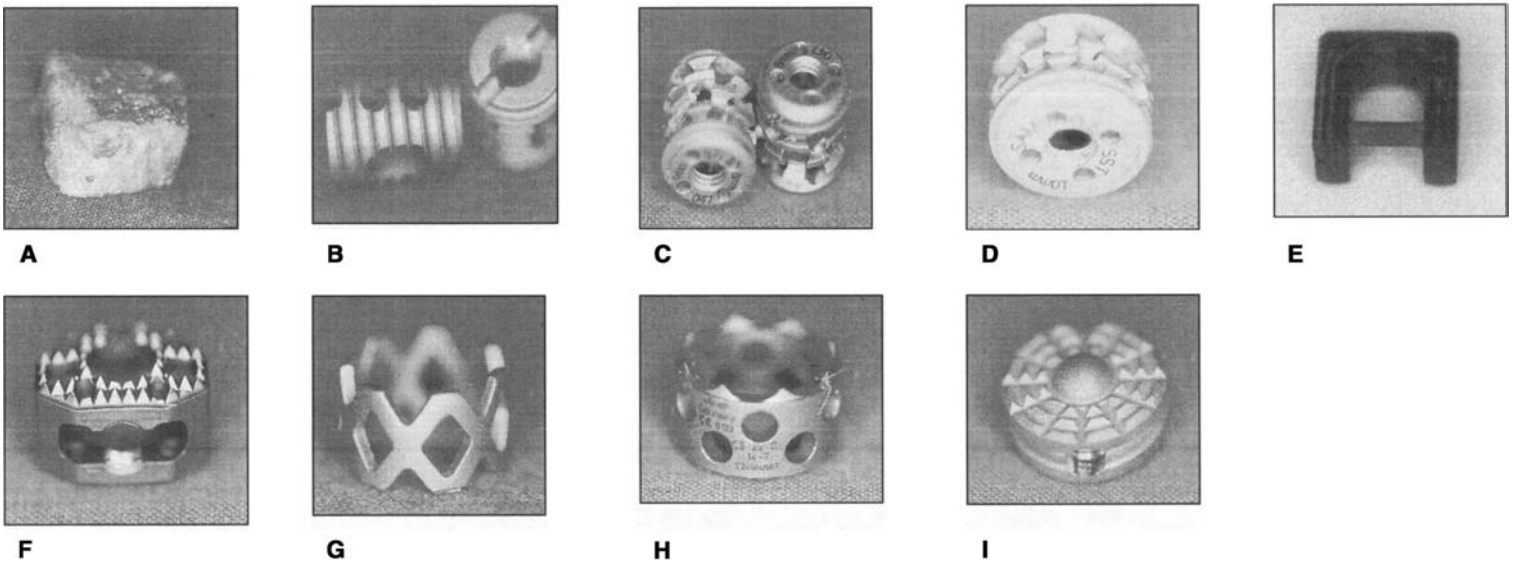

Figure 1 Stiffness of different cervical spine interbody fusion cages normalized to the intact motion segment C3–C4 in response to flexion, extension, rotation, and bending.

Table 1 Height, Width, and Depth of Cervical Spine Interbody Fusion Cages

Group	Cage	Type	Company	Material	Height (mm)	Width (mm)	Depth (mm)
2	Iliac bone graft	—	—	Bone	8	14	14
3	Novus CTTi[a]	Screw	Sofamor Danek	Titanium	8	8	12
4	BAK-C[a]	Screw	SulzerMedica	Titanium	8	8	12
5	BAK-C	Screw	SulzerMedica	Titanium	12	12	12
6	Novus CRSC	Box	Sofamor Danek	Carbon	7	8	12
7	Syncage C	Box	Synthes	Titanium	7	15	13
8	Harms	Cylinder	DePuyAcroMed	Titanium	8	14	14
9	MSD	Cylinder	Ulrich	Titanium	8	14	14
10	Kaden	Cylinder	BiometMerck	Titanium	7	16	15

[a] The producer recommends the use of two parallel inserted cages of this height for cervical interbody fusion.

given as mean ± standard deviation. SPSS (release 7.5) (SPSS Inc., Chicago, IL) software supported statistical evaluation.

III. RESULTS

The results of volume and endplate-implant contact area measurements are depicted in Table 2. Figure 2 summarizes the stiffness of cervical spine interbody fusion cages normalized with respect to the intact motion segment during flexion, extension, rotation, and bending.

A. Comparison Between Cages and Intact Motion Segment

1. Screw Designs

In comparison with the intact motion segment, all cages with screw designs were able to stabilize the motion segment during flexion ($p < 0.01$). There was no significant difference in stiffness

Table 2 Results of Volume Measurements of Cervical Spine Interbody Fusion Cages

Group	Cage	Type	Company	Volume (cm^3)	uEICA (cm^2)	lEICA (cm^2)
2	Iliac bone graft	—	—	1.32	—	—
3	Novus CTTi[a]	Screw	Sofamor Danek	0.58[a] (2 screws)	0.23	0.23
4	BAK-C 8mm[a]	Screw	SulzerMedica	0.56[a] (2 screws)	0.25	0.25
5	BAK-C 12 mm	Screw	SulzerMedica	0.38	0.30	0.30
6	Novus CRSC	Box	Sofamor Danek	0.30	0.20	0.20
7	Syncage C	Box	Synthes	0.26	0.26	0.21
8	Harms	Cylinder	DePuyAcroMed	0.10	0.10	0.10
9	MSD	Cylinder	Ulrich	0.20	0.32	0.32
10	Kaden	Cylinder	BiometMerck	0.84	1.21	1.21

[a] The producer recommends the use of two parallel inserted cages of this height for cervical interbody fusion.
EICA = endplate implant contact area; u = upper; l = lower.

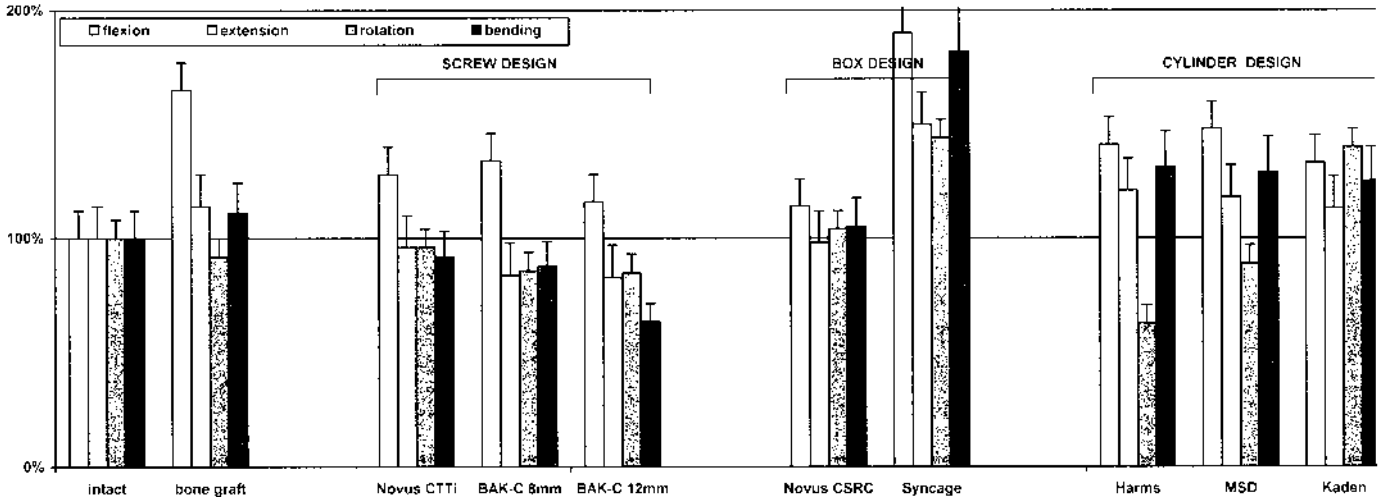

Figure 2 The different groups tested in the study. Depicted are the implanted cages. 1a: Control group: (1a) autologous iliac bone graft. 1b–d: Screw designs: (1b) two titanium screws (Novus CTTi, Sofamor Danek); (1c) two titanium screws (BAK-C 8 mm, Sulzer Orthopedics); (1d) one titanium screw (BAK-C 12 mm, Sulzer Orthopedics). 1e–f: Box designs: (1e) carbon box (Novus CSRC, Sofamor Danek); (1f) titanium box (Syncage, Synthes). 1g–i: Cylinder designs: (1g) titanium mesh cylinder (Harms, DePuy Acromed); (1h) titanium cylinder (MSD, Ulrich); (1i) titanium cylinder (Kaden, BiometMerck).

between the Novus CTTi and the intact motion segment in extension, rotation, and bending. The BAK-C cages (8 and 12 mm) were not able to restore stiffness of the intact motion segment in extension, rotation, and bending ($p < 0.05$).

2. Box Designs

In comparison with the intact motion segment, flexional stiffness of Novus CSRC was significantly larger ($p < 0.05$). There was no significant difference in stiffness between the Novus CSRC and the intact motion segment in extension, rotation, and bending. In comparison with the intact motion segment, stiffness of Syncage was significantly larger in all directions ($p < 0.001$).

3. Cylinder Designs

In comparison with the intact motion segment, flexional, extensional, and rotational stiffness of all cages with cylinder design were significantly larger ($p < 0.05$). Rotational stiffness of cages increased with the endplate-implant contact area. Therefore, in comparison with the intact motion segment, rotational stiffness of Harms and MSD cage was significantly lower ($p < 0.05$), whereas rotational stiffness of the Kaden cage was significantly higher ($p < 0.01$).

B. Comparison Between Cages and Tricortical Bone Graft

1. Screw Designs

In comparison with bone graft, all cages with screw designs were less stable during flexion, extension, and bending ($p < 0.01$). There was no significant difference in rotational stiffness between the three cage types with screw design and bone graft.

2. Box Designs

In comparison with bone graft, flexional stiffness of Novus CSRC was significantly lower ($p < 0.01$). There was no significant difference in extensional and bending stiffness between the Novus CSRC and bone graft fixated motion segment. Rotational stiffness was higher in the Novus CSRC ($p < 0.05$). In comparison with bone graft, stiffness of Syncage was significantly larger in all directions ($p < 0.001$).

3. Cylinder Designs

In comparison with the bone graft, the flexional stiffness of all cages with cylinder design was significantly lower ($p < 0.05$), whereas extensional stiffness was not different. Bending stiffness was significantly higher ($p < 0.05$). In comparison with bone graft, rotational stiffness was higher for the Kaden-cage ($p < 0.05$), not different for the MSD cage, and significantly lower for the Harms cage ($p < 0.05$).

C. Intragroup Comparison

1. Screw Design

There was no significant difference between the three cage types in screw design except for bending stiffness of the BAK 12 mm, which was significantly lower than bending stiffness of the other two cage types ($p < 0.01$).

2. Box Design

The stiffness of Syncage was significantly higher than the stiffness of Novus CSRC in all directions ($p < 0.01$).

3. Cylinder Design

There was no difference between the three cage types with cylinder design for flexion, extension, and bending stiffness. Rotational stiffness of cylindrical cages increased with the endplate-implant contact area. Therefore, rotational stiffness of the Kaden cage was significantly higher compared to the Harms cage ($p < 0.001$) and MSD cage ($p < 0.01$).

D. Intergroup Comparison

1. Screw Design Versus Box Design

Stiffness of all screw designs was significantly lower than stiffness of Syncage in all directions ($p < 0.01$). If two screws were inserted (Novus CTTi and BAK-C 8mm) flexional stiffness for screw designs was higher than for Novus CSRC ($p < 0.05$). There was no difference if one screw was inserted (BAK-C 12 mm). There was no significant difference between the Novus CTTi and Novus CSRC in extension, rotation, and bending. Extensional, rotational, and bending stiffness was significantly higher for Novus CSRC than for both BAK-C cages ($p < 0.05$).

2. Screw Design Versus Cylinder Design

If two screws were inserted (Novus CTTi and BAK-C 8 mm) there was no significant difference in flexional stiffness between both design groups. If one screw was inserted (BAK-C 12 mm) flexional stiffness was higher for cylinder designs ($p < 0.05$). Extensional and bending stiffness were always higher with cylinder designs ($p < 0.05$). If two screws were inserted (Novus CTTi and BAK-C 8mm) rotational stiffness was higher in comparison with the Harms cage ($p < 0.01$), not different in comparison with the MSD cage, and lower in comparison with the Kaden cage ($p < 0.01$). If one screw was inserted (BAK-C 12 mm) rotational stiffness was not different in comparison with the Harms cage and lower in comparison with the MSD cage ($p < 0.05$) and Kaden cage ($p < 0.01$).

3. Box Design Versus Cylinder Design

Stiffness of all cylinder designs was significantly lower than stiffness of Syncage in all directions ($p < 0.01$). Flexional, extensional, and bending stiffness was higher for cages with cylinder design than for Novus CSRC. Rotational stiffness of Novus CSRC was higher in comparison with the Harms cage ($p < 0.001$) and MSD cage ($p < 0.05$) but, lower in comparison with Kaden cage ($p < 0.01$).

E. Volume-Related Stiffness

Figure 3 summarizes the volume-related stiffness results of cervical spine interbody fusion cages normalized with respect to the bone graft during flexion, extension, rotation, and bending.

In comparison with bone graft, all cages increased volume-related stiffness significantly. Volume-related stiffness for flexion extension and bending was significantly highest for the Harms cage ($p < 0.01$). There was no difference for rotational volume-related stiffness between the Harms cage and Syncage.

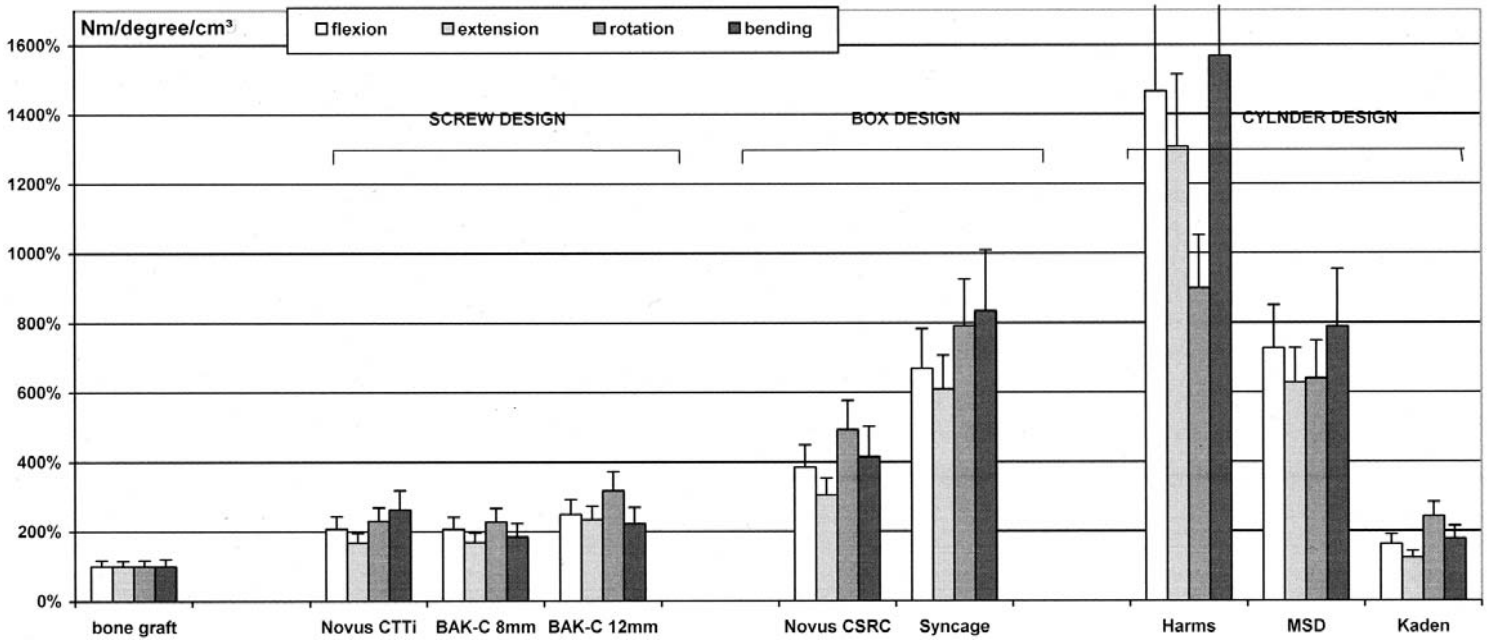

Figure 3 Volume-related stiffness of different cervical spine interbody fusion cages normalized to the bone graft in response to flexion, extension, rotation, and bending.

IV. DISCUSSION

A. Study Limitations

Many different test loading conditions have been used in the past, making a comparison of the results from different groups almost impossible. According to previously published recommendations [47], these in vitro tests were performed under pure moment loading conditions. Due to the complex and still widely unknown loading of the cervical spine in vivo, it is impossible to transfer the results of this sheep in vitro study directly on to the human cervical spine in vivo. Therefore, the biomechanical performance of the tested implants in the human in vivo may differ significantly from the results obtained in this sheep in vitro study. Additionally, it is not possible to determine the correlation between the 25 N compression load and the 6 Nm moment in this in vitro sheep experiment with in vivo human loading conditions because of the complex loading conditions of the human cervical spine in vivo. However, new implants should be tested in vitro for primary stability in standardized laboratory tests in order to decide the most appropriate before being accepted for clinical use.

B. Animal Model

The sheep spine is frequently used as a model for the human spine in spine research [1,5,7,24,25,27,29,38,45,46,49]. Recently, anatomical biomechanical and bone mineral density evaluation of the sheep cervical spine showed good comparability to the human spine [25,45,46]. Anatomical evaluation has demonstrated an average disc space height for the sheep cervical spine of 6 mm, which is approximately 1 mm higher than that in the human cervical spine [31]. Additionally, similar upper endplate parameters of C4 and C5 for both species were observed. Therefore, human implants fit in the sheep cervical spine. Wilke et al. [45] were the first to describe biomechanical analogies in sheep and human spine by testing sheep spines and comparing the data to literature. Although many data are available from in vitro and in vivo tests of the normal human cervical spine [30,42,44], comparison remains difficult because of the large variety of test setups. Kandziora et al. [15] compared both species biomechanically using the same test setup. Although significant differences were observed between the two species, especially for rotation parameters, ROM and stiffness data were mainly comparable in their craniocaudal trends. They concluded that if the sheep animal model is used, motion segments C2–C3 and C3–C4 were the most suitable for biomechanical tests. Bone mineral density has an influence on primary stability of cervical spine fixation techniques [8,13,18,20,36,48]. A linear correlation was observed between axial compression strength of cages and bone mineral density (BMD) [12]. Currently, no data are available comparing BMD of severely degenerated human cervical spine motion segments for which surgery is indicated with the sheep cervical spine. However, in a study comparing BMD values of human and sheep cervical spines [15], no significant difference could be registered with regard to BMD between the two species. The least percentile difference was found for C4. Standard deviations for bone mineral density of the human cervical spine were fourfold higher compared to the sheep cervical spine. Therefore, the sheep animal model—in particular, the motion segment C3–4—seems to allow a quasi ''BMD-independent,''l biomechanical evaluation of human size implants.

C. Stiffness Tests

Primary stability in cervical spine interbody fusion is essentially determined by the biomechanical effects of the fixation devices. Several biomechanical studies were performed to evaluate lumbar interbody fusion cages with screw designs [2,9,10,12,16,21,28 32–34,40,41,50]. The

main aim of these studies was to compare different screw designs or to evaluate the biomechanical effects of additional posterior fixation techniques. Zdeblick et al. [50] and Rapoff et al. [34], using two BAK devices in calf spines, found that bending and flexion/extension stiffness increased twofold in comparison with noninstrumented motion segments. Comparable results were obtained by Nibu et al. [28], Rapoff et al. [34], and Rathonyi et al. [35] in the human spine. Tencer et al. [40] and Kettler et al. [16] observed the same using the Ray device, another interbody fusion cage with screw design. In contrast, Pitzen et al. [32,33], using PLIF techniques with the BAK cage in an in vitro biomechanical and a finite element model, showed a loss of stiffness in compression, shearing, and especially torsion. Interestingly, all investigators noted that in comparison with the intact spine, torsional stiffness was minimally changed or decreased by using screw-like implants.

Very little information on biomechanical testing of cages with cylinder designs is available. Heller et al. [9] used the Harms titanium cage in a calf lumbar spine corporectomy model. They showed that only a combined anterior/posterior construct was able to restore stability comparable to the intact state. To our knowledge, Hollowell et al. [10] were the first to use the Harms titanium cage in a biomechanical study applying a discectomy model of the human thoracic spine. They focused mainly on subsidence without testing three-dimensional displacement stiffness of this implant. Pitzen et al. [32,33] used the Harms titanium cage in a lumbar spine discectomy model. They showed a higher initial stability of PLIF with the Harms titanium cage and posterior instrumentation than PLIF with the BAK cage alone.

Similar to cylinder designs, information about biomechanical data of cages with box designs is scarce. Brantigan et al. [2], using a PLIF model in the lumbar spine, demonstrated that their carbon fiber implant showed superior biomechanical properties in comparison to the bone graft. To our knowledge, Shono et al. [37] were the only ones who performed biomechanical studies in the cervical spine. They demonstrated that the Brantigan carbon fiber cage [2] was more rigid than an iliac bone graft.

The aim of this study was to evaluate the biomechanical effects of cervical spine interbody fusion cages and to compare three CSIFC design groups. To our knowledge no biomechanical study is currently available addressing different cervical spine interbody fusion cages. Additionally, no data are available concerning comparison of different cage design groups. Cage size has a significant influence on the biomechanical behavior of different cages [6]. Therefore, to allow comparison between the different cage designs, cages of similar height, width, and depth were used in this study.

Any cage implantation increased flexional stiffness compared to the intact motion segment. On the contrary, rotational stiffness decreased after implantation of a CSIFC, except for the Novus CSRC, Syncage, and Kaden cage. In comparison with the intact motion segment, extensional and bending stiffness increased with the cylinder designs and with the Syncage, a box design, whereas extensional and bending stiffness for screw designs decreased or remained unchanged.

Comparison between the different cage designs showed that if two screws were inserted (Novus CTTi and BAK-C 8mm) no significant difference in flexional stiffness between screw and cylinder design groups was registered. Yet, if one screw was inserted (BAK-C 12mm) flexional stiffness was higher for cylinder designs ($p < 0.05$). Extensional and bending stiffness were always higher with cylinder designs ($p < 0.05$). The best biomechanical results were observed in the Syncage, a box design.

D. Volume-Related Stiffness

Secondary stability in cervical spine interbody fusion is determined biologically resulting from the amount of bony fusion. The ideal biological environment for spondylodesis is influenced

by several factors, including optimal grafting techniques, a maximum graft filling of the intervertebral space, a mechanical protection of the graft in the intervertebral space, and an optimal surface contact area of graft and vertebral body [43]. But as cage volume increases, graft volume decreases. Therefore, there is some kind of competition between cage and graft volume. In conclusion, one important biological factor for a fusion cage is to have the smallest possible cage volume and as a result to allow the maximum graft filling of the intervertebral space [43]. However, cages also have to provide adequate mechanical stability. In an attempt to take these two factors into consideration, the volume-related stiffness was determined by dividing stiffness results through cage volume. This parameter should allow the interpretation of biomechanical test results from a more biological point of view.

The volume-related stiffness was significantly highest with the Harms cage and the Syncage. In conclusion, with these cages less implant is needed for mechanical stabilization. Therefore, sufficient space remains, which may be filled by bone graft, which in turn might lead to a better biological environment for bony fusion. Several studies [17,39] have documented that if graft volume increased, the chance for bony fusion increased, too. Therefore, the data suggest that the Harms cage and the Syncage will probably provide a better biological environment for spondylodesis than the other cages tested. Further in vivo studies with different cage designs are necessary to determine if the parameter volume-related stiffness is able to predict secondary stability in cervical spine interbody fusion.

V. CONCLUSION

The ideal CSIFC should correct an existing deformity, provide stability to the segment until fusion occurs, and supply a good environment for successful spondylodesis without concurrent morbidity associated with its use [43]. The purpose of this study was to evaluate the mechanical properties of CSIFC and to compare three CSIFC design groups. From a biomechanical perspective the results suggest that intragroup design variations in the screw and cylinder design groups are of little importance. However, cages with a cylinder design were able to control extension and bending more effectively than cages with a screw design.

A question that cannot be answered by this in vitro study concerns the level of rigidity required to obtain long-term stability and fusion by cervical spine interbody fixation methods. But it may be assumed that the more spinal motion is eliminated, the greater the chance of definite spinal fusion. Therefore, it seems reasonable that the most reliable and rigid fixation method would be the method of choice. In conclusion, the authors suggest the use of cylinder or box design cages for cervical spine interbody fusion.

Another unanswered question refers to secondary stability of CSIFC. Volume-related stiffness may allow the interpretation of mechanical test results from a more biological point of view, but further in vivo investigations are necessary.

REFERENCES

1. Ahlgren BD, Vasavada MS, Brower RS, Lydon C, Herkowitz MD, Panjabi MM. Annular incision technique on the strength and multidirectional flexibility of the healing intervertebral disc. Spine 1994; 19:948–954.
2. Brantigan JW, Steffee AD, Geiger JM. A carbon fiber implant to aid interbody lumbar fusion. Mechanical testing. Spine 1991; 16:277–282.
3. Brooke NS, Rorke AW, King AT, Gullan RW. Preliminary experience of carbon fibre cage prostheses for treatment of cervical spine disorders. Br J Neurosurg 1997; 11:221–227.

4. Brodke DS, Dick JC, Kunz DN, McCabe R, Zdeblick TA. Posterior lumbar interbody fusion. A biomechanical comparison, including a new threaded cage. Spine 1997; 22:26–31.
5. Cain CC, Fraser RD. Bony and vascular anatomy of the normal cervical spine in the sheep. Spine 1995; 20:759–765.
6. Goh JC, Wong HK, Thambyah A, Yu CS. Influence of PLIF cage size on lumbar spine stability. Spine 2000; 25:35–39.
7. Gunzburg R, Fraser RD, Moore R, Vernon-Roberts B. An experimental study comparing percutaneous discectomy with chemonucleolysis. Spine 1993; 18:218–226.
8. Halvorson TL, Kelley LA, Thomas HA, Whitecloud TS, Cook SD. Effects on bone mineral density on pedicle screw fixation. Spine 1994; 19:2415–2420.
9. Heller JG, Zdeblick TA, Kunz DA, McCabe R, Cooke ME. Spinal instrumentation for metastatic disease: in vitro biomechanical analysis. J Spinal Disord 1993; 6:17–22.
10. Hollowell JP, Vollmer DG, Wilson CR, Pintar FA, Yoganandan N. Biomechanical analysis of thoracolumbar interbody constructs. How important is the endplate?. Spine 1996; 21:1032–1036.
11. Jensen J, Kragskov J, Wenzel A, Sindet-Pedersen S. Volumetry of bone grafts by three-dimensional computed tomographic reconstruction: an animal study in the minipig. Dentomaxillofac Radiol 1998; 27:41–44.
12. Jost B, Cripton PA, Lund T, Oxland TR, Lippuner K, Jaeger P, Nolte LP. Compressive strength of interbody cages in the lumbar spine: the effect of cage shape, posterior instrumentation and bone density. Eur Spine J 1998; 7:132–141.
13. Kandziora F, Mittlmeier T, Kerschbaumer F. Stage related surgery for cervical spine instability in rheumatoid arthritis. Eur Spine J 1999; 8:371–381.
14. Kandziora F, Kerschbaumer F, Starker M, Mittlmeier T. Biomechanical assessment of the transoral plate fixation for atlantoaxial instability. Spine 2000; 25:1555–1561.
15. Kandziora F, Pflugmacher R, Scholz M, Schnake K, Schröder R, Hoffmann J, Mittlmeier T. The sheep cervical spine in comparison to the human spine. An anatomic, radiographic, bone mineral density and biomechanical study. Spine 2001; 26:1028–1037.
16. Kettler A, Wilke HJ, Dietl R, Krammer M, Lumenta C, Claes L. Stabilising effect of posterior lumbar interbody fusion cages before and after cyclic loading. J Neurosurg 2000; 92:87–92.
17. Kim KW, Ha KY, Moon MS, Kim YS, Kwon SY, Woo YK. Volumetric change of the graft bone after intertransverse fusion. Spine 1999; 24:428–433.
18. Kumano K, Hirabayashi S, Ogawa Y, Aota Y. Pedicle screws and bone mineral density. Spine 1994; 19:1157–1161.
19. Kumaresan S, Yoganandan N, Pintar FA. Finite element analysis of anterior cervical spine interbody fusion. Biomed Mater Eng 1997; 7:221–230.
20. Lim TH, An HS, Evanich C, Hasanoglu KY, McGrady L, Wilson CR. Strength of vertebral screw fixation in relationship to bone mineral density. J Spinal Disord 1995; 8:121–125.
21. Lund T, Oxland TR, Jost B, Cripton P, Grassmann S, Etter C, Nolte LP. Interbody cage stabilisation in the lumbar spine: biomechanical evaluation of cage design, posterior instrumentation and bone density. J Bone Joint Surg Br 1998; 80:351–359.
22. Majd ME, Vadhva M, Holt RT. Anterior cervical reconstruction using titanium cages with anterior plating. Spine 1999; 24:1604–1610.
23. Matge G. Anterior interbody fusion with the BAK-cage in cervical spondylosis. Acta Neurochir 1998; 140:1–8.
24. Melrose J, Ghosh P, Taylor TKF, Hall A, Osti OL, Vernon-Roberts B, Fraser RD. A longitudinal study of the matrix changes induced in the intervertebral discs by surgical damage to the annulus fibrosus. J Orthop Res 1992; 10:665–676.
25. Moore RJ, Osti OL, Vernon-Roberts B, Fraser RD. Changes in endplate vascularity after an outer annulus tear in the sheep. Spine 1992; 17:874–878.
26. Munoz FLO, de las BG, Lopez VC, Siguero JJA. Comparison of three techniques of anterior fusion in single-level cervical disc herniation. Eur Spine J 1998; 7:512–516.
27. Nagel DA, Kramers PC, Rahn BA, Cordey J, Peeren SM. A paradigm of delayed union and nonunion in the lumbosacral joint: a study of motion and bone grafting of the lumbosacral spine in sheep. Spine 1991; 16:553–559.

28. Nibu K, Panjabi MM, Oxland T, Cholewicki J. Multidirectional stabilising potential of BAK interbody spinal fusion system for anterior surgery. J Spinal Disord 1997; 10:357–362.
29. Osti OL, Vernon-Roberts B, Fraser RD. Annulus tear in intervertebral disc degeneration: an experimental study using an animal model. Spine 1990; 15:431–435.
30. Panjabi MM, Duranceau J, Goel V, Oxland T, Takata K. Cervical human vertebrae. Quantitative three-dimensional anatomy of the middle and lower regions. Spine 1991; 16:861–869.
31. Pait GT, Killefer JA, Arnautovic KI. Surgical anatomy of the anterior cervical spine: the disc space, vertebral artery, and associated bony structures. Neurosurgery 1996; 39:769–776.
32. Pitzen T, Caspar W, Matthis D, Müller-Storz H, König J, Georg T, Wurm EM, Steudel WI. Primary stability of 2 PLIF (posterior lumbar interbody fusion)—a biomechanical in vitro comparison. Z Orthop 1999; 137:214–218.
33. Pitzen T, Matthis D, Caspar W, Müller-Storz H, Steudel WI. Initial stability of two PLIF techniques. A biomechanical comparison using a finite element model. Orthopädie 2000; 29:68–72.
34. Rapoff AJ, Ghanayem AJ, Zdeblick TA. Biomechanical comparison of posterior lumbar interbody fusion cages. Spine 1997; 22:2375–2379.
35. Rathonyi GC, Oxland TR, Gerich U, Grassmann S, Nolte LP. The role of supplemental translaminar screws in anterior interbody fixation: a biomechanical study. Eur Spine J 1998; 7:400–407.
36. Ryken TC, Goel VK, Clausen JD, Traynelis VC. Assessment of unicortical and bicortical fixation in a quasistatic cadaveric model. Role of bone mineral density and screw torque. Spine 1995; 20: 1861–1867.
37. Shono Y, McAfee PC, Cunningham BW, Brantigan JW. A biomechanical analysis of decompression and reconstruction methods in the cervical spine. Emphasis on a carbon-fiber-composite cage. J Bone Joint Surg Am 1993; 75:1674–1684.
38. Slater R, Nagel R, Smith RL. Biochemistry of fusion mass consolidation in the sheep spine. J Ortho Res 1988; 6:138–144.
39. Stevenson S, Emery SE, Goldberg VM. Factors affecting bone graft incorporation. Clin Orthop 1996; 324:66–74.
40. Tencer AF, Hampton D, Eddy S. Biomechanical properties of threaded inserts for lumbar interbody spinal fusion. Spine 1995; 20:2408–2414.
41. Volkman T, Horton WC, Hutton WC. Transfacet screws with lumbar interbody reconstruction: biomechanical study of motion segment stiffness. J Spinal Disord 1996; 9:425–432.
42. Voo LM, Pintar FA, Yoganandan N, Liu YK. Static and dynamic bending response of the human cervical spine. J Biomech Eng 1998; 120:693–696.
43. Weiner BK, Fraser RD. Spine update lumbar interbody fusion cages. Spine 1998; 23:634–640.
44. Wen N, Lavaste F, Santin JJ, Lassau JP. Three-dimensional biomechanical properties of the human spine in vitro. Eur Spine J 1993; 2:2–47.
45. Wilke HJ, Kettler A, Claes LE. Are sheep spines a valid biomechanical model for human spines?. Spine 1997; 22:2365–2374.
46. Wilke HJ, Kettler A, Wenger KH, Claes LE. Anatomy of the sheep spine and its comparison to the human spine. Anat Rec 1997; 247:542–555.
47. Wilke HJ, Wenger K, Cleas L. Testing criteria for spinal implants: recommendations for the standardization of in vitro stability of spinal implants. Eur Spine J 1998; 7:148–154.
48. Wittenberg RH, Shea M, Swartz DE, Lee KS, White AA, Hayes WC. Importance of bone mineral density in instrumented spine fusions. Spine 1991; 16:647–652.
49. Yamamuro T, Shikata J, Okumura H, Kitsugi T, Kakutani Y, Matsui T, Kokubo T. Replacement of the lumbar vertebrae of sheep with ceramic prostheses. J Bone Joint Surg Br 1990; 72:889–893.
50. Zdeblick TA, Warden KE, Zou D, McAfee PC, Abitbol JJ. Anterior spinal fixators. A biomechanical in vitro study. Spine 1993; 18:513–517.

26
In Vivo Performance of Cervical Spine Cages

F. Kandziora, R. Pflugmacher, M. Scholz, J. Schaefer, K. Ludwig, T. Eindorf, and N. P. Haas
Universitätsklinikum Charité der Humboldt-Universität Berlin Berlin, Germany

I. INTRODUCTION

Anterior decompression and interbody fusion is a widely accepted surgical treatment for patients with cervical spondylosis. Tricortical iliac crest bone graft has been the gold standard up to now but is associated with high donor site morbidity. Additional problems such as pseudarthrosis, graft collapse with kyphotic deformity, and graft extrusion have led to a rapid increase in the use of cervical spine interbody fusion cages as an adjunct to spondylodesis [3,16,21,24,25,27], although experimental data are lacking [37].

Several interbody construct designs have been developed. According to Weiner and Fraser [37] cage designs can be subdivided into three groups: screw (horizontal cylinder), box, or cylinder (vertical ring) designs.

Devices for interbody stabilization have to ensure good primary stability. Cages have especially been promoted with the aim to provide immediate strong anterior column support. This has already been proven in several biomechanical in vitro studies for all cage designs [1,4,11–14,19,21,23,28,31–33,35,36]. In vitro biomechanical fixation properties of screw-design cages have been evaluated extensively [4,11,14,19,23,28,31,32,35]. However, little information is available for comparative evaluation of different cage designs. Oxland et al. [29] compared box and cylinder cages in a biomechanical human in vitro study showing no differences between the two designs. In contrast, Mittlmeier et al. [26] determined fundamental differences between box, screw and cylinder type cages using a sheep cervical spine model. They showed that cylinder and box type cages were able to control extension and bending more effectively than screw design types.

Additionally, interbody cages have been developed in the quest for interspace structural stability during bony fusion. Cages should retain interbody distraction and should be resistant against subsidence into the adjacent vertebrae in order to obtain a biological environment that guarantees bony fusion of desired quality. However, this can only be evaluated by in vivo investigations. The structural stability of screw type cages has already been proven by some in vivo studies [34,38], showing that they were able to preserve interbody distraction more effectively than an autologous tricortical iliac crest bone graft. However, experimental in vivo data for cylinder or box design cages are not available. Additionally, no information is available concerning comparative experimental in vivo evaluation of different cage designs.

The purpose of this study was to compare interbody fusion of an autologous tricortical iliac crest bone graft with a cylinder and a box type cage in a sheep cervical spine interbody

fusion model. It was designed to determine whether there are differences at a given early time point in a developing fusion between the three interbody fusion techniques in (1) the ability to preserve postoperative distraction, (2) biomechanical stability, and (3) the histological characteristics of intervertebral bone matrix formation.

II. MATERIALS AND METHODS

Twenty-five adult female merino sheep (2 years old) underwent C3-C4 discectomy and fusion: one animal was lost at follow-up. The remaining 24 sheep were randomly assigned to the following groups: group 1, autologous tricortical iliac crest bone graft ($n = 8$); group 2, cylinder-design titanium cage filled with autologous cancellous iliac crest bone graft ($n = 8$); group 3, box-design titanium cage filled with autologous cancellous iliac crest bone graft ($n = 8$). The sheep were evaluated prospectively for 12 weeks. Afterward all sheep were sacrificed and radiographic, biomechanical, and histological evaluations were performed. All animal experimental work was approved by local authorities.

A. Surgical Technique and Postoperative Care

All sheep received 2 g amoxicillin intravenously (Augmentan i.v.®, SmithKline Beecham Pharma) before surgery. The animals underwent the surgical procedure under general endotracheal anaesthesia. For induction of anaesthesia 0.5 g thiopental-natrium (Trapanal®, Byk Gulden) and 0.1 mg fentanyl dihydrogen citrate (Fentanyl–Janssen®, Janssen-Cilag) were used. For maintenance of anesthesia, inhalation of isofluran (Isofluran-Lilly®, Lilly) and intravenous dosages of 0.2 mg fentanyl dihydrogen citrate (Fentanyl–Janssen®, Janssen-Cilag) were applied. The anterior part of the neck and the left iliac crest were prepared in a sterile fashion and a left anterolateral approach to the cervical spine was carried out through a longitudinal skin incision. The longus coli muscle was incised in the midline, and the intervertebral disc C3-C4 was exposed. After distraction of the motion segment with a Caspar distractor, anterior discectomy C3-C4 was performed. The endplates were shaved with a 2 mm high-speed diamond drill down to bleeding bone, resulting in a excision of 1 mm of each endplate. No attempt was made to excise the posterior longitudinal ligament or expose the spinal canal. For interbody stabilization, titanium cylinder-design cages (group 2, Harms cage, Motech GmbH, Schwenningen, Germany, width 14 mm, depth 14 mm, cage volume 0.10 cm^3) or box-design cages (group 3, SynCage-C, Synthes GmbH, Bochum, Germany, width 15 mm, depth 13 mm, cage volume 0.26 cm^3) of appropriate height (average height 8 mm for both groups) were used. Prior to insertion, both cages were filled with autologous cancellous bone grafts. In group 1 a tricortical autologous bone graft of 8 mm average height, 14 mm average depth and 11 mm average height was taken from the left iliac crest. Prior to insertion the volume of the cages filled with autologous bone or the volume of the bone grafts was determined using water-displacement technique (Archimedes principle). The tricortical bone graft was inserted press-fit into the intervertebral space with the cortical shape of the graft anterior (Robinson's technique). Finally, the wound was irrigated with saline and the longus coli muscle was closed with a running suture. The subcutaneous tissue and the skin were reapproximated with interrupted sutures, and a soft bandage was applied to the neck.

After surgery, the animals were maintained under observation until fully recovered from general anesthesia. They received two doses of 0.5 g metamizol-natrium (Novaminsulfon®, Lichtenstein) per day for 5 days intramuscularly. Clinical examination was performed daily for the first 10 days, then weekly. The sheep were allowed ad libitum activity for the remainder of the experiment. Fluorochrome sequential labels were administered at 3, 6, and 9 weeks

postoperatively consisting of oxytetracycline (25 mg/kg IV) at 3 weeks, calcein green (15 mg/kg IV) at 6 weeks, and xylenol orange (90 mg/kg IV) at 9 weeks. Twelve weeks after surgery the animals were killed after induction of anesthesia with 0.5 g thiopental-natrium (Trapanal®, Byk Gulden) and 0.1 mg fentanyl dihydrogen citrate (Fentanyl–Janssen®, Janssen-Cilag) by an intravenous injection of potassium chloride. The complete cervical spine including parts of the occiput and Th1 was then excised and cleaned from the surrounding tissue.

B. Radiographic Analysis

To allow comparable radiographic evaluation, special fixation devices for the sheep cervical spine were developed. The reproducibility of the positioning of the sheep cervical spine in this fixation device was investigated by repeated measurements. Prior to surgery one sheep in each group was selected randomly to have 10 lateral and 10 p.a. digital radiographic scans. Between the radiographic scans the sheep was removed from the fixation device, turned around, and then refixed in the fixation device. Subsequently, the complete series of linear and angular measurements was performed on each radiographic scan.

Lateral and p.a. digital radiographic scans (x-ray unit: Mobilett Plus, Siemens AG, Germany; x-ray films: Fuji CR 24x30, Fuji, Germany) were performed pre- and postoperatively and after 1, 2, 4, 8, and 12 weeks, respectively. At the same time periods, anterior, middle, and posterior intervertebral disc space heights (DSH), intervertebral angle (IVA), and lordosis angle (LA) of the motion segment C3-C4 were measured on lateral radiographic scans (Fig. 1). Average intervertebral DSH was calculated from anterior, middle, and posterior DSH measurements. After 12 weeks bony fusion was categorized using the following parameters: (1) no bony fusion, (2) maximum intervertebral gap of more than 5 mm, (3) maximum intervertebral gap of less than 5 mm, or (4) complete bony fusion. The maximum intervertebral gap in cranio-caudal direction was measured directly on lateral x-rays using a ruler. All radiographic measurements were evaluated by three independent observers.

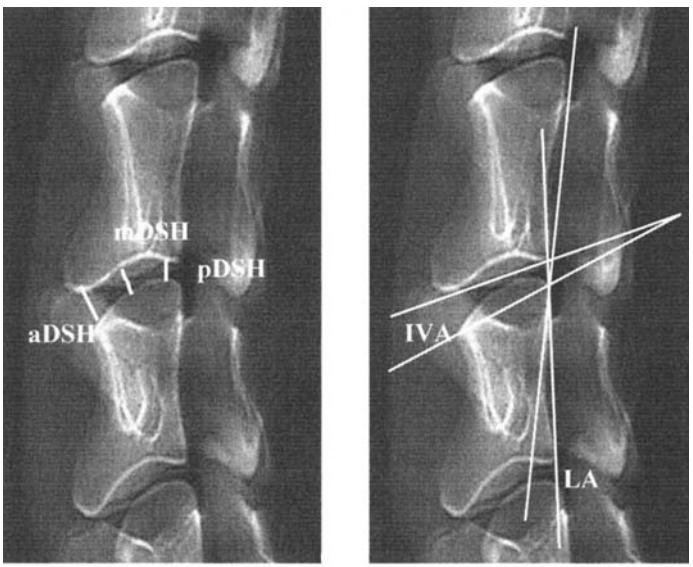

Figure 1 Radiographic measurements of (A) anterior disc space height (aDSH), posterior disc space height (pDSH), middle disc space height (mDSH), (B) intervertebral angle (IVA) and lordosis angle (LA).

C. Functional Radiographic Analysis

Fusion sites were evaluated using lateral digital functional radiographic scans in flexion and extension (Fig. 2) (x-ray unit: Mobilett Plus, Siemens AG, Germany; x-ray films: Fuji CR 24×30, Fuji, Germany). For this purpose, Th1 was rigidly fixed with a Steinmann pin while 60 N load was applied through C1 using a newtonmeter (Inha GmbH, Berlin, Germany). Flexion/extension differences of IVA and LA were calculated. All functional radiographic measurements were evaluated by three independent observers.

D. Quantitative Computed Tomographic Analysis

After sacrifice, quantitative computed tomographic scans (QCT) were performed using a Siemens Somatom plus 4 scanner (Siemens Inc., Erlangen, Germany). Axial cuts with 1 mm slice thickness were made parallel to the intervertebral disc space. Bone mineral density (BMD) measurements of the bony callus have been described in detail [18]. Measurements were calibrated with a 6-point bone mineral density phantom and were performed using specific software of the scanner (Sienet Magic View VA 30A, Siemens, Inc., Erlangen, Germany). Bony callus volume (BCV) was measured using an image analyzing system (Zeiss KS 400, Zeiss GmbH, Germany).

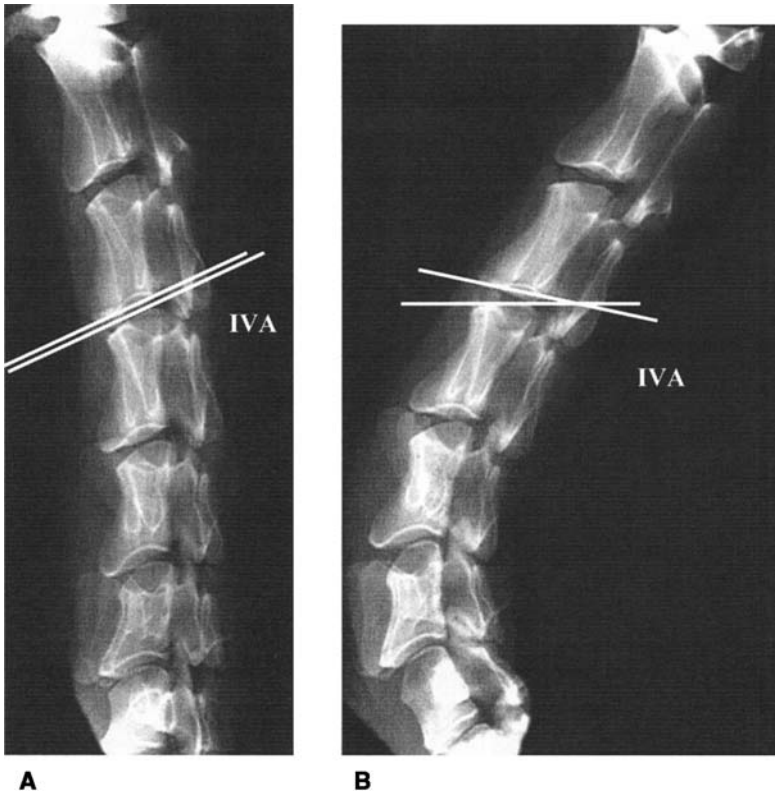

Figure 2 The motion segment C3-C4 was evaluated using lateral digital functional radiographic scans in (A) flexion and (B) extension. Flexion/extension differences of intervertebral angle (IVA) and lordosis angle were calculated.

Bone mineral content (BMC) was calculated from BMD and BCV measurements (BMC = BCV × BMD). After 12 weeks bony fusion was categorized on sagittal and coronal two-dimensional CT (2D-CT) reconstructions using the parameters described above: (1) no bony fusion, (2) maximum intervertebral gap of more than 5 mm, (3) maximum intervertebral gap of less than 5 mm, and (4) complete bony fusion. The maximum intervertebral gap in cranio-caudal direction was measured directly on midsagittal 2D-CT reconstructions using the scanner software described above. All radiographic CT measurements were evaluated by three independent observers.

E. Biomechanical Analysis

After euthanasia biomechanical testing was performed by a nondestructive flexibility method using a nonconstrained testing apparatus described in detail elsewhere [17,18]. Pure bending moments were applied to the motion segments C3-C4 using a system of cables and pulleys to induce flexion, extension, left and right lateral bending, and left and right axial rotation. Tension was applied to the cables with an uniaxial testing machine (1456, Zwick GmbH, Ulm, Germany). Three-dimensional displacement of each motion segment was measured using an optical measurement system (Qualysis Inc., Sävebalden, Sweden). Triangular markers with three diodes (Qualysis Inc., Sävebalden, Sweden) were attached to the bodies of C3 and C4. Marker positions were detected with two cameras and recorded with a computerized motion analysis system (PC-Reflex, Qualysis Inc., Sävebalden, Sweden). Angular displacement of the upper vertebra (C3) in relation to the lower vertebra (C4) was calculated from marker position using custom-made computer software. The experimental error associated with this method was ± 0.1 degrees [18].

The vertebrae were mounted in pots using PMMA (Technovit 3040; Heraeus Kulzer GmbH, Wehrheim/Ts, Germany). The lower pot was rigidly attached to the base of the testing apparatus. This test setup resulted in a compressive preload of 25 N, due to the weight of the upper fixation pot, which represents the average weight of the head of the sheep. Moments were applied in a quasistatic manner in increments of 1 Nm to a maximum of 6 Nm. Specimens were preconditioned with three cycles of 6 Nm load with a velocity of 1.2 mm/sec of the traverse bar. The fourth cycle was measured.

The mean apparent stiffness values in the elastic zone were calculated from the corresponding load-displacement curves. Range of motion (ROM), and neutral (NZ) and elastic (EZ) zones were determined.

F. Histomorphological, Histomorphometric, and Fluorochrome Analysis

All C3-C4 motion segments were harvested at 12 weeks for bone histology. The motion segments were fixed for 7 days in 10% normal buffered formaldehyde followed by dehydration in ascending concentrations of ethanol and embedded undecalcified in methylmethacrylate (Technovit 9100, Heraeus Kulzer GmbH, Germany). For histomorphological and histomorphometric analysis, longitudinal sections in the sagittal plane were cut at 6 μm with a Leica SM 2500S microtome and a 40° stainless steel knife. Afterwards the residual parts of the cages were removed and the following stains were used: (1) Safranin-O/Lightgreen, (2) Safranin-O/v. Kossa, (3) Astrablue, and (4) Masson-Goldner. Masson-Goldner stainings were used for histomorphological analysis.

Histomorphological analysis included evaluation of bony fusion using the above-defined four parameters, The maximum intervertebral gap in cranio-caudal direction was measured directly on midsagittal sections using an image analyzing system (Zeiss KS 400, Zeiss GmbH, Germany).

Histomorphometric parameters were measured on the residual stainings using a Leica DM-RB microscope and the image analyzing system (Zeiss KS 400, Zeiss GmbH, Germany). Parameters were measured at a magnification of 1.6×. The sagittal diameter distance (S) of C3 and the average preoperative DSH were determined to define the size of the region of interest (ROI) for histomorphometric evaluation. The complete intervertebral fusion area was included in this ROI. The following structural indices were calculated in the ROI: bone volume/total volume (BV/TV), cartilage volume/total volume (CV/TV), mineralized cartilage volume/cartilage volume (mCV/CV).

For fluorochrome analysis, longitudinal sections in the parasagittal plane were cut at 400 μm with a precise macrogrinding machine (Fa. Exact, Norderstedt, Germany). These slices were then ground to a thickness of 80 μm using a precise microgrinding machine (Fa. Exact, Norderstedt, Germany). Fluorochrome markers were analyzed under appropriate lighting conditions using a Leica DM-RB microscope and an image analyzing system (Zeiss KS 400, Zeiss GmbH, Germany). Parameters were measured at a magnification of 1.6×.

Fluorochrome analysis of intervertebral fusion areas has been described in detail [49]. The first appearance of the marker served to time formation of new bone matrix. The presence or absence of each marker around or within the cage or the bone graft, respectively, was used to determine the relative time frame of new bone formation.

G. Statistical Analysis

Comparison of data was performed using one-way ANOVA for independent samples followed by TUKEY post hoc analysis for multiple comparison procedures with Bonferroni correction for multiple measurements. Intraobserver variability for radiographic, functional radiographic evaluation, and CT measurements was determined using kappa statistics. The above-described parameters were used to categorize semiquantitative bony fusion on plain radiographs, CT scans, and histological stainings, but no statistical evaluation of this score was performed.

Statistical significant differences were defined at a 95% confidence level. The values are given as mean ± standard deviation. SPSS (release 7.0) (SPSS Inc., Chicago, IL) software supported statistical evaluation.

III. RESULTS

A. Failure Parameters and Complications

One animal died due to anesthesiological complication at day 0. This animal was excluded from the study and replaced by another animal. In group 1 one animal (animal number 6) developed a hematoma at the donor site of the iliac crest graft. In group 3 one animal (animal number 6) developed wound-healing problems at the donor site. Both complications healed without further difficulties under conservative treatment.

B. Volume of the Implants

Volume of the implants was evaluated prior to insertion using water-displacement technique. The average volume of the autologous tricortical iliac crest bone graft was 1.30 ± 0.1 cm^3. The average volume of the cylinder- and box-design cage filled with autologous iliac crest bone graft was 1.52 ± 0.1 cm^3 and 1.50 ± 0.1 cm^3, respectively.

C. Radiographic Results

The reproducibility of the positioning of the sheep cervical spine in the fixation devices for radiographic evaluation was investigated by repeated measurements. Reproducibility of average DSH and IVA was high showing a maximum difference on 10 radiographic scans of 0.8 mm (approximately 10% of total value) and 1.5 degrees (approximately 10% of total value), respectively. However, reproducibility of LA was moderate, showing a maximum difference on 10 radiographic scans of 4.0 degrees (approximately 60% of total value).

Intraobserver agreement for radiographic measurements was good, showing kappa values ranging between 0.76 and 0.92.

Preoperative baseline values of all radiographic parameters did not show any differences between the groups. At 8 and 12 weeks, both cage groups showed significantly higher values for average DSH than group 1 ($p < 0.05$) (Fig. 3a). At 1 week average DSH values for the box-design cage were significantly higher than for the cylinder-design cage and the tricortical iliac crest bone graft ($p < 0.05$). No other differences were found for DSH between both cage types during the experimental period. At 2, 4, 8, and 12 weeks, both cage groups (groups 2 and 3) showed significantly higher values for IVA ($p < 0.05$) (Fig. 3b) compared to the autologous tricortical iliac crest graft group (group 1). During the experimental period, no significant differences of the IVA were found between the cage groups, except for at the 2-week time point, where the box-design cage showed a significantly higher IVA than the cylinder-design cage ($p < 0.05$). At 1, 4, 8, and 12 weeks, the box-design cage (group 3) showed significantly higher values for LA ($p < 0.05$) (Fig. 3c) compared to the autologous iliac crest graft group (group 1) and the cylinder-design cage group (group 2).

After 12 weeks bony fusion was evaluated on radiographic scans (Fig. 4). In the cage groups (groups 2 and 3) a slightly progressed interbody fusion was found in comparison to group 1 (Table 1).

D. Functional Radiographic Results

Intraobserver agreement for functional radiographic measurements was excellent, showing kappa values ranging between 0.84 and 0.96.

Flexion/extension differences of LA did not show any significant difference between group 2 and group 3 (Table 2). Functional radiographic assessment revealed significantly lower residual flexion/extension movement in the cylinder design cage group (group 2) than in the tricortical iliac crest graft group (group 1) ($p < 0.05$).

E. Quantitative Computed Tomographic Results

Intraobserver agreement for CT measurements was excellent, showing kappa values ranging between 0.82 and 0.92.

After 12 weeks there were no significant differences for BMD between the tricortical iliac crest graft group (group 1) and the cage groups (groups 2 and 3). In the cylinder-design cage group (group 2), bone mineral content of the callus was significantly higher than in groups 1 and 3 ($p < 0.05$). The cylinder-design cages (group 2) showed significantly higher values for BCV ($p < 0.05$) than the other groups (Fig. 5, Table 3).

Bony fusion was evaluated on 2-D-CT-reconstruction (Table 4). In the cage groups (group 2 and 3) a slightly advanced interbody fusion was found in comparison to group 1 (Table 1).

F. Biomechanical Results

Results for stiffness, range of motion (ROM), neutral zone (NZ), and elastic zone (EZ) are depicted in Fig. 6 and Table 5. The highest stiffness values and the lowest ROM, NZ, and EZ

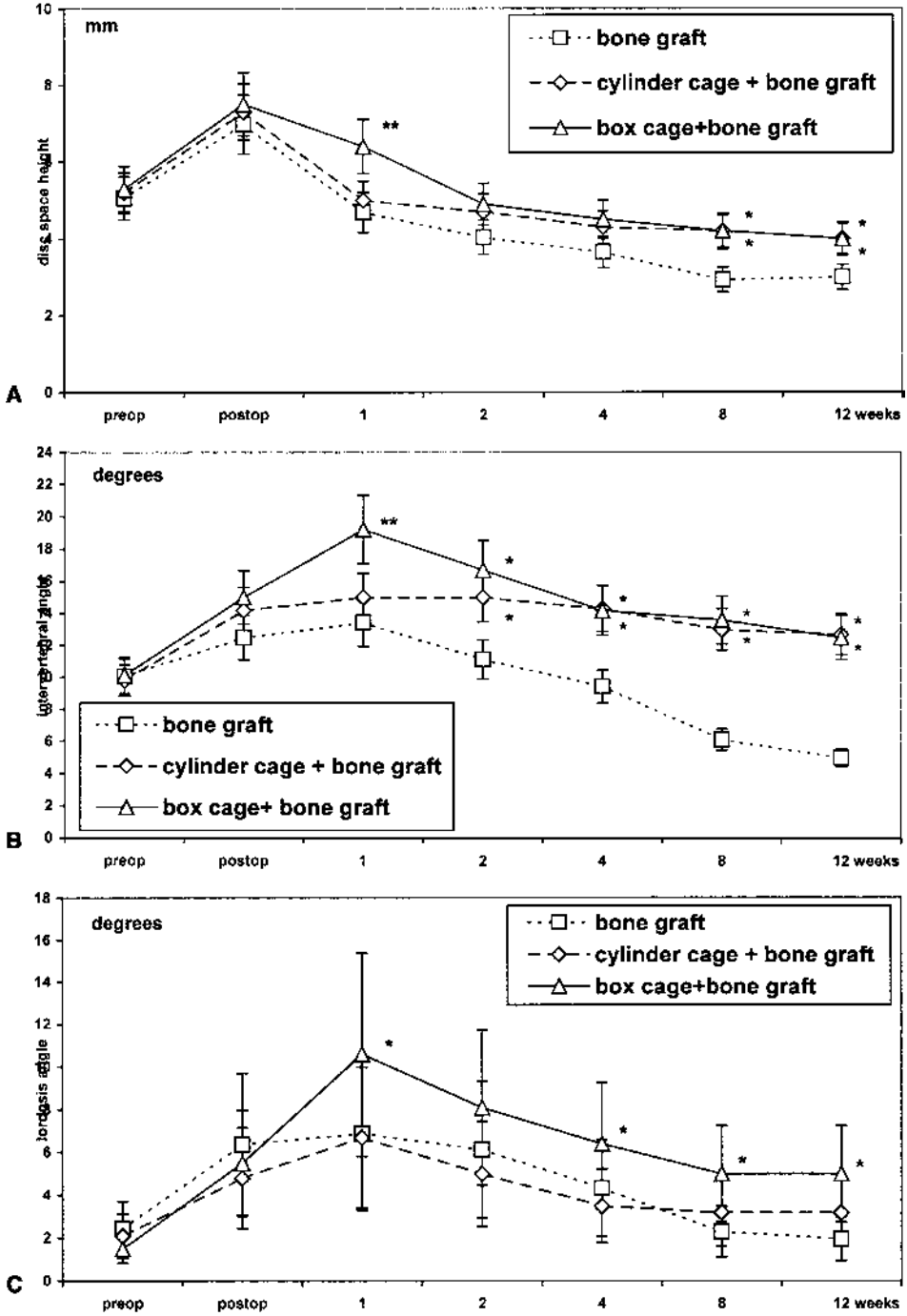

Figure 3 (A) Radiographic analysis: average disc space height of the different groups throughout the observation period. * $p < 0.05$ in comparison to the bone graft; ** $p < 0.05$ in comparison to the bone graft and the cylinder-design cage. (B) Radiographic analysis: average intervertebral angle of the different groups throughout the observation period. * $p < 0.05$ in comparison to the bone graft ** $p < 0.05$ in comparison to the bone graft and the cylinder-design cage. (C) Radiographic analysis: average lordosis angle of the different groups throughout the observation period. * $p < 0.05$ in comparison to the bone graft.

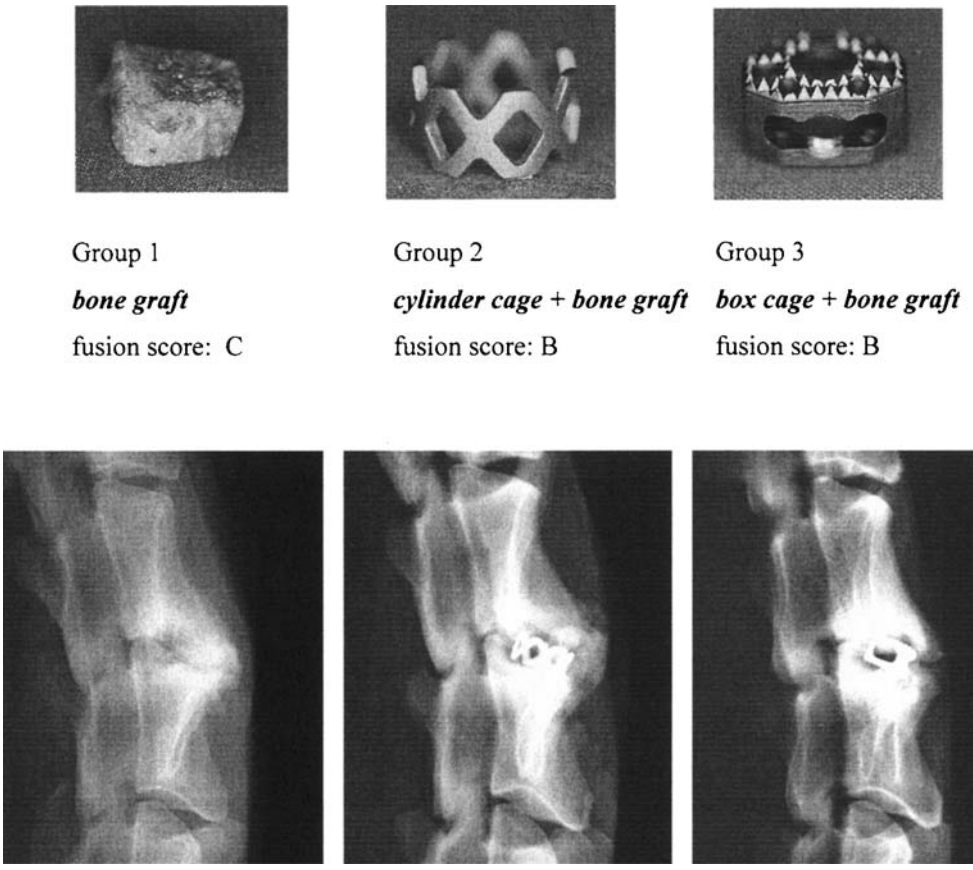

Figure 4 Radiographic analysis: bony fusion evaluated after 12 weeks on radiographic scans (example). The small pictures show the different implants. Notice the larger contiguous cranial pore in the cylinder design cage. The results of the fusion score are depicted: (A) no bony fusion; (B) maximum intervertebral gap of more than 5 mm; (C) maximum intervertebral gap of less than 5 mm; (D) complete bony fusion.

Table 1 Radiographic Analysis

Bony fusion parameter (score)	Group 1 ($n = 8$), bone graft	Group 2 ($n = 8$), cylinder cage + bone graft	Group 3 ($n = 8$), box cage + bone graft
A	0	0	0
B	5	4	5
C	3	3	3
D	0	1	0

Bony fusion was determined after 12 weeks on radiographic scans using following parameters: (A) no bony fusion, (B) intervertebral gap >5 mm, (C) intervertebral gap <5 mm, (D) complete bony fusion. All radiographic measurements were evaluated by three independent observers.

Table 2 Functional Radiographic Evaluation of Flexion/Extension at 12 Weeks

Flexion/extension (difference in degrees)	Group 1 ($n = 8$), bone graft	Group 2 ($n = 8$), cylinder cage + bone graft	Group 3 ($n = 8$), box cage + bone graft
IVA	13.6 ± 3.7 (6.0–13.5)	7.7 ± 3.0[a] (4.5–11.0)	9.6 ± 2.8 (7.0–12.5)
LA	14.1 ± 5.0 (6.5–17.0)	7.9 ± 3.4[a] (4.5–11.5)	10.1 ± 3.2 (6.0–13.5)

Flexion/extension differences of intervertebral angle (IVA) and lordosis angle (LA) were calculated.
[a] $p < 0.05$ in comparison to the bone graft (group 1).

values in rotation and bending were constantly found in group 2. Average stiffness in axial rotation and lateral bending was significantly higher ($p < 0.05$) in the cylinder-design cages than in any other group. ROM in rotation was significantly lower ($p < 0.05$) in group 2 than in both other groups.

G. Histomorphological Results

Histomorphological analysis supported the findings of radiographic and biomechanical examinations (Fig. 7).

Group 1 (autologous iliac crest bone graft) showed extensive callus formation with cartilage and connective tissue cells. The tricortical bone graft, however, collapsed and was mainly reabsorbed. Osteoclastic activity was noted as an indicator of graft resorption. Most of the callus was seen ventrally. Groups 2 and 3, stabilized with cages, showed bony islands between the endplates with cartilage and fibrous tissue components. These findings were accompanied by capillary ingrowth and resorptive lacunae. The tissue surrounding the cages appeared similar in both groups. However, inside the cage of group 3, extensive osteoclastic activity was noted as an indication of graft resorption.

Bony fusion was evaluated histomorphologically (Table 6). In the cage groups (groups 2 and 3) a progressed interbody fusion was found in comparison to the tricortical iliac crest graft group (group 1). However, the cylinder-design cage showed a slightly more progressed bone matrix formation than the box-design cage.

H. Histomorphometric Results

The results of histomorphometric analysis are depicted in Table 7. In histomorphometric analysis no significant differences of sagittal diameter distance (baseline) were determined between all groups. Compared to the bone graft group and the box-design cage group, histomorphometric parameters showed significantly progressed bone formation (BV/TV) in the cylinder-design cage group ($p < 0.05$). The bone graft group showed significantly higher histomorphometric values for CV/TV and mCV/TV than both cage design groups ($p < 0.05$).

I. Fluorochrome Analysis Results

The results of fluorochrome analysis are depicted in Table 8. Both cage designs exhibited earlier new bone formation both within and around the cages compared to the bone graft group at all

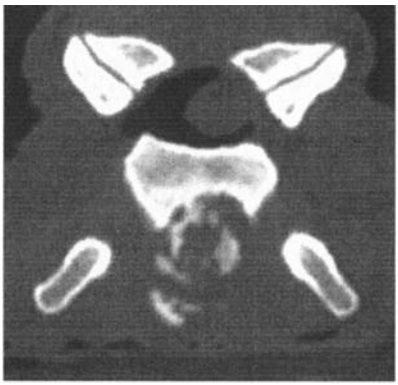

Group 1 bone graft

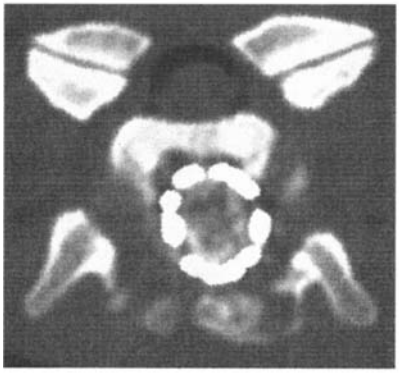

Group 2 cylinder cage + bone graft

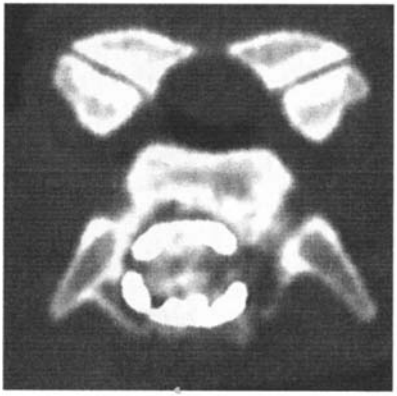

Group 3 box cage + bone graft

Figure 5 CT analysis: interbody fusion evaluated after 12 weeks on axial computer tomographic scans parallel to the intervertebral space (example).

time points. In comparison to the box-design cage, the cylinder-design cage showed more new bone formation both within and around the cages at 6 and 9 weeks.

IV. DISCUSSION

The objective of this study was to compare interbody fusion of an autologous tricortical iliac crest bone graft with a cylinder- and a box-design cage in a sheep cervical spine interbody

Table 3 QCT Analysis to Measure Bone Mineral Density, Bone Mineral Content, and Bony Callus Volume at 12 Weeks

QCT	Group 1 ($n = 8$), bone graft	Group 2 ($n = 8$), cylinder cage + bone graft	Group 3 ($n = 8$), box cage + bone graft
BMD (g/cm^3)	0.58 ± 0.04 (0.56–0.64)	0.55 ± 0.05 (0.52–0.59)	0.58 ± 0.07 (0.52–0.59)
BMC (g)	2.3 ± 1.0 (1.7–3.1)	3.2 ± 0.3[a,b] (2.8–3.7)	2.2 ± 0.3 (1.8–3.6)
BCV (cm^3)	4.0 ± 1.0* (3.8–5.1)	5.4 ± 1.4*[a,b] (3.8–6.3)	3.8 ± 0.3* (3.0–4.4)

[a] $p < 0.05$ in comparison to the bone graft (group 1).
[b] $p < 0.05$ in comparison to the box-design cage (group 3).
* Initial volume of the bone graft, the cylinder, and box design cage filled with bone graft was 1.30, 1.50, and 1.52 cm^3, respectively.

fusion model. This study was designed to determine whether there were differences between the three interbody fusion techniques in (1) the ability to preserve postoperative distraction, (2) the biomechanical stability, and (3) the histological characteristics of intervertebral bone matrix formation.

A. Distractive Properties

Several clinical studies demonstrated that tricortical iliac crest grafts used for interbody fusion developed disc space height decreases during the postoperative period [10,20]. These clinical investigations are in concordance with the experimental results of this study, showing significant decrease of disc space height in the bone graft group. Interbody cages have especially been developed in the quest for interspace structural stability during bony fusion. Cages should retain interbody distraction and should be resistant against subsidence into the adjacent vertebrae in order to guarantee bony fusion in a desired quality [37]. However, currently subsidence of cages has only been investigated in one animal experimental in vivo study. Sandhu et al. [34] showed using a sheep animal model that screw-design cages were able to preserve interbody distraction

Table 4 CT Evaluation

Bony fusion parameter (score)	Group 1 ($n = 8$), bone graft	Group 2 ($n = 8$), cylinder cage + bone graft	Group 3 ($n = 8$), box cage + bone graft
A	0	0	0
B	5	4	6
C	3	3	2
D	0	1	0

Bony fusion was determined after 12 weeks on Two-Dimensional CT reconstruction using the following parameters: (A) no bony fusion, (B) intervertebral gap of more than 5 mm, (C) intervertebral gap of less than 5 mm, (D) complete bony fusion. All radiographic measurements were evaluated by three independent observers.

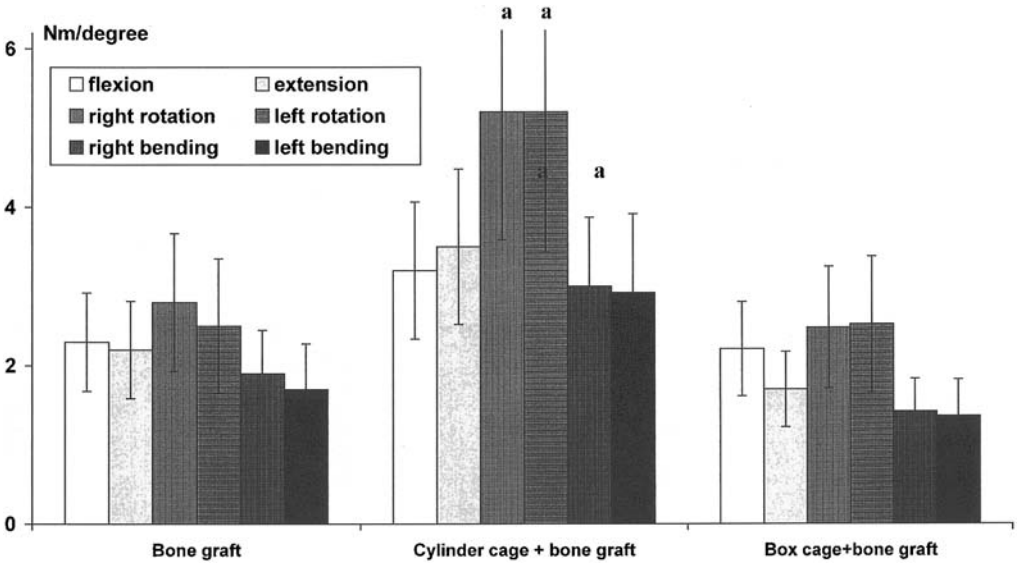

Figure 6 Biomechanical analysis: stiffness of the different groups for the different test modes.$^{>a}$ $p < 0.05$ in comparison to the bone graft (group 1) and to the box-design cage (group 3).

more effectively than an autologous iliac crest bone graft. Experimental in vivo data for cylinder- or box-design cages are not available at present. The data in the present study demonstrated that, at the time of surgery, both cages and the tricortical iliac crest bone graft were able to distract intervertebral spaces beyond their baseline measures to almost similar values. However, all conditions developed significant subsidence beyond normal disc space height values during the 12-week observation period. Whereas the loss of disc space height of the metallic cages resulted from subsidence into the subchondral bone of the adjacent vertebral bodies, the loss of the intervertebral space in the tricortical iliac crest graft group resulted mainly from gradual graft collapse. Both cages were able to decrease the loss of disc space height significantly in comparison to the tricortical iliac crest bone graft. Although the box-design cage showed significantly less subsidence after 2 weeks, both cages demonstrated similar disc space height values at final measurements.

B. Biomechanical Properties

In this in vivo experiment the tricortical iliac crest bone graft has shown significantly less biomechanical stiffness in bending and rotation and a higher range of motion in rotation than the cylinder-design cage. These in vivo results are in concordance with several in vitro studies showing a higher biomechanical stiffness for the cylinder-design cage used in this study than for a bone graft [22,26]. Previous biomechanical in vitro studies by Mittlmeier et al. [26] had demonstrated a significantly higher biomechanical stiffness for the box-design cage than for the tricortical bone graft. In contrast, no significant biomechanical difference could be determined between the box-design cage and the bone graft in this study after 12 weeks in vivo. Additionally, in this study there was a higher biomechanical stiffness in rotation and bending and a lower range of motion in rotation for the cylinder-design cage than for the box-design cage. These in vivo results are also in crucial contrast to in vitro results obtained by our own working group

Table 5 Biomechanical Analysis After 12 Weeks to Measure Range of Motion (ROM) and Neutral (NZ) and Elastic Zones (EZ) for Different Test Modes

Test modes (degrees)	Group 1 ($n = 8$), bone graft	Group 2 ($n = 8$), cylinder cage + bone graft	Group 3 ($n = 8$), box cage + bone graft
Flexion			
ROM	2.9 ± 1.0	3.9 ± 1.3	3.9 ± 1.4
NZ	0.7 ± 0.5	1.3 ± 0.9	1.6 ± 1.0
EZ	1.9 ± 0.7	2.6 ± 0.8	2.3 ± 0.9
Extension			
ROM	3.3 ± 1.5	3.8 ± 1.2	3.9 ± 1.4
NZ	0.9 ± 0.7	1.4 ± 0.9	1.7 ± 1.0
EZ	2.4 ± 0.8	2.4 ± 1.0	2.3 ± 1.0
right rotation			
ROM	3.3 ± 1.4	2.0 ± 1.0[a,b]	2.9 ± 0.8
NZ	0.7 ± 0.3	0.4 ± 0.2	0.6 ± 0.3
EZ	2.7 ± 1.1	1.6 ± 0.9[a]	2.3 ± 0.9
left rotation			
ROM	3.3 ± 1.4	2.1 ± 1.0[a,b]	2.9 ± 0.9
NZ	0.7 ± 0.5	0.5 ± 0.3	0.6 ± 0.3
EZ	2.7 ± 1.8	1.6 ± 0.9	2.3 ± 0.7
right bending			
ROM	4.5 ± 2.4	4.2 ± 2.2	5.6 ± 2.2
NZ	1.5 ± 1.5	1.2 ± 1.2	1.9 ± 1.0
EZ	3.0 ± 1.3	3.0 ± 1.9	3.7 ± 1.8
left bending			
ROM	4.6 ± 2.2	4.1 ± 2.1	5.6 ± 2.2
NZ	1.7 ± 1.6	1.3 ± 1.2	2.0 ± 1.3
EZ	2.9 ± 0.7	2.8 ± 1.9	3.6 ± 1.8

[a] $p < 0.05$ in comparison to the bone graft (group 1).
[b] $p < 0.05$ in comparison to the box-design cage (group 3).

[26]. In our previous in vitro studies [26] we were able to show significantly higher stiffness for the box-design cage than for the cylinder-design cage. This differences between biomechanical in vitro and in vivo results may be a result of the ''biological qualities'' of different cage designs in vivo, suggesting that currently available biomechanical in vitro tests are not highly predictive for the in vivo performance of any interbody fusion cage. Provisos against the predictive value of biomechanical in vitro tests for the in vivo performance of spinal implants have also been expressed by other authors [6,22,26,32,36].

C. Histological Characteristics

Histomorphometric analysis showed significantly higher intervertebral bone volume in the cylinder-design cage group than in the bone graft group. Additionally, significantly higher values for bone matrix formation were found in the cylinder design-group than in the box-design group. There are various possible explanations for these findings.

The limited biomechanical properties of the tricortical iliac crest bone graft resulted in a compression and sometimes fragmentation of the graft followed by extensive osteoclastic activity

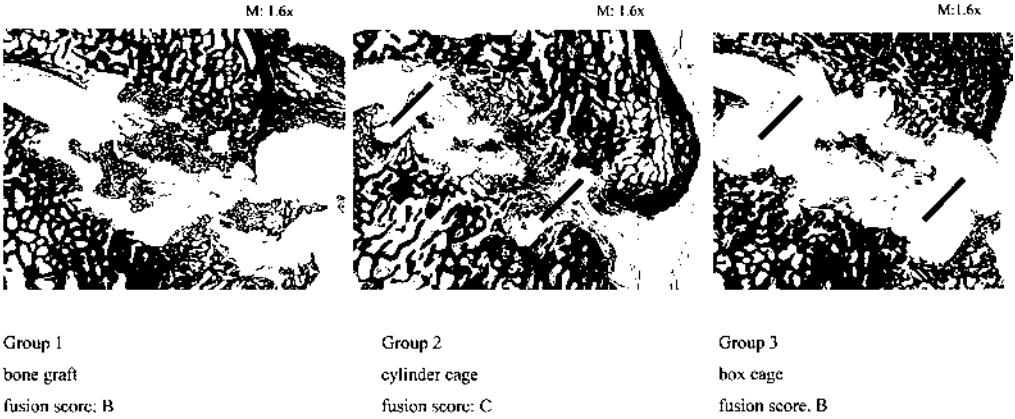

Figure 7 Histomorphological analysis: after 12 weeks interbody fusion was evaluated histomorphologically and histomorphometrically (example). M: = magnification; microradiograpy-like Safranin-O/v. Kossa staining. The results of the fusion score are depicted: (A) no bony fusion; (B) maximum intervertebral gap of more than 5 mm; (C) maximum intervertebral gap of less than 5 mm; (D) complete bony fusion.

and finally graft resorption. In contrast, the bone grafts packed inside the cages have a biomechanically protected and as a result biologically improved environment for fusion [37], resulting in a higher interbody fusion mass, especially in the cylinder-design cage group.

The initial biomechanical in vivo stability of the cage plus graft composite is nearly exclusively a result of the biomechanical properties of the cage [15,26]. Only secondarily does the interbody fusion mass arising from the incorporated bone graft contribute to biomechanical stability [15]. Having the biomechanical in vitro results of both cages in mind [26], the significantly higher biomechanical stability in the cylinder-design cage group compared to the box-design cage group in vivo was an effect of an accelerated interbody fusion in the cylinder-design group. Biomechanical loads in vivo consist of shear and compression. Whereas shear loads have proven to promote bone matrix formation, compressive loads do not [5,7,30]. In contrast to the bone graft, the cage mainly functions as a protector against compressive loads. Therefore, this characteristic of the cages contributed to the higher interbody fusion mass in the cylinder-design cage group compared to the bone graft group.

The ideal biological environment for spondylodesis is achieved by optimal grafting techniques and the maximum graft filling of the intervertebral space [37]. But as cage volume

Table 6 Histomorphological Analysis Evaluating Bony Fusion After 12 Weeks

Bony fusion parameter (score)	Group 1 ($n = 8$), bone graft	Group 2 ($n = 8$), cylinder cage + bone graft	Group 3 ($n = 8$), box cage + bone graft
A	0	0	0
B	5	4	5
C	3	3	3
D	0	1	0

(A) No bony fusion, (B) intervertebral gap of more than 5 mm, (C) intervertebral gap of less than 5 mm, (D) complete bony fusion.

Table 7 Histomorphometrical Analysis After 12 Weeks

Indices	Group 1 ($n = 8$), bone graft	Group 2 ($n = 8$), cylinder cage + bone graft	Group 3 ($n = 8$), box cage + bone graft
SDD	26.2 ± 1.0	25.5 ± 1.1	26.1 ± 0.8
(mm)	(25.0–28.3)	(24.6–27.8)	(25.2–28.0)
BV/TV	31.4 ± 3.9	45.5 ± 6.7[a,b]	31.6 ± 3.8
(%)	(24.8–39.0)	(38.5–61.3)	(20.5–42.3)
CV/TV	10.1 ± 2.8	4.6 ± 2.7[a]	4.2 ± 1.1[a]
(%)	(1.0–22.1)	(0.8–9.4)	(2.8–6.4)
mCV/CV	5.5 ± 2.0	2.8 ± 1.3[a]	3.2 ± 1.4[a]
(%)	(0.6–9.4)	(0.2–7.6)	(1.0–5.1)

Sagittal diameter distance (SDD, baseline), bone volume/total volume (BV/TV), cartilage volume/total volume (CV/TV), mineralized cartilage volume/cartilage volume (mCV/CV).

[a] $p < 0.05$ in comparison to the bone graft (group 1).

[b] $p < 0.05$ in comparison to the box-design cage (group 3).

Initial volume of the bone graft and the cylinder and box-design cage filled with bone graft was 1.30, 1.50, and 1.52 cm^3, respectively.

increases, graft volume decreases. Therefore, from the biological perspective the ideal cage would be the one with the smallest cage volume that will provide adequate mechanical stability, because this cage will allow the maximum graft filling of the intervertebral space [37]. Although both cages in this study showed nearly similar volumes when filled with bone grafts (cylinder-design cage: 1.52 cm^3; box-design cage: 1.50 cm^3), the volume of the isolated cages was substantially different (cylinder-design cage: 0.1 cm^3; box-design cage: 0.26 cm^3). Therefore, a higher bone graft volume was incorporated in the cylinder-design cage, which has potentially contributed to the higher intervertebral fusion mass in this group.

Kanayama et al. [15] showed in an in vitro study that the cage design has a significant influence on the loads of a graft within a cage. They demonstrated that a larger contiguous pore is important to decrease the stress-shielding effect on a graft within a interbody fusion device. He assumed that the lower the stress-shielding effect on a graft, the higher the possibility for interbody fusion. Finally, he stated that ''it remains unclear whether the stress-shielding environment influences the bone quality of the developing interbody fusion mass'' in vivo [15]. The incorporation and remodeling of a bone graft within a interbody cage was investigated in several animal experiments. Brantigan et al. [2] used carbon cage implants in a goat model and was

Table 8 Fluorochrome Analysis After 12 Weeks

	Group 1 ($n = 8$), bone graft		Group 2 ($n = 8$), cylinder cage + bone graft		Group 3 ($n = 8$), box cage + bone graft	
Indices	Adjacent	Within	Adjacent	Within	Adjacent	Within
3 weeks	0	0	0	1	1	0
6 weeks	1	0	4	6	2	4
9 weeks	1	0	4	6	4	4

Depicted are the number of fusion sites (of the different groups at different time points) in which the fluorochrome marker was present adjacent or within the cage or bone graft, respectively.

able to demonstrate a complete incorporation of the autograft and continuous trabecular bridging within the cage. Cunningham et al. [9] and Zdeblick et al. [38] investigated the efficacy of a screw-design cage in a sheep model. They did not find any significant difference in bone quality of the interbody fusion mass between the screw-design cage packed with autologous bone and the tricortical iliac crest graft during a short-term postoperative observation period. In the presented study bone matrix formation was evaluated inside both cages. However, the cylinder-design cage showed a significantly higher interbody bone volume and an accelerated interbody fusion in polychrome sequential labeling than the box-design cage. Therefore, it can be assumed that both cage designs were able to provide an adequate biological environment for interbody fusion, but the cylinder-design cage was more effective than the box-design cage. Comparing both cage designs a significantly larger contiguous pore is obvious in the cylinder-design cage (Fig. 5). Therefore, on the basis of Kanayama et al.'s results [15], the cylinder-design cage apparently has a significant lower stress-shielding effect on the incorporated bone graft than the box-design cage. In conclusion, the significantly lower stress-shielding effect of the bone graft within the cylinder-design cage might be the most important reason for the significantly higher interbody fusion mass found in this cage design.

V. CONCLUSION

In comparison to the tricortical bone graft, both cage designs showed significantly better distractive properties. The cylinder-design cage demonstrated a significantly higher biomechanical stiffness in rotation and bending and an accelerated interbody fusion in comparison to the box-design cage and the tricortical bone graft. The differences in bone matrix formation inside both cages were mainly a result of the significantly lower stress shielding of the bone graft within the cylinder-design cage. Further investigations are necessary to determine quantitatively the small borderline between biomechanical protected environment of the graft within a cage accelerating interbody fusion and stress shielding of a graft within the cage inhibiting interbody fusion.

REFERENCES

1. Brantigan JW, Steffee AD, Geiger JM. A carbon fiber implant to aid interbody lumbar fusion. Mechanical testing. Spine 1991; 16:277–282.
2. Brantigan JW, Mc Afee PC, Cunningham BW. Interbody lumbar fusion using a carbon fiber implant versus allograft bone. An investigational study in the Spanish goat. Spine 1994; 19:1436–1444.
3. Brooke NS, Rorke AW, King AT, Gullan RW. Preliminary experience of carbon fibre cage prostheses for treatment of cervical spine disorders. Br J Neurosurg 1997; 11:221–227.
4. Brodke DS, Dick JC, Kunz DN, McCabe R, Zdeblick TA. Posterior lumbar interbody fusion. A biomechanical comparison, including a new threaded cage. Spine 1997; 22:26–31.
5. Burger EH, Klein-Nulend J, Veldhuijzen JP. Mechanical stress and osteogenesis in vitro. J Bone Miner Res 1992; 7:327–401.
6. Cain CC, Fraser RD. Bony and vascular anatomy of the normal cervical spine in the sheep. Spine 1995; 20:759–765.
7. Carter DR, Wong M. Mechanical stresses and endochondral ossification in the chondroepiphysis. J Orthop Res 1988; 6:148–154.
8. Cloward RB. The anterior surgical approach to the cervical spine: the Cloward procedure: past, present, and future. The presidential lecture, Cervical Spine Research Society. Spine 1988; 13: 823–827.

9. Cunningham BW, Kanayama M, Parker LM. Osteogenic protein versus autologous interbody arthrodesis in the sheep thoracic spine. A endoscopic study using the Bagby and Kuslich interbody fusion device. Spine 1999; 24:509–518.
10. Dennis S, Watkins R, Landaker S, Dillin W, Springer D. Comparison of disc space heights after anterior lumbar interbody fusion. Spine 1989; 14:876–878.
11. Goh JC, Wong HK, Thambyah A, Yu CS. Influence of PLIF cage size on lumbar spine stability. Spine 2000; 25:35–39.
12. Heller JG, Zdeblick TA, Kunz DA, McCabe R, Cooke ME. Spinal instrumentation for metastatic disease: in vitro biomechanical analysis. J Spinal Disord 1993; 6:17–22.
13. Hollowell JP, Vollmer DG, Wilson CR, Pintar FA, Yoganandan N. Biomechanical analysis of thoracolumbar interbody constructs. How important is the endplate?. Spine 1996; 21:1032–1036.
14. Jost B, Cripton PA, Lund T, Oxland TR, Lippuner K, Jaeger P, Nolte LP. Compressive strength of interbody cages in the lumbar spine: the effect of cage shape, posterior instrumentation and bone density. Eur Spine J 1998; 7:132–141.
15. Kanayama M, Cunningham BW, Haggerty CJ, Abumi K, Kaneda K, McAfee PC. In vitro biomechanical investigation of the stability and stress-shielding effect of lumbar interbody fusion devices. J Neurosurg (Spine 2) 2000; 93:259–265.
16. Kandziora F, Mittlmeier T, Kerschbaumer F. Stage related surgery for cervical spine instability in rheumatoid arthritis. Eur Spine J 1999; 8:371–381.
17. Kandziora F, Kerschbaumer F, Starker M, Mittlmeier T. Biomechanical assessment of the transoral plate fixation for atlantoaxial instability. Spine 2000; 25:1555–1561.
18. Kandziora F, Pflugmacher R, Scholz M, Schnake K, Schröder R, Hoffmann J, Mittlmeier T. The sheep cervical spine in comparison to the human spine. An anatomic, radiographic, bone mineral density and biomechanical study. Spine 2001; 26:1028–1037.
19. Kettler A, Wilke HJ, Dietl R, Krammer M, Lumenta C, Claes L. Stabilising effect of posterior lumbar interbody fusion cages before and after cyclic loading. J Neurosurg 2000; 92:87–92.
20. Kumar A, Kozak JA, Doherty BJ, Dickson JH. Interspace distraction and graft subsidence after anterior lumbar fusion with femoral strut allograft. Spine 1993; 18:2393–2400.
21. Kumaresan S, Yoganandan N, Pintar FA. Finite element analysis of anterior cervical spine interbody fusion. Biomed Mater Eng 1997; 7:221–230.
22. Lee SW, Lim TH, You JW, An HS. Biomechanical effects of anterior grafting devices on the rotational stability of spinal constructs. J Spinal Disord 2000; 13:150–155.
23. Lund T, Oxland TR, Jost B, Cripton P, Grassmann S, Etter C, Nolte LP. Interbody cage stabilisation in the lumbar spine: biomechanical evaluation of cage design, posterior instrumentation and bone density. J Bone Joint Surg Br 1998; 80:351–359.
24. Majd ME, Vadhva M, Holt RT. Anterior cervical reconstruction using titanium cages with anterior plating. Spine 1999; 24:1604–1610.
25. Matge G. Anterior interbody fusion with the BAK-cage in cervical spondylosis. Acta Neurochir 1998; 140:1–8.
26. Mittlmeier T, Pflugmacher R, Schäfer J, Hoffmann J, Duda G, Kandziora F. Cervical interbody fusion cages. Biomechanical comparison of screw, box and cylinder designs. Eur Spine J 2000; 9: 297–298.
27. Munozu FLO, de las Heras BG, Lopez VC, Siguero JJA. Comparison of three techniques of anterior fusion in single-level cervical disc herniation. Eur Spine J 1998; 7:512–516.
28. Nibu K, Panjabi MM, Oxland T, Cholewicki J. Multidirectional stabilising potential of BAK interbody spinal fusion system for anterior surgery. J Spinal Disord 1997; 10:357–362.
29. Oxland TR, Hoffer Z, Nydegger T, Rathonyi GC, Nolte LP. A comparative biomechanical investigation of anterior lumbar interbody cages: central and bilateral approches. J Bone Joint Surg Am 2000; 82:383–393.
30. Patwardhan AG, Havey RM, Ghanayem AJ, Diener H, Meade KP, Dunlap B, Hodges SD. Load-carrying capacity of the human cervical spine in compression is increased under a follower load. Spine 2000; 25:1548–1554.

31. Pitzen T, Caspar W, Matthis D, Müller-Storz H, König J, Georg T, Wurm EM, Steudel WI. Primary stability of 2 PLIF (posterior lumbar interbody fusion)—a biomechanical in vitro comparison. Z Orthop 1999; 137:214–218.
32. Rapoff AJ, Ghanayem AJ, Zdeblick TA. Biomechanical comparison of posterior lumbar interbody fusion cages. Spine 1997; 22:2375–2379.
33. Rathonyi GC, Oxland TR, Gerich U, Grassmann S, Nolte LP. The role of supplemental translaminar screws in anterior interbody fixation: a biomechanical study. Eur Spine J 1998; 7:400–407.
34. Sandhu HS, Turner S, Kabo M, Kanim LE, Liu D, Nourparvar A, Delamater RB, Dawson EG. Distractive properties of threaded interbody fusion device. An in vivo model. Spine 1996; 21: 1201–1210.
35. Tencer AF, Hampton D, Eddy S. Biomechanical properties of threaded inserts for lumbar interbody spinal fusion. Spine 1995; 20:2408–2414.
36. Volkman T, Horton WC, Hutton WC. Transfacet screws with lumbar interbody reconstruction: biomechanical study of motion segment stiffness. J Spinal Disord 1996; 9:425–432.
37. Weiner BK, Fraser RD. Spine update lumbar interbody fusion cages. Spine 1998; 23:634–640.
38. Zdeblick TS, Ganayem AJ, Rapoff AJ, Swain C, Bassett T, Cooke ME, Markel M. Cervical interbody fusion cages. An animal model with and without bone morphogenetic protein. Spine 1998; 23: 758–765.

27

Autologous Growth Factors and Progenitor Cells as Effective Components in Bone Grafting Products for Spine

Terri A. Kapur, Sudha Kadiyala, and David J. Urbahns
DePuy Biologics
Raynham, Massachusetts, U.S.A.

Scott P. Bruder
DePuy Biologics, Raynham, Massachusetts, and
Case Western Reserve University, Cleveland, Ohio, U.S.A.

The miracle of tissue healing and repair can be ascribed to the collective activities of the body's own biological building blocks. As in embryological development, the dynamic interplay between cells, bioactive factors, and extracellular matrix scaffolds is responsible for the formation of new tissues and organs. From a functional perspective, the bioactive factors provide the instructional cues that direct the behavior of the cellular components. The extracellular matrix molecules provide a substrate for bioactive factor presentation and/or cellular attachment, proliferation, and differentiation. And lastly, the responding cells provide the biosynthetic machinery responsible for creating the new structural tissues. Within that context, the aims of this chapter are fourfold: (1) to review the basic cell and molecular events that occur during tissue injury and repair, (2) to articulate the role of specific contributory elements in this process, such as platelets, fibrin clots, and stem cells, (3) to outline the logic and data supporting therapeutic manipulation, or engineering, of these autologous materials, and (4) to provide appropriate examples of the benefit of such strategies for musculoskeletal tissue repair and regeneration.

I. FUNDAMENTALS OF NATURAL TISSUE HEALING

The basic paradigm of tissue healing is found throughout the systems of the body. To summarize, injury can cause release of specific growth factors into the surrounding environment and activation of the platelet-mediated wound-healing response. The released factors, at a given concentration gradient, act as ''attracting agents,'' causing white blood cells and stem cells to migrate to the wound site, a process termed chemotaxis. The white blood cells clear the wound of damaged and necrotic tissue and also release chemotactic factors to attract other cells. Once the stem cells and other progenitor cells arrive at the site, they begin to multiply to reach a critical mass

that is required for the healing process. Following this proliferative phase, the cells differentiate, undergo maturation, and begin to deposit extracellular matrix. The entire process can be summed as a sequence of steps starting with chemotaxis followed by proliferation and differentiation, and finally ending with optimal differentiated function (Fig. 1).

In the case of bone injury, the sequence of events follows the generalized case outlined above. Specifically, if a simple bone fracture occurs, hemorrhaging takes place, which activates certain proteins in the plasma by exposing blood to a subendothelial tissue factor. The blood proteins that are initially activated will in turn activate a very potent protein called thrombin. The thrombin molecule then cuts off two portions of the fibrinogen molecule and converts it to fibrin. The excision of these two portions allows the fibrin molecules to self-assemble, resulting in fibrin threads or fibrils. These fibrin threads come together to form a three-dimensional mesh. This mesh provides an ideal scaffold for the cells that migrate in later to repair the wound. The fibrin mesh is then cross-linked by the action of another molecule called fibrin-stabilizing factor (Factor XIII) that is present in the plasma and is activated by thrombin as well. Cross-linking of the mesh provides mechanical strength. The presence of calcium is essential for the progression of a number of steps in the clotting cascade, and in the absence of calcium the clotting cascade cannot proceed. The result of the clotting cascade is the formation of a stabilized fibrin mesh. The platelets, blood cells, and macromolecules that are present in the serum during the formation of the fibrin mesh are trapped within the developing fibrin network. The collective coagulum of the platelets, blood cells, and proteins in the fibrin mesh is referred to as the clot. The fibrin-rich clot serves as a ''sticky'' matrix for platelet adhesion and further activation, which leads to the release of factors such as platelet-derived growth factor (PDGF) and transforming growth factor (TGF-β) to attract macrophages, osteoprogenitors, and fibroblasts to the wound site [1]. The macrophages also become activated and clear the area of debris. The progenitor cells start to proliferate to reach a critical mass and then undergo differentiation into chrondrocytes or osteoblasts under the influence of locally occurring stimuli. These influences include biochemical signals released from the bone, such as growth factors, and also mechanical factors such as micromotion in the defect site. In the case of intramembraneous bone formation, osteoblasts

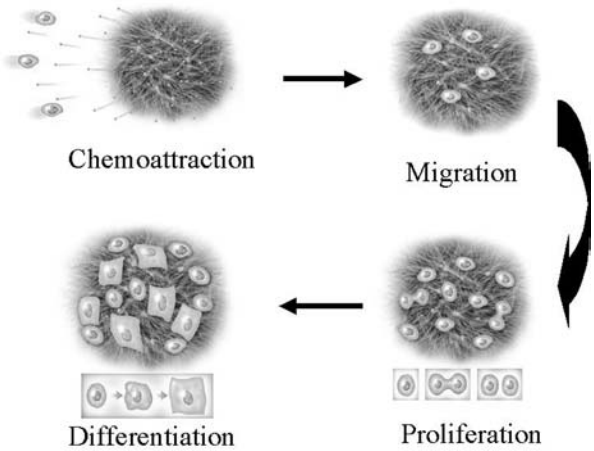

Figure 1 The basic paradigm of natural tissue healing is found throughout the body and can also be applied to bone healing. After injury, a chemotactic gradient causes cell migration to the wound site. After arriving, the cells will proliferate to reach a critical mass. Following proliferation, the cells will differentiate, undergo maturation, and begin to deposit extracellular matrix. (From Ref. 2.)

directly form the bone uniting the defect. In the case of endochondral bone formation, the chondrocytes initially lay down a cartilaginous bridge that is later mineralized. In either case, the first bridge formed is remodeled under the influence of Wolff's law to yield a structure of the appropriate density and architecture to bear the load placed upon it.

Bone healing following injury as outlined above is quite efficient if the defect size is small. In larger defects, however, the initial clot formation and the subsequent healing response is not sufficient to bridge the gap effectively. This necessitates to the need for bone grafting to achieve healing. Due to the multistep nature of the bone-healing process, it is possible to manipulate various stages of the healing cascade to increase the rate and efficiency of healing large defects. Thus, various types of graft materials have been developed, or are under investigation, for use in the clinic. These graft materials have been engineered to overcome a specific biological challenge encountered during bone healing. As the barriers become more difficult to cross, the bone graft materials become more complex, often requiring combinations of one or more types. For example, in a critical sized defect there is often a lack of endogenous growth factors and osteoblast precursors at the defect site. In order to overcome this, a graft material may be engineered to deliver certain bioactive factors and osteoprogenitors, thereby augmenting the natural healing process and therefore increasing the incidence and rate of fusion. Often these graft materials are classified according to their principal mode of action: osteoconductive, osteopromotive, osteoinductive, or osteogenic. The following sections will further expand on how the materials in each group are classified and engineered to overcome the biological barriers within the bone healing process.

II. SELECTION OF COMPONENTS IN FORMING BONE GRAFT MATERIALS

To prepare bone graft material, the surgeon must first consider the type of defect and understand the capabilities of the graft material. For a successful bone graft, three basic technologies must come together: a matrix, biological stimulants, and cells, as summarized in Fig. 2. Larger defects may require a combination of graft materials, whereas smaller defects may require only a single component. The same defect in different patients with different clinical histories, such as smoking or diabetes, might require different combinations of graft material. An outline of the ingredients one might choose to fabricate bone graft material follows in the next section and is summarized in Table 1 [2].

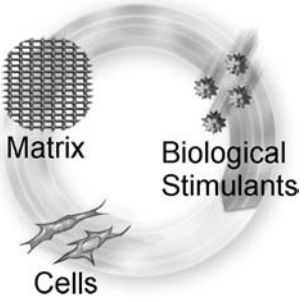

Figure 2 Basic biological essentials for successful bone graft materials. For a successful graft, three basic technologies must come together: a matrix, biological stimulants, and cells. A matrix provides conductivity; stimulants are necessary for increasing activity, and cells are essential for producing bone.

Table 1 Classification of Bone Graft Materials

	Physiological principle	Examples
Osteoconduction	Ingrowth of bone from margins of defect with gradual resorption of scaffold	Allograft cancellous chips, ceramic scaffolds, calcium phosphate
Osteopromotion	Enhancement or acceleration of the natural cascade of bone repair	Platelet rich plasma, electromagnetic stimulation, certain bioactive factors (FGF)
Osteoinduction	Promotes phenotypic conversion of undifferentiated cells into osteoblasts	Demineralized bone matrix, bone extracts, peptides, recombinant morphogenetic proteins
Osteogenesis	Transplantation of viable osteoblasts and precursors	Autogenous cancellous bone, marrow, and periosteum

Source: Ref. 2.

A. Osteoconductive Grafts

Osteoconductive materials refer to scaffolds that provide the appropriate framework for bone to grow in sites where bone naturally occurs. They function as substrates on which locally residing osteoblasts can attach. These materials rely on the presence of sufficient cues in the local environment to direct the bone formation process and depend on direct physical contact with exposed surfaces of viable bone.

Examples of osteoconductive scaffolds include naturally occurring materials such as mineralized cancellous chips (allograft), as well as synthetic substrates such as tricalcium phosphates (TCP) or hydroxyapatite (HA). Due to their relatively passive role, these materials have limited utility on their own. However, they can be mixed with autograft and adequately serve as autograft extenders. Also, they are essential for the delivery of cells and/or stimulatory signals.

B. Biological Stimulants

Biological stimulants refer to signals that direct the activity of cells. The general class of grafts where the primary mode of action is based on stimulatory signals can be subdivided into two major categories: osteoinductive and osteopromotive grafts.

1. Osteoinductive Grafts

Osteoinductive grafts are those that have the capacity to induce bone formation when placed into a site where normally no bone formation occurs. The ability of the graft to function in an osteoinductive manner is based on the presence of signals that can cause differentiation of locally occurring progenitor cells into osteoblasts. Since these grafts do not contain the necessary responding cells, they are dependent on an adequate supply of cells in the local tissue to respond to their stimuli.

Demineralized Bone Matrix. Demineralized bone matrix (DBM) is the best known and most widely used example of osteoinductive grafts. DBM is prepared by decalcifying allograft bone to expose the organic matrix, along with a plethora of stimulatory signals that were trapped in the organic matrix during bone formation. The factors contained within the DBM are capable of causing mesenchymal stem cell (MSC) chemotaxis, proliferation, and differentiation that

leads to new bone formation. Also, the underlying matrix provides a suitable scaffold for cell attachment.

The majority of DBM used is in the form of particulates (powders or fibers) requiring the use of a carrier to impart desirable handling properties to the graft. A variety of inert carriers have been used, including glycerol and gelatin. These carriers are largely considered noncontributory to the biological events but work solely to improve handling characteristics. DBM is typically considered to be an autograft extender rather than a replacement. This is due to the limited and variable bioactivity of DBM [3]. However, when combined with the appropriate supplement such as platelet-rich plasma (PRP), the biological potency may be raised to a level that imparts greater function as a bone graft substitute.

Bone Morphogenetic Protein. Urist postulated that the osteoinductivity of DBM was due to the presence of specific proteins trapped within the organic phase of the matrix [4], and he coined the term ''bone morphogenetic protein'' (BMP) to describe them [5]. Although it took another 20 years of study, a large family of BMPs was eventually purified from the DBM and cloned [6–9]. During this process it was determined that rather than a single protein, there exists a series of BMP molecules, as well as related molecules, that may also be isolated from nonbony tissue including cartilage. The BMPs are members of the TGF-β superfamily of growth factors [10–12] that includes the TGF-βs, cartilage-derived growth factors, and other proteins termed growth and differentiation factors.

While there have been some attempts to concentrate BMPs from naturally occurring sources [13], the majority of clinical development effort has been in the arena of recombinant molecules. In this approach, dimeric BMP molecules are synthesized using recombinant DNA technology, which involves the introduction of selected genes into mammalian cells or bacteria and their massive secretion of the gene product. Recombinant BMPs have been shown to be very potent in a variety of preclinical animal models and recently were approved by the U.S. Food and Drug Administration for use in limited indications in humans. This narrow FDA approval is in part based on the safety concerns that arise due to the very high doses needed for efficacy thus far.

2. Osteopromotive Grafts

Osteopromotive grafts have the ability to enhance the natural bone formation process by providing stimulatory signals at selected stages of the bone-healing process. However, they differ from osteoinductive grafts in that they do not have the capacity, by themselves, to induce new bone formation at nonorthotopic sites. Thus, osteopromotive grafts are best used where there are (1) natural differentiation cues sufficient to initiate bone formation in the local environment; (2) osteoinductive graft materials, such as DBM, present; or (3) osteogenic graft materials, such as autograft bone and marrow, present at the wound site. The best example of an osteopromotive graft material is PRP, which can be used in all the aforementioned settings.

3. Osteogenic Grafts

Osteogenic material refers to a mixture that contains all the necessary elements required for direct bone formation. Upon implantation into the body, such grafts can form bone without any additional elements from the surrounding environment other than nutritional and metabolic support. The basis of such powerful bone-forming potential lies in the fact that these grafts contain the necessary synthetic machinery; namely, living cells. Not only must these grafts contain the cells, they must include a scaffold that orients the cells and provides access to the stimulatory signals, which may be synthesized by the cells themselves.

Cortico-Cancellous Bone Autograft. Today's gold standard in bone grafting continues to be autologous bone harvested from the iliac crest. This autogenous graft provides a mixture of cells from fully differentiated osteoblasts lining the cancellous bone to undifferentiated stem cells in the marrow compartment. The cells, combined with the matrix and signals provided by the bone morsels, yield a mixture that leads to bone formation when placed into the surgical site.

There are, however, many drawbacks associated with the harvesting and use of iliac crest autograft. One major drawback is the potential morbidity and a resulting postoperative pain that can last for several years [14]. Some studies show the incidence of such complications, including infection, to be as high as 20% [15]. Limited supply and quality of autograft is also an issue for patients undergoing procedures that require large graft volumes or repeat surgeries. Due to these considerations, some surgeons have reverted to using autograft from the local cite, but local bone does not possess the same level of biological activity as iliac crest autograft due to the poor cellularity. Furthermore, the quantity of local bone available is often insufficient and requires combination with DBM or another graft extender.

Another limitation in the use of autograft is its poor handling characteristics. Autograft is typically morselized during harvest and is not easily placed or retained at the surgical site. More recently, however, PRP has been used effectively to impart desirable handling characteristics to autograft as well as to provide a source of concentrated growth factors that may further enhance the bone-healing process.

Bone Marrow–Based Grafts. Another class of potent osteogenic graft material is based on cells and stimulatory signals from bone marrow. Though not widely used in patients at present, the biological potential of marrow was first appreciated by surgeons over 100 years ago [16]. Unlike autograft, bone marrow can be obtained from the iliac crest using a simple percutaneous needle aspiration, which does not cause morbidity. These grafts typically have been prepared by mixing small amounts of aspirated marrow with an osteoconductive graft such as TCP granules or osteoinductive grafts such as DBM. The bone marrow provides a rich source of cells ranging from the MSCs, which are the undifferentiated stem cells, to cells that have already committed down the osteogenic lineage and are destined to become osteoblasts.

Despite the favorable bone-forming capacity of bone marrow–based grafts, they have not enjoyed widespread use as a replacement for iliac crest cancellous autograft for three reasons: (1) the variability resulting from inconsistent and substandard aspiration technique; (2) the very low osteoprogenitor content of these small aspirates; and (3) the combination of marrow cells with suboptimal scaffold materials. The osteoprogenitors constitute a very small fraction of the cells in the marrow and may occur as infrequently as one in 100,000 nucleated cells [17]. Thus, optimizing the aspiration, cell selection, and delivery system is critical to graft success. Despite the relative scarcity of these progenitors, it is important to remember that the bone marrow and periosteum provide a richer source of these cells than any other tissue.

III. EXAMPLES OF THERAPEUTIC BONE GRAFT MATERIALS

In the previous sections, the background of fundamental bone healing and the logical selection of bone graft materials were presented. These topics are integral to understanding the basis of developing therapies that encourage bone healing. In the following sections we will provide two examples of therapeutic bone graft materials and discuss outcomes of recent studies performed using these materials.

A. PRP as a Therapeutic Bone Graft Material

Platelets are a rich source of multiple growth factors, and thus by concentrating platelets from blood, the surgeon has a ready and ample source of autologous growth factors. Platelet-rich plasma is prepared by collecting and concentrating platelets from whole blood obtained from the patient immediately prior to or during surgery. When an appropriate method is used to concentrate platelets from whole blood, the growth factors in the resulting suspension increased proportionally to the increased platelet concentration [18].

Some of the growth factors shown to be concentrated in platelets are TGF-β, PDGF, and vascular endothelial growth factor (VEGF). TGF-β is one of the most potent chemotactic agents for osteoprogenitor cells and also has a very important role in supporting differentiated function of the osteoblasts [19]. PDGF is a potent mitogenic agent as well as possessing chemotactic properties [20]. VEGF is the best known inducer of angiogenesis, or blood vessel formation [21]. Thus, by providing a variety of concentrated growth factors, PRP can play an important role in enhancing the bone-healing process and, when used with the appropriate bone graft such as DBM or autograft, contributes to an optimal bone-healing environment. In addition, since platelet concentrates readily form a fibrin-based clot, this attribute may be used as an adjuvant to impart desirable handling characteristics to bone grafts used in surgery. Furthermore, the fibrin mesh that is formed during the clotting process also provides scaffolding needed for bone repair.

The effect of PRP on human mesenchymal stem cells has been directly evaluated in vitro. Specifically, PRP stimulates chemotactic migration of stem cells in a dose-dependent manner [22]. This is important because it demonstrates that concentrated platelets may effectively expedite the healing process by increasing the number of osteoprogenitors at the wound site through chemotaxis. Additionally, serum-free media supplemented with PRP encouraged MSCs to proliferate in a dose-dependent manner, as summarized in Fig. 3. This demonstrates that concentrated platelets not only attract MSCs, but also encourage them to divide to achieve a critical cell mass. Further, it was shown that there was no decrease in their osteogenic potential following exposure to PRP. Thus, the chemotactic migration followed by increased MSC proliferation may lead to a net increase in the production of bone matrix. These observations are consistent with in vivo wound-healing models, including the wound-healing cascade where degranulated platelets initiate chemotactic attraction and mitotic stimulation of reparative cells, which is then followed by differentiation and bone matrix production, finally resulting in new bone formation.

Other in vitro studies have demonstrated the direct involvement of platelets in stimulating osteogenic activity [23]. A proliferation increase of more than fourfold was observed in short-term cultures with the addition of PRP supplement in a culture of bone cells from the trabecular ends of human fetal long bones. Further, over long-term cultures, the number of bone-derived cells in PRP-treated medium increased significantly compared to those cultured in serum-free medium or medium supplemented with growth media. This effect was dose-dependent at 8 days, as summarized in Fig. 4. Still longer time points demonstrated osteogenic cell layers increasing as much as 36-fold at 30 days. This study, when considered with other results, demonstrates that platelet-rich plasma provides a readily accessible source of growth factors that offer a chemotactic and proliferative supplement to other forms of treatment when bone augmentation is desirable.

In a recent in vivo study, platelet concentrate was used in a rabbit posterolateral fusion model [24]. Fusion rates at the L5–L6 region were compared using two different volumes of iliac crest autograft with and without PRP. The study showed that the use of PRP significantly improved the handling characteristics of autograft. Histological evaluation of the fusion masses showed a trend towards greater osteoblastic activity, higher histological scores and a more robust

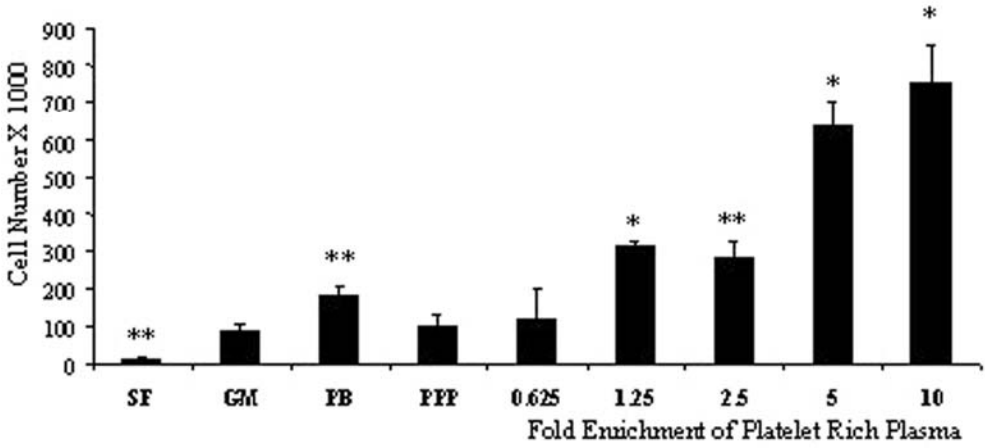

Figure 3 The effect of platelet rich plasma on proliferation of mesenchymal stem cells. Serum free media supplemented with platelet rich plasma encourages mesenchymal stem cells to proliferate in a dose dependent manner. (SF = serum free, GM = growth media, PB = peripheral blood, PPP = platelet poor plasma.) (From Ref. 22.)

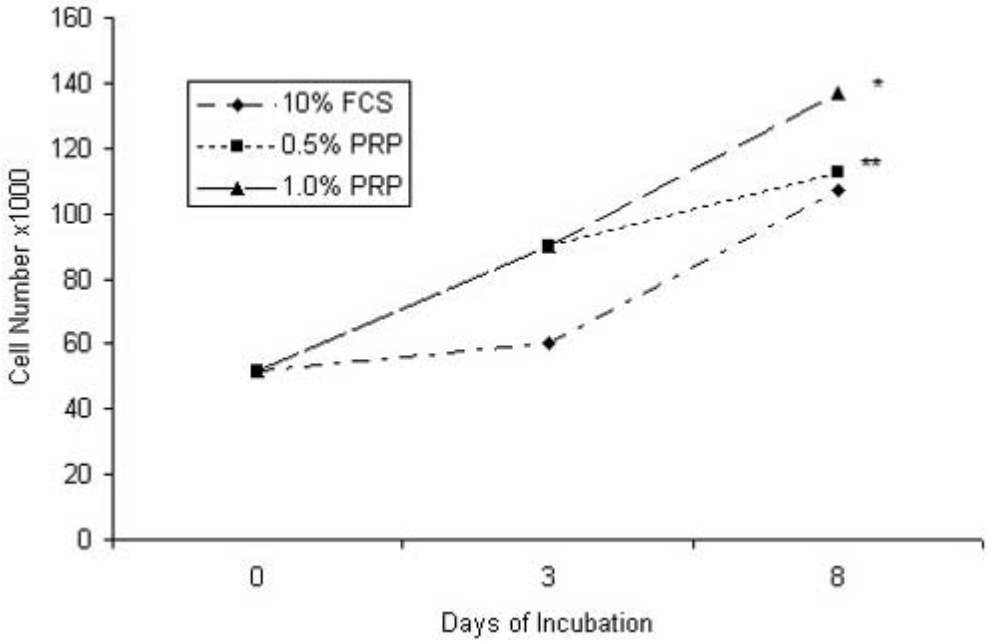

Figure 4 Number of bone-derived cells after incubation in various media. An increase in proliferation rate is observed when bone derived cells are supplemented with platelet concentrate. The results for the platelet-treated cultures (* and **) are significantly different from the 10% FCS control group. (FCS: fetal calf serum, SF: serum free medium, PC: platelet concentrate.) (From Ref. 23.)

active front of mineralization in the groups with PRP supplementation. When 1.5 cc of autograft was used in conjunction with PRP, there was a marked improvement in the biomechanical performance of the graft. Not surprisingly, when a sufficient amount of autograft was used in this model, no benefit of PRP could be shown. These data demonstrate that PRP can augment the incidence of fusion, especially in cases where the amount of available bone graft is limited.

In the clinical arena, extensive data are available in the context of bone reconstruction in oral and maxillofacial surgery [25]. For instance, Marx et al. [26] demonstrated a significant benefit in the healing rate and bone density due to the addition of PRP to autograft. In the setting of spine, studies showing the effects of PRP have just recently appeared in the literature [24,27,28]. While most reports show an improved outcome with the use of PRP, one abstract has reported a negative result associated with the use of PRP. The discrepancy between the various studies may be based, in part, on the differences in the quality and reproducibility of the PRP that is obtained using the various commercially available platelet concentrate systems. Kevy et al. [29] have compared two different systems on the basis of efficiency of platelet collection as well as quality of platelets with special regard to the extent of platelet activation and bioactive protein content. Their study documents major differences in both efficiency and quality of the platelet product, with the centrifugation-based system performing superior to an ultrafiltration-based method.

A recent human clinical study showed that autograft supplemented with PRP in posterolateral fusion resulted in a significantly higher number of fused levels compared to autograft alone after 7–9 months. In this 46-patient study, at 4–6 months group 1 (autograft only) had 61.1% fusion of all operated levels, while group 2 (autograft and PRP) had 77.3% fusion of all operated levels. By 7–9 months the difference in the two treatment groups had increased to the level of statistical significance with a fusion rate of 65.6% for group 1 and 89.4% for group 2 [28]. This study corroborates preclinical data where the addition of PRP increases the incidence of posteriolateral fusion [24]. Further, these studies lend credence to the overall bone-healing model outlined in the next section.

We have developed a hypothetical model for the role of PRP in bone healing. In summary, we suggest that the local application of PRP causes migration of MSCs to the wound site, followed by their replication to form a repair blastema. As the bioactive factors diffuse away from the fibrin scaffold, now densely populated by MSCs, the cells cease dividing and are primed to respond to the endogenous inductive cues that stimulate differentiation phase. The local and transient activity of PRP in this model of tissue repair is responsible for initiating and accelerating the natural healing cascade and thus increasing the rate of bone fusion.

B. Osteoprogenitor Cells as a Therapeutic Bone Graft Material

Bone fusion is directly affected by the number of osteoblasts in the healing environment. Since bone formation can be augmented by the addition of such cells and their progenitors, investigators have sought ways to isolate these cells for therapeutic use. For example, osteoprogenitors are readily available in the bone marrow and easily harvested, thus making marrow a good choice as a therapeutic bone graft material. However, as pointed out, there are limitations to the effectiveness of bone marrow as a graft material, principally due to the limited concentration of osteoprogenitor cells in the marrow. Thus, various strategies are being employed to increase the number of available osteoprogenitor cells.

1. Culture-Expanded Cell Technology

One method to increase the number of available osteoprogenitor cells is to expand their number ex vivo. In this method, a small aliquot of bone marrow aspirate, or an alternate cell source, is

shipped to site where cells of interest are isolated and seeded into culture dishes under specific conditions that encourage growth of a particular cell type or types. At a set time, usually on the order of a few weeks, the cells are harvested and sent back to the clinical site for reimplantation into the patient. This reimplantation method is being developed with autologous MSCs. To show clinical applicability of tissue regeneration therapies using such MSCs, a series of preclinical studies were performed. These investigations, all aimed at achieving osseous regeneration in a critical-sized defect of the femur, were designed to compare the efficacy and effective dosing when the cellular source was escalated from rodents to large animals. In the first study, culture expanded, marrow-derived MSCs were used to repair a segmental defect in the femur of rats [30]. When syngeneic MSCs were loaded onto hydroxyapatite/tricalcium phosphate (HA/TCP) cylinders and implanted, by 8 weeks nearly every pore of the implants contained considerable new bone. In contrast, cell-free implants were well vascularized, but displayed little if any bone formation within the pores. These studies established the proof of principle for MSC-based tissue regeneration therapy in bone.

The ability of MSC-loaded implants to repair defects in larger animals was examined in a critical-sized canine femoral gap defect model [31,32]. Ceramic implants made from porous HA/TCP were loaded with autologous culture expanded MSCs. At 16 weeks, radiographic union was established in all the implants loaded with MSCs, atrophic nonunion occurred in all of the femurs that had untreated defects, and only a small amount of trabecular bone formed at the cut ends of the cortex of the host bone in this group.

While these culture-expanded techniques have the potential to yield a large number of repair-competent cells, the logistics of the process pose considerable challenges for use in a hospital or private practice setting. We believe that intraoperative manipulation of bone marrow has the potential to revolutionize treatment options for patients requiring augmentation of bone formation [33]. The next section will outline results from studies utilizing a technique for concentrating osteoprogenitors quickly, easily, and effectively.

2. *Selective Cell Retention Technology*

A simple, automated methodology for the intraoperative concentration of cells that participate in the bone-healing process is currently in the late stages of development. This technique relies on the selective retention of the osteoprogenitor cells from bone marrow onto substrates that are directly implantable. The principle behind the technology is that when bone marrow is flowed through selected porous matrices under specific conditions, the osteoprogenitor cells are retained within the matrix with high efficiency. Other cells within the bone marrow, including a variety of white blood cells and their progenitors, are also retained within the matrix, but with a much lower efficiency. Consequently, the matrix is selectively enriched with a concentrated complement of osteoprogenitors. A schematic view of the selective retention process is shown in Fig. 5. This technology, coupled with recent advances that optimize the cellular yield during bone marrow aspiration [34], facilitates the preparation of potent grafts with a high level of osteoprogenitor cells.

Selective retention of the osteoprogenitors is influenced by the choice of matrix material used to capture the cells. For instance, osteoprogenitors have high affinity for substrates such as calcium phosphate ceramics or bone matrix. In addition to the chemical composition of the scaffold, the physical formulation of the matrix also has an effect on the cell retention, and thus one can manipulate parameters such as surface area, porosity and surface chemistry, or electrostatic charge to optimize cell retention. While the matrix component of the system may have a profound effect on the selective cell retention process, there are other parameters that can be manipulated to improve the osteoprogenitor retention and obtain efficiencies in the range of

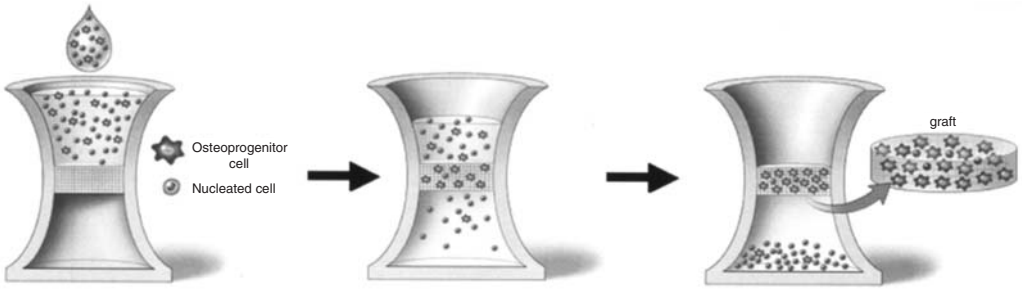

Figure 5 A schematic view of the selective retention process for concentrating stem cells. A bone graft matrix and bone marrow aspirate are placed into a concentrator. The aspirate is drawn through the graft material, selectively concentrating the osteoprogenitor cells on the matrix. The cell laden matrix can be removed from the concentrator and then implanted to promote bone healing.

70–90%. These parameters include the flow rate of the marrow through the matrix, the direction of the flow, the number of flow cycles, and the type of flow (i.e., turbulent versus steady). Grafts prepared using the selective retention technology have been shown to be highly osteogenic in a variety of in vivo models, as described below.

For instance, Takigami et al. [35] used the selective cell retention technique to capture the osteoprogenitor cells on a bed of DBM powder. Using this cell-enhanced mixture of allograft, they were able to reproducibly obtain spine fusion in a canine model. The results were comparable to those achieved with autograft alone and significantly better than that observed with allograft alone or allograft mixed with whole marrow [35].

Initial clinical results in interbody spine fusion and long bone defect repair using this technique at the Cleveland Clinic Foundation have also yielded encouraging results [36,37]. While the selective cell retention method has great promise, the widespread use of this technique requires the development of standardized kits that allow easy integration into the flow and timing of the surgical procedure. Moreover, identification of substrate mixtures that provide optimal cell capture, orientation, and presentation to the stimulatory signals could transform the way we think about, and practice, the art of bone grafting [35].

Recently, we have evaluated the efficacy of grafts prepared by the selective retention process in a critical-sized femoral defect model in large canines. The grafts were created using a matrix consisting of a mixture of allogeneic demineralized bone fibers and undemineralized cancellous bone chips (DBM-CC). The experimental group contained grafts prepared by flowing marrow through the matrix under controlled conditions that selectively retain the osteoprogenitors. To prepare 4 cc of graft material, approximately 16 cc of bone marrow was flowed through the matrix. As part of the final step of graft preparation, the concentrated osteoprogenitor-graft was clotted together with PRP (Con Osteoprogenitor-PRP). The control groups consisted of an iliac crest bone graft, allogeneic DBM-CC mixture alone or the DBM-CC mixture loaded with approximately 4 cc of whole marrow obtained via two different aspiration techniques (DBM-CC-Marrow). There was a minimum of five canines in each group. The rate and incidence of union was assessed by radiographic analysis, including plain films every 4 weeks and CT scan upon sacrifice at 16 weeks. Representative images from the autograft and the Con Osteoprogenitor-PRP group are shown in Fig. 6. In both of these groups, fusion was achieved in all animals (Fig. 7). In contrast, when the allogeneic DBM-CC mixture was used alone or in combination with native bone marrow, there was an unsatisfactory healing response, with approximately half to 67% of the canines going on to fusion respectively.

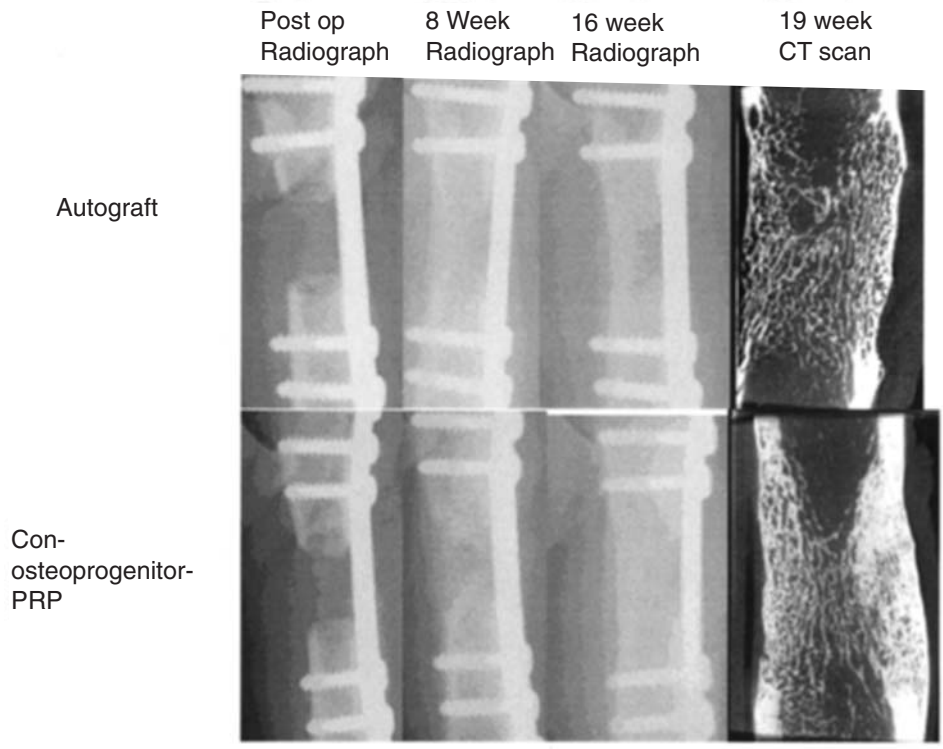

Figure 6 Results from canine femoral gap study: radiographic results from 0, 8 and 16 weeks, and CT scans from 16 week timepoints are shown. Femoral bone healing rate using a matrix with autologous platelet rich plasma and concentrated progenitor cells is similar to the femoral bone healing rate using autograft bone.

IV. AUTOLOGOUS POINT OF CARE THERAPIES IN THE SURGEON'S ARSENAL

Currently, there is a wide variety of bone grafts available to the surgeon for the repair or augmentation of bone. While the specific mode of action and intrinsic ability to form bone may be different for each of the graft materials, the underlying physiological processes that lead to bone formation are the common target. The cellular events of bone formation rely on the recruitment of osteoprogenitors to the site, followed by proliferation to increase cell number and then differentiation into osteoblasts. These differentiated cells are responsible for the synthesis of the new bone, which is then remodeled under the influence of the mechanical environment. Different graft materials function by specifically enhancing one or more of the steps in the bone formation cascade. Based on their mode of action, these grafts can be classified into the four categories summarized in Table 1.

It is important for the surgeon to understand the efficacy of each type of graft relative to other grafts. In general, osteoconductive grafts have limited potency and should be restricted to small voids or defects when used alone. Osteoinductive grafts have a wide spectrum of efficacy ranging from moderate (DBM) to high (purified or recombinant BMP). With a highly osteoinductive molecule, such as BMP-2 or BMP-7, the identification of an appropriate carrier for the delivery and presentation of the growth factor is critical. Osteopromotive grafts, such as PRP, are not used in isolation, but are typically added to the surgeon's graft of choice to improve

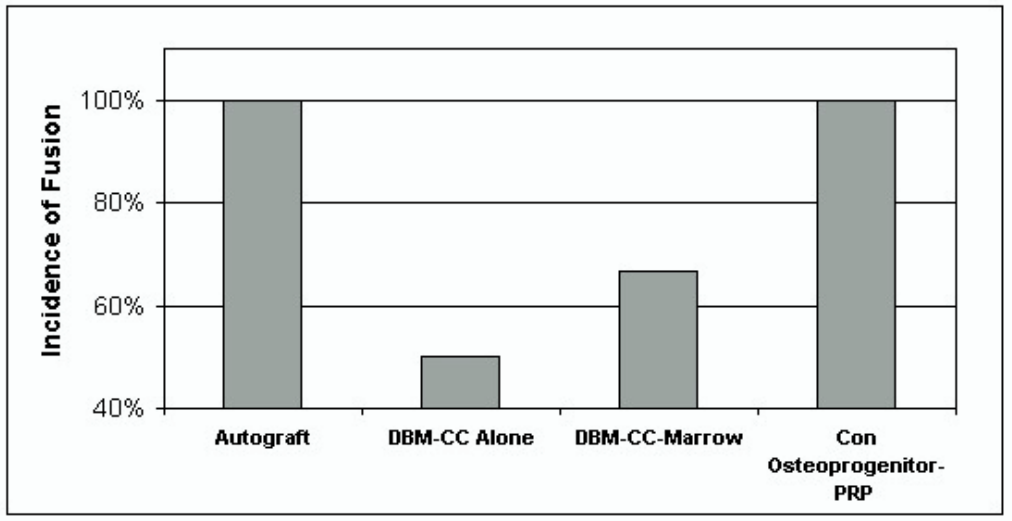

Figure 7 Summary of canine femoral gap study. 100% fusion was observed in the autograft and the graft treated with concentrated osteoprogenitor cells and platelet rich plasma.

graft handling and potentially enhance the bone-formation process. Thus, the efficacy of the combination graft containing osteopromotive material is driven, in part, by the performance characteristics of the underlying graft material. Osteogenic grafts rely on the presence of competent osteoprogenitor cells for their ability to form bone, and their efficiency is governed in part by the concentration of these cells.

In choosing the appropriate graft for the application, the surgeon has to consider a variety of factors in addition to the efficacy of the graft. These factors include morbidity to, and safety of, the patient, and the economic burden on both the patient and the health care system. The majority of the bone grafts available today rely on a single mode of action, such as potent growth factors. In humans, while some materials have been shown to be equivalent to autograft in a very narrow indication, none have been shown to be superior to autograft or as versatile as autograft. However, as our understanding of the complex phenomena of bone formation increases, potent combination grafts that are based on osteoprogenitor cells delivered on the appropriate scaffold in the presence of the proper stimulatory signals will become more widely available and, clearly, the superior alternative.

It is our view that new versatile choices for bone grafting are emerging. This new paradigm will revolutionize the field of bone regeneration by providing a family of choices for bone grafting based on an autologous biological platform. This paradigm was developed by first understanding the requirements for bone repair and regeneration and then harnessing the body's natural power to heal.

REFERENCES

1. Beutler E, Lichtman M, Coller B, Kipps T, Seligsohn U. Hematology. New York: McGraw-Hill, 2001.
2. Attawia M, Kadiyala S, Fitzgerald K, Kraus KH, Bruder SP. Cell Based Approaches for Bone Graft Substitutes. Bone Graft Substitutes. Pennsylvania: ASTM International, 2001:126–141.

3. Wang J, Davies M, Kanim L, Ukatu C, Dawson E, Lieberman JR. Prospective Comparison of Comercially Available Demineralized Bone Matrix for Spinal Fusion. San Francisco, CA: Orthopedic Research Society, 2001:276.
4. Urist MR. Bone Formation by Autoinduction. Science 1965; 150:893–899.
5. Urist MR, DeLange RJ, Finerman GAM. Bone Cell Differentiation and Growth Factors. Science 1983; 220:680–686.
6. Bentz H, Nathan RM, Rosen DM, Armstrong RM, Thompson AY, Segarini PR, Mathews MC, Dashch JR, Piez KA, S.M. S. Purification and Characterization of a Unique Osteoinductive Factor from Bovine Bone. Journal of Biological Chemistry 1989; 264:20805–20810.
7. Luyten FP, Cunningham NS, Ma S, Muthukumaran N, Hammonds RG, Nevins WB, Wood WI, Reddi AH. Purification and Partial Amino Acid Sequence of Osteogenin, a Protein Initiating Bone Differentiation. Journal of Biological Chemistry 1989; 264:13377–13380.
8. Wang EA, Rosen V, D'Alessandro , Bauduy M, Cordes P, Harada T, Israel DI, Hewick RM, Kerns KM, LaPan P, Luxenberg DP, McQuaid D, Moutsatsos IK, Nove J, Wozney JM. Recombinant Human Bone Morphogenetic Protein Induces Bone Formation. Proceedings of the National Academy of Science USA 1990; 87:2220–2224.
9. Wozney JM, Rosen V, Celeste AJ, Mitsock LM, Whitters MJ, Kriz RW, Hewick RM, Wang EA. Novel Regulators of Bone Formation: Molecular Clones and Activity. Science 1988; 242:1528–1534.
10. Lyons K, Graycar JL, Lee A, Hashami S, Lindquist PB, Chen EY, Hogan BLM, Derynck R. A Mammalian Gene Related Xenopus Vg-1 is a Member of the Transforming Growth Factor Beta Gene Superfamily. National Academy of Science USA 1989; 86:4554–4558.
11. Ozkaynak E, Rueger DC, Drier EA, Carbett C, Ridge RJ, Sampath TD, Oppermann H. OP-1 cDNA Encodes and Osteogenic Protein in the TGF beta family. EMBO (Eur. Mol. Biol. Organ.) 1990; 9: 2085–2093.
12. Wozney JM. Bone Morphogenetic Proteins. Progress of Growth Factor Research 1989; 1:267–280.
13. Damien C, Grob D, Boden S, Benedict J. Purified Bovine BMP Extract and Collagen for Spine Arthrodesis: Preclinical Safety and Efficacy. Spine 2002; 27:S50–58.
14. Gupta AR, Shah NR, Patel TC, Grauer JN. Perioperative and Long-Term Complications of Iliac Crest Bone Graft Harvesting for Spinal Surgery: A Quantitative Review of Literature. International Medical Journal 2001; 8:163–166.
15. Chapman MW, Younger EM. Morbidity at Bone Graft Donor Sites. Journal of Orthopaedic Trauma 1989; 3:192–195.
16. Goujon E. Recherches experimentals sur les proprietes physilogiques de la moelle des os. Journal de l'Anatomie et de Physiologic Normals et Pathologiques de l'Homme et des Animaux 1869; 6: 399.
17. Bruder SP, Jaiswal N, Haynesworth SE. Growth Kinetics, Self Renewal and the Osteogenic Potential of Purified Human Mesenchymal Stem Cells During Extensive Subcultivation and Following Cryopreservation. Journal of Cellular Biochemistry 1997; 64:278–294.
18. Kevy SV, Jacobson MS, Blasetti L, Fagnant A. Preparation of Growth Factor Enriched Autologous Platelet Gel. Vol. XXIV. St. Paul, Minnesota: Society for Biomaterials, 2001:262.
19. Wergedal JE, Mohan S, Lundy M, Baylink DJ. Skeletal Growth Factor and Growth Factors Known to be Present in Bone Matrix Stimulate Proliferation and Protein Synthesis in Human Bone Cells. Journal of Bone Mineral Research 1990; 5:179–186.
20. Cho M, Lin W, RJ G. Platelet-derived growth factor-modulated guided tissue regenerative therapy. Journal Periodontol 1995; 66:522–530.
21. Stephan C, Brock T. Vascular Endothelial Growth Factor, a Multifunctional Polypeptide. P R Health Sci J 1996; 15:169–178.
22. Haynesworth SE, Kadiyala S, Liang L-N, Thomas T, Bruder SP. Chemotactic and Mitogenic Stimulation of Human Mesenchymal Stem Cells by Platelet Rich Plasma Suggests a Mechanism for Enhancement of Bone Repair. Vol. 27. Dallas, TX: Orthopaedic Research Society, and Society for Biomaterials, 2002:462.
23. Slater M, Patava J, Kingham K, Mason R. Involvement of Platelets in Stimulating Osteogenic Activity. Journal of Orthopaedic Research 1995; 13:655–663.

24. Sethi P, Miranda J, Grauer JN, Fridlaender S, Kadiyala S, Patel TC. The use of Platelet Concentrate in Poterolateral Fusion. Biomechanical and Histologc Analysis. Edinburgh, Scotland: International Society for the Study of the Lumbar Spine, 2001:27.
25. Whitman DH, Berry RL, Green DM. Platelet gel: An Autologous Alternative to Fibrin Glue with Applicaitons in Oral and Maxillofacial Surfery. Journal of Oral Maxillofacial Surgery 1997; 55: 1294–1299.
26. Marx RE, Carlson ER, Eichstaedt RM, Schimmele SR, Strauss JE, Georgeff KR. Platelet Rich Plasma. Growth Factor Enhancement for Bone Grafts. Oral Surg Oral Med Oral Pathol Oral Radiol Endod 1998; 85:638–46.
27. Weiner B, Walker M, McCulloch J. Do Autologous Growth Factors Inhibit Lumbar Intertransverse Fusions?. Toronto, ON: International Society for the Study of the Lumbar Spine, 2002:127.
28. Edwards S, Hendrix R, Schafer M, Daryko G, Delbridge E. Radiographic Assessment of Posterolateral Spine Fusion With and Without Platelet Rich Plasma. Vancouver, BC: International Society for the Study of the Lumbar Spine, 2003:117.
29. Kevy SV, Jacobson MS, Lazar MD. Autologous Platelet Gel-Theory and Practice. Wisconsin Dells, WI: Wisconsin Perfusion Society, 2003.
30. Kadiyala S, Jaiswal N, Bruder SP. Culture-expanded, Bone Marrow-derived Mesenchymal Stem Cells Can Regenerate a Critical-Sized Segmental Bone Defect. Tissue Engineering 1997; 3:173–185.
31. Bruder SP, Kraus KH, Goldberg VM, Kadiyala S. The Effect of Implants Loaded with Autologous Mesenchymal Stem Cells on the Healing of Canine Segmental Bone Defects. Journal of Bone Joint Surgery 1998; 80A:985–99.
32. Kraus KH, Kadiyala S, Wotton HM, Kurth A, Shea M, Hannan M, Hayes WC, Kirker-Head CA, Bruder SP. Criticaly Sized Osteo-Periosteal Femoral Defects: A Dog Model. Journal of Investigative Surgery 1999; 12:115–124.
33. Bruder SP. Bone Regeneration: From Embryonic Chicks to Human Clinical Therapy. Vol. 52. San Antonio, TX: Association of Bone and Joint Surgeons, 2002:26.
34. Muschler GF, Boehm C, Easley K. Aspiration to Obtain Osteoblast Progenitor Cells from Human Bone Marrow. The Influence of Aspiration Volume. The Journal of Bone Joint Surgery 1997; 79-A:1699–1709.
35. Takigami H, Muschler GF, Matsukura Y, Boehm C, Valdevit A, Kambic H, Davros W, Powell K, Easley K. Spine Fusion Using Allograft Bone Matrix Enriched in Bone Marrow Cells and Connective Tissue Progenitors. Vol. 27. Dallas, TX: Orthopaedic Research Society, 2002:807.
36. Takigami H, Matsukura Y, Muschler GF. Osteoprogenitor Cell Enriched Bone Grafts Prepared Using Selective Cell Retention Technology: Clinical Application in Four Patients. Unpublished Data, 2003.
37. Lieberman IH, Reinhardt MK, Fleming J, Muschler GF. A Bone Marrow-Augmented Graft Prepared Using Selective Cell Retention Technology Provides an Effective Alternative to Iliac Crest Autograft: A Report of Two Spine Fusion Cases. Unpublished Data, 2003.

28

Process of Lumbar Spinal Degeneration: Interrelationships Between Disc Degeneration and Facet Joint Osteoarthritis

Yuichi Kasai, Kenji Takegami, Koichiro Morishita, and Atsumasa Uchida
Mie University Faculty of Medicine
Tsu, Mie, Japan

I. INTRODUCTION

The intervertebral disc and facet joints form the functional spinal unit, and disc degeneration and facet joint osteoarthritis play an important role in spinal degeneration [1–4]. Animal and clinical studies have demonstrated that lumbar spinal degeneration begins with degeneration of the intervertebral disc, and after a sufficient period of time osteoarthritis of the facet joints develops [5–7]. Although degenerative changes gradually progress with aging in both discs and facet joints [8], degenerative changes do not follow an identical course in all individuals. In order to determine the details of lumbar spinal degeneration, the present study utilized magnetic resonance imaging (MRI) and computed tomography (CT) findings to evaluate interrelationships between disc degeneration and osteoarthritis of facet joints. Two possible processes in lumbar spinal degeneration were identified.

II. SUBJECTS AND METHODS

Subjects comprised 97 patients (51 males, 46 females) who underwent surgery in our department for lumbar spinal stenosis, spondylolisthesis of the lumbar spine, or lumbar instability between 1995 and 2001, for whom MRI and CT images were obtained. Mean age at surgery was 66.5 years (range 39–92 years). All cases underwent decompression and fusion at L4–L5, L5–S1, or both levels.

For evaluation of intervertebral disc degeneration, Gibson's classification [9] on MRI is well known and Pathria's classifications [10] have been used for evaluation of osteoarthritis of the facet joints on CT. However, degenerative changes in the subjects of the present study had progressed so far that it was difficult to use the above-mentioned classifications to evaluate both discs and facet joints. We therefore evaluated disc degeneration and osteoarthritis of facet joints using the methods described below. For assessment of disc degeneration, those with hyperintensity in the nucleus pulposus at the most degenerated level (L4–L5 or L5–S1) on T2-weighted MRI image were classified as D(−), while those without this hyperintensity were classified as D(+) (Fig. 1). For osteoarthritis of facet joints, patients with remnant facet joint space at the

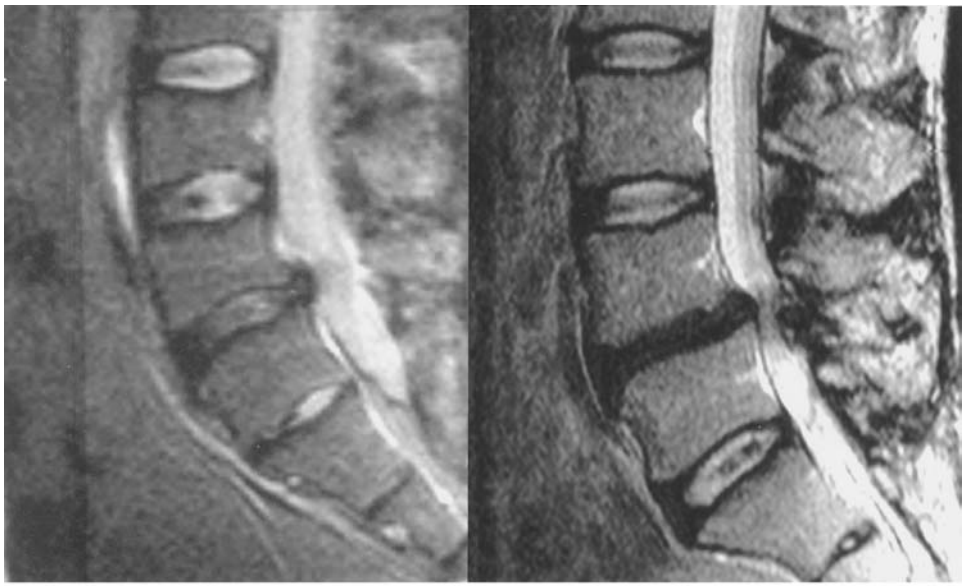

Figure 1 Evaluation of intervertebral disc degeneration (a): D(−); (b): D(+)

most degenerated level on lumbar CT images were classified as F(−), while those with complete or near-complete obliteration of facet joint space were classified as F(+) (Fig. 2).

The MRI device used was a 1.5 T unit (General Electric). T2 images were obtained according to the gradient echo method under the following conditions: echo time, 13 ms; repetition time, 200 ms; slice thickness on sagittal plane, 5 mm; and number of slices, 7. Degree of disc degeneration and osteoarthritis of facet joints was assessed by two of the authors (K.T. and K.M.). The coincidence rate of their assessment was 97.9% for both degree of disc degeneration and osteoarthritis of the facet joints, demonstrating extremely high interjudge reliability.

The following parameters were investigated in each subject: (1) age at operation, (2) sex, (3) body weight, (4) history of heavy labor, (5) history of participation in contact sports, and (6) present history of arthralgia of the extremities. Subjects were divided into the following four groups, and results of above parameters were compared among groups:

D(−)F(−) group: less severe disc degeneration and less severe facet joint osteoarthritis ($n = 12$, Fig. 3);

D(−)F(+) group: less severe disc degeneration and severe facet joint osteoarthritis ($n = 33$, Fig. 4);

D(+)F(−) group: severe disc degeneration but less severe facet joint osteoarthritis ($n = 5$, Fig. 5); and

D(+)F(+) group: severe disc degeneration and severe facet joint osteoarthritis ($n = 47$, Fig. 6).

Data were analyzed using the *t*-test and chi-square test, with the level of statistical significance set at $p < 0.05$.

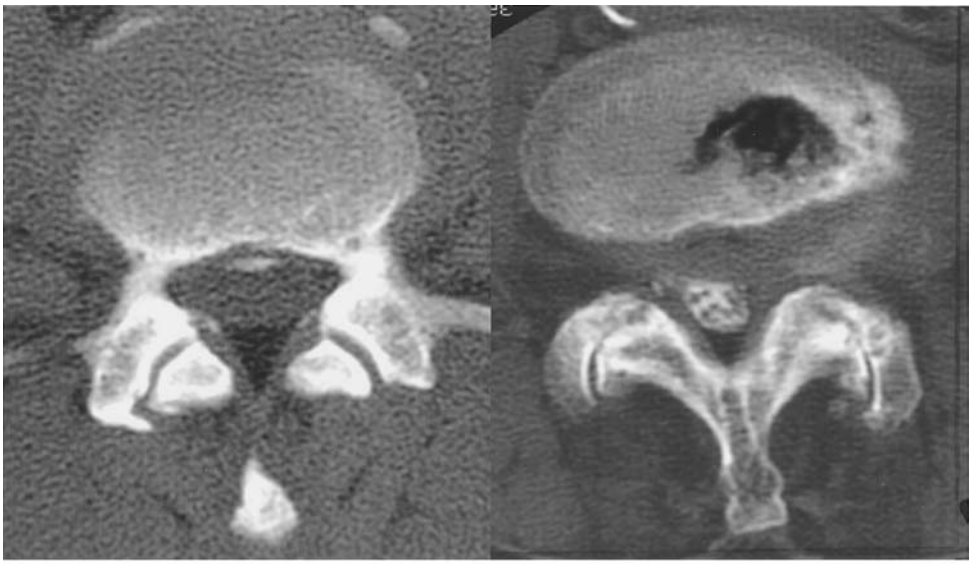

Figure 2 Evaluation of facet joint osteoarthritis (a): F(−); (b): F(+).

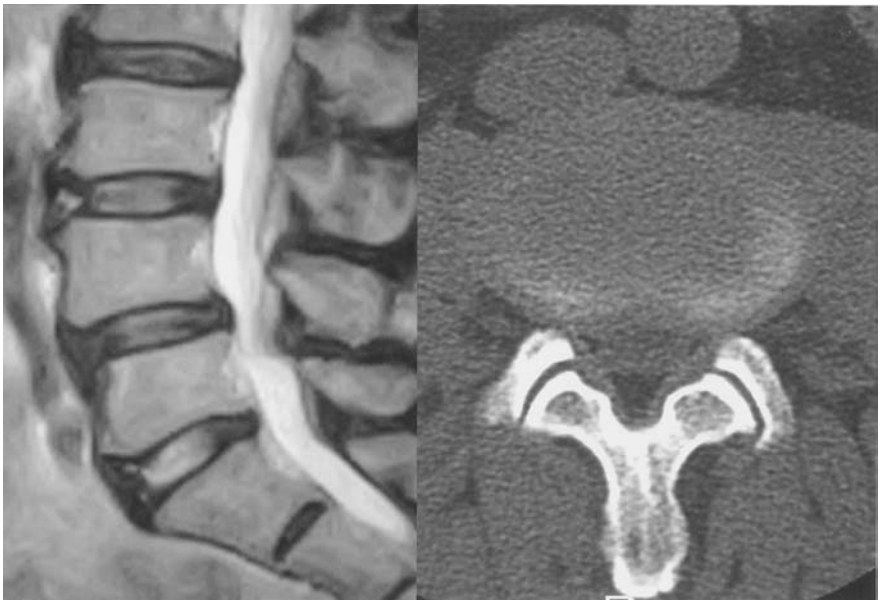

Figure 3 D(−)F(−)group: less severe disc degeneration and less severe facet joint osteoarthritis.

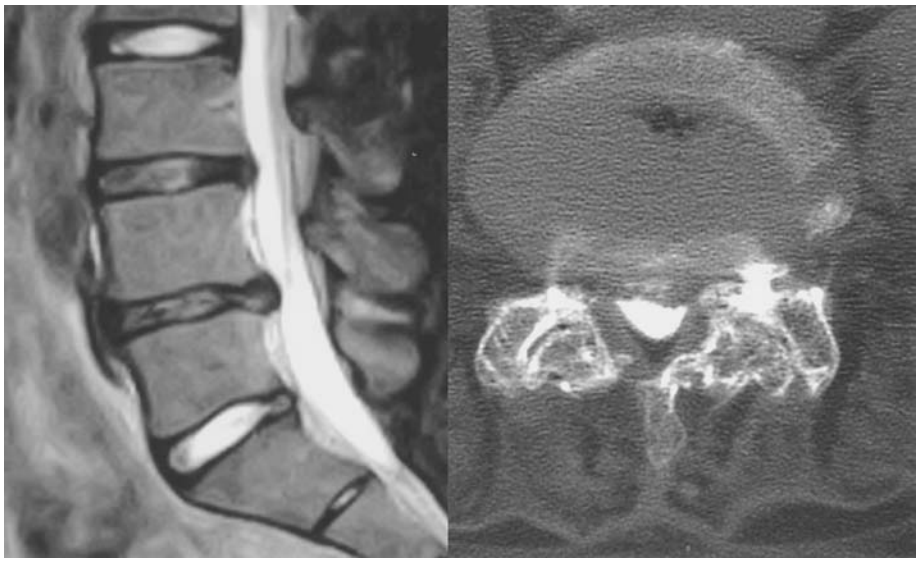

Figure 4 D(−)F(+)group: less severe disc degeneration and severe facet joint osteoarthritis.

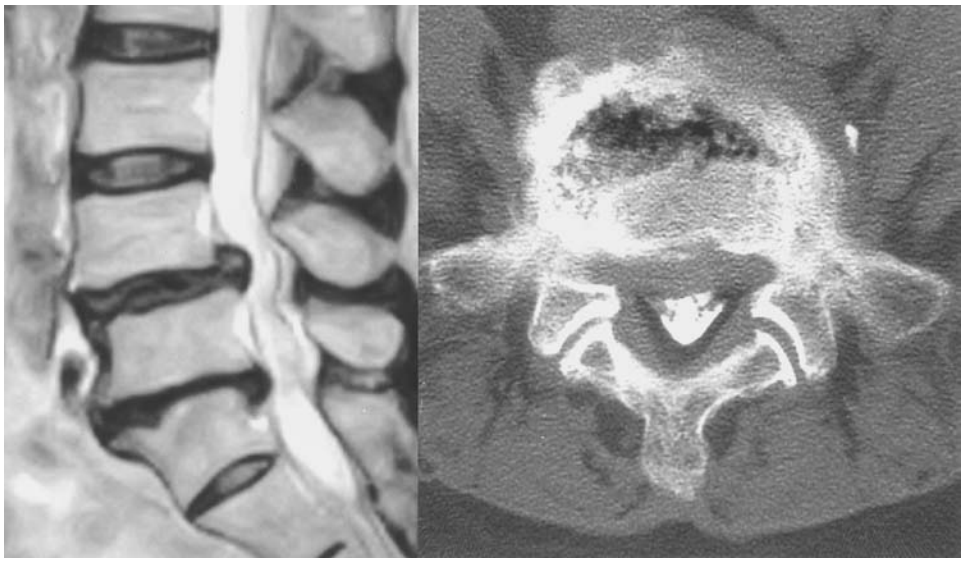

Figure 5 D(+)F(−)group: severe disc degeneration and less severe facet joint osteoarthritis.

III. RESULTS

As shown in Table 1, the subjects in the D(−)F(−) group were significantly younger at surgery than those in other groups ($p < 0.01$), while subjects in the D(−)F(+) and D(+)F(+) groups were significantly older than those of the other groups ($p < 0.05$). The proportion of males was significantly higher in the D(−)F(+) group ($p < 0.01$). No significant differences among groups

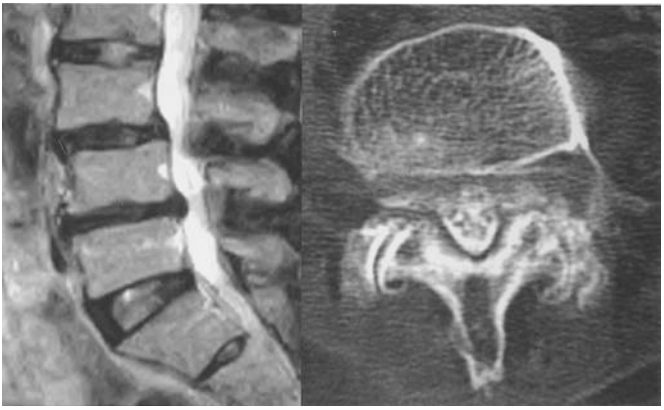

Figure 6 D(+)F(+)group: severe disc degeneration and severe facet joint osteoarthritis.

were observed in body weight or history of heavy labor or contact sports. Painful arthralgia of the extremities was observed in 20 of the 33 subjects (69.7%) in the D(−)F(+) group, and this frequency was significantly higher than that of the other groups ($p < 0.01$).

IV. DISCUSSION

The intervertebral disc and a pair of right and left facet joints are involved in lumbar spinal degeneration. Changes due to disc degeneration include torn annulus fibrosus, necrosis of chondrocytes, and decreased water content, while changes due to degeneration of the facet joints include disappearance of articular cartilage, hardened subchondral bone, and spur formation. Proposed risk factors for disc degeneration include aging, dynamic stress, and genetic predisposition, while proposed risk factors for osteoarthritis of the facet joints include anatomical abnormalities of the facet joints such as increased facet angle and tropism [11,12].

In the present study, both the D(−)F(+) (less severe disc degeneration and severe facet joint osteoarthritis) and D(+)F(−) (severe disc degeneration and less severe facet joint osteoarthritis) groups were represented, indicating that the process of degeneration of the disc and facet

Table 1 Characteristics of Surgical Subjects

	D(−)F(−) ($N = 12$)	D(−)F(+) ($N = 33$)	D(+)F(−) ($N = 5$)	D(+)F(+) ($N = 47$)
Mean age at operation, y	51.2	66.6	61.9	67.5
Sex				
male	4	25	2	20
female	8	8	3	27
Mean body weight, kg	60.2	62.5	60.5	61.7
History of heavy labor	3 (25.0%)	8 (24.2%)	1 (20.0%)	12 (25.5%)
History of participation in contact sports	2 (16.7%)	7 (21.2%)	1 (20.0%)	11 (23.4%)
Present history of arthralgia of the extremities	2 (16.7%)	23 (69.7%)	1 (20.0%)	14 (29.8%)

joints varies among individuals and that a single all-encompassing process does not exist. Vernon-Roberts and Pirie [13] examined the lumbar spine in more than 100 human cadavers and reported that in some cases the structure of intervertebral discs was sufficiently maintained despite severe degeneration of the facet joints.

In the main progressive pathway of degenerative change, D(−)F(−) progresses to D(+)F(+) via D(+)F(−). In the present study, it is of great interest that the mean age of the D(−)F(+) and D(+)F(+) groups was almost identical, at 66.6 and 67.5 years, respectively. The number of patients in the D(−)F(+) and D(+)F(+) groups was large, and we assumed that the end phases of degenerative change in the lumbar spine were represented by both D(−)F(+) and D(+)F(+) criteria. We therefore speculate that two processes of lumbar spinal degeneration may exist (Fig. 7), comprising a main process, in which both disc degeneration and osteoarthritis of the facet joints is severe (primarily in females), and another process in which osteoarthritis of the facet joints is severe despite less severe disc degeneration (primarily in males).

Postmortem and radiographic studies have indicated no difference in gender distribution in facet joint osteoarthritis and the process of lumbar spinal degeneration. We therefore performed an animal study to measure the hardness of the discs in rats according to sex and found that discs were significantly softer in females than in males [14]. Although this result cannot be directly applied to human beings, if the discs are also softer in human females than males, such a dynamic characteristic may result in a gender difference in the processes of lumbar spinal degeneration. Fujiwara et al. [15] performed bioengineering experiments using 110 spinal motion segments obtained from human cadavers and reported that the range of motion was significantly larger in females than males. This result indicates that the spine is more flexible in females, and this flexibility may promote disc degeneration. Moreover, this dynamic characteristic is considered to contribute to the clinical observation that idiopathic scoliosis, lumbar degenerative scoliosis, and degenerative spondylolisthesis of the lumbar spine occur more frequently in females than males, in addition to the pathology of spinal diseases.

In comparison with the two processes of lumbar spinal degeneration mentioned above, we performed hematological tests including parathyroid hormone, sexual hormone, growth hormone, blood glucose, serum calcium, phosphorus level, and alkaline phosphatase, in addition to plain radiography of the knee joint for 10 males each of the D(−)F(+) and D(+)F(+) groups. However, hematological findings and plain x-rays of the knee joint were not significantly different between the two groups, and thus the reasons for differences between the D(−)F(+) and D(+)F(+) groups remain unknown. Further studies of more cases and with longer follow-up are required to elucidate the process of lumbar spinal degeneration.

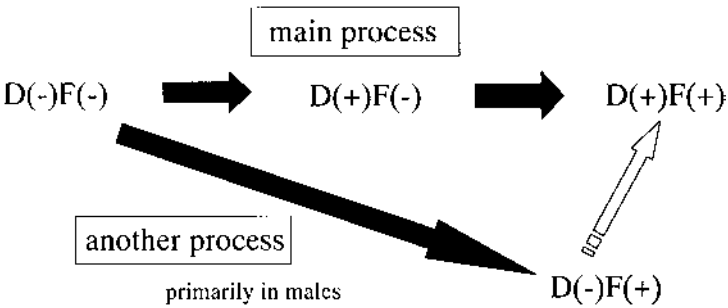

Figure 7 Two processes of lumbar spinal degeneration.

V. CONCLUSION

Two types of lumbar spinal degeneration processes were identified: cases with severe disc degeneration and osteoarthritis of facet joints and those with osteoarthritis of the facet joints despite less severe disc degeneration. Most of the latter cases were males and were accompanied by painful arthralgia of the extremities.

REFERENCES

1. Videman T, Battie MC, Gill K, Manninen H, Gibbons LE, Fisher LD. Magnetic resonance imaging findings and their relationships in the thoracic and lumbar spine; insight into the etiopathogenesis of spinal degeneration. Spine 1995; 20:928–935.
2. Lewin T. Osteoarthritis in lumbar synovial joints. Acta. Orthop. Scand 1964; 73:1–111.
3. Oegema TR, Bradford DS. The inter-relationship of facet joint osteoarthritis and degenerative disc disease. Br. J. Rheumatol 1991; 30:16–20.
4. Dunlop RB, Adams MA, Hutton WC. Disc space narrowing and the lumbar facet joints. J.Bone Joint Surg 1984; 66-B:706–710.
5. Fujiwara A, Tamai K, Yamato M, An H, Yoshida H, Saotome K, Kurihashi A. The relationship between facet joint osteoarthritis and disc degeneration of the lumbar spine: an MRI study. Eur. Spine J 1999; 8:396–401.
6. Moore RJ, Crotti TN, Osti OL, Fraser RD, Vernon-Roberts B. Osteoarthritis of the facet joints resulting from anular rim lesions in sheep lumbar discs. Spine 1999; 24:519–525.
7. Butler D, Trafimow JH, Andersson GB, McNeill TW, Huckman MS. Discs degenerate before facets. Spine 1990; 15:111–113.
8. Miller JAA, Schmatz C, Schultz AB. Lumbar disc degeneration: correlation with age, sex, and spine level in 600 autopsy specimens. Spine 1988; 13:173–178.
9. Gibson MJ, Buckley J, Mawhinney R, Mulholland RC, Worthington BS. Magnetic resonance imaging and discography in the diagnosis of disc degeneration. A comparative study of 50 discs. J. Bone J. Surg 1986; 68-B:369–373.
10. Pathria M, Sartoris DJ, Resnick D. Osteoarthritis of the facet joints: accuracy of oblique radiographic assessment. Radiology 1987; 164:227–230.
11. Riew KD, Yamaguchi K, Branch TP, Schellinger D, Wiesel SW. Orientation of the lumbar facet joints: association with degenerative disc disease. J. Bone J. Surg 1996; 78-A:403–411.
12. Vanharanta H, Floyd T, Ohnmeiss DD, Hochschuler SH, Guyer RD. The relationship of facet tropism to degenerative disc disease. Spine 1993; 18:1000–1005.
13. Vernon-Roberts B, Pirie CJ. Degenerative changes in the intervertebral discs of the lumbar spine and their sequelae. Reumatol. Rehab 1977; 16:13–21.
14. Kasai Y, Ikemura S, Takegami K, Uchida A. Hardness of lumbar intervertebral disc in rats: influence of aging and sex. Seikeigeka 2002; 53:576–577. (in Japanese).
15. Fujiwara A, Lim TH, An HS, Tanaka N, Jeon CH, Andersson GB, Haughton VM. The effect of disc degeneration and facet joint osteoarthritis on the segmental flexibility of the lumbar spine. Spine 2000; 25:3036–3044.

29

Relationships Between Lumbar Sagittal Alignment and Clinical Outcomes After Decompression and Posterolateral Spinal Fusion for Degenerative Spondylolisthesis

Mamoru Kawakami and Tetsuya Tamaki
Wakayama Medical University
Wakayama City, Wakayama, Japan

I. INTRODUCTION

Degenerative lumbar spondylolisthesis is a common condition of the aging spine. The clinical presentation of patients is one of a long history of low back pain with insidious onset of radicular leg pain and/or neurogenic claudication. This condition is recognized as the classic example of chronic lumbar instability [1]. However, the selection of surgical methods for patients with degenerative lumbar spondylolisthesis is still controversial. Although decompression without spinal fusion has yielded good results [2–4], the indication for posterior decompression alone is limited in some, but not all, patients with degenerative lumbar spondylolisthesis. That is, according to the mobility of the level with spondylolisthesis, severity of stenosis, and method of decompression, the appropriate operative methods need to be selected for patients with degenerative lumbar spondylolisthesis. Herkowitz and Kurz [5] reported, in a randomized and prospective study, that 25 patients treated with laminectomy and posterolateral spinal fusion had good clinical outcomes at 3 years mean follow-up, compared with those seen in 25 patients treated with laminectomy alone. Therefore, decompression and spinal fusion are thought to be effective for patients with degenerative lumbar spondylolisthesis.

We have evaluated as spinal instability if patients have more than 3 mm of sagittal translation and/or more than 15° of rotational instability at the segment of the spondylolisthesis in flexion and extension radiographs [2] taken in the standing position. We have also evaluated improvement of clinical symptoms after external fixation with cast or hard corset and finally decided whether to perform spinal fusion. In addition, we have used spinal instrumentation surgery for patients who have degenerative lumbar spine and instability with kyphosis of the relevant segments on the upright-standing radiographs and who were considered unable to undergo strict postoperative treatments such as bedrest and external fixation with cast and/or corset. According to our strategy for patients with spinal instability, we have evaluated patients with degenerative lumbar spondylolisthesis, in which the segment of slippage has instability radiologically, and we have treated with laminectomy and posterolateral spinal fusion.

The clinical outcomes of decompression and posterolateral spinal fusion for patients with degenerative lumbar spondylolisthesis may be influenced by a variety of pathophysiological

factors. These are thought to include residual compression of the neural tissues and recurrence of spinal canal stenosis, instability, deterioration of spondylolisthesis, lumbar kyphosis, nonunion, disturbance of adjacent segments, and irreversible changes to the nerve root or cauda equina.

Many reports described the surgical outcomes for patients with degenerative lumbar spondylolisthesis. Postoperative slippage and kyphosis at the operated levels have been used for the radiological evaluation of lumbar sagittal alignment [3,4,6–9]. However, little is known about whether the sagittal vertical axis influences the clinical outcomes in cases of degenerative lumbar spondylolisthesis, as measured by low back pain and neurogenic functions.

II. EVALUATION OF LUMBAR SAGITTAL BALANCE

As an index for the radiological evaluation of lumbar sagittal alignment we have used the L1 axis S1 distance (LASD)—the horizontal distance from the plumb line of the center in the first lumbar vertebral body (L1) to the back corner of the first sacral vertebral body (S1) (Fig. 1) [10–13]. This was measured on lateral x-rays of patients in a neutral standing position. The C7 plumb line has been used as the axis of loading in a lateral standing view [14,15]. Jackson and McManus [15] found that a plumb line dropped vertically from the center of C7 tended to transect the L1 vertebral body more frequently in patients with low back pain and the L1–L2 disc more frequently in healthy volunteers. The LASD, which is measured with a plumb line dropped from the center of L1 body and used as an index of lumbar sagittal balance, is thought to reflect the axis of loading.

III. PATIENTS AND METHODS

Fifty-three patients who underwent posterolateral spinal fusion for degenerative lumbar spondylolisthesis at our hospital were retrospectively reviewed. All patients had more than 3 mm of the vertebral body slippage in plain lateral radiographs taken in the neutral standing position and spinal instability described above. There were 16 men and 37 women, ranging in age from 41 to 79 years, with a mean age of 62.7 years. Nine, 28, and 16 patients had radiculopathy, symptoms of the cauda equina, and combined symptoms thereof, respectively. Spondylolisthesis was at level L4 in 44 patients, L3 in eight patients, and at L5 in one. Twenty-five and 28 patients underwent laminectomy and fenestration, respectively. Posterolateral spinal fusion was performed at one level in 39 patients, two levels in 11 patients, and three levels in 3 patients. Autologous bone grafts were obtained from the posterior iliac crest. Twenty-nine patients underwent arthrodesis with spinal instrumentation using the Texas Scottish Rite Hospital (TSRH) pedicular screw system (Sofamor Danek, Memphis, TN). During surgery, the patients were kept in the prone position on a U-shaped mat, and in situ internal fixation was performed without intentional reduction of the slippage. The mean duration of symptoms before surgery was 2.2 years (range 3 months to 10 years), and patients were followed for an average of 3.4 years (range 2–7 years).

The severity of low back pain was evaluated using a visual analog pain scale. The respective evaluation scores for lumbar lesions were assessed using those proposed by the Japanese Orthopedic Association (JOA score), (Table 1) [16]. Recovery rate was evaluated using Hirabayashi's method [17]. Slippage, LASD, lumbar lordosis, lordosis at the fused segment, bony union at the surgically managed segments, and disturbance of adjacent segments including instability and progressive loss of disc height loss were assessed clinically and radiologically [13].

Lateral radiographs of the lumbar spine used to measure the LASD were taken with patients in a relaxed standing position, their shoulders elevated at 45° anteriorly [10–13]. The distance

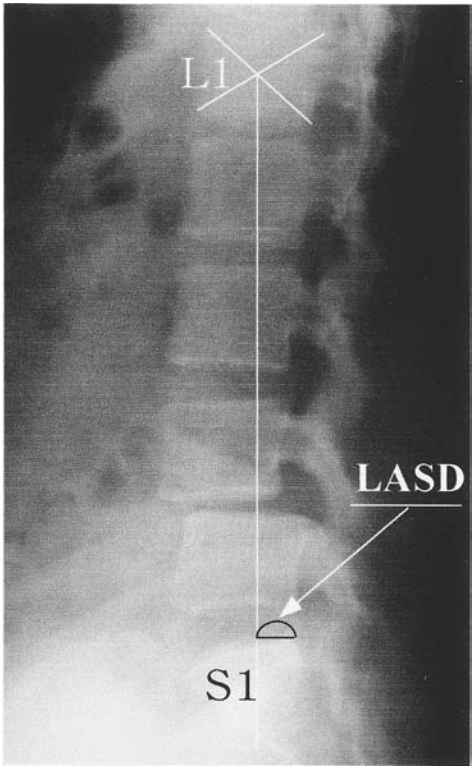

Figure 1 The L1 axis S1 distance (LASD): the horizontal distance from the L1 plumb line to the back corner of the S1 body, as observed on a lateral x-ray taken with the patient in the neutral standing position. (From Refs. 10–13.)

between lines on the posterior wall of the upper and lower vertebral bodies, at the level of spondylolisthesis, was measured as slippage in millimeters. Lumbar lordosis at L1 and S1 and lordosis at fused segments were measured by Cobb's method. A solid union of posterolateral spinal fusion was determined when the grafted bone was continuous on the transverse processes and when the intervertebral bodies at the fused segments were not shifted in superimposed lateral radiographs of the lumbar spine in flexion and extension with the patient in the standing position at follow-up assessment. Disturbance of adjacent segments after surgery was defined as instability or decreases in the height of the intervertebral disc space observed at follow-up assessment [10–13].

Two examiners judged the results of the imaging examinations. If their judgments differed, reevaluation by the two examiners was performed at the same time until they reached agreement. In the previous study, which evaluated surgical outcomes after posterolateral spinal fusion for an unstable lumbar spine, the findings showed that patients with more than 35 mm of LASD had greater slippage during the follow-up period [11,12]. Therefore, patients with degenerative lumbar spondylolisthesis were divided into two groups according to the LASD value and the changes in slippage during the follow-up period: the patients with LASD $>$ 35 mm (Group A) and those with $<$ 35 mm (Group B). Patients in Group A were divided into two subgroups: patients with in situ fusion (Group A1) and patients with reduced slippage (Group A2). Radiological factors and clinical outcomes were compared among these groups using statistical analysis.

Table 1 Japanese Orthopedic Association Scoring System for Treatment of Low Back Pain

Items			Score
Subjective symptoms	Low back pain (3 points)	None	3
		Occasional mild pain	2
		Frequent mild or occasional severe pain	1
		Continuous severe pain	0
	Leg pain and/or tingling (3 points)	None	3
		Occasional mild symptoms	2
		Frequent mild or occasional severe symptom	1
		Continuous severe symptom	0
	Gait (3 points)	Normal	3
		Able to walk father than 500 m although it results in pain, tingling, and/or muscle weakness	2
		Unable to walk father than 500 m owing to pain, tingling, and/or muscle weakness	1
		Unable to walk father than 100 m owing to pain, tingling, and/or muscle weakness	0
Objective symptoms	Straight leg raising test (2 points)	Normal	2
		30–70 degrees	1
		Less than 30 degrees	0
	Sensory abnormality (2 points)	No r mal	2
		Mild disturbance (not subjective)	1
		Marked disturbance	0
	Motor disturbance (MMT) (2 points)	Normal (Grade 5)	2
		Slight weakness (Grade 4)	1
		Marked weakness (Grade 3–0)	0
Restriction of ADL (14 points)	Turn over while lying Standing Washing Leaning forward Sitting (about 1 hour) Lifting or holding heavy objects Walking	No restriction Moderate restriction Severe restriction	2 1 0
Urinary bladder function (−6 points)		Normal	0
		Mild dysuria	−3
		Severe dysuria	−6
Total score			29

Recovery rate = (Final score – Preoperative score)/(29 – Preoperative score) × 100(%) (Hirabayashi's method); ADL = activities of daily living.
Source: Refs. 13, 16, 17.

IV. RESULTS

The JOA scores were 12.3 ± 5.1 preoperatively and 22.3 ± 4.7 at follow-up assessment. The recovery rate was 57.1 ± 26.3%. No significant difference could be detected in relationships among preoperative slippage (5.9 ± 5.2 mm), lumbar lordosis (35.3 ± 14.8°), lordosis at the fused segments (9.0 ± 8.2°), and recovery rates.

There were 19 patients classified into Group A and 34 into Group B. No significant differences were found between the groups in terms of age at surgery, gender, duration of symptoms before surgery, preoperative JOA score, methods of decompression, number of fused segments, or supplementation with spinal instrumentation. However, there was a negative correlation between preoperative LASD and recovery rate. Recovery rates were 42.8 ± 36.1% and 63.2 ± 23.8% in groups A and B, respectively ($p < 0.05$). Although there were no significant correlations among lumbar lordosis (35.7 ± 12.1°), LASD (20.4 ± 32.4 mm), slippage (4.5 ± 5.4 mm), and recovery rates at follow-up, there was a positive correlation between lordosis at the fused segments and recovery rates ($p = 0.01$) (Fig. 2).

Nine, 10, and 34 patients were classified in Groups A1, A2, and B, respectively. There were no statistically significant differences in age at surgery, gender, duration of symptoms before surgery, preoperative JOA score, methods of decompression, or number of fused segments (Table 2). All patients in Group A2 were treated with the TSRH pedicle screw system. The JOA scores at follow-up assessment were 18.3, 24.1, and 23.7 points in Groups A1, A2, and B, respectively. Recovery rates were 28.4, 64.4, and 62.0% in Groups A1, A2, and B, respectively. The JOA score and recovery rate at follow-up assessment in Group A1 were poorer than those in Groups A2 and B ($p < 0.05$) (Table 3). Although no difference in the prevalence of low back pain was found among Groups A1, A2, and B, the visual analog scale and JOA score

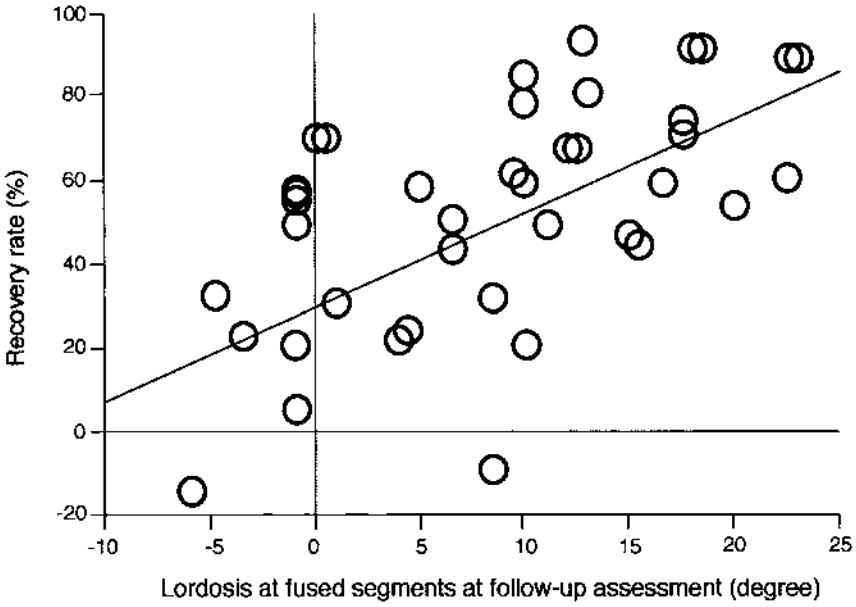

Figure 2 A positive correlation was found between lordosis at the fused segments and recovery rates ($p = 0.01$). (From Ref. 13.)

Table 2 Demographic and Surgical Data for Patients in Groups A1, A2, and B

	Group		
	A1	A2	B
Number of patients	9	10	34
Age at surgery (yr)	67.5 ± 6.4	66.3 ± 4.8	63.4 ± 9.9
Gender	Male 2, female 7	Male 2, female 8	Male 13, female 21
Duration symptoms prior to surgery (months)	41.6 ± 42.8	33.0 ± 31.8	28.2 ± 30.6
Preoperative JOA score	14.1 ± 6.3	11.7 ± 5.0	12.4 ± 5.1
Fenestration	5	5	15
Laminectomy	4	5	19
Supplementation of pedicular screw system	2	10*	17
Number of fused segments	1.3 ± 0.5	1.1 ± 0.5	1.2 ± 0.4

* $p < 0.05$.
JOA = Japanese Orthopedic Association.
Source: Ref. 13.

at follow-up assessment for low back pain in Group A1 were significantly poorer than those in Groups A2 and B (Table 4) ($p < 0.05$).

Although there were no significant differences in lumbar lordosis and preoperative lordosis at fused segments among three groups, significant lordosis at the fused segments was observed in the follow-up assessment of Group A2 as compared with that in Groups A1 and B ($p < 0.05$) (Fig. 3). Preoperative slippage was greater in Group A2 than in Groups A1 and B ($p < 0.05$) (Fig. 4). Slippage observed at follow-up assessment was greater in Group A1 than in Groups A2 and B ($p < 0.02$) (Fig. 4). Nonunion (two patients each in Groups A1 and B) and disturbance at the adjacent segments (three in Group A1, one in Group A2, and six in Group B) were not related to the clinical outcomes.

V. CONCLUSIONS

Radiological factors such as lordosis at the fused segments and LASD influence clinical outcomes after decompression and posterolateral spinal fusion for degenerative lumbar spondylolisthesis.

Table 3 Final JOA score and Recovery Rate in Groups A1, A2, and B

	Group		
	A1	A2	B
JOA score (points)	18.3 ± 6.2*	24.1 ± 6.7	23.7 ± 4.8
Recovery rate (%)	28.4 ± 29.7*	64.4 ± 33.9	62.0 ± 21.6

* $p < 0.05$.
JOA = Japanese Orthopedic Association.
Source: Ref. 13.

Table 4 Low Back Pain at Follow-Up in Groups A1, A2, and B

	Group		
	A1	A2	B
Low back pain (JOA score)	1.9*	2.6	2.4
Visual analog pain scale	3.8*	1.5	2.8
Number of patients with low back pain	8	5	20

* $p < 0.05$.
JOA = Japanese Orthopedic Association.
Source: Ref. 13.

In patients with an LASD of >35 mm, an increase in rotational or shear forces at the fused segments in the standing position may result in increased slippage and decreased lordosis for the fused segments observed at follow-up assessment. Changes in lumbar sagittal alignment, such as kyphosis and progression of the slippage, may result in poor outcomes after surgery. Our current study suggests that a sagittal vertical axis such as LASD should be considered in the choice of treatment strategy when posterolateral spinal fusion is indicated for patients with degenerative lumbar spondylolisthesis. In addition, it is possible that reduction in slippage with a pedicular screw system is useful to give improvement of clinical outcomes for patients with an LASD of >35 mm when posterolateral fusion is indicated for degenerative lumbar spondylolisthesis.

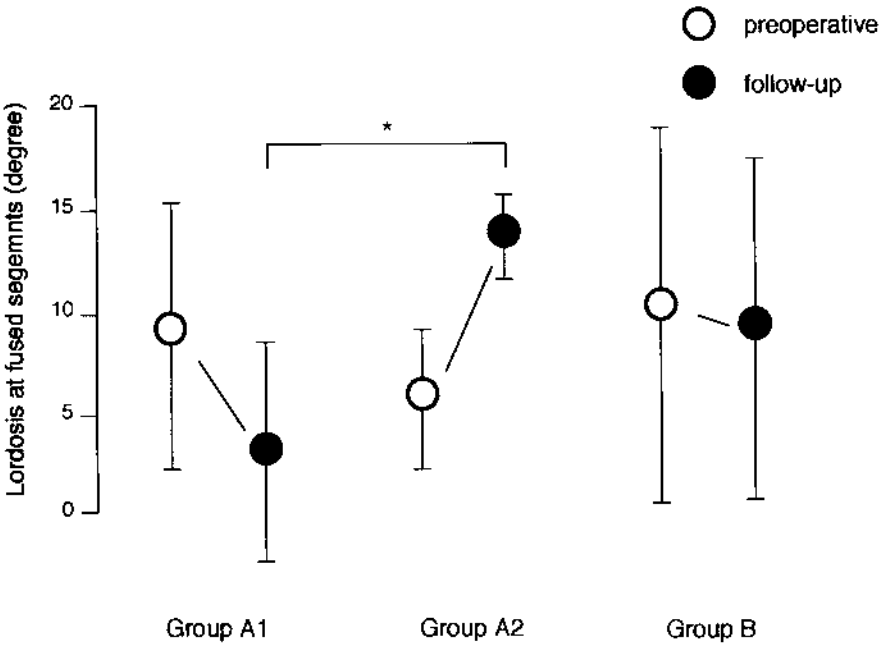

Figure 3 There was no significant difference in preoperative lordosis at the affected level among Groups A1, A2, and B. However, lordosis at fused segments in Group A2 was significantly increased at follow-up assessment, as compared with that observed in Groups A2 and B ($p < 0.05$). (From Ref. 13.)

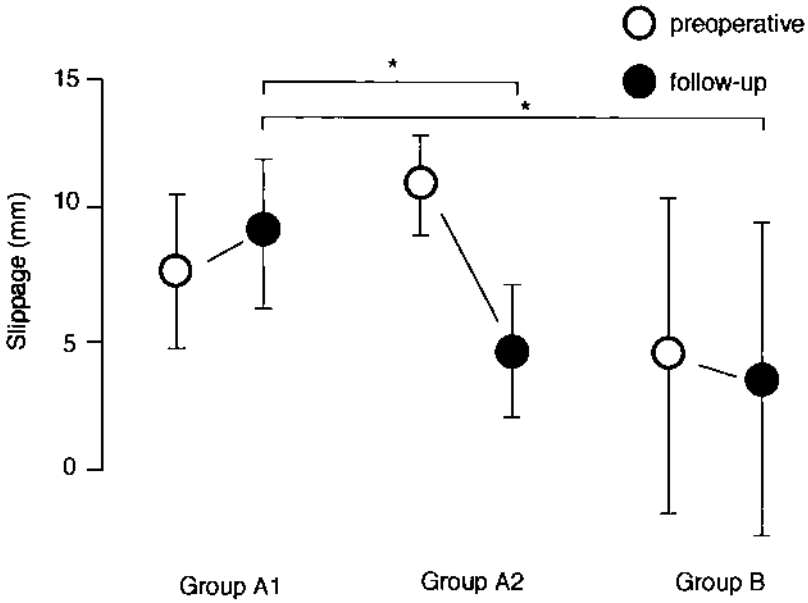

Figure 4 The preoperative slippage was greater in Group A2 than in Groups A1 and B, and slippage at follow-up assessment was greater in Group A1 than in Groups A2 and B ($p < 0.05$). (From Ref. 13.)

ACKNOWLEDGMENTS

This work was supported in part by a grant of the Research Foundation in the Department of Orthopedic Surgery, Wakayama Medical University, Wakayama, Japan.

REFERENCES

1. Lombardi JS, Wiltse LL, Reynolds J, Widell EH, Spencer C. Treatment of degenerative spondylolisthesis. Spine 1985; 10:821–827.
2. Iida Y, Kataoka O, Sho T, Sumi M, Hirose T, Bessho Y, Kobayashi D. Postoperative lumbar instability secondary to laminectomy. Rinsho Seikeigeka (Clini Orthop Surg) 1990; 25:449–453. (in Japanese).
3. Kobayashi H, Yasukawa Y, Akizuki A. Clinical results of posterolateral fusion (non instrumentation) for degenerative lumbar spondylolisthesis. Central Jpn J Orthop Traumat 1998; 41:941–942. (in Japanese).
4. Nishimura Y, Tuneoka T, Ookubo T. Long-term results of posterior decompression for degenerative spondylolisthesis. Seikei Saigai Geka 1998; 41:795–799. (in Japanese).
5. Herkowitz HN, Kurz LT. Degenerative lumbar spondylolisthesis with spinal stenosis. J Bone Joint Surg (Am) 1991; 73:802–807.
6. Sawamoto T, Yamamoto H, Tani S, Taniguchi S, Kamioka T. Results of surgical treatment with lumbar trapezoid plate for lumbar degenerative spondylolisthesis. Central Jpn J Orthop Traumat 1996; 34:77–78. (in Japanese).
7. Soshi S, Shiba R, Funasaki Y. Results of treatment for degenerative lumbar spondylolisthesis with Steffee VSP system and factors effected on correction. Rinsho Seikei Geka 1996; 31:1149–1153. (in Japanese).
8. Yamazaki T, Shimamura T, Endo K. Operative treatment for lumbar degenerative spondylolisthesis—postoperative evaluation between a group with spinal fusion and without spinal fusion. J Jpn Orthop Ass 1995; 69:S803. (in Japanese).

9. Yokoyama H, Kataoka H, Sho T. Clinical study of failed back surgery syndrome secondary to lumbar spinal canal stenosis. Rinsho Seikei Geka 1992; 27:465–471. (in Japanese).
10. Kawakami M, Tamaki T, Yoshida M, Ando M, Hayashi N, Yamada H. Radiological factors influence clinical outcomes in patients with posterolateral fusion for unstable lumbar spine. Rinsho Seikei Geka 1996; 31:1245–1252. (in Japanese).
11. Kawakami M, Tamaki T, Yoshida M, Ando M, Hayashi N, Yamada H. Lumbar complaints after posterolateral fusion in the lumbar spine. Sekitui Sekizui 1997; 10:599–604. (in Japanese).
12. Kawakami M, Tamaki T, Yoshida M, Hayashi N, Ando M, Yamada H. Radiological factors influence clinical outcomes in posterolateral fusion for unstable lumbar spine. J Musculoskeletal Res 1998; 2: 197–208.
13. Kawakami M, Tamaki T, Ando M, Yamada H, Hashizume H, Yoshida M. Lumbar sagittal balance influences the clinical outcome after decompression and posterolateral spinal fusion for degenerative lumbar spondylolisthesis. Spine 2002; 27:59–64.
14. Gelb DE, Lenke LG, Bridwell KH, Blanke K, McEnery KW. An analysis of sagittal spinal alignment in 100 asymptomatic middle and older aged volunteers. Spine 1995; 20:1351–1358.
15. Jackson RP, McManus AC. Radiographic analysis of sagittal plane alignment and balance in standing volunteers and patients with low back pain matched for age, sex, and size. Spine 1994; 19:1611–1618.
16. Yone K, Sakou T, Kawauchi Y, Yamaguchi M, Yanase M. Indication of fusion for lumbar spinal stenosis in elderly patients and its significance. Spine 1996; 21:242–248.
17. Hirabayashi K, Watanabe K, Wakano K, Suzuki N, Satomi K, Ishii Y. Expansive open-door laminoplasty for cervical spinal stenotic myelopathy. Spine 1983; 8:693–699.

30

Histological Findings in Revision Surgery of Instrumented Spine Fusion with the Use of Coralline Hydroxyapatite

Panagiotis Korovessis, Maria Repanti, and Giorgos Koureas
General Hospital Agios Andreas
Patras, Greece

I. INTRODUCTION

The rate of failure to obtain a solid spine bony fusion may be as high as 45%, and the incidence of morbidity associated with autogenous iliac crest bone graft harvest may approach 30% [1,2,12,14,19,29,31,33]. Recently, the search for acceptable bone graft substitutes has received increased attention. Ceramics, including sea coral, have been investigated as potential bone substitutes [11]. There are two primary types of coral under investigation. Natural sea coral comprised of calcium carbonate has been used in anterior and posterior spine fusions [7,15,16,23,27]. Coralline hydroxyapatite is made by a hydrothermal conversion of most of the calcium carbonate to hydroxyapatite. This converted coralline material has been used in metaphyseal bone defects, and its use in the spine has been reported anecdotally [10,17,21,22,25]. Boden et al. [8] showed in animals that healing of the intertransverse process spine fusion is considerably more challenging than in the highly vascular environment of a long bone metaphysis [2,5].

Coralline hydroxyapatite served as an excellent carrier for the bovine osteoinductive bone protein extract yielding superior results to those obtained with autograft or bone marrow [4]. When combined with autogenous iliac crest bone graft, coralline hydroxyapatite served in animal as a graft extender yielding results comparable to those obtained with autograft alone [8].

Although some surgeons are currently using coralline hydroxyapatite in patients undergoing spine fusion as a bone graft extender or substitute, there are no data to support and define the limits of use of coralline hydroxyapatite in the human spine.

The purpose of this study was to investigate histologically the incorporation of coralline hydroxyapatite in posterior and posterolateral instrumented spine fusion.

II. MATERIAL AND METHODS

Coralline hydroxyapatite (Pro Osteon 500 porous hydroxyapatite; Interpore International, Irvine, CA) was used in granules of 2–5 mm diameter. Intraoperatively, autogenous blood was taken with sponges from the bleeding operation field and was mixed with the coralline hydroxyapatite

granules and applied on the decorticated posterior spinal elements. The mixture composed of coralline hydroxyapatite and blood was applied bilaterally on the transverse processes, lamina, and spinous processes, after removal of articular cartilage of facet joints. Coralline hydroxyapatite was applied immediately after insertion of the pedicle screws and before the application of the hooks and rods, in close contact with the posterior surface of the instrumented spine, which had been previously meticulous cleaned from soft tissues and decorticated. Anteroposterior, lateral, and oblique roentgenograms of the instrumented spine were taken immediately postoperatively, 3, and 6 months postoperatively and thereafter once annually for radiographic analysis of the fusions. The radiographic analysis was performed by two unbiased observers, who rated the fusion in each particular spine from 1 to 3. During revision surgery, which was performed for different reasons (Table 1), biopsy was taken from 15 spines, which belonged to 13 patients, who had primarily received instrumented fusion with addition of coralline hydroxyapatite (Table 1). The diagnosis for primary fusion was degenerative lumbar disease, spine trauma, idiopathic scoliosis, while the material of instrumentation used was titanium alloy. The instrumentation used was CD-Horizon (Sofamor-Danek) for the thoracic and lumbar spine and Cervical Compact CD (Sofamor-Danek) for the cervical spine. The age of the patients at the time of revision surgery was 46 $\pm$ 20 years (range 16–78 years). The time lapsed between the two surgeries was 11 $\pm$ 11 months (Table 1). The indications for revision surgery were infection, pain related to bulky hardware, adjacent segment degeneration, and progression of unfused scoliotic curve in double major scoliosis (Table 1). Material from 10 different areas within the spine fusion mass was intraoperatively taken from all patients during the revision surgery and sent to the second author for histological evaluation. The second author was used as unbiased observer because she did not know the diagnosis, the site of fusion from which the specimen was taken, and the radiographic picture of the fusion progress and made the histological investigation of all specimens. The histological evaluation was made with the use of a photomicroscope, while the histological strain technique used the hematoxylin-eosin. The presence of bone surrounding the coralline hydroxyapatite granules was graded as 0 for absence of bone, + for mild presence of bone, and ++ for strong evidence of bone. Statistical analysis was performed using the Pearson correlation coefficient (r).

III. RESULTS

There was no difference between the radiologists of more than one degree in rating spine fusion; when there was a difference in the degree of fusion between the two radiologists, the average was taken. The inter-intraobserver agreement as expressed by the kappa-value ranged between 0.96 and 0.98.

During the revision operation there was no pseudarthrosis or material failure in any patient. There was a continuous fusion mass in all revised spines with follow-up more than 6 months.

The specific histological picture, observed in all 10 specimens derived from each individual spine was the same: there was a concentration of ''foreign-body'' like giant cells around the hydroxyapatite granules, associated with development of inflammatory granulation tissue, which were gradually with the time lapsed from initial and revision operation replaced by dense connective collagen tissue. Both inflammatory granulation and collagen tissues showed areas with foreign body reaction (Fig. 1). In the cases where bone developed, the most initial finding was the presence of osteoblasts and apposition of osteoid close to the hydroxyapatite granules (Fig. 2). In a later phase, development of cancellous or cortical bone seems to be the result of intercartilaginous ossification (Fig. 3).

Other findings were the presence of newly formed articular-type synovial membrane, as well as extracellular apposition of metal (titanium) at the margins of the specimens. Bone forma-

Table 1 Commulative Data on 15 Revised Spines with Use of Coralline Hydroxyapatite

No.	Age	Gender	Diagnosis for first operation	Levels of instrumentation	Diagnosis for revision	Time (days) between surgeries	Histological findings				Radiographic rating of fusion[a]	Intraoperative evaluation + of fusion (Y/N)
							Osteoblasts and osteoid	Bone	Synovial membrane	Metal debris		
1**	60	F	Degenerative disease	L1–L5	Deep infection	30	0	0	+	0	Early	N
2	78	F	T12& L1 fracture	T10–L4	Bulky hardware	150	0	+	0	0	Early	N
3	65	M	Degenerative disease	L4 & L5	Subcutaneous seroma	40	0	0	0	+/–	Early	N
4	55	M	Fracture/ dislocation C6–C7	C5–Th2	Bulky hardware	360	0	+	0	0	2.5	Y
5	57	M	Spinal stenosis	L4–S1	Deep infection	30	0	0	0	0	Early	N
6*	29	F	L3-fracture	L2–L4	Superficial infection	45	++	+	+	0	Early	N
7*	29	F	L3-fracture	L2–L4	Infection	60	++	+	0	0	Early	N
8	56	F	Spinal stenosis	L2–L5	Adjacent segment degeneration	360	++	++	+	++	3	Y
9	23	F	L4, L5 fracture	L3–S1	Deep infection	42	0	+	+	+	Early	N
10	25	F	Idiopathic scoliosis	Th10–L5	Bulky hardware	540	0	+	0	0	3	Y
11	46	F	Degenerative disease	L4–L5	Adjacent segment degeneration	360	0	+	+	0	2.5	Y
12	30	F	Osteoid osteom T12	Th12–L1	Bulky hardware	720	0	++	0	0	3	Y
13	16	M	Idiopathic scoliosis	Th12–L4	Progression unfused curve	720	0	+	0	0	3	Y
14	70	M	Th12-fracture	T10–L2	Bulky hardware	90	0	0	+	++	Early	N
15**	63	F	Degenerative disease	L2–L5	Bulky hardware	1080	0	+	0	+	3	Y

M = male; F = female.
Both cases signed with (*) correspond to the same patient. Both cases signed with (**) is the same patient.
[a] Radiographic fusion rating in cases with follow-up more than 6 months: 1 = not fused; 3 = fused.
+ = intraoperative evaluation of fusion made by the surgeon: Y = fused; N = not fused.
Early = too early (<6 months) for radiographic evaluation.

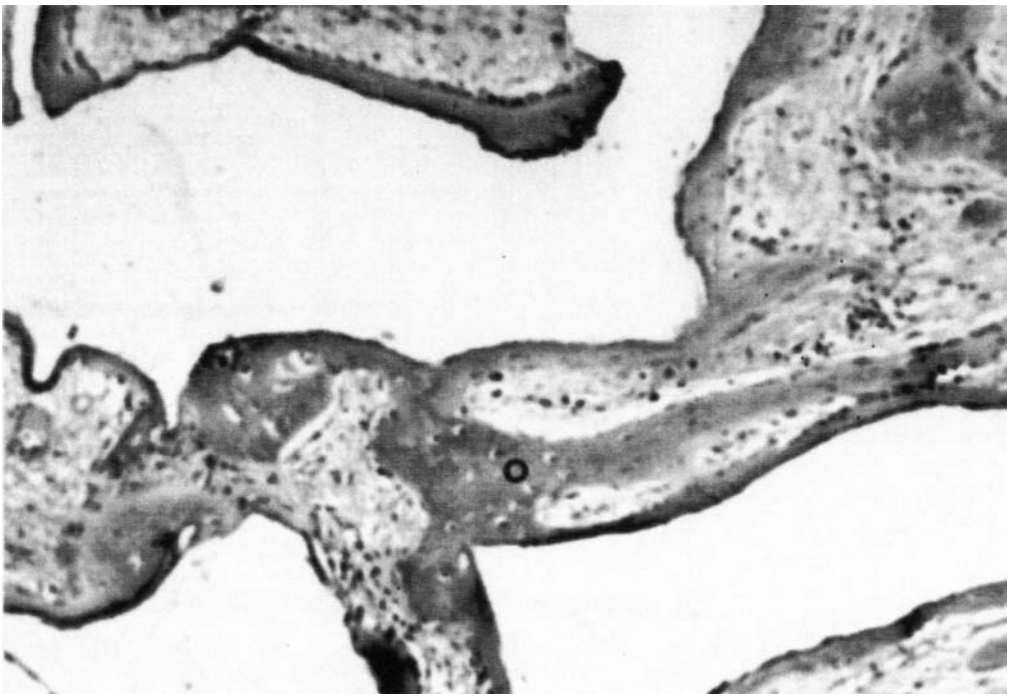

Figure 1 Granulation tissue comprising foreign body giant cells and newly formed collagen around coralline hydroxyapatite (CH) granules, which look like empty spaces following tissue processing (He $\times 100$).

tion was observed in 11 of the 15 operated cases and it was related to age, in favor of young patients ($r = 0.56, p < 0.05$), while there was no correlation with time elapsed from the primary operation.

Bone islands were observed around some hydroxyapatite granules, which were within the paravertebral muscles, away from the main instrumented fusion area (cases 6, 7). The presence of infection in this series seems not to have affected bone formation around hydroxyapatite granules.

All histological data are summarized in Table 1. The patient referred to as cases 1 and 15 is the same and was revised twice. The patient shown as cases 6 and 7 is the same and was also operated twice.

IV. DISCUSSION

Bone grafting is an integral part of spinal surgeries. The two choices of bone are autograft and allograft. Each source has its advantages and disadvantages. Currently, autogenous bone graft, usually from the iliac crest, is the gold standard against which all graft alternatives are compared. This study was conducted to determine if coralline hydroxyapatite induces bone formation in vivo in posterior spine fusion in human beings.

Several important results emerged from this histological investigation. First coralline hydroxyapatite applied on the decorticated posterior elements of the spine could induce bone

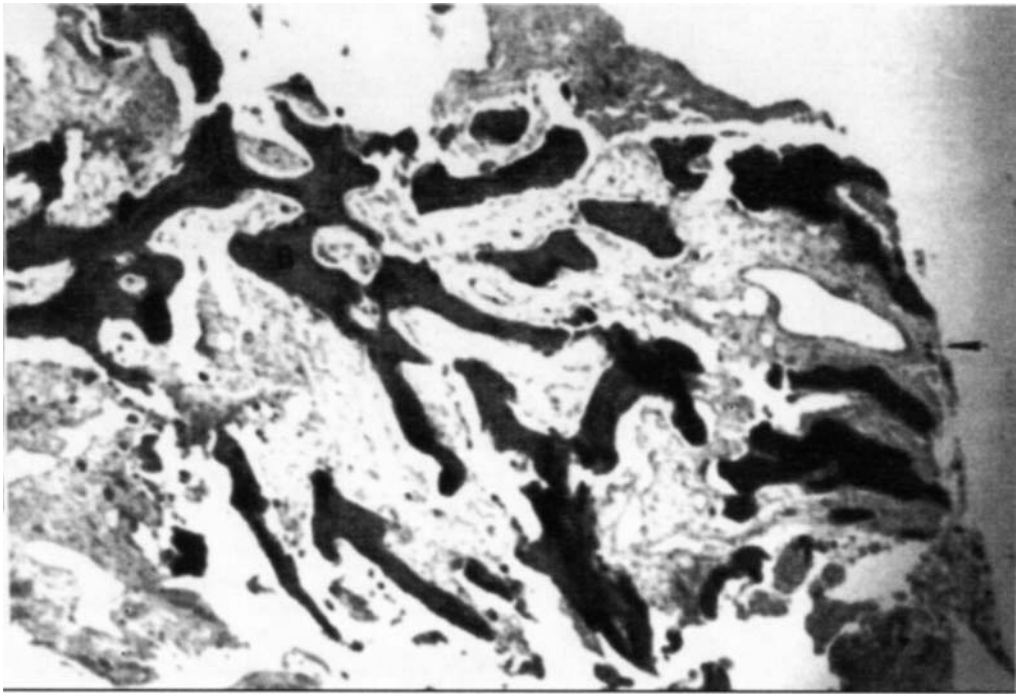

Figure 2 Osteoblasts rimming osteoid (O) apposition and development of cancellous bone in the connective tissue surrounding hydroxyapatite granules (HE $\times 100$).

formation within the fusion mass in the vast majority of the cases (73%) as early as 6 weeks postoperatively. Second, bone formation was induced by coralline hydroxyapatite in any region of the spine in which it was used. Third, bone appeared around the hydroxyapatite independently from the indication for spine fusion. Fourth, bone presence was most evident in young patients.

Few materials available today qualify as a stand-alone bone graft substitute and yield equivalent or better results than autogenous iliac crest bone graft. Although coralline hydroxyapatite is not advocated by the manufacturer as a complete bone graft substitute for use in the posterolateral spine, anecdotal information in reports indicates that some surgeons are attempting to use the material in this manner [17].

Although a previousse animal study in rabbit [8] showed that the use of coralline hydroxyapatite alone or with bone marrow is not sufficiently osteogenic for posterolateral lumbar spine fusion, our study showed that osteoid and bone formation within the fusion mass in the lumbar spine underwent posterolateral instrumentation and fusion. It seems that the results shown in experimental studies in animals cannot be completely compared with those in humans [3–8].

In the current study, bone, osteoblasts, and osteoid were histologically shown around coralline hydroxyapatite granules in cases with deep and superficial infection. Although the number of the cases with infection included in this study was small, it seems that the presence of infection does not seriously suspend bone formation.

In rabbits, Boden et al. [8] showed that coralline hydroxyapatite has some potential as a bone graft extender when combined 1:1 with autogenous bone graft. In the present study the coralline hydroxyapatite granules were applied on the decorticated posterior elements of the spine without any intended mixture with autologous bone graft. This difference should be related to the differences in osteogenic reaction between animals and human beings, the presence of

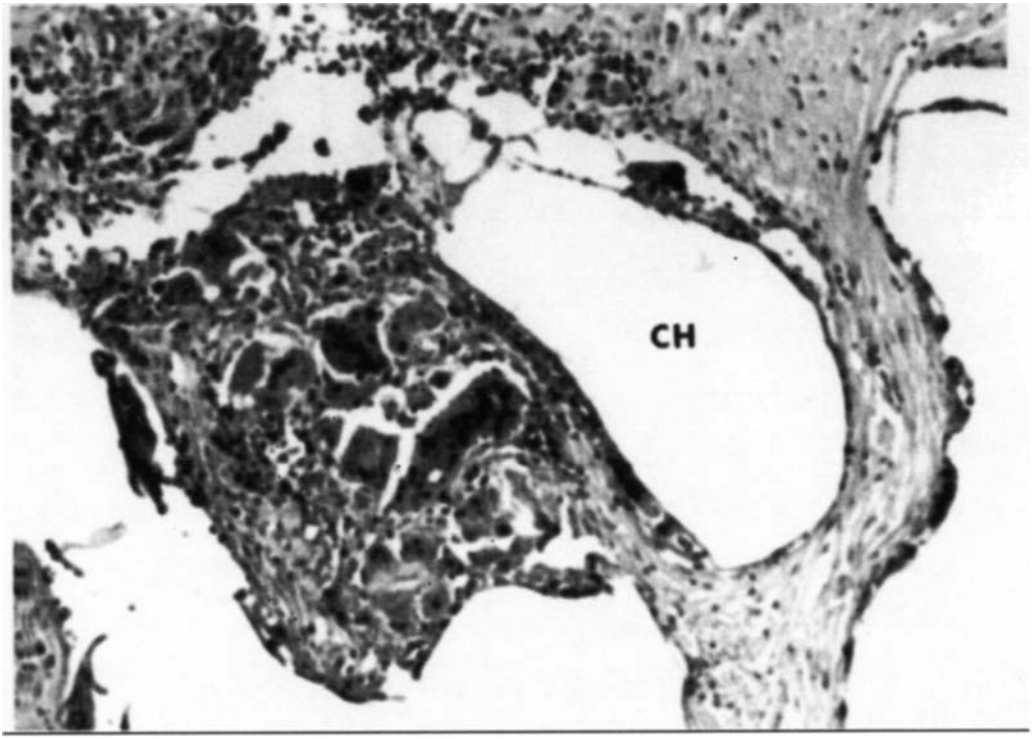

Figure 3 Well-formed cancellous bone (B) spicules. The position of hydroxyapatite granules is shown with arrow (HE $\times 100$).

stabilized material, and the significant more time elapsed from coralline hydroxyapatite application and histological examination. The successful fusion rate in animals with the use of coralline hydroxyapatite was reported to be 50% [8], a rate comparable to the fusion success rates of 50–70% seen with autogenous bone graft in previously published studies with the same model [3,4,13,28].

One advantage in the current study was the great range of the time elapsed from the implantation of coralline hydroxyapatite to the time of revision operation, because it allowed us to investigate the process of bone formation around the coralline hydroxyapatite granules in different phases of ossification.

There are two potential limitations of the validity of the current study: first the healing endpoint time was different among the 15 spines, because histology was performed in patients who underwent revision operation and histological examination at different times after the initial operation, ranging from one month to 3 years. Thus, although bone and osteoid islands were observed around coralline hydroxyapatite granules, one month seems to be inadequate time for coralline hydroxyapatite to be incorporated or even replaced by bone. It is possible, as seen in other models, that ingrowth into coral may have increased gradually for up to one year postoperatively [20–21, 26]. Second, all revision operations were made because of complications after surgery, none related to fusion. However, revision operations were not otherwise ethically feasible.

Thalgott et al. [32] radiologically studied the incorporation of coralline hydroxyapatite used in cervical spine for anterior interbody fusion with rigid anterior platting and showed a

100% incorporation rate. However, it is not possible to evaluate the viability of a fusion mass with coralline hydroxyapatite on the basis of radiological signs only.

Bozic et al. [9] evaluated coralline hydroxyapatite under current electrical stimulation in rabbit lumbar spine fusion and concluded that stimulation increased fusion rates.

Previous experimental animal studies have supported the notion that an osteoinductive material that is ceramic, such as coralline hydroxyapatite, may function as a bone graft substitute alone or with autogenous bone graft in a vascular bony environment such as the tibial-femoral metaphysis, but it may fail in a less vascular environment such as the posterolateral lumbar spine [18,20,21,24,26]. It is important to consider that the healing environments are dramatically different in a metaphyseal defect, the anterior intervertebral disc space, and the posterolateral spine. Clearly this study showed that coralline hydroxyapatite was useful when used as an osteoinductive graft substitute in posterior and posterolateral instrumented fusion in human beings with different pathologies, ages, and spine regions.

This histological study on human beings supports the use of coralline hydroxyapatite in spine surgery in combination with small amounts of cortico-cancellous bone chips taken from decortication of the posterior spine elements. This method avoids the use of autogenous iliac bone graft and the related donor site complications and the increased morbidity associated with harvesting iliac crest bone, but it is cost effective.

REFERENCES

1. Arrington ED, Smith WJ, Chambers HG, Bucknell AL, Davino NA. Complications of iliac crest bone graft harvesting. Clin Orthop 1996; 329:300–309.
2. Banwart JC, Asher MA, Hassanein RS. Iliac crest bone graft harvest donor site morbidity. A statistical evaluation. Spine 1995; 20:1055–1060.
3. Boden SD, Schimandle JH, Hutton WC. 1995 Volvo Award in Basic Sciences. The use of an osteoinductive growth factor for lumbar spinal fusion. Part II: study of dose, carrier, and species. Spine 1995; 20:2633–2644.
4. Boden SD, Schimandle JH, Hutton WC. Lumbar intertransverse process spine arthrodesis using a bovine-derived osteoinductive bone protein. J Bone Joint Surg (Am) 1995; 77-A:1404–1417.
5. Boden SD, Schimandle JH, Hutton WC. An experimental lumbar intertransverse process spinal fusion model: radiographic, histologic, and biomechanical healing characteristics. Spine 1995; 20:412–220.
6. Boden SD, Schimandle JH, Hutton WC, Chen MI. 1995 Volvo Award in Basic Sciences. The use of an osteoinductive growth factor for lumbar spinal fusion. Part I: The biology of spinal fusion. Spine 1995; 20:2626–2632.
7. Boden SD, Schimandle JH, Hutton WC. In vivo evaluation of a resorbable osteoinductive composite as a graft substitute for lumbar spinal fusion. J Spinal Disord 1997; 10:1–11.
8. Boden SD, Martin JG, Morone M, Ugbo JL, Titus L, Hutton CW. The use of coralline hydroxyapatite with bone marrow, autogenous bone graft, or osteoinductive bone protein wxtract for posterolateral lumbar spine fusion. Spine 1999; 24:320–327.
9. Bozic JK, Glazer PA, Zurakowski D, Simon JB, Lipson SJ. In vivo evaluation of coralline hydroxyapatite and direct current electrical stimulation in lumbar spinal fusion. Spine 1999; 24.
10. Canosa R, Del Pino JG. Effect of methotrexate in the biology of free vascularized bone grafts: a comparative experimental study in the dog. Clin Orthop 1994; 301:291–301.
11. Chiroff RT, White EW, Weber JN, Roy DM. Tissue ingrowth of replamine-form implants. J Biomed Res Symp 1975; 6:29–45.
12. DePalma AF, Rothman RH. The nature of pseudarthrosis. Clin Orthop 1968; 59:113–118.
13. Feiertag MF, Boden SD, Schimandle JH, Norman JT. A rabbit model for nonunion of lumbar intertransverse process spine arthrodesis. Spine 1996; 21:27–31.

14. Fernyhough JC, Schimandle JH, Weigel MC, Edwards CC, Levine AM. Chronic donor site pain complicating bone graft harvesting from the posterior iliac crest for spinal fusion. Spine 1992; 17: 1474–1480.
15. Guigui P, Plais PY, Flautre B. Experimental model of posterolateral spinal arthrodesis in sheep. Part 2. Application of the model: evaluation of vertebral fusion obtained with coral (Porites) or with a biphasic ceramic (Triosite). Spine 1994; 19:2798–2803.
16. Kehr PH, Graftiaux AG, Gosset F, Bogorin I, Bencheikh K. Coral as graft in cervical spine surgery. Orthop Traumatol 1993; 3:287–293.
17. Korovessis P, Papazisis Z, Petsinis G. Unilateral psoas abscess following posterior transpedicular stabilization of the lumbar spine. Eur Spine J 2000; 9:588–590.
18. Kuhne JH, Bartl R, Frisch B, Hammer C, Jansson V, Zimmer M. Bone formation in coralline hydroxyapatite. Effects of pore size studied in rabbits. Acta Orthop Scand 1994; 65:246–252.
19. Laurie SWS, Kaban LB, Mulliken JB, Murray JE. Donor-site morbidity after harvesting rib and iliac bone. Plast Reconstr Surg 1984; 73:933–938.
20. Martin G, Boden SD, Morone MA, Titus L. Evaluation of two new forms of demineralized bone matrix in posterolateral lumbar spine arthrodesis. Spine 1999.
21. Martin RB, Chapman MW, Sharkey NA, Zissimos SL, Bay B, Shors EC. Bone ingrowth and mechanical properties of coralline hydroxyapatite one year after implantation. Biomaterials 1993; 14:341–348.
22. Okumura M, Ohgushi H, Tamai S. Bonding osteogenesis in coralline hydroxyapatite combined with bone marrow cells. Biomaterials 1991; 12:411–416.
23. Pouliquen JC, Noat M, Verneret C, Guillemin G, Patat J. Coral as a substitute for bone graft in posterior spine fusion in childhood. French J Orthop Surg 1989; 3:272–280.
24. Preidler KW, Lemperle SM, Holmes RE. Coralline hydroxyapatite bone graft substitutes. Evaluation of bone density with dual energy x-ray absorptiometry. Invest Radiol 1996; 31:716–723.
25. Rahimi F, Maurer BT, Enzweiler MG. Coralline hydroxyapatite: a bone graft alternative in foot and ankle surgery. J Foot Ankle Surg 1997; 36:192–203.
26. Sartoris DJ, Holmes RE, Bucholz RW, Mooney V, Resnick D. Coralline hydroxyapatite bone-graft substitutes in a canine diaphyseal defect model. Radiographic-histometric correlation. Invest Radiol 1987; 22:590–596.
27. Schimandle JH, Boden SD. The use of animal models to study spinal fusion. Spine 1994; 19: 1998–2006.
28. Schimandle JH, Boden SD, Hutton WC. Experimental spinal fusion with recombinant human bone morphogenetic protein-2 (rhBMP-2). Spine 1995; 20:1326–1337.
29. Schnee CL, Freese A, Weil RJ, Marcotte PJ. Analysis of harvest morbidity and radiographic outcome using autograft for anterior cervical fusion. Spine 1997; 22:2222–2227.
30. Silcox DH, Daftari T, Boden SD, Schimandle JH, Hutton WC, Whitesides TE. The effect of nicotine on spinal fusion. Spine 1995; 20:1549–1553.
31. Steinmann JC, Herkowitz HN. Pseudarthrosis of the spine. Clin Orthop 1992; 284:80–90.
32. Thalgott JS, Fritts K, Giuffre JM, Timlin M. Anterior interbody fusion of the cervical spine with coralline hydroxyapatite. Spine 1999; 24:1295–1304.
33. Younger EM, Chapman MW. Morbidity at bone graft donor sites. J Orthop Trauma 1989; 3:192–195.

31

New Developments in Spinal Cord Monitoring

Danielle D. Langeloo, Henricus L. Journée, and Marinus de Kleuver
Sint Maartenskliniek
Nijmegen, The Netherlands

I. THE USE OF NEUROMONITORING

Surgery to correct spinal deformities, such as scoliosis, carries a small but significant risk of neurological damage. The consequences of this complication, especially if motor in origin, can be disastrous to the patient and all others involved.

The frequency of postoperative neurological deficits after scoliosis surgery is well illustrated in a study conducted in 1975 by the Scoliosis Research Society (SRS). Of 7558 corrective scoliosis surgeries performed between 1965 and 1971, an incidence of postoperative neurological deficits of 0.72% was found [13].

The realization that some of the neurological complications of spinal surgery could be avoided by early surgical management has led to the development of intraoperative spinal cord monitoring.

Damage to the spinal cord during surgery is caused by inadvertent compression of neurological structures or by interference with the blood supply. For example, a misplaced screw or overcorrection of a deformity can cause immediate neurological deficits. Surgeries that are considered to carry an increased risk of neurological complications are those in which corrective forces will be applied to the spine, the patient has preexisting neurological damage, the spinal canal will be invaded, or an osteotomy or other procedure will be carried out in immediate juxtaposition to the spinal cord.

Acute ischemia of the neurological structures leads to a pathophysiological state called ischemic penumbra. In this state the neurons are nonfunctional but still alive and salvageable by reperfusion. If this neurological dysfunction can be immediately detected by neuromonitoring, there is time to reverse the processes and prevent irreversible structural damage [1].

The primary purpose of intraoperative monitoring is to detect as early as possible any deterioration in neurological function so that treatment or correction can be implemented before the impairment becomes permanent. The secondary purpose of monitoring is to inform the surgeon if the recovery of the trace has occurred after the modification.

Neuromonitoring techniques have to fulfill the high demands of spinal deformity surgery. All deformity surgery on the spine has the following characteristics. It involves a large part of the spine, spinal cord, and cauda equina. Often large mechanical forces are applied during correction. Blood loss is often extensive, and ischemia associated with profound systemic hypo-

tension can cause neurological deficits and change the evoked responses. Last but not least, spinal surgery is time consuming, and the spine surgeon does often not welcome any additional time required for neuromonitoring.

Several techniques are available to monitor the spinal cord during surgery. These include the intraoperative wake-up test, somatosensory evoked potential monitoring (SSEP), and, more recently, motor evoked potential monitoring (MEP) with diverse application methods such as transcranial electrical motor evoked potential monitoring (TCE-MEP), transcranial magnetic motor evoked potential (TCM-MEP), and neuromotor evoked potential monitoring (NMEP).

The intraoperative applications of all these techniques have been reported in several large studies. In order to interpret these study outcomes, it is extremely important to realize that any study of a clinical intraoperative monitoring technique is ethically and methodologically difficult. For example, it is ethically unacceptable to ignore neuromonitoring outcomes and to wait until postoperative evaluation in order to determine whether these signal changes were indeed true positives or false positives. Therefore, clinical studies of neuromonitoring are usually descriptive cohort studies and can provide only limited information on sensitivity and specificity.

II. THE WAKE-UP TEST

As described in 1973, the wake-up test consists of lightening the anesthetic state to a point at which the patient can respond to a command [41]. The wake-up test is highly specific for intraoperative motor function. However, the use of the wake-up test has many limitations. First, as the patients wake up, inadvertent extubation, possible loss of intravenous lines, or dislodgement of instruments is possible. Second, the test is difficult to perform in young children or in mentally retarded patients. Furthermore, the test can be repeated only a limited number of times. Therefore, the test cannot be used to pinpoint the onset of a neurological injury, and it can only provide a momentary impression of motor functions at the wake-up moment. Any neurological injury that might have occurred before the final surgical handling may already have resulted in irreversible spinal cord damage by the time the wake-up test is performed.

Nowadays, the wake-up test has been replaced by more continuous intraoperative monitoring such as SSEP and MEP. However, the wake-up test is still commonly used in conjunction with evoked potential monitoring or when evoked potentials show abnormal responses [7]. It is the only intraoperative test of voluntary motor function.

III. SOMATOSENSORY EVOKED POTENTIAL MONITORING

Although no neurological deficit is acceptable, surgically induced motor deficits, such as paraplegia, are of greater concern than sensory deficits. Ironically, SSEP was the first intraoperative electrophysiological monitoring procedure to protect the spinal cord. Although SSEP has its limitations, SSEP monitoring is today the most widely used intraoperative monitoring technique. The first clinical application of SSEP was described in the early 1970s when the development of computer averaging techniques made the clinical application feasible [6].

To elicit an SSEP, a peripheral nerve is stimulated. Usually the posterior tibial nerve at the ankle is used. After stimulation of the nerve, the impulse normally reaches the sensorimotor cortex in about 40 msec. Electrodes positioned over the somatosensory cortex or at a spinous process record the evoked potential (Fig. 1).

Evoked potentials are in fact small-amplitude responses that are not identifiable with a single stimulus. Using signal averaging, the SSEP is extracted from the background noise.

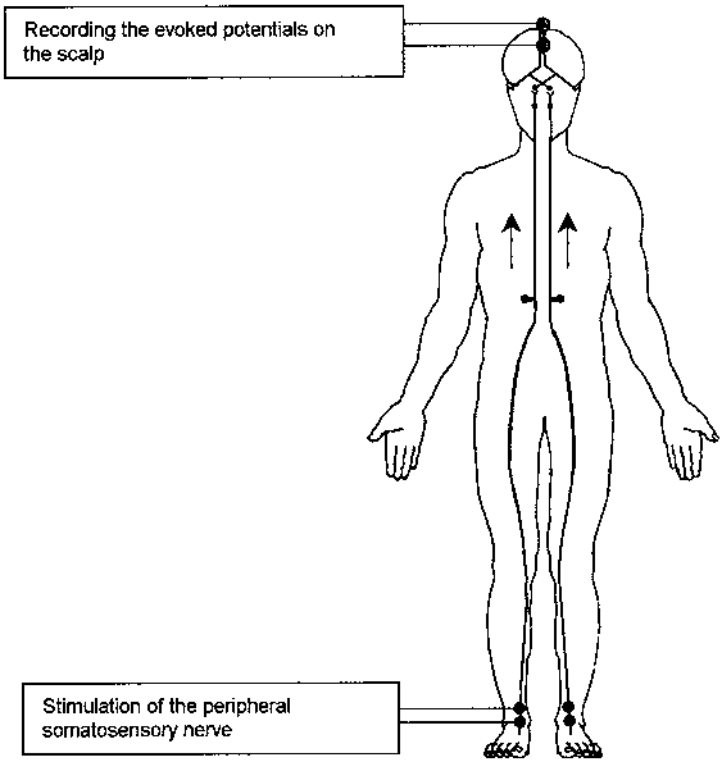

Figure 1 Position of the stimulation and recording electrodes in somatosensory evoked potential monitoring (SSEP).

Usually several hundred stimuli are needed to extract the evoked potential waveform. Because the averaging process takes several minutes, a drawback to this method is the monitoring delay.

During surgery, the latency and amplitude of the acquired response are measured and compared with baseline data. If necessary, a control site above the level of surgery can be used. A decrease of amplitude (over 50% of baseline) or by some authors a latency increase (of 10%) is suggestive of neurological damage [7,32,42].

In all evoked potential neuromonitoring there are environmental and physiological factors that influence the response measurements. For example, administration of anesthetic drugs may depress SSEP amplitudes and increase latencies. This is particularly true for the volatile anesthetic agents, which cause a marked dose-related depression of amplitudes and latency prolongation. Intravenous anesthetic drugs produce only minor effects. In addition, physiological changes in temperature and/or blood pressure (hypotension) can cause SSEP changes that disturb a correct interpretation of the SSEP response [21].

The rationale for using a sensory-based response to monitor motor tract function is based on the relative proximity of spinal cord sensory tracts to the spinal cord motor tract. It is thought that, because of their proximity, damage to the motor tracts indirectly affects the sensory responses, which results in a change of the SSEP. Most spinal cord damage due to spine distraction or rotation results from more diffuse damage involving both the anterior and the posterior spinal cord.

The reported high sensitivity of SSEP shows this hypothesis to be correct in most patients [32]. However, the anterior and lateral spinal cord is the most vulnerable to damage by surgical action. Not surprisingly, several studies have demonstrated that selective anterior cord damage due to surgery can result in a change in motor tract function without significant SSEP response changes: i.e., a false-negative outcome [3,11,29,43]. In addition, a survey of SRS by Dawson in 1991 revealed that 5 of the 30 major surgically induced neurological deficits were not detected by SSEP [7].

However, Nuwer performed a large multicenter survey, published in 1995, in which a questionnaire was sent to 173 surgeons in the United States. In this study the false-positive rate was 1.51%, and the false negative rate measured 0.13% [32].

In conclusion, somatosensory evoked potential monitoring has been shown to be a reliable and valid method for monitoring spinal cord function during surgery for spinal deformities. However, SSEP is an indirect method of intraoperative motor pathway monitoring in which selective motor pathway disturbances can be missed. Furthermore, the averaging procedures required for SSEP monitoring lead to several minutes' delay in detecting neurological damage.

IV. MOTOR EVOKED POTENTIAL MONITORING

Since the late 1980s, a concerted effort has been made to create a technique that directly monitors spinal cord motor tract function. Techniques with different methods of stimulation and response recording have been developed and refined.

A. Recording Techniques

Two types of potential recording have been described: myogenic and neurogenic. A myogenic response is a direct muscle contraction that can be registered by an EMG. A neurogenic response is the compound nerve action potential that evokes the contraction of the muscle innervated by that nerve.

In neurogenic motor evoked potential monitoring, the responses are most commonly recorded from the sciatic nerve. This invasive technique involves placing a needle electrode at the ischial tuberosity or popliteal fossa, (Fig. 2). When recording from a mixed nerve, complete neuromuscular blockade during surgery is optional. The neurogenic response contains an antidromic sensory activity. Various authors have questioned the presence and degree of true motor activity in this response [9,14,15]. Regardless of its neurological composition, however, NMEP has proven sensitive to neurological pathology [34]. The peripheral nerve response is small, about 1 mV. Therefore, similar to the averaging process in SSEP, it is necessary to average at least 100 responses in order to obtain a reproducible signal.

Myogenic recording can be performed at one or multiple peripheral muscles of choice by using surface or needle electrodes (Fig. 2). The motor response is recorded as a compound muscle action potential (CMAP). Logically, muscle relaxants influence the use of this potential. Hence, complete neuromuscular blockade must be avoided during monitoring, and if muscle relaxants are needed, the administration of muscle relaxants has to be titrated to such level that it is still possible to record muscle responses. The great advantage of myogenic monitoring is that the amplitudes are large and the latencies are reliable so that no averaging processes are needed. Furthermore, the surface electrodes can be placed on several different muscles providing a practical and simple monitoring method that also allows monitoring of individual muscle groups.

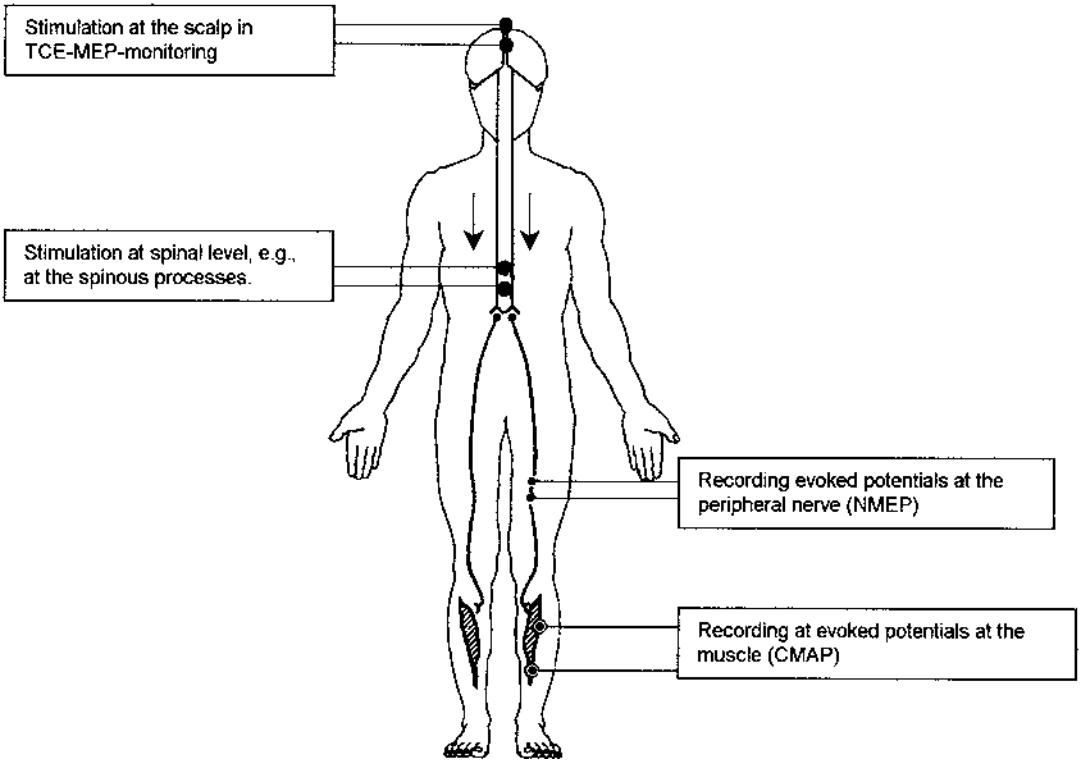

Figure 2 The position of the stimulation and recording electrodes in motor evoked potential monitoring (MEP).

B. Stimulation Techniques

Three different stimulation techniques can be used for motor evoked potential monitoring. Good monitoring results have been described in various studies for all three methods.

First, by placing an electrode on or near the dural sac, the potential can be elicited by stimulating the spinal cord proximal to the operative site. This can be done in the surgical wound or further proximally by placing an electrode percutaneously between the spinous processes (Fig. 2). This technique of spinal cord stimulation, introduced by Owen, was originally described in combination with neurogenic response monitoring [33]. This combination carries the advantage that neither anesthesia nor muscle relaxants need to be taken into consideration. Several variations of these methods have been reported that place needle electrodes in either the laminae in the cervical spine or in the disc spaces or that place epidural catheter proximal to the surgical site. Unfortunately, with spinal cord stimulation the examiner has no direct control over the stimulation. A further disadvantage of placing the electrodes in the surgical area is the accumulation of fluid that could lead to current shunting with a subsequent loss of the response. Current shunting may also occur if spinal instrumentation, metal implants, or instruments touch the stimulation electrodes.

Transcranial stimulation elicits a response to the stimulation on the scalp (Fig. 3). Transcranial evoked potential monitoring can be performed either electrically or magnetically. These

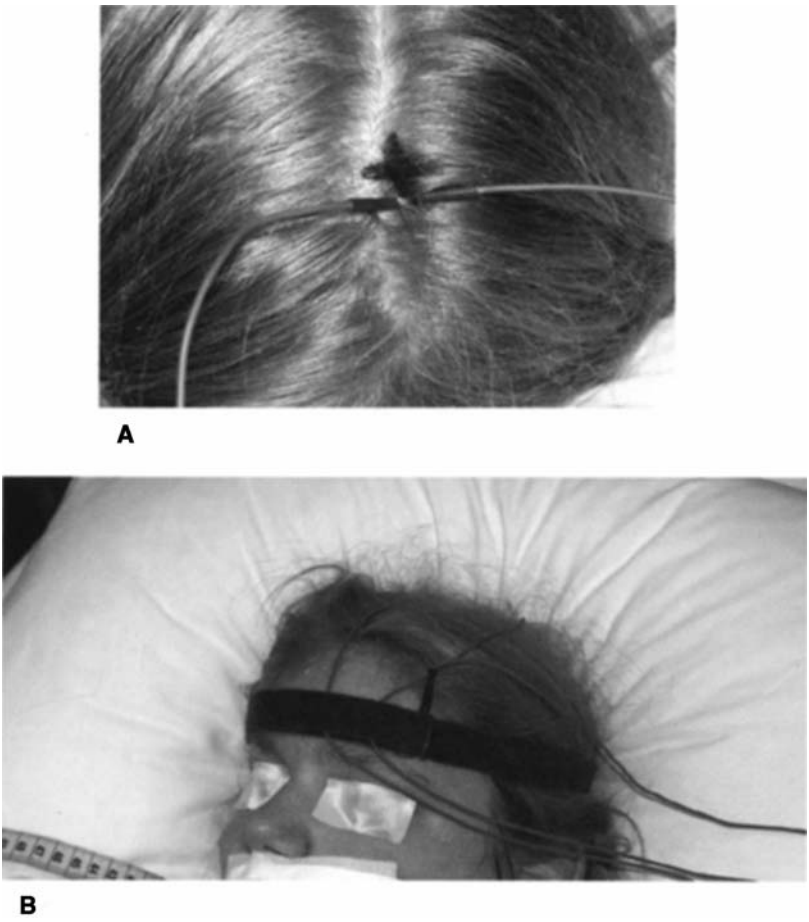

Figure 3 The location and fixation of the anode (A) and cathode (B) on the scalp in TCE-MEP.

methods are called transcranial magnetic or electrical motor evoked potential monitoring (TCM-MEP/TCE-MEP). The monitoring principles using TCE-MEP or TCM-MEP are similar.

In 1985 Barker described the first application of TCM-MEP [2]. Initially, magnetic stimulation was developed as a painless method to be used in neurophysiological settings in awake patients. Since its first report, several studies have reported the successful intraoperative use of TCM-MEP [9,14,26,25]. TCM-MEP is contraindicated in patients with pacemakers, skull defects, or metal implants in the skull. A disadvantage of TCM-MEP versus TCE-MEP is that continuous access to the head is required and small displacements of the magnet will result in considerable amplitude variability. Futhermore, the technique is highly sensitive to use of anesthetics, which complicates its intraoperative use.

In 1980 Merton and Morton introduced transcranial electrical stimulation, and the technique has since been further refined [30]. The assessment of trans-cranial electrical motor evoked potential monitoring has therefore has become more popular. Successful intraoperative use of TCE-MEP has been reported in several studies [4,5,17,19,31,35,37,38]. In August 2002, the U.S. Food and Drug Administration (FDA) approved transcranial stimulation for (intraoperative) use

and marketing. In the following section this technique and the recent developments of TCE-MEP will be discussed.

V. TCE-MEP TECHNIQUE BASICS

A. TCE-MEP Monitoring Devices

Transcranial electrical stimulation of the motor cortex is performed using specifically designed stimulators; originally these were voltage stimulators. Generally during idiopathic scoliosis surgery, the voltage of the stimulus needed to elicit a muscle response is generally around 150–250 V. The electrical current flows primarily through the skin; only a small portion of current flow reaches the motor cortex, where it may cause direct depolarization of the pyramidal tract neurons.

Outside the United States, most centers apply a special designed transcranial electrical stimulator, usually the Digitimer®. We use a similar stimulator, called the Neuro-guard® (JS-Center, Bedum, The Netherlands), which is a so-called custom design. Some inconveniences of the Digitimer, such as lack of accuracy of pulse shape and voltage, have been improved in this device. These voltage stimulators have a low output impedance (Digitimer: 120 Ohm; Neuro-guard: 22 Ohm) and current limits of 1 Å. Since FDA approval of these voltage stimulators in August 2002, current limits no longer apply.

B. TCE-MEP Stimulation

To perform transcranial electrical stimulation, subdermal needle electrodes are placed on the surface of the scalp over the motor cortex (Fig. 3A). One or more anodal 3 cm needle electrodes are inserted subcutaneously 2 cm behind the central Cz position (according to the international 10–20 system for the placement of the EEG electrodes). For a cathode, single electrodes or a metal strip can be used. We use a Velcro ground strip immersed in saline placed across the forehead (Fpz-position) (Fig. 3B). Before the actual stimulation, the electrode impedance calibration has to be performed. Therefore, the stimulus intensity is increased in 25 V increments, from 0 V to the maximum output of the stimulation or until all muscles respond to stimulation. A train of four pulses with an interpulse interval (IPI) of 2 ms and pulse width (PW) of 100 μs is used. The amplitude of the muscle response to the selected amplitude voltage is defined as the baseline amplitude. This baseline amplitude is different for each muscle group selected. During surgery, it is recommended that transcranial stimulation be performed at voltages slightly higher (25 V increment) than the determined maximum value (Fig. 4).

C. TCE-MEP Recording

When cortical stimulation reaches anterior horn cell synapse, an excitatory post-synaptic potential is generated. If there is sufficient temporal and spatial summation of potentials, the anterior horn cells will fire and trigger a motor unit and a muscle response (Fig. 2). The response signal consists of an initial direct D-wave, followed by several indirect I-waves. The D-wave is the result of direct activation of pyramidal cells in the motor cortex, while the I-waves are the result of transsynaptic activation of the corticospinal tract by cortical interneurons.

To record the response, subdermal needle electrodes or surface electrodes are placed in or on the muscles from which data are to be recorded (Fig. 5). An advantage of TCE-MEP is that multiple muscle sites can be selected according to the clinical situation. Generally, in anesthetized human subjects the myogenic motor response of the anterior tibial muscle is 100–1000 μV (Fig. 6).

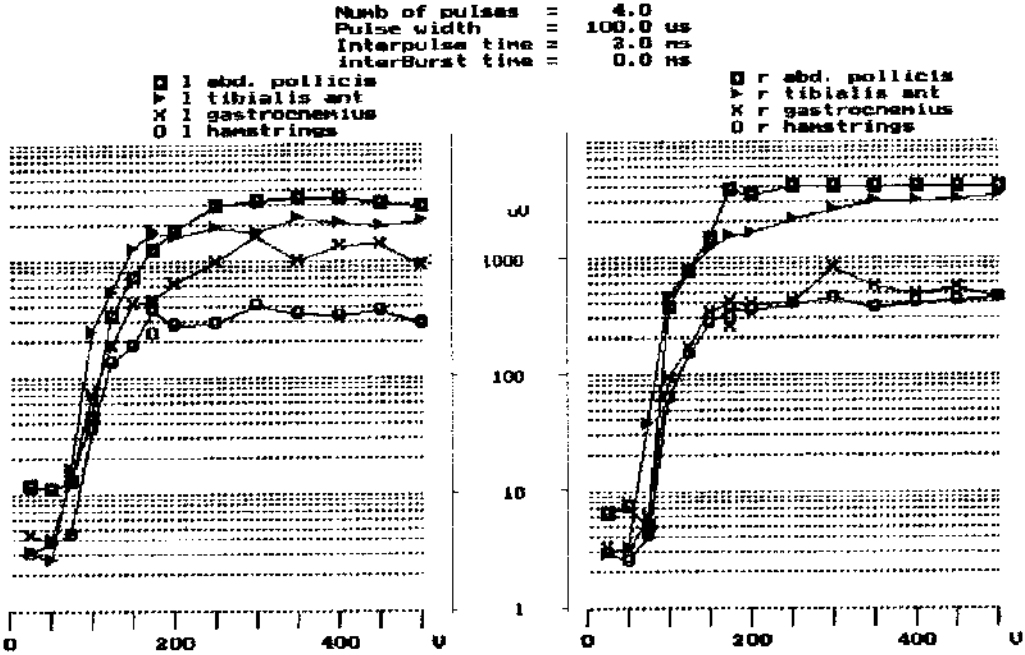

Figure 4 Graphs illustrating the determination of the threshold levels for each of the monitored muscles: x-axis: TCE-MEP stimulation amplitude in V; y-axis: response amplitude in μV (CAMP). The threshold was determined to be at 150V and intraoperative stimulation was therefore performed at 175 V (25 above threshold value).

During surgery, a decrease of response amplitude or, as noted by some authors, a increase of latency is an indication for possible for neurological ischemia (Fig. 7). Criteria and normal variations will be discussed in Sec. VI. C.

VI. NEW DEVELOPMENTS OF TCE-MEP

During the past 10 years, the intraoperative application of TCE-MEP has been further refined. First, multiple studies have focused on the influence of anesthetics on TCE-MEP amplitudes. Second, several new transcranial stimulation techniques to evoke high amplitudes have been developed that maintain responsiveness during surgery. Third, the normal amplitude variability of TCE-MEP responses during surgery and subsequently the criteria to indicate a neurological impediment have been determined. Fourth, the use of multiple monitoring sites in TCE-MEP has been applied in diverse patients categories. Fifth, TCE-MEP has been tested in patients with preexistent neurological deficits. These new developments in TCE-MEP monitoring will be discussed below.

A. Anesthetics and TCE-MEP Monitoring

The TCE-MEP amplitudes may be influenced by multiple factors: anesthetic-induced depression occurs most frequently. As in SSEP, most anesthetic agents depress the motor evoked response

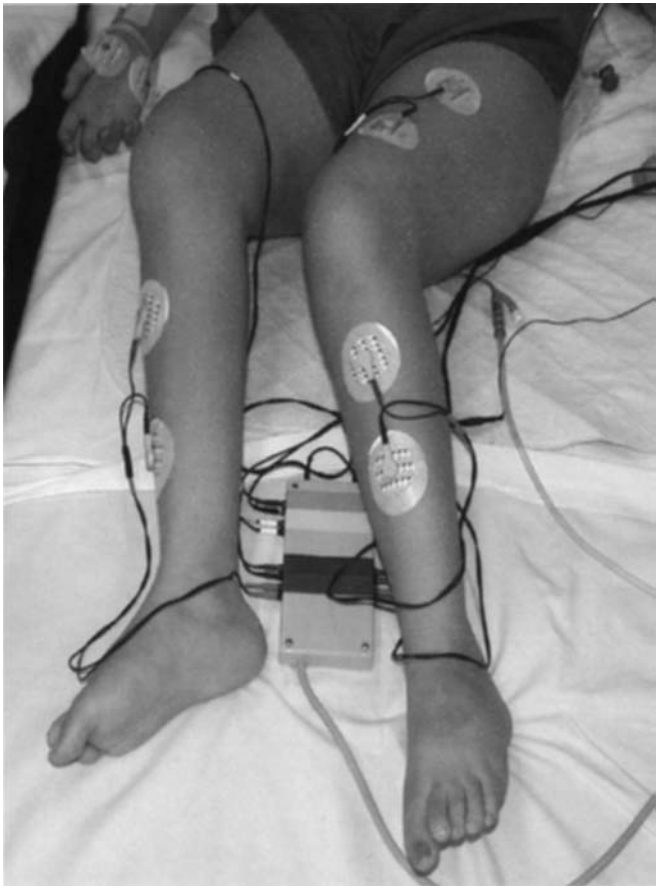

Figure 5 The position and fixation of the recording electrodes on the lower extremities in TCE-MEP monitoring.

amplitude. Volatile anesthetic agents have been confirmed to be the most potent TCE-MEP depressants [5,24]. The myogenic response is completely abolished with even very low concentrations of volatile anesthetic agents. For example, the myogenic response to single transcranial electrical stimulation is obliterated by end-tidal isoflurane concentrations as low as 0.3% [5,24].

Nitrous oxide is also a potent depressant of TCE-MEP, as are benzodiazepines and propofol [18,23,24,36]. In contrast, drugs known to increase or maintain muscle tone such as etomidate, ketamine, or synthetic opioids appear to have much less influence on TCE-MEP [39].

Two widely used successful anesthetic regimens during surgery in combination with TCE-MEP monitoring are nitrous oxide/opioid anesthesia and propofol/opioid total intravenous anesthesia. Propofol causes more depression of transcranial electric motor evoked responses than 50% N_2O. Injections of bolus propofol should be avoided to contain consistent response measurements [21].

B. Techniques to Increase TCE-MEP Amplitudes

Because of the variations in amplitude, it is important to evoke a high-amplitude muscle response in order to be able to monitor the entire surgical procedure. One method to increase the TCE-

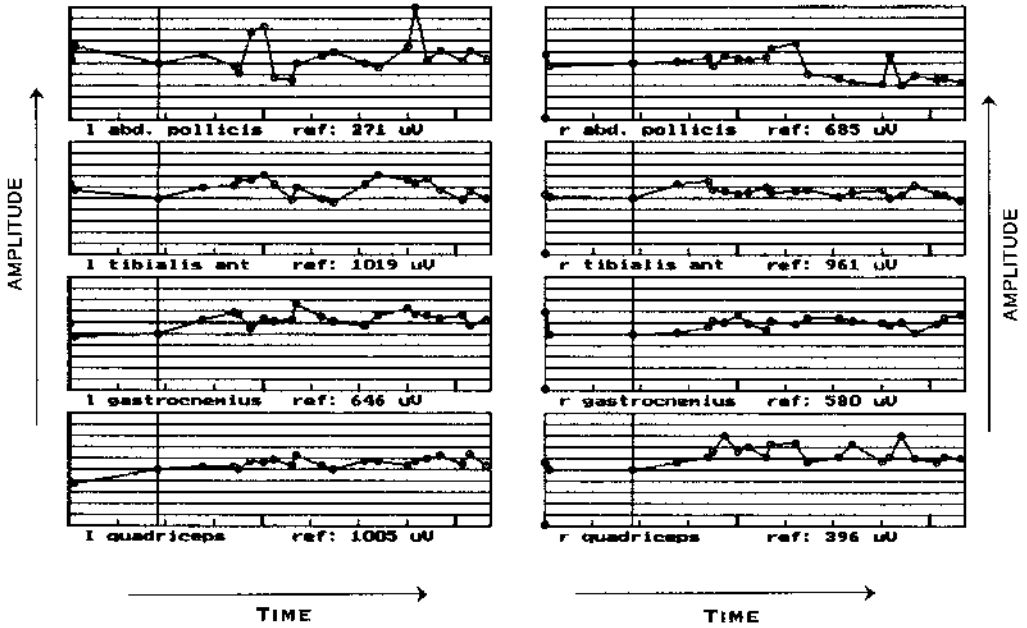

Figure 6 Time plots of intraoperative TCE-MEP amplitudes for eight muscle groups in a patient without amplitude decreases. In each time plot the amplitude (y-axis) is given as a percentage from the reference point indicated by the small vertical line. Time marks (x-axis) indicate 15 minutes.

MEP amplitude in anesthetized patients is the application of two or more successive stimuli, called a train or multipulse stimulation, with an interstimulus interval (ISI) of 2–3 ms [10,16,22]. With this technique the first stimulus lowers the excitation threshold of the motor neuron pool, thus facilitating depolarization by the second stimulus.

Multipulse stimulation has become popular in TCE-MEP monitoring [4,19,27,35]. It has been shown to provide higher, more reproducible amplitudes throughout surgery. We generally use a train of four stimuli. If responses are still too low, we can increase the train to seven stimuli. Similar to our experience, Deletis [8,9] have successfully applied TCE-MEP train monitoring using a custom-made current stimulator with a current range of 160–240 mA.

In our experience the success rate of current stimulators rose when the character of the transcranial stimulation was changed. For example, the use of a preconditioning train pulse, two trains of 4–7 pulses each with an ISI of 2 ms, with an intertrain interval of 10–30 ms (or $>$125 ms), enhances MEP amplitudes to 100–1000 μV. These high-amplitude responses to a two-train stimulus can often be achieved even if the single-train amplitude response is around 10 μV [20].

An alternative strategy for increasing TCE-MEP amplitude intraoperatively is to improve the efficiency of the stimulus delivery by changing the configuration of the stimulating electrodes. Ubags reported in 1996 that the use of a circumferential cathode might allow TCE-MEP monitoring in patients who do not have sufficiently reproducible responses when a single cathode is used [38]. The possible explanation for the improved efficiency is that the circumferential cathode alters the direction of electrical currents in the cortex, resulting in more efficient depolarization of cortical motor neurons.

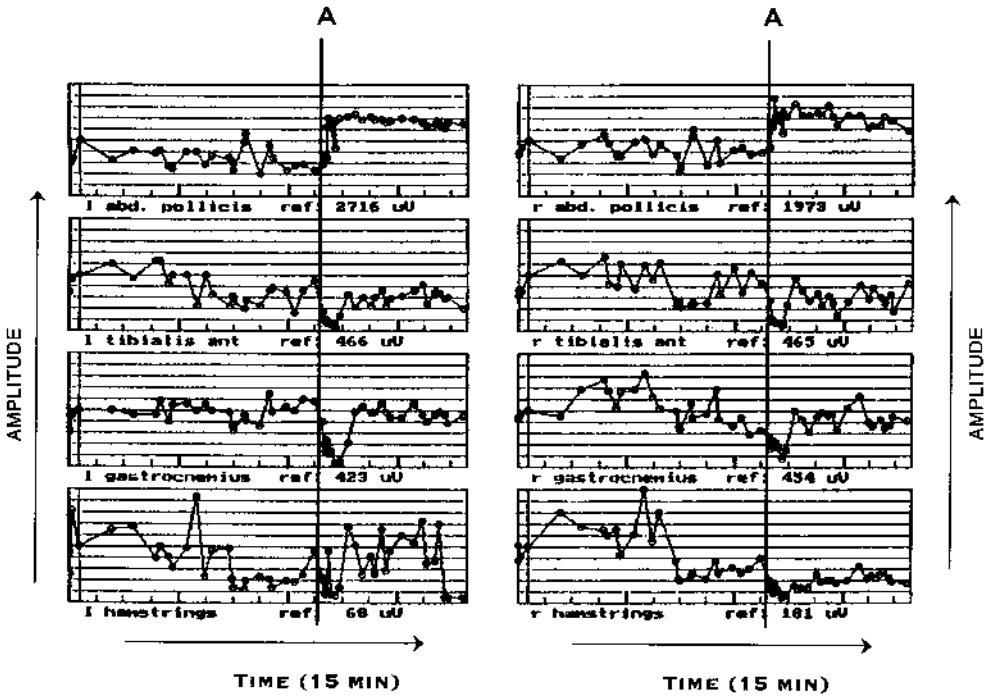

Figure 7 Time plots of intraoperative TCE-MEP amplitudes of eight muscle groups. In each time plot the amplitude (y-axis) is given as a percentage from the reference point indicated by the small vertical line. Time marks (x-axis) indicate 15 minutes. The vertical bar (marked A) indicates the time of the surgical maneuver that leads to decrease of amplitude in the six monitored leg muscles.

C. Normal Variations and Criteria Indicating Neurological Ischemia

Variations in TCE-MEP response values occur even in haemodynamically and anaesthetically stable patients. The amplitude changes are caused by varying number of excited motor units from one stimulus to the next.

Van Dongen reported in 1999 that in the lower limb in all patients with a partial neuromuscular blockade and a stable propofol/fentalyl/nitrous oxide anesthetic state, TCE-MEP with a multipulse stimulation produced reliable muscle responses with a coefficient of variation of approximately 20% [40].

In a recent study, we determined the actual amplitudes recorded at the time of impending neurological damage and derived criteria that could be used to warn the surgeon about spinal cord injuries in an early stage [28]. We included 145 patients undergoing corrective spinal surgery with TCE-MEP monitoring. In this TCE-MEP setting, three bilateral muscle sites and one bilateral reference site were used for recording. No additional monitoring device was used. Of the 145 patients, 106 were neurologically normal, 17 had cerebral palsy, 9 suffered from neuromuscular weakness (Duchenne, spinal dysraphism, spinal muscular atrophy), and 13 patients suffered from secondary compromised cord.

As mentioned in Sec. I, research of intraoperatively performed neuromonitoring is ethically and therefore methodologically difficult. We adhered therefore to the following strict definitions.

The clinical outcome was defined as the presence or absence of a neurological event. For the purpose of this study a neurological event was defined as the occurrence of (1) a postoperative

neurological deficit or (2) a marked decrease in TCE-MEP amplitude due to surgical maneuvers that recovered after further surgical intervention.

Negative clinical outcome: no neurological events due to surgical maneuvers
Positive clinical outcome: neurological event due to surgical maneuvers
Thus, the clinical outcome for each patient could be classified.

Negative monitoring outcome: no response amplitude decrease due to surgical maneuvers meeting the warning criteria
Positive monitoring outcome: responseamplitude decrease due to surgical maneuvers meeting the warning criteria

The success of neuromonitoring in detecting surgically induced neurological deficit could be expressed in terms of true/false-positive and true/false-negative monitoring outcomes.

It appeared that a safe warning criterion for neurological damage was one response amplitude decrease of 80% or more (i.e., lowered amplitudes of 20% or less of the reference values). Using this criterion, all neurological events were detected; there were no false negatives. The sensitivity was 1.0 (95% CI lowerbound 0.97) and a negative predictive value of 1.0 (95% CI lowerbound 0.97) (Fig. 8).

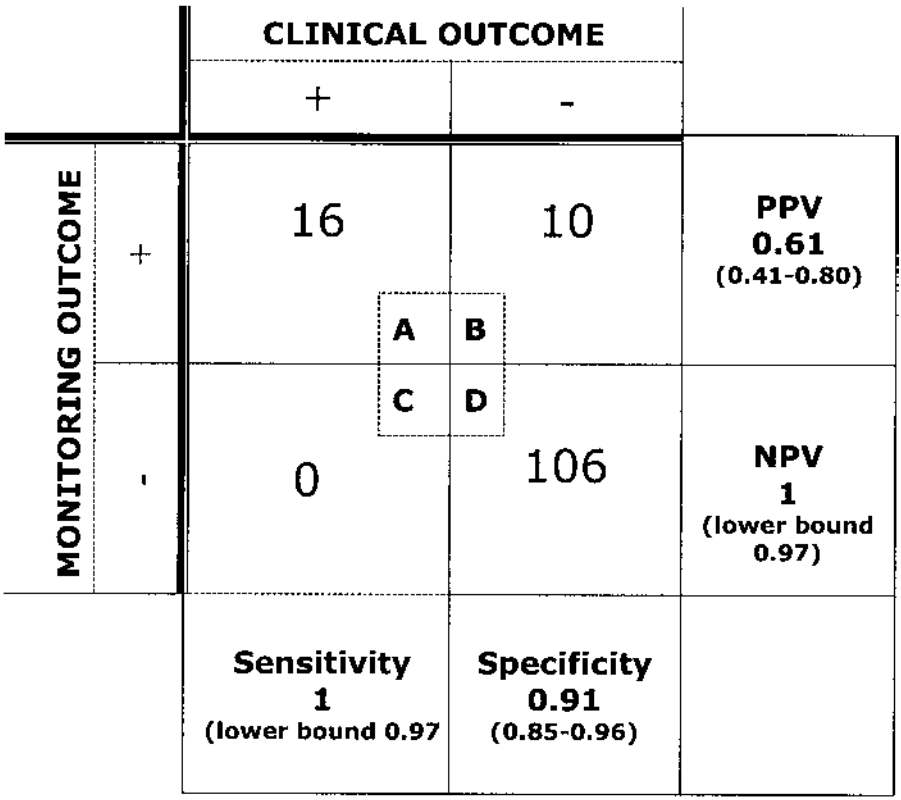

Figure 8 Analysis of criterion: 80% or more decrease of amplitude in any one of the six recordings. Comparison of clinical outcome to monitoring outcome and the calculated positive predictive value (PPV), negative predictive value (NPV), specificity, and sensitivity (and the 95% confidence interval) for criteria: 80% or more decrease of amplitude in any one of the six recordings. A, True positive; B, false positive; C, false negative; D, true negative.

D. Multiple Muscle Monitoring

TCE-MEP offers the possibility of recording the evoked potentials at multiple muscles. The target muscles are selected preoperatively. The neurophysiologist selects the muscles that are the most clinically relevant and important, with stable and high amplitudes.

One may assume that in terms of sensitivity and specificity, the results of monitoring are better using multiple muscle monitoring. In our study, we compared retrospectively the same criterion with six-muscle monitoring and two-muscle monitoring (anterior tibial muscles). The criterion was set to be a amplitude decrease of 80% or more compared to reference value (Fig. 9). Although there is a gain in specificity by using two instead of six muscle sites (n.s.), the use of the 80% decrease criterion for only two-muscle monitoring would have led to two false negative outcomes (n.s.). We consider the clinical importance of preventing a false negative (undetected neurological event) to be so great that the advantage of monitoring two instead of six muscle sites does not outweigh the cost of permanent neurological damage in the three patients who would not have been detected. Furthermore, in clinical practice, the great added advantage of monitoring six instead of two muscles is the greater ability to interpret and judge

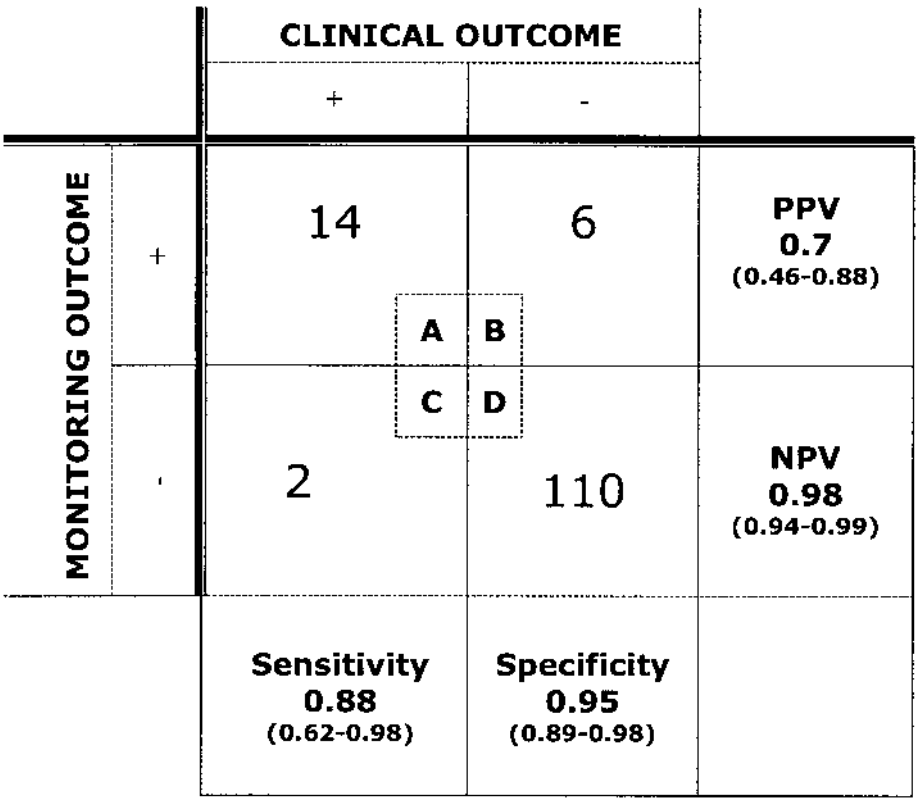

Figure 9 Analysis of criterion: 80% or more decrease in amplitude in either one of the two anterior tibial muscle recordings. Comparison of clinical outcome to monitoring outcome and the calculated positive predictive value (PPV), negative predictive value (NPV), specificity, and sensitivity (and the 95% confidence interval) for criteria: 80% or more decrease of amplitude in one of the two anterior muscle recordings. A, True positive; B, false positive; C, false negative; D, true negative.

changes intra-operatively when strict criteria cannot be applied, such as in patients with complex neurology or during hypotension or hypothermia. Therefore, in our opinion the use of multiple monitoring sites should be encouraged considering the minimal extra effort required.

E. TCE-MEP in Patients with Preexisting Neurological Deficits

In a study published in 2000, TCE-MEP was applied to patients with neuromuscular and severe muscle weakness undergoing scoliosis surgery [27]. TCE-MEP monitoring was used in nine patients. They had the following diagnoses: four myelomeningocele, four Duchenne muscular dystrophy, and one spinal muscular atrophy. All still had some minor function of the lower extremities. This made spinal cord monitoring important because increased neurological deficits would have huge consequences. TCE-MEP stimulation was performed as described in Sec. V. However, recording was adapted to the preserved neurological functions. The muscles that showed some clinical functions were selected for monitoring. In all patients the best three bilateral muscles were selected. In two patients the anal sphincter muscle was used. In this study TCE-MEP monitoring was possible in all patients. The responses were low, but reliable and consistent.

The study with 145 patients included 39 patients who had preexistent deficits. There were no false negatives, in other words, no unnoticed postoperative increased neurological deficits occurred. This confirms the result of the first study mentioned that TCE-MEP monitoring in patients with neurological deficit is possible and reliable [28].

VII. PITFALLS OF TCE-MEP

A. False Positives

During surgery, muscle responses are influenced by multiple factors that could potentially reduce the amplitude below the accepted criteria, which would produce false positive outcomes. Factors that influence response amplitude are blood pressure, temperature, anesthetics, and technical disturbances.

To our knowledge, no studies of false negatives have been reported confirming the high sensitivity of TCE-MEP monitoring. However, false positives do occur, causing inconvenient interruptions during the surgical procedure. In our study, the chosen criterion of one muscle group showing a response amplitude decrease of 80% or more resulted in 10 false positives out of 145 patients. We defined a false positive as a nonsurgical induced amplitude decrease, for which no technical, anesthetic, or hemodynamic cause could be found [28].

A stricter criterion creates fewer false positives, but as a consequence, the sensitivity decreases. In our opinion, a 100% sensitivity of TCE-MEP has the highest priority, which inevitably results in some false-positive outcomes. Obviously, it is much better to have false-positive than false-negative readings, when the consequence of a false negative could be a permanent neurological deficit.

In order to lower the false-positive results it is important to distinguish the surgically induced neurological ischemia from technically, anesthetically, and hemodynamically induced changes. Therefore it is important to work with an experienced trained team, an anesthetic protocol (see Sec. VI. A), optimal technical monitoring (see Sec. VI. B), and a protocol checklist.

A three-step protocol checklist should be used whenever a decrease in amplitude occurs. First, equipment should be checked for technical malfunctions (such as loose electrodes) that could cause amplitude disturbance and any such problems should be solved. Second, systemic and anesthetic circumstances have to be checked and normalized when possible. Systemic and

anesthetic problems, such as a drop in mean arterial pressure (MAP) below 60 mmHg, major blood loss, and/or a decrease in body temperature, must be identified and solved. After technical failure and systemic or anesthetic problems have been ruled out as the cause for the decreased response amplitude, the most recent surgical action can be considered to be the probable cause of the amplitude decrease.

B. TCE-MEP and Preexisting Neurological Deficits

TCE-MEP monitoring has been shown to be possible in patients with preexisting neurological deficits (see Sec. VI. E). TCE-MEP monitoring has proven to be reliable. However, it appears that variation of amplitude occurs more often in this patient category. In the study we performed, 39 of 145 patients had preoperative neurological deficits. TCE-MEP amplitude decreases occurred in 26% of these neurological compromised patients: in 5 patients due to neurological damage and in 5 patients due to systemic or anesthetic changes. This was more than in the group of preoperatively neurological intact patients (11%), but the differences are not statistically significant [28].

VIII. CONCLUSIONS

The improvements in TCE-MEP monitoring have led to the reliable use of this technique in a broad surgical area. TCE-MEP offers some important advantages compared to SSEP. TCE-MEP provides reliable and immediate monitoring of the motor pathways, and to date no false negatives have been reported. The multiple monitoring sites make selective monitoring possible, even in patients with preexisting neurological deficits. For a warning of impending neurological damage, the criterion of one muscle site showing a decrease of 80% or more from baseline value makes TCE-MEP a practical and valuable monitoring device for spinal surgery. Therefore, we consider TCE-MEP to be superior to SSEP in neuromonitoring during spinal surgery for monitoring the motor pathways.

REFERENCES

1. Astrup J, Siesjö B, Symon L. Thresholds in cerebral ischemia: the ischemic penumbra zone. Stroke 1981; 12:723–725.
2. Barker AT, Jalinous R, Freeston IL. Non-invasive magnetic stimulation of the human motor cortex. Lancet 1985; 1:1106–1107.
3. Ben-David B, Haller G, Taylor P. Anterior spinal fusion complicated by paraplegia. A case report of false negative somatosensory evoked potential. Spine 1987; 12:536–539.
4. Calancie B, Harris W, Broton JG. Threshold-level multipulse transcranial electrical stimulation of motor cortex for intraoperative monitoring of spinal motor tracts: description of method and comparison to somatosensory evoked potential monitoring. J. Neurosurg 1998; 88(3):457–470.
5. Calancie B, Klose KJ, Baier S. Isoflurane-induced attenuation of motor evoked potentials caused by electrical motor cortex stimulation during surgery. J. Neurosurg 1991; 74:879–904.
6. Dawson GD. Cerebral response to electrical stimulation of peripheral nerve in man. J. Neurol. Neurosurg. Psychiatry 1947; 10:137–140.
7. Dawson GD, Sherman JE, Kanim L. Spinal cord monitoring: results of the scoliosis research society and the European Spinal Deformity Society survey. Spine 1991; 16:S361–264.
8. Deletis V, Isgum V, Amassion VE. Neurophysiological mechanisms underlying motor evoked potentials in anesthetized humans. Part 1. Recovery time of corticospinal tract direct waves elicited by pairs of transcranial electrical stimuli. Clin Neurophysiol 2001; 112:438–444.

9. Deletis V, Rodi Z, Amassian VE. Neurophysiological mechanisms underlying motor evoked potentials in anesthetized humans. Part 2. Relationship between epidurally and muscle recorded MEPs in man. Clin. Neurophysiol 2001; 112:445–452.
10. Deletis V, Isgum V, Rodi Z. New evidence on corticospinal tract behavior after repetitive stimulation of the motor cortex. Electroenceph. Clin. Neurophysiol 1995; 97:S195–S196.
11. Deutch H, Arginteanu M, Manhart K. Somatosensory evoked potential monitoring in anterior thoracic vertebrectomy. J Neurosurg 2000; 92(3):155–161.
12. Edmonds HL, Paloheimo MP, Backman MH. Trans cranial magnetic motor evoked potentials (tc-mmep) for functional monitoring of motor pathways during scoliosis surgery. Spine 1989; 14: 683–686.
13. mc Ewen GD, Bunnel WP, Sriram K. Acute neurological complication in the treatment of scoliosis. J. Bone Joint Surg 1975; 57:404–408.
14. Gugino LD, Aglio LS, Segal ME. Use of transcranial magnetic stimulation for monitoring spinal cord motor pathways. Semin Spinal Surg 1997; 9:315–336.
15. Haghighi SS, York DH, Gaines RW. Monitoring of motor tracts with spinal cord stimulation. Spine 1994; 19:1518–1523.
16. Inghilleri M, Berardelli A, Cruccu G. Motor potentials after paired cortical stimuli. Electroenceph. Clin. Neurophysiol 1990; 77:382–389.
17. Jellinek D, Jewkes D, Jewkes FFRACS. Noninvasive intra-operative monitoring of motor evoked potentials under propofol anesthesia: effects of spinal surgery on the amplitude and latency of motor evoked potentials. Neurosurgery 1991; 29:551–557.
18. Jellinek D, Platt M, Jewkes D. Effects of nitrous oxide on motor evoked potentials recorded from skeletal muscle in patients under total anesthesia with intravenously administered propofol. Neurosurgery 1991; 29:558–562.
19. Jones SJ, Harrison R, Koh KF. Motor evoked potential monitoring during spinal surgery: responses of distal limb muscles to trans-cranial cortical stimulation with pulse trains. Electroencphalogr Clinical Neurophysiol 1996; 100:375–383.
20. Journee HL, Polak HE, Langeloo DD. Double train transcranial stimulation may improve the success rate of MEP monitoring with FDA approved electrical stimulators. Clin Neurophysiol 2002.
21. Kalkman CJ, Been HD, Ongerboer de Visser BW. Intraoperative monitoring of spinal cord function: a review. Acta Orthop. Scand 1993; 64(3):114–123.
22. Kalkman CJ, Been HD, Ubags JH. Improved amplitude of intraoperative myogenic evoked response after paired and transcranial electrical stimulation. Anesthesiology 1993; 79:A179.
23. Kalkman CJ, Drummond JC, Kennelly NA. Intraoperative monitoring of tibialis anterior muscle motor evoked responses to transcranial electrical stimulation during partial neuromuscular blockade. Anesth Analg 1992; 75:584–589.
24. Kalkman CJ, Drummond JC, Ribberink AA. Low concentrations of isoflurane abolish motor evoked responses to transcranial electrical stimulation during nitrous oxide/opioid anesthesia in humans. Anesth. Analg 1991; 73:410–415.
25. Kalkman CJ, Drummond JC, Ribberink AA. Effects of propofol, etomidate, midazolam, and fentanyl on motor evoked responses to transcranial electrical or magnetic stimulation in humans. Anesthesiology 1992; 76:502–509.
26. Lang EW, Beutler AS, Chesnut RM. Myogenic motor evoked potential monitoring using partial neuromuscular blockade in surgery of the spine. Spine 1996; 21(3):1676–1686.
27. Langeloo DD, Journee HL, Polak B. A new application of TCE-MEP: spinal cord monitoring in patients with severe neuromusular weakness undergoing corrective spine surgery. J. Spinal Disord 2001; 14(3):445–448.
28. Langeloo DD, Lelivelt A, Journee HL. M. TCE-MEP monitoring during spinal deformity surgery. A study of 145 patients. Spine 2002; 28(10).
29. Lesser RP, Raudzens P, Luders H. Post-operative neurological deficits may occur despite unchanged intraoperative somatosensory evoked potentials. Ann Neurol 1986; 19:22–25.
30. Merton PA, Morton HB. Stimulation of the cerebral cortex in the intact human subject. Nature 1980; 22:285–287.

31. Nagle KJ, Emerson RG, Adams DC. Intraoperative monitoring of motor evoked potentials: a review of 116 cases. Neurology 1996; 47:999–1004.
32. Nuwer MR, Dawson EG, Carlson LG. Somatosensory evoked potential spinal cord monitoring reduces neurological deficits after scoliosis surgery: results of a large multi-center survey. Electroencephalogr. Clin. Neurophysiol 1995; 96:6–11.
33. Owen JH, laschinger J, Bridwell KH. Sensitivity and specificity of somatosensory and neurogenic motor evoked potentials in animals and humans. Spine 1988; 13:1111–1118.
34. Padberg AM, Wilson-Holden TJ, Lenke LG. Somatosensory and motor evoked potential monitoring without a wake-up test during idiopathic scoliosis surgery: an accepted standard of care. Spine 1998; 23:1392–1400.
35. Pechstein U, Cedzich C, Nadstawek J. Transcranial high-frequency repetitive electrical stimulation for recording myogenic motor evoked potentials with the patient under general anesthesia. Neurosurgery 1998; 39:335–343.
36. Schonle PW, Isenberg C, Crozier TA. Changes of transcranially evoked motor responses in man by midazolam, a short acting benzodiazepine. Neurosci Lett 1989; 101:321–324.
37. Tabaraud F, Boulesteix JM, Moulies D. Monitoring of the motor pathway during spinal surgery. Spine 1993; 18(3):546–550.
38. Ubags LH, Kalkman CJ, Been HD. The use of a circumferential cathode improves amplitude of intraoperative electrical transcranial myogenic motor evoked responses. Anesth Analg 1996; 82(3): 1011–1014.
39. Ubags LH, Kalkman CJ, Been HD. The use of ketamine or etomidate to supplement sufentanil/N20 anesthesia does not disrupt monitoring of myogenic transcranial motor evoked responses. J Neurosurg Anesth 1997; 9:228–233.
40. Van Dongen EP, Ter Beek HT, Schepens MA. Within patient variability of lower extremity muscle responses to transcranial electrical stimulation with pulse trains in aortic surgery. Clin Neurophysiol 1999; 110:1144–1148.
41. Vauzuelle C, Stagnara P, Jouvinrouw P. Functional monitoring of spinal cord activity during spinal surgery. Clin. Orthop 1973; 93:173–178.
42. York DH. A critical evaluation of the 50% criterion in SEP monitoring. Proceedings of the American Society of Neuropsychological Monitoring Annual Meeting. MO: St. Louis, 1995.
43. Zornow MH, Grafe MR, Swenson MR. Preservation of evoked potentials in a case of anterior spinal artery syndrome. Electroencephalogr. Clin Neurophysiol 1990; 77:137–139.

32

The Physical Properties and Biocompatibility of Plasma-Sprayed Hydroxyapatite Coating

T. M. Lee and E. Chang
National Cheng Kung University
Tainan, Taiwan

C. Y. Yang
National Cheng Kung University Medical Center
Tainan, Taiwan

I. INTRODUCTION

The increasingly widespread use of biomedical devices manufactured from titanium or its alloys is due to their relative excellent to corrosion, and thus favorable biocompatibility, compared to stainless steel and cobalt chromium alloys [1,2]. The apparent success of titanium or its alloys in implants has been attributed to the existence of a thin, stable passivating oxide layer of TiO_2. Having the same chemical and crystallographic structure as the apatite of living bone, bioactive hydroxyapatite (HA) ceramic can bond physicochemically with bone and promote bone growth onto its surface [3,6]. HA is therefore considered an excellent bone substitute [7,8]. However, it was reported to be susceptible to fatigue failure [9], a property common to all ceramic materials. As a result, the HA implant can be applied only if either no forces at all or only compressive forces act on the implant. This problem can theoretically be solved by applying an HA coating (HAC) to a metal substrate; this device has both the required biocompatibility and the required mechanical properties. Plasma-sprayed HA-coated Ti alloy implants exhibiting excellent biocompatibility and satisfactory mechanical properties have been investigated as an approach to achieving reliable implant-to-bone fixation in clinical studies [10,11].

The microstructure and phase composition of HACs, which vary according to the plasma-spraying parameters used, have been evaluated in vitro [12]. However, the detailed characteristics of HACs are not completely clear. According to some studies [13,14], coating characteristics such as microstructure, thickness, mechanical properties, phase composition, crystallinity and chemical composition of HACs influenced biological responses. Therefore, these characteristics must be studied. In addition, some studies with regard to plasma-sprayed HACs can promote the formation of mineralized new bone at its surface [15,16]. Therefore, it is generally described as osteoconductive. However, there are few quantitative studies on osteoconductivity and osseointegration of HACs reported. By introducing the Chinese Coin implant model initiated by Yang et al. [15], the osteoconduction and the osseointegration of the implants was quantitatively assessed. One of the advantages of this implant model was that the histological properties of different surface-treated implants could be compared simultaneously.

The interaction occurring at the bone/biomaterial interface largely determines the success or failure of an implant [16,17]. The outcome at this site is dependent, in part, on successful bone formation. The osteoblast is the cell type responsible for deposition of bone within the interface zone between implant and host tissue. It plays a fundamental role in the successful clinical outcome of an implant. Since these responses may subsequently affect the fixation of implants, it is important to understand the reaction between osteoblasts and biomaterials. The osteoblast culture model has been widely adopted to evaluate the biocompatibility of biomaterials because the tissue/implant interface can be partially reproduced. This system allows early evaluation of the degree of cytocompatibility under controlled condition.

The aim of this chapter is to clarify in vitro the various characteristics of plasma-sprayed HACs and to evaluate in vivo the effect of the coating characteristics on the biological responses and fixation of HACs.

II. EFFECT OF PLASMA-SPRAYED PARAMETERS ON THE CHARACTERISTICS OF HYDROXYAPATITE COATINGS

To improve the bioactivity of metal implants, HA are generally applied as coatings. Various techniques, such as sputtering [18,20], electron beam deposition [19], laser deposition [21,22], and plasma spraying [10,11,23], have been employed to deposit HAC on various metal substrates. Among these techniques, plasma spraying has been widely used in the commercial product of HA-coated implants, because the plasma-sprayed coatings are a highly cost-effective, straightforward, simple, qualitatively controlled, and versatile method. Simply stated, the plasma gun incorporates a cathode (electrode) and an anode (nozzle) separated by a small gap forming a chamber between the two. DC power is applied to the cathode and arcs across to the anode. At the same time, gases are passed through the chamber. The powerful arc is sufficient to strip the gases of their electrons, and the state of matter known as plasma is formed. As the unstable plasma recombines back to the gaseous state, thermal energy is released. Because of the inherent instability of plasma, the ions in the plasma plume rapidly recombine to the gaseous state and cool. At the point of recombination, temperatures can be 6,000–16,000°C. When the coating material is injected into the gas plume, it is melted and propelled towards the target substrate. Because of the high temperature and enthalpy during the plasma-sprayed process, the impurity phases [α-$Ca_3(PO_4)_2$, β-$Ca_3(PO_4)_2$, $Ca_4P_2O_9$, and CaO] and amorphous phases are generally identified in the plasma-sprayed HAC. The amorphous and impurity phases have a high dissolution rate in aqueous solutions, and this will decrease the mechanical properties and loose in the firm fixation between the implant and surrounding bone tissue. Decreasing the amorphous and impurity phases is very important for the plasma-sprayed HAC.

Table 1 shows three groups of HACs on Ti-6Al-4V substrates (ASTM F-136) using different spraying parameters [24]. For P1-HAC, only Ar gas was used; for P2-HAC, helium (He) was added to argon; and for P3-HAC, hydrogen (H_2) was added to argon. Other spraying parameters, including the flow rate of carrier gas, powder feed rate, spray power, stand-off distance, and surface speed, were fixed. After plasma spraying, the microstructure of the HACs with different spraying parameters was examined by scanning electron microscopy (SEM). Three types of surface morphologies were distinguished: P1-HAC was a partially molten coating with some unmelted powder and a higher porosity (Fig. 1a); P2-HAC was a molten coating containing molten splats and lower porosity (Fig. 1b); P3-HAC was a completely molten coating with well-flattened splats and the lowest porosity (Fig. 1c). The main difference between these coatings was the extent of melting, attributed to either the heat transfer ability or the level of energy

Table 1 Plasma-Spraying Parameters Employed for preparing HACs

Parameters	Hydroxyapatite coatings		
	P1	P2	P3
Primary gas, flow rate (L/min)	Ar, 41	Ar, 41	Ar, 41
Secondary gas, flow rate (L/min)	—	He, 30	H_2, 8
Powder carrier gas, flow rate (L/min)	Ar, 3.2	Ar, 3.2	Ar, 3.2
Powder feed rate (g/min)	20	20	20
Power (kW)	40.2	40.2	40.2
Stand-off distance (cm)	7.5	7.5	7.5
Surface speed (cm/min)	2400	2400	2400
Transverse speed (cm/min)	60	60	60

Source: Ref. 24.

content exerted by different combinations of plasma gases. For P1-HAC, as unmelted powder appeared all over the surface, the extent of coating melting was apparently poor. As a consequence, large-scale porosities formed during the deposition of unmelted powders. For P2-HAC, the extent of melting was improved; instead of unmelted powder, molten splats appeared as the major part of the surface, hence the porosity decreased. Because of the molten, well-flattened splats in the topography of P3-HAC, the extent of coating melting of this specimen was superior to that of the others. The porosity of the P3-HAC specimens, as a result, was minimized.

By x-ray diffractometry (XRD) analysis (Fig. 2a) [24], the HA powder show a well-crystallized single phase of $Ca_{10}(PO_4)_6(OH)_2$. Comparing Figure 2a with Figure 2b–d (the XRD patterns of HACs), the differences in the composition and crystallinity between the HACs and HAP can be seen. Several impurity phases, including α-$Ca_3(PO_4)_2$ (α-TCP), β-$Ca_3(PO_4)_2$ (β-TCP), $Ca_4P_2O_9$ (TP), and CaO, were identified in the HACs, which is consistent with other studies [12,25]. The impurity phase contents in HACs and crystallinity of $Ca_{10}(PO_4)_6(OH)_2$ is shown in Table 2. It is clearly seen from Table 2 and Figure 1 that P3-HAC contained the highest amount of impurity phases and the least crystallinity. The formation of impurity phases and decreased crystallinity of $Ca_{10}(PO_4)_6(OH)_2$ in HACs was due to the fact that the HA material was supercooled from a very high temperature to room temperature during plasma spraying and the HA phase decomposed to form impurity phases and tended to be amorphous with less crystallinity. The decomposition of HA probably proceeds via several steps. First, at a high temperature (possibly above 1400°C), HA can decompose to form an α-TCP and TP phase as follows [26]:

$$Ca_{10}(PO_4)_6(OH)_2 \rightarrow 2\alpha\text{-}Ca_3(PO_4)_2 + Ca_4P_2O_9 + H_2O \quad (1)$$

Subsequently, upon cooling, decomposition of $Ca_4P_2O_9$ occurs [26]:

$$3Ca_4P_2O_9 \rightarrow Ca_{10}(PO_4)_6O_2 + 2CaO \quad (2)$$

Finally, α-$Ca_3(PO_4)_2$ transforms β-$Ca_3(PO_4)_2$ at about 1100°C [26]. When the spraying parameters result in high enthalpy, the impurity phase might increase and the crystallinity decrease. Because P3-HAC was produced using spraying parameters that provided high enthalpy, it had the highest amount of impurity phases and, the least crystallinity. The appearance of impurity

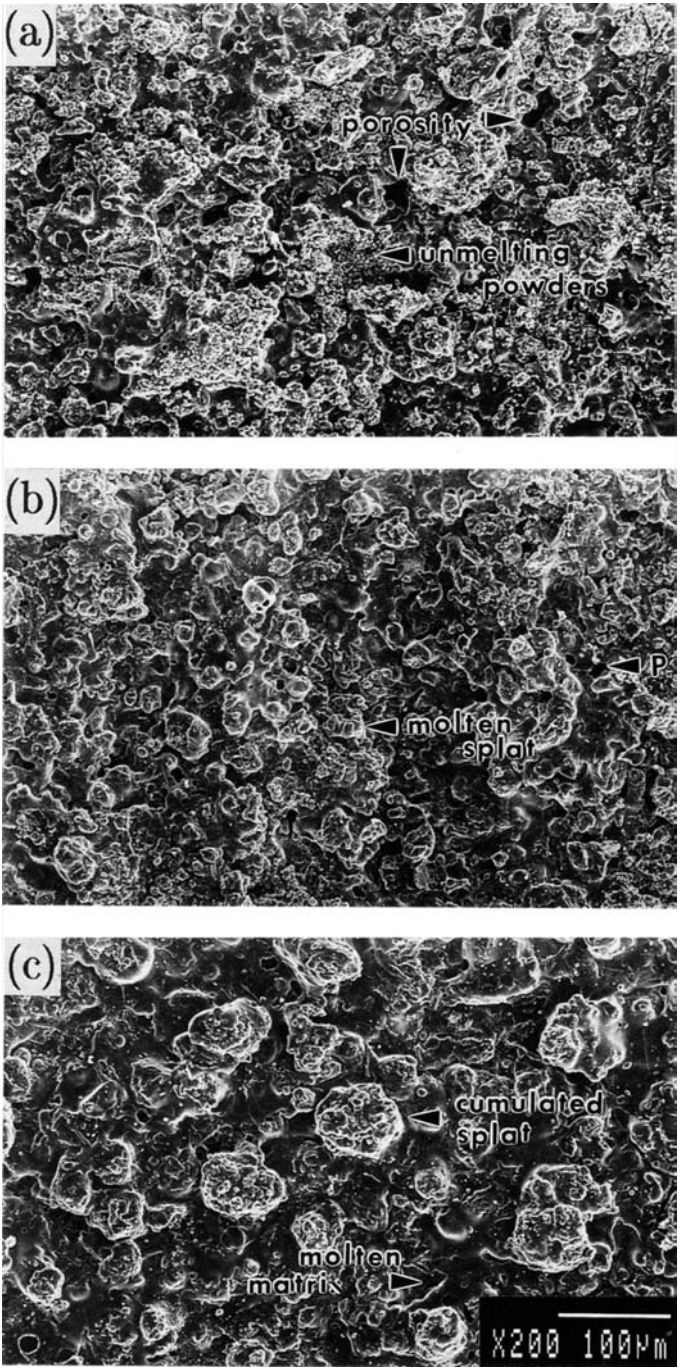

Figure 1 Surface morphology of (a) P1-HAC with unmelted powder and higher porosity, (b) P2-HAC with molten splats and lower porosity, and (c) P3-HAC with well-flattened splats and the lowest porosity. (From Ref. 24.)

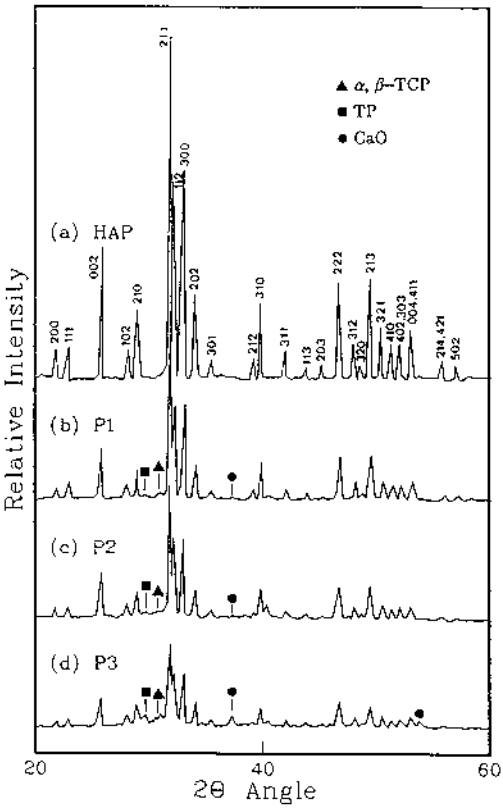

Figure 2 x-ray diffraction pattern (Cu Kα) for (a) HAP, (b) P1-HAC, (c) P2-HAC, and (d) P3-HAC. It was revealed that the HAP has a well-crystallized single phase of $Ca_{10}(PO_4)_6(OH)_2$. P3-HAC contained the highest amount of CaO phase and the lowest crystallinity. (From Ref. 24.)

Table 2 Characteristics of Hydroxyapatite Coatings

	HA coatings		
Characteristics[a]	P1	P2	P3
Concentration of impurity phases, wt%			
$Ca_4P_2O_9$	0.05	6.67	15.23
α-$Ca_3(PO_4)_2$	5.32	4.26	16.38
β-$Ca_3(PO_4)_2$	4.61	4.46	12.77
CaO	0.11	0.58	5.99
Index of crystallinity, %	81.39	70.01	48.53

[a] The concentration of the impurity phases and the index of crystallinity of the HACs were quantitatively determined by the internal standard method and the intensity ratio method, respectively.
Source: Ref. 24.

phases and the biological responses of these phases in HACs are of concern. Because α-TCP and β-TCP were reported to be quickly bioresorbed [27,28], the resolvability within the body would leave a loosened structure, which might significantly decrease the mechanical strength of HACs. Therefore, it is suggested that the appearance of the TCP phase in HACs should be avoided. With respect to the TP phase, some reports showed that TP could hydrolyze to form HA and $Ca(OH)_2$ according to the following reaction [29]:

$$3Ca_4P_2O_9 + 2H_2O \rightarrow Ca_{10}(PO_4)_6O_2 + 2Ca(OH)_2 \quad (3)$$

The existence of $Ca(OH)_2$ was suggested to be detrimental to the implantation. Since the CaO phase had no biocompatibility at all, it was considered to be the most detrimental phase for implantation. In summary, the level of impurity phases, especially the CaO phase, present in the HAC should be as low as possible, and the amorphous component in HACs is undesirable because of rapid resorption [30]. Well-crystallized HACs with pure phases are ideal for clinical application.

Except for the existence of amorphous and impurity phases, HACs also show an unstable state compared with original HA powder (HAP). The instability of HACs can be identified using differential thermal analysis (DTA). As shown in Figure 3, DTA tracing curves for HAP and HAC show three dominant endothermic peaks at specified temperatures: peak 1 at 1470°C, peak 2 at 1450°C, and peak 3 at 1315°C. For the HAP (Fig. 3d), only peak 1 was detected and referred to the decomposition of HA material [Eq. (1)]. In contrast to the HAP, however, the HACs (Fig. 3a–c) contained other peaks (2 and 3). Very close to peak 1, peak 2 at 1450°C was also regarded as due to decomposition of the HA phase. Peak 3, at a lower temperature (1315°C), was suggested to represent the phase decomposition of [Eq. (2)]. Because the temperature of peak 2 was lower

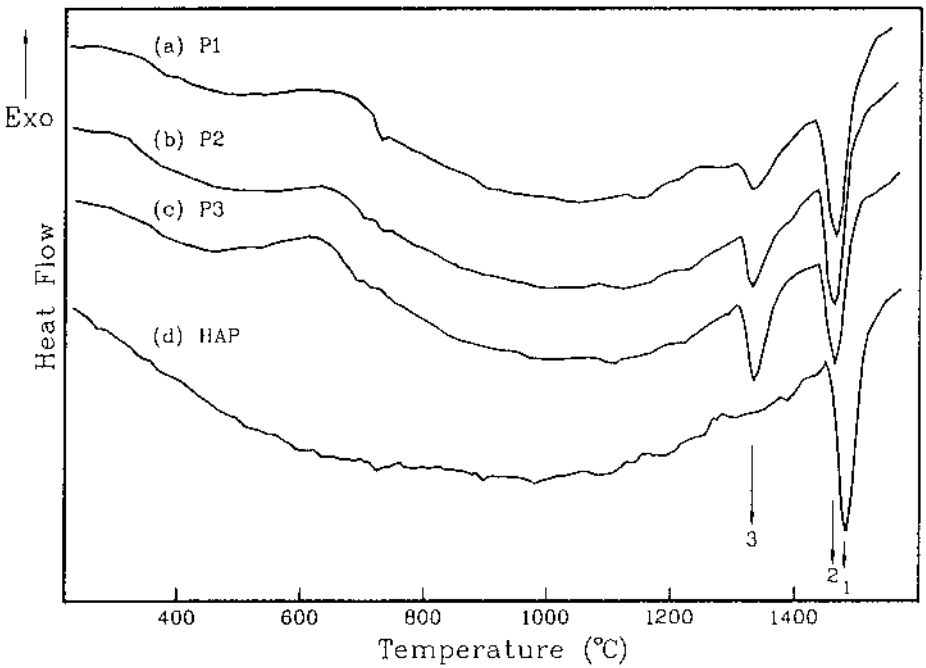

Figure 3 DTA tracing curves for (a) P1-HAC, (b) P2-HAC, (c) P3-HAC, and (d) HAP. Exo = exothermic. For an explanation of peaks 1, 2, and 3, see the text. (From Ref. 24.)

than that of peak 1, the HACs seemed to be less stable than HA powder. The reasons for unstable HACs are: (1) loss of OH^- ion in the HAC during plasma spraying, (2) the internal stress in the coating, and (3) vaporization of the elements of HAP, especially phosphorus, during the high temperature and enthalpy process. As shown in Figure 4 [24], the infrared (IR) spectra of HAP and HACs were recorded using Fourier transformation IR spectrometry. In the IR spectra, two peaks attributed to the vibrations of the OH^- ion were examined [31]: the stretching mode at 3600 cm^{-1} and flexural mode at 630 cm^{-1}. In the spectrum of HAP (Fig. 4d), two expected vibrations of OH^- ion were present. The spectra for the HACs (Fig. 4a–c), however, are considerably different. The OH^- stretching vibration disappears almost completely, and the bending vibration cannot be detected, indicating that the amount of OH^- ions present in the HAC has decreased. HA attains a stable phase at room temperature only if the ambient atmosphere contains water [26]. This indicates that it will be unstable and undergo a phase transformation when the partial vapor pressure of water is decreased. The observation of IR spectra is consistent with the results of DTA analysis given above. The decrease in the number of OH^- ions has a negative effect on the stability of HA phase. It is well known that residual stress is inherently induced in the coating by the plasma spray method [32]. The residual stress is caused by the difference in thermal properties between the coating and the substrate materials combined with the complicated solidification process of the coating. Generated from inhomogeneously distributed nonelastic changes of dimensions, residual stress is the internal stress existing in a body under no external load condition [33]. The research has shown that the measured stresses in plasma-

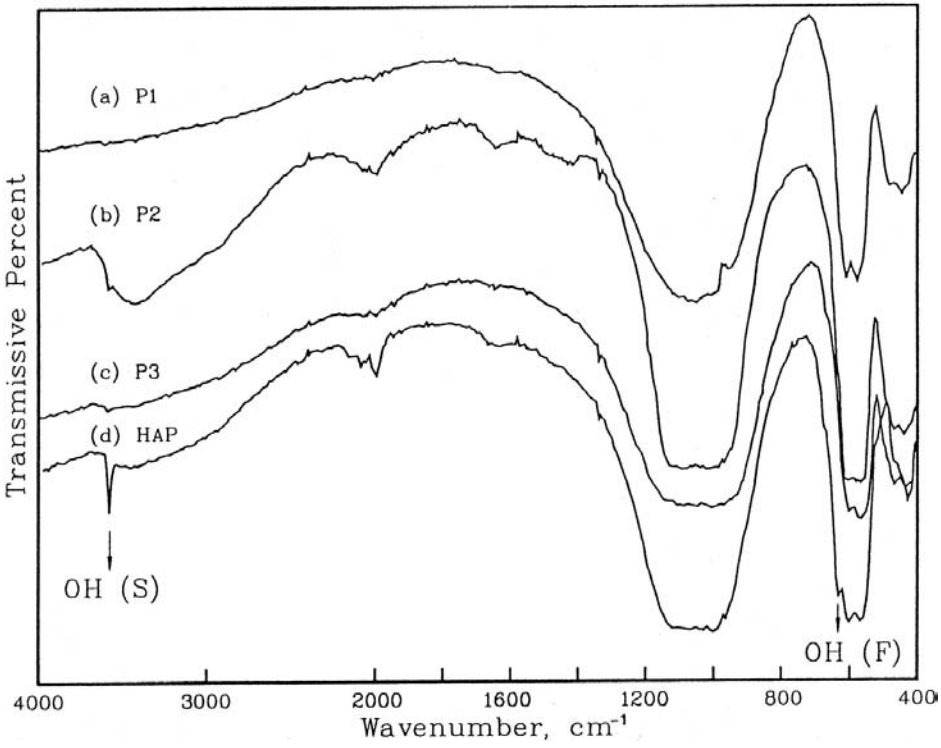

Figure 4 IR spectra for (a) P1-HAC, (b) P2-HAC, (c) P3-HAC, and (d) HAP. The OH^- ion content of the HACs was partially lost during plasma spraying. S = stretching; F = bending. (From Ref. 24.)

Table 3 Ca:P Molar Ratio Measurements for HAP and HACs

Sample	Ca:P molar ratio
HAP	1.69
P1-HAC	1.79
P2-HAC	1.80
P3-HAC	1.85

Source: Ref. 24.

sprayed HAC were in compressive states. The residual stress is suggested to decrease the stability of HAC compared with HAP. Table 3 shows the the Ca:P molar ratios for HAP and HACs (spalling coatings) calculated from atomic emission spectrometry (AES). Because the Ca:P molar ratio of stoichiometric HA is 1.67, the value for HA powder (Ca:P = 1.69) suggests that HA powder has a near-theoretical chemical composition. However, for each coating the measured Ca/P value increases. Because of the high temperature and enthalpy involved in the spraying process, the elements of HAP, especially phosphorus, with a low melting point (44°C) and boiling point (280°C), have a greater opportunity to vaporize during the spraying process. This is expected to cause an increase in the Ca:P values for each coating. Since the P3-HAC was sprayed using the highest temperature, the maximum value of Ca:P (1.85) was measured for this coating.

Although firm fixation of HA-coated implants was achieved, the failure mode of HAC was mainly observed within the coating layer itself or at interface of coating/metal substrate by push-out test [34, 35]. The mechanical properties, especial in interface bonding strength, of HAC are very important in clinical use. Table 4 shows the bonding strength data of P1-, P2-, and P3-HAC measured from the adhesion test (ASTM C-633) [24]. As shown in the table, P3-HAC displayed a significantly higher bonding strength than the other coatings, which could be explained by the spraying parameters of HACs. Among the three types of HAC, P3-HAC showed the densest structure and lowest porosity because of the high temperature and enthalpy of the spraying process. To provide long-term implant fixation, the bonding strength at the HAC/Ti-6 Al-4V interface should be as high as possible.

To summarize, impurity phases and less crystallinity were identified in plasma-sprayed HACs on Ti-6Al4V substrates because of high temperature and enthalpy and HACs compared with HAP become unstable because of OH^- ion loss, residual stress, and higher Ca:P molar ratio. Among three different HACs, P1-HAC, with the lowest impurity phases and higher crystallinity, showed a looser structure and the lowest bonding strength. It is difficult to achieve both high

Table 4 Bonding Strength Measurements for HACs

Sample	Bonding strength (MPa)
P1-HAC	23.51
P2-HAC	27.15
P3-HAC	30.25

Source: Ref. 24.

bonding strength and good biocompatibility for plasma-sprayed HAC on metal substrates. Thus, a compromise of spraying parameters is recommended for optimization of plasma-sprayed HAC.

III. EFFECT OF HYDROXYAPATITE COATING SURFACE ON CELL ATTACHMENT OF NEONATAL RAT CALVARIAL OSTEOBLASTS

In the application of biomaterials in orthopedic surgery, bone cell response and biocompatibility of material play important roles in the bone/implant interface for long-term survival of the prosthetic implant fixation. The effect of the biocompatibility on bone apposition and bone formation is associated with the bone cell response induced by biomaterials. Recent studies used the model of cell culture to investigate the biological response of bone/implant interface during the early phase [36,37]. The factors of chemical composition, surface topography, surface energy, and surface roughness of biomaterials would affect the bone cell response of implants and further influence the biocompatibility in clinical use.

Some researches have investigated the influence of surface roughness on bone integration of implants [38,39]. In vivo, rough surfaces were found to produce better bone fixation than smooth surfaces [38,39], suggesting that this surface property might have a direct effect on the attachment of osteoblasts and their subsequent proliferation and differentiation. However, surface roughness of HAC could be manipulated by using different plasma-sprayed parameters. As described above, the different phase contents and crystallinity of HAC would be changed by different plasma spray parameters. Maintaining the physical properties of HAC is very important for the evaluation of roughness on cellular responses.

As shown in Table 5 [40], the average surface roughness of as-sprayed HAC is significantly higher than the polished HAC (HAC-p), ground by SiC papers and finally polished using a 1.0 μm Al_2O_3 slurry. By XRD analysis, the phase composition of HAC consisted of HA phase and several impurity phases. These impurity phases include α-$Ca_3(PO_4)_2$ (α-TCP), β-$Ca_3(PO_4)_2$ (β-TCP), $Ca_4P_2O_9$, and CaO. After polishing, the phase composition of HAC-p is consistent with HAC specimens. The results indicate that the polishing treatment has not changed the phase composition and contents in HACs. Figure 5 shows the number of neonatal rat calvarial cells of different specimens (HAC and HAC-p) after 3-, 6-, and 24-hour culture in medium containing 4% fetal bovine serum (FBS) in Dulbecco's modified Eagle medium (DMEM) [40]. The level of cell attachment to the surface of HAC-p is significantly higher than for HAC during all culture periods. These higher levels of cell attachment on HAC-p could be explained by the cell morphology. The osteoblasts on the smoother surface exhibit a broadly spread and flattened morphology compared to cuboidal morphology on the rougher surface. Other researchers concluded that more flattened and well-spread cells would show higher proliferation rates than would round spherical cells. For example, Folkman and Moscona [41] and Archer et al. [42] reported that one of the main regulators of proliferate rate in anchorage dependent cells is shape.

Table 5 Surface Roughness of As-Sprayed HAC and Polished HAC

Sample	Roughness (μm)
As-sprayed HAC	0.67
Polished HAC	10.37

Source: Ref. 40.

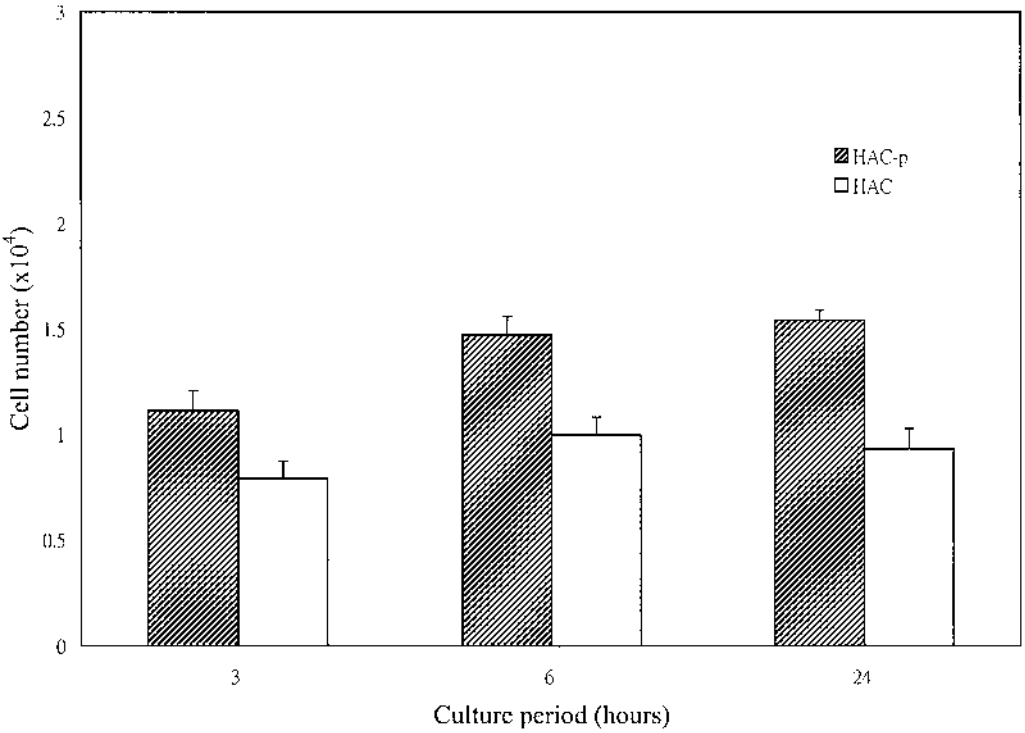

Figure 5 Under 4% serum condition, the growth of osteoblasts on different specimens. Values are the mean ± standard deviation ($n = 5$). (From Ref. 40.)

In their studies, the cells attached to materials with less spread showed lower proliferation rates than those on the material with better spreading. Similar results were also observed by Hunter et al. [43], who found that the surface of biomaterials with the greatest number and area of adhesion plaque spread well and flattened, while those materials with the least number of adhesion plaque were more rounded and less spread.

Figure 6 illustrates osteoblast attachment versus time for HAC and HAC-p under 10% FBS in DMEM [40]. Increasing the content of FBS from 4 to 10% in medium, the higher level of osteoblast attachment is found on the surface of specimens under 10% serum, and significant differences are found between the same specimens cultured with two different contents of FBS in all experimental periods. However, a significantly higher level of osteoblast attachment on HAC-p is also found than on HAC during all culture periods. The results indicate that the increasing FBS content has not diminished the factor of HAC surface roughness. As a general rule, cells do not directly bind to material surfaces. According to the results of Eriksson et al. [44], cells associated with the implant surface were almost never seen directly apposed to the implant but were attached to the surface via fibrin strands. After plating, the serum conditioned the reaction of material surface to provide better environment for cell attachment and spreading. In studies by Schneider and Burridge [45] and Bagambisa et al. [46], cell adhesion proteins in serum enhanced cell attachment and spreading. However, the precise composition of the material surface adsorbed protein is not clear. The physical properties of the surface are different from the corresponding bulk of the material. For thermodynamic reasons they contain unsaturated bonds, which lead to the formation of the surface reactive layers and adsorbed contamination

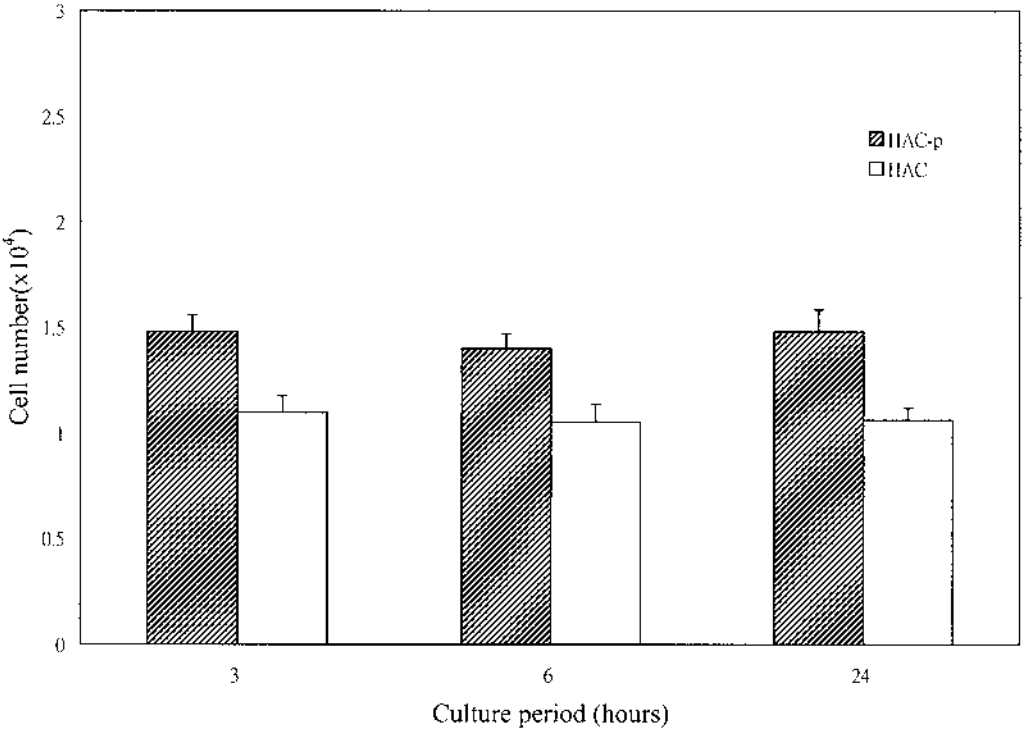

Figure 6 Under 10% serum condition, the growth of osteoblasts on different specimens. Values are the mean ± standard deviation ($n = 5$). (From Ref. 40.)

layers [47]. Although the 4% and 10% FBS conditions show higher cell attachment at the smoother surface (HAC-p) than the rougher surface (HAC) during 3-, 6-, and 24-hour cultures, the results show the optimal surface properties of HAC for osteoblasts attachment only during early periods (up to 24 hours). In both in vivo and in vitro, bone formation is a serial process, and the cell behavior is modified with serial changes of environment. Although HAC-p provides a better surface for osteoblast adhesion during early phase, the effect of biomaterials on later stages of osteoblast differentiation, matrix production, and calcification is as important as cell attachment and plays a major role in long-term implant success. However, in order to comprehend the effects of biomaterials and to obtain a complete interpretation of these events, further investigation of a series experiment at different stages is required.

IV. EFFECTS OF HYDROXYAPATITE COATING ON THE BIOLOGICAL RESPONSES AND FIXATION: A QUANTITATIVE STUDY

Plasma-sprayed HA-coated Ti alloy implants, exhibiting excellent biocompatibility and satisfactory mechanical properties, are currently being investigated as an approach to achieving reliable implant-to-bone fixation. Some studies of plasma-sprayed HA-coated titanium implants have demonstrated that the HAC can promote the formation of normal bone at its surface [10,14]. Therefore, it is generally described as osteoconductive. Furthermore, at the optical microscopic (OM) [10,14] and the SEM levels [48, 49], the evidence of ossseointegration, a direct bone-to-

HAC contact, has been reported. However, few quantitative studies on osteoconduction and osseointegration of HA-coated implant have been reported. The results of biological responses to implants are also influenced by many factors, such as implant models, experimental animals, surgical technique, mechanical testing parameters, sample preparation, etc. Developing the implant model for evaluation of biocompatibility of an orthopedic implant is very important. As shown in Figure 7, the osteoconduction and the osseointegration of Ti-6Al-4V implants with different coatings were evaluated using the Chinese coin implant model. One of the advantages of this implant model was that the histological properties of different surface-treated implants could be compared simultaneously and quantitatively. The concepts of the Chinese coin implant model are rectangular specimens implanted into the predrilled hole in the lateral cortices of dogs. After implantation, the cross-sectional view of the hole with the implant containing simultaneously four different surfaces, and four defective bone regions with approximately equal area, is quite like a Chinese coin (Fig. 7d). The defective bone regions were designed for new bone healing. Therefore, the osteoconductivity and osseointegration of different coatings could be simultaneously and quantitatively compared in the same specimens.

As shown in Figure 8 [24], the defective bone regions at 4-week healing were prominently repaired with new bone for P1-HAC by backscattered electron image (BEI) of SEM. Using a computer-assisted image analysis system, the quantity of defective bone and new bone area of the implants could be precisely measured. Then the osteoconductivity of the implant was represented in terms of the new bone healing index (NBHI), (Fig. 9). The osseointegration of implants was assessed using the apposition index (AI), (Fig. 9). Along the P1-HAC surface, direct bone-to-HAC contact (osseointegration) was observed within a limited area at the interface (Fig. 8), while in other regions bone marrow was apposed to the HAC. At the longer survival time of 6 weeks, the amount of mineralized new bone had increased for all coatings as compared with the amounts after 4 weeks of implantation. Moreover, the new bone showed better direct contact

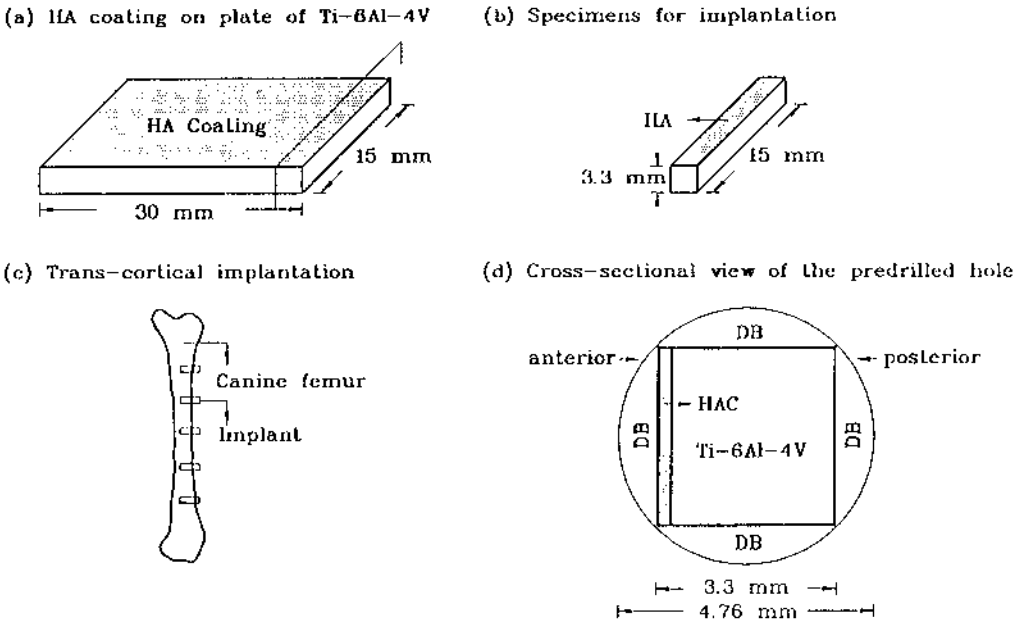

Figure 7 Schematic configuration of the implant model. (From Ref. 50.)

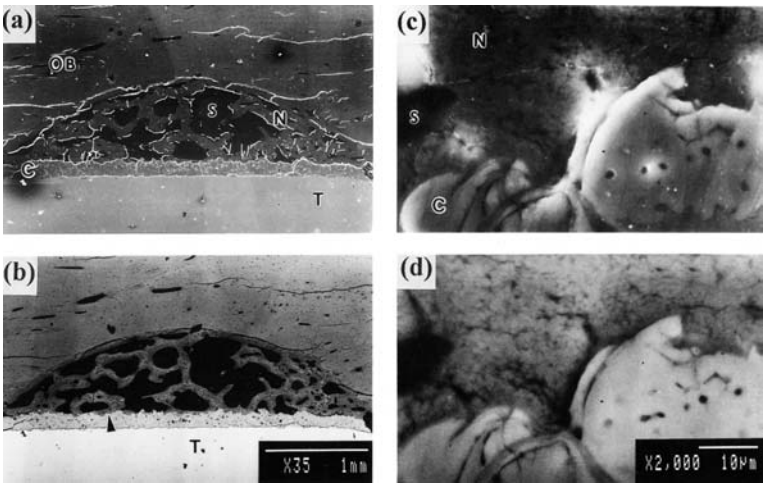

Figure 8 Images of histological section at the defective bone region at the P1-HAC face 4 weeks post/implantation: (a) secondary electron images (SEI)–SEM, (b) back-scattered electron image (BEI)–SEM at the bone-HAC interface, revealing osseointegration; direct bone-to-HAC contact at the of arrow-identified section by higher magnification of (c) SEI-SEM and (d) BEI-SEM. OB, original cortical bone; S, soft tissue; N, new bone; C, HA coating, T, Ti alloy. (From Ref. 24.)

to the HAC. However, after 12 weeks of implantation, the histological features were different from those at 6 weeks. With enormous remodeling canals observed at the P3-HAC/bone interface after 12 weeks (Fig. 10), it was noted that the regions of direct bone/P3-HAC contact had significantly decreased. Moreover, granular particles of about 1–3 μm (Fig. 11) [50], dissociated from the P3-HAC, were obviously observed within the remodeling canal. The granular particles were further proved to be HA by means of energy dispersive spectroscopy (EDS) (Fig. 12) [50].

To evaluate the osteoconduction quantitatively, the NBHI of each implant was calculated for the BEIs. As shown in Table 6 [24], the maximum NBHI of about 90% for all HACs was

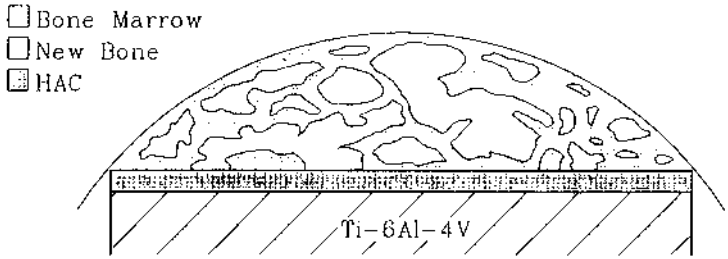

Figure 9 Schematic representation of new bone healing index (NBHI) and apposition index (AI).

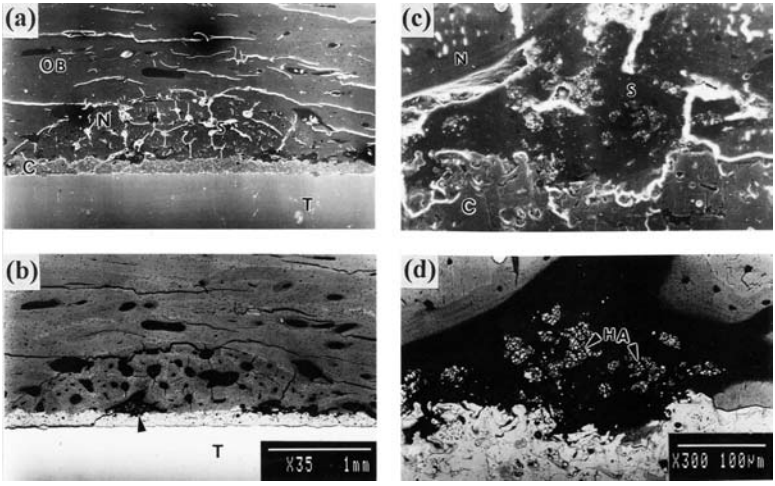

Figure 10 Images of histological section at the defective bone region at the P3-HAC face 12 weeks postimplantation: (a) SEI–SEM, (b) BEI-SEM at the bone/HAC interface, revealing the remodeling canal; partial dissolution of HAC observed at the arrow-identified section by higher magnification of (c) SEI-SEM and (d) BEI-SEM. OB, original cortical bone; S, soft tissue; N, new bone; C, HA coating, T, Ti alloy. (From Ref. 24.)

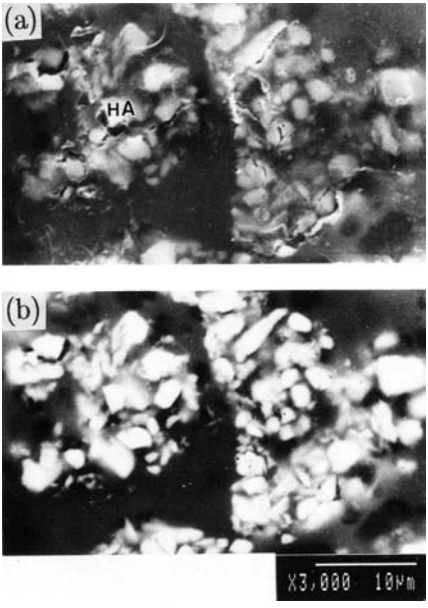

Figure 11 Granular HA particles, 1–3 μm, dissociated from the surface of P3-HAC (arrow, Fig. 10b): (a) SEI-SEM and (b)BEI-SEM. (From Ref. 50.)

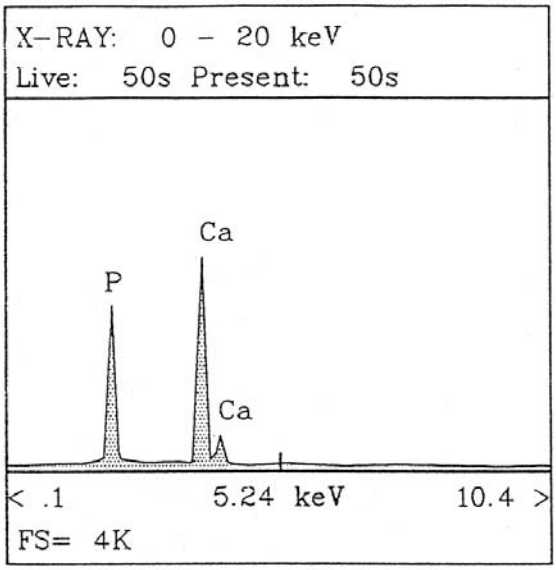

All elements analyzed, NORMALIZED

ELMT	ZAF	% ELMT	ATOM.%
CaK : 2	1.007	68.845	63.084
P K : 2	1.491	31.086	36.863
TiK : 2	0.714	00.070	00.053
AlK : 2	0.904	00.000	00.000
TOTAL		100.00	100.00

Figure 12 EDS analysis of granular particles confirming that these particles were HA. (From Ref. 50.)

reached at 6 weeks postimplantation. This finding led to an important conclusion that the different coating characteristics such as microstructure, phase composition, crystallinity, and chemical composition did not affect the results of NBHI within 6 weeks of healing. However, the NBHI for P3-HAC decreased with significant differences ($p < 0.005$) compared with the other HACs at 12 weeks. Since the maximum NBHI was reached at 6 weeks for all HACs, it was believed that the HACs had a stimulating effect on osteoconductivity within 6 weeks of healing regardless of the differences in coating characteristics. This finding was similar to those of other studies where the simulating influence on bone apposition of plasma-sprayed HACs was reported [38,51]. However, at 12 weeks it was found that the NBHI of the P3-HAC was reduced, showing different behavior compared with the other HACs. Thus, the different coating characteristics seemed to influence the NBHI at this time. Because P3-HAC contained the highest amount of impurity phases and the least crystallinity and highest calcium:phosphorus molar ratio, it was considered to be less stable and prone to biological degradation. As the biodegradation of HAC occurred, more or larger remodeling canals were thought to form, leading to a decrease in NBHI. The finding of partial dissociation of P3-HAC within the remodeling canal, consistent with the

Table 6 New Bone Healing Index (NBHI) Values for HACs

	HA coatings		
Weeks	P1	P2	P3
4	64.50 ± 11.31	64.37 ± 10.01	63.87 ± 10.84
6	90.12 ± 1.95	89.00 ± 4.37	90.00 ± 4.30
12	89.13 ± 3.87	90.15 ± 2.91	80.12 ± 2.99

Unit: %.
Values given is the mean ± standard deviation. In each case, 36 slices were taken for histomorphometry.
The P3-HAC has a lower NBHI ($p < 0.005$) than the other HACs at 12 weeks.
Source: Ref. 24.

results of Gottlander and Albrektsson [52] and Denissen et al. [53], seemed to support the above proposition. The pieces of HA loosened from the HAC were observed within the remodeling canals at the OM level 1 year and 9 months after implantation.

From the observations of BEIs, the evidence of osseointegration was found for all HACs. Apposition index measurements are listed in Table 7. At 4 weeks, an AI value of around 58% was measured for all HACs, and there were no significant differences among the three different HACs. With increasing survival time to 6 weeks, an obvious increase in the mean AI value from approximately 58% to approximately 81% was found. There still were no significant differences in AI data among all HACs 6 weeks postimplantation. With increasing survival time to 12 weeks, the values of AI for P1-HAC and P2-HAC were around 80%, and no statistical difference was observed between 6 and 12 weeks for P1-HAC or P2-HAC. However, an obvious decrease in AI from 81.26% to 65.38% was found for P3-HAC at 12 weeks, and the AI data for P1-HAC and P2-HAC were significantly higher than for P3-HAC. The appearance of remodeling canals was suggested to account for the decrease in AI 12 weeks after implantation.

Although P1-HAC contained few impurity phases, higher crystallinity, better osteoconductivity, and excellent osseointegration, the bonding strength may be too low to acquire strong fixation when implanted in bone. Evaluating the performance and stability of this implant design in the load-bearing situation after long-term follow-up, special considerations should be given to two interfaces, namely, the Ti-6Al-4V/HAC interface and the HAC/bone interface. The me-

Table 7 Apposition Index (AI) Values for HACs

	HA coatings		
Weeks	P1	P2	P3
4	59.34 ± 15.74	57.95 ± 18.47	57.44 ± 17.18
6	80.17 ± 8.41	81.24 ± 7.35	81.26 ± 8.80
12	79.34 ± 7.88	80.22 ± 4.96	65.38 ± 9.87

Unit: %.
Values given is the mean + standard deviation. In each case, 36 slices were taken for histomorphometry.
The P3-HAC has a lower NBHI ($p < 0.005$) than the other HACs at 12 weeks.
Source: Ref. 24.

chanical strengths of both interfaces are required to be as strong as possible. Although there was evidence of a chemical reaction observed at the Ti-6Al-4V/HAC interface [54,55], research suggested the presence of a potentially weak Ti-6Al-4V/HAC interface [54,56,57], particularly where the HAC was used as the primary means of fixation. Therefore, for clinical applications, the question was raised whether the weak Ti-6Al-4V/HAC interface would degrade with time in a physiological medium, since the dissolution of the HAC was evident in vitro and the sign of resorption of the HAC was documented in vivo [58,62]. After soaking in simulated body fluid for 4 weeks [63], the bonding degradation of HACs was approximately 25–33% of the original strength. Therefore, the exact coating characteristics that influenced the mechanical stability of the HAC in vivo need to be further investigated.

As shown in Table 8 [64], the shear strength at the HAC/bone interface was investigated in a canine transcortical femoral model after 12 and 24 weeks of implantation. The interface shear strength data of implants were evaluated by a push-out test with a loading rate of 0.2 mm/min. It is apparent that the shear strengths of P3-HACs were significantly ($p < 0.05$) higher than those of P1-HACs at each implant period. After 24 weeks of implantation, shear strength as high as 16.65 MPa was observed for P3-HAC. The failure site of implants after the push-out tests was conclusively at or near the HAC/bone interface. No failure was found at the Ti-6Al-4V/HAC interface. This finding could be explained by the bonding strength at the Ti-6Al-4V/HAC interface in simulated body fluid. By the method of adhesion test (ASTM C-633), the original bonding strength of P3-HAC (30.25 MPa) was higher than that (23.51 MPa) of P1-HAC. After 1 week of immersion, the bonding reduction of the P3-HAC (3.4%) was significantly lower than that of the P1-HAC (27%). This finding indicated that HAC with denser microstructure would revealed little degradation, though this kind of HAC (P3-HAC) contained the highest impurity phases and the lowest crystallinity (Table 1); the latter constituent had been demonstrated to increase the dissolution rate in SBF [58,59]. Accordingly, at 1 week the effect of microstructure in preventing the bonding from degradation was more important than the effect of crystallinity and the content of impurity phases in SBF. By the results of shear strength and bonding strength, the higher the bonding strength at the Ti-6Al-4V/HAC interface in SBF, the higher the shear strength at the implant (HAC on Ti-6Al-4V)/bone interface would be in vivo. This meant that among the coating characteristics evaluated in this study, the constructed microstructure of HACs played the key factor in determining the mechanical stability of the HACs both in SBF and in vivo, no matter what the content of the impurity phases and the index of crystallinity in the HACs.

To summarize, the maximum NBHI and AI were reached for all HACs at 6 weeks, indicating apparently that the different coating characteristics did not affect the osteoconductivity and

Table 8 Results of Shear Strength (MPa) Measurements

Weeks	P1-HAC	P3-HAC
12	14.72 ± 2.84 ($n = 12$)	16.27 ± 2.78* ($n = 12$)
24	14.64 ± 2.14 ($n = 12$)	16.65 ± 3.58* ($n = 12$)

Values are given as mean ± SD.

* Denotes statistical differences ($p < 0.05$) between P1-and P3-HAC.

Source: Ref. 64.

osseointegration of HACs within 6 weeks of healing. The HAC with dense microstructure and high bonding strength (P3-HAC) had undergone adverse biological degradation in terms of NBHI and AI after 12 weeks of implantation, because the denser HAC (P3-HAC) also exhibited a higher amount of impurity phases, less crystallinity, and off Ca:P stoichiometry. However, among coating characteristics, the microstructure was the key factor in influencing the mechanical stability of HACs both in SBF and in vivo. As a consequence, a denser HAC was needed to ensure the mechanical stability at both interfaces.

V. CONCLUSION

The physical and chemical characteristics, in vivo biological responses, and the mechanical property of plasma-sprayed HA coatings were evaluated. Three types of HAC with differences in microstructure, concentration of impurity phases, and index of crystallinity were prepared, varying the plasma-spraying parameters. The HAC revealing the largest extent of coating melting resulted in a denser microstructure, higher content of impurity phases, less crystallinity, and higher calcium:phosphorus molar ratio. The P3-HAC with the denser microstructure resulted in higher bonding strength at the HAC/Ti-6Al-4V interface. Employing the Chinese coin implant model in the cortex of canine femora, it was determined that different coating characteristics do not influence the NBHI or the AI within 6 weeks of healing. However, P3-HAC causes adverse biological responses after 12 weeks of implantation. After push-out measurements, P3-HAC shows higher shear strength than P1-HAC at each implant period, indicating that the coating characteristics of HACs would also influence the testing results, especially the constructed microstructure of the HACs. In addition, the osteoblast responses were influenced by the surface roughness of HAC during early periods, and the cell attachment at the smoother surface of HAC is significantly higher than at a rougher surface. Finally, the coating characteristics of HACs would influence the biological responses. How to decrease the impurity phases and increase the mechanical strength is important for clinical use of HACs. Using heat treatment to decrease impurity phases and bond coats to increase mechanical strength, a HAC with good biocompatibility and high bonding strength could be achieved and used in clinical application.

ACKNOWLEDGMENTS

This work was supported by grant NSC-90-2218-E-242-003 and NSC-91-2213-E-242-001 from the National Science Council, Taiwan, ROC. The authors wish to thank Dr. B. C. Wang, Z. S. Lee, Y. J. Wu, and M. R. Yang for their help with this chapter.

REFERENCES

1. Galante J, Rostoker W, Lueck R, Ray RD. Sintered fiber metal composites as a basis for attachment of implants to bone. J. Bone Joint Surg 1971; 53A:101–114.
2. Albrektsson T, Branemark PI, Hansson HA, Kasemo B, Larsson K, Lundstrom I, McQueen DH, Skalak R. The interface zone of inogranic implants in vivo: titanium implants in bone. Ann. Biomed. Eng 1983; 11:1–27.
3. Blitterswijk CA, Grote JJ, Kuijpers W, Daems WT, Groot K. Macropore tissue ingrowth: a quantitative and qualitative study on hydroxyapatite ceramic. Biomaterials 1986; 7:137–143.
4. Blitterswijk CA, Grote JJ, Kuijpers W, Hoek CJG, Daems WT. Bioreactions at the tissue/hydroxyapatite interface. Biomaterials 1985; 6:243–251.

5. Hoogendoorn HA, Renooij W, Akkermans LMA, Visser W, Wittebol P. Long-term study of large ceramic implants (porous hydroxyapatite) in dog femora. Clin. Orthop 1983; 187:281–288.
6. Kitsugi T, Yamamuro T, Takeuchi H, Ono M. Bonding behavior of three types of hydroxyapatite with different sintering temperatures implanted in bone. Clin. Orthop 1988; 234:280–290.
7. Holmes RE, Bucholz RW, Mooney V. Porous hydroxyapatite as a bone-graft substitute in metaphyseal defects. J. Bone Joint Surg 1986; 68A:904–911.
8. Bucholz RW, Carlton A, Holmes R. Interporous hydroxyapatite as a bone graft substitute in tibial plateau fractures. Clin. Orthop 1989; 240:53–62.
9. With G, Vandijk HJA, Hattu N, Prijs K. Preparation, micro-structure and mechanical properties of dense polycrystalline hydroxyapatite. J. Mater. Sci 1981; 16:1592–1598.
10. Geesink RGT, Groot K, Klein CAT. Chemical implant fixation using hydroxy-apatite coatings. Clin. Orthop 1987; 225:147–170.
11. Bauer TW, Geesink RGT, Zimmerman R, McMahon JT. Hydroxyapatite-coated femoral stems. J. Bone Joint Surg 1991; 73(A):1439–1452.
12. Gross KA, Berndt CC. Optimization of spraying parameters for hydroxyapatite. Proc. 2nd Plasma-Technik Symposium 1991; 3:159–170.
13. Geesink RGT, Groot K, Klein CAT. Chemical implant fixation using hydroxy-apatite coatings. Clin. Orthop 1987; 225:147–170.
14. Geesink RGT, Groot K, Klein CAT. Bonding of bone to apatite-coated implants. J. Bone Joint Surg 1988; 70B:17–22.
15. Yang CY, Lin RM, Wang BC, Chang E. Interface of bone and hydroxyapatite-coated titanium alloy implant. Chin J. Med. and Biol Eng 1991; 11(4):271–274.
16. Soballe K, Hansen ES, Rasmussen HB, Pedersen CM, Bunger C. Hydroxyapatite coating enhances fixation of porous coated implants. Acta Orthop. Scand 1990; 61(4):299–306.
17. Hayashi K, Uenoyama K, Matsuguchi N, Sugioka Y. Quantitative analysis of in vivo tissue responses to titanium-oxide- and hydroxyapatite-coated titanium alloy. J. Biomed. Mater. Res 1991; 25: 515–523.
18. Schaeken HG, Wolke JGC, Jansen JA. Influence of annealing temperature on r.f. magnetron sputtered calcium phosphate coatings. Biomaterials 1996; 17:405–10.
19. Ong JL, Lucas LC, Lacefield WR, Rigney ED. Structure, solubility and bond strength of thin calcium phosphate coatings produced by ion beam sputter deposition. Biomaterials 1992; 13:249–54.
20. Yoshinari M, Ohtsuka Y, Derand T. Thin hydroxyapatite coating produced by the ion beam dynamic mixing method. Biomaterials 1994; 15:529–35.
21. Singh RK, Qian F, Nagabushnam V, Damodaran R, Moudgil BM. Excimer laser deposition of hydroxyapatite thin films. Biomaterials 1994; 15:522–8.
22. Cotell CM, Chrisey DB, Grabowski KS, Spregue JA. Pulsed laser deposition of hydroxyapatite thin films on Ti-6Al-4V. J. Appl. Biomater 1992; 8:87–93.
23. Ducheyne P, Raemdonck WV, Heughebaert JC, Heughebaert M. Structural analysis of hydroxyapatite coating on titanium. Biomaterials 1986; 7:97–103.
24. Wang BC, Chang E, Yang CY, Tu D, Tsai CH. Characteristics and osteoconductivity of three different plasma-sprayed hydroxyapatite coatings. Surf. Coat. Tech 37:55–63.
25. Ducheyne P, Cuckler J, Radin S, Nazar E. Plasma sprayed calcium phosphate ceramic linings on porous metal coatings for bone ingrowth. In: Yamamuro T, Hench LL, Wilson J, eds. CRC Handbook of Bioactive Ceramics Vol. II. Boca Raton. FL: CRC Press Inc., 1990:123–131.
26. Phase Diagrams for Ceramists Vol. 5. Washington, DC: American Ceramic Society, 1983:321–322.
27. Groot K, Klein CAT, Wolke JGC, Blieck-Hoger-vorst JMA. Chemistry of calcium phosphate bioceramics. In: Yamamuro T, Hench LL, Wilson J, eds. CRC Handbook of Bioactive Ceramics Vol. II. Boca Raton. FL: CRC Press Inc., 1990:3–16.
28. Koch B, Wolke JG, Groot K. X-ray diffraction studies on plasma-sprayed calcium phosphate-coated implants. J. Biomed. Mater. Res 1990; 24:655–667.
29. Xie L, Monroe EA. Yamamuro T, Hench LL, Wilson J, eds(). CRC Handbook of Bioactive Ceramics Vol. II. Boca Raton. FL: CRC Press Inc., 1990:29–38.

30. Buser D, Schenk RK, Steinemann S, Fiorellini JP, Fox CH, Stich H. Influence of surface characteristics on bone integration of titanium implants. A histomorphometric study in miniature pigs. J. Biomed. Mater. Res 1991; 25:889–902.
31. Fowler BO. Infrared studies of apatite: I. Inorg. Chem 1974; 13(1):194–207.
32. Elsing R, Knotek O, Balting U. The influence of physical properties and spraying parameters on the creation of residual thermal stresses during the spraying process. Surf. Coat. Technol 1990; 41: 147–56.
33. Yang YC, Chang E, Hwang BH, Lee SY. Biaxial residual stress states of plasma-sprayed hydroxyapatite coatings on titanium alloy substrate. Biomaterials 2000; 21:1327–1337.
34. Wang BC, Lee TM, Chang E, Yang CY. The shear strength and the failure mode of plasma-sprayed hydroxyapatite coating to bone: the effect of coating thickness. J. Biomed. Mater. Res 1993; 27: 1315–1327.
35. Lee TM, Wang BC, Yang YC, Yang CY, Chang E. Comparison of plasma-sprayed hydroxyapatite coatings and hydroxyapatite/tricalcium phosphate composite coatings. in vivo study. J. Biomed. Mater. Res 2001; 55:360–367.
36. Schwartz Z, Boyan BD. Underlying mechanisms at the bone-biomaterials interface. J. Cellular Biochem 1994; 56:340–347.
37. Sinha RK, Tuan RS. In vitro analysis of the bone-implant interface. Semin Arthroplasty 1996; 7: 47–57.
38. Buser D, Schenk RK, Steinemann S, Fiorellini JP, Fox CH, Stich H. Influence of surface characteristics on bone integration of titanium implants: a histomorphometric study in miniature pigs. J. Biomed. Mater. Res 1991; 25:889–902.
39. Stanford CM, Keller JC, Solursh M. Bone cell expression on titanium surfaces is altered by sterilization treatments. J. Dent. Res 1994; 73(5):1061–1071.
40. Lee TM, Tsai RS, Chang E, Yang CY, Yang MR. The cell attachment and morphology of neonatal rat calvarial osteoblasts on the surface of Ti-6Al-4V and plasma-sprayed hydroxyapatite coating: effect of surface roughness and serum contents. J. Mat. Med.: Mat. Med 2002; 13:341–350.
41. Folkman J, Moscona A. Role of cell shape on growth control. Nature 1978; 273:345–9.
42. Archer CW, Rooney P, Wolpert L. Cell shape and cartilage differentiation of early chick limb bud cells in culture. Cell Differentiation 1982; 11:245–51.
43. Hunter A, Archer CW, Walker PS, Blunn GW. Attachment and proliferation of osteoblasts and fibroblasts on biomaterials for orthopaedic use. Biomaterials 1995; 16:287–295.
44. Eriksson AS, Ericson LE, Thomsen P, Lindblad R. Distribution of cells in soft tissue and fluid space around hollow and solid implants in the rat. J. Mater. Sci.: Mater. in Med 1994; 5:269–278.
45. Schneider BG, Burridge K. Formation of focal adhesions by osteoblasts adhering to different substrata. Expe Cell Res 1994; 214:264–269.
46. Bagambisa FB, Kappert HF, Schilli W. Cellular and molecular biological events at the implant interface. J. Cranio-maxillo-facial Surg 1994; 22:12–17.
47. Anselme K. Osteoblast adhesion on biomaterials. Biomaterials 2000; 21:667–681.
48. Denissen HW, Kalk W, Nieuport HM, Maltha JC, Hooff A. Mandibular bone response to plasma-sprayed coatings of hydroxyapatite. Int. J. Prosth 1990; 3:53–58.
49. Garcia R, Doremus RH. Electron microscopy of the bone-hydroxyapatite interface from a human dental implant. J. Mater. Sci.: Mater. Med 1992; 3:154–161.
50. Wang BC, Chang E, Yang CY, Tu D. A histomorphometric study on osteoconduction and osseointegration of titanium alloy with and without plasma-sprayed hydroxyapatite coating using back-scattered electron images. J. Mater. Sci.: Mater. Med 1993; 4:394–403.
51. Maxian SH, Zawadsky JP, Dunn MG. Mechanical and histological evaluation of amorphous calcium phosphate and poorly crystallized hydroxyapatite coatings on titanium implants. J. Biomed. Mater. Res 1993; 27:717–728.
52. Gottlander M, Albrektsson T. Histomorphometric studies of hydroxy-apatite-coated and uncoated CP titanium threaded implants in bones. Int. J. Oral Maxillofac. Imp 1991; 6:339–404.
53. Denissen HW, Kalk W, Nieuport HM, Maltha JC, Hooff A. Mandibular bone response to plasma-sprayed coatings of hydroxy-apatite. Int. J. Prosth 1990; 3:53–58.

54. Filiaggi MJ, Coombs NA, Pilliar RM. Characterization of the interface in the plasma-sprayed HA coating/Ti-6Al-4V implant system. J. Biomed. Mater., Res 1991; 25:1211–1229.
55. Ji H, Ponton CB, Marquis PM. Microstructural characterization of hydroxyapatite coating on titanium. J. Mater. Sci.: Mater. Med 1992; 3:283–287.
56. Kangasniemi IMO, Verheyen CPM, Velde EA, Groot K. in vivo tensile testing of fluorapatite and hydroxyapatite plasma-sprayed coatings. J. Biomed. Mater. Res 1994; 28:563–572.
57. Spivak JM, Ricci JL, Blumenthal NC, Alexander H. A new canine model to evaluate the biological responses of intramedullary bone to implant materials and surfaces. J. Biomed. Mater. Res 1990; 24:1121–1149.
58. Klein CAT, Wolke JGC, Blieck-Hogervorst JMA, Groot K. Features of calcium phosphate plasma-sprayed coatings: an in vitro study. J. Biomed. Mater. Res 1994; 28:961–967.
59. Gross KA, Berndt CC. in vitro testing of plasma-sprayed hydroxyapatite coatings. J. Mater. Sci.: Mater. Med 1994; 5:219–224.
60. Dhert WJA, Klein CAT, Wolke JGC, Velde EA, Groot K, Rozing PM. A mechanical investigation of fluorapatite, magnesiumwhitlockite, and hydroxyapatite plasma-sprayed coatings in goats. J. Biomed. Mater. Res 1991; 25:1183–1200.
61. Klein CAT, Patka P, Lubbe HBM, Wolke JGC, Groot K. Plasma-sprayed coatings of tetracalciumphosphate, hydroxyapatite, and α-TCP on titanium alloy: an interface study. J. Biomed. Mater. Res 1991; 25:53–65.
62. Jansen JA, Waerden JCM, Wolke JGC, Groot K. Histological evaluation of the osseous adaptation to titanium and hydroxyapatite-coated titanium implants. J. Biomed. Mater. Res 1991; 25::973–989.
63. Yang CY, Wang BC, Chang E, Wu BC. Bond degradation at the plasma-sprayed HA coating/Ti-6Al-4V alloy interface: an in vitro study. J. Mater. Sci.: Mater. Med 1995; 6:258–265.
64. Yang CY, Lin RM, Wang BC, Lee TM, Chang E, Hang YS, Chen PQ. in vitro and in vivo mechanical evaluations of plasma-sprayed hydroxyapatite coatings on titanium implants: the effect of coating characteristics. J. Biomed. Mater. Res 1997; 38:335–345.

33

Biomechanical Efficacy of Vertebroplasty and Kyphoplasty

Michael A. K. Liebschner and Kay Sun
Rice University
Houston, Texas, U.S.A

I. HISTORY OF VERTEBROPLASTY

Percutaneous application of an acrylic bone cement, polymethylmethacrylate (PMMA), to vertebral defects was pioneered in France in 1984 by Galibert et al. [1]. This procedure, called vertebroplasty, was first used to treat aggressive vertebral hemangioma and resulted in good pain relief. In 1991, Debussche-Depriester et al.[2] focused the treatment on osteoporotic compression fractures and also experienced success in pain control. Indications were subsequently extended to other weakening lesions, such as vertebral myeloma or metastatic vertebral lesions. In 1993, vertebroplasty was introduced to North America, but unlike in Europe, where vertebroplasty is mainly performed to manage pain due to tumor-related bone diseases [3–8], the focus in North America has been on the relief of pain associated with osteoporotic vertebral fractures that has failed to respond to conservative therapy [9,10].

The aim of vertebroplasty is to achieve rapid analgesic effect through the stabilization of vertebral bodies in patients experiencing back pain related to diseases that weaken the vertebral body [11]. The high success rate of pain relief with vertebroplasty has prompted the development of new surgical techniques and devices as well as patient-selection guidelines that aid in the reduction of procedural time and the improvement of safety. Unfortunately, information on the effects of vertebroplasty on the biomechanics of the vertebral body and the entire vertebral column is still limited. This knowledge, when available, will permit the optimization of the procedure, specifically with regards to cement volume, placement, and type of filler material, for biomechanical efficacy and minimal risk of complications.

II. PATIENT SELECTION

The main indications for vertebroplasty are osteoporotic vertebral compression fracture, vertebral angioma, and osteolytic metastasis and myeloma. The decision to perform this procedure must be made only after careful consideration of the severity of the local and systemic disease spread, vertebral level involved, pain intensity, neurological status, state of health, life expectancy, and other treatment options such as surgery, radiation therapy, pharmacological drugs, or a combination of these methods [3]

A. Osteoporotic Vertebral Collapse

Osteoporosis is a systemic skeletal disorder characterized by low bone mass and deterioration in the microarchitecture of bone tissue. The reduction in bone density and quality weakens the mechanical strength of the bone, leading to enhanced bone fragility and a consequent increase in fracture risk [12]. Over 10 million Americans are diagnosed with this bone disorder, and more than one third of women older than 65 have sustained at least one vertebral compression fracture [13]. Vertebral fractures may be defined as the reduction in vertebral height by 15% or more [14] and are classified by the degree and type of deformity (wedge, biconcavity, or compression) [15]. Clinical consequences of vertebral fracture include chronic back pain, loss of height, kyphosis or deformity, reduced pulmonary function, disability, diminished quality of life, and an increased mortality rate. Of the over 1.5 million fragility fractures that occur every year in the United States due to osteoporosis, approximately 700,000 are vertebral fractures [13,14]. Compared with fractures at other sites, where up to 90% are due to falls, 58% of osteoporotic vertebral fractures occur spontaneously during routine activities [17]. Fractures with little or no trauma are sustained when the amount of bone available for mechanical support falls below the fracture threshold. Vertebral crush fractures occur most frequently in postmenopausal women, where the lifetime vertebral fracture risk from age 50 years onwards was estimated to be almost 16% in Caucasian women and only 5% in Caucasian men [18]. The prevalence of vertebral fractures can reach as high as 50% in the older age groups [19–22].

Current therapy of vertebral fractures places an emphasis on pain control using either narcotic or anti-inflammatory medications in conjunction with immobilization [23]. Surgical interventions, including anterior or posterior stabilization with placement of internal fixation devices such as screws, plates, cages, or rods, are uncommon. Devices of this type are typically reserved for gross spinal deformity or for threatened or existing neurological impairment. Injury involving the adjacent disc may require fusion of the entire motion segment. The reasons for the conservative treatment stem from the high risks involved in performing open spinal surgery on the elderly, as well as the difficulty in achieving adequate anchorage of hardware in adjacent osteoporotic bone. Approximately one third of patients with vertebral fractures do not respond to medical therapy [14], and only when conservative therapy fails is surgery, i.e., percutaneous vertebroplasty, indicated. The primary goal of vertebroplasty is to alleviate pain and improve mobility, with a secondary goal of stabilization of the vertebral body [24].

B. Vertebral Angiomas

Vertebral angiomas are typically asymptomatic, benign lesions of the spine [3,11,25]. The pain accompanying this condition is caused by fracture, mass effect, and thecal sac compression or by neural foraminal narrowing [8]. Aggressive vertebral angiomas can be identified either by clinical symptoms or radiographic evaluations. Clinical symptoms consist of severe back pain or neurological signs signifying spinal cord or nerve root compression. Radiographically, aggressive vertebral angiomas appear as irregular and vertical trabeculation on plain x-ray films. On computerd tomography (CT) scans, they contain a distinct decrease in fat density with soft tissue content after an intravenous injection of contrast media. On magnetic resonance (MR) imaging, they are characterized by low signal intensity at focal, well-circumscribed lesion in T1-weighted images, which show a mild signal enhancement after intravenous injection of gadolinium [26]. Other radiographic signs include involvement of the whole vertebra, perivertebral invasion with an epidural extension and compression of the spinal cord or nerve roots, and occasionally, vertebral collapse [11,25].

Aggressive angioma with the following clinical signs and symptoms is indicated for vertebroplasty: (1) intense back pain without radiographic signs of aggressive vertebral angioma; (2) asymptomatic vertebral angioma with radiographic signs of aggressiveness; and (3) vertebral angioma with radiographic signs of aggressiveness and clinical signs of either acute spinal cord or cauda equina compression or progressive myelopathy or cauda equina syndrome [8,11]. Ethanol ablation is usually associated with vertebroplasty for vertebral angioma in asymptomatic patients with radiographical signs of aggressiveness and in patients with progressive neurologic signs. The ethanol injection has a sclerosing effect on vertebral angioma and cures vascular dysplasia. The ethanol also increases the risk of subsequent vertebral collapse, which can be prevented with proper strengthening from the injection of bone cement. For patients complaining of an acute myelopathy or cauda equina syndrome, a combination of vertebroplasty and surgery is indicated [11,27]. The surgical option is corpectomy, followed by cage placement, stabilization above and below with pedicle screws, and internal fixation. These surgical methods require significant postprocedural recovery and have associated morbidity and mortality. The injection of PMMA directly into the lesion serves to reduce pain, strengthen the compromised vertebral body structure, and embolize the hemangiomatous body, blocking off the arteries feeding it [1,8]. Vertebroplasty after decompression surgery, such as laminectomy or excision of epidural hemangioma, may make more invasive and high-risk surgery like vertebrectomy (excision of a portion of vertebral body) unnecessary [3].

C. Malignant Spinal Tumors

Osteolytic metastases and myeloma are the most frequent malignant osteolytic lesions of the spine, occurring in 30–70% of patients with cancer [25]. Tumor cells may access the spinal column via hematogenous, perineural, or lymphatic spread by direct extension from a paravertebral tumor. The affected patients usually experience severe pain and disability caused by tumor impingement on nerve roots or the spinal cord. Conventional therapy for malignant disease consists of bedrest, bracing, anti-inflammatory or opiate medications, and radiation therapy. Using radiation therapy, partial or complete relief of pain is attained in over 90% of patients [28], but is achieved only after a delay of 10–20 days [11]. Unfortunately, there is a longer-term effect of osteoblastic impairment due to the radiation, and 2–4 months suspension in bone strengthening is required, increasing the risk of vertebral collapse and, consequently, neural compression [3].

Vertebroplasty for the palliative treatment of malignant spinal tumors has two goals: vertebral stabilization when the lesion threatens the stability of the vertebrae and analgesic effect. Spinal pain, experienced in more than 70% of affected patients [25], is caused by mechanical micromotion within the osteolytic vertebral bodies [11]. The in situ polymerization and hardening of PMMA immobilizes the vertebral body fracture, contributing to the analgesic effect. Over 80% of vertebroplasty cases demonstrated significant rapid pain relief and improvement in mobility 24–48 hours after the procedure, and in two thirds of cases prolonged pain relief was observed [4,29]. Sufficient vertebral stabilization and strengthening require bone cement filling of both the osteolytic area of the lesion as well as the surrounding regions of the vertebral body that seem structurally normal [11]. However, the desire to inject excess bone cement into the lesion must be avoided for fear of complications due to cement leakages (discussed below). Another explanation for the alleviation of pain is the destruction of nerve endings by the cytotoxic effect of methylmethacrylate (MMA) and the heat released from the exothermic polymerization reaction. These two factors, along with ischemia also brought on by the introduction of PMMA, may also account for the anti-tumoral effect of vertebroplasty; recurrence of more spinal tumors at the site of injection is extremely rare [4].

The only limitation of vertebroplasty for this indication is the inherent problem in attempting to apply localized treatment to a disease that is multifocal in nature. Thus, vertebroplasty is commonly only indicated in cases where the osteolytic metastases or myelomatous are located in a single diseased vertebral body site. This shortcoming can be overcome by combining vertebroplasty with other methods of treatment such as radiation and surgery. Radiation therapy and vertebroplasty complement each other provided radiation is preceded by vertebroplasty. The irradiation increases the analgesic effect from vertebroplasty, while having no adverse effect on the mechanical properties of PMMA [30]. The bone cement similarly does not affect the results of radiation therapy. For the combination of vertebroplasty and surgery to be indicated, vertebroplasty must serve to facilitate the surgery by consolidating vertebral bodies to provide stabilization of the anterior vertebral column, thereby bypassing surgical fixation of the anterior column and allowing posterior surgical stabilization with a smaller fixation [4,31]. Because of the high viscosity of PMMA and its substitutes, vertebroplasty can be performed even in patients with varying degrees of destruction of the posterior cortex of the vertebral body, which would naturally increase the risk of cement leaks. Vertebroplasty is also strongly recommended as a preventive treatment in the case of an asymptomatic metastatic vertebral body lesion with a high risk of vertebral collapse [11]. Short of spinal cord compression or epidural involvement by the tumor, vertebroplasty is a viable option for the treatment of spinal tumors.

III. VERTEBROPLASTY TECHNIQUE

A. Procedure

Radiographs and CT scans are taken a few days before vertebroplasty to assess (1) the extent of the vertebral collapse; (2) the location and extent of the lytic process; (3) the visibility and degree of involvement of the pedicles; (4) the presence of cortical destruction or fracture; and (5) the presence of epidural or foraminal stenosis caused by tumor extension or repulsion of bone fragment [3]. These assessments allow the orthopedic surgeon to plot the best route that attains sufficient pain relief with minimal risk of complications. Thirty minutes prior to the procedure, the patient is given a prophylactic antibiotic and subsequently placed in a prone position for a thoracic or lumbar vertebroplasty and in a supine position for cervical vertebroplasty. The skin, subcutaneous soft tissue, and pedicular periosteum are anesthetized. General anesthesia is typically unnecessary unless patient movement needs to be eliminated for CT scanning or if pain due to the heat released from the exothermic polymerization of the bone cement is too intense. A small skin incision is made to allow easy passage of the vertebroplasty needle, which consists of a trocar with a cannula that ranges in size from 11 to 13 gauge. The cannula advancement is guided using standard fluoroscopy [3,11], CT guidance [32], or CT fluoroscopy. The preferred placement of the cannula is via the transpedicular approach to the posterior of the vertebral body in order to avoid cement leaking into the intervertebral foramina [25]. The cannula enters trabecular cortex of the vertebral body by boring through the pedicle either by a slight back-and-forth twisting motion or gentle tapping on the needle handle. Frequent fluoroscopic checks are made as the cannula traverses the pedicle to ensure proper alignment [24]. In the event that there is inadequate visualization under fluoroscopic guidance due to osteolysis involvement at the pedicles, transpedicular access is not possible. A posterolateral approach may be used instead, but the risk of pneumothorax associated with this route is relatively high. Furthermore, if the posterolateral movement of the needle is incorrect, nerves can be damaged and the cement can leak into paravertebral tissue when the needle is removed [3].

The risk of cement extravasations can be minimized by performing intraosseous venography prior to the vertebroplasty procedure. The contrast material, iohexol, is injected into the

vertebral body, which outlines the perivertebral venous drainages and fracture lines. This identification allows the evaluation of the trabecular space so that the needle can be positioned safely away from the venous plexus so as to avoid venous leakages and potential leaks along the fracture lines [11,24,25]. Unfortunately, there are limitations to this method; first, due to the different flow characteristics of the contrast material and bone cement, it is difficult to ascertain whether there is accurate correlation between the flow paths of the two agents. This means that venography is unable to accurately predict the final casting of PMMA, and a chance remains that cement may leak into the vertebral veins. Second, surgeons rarely alter the technique that they are accustomed to, even if there is a clear demonstration of extracorporeal venous filling based on the information from the venograms. Thus, in vertebroplasty cases where no venography was performed, the complication rates are typically no higher than cases with venography [3,11,32]. Third, the contrast material can leak into the intervertebral disc in the event that fractures have affected the endplates and can subsequently interfere with the detection of similar leaks of PMMA [33]. Lastly, venography adds cost and increases the amount of radiation exposure to the patient. The usefulness of venography is still debatable and the decision to perform the procedure is at the discretion of the surgeon.

B. PMMA Bone Cement Preparation

Currently, there is no commercially available PMMA that is U.S. Food and Drug Administration (FDA) approved for vertebroplasty. The PMMA used in vertebroplasty is a modified compound with lower viscosity that provides a longer working time [34]. A less viscous and more injectable PMMA is achieved by adding more liquid MMA monomer than is recommended by the manufacturer to the mixture of powdered PMMA component, radiopaque barium sulfate, and tobramycin powder (for prophylaxis) [9,25,35]. Although changes to the monomer-to-powder ratio can reduce the elastic modulus, yield strength, and ultimate strength of PMMA by as much as 24% [35], most orthopedic surgeons believe that the benefit of the longer working time outweighs the improved biomechanics, especially since the alteration to the cement material properties has no apparent clinical complications attributed to cement failure or to insufficient cement strength or stiffness [24]. Once a thin paste-like consistency is obtained, the surgeon has approximately 3–5 minutes to inject PMMA with a syringe into the vertebral body before polymerization causes it to harden [34]. PMMA cement typically sets within 20 minutes and achieves about 90% of its ultimate strength within 1 hour of injection [24].

The flow of PMMA within the vertebral body is monitored continuously under fluoroscopy. The injection is stopped immediately whenever the cement begins to extend to untoward locations, such as intervertebral disc space, the posterior vertebral wall, or when it approaches the paraverterbal veins at the posterior quarter of the vertebral body, which may result in extravasations [11,24]. Injection is also terminated when sufficient vertebral filling is attained. The average PMMA volume injected into a vertebral body is 4–6 cm^3, up to a maximum of 8 to 12 cm^3 [36,37]. Once the vertebra is filled, the needle is rotated to separate any stream of cement that may still be attached within the needle's dead space, and the needle is removed [24].

IV. CLINICAL SUCCESS

A vast majority of the reported results of vertebroplasty have been clinical case studies. Although there have been no prospective, randomized, controlled studies comparing vertebroplasty with standard medical therapy, the clinical studies for all indications demonstrated high rates of rapid pain relief [4,5,38–43], increase in mobility [38–40,44], and decreased medication use

[4,5,38–40,45]. Between 80 and 90% of patients treated with vertebroplasty attained partial to complete pain relief within the first 72 hours of the procedure and were capable of standing and walking 24 hours after the procedure [3–5,25,29,46]. The analgesic effect was durable as proven in long-term follow-up from 9 to 18 months [25,44,46].

The exact mechanism of pain relief associated with vertebroplasty is unclear, but several mechanisms have been proposed including thermal necrosis and chemotoxicity of the intraosseous pain receptors, as well as ischemia and mechanical stabilization of the vertebral body [33,47,48]. The heat produced during the exothermic polymerization reaction of PMMA may cause destruction of the neighboring pain fibers [49]. In a recent cadaveric vertebroplasty experiment, the temperature of the vertebral bodies rose as high as 60–70°C on the vertebral shell surface during PMMA curing [50]. Coincidentally, this is the target temperature for killing tumor cells during radiofrequency ablation. The same in vitro study suggested that temperatures generated during vertebroplasty are not likely to be sufficient to result in widespread thermal necrosis of osteoblasts [51] or neural tissue [52]. Therefore, there is no risk of thermal damage to the spinal cord or nerve roots, provided the cement is contained within the vertebral body [50].

The neurotoxicity of the MMA monomer [48,53,54] may play a role in pain reduction in vertebroplasty, especially when extra monomer is added to the PMMA powdered mixture than is recommended by the manufacturer in order to create a less viscous and more injectable cement with a longer working time. Such toxicity may account for the necrotic zone reported around the site of injection [49]. Another possible mechanism responsible for the zone of necrosis in tumors is ischemia, which may result from direct (cement intrusion) or indirect (compression) occlusion of tumor vessels.

The most probable mechanism for pain relief after vertebroplasty is believed to be the mechanical stabilization of the vertebral body [50,55–57]. Stabilization of the microfractures through hardening of the injected cement prevents painful micromotion at fracture site. The cement also has a strengthening and stiffening effect, which helps to regain the lost mechanical properties of the vertebral body [55–57].

V. COMPLICATIONS OF VERTEBROPLASTY

Complications associated with vertebroplasty include nerve root or spinal cord compression, pulmonary embolism, fracture of the rib, transverse process or pedicle, paravertebral hematoma, epidural abscess, and seizure or respiratory arrest from oversedation [24]. The complication rates are low, ranging from 1 to 10%, with different frequencies depending on the initial indications of percutaneous vertebroplasy (PVP). For osteoporotic vertebral collapse and vertebral angioma, complications are uncommon, with rates of only 1–3% and 2–5%, respectively [8]. The complication rates are much higher for malignant spinal tumors, up to 10%, due to the higher risk of cement extravasations resulting from vertebral cortex destruction associated with the osteolytic processes [11,31]. The most common causes for the complications are (1) inappropriate patient selection; (2) poor visualization due to inadequate fluoroscopic equipment, poor patient cooperation or unsatisfactory cement opacification; (3) operator error, such as lack of knowledge of the radiographic spinal anatomy and poor fluoroscopic triangulation skills; (4) lack of patient monitoring; and (5) improper aseptic technique [24].

A. Cement Leakage

The cause of most procedural complication is leakage of PMMA into adjacent structures as a result of vertebral cortical destruction or fracture, inadvertent injection of cement into the verte-

bral venous plexus, or excess vertebral filling. Cement leaks have been reported in 30–67% of patients who underwent vertebroplasty [58]. The majority of PMMA leakages have no clinical consequence, but when they do, the consequences are severe, at times even fatal. There are three types of cement leakage:

1. Venous extravasations, which occur in the perivertebral or epidural veins, are common in more than 10% of vertebroplasty cases, but are only symptomatic in less than 3% of patients [11]. Venous leaks can lead to compression of the spinal cord and nerve roots, as well as pulmonary embolism.
2. Soft tissue leakage occurs around the spine, in the epidural space, or along the needle track. It is rarely symptomatic, but if the leakage occurs in the epidural space or intervertebral foramina, there is a high risk of nerve root or spinal cord compression [25]. Cement leaks into the paravertebral soft tissues are more frequent during vertebroplasty indicated for osteoporotic collapse fracture or malignant spinal tumors since PMMA can easily leak through fractures or microfractures of the vertebral body and through paravertebral extension of the spinal tumor [11].
3. Leak into an intervertebral disc from a disc herniation are frequent and mostly asymptomatic. However, the presence of bone cement in the disc may have altered the mechanical dynamics of the vertebral column, provoking fractures in the adjacent vertebrae, particularly in osteoporotic patients with risk of secondary vertebral collapse [11].

One way to improve the safety of vertebroplasty is to minimize cement leakage by using less cement since complication rates due to cement extravasations are directly related to the amount of cement injected. A study by Cotton et al. [29] has shown that pain relief is not dependent on the percent volume of cement used, but rather on the distribution of cement within the vertebral body, specifically within the fracture planes. Therefore, adequate pain relief with minimal cement fill can be attained through the strategic placement of cement at fracture locations.

B. Damage to Adjacent Tissue

Approximately 3–6% of vertebroplasty patients suffer from radiculopathy [3,29], which is attributed to damage caused by the exothermic effect of PMMA during polymerization and an inflammatory reaction produced by PMMA [7]. Radicular pain can be successfully resolved in 2–4 days when treated with steroids and anti-inflammatory medications. However, persistent radiculopathy can occur in about 2–3% of patients, and surgical intervention is required to remove the bone cement [11,31].

C. Adjacent Vertebrae Failure

Recent studies have suggested that PMMA filling may promote fractures in the adjacent vertebrae due to the sharp increase in stiffness of the augmented vertebra [59,60]. It is hypothesized that drastic changes in the mechanical dynamics and kinematics of the vertebral column lead to an increase in mechanical demands on the neighboring vertebrae, thereby increasing the risk of fracture. A similar phenomenon is observed with regards to spinal fusion, where increased risk for disc degeneration in vertebrae adjacent to a fusion is observed. There is, however, limited information on this phenomenon. Retrospective reviews of vertebroplasty clinical studies are inconclusive. A retrospective review of 109 patients with 174 fractures by Jenson and Dion [24] demonstrated no statistical difference in the rate of adjacent level fractures between patients

who returned with new fractures following vertebroplasty ($n = 19$; fractures = 27) and a control group consisting of patients who presented with multiple fractures of the same acuteness ($n = 21$; fractures = 43). This indicated that fractures may occur in any patient at all vertebral levels during the follow-up of osteoporotic disease, since existing fractures are strong independent predictors of the risk of future vertebral fracture [61]. Therefore, the vertebrae adjacent to the site of cement injection are at no higher risk of fracture than any other vertebrae. On the other hand, in another uncontrolled, retrospective study of 25 (67%) of 40 patients with symptomatic osteoporotic vertebral compression fracture, the odds ratio (OR) of a vertebral compression fracture adjacent to a cemented vertebra was higher, at 2.27 (95% CI 1.11–4.56) compared with 1.44 (95% CI 0.82–2.55) for a compression fracture adjacent to an uncemented vertebral collapse (mean duration of follow-up was 48 month, ranging from 12 to 84 months) [42]. Due to the contradictory results of different retrospective studies, an alternate approach with direct analysis of the biomechanical consequences of vertebroplasty on the whole vertebral column may yield more consistent findings.

A recent biomechanical investigation on the failure of adjacent vertebrae by Berlemann et al. [62] showed a lower ultimate failure load for treated intact vertebrae compared to the untreated control. The caudal vertebrae of osteoporotic two-vertebra functional spine units (FSUs) were augmented with PMMA and were subjected to cyclic sinusoidal dynamic compression at a constant displacement rate of 0.5 mm/sec. The untreated FSUs acted as a control. The geometric mean treated-to-untreated ratio of the failure load was 0.81 (95% CI 0.70–0.92). There was no significant difference in overall FSU stiffness. In the treated FSUs, failure always occurred in the nonaugmented, cranial vertebral body, while in the untreated control FSUs, both cranial and caudal vertebrae sustained fractures. The authors suggested that the mechanism for such failure may be due to the alteration of the biomechanics of load transfer to the adjacent vertebrae caused by the increase in stiffness of the augmented fractured vertebrae. The early failure of the adjacent, nonaugmented level may be a result of a 'stress-riser' effect and a significant disparity in biomechanical properties between the two involved vertebral bodies.

VI. BIOMECHANICS OF VERTEBROPLASTY

A. In Vitro Experimental Designs

Despite the growing usage of vertebroblasty in surgical procedures, the underlying biomechanical effects of the procedure are yet unknown. Although the short-term effects of pain reduction, height recovery, and fracture repair have been demonstrated, long-term effects have yet to be shown (Table 1). Most current experimental designs have focused on the short-term reparative effects of vertebroblasty for osteoporotic or fractured spines [36,57,63–65]. Additional studies have focused on the ability of vertebroblasty to augment the strength of vertebral bodies weakened by conditions such osteopenia or osteoporosis (Table 2) [66–68]. In both types of study researchers have focused on the biomechanical aspects of the injectable bone cements. Experimental design for all groups is similar; the only difference between augmentation and fracture repair is the time of injection. In vitro studies exploring usage of the technique for fracture repair use vertebrae loaded beyond the ultimate point, whereas studies of augmentation effects explore unfractured vertebrae injected with bone cement. Most studies have used similar values for the vertebral body selection, compression rates, and injection volumes.

Because most vertebroplasty procedures are performed on vertebrae from the thoracolumbar region of the spine, this chapter will focus on in vitro biomechanics studies performed in this region. Many studies have used single vertebral bodies showing no predilection for either the thoracic or lumbar regions, while others examine the spinal segments. Lu et al. [69]and

Table 1 Biomechanical Data Obtained Through In Vitro Experiments

Spinal region	*N*	Procedure	*t*-score	Bone mineral density (g/cm^2)	Augmentation volume (mL)	Filler material	Mean filling (%)	Initial strength (N)	Treatment strength (N)	Initial stiffness (N/mm)	Treatment stiffness (N/mm)	Initial height (mm)	Postcompression height (mm)	Posttreatment height (mm)	Ref.
Thoracic	9	Bp			4	Simplex P		2522 ± 347	4058 ± 347	1559 ± 102	1097 ± 102	21.04 ± 0.12	19.99 ± 0.16	20.98 ± 0.12	
	10	Bp			4	Modified Simplex P		2710 ± 330	4146 ± 330	1783 ± 97	1224 ± 97	20.26 ± 0.12	19.97 ± 0.16	20.55 ± 0.12	
	10	Bp			4	BoneSource		2336 ± 330	2476 ± 330	1298 ± 97	797 ± 97	20.53 ± 0.12	19.67 ± 0.16	20.55 ± 0.12	
Lumbar	10	Bp	−3.8 ± 1.1	0.75 ± 0.15	6	Simplex P		2813 ± 364	4208 ± 364	1842 ± 74	1371 ± 74	26.19 ± 0.87	25.39 ± 1.24	26.31 ± 0.87	
	10	Bp			6	Modified Simplex P		2696 ± 364	3134 ± 364	1794 ± 74	1301 ± 74	27.08 ± 0.87	23.02 ± 1.12	27.37 ± 0.87	
	10	Bp			6	Bone Source		2630 ± 364	2450 ± 364	1834 ± 74	1301 ± 74	26.80 ± 0.87	26.27 ± 1.23	27.37 ± 0.87	
T3-L4	14	Bp		1.160 ± 0.100	6.4 ± 2.129	Palacos E-Flow PMMA	24.7 ± 5.1	2019 ± 979	2543.94	9667	8690 ± 2349				
T2-L3	14	Bp		0.659 ± 0.061	12.9 ± 6.875	Palacos E-Flow PMMA	47.0 ± 4.1	2019 ± 979	4764.84	1982	5772 ± 2002				
T3-L4	14	Bp		0.596 ± 0.056	6.1 ± 2.416	Palacos E-Flow PMMA	26.4 ± 4.2	2019 ± 979	7147.26	1982	5186 ± 2740				
T2-L3	14	Bp		0.653 ± 0.078	8.4 ± 3.812	Brushite Cement	41.4 ± 8.5	2019 ± 979	4118.76	1982	4156 ± 2060				
T4-L1	10	Bp		0.987 ± 0.085	11.8 ± 3.60	Brushite Cement	48.4 ± 5.5	2019 ± 979	4556.883	9667	5430				
L1-L4	30	Bp			4.3 ± 1.6	PMMA CMW 3		2561 ± 1188	3094 ± 1106						
L1-L5	10	Bp	−5		8	Orthocomp		1699 ± 462	6685 ± 462	1098 ± 99	1110 ± 99				
	10	Bp	−5		8	Simplex P		1645 ± 523	3590 ± 462	1180 ± 109	728 ± 99				
	13		−5.5					2375 ± 437	1687 ± 450	1105 ± 63	695 ± 63				
	12	Up	−5.5		6	Simplex P		2225 ± 437	4250 ± 450	1078 ± 63	964 ± 63				
	14	Bp	−5.5		10	Simplex P		2188 ± 375	6862 ± 450	1073 ± 63	1059 ± 63				
T9-L5	15			0.461 ± 0.069				7103 ± 773				22.7 ± 3.2			
	15	Bp/CH		0.452 ± 0.105		CPC		7684 ± 1012				24.2 ± 3.1			
	15	Bp		0.508 ± 0.145		CPC		11936 ± 1985				25.4 ± 2.4			
T12-L1	8	Bp/Ky	−5.3 ± 1.7	0.56 ± 0.2	9.4 ± 3.5	Cranioplastic		2118 ± 653	4792 ± 653	1125 ± 108	996 ± 108	25.7 ± 1.6	23.1 ± 0.7	25.6 ± 0.7	
	8	Bp	−5.3 ± 1.7	0.56 ± 0.2	9.4 ± 1.4	Cranioplastic		2138 ± 653	7832 ± 653	1239 ± 108	904 ± 108	25.9 ± 2.0	23.0 ± 0.9	23.8 ± 0.9	
T6-L5	18	Bp	−5.2		2	Orthocomp		2241 ± 617	2292 ± 359	1353 ± 68	848 ± 84	25.25 ± 0.05	24.86 ± 0.05	25.14 ± 0.05	
	18	Bp	−5.2		4	Orthocomp		1906 ± 254	2771 ± 952	1187 ± 274	844 ± 133	25.25 ± 0.05	24.86 ± 0.05	25.14 ± 0.05	
	18	Bp	−5.2		6	Orthocomp		1996 ± 473	3790 ± 888	1105 ± 148	1077 ± 187	25.25 ± 0.05	24.86 ± 0.05	25.14 ± 0.05	
	18	Bp	−5.2		8	Orthocomp		2191 ± 531	5156 ± 1135	1297 ± 216	1140 ± 51	25.25 ± 0.05	24.86 ± 0.05	25.14 ± 0.05	
	18	Bp	−3.9		2	Simplex 20		2188 ± 263	2168 ± 308	1259 ± 136	838 ± 226	24.47 ± 0.04	24.31 ± 0.04	24.14 ± 0.05	
	18	Bp	−3.9		4	Simplex 20		2425 ± 402	3166 ± 787	1194 ± 238	956 ± 98	24.47 ± 0.04	24.31 ± 0.04	24.14 ± 0.05	
	18	Bp	−3.9		6	Simplex 20		2178 ± 328	4425 ± 1530	1389 ± 13	1144 ± 115	24.47 ± 0.04	24.31 ± 0.04	24.14 ± 0.05	
	18	Bp	−3.9		8	Simplex 20		2364 ± 65	5332 ± 1319	1279 ± 123	1129 ± 65	24.47 ± 0.04	24.31 ± 0.04	24.14 ± 0.05	
L1-L5	8		−2.3 ± 2.4					2274 ± 508	2692 ± 508	756 ± 148	513 ± 148				
	9		−2.3 ± 2.4		8	Simplex P		2108 ± 479	6677 ± 479	954 ± 139	1005 ± 139				
	8		−2.3 ± 2.4		8	Cranioplastic		1704 ± 508	3584 ± 508	1163 ± 148	642 ± 148				
	8		−2.3 ± 2.4		8	Osteobond		1998 ± 508	4193 ± 508	990 ± 148a	774 ± 148				
T2-L1	10			0.56–0.89											
	10				6.11 ± 2.3	Simplex									
	10				6.8 ± 0.9	CaP									
	5				6.0 ± 3.4	Simplex									
	5				4.82 ± 2.0	CaP									

Bp = bipedicular vertebroplasty; PL = posterolateral vertebroplasty; Up = unipedicular vertebroplasty; Bp/Ky = bipedicular kyphoplasty; FFT = formalin-fixed tissue; CH = injection only in the cranial half; CPC = calcium phosphate cement;

Table 2 Biomechanical Data Obtained Through In Vitro Vertebroplasty Experiments for Reinforcement

Spinal region	*N*	Procedure	Bone mineral density (g/cm^2)	Augmentation volume (mL)	Filler material	Mean filling (%)	Initial strength (N)	Treatment strength (N)	Initial stiffness (N/mm)	Treatment stiffness (N/mm)	Ref.
T8-L3	8	BP		15	CaP		527 ± 43	1063 ± 127	84 ± 11	157 ± 21	[63]
	8	BP		15	PMMA		527 ± 43	1036 ± 100	84 ± 11	156 ± 8	
T9,T12,L3	15		0.461 ± 0.069				7103 ± 773				[73]
T10, L1, L4	15	BP/CH	0.452 ± 0.105		CaP			7684 ± 1012			
T11,L2,L5 FFT	15	BP	0.508 ± 0.145		CaP			11936 ± 1985			
T3-L4	14	BP	1.160 ± 0.100	6.4 ± 2.1	Palacos E-Flow PMMA	24.7 ± 5.1	2019 ± 979	2540	9667	8690	[36]
T2-L3	14	BP	0.659 ± 0.061	12.9 ± 6.9	Palacos E-Flow PMMA	47.0 ± 4.1	2019 ± 979	7145	2000	5772	
T3-L4	14	BP	0.596 ± 0.056	6.1 ± 2.4	Palacos E-Flow PMMA	26.4 ± 4.2	2019 ± 979	4765	2000	5186	
T2-L3	14	BP	0.653 ± 0.078	8.4 ± 3.8	Brushite Cement	41.4 ± 8.5	2019 ± 979	4119	2000	4156	
T4-L1	10	BP	0.987 ± 0.085	11.8 ± 3.6	Brush Cement	48.4 ± 5.5	2019 ± 979	4557	2000	4616	
T2-L1	10		0.56–0.89	6.11 ± 2.3	Simplex		4333 ± 1333	8000 ± 1667	4250 ± 1583	5333 ± 2000	[70]
	10		6.8 ± 0.9	CaP		4333 ± 1333	6333 ± 2333	4250 ± 1583	4750 ± 1583		

Hitchon et al. [70] used functional units of thoracic and lumbar bodies to compare different cements in spinal fracture. Hitchon et al. [70] used a functional segment of T9–L3 while Lu et al. used T10–L1 of a porcine segment. Other studies utilize functional units from the same spinal region [64,68]. Wilson et al. [75] used functional units from the same thoracic region, T7-T9 and T10-T12. In the experiments utilizing functional spine segments, the posterior elements are typically left attached; in studies utilizing single vertebral bodies, the posterior elements are commonly removed along with the surrounding soft tissue prior to compression tests in order to ensure plano-parallel ends.

Compression tests are employed almost universally to measure the strength and stiffness of the augmented or repaired vertebrae. Wilson et al. used a flexion and extension test to create a wedge fracture in addition to a compression test [68]. Compression tests are commonly performed using hydraulic machines, such as Instron, MTS, and Zwick, and Nihoi Koni. Compression rates for all tests were generally 5 mm/min to fracture, although faster compression rates of up to 2 mm/sec have been reported [67]. Nevertheless, the compression conditions are still considered quasi static for which hydraulic strengthening effects of the bone marrow and other viscoelastic materials are negligible. Although virtually all studies utilize a compression to fracture test, the definition of fracture is somewhat debatable. Fracture can be defined as a variety of conditions; a defined percent reduction in total height, a reduction in load with an increase of compression, or simply an audible cracking sound.

The general experimental design of most vertebroplasty studies is to evaluate the biomechanical efficacy of the procedure, by comparing the compressive stiffness and strength of the single vertebral bodies before and after the injection of the bone cement. There is much room for variations within this framework. The human spine experiences a wide variety of physiological loading conditions *in vivo* and it is under these complicated loads that fractures occur. Initial studies by Wilson et al. [75] and Hitchon et al. [69] assessed flexion, extension, lateral and rotational compliance after vertebroplasty repair of fractured spinal segments and both observed compliance values approach normal levels. Further studies into the effects of range of motion of the spine more complex loading conditions after vertebroplasty need to be explored.

B. Changes in Stiffness and Strength After Vertebroblasty

In an osteoporotic vertebra, the most important mechanical qualities determining fracture risk are the strength and stiffness of the vertebrae. As such, experimental design has focused on the examination of the changes of these properties resulting from vertebroblasty. Increase in vertebral strength is the most common measure of treatment effectiveness, though vertebral stiffness is often of note as it also contributes significantly to the viability of both the treated and neighboring vertebrae. Recent studies have attempted to analyze the biomechanical effects of different fill volumes in order to resolve the debate as to the optimal cement volume to be used clinically [67,76]. The volume of cement needed to restore stiffness and strength to prefractured values were considered to have achieved the biomechanical aim of vertebroplasty, and were therefore recommended. Belkoff et al. [67] conducted cadaveric studies on single vertebral bodies and found that only 2 mL of PMMA (Simplex P) was required to restore strength. To restore stiffness, the thoracic and lumbar regions needed 4 mL, while the thoracolumbar region required 8 mL. Liebschner et al. [76] simulated vertebroplasty on experimentally calibrated finite element models and also determined that only 3.5 mL was sufficient to restore stiffness on L1 vertebral body. Besides cement volume, there are a large number of factors contributing to vertebroplasty effectiveness, from treatment parameters, such as bone cement placement and material properties, to individual bone properties, such as bone mineral density, microarchitecture as well as severity and type of fracture. Previous studies on vertebral reinforcement of intact, osteoporotic vertebral

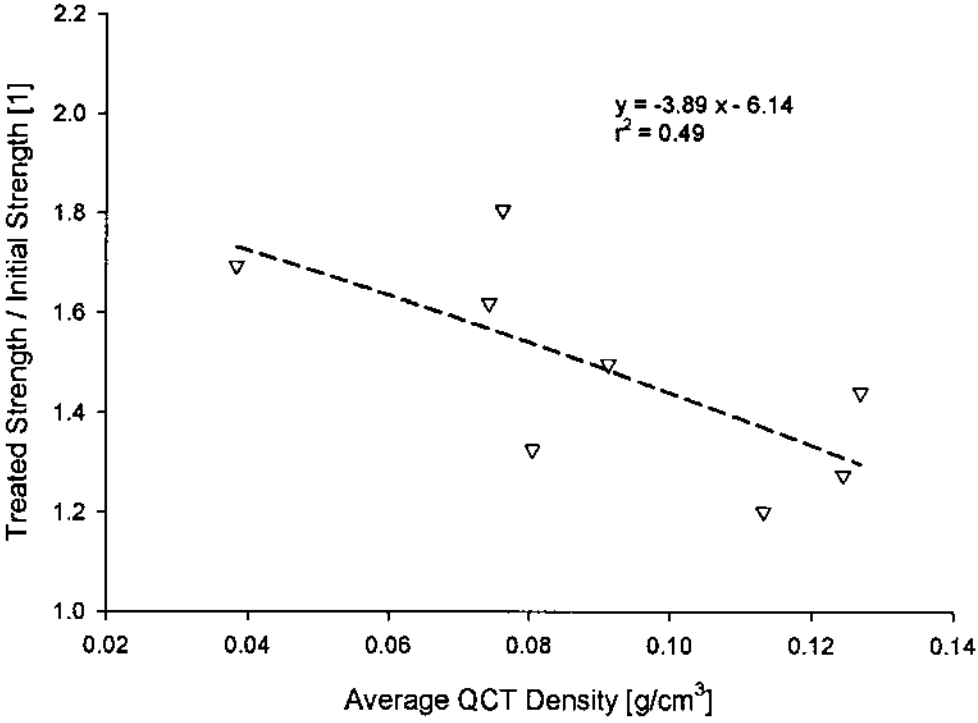

Figure 1 Strength increase as a function of bone mineral density. Increase in ultimate force of intact, osteoporotic vertebral bodies after injection of 5 mL of PMMA via bipedicular vertebroplasty is inversely proportional to the initial vertebral bone mineral density, implying that a greater increase in ultimate force can be gained in vertebrae with lower bone mineral density (unpublished data).

bodies injected showed strength augmentations be influenced by bone density, where lower bone mineral density experienced greater increase in strength [36,73] (Fig. 1).

Changes in the mechanical properties of the vertebrae can also be examined by combining stiffness and strength. Energy absorption can be calculated from the area under the load-deformation curve. Schildhauer et al. [71] demonstrated that the energy absorption of fractured single vertebrae (T1-T4) treated with carbonated apatite bone cement was considerably higher than for the untreated vertebrae. The results suggested that after the initial fracture, the carbonated apatite cement could augment the vertebrae to prevent further fractures and also had the potential to actually repair the damaged trabecular bone by remodeling due to the osteconductive nature of the cement.

C. Strengthening Effect and Energy Absorption

Injection of bone cement into a vertebral body provides not only an increase in the overall strength but also a strengthening effect and an increase in overall energy absorption. Few papers have addressed either of these effects, though they may have a significant effect on the viability of the treated vertebra. Injection of the cement results in a higher overall strength throughout the vertebra; however, in the immediate area surrounding the injection point the vertebra is actually weakened over time due to stress shielding by the stronger, injected material [62]. The

result of this uneven strengthening of the vertebra may promote fracture in the untreated region of the vertebra, which is still as weak as the untreated value. The effect of this is that the fracture point of the vertebra may shift away from the treated areas. Ikeuchi et al. [67] explored injection of the material at the top of the vertebra and in another sample through the entire vertebra. When compression tests were run, two peaks were seen in the load-deformation curve for the vertebra that was injected on the top.

A simple calculation using a series of springs representing the regions of bone and cement (Fig. 2) can show the effect of vertebroplasty on the strain experienced by surrounding bone. The range of possible strain values from a single applied load can be attained by examining an isostress condition=Min which the increase in strain is minimized=Mand the isostrain condition, resulting in the maximum effect. Assuming a 5 kN load (3.5 kN of which is experienced by the anterior portion of the vertebral body) and a fill volume of 30%, the strain in the isostress condition can be calculated as 0.0177, the same as that experienced under the intact condition (assuming elastic moduli of 600 MPa for cortical bone, 200 MPa for trabecular, and 800 MPa for PMMA). In the isostrain condition, this strain is raised to 0.025. The true increased strain lies between the two numbers, a number affected by several parameters such as the shape of the PMMA, but it is indisputable that the PMMA, if it has a higher stiffness than the surrounding bone, will cause an increased strain, possibly promoting fracture.

Only a few publications have adequately addressed the energy absorption of the vertebra as well. Schildhauer et al. demonstrated that the energy absorption of the treated vertebrae was considerably higher than for vertebrae of the untreated specimens [74]. The energy absorption,

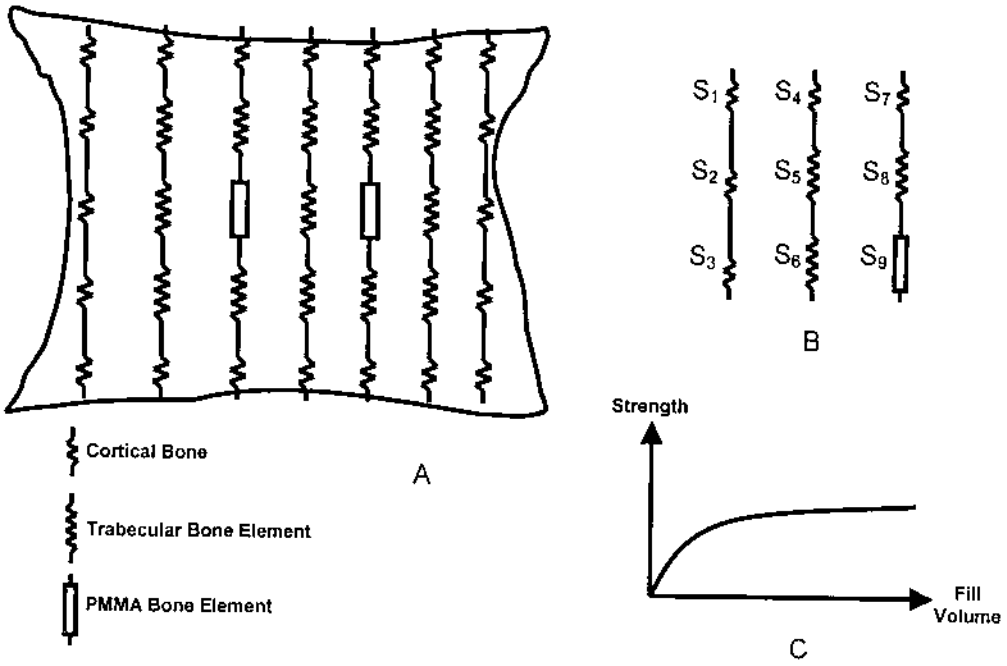

Figure 2 Modeling of the vertebral stiffness resulting from vertebroplasty. (A) Cross section of a vertebral body represented as a conglomeration of springs in series and parallel; (B) simplification of the model of a vertebral cross section; (C) graph showing the theoretical increase in strength as a function of volume fill.

calculated using the area under the curve of the load-deformation curve, is maximal in cases where there is a slow decline to failure after the ultimate point, as opposed to a sharp fracture.

D. Fatigue Strengthening of the Vertebroblasty

One of the adjunct goals of vertebroblasty is to prevent fractures caused by fatigue loading. Fatigue fractures result from cyclically applied forces smaller in magnitude than the ultimate strength of the vertebrae, which may simulate daily activities of a patient who underwent this type of treatment. Repeated loading can slowly weaken the vertebral body through microfractures that accumulate over time, leading to a decreased overall strength of the vertebral body. Although vertebroblasty is designed to prevent fracture by increasing the ultimate strength through augmentation, the efficacy of the treatment in the prevention of fatigue failure is not clear. One study by Lu et al. approached the subject of fatigue testing of treated vertebrae [69]. In this study, functional spinal segments from a porcine model were loaded in a compression machine (MTS). The load on the vertebrae was applied cyclically to induce failure by fatigue. The loading range was periodically applied from 100 to 1000N at 1 Hz for up to 3000 cycles in 10 specimens and up to 20,000 cycles in the remaining specimens. The stiffness of the segment was measured every 500 cycles with 1000 N. The design of this loading pattern was to simulate normal loading conditions of the human spine. Under experimental conditions with normal loads, the required test time would be in months [75], so the load was increased and 20,000 cycles were used to simulate a period of several months. The results of the study showed restoration of the failure load up to 20,000 cycles. However, a decrease in stiffness was observed at 3000 loading cycles. A total of 10,000 cycles equates to 2 weeks of regular daily activity [76], after which a healing mechanism starts repairing at least partially the accumulated damage. This study implies that vertebroplasty can be an effective means to reduce the effects of fatigue loading on the failure strength of the vertebral body. Conversely, stiffness regained by vertebroplasty can be lost through fatigue loading. It remains to be seen in further studies how fatigue loading damages the cement bone composite and influences the biomechanics of the surrounding tissue.

E. Possible Effects of Asymmetrical Augmentation

Vertebroplasty can be administered using different application techniques. The most common applications are the transpedicular approaches [9]. In each case, cement is applied to reinforce the vertebral body by injection through the pedicle of the vertebral body. The two approaches differ only in that one (unipedicular) fills the vertebral body on one side of the vertebral body, whereas the other (bipedicular) fills the vertebral body from both sides. Generally unilateral transpedicular treatment occurs when circumstances prohibit bilateral treatment, and the procedure is completed at a later time. Doubling of the number of procedures increases the expense incurred and the possibility for morbidity.

It is important to compare the effects of unilateral versus bilateral treatment for efficacy and effects on the biomechanics of the spine. One such investigation by Tohmeh et al. investigated the effect of unipedicular vertebroplasty on restoration of strength and stiffness of vertebral bodies and compared this result with that of bipedicular vertebroplasty [57]. In this study, vertebral bodies were loaded to failure and then treated with either unilateral or bilateral transpedicular vertebroplasty or used as an untreated control. The experimental setup used contained a compression platen mounted to a ball joint to allow rotation of the platen. Upon treatment, the vertebral bodies were again tested and strength and stiffness comparisons were made. In the case of both the bipedicular and unipedicular vertebroplasty–treated groups, strength was increased to a level above those seen prior to failure. The bipedicular did show a significantly higher increase in

strength than did the unipedicular treatment. Stiffness was also increased with both transpedicular vertebroplasty treatments, but the stiffness did not vary significantly from those observed prefailure. An interesting finding of the study was that there was no significant loss of height on either side of the vertebral bodies that received unilateral treatment resulting in toggle. Toggle occurs when the treated side of the vertebral body becomes significantly stronger than the untreated side of the vertebral body. Under loading this could lead to failure on the untreated aspect of the vertebral body, leading to a loss of height skewed to one side of the vertebral body. The resulting kyphosis could be detrimental. A possible reason for the absence of this finding in the study by Tohmeh et al. is that the experimental design forces the instantaneous center of rotation outside of the vertebral body (Fig. 3). As such, collapse would have to occur in an entire half of the vertebral body before toggle could be observed.

To investigate the possible occurrence of toggle, a study by Liebschner et al. used computer simulations to apply a pressure load to vertebral bodies that underwent various vertebroplasty procedures. Pressure loading conditions are believed to be the load transfer mechanism between intervertebral discs and the underlying vertebral bone. In the experiments, finite element models of CT scanned vertebral bodies, which were mechnically tested, were used to simulate bipedicular vertebroplasty, unipedicular vertebroplasty on the right side, unipedicular vertebroplasty on the left side, and postereolateral vertebroplasty. A calibration of the theoretical model to experimental results ensured realistic results. The virtually treated specimens were then loaded with a pressure boundary condition, which allowed for the deformation of the vertebral body without a fixed center of rotation outside of the vertebral body. The study found that unstable conditions resulted from the single-sided load transfer under the pressure load, which was proportional to filler volume. In the case of unipedicular treatments, a significantly greater relative motion was seen toward the untreated side of the vertebral body compared to the cases of bipedicular and posterolateral treatments (Fig. 4). Additionally, as the fill amount of the treatment increased, a corresponding increase was seen in the degree of toggle that occurred in the unipedicular case. In high fill vertebral bodies, the toggle was beyond the values of the untreated vertebral body, causing it to lose its stability.

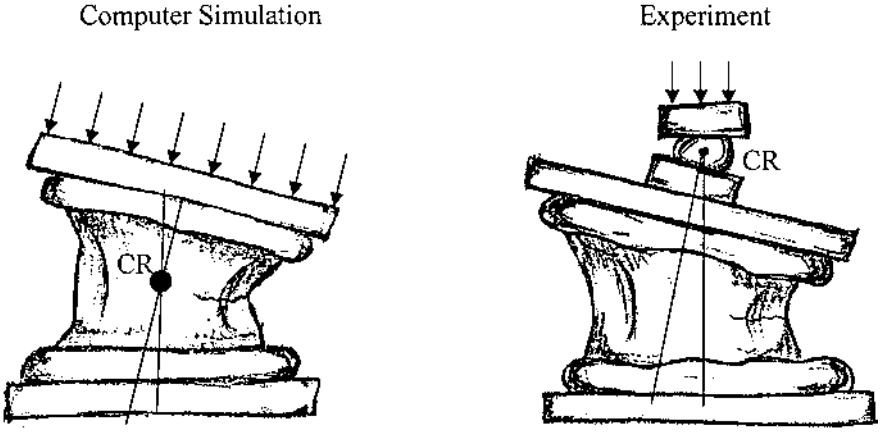

Figure 3 Comparison of techniques to investigate toggle. The computer simulation shows the effect of a pressure boundary on the center of rotation and the subsequent toggle that occurs. The experimental design shows the center of rotation located outside the vertebral body, where toggle cannot occur without dameage to a large portion of the vertebra.

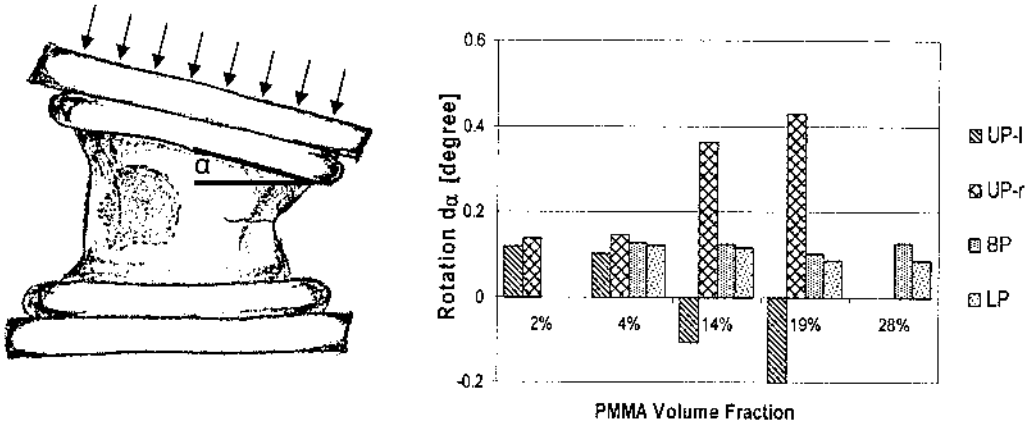

Figure 4 Effect of single-sided load transfer with unipedicular vertebroplasty. The image shows how toggle angle (α) results in a pressure boundary in unipedicular vertebroplasty. The graph shows how the toggle increases with fill volume. Different cases include unipedicular on the right side (UP-r), unipedicular on the left side (UP-l), bipedicular (BP), and posterolateral (LP) vertebroplasty.

Asymmetrical augmentation has been shown to have the ability to restore strength and stiffness as well as symmetrical augmentation in an in vitro setup. However, current testing methods do not allow for the application of a pressure load, which may be more relevant clinically. Only under this loading condition, which has heretofore been successfully completed virtually, can the effects of single-sided load transfer and the resultant toggle be investigated, pointing to the need for further development of models to investigate the effects of asymmetrical augmentation.

F. Biomechanical Goal of Vertebroplasty

The majority of vertebroplasty procedures performed are geared towards fracture repair. Several studies have investigated the changes in stiffness and strength experienced by vertebral bodies with osteoporotic vertebral compression fractures undergoing the procedure. Nevertheless, the optimum biomechanical effect of the procedure is not fully understood; while most studies the recovery of a fractured vertebral body to prefracture biomechanical properties, it can be argued that this does lower the fracture risk to a significant level.

Much of the abstruseness of the ultimate biomechanical goal of vertobroplasty stems from the highly debated issue of what comprises fracture risk. Newton-John and Morgan [77] suggested that a fracture threshold is reached when bone mass falls 2.5 standard deviations below the mean of normal young women. Because this is a relatively easily monitored value in a clinical setting, it has been adopted as the most common technique for vertebral risk assessment. However, Riggs et al. found that bone mineral density values in patients with and without vertebral fractures overlap widely, demonstrating a low sensitivity of the criteria [78].

A few studies reported in the literature have been geared towards calculating vertebral strength to estimate fracture risk, which is an intuitively more relevant mechanical parameter if one can approximate the loads experienced in daily activities. Nackemson [79] found that loads between 2.1 and 3.4 kN were generated at the L3–L4 region by lifting a 20 kg object, as measured by the intradisc pressure method. In a study by Biggemann et al. [80], fracture risk

was evaluated for 75 patients both by calculated vertebral strength and by bone mineral density alone. Vertebral compressive strength was calculated from the regression formula:

$$\text{Strength (kN)} = 0.32 + 0.00308 \times \text{density (mg/mL)} \times \text{endplate area (cm}^2\text{)} \quad (1)$$

and the patients were distributed into categories of high risk (compressive strength < 3 kN), medium risk (3–5 kN), and low risk (>5 kN). When examining the density risk groups (normal, slight osteoporosis, modest osteoporosis, severe osteoporosis), it was found that the strength range contained in each of the four groups exhibit a wide overlap with the neighboring groups. Strength ranges were as follows: normal group, 4.4–9.9 kN; for slight osteoporosis group, 2.5–5.8 kN; modest osteoporosis group 2.0–5.5 kN; severe osteoporosis group, 0.6–3.2 kN. This further supports the opinion that density alone does not fully predict fracture strength.

Since the overall goal of the procedure is to prevent further fracture, the augmentation of fractured vertebrae to low-risk strength accomplishes a significant step. However, it is a vital concern of the procedure to avoid complications; drastic changes in the mechanical properties of one vertebral body will have a severe impact on the dynamics of the surrounding segment. The balance of need for increased strength versus risk caused by drastically changed properties may limit the indications for treatment using vertebroplasty.

VII. INJECTABLE BONE SUBSTITUTES FOR VERTEBROPLASTY

A. Variability in PMMA Cements

While PMMA is currently not approved by FDA for vertebroplasty it is still the most widely used augmentation material. The mechanical properties of PMMA can vary widely based upon the manufacturer. The European clinicians who perform this technique typically use Simplex P (Howmedica, Rutherford, NJ), whereas U.S. clinicians commonly use Cranioplastic (Johnson & Johnson, Raynham, MA) or Osteobond (Zimmer, Warsaw, IN).

In a study comparing the biomechanics of treated vertebral body compression fractures with different bone cements in bipedicular vertebroplasty, Belkoff and colleagues mechanically tested 33 isolated vertebral bodies in an offset compression experiment [55]. A compression fracture was generated, stopping the deformation at a height reduction of the anterior wall of 25%. The specimens were then treated with respect to assigned group. After treatment, the test was repeated and stiffness and strength recorded. The augmentation volume was 4 mL through each pedicle (a total of 8 mL filler). The vertebral bodies treated with Cranioplastic were the only treated vertebral bodies that did not regain their initial stiffness. However, the results of a CANOVA test suggested that vertebral bodies injected with Cranioplastic were not significantly different in strength or stiffness than those injected with Osteobond. That the specimens injected with Cranioplastic did not recover their initial stiffness was attributed in part to the magnitude of the initial stiffness of the vertebral bodies in that group being higher and to the manner in which the cement was prepared. Typically, more monomer liquid is used during the preparation of the material than is recommended by the manufacturer. The additional amount of monomer allows for an increased working time and lower viscosity; it also, however, decreases the magnitude of the material properties. An unexpected result was that the vertebral bodies left untreated were not significantly weaker or less stiff than in the initial state. This finding may be related to the quality of vertebral specimens used and to the experimental limitations. The bone mineral density score of the specimens ranged from 0.7 to -6.9. Percutaneous vertebroplasty is used clinically for the treatment of compression fractures in osteoporotic vertebrae. Patients are considered to be osteoporotic only if their bone mineral density is 2.5 standard deviations below

the mean for gender- and weight-matched young adults ($t \leq 2.5$) [81]. In the study by Belkoff, only half of the cadaveric specimens met this criterion and could be considered osteoporotic [55]. Strength and stiffness of trabecular bone has been strongly correlated to density [82], and it is possible that those vertebral bodies with normal or near-normal bone density may exhibit less of an effect of vertebroplasty relative to those whose density is well below normal levels.

B. Disadvantages of PMMA

There are potential late complications of procedures using PMMA. Certainly one of the chief concerns surrounding vertebral augmentation is that because cement augmentation produces an exothermic reaction near bone and reduces fragment motion at the fracture site, and because cement flows into sites of potential repair, the procedure may hinder bone healing. Bioactive cements currently under development may be useful for augmentation and allow healing of the bone, which is the ultimate aim of fracture stabilization [68].

Even in contained cases, temperature elevations up to 70(C were recorded after injection of PMMA at the posterior vertebral cortex, albeit only in vertebrae with maximal cement filling. It has been hypothesized that this exothermic reaction of the PMMA in combination with the neurotoxic effect of the cement contributes to the marked pain relief of the patients, especially as the clinical improvement is not necessarily related to the injected volume of cement [29].

C. Alternative Materials

The various disadvantages of using PMMA in vertebroplasty procedures has led to investigation of other filler materials that reduce the negative aspects of PMMA usage. One such material is Orthocomp (Orthovita, Malvern, PA), a bioactive cement made of a glass-ceramic–reinforced composite material. The material is biocompatible, has a lower setting exotherm than PMMA, and has greater material properties than PMMA [25,83]. This particular material was examined in a study by Belkoff et al. [56]. The study compared the use of Orthocomp with a polymethylmethacrylate currently used for vertebroplasty in Europe, Simplex P (Howmedica, Rutherford, NJ). The study used 20 vertebral bodies (five each L1–L5 from four spines) with *t*-scores for bone mineral density ranging from -3.4 to -6.4. The specimens were split into two groups using a Latin square design. The specimens were measured for stiffness and strength, followed by a simulated compression fracture. Both groups showed similar values for both strength and stiffness. Vertebral bodies were then treated with a bipedicular vertebroplasty. Each vertebral body was injected with a 4 mL bolus of cement through each pedicle. The material injected was based upon the group assignments previously made. The results indicated that both cements restored strength to a value higher than that of the initial strength, but with a significantly higher increase in the group injected with Orthocomp. Upon examination of the stiffness, the results showed that the vertebral bodies injected with Simplex P failed to return to prefracture stiffness levels, while Orthocomp returned the stiffness to levels of those seen prior to fracture. The indications of this study show the possible effectiveness clinically for a material such as Orthocomp, especially when combined with the increased improvement over PMMA, the lower exotherm, and the ability of bone to bond to the cement.

Another material investigated for use in vertebroplasty procedures is an Experimental Brushite Cement (EBC). Heini et al.[36] used an EBC composed of 60% w/w β-tricalcium phosphate (β-TCP) and 40% w/w monocalciumphosphate monohydrate (MCPM). A small amount of $Na_2H_2P_2O_7$ was added to control the setting time. This was mixed with a solution of 0.1 mol H_2SO_4 solution containing 0.45 wt% Xanthan. The solid-to-liquid ratio was adjusted to 2.8 g/mL to obtain a viscosity of 2 Pa(s, which approaches the viscosity of PMMA cement.

EBC is a biocompatible cement that has a shear-thinning behavior, which is favorable for injection. Through direct comparison of PMMA- and EBC-reinforced spines, a higher ΔF_{max} and ΔS was observed with PMMA for the same degree of filling than with EBC. Also, for the same degree of reinforcement, less filling was necessary with PMMA than with EBC. This showed that while EBC could be used for vertebroplasty treatments, a larger fill volume would be required to gain the same increase in strength.

D. Biodegradable Materials

A biologically more inert material than PMMA for augmentation would be desirable [66]. The study by Heini et al. [36] evaluated one CaP cement, which showed less exothermic reaction. Schildhauer et al. used a special pressure-suction device to augment lumber vertebrae with an earlier version of Norian [74]. Under axial compression it was shown that augmentation resulted in a significant increase in energy absorption capabilities, albeit after initial collapse of about 25%. However, in order to prevent vertebral collapse, it seems important to augment the vertebral body at its maximal possible height. Other experimental studies have shown that CaP cements can have a favorable effect over time. Frankenburg et al. used Norian for filling proximal tibial and distal femoral metaphyseal defects in dogs [84]. Histological follow-up confirmed that the cement was osteoconductive and that gradual remodeling resulted in almost normal cortical and cancellous bone. Whether human osteoporotic bone reacts in a similar pattern remains an open question.

An alternative calcium phosphate cement (Mitsubishi Materials, Tokayo, Japan) has been examined by Ikeuchi et al. [67]. The CPC used in the study consisted of the cement [75% w/w α-tricalcium phosphate ($Ca_3(PO_4)_2$], 18% w/w tetracalcium phosphate [$Ca_4(PO_4)_2O$], 5% w/w dicalcium phosphate ($CaHPO_4{\cdot}H_2O$), and 2% w/w hydroxyapatite [$Ca_{10}(PO_4)_6(OH)_2$)] and a weakly basic hardening liquid (5% w/w chondroitin sodium sulfate, 12% w/w sodium succinate, 83% w/w water). The material in the study was prepared with a powder-to-liquid ratio of 2.8. The material was kneaded for 7 minutes to form a paste-like substance which was easy to infuse with a syringe and had a durable strength. The material progressively hardens to form hydroxyapatite by a hydration reaction. The resultant material has a compressive strength of about 80 MPa 1 week after hardening. The hardening characteristics of the cement vary with the weight ratios of the powder and liquid components. The material has been shown to be osteoconductive in vivo and bonds to newly formed bone. The results of the study showed that strength could be increased by using the CPC. Further, they showed an increase in strength with an increase in fill volume. Nevertheless, the CPC was utilized in this study as a prophylactic treatment of osteoporotic vertebral bodies at risk of fracture, therefore, the use of a 'weaker' material compared to PMMA may be beneficial in order to prevent stress-riser.

Hydroxyapatite (HA) cements are another biodegradable alternative to PMMA for use in vertebroplasty. The osteoconductivity and absence of exotherm of hydroxyapatite-forming materials make newly developed materials an attractive alternative to PMMA cement. However, difficulties associated with introducing the materials into vertebral bodies, primarily because of their poor flow characteristics, have impeded their acceptance and use by PVP practitioners. One example, BoneSource (Stryker-Howmedica-Osteonics, Rutherford, NJ), is a hydroxyapatite cement currently available and approved by FDA as a cranial defect filler. A study by Belkoff et al. [63] has shown that bipedicular vertebroplasty using BoneSource is able to restore strength to a level not significantly different from the prefracture values. However, the stiffness of the vertebral bodies is significantly lower posttreatment than prefracture. The same BoneSource material was examined by Hitchon et al. [70]. In this study, compression fractures were created in cadaveric vertebral bodies, which were then treated with a unipedicular vertebroplasty using

either PMMA or BoneSource. The study looked at the ability of each cement to restore the flexion, extension, axial rotation, and lateral bending. The results showed similar restoration of values for both PMMA and the HA-based BoneSource. In both cases, bending was improved on the side of treatment, but not on the collateral side, which did not receive filler materials. This merely illustrates the effect of the technique used for the vertebroplasty. The effectiveness of the HA material in restoring strength to fractured vertebral bodies without generation of excess heat is notable. Another benefit of this type of material is the osteoinductive nature and biodegradable of the material.

VIII. KYPHOPLASTY

A recent prospective randomized study [85] showed that vertebral compression fractures are associated with increased primarily pulmonary-related mortality. The presence of one vertebral compression fracture indicates that the chance of experiencing a second vertebral compression fracture during the next 5 years increases by fivefold [86]. If multiple vertebral bodies were to succumb to compression fractures and to lose height, it would be expected that the resultant progressive kyphosis would greatly affect normal spine function, pulmonary capacity, and activities of daily living [85]. In such cases, restoration of vertebral body height over several levels may have the most pronounced and desirable effect.

Treatment of vertebral compression fractures with PVP consists of injecting cement into the cancellous bone of the fractured vertebral body, presumably to stabilize the fracture. Although the technique increases strength and restores vertebral body stiffness, it does not restore vertebral body height. A new device, the inflatable bone tamp, has been developed as a means of restoring height. Height restoration has the potential benefit of reducing postfracture kyphosis and its associated squelae. The tamp is placed inside the vertebral body under fluoroscopic guidance through a percutaneously introduced cannula. The tamp is inflated, thereby compressing the cancellous bone, creating a void, and concurrently lifting the endplates in an en masse reduction. After tamp removal, the void can be filled under lower pressure than that needed for PVP. This procedure has been termed kyphoplasty (Fig. 5).

In a study by Belkoff and colleagues [87], a tamp treatment (kyphoplasty), followed by injection of Simplex P bone cement (Howmedica), resulted in stiffness restoration. Restoration of vertebral body stiffness should prevent any stress-riser effects or altered kinematics that would be expected if the stiffness were significantly more or less than that in the initial condition, respectively. The result that vertebral body stiffness is restored or nearly restored by augmentation (tamp or PVP) (PVP = percutaneous transpedicular vertebroplasty) is supported by a complementary investigation of spinal segment compliance [68].

The *t*-score for the vertebral bodies ranged from -3.7 to -8.8, with a mean of -5.3 ± 1.7 (SD). The average bone mineral density was 0.56 ± 0.2. Initially, vertebral body strength for the tamp group (2117 ± 579 N) was similar to that of the PVP group (2138 ± 740 N). Although strength after treatment increased significantly in both groups, vertebral body strength after treatment was significantly greater in the PVP group (7832 N) than in the tamp group (4792 N). The vertebral bodies in the PVP group were significant less stiff after treatment than they were in their initial condition. Posttreatment stiffness values for vertebral bodies in the tamp group were not significantly different than the initial stiffness values. There was no significant difference in posttreatment stiffness between the vertebral bodies in the tamp group and those in the PVP group.

The average cement volumes for the tamp and PVP groups were 9.4 ± 3.5 and 9.4 ± 1.4 mL, respectively. This difference was not statistically significant. Initial heights for the tamp

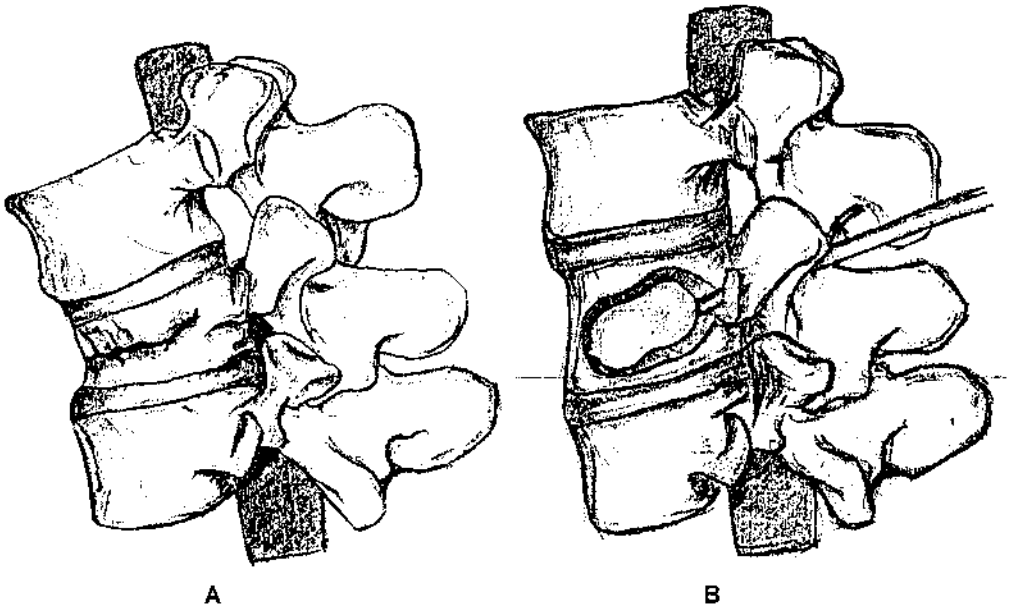

Figure 5 Kyphosis reduction through kyphoplasty. (A) A damaged vertebral body which has suffered a major fracture and accompanying kyphosis. (B) Inflation of the bone tamp in the interior of the vertebral body, creating a restoration of height and a reservoir for cement filling.

and PVP vertebral bodies were 25.7 ± 1.6 and 25.9 ± 2.0 mm, respectively. Postcompression height losses for the tamp and PVP groups were 2.6 ± 0.7 and 2.9 ± 0.9 mm, respectively. Height restored by the tamp treatment (2.5 ± 0.7 mm) was significantly more than that restored by the PVP treatment (0.8 ± 0.2mm).

Additionally, use of kyphoplasty in phase I trials has been shown to lead to a restoration of vertebral height. In studies by Lieberman et al. [88], restoration of height was seen in 70% of the cases, with a mean height restoration of 46.8% in this population. Similar results were seen by Dudeney and Lieberman; restoration of height was seen in 60% of the cases [89]. A mean height restoration of 56% was seen in this group.

As with vertebroplasty, other materials can be used as a filler material for restoration of strength. Verlaan et al. [90] investigated the use of calcium phosphate as a filler material for the kyphoplasty technique in a cadaveric model. The study showed the feasibility of using calcium phosphate in such a procedure, though the actual improvement of strength was not investigated.

The discrepancy between in vitro experimental results and data obtained through clinical studies elucidates the complexity of the mechanisms that influence the biomechanics of the spine and makes us realize how little we know about the fracture mechanics of the spine.

IX. FUTURE DIRECTIONS

In the clinical setting, vertebroplasty is currently used solely for fracture repair. However, the predictability of the procedure in these circumstances is typically very low. Vertebral fracture itself is an erratic phenomenon both in terms of circumstances of occurrence and in change in

mechanical properties affected. Thus, the biomechanical outcome of reparative vertebroplasty is very difficult to anticipate. Additionally, the degradation of mechanical properties of fractured vertebral bodies is commonly so severe that the vertebral strength, though it may be increased, relieving pain, will commonly remain at at-risk levels without injection of unsafe volumes of material [91].

Unfractured vertebrae in spines affected by osteoporosis have decreased mechanical properties to varying degrees and can benefit from vertebroplasty in much the same fashion as fractured vertebrae. Moreover, the mechanical property changes in osteoporotic spines are far more predictable and consistent than those in fractured spines, leading to a far more measurable effect from treatment. Under these circumstances, treatment optimization is far more accessible.

Optimization of vertebroplasty for efficacy in recovering the biomechanics of the vertebrae allows a smaller filler material volume to be used, which diminishes risk of complications due to cement leakages, while successfully enhancing structural behavior to reduce fracture risk, thereby improving long-term clinical outcomes. This can be accomplished by identifying damaged regions in the case of vertebral repair or regions at high risk of fracture for vertebral reinforcement and injecting filler material into those regions compared to injecting filler material into general anatomic locations (unipedicular, bipedicular, and posterolateral).

Though treatment with bone cements has been shown to be effective, the fact remains that it conventionally leaves behind an inert and foreign substance. Some present research is geared towards the use of bioresorbable compounds such as biodegradable polymers and calcium phosphate [65]. In this case, the ultimate goal of the procedure is to provide support and relief while giving the bone an opportunity to re-grow. To this end, growth factors and other hormones can be incorporated into the material injected [92], making them so-called biomimetric materials.

X. CONCLUSION

The percutaneous application of an acrylic bone cement, polymethylmethacrylate, to vertebral defects associated with osteoporotic vertebral compression fracture, vertebral angioma, and osteolytic metastasis and myeloma has proven successful in alleviating back pain. Vertebroplasty is able to restore biomechanical properties of the vertebrae to prefracture values. However, since fracture often occurred at the pre-fracture values, mechanical support offered through this procedure could be insufficient. Strength of the vertebral body must be increased beyond fracture risk levels (>5 kN) so as to prevent further fractures. Unfortunately, in order to attain such strength levels using PMMA, the volume of bone cement needed would be significant. Large cement fills increases the risk of extravasations and, subsequently, complications that threaten the health and life of the patient. Therefore, vertebroplasty may not be beneficial in treating vertebral compression fractures of severely osteoporotic patients with biomechanical properties that are well below the low fracture risk level. Another risk associated with vertebroplasty recently discovered is the increased risk of fracture in the vertebral body adjacent to the repaired vertebral body. The heightened risk has be attributed to the increased stiffness or rigidness of the treated vertebral body that leads to a ‘stiffness-riser’ effect, altering the biomechanics of load transfer to the adjacent vertebrae. This effect can be avoided with the use of alternative filler materials that increase strength while the increase in stiffness is minimal. The materials currently being investigated as potential alternatives, calcium phosphate, hydroxyapatite, and glass ceramics, are all too soft. The focus has to be directed on other materials with the desired mechanical properties. Analyzing current biomechanical data and using computer simulations, mechanical properties of an ideal material to be used in vertebroplasty may be found, which will then aid in the decision process for selecting alternatives to PMMA.

Vertebroplasty too has taken a new turn, from repair of fractured vertebrae to prophylactic vertebral reinforcement of intact but osteoporotic vertebrae, especially in patients who have previously sustained fractures and are at a high risk for subsequent fractures. Instead of injecting with a permanent material, biodegradable filler materials infused with bioactive factors, such as bone morphogenic proteins and growth factors, may be more suitable. The biodegradable material provides a temporary scaffold onto which new bone can grow. As the degradable material starts to be resorbed by the body, bioactive factors are released, inducing new bone growth, which replaces the resorbed material. Due to new bone growth, bone mass and strength will increase, thereby reducing the risk of fracture. This new application for vertebroplasty also faces the same complication risks associated with leakage of filler material. The risk of extravasation can be minimized by optimizing the amount of filler material needed for biomechanical efficacy through the strategic placement of the material at either high risk of fracture regions within the vertebral body for vertebral reinforcement or fracture sites for vertebral repair. As a result, by focusing research on the optimization of filler material, volume and placement for vertebral repair, vertebroplasty will enjoy success in pain relief and biomechanical enhancements with minimal risk of complications. Vertebroplasty for vertebral reinforcement may even help in reversing the effects of osteoporosis when combined with systemic pharmacological therapy.

REFERENCES

1. Galibert P. [Preliminary note on the treatment of vertebral angioma by percutaneous acrylic vertebroplasty]. Neurochirurgie 1987; 33(2):166–168.
2. Debussche-Depriester C. Percutaneous vertebroplasty with acrylic cement in the treatment of osteoporotic vertebral crush fracture syndrome. Neuroradiology 1991; 33(suppl):149–152.
3. Cotten A. Percutaneous vertebroplasty: state of the art. Radiographics 1998; 18(2):311–323.
4. Weill A. Spinal metastases: indications for and results of percutaneous injection of acrylic surgical cement. Radiology 1996; 199(1):241–247.
5. Martin JB. Vertebroplasty: clinical experience and follow-up results. Bone 1999; 25(2 suppl): 11S–15S.
6. Ide C. Vertebral haemangiomas with spinal cord compression: the place of preoperative percutaneous vertebroplasty with methyl methacrylate. Neuroradiology 1996; 38(6):585–589.
7. Cortet B. Percutaneous vertebroplasty in patients with osteolytic metastases or multiple myeloma. Rev Rheum Engl Ed 1997; 64(3):177–183.
8. Murphy KJ, Deramond H. Percutaneous vertebroplasty in benign and malignant disease. Neuroimaging Clin North Am 2000; 10(3):535–545.
9. Jensen ME. Percutaneous polymethylmethacrylate vertebroplasty in the treatment of osteoporotic vertebral body compression fractures: technical aspects. AJNR Am J Neuroradiol 1997; 18(10): 1897–1904.
10. Mathis JM, Petri M, Naff N. Percutaneous vertebroplasty treatment of steroid–induced osteoporotic compression fractures. Arthritis Rheum 1998; 41(1):171–175.
11. Deramond H. Percutaneous vertebroplasty with polymethylmethacrylate. Technique, indications, and results. Radiol Clin North Am 1998; 36(3):533–546.
12. Osteoporosis prevention, diagnosis, and therapy. JAMA 2001; 285(6):785–795.
13. www.osteo.org/osteo.html.
14. Silverman SL. The clinical consequences of vertebral compression fracture. Bone 1992; 13(suppl 2): S27–31.
15. Eastell R. Classification of vertebral fractures. J Bone Miner Res 1991; 6(3):207–215.
16. Riggs BL, Melton LJ. The worldwide problem of osteoporosis: insights afforded by epidemiology. Bone 1995; 17(5 suppl):505S–511S.

17. Cooper C. Incidence of clinically diagnosed vertebral fractures: a population-based study in Rochester, Minnesota, 1985–1989. J Bone Miner Res 1992; 7(2):221–227.
18. Melton LJ. How many women have osteoporosis now?. J Bone Miner Res 1995; 10(2):175–177.
19. Melton LJ. Epidemiology of vertebral fractures in women. Am J Epidemiol 1989; 129(5):1000–1011.
20. Ettinger B. Contribution of vertebral deformities to chronic back pain and disability. The Study of Osteoporotic Fractures Research Group. J Bone Miner Res 1992; 7(4):449–456.
21. Jensen KS, Mosekilde L. A model of vertebral trabecular bone architecture and its mechanical properties. Bone 1990; 11(6):417–423.
22. Johansson C. A community-based population study of vertebral fractures in 85-year-old men and women. Age Ageing 1994; 23(5):388–392.
23. Rapado A. General management of vertebral fractures. Bone 1996; 18(3 suppl):191S–196S.
24. Jensen ME, Dion JE. Percutaneous vertebroplasty in the treatment of osteoporotic compression fractures. Neuroimaging Clin North Am 2000; 10(3):547–568.
25. Deramond H. Percutaneous vertebroplasty. Semin Musculoskelet Radiol 1997; 1(2):285–296.
26. Galibert P, Deramond H. [Percutaneous acrylic vertebroplasty as a treatment of vertebral angioma as well as painful and debilitating diseases]. Chirurgie 1990; 116(3):326–334.
27. Dufresne AC. [Percutaneous vertebroplasty of the cervico-thoracic junction using an anterior route. Technique and results. Report of nine cases]. J Neuroradiol 1998; 25(2):123–128.
28. Shepherd S. Radiotherapy and the management of metastatic bone pain. Clin Radiol 1988; 39(5): 547–550.
29. Cotten A. Percutaneous vertebroplasty for osteolytic metastases and myeloma: effects of the percentage of lesion filling and the leakage of methyl methacrylate at clinical follow-up. Radiology 1996; 200(2):525–530.
30. Murray JA, Bruels MC, Lindberg RD. Irradiation of polymethylmethacrylate. In vitro gamma radiation effect. J Bone Joint Surg Am 1974; 56(2):311–312.
31. Chiras J. [Percutaneous vertebral surgery. Technics and indications]. J Neuroradiol 1997; 24(1): 45–59.
32. Gangi A, Kastler BA, Dietemann JL. Percutaneous vertebroplasty guided by a combination of CT and fluoroscopy. AJNR Am J Neuroradiol 1994; 15(1):83–86.
33. Mathis JM. Percutaneous vertebroplasty: a developing standard of care for vertebral compression fractures. AJNR Am J Neuroradiol 2001; 22(2):373–381.
34. Eck JC, Hodges SD, Humphreys SC. Vertebroplasty: a new treatment strategy for osteoporotic compression fractures. Am J Orthop 2002; 31(3):123–128.
35. Jasper LE. The effect of monomer-to-powder ratio on the material properties of cranioplastic. Bone 1999; 25(2 suppl):27S–29S.
36. Heini PF. Augmentation of mechanical properties in osteoporotic vertebral bones=Ma biomechanical investigation of vertebroplasty efficacy with different bone cements. Eur Spine J 2001; 10(2): 164–171.
37. Murphy KJ, Lin DD. Vertebroplasty: a simple solution to a difficult problem. J Clin Densitom 2001; 4(3):189–197.
38. Amar AP. Percutaneous transpedicular polymethylmethacrylate vertebroplasty for the treatment of spinal compression fractures. Neurosurgery 2001; 49(5):1105–1115.
39. Kaufmann TJ. Age of fracture and clinical outcomes of percutaneous vertebroplasty. AJNR Am J Neuroradiol 2001; 22(10):1860–1863.
40. Cortet B. Percutaneous vertebroplasty in the treatment of osteoporotic vertebral compression fractures: an open prospective study. J Rheumatol 1999; 26(10):2222–2228.
41. Barr JD. Percutaneous vertebroplasty for pain relief and spinal stabilization. Spine 2000; 25(8): 923–928.
42. Grados F. Long-term observations of vertebral osteoporotic fractures treated by percutaneous vertebroplasty. Rheumatology (Oxford) 2000; 39(12):1410–1414.
43. Cyteval C. Acute osteoporotic vertebral collapse: open study on percutaneous injection of acrylic surgical cement in 20 patients. AJR Am J Roentgenol 1999; 173(6):1685–16890.
44. Zoarski GH. Percutaneous vertebroplasty for osteoporotic compression fractures: quantitative prospective evaluation of long-term outcomes. J Vasc Interv Radiol 2002; 13(2 Pt 1):139–148.

45. Gangi A. CT-guided interventional procedures for pain management in the lumbosacral spine. Radiographics 1998; 18(3):621–633.
46. Jensen ME, Dion JE. Vertebroplasty relieves osteoporosis pain. Diagn Imaging (San Franc) 1997; 19(9):68, 71–72.
47. Cotten A, Duquesnoy B. Vertebroplasty: current data and future potential. Rev Rhum Engl Ed 1997; 64(11):645–649.
48. Bostrom MP, Lane JM. Future directions. Augmentation of osteoporotic vertebral bodies. Spine 1997; 22(24 suppl):38S–42S.
49. Ruiz D. Pathology findings with acrylic implants. Bone 1999; 25(2 suppl):85S–90S.
50. Deramond H, Wright NT, Belkoff SM. Temperature elevation caused by bone cement polymerization during vertebroplasty. Bone 1999; 25(2 suppl):17S–21S.
51. Eriksson RA, Albrektsson T, Magnusson B. Assessment of bone viability after heat trauma. A histological, histochemical and vital microscopic study in the rabbit. Scand J Plast Reconstr Surg 1984; 18(3):261–268.
52. De Vrind HH, Wondergem J, Haveman J. Hyperthermia-induced damage to rat sciatic nerve assessed in vivo with functional methods and with electrophysiology. J Neurosci Methods 1992; 45(3): 165–174.
53. Danilewicz-Stysiak Z. Experimental investigations on the cytotoxic nature of methyl methacrylate. J Prosthet Dent 1980; 44(1):13–16.
54. Dahl OE, Garvik LJ, Lyberg T. Toxic effects of methylmethacrylate monomer on leukocytes and endothelial cells in vitro. Acta Orthop Scand 1994; 65(2):147–153.
55. Belkoff SM. An in vitro biomechanical evaluation of bone cements used in percutaneous vertebroplasty. Bone 1999; 25(2 suppl):23S–26S.
56. Belkoff SM. Biomechanical evaluation of a new bone cement for use in vertebroplasty. Spine 2000; 25(9):1061–1064.
57. Tohmeh AG. Biomechanical efficacy of unipedicular versus bipedicular vertebroplasty for the management of osteoporotic compression fractures. Spine 1999; 24(17):1772–1776.
58. Lin JT, Lane JM. Nonmedical management of osteoporosis. Curr Opin Rheumatol 2002; 14(4): 441–446.
59. Watts NB, Harris ST, Genant HK. Treatment of painful osteoporotic vertebral fractures with percutaneous vertebroplasty or kyphoplasty. Osteoporos Int 2001; 12(6):429–437.
60. Hardouin P. Should percutaneous vertebroplasty be used to treat osteoporotic fractures? An update. Joint Bone Spine 2001; 68(3):216–221.
61. Ross PD, Davis JW, Epstein RS, Wasnich RD. Pre-existing fractures and bone mass predict vertebral fracture incidence in women. Ann. Intern Med 1991; 114:919–923.
62. Berlemann U. Adjacent vertebral failure after vertebroplasty. A biomechanical investigation. J Bone Joint Surg Br 2002; 84(5):748–752.
63. Belkoff SM. An ex vivo biomechanical evaluation of a hydroxyapatite cement for use with vertebroplasty. Spine 2001; 26(14):1542–1546.
64. Dean JR, Ison KT, Gishen P. The strengthening effect of percutaneous vertebroplasty. Clin Radiol 2000; 55(6):471–476.
65. Lim TH. Biomechanical evaluation of an injectable calcium phosphate cement for vertebroplasty. Spine 2002; 27(12):1297–1302.
66. Bai B. The use of an injectable, biodegradable calcium phosphate bone substitute for the prophylactic augmentation of osteoporotic vertebrae and the management of vertebral compression fractures. Spine 1999; 24(15):1521–1526.
67. Ikeuchi M. Mechanical augmentation of the vertebral body by calcium phosphate cement injection. J Orthop Sci 2001; 6(1):39–45.
68. Wilson DR. Effect of augmentation on the mechanics of vertebral wedge fractures. Spine 2000; 25(2):158–165.
69. Lu WW. Bioactive bone cement as a principal fixture for spinal burst fracture: an in vitro biomechanical and morphologic study. Spine 2001; 26(24):2684–2691.
70. Hitchon PW. Comparison of the biomechanics of hydroxyapatite and polymethylmethacrylate vertebroplasty in a cadaveric spinal compression fracture model. J Neurosurg 2001; 95(2 suppl):215–220.

71. von Stechow D. Does vertebroplasty alter the mechanical competence of severely osteoporotic vertebrae (abstr)? 48th Annual Meeting of the Orthopaedic Research Society. Poster Number 0557, 2002.
72. Alkalay R. Direct augmentation approach restores the structural competence of failed metastatic defect vertebrae (abstr). 48th Annual Meeting of the Orthopaedic Research Society. Poster Number 0765, 2002.
73. Belkoff SM. The biomechanics of vertebroplasty. The effect of cement volume on mechanical behavior. Spine 2001; 26(14):1537–1541.
74. Schildhauer TA. Intravertebral body reconstruction with an injectable *in situ*-setting carbonated apatite: biomechanical evaluation of a minimally invasive technique. J Orthop Res 1999; 17:67–72.
75. Ashman RB. Mechanical testing of spinal instrumentation. Clin Orthop 1988; 227:113–25.
76. Brinckmann P, Biggemann M, Hilweg D. Prediction of the compressive strength of human lumbar vertebrae. Spine 1989; 14(6):606–610.
77. Newton-John HF, Morgan DB. The loss of bone with age, osteoporosis, and fractures. Clin Orthop 1970; 71:229–252.
78. Riggs BL. Effect of the fluoride/calcium regimen on vertebral fracture occurrence in postmenopausal osteoporosis. Comparison with conventional therapy. N Engl J Med 1982; 306(8):446–450.
79. Nachemson A. Lumbar intradiscal pressure. In:Jayson M.I. Nachemson A, ed. The Lumbar Spine and Back Pain. London. Pitman, 1985:341.
80. Biggemann M. Risk of vertebral insufficiency fractures in relation to compressive strength predicted by quantitative computed tomography. Eur J Radiol 1991; 13(1):6–10.
81. Kanis JA. Assessment of fracture risk and its applications to screening for postmenopausal osteoporosis: synopsis of a WHO report. Osteoporos Int 1994; 4:368–381.
82. Hayes WC. Biomechanics of cortical and trabecular bone: implications for assessment of fracture risk. In:Mow, V C Hayes WCHayes, W C, Hayes WC, eds. Basic Orthopaedic Biomechanics. New York. Raven, 1991:93–142.
83. Dallap BL. Histological, radiological, and mechanical comparison of polymethylmethacrylate (PMMA) and a bioactive bone cement in an ovine model. (abstr). Trans Orthop Res Soc 1999; 24: 503.
84. Frankenburg EP. Biomechanical and histological evaluation of a calcium phosphate cement. J Bone Joint Surg Am 1998; 80:1112–1124.
85. Kado DM. Vertebral fractures and mortality in older women: a prospective study. Study of Osteoporotic Fractures Research Group. Arch Intern Med 1999; 159(11):1215–1220.
86. Ross PD. Pre-existing fractures and bone mass predict vertebral fracture incidence in women. Ann Intern Med 1991; 114(11):919–923.
87. Belkoff SM. An ex vivo biomechanical evaluation of an inflatable bone tamp used in the treatment of compression fracture. Spine 2001; 26(2):151–156.
88. Lieberman IH. Initial outcome and efficacy of 'kyphoplasty' in the treatment of painful osteoporotic vertebral compression fractures. Spine 2001; 26(14):1631–1638.
89. Lieberman I. Percutaneous vertebroplasty in the treatment of osteoporotic vertebral compression fractures: an open prospective study. J Rheumatol 2000; 27(10):2526.
90. Verlaan JJ. Balloon vertebroplasty with calcium phosphate cement augmentation for direct restoration of traumatic thoracolumbar vertebral fractures. Spine 2002; 27(5):543–548.
91. Heini PF, Berlemann U. Bone substitutes in vertebroplasty. Eur Spine J 2001; 10(suppl 2):S205–213.
92. Baylink D, Finkelman R, Mohan S. Growth factors to stimulate bone formation. J Bone Miner Res 1993; 8(2):C565–S572.

34

Bioactive Bone Cement for the Treatment of Osteoporotic Vertebral Compression Fracture

W. W. Lu and G. X. Ni
The University of Hong Kong
Hong Kong

I. INTRODUCTION

Vertebral compression fractures (VCFs) affect about 500,000 individuals annually in the United States, costing an estimated $250 million (Melton, 1989). These fractures occur when the load transmitted by a vertebra exceeds its failure load (Myers, 1997). Reduction in individual vertebral strength may result from infiltrative processes created by benign or malignant tumors or, more commonly, from bone mineral loss precipitated by osteoporosis (Peck, 1988; Hayes, 1991).

Osteoporosis, which may be age-related (primary) or due to steroid use (secondary), is a systemic disease affecting more than 24 million Americans. It results in progressive bone mineral loss and concurrent changes in bony architecture, which leave the spinal column vulnerable to compression fractures. It is estimated that the prevalence of vertebral fractures in postmenopausal women to be 25% and that the prevalence of fractures in men may approach that in women of the same age group (Melton, 1997).

The primary complication of VCFs is acute pain: 84% of patients with radiographic evidence of compression fractures report associated back pain (Cooper, 1992). Other complications include kyphotic deformity, transient ileus or urinary retention, and, rarely, cord compression (Lukert, 1994). The pain, discomfort, and deformity associated with compression fractures often lead to significant physical, psychological, and functional impairments and frequently have a substantial impact on quality of life (Lyles, 1993; Gold, 1996).

On the other hand, few effective, low-risk interventions are available for the treatment of VCFs. The traditional treatment of these fractures is commonly nonoperative and includes bracing and external orthoses, pain medications, physical therapy, and medical therapies for osteoporosis. Many elderly patients, unfortunately, have chronic pain and develop progressive kyphotic deformities. Surgical treatment for VCFs is indicated only when significant neurological dysfunction and progressive deformity exist. Such treatment is fraught with complications that are amplified by osteoporosis, including graft dislodgment and subsidence, loss of implant fixation, and junctional kyphosis.

Fortunately, there is another effective option for the treatment of VCFs. Percutaneous vertebroplasty (PVP) is a minimally invasive, radiologically guided interventional procedure originally performed in France in 1987 and in the United States in 1993. Furthermore, more

recently, a new method for augmenting fractured vertebrae, which includes a fracture reduction step, called kyphoplasty, is emerging. Kyphoplasty is a modification of the vertebroplasty procedure that attempts correction of the spinal deformity and restoration of vertebral body (VB) height prior to fracture stabilization with bone cement.

During the last 15 years, technical innovations and instrumentation enhancements of the PVP procedure have improved so that it may ultimately become the standard of care for the treatment of painful VCFs (Mathis, 2001). Clinical studies have shown that PVP/ kyphoplasty can relieve the acute pain associated with VCFs and reduce the duration of immobilization. In this chapter we will provide a brief overview of the clinical outcome of PVP/ kyphoplasty for the treatment of VCFs, as well as the basic science and biomechanics research related to this procedure. We will also introduce some potential bone cements for PVP/kyphoplasty, especially a bioactive bone cement (SrHAC) exclusively designed for PVP.

II. CLINICAL OUTCOMES AND COMPLICATIONS

Table 1 indicates that the PVP procedure provided excellent pain relief in 63–100% of treated patients. Compared with PVP, kyphoplasty is a relatively newer technique and has only been used actively in the last few years since the U.S. Food and Drug Administration (FDA) approved inflatable bone tamps in 1998. Several clinical studies have shown that this procedure also provided significant improvement in pain and functional status and an additional advantage of restoration in VB height (Table 2).

Table 1 Clinical Studies of Percutaneous Vertebroplasty

Reference	Patient number	Levels treated	Duration of f/u	Pain improved
Kaemmerlen et al, 1989 (54)	37	48	6mos-1yrs	100%–65%
Gangi et al, 1994 (37)	4	8	4–15mos	100%
Weill et al, 1996 (92)	24	33	6mos	73%
Cotten et al, 1996 (23)	16	17	2dys-6mos	97.3%–75%
Jensen et al, 1997 (53)	29	4.7	Up to 3 yrs	90%
Mathis et al, 1998 (71)	1	7	9mos	100%
Deramond et al, 1998 (31)	80	Not reported	Up to 10yrs	90+%
Martin et al, 1999 (69)	11	Not reported	Not reported	78%
Cortet et al, 1999 (22)	16	20	6 mos	88%
Cyteval et al, 1999 (25)	20	23	6 mos	90%
Barr et al, 2000 (8)	38	70	2–42mos	95%
O'Brien et al, 2000 (79)	6	6	3 mos	67%
Heini et al, 2001 (48)	17	45	12 mos	76%
Maynard et al, 2001 (73)	27	35	1w-32mos	93%
Diamond et al, 2001 (32)	4	Not reported	7 days	100%
Kaufmann et al, 2001 (55)	72	122	Within 1 mo	Significantly
Amar et al, 2001 (2)	97	258	2–35mos	63%
Gaughen et al, 2002 (39)	48	84	Up to 1mo	95%
Rami et al, 2002 (82)	1	1	17mos	100%
Ryu et al, 2002 (84)	159	347	3 mos	87%
Zoarski et al, 2002 (96)	30	54	15–18mos	96%
Tsou et al, 2002 (91)	16	17	18mos	100%

Table 2 Clinical Studies of Kyphoplasty

Reference	Patient number	Level treated	Duration of follow-up	VB height improved	Clinical outcome	Complication
Garfin et al, 2001 (38)	340	603	Up to 18mos	>50%	95%patients with significant pain and functional improvement	1 with transient fever, 1 epidural hematoma, 1 partial motor loss to lower extremities required surgery; and 1 anterior cord syndrome.
Lieberman et al, 2001 (64)	30	70	6.7mos	47%	Significant improvement in bodily pain and physical function	6 (8.6%) of 77 levels with leakage, 1 with pulmonary edema and 2 with rib fractures.
Theodorou et al, 2001 (89)	15	24	6–8mos	62.4%	100% pain relief, 2(13%) patients with significant improvement in respiratory function	No serious complications
Dudeney et al, 2002 (33)	18	55	7.4mos	34%	Significant improvement in bodily pain, physical function, vitality, and social functioning	2 (4%) of 55 levels with asymptomatic leakage

Cement extravasation is the most common complication associated with PVP/kyphoplasty. Other complications include transitory fever, transient worsening of pain, radiculopathy, rib fractures, cement pulmonary embolism, infection, and spinal cord compression. The rate of complications varies considerably with the indications. With osteoporotic VCFs, complications are few (usually 1–2%) and most often are nonneurological and transient (Weill, 1996; Jensen, 1997; Mathis, 1998; Barr, 2000). Transient radiculopathy has been reported in 3–6% of cases and has been successfully treated with steroids and antiinflammatory medications (Cotten, 1996, 1998; Chiras, 1997; Deramond, 1999); however, persistent radiculopathy occurred in 2–3% of patients and required surgical intervention for cement removal.

In conclusion, both PVP and kyphoplasty are efficacious treatments for VCFs, especially for those secondary to osteoporosis. However, long-term controlled clinical trails should precede widespread implementation of these techniques.

III. BIOMECHANICS

Several benchtop studies have been conducted to gain a better understanding of the underlying mechanics responsible for the success of PVP with cement augmentation as well as basic information on the materials used in the procedure (discussed later). Such investigations are giving impetus to the development of new devices and materials to improve efficacy of the treatment.

Several mechanisms have been proposed to explain the pain relief associated with PVP, including thermal necrosis and chemotoxicity of the intraosseous pain receptors as well as

mechanical stabilization (Bostrom, 1997). Among them, mechanical stabilization is thought to be the most likely mechanism (Belkoff, 1999, 2000; Deramond, 1999; Tohmeh, 1999).

After cement augmentation, microfractures in the bone are immobilized by the cement. Many studies have demonstrated that augmented vertebrae, either by unipedicular injection or bipedicular injection (Tohmeh, 1999), were significantly stronger in compression than unaugmented specimens (Bostrom, 1997; Schildauer, 1999), which suggests that the cement transmits part of the compressive load in an augmented vertebral body. Further study showed that this effect seems to be dose-dependent and region-dependent, and moreover that the restoration of strength and stiffness are not synchronous (Fig. 1). In a cadaveric study, Belkoff et al. (2001) found that the strength of vertebrae was restored for all regions (thoracic, thoracolumbar, and lumbar regions) when 2 mL of either Orthocomp or Simplex P cement was injected. To restore stiffness with Orthocomp, the thoracic and thoracolumbar regions required 4 mL, but the lumbar region required 6 mL. To restore stiffness with Simplex P, the thoracic and lumbar regions required 4 mL, but the thoracolumbar region required 8 mL.

Using an experimentally calibrated, anatomically accurate finite-element model, Liebschner et al. (2001a) found that vertebral stiffness recovery after vertebroplasty was strongly influenced by the volume fraction of the implanted cement. Only a small amount of bone cement (14% fill or 3.5 cm^3) was necessary to restore stiffness of the damaged vertebral body to the predamaged value. Use of a 30% fill increased stiffness by more than 50% compared with the predamaged value. The authors suggested that large volume fractions may not be the most biomechanically optimal configuration, and an improvement might be achieved by use of lower fills with symmetrical placement.

However, these studies are limited because only compressive loads were studied. For a more complete mechanical assessment of augmentation, relative motion of spine segment verte-

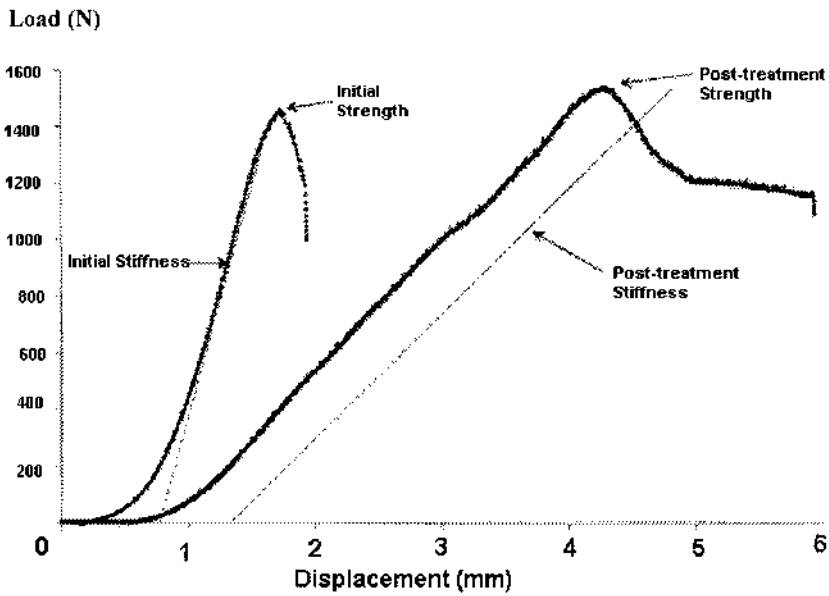

Figure 1 Initial and posttreatment VB strength and stiffness response to compression. The strength of VB may be restored with the injection of 2 mL of bone cement, however, 4 mL is needed to restore the stiffness. (Modified from Belkoff et al., 2001.)

brae in response to applied ''pure'' anterior/posterior and lateral bending moments must be determined.

To assess the mechanical effects of cement augmentation of vertebral wedge fractures, as well as to determine whether the kyphoplasty procedure has the same mechanical effects as the PVP procedure, Wilson et al. (2000) observed the effect of cement augmentation of wedge-fractured vertebral bodies on spine segment compliance in 16 cadaver specimens. In this study, neutral and full-load compliance of each fractured spine segment in flexion/extension and lateral bending were assessed by measuring the relative rotation of the vertebral bodies in response to applied moments. Eight of the fractured vertebral bodies were then augmented using PVP, while the others were augmented using kyphoplasty. Compliance of the augmented segments was then assessed. The results showed that cement augmentation reduced the compliance of the wedge-fractured spine segments, and both the neutral and full-load compliance were reduced by augmentation for flexion/extension and lateral bending. What is more, no significant differences were found between PVP and kyphoplasty for either compliance parameter in either direction (Fig. 2).

Cement augmentation seems to have different effects on wedge and burst fractures. The restoration of spine segment compliance to normal after a wedge fracture was created would require a 34% decrease in the flexion/extension range of motion and a 34% decrease in the lateral range of motion. However, Wilson et al.'s study showed that augmentation reduced flexion/extension and lateral full-load compliance by 23% and 26%, respectively. That suggests that cement augmentation restores more than one half of the spine segment stiffness lost due to wedge fracture and shows that the mechanical effect of augmentation is substantial. This partial restoration of normal compliance is due to the possible damage of the soft tissues when the fracture is produced.

On the other hand, Mermelstein et al. (1998) also found that cement augmentation of fractured vertebral bodies had a significant effect on spine segment compliance. These authors studied transpedicular reconstruction of a vertebral body with calcium phosphate (CaP) cement to reinforce a burst fracture initially stabilized using short segment pedicle screw instrumentation.

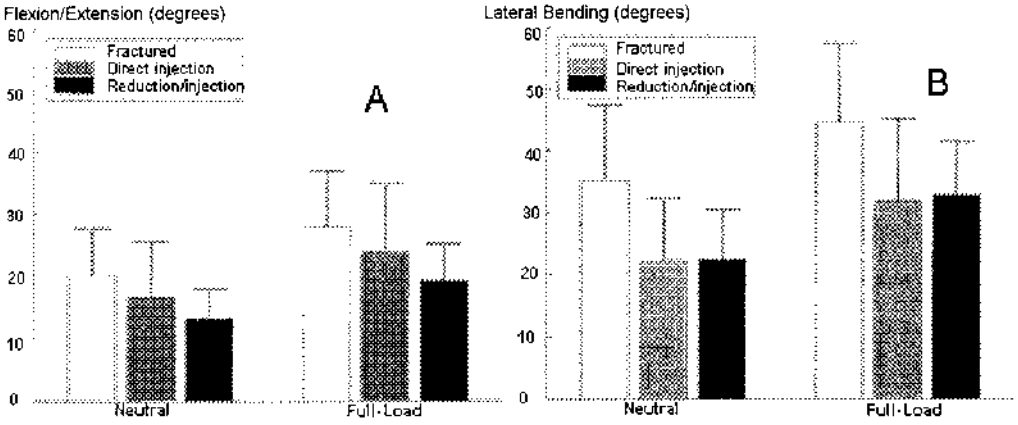

Figure 2 Compliance of the specimens before and after augmentation. (A) In flexion/extension, augmentation (direct injection and kyphoplasty) significantly reduced both the neutral and full-load compliance significantly. (B) In lateral bending, augmentation reduced both the neutral and full-load compliance significantly. No significant difference in compliance was detected between the two procedures. (Modified from Wilson et al., 2000.)

They found that vertebral body augmentation increased initial stiffness in flexion/extension by 40%, but found no significant differences in torsional stiffness. Also, augmentation had no significant effect on lateral stiffness. This contrast with Wilson's study is likely explained by the difference in fracture (burst versus wedge).

Unlike direct injection in PVP, during kyphoplasty a tamp is placed inside the VB under fluoroscopic guidance through a percutaneously introduced cannula. The tamp is inflated, thereby compressing the cancellous bone, creating a void, and concurrently lifting the end plates in an en masse reduction. After tamp removal, the void can be filled under lower pressure than that needed for PVP. In addition to increasing strength and restoring VB stiffness, this procedure seeks to restore VB height, thus reducing postfracture kyphosis and its associated sequelae (Tencer, 1981; Silverman, 1992; Lyles, 1993; Lukert, 1994).

To determine whether the tamp restores VB height in simulated compression fractures and whether the procedure results in VB strength and stiffness values different from those obtained using PVP alone, an ex vivo study was conducted on 16 osteoporotic cadaveric VBs that had been subjected to simulated compression fractures (Belkoff, 2001). Results showed that the tamp treatment resulted in significant restoration (97%) of VB height lost after compression, whereas PVP treatment resulted in a significantly lower restoration of lost height (30%). Both treatments resulted in significantly stronger vertebral bodies relative to their initial state. The tamp treatment restored vertebral body stiffness to initial values, but the PVP treatment did not. The authors concluded that tamp treatment resulted in significantly greater height restoration than did percutaneous vertebroplasty, without loss of vertebral body strength or stiffness.

Similar recovery phenomenon reportedly occurs in vivo. Table 1 illustrated that kyphoplasty can result in VB height restoration between 34 and 62.4%. The reason that less VB height recovery is found in in vivo studies than in vitro studies is that muscle forces and body weight might prevent such recovery.

IV. BONE CEMENTS IN VERTEBROPLASTY

So far, clinical series of PVP have exclusively reported the use of PMMA. This material is easy to handle, the radiopacity can be adapted by adding contrast dye, and it is mechanically efficient. Among PMMA cements, however, what type of cement is best suited for vertebroplasty is still unknown. European clinicians typically use Simplex P, whereas clinicians in the United States commonly use Cranioplastic (Galibert, 1987; Deramond, 1997; Jensen, 1997; Mathis, 1998). Regardless of the cement used, no cement is approved by FDA for use with the vertebroplasty procedure (Belkoff, 2000). Furthermore, when used for vertebropalsty, cements approved for other applications are altered by the addition of various opacifiers designed to increased cement visibility under fluoroscopy, thus preventing extravasation (Jensen, 1997; Cotton, 1998).

The use of PMMA for this application has risks of intraoperative and long-term complications. The PMMA cement cures by an exothermic reaction and may reach temperatures of 100–120°C, which can damage adjacent tissues including the spinal cord and nerve roots (Berman, 1984; Konno, 1994; Wilkes, 1994; Allen, 1998). During injection, hypotension and fat embolism can occur, resulting from absorption of PMMA monomer (Phillips, 1971; Harris, 1975; Daumas-Duport, 1977). The development of foreign-body response at the bone/cement interface can cause bone to be resorbed over time, resulting in lower strength (McAfee, 1986). Also, PMMA is not biodegradable, osteoconductive, or remodeled to bone (Bartucci, 1985). Once inserted, PMMA becomes a permanent resident and may interfere in the natural remodeling process of bone. In addition, with maximal PMMA filling, adjacent vertebral overload has been reported, possibly provoking fractures (Heini, 2001). For these reasons, Halligan and Hubsch-

mann (1993) strongly recommended against using PMMA alone in anterior procedures involving the spine except to treat malignant disease in patients with short life expectancies.

PMMA seems to be a successful, but not an optional material. Researchers and clinicians therefore have to consider and evaluate alternative substances for use in vertebroplasty. An optimized cement formula is definitely required for vertebroplasty. Li (2000) and Lu (2001) advocated that the bone cement suitable for use in vertebral fracture surgery should have the following characteristics:

1. An injectable nature, which allows it to conform precisely to its placement area
2. Rapid setting and adequate stiffness, which confers immediate load-bearing capacity and stiffness more closely resembling natural bone than metal or pure ceramic
3. Bioactivity, that allows for osseous integration, thus enhancing bone strength
4. Low setting temperature, reducing potential thermal injury to surrounding bone or neural elements
5. Radiopacity, allowing easy radiographic imaging during surgery, thus accurately controlling cement location and depth

In addition, Heini et al. (2001) thought, for an optimal substitute for vertebroplasty, other requirements, such as lasting, constant viscosity, low price, and slow biodegradation, should also be met.

Recently, attempts have been made to develop new bone cements that can meet these requirements. A large number of bone cements tested for vertebropalsty are now available. Here we introduce several promising bone cements, including Orthocomp and two CaP cements (α-BSM and Bone Source). Another new bioactive bone cement (SrHAC) will be introduced later in more detail.

Orthocomp is a bioactive, glass-ceramic–reinforced composite material with a matrix of Bis-phenol glycidyl dimethacrylate (BisGMA), Bis-phenol ethoxy dimethacrylate (BisEMA), and triethyleneglycol dimethacrylate (TEGDMA). The material is biocompatible and exhibits a lower setting exotherm and greater material properties compared with PMMA (Fujita, 1998; Dallap, 1999; Deramond, 1999). Orthocomp is also naturally more radiopaque than commercially available PMMA cements, even with 20% barium sulfate content (Belkoff, 1999). The cement is not resorbable, but the hydrophilic surface allows bone to bond chemically to the cement.

A study (Belkoff, 2000) compared the biomechanical performance of this material with that of Simplex P, which can result in VB stiffness restoration and the greatest increase in strength among various commercially available bone cements (Belkoff, 1999). In this cadaveric study, strength and stiffness of osteoropotic VBs were measured before and after either bone cement was injected. Results showed that VBs treated with either Orthocomp or Simplex P were significantly stronger than they were in their initial conditions. Augmentation with Simplex P, however, did not restore initial VB stiffness, whereas augmentation with Orthocomp did.

Compared with Simplex P, Orthocomp has two more advantages. Although the radiopacity of these two cements was not quantified, Orthocomp, however, is notably more radiopaque than Simplex P. Another potential advantage of Orthocomp compared with other PMMA cements is its biocompatibility as demonstrated by direct bone bonding in this class of bioactive cements (Fujita, 1998; Dallap, 1999).

Several in vivo studies have shown that CaP bone substitute materials are biocompatible. The histological response to these materials has been minimal and with no inflammation or foreign-body giant-cell reaction to the implanted materials (Bai, 1990; Fujikawa, 1995; Hollinger, 1996). The CaP material can be resorbed progressively from the outer surface and replaced by bone tissue in the normal bone remodeling process (Goad, 1997; Knaack, 1998; Knaack, 1998a).

Bone Source has been used since the early 1990s, primarily in cranial and maxillofacial defect-filling applications. It has been shown to be biocompatible, osteoconductive, and resorbable, slowly being replaced by host bone (Hansson, 1980; Knaack, 1998a). BoneSource is also known to have a high 24-hour wet compressive strength (51.0 ± 4.5 MPa) (Chiras, 1997). The infiltration properties of BoneSource have been significantly improved by a slight change in formulation, allowing it to be used for the transpedicular injection to the vertebral bodies for vertebroplasty or augmentation of osteoporotic vertebral body.

In a comparative ex vivo study (Belkoff, 2001), the biomechanical effectiveness of three cements in providing internal support to osteoporotic vertebrae subjected to simulated VCFs, including Simplex P, Simplex P formulated consistent with the practice of vertebroplasty (F2), and Bone Source. Simplex P is mixed as directed by the manufacturer, namely, mixing a 20 mL vial of monomer with the 40 g packet of powder that contains 36 g of PMMA and 4 g of $BaSO_4$. However, F2 is modified by adding a 20 mL vial of monomer liquid to 40 g of powder that contains 28 g of PMMA and 12 g of $BaSO_4$. For all three cements, 4 mL was injected for thoracic and 6 mL for lumbar vertebrae. The results showed that VBs repaired with Simplex P resulted in significantly greater strength relative to their prefracture states, those repaired with Bone Source resulted in the restoration of initial strength for both the thoracic and level, and those repaired with F2 resulted in significantly greater strength in the thoracic region and restoration of strength in the lumbar region. All cement treatments resulted in significantly less stiffness compared with initial values. The authors concluded that both the latter two bone cements showed promise for use in PVP, but they needed further clinical evaluation.

In a recent study (Lim, 2002), destructive biomechanical tests using fresh cadaveric thoracolumbar vertebral bodies were conducted to evaluate the compression strength for vertebroplasty in comparison with PMMA injection. Results demonstrated that the Bone Source cement can be injected and infiltrates easily into the vertebral body. During cement injection, extravasation of Bone Source was observed mostly at the needle insertion site in the pedicles, whereas extravasation of the PMMA cement was most common at the anterolateral wall of the vertebral body. It was also found that injection of Bone Source can improve the strength of a fractured vertebral body to at least the level of its intact strength. Thus, the authors concluded that this new CaP cement may be a good alternative to PMMA cement for vertebroplasty, although further in vivo animal and clinical studies should be done. In addition, Bone Source may be more effective in augmenting the strength of osteoporotic vertebral bodies for preventing compression fractures considering the biomechanical testing data and the known potential for biodegradability of Bone Source.

Recently, several new biodegradable CaP bone substitute materials have been developed. As with PMMA, these materials can be mixed into an injectable paste. One of these pastes consists of a precursor powder mixed with isotonic saline that hardens into a solid mass and cures at physiological temperature and pH and in an aqueous environment to reach a final maximum compressive strength in about 4 hours (Knaack, 1997, 1998a). Unlike PMMA, the paste remains workable for several hours at room temperature and the solidification proceeds endothermically. Most importantly, this material is similar to bone in chemical composition and crystalline size and is biocompatible and bioresorbable (Goad, 1997; Knaack, 1997, 1998a).

α-BSM, a new biodegradable CaP bone cement, was originally designed for dentistry and craniofacial surgery. In a cadaveric model, Bai et al. (1999) compared this bone cement with PMMA for strengthening osteoporotic vertebral bodies and improving the integrity of vertebral compression fractures. The results showed that both this CaP bone substitute and PMMA groups were significantly stronger than the intact control group, and no significant difference was found between the CaP bone substitute and the PMMA group. For the compression fracture study,

anterior vertebral height was increased 58.5% in the α-BSM group and 58.0% in the PMMA group as compared with preinjection fracture heights.

With α-BSM or PMMA augmentation, fracture strengths were significantly stronger than in the intact control group. Stiffness for both α-BSM and PMMA augmentation also was significantly higher than in the intact control group. Moreover, the injection of these materials into a vertebral compression fracture can partially restore vertebral height and prevent further vertebral collapse. However, this study demonstrated that α-BSM compares favorably with PMMA for strengthening vertebral bodies in cadaveric spines because CaP bone substitute may avoid the potential problems associated with the use of PMMA cement in this clinical setting.

This study determined only the immediate effects of CaP bone substitute augmentation. Clearly, the mechanical property of CaP bone substitute–bone composite during the resorptive phase is important and should be evaluated. In an in vivo study performed by Ikenaga et al. (1998), a biodegradable CaP cement was implanted in bone cavities created in the distal epiphysis of rabbit femurs. Within 16 weeks, the cement was replaced by new bone with mechanical properties similar to those of the original bone or better. Furthermore, Knaack et al. (1997, 1998a) showed similar new bone formation with autograft and α-BSM bone substitute in a canine femoral slot defect model. The defects were filled with trabecular bone in the first 3–4 weeks after implantation, and lamellar bone formation was established by week 12. However, whether CaP bone substitute provides adequate mechanical strength in vivo over longer time periods remains to be determined in future studies.

V. SRHAC—A NEW BIOACTIVE BONE CEMENT

A new injectable bioactive bone cement, strontium-containing hydroxyapatite cement (SrHAC), has recently been developed. This cement is made of strontium-containing hydroxyapatite (Sr-HA) powder and Bisphenol A Diglycidylehter Dimethacrylate (D-GMA) resin. Sr-HA has stronger mechanical properties and better bioactivity than pure hydroxyapatite (HA) and similar biocompatibility to HA (Aoki, 1994). Strontium has effects on bone strengthening and is associated with improving osteoporosis (Boivin, 1996; Christoffersen, 1997; Reginster, 1997). Furthermore, its radiopacity (Gedalia, 1978) makes it unnecessary to add another radiopaque agent to the cement.

SrHAC was designed especially for spinal surgery. Its characteristics of injectability, fast-setting ability, good biomechanical compatibility, comparative lower peak temperature, radiopacity, and potential bioactivity indicate that it meets the requirements for use in spinal surgery. In addition, SrHAC could also be formulated to allow controllable setting times, varied viscosity, and different strength levels. The bioactivity of SrHAC is currently being performed in large animal models.

Figure 3a showed the characterization of SrHA tested by Fourier transform infrared (FTIR) spectroscopy. The spectra of the Sr-HA powder and that of standard HA were found to be very similar (Aoki, 1994; Gibson, 1999). Three peaks (at 1097, 1030, and 959 cm^{-1}) identified phosphate at the λ3 and λ1 bands, while the λ4 band was distinguished by two peaks (at 604 and 564 cm^{-1}). Carbonate λ3 band was also observed as peaks (at 1458 and 1418 cm^{-1}), and carbonate λ2 band as a single peak (at 874 cm^{-1}).

X-ray diffraction (XRD) spectroscopy of Sr-HA power is shown in Figure 3b. The two strong characteristic peaks of HA (Aoki, 1991, 1994) were shown from the Sr-HA powder. The pattern of Sr-HA was very similar to HA, with no detectable secondary phases, such as tricalcium phosphate (TCP) or CaO, detected. According to present testing conditions, the strontium substitution did not appear to affect the diffraction pattern of HA.

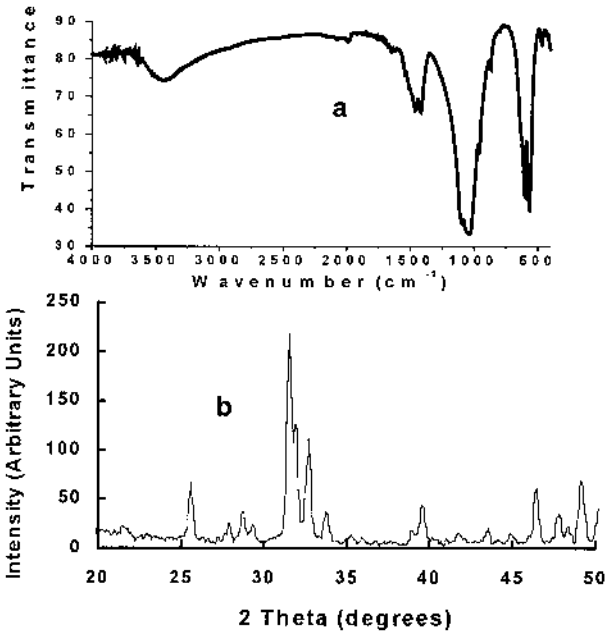

Figure 3 Fourier transform (a) infrared spectrum and (b) x-ray diffraction pattern of strontium-containing hydroxyapatite (Sr-HA) powder.

Setting time and temperature is a key issue for orthopedic surgery using bone cement. The amount of initiator and accelerator in the reaction mixture control the polymerization rate (setting time) and the heat released during polymerization (setting temperature). The ratio of benzoyl peroxide (BPO) and *N*,*N*-dimethyl-*p*-toluidine in the filler and resin blend was adjusted and the setting time and temperature were monitored during the mixing of bone cement. After many trials, the setting time of the bone cement can be adjusted from 10 to 25 minutes. However, the maximum temperature measured was between 35 and 70°C (unpublished data).

The cell relative growth rate (RGR) test and tetrazolium bromide (MTT) test are two different cytotoxicity tests with different biological endpoints. In general, cell culture testing methods have been shown to correlate well with animal assays and are often more sensitive than in vivo assays with limited acute toxicity testing (Spangberg, 1982). Hence, these cell tests verified one another and confirmed initial nontoxicity of the new bioactive bone cement.

In the RGR test, cytotoxicity ratios of the tested biomaterial were calculated from the average optical density (OD) values and classified according to the following criteria for cytotoxicity (Zhang, 1990; Li, 1999): If RGR $>$ 100%, the corresponding cytotoxicity type was class 0, indicating no toxicity. If RGR $=$ 0%, the corresponding cytotoxicity type was class 5, indicating the highest toxicity. 75–99%, 50–74%, 24–49%, and 1–25% RGR was catergorized as Class 1, 2, 3, and 4, respectively. The MTT test is sensitive, convenient, and quick to detect cytotoxicity of the new biomaterials (Kirkpatrick, 1998). In the MTT test, RGR of cells and classification of cytotoxicity were calculated according to the above equation and criteria for cytotoxicity.

To determine the cytotoxicity of SrHAC, these two tests were performed concurrently. In the RGR test, RGR at day 2, 4, and 7 was 87.8%, 93.4%, and 91.8%, respectively. Cells with extracts of the bioactive bone cement grew as fast as the negative group, and extract of the

cement was favorable for cell growth. The MTT test showed that RGR was 84.9% and 79.1% after cells interacted for 48 hours with 50% and 100% (twice the normal testing concentration) cement extract, respectively. According to criteria for cytotoxicity, these results demonstrated that cytotoxicity of SrHAC was Class 1, indicating no cytotoxicity.

Hemolysis test was conducted by Li et al. (2000) to further understand the biocompatibility of SrHAC. This test is a very important screening test, as elevated plasma hemoglobin levels may suggest hemolysis and reflect red blood cell membrane fragility when blood contacts with biomaterials (ISO 10993, 1992; Anderson, 1997; Demian, 1998). Results indicated that the hemolysis of SrHAC was lower than the criterion set by ISO (reference—5%) (Demian, 1998), proving that SrHAC has no potential to induce hemolysis.

Any new bone cement must demonstrate feasibility in spinal surgery from both biomechanical and morphological perspectives. In vitro spinal biomechanical testing and morphological observation after injection of SrHAC were performed on pig spines (Li, 2000). In this study, 17 pig spine specimens were divided into two groups: intact and cemented. Instant stiffness after bone cement injection was recorded, and a fatigue cyclic loading ranging from 100 to 1000 N was then conducted at 1 Hz for up to 3000 cycles, simulating 3 months of motion of the human spine. Following cyclic loading, spinal stiffness was recorded again for each specimen under the same loading conditions. Finally, failure strength was recorded when applying compressive failure load to the spine.

The results showed that, after inducing the fracture, the stiffness of the spine dropped significantly (53.3% of intact condition). However, after bone cement injection, it was 112% of the initial stiffness. Stiffness after fatigue loading decreased slightly (95%), suggesting that the bone cement stabilized the collapsed spine.

Review of the radiographs obtained before and after introduction of SrHAC into the fractured vertebral body displayed a nearly completed restoration of vertebral body dimensions (Fig. 4). There was no evidence of the bioactive bone cement retropulsion into the canal in any of the specimens. On review of the cross sections (Fig. 5), there was cement interdigitation into the fracture site and into the cancellous bone of the vertebral body in all specimens.

Another in vitro study was performed to further determine the mechanical stability of the fractured spine after injection of SrHAC under quasi-static and cyclic loading regimens (Lu, 2001). In this study, 26 fresh porcine specimens were used and divided into three groups: pilot, intact, and cemented. Spinal stiffness and failure strength were recorded in the intact group with the specimen flexed at 10°. Uniform injuries were created in all specimens of the cemented group, and compressive loading was applied with 10° of flexion until a fracture occurred. The bone cement was injected into the fractured spine, and stiffness was evaluated after 1 hour. Failure strength was also recorded after 3,000 and 20,000 fatigue load cycles. The results showed that spinal stiffness significantly decreased after fracture (47.5% of intact condition) and instant stiffness of the spine recovered to 107.8% of the intact condition after bone cement injection. After 3,000 and 20,000 cycles of fatigue loading, stiffness of the cemented spine was found to be 93.5% and 94.4% of intact stiffness, respectively. Average failure strength of the spine was 5056 N (after 3,000 cycles) and 5301 N (after 20,000 cycles) following bone cement injection and fatigue loading, equivalent to 86% and 90.5% of the intact values, respectively.

Review of the radiographs obtained before and after bone cement injection displayed a near-complete restoration of the vertebral body's dimensions. On observing the cut sections (Fig. 6), there was good cement dispersion into the fracture site and into the cancellous bone of the vertebral body in all specimens. Cement-bone bonding quality was satisfactory even after failure loads, as the failure mode did not include fracture at the cement/bone interfaces. It was noted, however, that 2 out of the 16 cemented specimens showed cement extrusion from the

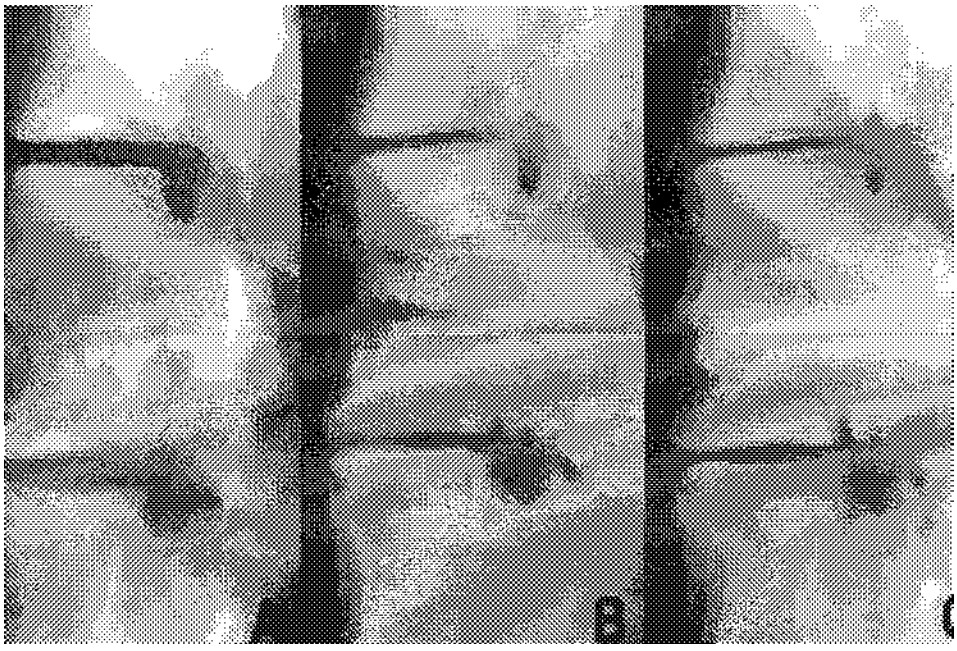

Figure 4 Radiographs of (A) intact, (B) fractured, and (C) bone-cemented spine specimen. Radiograph C was taken after fatigue testing. Note complete filling of the gaps in fracture site.

vertebral body into the canal space following injection, suggesting that precautions should be taken during injection to prevent possible leakage of cement into the canal.

While results from a limited (anterior column) mild burst fracture model are encouraging, clinical spinal fractures can vary from a mild compression fracture to a severe three-column burst fracture, and to what extent bone cement can restore the mechanical properties under different fracture conditions has yet to be determined. The indications for use of this cement are expected to be similar to those of PMMA cements, as similar mechanical properties have been found. PMMA and calcium phosphate cements have a tensile strength in the region 23–45 MPa and a modulus of 1.1–4.1 GPa, while this bone cement has a tensile strength of 8–13 MPa and a modulus of 2.4–4 GPa. However, the strength and stiffness of the cement fixation under loading conditions apart from flexion-compression also need to be tested, including axial rotation and lateral bending. Possible extrusion of the cement into the spinal canal would also tend to preclude the use of this cement in severe burst fractures where the vertebra is severely disrupted and unlikely to be able to contain the cement. However, further research may help in determining the mechanism of extrusion and fine-tuning the properties of the cement to prevent this possible complication. While the curing time for this new cement is longer than that of most typical PMMA cements, this is necessary both to minimize the curing temperature and to allow time to prepare and inject the cement under radiographic control.

Lu's study (2001) demonstrated that injection of SrHAC alone can restore the mechanical properties of a mild anterior column burst fracture model. Potential for clinical applications is currently under investigation. While the exact indications for use of this cement alone in the minimally invasive treatment of vertebral fractures are unclear, this study has demonstrated the clinical potential of the bioactive bone cement and justifies further investigations into the application of similar minimally invasive techniques to stabilize vertebral fractures. Most importantly,

Figure 5 Photograph of sagittal plane through a vertebral body filled with SrHAC bioactive bone cement and after fatigue loading. Noting cement interdigitation into the fracture site and good concellous bone-cement bonding.

it must demonstrate superiority to the current forms of PMMA, which have served the spinal community well for over 20 years (Lane, 2001).

VI. FUTURE DIRECTIONS

The clinical application of bioactive bone cement has been extending. In addition to direct injection (PVP) and reduction/injection (kyphoplasty), mentioned previously, injectable bone cements have shown their potential to replace metallic implants currently mainly used to stabilize fractured spine in many other ways, such as in pedicle screws and augmentation of CT instrumentation (Fig. 7). More efforts should be made to make full use of the bioactive bone cements in the clinical application of orthopedic surgery.

PVP, with cement augmentation, has been widely accepted as an effective treatment for VCFs with low complication rate, however, its long-term effect is still uncertain. Investigation of the prophylactic treatment of vertebrae at risk is just beginning. Because of the increased risk of additional fractures in patients with osteoporosis after their first VCF, there may be a substantial need for prophylactic augmentation to prevent future collapse in these at-risk vertebrae. Epidemiological and bone densitometric data may help provide the information needed to select the patients and the specific vertebrae that would most benefit from augmentation.

On the other hand, the bioactive bone cement does not effectively induce bone formation in the fractured sites and the long-term effectiveness is limited. As an alternative, tissue-engineer-

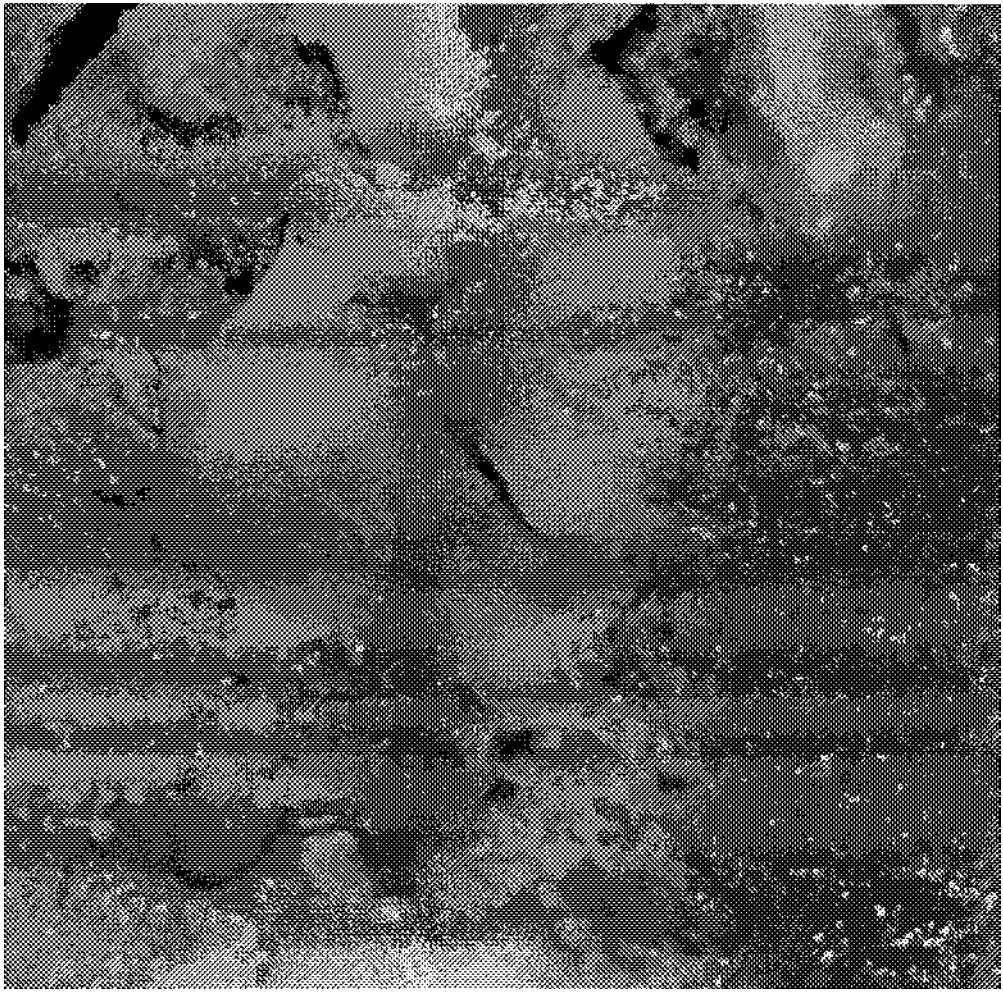

Figure 6 Transverse plane showing morphology of bone-cement bonding after 3000 cycle fatigue loads and failure testing.

ing is considered to be the next breakthrough development. Three new approaches for inducing new bone tissues are coming to fruition: (1) implantation of cytokines such as bone morphogenic proteins (BMPs) in combination with appropriated delivery systems, (2) transduction of genes encoding cytokines with osteogenic capacity to cells at the repair sites, and (3) transplantation of cultured osteogenic cells derived from bone marrow that will lead to new healthy bone formation at the target site. The third technique could be viewed as most promising in terms of practical use due to the current development focused on the gene transfer technology, stem cell therapy, and recombinant signaling molecules. Stem cells can differentiate fully into the various connective tissue species, including bone, cartilage, and tendons. Stem cells could differentiate into osteoblast under correct micromechanical environment with bone-inducing growth factors. Future studies should consider using mesenchymal stem cells (MSCs) encapsulated in a novel class of alginates for treating osteoporotic spinal fractures. The advantages of using MSCs

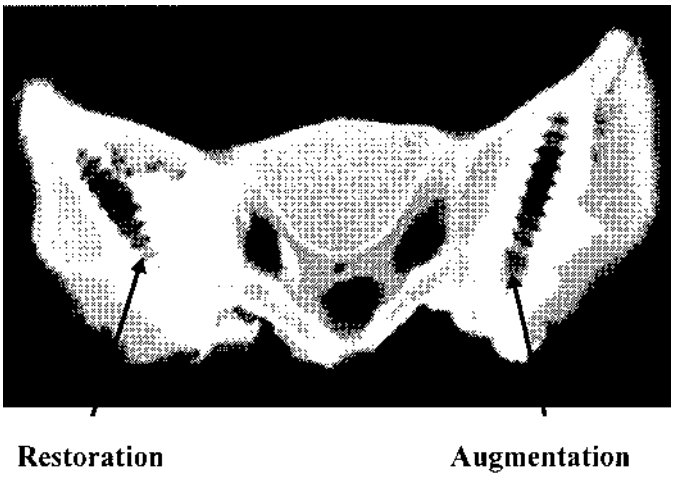

Figure 7 Transverse CT scan of spinal internal fixation: augmentation (right arrow) shows the use of bone cement before sacral screw fixation (SSF); whereas restoration (left arrow) indicates that bone cement is used to repair a failed SSF.

include easy aspiration of bone marrow and quick proliferation of cells compared with using osteocytes.

REFERENCES

1. Allen MJ, Park CK, Yuan PS. Barrier techniques for preventing PMMA-induced thermal injury of the spinal cord. Proceedings of 44th Annual Meeting of the Orthopaedic Research Society, Rider Dickerson Inc., Chicago, IL, 1998.
2. Amar AP, Larsen DW, Esnaashari N. Percutaneous transpedicular polymethylmethacrylate vertebroplasty for the treatment of spinal compression fractures. Neurosurgery 2001; 49:1105–1115.
3. Anderson JM. Interaction with blood. In: Braybrook JH, ed. Biocompatibility assessment of medical devices and materials. Chichester: John Wiley & Sons, 1997:140–142.
4. Aoki H. Science and medical application of hydroxyapatite. Tokyo: JAAS, 1991:vii, xv, 214.
5. Aoki H. Medical applications of hydroxyapatite. Tokyo: Ishiyaku EuroAmerica, 1994:205–305.
6. Bai B, Huang C. Osteogenesis effect of hydroxyapatite combine with autologous red bone marrow : An experimental study. Chin J Orthop 1990; 10:442–446.
7. Bai B, Jazrawi LM, Kummer FJ. The Use of an Injectable, Biodegradable Calcium Phosphate Bone Substitute for the Prophylactic Augmentation of Osteoporotic Vertebrae and the Management of Vertebral Compression Fractures. Spine 1999; 24:1521–1526.
8. Barr JD, Barr MS, Lemley TJ. Percutaneous vertebroplasty for pain relief and spinal stabilization. Spine 2000; 25:923–928.
9. Bartucci EJ, Gonzalez MH, Cooperman DR. The effect of adjunctive methylmethacrylate on failures of fixation and function in patients with intertrochanteric fractures and osteoporosis. J Bone Joint Surg [Am] 1985; 67:1094–107.
10. Bascoulergue Y, Duquesnel J, Leclercq R. Percutaneous injection of methyl methacrylate in the vertebral body for the treatment of various diseases: percutaneous vertebroplasty. Radiology 1988; 169:372–382.

11. Belkoff SM, Maroney M, Fenton DC. An *in vitro* biomechanical evaluation of bone cements used in percutaneous vertebroplasty. Bone 1999; 2:3S–6S.
12. Belkoff SM, Mathis JM, Erbe EM. Biomechanical evaluation of a new bone cement for use in vertebroplasty. Spine 2000; 25:1061–1064.
13. Belkoff SM, Mathis JM, Jasper LE. The biomechanics of vertebroplasty: the effect of cement volume on mechanical behavior. Spine 2001; 26:1537–1541.
14. Berman AT, Reid JS, Yanicko DR. Thermally induced bone necrosis in rabbits : Relation to implant failure in humans. Clin Orthop 1984; 186:284–92.
15. Boivin G, Deloffre P, Perrat B. Strontium distribution and interactions with bone mineral in monkey iliac bone after strontium salt (S12911) administration. J Bone Miner Res 1996; 11:1302–11.
16. Bostrom MPG, Lane JM. Future directions: Augmentation of osteoporotic vertebral bodies. Spine 1997; 22:38S–42S.
17. Chiras J, Depriester C, Weill A. Percutaneous vertebral surgery: Technics and indications. J Neuroradiol 1997; 24:45–59.
18. Chiras J, Dermond H. Complications des vertebroplastics, in. Saillant G (eds), Laville C, eds. Paris: Sauramps Medical, 1995:49–153.
19. Christoffersen F, Christoffersen MR, Kolthoff N. Effect of strontium ions on growth and dissolution of hydroxyapatite and on bone mineral detection. Bone 1997; 20:47–54.
20. Cohen LD. Fractures of the osteoporotic spine. Orthop Clin North Am 1990; 21:143–150.
21. Cooper C, Atkinson EJ, O'Fallon WM. Incidence of clinically diagnosed vertebral fractures: A population-based study in Rochester, Minnesota, 1985–1989. J Bone Miner Res 1992; 7:221–227.
22. Cortet B, Cotton A, Boutry N. Percutaneous vertebroplasty in the treatment of osteoporotic vertebral compression fractures: an open prospective study. J Rheumatol 1999; 26:2222–2228.
23. Cotten A, Dewatre F, Cortet B. Percutaneous vertebroplasty for osteolytic metastases and myeloma: effects of the percentage of lesion filling and the leakage of methyl methacrylate at clinical follow-up. Radiology 1996; 200:525–530.
24. Cotten A, Boutry N, Cortet B. Percutaneous vertebroplasty: State of the art. Radiographics 1998; 18:311–320.
25. Cyteval C, Sarrabere MP, Roux JO. Acute osteoporotic vertebral collapse: open study on percutabeous injection of acrylic surgical cement in 20 patients. Am J Roentgenol 1999; 173:1685–1690.
26. Dallap BL, Gadaleta S, Erbe E. Histological, radiological, and mechanical comparison of polymethylmethacrylate (PMMA) and a bioactive bone cement in an ovine model. [abstr] Trans Orthop Res Soc 1999; 24:503.
27. Daumas-Duport C, Hanau J, Abelanet R. Cerebral fat emboli: Apropos of a case of a peroperative complication associated with the use of a bone cement in orthopedic surgery. Ann Anat Pathol (Paris) 1977; 22:269–278.
28. Demian HW, McDermott K. Regulatory perspective on characterization and testing of orthopaedic bone cements. Biomaterials 1998; 19:1607–1618.
29. Deramond H, Wright NT, Belkoff SM. Temperature elevation caused by bone cement polymerization during vertebropasty. Bone 1999; 25:17S–21S.
30. Deramond H, Depriester C, Toussaint P. Percutaneous vertebroplasty. Semin Musculoskelet Radiol 1997; 1:285–295.
31. Deramond H, Depriester C, Galibert P. Percutaneous vertebroplasty with polymethylmethacrylate: technique, indications, and results. Radiol Clin North Am 1998; 36:533–546.
32. Diamond TH, Clark WA. Percutaneous vertebroplasty: a novel treatment for acute vertebral fractures. Med J Aust 2001; 174:398–400.
33. Dudeney S, Lieberman IH, Reinhardt MK. Kyphoplasty in the treatment of osteolytic vertebral compression fractures as a result of multiple myeloma. J Clin Oncol 2002; 20:2382–2387.
34. Fujikawa K, Sugawara A, Murai S. Histopathological reaction of calcium phosphate cement in periodontal bone defect. Dent Mater J 1995; 14:45–57.
35. Fujita H, Nakamura T, Tamura J. Bioactive bone cement: Effect of the amount of glass-ceramic powder on bone-bonding strength. J Biomed Mater Res 1998; 40:145–152.
36. Galibert P, Deramond H, Rosat P. [Preliminary note on the treatment of vertebral angioma by percutaneous acrylic vertebroplasty]. Neurochirurgie 1987; 33:166–168.

37. Gangi A, Kastler A, Dietemann L. Percutaneous vertebroplasty guided by a combination of CT and fluoroscopy. Am J Neuroradiol 1994; 15:83–86.
38. Garfin SR, Yuan HA, Reiley MA. New technologies in spine: kyphoplasty and vertebroplasty for the treatment of painful osteoporotic compression fractures. Spine 2001; 26:1511–1515.
39. Gaughen JR, Jensen ME, Schweickert PA. Relevance of antecedent venography in percutaneous vertebroplasty for the treatment of osteoporotic compression fractures. Am J Neuroradiol 2002; 23: 594–600.
40. Gedalia I, Brayer L, Kalter N. The effect of fluoride and strontium application on dentin: in vivo and in vitro studies. J Periondontol 1978; 49:269–272.
41. Gibson IR, Best SM, Bonfield W. Chemical characterization of silicon-substituted hydroxyapatite. J Biomed Mater Res 1999; 44:422–428.
42. Goad MEP, Aiolova M, Tofighi A. Resorbable apatitic bone substitute material, alpha-BSM, is associated with rapid bone regrowth in defects of rabbits tibias. J Bone Miner Res 1997; 12:S518.
43. Gold DT. The clinical impact of vertebral fractures: Quality of life in women with osteoporosis. Bone 1996; 18:185S–189S.
44. Halligan M, Hubschmann OR. Short-term and long-term failures of anterior polymethylmethacrylate construct with esophageal perforation. Spine 1993; 18:759–761.
45. Hansson T, Roos B, Nachemson A. The bone mineral content and ultimate compressive strength of lumbar vertebrae. Spine 1980; 5:46–55.
46. Harris NH, Miller AJ, Bourne R. Proceedings: Experimental investigation of fat embolism after the use of acrylic cement in orthopaedic surgery. J Bone Joint Surg [Br] 1975; 57:245–246.
47. Hayes WC, Piazza SJ, Zysset PK. Biomechanics of fracture risk prediction of the hip and spine by quantitative computed tomography. Radiol Clin North Am 1991; 29:1–18.
48. Heini PF, Berlemann U, Kaufmann M. Augmentation of mechanical properties in osteoporotic vertebral bones–a biomechanical investigation of vertebroplasty efficacy with different bone cements. Eur Spine J 2001; 10:164–171.
49. Heini PF, Berlemann U. Bone substitutes in vertebroplasty. Eur Spine J 2001; 10:S205–S213.
50. Hollinger JO, Brekke J, Gruskin E. Role of bone substitutes. Clin Orthop 1996; 324:55–65.
51. ISO 10993: Biological evaluation of medical devices. Part 4: Selection of tests for interaction with blood. ISO, Geneva, Switzerland, 1992.
52. Ikenaga M, Hardouin P, Lemaitre J. Biomechanical characterization of a biodegradable calcium phosphate hydraulic cement : A comparison with porous biphasic calcium phosphate ceramics. J Biomed Mater Res 1998; 40:139–44.
53. Jensen ME, Evans AJ, Mathis JM. Peercutaneous polymethylmethacrylate vertebroplasty in the treatment of osteoporotic vertebral body compression fractures: technical aspect. Am J Neuroradiol 1997; 18:1897–1904.
54. Kaemmerlen P, Thiesse P, Jonas P. Percutaneous injection of orthopedic cement in metastatic vertebral lesions. N Engl J Med 1989; 321:121.
55. Kaufmann TJ, Jensen ME, Schweickert PA. Age of fracture and clinical outcomes of percutaneous vertebroplasty. Am J Neuroradiol 2001; 22:1860–1863.
56. Kirkpatrick CJ, Bittinger F, Kohler H. Current trends in biocompatibility testing. Proc Instn Mech Engrs 1998; 212(part H):75–84.
57. Knaack D, Goad EB, Aiolova M. Novel fully resorbable calcium phosphate bone substitute. J Bone Miner Res 1997; 12:S202.
58. Knaack D, Goad EB, Aiolova M. Resorbable calcium phosphate bone substitute. J Biomed Mater Res 1998; 43:399–409 (A).
59. Knaack D, Aiolova M, Tofighi A. A Fully Resorbable Calcium Phosphate Bone Substitute. Proceedings of the 9th CIMTEC Meeting, World Ceramics Congress and Forum on New Materials, Florence, Italy, June 1998.
60. Konno S, Olmarker K, Byrod G. The European Spine Society AcroMed Prize 1994. Acute thermal nerve root injury. Eur Spine J 1994; 3:299–302.
61. Lane JM. Point of view. Spine 2001; 26:2690–2691.
62. Li YW, Leong JCY, Lu WW. A novel injectable bioactive bone cement for spinal surgery: a developmental and preclinical study. J Biomed Mater Res 2000; 52:164–170.

63. Liebschner MAK, Rosenberg WS, Keaveny TM. Effects of bone cement volume and distribution on vertebral stiffness after vertebroplasty. Spine 2001; 26:1547–1554.
64. Lieberman IH, Dudeney S, Reinhardt MK. Initial outcome and efficacy of ''kyphoplasty'' in the treatment of painful osteoporotic vertebral compression fractures. Spine 2001; 26:1631–1638.
65. Lim TH, Brebach GT. Biomechanical Evaluation of an Injectable Calcium Phosphate Cement for Vertebroplasty Spine. Vol. 27, 2002:1297–1302.
66. Lu WW, Cheung KMC. Bioactive bone cement as a principal fixture for spinal burst fracture. A in vitro biomechanical and morphological study. Spine 2001; 26:2684–2691.
67. Lukert BP. Vertebral compression fractures: How to manage pain, avoid disability. Geriatrics 1994; 49:22–27.
68. Lyles KW, Gold DT. Association of osteoporotic vertebral compression fractures with impaired functional status. Am J Med 1993; 94:595–601.
69. Martin JB, Sugiu BJK. Vertebroplasty: clinical experience and follow-up results. Bone 1999; 25(2S): 11S–15S.
70. Mathis JM, Eckel TS. Percutaneous vertebroplasty: a therapeutic option for pain associated with vertebral compression fracture. J Back Musculoskel Rehab 1999; 13:11–17.
71. Mathis JM, Petri M, Naff N. Percutaneous vertebroplasty treatment of steroid-induced osteoporotic compression fractures. Arthritis Rheum 1998; 41:171–175.
72. Mathis JM, Barr JD. Percutaneous vertebroplasty: a developing standard of care for vertebral compression fractures. Am J Neuroradiol 2001; 22:373–381.
73. Maynard AS, Jensen ME. Value of bone scan imaging in predicting pain relief from percunateous vertebroplasty in osteoporotic vertebral fractures. Am J Neuroradiol 2000; 21:1807–1812.
74. McAfee PC, Bohlman HH. Failure of stabilization of the spine with methylmethacrylate : A retrospective analysis of twenty-four cases. J Bone Joint Surg [Am] 1986; 68:1145–57.
75. Melton LJ, Kan SH. Epidemiology of vertebral fractures in women. Am J Epidemiol 1989; 129: 1000–1011.
76. Melton LJ. Epidemiology of spinal osteoporosis. Spine 1997; 22:2S–11S.
77. Mermelstein LE, McLain RF, Yerby SA. Reinforcement of thoracolumbar burst fractures with calcium phosphate cement: A biomechanical study. Spine 1998; 23:664–671.
78. Myers ER, Wilson SE. Biomechanics of osteoporosis and vertebral fracture. Spine 1997; 22:25S–31S.
79. O'Brien JP, Sims JT, Evans AJ. Vertebroplasty in patients with sever vertebral compression fractures: a technical report. Am J Neuroradiol 2000; 21:1555–1558.
80. Peck WA, Riggs BL. Research directions in osteoporosis. Am J Med 1988; 84:275–282.
81. Phillips H, Cole PV, Lettin AW. Cardiovascular effects of implanted acrylic bone cement. BMJ 1971; 3:460–461.
82. Rami PM, McGraw JK. Percutaneous vertebroplasty in the treatment of vertebral body compression fracture secondary to osteogenesis imperfecta. Skeletal Radiol 2002; 31:162–165.
83. Reginster JY. Miscellaneous and experimental agents. Am J Med Sci 1997; 3:33–40.
84. Ryu KS, Park CK. Dose-dependent epidural leakage of polymethylmethacrylate after percutaneous vertebroplasty in patients with osteoporotic vertebral compression fractures. J Neurosurg 2002; 96: 56–61.
85. Schildauer TA, Bennett AP. Intravertebral body reconstruction with an injectable in situ-setting carbonated apatite: Biomechanical evaluation of a minimally invasive technique. J Orthop Res 1999; 17:67–72.
86. Silverman SL. The clinical consequences of vertebral compression fracture. Bone 1992; 13:S27–S31.
87. Spangberg LSW. Endodontic filling materials. In: Smith DC editor, Williams DF, eds. Biocompatibility of dental materials. Volume □ Biocompatibility of dental restorative materials. Boca Raton. Florida: CRC press, 1982:161–222.
88. Tencer AF, Ahmed AM. The role of secondary variables in the measurement of the mechanical properties of the lumbar intervertebral joint. J Biomech Eng 1981; 103(3):129–137.
89. Theodorou DJ, Theodorou SJ. Percutaneous balloon kyphoplasty for the correction of spinal deformity in painful vertebral body compression fractures. J Clin Imaging 2002; 26:1–5.
90. Tohmeh AG, Mathis JM. Biomechanical efficacy of unipedicular versus bipedicular vertebroplasty for the management of osteoporotic compression fractures. Spine 1999; 24:1772–1776.

91. Tsou IY, Goh PY. Percutaneous vertebroplasty in the management of osteoporotic vertebral compression fractures: initial experience. Ann Acad Med Singapore 2002; 31:15–20.
92. Weill A, Chiras J. Spinal metastases: Indications for and results of percutaneous injection of acrylic surgical cement. Radiology 1996; 199:241–247.
93. Wilson DR, Myers ER. Effect of augmentation on the mechanics of vertebral wedge fractures. Spine 2000; 25:158–.
94. Wilkes RA, Mackinnon JG, Thomas WG. Neurological deterioration after cement injection into a vertebral body. J Bone Joint Surg [Br] 1994; 76:155.
95. Zhang CX, Sun J, Meng AY. A new method of measuring the cytotoxicity by spectrophotometer for amalgam of different cupric quantity. Chung Hua Kou Chiang Hsueh Tsa Chih 1990; 25:216–218.
96. Zoarski GH, Snow P. Percutaneous vertebroplasty for osteoporotic compression fractures: quantitative prospective evaluation of long-term outcomes. J Vasc Interv Radiol 2002; 13:139–148.

35

Advances in Technology and Spinal Fusion: A Clinician's Perspective

Stefano Lupparelli and Sergio Cecconi
Centro Ortopedico Umbro
Perugia, Italy

I. INTRODUCTION

Spinal fusion, or spinal arthrodesis, is a surgical procedure aimed at creating enduring nonphysiological constraints within one or more motion segments of the spine, thus attempting to abolish the degrees of freedom of a predetermined set of functional spinal units (FSUs). This functional outcome is surgically pursued with the decortication of adjacent elements of two or more vertebrae and the deposition of bone grafts over the decorticated bed. A successful fusion is achieved, both in biomechanical and anatomical terms, when bone grafts eventually form a solid osseous mass bridging two or more vertebrae and, as a consequence, motion among one or more FSUs is abolished.

The rationale underlying spinal fusion stems from the theoretical assumption that, by permanently suppressing motion, surgery can somehow address the cause of a patient's actual (e.g., a degenerative disorder) or expected (e.g., a progressive deformity) pain, impairment, disability, and handicap following a great variety of spine diseases. Hence, regardless of the etiology specific to each spinal disorder, spinal surgeons regard fusion as the final procedure to treat heterogeneous conditions such as trauma and degeneration. This conceptual model, along with the broadening of indications to fusion, remarkably for the degenerative spine, and the extended life expectancy in the elderly are some of the factors that may account for the huge number of fusion procedures performed each year in the United States and in the European Union [1–3], with a resultant dramatic increase in health care–related expenditures. However, the generalized health care cost increase in industrialized countries is urging policymakers to rationalize the allocation of health care resources in order to trade off reduced budgets and the greatest benefit for patients. Merging of the traditional clinical decision and health economics models into a new clinical resource management model has been advocated [4]. In this perspective, medical or surgical interventions are expected to rely on standards or guidelines originated in evidence-based medicine (EBM).

Spinal surgery is not immune from the ongoing process of a rigorous health care economic analysis, and spinal surgeons are being asked to supply evidence about the effectiveness of their interventions based on a sound methodology assessed by peer review [5]. However, despite the widespread use of fusion in spinal surgery, a survey of the available knowledge reveals a great deal of unsolved problems, uncertainties, and controversy, which can be summarized as follows:

1. Our understanding of spinal fusion in humans on a basic science level is poor. Particu-

larly, a disproportion exists between the information accumulated from extensive research conducted on animal models and the paucity of in-depth data regarding the biological events characterizing spinal fusion in humans, including the crucial issue of timing the steps leading to bone graft incorporation and remodeling.

2. Harvesting of autogeneic bone graft, so far the golden standard material in spinal fusion, is associated with a nonnegligible rate of complications.
3. The role of both mechanical stimuli and fixation in spinal fusion has not been conclusively elucidated, which explains the great variety of commercially available systems whose underlying engineering principles swing from load-bearing to load-sharing.
4. Although a recent meta-analysis indicated that fixation leads to higher fusion rates, unsuccessful fusion, namely nonunion or pseudoarthrosis, does occur. However, a seeming lack of correlation would exist between clinical outcome and pseudoarthrosis for degenerative conditions of the spine. The question of whether fixation has any clinical correlation has consequently been raised.
5. The aspects outlined in points 2, 3, and 4 have prompted researchers to focus on bone substitutes, growth factors, gene therapy, and stem cell cultures, which are expected to supply the surgeons with new tools for reducing patients' morbidity and the rate of fusion failure. However, practical application is yet in a preclinical or early clinical phase.
6. The indications for fusion are not unanimously defined and agreed upon by spinal surgeons, particularly for challenging conditions such as instability, and the appropriateness of many fusion procedures performed for some types of spinal disorders has therefore been questioned.

A concise review pertaining to each of the above-mentioned issues is presented in this chapter in order to provide the reader with an update and critical knowledge derived from the best clinical research.

II. BIOLOGY OF SPINAL FUSION

A perusal of the available literature reveals little in-depth information regarding the biology of spinal fusion in humans. Furthermore, current knowledge is mainly derived by the process of bone graft incorporation in spinal fusion to the bone-healing process that takes place in fractured long bones [6,7]. Three distinct phases are generally distinguished in the latter: (1) the inflammatory stage; (2) the repair stage; and (3) the remodeling stage: In the inflammatory stage, a hematoma is produced within the fracture site during the first few hours and days. Inflammatory cells and fibroblasts migrate to the injured area and the formation of granulation tissue and migration of mesenchymal cells follows. In the repair stage, fibroblasts synthesize a stroma that supports vascular in-growth. As angiogenesis progresses, a collagen matrix is deposited. Osteoid is secreted and subsequently mineralized, which leads to the formation of a soft callus around the repair site. Eventually the callus ossifies, forming a bridge of woven bone between the fracture fragments. In the remodeling stage, woven bone is slowly replaced by lamellar bone via the remodeling cycle, mechanical stresses significantly affecting the internal architecture of bone.

Unlike the fragments in a fracture site, however, bone grafts used in spinal surgery are not vascularized and consequently undergo necrosis during their incorporation, which is paralleled by a resorption phase during which new viable bone is laid down. This complex coupling of resorption of necrotic bone and synthesis of viable bone is termed creeping substitution [8].

It is worth observing that the sequential timing of the events leading to bone graft incorporation has never been described in humans, nor has it been correlated to imaging. Studies combining histological and diagnostic imaging signs would help spinal surgeons to monitor spinal fusion

throughout the lengthy process of bone healing, possibly detecting abnormal behavior and instituting appropriate countermeasures.

On a cellular and molecular level, the process of bone graft incorporation is far more complex than this description would suggest. A great variety of cells, local and systemic factors, which have been only recently and partially elucidated, are involved. In this framework, three key concepts may aid in understanding better the biology of spinal fusion, namely osteoinduction, osteoconduction, and osteogenesis [9].

Osteoinduction refers to the process whereby undifferentiated cells are stimulated by inductive agents to develop into the bone-forming lineage. These undifferentiated cells are represented by multipotent mesenchymal stem cells. Although an aliquot of mesenchymal cells are located in the deep periosteal and in the endosteal layers of bones, the most abundant reservoir of stem cells is represented by the bone red marrow [10]. Hence, it is important to regard both bone and bone marrow as a functional unit as far as bone graft incorporation is concerned. Since trabecular bone, unlike cortical bone, is rich in bone marrow, cancellous bone grafts, all factors being equal, are much more osteoinductive than cortical or cortico-cancellous ones.

What are the inductive agents involved in the process of osteoinduction? A large body of evidence has accumulated indicating that the recruitment of undifferentiated cells and their subsequent differentiation into preosteoblasts, osteoblasts, and osteocytes is regulated by a complex system of local messengers called growth factors. [11]. Among the growth factors expressed by cells during bone healing, five are currently being investigated for future clinical applications: Transforming growth factor-beta (TGF-β), bone morphogenetic protein (BMP), fibroblast growth factor (FGF), insuline like growth factor (IGF), and platelet-derived growth factor (PDGF). More detailed descriptions will be presented below. Suffice it to say here that only BMPs are true osteoinductive agents, all other molecules intervening during the bone healing process as mitogenic or angiogenetic factors.

Osteoconduction is the property by which a biomaterial allows bone to grow on and into its structure. The biomaterial acts as a scaffold on which both preexisting osteoprogenitor cells and recruited multipotent stem cells grow following osteoinduction. The term has a slightly different implication according to what type of biomaterial is implanted. When spinal fusion is performed, osteoconductivity may refer either to the property of the autogeneic/allogeneic bone grafts or to the characteristics of the metal implant. In the former case, osteoconductivity along with osteoinductivity and osteogenesis are the integrated steps to obtain a successful fusion. In the latter, osteoconductivity is a metal structure property affecting the implant osteointegration.

Osteogenesis indicates the process whereby new bone is laid down by osteoinducted cells that have migrated on and into an osteoconductive structure through new vascular channels. In an experimental model analyzing an intertrasverse fusion in rabbit, a sequential expression of BMPs during bone graft maturation suggested that the process of osteogenesis is modulated in a complex fashion [12,13], whose understanding in humans would allow for an optimal use BMPs as therapeutic agents.

III. AUTOGENEIC BONE GRAFTS

Autogeneic bone grafts are the gold standard materials recommended for use in spinal fusion [14]. The term autogeneic indicates that the bone grafts are harvested from one site and subsequently transplanted to a different site in the same organism. The anterior or the posterior iliac crests are the harvesting sites of choice in spinal surgery. The importance of a meticulous surgical technique obtaining grafts free of soft tissues should be constantly emphasized. An equally punctilious preparation of the recipient bed that is abundantly vascularized and debrided from soft tissues should

be pursued to optimize graft incorporation [10,15]. No technology breakthrough can in fact make up for any poor surgical technique (Fig. 1).

According to the harvesting technique, cancellous, nonvascularized cortical and cortico-cancellous grafts of various shape and size may be retrieved.

Cortical grafts are preferred when an immediate structural support is desired. It should be noted, however, that the creeping substitution phenomenon significantly decreases the initial graft strength in the later phase of graft incorporation in animal models [16,17]. Cortical grafts are mainly osteoconductive, having little osteoinductive properties [10].

Cancellous grafts have no initial mechanical strength but possess the largest amount of bone marrow entangled in their bone trabeculae, therefore representing the best osteoinductive type of autogeneic bone grafts; they are easily vascularized and rapidly incorporated [10]. Cortico-cancellous grafts have intermediate mechanical and biological properties and are generally used in combination with cancellous grafts.

Autogeneic bone grafts are osteoinductive, osteoconductive, osteogenic, and histocompatible. The risk of transferring an infection or a neoplastic lesion from the donor to the recipient site is low if an accurate preoperative screening focusing on the patient's clinical history, examination, and imaging of the donor site, if required, is routinely performed. Unfortunately, two factors affect the use of autogeneic bone grafts: the donor site morbidity and the amount of available graft per

Figure 1 Surgical field pertaining to the clinical case shown in Figure 5. Lumbar spine L4–L5 and L5-S1 fenestrectomy can be observed in the midline (photograph top margin) showing the dural sac covered by cotonoids used for dural sac protection during autograft implanting. Abundant autogeneic cancellous and cortico-cancellous chips harvested from the posterior iliac crest were deposited over the decorticated and bleeding transverse processes and the facet joint lateral aspect (photograph low margin). Encroaching soft tissues were carefully debrided before implanting autografts.

single patient, especially if a large quantity of bone is required and/or a patient scheduled for revision surgery previously underwent bone graft harvesting.

Donor site morbidity indicates the set of complications that may ensue after bone graft harvest from the iliac crest, with a reported rate of major and minor complications of 8.6% and 20.6%, respectively [18]. The complications shared by both anterior and posterior iliac crest graft harvest [19] include chronic pain at the donor site, hematoma, infection, cosmetic defects, and herniation of the abdominal content through iatrogenic defects in the ilium. Chronic pain and hematoma have the highest prevalence. Donor site morbidity associated with anterior iliac crest graft harvesting specifically follows from fracture of the anterior superior iliac spine and lesions to the lateral femoral cutaneous or ileoinguinal nerve. Harvesting from the posterior iliac crest has been associated with injuries to the cluneal nerves, to the superior gluteal artery, to the ureter, and with pelvic instability following destabilization of the sacro-iliac joint. It is worth remarking, however, that complications could be minimized if a careful and rigorous surgical technique is adhered to during graft harvesting, which should not be looked upon as a procedure to be carried out hurriedly.

When large amounts of bone grafts are required, as in fusion procedures for spine deformities, or a previously graft-harvested patient is to undergo revision surgery, the only feasible option to obtain autogeneic bone grafts is harvesting a virgin site, such as the opposite iliac crest, provided the violated crest is identifiable through surgical scar, clinical charts, or x-rays. Cancellous grafts can also be obtained from Gerdy's tubercle, the distal part of the radius, and the distal part of the tibia, while cortical grafts can be harvested from the fibula and the ribs [10].

In addition to the aforementioned drawbacks, autogeneic bone graft harvesting is admittedly a time-consuming procedure increasing the perioperative risk for patients. Furthermore, a consistent rate of nonunion ranging from 5 to 30% has been reported in the literature [20]. The summation of all these factors, which may weigh on the outcome, accounts for the new research trend in the field of bone substitutes, growth factors, and gene therapy.

IV. BIOMECHANICS OF SPINAL FIXATION

Bone responds to mechanical stimuli as postulated by Wolff's axiom stating that bone is able to change its architecture according to the stresses that are imparted to bone. Although the intimate processes regulating the transduction of mechanical stimuli into an integrated cellular response remain elusive, it is admitted that the remodeling cycle can build up a bone structure that is mechanically competent to sustain the stresses imposed by the functional demands. Loads are consequently necessary for proper functioning of the musculo-skeletal system provided they do not exceed the strength of each bone segment, which is determined by the structural properties of the segment itself.

As far as bone healing is concerned, a variety of factors comes into play for a successful union to take place, including the modulating action of loads [21,22]. Since any load is bound to bring about a given action, a balance exists between the favorable and adverse effects of mechanical stimuli on bone repair.

It is a basic traumatology principle that motion in a fracture site impairs healing, which is why fracture segments are immobilized to prime the healing process. A similar problem pertains to bone fusion in spinal surgery: Although transmission of stresses through the arthrodesis area is thought to be beneficial for a union to take place, undue motion may impair healing, thus leading to graft pseudoarthrosis. Spinal surgeons are therefore faced with a difficult task: creating a dynamic stable equilibrium in the spine segments to be fused so as to facilitate graft union without simultaneously shielding the stresses that are beneficial to graft incorporation and remodeling. In this perspective, two tools are at hand in the therapeutic armamentarium: braces and internal fixation.

Braces, which can be classified into elastic, semi-rigid, and rigid [23], have an unclear biomechanical action when used to limit spine motion in noninstrumented or instrumented spinal fusion. No studies demonstrated convincingly that braces provide any constraint on the spine on a segmental level, their action being limited to reducing the overall trunk motion [24–26], provided they extend to include at least one thigh [27]. Patients' lack of tolerance for wearing cumbersome orthoses is an additional issue that limits the clinical applicability of braces.

Internal fixation consists of the application of metal implants for a variety of conditions wherein the spine is to be maintained in a given configuration until grafts are fused. Since fixation devices, once implanted, allow external forces to be imparted, a pathological spine configuration can also be totally or partially corrected. Three types of spine instrumentations can be applied for internal fixation: laminar hooks, wires, and rods; pedicular screws; and interbody devices [15,28,29]. Although fads and industrial innovations may dictate the extinction of older instrumentations and the emergence of newer ones, each type of device is objectively characterized by mechanical properties that may be suitable to the surgical procedure to be performed for a given spinal disorder. Laminar hooks, wires, and rods allow for distraction, compression, and lateral deflection to be exerted on the spine, but they offer three main disadvantages: no rotational forces can be applied and no reduction in the sagittal plane can be carried out; the limited strength of the vertebral laminae restricts the magnitude of the applicable forces; selective segmental control cannot be accomplished [15].

The introduction of pedicular screws has represented a major breakthrough in internal spine fixation, since pedicles offer the strongest anchor point among vertebral elements [15,30]. Pedicular fixation provides superior advantages from a pure mechanical viewpoint, not only in terms of construct rigidity but also because external forces can be three-dimensionally and segmentally applied [15,30–32]. Two types of pedicular screws are currently manufactured: cylindrical and conical. Pedicular screws are cyclically subjected to bending moments at their ventral extremity via a cantilever mechanism, which predisposes them to fatigue fracture proximally to their connection to rods or plates [33]. By varying the screw section, thus modulating the area moment of inertia, conical screws are thought to have a better stress distribution along their axis than cylindrical ones [34,35]. Numerous variables determine the strength of a pedicular construct, including pedicle geometry [36], the implant material and design [31,32], the insertion technique [37,38], and the mineral density of local bone [31,32,39]. Pedicular screw insertion is technically challenging, with objective risks of screw misplacement and secondary neurological damage [40]. They have been classified by the U.S. Food and Drug Administration (FDA) as a class 3 device for use in the United States. Conversely, their clinical application is not restricted in the European Union.

Interbody fixation is achieved by using interbody devices termed cages. The development of interbody cages derived from the hypothesis that cages offer theoretical biomechanical advantages over other types of internal fixation [41,42]: they provide initial structural support in the axial plane; they provide distraction of the spine motion segment and restore disc height and sagittal balance; distraction allows for clearance of the intervertebral foramina in cases of foraminal stenosis; favorable conditions exist for an interbody fusion to occur because the anterior column is expected to bear some 80% of the compressive stresses acting on a motion segment . According to their shape, two types of cages are classified [43]: cylindrical or conical cages (threaded cages) and box-shaped or rectangular cages (nonthreaded cages). Threaded cages are inserted by a threaded device after the vertebral endplates have been prepared with a reamer. Nonthreaded cages are placed after removal of the endplate cartilage. Interbody cages can be inserted through an anterior or posterior surgical approach. Whereas the anterior approach is mandatory in the cervical spine, either approach is feasible in the lumbar spine (ALIF: anterior lumbar interbody fusion; PLIF: posterior lumbar interbody fusion; TLIF: transforaminal lumbar interbody fusion) [44–46]. Doubts have been raised whether a thorough clearance of soft tissues and cartilage can actually be achieved

when posterior approaches are used to insert both threaded and nonthreaded cages [43]. Although initially used as stand-alone fixation devices, biomechanical testing showed that the initial stability provided by cages in extension and axial rotation is not optimal [47]. Supplementing cage fixation with posterior instrumentation is strongly recommended to achieve primary stability from a biomechanical viewpoint [48] (Fig. 2).

A great variety of fixation devices is currently available in the market because both the design and the material used permit an engineering modulation of the mechanical properties of a construct, provided quality control during industrial production ensures a uniform manufacturing process. The ultimate goal is represented by the ideal implant combining primary stability without shielding

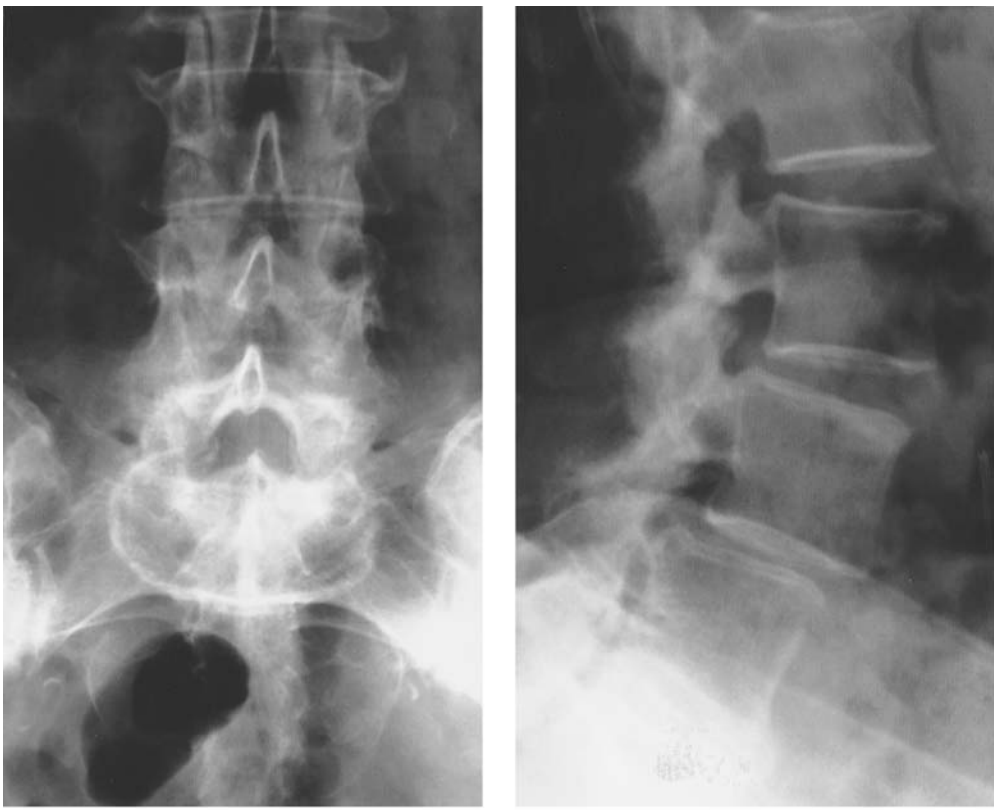

Figure 2 (A,B) Preoperative lumbar spine AP and LL roentgenogram views showing degenerative spondylolisthesis in a 68-year-old retired woman affected by neurogenic claudicatio intermittens and right L5 and S1 radiculopathy at rest. A severe central and lateral stenosis was observed at the L4-L5 and L5-S1 levels in the preoperative CT scans (not reported here). She was scheduled for L4-L5 and L5-S1 decompression by laminotomy and lateral recess enlargement, and instrumented interbody fusion. (C,D) Postoperative lumbar spine AP and LL roentgenogram views showing decompression and interbody fusion instrumented by nonthreaded mesh cages and polyaxial transpedicular screws (Moss®-Miami System). Note the L4-L5 intervertebral disc space increase and the foraminal clearance that did not require foraminotomy at this level. Bone graft were impacted in front of the mesh cages as described in the original surgical technique to help monitoring fusion in the postoperative time (sentinel graft). The patient is free from low back and lower limb pain at 2-year follow-up.

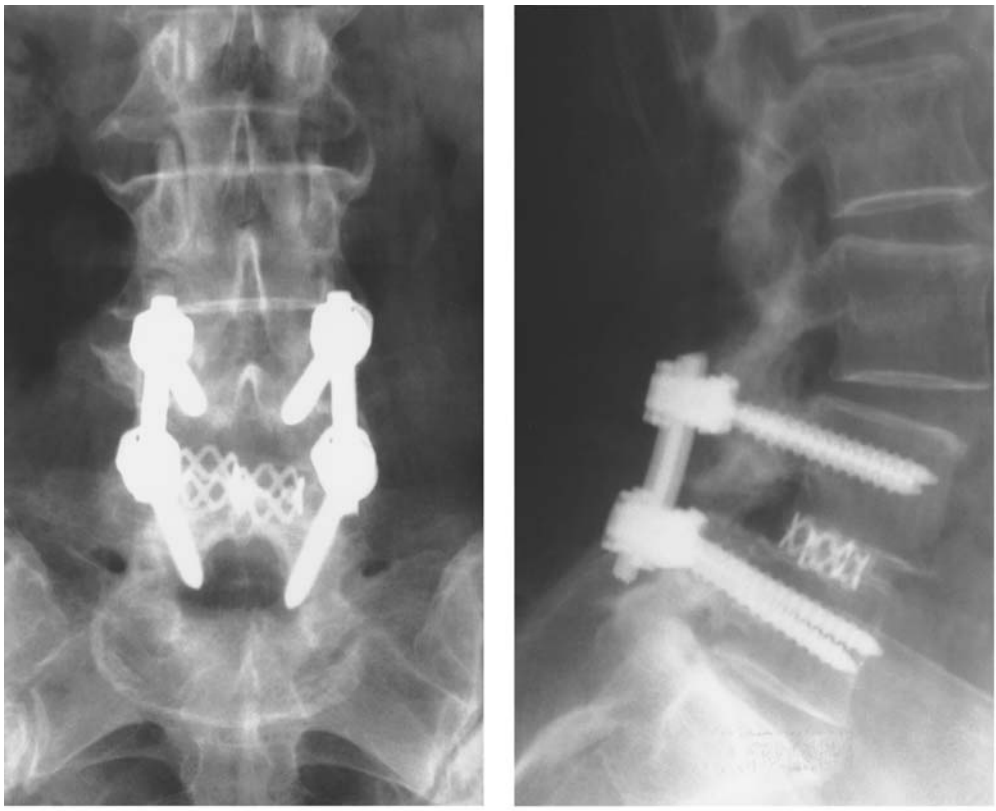

C D

Figure 2 Continued.

those stresses that are beneficial for fusion to occur. However, even assuming that the ideal implant be contrived, it has been suggested that the fusion mass bridging one or more motion segment may itself exert a shielding effect and transmit stresses on the neighboring segments [31,32].

As a consequence, fusion has brought about a iatrogenic pathology that is referred to as junctional pathology [49]. Although it has not been clearly elucidated whether degeneration in discs adjacent to an arthrodesis area is a direct effect of fusion or an occurrence related to the aging process and whether junctional pathology diagnosed through imaging has any clinical correlation, it may be reasonable to hypothesize that the nonphysiological constraints following fusion can cause a functional overload on the adjacent levels [50–52]. At present this aftermath appears to be inherent to the arthrodesis procedure itself, which accounts for alternatives to fusion, such as artificial disc replacement, being developed for degenerative disorders [53].

V. THE ROLE OF INTERNAL FIXATION IN SPINE FUSION

Treatment outcome can be assessed through a variety of methods including physician's objective findings (physical examination, laboratory tests, diagnostic imaging) and patient-based evaluation of pain, quality of life, disability, satisfaction, and fitness for work [54]. Following the introduction

of EBM concepts [55], the focus of outcome assessment has switched from surgeon-based to patient-based evaluation, assuming that the ultimate goal of treatment is returning to work a pain-free, functioning patient who is satisfied with his or her quality of life. Although patient-centered outcome measures are certainly paramount in evaluating the treatment effect of any medical intervention, which is currently agreed upon by all authoritative medical journals, surgeons continue to assess diagnostic imaging or other objective findings in their daily practice. A spinal surgeon performing a spinal fusion, in addition to administering outcome tools to patients, will also monitor the incorporation of grafts until a diagnosis of fusion may reasonably be made on imaging [56].

Spinal fusion, which can be noninstrumented or instrumented, is an expensive procedure in terms of direct and indirect costs sustained by health care givers and patients [57]. Perioperative complications and revision surgery in cases of nonunion are additional factors increasing the overall health care expenditures [58]. From a surgeon-based viewpoint, the occurrence of fusion, as diagnosed on a roentgenogram, consequently represents the final endpoint to assess the success of the operation he or she performed, thus relieving the health care professional from the concerns that inevitably arise when nonfusion is suspected or diagnosed. Although nonunion is not necessarily related to the clinical outcome [59], fusion does represent a priority for a spinal surgeon. Spinal instrumentation has been accordingly developed and introduced into surgical practice not only to reduce patients' discomfort caused by the immobilization imposed by burdensome braces but also to improve the chances of bone graft incorporation. However, fixation devices further increase costs due to the implant itself and to the longer operative time and related perioperative complications [60].

The research trend to evaluate the effect of treatment is currently represented by grading the methodological quality of the studies purporting the effectiveness of a given medical or surgical intervention [61]. A host of biases and confounding variables, if not properly recognized and controlled by study design and statistical methodology, can in fact invalidate the conclusions of a seemingly well-conducted study. Since randomization allows a truly casual distribution of confounding variables among groups, provided the randomization procedure is concealed, only randomized studies can reach conclusions at a low risk of being distorted by the unbalanced weight of confounding variables [55]. Moreover, any treatment effect has to be compared to the effect induced by something else (the control), may it be an event natural history (e.g., a disease) or a placebo or a golden standard treatment. Hence, randomization with a control group is the only method of establishing a reasonably likely cause-effect relationship between a treatment and an observed outcome, if any, all factors being equal.

The spreading of the stringent scientific methodology derived from the cultural revolution fostered by EBM has generated levels of evidence supporting the conclusions of published studies. Four levels of evidence grading are currently used [61]. Grade A: support is derived from meta-analysis or a good quality systematic review of two or more randomized controlled trials (RCTs); grade B: support is provided from one or more RCTs or good observational studies; grade C: evidence is insufficient or inconclusive (no or poor randomized controlled trials or observational studies); grade D: no scientific support exists. In this framework, grade A evidence provides physicians with the best research assessment of the validity of a given treatment. Grade B evidence is lower ranked but acceptable when surgical treatments are assessed due to the inherent problems of randomization in surgical disciplines. In this evaluation system, meta-analysis is credited to be the most reliable method for judging the effectiveness of treatment [55].

Meta-analysis is a statistical technique used to assess the effectiveness of clinical interventions [62]. It merges the results from two or more randomized controlled trials and supplies a precise estimate of the treatment effect giving due weight to the size of the different studies included. The validity of meta-analysis depends on the quality of the systematic review on which it is based, which implies that rigid criteria should be applied when meta-analyzing studies [63–65]. Although

surgical disciplines including orthopedics have objective difficulties in designing randomized controlled trials [66], the issue of whether randomizing patients is ethical also being raised, RCTs have been conducted and meta-analyses regarding spinal surgery have been elaborated upon by credited agencies such as the Cochrane Collaboration.

The one and only published meta-analysis dealing with the role of instrumented versus noninstrumented spinal fusion in degenerative lumbar spine conditions was derived by pooling RCTs selected by a careful systematic review [67]. However, these trials dealt with heterogeneous pathological conditions for which different indication criteria and instrumentation systems were employed. Despite these limitations, the Cochrane metaanalysis suggested that strong evidence exists that instrumented fusion leads to a higher fusion rate. This conclusion has been confirmed by the findings of a RCT published by the Swedish Lumbar Spine Group comparing, among other outcomes, the rate of successful fusion in three groups: instrumented postero-lateral fusion, instrumented postero-lateral and interbody (ALIF or PLIF) fusion, and noninstrumented postero-lateral fusion of the lumbar spine performed for chronic low back pain [68]. Higher fusion rates were observed in the instrumented group, and no significant differences were noted between posterolateral and circumferential fusion.

Current evidence would therefore warrant the use of internal fixation to increase the likelihood of successful fusion. However, even if instrumentation seems to be beneficial to the biology of spinal fusion by reducing harmful mechanical stresses, two considerations deserve brief comment. First, despite internal fixation pseudoarthrosis is still a frequent complication in spinal surgery. New strategies are therefore being investigated to further improve the rate of fusion. Second, evidence is lacking as to whether the rate of fusion is correlated with clinical outcome, at least in lumbar spine surgery. Since patients' well-being is the ultimate goal of spinal fusion, RCTs should be conducted to prove that a solid fusion is clinically meaningful, not only from a surgeon-based but primarily from a patient-based viewpoint. Until then, health economists may legitimately raise the question of whether a radiographic outcome (e.g., fusion) not necessarily related to the clinical outcome warrants the increased costs related to instrumentation.

VI. BONE SUBSTITUTES AND GROWTH FACTORS

The nonnegligible rate of pseudoarthrosis in spinal fusion, the donor site morbidity related to autogeneic bone harvesting, and the limited availability of autogeneic bone grafts retrievable during surgery are all factors that have caused scientific investigation to expand its interest area and focus on new research fields such as biomaterials, molecular biology, and tissue engineering after decades of study and application of metal fixation devices. Biology, rather than metallurgy, currently seems to be endowed with the opportunity of improving the performance of spinal fusion in terms of both predictability and reliability. However, technological innovations are being introduced at a very fast pace as opposed to the lengthy process required to test medical devices in preclinical and clinical trials in humans. As a result, few high-quality papers are currently listed in the literature yielding clinically applicable data about the newest biomaterials and molecules that the industry presents to spinal surgeons as the philosopher's stone to predictably transmute bone grafts into a solid fusion mass.

Since any graft biomaterial different from autografts is expensive and is potentially risky for health, clinical studies on the treatment effects of new biomaterials yield meaningful information and justify the use of the tested product provided they are randomized and compare a new treatment to autografts. Hence, RCTs are mandatory when we wish to assess if a bone substitute and/or a growth factor is able either to obtain at least the same fusion rate as autografts while eliminating donor site morbidity or to reduce the nonunion rate. Prospective observational studies may be ac-

ceptable when primary or revision spine surgery requires large amounts of bone that could not be harvested, the purpose being observing results rather than comparing treatments.

A survey of these new trends in research is presented in this section, focusing on those bone substitutes and growth factors for which RCTs or at least systematic reviews may currently be available. The numerous and valuable experimental studies about bone substitutes and growth factors are not reported here in order to supply spinal surgeons with concise but clinically meaningful reference information.

A. Bone Substitutes

The term bone substitutes refers to a heterogeneous group of biomaterials intended for use as (1) sheer substitutes for or extenders/expanders to autogeneic bone grafts and (2) carriers of growth factors or multipotent mesenchymal stem cells in fusion procedures. Since any biomaterial implanted into an organism triggers an interaction between the biomaterial and the surrounding host environment, the concepts of biocompatibility and bioreactivity need to be introduced in addition to those of osteoinductivity, osteoconductivity, and osteogenesis.

Biocompatibility refers to the ability of a biomaterial to perform with an appropriate host response in a specific application [69]. Bioreactivity pertains to the type of interaction occurring between a material and the host environment, which allows classifying a material into [69]: 1) bioinert: when its shape and structure are preserved through time; 2) bioactive: when its shape and structure are maintained through time but its surface attaches to the surrounding environment; 3) biodegradable: when its shape and structure are retained and surface attachments are formed within a given time interval, past which the material eventually loses its shape and structure and is replaced by host tissue; the replacement process is referred to as bioresorption.

The ultimate goal of bone substitute technology is to supply spinal surgeons with an ideal material that should be osteoinductive, osteoconductive, osteogenic, biocompatible, and biodegradable; load-bearing properties may also be required. No bone substitute as yet possesses all of these ideal properties, and currently available biomaterials have variable properties, knowledge of which is essential to choose to best biomaterial for the best performance in a spinal fusion procedure.

1. Allogeneic Bone

Allogeneic bone (allografts) is available in three main preparations: fresh-frozen, freeze-dried, and demineralized [10,70,71]. The processing method significantly modifies the allograft strength, capacity for incorporation, immunogenicity, and potential for disease transmission.

Fresh-frozen allografts are obtained from cadaveric donors or from living donors usually operated on for joint replacement following a careful donor screening. Frozen bone is recovered aseptically to reduce the risk of bacterial contamination and is consequently processed to remove surface tissues, internal blood, marrow elements, and fat. Fresh-frozen bone is osteoinductive, osteoconductive, osteogenic, and preserves most of its mechanical strength [72]. Depending on the processing methodology, fresh-frozen bone may contain, to a variable extent, viable elements stimulating the formation of antibodies to histocompatibility antigens and blood group antigens [70]. Moreover, unless undergoing sterilization, which greatly affects its osteoinductive and osteogenic properties, the potential for disease transmission is high. This limits its clinical application [10].

Freeze-dried or lyophilized bone is obtained through extensive processing following donor and tissue screening, including aseptic retrieval and removal of superficial and internal tissues. Bone is subsequently lyophilized and vacuum-packed; sterilization may optionally be added during bone processing [70]. Freeze-dried bone is osteoconductive but has weaker osteoinductive

properties, especially when it is subjected to sterilization. Processing minimizes the potential for immunogenicity and disease transmission. Lyophilization alters the mechanical properties of bone up to 50%, especially as far as torsional and bending strength are concerned, compressive strength being affected to a lesser extent [71,73]. Freeze-dried bone is available in a great variety of preparations and may be subdivided in relation to both shape (strips, blocks, dowels, struts, cubes, and ground powder) and composition (primarily cancellous or cortical). Freeze-dried autografts are classified into two main varieties accordingly: structural cortical grafts and cancellous and particulate (cortical and cancellous) grafts [71].

Either method of preparation affects the relevant biological properties between graft types in a fashion that should be borne in mind to optimize their clinical application [73–75]. Cortical grafts supply an initial structural support but are slowly revascularized and incompletely resorbed; their incorporation occurs through a process of periosteal osteogenesis that encircles the allograft and forms an external callus [76]. Conversely, cancellous and particulate allografts offer no structural support but are rapidly revascularized and resorbed; their incorporation takes place as new bone is laid down on the surfaces of the trabeculae, which increases the area available for osteogenesis [77,78].

Although no meta-analysis is currently available for critically appraising the role of freeze-dried bone grafts in spinal fusion, a review of clinical studies suggested that the indications for allograft use in spinal surgery would depend on the type of allograft preparation, the anatomical fusion site and the patient's age [79]. Particularly, structural allografts, which supply an osteoconductive but limited osteoinductive scaffold, are recommended for an anterior single-level lumbar and cervical interbody fusion, fusion rates being comparable to those obtained when autografts were employed. These findings have been recently confirmed by a RCT comparing the rate of fusion in patients undergoing cervical interbody fusion by autografts, allografts, and xenografts [80]. Particulate allografts may be used as autograft extenders in instrumented fusion procedures performed for thoracolumbar deformities, but they yield unreliable fusion rates, especially in the adult population. In posterolateral fusion at the lumbar spine level, particulate allografts yielded the lowest fusion rates when prospectively compared to autogeneic bone grafts, a mixture of autografts and allografts, and fresh-frozen grafts.

Demineralized bone matrix (DBM) is obtained by a standardized method whereby processed allogeneic bone is crushed to a particle size ranging from 74 to 420 μm and subsequently demineralized in a 0.5 N HCl mEq/g acid bath for 3 hours. The residual acid is washed out in sterile water, ethanol, and ethyl ether [10]. DBM is osteoconductive and possibly osteoinductive since the growth factors present in the bone matrix would be made available to the host environment by the decalcification process [10]. It should be noted, however, that since the American Association of Tissue Banks and FDA regulate that each batch of DBM be obtained from a single donor for safety reasons, the biological properties may widely vary among batches as a function of the biological diversity of the donors [81]. The potential for immunogenicity and disease transmission is low, the latter being further reduced by the demineralization process that is able to inactivate human immunodeficiency virus (HIV) [82]. DBM offers no structural support and is manufactured as freeze-dried powder, crushed granules or chips, and a gel or paste [10]. It has been suggested that DBM may be used alone, as an augmentation and expanding material in combination with autografts, and as a carrier for autologous stem cells taken from the recipient's iliac red bone marrow [83,84]. Although experimental data obtained in animal models showed that DBM favorably affected spinal fusion, clinical application in humans has given disappointing results. In a prospective multicenter study, higher nonunion rates were recorded when DBM was used alone in comparison with the fusion rates obtained when autogeneic bone was employed [85]. One proposed reason for such a discrepancy may be the variability in the osteoinductive properties of commercial preparation of DBM as evidenced by submolecular assay [86]. Another possible explanation may be that DBM osteoin-

ductivity is thought to be dependent on the activity of growth factors unmasked by demineralization. As a consequence, the response of the host bone to DBM may not be dose-optimized in humans who, like other primates, show a dose-response effect to growth factors, as will be detailed further on in this chapter. Current evidence therefore suggests the use of DBM as graft extender or expander in addition to autogeneic bone, when required [71].

2. *Ceramics*

Ceramics encompass a heterogeneous group of materials that are composed of metallic and nonmetallic elements and share the characteristics of being refractory, inorganic, and of having nonmetallic properties [71]. Ceramics can be classified as either crystalline (having a repeating three-dimensional unit cell) or amorphous (having no long-range atomic order). Ceramics used for application in orthopedic surgery are typically calcium phosphates [10]. Calcium phosphate ceramics can be subdivided into high-temperature and low-temperature calcium phosphates [87]. Low-temperature calcium phosphates, also referred to as calcium phosphate cements, are not classified as ceramics in some published papers [88].

High-temperature calcium phosphates are synthesized by a thermal reaction that takes place at approximately 1000°C. They have a polycrystalline structure in that they are obtained from individual crystals that have been fused together [71]. They include β-tricalcium phosphate (β-TCP), hydroxyapatite (HAP), and β-TCP/HAP composites [87]. All high-temperature calcium phosphates are osteoconductive since they possess a polycrystalline lattice that mimics that of cancellous bone [10]. They are biocompatible, and their bioreactivities vary as a function of both their crystalline structure and composition [71]. High-temperature calcium phosphate ceramics are brittle materials (they fail suddenly with little plastic deformation), and their compressive strength is higher than their tensile and shear strength [89].

β-TCP is a random porous biomaterial, commercially available in blocks or granules. It is biodegraded by osteoclastic activity within 1–2 years [90]. However, a fraction of β-TCP undergoes a partial conversion into HAP so that the overall biodegradability profile of β-TCP is deemed unpredictable by some authors [10].

HAP is obtained by sintering (a process of coalescence of individual ceramic particles into a solid phase) precipitated hydroxyapatite. [88]. Sintered HAP should not be confused with coralline HAP, which is also a synthetic material obtained by a hydrothermal exchange method wherein the calcium carbonate skeleton of the coral *Porites asteroides* is heated in the presence of an aqueous phosphate solution so that a calcium phosphate copy of the coral skeleton is obtained [91]. The microscopic architecture of both sintered and coralline HAP closely resembles that of cancellous bone, which accounts for HAP being considered the most biocompatible bone substitute [92]. HAP biodegradation takes place over decades so that it is actually regarded as a nonresorbable biomaterial [88]; concerns exist that the persistence of HAP in a fusion mass may hinder the subsequent remodeling phase during graft incorporation in spinal fusion.

β-TCP/HAP composites are biphasic compounds that have intermediate properties compared with β-TCP and HAP. Most commercial products contain 40% β-TCP and 60& HAP [88].

Low-temperature calcium phosphates are obtained by mixing one or several calcium phosphates in an aqueous solution at low temperature. Calcium phosphates precipitate and form a less soluble end product. Whatever the number of mixed calcium phosphates, four end products are currently obtainable [88]: precipitated hydroxyapatite (apatite), carbonated precipitated hydroxyapatite (carbonated apatite), dicalcium phosphate dihydrate (brushite), and amorphous calcium phosphate. Since one study indicated that amorphous calcium phosphate is converted to precipitated hydroxyapatite [93], all cement formulations can be classified into apatite, carbonated apatite, and brushite cements.

Calcium phosphate cements are osteoconductive and, thanks to their large specific area, are more bioreactive than high-temperature calcium phosphates [88]. Biodegradation occurs via osteoclastic activity, and the resorption rate is a function of both crystal size and porosity in that a longer rate is expected when crystal size increases or porosity decreases [88]. Calcium phosphate cements have a porosity ranging from 30 to 60% with a mean pore size of 1 μm; since the pore size prevents a fast bone ingrowth, they are resorbed layer by layer [88].

Most calcium phosphate cements are rigid, because during the setting reaction crystal growth occurs. Their mechanical properties increase as porosity decreases [88]. Moreover, some studies indicated that their mechanical properties vary as a function of time in a fashion peculiar to each cement type [94,95]. Like high-temperature calcium phosphates, they have poor tensile and shear strength.

Commercially available calcium phosphate cements are prepared from mixing a liquid and a powder. In all cases, a paste is obtained following setting via either an exothermic or an endothermic reaction. The calcium phosphate cement exothermic reactions are either not as intense as those of polymethylmethacrylate cements or, when they are, the heat release rate is slower, which eases the dissipation of the thermal energy [88]. Different biodegradability profiles and mechanical properties characterize the commercialized available apatite, carbonated apatite, and brushite cements, in that the resorption rate of brushite cements is slower than that of apatite cements [88] and the mechanical properties of apatite increase throughout bone growth, whereas those of brushite first decrease and then increase. These variations should be considered by the spinal surgeon choosing among different products.

Following experimental research, ceramics were introduced into surgical practice, and two RCTs are currently found in the literature. In two studies patients affected by idiopathic scoliosis were randomized to instrumented spine fusion using either autografts or β-TCP/HAP composite blocks as graft material. A complete ceramic graft incorporation and good radiographic results were obtained in the investigational group at a minimum 2-year follow-up [96,97]. In a prospective nonrandomized study, patients with adolescent idiopathic scoliosis were treated to instrumented spine fusion using a mixture of either autografts plus allografts or autografts plus β-TCP. Successful fusion was attained in both groups, and complete β-TCP resorption was observed [98]. As a result, preliminary evidence would suggest that β-TCP may be an effective substitute for autogeneic bone as a graft material in instrumented posterior fusion for adolescent idiopathic scoliosis. Its usefulness in other spine disorders awaits validation from RCTs.

B. Growth Factors

Growth factors are proteins that are synthesized and secreted by cells in response to appropriate stimuli during bone healing. According to a theory advocated by Frost [99,100], the local bone, bone marrow, and soft tissue damage initiated by surgery sensitizes the viable surviving cells and induces the secretion of growth factors regulating the cell response aiming at tissue repair. Growth factors, which influence cellular activity by an autocrine, paracrine, or endocrine mechanism, act on target cells by binding to specific cell receptors (ligand-receptor interaction). The ligand-receptor interaction causes the receptor intracellular domain to modify its configuration, which activates an intracellular system, ultimately leading to the expression of a gene or a set of genes [101].

According to the type of response elicited in target cells, growth factors may be distinguished into mitogenic and osteoinductive factors. Mitogenic growth factors act on multipotent mesenchymal cells, stimulating their proliferation, whereas osteoinductive growth factors induce the differentiation of stem cells towards the osteogenic lineage.

Five types of growth factors have been considered for current or future clinical application: TGF-β, FGF, IGF, PDGF, and BMP. To date, only BMPs have been proved to have osteoinductive

activity, accounting for the extensive experimental research conducted leading to their commercialization and use in clinical settings.

1. TGF-β

TGF-β is a growth factor that is included in the so-called TGF-β superfamily, which also includes BMPs, growth differentiation factors (GDFs), activins, inhibins, and Mullerian substance [102,103]. TGF-β exists in five isoforms (TGF-β1 to TGF-β5) and is found in platelets, bone, and cartilage matrix [104], a fact fostering the deductive hypothesis that TGF-β is somehow involved in the phases of bone healing. TGF-β induces the proliferation of stem cells by binding to a specific membrane receptor complex (type I and II serine/threonine kinase receptors) and activating a group of intracellular messengers called Smad proteins [105]. A number of experimental studies have suggested the role of TGF-β as a mitogen in bone healing, although its osteoinductive activity appears to be limited. However, since TGF-β acts on a variety of cellular phenotypes, unpredictable adverse events might be expected, which has so far hindered its clinical application [101].

2. FGFs

The term fibroblast growth factor encompasses a group of nine polypeptides that share an affinity for cellular glycosaminoglycan heparin-binding sites [106]. FGFs are secreted by macrophages, mesenchymal cells, chondrocytes, and osteoblasts and act as mitogens on a variety of cellular phenotypes, such as epithelial cells, myocytes, chondrocytes, and osteoblasts via their interaction with a tyrosine kinase receptor [107]. Among FGFs, two types are found in adult human tissues: acid FGF (α-FGF or FGF-1) and basic FGF (β-FGF or FGF-2), which have been shown to be involved in chondrocyte and osteoblast proliferation, respectively [108,109]. Since experimental research has indicated that FGFs can accelerate bone healing, their clinical application as bone-healing enhancers may be hypothesized [101].

3. IGFs

IGFs are secreted by target cells in response to the action of growth hormone released by the pituitary gland following stimulation by growth hormone–releasing hormone secreted by the hypothalamus [101]. IGFs are present in chondrocytes and osteoblasts and have a mitogenic action via their interaction with a tyrosine kinase receptor. Two types of IGF (IGF-1 and IGF-2) are distinguishable in humans, the former being located in fracture sites in humans [110]. Since experimental studies demonstrated that IGF-1 promotes bone healing through intramembranous ossification, its relevant use as bone healing enhancer has been suggested [111].

4. PDGF

PDGF is a growth factor secreted by platelets during the hemorrage phase of bone healing [112]. It acts as a mitogen for osteoblasts via a tyrosine kinase receptor, but its role in bone healing and consequently its potential clinical applications are still uncertain [113].

5. BMPs

BMPs are a family of proteins belonging to the TGF-β superfamily. They are structurally related owing to homology in the amino acid sequence, yet they are multifunctional in that they have a great variety of effects in different tissues throughout life [114]. Of the 20 BMPs so far identified, 6 (BMP-2, 4–8) have been shown to have structure and function similarities based on both their amino acid sequence and their action [115].

All six BMPs structurally share two features: (1) they are synthesized as precursors whose propeptide is clipped from the mature protein during secretion, leaving a carboxylic terminus with a highly conserved seven-cystein repeat; (2) each mature BMP is a homologous or heterologous dimeric chain derived from two monomers undergoing disulfide linkage dimerization. Structural similarities allow for BMPs being further subdivided into a subclass comprising BMP-2 and BMP-2, which are highly related and differ mainly in the terminal regions, and BMP-5, BMP-6, BMP-7 (or osteogenic protein-1, OP-1), and BMP-8 (or osteogenic protein-2, OP-2), which share roughly a 70% amino acid identity [115].

Functional analogies pertain to the role that these BMPs play during development and in adulthood. During formation of the embryo, BMPs regulate the morphogenesis of skeletal and nonskeletal tissues, each BMP having a specific role [116,117]. In adult life, BMPs act as local osteoinductive agents during bone healing via a complex, strictly regulated, and self-limiting process. BMPs act on target cells, which are represented by multipotent mesenchymal stem cells, through the interaction with a cell membrane receptor complex formed by two different types (1 and 2) of serine-threonine kinase receptors; in mammals Type 1 includes Type A1 and Type B1 receptors, each activating intracellular signaling in a different fashion [118]. BMP interaction with Type 1 and Type 2 receptors triggers an intracellular signaling pathway whose messengers are represented by a group of proteins called Smad; Smad proteins subsequently form complexes that migrate into the nucleus, where they regulate the transcription of target genes [119].

Extensive experimental studies have demonstrated that BMPs are chemotactic, mitogenic, and osteoinductive agents that initiate a complex series of cellular events ending up with osteogenesis when implanted in vivo [12]. However, the same studies also indicated that BMPs exhibit a threshold concentration affecting bone formation, a property referred to as the dose-response effect. This dose-response effect appears to be dependent on a number of factors including the type of BMP, the type of carrier, the anatomical location, and the animal species [114,115]. In general terms higher doses are required for BMPs to act as osteoinductive agents in complex organisms such as nonhuman and human primates, which has raised the question of the safety profile of BMPs in clinical settings [120]. Moreover, since the in vivo implantation of individual BMPs suffices for the osteoinductive process leading to bone formation to take place, one wonders whether the apparent redundancy of BMPs in adulthood has any functional role or if it is a vestige of the BMP differential role during embryogenesis [115]. Research conducted on an animal model indicated that BMP expression is a complex process wherein BMPs are released according to a well-defined spatial and temporal pattern [12], which would suggest that the apparent redundancy may actually have an undiscovered functional meaning.

Although the results obtained from animal models are not directly applicable to humans, the large body of experimental evidence as to BMP osteoinductivity and safety prompted BMP manufacturing, commercialization, and possible clinical application; however, it is important to note that the legislation regulating the clinical use of medical devices differs between the United States and Europe, so that devices employed in clinical trials in Europe may not be FDA-approved in the United States.

One fundamental point to bear in mind when assessing the results of studies analyzing the efficacy of BMPs versus autografts in spinal fusion procedures is that evidence, if any, of BMPs being as effective as autogeneic bone in achieving fusion does not automatically imply that BMPs are superior to autografts, since a cost-effectiveness analysis should be performed to prove that lower donor site morbidity and/or faster functional recovery rate make up for the adjunctive costs related to BMP use. Only studies indicating that the use of BMPs can reduce the current nonunion rate in spinal surgery may warrant their clinical application.

Three BMP-based formulations are currently produced for possible clinical applications in spinal surgery: bovine BMP extract and human BMP-2 and BMP-7.

Bovine BMP extract (bBMPx) is manufactured from bovine bone undergoing sequential processing consisting of fat and mineral content removal, extraction of BMPs from the demineralized matrix, and purification by chromatography. The final product contains a mixture of growth factors represented by BMP-2, BMP-3, BMP-4, BMP-5, BMP-6, BMP-7; TGFβ_1, TGF-β_2, TGF-β_3; FGF-1 and other noncollagenous proteins [121]. bBMPx offers theoretical advantages and disadvantages over human BMPs. The former include the presence of both BMP heterodimers, which are more potent than homodimers [122], and several BMP and non-BMP proteins, which may act synergistically. The latter encompass the potential immunogenicity of bovine-derived BMP extracts and the possible presence of contaminants having either inactive or inhibitory effects on the osteoinductivity process. bBMPx is not consequently FDA-approved as an osteoinductive agent in clinical settings and is not commercially available in the United States. However, experimental studies conducted on animal models (rabbits and nonhuman primates) demonstrated that bBMPx is as safe and effective as autografts in achieving postero-lateral fusion of the lumbar spine, although the results also indicated that bBMPx shows a definite dose-response effect depending on the animal species [123]. A clinical trial is currently being performed in Europe on 22 patients to test the efficacy of bBMPx versus autografts in lumbar posterolateral fusion. It showed early promising results but also revealed that higher doses than those used in nonhuman primates are required to achieve fusion [121].

BMPs can be obtained via recombinant DNA technology starting from mammalian cells. The advantage of biotechnology-derived BMPs over bBMPx is that molecules identical to human BMPs can be obtained in unlimited quantities. The biotechnology processes involved in rhBMP synthesis are based on sequential steps [115]. The human DNA sequence specific to a BMP is first linked to a vector that is transfected into a selected mammalian host cell. The BMP coding sequence is subsequently amplified, and the cell line is expanded and frozen. Finally, lots of the cell line retrieved from the cell bank for production are thawed and made to grow in larger and larger culture medium volumes, from which BMPs are purified. Two types of recombinant human BMP are currently available: recombinant human BMP-2 (rhBMP-2) and BMP-7 or OP-1 (rhBMP-7or rhOP-1).

rhBMP-2 is the only type of BMP that FDA advised be approved for clinical application in spinal fusion [124]. The FDA advice stems from a huge body of experimental evidence and, more importantly, from clinical pilot studies indicating that rhBMP-2 is osteoinductive in humans. The one and only published pilot clinical study is a multicenter, independent observer, nonblinded RCT with a 2-year follow-up [125]. Fourteen patients with a single-level symptomatic degenerative disc at the lumbar spine level undergoing ALIF were randomized to two treatment groups: one group (11 patients) was implanted with threaded cages filled with a sponge containing rhBMP-2, while the control group (3 patients) received a threaded cage packed with autogeneic bone grafts. The study results indicated that fusion occurred more reliably in the group receiving rhBMP-2, which also showed satisfactory clinical outcome, as assessed through validated patient-based self-evaluation tools. A group of FDA-approved investigational trials involving more than 480 patients has been recently quoted in the literature, although, to our best knowledge, the bibliographical references refer to results listed in conference abstracts rather than to papers published in peer-review journals [126–131]. Despite these limitations, the preliminary results related to the use of rhBMP-2 versus autografts to achieve cervical and lumbar interbody fusion and lumbar postero-lateral fusion would appear to be promising. Technical challenges inherent to adapting both rhBMP-2 doses and delivery systems in different anatomic locations in humans are reported by the authors [124].

rhBMP-7 (rhOP-1) has been used in experimental models indicating that rhBMP-7 is effective in promoting both interbody and postero-lateral spinal fusion [132]. A number of FDA-approved investigational clinical trials inquiring the efficacy of rhBMP-7 in achieving posterolateral

fusion in the lumbar spine, which are currently ongoing or completed, would suggest that rhBMP-7 is as effective as autografts to achieve fusion in human lumbar spines [133–135]. However, the relevant results only appear in gray literature, which precludes a rigorous assessment of these studies.

Although early clinical trials would suggest that BMPs are biologically effective when therapeutically used as osteoinductive agents, one crucial point is that they cannot be directly discharged into a decorticated area free of soft tissues for a successful fusion to occur. BMPs consequently require appropriate delivery systems or carriers to carry out their osteoinductive action at a fusion site.

A number of reasons exist for the fundamental role of carriers in BMP-induced spinal fusion [101]: (1) the BMP release has to be controlled at the fusion site because an appropriate BMP concentration has to be retained for a time interval necessary and sufficient to induce bone formation; (2) a void structure has to be interposed between the decorticated areas to allow for cellular migration and angiogenesis, at the same time preventing soft tissue encroachment; (3) the void structure has to be osteoconductive to enhance the attachment of recruited stem, thus promoting osteogenesis in osteoinducted cells. It ensues that an ideal BMP carrier should not only deliver BMPs at an appropriate rate and dose in an osteoconductive environment, but also possess suitable biocompatibility and bioreactivity characteristics. Specifically, a delivery biomaterial should biodegrade without evoking any immunogenicity and producing any local degradation wastes that may impair the bone-healing process; at the same time, however, the biodegradation rate should parallel the bone formation rate to prevent soft tissue from invading the fusion area. Finally, the carrier itself or its secondary biodegradation products should not interfere with the pharmacokinetics of the BMP release.

A great variety of biomaterials has been employed or is currently under investigation for use as BMP delivery systems. They can be classified into five categories: (1) allografts; (2) ceramics; (3) natural polymers; (4) synthetic polymers; (5) composites of ceramics, natural and synthetic polymers. Since a detailed discussion about the properties of delivery biomaterials listed in the five categories would be beyond the scope of this clinically oriented chapter, the reader is advised to refer to dedicated bibliographical references for an in-depth study [136].

VII. GENE THERAPY AND CELL-BASED THERAPY

Gene therapy and cell-based therapy are the ultimate biotechnology frontier in spinal fusion. Although no study has yet supplied evidence about their efficacy in humans, they are briefly discussed here to offer the reader a survey of the latest biotechnology advances holding promise of improving the outcome of patients undergoing spinal fusion.

Gene therapy consists of the insertion of one or more specific gene(s), referred to as transgene(s), into target somatic cells that are made to synthesize the proteins encoded by the transgene(s) [138]. The transgene insertion into target cells is accomplished by a vector, which is an agent that enhances the access and the expression of a given DNA sequence in a host cell. According to the type of vector, which may be viral or nonviral, two modalities of genetic material transferring may be distinguished [137]: transduction, which refers to the insertion of genetic material into a host cell via a viral vector, and transfection, which is the process whereby a cell can take up DNA from the environment.

The genes encoding for BMPs or other growth factors are ideal candidates for gene therapy being applied to spinal fusion. Two main strategies for BMP gene therapy may be envisaged [138]. The first is an in vivo approach wherein a vector directly inserts the BMP transgene into the host cells in a specific anatomical location. The second is an ex vivo approach wherein target cells are

obtained from the host, genetically modified with a transgene and implanted into the original host. According to the insertion technique used, short- or long-term genetic expression, and consequently protein synthesis, can be obtained [101].

Two types of vectors for gene therapy are currently under investigation: viral and nonviral vectors. Viral vectors comprise a number of viral agents that undergo a process known as homologous recombination before being used for gene therapy. Homologous recombination consists of the deletion of portions of the viral genome so to make the virus replication-deficient and ready to accommodate the therapeutic transgene [101]. The genetically modified virus subsequently binds to and enters the host cell, and transduction begins with the injected DNA being incorporated into the host cell genome or remaining extrachromosomal. In either case, the transduced target cell is able to synthesize and secrete the protein encoded by the transgene. A number of viral vectors are being investigated, including adenovirus, adeno-associated virus, retrovirus, and herpes simplex viruses, each offering theoretical advantages and disadvantages related to the virus life cycle [139]. Nonviral vectors include a heterogeneous group of substances and techniques represented by naked DNA injection, electroporation, biolistics or gene gun, liposomes, and polymer-DNA complexes [137].

In general terms, transduction rates are higher than transfection rates, and current research has consequently focused on viral vectors, especially adenovirus. However, a number of problems has so far hindered the application of viral vector–based gene therapy in humans such as the possibility that a defective virus may recombine with viruses present in the host cell, the ability of certain viruses like adenovirus to keep on producing undesired viral proteins, and the host immunogenic response limiting the duration of gene expression [140].

Cell-based therapy includes a variety of techniques based on the properties of mesenchymal stem cells to respond to appropriate osteoinductive stimuli and to differentiate towards the osteogenic lineage.

A definition of terms is required when discussing mesenchymal stem cells in order to avoid incorrect terminology utilization. Three types of mesenchymal stem cells must be distinguished accordingly [141]:

Totipotent mesenchymal stem cells are formed at conception and persist until the embryo is 4 days old. These cells can develop into all of the cells of the body.

Pluripotent mesenchymal stem cells (also known as embryonic stem cells) begin forming when the embryo is 4 days old and exist until the embryo is 8 months old. These cells can develop into most of the cells in the body.

Multipotent mesenchymal stem cells begin forming when the embryo is 8 months old and exist throughout life. They are found in a number of postnatal tissues and are characterized by their ability to differentiate into cell lineages that are phenotypically unrelated to their tissue of origin.

Postnatal bone marrow is one of the tissues harboring multipotent stem cells that have been recognized as the osteoprogenitor cells of skeletal tissues [142], although some authors claim that evidence of the existence of stem cells in bone marrow has not yet been rigorously supplied [143]. These multipotent stem cells would seem to be identifiable in the nonhematopoietic, stromal cell population and have been termed bone marrow stromal cells (BMSCs). In fact, like stem cells, BMSCs exhibit the property of rapidly adhering to a culture plate, forming distinct colonies, each of which is derived from a single precursor cell called the colony-forming unit–fibroblast (CFU-F). It has been proposed that BMSCs and the pericytes located in the bone marrow vascular network are the same entity [142].

Harvesting of autogeneic bone marrow by aspiration from the posterior iliac wing has consequently been advocated as an autogeneic bone substitute that is osteogenic and potentially osteoin-

ductive [10]. However, since only 0.001% of the nucleated cells present in the bone marrow are thought to be mesenchymal stem cells [144,145], simply aspirating and implanting bone marrow to a fusion site may not supply enough stem cells to achieve arthrodesis. Biotechnology techniques for stem cell isolation and culturing are consequently being developed to obtain expanded cultures of osteoprogenitor cells which may be either predifferentiated into osteoblasts or used as target cells for BMP gene therapy [145]. The choice of appropriate biomaterials to act as stem cell culture carriers is as crucial here as in selecting systems delivering BMPs.

VIII. INDICATIONS TO SPINAL FUSION

The issue of clinical indications for spinal fusion is most disputed in spinal surgery [146]. It has already been mentioned that the purpose of spinal fusion is abolishing or reducing the degree of motion in a set of FSUs, but in what instances is fusion thought to be beneficial to patients ?

The performance of spinal arthrodesis, which may be supplemented by internal fixation, is generally based on an existing or expected diagnosis of instability of the spine, one exception being discogenic neck and low back pain, which is increasingly being treated with fusion [147] (Fig. 3). The pertinent crucial point is consequently defining the concepts of stability and instability of the spine.

The terms stability and instability have been borrowed from mechanics, wherein they refer to the equilibrium state of either a rigid or an elastic body [34,35]. A body is conventionally regarded as rigid when the mechanical analysis focuses on the variations of the body's rest or motion state that are caused by forces acting on the body itself. Conversely, a body is conventionally defined as elastic when the mechanical analysis concentrates on stresses and strains caused by forces acting on the body itself. In the case of a rigid body, a static and a dynamic equilibrium are distinguished depending on the body being at rest or in motion; the static or dynamic equilibrium can be further subdivided into a stable, unstable, and neutral equilibrium. In the case of an elastic body, stable or unstable equilibria are similarly distinguished.

Since stability and instability are mechanical definitions having different implications according to the type of mechanical analysis one wishes to perform on a system, their direct application in a clinical setting is at best methodologically incorrect unless the following goals are achieved.

1. A model wherein the spine is considered as a series of either rigid or elastic linked bodies should be elaborated and validated for clinical use, so that pertinent definitions of stability and instability could be applied; although in either case the model would be a rough approximation of the living spine, it would at least provide a unified model and terminology to describe spine disorders from a mechanical viewpoint.
2. The living spine is a highly variable multisegmental structure composed of visco-elastic materials that adapt and respond to mechanical stimuli throughout life so that its structural properties vary, among other factors, as a function of time; obtaining normative data (stratified by age and other significant parameters) from healthy individuals and incorporating them in a model would consequently help classify a spine as physiologically or pathologically unstable.
3. Even assuming that a spine model and index values may become available, clinicians should further avail of both a noninvasive, reliable measuring method and a way to correlate measures pertaining to mechanical aspects to subjective and objective clinical findings. Unfortunately, few efforts have been directed towards the creation of a comprehensive clinical algorithm allowing spinal surgeons to diagnose a clinically meaningful condition of current or expected instability [148]. The large number of definitions of

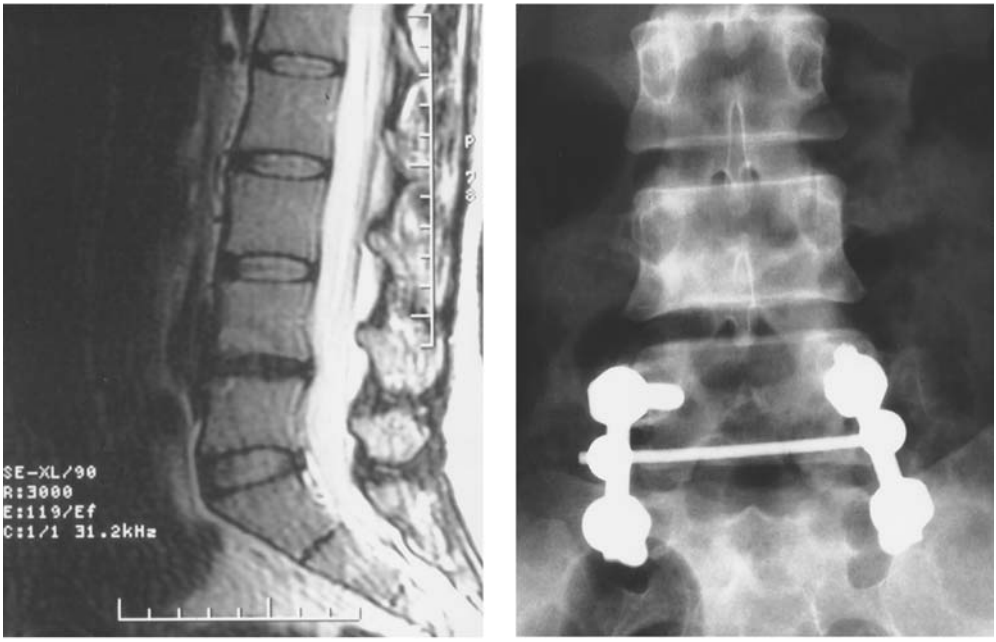

Figure 3 (A) Preoperative T2-weighted sagittal MRI of the lumbar spine in a 36-year-old female farmer affected by discogenic chronic low back pain unresponsive to several conservative treatment modalities over the last 2 years. Both the L4-L5 and the L5-S1 intervertebral discs show a hyperintensity zone (HIZ) in the posterior anulus. The L4-L5 disc reveals a severe degeneration when compared to the L5-S1 disc on imaging. Following provocative discography, however, only the L5-S1 disc reproduced a concordant pain and surgical indication to instrumented postero-lateral fusion at the L5-S1 level only was decided. (B) Postoperative lumbar spine roentgenogram AP view showing postero-lateral fusion with autogeneic bone grafts and transpedicular polyaxial screw/rod fixation supplemented by a transverse connector (Moss®-Miami System) at he L5-S1 level. Screws were inserted according to the inward technique described by Magerl because a synthetic model study suggested that cranially or caudally directed screws as in the up-and-in technique advocated by Levine and Edwards are prone to undergo fatigue stress; the transverse connector was added to increase rotational stability and, according to some authors, lateral bending stability as well. (C) Postoperative lumbar spine LL roentgenogram view showing sacral screws purchasing the ventral sacral cortical to increase the screw pull-out strength. The low back pain resolved after surgery, and the patient is well at a 2-year follow-up. She was advised at hospital discharge to take up a lighter job.

spine instability retrievable in the literature testifies to the uncertainties relevant to this tricky field of spinal surgery [149].

Despite these conceptual limitations, however, clinical experience empirically demonstrates that a number of spinal disorders and/or surgical procedures aimed at decompressing the neural structures can alter motion segment constraints to such a point that the spine becomes unstable, namely loses its capacity, under physiological loads, to maintain its configuration in such a way that initial or subsequent damage to the spinal cord or nerve roots and incapacitating deformity or severe pain occur, according to a most credited definition of spinal instability [148].

Trauma, tumor, and infection are typical spinal disorders directly or indirectly creating gross instability requiring fusion and internal fixation [150]. Pediatric progressive deformities unrespon-

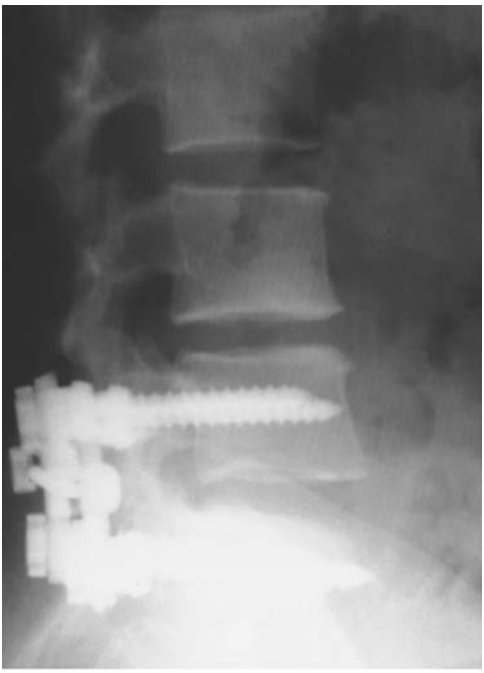

C

Figure 3 Continued.

sive to conservative treatment, high-grade deformities with no indications for conservative treatment at the time of first observation, and deformities whose angular value at growth completion suggests a high risk of progression in adulthood are further examples of conditions warranting the indication to instrumented fusion [151].

Conversely, degenerative diseases challenge the decision-making ability of a spinal surgeon, who is faced with the dilemma of whether to perform fusion or not [152]. As a rule of thumb, most authors agree that no fusion is needed when no instability is detected on either static or dynamic roentgenograms and when the decompressing surgical procedures does not impair physiological (e.g., facet joints or posterior anulus) or pathological (e.g., osteophytes) constraints beyond a certain extent [148]. As far as the radiographic evaluation of instability is concerned, however, spinal surgeons should be encouraged to strictly adhere to those index translational and rotational values that literature data, when available, regard as evidence of vertebral hypermobility [146]. In borderline situations the surgeon is advised to refer to the literature, if any, rather than to personal beliefs. An example is represented by a symptomatic degenerative spondylolisthesis with a slippage that does not exceed index values in either static or dynamic x-rays but may increase postoperatively when sagittally oriented and osteophyte-locked facet joints are undercut to release the dural sac and nerve roots (Fig. 4). Although some authors claim that a good clinical outcome may be obtained by decompression only [153], a prospective RCT showed that better results are achieved when fusion is added [154].

Symptomatic isthmic spondylolysis/spondylolisthesis is a spine disorder for which the surgical indication to instrumented fusion, and decompression if required, is advocated by most authors (Fig. 5) [155].

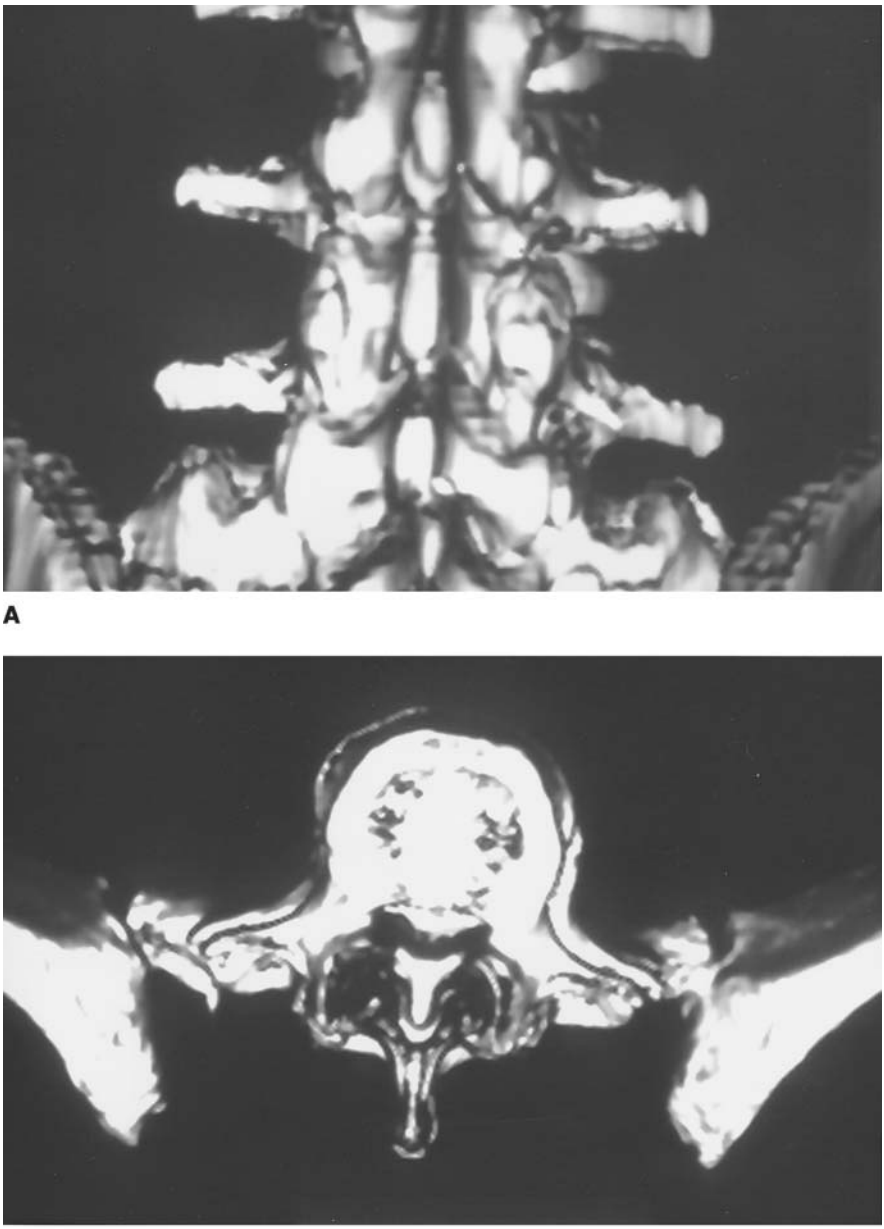

Figure 4 (A–B) Preoperative lumbar spine 3D-CT PA and axial views at the L4-L5 level showing degenerative spondylolisthesis in a 66-year-old retired woman affected by neurogenic claudicatio intermittens over the last 5 years. A marked facet joint hypertrophy can be observed in the PA image, also suggesting spontaneous ossification of the zygapophyseal complex, which finding was confirmed during surgery. The axial view reveals a trefoil canal with sagittal orientation of the L4-L5 facet joint. During preoperative planning indication to decompression without fusion was advised due to associated comorbidities hindering time-consuming surgical procedures (noninstrumented or instrumented fusion).

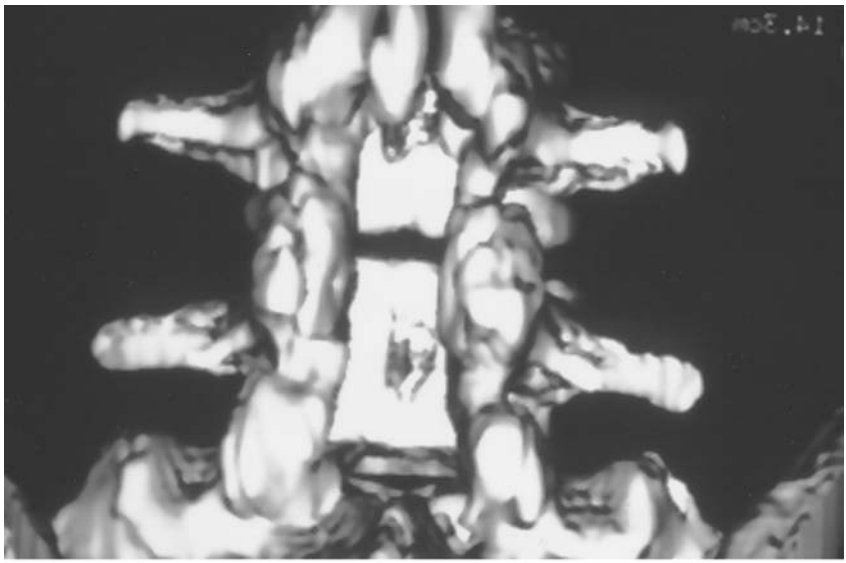

C

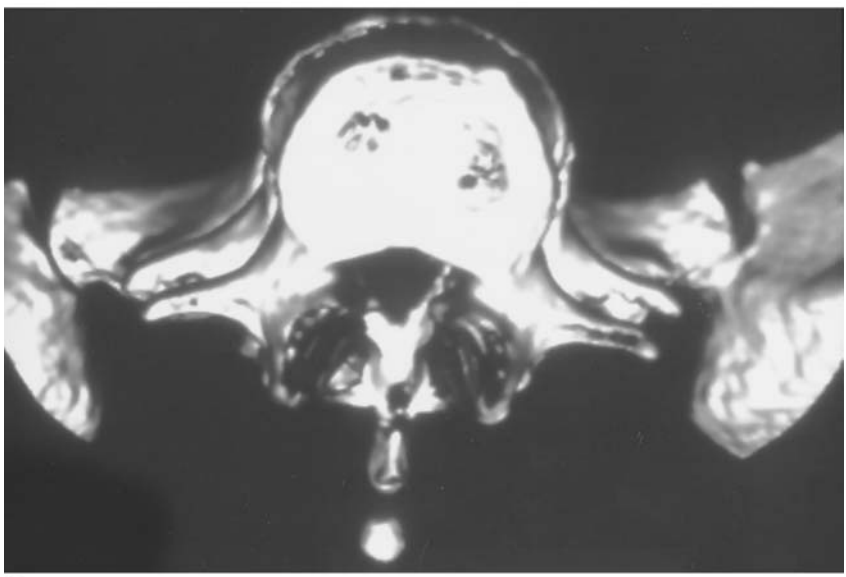

D

Figure 4 (C,D) Postoperative lumbar spine 3D-CT PA and axial views at the L4-L5 level showing laminectomy and partial arthrectomy at the L4-L5 joint complex level. Note that facetectomy was carefully performed balancing the amount of lateral recess decompression and the risk of slippage increase following iatrogenic removal of the natural constraints (facet joint ventral ostephytes) in these sagittally oriented joints. The patient recovered from claudicatio intermittens, but low backpain was not completely resolved by surgery and a part-time semi-rigid brace was prescribed. She was on the whole satisfied with her operation because she resumed walking with her pals without any lower limb pain.

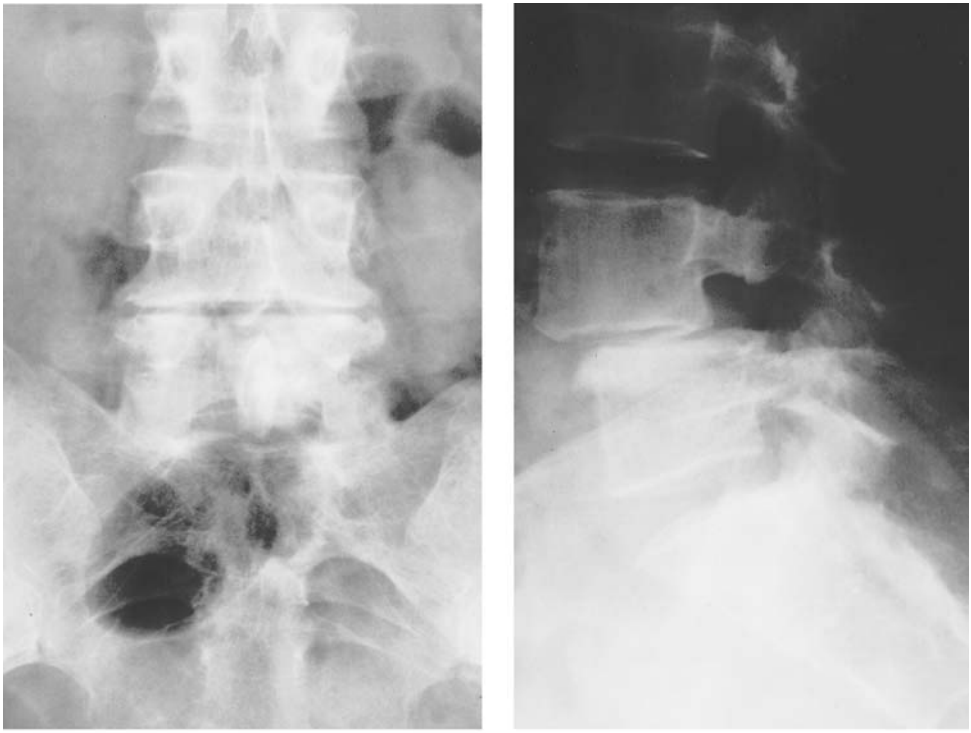

Figure 5 (A,B) Preoperative lumbar spine AP and LL roentgenogram views showing a II degree L4-L5 isthmic spondylolisthesis in a 46-year-old female employee affected by low back pain and bilateral L4, L5, and S1 radiculopathy over the last 3 years. A large Gill's nodule and lateral recess stenosis were observed encroaching the L4-L5 and S1 roots at the L4-L5 and L5-S1 levels, respectively, on MRI (not reported here). (C,D) Preoperative lumbar spine roentgenogram oblique views showing the lytic defect in the L4 pars interarticularis. The patient was scheduled for an instrumented L4-L5 postero-lateral fusion and L4-L5, L5-S1 decompression by lamino-foraminotomy (fenestrectomy). (E,F) Postoperative lumbar spine roentgenogram AP and LL views showing postero-lateral fusion with autogeneic bone grafts (see also Fig. 1) instrumented by transpedicular monoaxial screw fixation augmented by a transverse connector (Isola® System). The patient was well at 3-year follow-up.

IX. CONCLUSIONS

After the metal age that has dominated the spinal surgery scenario over the last decades, spinal surgeons impatiently await the advent of the biotechnology era. Refined techniques are offering potentially new solutions to unsolved problems inherited from the past, and a legitimate enthusiasm excites scientists and clinicians. Preliminary results of ongoing clinical trials, current concept reviews, and instructional courses proliferate in the literature.

The present descriptive chapter reviewed the current knowledge about spinal fusion integrating the new trends in biotechnology and biomaterial research. The purpose was not to supply the reader with a spinal fusion checklist but to stimulate some fruitful reflections about how much of our current and future surgical practice is opinion- or evidence-based. The ever-increasing cuts in health care budgets compel all health care professionals to employ the allocated resources judiciously, for the latest marketed biomaterials and biotechnologies may further increase the current costs of spinal fusion procedures. As a consequence, the clinical application of technology ad-

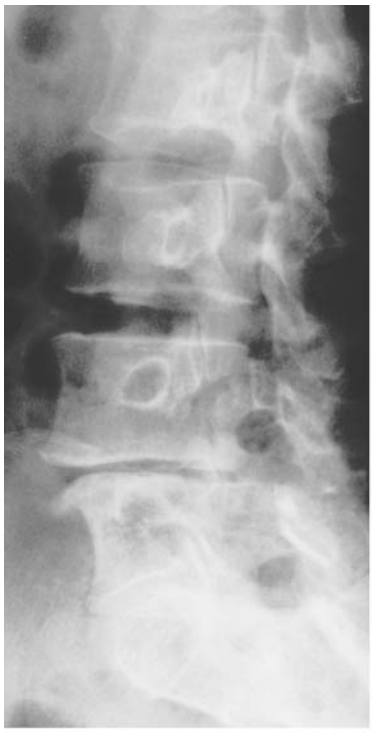

C

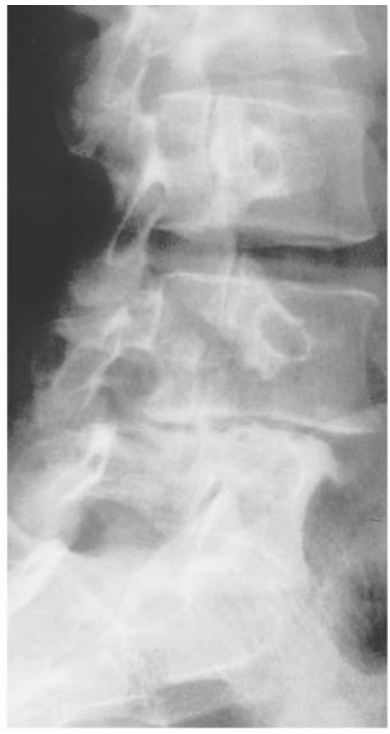

D

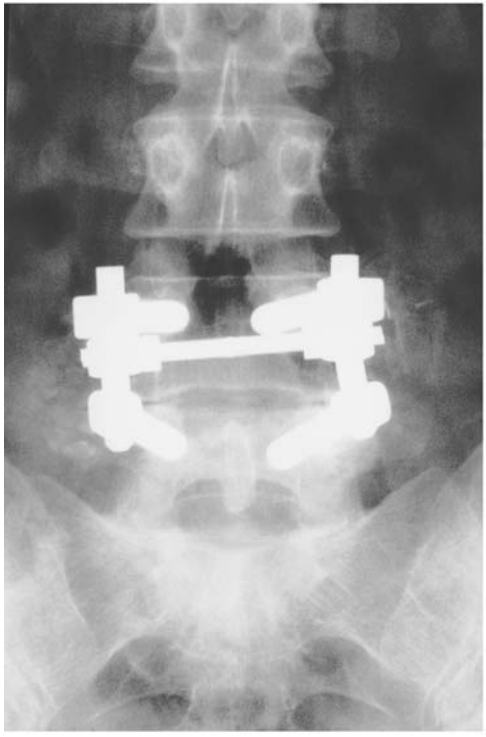

E

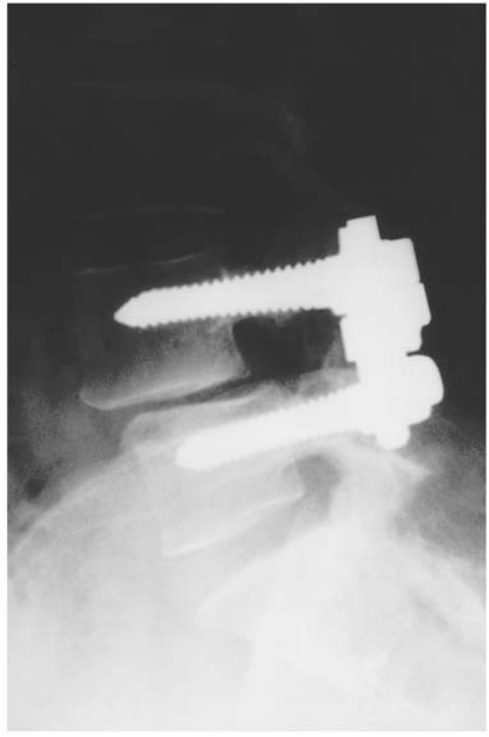

F

Figure 5 Continued.

vances in the field of spinal surgery should be founded not only on evidence but also on health economical analyses (cost-effectiveness, cost-utility, and cost-benefit) [156,157].

The concise literature survey presented in this chapter unfortunately shows that this is not the case. Most of our current knowledge is based on clinical series and is consequently amenable to bias, confounding factors, and error, which may partly explain the great variety of surgical techniques and devices used to treat spine disorders. Although the importance of designing studies capable of providing evidence-based data is increasingly being recognized and encouraged, spinal surgery is still lagging behind [158]. The introduction of new biomaterials and biotechnologies may further amplify the problem if stringent methodological criteria are not adopted to warrant the clinical application of new devices and techniques. The fast pace of technology advances also requires dedicated study designs to be applied in clinical research due to the large number of variants introduced by biomaterial and technique modifications [159]. Even if it may prove demanding, the conduction of tracker studies would represent a sensible compromise between the need for excellence in research and the tumultuous progression of technological innovations. Only when technology advances and the quality of clinical research progress hand in hand may we foresee a turning point in the potential for improving the outcome of spinal fusion.

REFERENCES

1. Katz J. Lumbar spinal fusion: surgical rates, costs and complications. Spine 1995; 20:S78–S83.
2. Cherkin DC, Deyo RA, Loeser JD, et al. An international comparison of back surgery rates. Spine 1994; 19:1201–1206.
3. Volinn E, Mayer J, Diehr P, et al. Small area analysis of surgery for low-back pain. Spine 1992: 575–579.
4. Mélot C. Principles of cost-benefit-analysis. In: Szpalski M, Gunzburg R, Pope MH, eds. Lumbar Segmental Instability. Philadelphia: Lippincott Williams and Wilkins, 1999:259–273.
5. Heckman JD. Excellence through peer review. J Bone Joint Surg 2001; 83-A:1–2.
6. Axhausen W. The osteogenetic phases of regeneration of bone. A historical and experimental study. J Bone Joint Surg 1956; 38-A:593–600.
7. Kaufman HH, Jones E. The principles of bony spinal fusion. Neurosurgery 1989; 24:264–270.
8. Burchardt H. Biology of bone transplantation. Orthop Clin North Am 1987; 18:187–196.
9. Albrektsson T, Johansson C. Osteoinduction, osteoconduction and osseointegration. Eur Spine J 2001; 10:S96–S101.
10. Finkemeier CG. Current concept review. Bone grafting and bone graft substitutes. J Bone Joint Surg 2002; 84-A:454–464.
11. Lieberman JR, Daluiski A, Einhorn TA. The role of growth factors in the repair of bone. Biology and clinical applications. J Bone Joint Surg 2002; 84-A:1032–1044.
12. Boden SD. The biology of posterolateral lumbar spinal fusion. Orthop Clin North Am 1998; 29: 603–619.
13. Boden SD. Overview of the biology of lumbar spine fusion and principles for selecting a bone graft substitute. Spine 2002; 27:S26–S31.
14. Friedlaender GE, Curtin SL, Huo MH. Bone grafts and bone graft substitutes. In: Frymoyer JH, ed. The Adult Spine. Principles and Practice. 2nd ed. Philadelphia: Lippincott-Raven Publishers, 1997:719–732.
15. Zindrick MR, Lorenz MA. Posterior lumbar fusion. Overview of options and internal fixation devices. In: Frymoyer JH, ed. The Adult Spine. Principles and Practice. 2nd edition. Philadelphia: Lippincott-Raven Publishers, 1997:2175–2203.
16. Dell PC, Burchardt H, Glowczewskie FP. A roentgenographic, biomechanical and histological evaluation of vascularized and non-vascularized segmental canine fibular autografts. J Bone Joint Surg 1985; 67-A:105–112.

17. Enneking WF, Burchardt H, Puhl JJ, Plotrowski G. Physical and biological aspects of repair in dog cortical-bone transplant. J Bone Joint Surg 1975; 57-A:237–252.
18. Younger EM, Chapman MW. Morbidity at the bone graft donor site. J Orthop Trauma 1989; 3: 192–195.
19. Seiler JG, Johnson J. Iliac crest autogenous bone grafting: donor site complications. J South Orthop Assoc 2000; 9:91–97.
20. Lind M, Bünger C. Factors stimulating bone formation. Eur Spine J 2001; 10:S102–S109.
21. Marchesi DG. Spinal fusion: bone and bone substitutes. Eur Spine J 2000; 9:372–378.
22. Ogilvie JW. Spinal Biomechanics. In: Lonstein JE, Bradford DS, Winter RB, Ogilvie JW, eds. Moe's Textbook of Scoliosis and Other Spinal Deformities. 3rd edition. Philadelphia: W.B. Saunders Company, 1995:7–22.
23. Ogilvie JW. Orthotics. In: Lonstein JE, Bradford DS, Winter RB, Ogilvie JW, eds. Moe's Textbook of Scoliosis and Other Spinal Deformities. 3rd edition. Philadelphia: W.B. Saunders Company, 1995:95–106.
24. Fidler MW, Plasmans MT. The effect of four types of support on the segmental mobility of the lumbosacral spine. J Bone Joint Surg 1983; 65-A:943–947.
25. Axelsson P, Johnsson R, Strömqvist B. Effect of lumbar orthosis on intervertebral mobility. A roentgen stereophotogrammetric analysis. Spine 1992; 17:678–681.
26. Axelsson P, Johnsson R, Strömqvist. B. Lumbar orthosis with unilateral hip immobilization. Effect on intervertebral mobility determined by roentgen stereophotogrammetric analysis. Spine 1993; 18: 876–879.
27. Petersen BP, Panjabi MM, White AA. A user's guide to lumbar orthoses: theoretical, scientific and clinical rationale. In: Szpalski M, Gunzburg R, Pope MH, eds. Lumbar Segmental Instability. Philadelphia: Lippincott Williams and Wilkins, 1999:275–281.
28. Bradford DS. Master Techniques in Orthopaedic Surgery. The Spine. Philadelphia: Lippincott-Raven Publishers, 1997.
29. An HS, Cotler JM. Spinal Instrumentation. 2nd edition, Lippincott Williams and Wilkins. 1999.
30. Gaines RW. The use of pedicle-screw internal fixation for the operative treatment of spinal disorders. J Bone Joint Surg 2000; 82-A:1458–1476.
31. Vanichkachorn JS, Vaccaro AR, An HS. Transpedicular screw instrumentation. In: An HS, Cotler JM, eds. Spinal Instrumentation. 2nd edition. Philadelphia: Lippincott Williams and Wilkins, 1999: 257–276.
32. Lim TH, An HS. Biomechanics of spinal instrumentation. In: An HS, Cotler JM, eds. Spinal Instrumentation. 2nd edition. Philadelphia: Lippincott Williams and Wilkins, 1999:59–72.
33. Haher TR, Merola AA, Caruso SA, Paskoff R. Implants: Modes of Failure. In: Margulies JY, Aebi M, Farcy JPC, eds. Revision Spine Surgery. 1st edition. St. Louis: Mosby Inc., 1999:114–127.
34. Feodosev VI. La Resistenza dei Materiali. Rome: Editori Riuniti, 2001.
35. Frankel VH, Burstein AH. Orthopaedic Biomechanics. Philadelphia: Lea and Febiger, 1970.
36. McKinley TO, McLain RF, Yerby SA, Sarigul-Klijn N, Smith TS. The effect of pedicle morphometry on pedicle screw loading. Spine 1997; 22:246–252.
37. McKinley TO, McLain RF, Yerby SA, Sharkey NA, Sarigul-Klijn N, Smith TS. Characteristics of pedicle screw loading. Effect of surgical technique on intravertebral and intrapedicular bending moments. Spine 1999; 24:18–25.
38. Youssef JA, McKinley TO, Yerby SA, McLain RF. Characteristics of pedicle screw loading. Effect of sagittal insertion angle on intrapedicular bending moments. Spine 1999; 24:1077–1081.
39. McLain RF, McKinley TO, Yerby SA, Smith TS, Sarigul-Klijn N. The effect of bone quality on pedicle screw loading in axial instability. A synthetic model. Spine 1999; 22:1454–1460.
40. Lonstein JE, Denis F, Perra JH, Pinto MR, Smith MD, Winter RB. Complications associated with pedicle screws. J Bone Joint Surg 1999; 81-A:1519–1528.
41. Weiner BK, Fraser RD. Spine update. Lumbar interbody cages. Spine 1998; 23:634–640.
42. McAfee PC. Interbody fusion cages in reconstructive operations of the spine. J Bone Joint Surg 1999; 81-A:859–880.
43. Steffen T, Tsantrizos A, Fruth I, Aebi M. Cages: design and concepts. Eur Spine J 2000; 9:S89–S94.

44. Schlegel JD, Yuan HA, Fredricksen BE. Anterior interbody fixation devices. In: Frymoyer JH, ed. The Adult Spine. Principles and Practice. 2nd edition. Philadelphia: Lippincott-Raven Publishers, 1997:2157–2174.
45. Simmons JW. Posterior lumbar interbody fusion. In: Frymoyer JH, ed. The Adult Spine. Principles and Practice. 2nd edition. Philadelphia: Lippincott-Raven Publishers, 1997:2225–2252.
46. Humphreys SC, Hodges SD, Patwardhan AG, Eck JC, Murphy RB, Covington LA. Comparison of posterior and transforaminal approaches to lumbar interbody fusion. Spine 2001; 26:567–571.
47. Tsantrizos A, Andreou A, Aebi M, Steffen T. Biomechanical stability of five stand-alone anterior lumbar interbody fusion constructs. Eur Spine J 2000; 9:14–22.
48. Oxland TR, Lund T. Biomechanics of stand-alone cages and cages in combination with posterior fixation: a literature review. Eur Spine J 2000; 9:S95–S101.
49. Hambly MF, Wiltse LL, Raghavan N, Schneiderman G, Koenig C. The transition zone above a lumbosacral fusion. Spine 1998; 23:1785–1792.
50. Wiltse LL, Radecki SE, Biel HM, DiMartino PP, Oas RA, Farjalla G, Ravesspus FA, Wohletz C. Comparative study of the incidence and severity of degenerative change in the transition zone after instrumented versus non-instrumented fusion of the lumbar spine. J Spinal Disord 1999; 12:27–33.
51. Kumar MN, Baklanov A, Chopin D. Correlation between sagittal plane changes and adjacent segment degeneration following lumbar spine fusion. Vol. 10, 2001:314–319.
52. Rohlmann A, Neller S, Bergmann G, Graichen F, Claes L, Wilke H-J. Effect of an internal fixator and a bone graft on intersegmental spinal motion and intradiscal pressure in the adjacent regions. Eur Spine J 2001; 10:301–308.
53. Kostuik JP. Alternatives to spinal fusion. Orthop Clin North Am 1998; 29:701–716.
54. Bombardier C. Outcome assessment in the evaluation of treatment of spinal disorders. Summary and general recommendations. Spine 2000; 24:3100–3103.
55. Sackett DL, Straus SE, Richardson WS, Rosenberg W, Haynes RB. Evidence-Based Medicine. How to Practice and Teach EBM. 2nd edition. London: Churchill Livingstone, 2000.
56. Hilibrand AS, Dina TS. The use of diagnostic imaging to assess spinal arthrodesis. Orthop Clin North Am 1998; 29:591–601.
57. Greenough CG. Cost and ethics of surgery for instability. In: Szpalski M, Gunzburg R, Pope MH, eds. Editors. Lumbar Segmental Instability. Philadelphia: Lippincott Williams and Wilkins, 1999: 275–281.
58. Brown CA, Eismont FJ. Complications in spinal fusion 1998; 29:679–699.
59. Waddell G, Gibson JNA, Grant I. Surgical treatment of lumbar disc prolapse and degenerative lumbar disc disease. In: Nachemson A, Jonsson E, eds. Neck and Back Pain: The Scientific Evidence of Causes, Diagnosis, and Treatment. Philadelphia: Lippincott Williams and Wilkins, 2000:305–325.
60. Kuntz KM, Snider RK, Weinstein JN, Pope MH, Katz JN. Cost-effectiveness of fusion with and without instrumentation for patients with degenerative spondylolisthesis and spinal stenosis. Spine 2000; 25:1132–1139.
61. Nachemson A. Introduction. In: Nachemson A, Jonsson E, eds. Neck and Back Pain: The Scientific Evidence of Causes, Diagnosis, and Treatment. Philadelphia: Lippincott Williams and Wilkins, 2000:1–12.
62. Bhandari M, Morrow F, Kulkarni AV, Tornetta P. Meta-analysis in orthopaedic surgery. A systematic review of their methodologies. J Bone Joint Surg 2001; 83-A:15–24.
63. Egger M, Davey Smith G, Phillips AN. Meta-analysis: principles and procedures. BMJ 1997; 315: 1533–1537.
64. Egger M, Davey Smith G. Meta-analysis: potentials and promise. BMJ 1997; 315:1371–1374.
65. Davey Smith G, Egger M. Meta-analysis: unresolved issues and future developments. BMJ 1998; 316:221–225.
66. McCulloch P, Taylor I, Sasako M, Lovett B, Griffin M. Randomised trials in surgery: problems and possible solutions. BMJ 2002; 324:1448–1451.
67. Gibson JNA, Grant I, Waddell G. The Cochrane review of surgery for lumbar disc prolapse and degenerative lumbar spine. Spine 1999; 24:1820–1832.
68. Fritzell P, Hagg O, Wessberg P, Nordwall A. and the Swedish Lumbar Spine Study Group, Spine. Chronic low back pain and fusion: a comparison of three surgical techniques. Spine 27:1131–1141.

69. Lemons JE. Ceramics. In: Callaghan JJ, Rosenberg AG, Rubash HE, eds. The Adult Hip. Philadelphia: Lippincott-Raven Publishers, 1998:97–104.
70. Eastlund DT. Bone transplantation and bone banking. In: Lonstein JE, Bradford DS, Winter RB, Ogilvie JW, eds. Moe's Textbook of Scoliosis and Other Spinal Deformities. 3rd edition. Philadelphia: W.B. Saunders Company, 1995:581–595.
71. Berven S, Tay BKB, Kleinstueck FS, Bradford DS. Clinical applications of bone graft substitutes in spine surgery: consideration of mineralized and demineralized preparations and growth factor supplementation. Eur Spine J 2001; 10:S169–S177.
72. Hamer AJ, Strachan JR, Black MM, Ibbotson CJ, Stockley I, Elson RA. Biomechanical properties of cortical allograft bone using a new method of bone strength measurement: a comparison of fresh, fresh-frozen and irradiated bone. J Bone Joint Surg 1996; 78-B:363–368.
73. Sandhu HS, Grewal HS, Parvataneni H. Bone grafting for spine fusion. Orthop Clin North Am 1999; 30:685–698.
74. Goldberg VM, Stevenson S. Natural history of autografts and allografts. Clin Orthop 1987; 225: 7–16.
75. Heiple KG, Chase SW, Herndon CH. A comparative study of the healing process following different types of bone transplantation. J Bone Joint Surg 1963; 45-A:1593–1616.
76. Enneking WF, Mindell ER. Observations on massive retrieved human allografts. J Bone Joint Surg 1991; 73-A:1123–1142.
77. Bauer TW, Muschler GF. Bone graft materials. An overview of the basic science. Clin Orthop 2000; 371:10–27.
78. Stevenson S, Horowitz M. The response to bone allografts. J Bone Joint Surg 1992; 74-A:939–949.
79. Butterman GR, Glazer PA, Bradfor DS. The use of bone allografts in the spine. Clin Orthop 1996; 324:74–85.
80. Lofgren H, Johansson V, Olsson T, Ryd L, Levander B. Rigid fusion after Cloward operation for cervical disc disease using autograft, allograft, or xenograft: a randomized study with radiostereometric and clinical follow-up assessment. Spine 2000; 25:1908–1916.
81. AATB information alert. McLean, VA: American Association of Tissue Banks, 1993.
82. Prewett AB, Moyer MP, O'Leary RK, Mellonig JT. Decalcification inactivates HIV in spiked and infected bone. Trans Orthop Res Soc 1992; 17:436.
83. Lindholm TS, Urist MR. A quantitative analysis of new bone formation by induction in compositive grafts of bone marrow and bone matrix. Clin Orthop 1980; 150:288–300.
84. Greer E, Hinton C, Triffitt JT. The effect of decalcified bone matrix on the osteogenic potential of bone marrow. Clin Orthop 1986; 205:292–298.
85. An HS, Simpson JM, Glover JM, Stephany J. Comparison between allograft plus demineralized bone matrix versus autograft in anterior cervical fusion. A prospective multicenter study. Spine 1995; 20:2211–2216.
86. Schwartz Z, Mellonig JT, Carnes DL, de la Fontaine J, Cochran DL, Dean DD, Boyan BD. Ability of commercial demineralized freeze-dried bone allograft to induce new bone formation. J Periodontol 1996; 67:918–926.
87. Bohner M. Physical and chemical aspects of calcium phosphates used in spinal surgery. Eur Spine J 2001; 10:S114–S121.
88. Seeherman H, Wozney J, Li R. Bone morphogenetic proteins delivery systems. Spine 2002; 27: S16–S23.
89. Jarcho M. Calcium phosphate ceramics as hard tissue prosthetics. Clin Orthop 1981; 157:259–278.
90. Eggli PS, Muller W, Schenk RK. Porous hydroxyapatite and tricalcium phosphate cylinders with two different pore size range implanted in the cancellous bone of rabbits. Clin Orthop 1988; 232: 127–138.
91. Roy DM, Linnehan SK. Hydroxyapatite formed from coral skeletal carbonate by hydrothermal exchange. Nature 1974; 247:220–222.
92. Spivak JM, Hasharoni A. Use of hydroxyapatite in spine surgery. Eur Spine J 2001; 10:S197–S204.
93. Driessens FCM, DeMayer EAP, Fernandez E, Boltong MG, Berger G, Verbeeck RMH, Ginebra MP, Planell JA. Amorphous calcium phosphate cements and their transformation into calcium deficient hydroxyapatite. Bioceramics 1996; 9:231–234.

94. Miyamoto Y, Ishikawa K, Fukao H, Sawada M, Nagayama M, Kon M, Asaoka K. In vivo setting behavior of fast-setting calcium phosphate cement. Biomaterials 1995; 16:855–860.
95. Ikenaga M, Hardouin P, Lemaitre J, Andrjanatovo H, Flautre B. Biomechanical characterization of a biodegradable calcium phosphate hydraulic cement: a comparison with porous biphasic calcium phosphate ceramics. J Biomed Mater Res 1998; 40:139–144.
96. Écrin J, Takahashi S, Gouin F, Passuti N. A synthetic porous ceramic as a bone graft substitute in the surgical management of scoliosis. A prospective randomized study. Spine 2000; 25:563–569.
97. Ransford AO, Morley T, Edgar MA, Webb P, Passuti N, Chopin D, Morin C, Michel F, Garin C, Pries D. Synthetic porous ceramic compared with autograft in scoliosis surgery. A prospective, randomized study of 341 patients. J Bone Joint Surg 1998; 80-B:13–18.
98. Muschik M, Ludwig R, Halbhubner S, Bursche K, Stoll T. β-Tricalcium phosphate as a bone substitute for dorsal spinal fusion in adolescent idiopathic scoliosis: preliminary results of a prospective clinical study. Eur Spine J 2001; 10:S178–S184.
99. Frost HM. The biology of fracture healing. An overview for clinicians, part I. Clin Orthop 1989; 248:283–293.
100. Frost HM. The biology of fracture healing. An overview for clinicians, part II. Clin Orthop 1989; 248:283–293.
101. Lieberman JR, Einhorn TA. Current concept review. The role of growth factors in the repair of bone. Biology and clinical applications. J Bone Joint Surg 2002; 84-A:1032–1044.
102. Joyce ME, Jingishi S, Bolander ME. Transforming growth factor-beta in the regulation of fracture repair. Orthop Clin North Am 1993; 21:199–209.
103. Sumner DR, Turner TM, Purchio AF, Gombotz WR, Urban RM, Galante JO. Enhancement of bone ingrowth by transforming growth factor-beta. J Bone Joint Surg 1995; 77-A:1135–1147.
104. Robey PG, Young MF, Flanders KC, Roche NS, Kondaiah P, Reddi AH, Termine JD, Spora MB, Roberts AB. Osteoblasts synthesize and respond to transforming growth factor-beta (TGF-beta) in vitro. J Cell Biol 1987; 105:457–463.
105. Heldin CH, Miyazono T, Diijke P. TGF-beta signalling from cell membrane to nucleus through SMAD proteins. Nature 390:465–471.
106. Lind M. Growth factors stimulation of bone healing. Effects on osteoblasts, osteotomies and implant fixation. Acta Orthop Scand Suppl 1998; 283:2–37.
107. Dionne CA, Jaye M, Schlesinger J. Structural diversity and binding of FGF receptors. Ann NY Acad Sci 1991; 638:161–166.
108. Jingushi S, Heydemann A, Kana SK, Macey LR, Bolander ME. Acidic fibroblast growth factor (aFGF) injection stimulates cartilage enlargement and inhibits cartilage gene expression in rat fracture healing. J Orthop Res 1990; 8:364–371.
109. Canalis E, Centrella M, McCarthy T. Effects of basic fibroblast growth factor on bone formation in vitro. J Clin Invest 1988; 81:1572–1577.
110. Andrew JG, Hoyland J, Freemont AJ, Marsh D. Insulin-like growth factor gene expression in human fracture callus. Calcif Tissue Int 1993; 53:97–102.
111. Trippel SB. Potential role of insulin-like growth factors in fracture healing. Clin Orthop 1998; 355: S301–S313.
112. Andrew JG, Hoyland JA, Freemont AJ, Marsh DR. Platelet-derived growth factor expression in normally healing human fractures. Bone 1995; 16:455–460.
113. Canalis E, McCarthy TL, Centrella M. Effects of platelet-derived growth factor on bone formation in vitro. J Cell Physiolg 1989; 140:530–537.
114. Helm G, Anderson DG, Andersson GBJ, Boden SD, Damien C, Ebara S, Lane JM, McKay B, Sandhu HS, Seeherman H, Wozney J. Summary statement: bone morphogenetic proteins. Basic science. Spine 2002; 27:S9.
115. Wozney JM. Overview of bone morphogenetic proteins. Spine 2002; 27:S2–S8.
116. Lyons KM, Jones CM, Hogan BLM. The DVR gene family in embryonic development. Trends Genet 1991; 7:408–412.
117. Hogan BLM. Bone morphogenetic proteins: multifunctional regulators of vertebrate development. Genes Dev 1996; 10:1580–1594.

118. Diijke P, Miyazono K, Heldin CH. Signaling via hetero-oligomeric complexes of type I and type II serine/threonine kinase receptors. Curr Opin Cell Biol 1996; 8:139–145.
119. Ebara S, Nakayama K. Mechanism for the action of bone morphogenetic proteins and regulation of their activity. 2002; 27:S10–S15.
120. Poynton AR, Lane JM. Safety profile for the clinical use of bone morphogenetic proteins in the spine. Spine 2002; 27:S40–S48.
121. Damien CJ, Grob D, Boden SD, Benedict JJ. Purified bovine BMP extract and collagen for spine arthrodesis. Preclinical safety and efficacy. Spine 2002; 27:S50–S58.
122. Boden SD, Schimandle JH, Hutton WC. Lumbar intertrasverse process spinal arthrodesis with use of a bovine bone-derived osteoinductive protein. J Bone Joint Surg 1995; 77-A:1404–1417.
123. Israel DI, Nove J, Kerns KM, et al. Heterodimeric bone morphogenetic proteins show enhanced activity in vitro and in vivo. Growth Factors 1996; 13:291–300.
124. McKay B, Sandhu HS. Use of recombinant human bone morphogenetic protein-2 in spinal fusion applications. Spine 2002; 27:S66–S85.
125. Boden SD, Zdeblick TA, Sandhu HS, Heim SE. The use of rhBMP-2 in interbody fusion cages. Definitive evidence of osteoinduction in humans: a preliminary report. Spine 2000; 25:376–381.
126. Gornet MF, Burkus K, Dickman CA. rhBMP-2 with tapered cages: a prospective randomized lumbar fusion study. Seattle, WA: North American Spine Society, 2001.
127. Alexander JT, Branch CL, Haid RW, Jr, et al. An analysis of the use of rhBMP-2 in PLIF constructs: clinical and radiographic outcomes. Presented at the 18th Annual Meeting of the American Association of Neurological Surgeons and Congress of Neurological Surgeons Section on Disorders of the Spine and Peripheral Nerves. Orlando, FL, February 27 to March 2, 2002:26.
128. Baskin DS, Ryan PG, Westmark RM, et al. ACDFP with Cornerstone-SR (allograft and plate: rhBMP-2 vs. autograft). Presented at the 18th Annual Meeting of the American Association of Neurological Surgeons and Congress of Neurological Surgeons Section on Disorders of the Spine and Peripheral Nerves. Orlando, FL, February 27 to March 2, 2002:26.
129. Burkus JK, Transfeldt E, Kitchel SH, et al. A prospective randomized study assessing the clinical and radiographic outcomes of patients treated with rhBMP-2 and threaded cortical bone dowels in the lumbar spine. New Orleans. LA: NASS, 2000:114.
130. Luque E. Latest clinical results using demineralized bone materials and rhBMP-2: the Mexican experience. In: Total Spine: Advanced Concepts and Constructs. Cancun, Mexico, 2000.
131. Zdeblick TA, Heim SE, Kleeman TJ, et al. Laparoscopic approach with tapered metal cages: rhBMP-2 vs. autograft. Seattle, WA: North American Spine Society, 2001:200.
132. Vaccaro AR, Anderson G, Toth C. Recombinant human osteogenic protein-1 (bone morphogenetic protein-7) as an osteoinductive agent in spinal fusion. Spine 2002; 27:S59–S65.
133. Patel TC, Erulkar JS, Grauer JS. OP-1 overcomes the inhibitory effects of nicotine on lumbar fusion. New Orleans. LA: North American Spine Society, 2000.
134. Patel TC, Vaccaro AR, Truumees E, et al. A safety and efficacy study of Op-1 (rhBMP-7) as an adjunct to posterolateral lumbar fusion. Presented at the North American Spine Society Meeting. Seattle, WA: NASS, 2001.
135. Patel TC, McCulloch JA, Vaccaro AR, et al. A pilot safety and efficacy study of OP-1 (rhBMP-7) in posterolateral lumbar fusion as a replacement for iliac crest autograft. Presented at the North American Spine Society 16th Annual Meeting. Seattle, WA: NASS, 2001.
136. Seeherman H, Wozney J, Li R. Bone morphogenetic protein delivery systems. Spine 2002; 27: S16–S23.
137. Hannallah D, Peterson B, Lieberman JR, Fu FH, Huard J. Gene therapy in orthopaedic surgery. J Bone Joint Surg 2002; 84-A:1046–1061.
138. Alden TD, Varady P, Kallmes DF, Jane JA, Helm GA. Bone morphogenetic protein gene therapy. Spine 2002; 27:S87–S93.
139. Kay MA, Glorioso JC, Naldini L. Viral vectors for gene therapy: the art of turning infectious agents into vehicles of therapeutics. Nat Med 2001; 7:33–40.
140. Crystal RG. Transfer of genes to humans: early lessons and obstacles to success. Science 1995; 270:404–410.

141. http://www.nih.gov/news/stemcell/primer.htm, 2003.
142. Bianco P, Riminucci M, Gronthos S, Robey PG. Bone marrow stem cells: nature, biology and potential applications. Stem Cells 2001; 19:180–192.
143. Aubin JE. Bone stem cells. J Cell Biochem Suppl 1998; 30/31:73–82.
144. Caterson EJ, Nesti LJ, Albert T, Danielson K, Tuan R. Application of mesenchymal stem cells in the regeneration of musculoskeletal tissues. http://www.medscape.com/viewarticle/408101, 2001.
145. Helm GA, Dayoub H, Jane JA. Bone graft substitutes for the promotion of spinal arthrodesis. http://www.medscape.com/viewarticle/405701, 2001.
146. Hanley EN, David SM. Who should be fused? Lumbar spine. In: Frymoyer JH, ed. The Adult Spine. Principles and Practice. 2nd edition. Philadelphia: Lippincott-Raven Publishers, 1997:2157–2174.
147. Fritzell P, Hagg O, Wessberg P, et al. Volvo award winner in clinical study. Lumbar fusion versus non-surgical treatment for chronic low back pain: a multicenter randomized control trial from The Swedish Lumbar Spine Study Group. Spine 2001; 26:2521–2536.
148. White AA, III, Bernhardt M, Panjabi M. Clinical biomechanics and lumbar spine instability. In: Szpalski M, Gunzburg R, Pope MH, eds. Lumbar Segmental Instability. Philadelphia: Lippincott Williams and Wilkins, 1999:275–281.
149. Krauss WE, McCormick PC. Biomechanical and clinical evaluation of segmental instability. In: Menezes AH, Sonntag VKH, eds. Principles of Spinal Surgery. McGraw-Hill, 1996:1029–1038.
150. Frymoyer JH, ed. The Adult Spine. Principles and Practice. 2nd edition. Philadelphia: Lippincott-Raven Publishers, 1997.
151. Lonstein JE. Bradford DS, Winter RB, Ogilvie JW, eds. Moe's Textbook of Scoliosis and Other Spinal Deformities. 3rd edition. Philadelphia: W.B. Saunders Company, 1995:581–595.
152. Krismer M. Indications for lumbar spinal fusion. In: Thorngren K-G, Soucacos PN, Horan F, Scott J, eds. European Instructional Course Lectures. Vol. 5. London: The British Editorial Society of Bone and Joint Surgery, 2001:124–137.
153. Herron LD, trippi AC. L4-L5 degenerative spondylolisthesis. The results of decompressive laminectomy without fusion. Spine 1989; 14:534–538.
154. Herkowitz HN, Kurz LT. Degenerative lumbar spondylolisthesis with spinal stenosis. J Bone Joint Surg 1991; 73-A:802–809.
155. Grobler LJ, Wiltse LL. Classification, and non-operative and operative treatment of spondylolisthesis. In: Frymoyer JH, ed. The Adult Spine. Principles and Practice. 2nd edition. Philadelphia: Lippincott-Raven Publishers, 1997:2157–2174.
156. Nachemson A. Scientific diagnosis or unproved label for back pain patients? In: Szpalski M, Gunzburg R, Pope MH, eds. Lumbar Segmental Instability. Philadelphia: Lippincott Williams and Wilkins, 1999:297–301.
156a. Mélot CA. Economic evaluation in health care. In: Gunzburg R, Szpalski M, eds. Lumbar Spinal Stenosis. Philadelphia: Lippincott Williams and Wilkins, 2000:357–365.
157. Manadiakis N, Gray A. Review article. Health economics and orthopaedics. J Bone Joint Surg 2000; 82-B:2–8.
158. Nachemson A. Scientific diagnosis or unproved label for back pain patients? In: Szpalski M, Gunzburg R, Pope MH, eds. Lumbar Segmental Instability. Philadelphia: Lippincott Williams and Wilkins, 1999:297–301.
159. Lilford RJ, Braunholtz DA, Greenhalgh R, Edwards SJL. Trials and fast changing technologies: the case for tracker studies. BMJ 2001; 320:43–46.

36

Replacement of Autograft with BMP for Spinal Arthrodesis: Future Perspectives Following Recent Research

Michael N. Magin
EuromedClinic
Fürth, Germany

I. INTRODUCTION

Increasing numbers of spinal fusions for various reasons of vertebral instability are being performed worldwide. Nearly 1 million procedures are performed each year [1]. Approximately one third of these procedures involve bone grafting. Sandhu [2] has estimated that in 2001, approximately 360,000 patients in the United States alone underwent some type of spinal arthrodesis. A similar enthusiasm for these techniques is being observed in developed countries worldwide. Among the indications are low back pain, postdiscectomy syndrome, spondylosis and spondylolisthesis, rheumatoid instabilities, unstable fractures, and other lesions, each contributing different challenges in improving solid permanent fixation of the affected motor segment.

Depending on the operative techniques applied, loss of correction, hardware failures, and development of pseudarthrosis are reported [3–10]. Furthermore, risk factors like smoking and metabolic alterations, e.g, diabetes, might increase the rate of complications in spinal surgery [11–18]. The gold standard in spinal fusion is the application of autogenous bone graft [7,19–21] from various sites (iliac crest, rib, fibula, locally from decompression procedures) with or without primary load-bearing capacity [3,6,22]. Ventral [23,24] or dorsal metal implants [25–29], including transpedicular instrumentation [30–32], screw fixation, and the use of various cages [33], are normally required to achieve primary stability and facilitate bone healing and graft incorporation [18,29,31,34–36].

Harvesting procedure morbidity [20,36–43], inconsistent bone quality [5–7], and physical and resource burdens of combined ventral and dorsal approaches [5,23,34] strongly motivate the search for alternative vertebral fusion protocols. Several types of material, including allogenic bone, tricalcium phosphate, different preparations of hydroxyapatite, and polymethyl methacrylate (PMMA), have been applied both in animal studies and in clinical settings [29,44–46].

In recent years, much research has been focused on bone morphogenetic proteins (BMPs) and their ability to enhance bone healing. Urist and his pioneering research have introduced a new era of understanding bone formation and, consecutively, osseous healing [47]. Elution of proteins from animal cortical bone by digestion of the demineralized bone matrix led to the understanding of a whole family of potent transforming growth factors belonging to the TGF-β superfamily [48] They were found not to be species specific; i.e., bovine-derived proteins

were able to induce bone formation in dogs, rabbits, and monkeys, and BMP extracted from human tissues induced new bone in sheep or mice [49].

The sole criterion for BMP classification is the ability to induce ectopic bone formation in a standard in vivo assay system [50]. So far nine proteins have been identified that meet this requirement. Nevertheless, research revealed that BMPs have a variety of signaling and differentiating properties even in extraskeletal tissues. To some extent their role in bioresearch nowadays is reminiscent of that of the glucocorticoids five decades ago [51].

A number of extraction schemes have been developed, but all are complex and hard to handle. Small extractable quantities (< 1 mg/100 kg of cortical bone) and lack of purity resulting in two problems—inconsistent reproduction of data and convection of blood-transmissible infections—reinforced the search for new sources. They were found with the application of recombinant DNA technology in the manufacturing of BMPs in the late 1980s [49]. Quasi-unlimited amounts of material generated a cascade of both experimental studies and clinical trials. Promising data were reported from fracture models, skull repair [52], and even restoration of critical size defects in long bones [53–56], as well as in spinal arthrodesis [57–65] in a variety of species like rats, rabbits, goats, dogs, and primates [66]. Early clinical trials have shown encouraging results in selected cases [2,54,67–70]. The current study seeks to determine whether the fusion rate achieved with BMP differs from the fusion rate achieved with autogenic grafting.

II. METHODS

The current study involved 18 adult female sheep ≤ 5 years of age with an average weight of 70–80 kg. They underwent a one-level lumbar spinal fusion. A dorsal median approach to the lower lumbar spine, with transsection of the skin followed by a bilateral fascia incision, was carried out. The back muscles were moved subperiosteally, and after exposure of the small vertebral joints of L4 and L5 and protection of the nerve root, the left transverse process of L5 was osteotomized, close to the vertebral body. Subsequently, while carefully protecting soft tissues, the intervertebral disc was removed and the adjacent vertebral endplates decorticated. Thereby, a defect of 5 mm height and two thirds of the diameter of the vertebral body was created, always ensuring protection of the spinal cord (Fig. 1).

After applying a mono-segmental transpedicular internal fixator (Fig. 2), either autograft or BMP was administered into the created cavity under fluoroscopic control. After suturing the wound and postoperative biplanar conventional control x-ray (Fig. 3), the animals were placed in individual boxes.

The cancellous chips used in the interbody fusion of the first group were harvested from the left dorsal iliac crest, via a separate approach, under the same anesthesia. The other group was administered 2.5 mg of rhOP-1 (Stryker Biotech, Hopkinton, MA) on 1 g of a bovine type-1 collagen carrier, diluted in 3 mL of 0.9% NaCl solution. Containment of the applied materials was ensured by preservation of adjacent soft tissue. Spinal canal intrusion was prevented by preserving the dorsal parts of the disc and longitudinal ligaments.

Fluorochrome sequential staining was performed to obtain information on the dynamics of osteoneogenesis. Xylenol orange, calcein green, and oxytretacycline were given during the first 3 months, starting with the first stain 4 weeks postoperatively (for details see Ref. 63). Six months after surgery the animals were sacrificed by injection of pentobarbital.

In addition to frequent clinical and laboratory checks during the healing process, postoperative monitoring included the following examinations:

1. Conventional biplanar x-ray examination every 4 weeks
2. CT imaging of the lumbar spine at the end of the trial

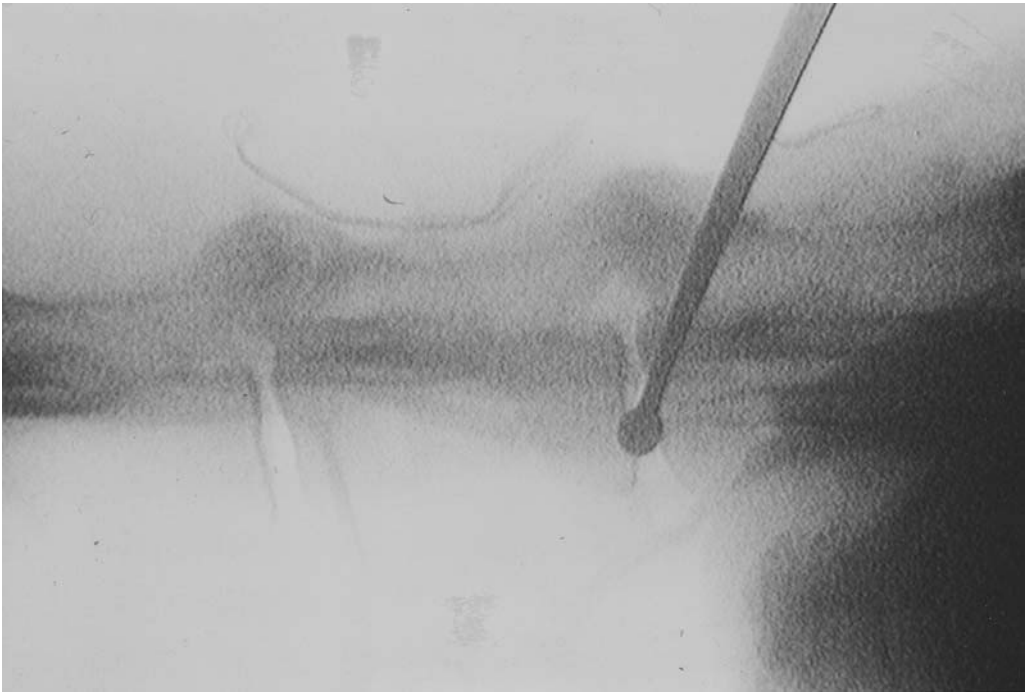

Figure 1 Creation of a defect between L4 and L5 under fluoroscopic control.

3. Nondestructive biomechanical testing in a spine-testing apparatus (e.g., Ref. 63)
4. Histological examination of nondecalcified saw cuts of 50 μm layer thickness after Giemsa staining

III. RESULTS

A. Histological Analysis

Spinal arthrodesis was performed with autograft in eight sheep and in a further 10 animals with BMP-7. In the autograft group (Fig. 4) bony bridging had developed, containing single fibrous areas and remaining islands of intervertebral cartilage. The bone tissue was densely structured. The more remote from the cancellous host bone, the more the graft appeared to be regular in structure. Extensive fluorochrome deposits in the osteosclerotic area were observed.

In the BMP group (Fig. 5), the intervertebral area was completely filled with sclerosed bone tissue. The proportion of newly formed bone tissue reached over 95%. The newly built trabeculae was almost cortex-like in structure, and a periosteal bridge over the fused vertebral bodies also appeared. (Fig. 6)

In polarized light (Fig. 7), a lamellar bone structure and osteons were observed, which showed central capillaries, as in the bony cortex. The central sections revealed newly formed cancellous bone, which consisted of broad trabecular structures with extended intertrabecular networks. Following Wolff's law, the trabeculae ran parallel like those of the original vertebral body in order to fulfill load-bearing requirements.

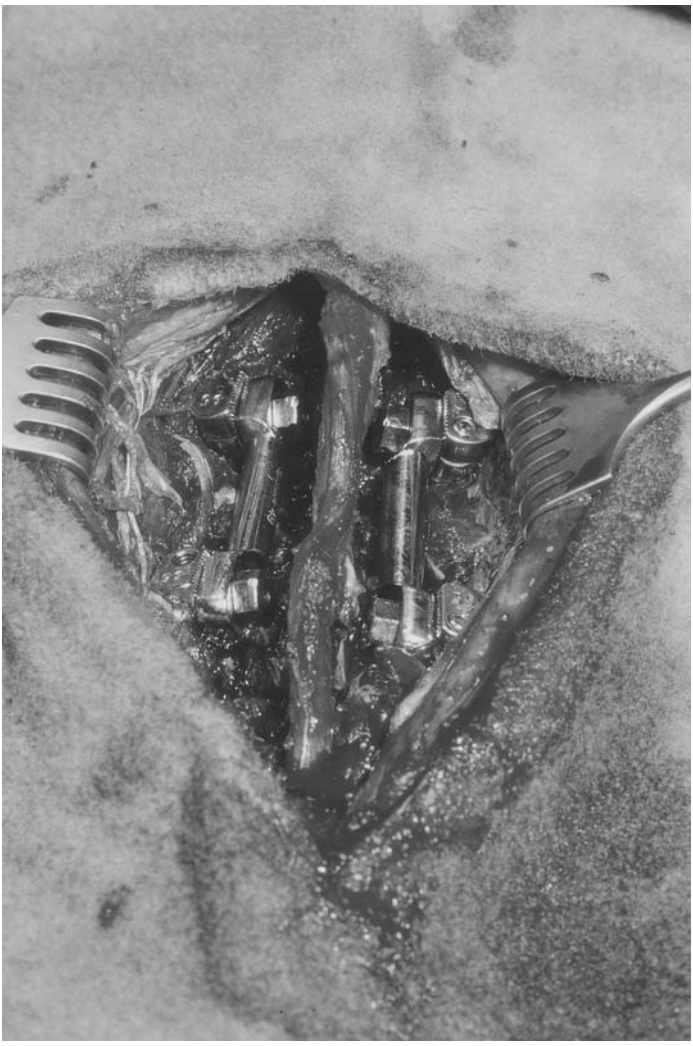

Figure 2 Operation situs after implantation of a monosegmental internal fixator. Preserved spinal process with dorsal longitudinal ligament in the median line.

Disc cartilage fragments were occasionally seen, completely integrated into the osseous structure at the border of the artificial defect. Residues of remaining endplates with areas of heavily mineralized bone matrix were noticed in some areas. The adjacent parts were fully incorporated into the osseous structure. Periosteally, there was visible new bone formation bridging the defect.

In the outer areas of the defect, little subperiosteal bone formation was observed, which slightly exceeded the original size of the vertebra. Periosteum covered the new bone, and no ectopic ossification in adjacent soft tissues, such as fat or striated muscle, was seen in any of the preparations.

UV light revealed the densest arrangement of fluorochrome deposits. Two preparations showed incomplete bone bridging, and there was evidence of some tiny remnants of the intervertebral disc and conversion to granulation tissue.

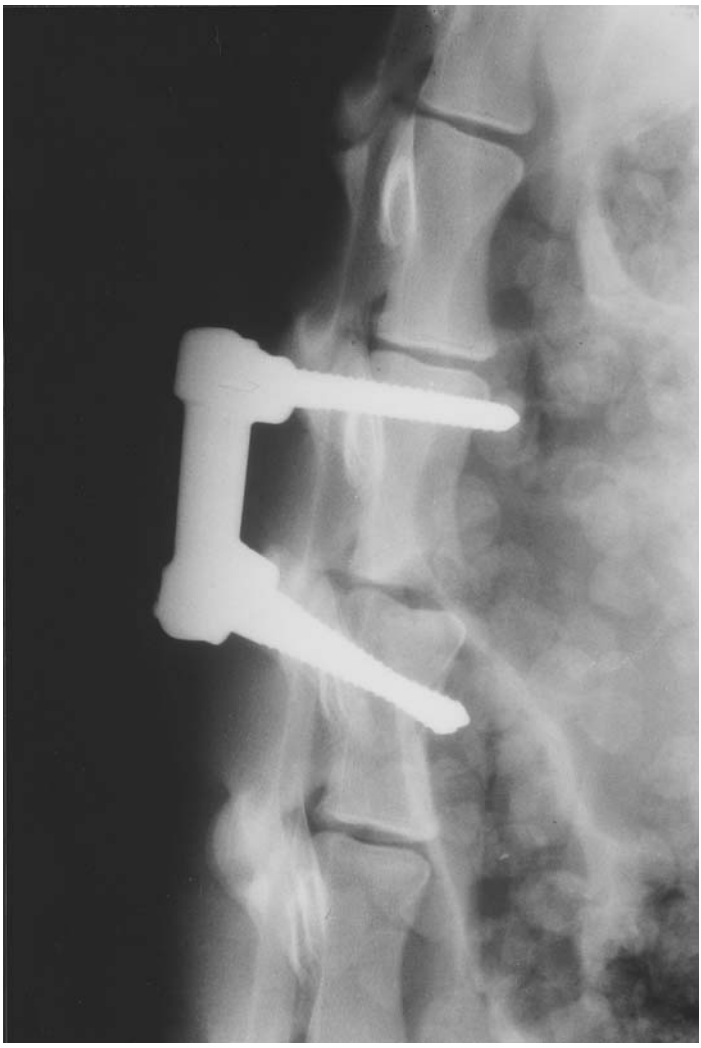

Figure 3 Lateral radiographic view of a sheep lumbar spine. Correct placement of the instrumentation. The anterior defect of the intervertebral space of L4 to L5 is filled with the radiolucent BMP-7 device.

B. Radiographic Analysis

Plain x-ray evaluation proved that all of the animals, when treated with autograft, showed significant bone remodeling after 6 months leading to good bony fusion (Fig. 8). The animals in the BMP group, however, consistently revealed complete bone healing after just 4 months, with good or excellent bone remodeling throughout the defect. Computed tomography (CT) evaluation of the two trial groups was based on a single postoperative assessment on the isolated spinal preparation. One animal in the autograft group had a complete bony fusion (Fig. 9), and a further seven showed a good to moderate result. The size of the bony defect in the vertebral bodies, after removal of the pedicular screws, did not indicate any sign of implant loosening. There were no signs of osteolysis or excess of bone formation.

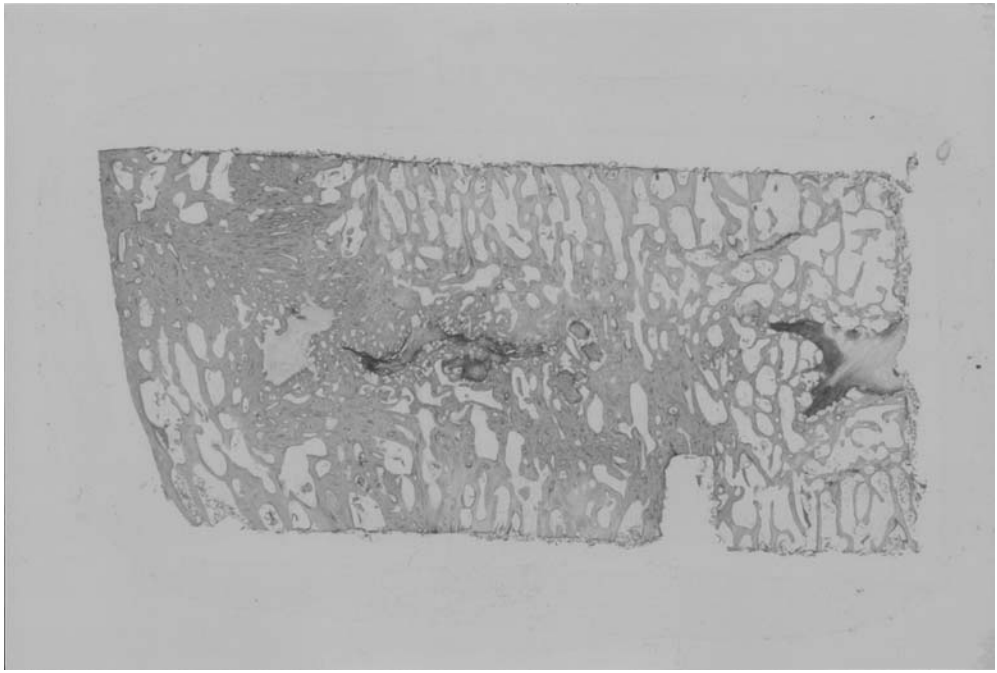

Figure 4 Midsagittal histological section of the fusion site. Endplate-to-endplate fusion after administration of autograft. Islands of cartilage and posterior remnants of the disc can be discerned. Anteriorly, at the left side of the image, some external bridging (see Figs. 8, 9) has occurred.

In 8 of 10 experimental animals treated with BMP (Fig. 10) CT scans showed that the defect had been bridged and filled by new bone. There was no evidence of implant loosening, hyperosteogeny, or ectopic ossification. In one animal, homogeneous bone formation did not occur although partial bridging was seen.

C. Biomechanical Analysis

The vertebral preparations were biomechanically, nondestructively tested for the range of motion (ROM) of the fused segment L4/5 and the neighboring nonfused segments L3/4 and L5/6 (Fig. 11). They were then examined to calculate the stiffness (Nm/°) of the individual vertebral motor segment in flexion and extension, lateral bending, and rotation. There was comparatively little movement in the fused versus the nonfused segments in all groups, resulting in higher stiffness values. In all six degrees of freedom, the autograft and the BMP samples did not differ significantly. The Kruskal-Wallis statistical analysis of stiffness of the nonfused segments did not result in any considerable differences between the test groups.

IV. DISCUSSION

Bone morphogenetic proteins are obviously capable of eliciting bone formation and lead to satisfactory results in arthrodesis of the lumbar spine in sheep [2,46,63]. The results show that the use of autograft prompts satisfactory osseous bridging [71], whereas applying BMP alone

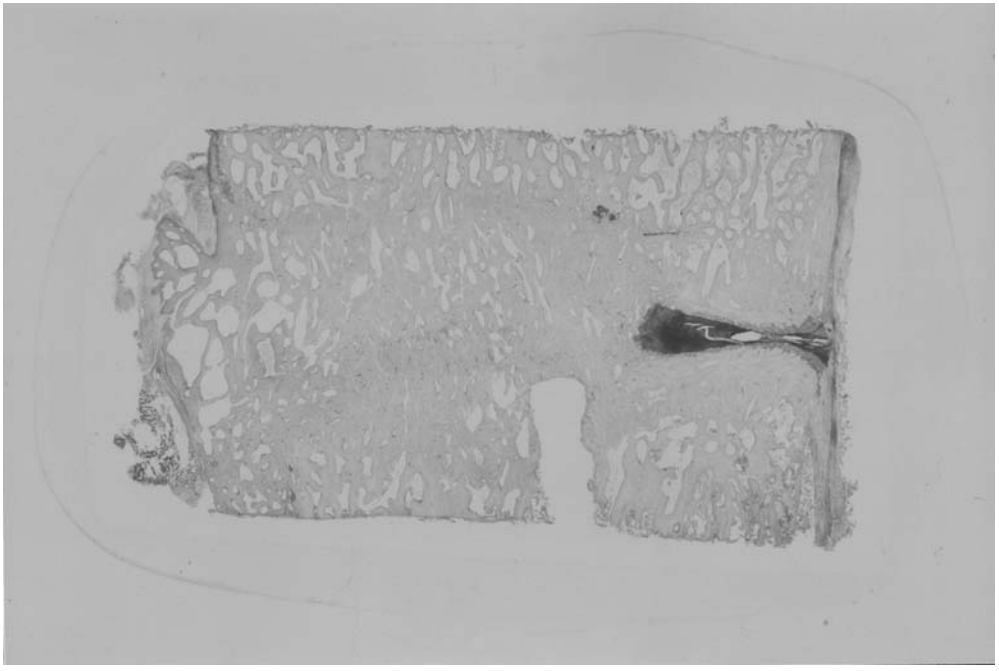

Figure 5 Same view as in Fig. 4 after fusion with BMP-7. Fusion appears to be very homogeneous.

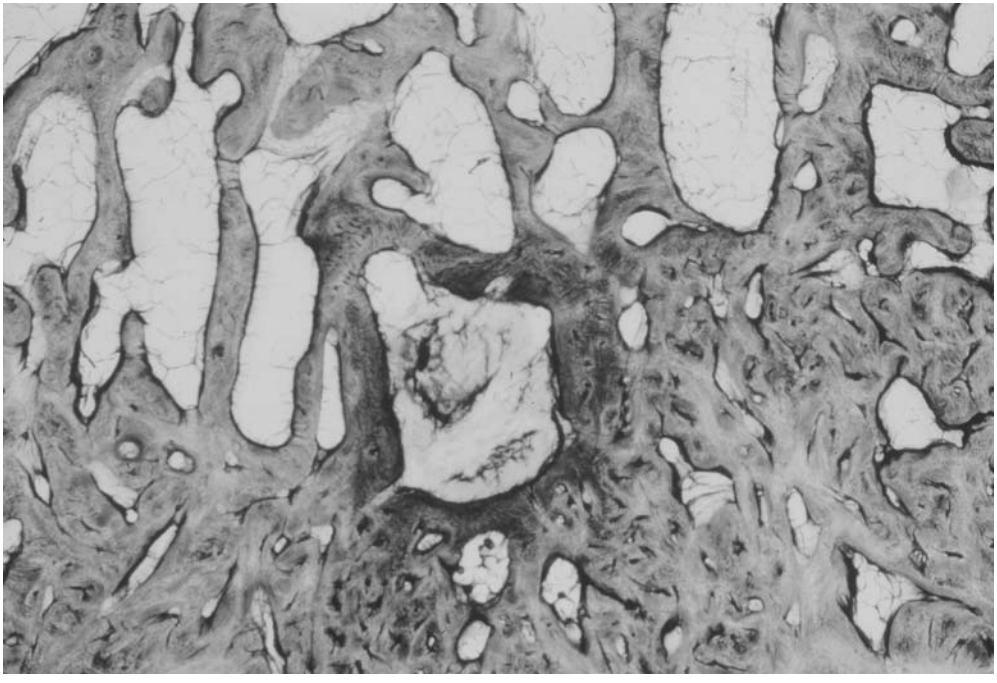

Figure 6 Intervertebral fusion with BMP-7. With higher magnification (50×) a remarkable transition from normal trabecular bone to newly formed bone tissue of a cortex-like high density can be noticed.

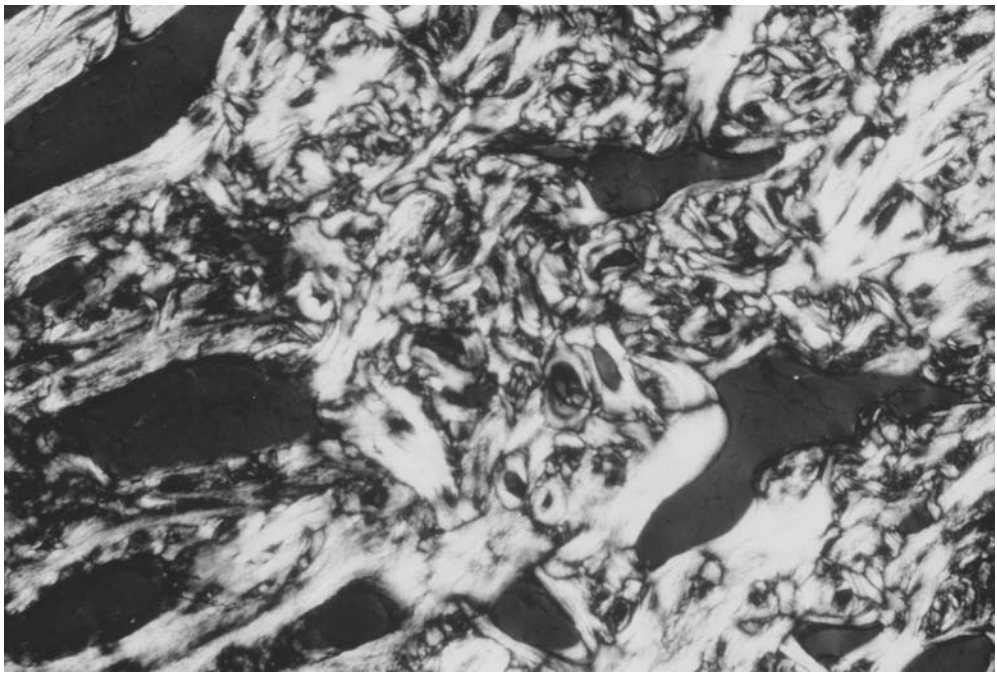

Figure 7 A similar view to Fig. 6 in polarized light reveals the formation of osteons as well as trabecular orientation.

with a bovine collagen carrier always resulted in a formation of remarkably dense bone, characterized by homogeneous, cortex-like structures with development of osteones [63,71].

The results of the study prove a reliable and reproducible lumbar spinal arthrodesis achieved by the mere BMP application into the intervertebral space, secured by a monosegmental instrumentation through a single dorsal approach [3,8,25–28,30,32,46]. There have been spinal fusion experiments before, but in smaller animals and nonhuman primates [59,60,62,64,72]. Others, in fact, have been performed in larger animals, but cages were used to achieve primary stability and containment of BMP [19,33].

Both autograft and BMPs function as osteoinducers, promoting bone formation [47,57] in the defect area. Compared with autograft, BMP leads to increased bone formation irrespective of vascularity at the replacement site, a generated tissue gap of at least two thirds of the intervertebral space and 5 mm in height [63]. Nevertheless, histological evaluation shows a remarkably good vascularization of the newly formed bone, especially in animals fused with BMP [19].

Formation of bone trabeculae growing into discal remnants proves the high osteogenic potential of BMPs. At the fusion site it is also observed that remaining intact endplate structures are completely rebuilt, with ingrowing trabecular structures (Fig. 12). Although the mere effect of the rhOP-1 carrier material was not evaluated in the current study, data from several other trials have revealed that the bovine bone–derived type I collagen does not have cartilage- or bone-inductive properties [56,66,53,73]. Nevertheless, small fragments consisting of demineralized bone matrix including single osteons could be noticed. This phenomenon was interpreted as a remnant rhOP-1 carrier.

Conventional x-ray diagnosis at 4-weekly intervals indicated that visible bone healing had already occurred in the BMP group after 4 months. None of the experimental animals gave evidence of dystopic bone formation or excessive growth of osteophytes.

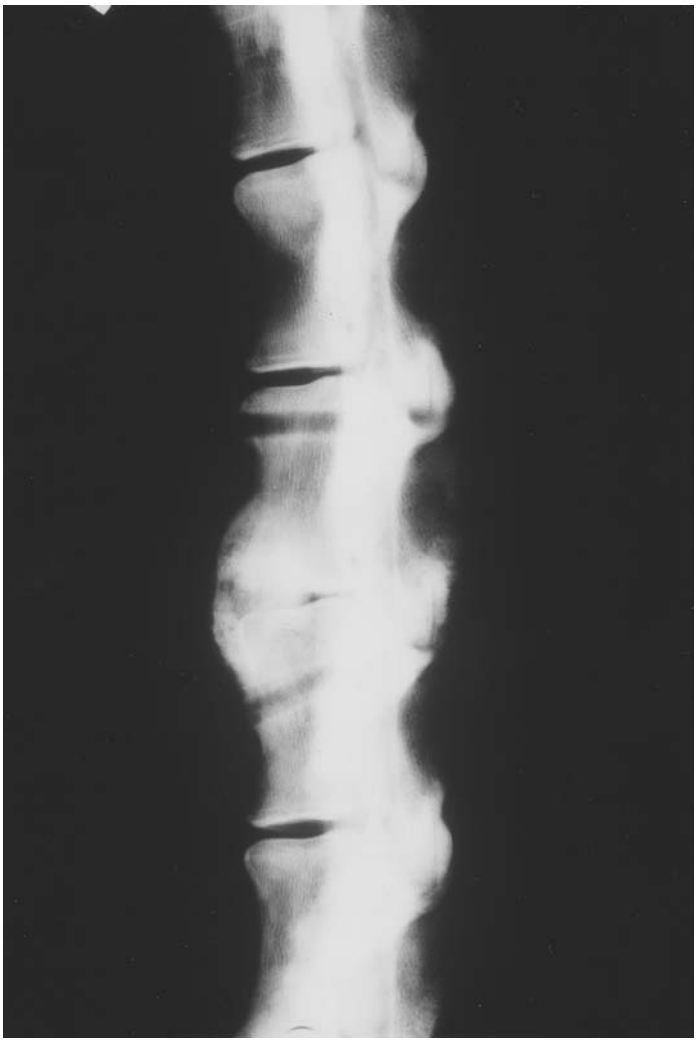

Figure 8 Plain lateral radiograph of the postmortem explanted lumbar specimen after fusion with autograft. The holes remaining in the adjacent vertebrae after removal of the hardware are visible.

The objective of this study was to answer the basic question of whether osteoinductive material can be used to achieve lumbar spine arthrodesis in a large animal. Nowadays, most lumbar spinal fusions in patients are instrumented, so it is important to use an appropriate procedure for animal experiments [46]. Taking into account the differences in species, this study suggests that lumbar spine interbody fusion can be improved by using the highly potent osteoinductive substance rhBMP-7. Repeatedly confirmed suitability of sheep lumbar spine justifies comparison [19] with the situation in humans in terms of bone healing, dimensions, and biomechanical behavior [46,74].

Our findings strongly support the preference for BMPs in spinal arthrodesis instead of autograft with its associated risks such as additional surgery, considerable rate of complications, and limited biological value due to inconsistent quality [5–7]. For a benefit analysis, the following should be taken into account: duration of operation and anesthesia, additional manpower,

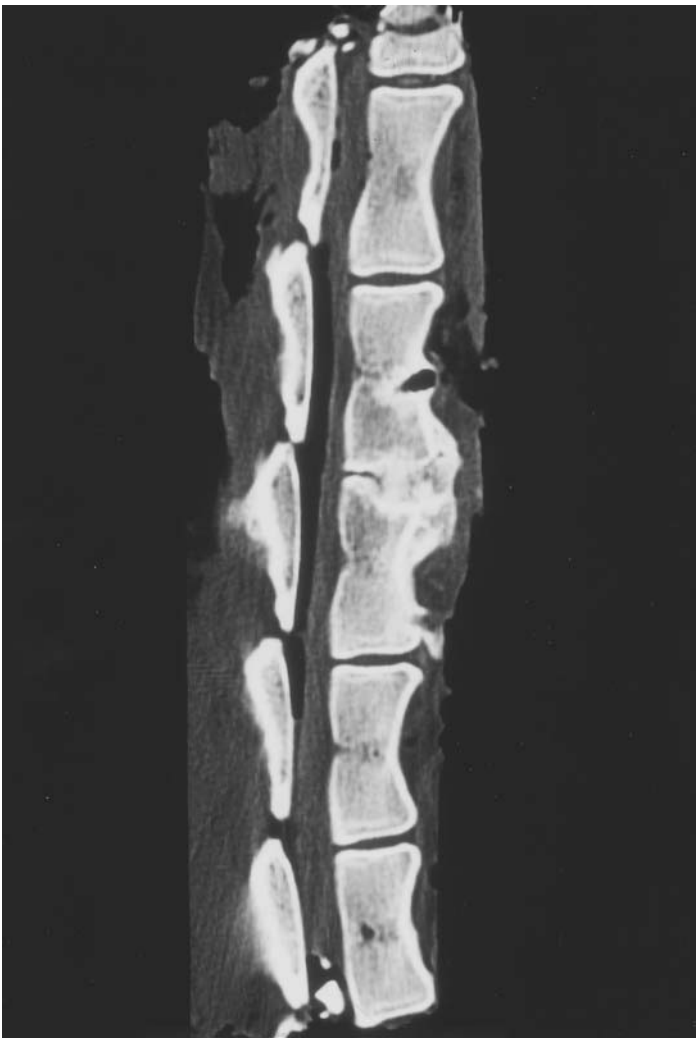

Figure 9 Same specimen as in Fig. 8 examined by computed tomography (CT): a solid fusion is obvious. Posterior remnants of the intervertebral disc (see Fig. 4) can be seen. Other vertebral segments appear to be regular.

hemorrhage, complications that require extensive treatment, such as nerve and vascular injury, hematoma, infection, fracture at the site of harvesting, violation of the sacroiliac joint, herniation of abdominal contents, cosmetic deformities associated with scar formation and alterations of the iliac crest, gait disturbances, and chronic donor-site pain [10,20,21,36–40].

With the use of BMPs in spinal arthrodesis, new therapeutic options might be introduced. In recent years, transpedicular or other merely dorsal approaches have been established, contributing to less invasive surgical treatments. In fact, the Daniaux procedure [8,25], in its initial setting, was not found to be a long-term success [7,75]. However, when applying BMPs, some sort of revival may be seen.

PLIF techniques with various cages can probably also be improved when carried out with potent osteoinducers like BMPs. Preliminary results of a clinical pilot study have already been

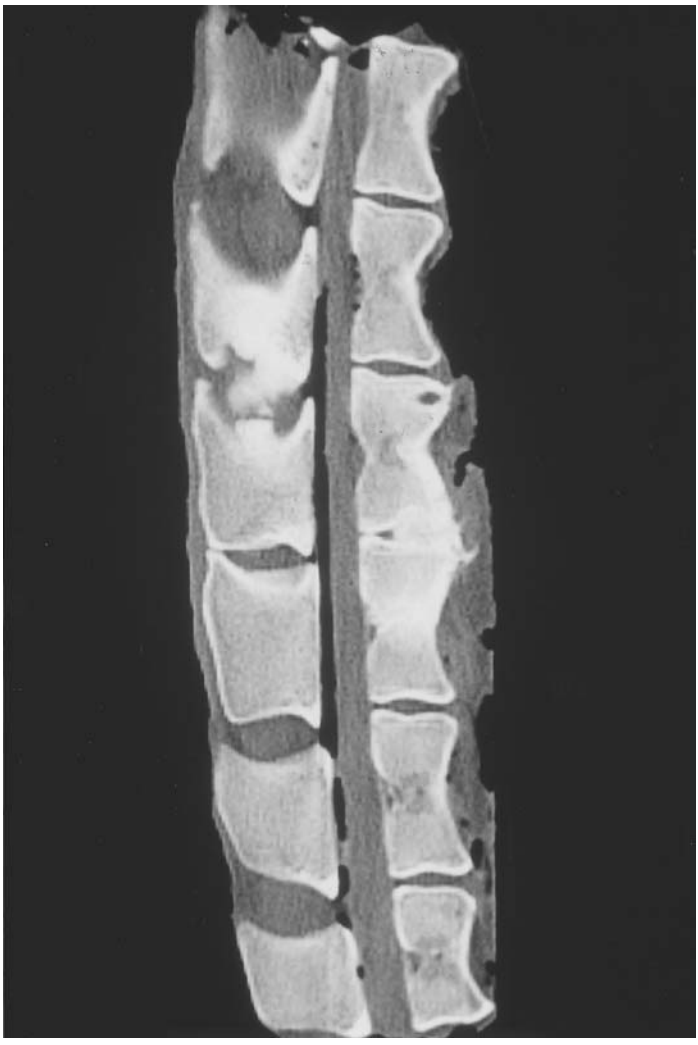

Figure 10 Longitudinal CT scan of a lumbar vertebral specimen showing fusion with BMP-7. Dense bone formation can be observed.

published by Boden et al. [76]. The sole use of rhBMP-2 on a collagen carrier without employing autograft succeeded in lumbar vertebral fusion at the L5-S1 level after 6 months. This finding was revealed in 11 patients treated with anterior spinal cages. The major objective, avoidance of anterior surgical procedures of the thoracic or lumbar spine, could be achieved by using these new technologies which provide a more rapidly loadable bone formation.

Kyphoplasty and vertebroplasty can furthermore be seen as innovative treatment options [77–79] in the context of applying growth factors capable of inducing and speeding up osteoneogenesis. At present, PMMA is the preferred substance for this kind of treatment in osteoporotic compression fractures with or without balloons. Composites of injectable calcium phosphate bone cements and BMPs may potentially combine both early load transmission capability and enhancement of biological bone repair.

Figure 11 The spine-testing apparatus in use allowed evaluation of lumbar vertebral specimen in all six degrees of freedom (flexion and extension, lateral bending, and rotation).

A variety of questions concerning the best carrier, timing of application, dosage, and the interplay of different growth and differentiating factors remain unanswered. The presence of one factor might result in the expression of another. Binding of two different BMPs has been observed, leading to an increase in BMP receptor affinity. For instance, the combination of BMP-2 and BMP-6 has been shown to be fivefold more potent in inducing bone formation than BMP-2 alone [80]. We have to realize that a whole cascade of factors merge one into the other, controlling stepwise expression of each other and thereby resulting in controlled bone formation [81].

Reflections on the complexity of biological systems led to the concern that a single-dose application even of potent growth factors might be too crude to sufficiently face the problem of bone healing, particularly in difficult situations. Adequate biological piloting is probably

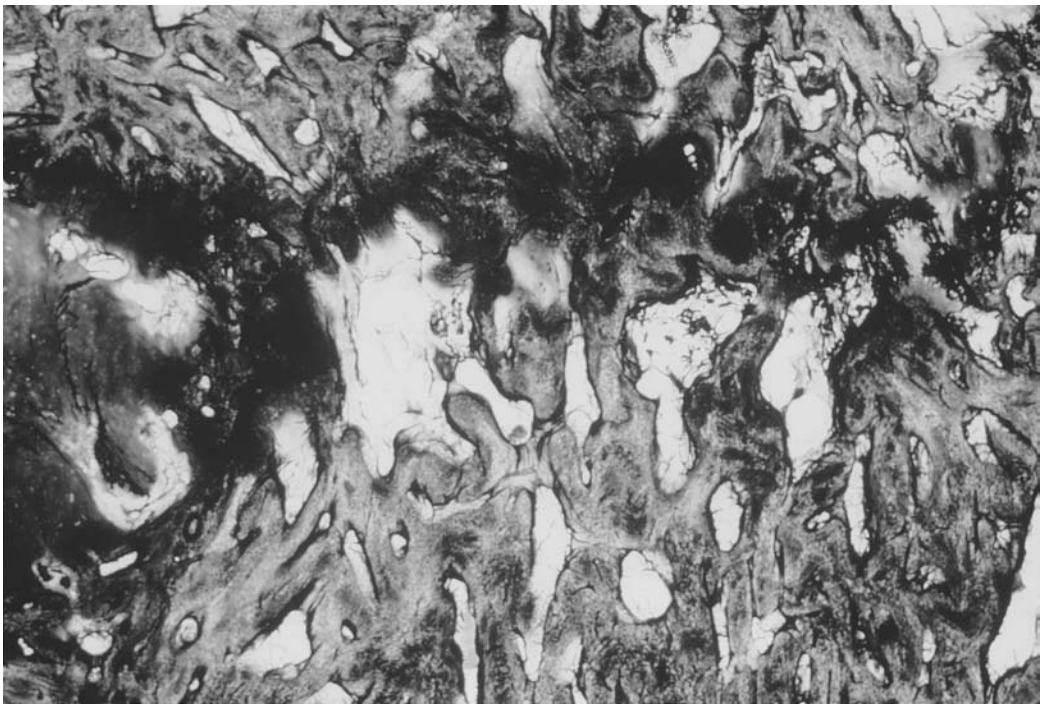

Figure 12 The histological section of the fusion site after BMP-7 shows a region with an intact endplate next to remaining parts of the intervertebral disc. Nevertheless, ingrowing trabecular structures reorganize this barrier and, thus, contribute to fusion.

provided best by means of gene therapy [1]. By transferring genetic information to the target cell, the cell is enabled to synthesize the protein encoded in the transferred gene. Several gene therapy options are currently in experimental use, enrolling both short-term and long-term expression of different growth factors. Viral and nonviral vectors to induce vertebral arthrodesis are under investigation [82,83]. Major concerns with this type of gene therapy are uncontrolled generation of replication-competent viruses in the host organism and the production of viral proteins other than the transgene product. Yet unknown genetic alterations leading to uncontrolled further disorders or malignant deterioration must also be considered.

The advantages and disadvantages of both kinds of treatment to promote osseous healing in the spine must be compared (Table 1). The advantages of autografts are histocompatibility, no disease transmission, no immunogenicity, and easy availability. The disadvantages are donor site morbidity, requirement of additional surgery, and inconsistent quality.

The advantages of growth factors like BMP include defined biological activity, general availability, enhanced osteogenicity, overcoming toxic effects of smoking [14,17], appropriate for minimally invasive techniques [72,82,83], no need for additional surgery and, therefore, less demanding. There has been limited experience with clinical applications of growth factors. The balance for both types of treatment, including economic impact, is still in flux. It can be expected to gradually change in favor of the new technology as long as the treatment costs decrease.

Although copious information about the behavior of BMPs in experimental settings has been obtained, clinical data are still sparse. A recent paper by Laursen et al. demonstrated a poor clinical outcome when the OP-1 device was applied transpedicularly in thoracolumbar

Table 1 Advantages and Disadvantages of Autografts and BMPs

	Advantage	Disadvantage
Autograft	Histocompatibility	Donor site morbidity
	No disease transmission	Additional surgery
	No immunogenicity	Inconsistent quality
	Easy availability	Limited resources
	Cost-effective?	Expensive?
BMP	Defined biological activity	Limited experience with clinical applications
	Unlimited availability	
	High osteogenic activity	Expensive
	Overcoming toxic effects	
	No additional surgery	
	Less demanding	
	Appropriate for minimally invasive techniques	
	Cost-effective?	

burst fracture [84]. The small number of cases (five patients) in this preliminary report has to be considered as does unexpected detrimental bone resorption as a possible primary event after BMP application at a certain stage of the bone repair cascade.

Clinicians must be critical in their assessment of BMPs and other principles for tissue engineering in terms of both efficacy and safety. Unexpected side effects should be evaluated carefully to offset excitement associated with an innovative treatment option.

ACKNOWLEDGMENTS

Supported by grants from Stryker Biotech (Hopkinton, MA) and Rhenish-Westphalian Technical University, (Aachen, Germany). Some of the technical equipment and the implants were provided by Stryker Biotech (Hopkinton, MA) and Endotec, (Leverkusen, Germany). We would like to thank the following for their assistance: G. Delling, A. Freund, S. Kinzel, W. Küpper, J. Neuerburg, S. Niesen, K. Scherer, and T. Stopinsky.

REFERENCES

1. Lieberman JR, Daluiski A, Einhorn TA. The role of growth factors in the repair of bone. Biology and clinical application. J. Bone Joint Surg 2002; 84-A:1032–1044.
2. Sandhu HS. Anterior lumbar interbody fusion with osteoinductive growth factors. Clin. Orthop 2000; 371:56–60.
3. Crawford RJ, Askin GN. Fixation of thoracolumbar fractures with the Dick fixator: the influence of transpedicular bone grafting. Eur Spine J 1994; 3:45–51.
4. Hadjipavlou A, Enker P, Dupuis P, Katzman S, Silver J. The causes of failure of lumbar transpedicular spinal instrumentation and fusion. Intern Orthop 1996; 20:35–42.
5. Katz JN. Lumbar spinal fusion. Surgical rates, costs, and complications. Spine 1995; 24S:78S–83S.
6. Kim CW, Abrams R, Lee G, Hoyt D, Garfin SR. Use of vascularized fibular grafts as a salvage procedure for previously failed spinal arthrodesis. Spine 2001; 26:2171–2175.

7. Knop C, Fabian HF, Bastian L, Blauth M. Late results of thoracolumbar fractures after posterior instrumentation and transpedicular bone grafting. Spine 2001; 26:88–99.
8. Liljenquist U, Mommsen U. Die operative Behandlung thorakolumbaler Frakturen mit dem Fixateur interne und transpedikulärer Spongiosaplastik. Unfallchirurgie 1995; 21:30–39.
9. Steinmann JC, Herkowitz N. Pseudarthrosis of the spine. Clin. Orthop 1992; 284:80–90.
10. Weckbach N, Vogel S. Einflu der transpedikulären intercorporellen Spongiosaplastik auf den Korrekturverlust nach alleiniger dorsaler Instrumentierung thoracolumbaler Wirbelsäulenverletzungen. Hefte Unfallchir 1997; 268:205–208.
11. Brown CW, Orme TJ, Richardson HD. The rate of pseudarthrosis (surgical nonunion) in patients who are smokers and patients who are nonsmokers: a comparison study. Spine 1986; 11:942–943.
12. Capen DA, Calderone RR, Green A. Peroperative risk factors for wound infections after lower back fusions. Orthop. Clin. North Am 1996; 27:83–86.
13. Hilibrand AS, Fye MA, Emery SE, Palumbo MA, Bohlman HE. Impact of smoking on the outcome of anterior cervical arthrodesis with interbody or strut-grafting. J. Bone Joint Surg 2001; 83-A: 668–673.
14. Patel TC, Erulkar JS, Grauer JN, Troiano NW, Panjabi MM, Friedlaender GE. Osteogenic protein-1 overcomes the inhibitory effect of nicotine on posterolateral lumbar fusion. Spine 2001; 26: 1656–1661.
15. Reibel GD, Boden SD, Whitesides TE. The effects of nicotine on incorporation of cancellous bone graft in an animal model. Spine 1995; 20:2198–2202.
16. Silcox DH, Daftari T, Boden SD. The effect of nicotine on spinal fusions. Spine 1995; 20:1549–1553.
17. Silcox DH, Boden SD, Schimandle JH. Reversing the inhibitory effect of nicotine on spinal fusion using an osteoinductive protein extract. Spine 1998; 23:291–297.
18. Stevenson S, Emery SE, Goldberg VM. Factors effecting bone graft incorporation. Clin Orthop 1996; 323:66–74.
19. Cunningham BW, Kanayama M, Parker LM. Osteogenic protein (rhOP-1) versus autologous interbody arthrodesis in the sheep thoracic spine. Spine 1999; 24:509–518.
20. Robertson PA, Wray AJ. Natural history of posterior iliac crest bone graft donation for spinal surgery. A prospective analysis of morbidity. Spine 2001; 26:1473–1476.
21. Wood GW, Boyd RJ, Carothers TA. The effect of pedicle screw/plate fixation of lumbar/lumbosacral autogenous bone graft fusions in patients with degenerative disc disease. Spine 1995; 20:819–830.
22. Gurwitz GS, Dawson JM, McNamara MJ. Biomechanical analysis of three surgical approaches for lumbar burst fractures using short-segment instrumentation. Spine 1993; 18:977–982.
23. Greenough CG, Taylor LJ, Fraser RD. Anterior lumbar fusion: results, assessment techniques and prognostic factors. Eur Spine J 1994; 3:225–230.
24. Zdeblick TA, Warden KE, Zou D, McAfee PC, Abitbol JJ. Anterior spinal fixators—a biomechanical in vitro study. Spine 1993; 18:513–517.
25. Daniaux H. Transpedikuläre Reposition und Spongiosaplastik bei Wirbelkörperbrüchen der unteren Brust und Lendenwirbelsäule. Unfallchirurgie 1986; 89:197–213.
26. Dick W, Kluger P, Magerl F, Wörsdorfer O, Zäch G. A new device for internal fixation of thoracolumbar and lumbar spine fractures: the fixateur interne. Paraplegia 1985; 23:225–232.
27. Dick W. The ''fixateur interne'' as a versatile implant for spine surgery. Spine 1987; 12:882–900.
28. Kluger P, Gerner HJ. Das mechanische Prinzip des Fixateur externe zur dorsalen Stabilisierung der Brust und Lendenwirbelsäule. Unfallchirurgie 1986; 12:68–79.
29. Wimmer C, Krismer M, Gluch H, Ogon M, Stöckl S. Autogenic versus allogenic bone grafts in anterior lumbar interbody fusion. Clin. Orthop 1999; 360:122–126.
30. Olerud S, Karlstrom G, Sjostrom L. Transpedicular fixation of thoracolumbar vertebral fractures. Clin Orthop 1988; 227:44–51.
31. Rommens PM, Van Calenbergh F, Goffin J, Broos PL. Mechanical performance of the Dick internal fixator: a clinical study of 75 patients. Eur Spine J 1995; 4:104–109.
32. Vacaro AR, Garfin SR. Internal fixation (pedicle screw fixation) for fusions of the lumbar spine. Spine 1995; 20:157S–165S.
33. McAfee PC. Interbody fusion cages in reconstructive operations on the spine. J Bone Joint Surg 1999; 81-A:859–880.

34. Fraser RD. Interbody, posterior, and combined lumbar fusions. Spine 1995; 20:167S–177S.
35. Goel VK, Pope MH. Biomechanics of fusion and stabilization. Spine 1995; 20:85S–99S.
36. Summers BN, Eissenstein SM. Donor site pain from the ilium. A complication of lumbar spine fusion. J Bone Joint Surg 1989; 71-A:677–680.
37. Arrington ED, Smith WJ, Chambers HG, Bucknell AL, Davino NA. Complications of iliac crest bone graft harvesting. Clin Orthop 1996; 329:300–309.
38. Banwart JC, Asher MA, Hassanein RS. Iliac crest bone graft harvest donor site morbidity. Spine 1995; 20:1055–1060.
39. Ebraheim N, Elgafy H, Xu R. Bone graft harvesting from iliac and fibular donor sites: techniques and complications. J. Am. Acad. Orthop. Surg 2001; 9:210–218.
40. Kurz LT, Garfin SR, Booth RE. Harvesting autogenous iliac bone grafts: a review of complications and techniques. Spine 1989; 14:1324–1331.
41. Massey EW. Meralgia paresthetica secondary to trauma of bone graft. J. Trauma 1980; 20:342–343.
42. Weikel AM, Habal MB. Meralgia paresthetica: a complication of iliac bone procurement. Plast. Reconstr. Surg 1977; 60:572–574.
43. Younger EM, Chapman MW. Morbidity at bone graft donor site. J Orthop Trauma 1989; 3:192–195.
44. Hamburger C, Festenberg FV, Uhl E. Ventral discectomy with PMMA interbody fusion for cervical disc disease. Long-term results in 249 patients. Spine 2001; 26:249–255.
45. Ragni P, Ala-Mononen P, Lindholm TS. Spinal fusion induced by porous hydroxyapatite blocks (HA). Experimental comparative study with HA, demineralized bone matrix and autogenous bone marrow. Ital J Orthop Traumatol 1993; 19:133–144.
46. Steffen T, Marchesi D, Aebi M. Posterolateral and anterior spinal fusion models in the sheep. Clin. Orthop 2000; 371:28–37.
47. Urist MR. Bone: formation by autoinduction. Science 1965; 150:893–899.
48. Reddi AH. Bone and cartilage differentiation. Curr. Opin. Genet. Dev 1994; 4:737–744.
49. Wozney JM, Rosen V, Celeste AJ. Novel regulators of bone formation: molecular clones and activities. Science 1988; 242:1528–1534.
50. Urist MR, Mikulski A, Lietze A. Solubilized and insolubilized bone morphogenetic protein. Proc. Natl. Acad. Sci. USA 1979; 76:1828–1832.
51. Vukiceciv S, Reddi AH, eds. First European Conference on Bone Morphogenetic Proteins. Zagreb, Oct. 7–11, 1998.
52. Lindholm TC, Lindholm TS, Marttinen A, Urist MR. Bovine bone morphogenetic protein (bBMP/NCP)-induced repair of skull trephine defects in pigs. Clin. Orthop 1994; 301:263–270.
53. Cook SD, Salkfeld SL, Brinker MR, Wolfe MW, Rueger DC. Use of an osteoinductive biomaterial (rhOP-1) in healing large segmental bone defects. J. Orthop. Trauma 1998; 12:407–412.
54. Geesink RG, Hoefnagels NH, Bulstra SK. Osteogenic activity of OP-1 bone morphogenetic protein (BMP-7) in a human fibular defect. J. Bone Joint Surg 1999; 81-B:710–718.
55. Ripamonti U, Van den Heever B, Sampath TK, Tucker MM, Rueger DC, Reddi AH. Complete regeneration of bone in the baboon by recombinant human osteogenic protein-1 (hOP-1), bone morphogenetic protein-7. Growth Factors 1996; 13:273–289.
56. Salkfeld SL, Patron LP, Barrack RL, Cook SD. The effect of osteogenic protein-1 on the healing of segmental bone defects treated with autograft or allograft bone. J. Bone Joint Surg 2001; 83-A: 803–816.
57. Boden SD, Schimandle JH, Hutton WC. The use of an osteoinductive growth factor for lumbar spinal fusion. Spine 1995; 20:2626–2644.
58. Boden SD, Martin GJ, Horton WC, Truss TL, Sandhu HS. Laparoscopic anterior spinal arthrodesis with rh BMP-2 in a titanium interbody threaded cage. J Spinal Disord 1998; 11:95–101.
59. Cook SD, Dalton JE, Tan EH, Whitecloud TS, Rueger DC. In vivo evaluation of recombinant human osteogenic protein (rhOP-1) implants as a bone graft substitute for spinal fusions. Spine 1994; 19: 1655–1663.
60. Fischgrund JS, James SB, Chabot MC. Augmentation of autograft using rhBMP-2 and different carrier media in the canine spinal fusion model. J Spinal Disord 1997; 10:467–472.
61. Grauer JN, Patel TC, Erulkar JS, Troiano NW, Panjabi MM, Friedlaender GE. Evaluation of OP-1 as a graft substitute for intertransverse process lumbar fusion. Spine 2001; 26:127–133.

62. Lovell TP, Dawson EG, Nilsson OS, Urist MR. Augmentation of spinal fusion with bone morphogenetic protein in dogs. Clin Orthop 1989; 243:266–274.
63. Magin MN, Delling G. Improved lumbar vertebral interbody fusion using rhOp-1. Spine 2001; 26: 469–478.
64. Muschler GF, Hyodo A, Manning T. Evaluation of human bone morphogenetic protein 2 in a canine spinal fusion model. Clin Orthop 1994; 308:229–240.
65. Paramore CG, Lauryssen C, Rauzzino C. The safety of OP-1 for lumbar fusion with decompression—a canine study. Neurosurgery 1999; 44:1151–1155.
66. Cook SD, Baffes GC, Wolfe MW, Sampath TK, Rueger DC. Recombinant human bone morphogenetic protein-7 induces healing in a canine long-bone segmental defect model. Clin. Orthop 1994; 301: 302–312.
67. Friedlaender GE, Perry CR, Cole JD. Osteogenic protein 1 (bone morphogenetic protein-7) in the treatment of tibial nonunions. J. Bone Joint Surg 2001; 83-A(suppl. 1):151–158.
68. Johnson EE, Urist MR. Human bone morphogenetic protein allografting for reconstruction of femoral nonunion. Clin. Orthop 2000; 371:61–74.
69. Cook SD, Barrack RI, Shimmin A. The use of osteogenic protein-1 in reconstructive surgery of the hip. J. Arthroplasty 2001; 16(suppl.1):88–94.
70. Giltaij LR. Bone morphogenetic protein-7 in orthopaedic applications. A review. J. Musculoskeletal Res 2002; 6:55–62.
71. Wang EA, Rosen V. Recombinant human bone morphogenetic protein induces bone formation. Proc Natl Acad Sci USA 1990; 87:2220–2251.
72. Boden SD, Moskovitz PA, Morone MA, Toribitake Y. Video-assisted lateral intertransverse process arthrodesis. Validation of a new minimally invasive lumbar spinal fusion technique in the rabbit and nonhuman primate (rhesus) models. Spine 1996; 21:2689–2697.
73. Sampath TK, Reddi AH. Dissociative extraction and reconstitution of extracellular matrix components involved in local bone differentiation. Proc. Natl. Acad. Sci. USA 1981; 78:7599–7603.
74. Wilke HJ, Kettler A, Claes LE. Are sheep spines a valid biomechanical model for human spines?. Spine 1997; 22:2365–2374.
75. Knop C, Fabian HF, Bastian L. Fate of the transpedicular intervertebral bone graft after posterior stabilisation of thoracolumbar fractures. Eur. Spine J 2002; 11:251–257.
76. Boden SD, Zdeblick TA, Sandhu HS, Heim SE, O'Brien J. The use of rhBMP-2 in interbody fusion cages. Spine 2000; 25:376–381.
77. Garfin SR, Yuan HA, Reiley MA. New technologies in spine. Kyphoplasty and vertebroplasty for the treatment of painful osteoporotic compression fractures. Spine 2001; 26:1511–1515.
78. Liebermann IH, Dudeney S, Reinhardt MK, Bell G. Initial outcome and efficiacy of ''kyphoplasty'' in the treatment of painful osteoporotic vertebral compression fractures. Spine 2001; 26:1631–1638.
79. Mathis JM, Petri M, Naff N. Percutaneous vertebroplasty treatment of steroid-induced osteoporotic compression fractures. Arthritis Rheum 1998; 41:171–175.
80. Mayer H, Scutt AM, Ankenbauer T. Subtle differences in the mitogenic effects of recombinant human bone morphogenetic proteins-2 to -7 on DNA synthesis on primary bone forming cells and identification of BMP-2/4 receptor. Calcif. Tissue Int 1996; 58:249–255.
81. Zlotolow DA, Vaccaro AR, Salamon ML, Albert TJ. The role of human bone morphogenetic proteins in spinal fusion. J. Am. Acad. Orthop. Surg 2000; 8:3–9.
82. Boden SD, Titus L, Hair G. Lumbar spine fusion by local gene therapy with a cDNA encoding a novel osteoinductive protein (LMP-1). Spine 1998; 23:2486–2492.
83. Alden TD, Pittman DD, Beres EJ. Percutaneous spinal fusion using bone morphogenetic protein-2 gene therapy. J. Neurosurg 1999; 90(1 suppl):109–114.
84. Laursen M, Hoy K, Hansen ES. Recombinant bone morphogenetic protein-7 as an intracorporal bone growth stimulator in unstable thoracolumbar burst fractures in humans: preliminary results. Eur. Spine J 1999; 8:485–490.

37

Occipitocervical Fusion for Rheumatoid Arthritis Patients with Myelopathy

Shunji Matsunaga and Takashi Sakou
Kagoshima University
Kagoshima, Japan

Nobuhiko Sunahara
Kagoshima Red Cross Hospital
Kagoshima, Japan

I. INTRODUCTION

Surgical treatments such as atlantoaxial fixation [1,2], occipitocervical fusion [3,4], and transoral dens resection [5], have been used to alleviate upper cervical lesions of patients with rheumatoid arthritis (RA). While many studies have reported the results of surgical treatment for upper cervical lesions [6–8], the final prognosis of patients who underwent this surgery has not been discussed. The prognosis for patients with rheumatoid arthritis is believed to be relatively poor, and their expected life span is shorter than that of healthy individuals [9,10]. Few studies of patients with upper cervical lesions due to rheumatoid arthritis have compared the prognosis of patients who underwent surgical treatment with that of matched controls. Since 1985, we have performed laminectomy of the atlas and occipitocervical fusion using a rectangular rod [4] on patients with irreducible atlanto-axial dislocation or vertical dislocation due to rheumatoid arthritis. In this study we examined the outcome of patients with occipitocervical fusion whom we followed for longer than 10 years. The prognosis of patients who underwent occipitocervical fusion was compared with that of matched patients who had upper cervical lesions due to rheumatoid arthritis and did not undergo surgery.

II. MATERIALS

For this study, 18 patients were chosen from a group of 42 RA patients who had undergone occipitocervical fusion with a rectangular rod for upper cervical lesion in order to obtain minimum 10-year follow-up study for the patients with myelopathy. All patients have atlanto-axial dislocation, and 12 of the 18 patients were associated with upward migration of the odontoid process. Occipito-cervical fusion of O-C2 was performed in 12 cases, of O-C3 in 4, and of O-C4 or O-Th1 in one case. Laminectomy of C1 was accompanied in all cases to decompress the spinal cord. The age at operation ranged from 44 to 72 years (mean 60.8 yr).

The matched controlled 21 RA patients with myelopathy due to the upper cervical lesion who were treated conservatively were studied to compare the results with those of surgery

patients. These patients were recommended to have surgery by clinicians but refused operation. All patients with conservative treatment had atlanto-axial dislocation, and 13 were associated with upward migration of the odontoid process. The subject characteristics of the two groups are presented in Table 1.

Radiographic determinations were performed on the lateral view of the cervical spine for anterior atlantoaxial dislocation, upward migration of the odontoid, and subaxial subluxation. Anterior atlanto-axial dislocation was defined as when atlanto-dental interval (ADI: distance between the posterior edge of the ring of C, and the anterior edge of the odentoid) in the flexion of the cervical spine is more than 3 mm. Upward migration of the odontoid was estimated by the Redlund-Johnell method [11,12]. Subaxial subluxation was defined as greater than 3 mm slippage of the posterior border of the vertebral body to that of the adjoining one below during flexion and extension of the neck.

The patients were evaluated with the respect to the following: radiographic results, recovery of clinical symptoms by Ranawat (pain and neural assessments) [3], functional recovery by the American Rheumatism Association [13], and survival rate.

A. Radiographic Examination

In cases of conservative treatment, ADI increased from 7.9 to 9.9mm during follow-up periods. Redlund-Johnell values were aggravated 30.8 mm on average to 24.4 mm. However, subaxial subluxation occurred in only 3 cases (14%).

As for oparative group, bone union was achieved in 17 (94 %) of 18 cases, with one case showing nonunion. ADI was reduced from 8.5 mm average preoperatively to 5.8 mm immediately after surgery and retained well at the final follow-up (Fig. 1). There was no significant difference in Redlund-Johnell values throughout the course (Fig. 2). Subaxial subluxation took place in 5 (28%) of 18 cases—at C4/5 in four and C5/6 in one.

B. Recovery from Clinical Symptoms

Pain and neural function were evaluated using Ranawat's classification. In the operated cases, occipital or nuchal pains improved well in all patients except one. As for neural recovery , one-level improvement was found in 8 (44%) of 18 patients, two-level improvement in 4 (22%), no

Table 1 Patient Characteristics

	Occipito cervical fusion ($N = 18$)	Conservative therapy ($N = 21$)
Sex	3 males, 15 females	4 males, 17 females
Age at onset of myelopathy (yr)	44–72 (mean 60.8)	43–69 (mean 59.2)
Length of time suffering from RA (yr)	9–21 (mean 14.8)	10–19 (mean 13.8)
Steinbrocker's stage	Stage III, 8; IV, 10	Stage III, 8; IV, 13
Neurological criteria by Ranawat's classification	Class II, 2; IIIA, 12; IIIB, 4	Class II, 2; IIIA, 14; IIIB, 5
Functional classification by the ARA	Class 2, 5; 3, 10; 4, 3	Class 2, 5; 3, 12; 4, 4

There is a statistical difference in the follow-up periods between the two groups. All patients of the conservative group died within 7 years. ARA, American Rheumatism Association.

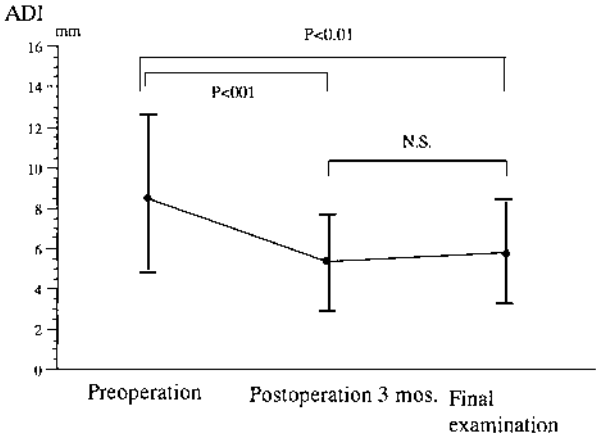

Figure 1 Change of atlanto-dental interval (ADI) in 18 operated-upon patients. Data represent mean ± SD. Statistical significance was evaluated by ANOVA. N.S., Not significant.

change in 5 (28%), and a worsening of the condition in one (6%) at the final follow-up (Fig. 3).

The patients with concervative treatment showed improvement of occipital or nuchal pain in 5 (25%). However, no signicant improvement of myelopathy was recognized, and deterioration of myelopathy during follow-up occurred in 16 (76%) of 21 cases.

C. Functional Recovery

Functional recovery in the operated group was varing in the final follow-up. Most subjects showed functional recovery at the relatively short follow-up, but some showed deterioration

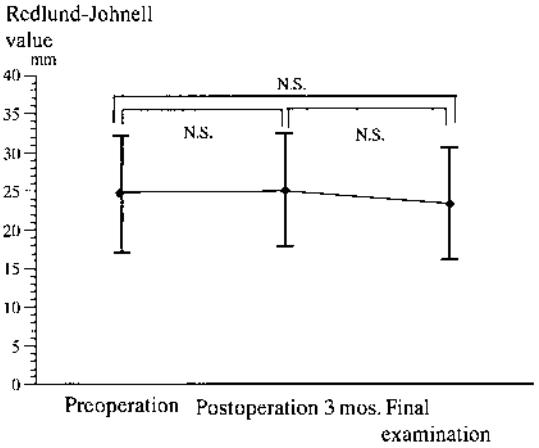

Figure 2 Change of Redlund-Johnell values in 18 patients with the oparation. Data represent mean ± SD. Statistical significance was evaluated by ANOVA. N.S., Not significant.

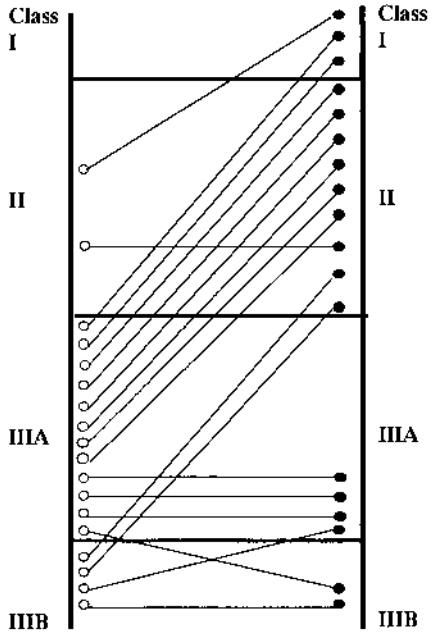

Figure 3 Neural evaluation by Ranawat criteria before and after operation.

during follow-up. (Fig. 4). All of the patients treated conservatively ended up bedridden within 3 years after the onset of myelopathy.

D. Survival Prognosis

Eight operated patients died in the final follow-up period. Causes were traffic accident, pulmonary fibrosis, renal failure, unknown cause, and heart failure in 1, 1, 1, 1, and 4 patients, respectively. No cause of death related to an operation was recognized. The average age at death was 66.5 years, and the time from operation to death ranged from 2 to 7 years (mean 4.1 yr). The survival rate following surgery as calculated by Kaplon-Meier's method [15] was 83% 5 years after surgery, and 39% in the first 10 years. Seven of 21 patients who had been treated conservatively died, including 3 who suffered sudden deaths. The survival rate was 0% in the first 7 years after the onset of myelopathy (Fig. 5).

III. CONCLUSION

A consensus supports surgical treatment for patients with upper cervical lesions and related myelopathy due to rheumatoid arthritis. Various surgical methods [1,2,4] are used, including posterior atlantoaxial transarticular screw fixation [15–17]. However, long-term results of this surgical method have not been studied. Occipitocervical fusion with a rectangular rod, the surgical method presented in this paper, is an operation, and long-term follow-up study can be performed. However, few studies have evaluated patients' prognosis after surgery compared with the results of conservative therapy. The subjects in our study were all patients with irreducible atlantoaxial dislocation from myelopathy due to upper cervical lesions, and many also had

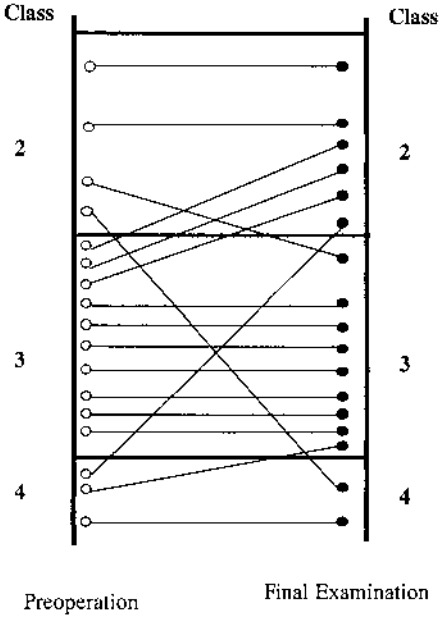

Figure 4 Functional evaluation by American Rheumatism Association criteria.

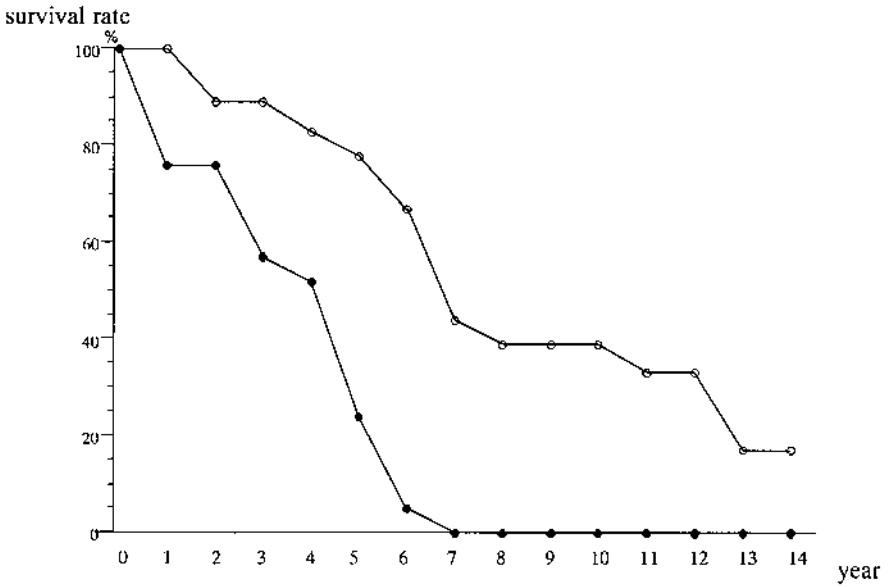

Figure 5 Survival rate of patients with myelopathy. White circles represent the survival rate of the operated group. The figures in transverse line show the postoperative time in the operated group. Black circles represent the survival rate of the conservative therapy group. The figures in transverse line show the time from the onset of myelopathy.

vertical dislocation. We evaluated radiographic changes, improvement of clinical symptoms, functional recovery, and the survival rates of these patients to determine any the advantage of this operation. Furthermore, we performed a long-term follow-up study of patients with upper cervical lesions and related myelopathy treated without surgery for comparison.

Some reports have discussed the prognosis of patients with rheumatoid arthritis and concluded that the lifespan of such patients was shorter than that of healthy individuals [6,7]. When Marks and Sharp [17] compared the merits of surgical and conservative treatments during a 6-month follow-up period, 3 of the 11 patients who underwent surgery and 12 of the 20 patients who were treated conservatively had died. The surgical group appeared to show a better prognosis, although accurate evaluation was impossible. Meijers et al. [19] reported that in 9 patients with myelopathy who did not undergo surgery, all died within 1 year, with 4 deaths resulting from cord compression. In the present study, patients with rheumatoid arthritis and myelopathy due to upper cervical instability who did not undergo surgery had a poor prognosis: all became bed-ridden and died within 8 years from the onset of myelopathy. Boden et al. [20] reported that neurological symptoms were minimally relieved by atlantoaxial fusion or occipitocervical fusion, if the posterior atlanto-odontoid interval (space available for the spinal cord) was less than 10 mm. He recommended spinal fusion before the posterior atolanto-odontoid interval because 14 mm or less. We agree, although our patients who underwent surgery showed good neurological recovery and satisfaction. We presumed that the considerable satisfaction of the patients who underwent occipitocervical fusion with a rectangular rod and the associated C1 laminectomy resulted from the pain relief and improvement of myelopathy by decompression of the spinal cord.

In the present study, the survival rate 10 years after surgery was 39%. This figure might appear discouraging, but the following considerations make it more encouraging. First, in this study the mean age at death was 71 years, very close to the generally accepted lifespan of patients with rheumatoid arthritis. Second, the survival rate of patients with rheumatoid arthritis 10 years after the development of myelopathy due to upper cervical lesions without surgical intervention was 0%.

On radiographic examination, occipitocervical fusion with a rectangular rod is useful for reducing and maintaining of ADI but could not maintain the reduction in Redlund-Johnell values. Some lesions, such as subaxial subluxation, are known to to develop long after occipitocervical fusion [7,21–23]. In our study this postoperative abnormality developed in 32% of patients. The rate of occurrence of subaxial subluxation after occipitocervical fusion is significantly higher than its rate in the absence of surgery. Our previous papers reported that increase of mechanical stress of adjacent vertebra is one of the factors associated with development of subaxial lesion following occipitocervical fusion [24,25]. New surgical methods such as atlantoaxial transarticular screw fixation should overcome these problems with occipitocervical fusion.

We conclude that occipitocervical fusion for patients with rheumatoid arthritis is useful for decreasing nuchal pain, reducing myelopathy, and improving prognosis.

REFERENCES

1. Gallie WE. Fractures and dislocations of the cervical spine. Am. J. Surg 1939; 46:495–499.
2. McGraw RW, Rusch RM. Atlanto-axial arthrodesis. J. Bone Joint Surg 1973; 55B:482–489.
3. Ranawat CS, O'Leary P, Pellicci P, Tsairit P, Marchisello P, Dorr L. Cervical spine fusion in rheumatoid arthritis. J. Bone Joint Surg 1979; 61A:1003–1010.
4. Sakou T, Kawaida H, Morizono Y, Matsunaga S, Fielding JW. Occipitoatlantoaxial fusion utilizing a rectangular rod. Clin. Orthop 1989; 239:136–144.

5. Crockard HA, Calder I, Ransford AO. One-stage transoral decompression and posterior fixation in rheumatoid atlanto-axial subluxation. J. Bone Joint Surg 1990; 72-B:682–685.
6. Cregan JCF. Internal fixation of the unstable rheumatoid cervical spine. Ann. Rheum. Dis 1966; 25: 242–252.
7. Crellin RQ, Maccabe JJ, Hamilton EBD. Severe subluxation of the cervical spine in rheumatoid arthritis. J. Bone Joint Surg 1970; 52B:244–251.
8. Ferlic DC, Clayton ML, Leidholt JD, Gamble WE. Surgical treatment of the symptomatic unstable cervical spine in rheumatoid arthritis. J. Bone Joint Surg 1975; 57A:349–354.
9. Rasker JJ, Cosh JA. The natural history of rhumatoid arthritis over 20 years; clinical symptoms, radiological signs, reatment, mortality and prognostic significans of early features. Clin. Rheumatol 1987; 6:5–11.
10. Scott DL, Symmons DPM, Coulton BL, Popert AJ. Long-term outcome of treating rheumatoid arthritis; results after 20 years. Lancet 1987; 348:1108–1111.
11. -Johnell I, Pettersson H. Radiographic measurements of the cranio-vertebral region. Designed for evaluation of abnormalities in rheumatoid arthritis. Acta. Radiol. Diagn 1984; 25:23–28.
12. Redlund-Johnell I, Pettersson H. Vertical dislocation of the C1 and C2 vertebrae in rheumatoid arthritis. Acta. Radiol. Diagn 1984; 25:133–141.
13. Steinbrocker O, Traeger CH, Batterman RC. Therapeutic criteria in rheumatoid arthritis. JAMA 1949; 140:659–662.
14. Eleraky MA, Masferrer R, Sonntag VKH. Posterior atlantoaxial facet screw fization in rheumatoid arthritis. J. Neurosurg 1995; 83:1095–1100.
15. Kaplan EL, Meier P. Non parametric estimation from incomplete observations. J Am Stat Assoc 1988; 53:457–481.
16. Grob D, Jeanneret B, Aebi M, Markwalder TM. Atlanto-axial fusion with transarticular screw fization. J. Bone Joint Surg 1991; 73B:972–976.
17. Margel F, Seemann PS. Stable posterior fusion of the atlas and axis by transarticular screw fization. In Kehr P, Weidner A, eds. Cervical Spine. Vienna: Springer-Verlag, 1986:322–327.
18. Marks JS, Shrap J. Rheumatoid cervical myelopathy. Q. J. Med 1981; 199:307–319.
19. Meijers KAE, Van Beusekom GT, Luyendijk W, Duijfjes F. Dislocation of the cervical spine with cord compression in rheumatoid arthritis. J. Bone Joint Surg 1974; 56B:668–680.
20. Boden SD, Dodge LD, Bohlman HH, Rechtine GR. Rheumatoid arthritis of the cervical spine. J. Bone Joint Surg 1993; 75A:1282–1297.
21. Agarwal AK, Peppelman WC, Kraus DR, Pollock BH, Stolzer BL, Eisenbeis CH, Donaldson WF, Jr. Recurrence of cervical instability in rheumatoid arthritis following previous fusion: Can disease progression be prevented by early surgery? J. Rheumatol 1992; 19:1364–1370.
22. Kraus DR, Peppelman WC, Agarwal AK, DeLeeuw HW, Donaldson WF. Incidence of subaxial subluxation in patients with generalized rheumatoid arthritis who had previous occipital cervical fusion. Spine 1991; 16:486–489.
23. Krieg JC, Clark CR, Goetz DD. Cervical spine arthrodesis in rheumatoid arthritis: a long-term follow-up. Yale J. Biol. Med 1993; 66:257–262.
24. Matsunaga S, Sakou T, Sunahara N, Onishi T, Maeda S, Nakanishi K. Biomechanical analysis of buckling alignment of cervical fusion. predictive value for subaxial subluxation after occipitocervical fusion. Spine 1997; 22:765–771.
25. Matsunaga S, Onishi T, Sakou T. Significance of occipitoaxial angle in subaxial lesion after occipitocervical fusion. Spine 2001; 26:161–165.

38

Validity of a Bioactive Ceramic Spacer in Posterior Lumbar Interbody Fusion with Studies of the Stability of the Pedicle Screw for the Osteoporotic Spine In Vivo and In Vitro

Naohisa Miyakoshi, Koichiro Okuyama, Tetsuya Suzuki, Eiji Abe, Yoichi Shimada, and Eiji Itoi
Akita University School of Medicine
Akita, Japan

I. INTRODUCTION

Posterior lumbar interbody fusion (PLIF) was proposed as one of the procedures to obtain solid mechanical efficacy [10,12] A successful PLIF maintains the anatomical intervertebral disc height, restores weight bearing to the anterior column, and immobilizes the unstable degenerated segment [5]. PLIF was first described by Briggs in 1944 [9], and it was popularized by Cloward [12] in the early 1950s. Cloward's technique consisted of interbody fusion using autologous iliac crest bone grafts without the additional use of an internal device [12]. Progressively, the original technique was modified and developed, and posterior instrumentation was added to increase the fusion rate. During the technique, as the screw is inserted through the pedicle into the vertebral body, it is possible to obtain a segmental and solid stability by using the posterior approach [61]. Steffee et al. [3,62,63] stated that PLIF in conjunction with pedicle screw fixation was mechanically ideal and that it enhanced the osteosynthesis and success rate of the spinal fusion. Recent studies have shown that the fusion rates of PLIF range from 88 to 94% [2,15,25,33,35,39,53,68].

However, problems do exist with PLIF. Collapse, slippage, and graft migration have been reported in 3–10% of cases where PLIF had been performed [15,25,35,54]. Generally, bony fusion in PLIF occurs if the stability of PLIF is well maintained [40,42,52], whereas loss of stability before the fusion tends to lengthen the fusion process or to result in nonunion [32]. A number of studies have reported that corticocancellous interbody bone grafts that lacked initial mechanical strength frequently collapsed, extruded, or were displaced [36,51,60].

Therefore, as a possible solution, the use of intervertebral implants (spacers and cages) has been proposed to restore the intervertebral disc height and to maintain the initial stability of PLIF in the operated segment [16,20,22,26,31,32,58,65,66,71]. Intervertebral implants can resist forces several times those measured in the disc space and those of a tricortical iliac graft

[6,7,31,41,49,54,57,71]. The use of intervertebral implants for PLIF is ideal to conserve the grafted bone and to stabilize fused segments immediately after surgery.

Another possible solution to the problems of collapse, slippage, and graft migration that exist with PLIF is to enhance the stability of the pedicle screws that are commonly used in PLIF. Incidences of pedicle screw bending or breakage are now decreasing with the increase in screw diameters and shank tapering [4,44]. However, the problems of pedicle screw loosening and other related failures still develop, especially in osteoporotic spines [24]. Therefore, enhancing the fixation strength of pedicle screw is extremely important for patients with osteoporotic spines.

II. INTERVERTEBRAL IMPLANTS FOR PLIF

Intervertebral implants used for PLIF surgery must have sufficient mechanical strength, provide long-term stability through fusion between the implant and the endplate or bone union between the grafted bone and the endplate, have a large enough contact area at the endplate/implant interface to obtain sufficient bone union, and preserve the exact disc height to provide good balance [13,15,34,38]. In recent years, numerous intervertebral implants have been introduced to treat symptomatic degenerative disc disease of the lumbar spine. Implants for the intervertebral disc space come in various configurations [67], ranging from horizontal cylinders (e.g., the BAK cage) [31,65], vertical rings (e.g., the Harms cage) [20,26], and open boxes (e.g., the Brantigan cage) [5,6], to solid rectangular parallel-piped spacers, such as the intervertebral spacer made of bioactive ceramics [e.g., the apatite- and wollastonite-containing glass ceramic (AW-GC) spacer] [71].

III. THE AW-GC INTERVERTEBRAL SPACER

Apatite- and wollastonite-containing glass ceramic (AW-GC), which was developed in 1982 at Kyoto University, Japan [28], is a hybrid material consisting of three phases of apatite, wollastonite, and glass with the composition MgO 4.6, CaO 44.9, SiO_2 34.2, P_2O_5 16.3, CaF_2 0.5 by weight ratio [28]. The compressive strength, bending strength, and elastic modulus of the AW-GC are higher than the strengths of human cortical bone (Table 1) [71]. AW-GC has the ability to form tight chemical bonds with living bone [28,71]. An experimental study that focused on the replacement of sheep lumbar vertebrae with an AW-GC prosthesis without bone grafting showed direct bone bonding with the prosthesis [71]. Clinical results of PLIF utilizing the AW-GC intervertebral spacer were first reported by Yamamuro and Shimizu [72] in 1994, showing that the AW-GC spacer was used in 11 patients and that good bone formation around the spacer was observed with time. There were no systemic or local toxic side effects associated with the AW-GC spacer, or any abnormalities associated with laboratory data. Therefore, Yamamuro and Shimizu concluded that the AW-GC spacer is a new biomaterial with excellent properties that can be successfully substituted for bone graft in spine surgery [72]. Based on these experimental and clinical results, the AW-GC intervertebral spacer (Fig. 1) has been shown to be excellent in bonding directly with adjacent living bone tissue and in having strong mechanical strength with no toxic effects. Similar to Yamamuro and Shimizu's use of the AW-GC intervertebral spacer, we have been using the spacer since 1992.

IV. THE PLIF PROCEDURE

Our PLIF procedure for unstable degenerative disorders has been performed by entire excision of the bilateral facets and augmented with pedicle screws since 1992. Complete excision of the

Table 1 Mechanical Properties of AW-GC

Bending strength	200–220 MPa
Compressive strength	1000 MPa
Elastic modulus	120 GPa
Vickers hardness	680 MPa
Density	3.08×10^3 kg/m^3
Fracture toughness	2.0 MPa/m$^{1/2}$

Source: Ref. 71.

bilateral facet joints, including the inferior portion of the superior lamina in the affected segment, has enabled us to increase the space available for the PLIF maneuver.

The AW-GC intervertebral spacer and the Akita Pedicle Screw System (Mizuho Co., Tokyo, Japan) were used (Fig. 2) in most of our cases. Two AW-GC spacers combined with autologous bone grafts from the posterior iliac crest were applied as a way to obtain intervertebral space. The parallel piped bioactive AW-GC prosthesis with a large surface area was suitable for spinal fusion in osteoporotic patients [27]. Ambulation was permitted 2–3 days after surgery. Soft braces were worn routinely for 6 months. Semi-hard braces were also applied for the first 3 months after surgery in osteoporotic cases. Finally, isometric muscle exercises were introduced 3–4 weeks after surgery.

V. OUTCOME OF OUR PLIF PROCEDURE AND CLINICAL APPLICATION OF THE AW-GC INTERVERTEBRAL SPACER

We evaluated the efficacy of our PLIF procedure and clinical application of the AW-GC intervertebral spacer in our patient series from 1992 to 1995 [45], during which we treated 148 consecutive patients (68 men and 80 women). The AW-GC spacer was applied in 117 cases. Patients' mean age at the time of surgery was 59 years (range: 19–80 yr). The mean follow-up period was 3.2 years (range: 2–6.5 yr). The disorders in this patient series were degenerative spondylolisthesis (79 patients), isthmic spondylolysis and spondylolisthesis (56 patients), degenerative lumbar scoliosis (6 patients), failed back syndrome (4 patients), and others (3 patients). Single-level fusion was performed at L4/5 in 81 cases and at L5/S1 in 38 cases. Two-level and three-level fusion was also performed in 12 and three cases, respectively. Radiographic assessment

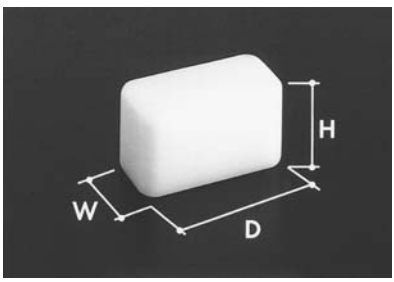

Figure 1 Intervertebral spacer made of AW-GC. Different sizes are available to accommodate different disc spaces: width (W), 10 mm; depth (D), 20 or 25 mm; height (H), 8, 10, 12, or 14 mm.

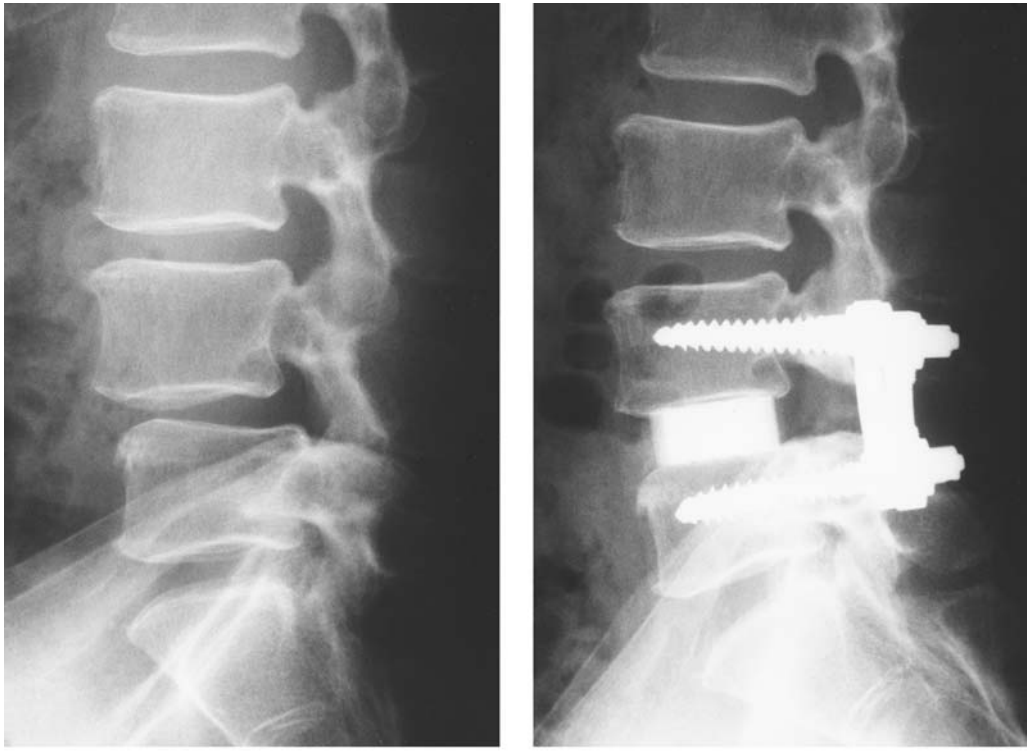

Figure 2 Lateral radiographs in a 63-year-old man with degenerative spondylolisthesis in L4–5 obtained before surgery (A), one year after surgery (B), and 5 years after surgery (C). Posterior lumbar interbody fusion was performed with the AW-GC intervertebral spacer and the Akita Pedicle Screw System. Bone union (trabecular bony bridging) was observed by time. No radiolucent zones around the AW-GC spacer and pedicle screws were seen.

was performed in all cases. Correction loss was defined an increase in kyphosis greater than 3 degrees or slippage of more than 2 mm. Screw loosening was defined as positive when a radiolucency of 1 mm or wider at the bone/screw interface was observed on plain radiograms.

At final follow-up, there was a case with a loss of correction (Table 2). Compression fracture in an upper vertebra adjacent to the fused segment was observed in four osteoporotic cases. Disc herniation of a disc space adjacent to the fused segment was also observed in two cases. Screw loosening and breakage were observed in four cases and one case, respectively. In regard to complications with the AW-GC spacer, one case developed L5 radiculopathy caused by an AW-GC spacer protrusion into the spinal canal 3 months after the operation. Breakage of an AW-GC spacer also developed in one case with no symptoms.

PLIF performed by our procedure was therefore associated with a very low incidence of osteosynthesis failure, such as screw loosening, breakage, and loss of correction ($<3\%$) [45]. Complications related to the AW-GC intervertebral spacer were reported in only 2 of 117 patients (1.7%) [45]. Based on these results, we concluded that our PLIF procedure is effective in treating lumbar degenerative disorders and that the AW-GC spacer is useful in the clinical application of PLIF.

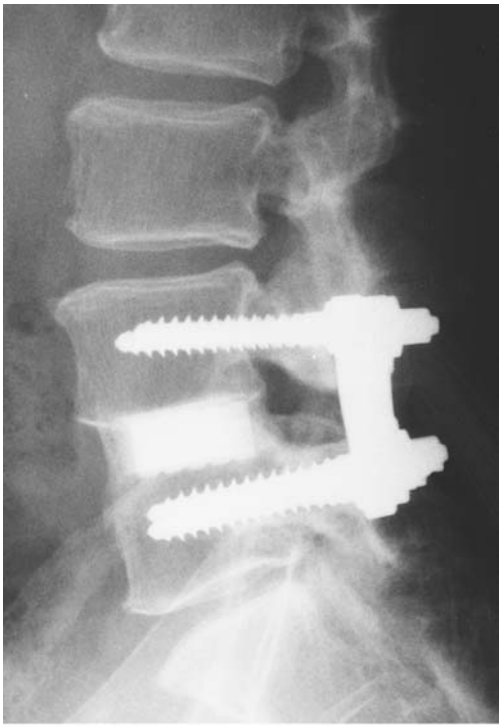

C

Figure 2 Continued.

Table 2 Postoperative Radiological Complications of PLIF with Pedicle Screw Fixation

	DGS ($n = 79$)	ISO ($n = 56$)	Degenerative scoliosis ($n = 6$)	Failed back ($n = 4$)	Others ($n = 3$)	Total ($n = 148$)
Screw loosening	3	1				4
Screw breakage	1					1
Correction loss	1					1
AW-GC protrusion	1					1
AW-GC breakage	1					1
Compression fracture of adjacent vertebra	2		2			4
Hemiation of adjacent disc	1	1				2

DGS, Degenerative spondylolisthesis; ISO, isthmic spondylosis/-olisthesis.
AW-GC spacers were used in 117 patients.
Source: Ref. 45.

VI. FACTORS AFFECTING THE STABILITY OF PEDICLE SCREWS

Pedicle screw fixation has been widely used for spinal fusion or reconstruction after spinal trauma, for degenerative disorders, and for spinal bone tumors, among others disorders [18,29,55,75]. The advantage of immediate rigid fixation with a minimum number of fused segments has been demonstrated in numerous studies. However, implant failures of pedicle screw fixation still occur, in spite of this advantage. Common problems include screw bending, breakage, loosening (radiolucency in the bone–screw interface), and other related failures. In a review of the literature, Esses et al. [17] found a selected survey conducted by the American Back Society that revealed that the rates of screw loosening and breakage were observed in 0.81% (range: 0.6–11%) and 2.9% (range: 0.6–25%) of 617 cases, respectively.

The stability of pedicle screws is mainly dependant on the bone/screw interface. If pedicle screws are inadequately anchored into the vertebral body through the pedicle, the screw can loosen, which could lead to a loss of correction and nonunion. Therefore, to predict development of screw loosening, objective evaluation of the stability in the bone/screw interface is very important. If surgeons could forecast which patients would be likely to develop screw loosening, with the potential increased risk for loss of correction and nonunion, then they could use supplementary augmentation and could choose more careful postoperative management.

Several factors affecting the stability of pedicle screws in vitro, such as the length, outer diameter, design, fitness in the pedicle, bone mineral density (BMD), and elasticity of the cancellous bone, have been mentioned [29]. In particular, a very high correlation between BMD and the stability of pedicle screw has been confirmed [11,14,48,61,70]. Thus, BMD is assumed by many to be a very important factor influencing the stability of pedicle screws.

Only a few studies have described the influence of BMD in vivo on the stability of pedicle screws. Kumano et al. studied the relationship between BMD and the rate of nonunion and loosening in patients in whom pedicle screw fixation augmenting posterolateral fusion was performed and found no statistical difference in the rate of nonunion and screw loosening between patients with high BMD (140.6 $\pm$ 30.0 mg/mL) and low BMD (72.0 $\pm$ 21.2 mg/mL), who had been evaluated by quantitative computed tomography (QCT) [30]. On the contrary, Yasukawa et al. have reported that patients with low BMD determined by QCT have the potential of increased risk of nonunion (94.9 $\pm$ 43.3 mg/mL) and loosening (85.8 $\pm$ 25.2 mg/mL) in pedicle screw fixation augmenting posterolateral fusion [73].

We evaluated the effect of BMD on the mechanical stability of pedicle screws in vitro [48] as well as in vivo [46,47]. In these studies, we proposed a specific threshold for BMD regarding the risk of screw loosening or loss of correction in osteoporotic cases to solve the problem of stability in the bone/screw interface.

VII. A STUDY OF THE MECHANICAL STABILITY OF THE PEDICLE SCREW FOR THE OSTEOPOROTIC SPINE IN VITRO

We evaluated the influence of BMD on the stability of pedicle screws in the human cadaveric lumbar vertebrae [48].

A. Materials and Methods

Spine specimens containing the 3rd, 4th, and 5th lumbar vertebrae were obtained from 15 human cadavers and used in this study. The specimens were preserved in a 1% phenol solution after dissection. The average donor age was 70 years at the time of death (range 49–95 yr). After BMD measurement using QCT (Toshiba E 400, Toshiba Co., Tokyo, Japan), each vertebra was

embedded in methylmethacrylate up to the base of the pedicles for testing. The screw used was an Akita Pedicle Screw, modified by us (outer diameter, 7.0 mm; core diameter, 4.0 mm; thread length, 40 mm; self-tapping type, SUS 316, Mizuho Co., Tokyo, Japan). During screw insertion, the maximum insertional torque was measured by a torque wrench of the Kanon type with a special connector (Nakamura Co., Tokyo, Japan).

Each embedded vertebra was mounted on the Electrohydraulic Materials Testing System (Shimadzu Autograph I-10T, Shimadzu Manufacturing Co., Kyoto, Japan) in which the maximum capacity of the load cell was limited to 4500 N, and the following mechanical tests were performed.

1. The pullout test: determination of the load needed to pull the screw out along its axial direction. The pullout load was defined as the maximum load observed just before an abrupt decrease on a load-displacement curve.
2. The tilting test: determination of the load needed at the screw-plate junction to tilt the screw approximately 4° in the cranial direction. The force was applied parallel to the axial direction. The end of a 3 cm length plate was displaced 2 mm through a universal joint. The displacement was confirmed by a special gauge that showed that the screw had not been displaced in its axial direction (Fig. 3).
3. The cut-up test: determination of the load needed to tip the superior end plate up. For this test, the superior endplate was not embedded in methylmethacrylate. The speed of the cross head was set at 1 mm/min. A typical load-displacement curve for the tilting and cut-up tests is shown in Figure 4. The curve was almost a linear line up to the 2 mm (elastic limit) point. After the 2 mm point, the line gradually curved. The cut-up of the endplate was also defined as an abrupt decrease of force, followed immediately by an increase of force, thereby creating a dip on the curve.

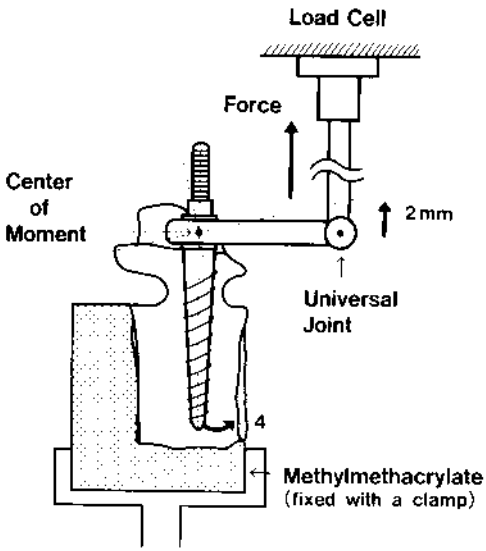

Figure 3 The schema of the apparatus for the tilting and cut-up tests. The load and displacement were measured through the universal joint by the load cell. A solid screw shows the direction of the load and displacement. (From Ref. 48. Published, with permission, from Okuyama K, et al. Stability of transpedicle screwing for the osteoporotic spine. An in vitro study of the mechanical stability. Spine 1993; 18: 2240–2245.)

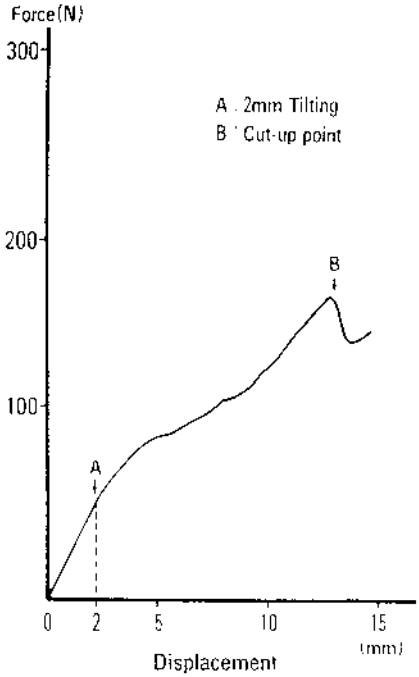

Figure 4 The typical load-displacement curve in the tilting and cut-up tests. The load-displacement curve was almost a linear line up to 2 mm point (A), after which it gradually curved. The cut-up by the screw was detected by a dip (B). (From Ref. 48. Published, with permission, from Okuyama K, et al. Stability of transpedicle screwing for the osteoporotic spine. An in vitro study of the mechanical stability. Spine 1993; 18: 2240–2245.)

B. Results

The mean BMD of lumbar vertebrae was 130 ± 53.2 mg/mL (mean ± SD; $n = 30$). The average maximum insertion torque was 0.4 ± 0.25 Nm. A positive correlation was found between the maximum insertion torque and BMD (Fig. 5). The average pullout force of 582 ± 431.2 N correlated with the BMD ($Y = 5.71X - 115.23$; $r = 0.737$; $n = 15$; $p < 0.01$) and with the maximum insertion torque ($Y = 1431.10X - 67.09$; $r = 0.925$; $n = 15$; $p < 0.01$). The average tilting moment of 2.4 ± 1.21 Nm correlated with BMD (Fig. 6a) and with the maximum insertion torque (Fig. 6b). The average cut-up force of 234 ± 159.9 N correlated with BMD (Fig. 7a) and also with the maximum insertion torque (Fig. 7b). A correlation was also found between the cut-up force and the tilting moment ($Y = 98.07X - 16.82$; $r = 0.797$; $n = 12$; $p < 0.05$).

This study confirmed that the pullout load of pedicle screws (i.e., the stability along its axial direction) was significantly affected by BMD, and that the tilting and cut-up loads (i.e., the stability in the sagittal rotation) were also influenced by BMD. It was suggested that preoperative measurement of BMD is necessary for pedicle screwing in osteoporotic cases. Based on the findings in this study, we concluded that the maximum insertion torque could predict the mechanical stability of pedicle screws.

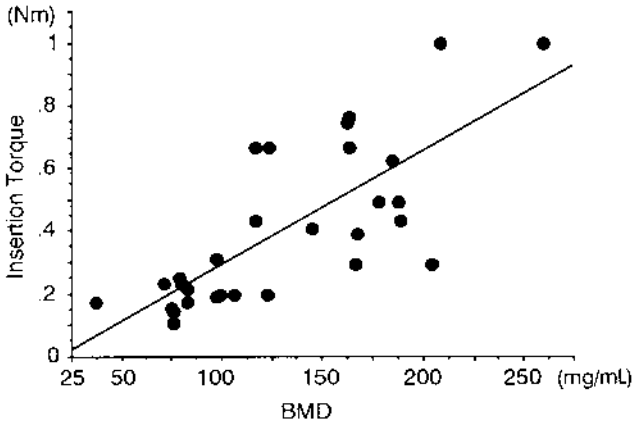

Figure 5 The correlation between the insertion torque and BMD in vitro ($y = 0.004x - 0.064$; $r = 0.755$; $n = 30$; $p < 0.01$). (From Ref. 48. Published, with permission, from Okuyama K, et al. Stability of transpedicle screwing for the osteoporotic spine. An in vitro study of the mechanical stability. Spine 1993; 18: 2240–2245.)

VIII. AN IN VIVO STUDY EVALUATING THE RELATIONSHIP BETWEEN THE INSERTIONAL TORQUE, BMD, AND SCREW LOOSENING IN PLIF

Based on our in vitro study [48], we performed an in vivo study to investigate the in vivo relationship between the intraoperative insertional torque of pedicle screws and BMD of the vertebra and whether the insertional torque could predict the development of screw loosening in PLIF.

A. Materials and Methods

In this study, the insertional torque of pedicle screws was intraoperatively measured in 62 consecutive patients (25 men and 37 women) in the time period between 1994 and 1996. The average age of the subjects was 58 years (range 34–74 yr) at the time of pedicle screw fixation augmenting PLIF. Disorders were divided into the following classes: degenerative spondylolisthesis (35 patients), isthmic spondylolysis and spondylolisthesis (21 patients), degenerative scoliosis (2 patients), and others (4 patients). Monosegmental and bisegmental fusion was done in 55 cases and in 7 cases, respectively. The mean follow-up period was 2.7 years (range 2–4.5 yr). PLIF was performed using the AW-GC spacer along with autologous iliac bone and the Akita Pedicle Screw System (Mizuho Co., Tokyo, Japan) [1,43,44]. A screw with an outer diameter of 7.0 mm was consecutively introduced in all patients. A screw made of stainless steel (SUS316) was used in 45 patients, and a titanium screw (Ti-6Al-4V) was used in 17 patients.

The insertional torque was measured as the same manner as in the previous in vitro study by us [48]. The BMD of L2 or L3 vertebra was quantitatively measured in the anteroposterior view by the dual energy x-ray absorptiometry (DXA) (Hologic QDR-4500SL, Waltham, MA). Screw loosening was defined as positive when a radiolucency of 1 mm or wider at the bonescrew

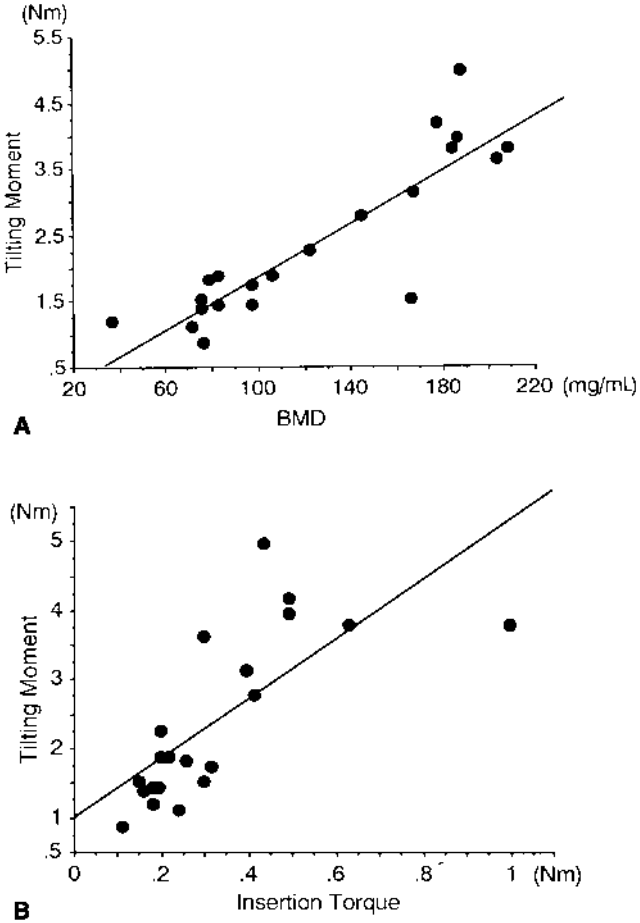

Figure 6 (a) The correlation between the tilting moment and BMD ($y = 0.020x - 0.090$, $r = 0.882$, $n = 21$, $p < 0.01$). (b) The correlation between tilting moment and insertion torque ($y = 4.30x + 1.02$; $r = 0.732$; $n = 21$; $p < 0.01$). (From Ref. 48. Published, with permission, from Okuyama K, et al. Stability of transpedicle screwing for the osteoporotic spine. An in vitro study of the mechanical stability. Spine 1993; 18: 2240–2245.)

interface was observed on plain radiograms. Development of osteoporotic compression fractures in the adjacent vertebrae was also evaluated.

B. Results

There was no significant difference between the mean insertion torque with screw loosening (1.28 ± 0.37 Nm; $n = 4$) and without screw loosening (1.50 ± 0.40 Nm; $n = 52$) (Fig. 8). The insertional torque without screw loosening was significantly higher than that of cases with compression fractures in the upper adjacent vertebra (0.83 ± 0.23 Nm; $n = 3$) ($p < 0.01$).

A quantitative evaluation of BMD with DXA was performed in 21 of 59 cases, whose mean BMD was 0.870 ± 0.233 g/cm^2. A high correlation was found between the mean insertion

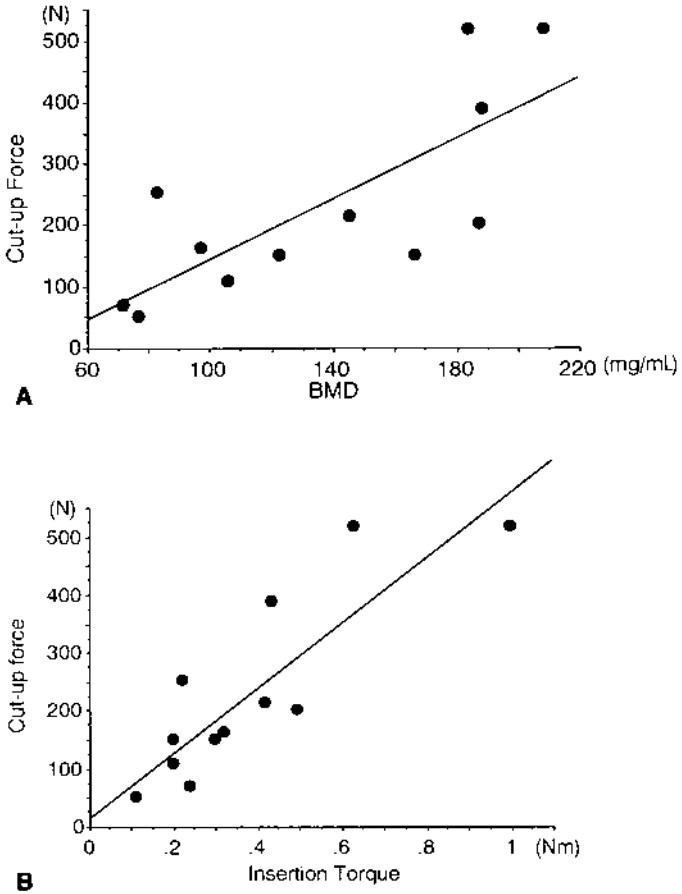

Figure 7 (a) The correlation between the cut-up force and BMD ($y = 2.44x - 97.61$; $r = 0.76$; $n = 12$, $p < 0.01$). (b) The correlation between cut-up force and insertion torque ($y = 558.80x + 24.08$; $r = 0.857$; $n = 12$; $p < 0.01$). Mean ± SD. (From Ref. 48. Published, with permission, from Okuyama K, et al. Stability of transpedicle screwing for the osteoporotic spine. An in vitro study of the mechanical stability. Spine 1993; 18: 2240–2245.)

torque and BMD (Fig. 9). Although a high correlation was found between the insertion torque of pedicle screws and BMD in vivo, the insertion torque could not objectively predict screw loosening.

IX. AN IN VIVO STUDY EVALUATING THE RELATIONSHIP BETWEEN BMD AND SCREW LOOSENING, LOSS OF CORRECTION, AND NONUNION IN PLIF IN THE OSTEOPOROTIC SPINE

We further investigated the in vivo relationship between BMD and screw loosening, loss of correction, and nonunion in patients who had undergone PLIF [47].

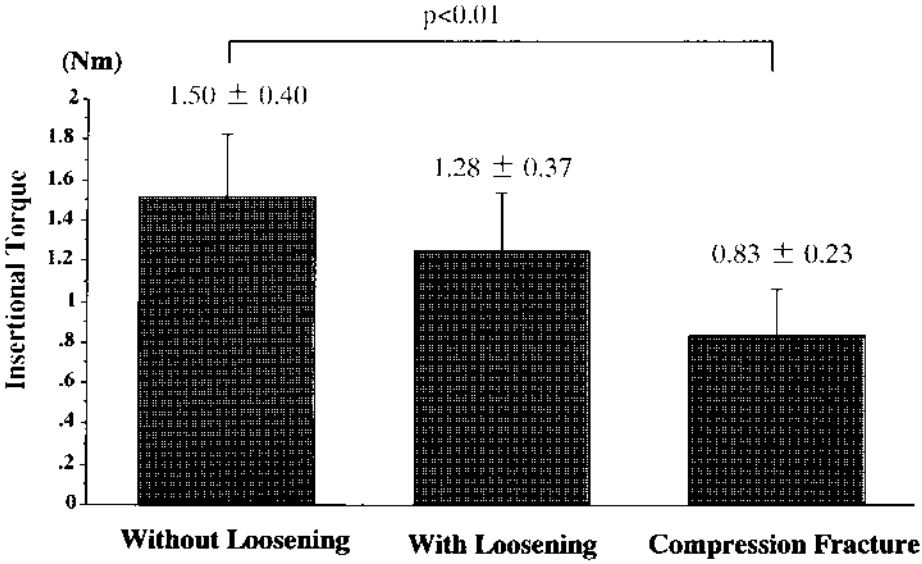

Figure 8 Means of the insertional torque in patients with screw loosening ($n = 4$), without screw loosening ($n = 52$), and with compression fractures in the upper adjacent vertebrae ($n = 3$), in patients who underwent PLIF. The mean insertional torque in cases without screw loosening was significantly higher than that of patients with compression fractures ($p < 0.01$). Mean ± SD. (From Ref. 46. Published, with permission, from Okuyama K, et al. Can insertional torque predict screw loosening and related failures? An in vivo study of pedicle screw fixation augmenting posterior lumbar interbody fusion. Spine 2000; 25: 858–864.)

A. Materials and Methods

Fifty-two consecutive patients (13 men, 39 women) in the time period between 1994 and 1998 were included in this study. The average age of patients at the time of surgery was 63 years (range 45–76 yr). The patients in this study were more osteoporotic than patients in our previous studies [45,46] because their mean age was higher and there were many female subjects. The disorders were divided into the following: degenerative spondylolisthesis (41 patients), isthmic spondylolisthesis (8 patients), degenerative scoliosis (2 patients), and lumbar disc herniation (1 patient). Monosegmental and bisegmental fusion was performed in 41 patients and in 11 patients, respectively. The mean follow-up period was 2.8 years (range 2–6 yr). PLIF was performed using the AW-GC spacer along with autologous bone and the Akita Pedicle Screw System (Mizuho Co., Tokyo, Japan) [1,43,44]. A screw with an outer diameter of 7.0 mm was consecutively introduced in all patients. A screw made of stainless steel (SUS316) was used in 12 patients, while a titanium screw (Ti-6Al-4V) was used in 40 patients.

BMD measurement by DXA, determination of screw loosening, and loss of correction on plain radiograms were the same as those described in the previous studies explained above [45,46]. If there was no movement seen on the lateral view in the flexion-extension and continuity of trabecular bony bridging between the grafted bone and the fused segment, it was termed ''union.'' If there was any movement seen on the lateral view in the flexion-extension or discontinuity of the trabecular bony bridging, it was termed ''nonunion.'' It was also termed ''undetermined union'' if continuity of the trabecular bony bridging was vague in spite of no movement

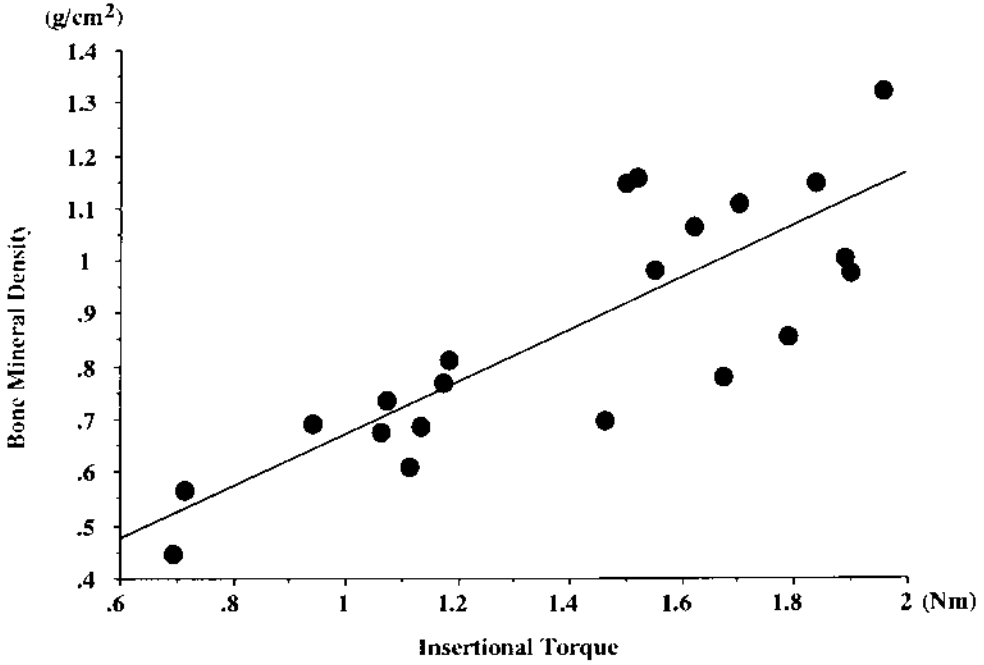

Figure 9 The correlation between the insertional torque and BMD in patients who underwent PLIF ($y = 448.8x + 185.0$; $r^2 = 0.679$; $n = 21$; $p < 0.01$). (From Ref. 46. Published, with permission, from Okuyama K, et al. Can insertional torque predict screw loosening and related failures? An in vivo study of pedicle screw fixation augmenting posterior lumbar interbody fusion. Spine 2000; 25: 858–864.)

of the fixed segment in the flexion-extension. The relationships between BMD, screw loosening, and its related failures were analyzed.

B. Results

In all, 29 of 230 screws (12.6%) in 11 of 52 patients (21.2%) loosened. The mean latency of screw loosening was 7 months (range 3–12 months) after surgery. ''Nonunion'' and ''undetermined union'' was observed in 4 (7.6%) and 8 (15.3%) of the patients, respectively. Loss of correction was found in all patients of ''nonunion,'' and 2 patients of ''undetermined union.'' Forty patients without screw loosening demonstrated ''union.'' One patient without screw loosening showed an ''undetermined union.'' The BMD of patients with screw loosening (0.720 ± 0.078 g/cm^2; $n = 11$) was significantly lower than the BMD of patients without loosening screws (0.922 ± 0.221 g/cm^2; $n = 41$) ($p < 0.01$) (Fig. 10). The BMD of patients with ''union'' (0.934 ± 0.210 g/cm^2; $n = 40$) was significantly greater than of patients with ''nonunion'' (0.674 ± 0.104 g/cm^2; $n = 4$) and ''undetermined union'' (0.710 ± 0.116 g/cm^2; $n = 9$) ($p < 0.05$) (Fig. 11).

In this study we found a significant difference of the mean BMD of the patients with and without screw loosening. Moreover, the mean BMD of patients with ''union'' was significantly greater than of patients with ''nonunion'' and ''undetermined union.'' Based on the findings of this study, we propose that the BMD values of 0.720 ± 0.078 g/cm^2 and 0.674 ± 0.104 g/

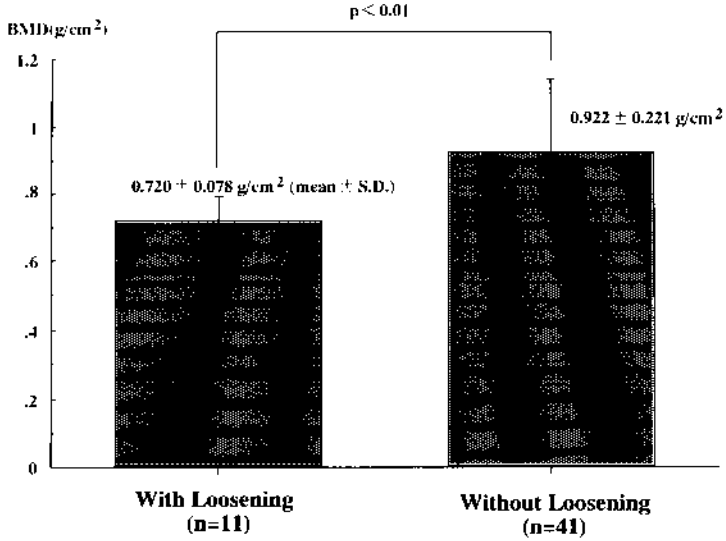

Figure 10 Means of BMD in patients with screw loosening ($n = 11$), without screw loosening ($n = 41$), in patients who underwent PLIF. The mean BMD in patients without screw loosening was significantly higher than that in patients with screw loosening ($p < 0.01$). Mean ± SD. (From Ref. 47. Reprinted from *The Spine Journal, Vol 1*, Okuyama, K., et al., Influence of bone mineral density on pedicle screw fixation: a study of pedicle screw fixation augmenting posterior lumbar interbody fusion in elderly patients, Pages 402–407, Copyright 2001, with permission from Elsevier Science.)

cm^2 in DXA are specific thresholds below which screw loosening and nonunion develop when pedicle screw fixation is performed in conjunction with PLIF.

X. STRATEGIES TO IMPROVE PULLOUT STRENGTH OF THE PEDICLE SCREW

When pedicle screwing is used in elderly patients with low BMD, various complications, such as screw loosening or loss of correction, often occur [19,30,47]. Therefore, establishing a method that minimizes such complications is a priority. Various biomechanical studies have been performed in which attempts have been made to enhance the pullout strength of pedicle screws by optimizing the diameter, depth, or direction of a screw, and by bone cementing [8,29,50,59,61,75]. However, all of these procedures are associated with the possibility of neurological or vascular injury. In particular there is a risk of perforating the medial or inferior wall of the pedicle and the anterior wall of the vertebra by screwing [69]. Making a connection between bilateral pedicle screws in the same vertebra using a coupler has been proposed as one method of enhancing pullout strength. This method is simple and safe. Ruland et al. [56] reported the strengthening of transpedicle screw fixation by screw coupling.

XI. AN IN VITRO STUDY TO IMPROVE THE PULLOUT STRENGTH OF THE PEDICLE SCREW BY SCREW COUPLING

We have also investigated the efficacy of screw coupling in improving the pullout strength of pedicle screws [64]. In addition, we have further examined the effect of the stiffness of a screw

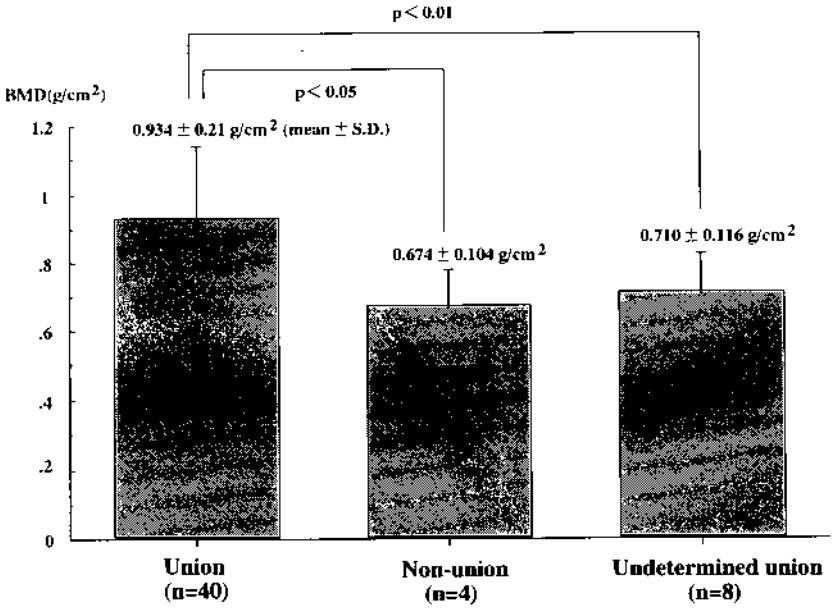

Figure 11 Means of BMD in patients with ''union'' ($n = 40$), with ''nonunion'' ($n = 4$), and with ''undetermined union'' ($n = 8$), in patients who underwent PLIF. The mean BMD in patients with ''union'' was significantly higher than that in patients with ''nonunion'' and ''undetermined union'' ($p < 0.05$ and $p < 0.01$, respectively). Mean + SD. (From Ref. 47. Reprinted from *The Spine Journal, Vol 1*, Okuyama, K., et al., Influence of bone mineral density on pedicle screw fixation: a study of pedicle screw fixation augmenting posterior lumbar interbody fusion in elderly patients, pages 402–407. Copyright 2001, with permission from Elsevier Science.)

coupler and BMD on the enhancement of the pullout strength of pedicle screws for screw coupling in the osteoporotic spine [64].

A. Materials and Methods

Spine specimens containing the 3rd to 5th lumbar vertebrae were obtained from 33 human cadavers and used in this study. The average donor age was 69 years at the time of death (range 46–89 years). The preparation of specimens, measurement of BMD by QCT, and pedicle screws used were the same as in the previous in vitro study explained earlier [48]. The screw coupler was made of stainless steel (6.0 mm in center width; 2.3 mm in thickness). The bending strength of the coupler was determined from the elastic limit in a three-point bending test with an interfulcral distance of 30 mm and was found to be 52.0 kgf.

The specimens were mounted on the Electrohydraulic Materials Testing System described earlier [48]. The shanks of the pedicle screws were jointed using a purpose-designed connector that allowed a rotational movement of the screws in the axial plane of the vertebra. The connectors of both screws were parallel to each other, and pullout force was applied in a posterior direction perpendicular to the coronal plane of the vertebra (Fig. 12). Pullout tests were carried out in the three series: screws without screw coupling (control group), screws connected by a single

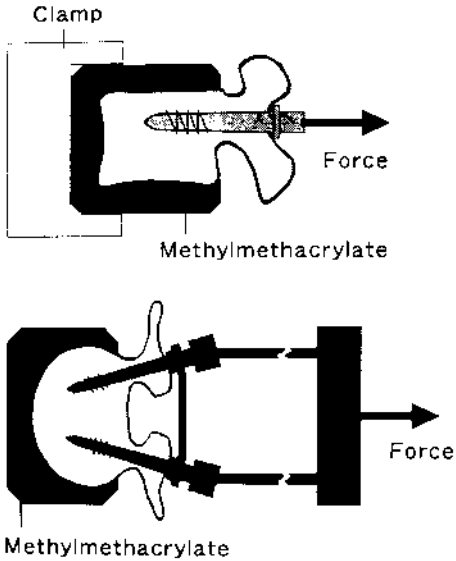

Figure 12 Schema of apparatus for pullout test. A posterior force was applied to each screw. (From Ref. 64. Published, with permission, from Suzuki T, et al. Improving the pullout strength of pedicle screws by screw coupling. J Spinal Disord 2001; 14: 399–403.)

screw coupler (single coupler group), and screws connected by double screw couplers (double coupler group).

B. Results

The average peak pullout strength in the control group was 909.3 ± 188.6 N. The single and double coupler groups exhibited approximately a 150% increase in pullout strength, an increase that was significantly different from that of the control group ($p < 0.05$) (Table 3). No significant difference in peak pullout strength was detected between the single and double coupler groups. The single and double coupler groups exhibited significantly smaller displacements at maximum pullout strength compared to control group ($p < 0.05$). The pullout strength at 1 mm displacement under initial loading was analyzed in order to evaluate the initial stability of the screws. The single and double coupler groups exhibited a significantly greater pullout strength than the control group ($p < 0.05$) in this case as well.

In order to investigate the effectiveness of screw coupling on enhancing pullout strength in osteoporotic spines, the control and coupler groups were divided into a high BMD group (≥90 mg/mL) and a low BMD group (<90 mg/mL). This criterion value of BMD was selected as the value for deciding whether a sample was osteoporotic or not. Pullout strength with screw coupling was significantly higher than without coupling in the high BMD group (Fig. 13). In the low BMD group, however, pullout strength with screw coupling was increased, but this increase was not statistically significant.

This study suggests that the coupling of the pedicle screw improves pullout strength. In addition, this study showed how the pullout strength obtained using the pedicle screw system is enhanced by screw coupling in reference to the grade of osteoporosis. Pullout strength was also improved but not significantly by screw coupling in the group with a BMD of less than

Table 3 Pullout Strength and Displacement of Screws With or Without Screw Coupling

Group	*n*	Peak pullout strength (N)	Displacement of screws (mm)[a]	Pullout strength at 1 mm displacement (N)
Control	9	909.3 ± 88.6	2.77 ± 0.53	531.8 ± 201.6
Single coupler	9	1409 ± 469.1**	2.05 ± 0.66**	1027.7 ± 310.0*
Double coupler	9	1494.0 ± 691.6**	1.81 ± 0.65*	1009.4 ± 358.9**

Mean ± SD.

[a] Displacement of the screws at the peak pullout strength from the initial loading.

*$p<0.001$; **$p<0.05$, compared to control group.

Source: Ref. 64.

90 mg/mL. Thus, the effectiveness of screw coupling may be less than expected in severely osteoporotic spines with less than 90 mg/mL BMD. Therefore, we concluded that the coupling of pedicle screws using a stiff screw coupler was found to enhance pullout strength in mild or moderately osteoporotic spines. In severely osteoporotic spines, however, the degree of strengthening was lower. Further clinical in vivo studies investigating screw coupling are needed.

XII. STRATEGIES TO IMPROVE INITIAL STABILITY OF PEDICLE SCREWING AUGMENTING PLIF

With the osteoporotic spine in mind, Yerby et al. demonstrated that the use of a laminar hook with pedicle screw can significantly reduce migration of the screw into the endplate in osteopo-

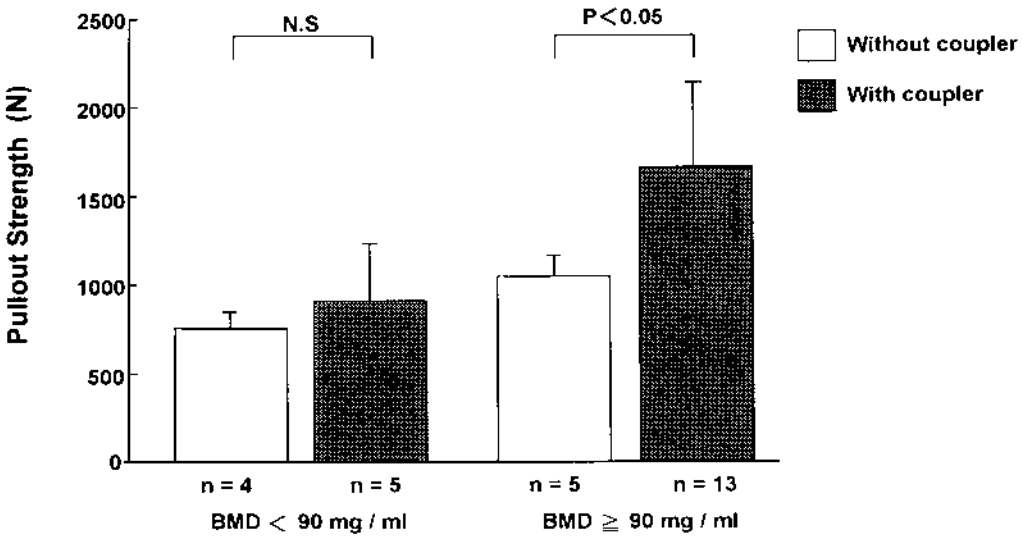

Figure 13 Screw coupling and pullout strength of screws for BMD groups. Mean ± SD. (From Ref. 64. Published, with permission, from Suzuki T, et al. Improving the pullout strength of pedicle screws by screw coupling. J Spinal Disord 2001; 14: 399–403.)

rotic cadavers [74]. Hasegawa et al. reported that stiffness of the pedicle screw in the bone–screw interface is significantly enhanced by adding a laminar hook [21]. Hilibrand et al. studied the efficacy of the pediculolaminar fixation in the compromised pedicle bone [23]. Lotz et al. suggested that augmentation with the carbonated apatite cancellous bone cement can enhance immediate screw fixation [37]. These biomechanical studies support an advantage of using the laminar hook or the carbonated apatite cement to reduce the risk of screw loosening and nonunion in pedicle screw fixation. However, these supplementary instrumentation procedures should be used only for the patients in whom screws are going to loosen. Considering our in vivo results [47], patients with a mean BMD of less than 0.674 ± 0.104 g/cm^2 by DXA could be good candidates for these supplementary procedures.

XIII. CONCLUSIONS

Our clinical study of PLIF using a bioactive ceramic intervertebral spacer (the AW-GC spacer) and the Akita Pedicle Screw System showed that screw loosening, breakage, and loss of correction were less than 3%, and that complications with the AW-GC spacer were 1.7%. We conclude that this procedure is satisfactory and that the AW-GC intervertebral spacer for PLIF is ideal for conserving the grafted bone and for stabilizing fused segments immediately after surgery.

The pullout load, tilting load, and cut-up load of the pedicle screws were significantly affected by BMD in vitro. High correlation was found between the insertion torque of pedicle screws and BMD in vivo as well as in vitro. A significant difference of the BMD of the lumbar spine with and without screw loosening was also found in vivo. Therefore, we conclude that BMD should be considered as a very important factor that influences the development of screw loosening. To minimize the screw loosening induced by low BMD, the pedicle screw coupler was considered. The coupling of pedicle screws using a stiff screw coupler was found to enhance the pullout strength in mild or moderately osteoporotic spines. However, in severe osteoporotic spines, the degree of strengthening was lower.

REFERENCES

1. Abe E, Arai M, Sato K, Yamamoto M, Chiba M, Mizutani Y. Pedicular screw fixation for the unstable spine (in Japanese with English abstract). Orthop. Surg. Traumatol 1991; 34:455–461.
2. Agazzi S, Reverdin A, May D. Posterior lumbar interbody fusion with cages: an independent review of 71 cases. J. Neurosurg 1999; 91:186–192.
3. Ani N, Keppler L, Biscup RS, Steffee AD. Reduction of high-grade slips (grades III-V) with VSP instrumentation: report of a series of 41 cases. Spine 1991; 16:S302–310.
4. Ashman RB, Galpin RD, Corin JD, Johnston CE. Biomechanical analysis of pedicle screw instrumentation systems in a corpectomy model. Spine 1989; 14:1398–1405.
5. Brantigan JW, McAfee PC, Cunningham BW, Wang H, Orbegoso CM. Interbody lumbar fusion using a carbon fiber cage implant versus allograft bone: an investigational study in the Spanish goat. Spine 1994; 19:1436–1444.
6. Brantigan JW, Steffee AD. A carbon fiber implant to aid interbody lumbar fusion. Two-year clinical results in the first 26 patients. Spine 1993; 18:2106–7.
7. Brantigan JW, Steffee AD, Geiger JM. A carbon fiber implant to aid interbody lumbar fusion. Mechanical testing. Spine 1991; 16:S277–282.
8. Brantley AGU, Mayfield JK, Koeneman JB, Clark KR. The effect of pedicle screw fit: an in vitro study. Spine 1994; 19:1752–1758.
9. Briggs H, Milligan PR. Chip fusion of the low back following exploration of the spinal canal. J. Bone. Joint. Surg 1944; 26A:125–130.

10. Capener N. Spondylolisthesis. Br. J. Surg 1932; 19:374–386.
11. Carlson GD, Abitbol JJ, Anderson DR, Krag MH, Kostuik JP, Woo SL, Garfin SR. Screw fixation in the human sacrum. An in vitro study of the biomechanics of fixation. Spine– 1992; 17.
12. Cloward RB. The treatment of ruptured lumbar intervertebral discs by vertebral body fusion. J. Neurosurg 1953; 10:154–168.
13. Cloward RB. Posterior lumbar interbody fusion updated. Clin. Orthop 1985; 193:16–19.
14. Coe JD, Warden KE, Herzig MA, McAfee PC. Influence of bone mineral density on the fixation of thoracolumbar implants: a comparative study of transpedicular screws, laminar hooks, and spinous process wires. Spine 1990; 15:902–907.
15. Collis JS. Total disc replacement: a modified posterior lumbar interbody fusion. Report of 750 cases. Clin. Orthop 1985; 193:16–19.
16. Dietl RH, Krammer M, Kettler A, Wilke HJ, Claes L, Lumenta CB. Pullout test with three lumbar interbody fusion cages. Spine 2002; 27:1029–1036.
17. Esses SI, Sachs BL, Dreyzin V. Complications associated with the technique of pedicle screw fixation. A selected survey of ABC members. Spine 1993; 18:2231–2239.
18. Gurr KR, McAfee PC. Cotrel-Dubousset instrumentation in adults: a preliminary report. Spine 1988; 13:510–520.
19. Halvorson TL, Kelley LA, Thomas KA, Whitecloud TS, Cook SD. Effects of bone mineral density on pedicle screw fixation. Spine 1994; 19:2415–2420.
20. Harms J, Stoltze D. The indications and principles of correction of post-traumatic deformities. Eur. Spine J 1992; 1:142–151.
21. Hasegawa K, Takahashi HE, Uchiyama S, Hirano T, Hara T, Washio T, Sugiura T, Youkaichiya M, Ikeda M. An experimental study of a combination method using a pedicle screw and laminar hook for the osteoporotic spine. Spine 1997; 22:958–962.
22. Hashimoto T, Shigenobu K, Kanayama M, Harada M, Oha F, Ohkoshi Y, Tada H, Yamamoto K, Yamane S. Clinical results of single-level posterior lumbar interbody fusion using the Brantigan I/F carbon cage filled with a mixture of local morselized bone and bioactive ceramic granules. Spine 2002; 27:258–262.
23. Hilibrand AS, Moore DC, Graziano GP. The role of pediculolaminar fixation in compromised pedicle bone. Spine 1996; 21:445–451.
24. Hu SS. Internal fixation in the osteoporotic spine. Spine– 1997; 22.
25. Hutter CG. Posterior intervertebral body fusion: a 25-year study. Clin. Orthop 1983; 179:86–96.
26. Ido K, Asada Y, Sakamoto T. A new-type titanium intervertebral spacer and its insertion device used in posterior lumbar interbody fusion. Biomed. Mater. Eng 2000; 10:127–130.
27. Kaneda K, Asano S, Hashimoto T, Satoh S, Fujiya M. The treatment of osteoporotic-posttraumatic vertebral collapse using the Kaneda device and a bioactive ceramic vertebral prosthesis. Spine 1992; 17:S295–303.
28. Kokubo T, Shigematsu M, Nagashima Y, Tashiro M, Nakamura T, Yamamuro T, Higashi S. Apatite- and wollastonite-containing glass-ceramics for prosthetic application. Bull. Inst. Chem. Res., Kyoto Univ 1982; 60:260–268.
29. Krag MH, Beynnon BD, Pope MH, Frymoyer JW, Haugh LD, Weaver DL. An internal fixator for posterior application to short segments of the thoracic, lumbar, or lumbosacral spine: Design and testing. Clin. Orthop 1986; 203:75–98.
30. Kumano K, Hirabayashi S, Ogawa Y, Aota Y. Pedicle screws and bone mineral density. Spine 1994; 19:1157–1161.
31. Kuslich SD, Ulstrom CL, Griffith SL, Ahern JW, Dowdle JD. The Bagby and Kuslich method of lumbar interbody fusion. History, techniques, and 2-year follow-up results of a United States prospective, multicenter trial. Spine 1998; 23:1267–1278.
32. Le Huec JC, Liu M, Skalli W, Josse L. Lumbar lateral interbody cage with plate augmentation: in vitro biomechanical analysis. Eur. Spine J 2002; 11:130–136.
33. Lee CK, Vessa P, Lee JK. Chronic disabling low-back pain syndrome caused by internal disc derangements: the results of disc excision and posterior lumbar interbody fusion. Spine 1995; 20:356–361.
34. Lin PM. Posterior lumbar interbody fusion technique: complications and pitfalls. Clin. Orthop 1985; 193:90–102.

35. Lin PM, Cautilli RA, Joyce MF. Posterior lumbar interbody fusion. Clin. Orthop 1983; 180:154–168.
36. Loguidice VA, Johnson RG, Guyer RD, Stith WJ, Ohnmeiss DD, Hochschuler SH, Rashbaum RF. Anterior lumbar interbody fusion. Spine 1988; 13:366–369.
37. Lotz JC, Hu CC, Chiu DFM, Yu M, Colliou O, Poser RD. Carbonated apatite cement augmentation of pedicle screw fixation in the lumbar spine. Spine 1997; 22:2716–2723.
38. Ma GWC. Posterior lumbar interbody fusion with specialized instruments. Clin. Orthop 1985; 193: 57–63.
39. Mardjetko SM, Connolly PJ, Shott S. Degenerative lumbar spondylolisthesis. A meta-analysis of literature 1970–1993. Spine 1994; 19:S2256–2265.
40. Moeini SM, Nasca RJ, Lemons JE, Montgomery RD. Intervertebral spacer as an adjunct to anterior lumbar fusion. Part I. Design, fabrication, and testing of three prototypes. J. Spinal Disord 1998; 11: 129–135.
41. Nachemson AL. Disc pressure measurements. Spine 1981; 6:93–97.
42. Nibu K, Panjabi MM, Oxland T, Cholewicki J. Multidirectional stabilizing potential of BAK interbody spinal fusion system for anterior surgery. J. Spinal Disord 1997; 10:357–362.
43. Okuyama K, Abe E, Ishikawa N, Sato K. The mechanical strength and influence of titanium pedicle screw on MR image (in Japanese with English abstract). Spine Spinal Cord 1995; 8:501–507.
44. Okuyama K, Abe E, Sato K, Kamata S, Nagata H, Miyano T. Bending strength and pull-out force of pedicle screws (in Japanese with English abstract). Orthop. Surg. Traumatol 1993; 36:1357–1363.
45. Okuyama K, Abe E, Suzuki T, Tamura Y, Chiba M, Sato K. Posterior lumbar interbody fusion: a retrospective study of complications after facet joint excision and pedicle screw fixation in 148 cases. Acta Orthop. Scand 1999; 70:329–334.
46. Okuyama K, Abe E, Suzuki T, Tamura Y, Chiba M, Sato K. Can insertional torque predict screw loosening and related failures? An in vivo study of pedicle screw fixation augmenting posterior lumbar interbody fusion. Spine 2000; 25:858–864.
47. Okuyama K, Abe E, Suzuki T, Tamura Y, Chiba M, Sato K. Influence of bone mineral density on pedicle screw fixation: a study of pedicle screw fixation augmenting posterior lumbar interbody fusion in elderly patients. Spine J 2001; 1:402–407.
48. Okuyama K, Sato K, Abe E, Inaba H, Shimada Y, Murai H. Stability of transpedicle screwing for the osteoporotic spine. An in vitro study of the mechanical stability. Spine 1993; 18:2240–2245.
49. Onesti ST, Ashkenazi E. The Ray threaded fusion cage for posterior lumbar interbody fusion. Neurosurgery 1998; 42:200–205.
50. Pfeifer BA, Krag MH, Johnson C. Repair of failed transpedicle screw fixation. A biomechanical study comparing polymethylmethacrylate, milled bone, and matchstick bone reconstruction. Spine 1994; 19:350–353.
51. Pfeiffer M, Griss P, Haake M, Kienapfel H, Billion M. Standardized evaluation of long-term results after anterior lumbar interbody fusion. Eur. Spine J 1996; 5:299–307.
52. Pilliar RM, Lee JM, Maniatopoulos C. Observations on the effect of movement on bone ingrowth into porous-surfaced implants. Clin. Orthop 1986; 208:108–113.
53. Prolo DJ, Oklund SA, Butcher M. Toward uniformity in evaluating results of lumbar spine operations. A paradigm applied to posterior lumbar interbody fusions. Spine 1986; 11:601–606.
54. Ray CD. Threaded titanium cages for lumbar interbody fusions. Spine 1997; 22:667–679.
55. -Camille R, Saillant G, Mazel C. Internal fixation of the lumbar spine with pedicle screw plating. Clin. Orthop 1986; 203:7–17.
56. Ruland CM, McAfee PC, Warden KE, Cunningham BW. Triangulation of pedicular instrumentation: a biomechanical analysis. Spine 1991; 16:S270–276.
57. Schultz A, Andersson G, Ortengren R, Haderspeck K, Nachemson A. Loads on the lumbar spine. Validation of a biomechanical analysis by measurements of intradiscal pressures and myoelectric signals. J. Bone Joint Surg 1982; 64A:713–720.
58. Shimizu K, Iwasaki R, Matsushita M, Yamamuro T. Posterior lumbar interbody fusion using AW-GC vertebral spacer. In: Yamamuro T, et al, ed. Bioceramics 5. Kobunshi Kankokai. Kyoto, 1992: 435–441.
59. Skinner R, Maybee J, Transfeldt E, Venter R, Chalmers W. Experimental pullout testing and comparison of variables in transpedicular screw fixation: a biomechanical study. Spine 1990; 15:195–201.

60. Soini J. Lumbar disc space heights after external fixation and anterior interbody fusion: a prospective 2-year follow-up of clinical and radiographic results. J. Spinal Disord 1994; 7:487–494.
61. Soshi S, Shiba R, Kondo H, Murota K. An experimental study on transpedicular screw fixation in relation to osteoporosis of the lumbar spine. Spine 1991; 16:1335–1341.
62. Steffee AD, Brantigan JW. The variable screw placement spinal fixation system: report of a prospective study of 250 patients enrolled in Food and Drug Administration clinical trials. Spine 1993; 18: 1160–1172.
63. Steffee AD, Sitkowski D. Posterior lumbar interbody fusion and plates. Clin. Orthop 1988; 227: 99–102.
64. Suzuki T, Abe E, Okuyama K, Sato K. Improving the pullout strength of pedicle screws by screw coupling. J. Spinal Disord 2001; 14:399–403.
65. Tencer AF, Hampton D, Eddy S. Biomechanical properties of threaded inserts for lumbar interbody fusion. Spine 1995; 20:2408–2414.
66. Van Dijk M, Smit TH, Sugihara S, Burger EH, Wuisman PI. The effect of cage stiffness on the rate of lumbar interbody fusion: an in vivo model using poly (L-lactic acid) and titanium cages. Spine 2002; 27:682–688.
67. Weiner BK, Fraser RD. Spine update: lumbar interbody cages. Spine 1998; 23:634–40.
68. Wetzel FT, LaRocca SH, Lowery GL, Aprill CN. The treatment of lumbar spinal pain syndromes diagnosed by discography. Lumbar arthrodesis. Spine 1994; 19:792–800.
69. Yahiro MA. Comprehensive literature review. Pedicle screw fixation devices. Spine 1994; 19: S2274–2278.
70. Yamagata M, Kitahara H, Minami S, Takahashi K, Isobe K, Moriya H. Mechanical stability of the pedicle screw fixation systems for the lumbar spine. Spine 1992; 17:S51–54.
71. Yamamuro T, Shikata J, Okumura H, Kitsugi T, Kakutani Y, Matsui T, Kokubo T. Replacement of the lumbar vertebrae of sheep with ceramic prostheses. J. Bone. Joint. Surg 1990; 72B:889–893.
72. Yamamuro T, Shimizu K. Clinical application of AW glass ceramic prosthesis in spinal surgery. J. Jpn. Orthop. Assoc 1994; 68:505–515.
73. Yasukawa Y, Akizuki A, Ryuzawa T, Kobayashi H, Kitahara J. Influence of BMD and BMI on the clinical results of posterolateral fusion for degenerative lumbar spondylolisthesis. J Jpn Spine Res Soc 1999; 10:S254.
74. Yerby SA, Ehteshami JR, McLain RF. Offset laminar hooks decrease bending moments of pedicle screws during in situ contouring. Spine 1997; 22:376–381.
75. Zindrick MR, Wiltse LL, Widell EH, Thomas JC, Holland WR, Field BT, Spencer CW. A biomechanical study of intrapeduncular screw fixation in the lumbosacral spine. Clin. Orthop 1986; 203:99–112.

39

Thoracic Pedicle Screws: Biomechanical Considerations of the Extrapedicular Approach

W. Morgenstern and P. Metz-Stavenhagen
Center of Spine Surgery, Werner Wicker Klinik
Bad Wildungen, Germany

S. J. Ferguson
University of Bern Orthopaedic Biomechanics Division
Bern, Switzerland

I. INTRODUCTION

The use of pedicle screws is an increasingly relevant method which has substantially improved the results in the operative treatment of spine diseases and deformities. A first report of pedicle screws was published over 40 years ago by Boucher, and knowledge of the technique was more widely propagated through the work of Roy-Camille in the 1960s [5,35]. Spine instrumentation with pedicle screws offers a potentially superior construction to instrumentation with hooks, as the pedicle offers the most stable anchorage possibility in the vertebral body. In comparison to ventral instrumentation, biomechanical advantages of pedicle fixation have been found [3,22]. Pedicle screws may be considered today as the gold standard of spinal internal fixation [16]. In connection with rigid longitudinal rods, they are recognized as a stable implant in the sacrum, lumbar spine, and the thoracolumbar junction and allow a three-dimensional control of the instrumented spine. Furthermore, with correct insertion, the spinal canal and neuroforamen are not constricted, as is the case with hook constructions. Recent clinical reviews demonstrate that, with careful patient selection and meticulous surgical technique, pedicle screw fixation is an effective and safe procedure with minimal complications [15,16,26].

There is not yet a consensus on the use of pedicle screw fixation in the thoracic spine. Numerous studies have been undertaken to improve the safety of the technique, in which morphological data about the anatomy of the pedicle in the thoracic region have been collected, as well as clinically oriented studies, which have compared current techniques with new alternatives [10,13,14,30,43]

A. Anatomy of the Thoracic Pedicle

The shape of the thoracic pedicle is complex; they are mostly teardrop or kidney-shaped, laterally concave, and medially convex [34]. Pedicle shapes in the thoracic spine demonstrate significant

regional variation. Morphological differences within a region also have been found, which makes a standardization of the technique difficult. The transverse and horizontal dimensions of the pedicle have been measured in several studies. At the fourth thoracic level, transverse diameters from 3.7 to 6.3 mm have been measured [14,34,51]. In these studies, the outer pedicle diameter has been determined. With these dimensions it appears to be complicated or even impossible to insert even thin pedicle screws with a diameter of 4.5 mm exactly into the pedicle, without the risk of damaging the medial or lateral cortex. On the other hand, the height of the pedicle is not a limiting factor. Here, the smallest dimensions have been measured at the first thoracic level (8.2–9.6 mm). The orientation of the pedicle axis in the transverse plane and the sagittal plane has also been determined. In the transverse plane, Zindrick et al. [51] found an average angle of the pedicle axis to the mid-line of 12.6° at the eighth thoracic level, whereas Panjabi et al. [34] and Ebraheim et al. [14] reported values of 19.5° and 24°, respectively. Substantial variations at other levels have also been measured, which again makes a standardization of thoracic pedicle screw placement difficult. Ebraheim et al. studied the projection of the pedicle axis onto the dorsal structures in order to gain information about the variability of the potential screw entry point. An assumption here is that the ideal entry point lies as near as possible to an extension of the pedicle axis. In this respect, they found somewhat less variable values. Between the third and twelfth thoracic vertebrae, the projections of the pedicle axes were described as 4–5 mm medial of the lateral border of the facet joint and 5–8 mm cranial of the mid-line of the transverse process.

The anatomical relationship of the thoracic pedicle to the adjoining neural structures, i.e., to the superior and inferior nerve roots and the dural sac, has also been meticulously studied. Ebraheim et al. [14] could find no epidural reserve space between the pedicle and the dural sack in the 15 cadaver specimens which were studied. Average distances of 1.9–3.9 mm to the superior nerve root and 1.7–2.8 mm to the inferior were found. This means that towards cranial and caudal, a reserve space between the pedicle and nerve root minimizes the risk of insertion, however no medial deviation can be allowed.

B. Pedicle Screws in the Thoracic Spine

Among spine surgeons, the use of pedicle screws in the thoracic spine remains a controversial theme. In this context, the incidence, extent, and clinical consequences of a penetration of the thoracic pedicle screw medially towards the spinal cord is of special interest. The reason for this fear of screw misplacement is naturally the knowledge of the anatomical conditions in the thoracic spine, as has been described in the previous section: that is, the close proximity of the spinal cord, as well as knowledge of the dimensions of the thoracic pedicle, which is much smaller than the lumbar pedicle [9,10,34,51].

C. Complications

In experimental studies on cadavers, a high incidence of misplaced screws has been found, despite insertion by experienced spine surgeons. Vaccaro et al. [44] reported damage of the pedicle cortex in 41% of 91 screws. Nevertheless, reports of clinical complications due to misplaced pedicle screws in the thoracic spine are rather rare. In 1999, Papin et al. [31] reported on diffuse neurological and abdominal symptoms after an operative scoliosis correction in a 15-year-old girl. Following computer tomographic clarification, a 4 mm pedicle screw was found to be encroaching the spinal canal in the lower thoracic spine. After removal of the screw, the patient recovered completely within a month. In 1996, Donovan et al. [12] described the case of a patient with a thoracolumbar fracture who showed neurological deficits after the operation as well as a continuous flow of spinal

fluid from the wound. The cause of these symptoms could be traced to three intraspinally placed screws, with a shift of the dural sac and a partial impingement of the nerve roots. Also here, the patient recovered completely from these symptoms following removal of the screws. Amiot et al. [1] reported in 2000 about 9 misplaced screws from a total of 70, which had been implanted conventionally in the thoracic spine. On the other hand, only one misplaced screw from 74 was reported for screws implanted with the help of a computer-assisted system. It is difficult to estimate how high the actual number of complications is following the use of pedicle screws in the thoracic spine. It is likely, however, to be much higher than the reported cases.

One unusual screw misplacement was found in a 67-year-old patient who presented 10 years after her scoliosis operation due to low back pain. During the diagnostic clarification, a pedicle screw was discovered in the fifth thoracic vertebra, passing through the middle of the spinal canal, which obviously had been inserted initially in this way. The neurological exploration revealed no deficits. During the revision, the screw was removed. The screw had run 10 mm medial to the pedicle wall, but had only minimally displaced the myelon, as the screw was located on the convex side of the scoliotic curve and the myelon is normally located towards the concave side. It is unlikely that such misplacement with a medially lying myelon would not have caused any neurological complications [28] (Fig. 1).

D. Pedicle Screw Technique in the Thoracic Spine

In order to improve the technique and to optimize safety, numerous studies have been carried out which have focused on both the anatomical relationship of the pedicle to the surrounding structures and on the varying techniques for screw insertion. In this context, entry points have been defined and preparation techniques have been evaluated. Xu et al. [49] compared the oldest technique from

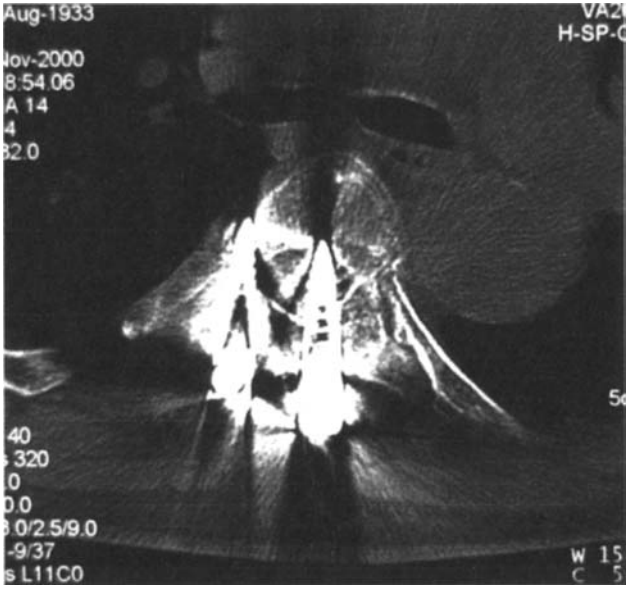

Figure 1 Misplaced thoracic pedicle screws at T5 10 years after scoliosis correction. The fact that the myelon lay on the opposite, concave side of the spinal canal led to this uneventful postoperative course without any neurological symptoms.

Roy-Camille with an open-lamina technique. Roy-Camille defined the entry point of the pedicle screw as the point at which the mid-line of the facet joint meets that of the transverse process (Fig. 2). Xu et al., on the other hand, carried out a partial laminectomy and could therefore palpate the borders of the pedicle in order to determine an exact entry point and a good orientation of the screw [49]. Overall, fewer misplacements have been recorded with the open-lamina technique. However, considering damage to the medial pedicle wall, the incidence for both techniques was comparable at 6%, although the extent of misplacement with Roy-Camille technique was somewhat greater.

In America, the so-called ''funnel technique'' has been favored, in which the entry point is defined through a decortication of the lamina, and a blunt instrument is carefully guided ventrally under the control of an image intensifier to define the screw path [16].

E. Extrapedicular Screw Insertion in the Thoracic Spine

Extrapedicular screw placement was first described by Dvorak et al. [13] in 1993. With this technique, screws are placed laterally to the pedicle. The entry point is found on the outer third of the transverse element tip (Fig. 2). The costotransverse and costovertebral joints are intersected by the screws. This technique guarantees a greater distance from the screw to the spinal canal and also anchors the screw in more cortices (ribs and vertebral body) and in the cancellous bone of the vertebra. In comparison to conventionally placed intrapedicular screws, longer screws can be used with this technique, and therefore the length of the screw/bone interface is increased. Therefore, the technique would appear to be safer. Dvorak et al., in a study of extrapedicular screw placement, was able to insert significantly longer screws and demonstrated a biomechanical advantage by measuring a significantly greater pull-out force. In their conclusions, however, Dvorak et al. wrote that while extrapedicular screw placement was a safe in vitro technique, due to the anatomical variability of the thoracic spine a standardization of the technique was not possible [13].

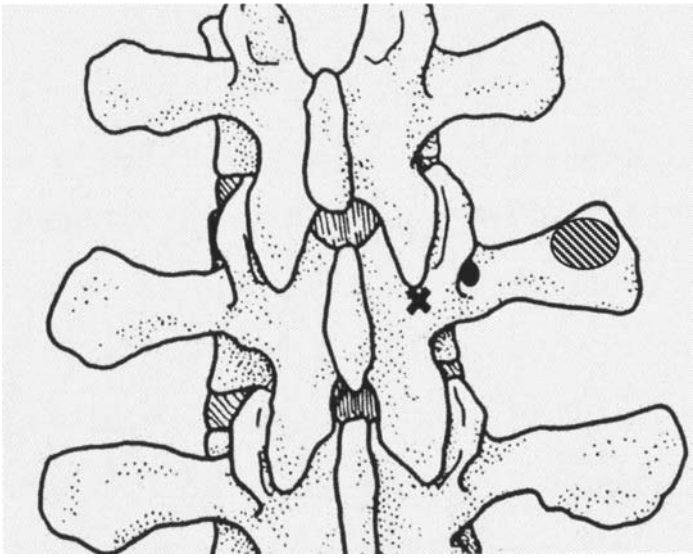

Figure 2 Entry points of different insertion techniques: (cross) RoyCamille's (dot) Weinstein, (hatched) extrapedicular technique.

In another study, the safety of the technique was examined by the definition of anatomical orientation points for screw insertion. An entry point in the proximal third of the tip of the transverse process is defined, with the screw orientation in the sagittal plane perpendicular to the posterior structures. In the transverse plane, the screw is oriented slightly lateral to the superior facet joints, in order to ensure that the screw does not end up too far medially and risk injury to the spinal canal (Fig. 3, 4) [27].

F. Computer-Assisted Screw Insertion

A variety of clinical [1,23,37,38] and experimental [6,29,30] studies have concerned themselves with the advantages and efficiency of computer-assisted pedicle screw placement and have evaluated the technique in terms of safety and accuracy. From 294 screws which were implanted with the computer assisted surgery (CAS) system, Amiot et al. [1] found 16 (5%) misplacements. In the conventionally inserted group, for which only fluoroscopic imaging was available, 81 screws were misplaced, and seven reoperations were required due to misplacement. For four patients, continuous neurological symptoms were present, which for two patients could be traced to the false screw placement. Amiot et al. judged the system to be a valuable instrument with which the safety of pedicle screw placement could be increased and the risk of neurological complications could be minimized.

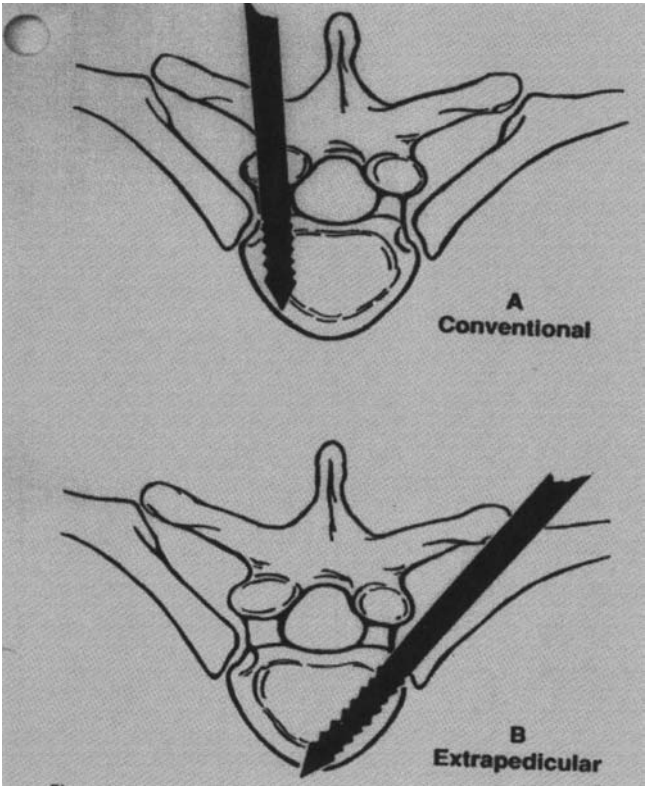

Figure 3 (A) Conventional intrapedicular screw placement and (B) novel extrapedicular technique. Note the distance of the screw to the spinal canal when using the extrapedicular technique

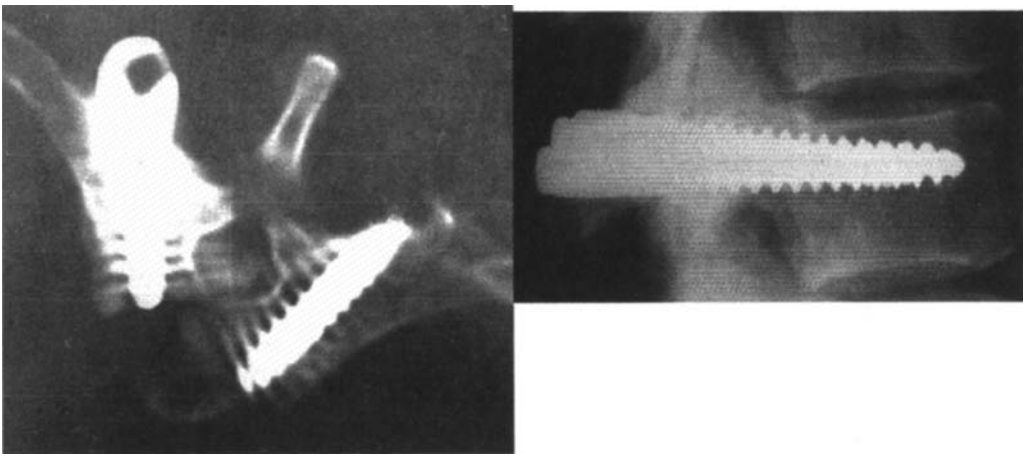

Figure 4 Computer (left) tomograph of an extrapedicular screw (6mm) at T4. Note the distance of the screw to the spinal canal. (Right) Lateral x-ray demonstrating extrapedicular screw placement at T4.

G. Goal of the Study

With the previously published results, information about the safety and pull-out strength of extrapedicular screw placement is available. However, no information is available about the biomechanical behavior of a multisegment thoracic spine construct, i.e., multiple spine segments plus implant. The following study evaluated the biomechanical characteristics of such an extrapedicular construct through motion analysis and fatigue testing and compared these with a construct in which the screws had been implanted intrapedicularly. The hypothesis was that extrapedicular screws would guarantee an equivalent or greater multidirectional spine stability to that of intrapedicular screws.

II. MATERIAL AND METHODS

A. Specimens

For the study, 12 human thoracic spine specimens were used (T4–T8), obtained from 9 male and 3 female cadavers. The donors were between 19 and 87 years old at the time of death. Following harvesting, specimens were preserved in vacuum-sealed plastic bags at -20°C until preparation for testing.

B. Specimen Groups and Bone Density

Due to the limited number of specimens, a randomized group allocation was not possible, as the variation in age, bone density, and kyphosis of the spine specimens was too high. Therefore, the specimens were allocated into two matching groups according to their bone mineral density (BMD) and the measured kyphosis (using Cobb's method). Furthermore, age, size, and weight were documented (Table 1).

Bone density was measured with dual energy x-ray absorptiometry (DEXA) (QDR 1000, Hologic Corporation, Waltham, MA). Bone density measurements were made by sagittal projections of four thoracic vertebrae (T4–T8), and the average for each specimen was documented.

Table 1 Matched Pairs for Intra- and Extrapedicular Screw Insertion

Group	Specimen ID	BMD (g/cm^2)	Sex	Age (y	Cobb angle (°) (T1–T12)	(T4–T8)
			Extrapedicular screws			
I	57	0.725	M	19	3	5
I	76	0.617	M	68	48	21
I	125	0.548	M	75	51	20
I	10	0.530	M	84	30	20
I	70	0.380	F	87	33	40
I	297	0.620	M	25		10
Average		0.570		59.7	33.0	19.3
Std. Dev.		0.116				
			Intrapedicular screws			
II	108	0.716	M	58	52	25
II	107	0.617	M	74	26	10
II	85	0.557	M	79	45	25
II	62	0.523	M	69	68	31
II	66	0.466	F	74	26	15
II	122	0.560	F	69		15
Average		0.573		70.5	43.4	20.2
Std. Dev.		0.086				

The average bone density for both groups was 0.573 ± 0.086 vs. 0.570 ± 0.116 g/cm^2 (Table 1).

C. Specimen Preparation and Instrumentation

Before testing, residual soft tissues were cleaned from the bone. However, to guarantee the biomechanical integrity of the specimen, special efforts were made to preserve all stabilizing structures such as ligaments or joint capsules. The cranial and caudal vertebral bodies were potted in polymethylmethacrylate (PMMA) to provide a solid fixation in a multidirectional testing machine, such that the middle vertebral body was oriented in the horizontal plane.

The AO Universal Spine System (USS) (Mathys Medical, Bettlach, Switzerland) was used for posterior pedicle screw stabilization. The USS incorporates side-opening pedicle screws and 6 mm connecting rods. Pedicle screws with a diameter of 5 mm were inserted between T5 and T8. Screw length was chosen so that the anterior cortex of the vertebra was not perforated. In Table 2, the screw lengths for the intrapedicular and extrapedicular groups are listed. Standardized screw length and accurate and consistent screw placement, either intrapedicularly or extrapedicularly, was ensured through the use of a CAS planning and navigation system (SurgiGate, Medivision, Stratec Medical, Oberdorf, Switzerland). Based on CT data for each specimen, the precise trajectory and length of each pedicle was planned and could be visualized on the computer monitor during specimen preparation. Real-time tracking of a navigated pedicle awl was used to accurately place the entrance point and complete the screw hole. Finally, the rod was placed after it had been contoured to match the position of the screw heads. Pre-bending of the rod should minimize residual stresses from being transferred to the specimen.

Table 2 Data for Screw Length for Intra- and Extrapedicular Screw Placement in Thoracic Spine

T5	T6	T7	T8
Extrapedicular screws			
55	55	55	55
50	55	55	55
55	55	55	55
55	55	55	55
50	55	55	55
45	45	45	45
51.67	53.33	53.33	53.33
Intrapedicular screws			
40	45	45	45
35	40	45	45
35	35	40	40
35	35	40	40
35	35	40	40
45	45	45	45
37.50	39.17	42.50	42.50

D. Intrapedicular Technique

During the planning with the CAS system, the entry point was determined in the dorsal structure of the lamina, along an elongation of the pedicle axis, with the screw direction oriented ventrally.

E. Extrapedicular Technique

For the extrapedicular technique, the entry point was chosen laterally on the transverse process and the screws were oriented converging ventrally, so that no damage to the medial pedicle wall could result. The screw length was chosen as for the intrapedicular technique, so that the ventral cortex would not be perforated.

F. Biomechanical Testing

Nondestructive flexibility measurements were performed in a custom testing machine which used bearing-mounted pneumatic cylinders and steel cables to apply pure, nonconstraining moments with an accuracy of ± 0.1 Nm. A standardized flexibility test was conducted that consisted of applying pure moments of flexion-extension, bilateral axial rotation, and bilateral lateral bending individually to a maximum of 8 Nm in four equal steps, for three cycles. Following two preconditioning loading cycles, motion data were collected during the final cycle. Each moment was sustained for 30 seconds to allow for equilibration of viscoelastic effects.

Four light-emitting diodes (LEDs) were attached to each vertebral body of the spine specimen. The spatial positions of the LEDs were tracked by an optoelectronic camera (Optotrak 3020, Northern Digital, Waterloo, Canada) and were recorded at the end of each load step (see Fig. 6). Using custom software, rotations of the T5 vertebra with respect to the lower fixed vertebra (T8) were calculated and expressed as Euler angles. For each applied moment and for all testing configurations, the movement in the direction of the moment was analyzed and the total movement under the maximum moment, the range of motion (ROM), was calculated.

G. Test Sequence

Biomechanical testing was performed first on the noninstrumented, intact specimen, then following instrumentation and stabilization with screws and rods, and finally again, following a fatigue loading sequence.

H. Fatigue Loading

For fatigue loading of the spine specimen, a MTS Bionix servo-hydraulic testing machine was used, which subjected the specimen to a cyclic compressive load of 0–200 N for 10,000 cycles at a frequency of 2 Hz, applied through a mobile connection to ensure pure axial loading.

I. Statistical Analysis

Due to the small number of specimens in each group ($n = 6$) and the non-normal distribution of the data, nonparametric methods were used. To determine the influence of instrumentation technique, the intervertebral range of motion was normalized with respect to the intact (uninstrumented) spine specimen and the Mann-Whitney U-test was performed comparing intrapedicular fixation to extrapedicular, with a significance level of $p = 0.05$.

To determine the sequential effects of posterior instrumentation and subsequent fatigue loading on specimen flexibility, the range of motion results for intrapedicular and extrapedicular groups were pooled and a Friedmann repeated-measures ANOVA was performed. Pooling of the data was only valid if the Mann-Whitney U-test demonstrated no differences between the two techniques. Individual differences between the sequential effects were tested using a Wilcoxon matched-Pairs test, with a significance level of $p = 0.05$.

J. Results

The median ratios of spine motion with instrumentation to motion of the intact specimen for the two instrumentation techniques for all loading directions are plotted in Figure 10 (below). The median ranges of motion in flexion-extension, axial rotation, and lateral bending, demonstrating the sequential effects of instrumentation and fatigue loading, are plotted in Figures 5–10.

K. Flexion-Extension

In flexion-extension, posterior instrumentation using intrapedicular or extrapedicular screws decreased the median range of motion to 17–43% of intact motion ($p < 0.01$). The differences between the two techniques were not statistically significant ($p = 0.52$) (Fig. 5).

Following the application of dynamic fatigue loading, the median range of motion of the instrumented specimens was 19–46% of the intact motion, significantly different ($p < 0.01$) from the intact motion but not significantly different from the motion measured before fatigue loading ($p = 0.06$) (Fig. 6). After fatigue loading, differences between the two techniques were not significant ($p = 0.42$).

L. Axial Rotation

The median ratios of instrumented to intact range of motion for axial rotation are plotted before (Fig. 7) and after (Fig. 8) fatigue loading. Posterior instrumentation decreased the range of motion to 41–45% of the intact motion ($p < 0.01$). The range of motion after fatigue loading was still

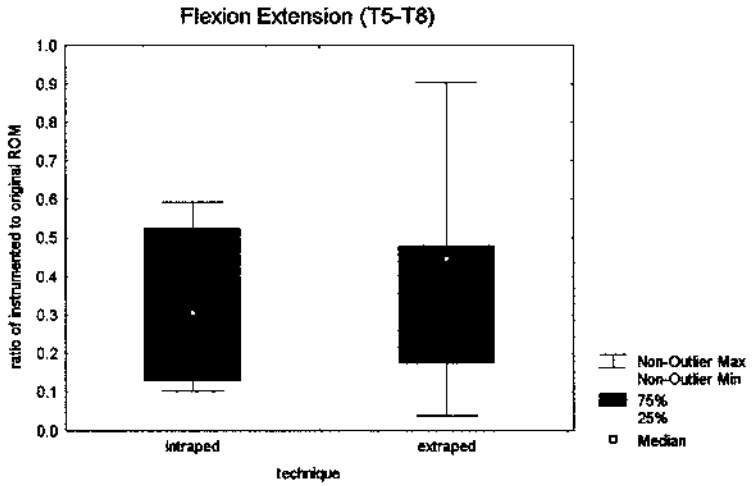

Figure 5 Decrease in range of motion (ROM) for flexion/extension: no significant difference between intra- and extrapedicular technique.

significantly lower than the intact motion (43–44%, $p < 0.01$). Differences between the two techniques were not statistically significant before ($p = 0.52$) or after ($p = 0.52$) fatigue loading. Fatigue loading did not result in a significant difference in segment flexibility ($p = 0.42$).

M. Lateral Bending

In lateral bending, posterior instrumentation using intrapedicular or extrapedicular screws decreased the median range of motion to 35% of intact motion ($p < 0.01$). After fatigue loading, a

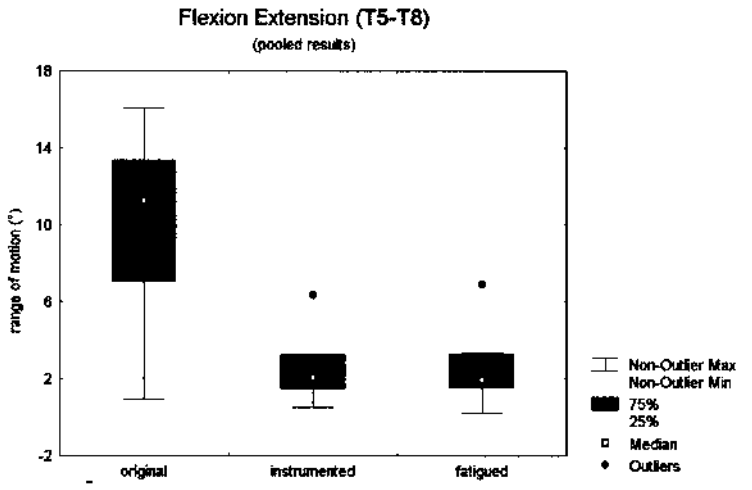

Figure 6 After dynamic fatigue loading, no significant increase was found in ROM for either of the techniques.

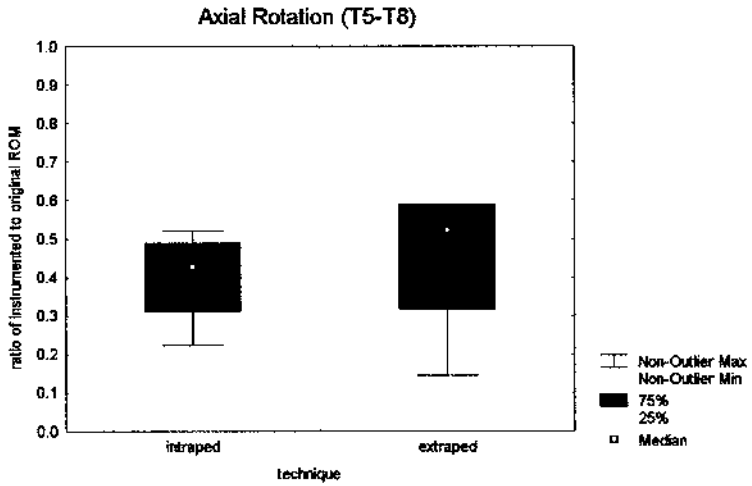

Figure 7 Decrease in range of motion (ROM) for axial rotation: no significant difference between intra- and extrapedicular technique.

reduction to 30–36% of intact motion ($p < 0.01$) was measured. Differences between the two techniques were not significant before or after fatigue loading ($p = 0.86$). Fatigue loading did not result in a significant difference in segment flexibility ($p = 0.06$) (Figs. 9, 10).

III. DISCUSSION

Indications for the use of pedicle screws in the thoracic spine have not yet been specifically defined. The number of surgeons who are using this technique for a variety of indications is steadily growing

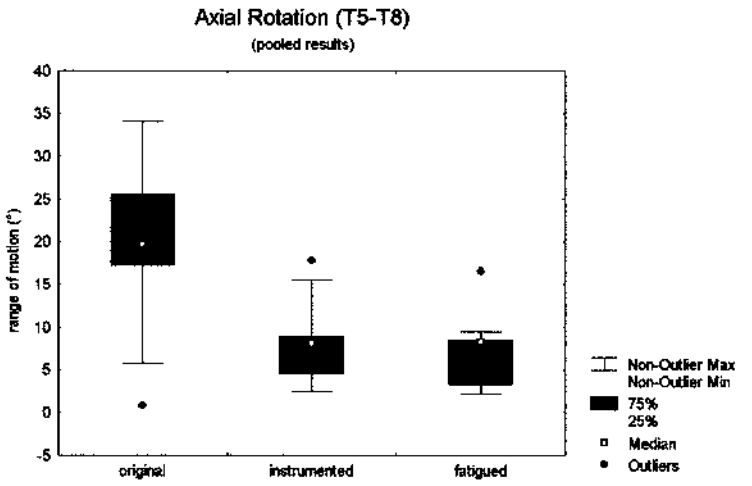

Figure 8 After dynamic fatigue loading, no significant increase was found in ROM for either of the techniques.

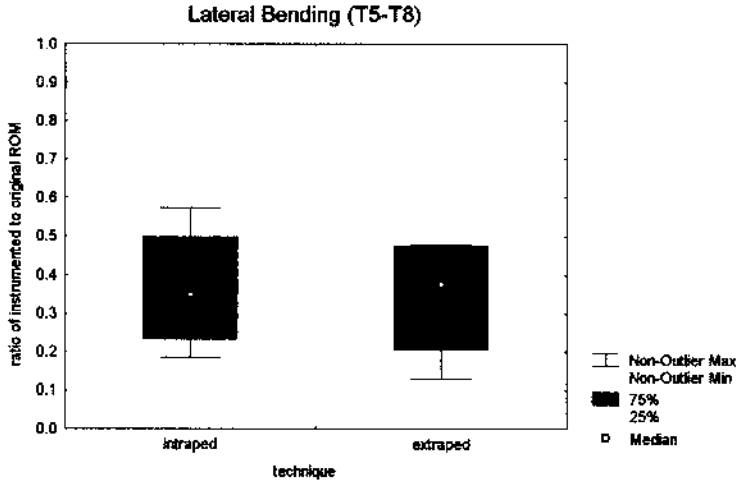

Figure 9 Decrease in range of motion (ROM) for lateral bending: no significant difference between intra- and extrapedicular technique.

[36,41,48], but the majority of surgeons avoid using pedicle screws in the mid- and upper thoracic spine. This is primarily due to the fear of neurological injury due to the close proximity of the screw to the spinal cord, the smaller size of the thoracic pedicles, and the more demanding surgical technique required for screw insertion [10,43,44].

A. Risks of Thoracic Pedicle Screw Insertion

The risk of intrapedicular screw placement in the thoracic spine is a controversial topic. On the one side, supporters of the technique report a large number of cases with few complications, whereas on

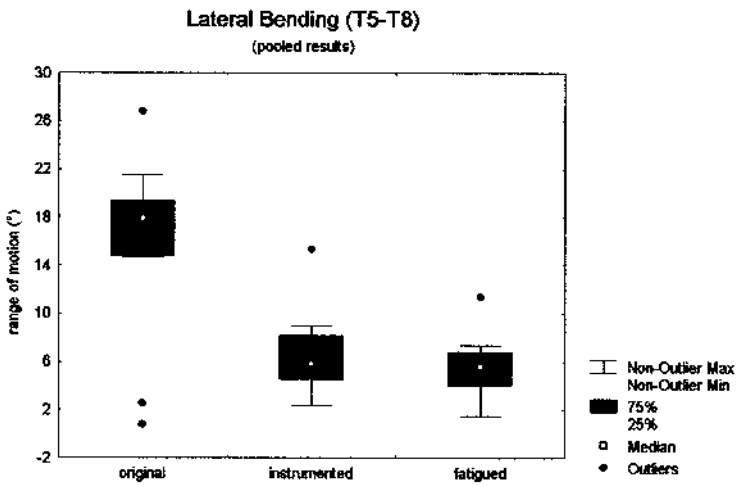

Figure 10 After dynamic fatigue loading, no significant increase was found in ROM for either of the techniques.

the other hand there are critics who have demonstrated in experimental studies the potential risks of the technique. Suk et al. [42] reported in 1994 on the use of pedicle screws for scoliosis correction and compared three methods: (1) instrumentation with hooks according to the method of Cotrel-Debusset, (2) pedicle screws inserted according to the example of Cotrel-Debusset, and (3) pedicle screws inserted in a segmental fashion, i.e., each pedicle in the instrumented region was fixed with a single pedicle screw. The best correction results were obtained with the segmental pedicle screw technique. Suk et al. favored this technique also for its safety and effectiveness. In this study, Suk et al. found only three misplaced screws, and there were no neurological or other major complications [42]. In a second study, Suk et al. [41] specifically analyzed the safety of thoracic pedicle screws and evaluated the results of over 4000 pedicle screws. They found 67 screw misplacements (1.5%) in 48 patients (10.4%). Neurological complications related to screw placement occurred in 4 patients (0.8%), with a transient paraparesis and three dural tears. They concluded that thoracic pedicle screw fixation is a reliable method of treating spinal deformities, with an excellent deformity correction and a high margin of safety [41].

Vaccaro et al. presented a study in which experienced spine surgeons implanted pedicle screws in cadaver spine specimens. Of the 90 screws inserted, 37 penetrated the cortices of the pedicle, of which 21 were misplaced medially and lay in the spinal canal, and a further 16 were misplaced laterally. Posterior mediastinal structures like the aorta and the esophagus were at greatest risk for injury after the pedicle screw had penetrated the anterior cortex. Vaccaro et al. recommended, based on these results, that pedicle screws should only be used when the overall stability of the spine is critical, and when sufficient data on the precise morphology of the pedicles can be obtained through preoperative computer tomography to improve the accuracy of screw insertion [43,44].

There are reports on the safety of pedicle screw instrumentation with respect to the biomechanical influence of a pedicle injury or iatrogenous pedicle fractures. Kothe et al. reported multidirectional instability for axial rotation and lateral bending in a fracture model after iatrogenous pedicle injury or after pedicle resection [21]. Clinical and experimental studies have shown that the lateral wall of the pedicle is most often damaged by screw insertion, which can be explained by a lateral cortical thickness which is only one third the thickness of the medial cortex. It has also been shown that the strength of screw fixation in pull-out testing decreases significantly following pedicle fracture in comparison to the intact pedicle [17].

B. Extrapedicular Technique

As an alternative to the conventional pedicle screw technique, Dvorak et al. first described an extrapedicular technique a decade ago [13]. In the study of Dvorak, the theoretical advantages of the technique were highlighted, but a standardized approach for extrapedicular instrumentation was not proposed until Morgenstern et al. [28] described reproducible anatomical landmarks to allow safe and reproducible placement of screws. The entry point was chosen in the proximal third of the tip of the transverse element (Fig. 2) and the screw was passed laterally to the facet joint. In the sagittal plane, the screw is oriented perpendicular to the dorsal structures (lamina). After the anatomical landmarks were defined, none of the 72 screws inserted in this study perforated the medial pedicle wall. In one case, the screw perforated laterally by a few millimetres out of the vertebra but remained covered by the pleura.

After the reproducibility of the technique had been demonstrated, the biomechanical characteristics of an extrapedicular construct, specifically the three-dimensional stability during motion analysis, had not yet been adequately evaluated. In their original study, Dvorak et al. demonstrated a significantly higher pull-out force for the extrapedicular screws in comparison to intrapedicular technique [13]. A possible reason for this could be the better screw-bone

fixation, due to the use of longer and larger-diameter screws, which the extrapedicular technique allows. This relationship had been described in previous studies [38,47,50]. The extrapedicular technique allows the selection of screw sizes independent of the pedicle diameter. The screw-bone contact is up to 50% greater, as extrapedicular screws find purchase in many cortices: in the transverse process, in the costotransverse joint, and finally in the costovertebral joint (Figs. 3, 4).

A further reason for the biomechanical advantages of the extrapedicular technique with respect to screw loosening is the convergence of the screws. Barber et al. concluded in a biomechanical study that two pedicle screws, implanted with a converging angle of 30°, would provide a greater resistance to axial pull-out and, furthermore, that convergent screws could withstand higher physiological loads before loosening than screws which were implanted parallel (0°) [4]. Although this study was conducted on lumbar specimens, the results should nevertheless be applicable to the thoracic spine. Due to the significantly lateral entry point of the extrapedicular screw in the thoracic spine, it is logical that a greater convergence will be achieved in comparison with the intrapedicular technique. The concern of a medial perforation of the screw into the spinal canal for convergent screws in the lumbar spine is not a factor for extrapedicular screw placement in the thoracic spine, as the distance from the screw to the spinal canal is much greater than for the intrapedicular technique, where the screws must be inserted, depending on the level, considerably more parallel.

In the treatment of rigid kyphoses, as is the case for a Scheuermann kyphosis, the correction results in considerable forces being applied to the implant. The success or failure of the instrumentation depends on the bone quality, the boneimplant interface, and the prestress in the vertical stabilizing rods. With extrapedicular instrumentation, the screws are not parallel to the sagittal plane and are therefore not in the same plane as the pull-out forces, as is the case for the intrapedicular technique. This could be considered a further advantage of the technique in clinical practice.

C. Biomechanical Testing

In the present study, the stabilizing potential of extrapedicular screw fixation has been determined using standard spine flexibility measurements and compared with the results for conventional intrapedicular fixation. Multidirectional biomechanical testing of spine segment flexibility is a well-established technique to characterize the stabilizing potential of various spinal fixation devices [2,11,18,25,35,39,40].

Instrumentation with extrapedicular or intrapedicular screws and longitudinal connecting rods substantially and significantly reduces the overall spine motion by, on average, more than 50% in all three principal motion directions. As there were no significant differences between the stabilizing effects for the extrapedicular and intrapedicular techniques, the results supported the hypothesis that extrapedicular screw placement is biomechanically equivalent to conventional intrapedicular instrumentation.

D. Computer Assisted Insertion of Thoracic Pedicle

Computer-assisted spine surgery appears to offer an ideal tool for improving the accuracy of insertion of thoracic pedicle screws. The definition of the optimal entry point and orientation of the screw can be determined exactly for each instrumented pedicle. Anatomical variations, resulting either from degenerative causes or as a consequence of fractures, tumors or congenital deformation, can be anticipated. The system provides the surgeon with continuous information about the position of surgical instruments and implants and helps to achieve an exceptional level

of surgical accuracy [29,30]. In the ideal case, the use of a computer et al. assisted technique would completely eliminate pedicle perforation. More realistically, Kim registered in an in vivo study 23 perforations from 120 screw insertions, of which nine were considered significant. In their opinion, the use of such systems exhibits a definite learning curve, which is especially dependent on overcoming technical problems with hardware and software [20]. In order to alleviate the technical uncertainty of a standardized screw placement in the present study, a navigation system was used for both the intrapedicular and extrapedicular screw placement. Although anatomical landmarks have been defined to ease extrapedicular screw insertion [27], the accuracy of the technique can be improved when the reference points in the thoracic spine can be clearly visualized in multiple anatomical planes, especially when dealing with the considerable variation in vertebral anatomy from level to level [10]. However, the technical feasibility was limited in the current study, as the screws were inserted in individual spine specimens and not in whole cadavers. Fixation of the specimen to the working surface was difficult to accomplish, which led to an occasional shift and necessitated repositioning. With instrumentation on a whole cadaver, a typical operative environment could be more closely recreated.

E. Limitations of the Study

As with all in vitro studies, the experimental protocol has certain limitations. The in vivo loading of the thoracic spine has not been adequately explored, and therefore a definitive physiological load cannot be defined. Based on the recommendations presented by Wilke et al. for a standardized testing protocol [45], pure moments were applied to provide a constant loading along the length of the specimen and to ensure identical loads for all specimens. It has been shown that muscle loads would further limit spinal motion through compressive loading [32,46]. Therefore, the stabilizing effect of posterior instrumentation measured here would be enhanced in vivo by muscle loading. The limited number of cadaver specimens available for testing resulted in a wide variability of the results. The full flexibility measurement, repeated three times, requires up to 8 hours to complete with the addition of fatigue loading. Although the specimens were kept moist throughout the tests, degradation of the specimens cannot be ruled out.

IV. CONCLUSIONS

The fact that, with this novel technique, the safe zone for screw insertion is larger would encourage the surgeon to prefer the extrapedicular technique (Fig. 11). Reproducible anatomical landmarks have been described and facilitate screw insertion in everyday clinical practice [27]. The biomechanical characteristics with respect to pull-out force have been shown to be better. In the current motion analysis, no significant differences in construct stability were found in comparison with the conventional intrapedicular technique. An image intensifier provides adequate intraoperative assistance, with which the screw orientation, especially in the sagittal place, must be controlled. However, it is recommended that each surgeon obtain sufficient training in the technique from a colleague who is experienced with the extrapedicular insertion of pedicle screws. Also, surgeons interested in adopting this technique would be encouraged to gain experience in cadaver spine preparations. We recommend the use of extrapedicular pedicle screw insertion for the treatment of spine diseases and deformities because of the aforementioned advantages of the technique. This technique has already been applied for several years with considerable success and has proven itself especially for the correction of kyphotic deformities (Figs. 12, 13).

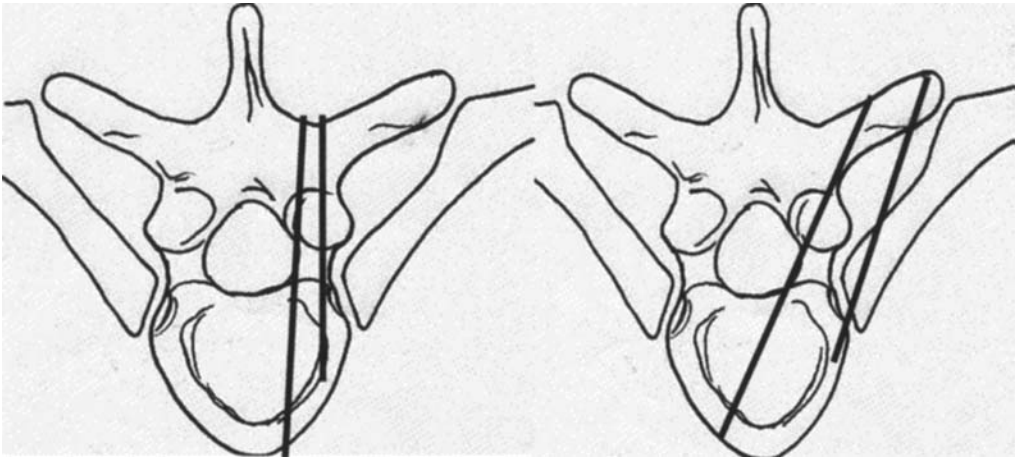

Figure 11 Safe zone for the (left) intra- and (right) extrapedicular technique.

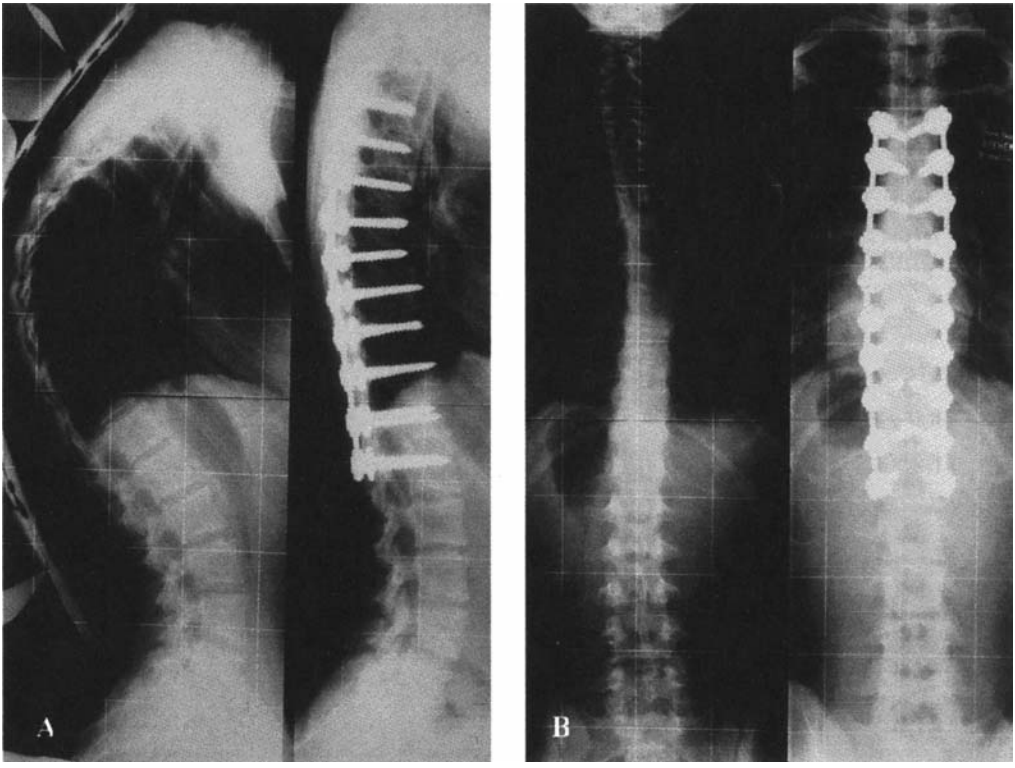

Figure 12 Compression and fusion for operative correction of Scheuermann's kyphosis using extrapedicular screw placement in the thoracic spine: (A) lateral and (B) anteroposterior views.

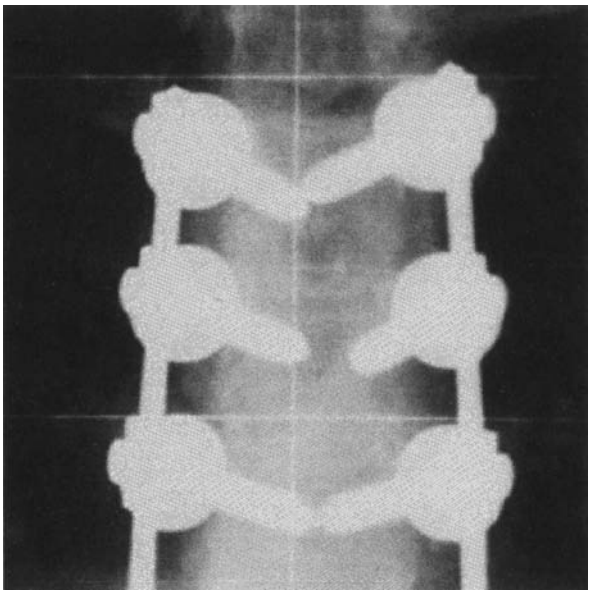

Figure 13 AP x-ray (close-up view) of upper thoracic spine demonstrating extrapedicular screws with far lateral entry point.

V. FUTURE STUDIES

In order to evaluate the efficiency of the technique, a clinical study should be initiated in which the extrapedicular technique is compared with the conventional technique. In this study the extrapedicular screws should be implanted exclusively with the assistance of fluoroscopic imaging and with the consideration of previously defined anatomical landmarks, whereas the intrapedicular screws would be placed with the assistance of a CAS system.

ACKNOWLEDGMENTS

This study was generously funded by the Robert Mathys Foundation, Bettlach, Switzerland. The junior author (W.M.) expresses gratitude to Dr. P. Metz-Stavenhagen, who has the technique for many years with considerable success. He standardized the technique as routine procedure.

REFERENCES

1. Amiot LP, Lang K, Putzier M. Comparative results between conventional and computer-assisted pedicle screw installation in the thoracic, lumbar, and sacral spine. Spine 2000; 25:606–614.
2. An HS, Lim TH, You JW, Hong JH, Eck J, McGrady L. Biomechanical evaluation of anterior thoracolumbar spinal instrumentation. Spine 1995; 20:1979–1983.
3. Ashman RB, Galpin RD, Corin JD, Johnston CE. Biomechanical analysis of pedicle screw instrumentation systems in a corpectomy model. Spine 1989; 14:1398–1405.
4. Barber JW, Boden SD, Ganey T, Hutton WC. Biomechanical study of lumbar pedicle screws: does convergence affect axial pullout strength?. J Spinal Disord 1998; 11(3):215–220.

5. Boucher HH. A method of spinal fusion. J Bone Joint Surg (Br) 1959; 41:248–259.
6. Berlemann U, Monin D, Arm E. Planning and insertion of pedicle screws with computer assistance. J Spinal Disord 1997; 10:117–124.
7. Carl AL, Tromanhauser SG, Roger DJ. Pedicle screw instrumentation for thoracolumbar burst fractures and fracture-dislocations. Spine 1992; 17:S317–S24.
8. Carson WL, Duffield RC, Arendt M, Ridgely BJ, Gaines RW. Internal forces and moments in transpedicular spine instrumentation—the effect of pedicle screw angle and transfixation—the 4-bar linkage concept. Spine 1990; 15:893–901.
9. Chesnut RM. Early failure of short-segment pedicle instrumentation for thoracolumbar fractures. A preliminary report [letter;comment]. J Bone Joint Surg (Am) 1994; 76A:153–154.
10. Cinotti G, Gumina S, Ripani M, Postacchini F. Pedicle instrumentation in the thoracic spine—a morphometric and cadaveric study for placement of screws. Spine 1999; 24:114–119.
11. Dick JC, Brodke DS, Zdeblick TA, Bartel BD, Kunz DN, Rapoff AJ. Anterior instrumentation of the thoracolumbar spine. A biomechanical comparison. Spine 1997; 22:744–750.
12. Donovan DJ, Polly DW, Ondra SL. The removal of a transdural pedicle screw placed for thoracolumbar spine fracture. Spine 1996; 21:2495–2498.
13. Dvorak M, MacDonald S, Gurr KR, Bailey SI, Haddad RG. An anatomic, radiographic, and biomechanical assessment of extrapedicular screw fixation in the thoracic spine. Spine 1993; 18:1689–1694.
14. Ebraheim NA, Xu RM, Ahmad M, Yeasting RA. Projection of the thoracic pedicle and its morphometric analysis. Spine 1997; 22:233–238.
15. Faraj AA, Webb JK. Early complications of spinal pedicle screw. Eur Spine J 1997; 6:324–326.
16. Gaines RW. The use of pedicle-screw internal fixation for the operative treatment of spinal disorders. J Bone Joint Surg (Am) 2000; 82-A:1458–1476.
17. George DC, Krag MH, Johnson CC, Van Hal ME, Haugh LD, Grobler LJ. Hole preparation techniques for transpedicle screws. Effect on pull-out strength from human cadaveric vertebrae. Spine 1991; 16:181–184.
18. James KS, Wenger KH, Schlegel JD, Dunn HK. Biomechanical evaluation of the stability of thoracolumbar burst fractures. Spine 1994; 19:1731–1740.
19. Kaus M, Steinmeier R, Sporer T. Technical accuracy of a neuronavigation system measured with a high-precision mechanical micromanipulator. Neurosurgery 1997; 41:1431–1437.
20. Kim KD, Johnson JP, Bloch O, Masciopinto JE. Computer-assisted thoracic pedicle screw placement. An in vitro feasibility study. Spine 2001; 26:360–364.
21. Kothe R, Panjabi MM, Liu W. Multidirectional instability of the thoracic spine due to iatrogenic pedicle injuries during transpedicular fixation. A biomechanical investigation. Spines 1997; 22: 1836–1842.
22. Krag MH, Weaver DL, Beynnon BD, Haugh LD. Morphometry of the thoracic and lumbar spine related to transpedicular screw placement for surgical spinal fixation. Spine 1988; 13:27–32.
23. Laine T, Lund T, Ylikoski M. Accuracy of pedicle screw insertion with and without computer assistance: a randomised controlled clinical study in 100 consecutive patients. Eur Spine J 2000; 9: 235–240.
24. Liljenqvist UR, Halm HFH, Link TM. Pedicle screw instrumentation of the thoracic spine in idiopathic scoliosis. Spine 1997; 22:2239–2245.
25. Lim TH, An HS, Hong JH. Biomechanical evaluation of anterior and posterior fixations in an unstable calf spine model. Spine 1997; 22:261–266.
26. Masferrer R, Gomez CH, Karahalios DG, Sonntag VK. Efficacy of pedicle screw fixation in the treatment of spinal instability and failed back surgery: a 5-year review. J. Neurosurg 1998; 89: 371–377.
27. Morgenstern W, Metz-Stavenhagen P, Merola A, Haher T. Extrapedicular screw placement in the thoracic spine: a cadaveric study. Proceedings of the International Meeting of Advanced Spine Techniques, Vancouder, Canada, 1999.
28. Morgenstern W, Fortser T, Jeszenszky D. Presentation of a misplaced intraspinal pedicle screw in thoracic scoliosis 10 years after the operation. Proceedings of the International Meeting of Advanced Spine Techniques, Bahamas, 2001.

29. Nolte LP, Zamorano L, Visarius H. Clinical evaluation of a system for precision enhancement in spine surgery. Clin Biomech 1995; 10:293–303.
30. Nolte LP, Visarius H, Arme E. Computer-aided fixation of spinal implants. J Image Guid Surg 1995; 1:88–93.
31. Papin P, Arlet V, Marchesi D, Rosenblatt B, Aebi M. Case report: unusual presentation of spinal cord compression related to misplaced pedicle screws in thoracic scoliosis. Eur Spine J 1999; 8(2): 156–159.
32. Panjabi M, Abumi K, Duranceau J, Oxland T. Spinal stability and intersegmental muscle forces. A biomechanical model. Spine 1989; 14:194–200.
33. Panjabi MM, Abumi K, Duranceau J, Crisco JJ. Biomechanical evaluation of spinal fixation devices: II. Stability provided by eight internal fixation devices. Spine 1988; 13:1135–1140.
34. Panjabi MM, O'Holleran JD, Crisco JJ, Kothe R. Complexity of the thoracic spine pedicle anatomy. Eur Spine J 1997; 6:19–24.
35. Roy-Camille R, Saillant G, Mazel C. Plating of thoracic, thoracolumbar, and lumbar injuries with pedicle screw plates. Orthop Clin North Am 1986; 17(1):147–159.
36. Sasso RC, Cotler HB, Reuben JD. Posterior fixation of thoracic and lumbar spine fractures using DC plates and pedicle screws. Spine 1991; 16:S134–139.
37. Schlenzka D, Laine T, Lund T. Computer-assisted spine surgery. Eur Spine J 2000; 9(suppl 1):57–64.
38. Schwarzenbach O, Berlemann U, Jost B. Accuracy of computer-assisted pedicle screw placement: an in vivo computed tomography analysis. Spine 1997; 22:452–458.
39. Shono Y, McAfee PC, Cunningham BW. Experimental study of thoracolumbar burst fractures. A radiographic and biomechanical analysis of anterior and posterior instrumentation systems. Spine 1994; 19:1711–1722.
40. Slosar PJ, Patwardhan AG, Lorenz M, Havey R, Sartori M. Instability of the lumbar burst fracture and limitations of transpedicular instrumentation. Spine 1995; 20:1452–1461.
41. Suk SI, Kim WJ, Lee SM, Kim JH, Chung ER. Thoracic pedicle screw fixation in spinal deformities—Are they really safe?. Spine 2001; 26:2049–2057.
42. Suk SI, Lee CK, Min HJ, Cho KH, Oh JH. Comparison of Cotrel-Dubousset pedicle screws and hooks in the treatment of idiopathic scoliosis. Int Orthop 1994; 18:341–346.
43. Vaccaro AR, Rizzolo SJ, Allardyce TJ. Placement of pedicle screws in the thoracic spine. Part I: Morphometric analysis of the thoracic vertebrae. J Bone Joint Surg (Am) 1995; 77:1193–1199.
44. Vaccaro AR, Rizzolo SJ, Balderston RA. Placement of pedicle screws in the thoracic spine. Part II: An anatomical and radiographic assessment. J Bone Joint Surg (Am) 1995; 77:1200–1206.
45. Wilke HJ, Wenger K, Claes L. Testing criteria for spinal implants: recommendations for the standardization of in vitro stability testing of spinal implants. Eur Spine J 1998; 7:148–154.
46. Wilke HJ, Wolf S, Claes LE, Arand M, Wiesend A. Stability increase of the lumbar spine with different muscle groups. A biomechanical in vitro study. Spine 1995; 20:192–198.
47. Wittenberg RH, Lee KS, Shea M, White AA, Hayes WC. Effect of screw diameter, insertion technique, and bone cement augmentation of pedicular screw fixation strength. Clin Orthop 1993; 296:278–287.
48. Wu SS, Hwa SY, Lin LC, Pal WM, Chen PQ, Au MK. Management of rigid post-traumatic kyphosis. Spine 1996; 21:2260–2266.
49. Xu RM, Ebraheim NA, Ou YJ, Yeasting RA. Anatomic considerations of pedicle screw placement in the thoracic spine Roy-Camille technique versus open-lamina technique. Spine 1998; 23:1065–1068.
50. Yamagata M, Kitahara H, Minami S. Mechanical stability of the pedicle screw fixation systems for the lumbar spine. Spine 1992; 17:S51–S54.
51. Zindrick MR, Wiltse LL, Doornik A. Analysis of the morphometric characteristics of the thoracic and lumbar pedicles. Spine 1987; 12:160–166.

40

Two-Cage Reconstruction Versus Single Mega-Cage or Dual Nested Cages for Lumbar Interbody Fusion

Hideki Murakami
Kanazawa University School of Medicine
Kanazawa, Japan

William C. Horton and William C. Hutton
Emory University School of Medicine, The Emory Spine Center
Decatur, Georgia, U.S.A.

I. INTRODUCTION

There has been an increase in the use of interbody cages as an adjunct to arthrodesis [6]. Interbody fusion should be carried out with the aim of providing stability to the segment until arthrodesis is obtained. While various designs exist, a threaded cylindrical type is commonly used. With the threaded cage it is usual to insert two cages side by side per disc space whenever possible.

There are several practical problems with using two cages:

1. Using two cages may place the posterior foramina at risk laterally, especially with a thick disc, when larger diameter cages are necessary.
2. Incomplete disc excision may occur with reaming, especially if the endplates are biconcave, thus limiting the fusion environment.
3. It is difficult to achieve symmetrical positioning with two cages.
4. A very wide lateral vascular mobilization and retraction is necessary with two cages.
5. Inserting two cages could result in higher direct costs to the patient, as well as extending operative time.

These drawbacks could be offset to some extent by the use of a single cage of larger diameter (i.e., a mega-cage) or by the use of reduced lateral profile cages (i.e., ''nested'' cages). The nested cages can be docked together. Docking significantly reduces the lateral profile of the implants and reduces the transverse diameter requirements.

Our purpose here was to compare the biomechanical properties of a reconstruction using two standard cages (18 mm diameter), with a reconstruction using a single mega-cage (24 mm diameter) and a reconstruction using dual nested cages (22 mm diameter) as well as to quantify the surface area of the cancellous bone bed created by reaming for cages. We considered that the surface area of the vascular bed should correlate positively to blood supply for eventual healing.

II. MATERIALS AND METHODS

Twenty-four L5-S1 motion segments were selected (as ''normal'') from fresh cadavers (age range 67–89 years). None of the cadavers had a history of spinal disease. Each motion segment was radiographed to ensure that no major structural abnormalities were present. These particular specimens were selected due to very similar characteristics of disc and vertebral morphology with minimal degenerative signs and very similar disc height. Templating was done using standard templates (Medtronic Sofamor Danek, Memphis, TN) to ensure that the distraction height of the segment was correctly determined for each. The 24 motion segments were then randomized so that 8 received two cages, 8 received a single mega-cage, and 8 received dual nested cages. In all groups, there were 5 males and 3 females, and four discs were templated to 8 mm high and the other four to 10 mm high. The mean age was 78.0 years (range 67–89 yr) in the two-cage group, 77.8 years (range 67–88 yr) in the single mega-cage group, and 79.4 years (range 69–86 yr) in the nested-cage group. All specimens were frozen to $-50^{\circ}C$ and stored until the day before testing, when they were allowed to thaw slowly to room temperature.

Each lumbar motion segment was carefully stripped of muscle, with great care taken to preserve all ligaments, joint capsule, disc, and bone structure. Each vertebra of a motion segment was then potted up to its midbody in a 10 cm diameter polyvinylchloride (PVC) end cap using dental cement (Fig. 1).

The PVC end cap, which contained S1, was clamped in a mechanical testing machine (MTS) (Minneapolis, MN), and after a cyclic compression conditioning period (500 ± 150 N at 1 Hz for 1000 cycles), the motion segment was mechanically tested according to the following eight-step loading sequence. At each step the load was applied three times and a load-deformation curve was obtained each time. The three load-deformation curves were always identical, and only one of the three was used to calculate stiffness.

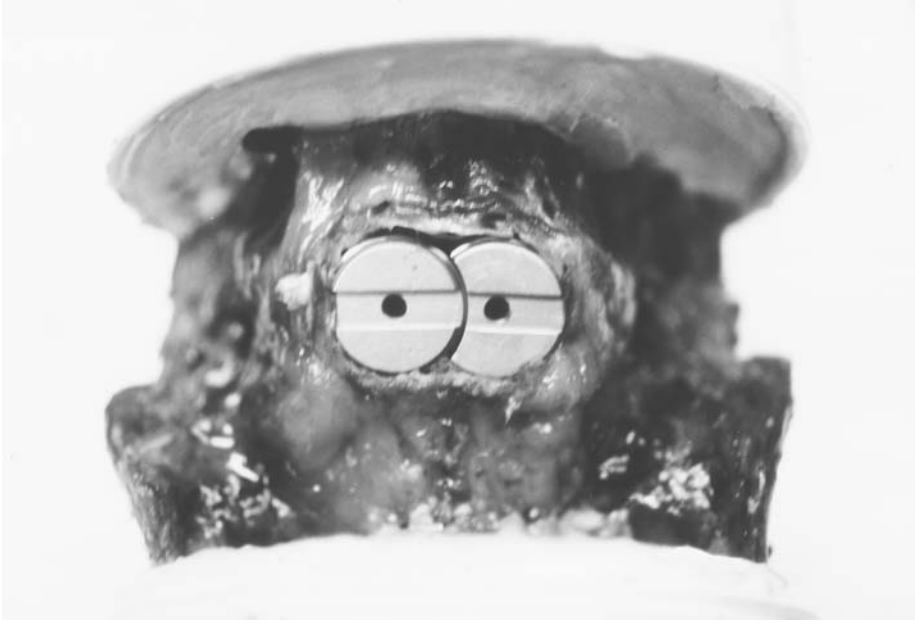

Figure 1 The motion segment with nested cages inserted is shown potted in dental cement.

Step 1 (Establishing the Center of Rotation): The center of rotation was established in the intact motion segment at the beginning of the experiment. This was accomplished as follows: a pure compressive load of 50 N was applied through a ball bearing to the top surface of the PVC end cap, which contained L5. The ball bearing was positioned and the load applied and then repositioned and applied until no angular rotation in the coronal or sagittal planes could be detected when a compressive force was applied to the upper end cap. This spot on the top surface of the end cap was designated the center of rotation and was clearly marked. This spot remained as the reference spot for the center of rotation for all the remaining steps carried out on that particular motion segment. These included the tests carried out after the cage, or cages, were inserted.

Step 2 (Compression): The specimen was then loaded in pure compression (with the load applied at the center of rotation) at a displacement rate of 0.25 cm/min. The load was applied up to a maximum of 900 N. The load limit of 900 N was chosen on the basis of it being a middle value within the range of 500–2000 N (500 N corresponds to erect standing, and 2000 N to light manual labor) [1]. A previous study [5] showed that this maximum load allowed repeated load cycles without causing irreversible damage to the intervertebral joint.

Step 3 (Flexion): The test was repeated with the 900 N load applied 2 cm anterior to the center of rotation, to produce a maximum bending moment of 18 Nm (i.e., 0.02 m $\times$ 900 N $=$ 18 Nm) in flexion. A bending movement of 18 Nm was chosen on the grounds that this was within the range of bending moments applied to an intervertebral joint in vivo (e.g., if the weight of the upper trunk is 300 N and one bends forward so that the center of gravity moves anteriorly from the center of rotation in the disc by 6 cm, a bending moment of 18 Nm is exerted on that disc).

Step 4 (Extension): The 900 N load was applied 2 cm posterior to the center of rotation, to send the specimen into extension.

Step 5 (Right Lateral Bending): The 900 N load was applied 2 cm to the right of the center of rotation, to send the specimen into right lateral bending.

Step 6 (Left Lateral Bending): The test was repeated with the same parameters for left lateral bending and a load-deformation curve was obtained.

Step 7 (Right Axial Torsion): To apply axial torsion the specimen was first compressed to 900 N and then an axial torque applied in a clockwise motion (about the center of rotation), to a maximum of 10 Nm. A torque-angular deformation curve was obtained.

Step 8 (Left Axial Torsion): The test was repeated with the same parameters in a counterclockwise motion.

Experimental protocol was carried out on each motion segment:

Condition 1 (intact specimen): The center of rotation for the intact specimen was determined (Step 1), and the intact specimen was tested according to the loading sequence described above (Steps 2–8).

Condition 2 (specimen with two cages, or a single mega-cage, or dual nested cages inserted): The motion segment with the inserted cage, or cages, was tested again according to Steps 2–8 of the loading sequence.

Interbody-threaded titanium spine cages (Sofamor Danek, Memphis, TN) were inserted in accordance with the manufacturer's instructions. All insertion was done by one investigator, using matched size-specific dilators and reamers. All cages were inserted using an anterior approach and were centered within the disc space. An anterior annulotomy, dilation, and reaming

was carried out with standard manual instrumentation. Maximum dilation was taken to 8 or 10 mm based on preoperative templating and observed disc tension during insertion.

From each load-deformation curve, the stiffness of the motion segment was determined as follows. It was noted what the deformation was when the curve reached 900 N (or 10 Nm in the case of torsion). This deformation was then divided by two and the slope of the latter half of the curve between these two points was measured. We reasoned that the first half of the curve could have concealed displacement artifacts caused by the experimental setup, and it was not until these were removed that the effective stiffness was revealed [5]. For each motion segment, each value of stiffness for a particular loading sequence after the cage, or cages, was inserted was normalized against the corresponding value of stiffness for the same loading sequence, when the motion segment was tested intact. This normalization allowed us to adjust for individual variation in motion segment stiffness.

At the end of the biomechanical testing the specimens were bisected through the disc and the surface area of the vascular bed that had been created in the cancellous bone (of both adjacent vertebrae) was measured and calculated for each motion segment.

Statistically significant differences in each of the measured values were tested for using a Wilcoxon rank sum test. Significance was established at the $p < 0.05$ level.

III. RESULTS

The average values of stiffness for each of the three groups of specimens tested intact showed no significant difference between the three in compression, flexion, extension, right lateral bending, left lateral bending, right axial torsion, or left axial torsion.

The average values of normalized stiffness are shown graphically in Figure 2. Overall, the nested cages provided the stiffest reconstruction. There were no significant differences between the two-cage group and the nested-cage group. There was a significant difference between the mega-cage group and nested-cage group in compression (0.68 vs. 0.85) ($p < 0.05$), flexion (0.74 vs. 1.11) ($p < 0.01$), and left lateral bending (0.82 vs. 0.99) ($p < 0.05$).

The normalized stiffness for the specimens with the mega-cage inserted was slightly less in compression, flexion, extension, and lateral bending than for the specimens with either two cages or nested cages inserted. In torsion, the standard dual cages were the least stiff. However, the only significant difference between the mega-cage group and standard-cage group was in flexion (0.74 vs. 1.08) ($p < 0.05$).

The average values of the surface area of the cancellous bone bed are given in Figure 3. The average surface area of the cancellous bed was least with the two-cage group (1236 mm^2), more with the mega-cage group (1341 mm^2), and significantly more with the nested-cage group (1873 mm^2). There was a significant difference between the two-cage group and the nested-cage group ($p < 0.01$) and between the mega-cage group and the nested-cage group ($p < 0.01$).

IV. DISCUSSION

There has recently been a rapid and progressive increase in the use of interbody fusion cages as an adjunct to arthrodesis in the treatment of a wide range of spinal disorders, including spondylolisthesis and degenerative disc disease. It is usual to insert two cages per disc space at the L5-S1 level. This practice is based on the presumption that two cages provide stability whereas a single cage may not be biomechanically adequate [4]. However, there are several practical problems. First, placement of two cages risks violation of the posterior foramina. This is especially an issue with a thick disc, when larger-diameter cages are necessary. Two larger-

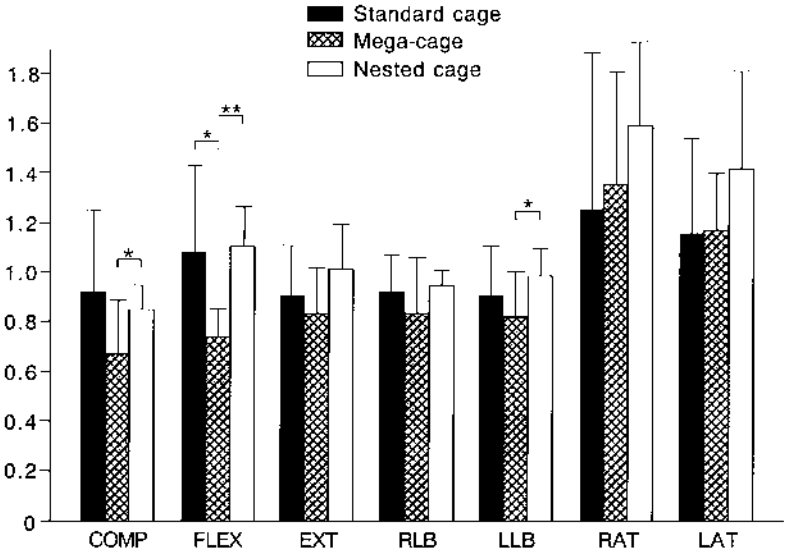

Figure 2 The average values of normalized stiffness for the two-cage group, the mega-cage group, and the nested-cage group. COMP, compression; FLEX, flexion; EXT, extension; RLB, right lateral bending; LLB, left lateral bending; RAT, right axial torsion; LAT, left axial torsion. Error bar = standard deviation. $*p < 0.05$; $**p < 0.01$.

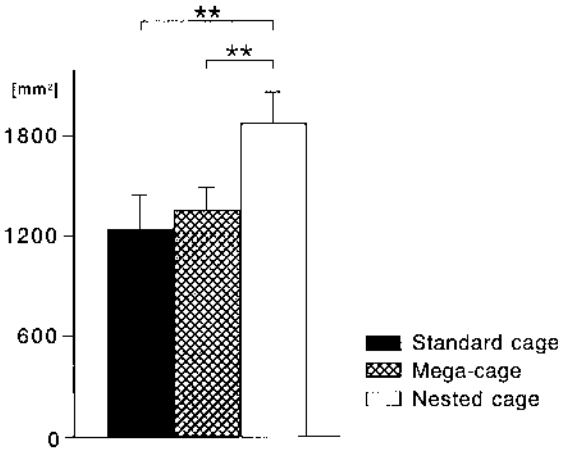

Figure 3 The values of exposed surface area of cancellous bone bed for the two-cage group, the mega-cage group, and the nested-cage group. Error bar = standard deviation. $**p < 0.01$.

diameter cages present as a wider overall reconstruction that may intrude into the foramen posterolaterally. This risk to the foramen is even further heightened if cage placement is asymmetrical in a left-to-right direction. Both extrusion of disc material into the foramen and intrusion of the posterolateral corner of the cage into the foramen have been reported [3]. Both of these can induce nerve root irritation postoperatively. Second, a very wide lateral vascular mobilization and retraction is necessary to provide a safe working zone for two cages side by side; this may place the iliac vessels at risk during reaming or insertion, especially with bifurcation or vascular scarring.

Using a single mega-cage or dual nested cages could offset these drawbacks to some extent. Both the mega-cage reconstruction and dual nested-cage reconstruction significantly reduce the lateral dimension required for insertion of cages into the lumbar interspace, hence reducing the risk to the foramen and minimizing lateral vascular exposure. For example, the transverse vertebral width required to insert two 22 mm nested cages is the same as that required to insert two 18 mm standard cages. Examination of the vertebral body after the motion segment was bisected revealed no risk to the posterior foramina in the single mega-cage reconstruction compared with two-cage reconstruction or the nested-cage reconstruction (Fig. 4).

Another problem presented by the placement of two smaller cages is that the midportion of the endplate may not be sufficiently decorticated to expose the cancellous blood supply for cellular ingrowth if there is marked endplate concavity. This potential problem is compounded if the smaller cage is not symmetrically placed across each endplate or if the smaller cage is not placed parallel to the endplates. One solution to this potential problem would be to insert a single mega-cage or dual nested cages. Both of these reconstructions offer greater surface area

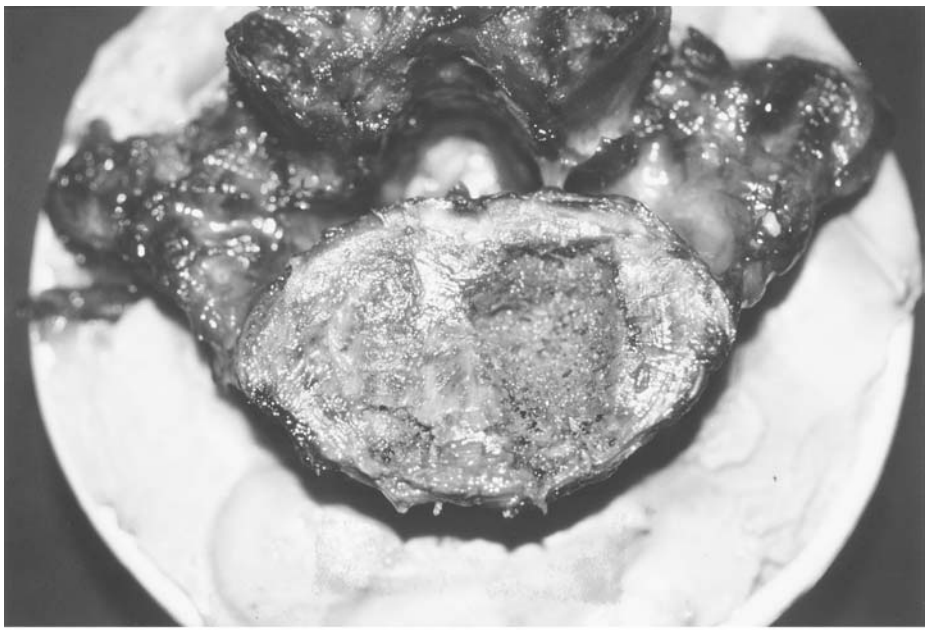

A

Figure 4 (A) A motion segment bisected through the intervertebral disc after removal of the two standard cages. The impression left by the cages reveals a lack of symmetry—very little exposed vascular bone bed on the left side. Note that the posterior foramina is at risk on the left side.

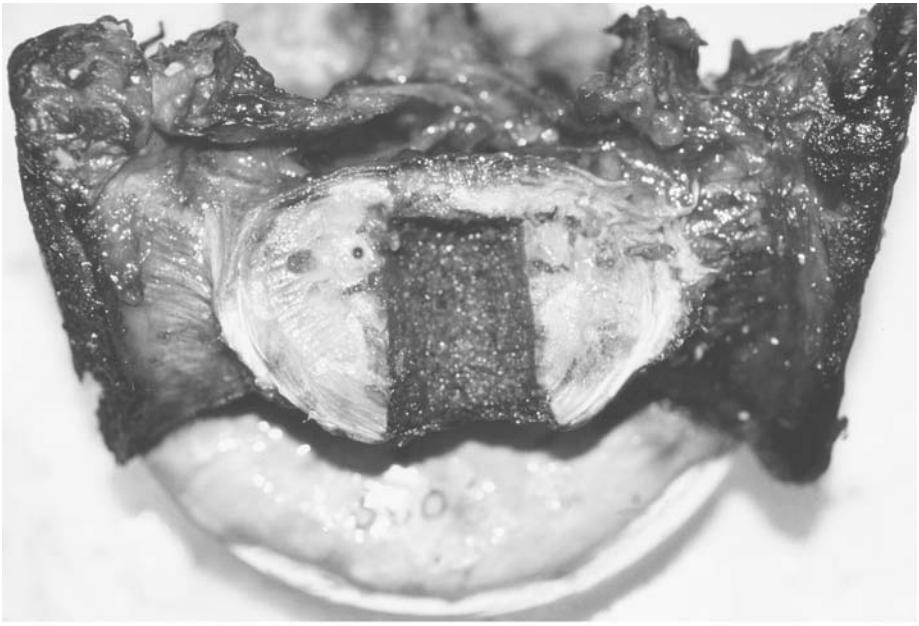

B

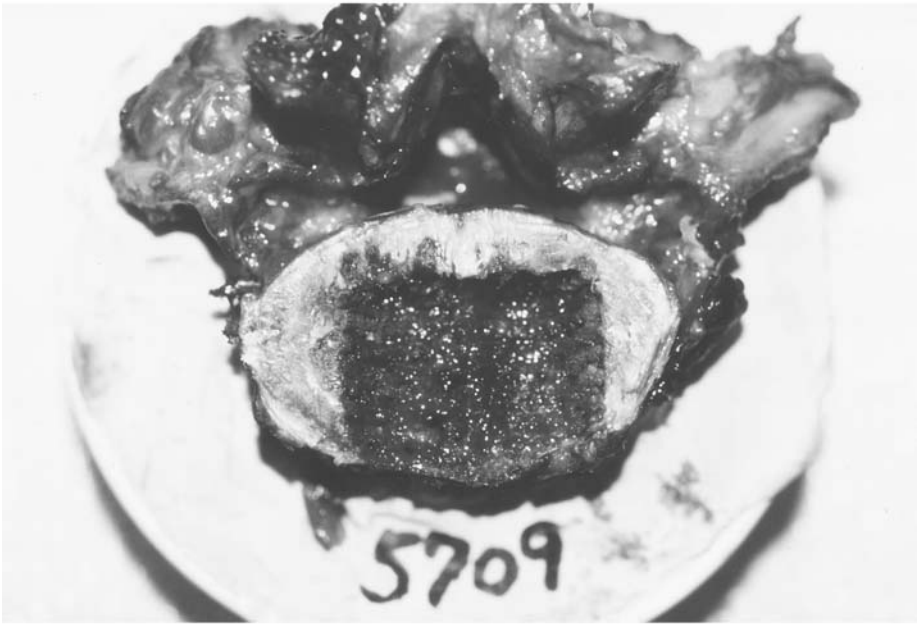

C

Figure 4 (B) A motion segment bisected through the intervertebral disc after removal of the single mega-cage. Note that the extent of cancellous bone bed exposed and the posterior foramina are no risk. (C) A motion segment bisected through the intervertebral disc after removal of the nested cages. Note the extent of cancellous bone bed exposed.

of cancellous bone bed. Reconstruction using two smaller-diameter cages has demonstrated extremely variable results, with fusion rates ranging from 19 to 95% [2]. Complete disc excision is hard to achieve routinely, especially with the recently developed laparoscopic techniques. The cartilaginous endplate represents a potential barrier that can impede solid arthrodesis in a reamed threaded system. We assume that exposed cancellous vertebral bone is a key for cellular differentiation and ingrowth in the interbody fusion environment. Figure 4A shows that the bone bed when using two cages may be low quality as compared to that offered by a mega-cage (Fig. 4B) or nested cages (Fig. 4C) because of the inclusion of endplate cartilage.

From the standpoint of potent safety, both the mega-cage and the nested cages offer potential advantages. They do not require the iliac vessels to be manipulated so widely, potentially reducing the risk of intraoperative bleeding. They do not protrude as widely and are thus less likely to protrude into the foramen. This gives a margin of safety should positioning be slightly off the midline. Additionally, we would anticipate some time savings in the operating room with both as compared to the two standard cages since less time is needed for vascular mobilization and a second independent docking step is not required.

The results of this study support both the mega-cage and nested cages as being good alternatives to two standard cages.

V. CONCLUSION

Comparison of the biomechanical properties of reconstruction using two standard cages with reconstruction using a single mega-cage and reconstruction using dual nested cages showed that dual nested cages produced, on balance, the stiffest reconstruction. The surface area of cancellous bone bed created for reaming for each of the three reconstructions showed that the surface area was greatest for the dual nested-cage reconstruction.

ACKNOWLEDGMENTS

This study was funded in part by a grant from the Yoshida Scholarship Foundation and in part by Medtronic Sofamor Danek.

REFERENCES

1. Nachemson AL. Disc pressure measurements. Spine 1981; 6:93–97.
2. Schlegel JD, Yuan HA, Fredricksen BE. Anterior interbody fixation devices. In: ed. Frymoyer JW. The Adult Spine. New York: Raven Press, 1997:2205–2223.
3. Taylor BA, Vaccaro AR, Hilibrand AS, Zlotolow DA, Albert TJ. The risk of foraminal violation and nerve root impingement after anterior placement of lumbar interbody fusion cages. Spine 2000; 26: 100–104.
4. Tencer AF, Hampton D, Eddy S. Biomechanical properties of threaded inserts for lumbar interbody fusion. Spine 1995; 20:2408–2414.
5. Volkman T, Horton WC, Hutton WC. Transfacet screws with lumbar interbody reconstruction: biomechanical study of motion segment stiffness. J. Spin Disord 1996; 9:425–432.
6. Weiner BK, Fraser RD. Spine update: lumbar interbody cages. Spine 1998; 23:634–640.

41

Spontaneous Remission of Intervertebral Disc Hernia and Responses of Surrounding Macrophages

Kensei Nagata and Michiyo Tsuru
Kurume University School of Medicine
Kurume, Japan

I. INTRODUCTION

An electron microscope was used to observe disc hernia degeneration at the cellular level as expressed in extruded tissue from a human intervertebral disc and in cultured chondrocytes. The mechanism of spontaneous regression was analyzed in order to investigate the effects of homologous macrophages, and the results of this analysis may be developed into a clinical therapy. Extruded tissue specimens excised during surgery on human intervertebral disc hernia and cultured chondrocytes isolated from the excised tissue were observed via electron microscopy. The intervertebral disc exhibits a matrix structure similar to that of cartilagenous tissue. Many studies have examined the destruction of the aricular cartilage due to degeneration or aging. However, there have been few studies regarding the destruction of the intervertebral disc due to degeneration or aging. The intervertebral disc is poor in vascularity. Therefore, it is believed that infiltration by various cells, such as vascular endothelial cells, lymphocytes, and macrophages, occurs during the course of degeneration. Cells in the intervertebral disc actively start to metabolize in response to mechanical and biochemical stimulations of the intervertebral disc via the matrix. Furthermore, it is also believed that cells in the intervertebral disc become activated by themselves, thus causing tissue destruction in the intervertebral disc. In addition to mechanical compression of the intervertebral disc tissue, inflammatory stimulations due to chemical substances derived from the degenerated intervertebral disc are believed to be involved in the development of lumbar disc herniation. It was previously reported that various optimal environmental factors (circulation, structural components, pH, etc.) as well as triggering factors, including cytokines, were involved in a mechanism of prolapse, regression, and elimination of hernia. We previously studied the extracellular matrix of herniated tissue from a patient with intervertebral disc hernia by using ELISA to measure MMP-3 and TIMP-1 at the protein level and the mRNA level [1]. Currently, extracellular matrix MMP has been discussed in relation to the extrusion and spontaneous regression of the herniated mass observed in lumbar disc herniation. However, the question remains as to whether degenerated protein is really the cause of this condition's pathogenesis. We confirmed immunologically by means of electron microscopy that extrusion is caused by the AGE (advanced glycation end products)–induced cross-linking of collagen and that spontaneous regression is due to AGE receptors on macrophages.

Further, AGEs were found to be already exposed during histogenesis, suggesting a relation to apoptosis. In lumbar disc herniation and aging, glucose-derived AGEs cross-link proteins and cause vascular tissue damage [2].

In that study we established chondrocytes derived from human herniated intervertebral disc tissue and analyzed them by means of an electron microscope in order to investigate the pathologies of intervertebral disc herniation in an in vitro disc hernia model. We also confirmed by electron microscopy that clinically observed spontaneous regression is caused by macrophages [3].

II. MATERIALS AND METHODS

A. Tissues

Herniated intervertebral discs obtained from patients with disc herniation were classified as protrusion, extrusion, or as sequestrastion types according to Macnab's classification [4]. The lumbar discs obtained from 23 autopsied cadavers (ranging from 11 to 90 years old) were examined. Herniated intervertebral discs were obtained during surgery from 25 patients (ranging from 18 to 52 years old) with lumbar disc herniation at L4/5. In particular, intervertebral disc with extrusion or sequestration type herniation was subclassified as extruded region or inside region (Table 1).

The cell line KTN-1 was derived from a human chondrocyte of the central region of the intervertebral disc hernia at L4/5, which was obtained from a 34-year-old Japanese male. He had not received previous lumbar surgery or chemical or irradiation therapy. His surgery was performed on November 11, 1997. The central region of extirpated disc material, which was of the subligamentous extruded disc herniation type, was processed for tissue culture immediately after operation. We examined in detail the conditions of these tissues. Small pieces of intervertebral disc tissue were immersed immediately in fixatives for analysis via electron microscopy and electron microscopic immunohistochemistry. Tissues were fixed in several kinds of fixative to optimize the fixative conditions and to avoid fixative-specific artifacts. The tissue specimen was washed with Hank's balanced salt solution (pH 7.4) containing penicillin (100 units/mL) and streptomycin (100 μg/mL) (Meiji Seika, Tokyo, Japan) for primary culture. All controlled subjects and patients gave written consent to the study.

B. Electron Microscopy

Tissue blocks of interest were sequentially fixed with 2.0% paraformaldehyde/2.5% glutaraldehyde/PBSem, 1.0% glutaraldehyde–0.1 M sodium cacodylate buffer, pH 7.4, and 1.0% OsO_4 followed by LR-White (Sigma, St. Louis, MO) embedding. Cultures were fixed with 1.0%

Table 1 Patient Characteristics

Prolapsed cadaver		Lumbar disc herniation	
Number of patients (M/F)	23 (12/11)	Number of patients (M/F)	25 (15/10)
Normal	6	Protrusion	5
Mild-moderate	9	Extrusion	14
Severe	8	Sequestration	6
Age (mean ± SD)	11–90 (50 ± 20)	Age (mean ± SD)	18–52 (39 ± 10)

glutaraldehyde and 0.1 M sodium cacodylate buffer, pH7.4, for 2 h at 4°C, washed in the same buffer, postfixed with 1.0% $OsO_4$0.1 M sodium cacodylate buffer, pH 7.4, at room temperature (RT) for 1 h, and washed twice with 0.1 M sodium cacodylate buffer [5]. The cells were dehydrated in their respective culture dishes by a graded series of alcohols and three changes of absolute ethanol. The culture dishes were immediately infused with 100% LR-White for 1 h at RT, followed by 100% LR-White overnight at 4°C, and 100% LR-White for 1 h at RT [6]. The culture dishes were cut into culture layers using a scalpel. The culture layer squares in the plane of the dish were assembled into a LR-White block using glue. Ultrathin sections were cut at 90 nm, stained with 2% uranyl acetate and Reynold's lead citrate, and viewed via a JEM2000EX electron microscope at 100 kV [7].

C. Electron Microscopic Immunohistochemistry

Samples were sliced, rinsed with PBSem, and fixed with 4.0% paraformaldehyde/0.1% glutaraldehyde in PBSem for 3 h at RT while being mixed. The fixed tissues were then rinsed in PBSem and cut into smaller blocks [8]. Following microwave oven (Yokogawa Electric Corporation, Tokyo, Japan) irradiation, the sample bottles were kept on ice for 10 min. [9] After being rinsed with a cold solution consisting of 100 mM lysine/100 nM sodium phosphate, pH 7.4/150 mM $NaCl_2$, the specimens were dehydrated in a graded series of cold ethanol and embedded in LR-White at 50°C. Ultrathin sections were cut on a MT-7000 ultramicrotome (Research and Manufacturing Company, Inc.) and collected on nickel grids with a polyvinylformal membrane. The sections were immunostained with monospecific antibodies and a protein A-gold solution with 15 nm to 5 nm gold particles (EY Laboratories, San Mateo, CA) [10]. Specimens were observed with a JEM2000 electron microscope at an accelerating voltage of 100 kV after being stained with uranylacetate and lead citrate. For the preparation of cultured cell specimens, the cell layers were removed from the dish and fixed in situ for 1 h at 4°C with 4.0% paraformaldehyde/0.1% glutaraldehyde in PBSem at pH 7.4. After being washed overnight at 4°C with 7.5% sucrose in 0.1 M sodium cacodylate at pH 7.4, the specimens were dehydrated in graded ethanols. Immediately before propylene oxide treatment, the samples were embedded in LR-White at 50°C.

D. Established Cell Line KTN-1

The tissue specimens were minced into small pieces, dispersed with 0.1% collagenase (Nitta Gelatin Inc, Osaka, Japan), 0.005% DNase (Sigma, St. Louis, MO) and 0.002% hyaluronidase (Sigma, St. Louis, MO) in Dulbecco's Modified Eagle Medium pH 7.4 (Life Technologies, Grand Island, NY), incubated for 30 min at 37°C, and centrifuged at 250 *g* for 5 min. The cells were suspended in 5 mL of 2 mM EDTA in Ca^{2+}-and Mg^{2+}-free phosphate-buffered saline and incubated for 15 min at 37°C. After centrifugation, the cells were resuspended in 0.2% collagenase in Dulbecco's Modified Eagle Medium, pH 7.4, and incubated for 30 min at 37°C. The cell suspension was then filtered through a mesh and centrifuged again. The cell pellet was finally suspended in Dulbecco's Modified Eagle Medium supplemented with penicillin and streptomycin and then seeded on a petri dish (Iwaki Glass, Tokyo, Japan) [11].

E. Isolation of Monocytes from Human Peripheral Blood

An indicator of the experiment's value was its ex vivo clinical application for each specimen of the blood taken from the same patient. Heparinized peripheral blood from a homologous donor was mixed with one volume of PBS and one volume of hydroxyethyl starch (Plasmasteril;

Fresenius, Bad Homburg, Germany) in a cylinder and allowed to rest for 30 min at 37°C to permit the sedimentation of erythrocytes. The resulting supernatant was centrifuged at 400 *g* for 7.5 min, and the pellet was washed and suspended in PBS. This cell suspension was loaded carefully onto three volumes of Ficoll-sodium metrizoate (Lymphoprep; Nyegaerd, Oslo, Norway; density = 1.077 g/mL) and centrifuged at 400 *g* for 30 min. The layer of mononuclear cells was washed and suspended in Hanks' balanced salt solution, supplemented with 0.5% human serum albumin (HBSS + 0.5% HAS), and used as a monocyte source. Monocytic cells were allowed to adhere to the surface of the plastic tissue culture vessel during incubation at 37°C for 16 h and were separated from non-adherent lymphocytic cells by being washed with prewarmed PBS/1% (v/v) FCS. Growth medium was added to the adherent cell cultures, which were then incubated at 37°C in a humidified atmosphere with 6% (v/v) CO_2 until ready for use. Cells were examined at 3 days postplating, at which time they had differentiated into monocyte-derived macrophages, regardless of their incubation temperature. More than 95% of the adherent cells were macrophages, defined by the recently identified KP-1 (CD68) (DAKO) mature macrophage marker [12]. Finally, color development was established by treating macrophages with AEC (DAKO) at room temperature for 5 min.

F. Alamar Blue Assay

The Alamar Blue assay is a good alternative to the [^{3}H]thymidine assay. The advantages of this assay include a simpler protocol, which saves time and reduces errors, allows rapid assessment of proliferation, allows less costly monitoring of proliferation during the culture period < $2.00 per 96-well plate), and permits additional analysis of proliferating cells. The stock solution of Alamar Blue was aliquoted and kept in darkness at 4°C. To the cultured cells, 20 μL of Alamar Blue (Alamar, Sacramento, CA) (10% of incubation volume) was added according to the manufacturer's instructions. The proliferation of cultures with Alamar Blue was determined under aseptic conditions at 24-h intervals during the culture period by measuring absorbance at 570 and 600 nm in a microELISA titer plate reader (Molecular Devices, Menlo Park, CA). Absorbance at 600 and 570 nm wave lengths determined the OD of oxidized and reduced forms of Alamar Blue, respectively [13].

G. Enzyme Linked Immunosorbent Assay

We determined the tissue and preoperative serum levels of MMP-3 and TIMP-1. That is, 50 mg tissue samples were homogenized and centrifuged at 10,000 rpm for 20 min to obtain the supernatant. Levels of MMP-3 and TIMP-1 in the supernatant of tissue homogenates as well as serum levels of MMP-3 and TIMP-1 were measured with a MMP-3 ELISA kit provided by BioSource Europe (Belgium) and a TIMP-1 ELISA kit provided by Amersham LIFE SCIENCE (England).

H. RT-PCR

Total cellular RNAs were extracted using Isogen (Nipopon Gene Co., Tokyo, Japan), and cDNAs were synthesized from 5 μg of total RNA using RAV-2 reverse transcriptase (Takara, Japan) in the presence of random primers (Takara) in a 20 μL reaction volume at 42°C for 60 min. One μL of cDNA solution was amplified by Taq polymerase (Takara) in a volume of 10 μL. For mRNA detection of IRS-1 and RAGE genes, the PCR procedure was performed with 36 cycles of denaturation at 94°C for 30 s, annealing at 54°C for 30 s, and extension at 72°C for 90 s, with a predenaturing time of 2 min and a final extension time of 5 min. The primer sequences were IRS-1, 5′-CTCGTCAAAGCTATGTGGATACC-3′ (sense) and 5′-GTTGCTTCTGGAAGTTGATGC-3′

(antisense); RAGE, 5′-GCAGTAGTAGGTGCTCAAAAC-3′ (sense) and 5′-GTGTCAGGTGT-TTAATCATCA-3′ (antisense).

I. Statistical Analyses

Values are expressed as mean ± SD. Statistical differences between groups were analyzed using the Mann-Whitney U test or Kruskal-Wallis test. Correlations were assessed using univariate linear regression analysis. A p-value of < 0.05 was considered significant.

III. RESULTS

Chondrocytes were cultured from extruded tissues excised during surgery for lumbar disc hernia and then established (Fig. 1). In vitro growth of the chondrocytes was evaluated by Alamar Blue assay (Fig. 2). Under the employed conditions, the absorbance reflected the total cell marker in the culture. From such data it was possible to identify when a given inoculation density exhibited exponential growth until day 7 of culture, when it reached plateau-phase growth. To investigate the role of macrophages infiltrated into the hernia tissues during a spontaneous regression, macrophages obtained from the same patient were added to the chondrocyte culture. Infiltration of macrophages among the chondrocytes was observed in the mixed culture. When herniated intervertebral disc–derived human chondrocytes were cultured under normal homeostatic conditions, spherical nuclei and the development of rough-surfaced endoplasmic reticula were observed under an electron microscope (Fig. 3a). When the same tissue was directly observed without culture, nuclei degeneration, the development of chromatin granules, changes in the osmotic pressure of the nuclear membrane and rough-surfaced endoplasmic reticulum, and the development of fat droplets were observed (Fig. 3b). These findings were consistent even when different fixatives were used. Subcellular localization of extracellular matrix proteins, MMP-3 and TIMP-1, was analyzed by immunoelectron microscopy. Both MMP-3 and TIMP-1 were localized in the endoplasmic reticulum of the cultured chondrocytes derived from the intervertebral disc obtained from patients with disc herniation (data not shown) [3] and in freshly isolated chondrocytes derived from the intervertebral disc obtained from patients with disc herniation (data not shown) [3]. Furthermore, macrophages obtained from the same tissue specimen were added to the extruded chondrocytes and observed under an electron microscope (Fig. 4), the macrophages from healthy individuals were co-cultured with intervertebral disc herniа-derived chondrocytes and observed by electron microscopy, and macrophages phagocytosing chondrocytes were observed (Fig. 5). Chondrocytes derived from the intervertebral disc obtained from patients with disc herniation were phagocytized by the macrophages. In order examine the expression of scavenger receptors, which have been characterized as phagocytizing apoptotic cells, the expression of CD36 on the macrophages was analyzed. As Figure 6 shows, scavenger receptors are a family of cell surface receptors expressed by macrophages. In addition, Figure 7 shows typical immunohistochemical findings with anti-human MMP-3 monoclonal antibody (Fuji Pharmaceutical Industry, Toyama, Japan) produced in a prolapsed cadaver and lumbar disc herniation. Compared to the control group, the degree of localization of MMP-3–producing cells was significantly increased in both the degenerated and herniated intervertebral discs. In the disc degeneration group, localization of MMP-3–producing cells was more prominent in the severe disc degeneration group than in the mild to moderate disc degeneration group. In the disc herniation group, localization of MMP-3–producing cells was more prominent in the extrusion-type or sequestration-type disc herniation groups than in the protrusion-type disc herniation group. Figure 8 shows that compared to the control group, the degree of localization

of TIMP-1–producing cells was significantly increased in both the degenerated and herniated intervertebral discs. In the disc degeneration group, localization of MMP-3–producing cells was more prominent in the severe disc degeneration group than in the mild to moderate disc degeneration group. In the disc herniation group, localization of TIMP-1–producing cells was more prominent in the severe disc degeneration group than in the mild to moderate disc degeneration group. In the disc herniation group, localization of TIMP-1–producing cells was more prominent in the extruded region than in the inside region in both the extrusion-type and sequestration-type disc herniation groups. There was significant positive correlation between the number of MMP-3–producing cells and that of TIMP-1–producing cells (Fig. 9). In intervertebral disc tissues obtained from autopsied cadavers, the expression of the MMP-3 gene was observed in all types of disc degeneration (Fig. 10c) and the expression of the TIMP-1 gene was observed in mild to moderate and severe disc degeneration. However, the expression of the TIMP-1 gene was weaker in the normal intervertebral disc compared to that in the other two disc degeneration groups. Meanwhile, the expression of the MMP-3 gene was observed in all types of disc herniation. As Figure 11 was zymography, in some normal control intervertebral disc tissues obtained from autopsied cadavers, the potential-type MMP-3 was not observed. However, potential-type MMP-3 was observed in the mild to moderate disc degeneration group as well as in the severe disc degeneration group. Moreover, activated-type MMP-3 was observed more frequently in the intervertebral disc with more prominent degeneration (Fig. 11a). Although potential-type MMP-3 was observed in all types of disc herniation, activated-type MMP-3 was observed in the extrusion-type and sequestration-type disc herniation groups (Fig. 11b). Using immunohistochemical study, compared to the control group, the degree of localization of MMP-3–producing cells was significantly increased in both the degenerated and herniated intervertebral disc. In the disc degeneration group, localization of MMP-3–producing cells was more prominent in the severe disc degeneration group than in the mild to moderate disc degeneration group. In the disc herniation group, localization of MMP-3–producing cells was more prominent in the extrusion-type or sequestration-type disc herniation groups than in the protrusion-type disc herniation group. Moreover, localization of MMP-3–producing cells was more prominent in the extruded region than in the inside region in both the extrusion-type and the sequestration-type disc herniation groups. Moreover, as for the enzyme-linked immunosorbent assay (ELISA), Figure 12 shows that, compared to the normal control group, the tissue levels of MMP-3 were significantly high in all groups, and Figure 13 shows that, compared to the normal control group, the tissue levels of TIMP-1 were significantly increased in all groups. In the intervertebral disc tissue obtained from autopsied cadavers, the MMP-3 levels increased with the severity of degeneration. In addition, the MMP-3 levels increased in disc herniation with the severity of herniation. Serum MMP-3 levels were significantly more increased in the degenerated or herniated intervertebral disc than in the normal control group as the severity of degeneration or herniation was increased (Fig. 14). Moreover, serum TIMP-1 levels were also more increased in the degenerated intervertebral disc than in the normal control group with the severity of degeneration. Among the disc herniation groups, there was no difference in serum TIMP-1 levels between the protrusion-type disc herniation group and the normal group. However, serum TIMP-1 levels were significantly higher in the extrusion-type and in the sequestration-type disc herniation groups than in the normal and protrusion-type disc herniation groups (Fig. 15). During the evaluation of correlations among the number of MMP-3–producing or TIMP-1–producing cells, the MMP-3 and TIMP-1 levels in the intervertebral disc, as well as serum MMP-3 and TIMP-1 levels determined by ELISA, positive correlations were observed between the number of MMP-3–producing cells and tissue levels of MMP-3, between the number of TIMP-1–producing cells and tissue levels of TIMP-1, between tissue levels of MMP-3 and TIMP-1 (Figs. 16–18), and between serum levels of MMP-3 and TIMP-1 (Fig. 19). In herniated intervertebral disc

patients complicated by diabetes, the expression of the RAGE gene was 1328bp (arrow) (Fig. 20a), and the IRS-1 gene was 243bp (arrow) (Fig. 20b).

IV. DISCUSSION

Tissue extruded from the intervertebral disc showed obvious signs of degeneration such as changes in osmotic pressure. Macrophages were observed to be the mechanism of spontaneous regression. In patients in whom the blood glucose level had been high in the past, the incidence remained high even though the blood glucose level was currently controlled, suggesting that AGEs affect a gene and that the effect is memorized. Our study may be significant in elucidating another pathological state of lumbar disc hernia. In summary, we have identified an inducible AGE as a novel mechanism for the cooperative interaction between tissue macrophages and lymphocytes during tissue homeostasis or repair. Under conditions of excessive AGE protein/lipid accumulation (in aging or chronic diabetes), this orderly system may be disturbed so that inappropriate lymphokine activity, in synergy with macrophage-derived cytokine activity, could lead to tissue injury. AGEs and insulin induce a wide variety of growth and metabolic responses and play important roles in the anabolic regulation of bone metabolism [2]. In a previous study we evaluated the correlation between disc herniation or degeneration and the levels of MMP-3 or TIMP-1 [1]. Furthermore, we demonstrated that activities of MMPs are regulated by their inhibitors, the tissue inhibitor of metalloproteinases (TIMPs). The previous study revealed that the number of MMP-3–producing or TIMP-1–producing cells increased during disc degeneration or progression of herniation. We also found that there were positive correlations between the number of MMP-3–producing or TIMP-1–producing cells and the tissue levels of MMP-3 or TIMP-1, respectively. It was believed that increased neovascularization, matrix neogenesis, and hydrolysis of matrix by matrix metalloproteases were induced in the intervertebral disc tissue as the severity of degeneration increased. Moreover, MMP-3 was believed to be closely related to the pathological conditions of disc herniation such as the development or elimination

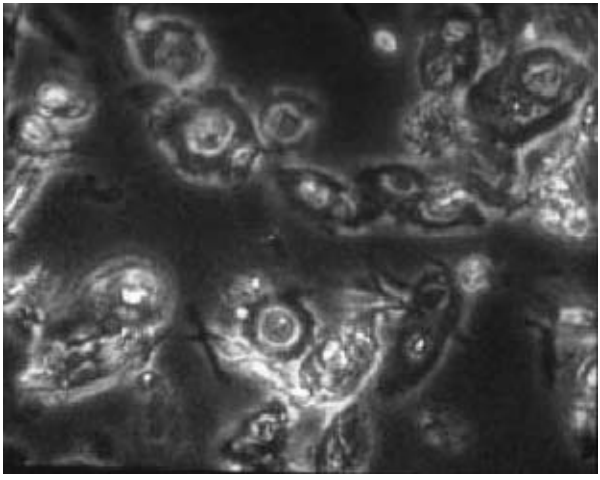

Figure 1 Photomicrographs of KTN-1 cells growing in monolayer culture. Phase-contrast optics, $\times 300$ (original magnification).

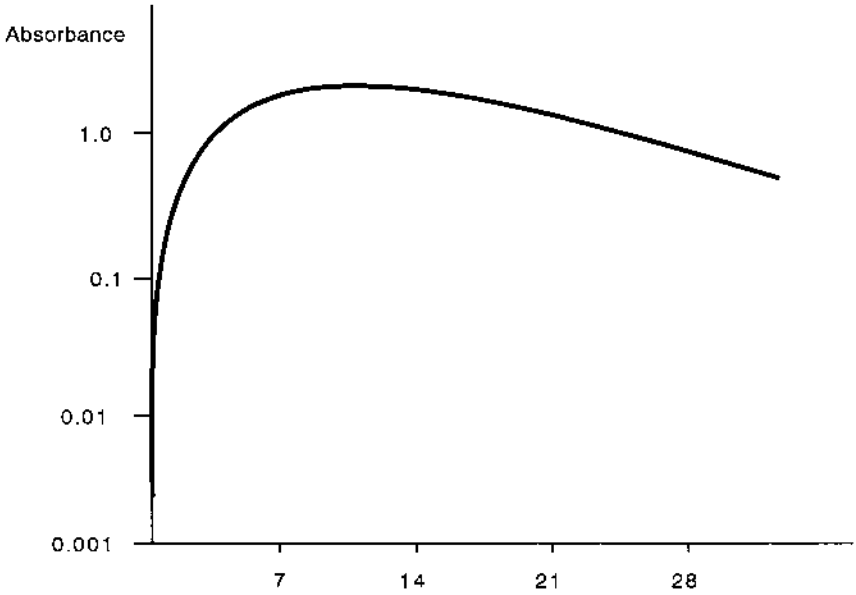

Figure 2 Growth profile assessments using the alamar blue KTN-1. Chondrocytes were cultured from extruded tissues excised during surgery for lumbar disc hernia and then established. In vitro growth of the chondrocytes was evaluated by Alamar blue assay.

of hernia. In a previous study, MMP-3 levels in herniated tissue or in the blood increased with the degree of herniation. Furthermore, the MMP-3 level showed a greater increase in the inside region of the sequestration-type disc herniation than in the extruded region of the extrusion-type disc herniation. These findings suggested that the production of MMP-3 increased further with the degree of herniation. Moreover, we speculated that the development of disc herniation induced changes in the intervertebral disc itself and that MMP-3 influenced not only the herniated tissue itself but also the remaining tissue of the intervertebral disc. In this study we observed the pathological state of a disc hernia at the cellular level. When chondrocytes from the same tissue were cultured under conditions similar to those in the intervertebral disc, the extruded tissue showed a clear difference. The differing cell morphology between an extruded disc and an unextruded disc was significant. The possibility that membrane osmotic pressure affects intervertebral disc hernia in patients and that protein transmission occurs in the endoplasmic reticulum was considered. The differing cell morphology signifies a degeneration of herniation. It was also believed that spontaneous regression is due to the infiltration of macrophages. Rapalino et al. [15] circumvented this by implanting macrophages, preexposed ex vivo to peripheral nerve segments, into a transected rat spinal cord. In recovered rats, retransection of the cord above the primary transection site led to loss of recovery, indicating the involvement of long descending spinal tracts. Postinjury recovery in most tissues requires an effective dialogue with macrophages; however, in the mammalian central nervous system, this dialogue may be restricted (possibly due to its immune-privileged status), which probably contributes to its regeneration failure. We also confirmed by electron microscopy that clinically observed spontaneous regression is caused by macrophages. Expression of CD36 on the macrophages was also demonstrated. Rigotti et al. [16] found that CD36 and SR-B1, members of the class B scavenger receptor family, were expressed on macrophages previously believed to phagocytose apoptotic cells

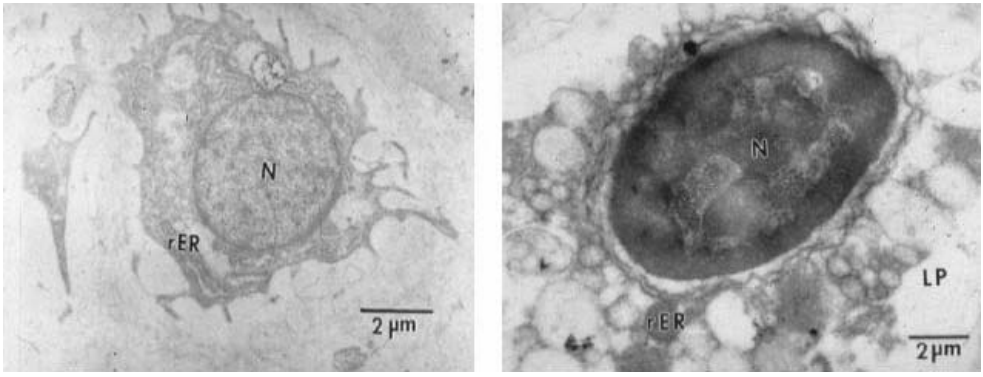

Figure 3 Established cell line KTN-1. The cell line KTN-1 was derived from a human chondrocyte of the central region of the intervertebral disc hernia at L4/5, which was obtained from a 34-year-old Japanese male. He has not received previous lumbar surgery, chemical, or irradiation therapy. His surgery was performed on November 11, 1997. The central region of extirpated disc material, which was subligamentous extruded disc herniation type, was processed for tissue culture immediately after operation. We examined in detail the conditions of these tissues. The tissue specimens were minced into small pieces, dispersed with 0.1% collagenase (Nitta Gelatin Inc, Osaka, Japan), 0.005% DNase (Sigma, St. Louis, MO) and 0.002% hyaluronidase (Sigma, St. Louis, MO) in Dulbecco's Modified Eagle Medium pH7.4 (Life Technologies, Grand Island, NY), incubated for 30 min at 37°C, and centrifuged at 250 *g* for 5 min. The cell pellet was finally suspended in Dulbecco's Modified Eagle Medium supplemented with penicillin and streptomycin and then seeded on a petri dish (Iwaki Glass. Tokyo, Japan). All controlled subjects and patients gave written consent to the study. Electric pulse delivery and electrodes. When herniated intervertebral disc-derived human chondrocytes were cultured under normal homeostatic conditions, spherical nuclei and the development of roughsurfaced endoplasmic reticula were observed under an electron microscope (A). Electron micrograph cultured chondrocytes derived from human intervertebral disc herniation (A) (bar = 2 μm). Electron micrograph of freshly isolated chondrocytes derived from human intervertebral disc herniation (B) (bar = 2 μm).

[17]. These results suggest that the scavenger receptors on the macrophaes may contribute to spontaneous regression through ingestion of apoptotic cells. There receptors are presumed to play an important part in the spontaneous regression of herniated tissue on macrophages; however, the function of the macrophages cannot be observed in chondrocytes from an undegenerative disc without herniation. Unfortunately, the macrophages cannot be obtained from normal human discs for culture. At present we can obtain them from established chondrocytes derived from normal human tissue. Haro et al. [18,19] also found that MMP-3 and macrophages were expressed in herniated intervertebral disc resorption. They concluded that macrophage induction of chondrocyte MMP-3 plays a major role in disc resorption by mechanisms that include the generation of a bioactive macrophage chemoattractant. Macrophages were observed to be the mechanism by which spontaneous regression occurs.

Macrophages incorporate LDL via the scavenger receptors. Point mutation in IRS-1 blocks the action of glucose transporter, $GLUT_4$, while PPAR γ simultaneously promotes differentiation/induction of fat cells, resulting in bulky fat cells. Large fat cells secrete various cytokines, feedback signals, and inhibit phosphorylation of insulin receptors and expression of $GLUT_4$, which transforms macrophages to foam cells, increasing fat cells (Fig. 21). The foam cells cannot phagocytose abnormally ossified cartilage tissues, and the disorder progresses.

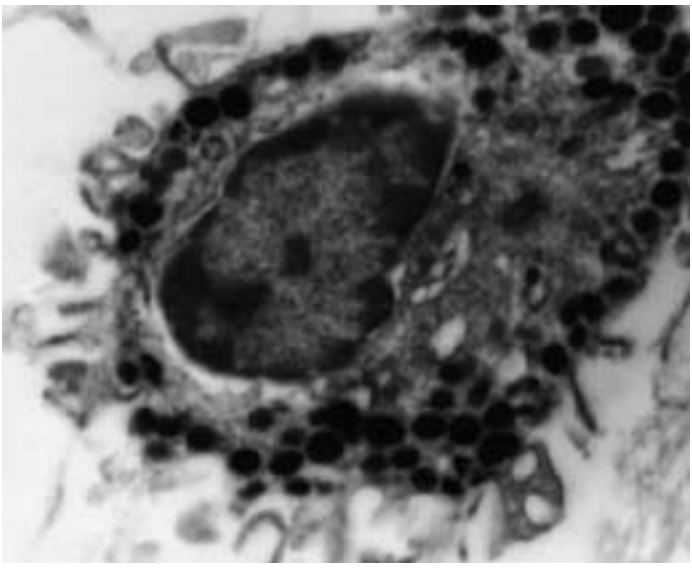

Figure 4 Electronic microphotograph of intervertebral disk hernia organization.

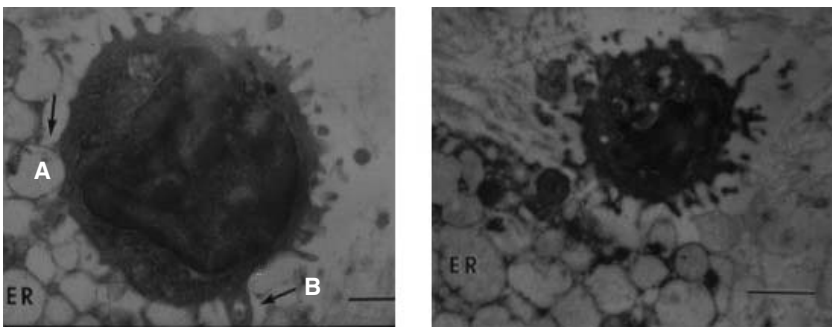

A **B**

Figure 5 It is possible to identify when a given inoculation density exhibited exponential growth until day 7 of culture, when it reached plateau-phase growth. To investigate the role of macrophages infiltrated into the hernia tissues during a spontaneous regression, macrophages obtained from the same patient were added to the chondrocyte culture. Infiltration of macrophages among the chondrocytes was observed in the mixed culture. When herniated intervertebral disc–derived human chondrocytes were cultured under normal homeostatic conditions, spherical nuclei and the development of rough-surfaced endoplasmic reticula were observed under an electron microscope. When the same tissue was directly observed without culture, nuclei degeneration, the development of chromatin granules, changes in the osmotic pressure of the nuclear membrane and rough-surfaced endoplasmic reticulum, and the development of fat droplets were observed. Electron micrographs showing the infiltration of macrophages and the chondrocyte culture cells derived from human intervertebral disc (a: bar $= 2\ \mu m$; b: bar $= 1\ \mu m$). (A) The taking-in mechanism in the cell, the zipper mechanism type. (B) A similar type of mechanism having to do with a crater of the macrophage.

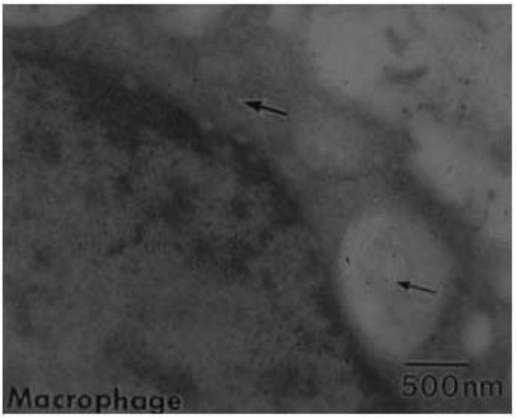

Figure 6 Chondrocytes derived from the intervertebral disc obtained from patients with disc herniation were phagocytized by macrophages. In order to examine the expression of scavenger receptors, which have been characterized as phagocytizing apoptotic cells, the expression of CD36 on the macrophages was analyzed. As shown, scavenger receptors are a family of cell surface receptors expressed by macrophages. Electron micrographs show the immunohistochemical localization of CD36 in human macrophage. Arrows indicate particles on macrophage. Immunogold labeling with mAb, CD36 (bar = 500 nm).

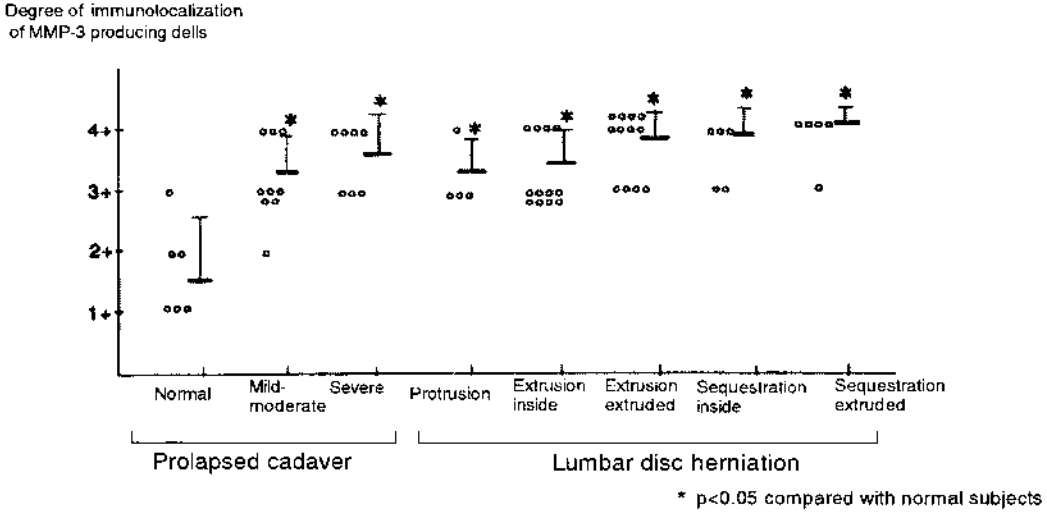

Figure 7 Degree of distribution of MMP-3-producing cells in prolapsed cadaver and lumbar disc herniation. In the intervertebral disc tissue obtained from autopsied cadavers, the number of MMP-3–producing cells increased with the severity of degeneration. The number of MMP-3–producing cells increased in the herniated intervertebral disc obtained from patients with disc herniation with the degree of herniation. The number of MMP-3–producing cells increased more in the inside region of the sequestration-type disc herniation than in the extruded region of the extrusion-type disc herniation. 1 +, less than 10% positive; 2 +, 10–40% positive; 3 +, 40–70% positive; 4 +, more than 70% positive. *$p < 0.05$ compared with normal subjects.

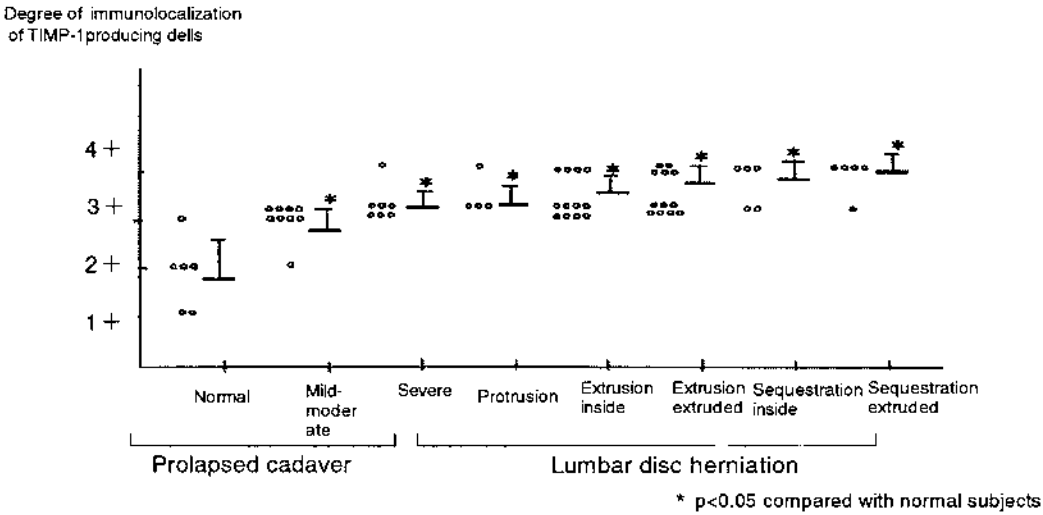

Figure 8 Degree of distribution of TIMP-1–producing cells in prolapsed cadaver and lumbar disc herniation. In the intervertebral disc tissue obtained from autopsied cadavers, the number of TIMP-1–producing cells increased with the severity of degeneration. The number of TIMP-1–producing cells increased in the herniated intervertebral disc obtained from patients with disc herniation with the degree of herniation. The number of TIMP-1–producing cells was more increased in the inside region of the sequestration-type disc herniation than in the extruded region of the extrusion-type disc herniation. 1 + , less than 10% positive; 2 + , 10–40% positive; 3 + , 40–70% positive; 4 + , more than 70% positive. *$p < 0.05$ compared with normal subjects.

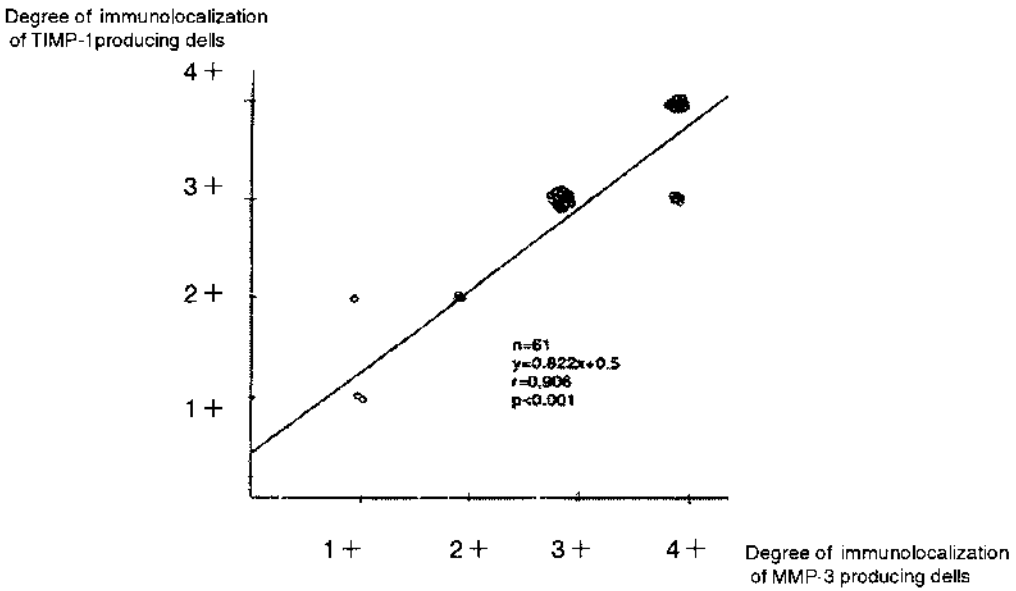

Figure 9 Correlation between the number of MMP-3–producing cells and that of TIMP-1–producing cells. There was a significantly positive correlation between the number of MMP-3–producing cells and that of TIMP-1–producing cells.

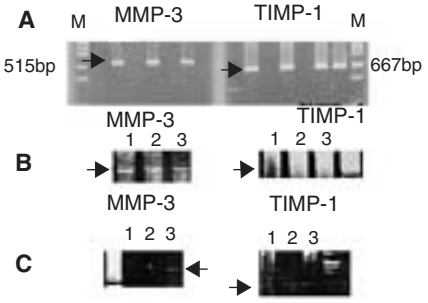

Figure 10 (A) Cloning MMP-3 cDNA and TIMP-1 cDNA. (B) RT-PCR in the degenerated intervertebral disc (line 1: normal, line 2: mild-moderate; line 3: severe). In the intervertebral disc tissue obtained from pathologically autopsied cadavers, the MMP-3 gene was expressed in all types of disc degeneration. The expression of the TIMP-1 gene was observed in the mild to moderately degenerated intervertebral disc as well as in the severely degenerated intervertebral disc. However, the expression of the TIMP-1 gene was weaker in the normal intervertebral disc compared to the other 2 disc degeneration groups. (C) RT-PCR in disc herniation (protrusion type, extruded and inside regions of the extrusion type) (line 1: protrusion type; line 2: extruded regions of the extrusion type; line 3: inside regions of the extrusion type). The MMP-3 gene was expressed in all types of disc herniation. The expression of TIMP-1 gene was clearly observed in the extruded region of the extrusion and sequestration types of disc herniation. However, the expression of the TIMP-1 gene was weaker in the inside region of the above types of disc herniation.

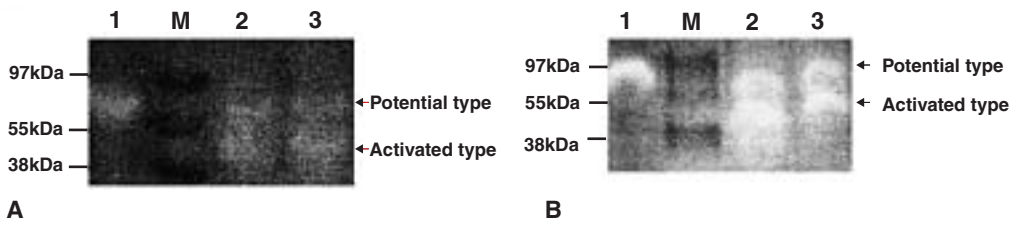

Figure 11 (A) Zymography of the degenerated intervertebral disc (M: marker; line 1: normal; line 2: mild-moderate; line 3: severe). Potential type MMP-3 was not observed in the normal intervertebral disc. However, potential type MMP-3 was observed in the mild to moderately degenerated intervertebral disc as well as in the severely degenerated intervertebral disc. Moreover, activated type MMP-3 was observed in the highly degenerated intervertebral disc. (B) Zymography in disc herniation (protrusion type, extruded and inside regions of the extrusion type) M: marker; line 1: protrusion type; line 2: extruded regions of the extrusion type; line 3: inside regions of the extrusion type). Potential type MMP-3 was observed in all types of disc herniation. However, activated type MMP-3 was observed in the extrusion and sequestration types of disc herniation.

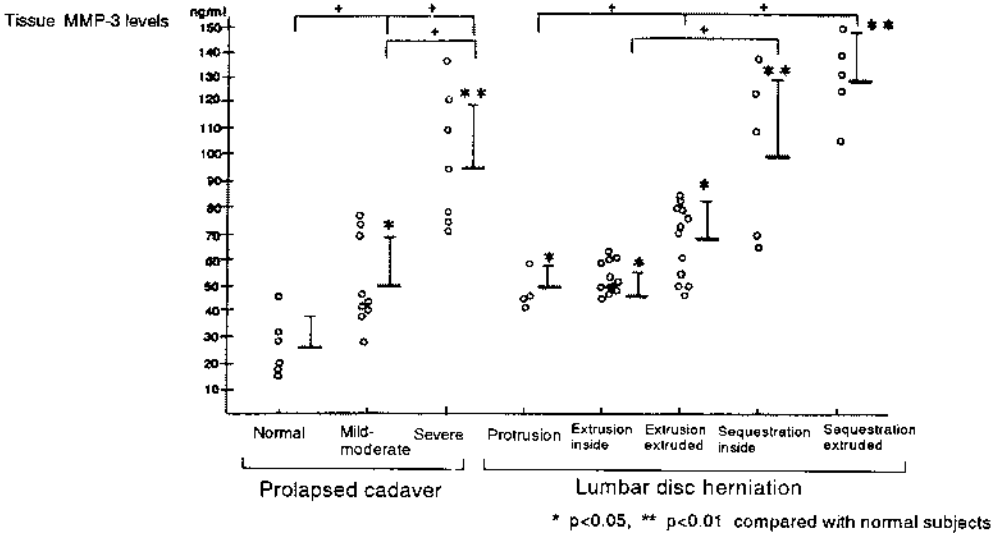

Figure 12 Determination of tissue MMP-3 levels in the intervertebral disc by ELISA. In the intervertebral disc obtained from autopsied cadavers, the tissue levels of MMP-3 increased with the severity of degeneration. The tissue levels of MMP-3 increased in the herniated intervertebral disc with the degree of herniation. The tissue levels of MMP-3 were more increased in the inside region of the sequestration type disc herniation than in the extruded region of the extrusion type disc herniation.

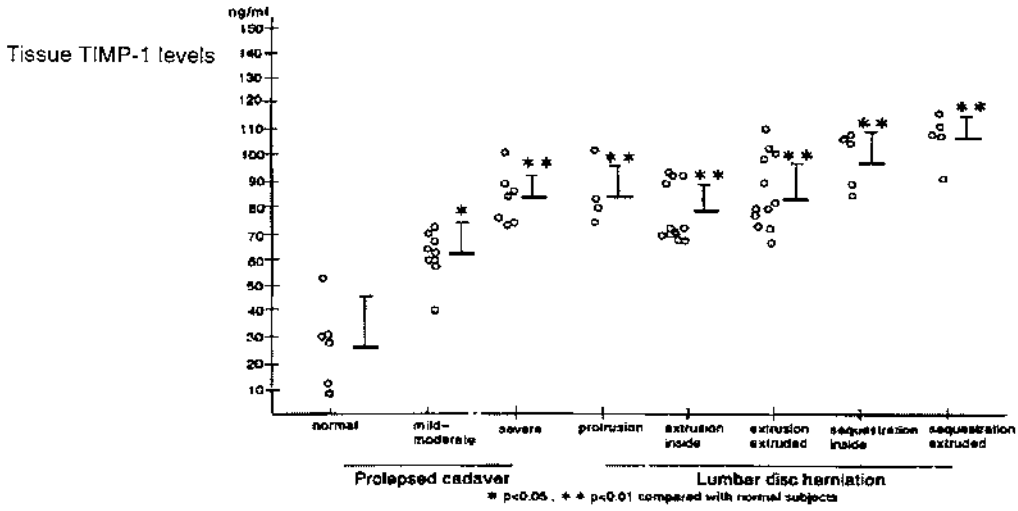

Figure 13 Determination of tissue TIMP-1 levels in the intervertebral disc by ELISA. In the intervertebral disc obtained from autopsied cadavers, the tissue levels of TIMP-1 increased with the severity of degeneration. The tissue levels of TIMP-1 increased in the herniated Intervertebral disc with the degree of herniation. The tissue levels of TIMP-1 were more increased in the inside region of the sequestration type disc herniation than in the extruded region of the extrusion type disc herniation.

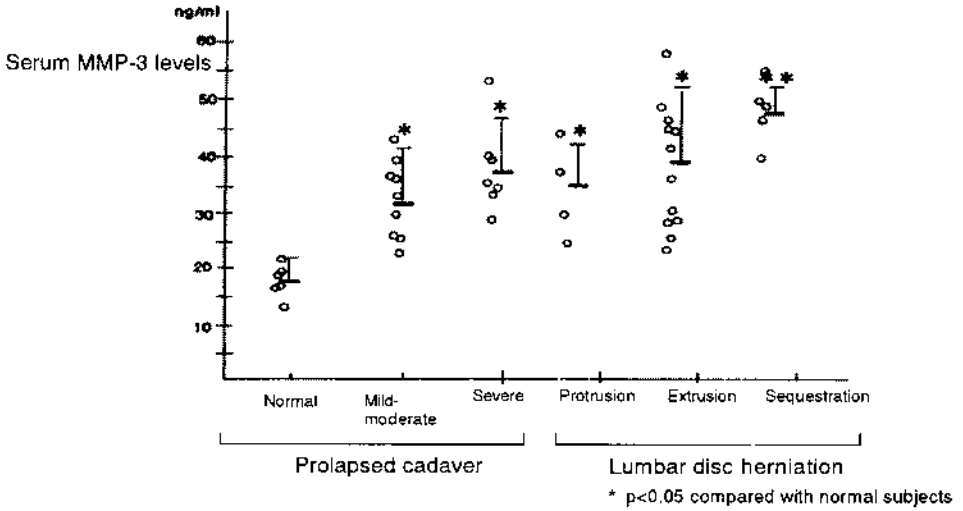

Figure 14 Determination of serum MMP-3 levels by ELISA. In the intervertebral disc obtained from autopsied cadavers, the serum MMP-3 levels increased with the severity of degeneration. The serum MMP-3 levels increased in the herniated intervertebral disc with the degree of herniation.

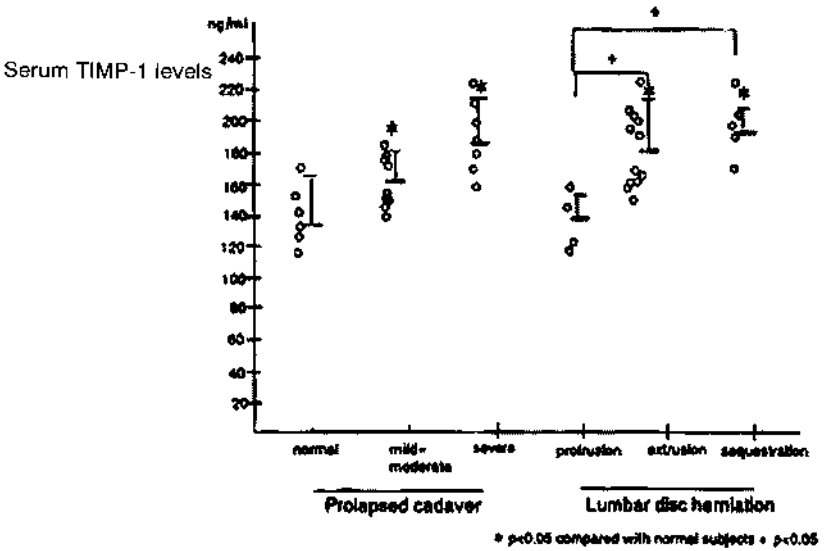

Figure 15 Determination of serum TIMP-1 levels by ELISA. In the intervertebral disc obtained from autopsied cadavers, the serum TIMP-1 levels increased with the severity of degeneration. The serum TIMP-1 levels increased in the herniated intervertebral disc with the degree of herniation.

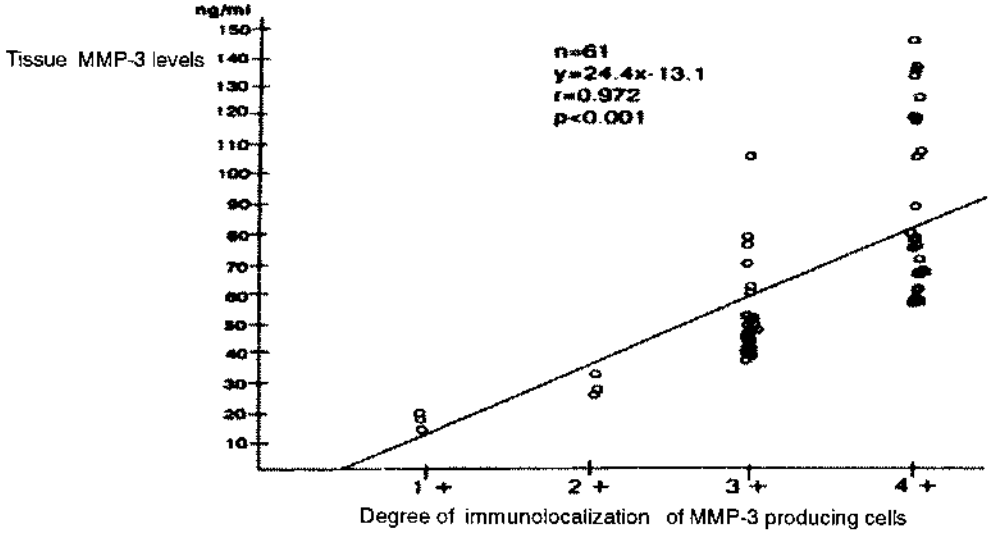

Figure 16 Correlation between the number of MMP-3–producing cells and levels of MMP-3 in tissue samples. Production of MMP-3 increased with the number of MMP-3–producing cells, and there was significant positive correlation between the number of MMP-3–producing cells and tissue MMP-3 levels.

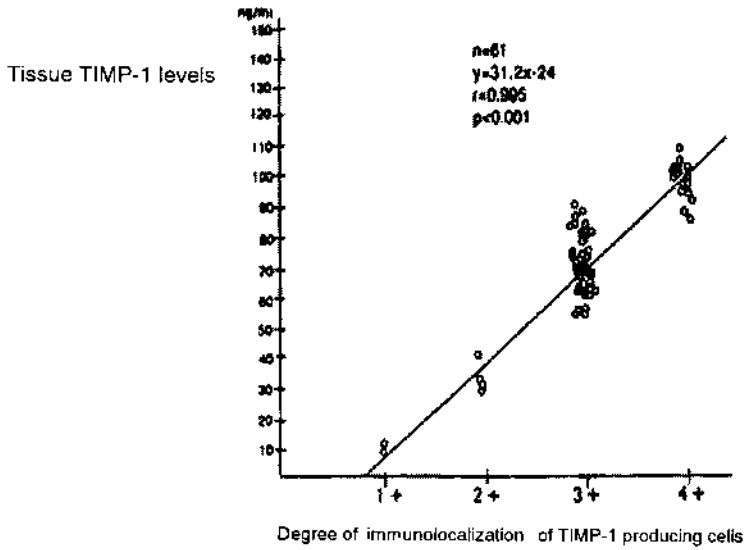

Figure 17 Correlation between the number of TIMP-1–producing cells and levels of TIMP-1 in tissue samples. Production of TIMP-1 increased with the number of TIMP-1–producing cells, and there was significant positive correlation between the number of TIMP-1–producing cells and tissue TIMP-1 levels.

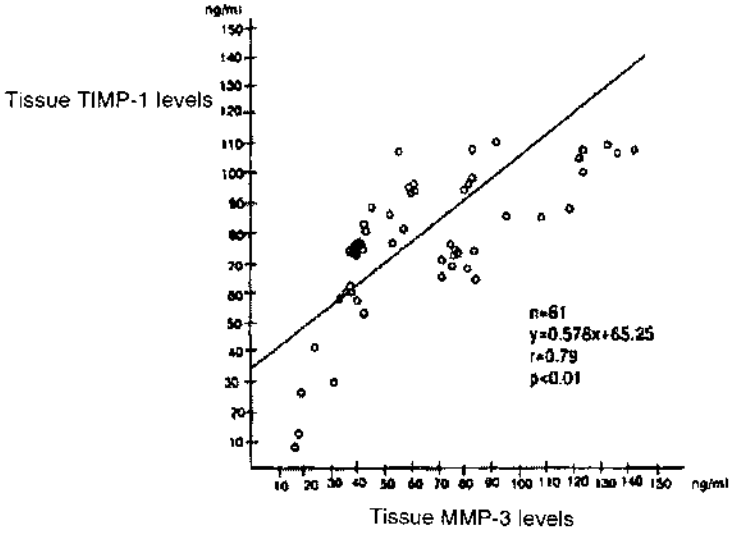

Figure 18 Correlation between levels of MMP-3 and TIMP-1 in tissue samples. There was a significant positive correlation between levels of MMP-3 and TIMP-1.

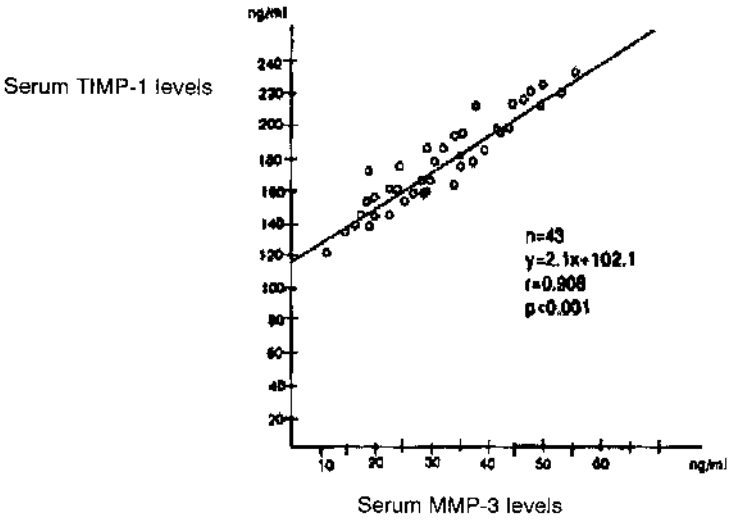

Figure 19 Correlation between blood levels of MMP-3 and TIMP-1. There was a significant positive correlation between blood levels of MMP-3 and TIMP-1.

In intervertebral discs, pH is generally acidic and few blood vessels are present, indicating a low metabolic environment. Under hyperglycemic conditions, accumulation of AGE progresses and degenerates the intervertebral disc and causes extrusion of tissues from the intervertebral disc, leading to herniation. Hyperglycemia transforms macrophages to fat cells and inhibits spontaneous remission. If blood sugar and fat are controlled, macrophages are mobilized and

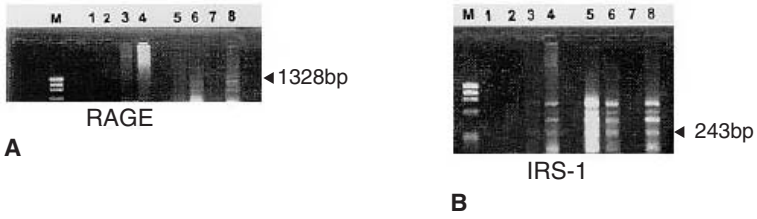

Figure 20 RT PCR. In herniated intervertebral disc patients complicated by diabetes, the expression of (A) the RAGE gene was 1328 bp (arrow) and (B) the IRS-1 gene was 243 bp (arrow). Lane M: Ø × 174 Hae I I I digest. Lanes 1–4: herniated intervertebral disc patients. Lanes 5–8: herniated intervertebral disc patients complicated by diabetes.

phagocytose tissues extruding from intervertebral discs even in the presence of other factors (smoking, physical factors), causing spontaneous remission, and compression of nerves and cytokines decrease, resulting in spontaneous healing.

ACKNOWLEDGMENTS

We are grateful to Professor Mitsuaki Yoshizuka (Department of Anatomy, Kurume University School of Medicine), Professor Takato Ueno (Research Center for Innovative Cancer Therapy,

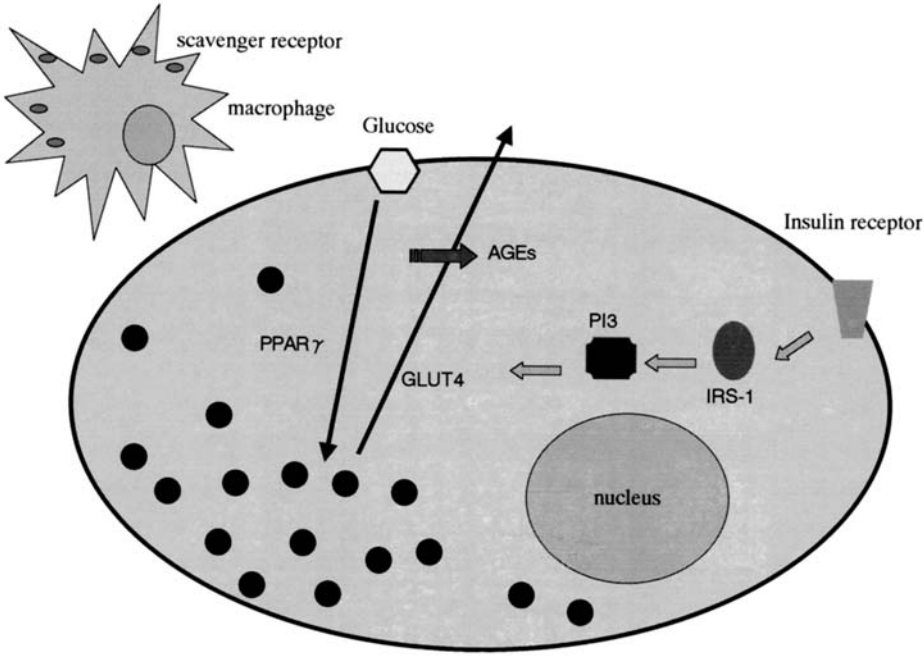

Figure 21 Mechanism of glucose transportation promotion by insulin in bone formation.

Kurume University School of Medicine), Assistant Professor Atsuo Jimi (Department of Pathology, Kurume University School of Medicine), Assistant Professor Akira Yamada (Department of Immunology, Kurume University School of Medicine) and Professor Michio Sata (Second Department of Medicine, Kurume University School of Medicine) for helpful suggestions and observations and a critical reading of the manuscript. Their contributions to our paper have been great, and the author takes pleasure in acknowledging the important part played by them. Thanks are also due to the many colleagues with whom I have discussed this problem.

REFERENCES

1. Nishida T. Kinetics of tissue and serum matrix metalloproteinase-3 and tissue inhibitor of metalloproteinases-1 in intervertebral disc degeneration and disc herniation. Kurume Med J 1999; 46:39–50.
2. Tsuru M, Nagata K, Jimi A, Irie K, Yamada A, Nagai R, Horiuchi S, Sata M. Effect of AGEs on human disc herniation: intervertebral disc hernia is also effected by AGEs. Kurume Med J 2002; 49: 7–13.
3. Tsuru M, Nagata K, Ueno T, Jimi A, Irie K, Yamada A, Nishida T, Sata M. Electron microscopic observation of established chondrocytes derived from human intervertebral disc hernia (KTN-1) and role of macrophages in spontaneous regression of degenerated tissues. Spine J 2001; 6:422–431.
4. Macnab BI. Williams & Wilkins. Baltimore, 1977:91–95.
5. Grutzkau A, Kruger-Krasagakes S, Kogel H, Moller A. Detection of intracellular interleukin-8 in human mast cells: flow-cytometry as a guide for immunoelectron microscopy. J Histochem Cytochem 1997; 45:935–945.
6. Raymond A, Sobrl A, Julian R, Hinojoza R, Atsuko Maeda, Michael Chen. Endothelial cell integrin laminin receptor expression in multiple sclerosis lesions. Am J Physiol 1998; 153:405–415.
7. Kuhn H. A simple method for the preparation of cell cultures for ultrastructural investigation. J Histochem Cytochem 1981; 29:84–86.
8. Brown RA, Kayser M, Mclaughlin B, Weiss JB. Collagenase and gelatinase production by calcifying growth plate chondrocytes. Exp Cell Res 1993; 208:1–9.
9. Login GR, Dvorak AM. Microwave energy fixation for electron microscopy. Am J Pathol 1985; 120:230–243.
10. Bendayan M. Protein A-gold electron microscopic immunocytochemistry: methods, applications and limitations. J Electron Microsc Tech 1984; 1:243–270.
11. Funakoshi A, Tateishi K, Tsuru M, Jimi A. Acetylcholine regulates pancreastatin secretion from the human pancreastatin-producing cell line (QGP-1N). J Clin E&M 1991; 73:151–155.
12. Burmester GR, Winchester RJ, Dimitriu-Bona A, et al. Delineation of four cell types comprising the giant cell tumor of bone: expression of Ia and monocyte-macrophage lineage antigen. J Clin Invest 1983; 71:1633–1648.
13. Ahmed AS, Gogal RM, Jr, Walsh JE. A new rapid way of determining the proliferation of lymphocytes: an alternative to [^{3}H]thymidine incorporation assay. J. Immunol. Methods 1994; 170:211–224.
14. Obata K, Okada K, Iwata K, Kohrin Y, Ohuchi E. A one-step sandwich enzyme immunoassay for human metalloproteinase-3 (stromelysin-1) using monoclonal antibodies. Clin Chim Acta 1992; 211: 59–72.
15. Rapalino O, Lazarov-Spiegler O, Agranov E,. Implantation of stimulated homologous macrophages results in partial recovery of paraplegic rats. Nat Med 1998; 4:814–821.
16. Rigotti A, Acton SL, Krieger M. The class B scavenger receptors SR-BI and CD36 are receptors for anionic phospholipids. J. Biol. Chem 1995; 270:16221–16224.
17. Ren Y, Silverstein RL, Allen J, Savill J. CD36 gene transfer confers capacity for phagocytosis of cells undergoing apoptosis. J. Exp. Med 1995; 181:1857–1862.
18. Haro H, Crawford HC, Fingleton B, MacDougall JR, Kenichi S, et al. Matrix metalloproteinase-3 dependent generation of a macrophage chemoattractant in a model of herniated disc resorption. J Clin Invest 2000; 105:133–141.
19. Haro H, Crawford HC, Fingleton B, Kenichi S, et al. Matrix metalloproteinase-7 dependent release of tumor necrosis factor-α in a model of herniated disc resorption. J Clin Invest 2000; 105:143–150.

42

Gene Expression Profiling During Osteochondrogenic Events in the Spinal Region: Use in the Development of Promising Spinal Fusion

Takanobu Nakase
Osaka University Graduate School of Medicine
Suita, Japan

I. INTRODUCTION

Recent advances in molecular biology have elucidated the characteristics of the cellular mechanisms involved in spine disorders and opened the way for promising, less invasive spinal fusion processes using new molecular technologies. What kind of molecules are locally involved in osteochondrogenic events occurring in spinal regions? What kinds of cells in what locations respond to what kinds of osteoinductive growth factors? The answers to such questions would help identify the targeted foci that induce osteochondrogenesis in the spine, leading to spinal fusion based on molecular or recombinant techniques. Therefore, gene expression profiling of various processes of osteoinductive events in the spine is an important step in the formulation of a strategy to develop these new approaches to promising spinal fusion methods. In this chapter, patterns of gene expression are introduced utilizing animal models and human specimens. Some targeting molecules, targeting sites, and cells are identified, and a strategy for the future development of successful spinal fusion is suggested.

II. STRATEGY FOR THE DEVELOPMENT OF MOLECULAR BIOLOGY–BASED SPINAL FUSION

If osteochondrogenesis, such as endochondral and intra-membranous ossification, is induced in spinal regions in vivo using molecular biology techniques, the process will become a powerful tool for less invasive spinal fusion. When this method is taken into consideration, all skeletal morphogens involved in the embryogenic process [1] become candidate molecules for spinal fusion. Thus, the existing research into the functions of these candidate molecules during osteochondrogenesis should be examined in detail.

The first step is confirmation of candidate molecules in the spine (Fig. 1). Both human surgical specimens and experimental animal models can provide such candidates. Systematic analysis can only be performed using experimental models. Investigations using human specimens need to be performed in parallel to confirm whether the experimental results suitably reflect the human condition.

The second step is the identification of delivery cells, cells responsive to these candidate factors, and the location of these cells. This information will help identify the targeting foci for less invasive spinal fusion. In situ hybridization and immunohistochemistry using histological sections can provide all of this data.

The final step is the use of the candidate molecules for spinal fusions. The procedures should be less invasive and more successful than the conventional surgical procedures. For example, injection of the target genes, targeting overexpression of the osteogenic molecules in the proper regions, gene-transfected cell transplantation, and application of recombinant proteins as well as upregulation of receptors are all possible procedures.

This chapter focuses on the first and second steps, i.e., identification of candidate molecules, cells, and sites for the osteochondrogenic events in the spine. Such information is of vital importance for molecular biology–based spinal fusion procedures.

III. GENE EXPRESSION PROFILING IN THE PROCESS OF OSTEOCHONDRO-INDUCTIVE EVENTS IN THE SPINE

Prominent osteochondrogenic events have been induced by mechanical stimuli in cervical spine regions in a mouse experimental model. This model was created by dissecting the posterior spinal segment (spinous process and related muscles) of 5-week-old mouse cervical spine [2,3]. In this model, mechanical overload stimulates and accelerates the osteochondrogenic process of the anterior spinal segment, leading to osteophyte formation. This phenomenon is most prominently observed in the C5/6 spine. The radiological and histological findings in this model resemble those occurring in the human condition.

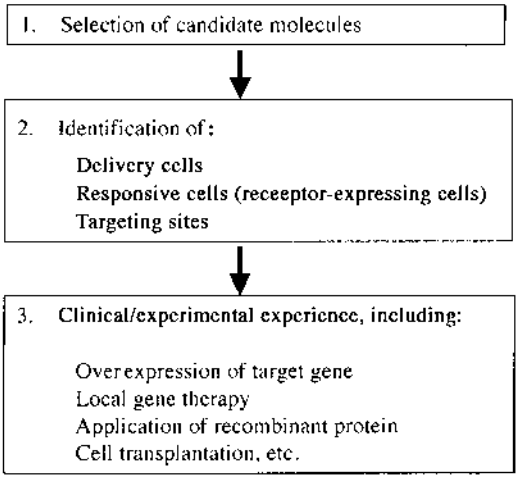

Figure 1 Strategy for development of molecular biology–based spinal fusion.

A. Molecular Mechanisms Underlying the Process of Experimental Spondylosis

1. Histological Process of Experimental Spondylosis

Histological examination of the cervical spines of preoperative mice shows normal morphology, i.e., the nucleus pulposus enriched by many layers of annulus fibrosus (Fig. 2). Cells in the annulus fibrosus are spindle shaped.

Histological events occurring in the postoperative stage are most clearly observed in the anterior (ventral) portion. In the early phase, the volume of nucleus pulposus decreases and some cells in the outer layer of the annulus fibrosus show metaplasia into round chondrocyte-like cells. No prominent osteophyte formation can be detected.

In the late phase, the nucleus pulposus disappears and the lamellar structure of the annulus becomes disorganized. Instead, enlargement of cartilaginous tissues together with osteophyte tissue is observed in the anterior margin of the intervertebral space. Spindle-shaped cells in the annulus are lost and replaced by mature chondrocytes. In age-matched control groups, these characteristic findings are not seen. These findings mimic the histology of human surgical specimens of spondylosis.

2. Candidate Molecules Involved in the Process of Experimental Spondylosis

Based on in situ messenger (m) RNA localization studies on histological sections (in situ hybridization), several candidate molecules in the process of the development of spondylosis have been

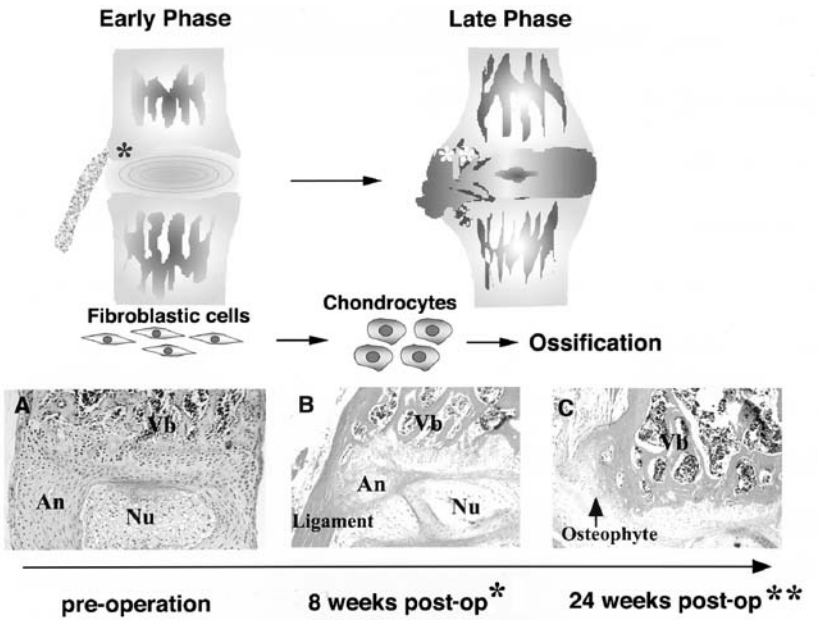

Figure 2 Histological transition seen in the process of experimental spondylosis model. (Upper) Schematic diagram of histological transition of experimental spondylosis. Fibroblastic undifferentiated cells differentiate into chondrocytes, leading to ossification. (Lower) Photomicrographs showing histology of the sagittal sections of the anterior margin of disc and vertebral junction (annular-ligament complex) of C5/6 in each phase. A: Safranin-O and fast-green staining; B and C: hematoxylin and eosin staining. (A) Normal 5-week old mouse; (B) early phase; (C) late phase. An, annulus fibrosus; Nu, nucleus pulposus; Vb, vertebral body. (magnification $\times 100$)

identified in this model [3,4]. These molecules are members of the BMP (bone morphogenetic protein) families [5–8], PTHrP (parathyroid hormone–related peptide), and Ihh (Indian hedgehog) [9–13], which are essential molecules for cartilage generation and endochondral ossification. Each of these molecules plays a specific role in the process of ossification through its specific receptor [9,14,15].

BMP and BMP Receptors. In the early stage, BMP-4 mRNA is localized predominantly in cells in the anterior margin of the discs (annular-ligament complex), together with ALK-6 (BMP receptor type IB) mRNA. GDF (growth/differentiation factor)-5 and BMP-6 mRNAs are not detected at this stage. In the late stage, the number of cells positive for BMP-4 decrease, whereas GDF 5 and BMP-6 mRNAs are localized in cells undergoing chondrogenesis. ALK-3 (BMP receptor type IA) mRNA begins to appear in this stage together with ALK-6 mRNA (Figs. 3A-3C, 3I, and Fig. 4).

Ihh, PTHrP, and Their Receptors. In the early stage, transcripts for Ihh are absent, but those for Ptc (patched: a receptor for Ihh), PTHrP, and PTHR (PTH receptor) are localized mainly in cells in the anterior margin of the discs. In the late stage, transcripts for Ihh and PTHrP are localized in mature, hypertrophic chondrocytes adjacent to the bone-forming area in osteophytes. At this stage, mRNAs for Ptc and PTHR continue to localize in the osteophytic region (Figs. 3D–3H and Fig. 4).

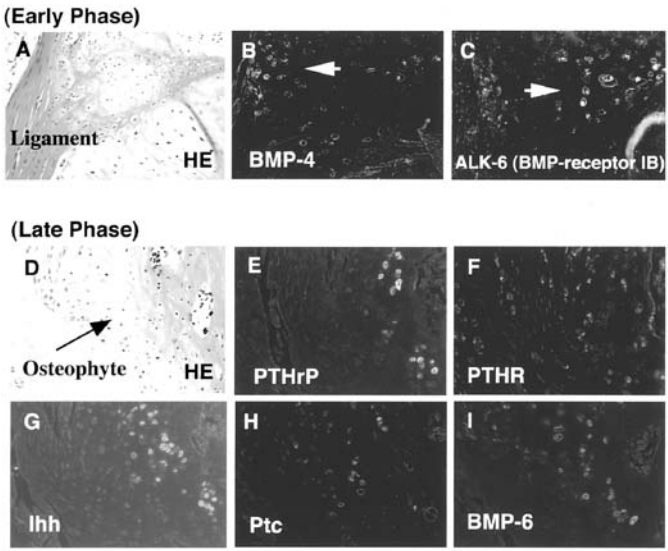

Figure 3 Examples of mRNA localization of osteochondrogenic factors in the mice spondylosis model as revealed by in situ hybridization. In the early phase, both BMP-4 (arrow in B) and ALK-6 (arrow in C) mRNAs are localized near the attachment of the spinal ligament. However, ALK-6 mRNA is localized in a rather more inner area than BMP-4 mRNA (A–C indicate higher magnification of Fig. 2B). In the late phase, both Ihh and Ptc mRNAs are localized in chondrocytes as well as their receptors in the newly formed osteophyte region. Ptc and PTHR mRNAs are localized more widely than those for their ligands. (D–I correspond to a higher magnification of Fig. 2A.) All are sagittal sections of C5/6 spine. HE: Hematoxylin and eosin staining. B, C, and E–I are the results of in situ hybridization. White spots show positive signals. A–C and D–I are serial sections, respectively. (magnification $\times 200$)

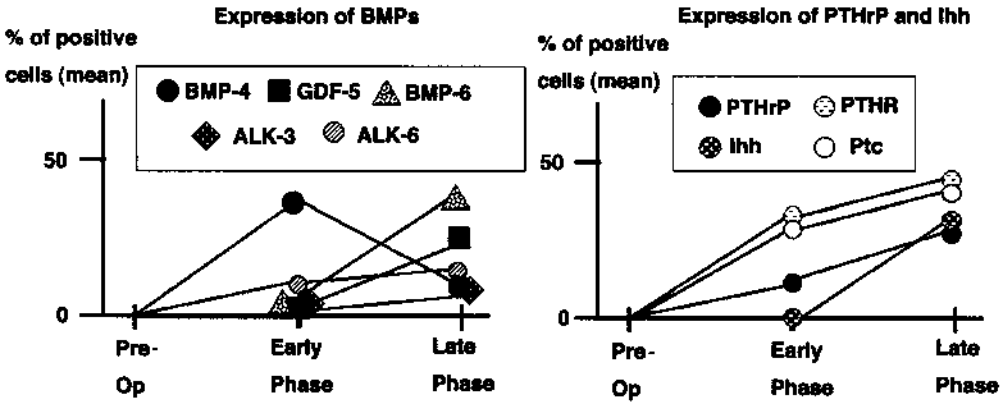

Figure 4 Semi-quantitative evaluation of mRNA expression in each phase of spondylosis model. Transition of the means of the number of cells positive for BMP members (left), and PTHrP and Ihh (right) as well as their receptors in the anterior one-third portion of C5/6 cervical spine region in murine experimental spondylosis.

B. Candidate Molecules in Osteochondrogenesis in the Spine and Their Potential Role: Possible Regulation of the Process of Spondylosis

Such expression profiling of genes during the process of spondylosis provides valuable information of the mechanism of spondylosis. At the very least, BMP-4, -6, GDF-5, PTHrP, and Ihh are involved in the process of spondyloyic osteophyte formation (Fig. 5). These molecules are reportedly essential growth factors for osteochondrogenesis in embryogenesis and fracture repair. Together with the reported roles of these molecules in endochondral ossification, the molecular mechanisms underlying the present model are thought to be as follows: BMP-4/ALK-6 [15] is activated, most likely by the mechanical stimuli, and regulates initial chondrogenesis at the annulus/ligament complex. PTHrP/PTHR [9–11,13] is also activated at similar sites and promotes early chondrocyte proliferation. BMP-4/ALK3 [15] and GDF-5/ALK-6 [7] promote cartilage formation and enlargement of cartilaginous matrix. PTHrP promotes proliferation and inhibits maturation of chondrocytes [9–11,13] located close to mature chondrocytes via PTHR. In mature chondrocytes, BMP-6 stimulates Ihh synthesis, and Ihh upregulates PTHrP expression via Ptc. In this location PTHrP inhibits expression of BMP-6 and Ihh (positive stimulators for PTHrP) and forms a negative feedback loop [8,10,13]. The rate of chondrocyte maturation leading to osteophyte formation in spondylosis is regulated by this negative feedback loop. Proper regulation of these groups of molecular signals would induce and promote osteochondrogenesis leading to spinal fusion.

IV. LOCAL MOLECULAR MECHANISMS INVOLVED IN HUMAN HYPEROSTOTIC SPINE DISORDER: PATHOLOGICAL OSSIFICATION IN SPINAL LIGAMENT

Ossification of the ligament flavum (OLF) is a unique pathological condition leading to compression of the spinal cord and nerve roots, thus sometimes causing severe myeloradiculopathy [16]. The process of OLF is reportedly a novel form of endochondral ossification, in which cartilagi-

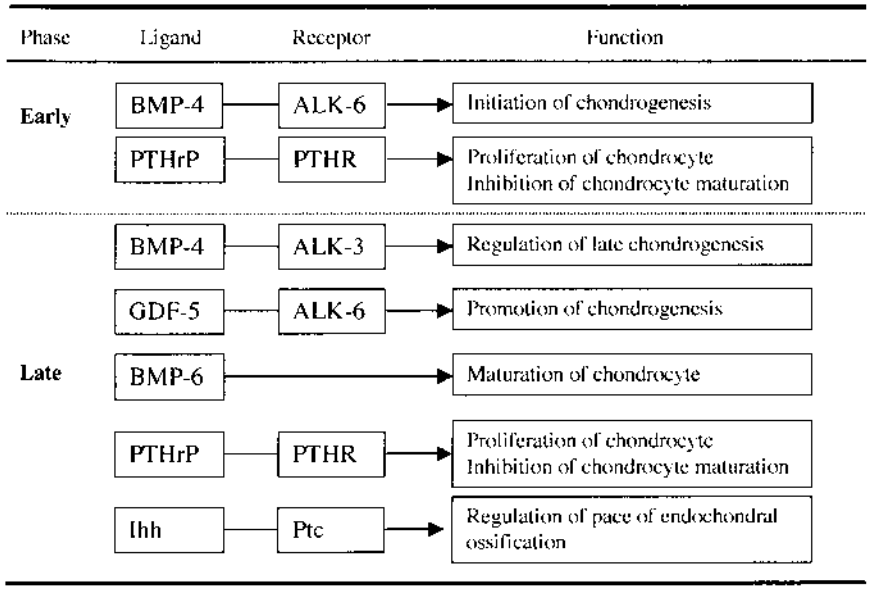

Figure 5 Proposed function of ligand and receptor complex in osteochondrogenesis induced in the present experimental spondylosis.

nous template determines the shape and volume of the skeleton [16]. Various growth factors are reportedly involved in this process, i.e., BMP families [17], transforming growth factor-beta (TGF-β) [18], and insulin-like growth factor (IGF) [19] as well as their receptors. In this chapter the gene expression profile of potent chondrogenic factors in the process of OLF is introduced.

A. Process of Ossification of the Spinal Ligament

The process of OLF is characterized by several histological and cellular events as follows (Fig. 6) [20]:

1. Portion distant from the ossification front: numerous undifferentiated fibroblastic cells in the spinal ligament proliferate in this portion.
2. Intermediate portion close to the ossification front: a few chondrocytes appear within disorganized ligament fibers.
3. Calcified ossification front: the number of chondrocytes is increased in this portion.

B. Local Activation of CDMP-1 and Its Receptors in OLF

CDMP (cartilage-derived morphogenetic protein)-1 is a potent mitogenic and chondrogenic factor belonging to the BMP superfamily [7]. Mutations of the CDMP-1 gene result in abnormal formation of the skeleton [21], and CDMP-1 is considered one of the key molecules in chondrogenic events in humans. Involvement of CDMP-1 in the development of OLF has been examined by in situ hybridization and immunohistochemical analysis (Fig. 6) [20]. The CDMP-1 gene is not detected in nonossification sites, but it is activated in proliferated fibroblastic cells and chondrocytes in OLF region. CDMP-1 protein is also localized in the similar regions. Therefore,

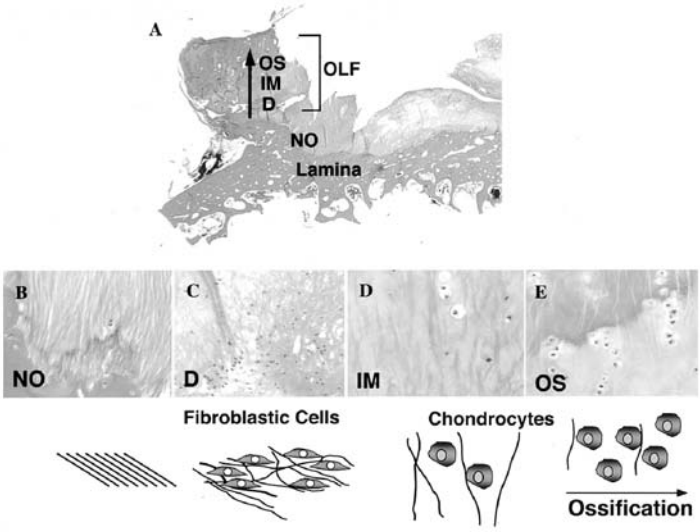

CDMP-1	NO	D	IM	OS
mRNA	-	++	++	+
Protein	-	++	++	+

Figure 6 Histological characteristics of OLF and CDMP-1 expression. (Upper) Histology and scheme of cellular events in areas of OLF (hematoxylin and eosin staining). OLF, ossification of ligamentum flavum; NO, nonossified region; D, an area distant from the ossification front; IM, an intermediate portion close to the ossification front; OS, ossification front. (A) Macroscopic magnification; (B–E) magnification $\times 200$). (Lower) CDMP-1 distribution in each area (+: ~25% cells stained; ++: 25–50% cells stained).

CDMP-1 is activated locally at the site of chondrogenic events prior to ossification. Receptors for CDMP-1 are reportedly activated at similar sites [17]. Thus, CDMP-1 may act as a potent chondrogenic factor in the mechanism of OLF. These findings indicate that cells in the spinal ligament are able to synthesize and respond to CDMP-1, leading to cartilaginous expansion, and CDMP-1 is one of the candidate molecules for chondrogenesis leading to ossification in the human condition.

V. TOWARDS PROMISING SPINAL FUSIONS BASED ON MOLECULAR BIOLOGY

A. Several Molecules Share Roles in Osteochondrogenesis in the Spine

As is the case with embryogenesis, several molecules share roles in the osteochondrogenic events in the spine. BMP-4 induces chondrogenesis, GDF-5 promotes cartilage enlargement, and BMP-6 regulates final ossification in concert with Ihh and PTHrP (Fig. 5). In therapeutic procedures, each molecule would play a specific role, and proper regulation of these molecules at the proper sites and times would result in more efficient processes. For example, BMP-4 would be a powerful tool for the induction of spinal fusion, PTHrP/GDF-5 would be an efficient

tool for cartilaginous enlargement, and BMP-6/Ihh would be useful for final ossification. For instance, in hypertrophic nonunion after surgery in which final ossification is absent, application of BMP-6/Ihh may be a more useful alternative than surgical fixation. When atrophic nonunion occurs, the application of BMP-4 may be more effective than bone grafting surgery. Careful consideration of the processes that are absent and of the most appropriate therapy for each specific spinal fusion situation is most important to develop the optimal procedure.

B. Targeting Sites and Cells for Osteochondrogenesis in the Spinal Region

Localization of mRNA for osteochondrogenic factor receptors provides information about the type and location of cells that respond to secreted growth factors. This is a particularly important issue because identification of sites and cells for targeting is essential prior to local application of osteochondrogenic factors. Most spine surgeons would recognize that undifferentiated mesenchymal cells exist in bone marrow and periosteum. This type of cell is pluripotent and can differentiate into osteoblasts/chondrocytes, which results in ossification. These cells therefore play important roles in the process of spinal fusion. However, the findings described in this chapter suggest that fibroblastic mesenchymal cells also exist in the intervertebral discs (especially in the annular-ligament complex) and spinal ligaments. Activation of BMP receptors in fibroblastic cells indicates potential responsiveness to osteoinductive factors. Chondrocytes synthesize receptors for various osteochondrogenic factors, such as BMP receptors, Ptc, and PTHR. These molecules propagate the signals for cartilage enlargement and endochondral ossification. Chondrocytes in the annulus fibrosus could become a target to stimulate the cartilaginous expansion and final endochondral ossification that are key events in spinal fusion.

Molecular biology–based therapy includes local gene therapy, targeting overexpression of specific molecules, transplantation of cells in which targeted genes have been transfected, or application of recombinant proteins as well as regulation of receptor expression. When considering molecular biology–based spinal fusion systems, gene expression profiles of the osteochondrogenic events in the spine will provide information regarding the best reagents to use, the targeting foci for osteogenesis, and the type of cells that are the focus in various types of spinal disorders.

VI. CONCLUDING REMARKS

A variety of molecular biology techniques hold the key to the formulation of new strategies for the development of molecular biology–based spinal fusion systems. Gene expression profiling in the process of spine disorders provides evidence for the possible application of new techniques and indicates the way forward for new advanced approaches for the treatment of spinal disorders. However, we should recognize that such profiling studies only provide observational evidence. Prior to the use of these strategies in clinical practice, confirmation of their role and effectiveness using animal studies or in vitro studies is required. Proper use of information about gene expression profiles will strongly support less invasive and more successful spinal fusion procedures.

ACKNOWLEDGMENTS

I thank Prof. Yoshikawa, Dr. K. Yonenobu, Dr. S. Miyamoto, Dr. M. Iwasaki, and Dr. N. Tsumaki for helpful advice, and thank Dr. K. Ariga and Mrs. Kaori Furuta for their technical

assistance. I also thank Dr. S. E. Gitelmann, Dr. D. Kingsley, Dr. M. P. Scott, G. N. Segre, Dr. T. Koke, and Dr. F. P. Luyten for providing us cDNAs.

REFERENCES

1. Olsen BR. Bone morphogenesis and embryonic developmen. In: Favus MJ, ed. Primer on the Metabolic Bone Diseases and Disorders of Mineral Metabolism. Fourth Edition. Philadelphia: Lippincott Williams & Wilkins, 1999:11–14.
2. Miyamoto S, Yonenobu K, Ono K. Experimental cervical spondylosis in the mouse. Spine 1991; 16:S495–500.
3. Nakase T, Ariga K, Miyamoto S, Okuda S, Tomita T, Iwasaki M, Yonenobu K, Yoshikawa H. Distribution of genes for bone morphogenetic protein-4, -6, growth differentiation factor-5, and bone morphogenetic protein receptors in the process of experimental spondylosis in mice. J. Neurosurg. (spine 1) 2001; 94:68–75.
4. Nakase T, Ariga K, Meng W, Iwasaki M, Tomita T, Myoui A, Yonenobu K, Yoshikawa H. Distribution of genes for parathyroid hormone (PTH)-related peptide, Indian hedgehog, PTH receptor and patched in the process of experimental spondylosis in mice. J. Neurosurg. (spine 1) 2002; 97:82–87.
5. Nakase T, Nomura S, Yoshikawa H, Hashimoto J, Hirota S, Kitamura Y, Oikawa S, Ono K, Takaoka K. Transient and localized expression of bone morphogenetic protein 4 messenger RNA during fracture healing. J. Bone Miner. Res 1994; 9:651–659.
6. Nakase T, Takaoka K, Sugimoto M, Hirota S, Sato M, Yoshikawa H, Nomura S. Expression of bone morphogenetic protein-4 mRNA during the process of bone formation in embryogenesis and fracture repair. Wound. rep. Reg 1996; 4:82–86.
7. Chang SC, Hoang B, Thomas JT, Vukicevic S, Luyten FP, Ryba NJ, Kozak CA, Reddi AH, Moos MJ. Cartilage-derived morphogenetic proteins. New members of the transforming growth factor-beta superfamily predominantly expressed in long bones during human embryonic development. J. Biol. Chem 1994; 269:28227–28234.
8. Grimsrud CD, Romano PR, D'Souza M, Puzas JE, Reynolds PR, Rosier RN, O'Keefe RJ. BMP-6 is an autocrine stimulator of chondrocyte differentiation. J. Bone Miner. Res 1999; 14:475–482.
9. Lanske B, Karaplis AC, Lee K, Luz A, Vortkamp A, Pirro A, Karperien M, Defize L, Ho C, Mulligan RC, Abou SA, Juppner H, Segre GV, Kronenberg HM. PTH/PTHrP receptor in early development and Indian hedgehog-regulated bone growth. Science 1996; 273:663–666.
10. Kronenberg HM, Lee K, Lanske B, Segre GV. Parathyroid hormone-related protein and Indian hedgehog control the pace of cartilage differentiation. J. Endocrinol 1997; 154:S39–45.
11. Lee K, Lanske B, Karaplis AC, Deeds JD, Kohno H, Nissenson RA, Kronenberg HM, Segre GV. Parathyroid hormone-related peptide delays terminal differentiation of chondrocytes during endochondral bone development. Endocrinology 1996; 137:5109–5118.
12. Nakase T, Miyaji T, Kuriyama K, Tamai N, Horiki M, Tomita T, Myoui A, Shimada K, Yoshikawa H. Immunohistochemical detection of parathyroid hormone-related peptide, Indian hedgehog, and patched in the process of endochondral ossification in the human. Histochem. Cell Biol 2001; 116: 277–284.
13. Vortkamp A, Lee K, Lanske B, Segre GV, Kronenberg HM, Tabin CJ. Regulation of rate of cartilage differentiation by Indian hedgehog and PTH-related protein. Science 1996; 273:613–622.
14. Chuang PT, McMahon AP. Vertebrate hedgehog signalling modulated by induction of a hedgehog-binding protein. Nature 1999; 397:617–621.
15. Zou H, Wieser R, Massague J, Niswander L. Distinct roles of type I bone morphogenetic protein receptors in the formation and differentiation of cartilage. Genes. Dev 1997; 11:2191–2203.
16. Sakou T, Matsunaga S, Koga H. Recent progress in the study of pathogenesis of ossification of the posterior longitudinal ligament. J. Orthop. Sci 2000; 5:310–315.
17. Hayashi K, Ishidou Y, Yonemori K, Nagamine T, Origuchi N, Maeda S, Imamura T, Kato M, Yoshida H, Sampath TK, ten Dijke P, Sakou T. Expression and localization of bone morphogenetic proteins (BMPs) and BMP receptors in ossification of the ligamentum flavum. Bone 1997; 21:23–30.

18. Kawaguchi H, Kurokawa T, Hoshino Y, Kawahara H, Ogata E, Matsumoto T. Immunohistochemical demonstration of bone morphogenetic protein-2 and transforming growth factor-beta in the ossification of the posterior longitudinal ligament of the cervical spine. Spine 1992; 17:S33–36.
19. Goto K, Yamazaki M, Tagawa M, Goto S, Kon T, Moriya H, Fujimura S. Involvement of insulin-like growth factor I in development of ossification of the posterior longitudinal ligament of the spine. Calcif. Tissue Int 1998; 62:158–165.
20. Nakase T, Ariga K, Yonenobu K, Tsumaki N, Luyten F, Mukai Y, Sato I, Yoshikawa H. Activation and localization of cartilage-derived morphogenetic protein-1 at the site of ossification of the ligamentum flavum. Eur. Spine J 2001; 10:289–294.
21. Storm EE, Huynh TV, Copeland NG, Jenkins NA, Kingsley DM, Lee SJ. Limb alterations in brachypodism mice due to mutations in a new member of the TGF beta-superfamily. Nature 1994; 368:639–643.
22. Tsumaki N, Tanaka K, Arikawa HE, Nakase T, Kimura T, Thomas JT, Ochi T, Luyten FP, Yamada Y. Role of CDMP-1 in skeletal morphogenesis: promotion of mesenchymal cell recruitment and chondrocyte differentiation. J Biol. Chem 1999; 144:161–173.
23. Tsumaki N, Nakase T, Miyaji T, Kakiuchi M, Kimura T, Ochi T, Yoshikawa H. Bone morphogenetic protein signals are required for cartilage formation and differently regulate joint development during skeletogenesis. J Bone Miner. Res 2002; 17:898–906.

43

Cells, Signals, and Scaffolds: The Future of Spinal Fusion

Leon J. Nesti
Walter Reed Army Medical Center, Washington, D.C., U.S.A. and
Thomas Jefferson University
Philadelphia, Pennsylvania, U.S.A.

Timothy R. Kuklo
Walter Reed Army Medical Center
Washington, D.C., U.S.A.

Edward J. Caterson
Thomas Jefferson University
Philadelphia, Pennsylvania, U.S.A

I. INTRODUCTION

The vertebral column is the center of the axial skeleton and provides structural support, bending motion, and protection of the spinal cord. The column is comprised of several components: bone, intervertebral disc, muscle tendons and ligaments, and neural elements. Failure of one or any combination of these components may lead to spinal disease in which the normal mechanics of the vertebral column is disrupted. This results in a variety of clinical sequela including back pain, stiffness, or neurological compromise.

The current therapy for many of these spinal disorders includes spinal fusion, in which segmental motion is sacrificed for pain relief and structural stability. Spinal fusion has inherent limitations, because restoration of structural stability, while necessary, is unable to address the entire spectra of underlying pathology. Questions arise as to the number of segments to fuse, the approach and method of fusion, and whether or not to use ''biologics'' to assist with the fusion process and minimize the potential complication of nonunion. In this chapter we do not present new methods of spinal fusion, nor do we claim to have the definitive technique in treating spinal disease; we do, however, present a basic foundation for the understanding of the cell biology and material science involved in novel tissue regeneration approaches for reconstruction of the spine. These approaches arise from the relatively new discipline of tissue engineering (TE) in which clinical considerations and scientific principles intersect to address disease pathology (Fig. 1). We have now gained a better understanding of the cells involved in bone and cartilage regeneration, the signals required to direct these cells, and the environment in which to create new tissue for use in spinal fusion.

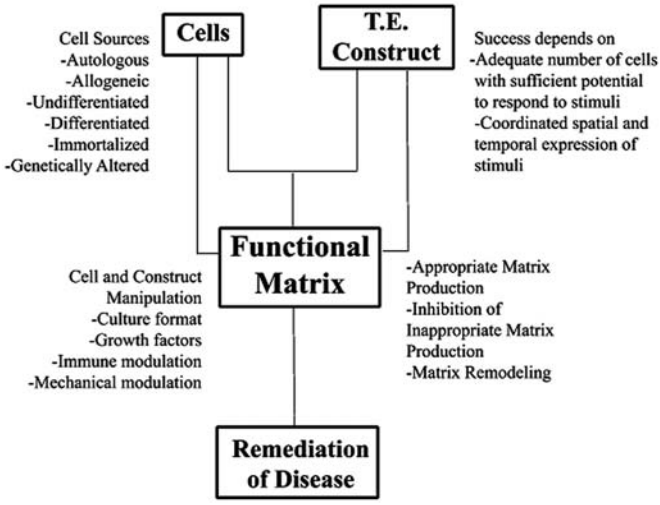

Figure 1 Paradigm of cell-based tissue engineering. In cell-based tissue engineering initiatives, one must consider a number of factors to include cell source, cell construct, and coordination of the spatial and temporal expression of stimuli in order to ensure success.

II. CELLS

The vertebral column is subject to traumatic injury, age-related deterioration, and disease pathology that may lead to significant compromise of its normal function, necessitating corrective intervention. The cells of the axial skeleton, namely, osteoblasts, osteoclasts, chondrocytes, and cells of the intervertebral disc, will attempt to correct structural defects; however, the regenerative limits of these cells are often exceeded, and thus TE approaches in the regenerative process are welcome.

The underlying principles of TE require that use of existing living tissue be maximized and utmost importance be placed on integration of any engineered construct with the existing microenvironment. In order to accomplish this, a thorough understanding of the cells involved in tissue formation must be gained.

A. Osteoblasts

Osteoblasts are bone-building cells and are responsible for bone formation, maintenance, and degradation through their influence on osteoclast function. They are mesenchymal stem cells (MSC) derivatives and proceed through a number of osteoblastic iterations throughout their lifecycle. This cycle begins after the MSC is exposed to the appropriate environmental cues, both chemical and mechanical, and starts to express various preosteoblast characteristics. This includes expression of nuclear transcription factors such as core binding factor alpha 1 (CBFA1), protein production to include alkaline phosphatase and collagen type I (col I), and responsiveness to growth factors and cytokines such as prostaglandin (PGE2), epidermal growth factor (EGF), and transforming growth factor β1 (TGF-β1) [1–3]. Determination of the osteoblast phenotype by morphology alone is near impossible; therefore, functional classification based on extracellular matrix (ECM) is preferred. As the osteoblast matures, protein production alters and the ECM develops into mature bone matrix with the addition of osteopontin, osteonectin, and osteocalcin,

all of which are important for mineralization of the osteoid either in the development or in the ossifying callus of the spinal fusion site.

B. Osteoclasts

The osteoclast is the bone-resorbing cell, and it plays a crucial role in bone formation, regeneration, and maintenance. One of the distinguishing characteristics of bone is its ability to respond to a changing environment, whether chemical or mechanical. In the environment of perfect homeostasis, osteoblast and osteoclast activity is matched so that the rate of bone resorption is equivalent to that of bone deposition. However, perturbation of the homeostatic condition leads to inequities in osteoblastic and osteoclastic activities. Situations in which osteoclast activity is disproportionately high include both chemical and mechanical stress, such as low serum Ca^{2+} levels and relief of bone compression. Repeated cycles of increasing and decreasing osteoclast activity ultimately result in complete skeletal turnover, a process that is required for maintenance of healthy bone. As such, the osteoclast is considered to be a critical cell for formation and maintenance of bone despite its seemingly contradictory function of bone resorption.

The osteoclast distinguishes itself from the other connective tissue cells of the skeleton in that it is of hematopoietic origin from the monocyte-macrophage lineage. Osteoclast precursors bear a strong resemblance to both mononuclear cells and fused mononuclear cells with the unique capability of dissolving mineralized bone matrix. These origins prevent the use of MSCs as potential precursors for osteoclasts, but their importance as modulators of a tissue engineered bone callus for spinal fusion cannot be ignored.

C. Chondrocyte

The chondrocyte is of mesenchymal origin, and it is responsible not only for producing the articulating surfaces between bones, but for the growth and formation of new bone through its role in endochondral ossification. The majority of bones are created through this process in which a cartilage anlage is created and then replaced with mineralized bony matrix (Fig. 2). This sequence is most prevalent during development when the skeleton is first created; however, it persists in the adult skeleton whenever bony defects occur. A bony defect initiates the inflammatory cascade, allows for hematoma formation, and permits interaction of naïve MSCs with various chemical mediators such as TGF-β1. The result is formation of a cartilage model that is subject to neovascularization, thus allowing infusion of additional stem cells into a microenvironment now appropriate for mineralized matrix deposition.

D. Cells of the Intervertebral Disc

The intervertebral disc consists of at least two unique cell types located in the annulus fibrosis (AF) and nucleus pulposis (NP). Despite their close proximity, these cells arise from two distinct origins and have significantly different properties reflected in their consistency and ECM composition. AF cells arise from the mesenchyme and are responsible for producing and maintaining a thick annular ring about the intervertebral disc. This ring serves as a structural support with great tensile strength to protect the inner NP. The AF cells produce a matrix that is rich in col I and col III, similar to fibroblastic cells of tendon and ligament. The matrix fibrils of the ring consist of primarily col I, whereas col III is largely restricted to the AF pericellular environment [4].

NP cells arise from the notochord and are similar to chondrocytes in that they secrete a collagenous ECM consisting predominantly of col IV and col II. The NP secretes an extracellular

Figure 2 The developing chick embryo at day 7 of gestation demonstrates a cartilage anlage that will be replaced by a mineralized boney matrix. Recapitulation of this process, to greater or lesser degrees, is thought to be necessary for functional success of a TE construct.

matrix with a gelatinous consistency rich in proteoglycans that attract a high number of water molecules imparting much of the shock absorbing properties to the disk. Additional differences in these two regions of the disk can be found in their proteoglycan makeup. Biglycan and decorin are found mostly in the AF, whereas aggrecan is distributed rather equally in both the AF and NP. The exact composition of these two regions is not completely understood and is currently an active area of research. Initial studies have found much variability in the subregions of the intervertebral disc that appears to be dependent upon aging and disease state [5,6].

E. Mesenchymal Stem Cells

The aforementioned cell populations are present and active to varying degrees in spinal disease, but for the purposes of reconstruction they often do not occur in sufficient quantities or in the appropriate metabolic state to be used primarily for significant tissue regeneration—thus the need for a readily available, plastic, and mitotically active cell source. We have found MSCs obtained from iliac crest biopsy to be an ideal source of cells used for TE purposes.

MSCs are multipotential and, as such, have the ability to differentiate into a variety of cell types, including osteoblasts, chondrocytes, adipocytes, myoblasts, fibroblasts, and marrow stroma (Fig. 3). The stem cell is unique in its ability to proliferate despite physiological or artificial removal from its native population, and it is not limited by a fixed number of cell divisions. Unlike transformed cells, however, the stem cell is sensitive to cell-contact inhibition and is responsive to negative control regulators from its differentiated progeny, a comforting property if the ultimate goal is to use these cells for tissue repair. As the stem cell divides and differentiates, its intrinsic genomic potential responds to extrinsic signals in the local environment to create a stepwise progression through the developmental pathway with each passing generation. The ultimate end of this developmental progression is tissue formation.

There are several sites from which mesenchymal stem cells can be harvested to include bone marrow, periosteum, fat, and muscle. Of these sites, the bone marrow is the most accessible source for spinal surgeons because of iliac crest bone grafting procedures in which bone marrow containing MSCs is readily available. Clinically, MSCs are obtained by aspiration of the anterior superior iliac crest and have been successfully used as adjuvant therapy in fracture healing

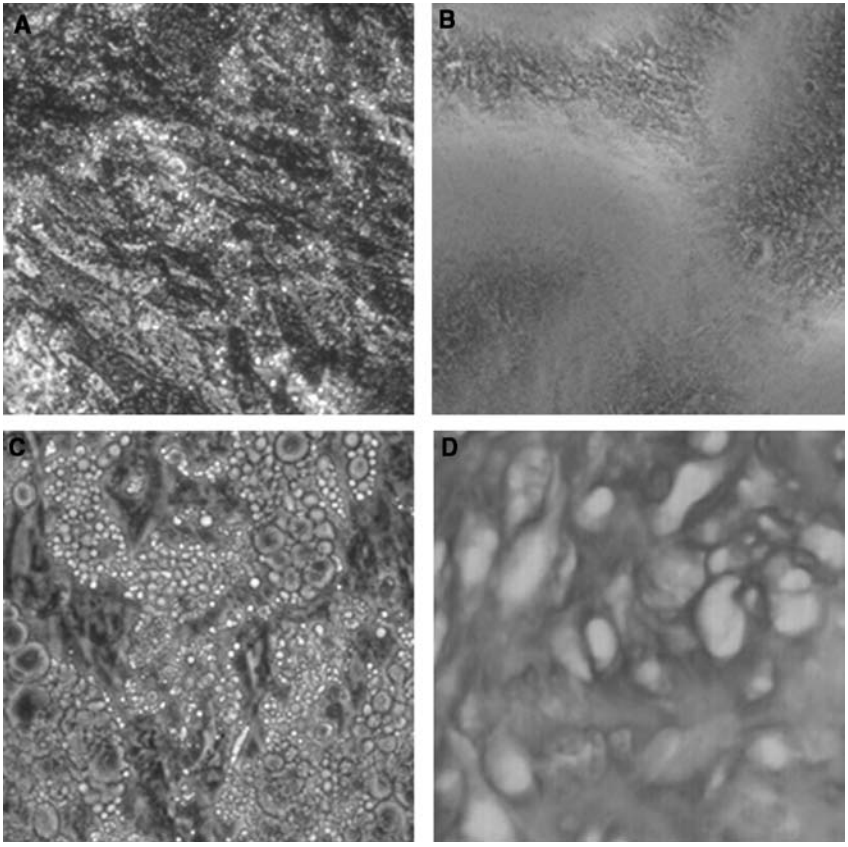

Figure 3 The pluripotent MSC has the ability to develop into an osteoblast, adipocyte, and chondrocyte depending upon its local environment. We have cultured MSCs in several different microenvironments to produces cells of bone, fat, and cartilage. Here, MSCs are stained with alkaline phosphatase (A) and alizarin red (B) demonstrating osteoblast lineage characteristics, oil red O (C) demonstrating adipocyte lineage, and alcian blue (D) demonstrating chondrocyte lineage.

through direct injection of the unmodified bone marrow into a fracture nonunion site. They have also been used in articular cartilage repair through the process of osteochondral picking. The number of stem cells obtained through this type of harvest depends upon the age of the patient, the aspiration site, and the presence of systemic disease. In using stem cells for tissue engineering purposes, a purified population is desired, so additional processing is performed on the raw bone marrow aspirate. There is approximately one MSC for every 100,000 nucleated marrow stromal cells in a young, healthy donor. These cells can be separated, and purified, from the raw aspirate by taking advantage of their intrinsic adhesive properties. Essentially, stem cells adhere to tissue culture polystyrene, a common tissue culture substrate, while cells of the hematopoietic lineage do not. Thus, a relatively pure population of MSCs can be obtained from a raw bone marrow aspirate by simply allowing the cells to adhere to a tissue culture plate and rinsing away the nonadherant cells [7].

MSCs, in the undifferentiated state, exhibit a combination of biological markers that distinguish them from common fibroblastic cells. These include col I, col II, fibronectin, basement membrane laminin, and often STRO-1 (Fig. 4) [8,9]. Recent studies have shown that the MSC actually expresses low-level messages of the ECM components for many potential differentiated states such as chondrocytes, osteoblasts, and adipocytes; however, when environmental or chemical cues are encountered, messages that are not lineage specific are suppressed and the genes particular to the selected cell lineage begin production in an orderly fashion.

The microenvironment within which the MSC resides provides the environmental cues that ultimately lead to stem cell differentiation. These cues may be structural, mechanical, or chemical, and all are likely to have significant influence on the differentiation process. This illustrates the importance of a scaffold in order to promote a microenvironment conducive to cartilage formation and is specifically demonstrated in MSCs cultured in an encapsulated state

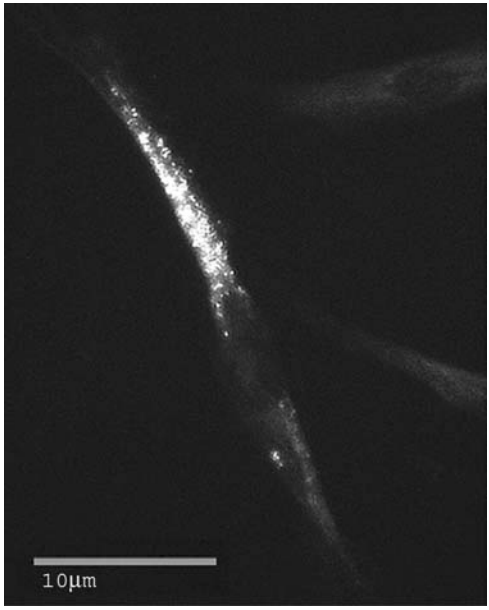

Figure 4 A low percentage of naïve, undifferentiated MSCs express STRO-1 in culture. Here, immunofluorescence staining demonstrates the presence of this elusive marker in our human bone marrow–derived cells.

in the presence of TGF-β1 (Fig. 5). Various methods can be used with novel scaffolding to achieve this purpose. In our studies we selected alginate as a polysaccharide gel to encase and surround a polymeric backbone serving as a biodegradable scaffold for cartilage production in vitro [10]. This encapsulated microenvironment coupled with the appropriate chemical stimulus (TGF-β1) will aid the stem cell in its journey towards chondrocyte differentiation and have applicability in spinal fusion.

III. THE SIGNALS

MSCs, by definition, are undifferentiated and in their native state demonstrate no preference for any particular cell type. Once they encounter a chemical cue to lead them down a particular differentiation pathway, they begin to express markers of a unique cell lineage. TGF-β1 is a potent osteoactive cytokine that has been shown to push MSCs through both chondrocytic and osteoblastic differentiation pathways. It is important to understand how TGF-β1 and other

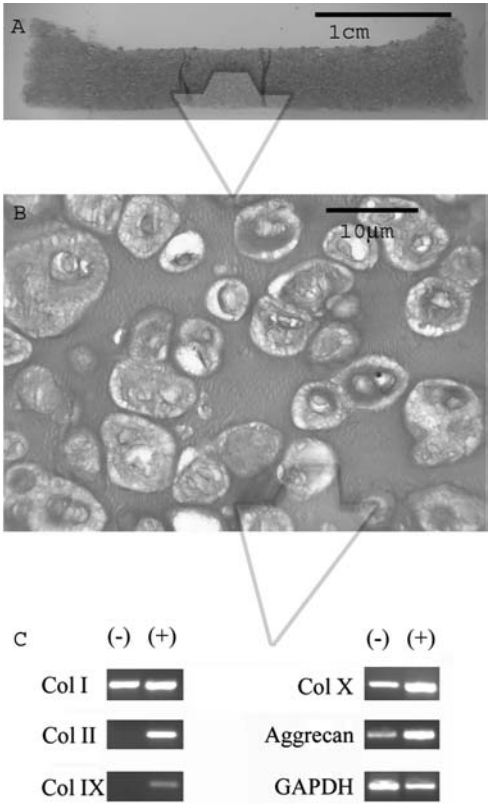

Figure 5 Three-dimensional culture systems are used to recreate in vivo microenvironments as they allow for improved cellular distribution and encapsulation. Here, alginate cultured chondrocytes, derived from our MSC pool, express cartilage specific markers. En bloc alcian blue staining of chondrocytes cultured in an alginate ''disc'' (A) depict cartilage-specific phenotypes at the cellular (B) and molecular (C) levels. RT-PCR techniques were used to detect various ECM message expression (C). Western blotting studies have confirmed subsequent protein production.

cytokines trigger cellular response so that greater control of MSC function can be attained and applied to the model of spinal fusion. A thorough understanding of signaling pathways is necessary to provide targets for small molecule intervention. Similar to the way COX-2 inhibitors block specific branches of the cyclooxygenase pathway, small molecule therapeutics allow for greater control of cell function through their actions on targeted components of a given signaling pathway.

TGF-β1 is the proteotypic member of the TGF-β superfamily consisting of activins, inhibins, müllerian-inhibiting substance, other TGF-βs and bone morphogenetic proteins (BMPs). This family of over 40 related growth and differentiation factors has gained many new members since the discovery of TGF-β1 (Fig. 6) [11]. TGF-β1 is synthesized as part of a larger inactive protein consisting of two disulfide linked, cysteine-rich 12–15 kDa polypeptides. Furin proteases activate this precursor molecule through enzymatic cleavage and release of the biologically active C-terminal region [12]. It is this active protein that serves as a potent osteoactive factor.

Our understanding of TGF-β1 signal transduction has come a long way in the past decade, but there is still much that is unknown. Although several TGF-β1 receptors have been discovered, two types of TGF-β1 receptors (TβRs) are generally believed to initiate the signal transduction cascade [13–15]. The TGF-β1 receptor complex consists of two type II and two type I receptors. TGF-β1 initially binds to the type II TGF-β1 receptor (TβRII), a constitutively active serine/threonine kinase specific for the type I TGF-β1 receptor (TβRI). This ligand-receptor complex then recruits and phosphorylates TβRI in a glycine and serine (GS)–rich domain upstream of

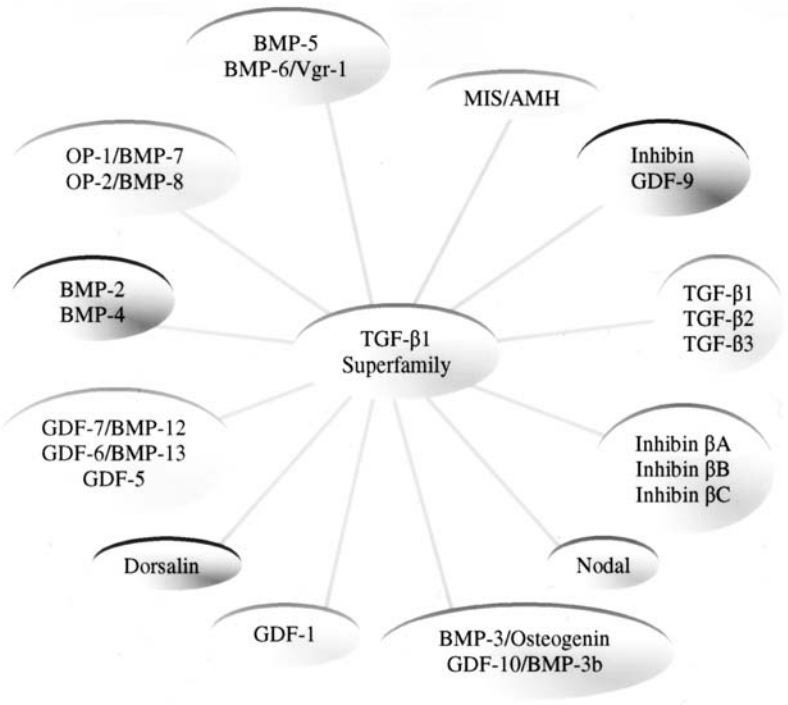

Figure 6 Diagram of the TGF-β1 superfamily. TGF-β family members are grouped based on evolutionary homology. All members of the family are synthesized as pre-promolecules and need to be posttranslationally modified before they become active. The members use hetero-oligomeric complexes of serine/threonine kinase receptors to transmit intracellular signals.

the kinase domain. This activates the TβRI kinase to form a heterotetrameric TGF-β receptor complex, thereby initiating signal transduction (Fig. 7). The function of the other TGF-β1 receptors in the signal transduction cascade is not clear.

The most commonly described intracellular targets for the TβRI kinase are the receptor-associated Smad proteins (rSmad). Studies first done in *Drosophila* led to the discovery of a group of related proteins called mothers against decapentaplegic (dpp), or Mad proteins, that were targets of receptor serine/threonine kinases (RSK) [16]. Subsequent identification of specific Mad-binding DNA domains demonstrated their direct regulation of gene transcription [16]. Smad proteins are the vertebrate homologs of Mad. Several Smad proteins have been discovered, and some of the receptor associated Smads, rSmads, are unique for specific TGF-β superfamily members. The rSmads specific for TGF-β1 are Smad 2 and Smad 3. Activated TβRI phosphoryl-

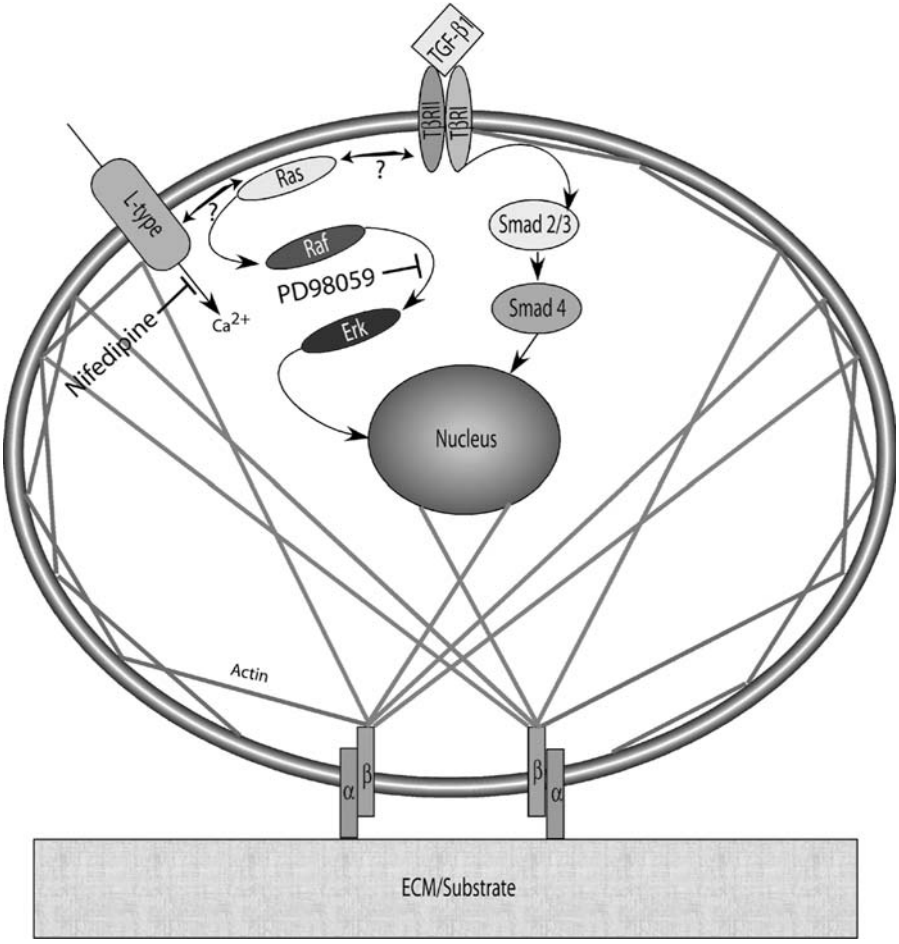

Figure 7 Simplified diagram of TGF-β1 intracellular signaling pathways. TGF-β1 signaling is initiated by ligand receptor interaction at the cell membrane. Three separate intracellular signaling pathways have been shown to be activated: Smad, MAPK, and Ca^{2+} flux. These pathways demonstrate several regions of potential ''crosstalk'' and possess many targets for therapeutic intervention. Of note is the undefined importance of the actin cytoskeleton in signaling mechanics after the cell adheres through specific integrin receptors to the ECM.

ates Smads 2 and 3 on a unique Ser-Ser-X-Ser motif resulting in dissociation from the TβRI. The phosphorylated Smad then forms a heteromeric complex with the universal partner, Smad 4, and translocates to the nucleus, where it may interact with specific nuclear targets such as the forkhead activin signal transducer (FAST, the first nuclear target identified), ATF2, Jun, and TFE3 (Fig. 7) [17–19].

The Smad proteins contain highly conserved NH_2- and COOH-terminal regions, termed Mad homology 1 and Mad homology 2 (MH1 and MH2). The linker between MH1 and MH2 is not conserved, but it contains targets for proline kinases like those of the MAPK pathway [20,21]. These regions are responsible for protein-protein interactions, protein-DNA interactions, and subcellular localization [22–24]. While the MH1 and MH2 domains are mostly involved in the direct signaling cascade and gene transcription, the linker region may prove to be important for ''crosstalk,'' or interaction of two or more signaling cascades, between signaling pathways within the cytosol. Other potential targets of signaling crosstalk have been identified within the nucleus.

TGF-β1 has also been shown to activate the mitogen-activated protein kinase (MAPK) signaling pathway. This pathway serves as a connection between membrane receptors and nuclear transcription that often result in changes in cell proliferation and differentiation. There are at least three MAPK cascades in mammalian cells. They are the extracellular signal-regulated kinase (ERK) cascade, the stress-activated protein kinase/c-jun N-terminal kinase (SAPK/JNK) cascade, and the p38MAPK/RK/HOG cascade. These pathways generally target a similar group of transcription factors that ultimately lead to activation of rapid response genes such as members of the fos and jun family. The MAPK family share common activation steps. Specifically, they are activated by phosphorylation on a threonine-Xaa-tyrosine motif and then act as proline-directed serine/threonine kinases [25].

The ERK cascade is activated when cells encounter signals to proliferate. Recent investigations have demonstrated TGF-β1 activation of the MAPK signaling cascade [26,27]. This cascade begins with the activation of MAPK-kinase-kinase (MAPKKK), or RAF, through a poorly defined mechanism that usually involves the membrane-bound, small G-protein, RAS [25,28]. Activated RAF then phosphorylates and thus activates MAPK-kinase (MAPKK), or MEK, that has the unique ability to phosphorylate ERK on a specific threonine-glutamic acid-tyrosine activation motif [25,29]. ERK phosphorylation/activation allows for translocation to the nucleus, where it can interact with its nuclear targets, namely transcription factors and the basal transcription complex [30,31].

Activated ERK has also been shown to interact with the Smad signaling pathway. Specifically, RAS-dependent phosphorylation of ERK may phosphorylate Smad1, Smad2, and Smad3 in the region linking MH1 and MH2 domain on four consensus phosphorylation sites [20,21]. This phosphorylation interrupts rSmad-Smad4 nuclear accumulation and thus blocks TGF-β and BMP-2 signaling [20,21]. The interaction of the ERK and Smad pathways in terms of ERK phosphorylation of the r-Smad-Smad4 complex appears to be antagonistic. Events that tip the scale in favor of either ERK or Smad signaling are not yet known, but the timing of pathway activation may play a role. The ERK cascade is often transient and is activated for a short period of time, whereas Smad activation persists longer. Factors that either increase the duration of ERK activation or decrease the length of Smad activation may alter the outcome of cytosolic Smad/ERK crosstalk.

Nuclear crosstalk of the ERK/Smad pathway is also possible given the number of common nuclear targets. One such target is fos of the AP-1 transcription factor. Fos is phosphorylated by ERK on sites that have been identified as transcriptional inhibitors [32,33], but it is also a functional target of the Smad 3 MH2 domain, which ultimately potentiates transcription of genes

containing AP-1–binding sites in their promoter [19]. Thus, ERK can antagonize Smad signaling at the nuclear level through interaction with common nuclear targets such as fos.

Recently we described a novel TGF-β1 Ca^{2+} signaling pathway in human osteoblasts (HOB) and found similar results in MSCs (Fig. 8) [34,35]. TGF-β1 stimulation of HOB results in an immediate and rapid rise in the $[Ca^{2+}]_i$ and stimulates subsequent Ca^{2+} oscillations. This TGF-β1–stimulated Ca^{2+} flux is required for TGF-β1 enhancement of cell adhesion, select protein production, and cell proliferation. Interestingly, the Ca^{2+} signal does not regulate receptor-associated Smad protein phosphorylation/activation.

Cell adhesion is often the first step in determining the fate of the cell, and factors within the local microenvironment may alter adhesion mechanics, thus leading to a less desirable outcome in tissue generation. This has been demonstrated extensively in studies examining osteoblast adhesion to implant biomaterials where failure of osseointegration leads to fibrous capsule formation and increases the probability of prosthetic loosening. The TGF-β1 Ca^{2+} signal is required for complete stimulation of α5 integrin expression, the quintessential component of the integrin complex, and is necessary for TGF-β1–stimulated focal contact formation and cytoskeletal organization—events closely associated with enhancing cell adhesion (Fig. 9) [34,35]. It is likely that TGF-β1 also stimulates cell proliferation through Ca^{2+} signaling activation of the MAPK signaling pathway, thus establishing evidence for TGF-β1 signaling crosstalk of at least three separate TGF-β1–activated signaling pathways.

Ca^{2+} signaling pathways are present in many cells and serve as rapid and expansive communication events that influence cellular activity. The specificity of the Ca^{2+} signal is largely dependent upon the Ca^{2+}-sensitive mechanisms within a specific cell type, the frequency of intracellular Ca^{2+} oscillations, and activation of concomitant signaling pathways with which crosstalk is possible [33]. Increases in $[Ca^{2+}]_i$ have been shown to control many cell functions such as adhesion, motility, gene expression, and proliferation [36,37]. It is thought that several Ca^{2+}-sensitive transcriptional regulators, including NF-κB [38], JNK [24], and NFAT [39], promote gene expression responsible for these responses. The specificity of the Ca^{2+} signal for these transcription factors has been attributed to both calcium-sensitive activating proteins, such as calcineurin—a Ca^{2+} sensitive phosphatase [39]—and the type of Ca^{2+} signaling pattern in response to a given stimulus [33]. Differential Ca^{2+} signaling patterns include single transients, repetitive oscillations, or sustained plateaus (Fig. 10) [36]. Studies are now beginning to investigate the association of these signaling patterns with specific intracellular events. Specifically,

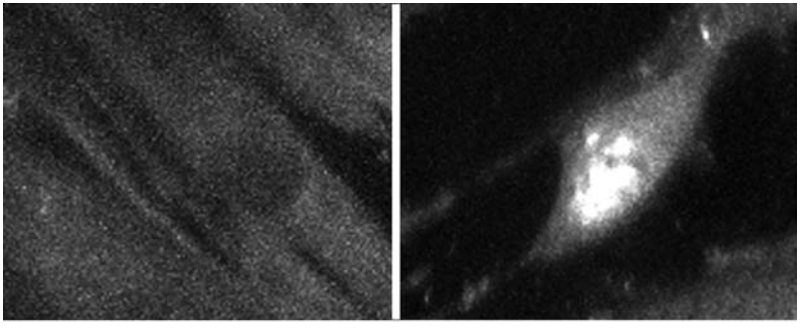

Figure 8 Immunofluoresence studies of MSCs stimulated with 10 ng/mL of TGF-β1 demonstrate nuclear accumulation and clustering of Smad-2 (B). In unstimulated cells, Smad-2 proteins remain in the cytosol (A).

Figure 9 Sequential $[Ca^{2+}]_i$ dynamics images in MSC after TGF-β1 stimulation. Red cells indicate increasing $[Ca^{2+}]_i$ relative to previous image, blue cells indicate decreasing $[Ca^{2+}]_i$ relative to previous image, and white indicates unchanged $[Ca^{2+}]_i$ relative to previous image.

Ca^{2+} oscillations, and to a lesser extent low-level, sustained Ca^{2+} plateaus, have been linked to NFAT activation, while single, transient Ca^{2+} signals appear to activate NF-kB and JNK [33].

We have found that TGF-β1 treatment of osteoblasts activates at least three major intracellular signaling pathways, receptor-associated Smad proteins, intracellular Ca^{2+} flux, and ERK. These pathways contain a number of potential overlap areas where signaling crosstalk may occur. TGF-β1 is notorious for eliciting a variety of different effects within many different cell types and within the same cell type. Many studies have found that these differences are associated with the concentration of TGF-β1 used, the cellular differentiation and maturation state, and cell culture conditions. However, little attention has been given to the potential interactions between various TGF-β1–activated signaling pathways. Once these interactions are understood,

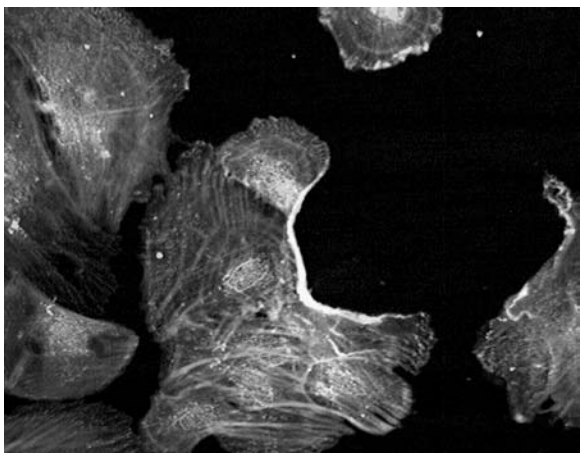

Figure 10 TGF-β1 stimulation of HOB demonstrates increased actin cytoskeleton production, organization, and colocalization with integrin receptors 3 hours after plating. Immunofluorescence imaging of cells stained with rhodamine phalloidin (actin, red) and antibodies to α5 integrin (green) demonstrate thickened actin stress filaments with ruffled boarder formation, increased integrin production, and a large degree of actin and integrin colocalization (yellow), suggesting a firmly adherent and maturing cell.

novel targets for key events in the signaling pathway can be identified and cellular response can be tailored for the appropriate conditions.

The TGF-β1 Ca^{2+} signal in HOB is not present at all times in culture. Our Ca^{2+} imaging studies have shown the TGF-β1–induced Ca^{2+} signal in HOB to be dependent upon cell density and time in culture. Whether differences in TGF-β1's functional effects on HOB are seen in the same time periods needs to be determined. However, it is likely that TGF-β1 stimulation of HOB during periods in which the Ca^{2+} signaling machinery is not intact will have functional effects similar to those seen when the TGF-β1 Ca^{2+} signal is artificially blocked.

We have demonstrated that initial, short-term treatment of MSCs with TGF-β1 leads to chondrocytic differentiation that persists in long-term cell culture (Fig. 11). This data suggests that it is early actions of TGF-β1 on the MSC that result in dedicated differentiation. Although the signaling pathway of TGF-β1 and related superfamily has not been completely elucidated, there appear to be several key events that result in cellular response. These events begin with TGF-β1 binding to its specific cell surface receptors and continue with the activation of independent, yet interacting intracellular signaling pathways, namely receptor-associated Smad proteins, MAPK signaling pathways, and intracellular Ca^{2+} signals.

The importance of this information is that it serves to arm the spinal surgeon with a foundation integral for directed growth factor modulation. Tissue engineering is progressing

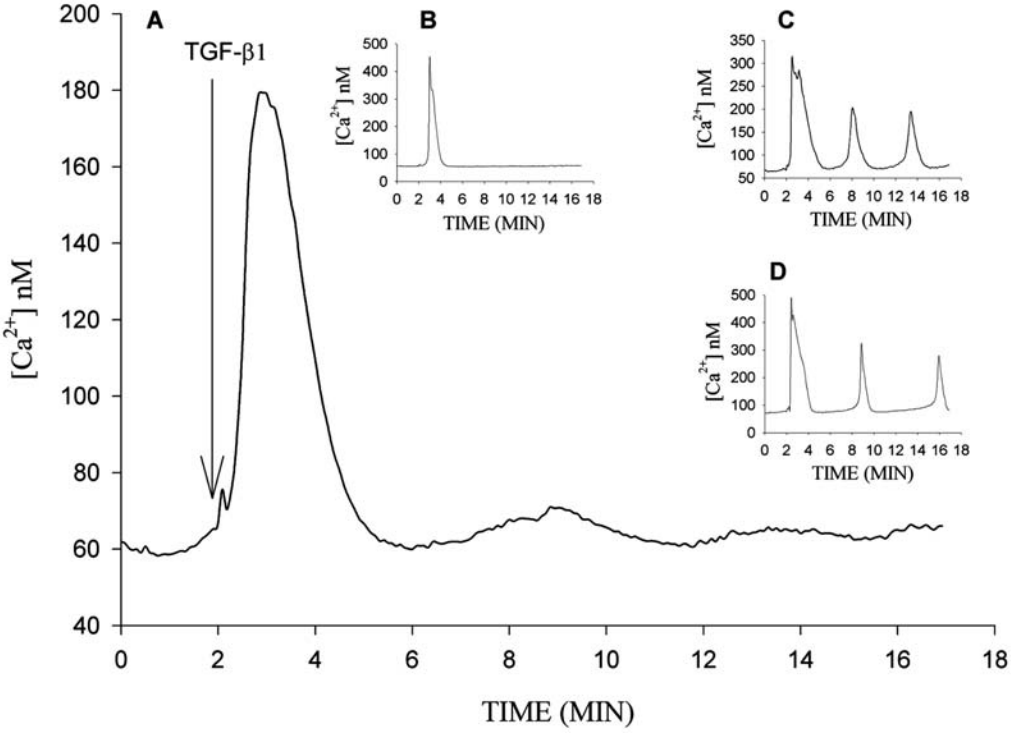

Figure 11 TGF-β1 treatment of HOB results in transient rise in $[Ca^{2+}]_i$. HOB were isolated, cultured, and treated with 10 ng/mL of TGF-β1 and monitored for $[Ca^{2+}]_i$ using Fura-2 ratiometric spectrofluorimetry. The results presented in the main figure (A) are an average from a population of cells ($n = 75$). Representative single cell responses include single spike (B) and initial spike with subsequent $[Ca^{2+}]_i$ oscillations (C,D).

rapidly, and within this emerging technology is the concept that growth factor and molecular modulations must be customized to control individual events in the progression towards the restoration of tissue damaged by disease and/or trauma. These principles encompass several components, cells capable of producing a functional matrix, an appropriate scaffold for transplantation and support of the cell-laden graft, and iatrogenic or autogenous bioactive molecules, which drive the processes of differentiation and maturation.

The importance of the TGF-β superfamily and a thorough understanding of its effects at the cellular level allow for multiple therapeutic interventions to be developed, which can enhance, accelerate, or aid in providing rigid fixation of the spine. The random application of growth factor to a fracture callus is suboptimal and will be replaced in the future with the targeting of individual signaling cascades associated with cell adhesion, proliferation, extracellular matrix production, and matrix remodeling in an effort to achieve a controlled progression of tissue regeneration.

IV. THE SCAFFOLD

The interactions of cells, signals, and scaffold will provide the orthopedic surgeon with new treatment solutions beyond the current achievement of rigid fixation through the fusion of osseous elements. TE methodology allows for the potential recreation of all structures and restoration of the balance between these functional elements compromised by spinal pathology. With this in mind, the future of spine TE will not only provide enhancement of the fusion process, but also provide novel strategies to approach a biological solution for disc pathology. Intensive study of the signals responsible for cartilaginous differentiation of the MSC has enabled us to utilize a single cell source exposed to unique microenvironments to be considered for multiple TE constructs. To this end, intervertebral disc tissue engineering has begun using the same starting materials, albeit in different combinations.

Historically, the culture of primary chondrocytes and chondrocyte cells lines has proven difficult. The culture techniques required that the starting cells be grown in a micromass culture system in which a high number of cells are grown in a small surface area so that three-dimensional layering occurs. If the cells are allowed to expand into a monolayer culture system, they dedifferentiate and become more fibroblast-like. These studies prove the need for three-dimensional culture systems for both chondrocytes and MSCs undergoing chondrogenic differentiation to maintain the precarious balance between differentiated chondrocytes and poorly differentiated fibroblasts (Fig. 12).

When considering MSCs as candidate cells for cartilage repair or for other autologous skeletal tissue engineering applications, two important issues need to be addressed. First, to complement the intrinsic regenerative functions of skeletal tissues, a mechanically stable, engineered cellular scaffold is preferred. Second, a biocompatible construct seeded with proliferative cells that have achieved and are capable of maintaining a specific differentiated phenotype is desirable to optimize interactions with the host tissue. In terms of mechanical stability, polymeric scaffolds, particularly those that are bioresorbable or biodegradable, have shown promise as delivery agents for MSCs or other marrow-derived cells [40]. Biodegradable polyester scaffolds of α-hydroxy acids, such as poly-l-lactic acid (PLA), have been shown to support cartilage and connective tissue ingrowths, and at the same time confer mechanical stability during tissue regeneration [41–44]. PLA undergoes hydrolytic degradation to lactic acid, a normal metabolite after serving as a biodegradable scaffold for tissue repair and regeneration [45]. The second issue concerns the finding that chondroprogenitor cells, which normally require maintenance at higher cell density for chondrogenic differentiation, are able to express a chondrogenic phenotype

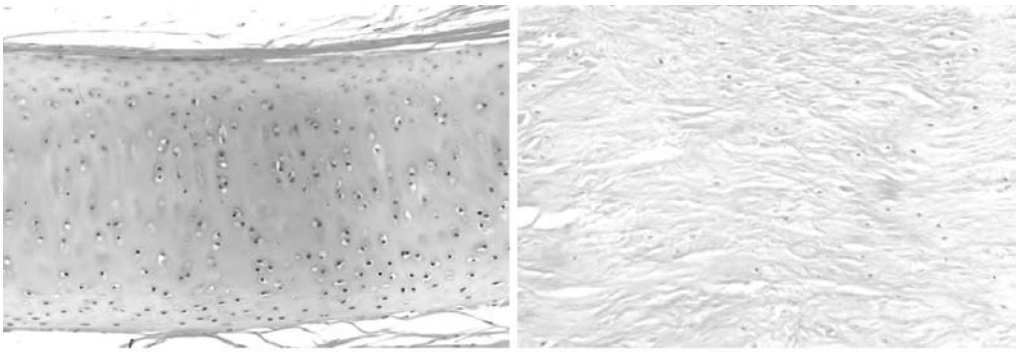

Figure 12 The cellular microenvironment influences the precarious balance between articular cartilage (A) and a similar, yet less structurally sound, fibrocartilage (B). The environmental cues instructing the cells down either pathway are central to the success of TE contructs.

when cultured as encapsulated cells within matrices such as collagen type I, agarose, and alginate [46]. This encapsulation of the tissue progenitor cells within a polymeric or macromolecular gel is believed to facilitate as well as enhance cell shape changes that favor chondrogenic differentiation [47]. Delivery of cells within such matrices should also improve cell loading and retention at the desired tissue site.

The use of this amalgam or composite of both a cartilage-promoting hydrogel, such as alginate, and polymeric macrostructure is to develop a rational approach towards the creation of a biological substitute for the interverterbral disc. The use of the alginate sol/gel or another hydrogel-like material to seed MSCs in the PLA, or similar polymeric macrostructure, ensures that the cells are first homogeneously distributed and, upon gelation of the polysaccharide medium, are then retained throughout the highly porous polymeric construct [47]. In addition, the alginate gel can be removed by chelating calcium after the resident cells have proliferated and become integrated within the scaffold. This allows for production of functional extracellular matrix, thus optimizing cell-matrix interactions. Alternatively, in vivo, alginate may be hydrolyzed into mannuronic acid and glucuronic acid [48,49], which are degraded further in metabolic pathways.

The polymeric amalgam construct has several technical advantages which are important in developing a strategy for cartilage tissue engineering of both spinal fusion and regeneration of the intervertebral disc. First, an alginate cell suspension can be loaded onto the construct of choice and a gel created intraoperatively within minutes to confine the cells in the construct. This characteristic can allow for immediate surgical handling of the cell-laden composite graft, circumventing the need for initial cellular adhesion to the polymer graft, which would take at least 2 hours under controlled conditions [40]. Second, the use of the polymeric PLA-alginate amalgam is potentially a functionally more desirable approach to cartilage tissue engineering than PLA polymer alone, because the addition of alginate to the scaffold prevents the formation of a fibrous tissue shell along the periphery of the graft. In previous studies of marrow-derived MSCs grown in pellet cultures and on gelatin sponge constructs, cells at the perimeter of the constructs do not exhibit significant cartilage matrix histology or immunohistochemical reactivity for collagen type II, but instead form a thin fibrous capsule around the constructs [40,50]. This fibrous tissue could prevent graft integration with the healing host tissue and lead to an inadequate repair process much in the same way that intervening fibrous tissue causes nonunion in fracture

repair [51]. A fibrous tissue layer is not seen in the polymer-alginate system because the alginate gel maintains a uniform, round cell shape over the entire PLA-alginate amalgam construct, including the perimeter regions, as shown by SEM and histology (Fig. 13).

This quality of the amalgam has considerable importance because it gives one the added flexibility to combine an outer polymeric mesh with the PLA-alginate amalgam to encase the entire hydrogel, with MSCs differentiating along the chondrogenic lineage. In this schema, a polymeric envelope surrounds the entire tissue engineered gel structure containing differentiating mesenchymal stem cells and mimics the functional character of an annulus that contains the tissue engineered intervertebral disc (Fig. 14) [52]. In addition, the polymeric mesh surrounding the hydrogel allows for collagen-based fibrous tissue ingrowth serving to recapitulate the tensile stability surrounding the biological disc replacement. This rationale schema for TE of the intervertebral disc has shown promise in vitro, and further work on biological replacements for the intervertebral disc and its restraining elements are a continued area of research and interest.

Because all biomaterials are foreign bodies, they carry an intrinsic risk of causing infection and/or eliciting inflammatory responses from the host [53,54]. It is thus desirable that the delivery scaffold of the TE construct not remain once it has served its initial purpose, whether mechanical or as a cell carrier. The PLA and the PLA-alginate amalgam constructs described here have been shown to be biocompatible and to be biodegradable via normal metabolic pathways

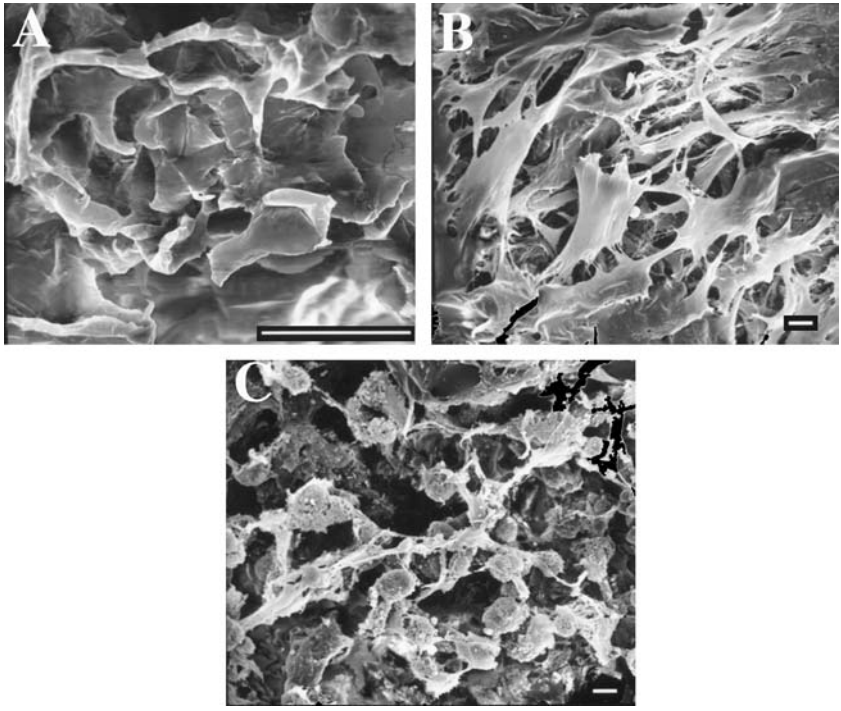

Figure 13 Scanning electron micrograph views demonstrate the importance of material science in the culture of chondrocytes. The panels demonstrate PLA scaffold alone (A), PLA seeded with MSCs (B), and PLA-alginate amalgam seeded with MSCs (C) after 7 days in culture in chondrogenic medium. Bone marrow–derived cells in the PLA-alginate amalgam construct (C) exhibited a round cell shape and produced extracellular matrix. Bone marrow–derived cells on plain PLA (B) qualitatively appeared more extended and spindle shaped. Bar (A) = 100 μm; bars (B, C) = 10 μm.

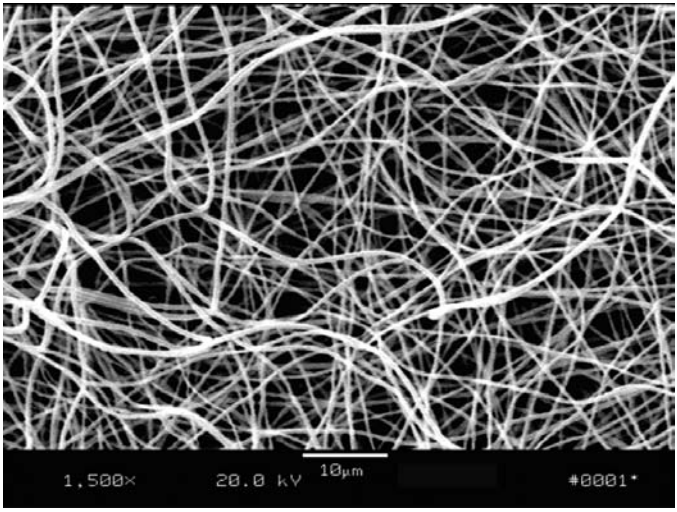

Figure 14 Scanning electron micrograph of PLA spun nanofibers. This technique allows for greater cell-biomaterial interaction and cell ingrowth in a TE construct that resembles flexible mesh. The fiber size, composition, and ''tightness of the weave'' are all variables that can be adjusted according to construct need. These variables permit greater control of biocompatibility and biomechanical properties. (Courtesy of Dr. Wan Ju I.i.)

[41,42,55–57]. Newly developed amalgams of other biomaterials with comparable properties may certainly be considered for this application in spine TE.

Based on the results presented here, the following scheme for cartilage engineering using the PLA-alginate amalgam scaffold is proposed. Initially, a large number of bone marrow–derived cells, including MSCs, are loaded into a polymeric construct, which is encased in alginate. An initial dose of TGF-β1 is then given for a period of 3 days to provide the inductive stimulus for chondrogenesis. After chondrogenic induction, the alginate that serves to confine the cells and relevant growth factors within the polymeric macrostructure may be removed by calcium chelation if necessary, with residual alginate to be broken down metabolically by the pathways mentioned above. Alternatively, the alginate gel could be retained in toto on the construct to be gradually degraded by these same pathways. The construct/graft is then surrounded with a biodegradable polymeric mesh, which will promote fibrous tissue ingrowth and serve as a bioengineered annulus and then subsequently implanted into the defect. The implanted cells delivered in such a construct, with a relatively uniform distribution, are likely to respond and interact with their microenvironment to facilitate the regeneration of functional tissue in locations that have been compromised by disease or trauma. It is for these reasons that the gel-polymer amalgam scaffolding for mesenchymal chondrogenesis or similar biomaterial combinations represent promising candidate TE approaches suitable for the repair of spinal pathology.

V. CONCLUSION

The foundation of spinal tissue engineering will rely on the restoration of a functional matrix in order to remediate disease. It is only through the cohesive interactions of cells, signals, and scaffolds that these goals will be achieved. Important to the creation of a functional matrix for

spinal fusion is the inherent flexibility for appropriate matrix production and the suppression of the signals and cells responsible for inappropriate matrix production as well as a conservation of the potential for matrix remodeling. The cell sources that can be used as the raw material for matrix production are vast and, as previously mentioned, include the cells present in the fusion callus as well as the recruitment of MSCs to bolster the repair mechanisms that have faltered. In cell-based TE initiatives proposed for spinal fusion models, one must consider a number of factors including cell source, cell construct, and the coordination of the spatial and temporal expression of stimuli in order to ensure success. It is only through a greater understanding of cells, signals, and scaffolds that novel mechanisms to aid in rigid fixation and restoration of the functional stability of the spine will be achieved. Tissue engineering will be at the forefront of these advances, and its progression will give the spine surgeon greater flexibility in the approach to and restoration of spinal pathology.

REFERENCES

1. Aubin JE, Liu F, Malaval L, Gupta AK. Osteoblast and chondroblast differentiation. Bone 1995; 17(2 suppl):77S–83S.
2. McCabe LR, Kockx M, Lian J, Stein J, Stein G. Selective expression of fos- and jun-related genes during osteoblast proliferation and differentiation. Exp Cell Res 1995; 218(1):255–262.
3. Liu F, Malaval L, Gupta AK, Aubin JE. Simultaneous detection of multiple bone-related mRNAs and protein expression during osteoblast differentiation: polymerase chain reaction and immunocytochemical studies at the single cell level. Dev Biol 1994; 166(1):220–234.
4. Urban JP, Roberts S. Development and degeneration of the intervertebral discs. Mol Med Today 1995; 1(7):329–335.
5. Johnstone B, Bayliss MT. The large proteoglycans of the human intervertebral disc. Changes in their biosynthesis and structure with age, topography, and pathology. Spine 1995; 20(6):674–684.
6. Oegema TR, Jr. Biochemistry of the intervertebral disc. Clin Sports Med 1993; 12(3):419–439.
7. Caterson EJ, Nesti LJ, Danielson KG, Tuan RS. Human marrow-derived mesenchymal progenitor cells: isolation, culture expansion, and analysis of differentiation. Mol Biotechnol 2002; 20(3): 245–256.
8. Gronthos S, Graves SE, Ohta S, Simmons PJ. The STRO-1 + fraction of adult human bone marrow contains the osteogenic precursors. Blood 1994; 84(12):4164–4173.
9. Friedenstein AJ, Chailakhyan RK, Gerasimov UV. Bone marrow osteogenic stem cells: in vitro cultivation and transplantation in diffusion chambers. Cell Tissue Kinet 1987; 20(3):263–272.
10. Caterson EJ, Nesti LJ, Li WJ, Danielson KG, Albert TJ, Vaccaro AR, Tuan RS. Three-dimensional cartilage formation by bone marrow-derived cells seeded in polylactide/alginate amalgam. J Biomed Mater Res 2001; 57(3):394–403.
11. Roberts CJ, Birkenmeier TM, McQuillan JJ, Akiyama SK, Yamada SS, Chen WT, Yamada KM, McDonald JA. Transforming growth factor beta stimulates the expression of fibronectin and of both subunits of the human fibronectin receptor by cultured human lung fibroblasts. J Biol Chem 1988; 263(10):4586–4592.
12. Gentry LE, Lioubin MN, Purchio AF, Marquardt H. Molecular events in the processing of recombinant type 1 pre-pro-transforming growth factor beta to the mature polypeptide. Mol Cell Biol 1988; 8(10): 4162–4168.
13. Alevizopoulos A, Mermod N. Transforming growth factor-beta: the breaking open of a black box. Bioessays 1997; 19(7):581–591.
14. Hill CS. Signalling to the nucleus by members of the transforming growth factor-beta (TGF-beta) superfamily. Cell Signal 199; 8(8):533–544.
15. Heldin CH, Miyazono K, ten Dijkei P. TGF-beta signalling from cell membrane to nucleus through SMAD proteins. Nature 1997; 390(6659):465–471.

16. Kim J, Johnson K, Chen HJ, Carroll S, Laughon A. Drosophila Mad binds to DNA and directly mediates activation of vestigial by Decapentaplegic. Nature 1997; 388(6639):304–308.
17. Chen RH, Juo PC, Curran T, Blenis J. Phosphorylation of c-Fos at the C-terminus enhances its transforming activity. Oncogene 1996; 12(7):1493–1502.
18. Sano Y, Harada J, Tashiro S, Gotoh-Mandevillei R, Maekawa T, Ishii S. ATF-2 is a common nuclear target of Smad and TAK1 pathways in transforming growth factor-beta signaling. J Biol Chem 1999; 274(13):8949–8957.
19. Zhang Y, Feng XH, Derynck R. Smad3 and Smad4 cooperate with c-Jun/c-Fos to mediate TGF-beta-induced transcription. Nature 1998; 394(6696):909–913.
20. Kretzschmar M, Doody J, Massague J. Opposing BMP and EGF signalling pathways converge on the TGF-beta family mediator Smad1. Nature 1997; 389(6651):618–622.
21. Kretzschmar M, Doody J, Timokhina I, Massague J. A mechanism of repression of TGFbeta/Smad signaling by oncogenic Ras. Genes Dev 1999; 13(7):804–816.
22. Chen YG, Hata A, Lo RS, Wotton D, Shi Y, Pavletich N, Massague J. Determinants of specificity in TGF-beta signal transduction. Genes Dev 1998; 12(14):2144–2152.
23. Dennler S, Itoh S, Vivien D, ten Dijkei P, Huet S, Gauthier JM. Direct binding of Smad3 and Smad4 to critical TGF beta-inducible elements in the promoter of human plasminogen activator inhibitor-type 1 gene. EMBO J 1998; 17(11):3091–3100.
24. Wu G, Chen YG, Ozdamar B, Gyuricza CA, Chong PA, Wrana JL, Massague J, Shi Y. Structural basis of Smad2 recognition by the Smad anchor for receptor activation. Science 2000; 287(5450): 92–97.
25. Whitmarsh AJ, Davis RJ. Transcription factor AP-1 regulation by mitogen-activated protein kinase signal transduction pathways. J Mol Med 1996; 74(10):589–607.
26. Hu PP, Shen X, Huang D, Liu Y, Counter C, Wang XF. The MEK pathway is required for stimulation of p21(WAF1/CIP1) by transforming growth factor-beta. J Biol Chem 1999; 274(50):35381–35387.
27. Yonekura A. Transforming growth factor-beta stimulates articular chondrocyte cell growth through p44/42 MAP kinase (ERK) activation. Endocr J 1999; 46(4):545–553.
28. Daum G, Eisenmann-Tappei I, Fries HW, Troppmair J, Rapp UR. The ins and outs of Raf kinases. Trends Biochem Sci 1994; 19(11):474–480.
29. Hunter T. Protein kinases and phosphatases: the yin and yang of protein phosphorylation and signaling. Cell 1995; 80(2):225–236.
30. Chen RH, Sarnecki C, Blenis J. Nuclear localization and regulation of erk- and rsk-encoded protein kinases. Mol Cell Biol 1992; 12(3):915–927.
31. Luo K, Stroschein SL, Wang W, Chen D, Martens E, Zhou S, Zhou Q. The Ski oncoprotein interacts with the Smad proteins to repress TGFbeta signaling. Genes Dev 1999; 13(17):2196–2206.
32. Chen RH, Abate C, Blenis J. Phosphorylation of the c-Fos transrepression domain by mitogen-activated protein kinase and 90-kDa ribosomal S6 kinase. Proc Natl Acad Sci USA 1993; 90(23): 10952–10956.
33. Ofir R, Dwarki VJ, Rashid D, Verma IM. Phosphorylation of the C terminus of Fos protein is required for transcriptional transrepression of the c-fos promoter. Nature 1990; 348(6296):80–82.
34. Nesti LJ, Caterson EJ, Wang M, Chang R, Chapovsky F, Hoek JB, Tuan RS. TGF-beta1-stimulated osteoblasts require intracellular calcium signaling for enhanced alpha5 integrin expression. Ann NY Acad Sci 2002; 961:178–182.
35. Caterson EJ, Li WJ, Nesti LJ, Albert T, Danielson K, Tuan RS. Polymer/alginate amalgam for cartilage-tissue engineering. Ann NY Acad Sci 2002; 961:134–138.
36. Cary LA, Chang JF, Guan JL. Stimulation of cell migration by overexpression of focal adhesion kinase and its association with Src and Fyn. J Cell Sci 1996; 109(pt 7):1787–1794.
37. Sastry SK, Horwitz AF. Adhesion-growth factor interactions during differentiation: an integrated biological response. Dev Biol 1996; 180(2):455–467.
38. Buckwalter JA, Glimcher MJ, Cooper RR, Recker R. Bone biology. II: Formation, form, modeling, remodeling, and regulation of cell function. Instr Course Lect 1996; 45:387–399.
39. Marks SC, Jr, Popoff SN. Bone cell biology: the regulation of development, structure, and function in the skeleton. Am J Anat 1988; 183(1):1–44.

40. Ponticiello MS, Schinagl RM, Kadiyala S, Barry FP. Gelatin-based resorbable sponge as a carrier matrix for human mesenchymal stem cells in cartilage regeneration therapy. J Biomed Mater Res 2000; 52(2):246–255.
41. Vacanti CA, Langer R, Schloo B, Vacanti JP. Synthetic polymers seeded with chondrocytes provide a template for new cartilage formation. Plast Reconstr Surg 1991; 88(5):753–759.
42. Freed LE, Vunjak-Novakovici G, Biron RJ, Eagles DB, Lesnoy DC, Barlow SK, Langer R. Biodegradable polymer scaffolds for tissue engineering. Biotechnology (NY) 1994; 12(7):689–693.
43. Lo H, Kadiyala S, Guggino SE, Leong KW. Poly(L-lactic acid) foams with cell seeding and controlled-release capacity. J Biomed Mater Res 1996; 30(4):475–484.
44. Rotter N, Aigner J, Naumann A, Planck H, Hammer C, Burmester G, Sittinger M. Cartilage reconstruction in head and neck surgery: comparison of resorbable polymer scaffolds for tissue engineering of human septal cartilage. J Biomed Mater Res 1998; 42(3):347–356.
45. Brady JM, Cutright DE, Miller RA, Barristone GC. Resorption rate, route, route of elimination, and ultrastructure of the implant site of polylactic acid in the abdominal wall of the rat. J Biomed Mater Res 1973; 7(2):155–166.
46. Diduch DR, Jordan LC, Mierisch CM, Balian G. Marrow stromal cells embedded in alginate for repair of osteochondral defects. Arthroscopy 2000; 16(6):571–577.
47. Marijnissen WJ, Osch GJ, Aigner J, Verwoerd-Verhoefi HL, Verhaar JA. Tissue-engineered cartilage using serially passaged articular chondrocytes. Chondrocytes in alginate, combined in vivo with a synthetic (E210) or biologic biodegradable carrier (DBM). Biomaterials 2000; 21(6):571–580.
48. Paige KT, Cima LG, Yaremchuk MJ, Schloo BL, Vacanti JP, Vacanti CA. De novo cartilage generation using calcium alginate-chondrocyte constructs. Plast Reconstr Surg 1996; 97(1):168–180.
49. Paige KT, Cima LG, Yaremchuk MJ, Vacanti JP, Vacanti CA. Injectable cartilage. Plast Reconstr Surg 1995; 96(6):1390–1400.
50. Mackay AM, Beck SC, Murphy JM, Barry FP, Chichester CO, Pittenger MF. Chondrogenic differentiation of cultured human mesenchymal stem cells from marrow. Tissue Eng 1998; 4(4):415–428.
51. Rosen H. The treatment of nonunions and pseudarthroses of the humeral shaft. Orthop Clin North Am 1990; 21(4):725–742.
52. Li WJ, Laurencin CT, Caterson EJ, Tuan RS, Ko FK. Electrospun nanofibrous structure: A novel scaffold for tissue engineering. J Biomed Mater Res 2002; 60(4):613–621.
53. Gristina AG. Biomaterial-centered infection: microbial adhesion versus tissue integration. Science 1987; 237(4822):1588–1595.
54. Wang ML, Hauschka PV, Tuan RS, Steinbeck MJ. Exposure to particles stimulates superoxide production by human THP-1 macrophages and avian HD-11EM osteoclasts activated by tumor necrosis factor-alpha and PMA. J Arthroplasty 2002; 17(3):335–346.
55. Meachim G. Meshwork patterns in the ground substance of articular cartilage and nucleus pulposus. J Anat 1972; 111(2):219–227.
56. Hollinger JO, Battistone GC. Biodegradable bone repair materials. Synthetic polymers and ceramics. Clin Orthop 1986; (207):290–305.
57. Bucholz RW, Henry S, Henley MB. Fixation with bioabsorbable screws for the treatment of fractures of the ankle. J Bone Joint Surg Am 1994; 76(3):319–324.

44

Roentgen Stereometric Analysis: A Novel In Vivo Method to Assess Spinal Fusion

Dietrich Pape, Frank Adam, Ekkehard Fritsch, and Dieter Kohn
University of Saarland
Homburg/Saar, Germany

I. INTRODUCTION

In the treatment of symptomatic spondylolisthesis, spinal fusion is an established method to achieve stability and restore physiological anatomical relations in the spondylolytic segment. Surgical management may vary with regard to approach (anterior, posterior, or combined), technique (open, endoscopic, or combined), fixation device (anterior plate, posterior pedicle screws, interbody implants), and bone graft material (autogenic, allogenic). A common problem with all constructs is difficulty in evaluating spinal stability and the presence of bony fusion.

Direct surgical exploration was previously the gold standard for evaluating the grafted area [1], but it cannot be recommended as a routine procedure due to the morbidity and expense involved [2]. A variety of imaging methods have been used to determine the presence of solid arthrodesis, but they have all been associated with a high misinterpretation rate and provide only static information about the fusion site [1,3,4].

Imaging methods can detect either structural or functional integrity of a fusion [5]. Structural integrity implies a firm attachment between the cage-surrounded bone graft and the adjacent vertebrae, as seen in conventional radiography, computed tomography (CT), and magnetic resonance imaging (MRI).

Functional integrity of fused vertebrae implies the absence of motion within the fused level despite manipulation of the fused area by flexion/extension or compression. These intervertebral translations of fused vertebrae are induced by a positional change of the patient and can be detected either by flexion-extension radiography or by roentgen stereometric analysis (RSA). Conventional radiography offers a low mean accuracy of 1–5 mm depending on the anatomical region and the number of investigators [6]. RSA is a precise quantifying method in evaluating the functional integrity of spinal arthrodesis. It provides information about persisting micromotion between fused vertebrae and is especially useful for testing the mechanical properties in vivo of different constructs within the unstable spine. RSA has already been proven to achieve an accuracy of 0.3–0.7 mm in spinal arthrodesis depending on the axis of motion [3,7–10]. In other orthopedic fields, RSA has gained wide acceptance in detecting early migration after prosthetic fixation in the hip or knee, in assessing joint stability, and in kinematics or fracture stability [6,11–14].

In our clinical studies, RSA was used to determine the functional integrity of lumbosacral anteroposterior fusions over time.

In the first study (primary lumbosacral stability), we examined the primary intervertebral stability of the lumbosacral segment after laparoscopic insertion of carbon cages following posterior pedicle screw fixation.

In a second study (lumbosacral stability after hardware removal), we determined the lumbosacral stability of spinal arthrodesis solely retained by bony integrated carbon fiber implants after removal of the internal fixator.

II. MATERIAL AND METHODS

A. Surgical Procedures and Techniques

To determine the primary lumbosacral stability, 15 patients (10 men, 5 women; mean age 48 yr) with no previous spinal surgery suffering from spondylolisthesis L5-S1 grade 2 underwent a two-stage operative procedure: an open posterior instrumentation using the BWM fixator [15] was followed after 4–10 days (mean 7 days) by an endoscopic anterior lumbar fusion using radiolucent carbon fiber cages (Brantigan I/F Cages) [16] filled with autologous cancellous bone grafts (Fig. 1). During the first stage, tantalum markers with a diameter of 1 mm were implanted into the fifth lumbar (L5) vertebral body, arch, transverse, and spinal processes in a standardized pattern avoiding the loose arches of L5. After the pedicle was manually tapped and an internal screw thread was assembled, tantalum markers were inserted into the left and right ventral aspects of the vertebral body using the transpedicular screw hole. The insertion of pedicle screws took place immediately after the implantation of vertebral body markers. Tantalum markers of the same size were placed in the lateral masses and central crest of the sacrum. During the second stage, laparoscopic lumbosacral discectomy was followed by the removal of disc material and curettage of the central end plates. After gradual distraction of the disc space using spreader blocks, the wedge-shaped carbon cages were inserted in the prepared space. During this anterior surgery, no further tantalum markers were implanted.

To determine lumbosacral stability after hardware removal of consolidated anteroposterior (AP) fusions, 10 patients (6 men, 4 women, mean age 44.6 yr) without previous spinal surgery and with spondylolisthesis L5-S1 grade 2 underwent a single-stage AP lumbosacral fusion using the same procedure as mentioned above. In all of these patients, two anterior endoscopic thoracolumbar implants cages (AETI/AcroMed) were inserted into the intervertebral space using a transperitoneal laparoscopic approach caudally from the aortic bifurcation. Patients were prepared for anterior surgery with routine enemas to empty the rectum and sigmoid colon. During anterior surgery, the patient was placed in a supine Trendelenburg position with the lumbar spine hyperextended and both legs in maximum abduction. Carbon dioxide insufflation was used to enable video-assisted visualization through a 10 mm 30° endoscope. The camera was positioned through a supraumbilical port, and endoshears and endodissectors or retractors were positioned through ports in the left and right lower quadrants.

The subsequent steps of the procedure, such as bowel reduction, exposure of sacral promonory, opening of the peritoneum, annulus and anterior disc space exposure, disc space and end plate preparation, and finally graft implantation, were consistent with reports published previously in greater detail [17–19].

All patients were fitted with a semi-rigid lumbosacral orthosis for 3 months postoperatively. Full weight bearing was permitted immediately after surgery.

B. Cage Implants

The cage-shaped implants, constructed of biologically inert carbon fiber–reinforced polymer composite, have struts that permit anterior load sharing and tooth-like ridges that resist pull-out

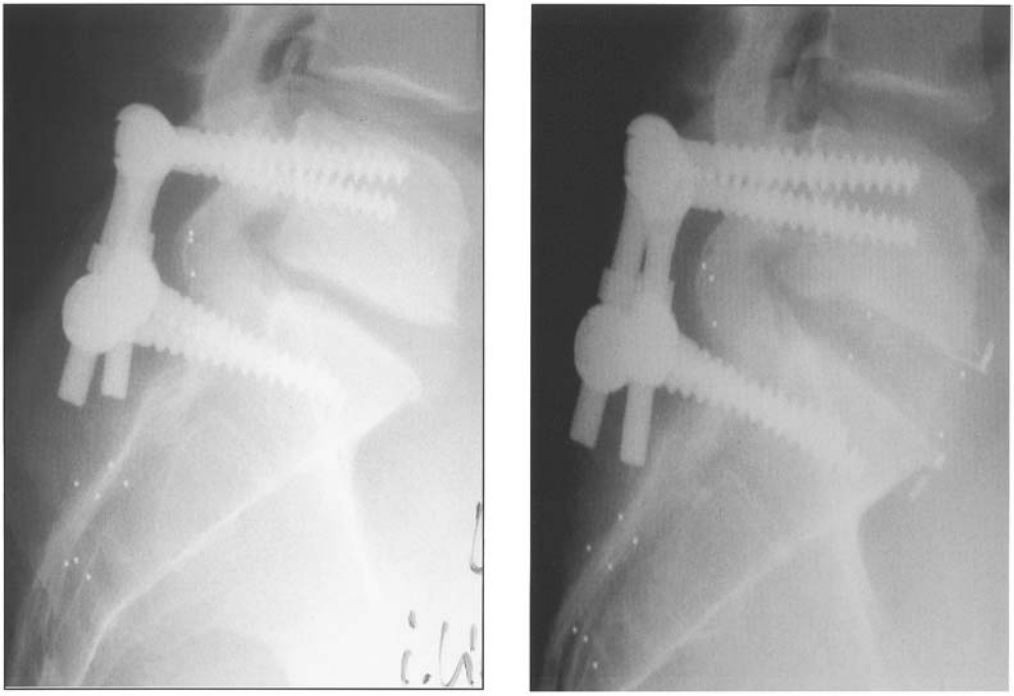

Figure 1 (A) Low-grade spondylolisthesis with a posterior pedicle screw fixation using the BWM fixateur. 1.0 mm tantalum indicators implanted into the fifth lumbar (L5) vertebral body (via the transpedicular approach), arche, transverse and spinal process in a standardized pattern avoiding loose arches of L5. (B) Anterior laparoscopic fusion using radiolucent carbon cages. (From Ref. 9.)

and expulsion [20]. Their flexibility and modulus of elasticity are similar to that of human cortical bone. They are radiolucent, allowing postoperative assessment of bone healing by conventional x-ray methods like RSA and plain radiography.

C. Roentgen Stereometric Analysis

RSA is known to provide highly accurate three-dimensional in vivo measurements using radiographs despite the presence of a pedicle screw system [8]. The insertion of five to nine radiopaque tantalum markers in each vertebra is required to determine the geometric characteristics of the vertebral anatomy.

All patients were examined by RSA after each operation. The RSA x-ray setup using two 40° angulated conventional x-ray tubes was identical in all patients. All patients were positioned above the combined reference plate and calibration device with 1 mm tantalum indicators, placed at known positions in front of the film plane [21].

X-rays were taken within 48 hours of the surgical procedures both in supine position at 45° inclination using a 45° angulated ramp and in neutral spine position to put load on the lumbosacral spine (Fig. 2).

The intervertebral translations of L5 against the Os sacrum were induced by this positional change, and relative movements (micromotion) of the transverse (x), vertical (y), and sagittal (z)

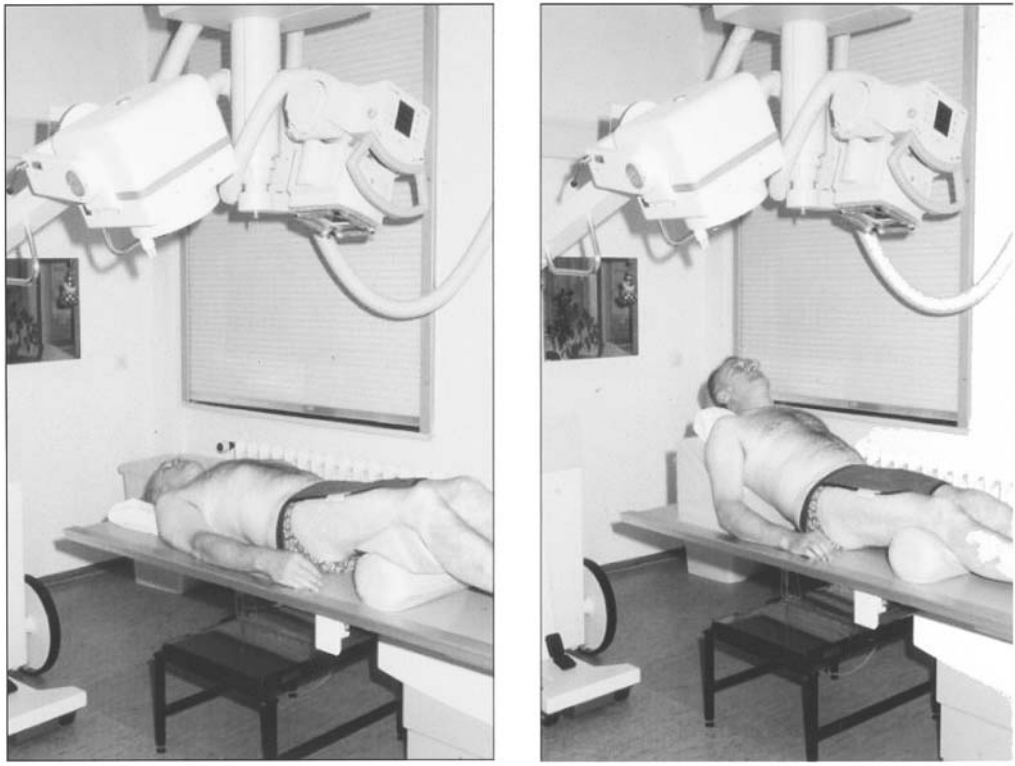

Figure 2 RSA setup: (A) patient in neutral supine position; (B) patient in 45° flexion lying on a ramp. (From Ref. 9.)

axes were calculated by repeated x-rays using the RSA-Kinematic software [22]. The calculated intervertebral translations allowed visualization of persisting micromotion between the fused vertebrae L5/Os sacrum. Patients were monitored post-operatively every 3 months after the procedures and 4 weeks after hardware removal.

D. Accuracy of RSA

To determine the experimental error of our RSA setup we examined five patients with RSA who had displayed osseous fusion on conventional x-rays 6 months postoperatively. The accuracy of RSA was determined by double examinations in the supine spine in 45° inclination and neutral spine position. The induced intervertebral displacements were calculated and the standard deviations of these displacements from zero were estimated. Zero is the theoretical difference within pairs. The minimum significant translations ($p < 0.01$) for the transverse (x), vertical (y), and sagittal (z) axes were calculated using Student's *t*-test distribution. Double examinations of the five patients revealed standard deviations for error for the three axes of motion of 0.08, 0.13, and 0.18 mm respectively. These values corresponded to the minimum significant translations ($p < 0.01$) of 0.25, 0.42, and 0.57 mm. In this study, measurements of lumbosacral fusion translation were not considered significant unless they exceeded 0.3, 0.5, and 0.7 mm along the

respective axes. The accuracy of our RSA setup was determined in a similar method to that used by Johnsson et al. [8], who published comparable minimum significant translations ($p < 0.01$) of 0.22, 0.49, and 0.64 mm for the transverse (x), vertical (y), and sagittal (z) axes, respectively.

E. Indications for Surgery

All patients had complained of progressive disabling back pain for at least 8 months without pain relief from conservative treatment such as physical therapy, anti-inflammatory drugs, and supervised exercise. Prior to surgery, a disability score of 60–80% on the Oswestry Low Back Pain Disability Questionnaire [23] was necessary. All patients gave informed consent for surgery, the marking process using tantalum balls and the RSA-radiographic examinations after surgery. A positive external fixation test 6 weeks prior to surgery was mandatory for all patients. Active workers' compensation or litigation claims were a contraindication to surgery. Hardware removal was undertaken at an average of 10 months after initial surgery once the following criteria were met:

1. Structural integrity of the fusion site seen as a bony bridging on conventional lateral x-rays.
2. Absence of pseudarthrosis according to RSA data gathered 6 months after fusion operation. Solid fusion was assumed if the measured translation of L5 against S1 did not exceed 0.3, 0.5, and 0.7 mm along the transverse (x), vertical (y), and sagittal (z) axes, respectively (Table 1).
3. Persistent lumbosacral discomfort consistent with soft tissue impingement in the absence of radicular pain.
4. 50% pain alleviation on a VAS after infiltration of affected soft tissue with 10 mL 0.25% bupivacaine.

F. Intraoperative Evaluation of Spinal Arthrodesis

At the time of hardware removal, solid fusion was determined by the following intra-operative methods: A towel clip was placed on the intact spinous process of L5 to distract, torque, and compress the fusion. Any motion visualized between the fused segment under lateral fluoroscopic control indicated a pseudarthrosis (towel clip test). Before removing the pedicle screws, two screwdrivers were inserted press-fit into the adjacent screws of one side. The same processes of distraction, compression, and torque were applied to the pedicle screws along these larger lever arms. Parallel movement of the two screw drivers indicated a solid bony fusion (screwdriver test) (4).

G. Radiographic Evaluation of Spinal Arthrodesis

In spinal arthrodesis with titanium cages, anterior bony bridge formation is the most important radiographic sign for the presence of bony fusion. In contrast to titanium cages, carbon fiber cages are radiolucent and allow for a postoperative radiographic assessment of trabecular bridging within the cage. We assumed a bony fusion of the arthrodesis when trabecular bridging was visible on conventional x-rays (Fig. 3).

H. Time Schedule

A physical exam was performed postoperatively, every 3 months after surgery and 4 weeks after hardware removal. This included a muscle strength test, a dermatomal sensory function

Table 1 RSA Data of Lumbosacral Stability After Hardware Removal

Case no.	1 week	3 months	6 months	After hardware removal
x-axis				
1	0.05	0.05	0.25	0.29
2	0.04	0.09	0.09	0.28
3	0.29	0.2	0.18	0.24
4	0.1	0.07	0.06	0.22
5	0.06	0.02	0.03	0.19
6	0.02	0.18	0.02	0.26
7	0.05	0.58	0.09	0.31
8	0.31	0.05	0.13	0.22
9	0.09	0.24	0.08	0.18
10	0.17	0.33	0.12	0.28
Mean	0.12	0.18	0.11	0.25
y-axis				
1	0.06	0.29	0.39	0.45
2	1.28	0.98	0.05	1.19
3	0.91	0.16	0.42	0.68
4	0.05	0.34	0.09	0.41
5	0.04	0.05	0.03	0.52
6	0.02	0.16	0.03	0.02
7	0.1	0.22	0.12	0.23
8	0.08	0.26	0.14	0.31
9	0.12	0.18	0.06	0.41
10	0.24	0.31	0.03	0.29
Mean	0.29	0.30	0.14	0.45
z-axis				
1	0.12	0.54	0.31	0.58
2	0.35	0.09	0.21	1.26
3	1.49	0.91	0.27	0.81
4	0.02	0.01	0.02	0.65
5	0.01	0.02	0.09	0.38
6	0.09	0.1	0.12	0.54
7	0.09	1.62	0.23	0.50
8	0.27	0.19	0.24	0.43
9	0.02	0.09	0.03	0.49
10	0.11	0.17	0.29	0.56
Mean	0.26	0.37	0.18	0.62

Measured intervertebral translations 1 week, 3 months, and 6 months after anteroposterior arthrodesis and 4 weeks after hardware removal. Significant translations ($p < 0.01$) along the transverse (x), vertical (y), and sagittal (z) axes are 0.3, 0.5, and 0.7 mm, respectively.

test, knee and ankle jerks, and passive straight leg raising test. Conventional radiographs with anteroposterior and lateral views were obtained at each follow-up.

I. Statistics

T-test for paired values was used to determine a statistical difference of residual intervertebral translations before and after additional fusion in the three axis of motion ($p < 0.05$).

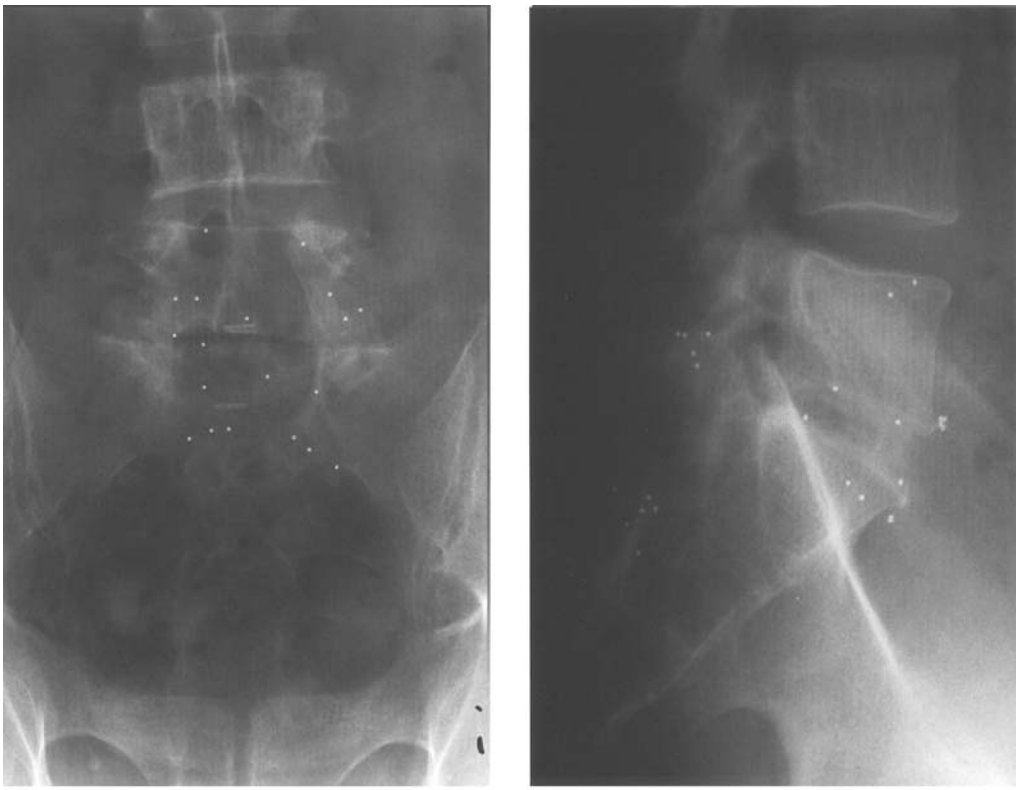

Figure 3 (A) Ap and (B) lateral views of the lumbosacral spine 6 weeks after hardware removal showing a solid bony fusion according to RSA. Radio-opaque tantalum markers were required to determine the geometric characteristics of the vertebral anatomy. Five to nine markers with a diameter of 1 mm were inserted in each vertebra during initial surgery. They were implanted in the fifth lumbar (L5) vertebral body, arch, transverse, and spinal process. A standardized pattern of marker distribution was used, avoiding loose arches of L5. (From Ref. 10.)

III. RESULTS

A. Radiographic Findings

In all patients conventional lateral x-rays revealed trabecular bridging 6 months after surgery, indicating bony lumbosacral fusion. Four weeks after hardware removal, lateral x-rays did not reveal pseudarthrosis.

B. RSA Data of Primary Lumbosacral Stability (Study 1)

After implantation of the posterior pedicle system, the mean intervertebral mobility as determined by RSA was 0.23, 0.54, and 1.2 mm in the transverse (x), vertical (y), and sagittal (z) axis, respectively. After additional anterior endoscopic fusion (ALIF) with carbon cages 7 days later, the remaining translation between the fused segments L5/S1 decreased to 0.17, 0.16, and 0.44 mm in x-,y-, and z-axis, respectively (Table 2).

C. RSA Data of Lumbosacral Stability After Hardware Removal (Study 2)

One week after fusion surgery, serial RSA showed an immediate lumbosacral stability in all patients with only minor mean translatory motions in the transverse (x = 0.12 mm), vertical (y = 0.29 mm), and sagittal (z = 0.26 mm) axes. Three months after surgery, RSA revealed no significant changes in intervertebral translations indicating a persisting stability of the lumbosacral junction after anteroposterior fusion (mean values for x-axis = 0.18 mm, y-axis = 0.3 mm, and z-axis = 0.37 mm).

Six months after surgery, RSA showed a reduction of residual mobility mainly in the vertical (y-axis) and sagittal (z-axis) direction (mean values for x-axis = 0.11 mm, y-axis = 0.14 mm, z-axis = 0.18 mm). In all 10 patients, these measured translations were below the significant values of 0.3, 0.5, and 0.7 mm, respectively.

Four weeks after hardware removal, RSA revealed increased intervertebral translation of 0.25, 0.45, and 0.62 mm in the transverse, vertical, and sagittal axes, respectively (see Table 1). In 8 of 10 patients, this average increase was still below the significant translation values (0.3, 0.5, and 0.7 mm for the x-, y-, and z-axis), which had been calculated for the 5 control patients with good osseous fusion. However, in two patients (patients 2 and 3; see Table 1) the measured translations exceeded the calculated values for a significant motion after removal of the internal fixator.

Table 2 RSA Data of Primary Lumbosacral Stability Before and After the Additional Insertion of I/F Cages in the Presence of a Pedicle Screw System.

	Mobility after first operation (mm)			Mobility after second operation (mm)		
Patient	x	y	z	x	y	z
1	0.12	0.29	2.77	0.13	0.29	1.01
2	0.54	1.58	2.45	0.07	0.06	0.17
3	0.03	0.12	0.09	0.20	0.03	0.40
4	0.47	1.59	1.67	0.29	0.23	0.10
5	0.06	0.70	0.99	0.19	0.22	0.51
6	0.02	0.52	0.98	0.09	0.03	0.05
7	0.24	0.59	1.12	0.05	0.43	0.25
8	0.02	0.11	0.11	0.20	0.01	0.43
9	0.32	0.14	0.93	0.15	0.08	0.88
10	0.44	0.47	0.43	0.08	0.18	0.29
11	0.26	0.56	1.02	0.40	0.22	0.66
12	0.20	0.07	0.66	0.24	0.05	0.40
13	0.21	0.53	1.56	0.21	0.19	0.51
14	0.31	0.61	1.29	0.18	0.31	0.49
15	0.19	0.24	1.92	0.11	0.14	0.47
Mean	0.23	0.54	1.20	0.17	0.16*	0.44*

Intervertebral translations induced by a change from 45° inclination to neutral position with the patient supine. Measurements were performed within 48 hours after the first (posterior instrumentation with pedicle screws) and second operation (additional anterior lumbar interbody fusion in endoscopic technique), respectively.
*Differences of mobility in the y- and z-axis are statistically significant, $p < 0.05$.
Source: Ref. 9.

D. Intraoperative Findings

Lateral fluoroscopic control during the towel clip test and the screwdriver test did not reveal any visible motion in the lumbosacral junction despite distraction, compression, and torque of the grafted area. No pseudarthrosis was diagnosed (Table 3).

E. Complications

No patient required conversion from endoscopic to an open procedure. Complications related to internal fixation, such as screw misplacement, breakage, bending, or loosening, did not occur in any patient. All patients had successful implantation of two AETI carbon cages in each disc space without any displacement in transverse or sagittal direction. One superficial wound infection was treated successfully with antibiotics. There were two neurological complications: a transient motor weakness involving the L5 root and a numbness involving the L5/S1 roots that persisted beyond the time of hardware removal.

IV. DISCUSSION

Posterior screw fixation in combination with interbody implants is widely recommended as a means of enhancing the early bony fusion of spinal arthrodesis [24–26]. Previous studies have demonstrated that anteroposterior fusion can create a stable mechanical environment by restoring the anterior column, thus prolonging instrumentation life and increasing fusion rate [9,27,28]. The aim of surgery should include both primary and long-term postoperative stability of the fused vertebrae [29], but this is difficult to evaluate, especially in the presence of radio-opaque pedicle screws and implants.

Direct surgical inspection is considered to be the gold standard for evaluation of fusion status [1], although various imaging methods are available. Previous studies failed to demonstrate a significant correlation between imaging methods (plain radiographs, flexion/extension radiographs, CT scanning, bone scintigraphy) and direct surgical inspection [30]. Plain radiography

Table 3 Patient Characteristics and Intraoperative Findings at Hardware Removal (HWR) Under Fluoroscopic Control.

Case no.	Sex	Age at fusion surgery (yr)	Time of hardware removal (month)	screwdriver test/towel clip test at HWR
1	f	44	9	Solid fusion
2	f	47	8.5	Solid fusion
3	f	62	11	Solid fusion
4	f	35	9.5	Solid fusion
5	f	37	12	Solid fusion
6	m	41	15	Solid fusion
7	m	49	7	Solid fusion
8	m	52	8.5	Solid fusion
9	m	39	9	Solid fusion
10	f	40	10	Solid fusion
Mean		44.6	10	

is certainly the most widely utilized method of evaluating spinal arthrodesis, but it is known to misinterpret the degree of fusion in 31% of cases [31]. In addition, plain radiography offers a low mean accuracy of 1–5 mm, depending on the anatomical region and the number of investigators [6]. Roentgen stereometric analysis might provide an alternative to this diagnostic dilemma, at least in a basic science setting. It is a more precise method of examining functional integrity of fused vertebrae and has already been proven to achieve an accuracy of 0.3–0.7 mm in spinal arthrodesis depending on the axis of motion [7,8,32,33]. RSA allows for a three-dimensional motion analysis [34] indicating the presence or absence of functionally fused but radiolucent premineralized osteoid in the early phase after arthrodesis [31].

Johnsson et al. [8] were one of the first study groups to apply RSA to spinal surgery. They demonstrated the efficacy of transpedicular screw fixation in posterolateral fusions and described a permanent intervertebral mobility mainly in sagittal direction using the RSA method. They saw a correlation between persisting intervertebral translation and the degree of bone removal such as laminectomy and partial pedicle excision, indicating a possible need for stabilizing the anterior vertebral column in unstable cases [32].

Biomechanical studies on human cadaver spines and a calf spine model showed that the insertion of interbody cages with different cage designs provided a significant stabilizing effect in flexion and lateral bending [35,36]. Animal studies in dogs and sheep confirm the efficacy of anterior instrumentation leading to higher fusion rates due to a more rigid spinal segment [37,38].

In our study of primary lumbosacral stability, the anterior endoscopic insertion of carbon fiber implants was performed 4–10 days after the pedicle screw fixation in 15 patients with low-grade spondylolisthesis. Due to the two-stage surgery, we were able to compare intervertebral translations before and after additional anterior insertion of cages.

Our RSA data confirm the stabilizing effect of cage insertion in vivo, which has already been seen in biomechanical studies: In our RSA patients, insertion of carbon fiber cages reduced the intervertebral mobility mainly in the sagittal (ventral-dorsal direction = z-axis) and longitudinal (cranial-caudal direction = y-axis) plane.

We did not detect a major change in the bending stability after the laparoscopic procedure (left-right direction = transversal x-axis) (see Table 1) because the x-ray position of the patients in 45° flexion does not exert much load onto the lateral aspect of the spine. In addition, the persisting residual mobility in sagittal direction after posterior instrumentation described in the RSA-study by Johnsson [32] disappeared in our patients after the additional anterior procedure.

Among the variety of surgical options, posterior distraction with pedicle screws combined with anterior insertion of bone packed cages appears to be a beneficial technique. Lack of primary stability between fused vertebrae seems to prolong bony fusion up to 6 months and longer, according to other RSA studies [13].

Meta-analysis (39) of literature regarding the spine and recent RSA studies indicate a pronounced range of interindividual lumbar spine mobility. They speak in favor of a positive fusion effect due to early stability following spinal instrumentation [40,41]. However, there are studies showing that the clinical outcome is not different with regard to presence or absence of internal fixation in groups of patients with grade II spondylolytic spondylisthesis [42,43].

Thus, the long-term stabilizing effect of spinal instrumentation is disputed: Sheep models on posterolateral fusion suggest a continuance of support for the anterior and middle column offered by transpedicular screw fixation beyond the presence of bony fusion [44]. In the same animal model, load-sharing of the spinal instrumentation decreases concurrently with the development of spinal fusion [45]. The remaining in vivo stability of consolidated AP fusion following hardware removal remains unclear.

Considering the difficulties in diagnostic imaging we have tried to confirm the presence of a solid fusion in our study of lumbosacral stability after hardware removal on the basis of different criteria. The lateral view in conventional x-rays reflects the structural integrity. The RSA data provide information about the functional integrity of the fused segments and mechanical stress tests during hardware removal verify the absence of motion with fluoroscopic control. We used serial RSA to examine intervertebral lumbosacral stability after AP fusion surgery. Our RSA data suggest a high primary stability of the construct, which is retained over 6 months after surgery without a significant change of intervertebral translations (see Table 1).

In patients with a bilateral posterolateral fusion without additional instrumentation Johnsson et al. [8] demonstrated that fusion healing may vary between 3 months and one year according to RSA. The addition of an internal fixator increased the primary stability, which has been retained during fusion healing but allowed persisting sagittal movements [3]. In our RSA patients, the sagittal movements (z-axis, Table 1) between the fused vertebrae disappear after the additional support of the anterior column with interbody implants indicating a further increase in construct stability [9].

Following hardware removal, our RSA data reveal an increase of intervertebral translations in all axes of motion. However, this increase in micromotion is small, 0.14, 0.31, and 0.44 mm in the transverse, vertical, and sagittal directions, respectively, and is not considered to be significant in 8 of 10 patients since significant translation is not exceeded (Table 1).

The detected increase in micromotion after hardware removal could be partially due to the individual characteristics of bone elasticity, which might come into effect again in bending forces after hardware removal. This may apply especially to patients 2 and 3 (Table 1), who demonstrated increased intervertebral micromotion after hardware removal that exceed the calculated values for a significant translation without demonstrating any signs of pseudarthrosis during surgical inspection. It can only be hypothesized that a potential loss of stabilizing effect following removal of the internal fixator might add to the increased intervertebral micromotion despite the integrated interbody implants. Biomechanical tests in vitro suggest an overall improved primary stability of cage arthrodesis after the addition of supplementary posterior fixation [46]. The in vivo stabilizing effect of an internal fixator in the presence of anterior spinal fusion has not yet been examined in humans.

Our RSA data, obtained 4 weeks after hardware removal, suggest that transpedicular screw fixation in consolidated AP fusion does not provide a persisting major stabilizing effect. It seems that the anterior column is sufficiently supported by integrated fusion cages despite hardware removal, since the functional integrity of the construct does not dramatically deteriorate according to RSA.

Previously, Kanayama et al. [45] demonstrated in an in vivo sheep model that load-sharing of the spinal instrumentation decreases concurrently over time following posterolateral arthrodesis. This might indicate that the stabilizing effect of spinal instrumentation gradually decreases with the progression of bony fusion and supports our findings in humans. However, the degree of stability needed remains unknown, and several studies have questioned the need for implant-supported fusion since functional outcome and fusion rate are comparable with and without instrumentation [42,43].

Seemingly, there are certain limitations to our study: No diagnosis of pseudarthrosis has been made by RSA 6 months after fusion surgery, which could imply that RSA as an in vivo test is not specific to detect false-positive ‘‘solid fusion’’ cases. However, RSA has previously been used to study vertebral motion after posterolateral fusion with transpedicular fixation and has proved to be effective in differentiating between patients with and without fusion [3,7,8].

Moreover, the applied forces to distract, compress, and torque the fusion site during hardware removal, as suggested by Kant et al. [4], are not standardized. We have tried to increase the reliability of the screw driver and towel clip test by adding fluoroscopy to the procedure.

V. CONCLUSION

Anterior endoscopic lumbosacral fusion significantly increases the primary stability of the posterior fusion with a pedicle screw system in two axes of motion. The internal fixator can be removed without endangering the stability of the spinal fusion. Direct surgical exploration has confirmed the adequacy of RSA as a reliable in vivo method to evaluate lumbosacral stability after AP fusion. Further studies are necessary to examine if an increased cage subsidence into the adjacent end plates will evolve due to increased compressive loads following hardware removal.

ACKNOWLEDGMENT

This study was supported by grants from the Medical Faculty of the University of Hamburg, Germany.

REFERENCES

1. Hilibrand AS, Dina TS. The use of diagnostic imaging to assess spinal arthrodesis. Orthop. Clin. North Am 1998; 29:591.
2. Brodsky AE, Kovalsky ES, Khalil MA. Correlation of radiologic assessment of lumbar spine fusions with surgical exploration. Spine 1991; 16:S261.
3. Johnsson R, Axelsson P, Gunnarsson G, Stromqvist B. Stability of lumbar fusion with transpedicular fixation determined by roentgen stereophotogrammetric analysis. Spine 1999; 24:687.
4. Kant AP, Daum WJ, Dean SM, Uchida T. Evaluation of lumbar spine fusion. Plain radiographs versus direct surgical exploration and observation. Spine 1995; 20:2313.
5. Lang P, Chafetz N, Genant HK, Morris JM. Lumbar spinal fusion. Assessment of functional stability with magnetic resonance imaging. Spine 1990; 15:581.
6. Karrholm J. Roentgen stereophotogrammetry: review of orthopedic applications. Acta Orthop. Scand 1989; 60:491.
7. Johnsson R, Stromqvist B, Axelsson P, Selvik G. Influence of spinal immobilization on consolidation of posterolateral lumbosacral fusion. A roentgen stereophotogrammetric and radiographic analysis. Spine 1992; 17:16.
8. Johnsson R, Selvik G, Stromqvist B, Sunden G. Mobility of the lower lumbar spine after posterolateral fusion determined by roentgen stereophotogrammetric analysis. Spine 1990; 15:347.
9. Pape D, Adam F, Fritsch E, Müller KKD. Primary lumbosacral stability after open posterior and endoscopic anterior fusion with interbody implants: a roentgen stereophotogrammetric analysis. Spine 2000; 25:2514.
10. Pape D, Fritsch E, Kelm J, Muller K, Georg T, Kohn D, Adam F. Lumbosacral stability of consolidated anteroposterior fusion after instrumentation removal determined by roentgen stereophotogrammetric analysis and direct surgical exploration. Spine 2002; 27(3.):269.
11. Karrholm J, Hansson LI, Selvik G. Mobility of the lateral malleolus. A roentgen stereophotogrammetric analysis. Acta Orthop. Scand 1985; 56:479.
12. Karrholm J, Snorrason F. Migration of porous coated acetabular prostheses fixed with screws: roentgen stereophotogrammetric analysis. J. Orthop. Res 1992; 10:826.
13. Karrholm J, Jonsson H, Nilsson KG, Soderqvist I. Kinematics of successful knee prostheses during weight-bearing: three-dimensional movements and positions of screw axes in the Tricon-M and Miller-Galante designs. Knee. Surg. Sports Traumatol. Arthrosc 1994; 2:50.
14. Ragnarsson JI, Eliasson P, Karrholm J, Lundstrom B. The accuracy of measurements of femoral neck fractures. Conventional radiography versus roentgen stereophotogrammetric analysis. Acta Orthop. Scand 1992; 63:152.

15. Bailey SI, Bartolozzi P, Bertagnoli R, Boriani S, van Beurden AF, Cross AT, Friedl HP, Gurr KR, Halm H, Kruls HJ, Metz-Stavenhagen P, Schulze KJ. The BWM spinal fixator system. A preliminary report of a 2-year prospective, international multicenter study in a range of indications requiring surgical intervention for bone grafting and pedicle screw fixation. Spine 1996; 21:2006.
16. Brantigan JW, Steffee AD, Geiger JM. A carbon fiber implant to aid interbody lumbar fusion. Mechanical testing. Spine 1991; 16:S277.
17. Olinger A, Pistorius G, Lindemann W, Vollmar B, Hildebrandt U, Menger MD. Effectiveness of a hands-on training course for laparoscopic spine surgery in a porcine model. Surg. Endosc 1999; 13: 118.
18. Zdeblick TA. Laparoscopic spinal fusion. Orthop. Clin. North Am 1998; 29:635.
19. Zucherman JF, Zdeblick TA, Bailey SA, Mahvi D, Hsu KY, Kohrs D. Instrumented laparoscopic spinal fusion. Preliminary results. Spine 1995; 20:2029.
20. Brantigan JW, Steffee AD. A carbon fiber implant to aid interbody lumbar fusion. Two-year clinical results in the first 26 patients. Spine 1993; 18:2106.
21. Selvik G. Roentgen stereophotogrammetric analysis. Acta Radiol 1990; 31:113.
22. Selvik G, Alberius P, Aronson AS. A roentgen stereophotogrammetric system. Construction, calibration and technical accuracy. Acta Radiol. [Diagn.] (Stockh.) 1983; 24:343.
23. Fairbank J, Mbaot JD. The Oswestry Low Back Pain Disability Questionnaire. Physiotherapy 1980; 66:271.
24. Esses SI, Doherty BJ, Crawford MJ, Dreyzin V. Kinematic evaluation of lumbar fusion techniques. Spine 1996; 21:676.
25. Kanayama M, Cunningham BW, Weis JC, Parker LM, Kaneda K, McAfee PC. The effects of rigid spinal instrumentation and solid bony fusion on spinal kinematics. A posterolateral spinal arthrodesis model. Spine 1998; 23:767.
26. Schwab FJ, Nazarian DG, Mahmud F, Michelsen CB. Effects of spinal instrumentation on fusion of the lumbosacral spine. Spine 1995; 20:2023.
27. Enker P, Steffee AD. Interbody fusion and instrumentation. Clin. Orthop 1994:90.
28. Kanayama M, Cunningham BW, Sefter JC, Goldstein JA, Stewart G, Kaneda K, McAfee PC. Does spinal instrumentation influence the healing process of posterolateral spinal fusion? An in vivo animal model. Spine 1999; 24:1058.
29. Evans JH. Biomechanics of lumbar fusion. Clin. Orthop 1985:38.
30. Larsen JM, Rimoldi RL, Capen DA, Nelson RW, Nagelberg S, Thomas JCJ. Assessment of pseudarthrosis in pedicle screw fusion: a prospective study comparing plain radiographs, flexion/extension radiographs, CT scanning, and bone scintigraphy with operative findings. J. Spinal. Disord 1996; 9: 117.
31. Blumenthal SL, Gill K. Can lumbar spine radiographs accurately determine fusion in postoperative patients? Correlation of routine radiographs with a second surgical look at lumbar fusions. Spine 1993; 18:1186.
32. Johnsson R, Axelsson P, Gunnarsson G, Stromqvist B. Stability of lumbar fusion with transpedicular fixation determined by roentgen stereophotogrammetric analysis. Spine 1999; 24:687.
33. Olsson TH, Selvik G, Willner S. Vertebral motion in spondylolisthesis. Acta Radiol. [Diagn.] (Stockh.) 1976; 17:861.
34. Karrholm J. Roentgen stereophotogrammetry: review of orthopedic applications. Acta Orthop. Scand 1989; 60:491.
35. Lund T, Oxland TR, Jost B, Cripton P, Grassmann S, Etter C, Nolte LP. Interbody cage stabilisation in the lumbar spine: biomechanical evaluation of cage design, posterior instrumentation and bone density. J.Bone Joint Surg. Br 1998; 80:351.
36. Lim TH, An HS, Hong JH, Ahn JY, You JW, Eck J, McGrady LM. Biomechanical evaluation of anterior and posterior fixations in an unstable calf spine model. Spine 1997; 22:261.
37. Zdeblick TA, Shirado O, McAfee PC, Warden KE, Degrot H. Anterior spinal fixation after lumbar corpectomy. J.Bone Joint Surg. Am 1999; 73:527.
38. Sandhu HS, Turner S, Kabo JM, Kanim LE, Liu D, Nourparvar A, Delamarter RB, Dawson EG. Distractive properties of a threaded interbody fusion device. An in vivo model. Spine 1996; 21:1201.

39. Mardjetko SM, Connolly PJ, Shott S. Degenerative lumbar spondylolisthesis: a meta-analysis ol literature 1970–1993. Spine 1994; 19(suppl):2256.
40. Axelsson P, Johnsson R, Stromqvist B. The spondylolytic vertebra and its adjacent segment. Mobility measured before and after posterolateral fusion. Spine 1997; 22:414.
41. Johnsson R, Stromqvist B, Axelsson P, Selvik G. Influence of spinal immobilization on consolidation of posterolateral lumbosacral fusion. A roentgen stereophotogrammetric and radiographic analysis. Spine 1992; 17:16.
42. Fischgrund JS, Mackay M, Herkowitz HN, Brower R, Montgomery DM, Kurz LT. 1997 Volvo Award winner in clinical studies. Degenerative lumbar spondylolisthesis with spinal stenosis: a prospective, randomized study comparing decompressive laminectomy and arthrodesis with and without spinal instrumentation. Spine 1997; 22:2807.
43. Thomsen K, Christensen FB, Eiskjaer SP, Hansen ES, Fruensgaard S, Bunger CE. 1997 Volvo Award winner in clinical studies. The effect of pedicle screw instrumentation on functional outcome and fusion rates in posterolateral lumbar spinal fusion: a prospective, randomized clinical study. Spine 1997; 22:2813.
44. Kotani Y, Cunningham BW, Cappuccino A, Kaneda K, McAfee PC. The role of spinal instrumentation in augmenting lumbar posterolateral fusion. Spine 1996; 21:278.
45. Kanayama M, Cunningham BW, Weis JC, Parker LM, Kaneda K, McAfee PC. Maturation of the posterolateral spinal fusion and its effect on load-sharing of spinal instrumentation. An in vivo sheep model. J.Bone Joint Surg. Am 1997; 79:1710.
46. Oxland TR, Lund T. Biomechanics of stand-alone cages and cages in combination with posterior fixation: a literature review. Eur Spine J 2000; 9:95.

45

The Morbidity of Autogenous Bone Graft Donation

Peter A. Robertson and Mark J. Sherwood
Auckland Hospital
Auckland, New Zealand

I. INTRODUCTION

The Hippocratic oath, the guiding dogma of medicine, states *primum non nocere* (first do no harm) [1], yet the procedure of spinal fusion has subjected an increasing number of patients to painful bone graft donation as an additional insult over and above that of the spinal fusion procedure.

Many patients preparing for spinal fusion with autogenous bone believe that the ''hip,'' or bone graft donation site, will be more painful that the index surgical site, yet there is little more than anecdotal evidence [2,3] to support this concern. It is a commonly held belief that the surgical insult from iliac crest bone graft donation causes more postoperative pain at the donor site than at the operative site. This belief has been promulgated over the years and is commonly discussed at the preoperative counseling session. It is interesting that much attention is paid to the immediate postoperative pain from the donor site but little mention is made of the likelihood of long-term morbidity.

No reference is made as to the origin of these assumptions. These concerns regarding bone graft donation pain are handed on from patient to patient, although it is infrequently quoted in publications. The scientific literature has made little attempt to evaluate and quantify the specific difference between operative site pain and that of the donor site. Intuitively, scientific evaluation of this difference is fraught with difficulty, as the patient's nociceptive system is flooded with afferent pain information from multiple sites while recovering and rehabilitating from the operation, not to mention the level of the patient's expectation that the overall ''surgical package'' is intended to bring relief to their suffering, trading their current morbidity for the graft site pain—a lesser of two evils! However, there is increasing evidence to suggest that long-term symptoms of significance from the donor site can impair quality of outcome.

As we become aware of an increasing array of growth factors, graft simulators and expanders, alternative bone options, and other options including disc replacement to avoid fusion, it is appropriate to reexamine the morbidity of autogenous bone graft donation for spinal fusion and to clearly define what this morbidity represents.

II. PURPOSE OF BONE GRAFTS

Bone grafting is performed in orthopedic surgery to enhance fracture and osteotomy healing, to treat nonunions, to achieve solid fusion of painful mobile joints, and to provide mechanical

strength in the form of a strut or onlay graft. Once incorporated, the bone graft provides a dynamic, living support, capable of withstanding normal biomechanical loads. Further remodeling over time leads to trabecular alignment of the bone graft according to applied cyclical stresses.

In spinal surgery, bone graft is used in a variety of ways to achieve spinal fusion. For posterior spinal procedures, corticocancellous bone is applied to decorticated bone adjacent to the region being fused. The posterolateral bone and transverse processes are decorticated, and the bone graft is laid in direct apposition to these areas, held in place by the vascular paraspinal muscles after wound closure. This provides an ideal graft bed in terms of blood supply. Instrumentation has, to a great extent, improved fusion rates and allowed patients to mobilize, usually without the encumbrance of external bracing. High fusion rates have been reported for instrumented procedures with posterolateral bone graft using morselized corticocancellous autogenous bone [58].

Corticocancellous structural grafts are occasionally used posteriorly in the cervical spine where they function in tension, spanning the posterior elements of adjacent vertebrae. The same structural grafts function anteriorly throughout the spine as compressive spacers between vertebral bodies following discectomy or corpectomy. Morselized bone graft is also used anteriorly to fill implantable cages so that the cage provides the biomechanical strength while the biologically active bone that promotes fusion is provided by the graft.

The science of bone graft function is not completely understood, and as newer products and methods are becoming available, they must be interpreted in the light of current knowledge of the basic science. Although vascularised cortical and cancellous autografts show optimum skeletal incorporation, host morbidity and limited bone availability make these techniques rarely practicable.

Muschler and Lane [4] defined: ''a bone graft is any implanted material that, alone or in combination with other materials, promotes a bone healing response by providing osteogenic, osteoconductive, or osteoinductive activity to a local site''. Bone graft materials broadly comprise autograft, allograft, xenograft, synthetic materials and combinations of these materials.

III. AUTOGRAFT: THE GOLD STANDARD

Autogenous bone graft is universally accepted as the gold standard against which other materials must be judged. Bone grafts come in an array of presentations and are classified by composition in Table 1. The biology of bone graft incorporation follows the five distinct stages described by Goldberg and Stevenson [6]: inflammation, vascularization, osteoinduction, osteoconduction, and remodeling [53].

Autograft incorporates more rapidly and more completely than allograft, as does cancellous bone compared to cortical bone. Within these two major categories, they behave quite differently.

When cancellous autograft is compared to cortical autograft, the more rapid incorporation of the cancellous bone occurs with more complete vascularization. Host progenitor cells are stimulated to differentiate to become osteoblasts, which lay down new bone upon the graft trabeculae, which are subsequently resorbed and remodeled. Cortical autograft is incorporated more slowly and less completely with a predominantly osteoclastic response followed by osteoblastic bone deposition. Therefore, cancellous autograft initially increases in mineral density as bone is laid down, whereas cortical autograft proceeds through an osteoclastic resorption leading to a reduction in mechanical strength while this process is occurring (Table 2).

Allograft, on the other hand, has an HLA-based immune-related inflammation phase much greater than autograft causing slower incorporation for both cancellous and cortical bone. The

Table 1 Bone Graft Materials Classified by Composition

1) Autograft
   a) Aspirated bone marrow
   b) Processed osteogenic cells
   c) Cancellous bone
   d) Cortico-cancellous bone
   e) Nonvascularized cortical bone
   f) Vascularized bone
2) Allograft
   a) Graft anatomy
      i) Cortical
      ii) Cancellous
      iii) Cortico-cancellous
      iv) Osteochondral
   b) Graft processing
      i) Fresh
      ii) Frozen
      iii) Freeze-dried
      iv) Demineralized
   c) Graft sterilization
      i) Sterile processed
      ii) Irradiated
      iii) Ethylene oxide
   d) Presentation of product
      i) Powder
      ii) Particulate
      iii) Gel
      iv) Paste or putty
      v) Chips
      vi) Strips or blocks
      vii) Massive
3) Synthetic materials
   a) Osteoconductive blocks or granules
   b) Osteoconductive cements
   c) Osteoinductive proteins
   d) Composites

Source: Ref. 5.

method by which the allograft is processed affects the biomechanical strength, the immunogenicity, and the transmissible infective risk (Table 3).

In clinical practice, higher rates of fusion have been reported with autograft than allograft [7]. Anterior cervical fusion represents an ideal fusion procedure highlighting this discussion and its clinical relevance. For cervical interbody fusion, tricortical autograft fusion rates of 97% are reported [8] for single-level modified Smith-Robinson [7] procedures. Results are also promising for fibular achieving solid fusion [9].

When fusion rates for single-level anterior cervical discectomy and fusion using allograft are compared, equally high success rates (95%) can be achieved [10]. However, in this study, the nonunion rate became disparate for two-level ACDF procedures, with nonunion rates of

Table 2 Structural Qualities of Bone Graft Materials

	Autograft			Allograft[a]		
	Cancellous	Cortical	Vascularized	Cancellous	Cortical	Xenograft
Initial strength	++	+++	+++	++	+++	+++
Trough strength	+++	+[b]	+++	++	+	(?)
Time to peak incorporation	<	>>	3–6/12[c]	>	>>>	>>>[d]
Peak incorporation strength	Late	Initially and then at maturity	+++	+	+++	?
Strength at maturity	+++	+++(?)	+++	+++	+++	?
Incorporation method	New bone laid onto graft trabeculae	Osteoclastic resorption, then bone deposition	Callus, like fracture healing	Creeping substitution	Incomplete osteoclastic resorption, then bone deposition	

[a] Mechanical characteristics depend on processing and preservation technique.
[b] Bone resorption occurs early followed by bone deposition.
[c] Heals like a fracture with callus at the grafthost interface. Initial strength maintained and modified by cyclical loading.
[d] Highly immunogenic—fibrous tissue walls off the area.

17% and 63% for autograft and allograft, respectively. It is also notable that the allograft procedures showed a high incidence of graft collapse (30% vs. 5%) consistent with the biological incorporation of allograft. The preservation technique of the allograft bone is now known to be an important factor in graft choice and performance [10].

Because single-level ACDF procedures performed with allograft and plating show an acceptably low rate of pseudarthrosis, compared with ACDF with autograft, discussion regarding the risks and benefits of donor site morbidity versus those of allograft bone use is warranted [7]. In the pediatric population, the much greater fusion potential of the growing skeleton means that allograft produces better and more acceptable fusion rates in patients who may have a limited volume of autograft available. In the lumbar spine, instrumented posterolateral single-level spine fusions show high fusion rates with morselized corticocancellous autograft [58]. It has been speculated that the higher ratio of cortical to cancellous bone and the greater amount of soft tissue adherent to the bone fragments may make local bone from a decompression site a less desirable alternative [11]. When morselized cancellous bone is used in posterolateral

Table 3 Effects of Allograft Processing on Mechanical Strength, Immunogenicity, and Infective Risk

	Fresh	Frozen	Freeze-dried
Mechanical strength	+++	+++(?)	+
Immunogenicity	+++	++	+
Infective risk	+++	++	+(?)

lumbar spine fusion, studies have shown the radiographic fusion mass to be larger with autograft than allograft [12].

IV. HARVEST SITES FOR AUTOGRAFT

Autograft availability is affected by a number of variables. First, patients may express preference either for or against autologous bone graft donation. Preoperative counseling must provide the patient with sufficient information to give informed consent regarding the options available for bone graft donation. Second, the operative procedure will demand a certain volume of bone graft in order to create a fusion mass of satisfactory bulk. Third, previous surgery will limit the sites at which bone graft is available. Finally, the anatomical location from which the graft is taken will directly affect the volume, composition, and graft site morbidity.

No literature is available regarding the composition and relative volumes of the various graft donor sites throughout the body, although surgeons who frequently harvest autologous bone graft rapidly develop a feeling for the volume and composition that a particular donor site will contribute. Patient positioning must be considered when planning a surgical approach in order to have adequate access to suitable bone. The chosen operative procedure will dictate whether a structural or morselized graft is required.

It is important to note that the age of the patient donating the bone graft will affect the structural qualities and may reduce the effective volume of cancellous bone available. Cortical bone undergoes age-related osteopenia, and the cancellous trabeculae are reduced in number with disease processes such as osteoporosis and age-related fatty infiltration of the bone marrow.

A. The Ilium

The ilium is the most frequently accessed site for bone graft. It provides a variety of types of bone for the different applications. A single posterior iliac crest yields a large volume of predominantly cancellous bone, sufficient for a four-level posterolateral lumbar fusion. There are always a few strips of cortico-cancellous bone from the outer table of the ilium. However, in most applications these are irrelevant as structural components of the graft. The anterior iliac crest is easily accessed in conjunction with anterior spinal procedures and provides a moderate source of cancellous bone. More importantly, the apex of the iliac crest is a tri-cortical structure with excellent compressive strength [13–17] and can provide lengths of up to 10 cm of cortico-cancellous apical strut graft. For the same-sized wound, a larger volume of uncompressed cancellous bone can usually be obtained from the posterior iliac crest compared to the anterior iliac crest.

B. The Fibula

The fibular diaphysis provides a ready source of cortical autograft for use as a compressive strut in anterior discectomy and corpectomy surgery throughout the spine. It is especially suitable in the cervical spine where the endplate or vertebral body surface area for graft apposition is similar. The fibula's shape and its possession of the highest cortical/cancellous ratio of any long bone and high cortical content makes it ideal in this setting.

The entry of the nutrient artery in a direction away from the knee joint, at the mid-diaphysis of the bone, makes this segment of the fibula ideal for a vascularized cortical strut graft in complex or revision spine surgery. In applications where a long strut is required, for example,

in pediatric spinal deformity, a vascularized graft is an excellent biological method of swinging the balance of graft fatigue versus incorporation towards incorporation.

As with the ilium (and as will be discussed later), fibular autograft harvest is not without complications.

C. Rib

Autograft from the rib is usually made available by the rib excision performed during thoracotomy for the anterior exposure of the thoracic and upper lumbar spine. It is uncommon to harvest rib autograft for a spinal procedure not requiring a thoracotomy.

The rib presents a curved, flattened shape, less ideally suited for use as a compressive strut. It has an approximately balanced content of cancellous and cortical bone. When morselized, the cortical bone has a predominantly cortical, ''splintery'' appearance, which is often difficult to morselize in a bone mill. The accessibility of the nutrient artety to the rib makes this bone suitable for use as a vascularized strut graft [18], although inferior in biomechanical properties to the fibula. Because of its location it can be swung on a vascular pedicle (intercostal vessels) into the spine—without the need for vascular reconstruction [19]. Many surgeons find the rib useful in the upper thoracic spine for anterior fusion, as the rib struts can be stacked to supplement the stability already provided by the rib cage [20].

D. Local Bone

Local bone is defined as that removed from the operative site as part of the operative procedure. This bone can be cleaned of soft tissue and morselized to provide sufficient bone for a single level postero-lateral spinal fusion. Although local bone is a term used with some frequency in the literature, there are limited studies quantifying its performance [21,52]. It has been speculated that it is an inferior graft material compared to freshly harvested iliac bone, less able to induce spinal fusion due to soft tissue presence and its high cortical content [11].

V. COMPLICATIONS OF BGD

The quest continues for a reliable, effective, low-morbidity bone graft alternative which can be used by all surgical specialities that employ bone grafting—both spinal and general orthopedic. The principal incentive to develop efficient bone graft alternatives is to reduce donor site morbidity. There are relatively few publications covering the topic of specific morbidities, and within these, it is hard to find prospective randomized controlled trials that clearly define these morbidities, their frequency, and the natural history of autologous bone graft donation.

Overall donor site complication rates have been reported to be much greater at the donor site than at the operative site [22]. Lesser incentives to the development of bone graft alternatives include reducing the pseudarthrosis rate and eradicating the occurence of bloodborne diseases. A morbidity-free, highly osteogenic, and disease-free synthetic bone graft substitute would be ideal.

A spectrum of complications has been reported by multiple authors. Key review articles [23–27] have revealed that there are a core of common complications that can be divided into minor and major. Complications can also be conveniently divided into three categories based on their temporal association: peri-operative, short-term postoperative, and long term.

Younger and Chapman [23] divided bone graft donor site complications into major and minor as well as early and late. Major complications were those that caused an increase in

hospital days, required additional surgery, or caused significant disability. Minor complications were those that responded to treatment such as local wound care or resolved without treatment and did not cause permanent disability. They defined early complications as those that occurred in the perioperative period, usually while the patient was still hospitalized. In their retrospective study of 243 autogenous bone grafts, 54.3% of the operations were spinal fusions; 89.5% of the grafts were obtained from the ilium. They observed a major complication rate of 8.6% and a minor rate of 20.6%. These authors also noted that there was a much higher complication rate (17.9% major) when the incision used for the surgery was the same as that used for the bone graft.

Most publications are retrospective analyses of series predominantly of iliac crest autograft donation. Few prospective, randomized studies exist, especially with respect to the ''natural history'' of symptoms from ABGD.

As there are many thorough reviews of the complications of ABG donation, the reader is referred to five suitable papers [23–27] as a basis for thorough coverage of the following summary of complications. Only references requiring direct quotation will be annotated.

VI. INTRAOPERATIVE COMPLICATIONS

A. Cutaneous Nerve Injury

The most commonly injured cutaneous nerves are the superior cluneal nerves (L1,2,3) when the posterior iliac crest is used [28]. It is recommended that these nerves be preserved when encountered intraoperatively, although in the author's personal experience it is rare to encounter them. Extending the midline incision where appropriate to enable exposure of the posterior iliac crest through a pocket created at the deep fascial level is an alternative and avoids making a separate skin incision. It must be remembered, though, that the cutaneous nerves pierce the fascia and so may still traverse the wound.

For the anterior iliac crest, the incision must be kept at least 2 cm posterior to the anterior superior iliac spine (ASIS) to avoid injury to the lateral femoral cutaneous nerve (LFCN) [29]. Mirovsky and Neuwith suggested a 20% rate of injury to the LFCN during spine surgery, identifying compression by positioning frames, retroperitoneal dissection and retraction, and harvesting bone from the iliac crest as the most common causes. Murata et al. [30] have shown that meralgia paraesthetica is more common after large anterior iliac crest grafts are taken where the depth of dissection down from the apex of the anterior iliac crest is greater than 30 mm.

Colterjohn and Bednar [31] described an alternative incision and approach to the posterior iliac crest by orientating the separate skin incision along the line of the cluneal nerves. There was a statistically significant reduction in postoperative numbness at 1 month and 6 months, and a statistically significant reduction in wound tenderness at the same intervals. There was a dramatic reduction in overall donor site pain at 6 months, also reaching statistical significance. These authors attributed the favorable difference in donor site morbidity between the control and study groups to the use of the modified incision.

B. Breech of Anatomical Cavities (Visceral Injury)

Visceral injury is rare and can occur with aggressive dissection or with inadvertant ''plunging'' with instruments such as osteotomes and curettes. Since some force is required to excavate the cancellous bone from the ilium, control of instrument pressure is essential. The ureter and sciatic nerve is at risk due to its close proximity to the superior gluteal artery and can be damaged by

retraction or dissection in the sciatic notch. A single case report was published by Escalas and DeWald concerning this injury, which resolved spontaneously [32].

C. Bleeding

The superior gluteal artery is the most common vessel injured [54]. Care with retraction around the sciatic notch is essential as the vessel will retract into the pelvis if it is transected. This can be difficult to control, and some suggest that anterior pelvic surgery is necessary to achieve control. A better option is to extend the wound distally, dissect the gluteal nuscles from the pelvis, and apply traction to ''deliver'' the superior gluteal artery into the wound [55]. General ooze from the raw cancellous bone edge is usually easily controlled with thrombostatic sponge or bone wax. Large postoperative blood loss into drain is rare [32–34].

D. Neurological Injury

Injury to major nerves of the lower limb is rare. Cases have been reported with relationship to subfascial hematomas affecting the femoral nerve [35]. The ilioinguinal nerve is also vulnerable to injury as it lies between the external oblique and internal oblique muscles at the pelvic brim. The sciatic nerve is vulnerable to inadvertent damage in the sciatic notch while bone is being harvested from the posterior iliac crest. Careful digital probing intraoperatively will allow the surgeon to determine the proximity to the sciatic notch.

F. Fracture

Fracture of the iliac crest is more common when bone graft is harvested from the anterior iliac crest. The ASIS is the most frequent portion of the ilium to fracture and is usually managed nonoperatively. Limiting the bone resection margin to 3 cm posterior to the ASIS will reduce the risk of fracture and also that of injury to the LFCN [36].

F. Joint Penetration

It is extremely rare for the hip joint to suffer damage from penetration during graft harvest. Inadvertent penetration may not be recognized at the time of surgery.

The sacro-iliac joint (SIJ) is in close proximity when bone is harvested from the posterior iliac crest. It is probably breached more often than is recognized. Fracture of the posterior portion of the ilium may destabilize the SIJ, leading to late instability (see below).

G. Tumor Transplantation

In cases where bone graft is required to be used in tumor reconstruction, it is important to maintain isolation of the graft site. Graft should be harvested at the beginning of the procedure and the wound closed, over sealed drains if appropriate, and covered with a carefully placed, occlusive dressing. The graft should be harvested in excess, having utilized appropriate imaging techniques preoperatively to gain information as to the likely volume of graft required.

VII. EARLY COMPLICATIONS

A. Pain

Early postoperative pain from the bone graft donor site may predominate over that of the surgical wound and is a major source of morbidity. Donor site pain that persists for more than 3 months

following iliac crest ABGD has been reported in up to 15% of patients [37–39]. The incidence seems to be the same for both anterior and posterior wounds and also appears to be proportional to the amount of dissection [40,41]. The authors' experience is that although donor site pain is a source of morbidity, peaking at 6 months, more than half of the 106 patients studied had no pain at one-year follow-up [45].

B. Hematoma and Infection (Superficial, Deep, and Osteomyelitis of the Ilium)

The incidence of infection is reported to be less than 1% of cases, although Arrington et al. [33] found an incidence of 1.2% superficial and 1.7% deep infection. These infections respond well to debridement and focused antibiotic treatment. Osteomyelitis of the ilium is rare but should be considered where deep infection or prolonged wound ooze is present. The use of thrombin-soaked polycrystalline collagen and drainage of the wound reduces the rate of hematoma formation and its morbidities. Many authors emphasize the importance of meticulous hemostasis and tight, multilayer closure to reduce hematoma formation, a potential risk factor for infection. It has been our experience that posterior iliac crest wound infection and breakdown is much higher in PIC donor sites where patients have paraplegia or quadriplegia following spinal cord injury. Immobility and sphincter dysfunction are likely contributors to this.

C. Herniation of Abdominal Contents Through Bony or Fascial Defect

A palpable defect is often present and asymptomatic, but up to 5% of cases have been reported to develop herniation of abdominal contents through the defect in the ilium when full thickness grafts are taken or there is breach of the inner cortex [25]. The rate of symptomatic herniation may be less than this, but symptomatic cases may present with vague aching or fullness over the site. The authors' experience supports the literature that reports this complication as rare [26,27]. These hernias can present as late as 15 years after surgery. Clinical signs of a reducible sac and auscultation of bowel sounds are supported by imaging modalities such as computed tomography. Known risk factors are advanced age, obesity, female sex, and a graft larger than 4 cm [34]. Although treatment of these hernias is highly individualized, attempted closed reduction precedes soft tissue reconstruction, which is usually attempted before more extensive procedures such as unicortical transfer graft from the opposite side. There have been cases of CT-proven herniation that have responded well to closed reduction.

D. Ileus

Patients may develop ileus following large, full-thickness iliac crest grafts. If the bone graft is used for anterior transabdominal surgery, there will be an additional direct insult on the gastrointestinal tract, which will further exacerbate and prolong the ileus.

VIII. LATE COMPLICATIONS

A. Gait Abnormality

Extensive muscular stripping or muscular release with inadequate repair of the fascial attachments may lead to an antalgic gait or an abductor lurch. This is an uncommon problem attributed directly to the surgical insult, given that the primary pathology and coexisting morbidity may cause gait disturbance independent of the graft site. Gait abnormality is equally likely to be

related to graft site complications such as neurological injuries, hematomas, fractures, and painful herniation of abdominal contents.

B. Stress Fractures

Stress fractures of the ilium have been reported as occurring only after removing full thickness grafts from the anterior ilium [35]. As mentioned previously, ensuring that the graft is taken a minimum of 3 cm posterior to the ASIS and paying particular attention to the orientation of the anterior osteotomy at the time of harvest will reduce the risk of this complication.

C. Late Instability of the SI Joint

Coventry and Tapper [42] reported six patients in whom late sacroiliac instability developed after bone graft harvesting of the posterior iliac crest. Authors reporting this late complication have postulated that the posterior sacro-iliac ligaments must have been transected during the graft harvest.

D. Chronic Pain and Dysesthesia

Chronic pain is an unavoidable result in a small number of patients undergoing ABGD and has been reported to have an incidence of 6–39% [43,44]. Predictors of those patients at risk of developing chronic pain are not known although it has been suggested that those with a poor result from their spinal surgery tend to have greater BGDS pain [44,45]. The BGDS may become a focus of pain to which new regional pain stimuli are localized [56].

E. Cosmesis

The superior contour of the iliac crest can be altered by the defect created by the harvesting of the bone graft. Techniques have been developed to reduce the incidence of this complication: the trap door method, the subcrestal window, and an oblique sectioning of the crest. These methods are described pictorially in the article by Kurz et al. [26]. Reconstruction for major pelvic iliac crest deformity in corpectomy surgery has included rib, cement, and other ''fillers'' to cover a major abnormality of iliac contour.

F. Compromise of Late Reconstruction Options

Posterior iliac crest donation may limit late reconstruction options where instrumentation extension to the pelvis using Galveston intrailiac rods or iliac bolts is required. Experience has suggested that as long as 2 cm of bone above the sciatic notch is preserved, then adequate iliac fixation of long constructs can be achieved [57].

IX. FIBULAR DONOR SITE MORBIDITY

Harvest of autograft from the fibula, although a rare procedure in spinal surgery currently, has been associated with postoperative tibial stress fractures (1–2%) [48], superficial and deep peroneal nerve injury (15%) [49], and persistent graft site pain. Short-term symptoms related to the graft site and the incision are common (15–61% [50], and long-term pain, motor, or sensory deficits have been reported in more than 24% of patients [51].

X. NATURAL HISTORY OF BONE GRAFT DONOR SITE PAIN

What, then, is the natural history of autologous bone graft donation from the posterior iliac crest? Can these observations be extrapolated to the anterior iliac crest and other, more distant donor sites? As we more closely advise patients about outcomes, can a surgeon recommend ABGD as a viable option given the accelerating availability of newer materials which are safe, effective and have highly focused biological activity? Can the surgical technique and the perioperative analgesia regimen be modified to minimize graft site morbidity? It is clear that ABGD pain is a many-headed beast that needs to be approached as such.

Few papers offer suitably robust study methodologies to describe the natural history of ABGD. The author's experience is with 106 adult patients undergoing autologous posterior iliac crest bone graft donation for posterior spinal fusion performed by a single, experienced, spinal surgeon [45]. Patients were excluded if they had undergone fixation to the ilium, did not speak English as their first language, or had spinal cord injury with neurology. All patients had bone graft harvested according to the technique of Coulterjohn and Bednar [31] using a separate incision parallel to the iliac crest. At 3, 6, and 12 months after surgery the patients completed a questionnaire and underwent a postoperative examination. Pain was recorded on a visual-analog scale (VAS) of 0 (no pain) to 10 (maximum pain imaginable). Overall surgical outcome was recorded at the final review.

Only two major complications were seen. In one patient a deep infection developed in an instrumented lumbosacral fusion and presented as a donor site infection. The patient developed osteomyelitis of the posterior iliac crest, eventually healing with radical resection of the posterior iliac crest. The second patient developed a gluteus maximus detachment requiring reattachment.

The minor complication rate was 35%, with the most frequently reported morbidity being donor site pain. The mean VAS was 1.640 at 3 months, 1.812 at 6 months, and 1.207 at 12 months. ANOVA showed the 12-month VAS to be significantly less ($p = 0.005$) than at 3 and 6 months, with a trend toward the highest scores at 6 months. The VAS was unaffected by gender, age, donor site, or primary versus revision surgery.

At 12 months, only 12% of the patients reported a VAS of greater than 3, and 55% of the patients had no pain at all. Other reported complications were scar numbness (13 patients), scar painful if knocked (6 patients), itchy scar (4 patients), and local sensory loss (10%) consistent with minor cluneal sensory loss. Harvesting graft from the same side as unilateral leg pain, when present, did not alter the donor site pain. This was an interesting finding, as many have suggested grafting should be performed from the same side as the leg pain (then the bone graft can be blamed for residual symptoms!) or from the opposite side to avoid exacerbating leg symptoms. As there was no relationship between unilateral leg pain and an increase in postoperative bone graft donation pain, we now ask patients which side they want the graft harvested from, suggesting they select the side they don't sleep on.

Palpable defects were present in 26, 28, and 35% of patients at 3, 6, and 12 months, respectively. It was unclear whether these defects were confined to subcutaneous tissue, or whether they represented muscle detachment from the side of the pelvis. There was a strong correlation between local tenderness and a palpable defect at 12 months. Almost twice as many scars were hypertrophic at 12 months than at 3 months. It is therefore tempting to suggest that local tenderness and both soft tissue defects and expanded scars have much to do with patients' personal tissue healing characteristics.

The residual bone graft donor site pain varied with spinal surgical level, with lower lumbar surgery worse than thoracolumbar and cervical procedures. Patients with poorer overall outcomes from surgery had significantly higher donor site VAS pain scores at six months.

The results of this study indicate that the major component of morbidity is donor site pain and that this pain scores relatively low on the VAS. Increased proximity of the donor site to

the wound and failure to isolate the surgical wound pain from the donor site in lower lumbar surgery may explain why these patients had a higher VAS. Even so, 55% of patients had no donor site pain, and it was the author's impression (subsequently supported by a recent paper by Lehmann et al. [46]) that many patients who did record pain only did so because they were asked, often having forgotten which side the graft came from. Indeed, the beneficial effects of studying a problem in an academic environment may have been offset by ''raising consciousness of the problem,'' which for many was trouble-free. Just over 1 in 10 patients had a pain score of greater than 3, and many patients reported that they only noticed the wound if they ''knocked it.''

The higher pain scores at 6 months may reflect increased rehabilitation activity prior to soft tissue maturation.

XI. COSTS OF BONE GRAFT DONATION

The costs of ABGD are difficult to measure objectively. Intraoperative complications will increase the operative time and subject the patient to the small but real risks of prolonged anesthesia, increased open wound time, and increased blood loss with its associated risk of allogenic blood transfusion. The author's personal experience is that a posterior iliac crest bone graft harvest adds between 20 and 30 minutes to the operative time, although good time management usually allows bone graft harvest to be performed during intervals in the operative procedure such as waiting for confirmatory radiographs or while imaging equipment is being brought in, set up, and positioned.

Although there are no studies addressing the issue of early postoperative pain from the donor site, it can be severe enough to delay mobilization in some cases even though the donor site is usually a smaller wound compared with the operative site. In radical surgeries, the bone graft site is the lesser hindrance to mobilization but in smaller, single-level, instrumented spinal fusions, the bone graft donor site can significantly delay mobilization [47].

In reality, carefully procured posterior iliac crest bone graft should not create excessive short-term pain and is well tolerated, with minimal long-term morbidity in most patients. Autologous bone graft donation remains the gold standard for appropriate indications in orthopedic surgery. Its favorable fusion rates, acceptable biomechanical qualities, and excellent biocompatibility all support its use. The appearance of newer bone graft substitutes and osteogenic agents present alternative bone graft materials, which are gaining increased acceptance. It must be stressed, however, that these products have specific label applications that should be adhered to.

XII. CONCLUSIONS

Autogenous bone graft donation in spinal surgery, predominantly harvested from the iliac crest, carries a real morbidity that can detract from surgical outcomes. Risks include intraoperative and later presenting complications in addition to chronic donor site pain. Alternatives exist but fall short of the performance of autogenous bone graft donation, which remains the gold standard. Patients should be made aware of the risks and benefits of the available methods of achieving solid fusion.

Despite the risk of chronic donor site pain, the incidence of which has been reported with some variability, overall functional results are good, with most patients having minimal discomfort from the donor site. Newer products, especially bone morphogenic proteins, appear to have

strong osteogenic potential and, although still limited in their designated applications, show promise as the solution to the morbidity of the donor site.

REFERENCES

1. The Hippocratic Oath: Text, Translation, and Interpretation, by Ludwig Edelstein. Baltimore: Johns Hopkins Press, 1943.
2. Heary RF, Schlenk RP, Sacchieri TA, Barone D, Brotea C. Persistent iliac crest donor site pain: independent outcome assessment. Neurosurgery 2002; 50(3):510–517.
3. Laurie SW, Kaban LB, Mulliken JB, Murray JE. Donor-site morbidity after harvesting rib and iliac bone. Plast Reconstruct Surg 1984; 73(6):933–938.
4. Muschler GF, Lane JM. Orthopaedic surgery. In: Habal MB, Reddi AH, eds. Bone Grafts and Bone Substitutes. Philadelphia: WB Saunders Co, 1998:1573–1589.
5. Bauer TW, Muschler GF. Bone graft materials. An overview of the basic science. Clin Orthop Rel Res 2000; 371:10–27.
6. Goldberg VM, Stevenson S. Natural history of autografts and allografts. Clin Orthop Rel Res 1987; 225:7–16.
7. Malloy KM, Hilibrand AS. Autograft versus allograft in degenerative cervical disease. Clin Orthop Rel Res 2002; 394:27–38.
8. Brodke DS, Zdeblick TA. Modified Smith-Robinson procedure for anterior cervical discectomy and fusion. Spine 1992; 17(10 suppl):S427–430.
9. Emery SE, Bohlman HH, Bolesta MJ, Jones PK. Anterior cervical decompression and arthrodesis for the treatment of cervical spondylotic myelopathy. Two to seventeen-year follow-up. J Bone Joint Surg 1998; 80(7):941–951.
10. Zdeblick TA, Ducker TB. The use of freeze-dried allograft bone for anterior cervical fusions. Spine 1991; 16(7):726–729.
11. Kanim LEA, Le Y, Davies MR, Campbell PA, Dawson EG, Wang JC. Direct comparison of human ''local'' bone versus human iliac crest bone for spinal fusion, International Society for Study of the Lumbar Spine Meeting, May 14–18, Cleveland, Ohio, 2002.
12. Jorgenson SS, Lowe TG, France J, Sabin J. A prospective analysis of autograft versus allograft in posterolateral lumbar fusion in the same patient. A minimum of 1-year follow-up in 144 patients. Spine 1994; 19(18):2048–2053.
13. Wolfinbarger L, Jr, Zhang Y, Adam BL, Sutherland V, Homsi D, Brame B. A comprehensive study of physical parameters, biomechanical properties, and statistical correlations of iliac crest bone wedges used in spinal fusion surgery. I. Physical parameters and their correlations. Spine 1994; 19(3): 277–283.
14. Wolfinbarger L, Jr, Zhang Y, Adam BL, Sutherland V, Gates K, Brame B. A comprehensive study of physical parameters, biomechanical properties, and statistical correlations of iliac crest bone wedges used in spinal fusion surgery. II. Mechanical properties and correlation with physical parameters. Spine 1994; 19(3):284–295.
15. Zhang Y, Wolfinbarger L, Jr. A comprehensive study of physical parameters, biomechanical properties, and statistical correlations of iliac crest bone wedges used in spinal fusion surgery. III. Multivariable regression analysis and practical formulas for strength prediction. Spine 1994; 19(3):296–303.
16. Zhang Y, Homsi D, Gates K, Oakes K, Sutherland V, Wolfinbarger L, Jr. A comprehensive study of physical parameters, biomechanical properties, and statistical correlations of iliac crest bone wedges used in spinal fusion surgery. IV. Effect of gamma irradiation on mechanical and material properties. Spine 1994; 19(3):304–308.
17. Brantigan JW, Cunningham BW, Warden K, McAfee PC, Steffee AD. Compression strength of donor bone for posterior lumbar interbody fusion. Spine 1993; 18(9):1213–1221.
18. Hendel PM, Hattner RS, Rodrigo J, Buncke HJ. The functional vascular anatomy of rib. Plast Reconstruct Surg 1982; 70(5):578–587.

19. McElvein RB, Nasca RJ, Dunham WK, Zorn GL, Jr. Transthoracic exposure for anterior spinal surgery. Ann Thorac Surg 1988; 45(3):278–283.
20. Nakamura H, Yamano Y, Seki M, Konishi S. Use of folded vascularized rib graft in anterior fusion after treatment of thoracic and upper lumbar lesions. Technical note. J Neurosurg 2001; 94(2 suppl): 323–327.
21. Keene JS, McKinley NE. Iliac crest versus spinous process grafts in posttraumatic spinal fusions. Spine 1992; 17(7):790–794.
22. Whitecloud TS. Complications of anterior cervical fusion. Am Acad Orthop Surg 1978; 27:223–227.
23. Younger EM, Chapman MW. Morbidity at bone graft donor sites. J Orthopa Trauma 1989; 3(3): 192–195.
24. Banwart JC, Asher MA, Hassanein RS. Iliac crest bone graft harvest donor site morbidity. A statistical evaluation. Spine 1995; 20(9):1055–1060.
25. Seiler JG, III, Johnson J. Iliac crest autogenous bone grafting: donor site complications. J South Orthop Assoc 2000; 9(2):91–97.
26. Kurz LT, Garfin SR, Booth RE, Jr. Harvesting autogenous iliac bone grafts. A review of complications and techniques. Spine 1989; 14(12):1324–1331.
27. Arrington ED, Smith WJ, Chambers HG, Bucknell AL, Davino NA. Complications of iliac crest bone graft harvesting. Clin Orthop Rel Res 1996; 329:300–309.
28. Fernyhough JC, Schimandle JJ, Weigel MC, Edwards CC, Levine AM. Chronic donor site pain complicating bone graft harvesting from the posterior iliac crest for spinal fusion. Spine 1992; 17(12): 1474–1480.
29. Mirovsky Y, Neuwirth M. Injuries to the lateral femoral cutaneous nerve during spine surgery. Spine 2000; 25(10):1266–1269.
30. Murata Y, Hanaoka E, Takahashi K, Yamagata M, Kuokawa M, Aoki Y, Moriya H. Does the size of iliac bone graft influence the incidence of meralgia parasthetica?. International Society for Study of the Lumbar Spine Meeting, May 14–18, Cleveland, Ohio, 2002.
31. Colterjohn NR, Bednar DA. Procurement of bone graft from the iliac crest. An operative approach with decreased morbidity. J Bone Joint Surg 1997; 79(5):756–759.
32. Escalas F, DeWald RL. Combined traumatic arteriovenous fistula and ureteral injury: a complication of iliac bone-grafting. J Bone Joint Surg 1977; 59(2):270–271.
33. Arrington ED, Smith WJ, Chambers HG, Bucknell AL, Davino NA. Complications of iliac crest bone graft harvesting. Clin Orthop Rel Res 1996; 329:300–309.
34. Kurz LT, Garfin SR, Booth RE. Jr. Harvesting autogenous iliac bone grafts. A review of complications and techniques. Spine 1989; 14(12):1324–1331.
35. Guha SC, Poole MD. Stress fracture of the iliac bone with subfascial femoral neuropathy: unusual complications at a bone graft donor site: case report. Br J Plast Surg 1983; 36(3):305–306.
36. Kuhn DA, Moreland MS. Complications following iliac crest bone grafting. Clin Orthop Rel Res 1986; 209:224–226.
37. Dawson EG, Lotysch M, Jr, Urist MR. Intertransverse process lumbar arthrodesis with autogenous bone graft. Clin Orthop Rel Res 1981; 154:90–96.
38. DePalma AF, Rothman RH, Lewinnek GE, Canale ST. Anterior interbody fusion for severe cervical disc degeneration. Surg Gynecol Obstet 1972; 134(5):755–758.
39. Flint M. Chip bone grafting of the mandible. Br J Plast Surg 1964; 17:184–188.
40. Bloomquist DS, Feldman GR. The posterior ilium as a donor site for maxillo-facial bone grafting. J Maxillofac Surg 1980; 8(1):60–64.
41. Scott W, Petersen RC, Grant S. A method of procuring iliac bone by trephine curettage. J Bone Joint Surg 1949; 31A:860.
42. Coventry MB, Tapper EM. Pelvic instability: a consequence of removing iliac bone for grafting. J Bone Joint Surg 1972; 54(1):83–101.
43. Cockin J. Autologous bone grafting—complications at the donor site. J Bone Joint Surg 1971; 53B: 153.
44. Summers BN, Eisenstein SM. Donor site pain from the ilium. A complication of lumbar spine fusion. J Bone Joint Surg 1989; 71B(4):677–680.

45. Robertson PA, Wray AC. Natural history of posterior iliac crest bone graft donation for spinal surgery: a prospective analysis of morbidity. Spine 2001; 26(13):1473–1476.
46. Lehmann TR, Spratt KF, Harding MK, Lehmann LK. Incidence of chronic donor site pain from posterior iliac bone harvesting, International Society for Study of the Lumbar Spine Meeting, May 14–18, Cleveland, Ohio, 2002.
47. Zdeblick TA, Heim SE, Kleeman TJ. Laparoscopic approach with tapered metal cages: rhBMP-2 versus autograft, International Society for Study of the Lumbar Spine Meeting, May 14–18, Cleveland, Ohio, 2002.
48. Emery SE, Heller JG, Petersilge CA, Bolesta MJ, Whitesides TE, Jr. Tibial stress fracture after a graft has been obtained from the fibula. A report of five cases. J Bone Joint Surg 1996; 78(8): 1248–1251.
49. Gore DR, Gardner GM, Sepic SB, Mollinger LA, Murray MP. Function following partial fibulectomy. Clin Orthop Rel Res 1987; 220:206–210.
50. Vail TP, Urbaniak JR. Donor-site morbidity with use of vascularized autogenous fibular grafts. J Bone Joint Surg 1996; 78(2):204–211.
51. Whitecloud TS, LaRocca H. Fibular strut graft in reconstructive surgery of the cervocal spine. Spine 1976; 1:33–43.
52. Keene JS, McKinley NE. Iliac crest versus spinous process grafts in posttraumatic spinal fusions. Spine 1992; 17(7):790–794.
53. Boden SD, Schimandle JH, Hutton WC. An experimental lumbar intertransverse process spinal fusion model. Radiographic, histologic, and biomechanical healing characteristics. Spine 1995; 20(4): 412–420.
54. Lim EV, Lavadia WT, Roberts JM. Superior gluteal artery injury during iliac bone grafting for spinal fusion. A case report and literature review. Spine 1996; 21(20):2376–2378.
55. Shin AY, Moran ME, Wenger DR. Superior gluteal artery injury secondary to posterior iliac crest bone graft harvesting. A surgical technique to control hemorrhage. Spine 1996; 21(11):1371–1374.
56. Carragee EJ, Tanner CM, Yang B, Brito JL, Truong T. False-positive findings on lumbar discography. Reliability of subjective concordance assessment during provocative disc injection. Spine 1999; 24(23):2542–2547.
57. Kuklo TR, Bridwell KH, Lewis SJ, Baldus C, Blanke K, Iffrig TM, Lenke LG. Minimum 2 year analysis of sacropelvic fixation and L5-S1 fusion using S1 and iliac screws. Spine 2001; 26(18): 1976–1981.
58. Yuan HA, Garfin SR, Dickman CA, Mardjetko SM. A historical cohort study of pedicle screw fixation in thoracic, lumbar, and sacral spinal fusions. Spine 19(20 suppl):2279S–2296S.

46

Loads on an Internal Spinal Fixation Device Measured In Vivo

Antonius Rohlmann, Friedmar Graichen, and Georg Bergmann
Free University of Berlin
Berlin, Germany

I. INTRODUCTION

Internal spinal fixation devices are commonly used for stabilizing lower thoracic and lumbar motion segments in patients with traumatic, degenerative, or tumorous disorders. Pedicle screw breakage in 6–7% of the cases [1,2], screw loosening, and correction loss are possible complications associated with these systems. Little is known about the loads acting in the spine and on the implants during daily activities. After stabilizing a spine with an internal fixation device, part of the spinal load is taken over by the implant. However, it is not known exactly how the load is shared between the implant and the spine at the level of the bridged vertebra. Direct measurement of the complete spinal load is not yet possible. Intradiscal pressure has been measured in different body positions [3–5] and was found to be significantly higher in an upright than in a recumbent position. Several groups [6–8] have performed measurements on external spinal fixators, but the loads on these implants differ from those on internal fixation devices. Data on implant loads are needed to perform realistic implant testing, refine implant design, choose the best rehabilitation program, identify physical activities that endanger implant stability, and evaluate the efficacy of aids like braces and crutches.

The aim of the study was to measure the loads acting on internal spinal fixation devices for different body positions and numerous activities. The influence of several parameters was determined. These included anterior interbody fusion, the postoperative temporal course, and wearing a brace.

II. INSTRUMENTED INTERNAL FIXATOR

The bisegmental internal spinal fixator described by Dick [9] was modified to measure three force and three moment components acting on the implant. The longitudinal threaded rod was provided with an integrated measuring cartridge containing six load sensors, a telemetry unit, and a coil for the inductive power supply of the electronic system (Fig. 1). The cartridge was hermetically sealed by electron-beam welding. The fixators were calibrated in the laboratory prior to implantation. The measurements were performed utilizing a flat coil and a small antenna placed on the patient's back to activate the paired spinal implants. The patient was videotaped during the measurements, and the load-dependent signals of both telemeterized fixators were stored together with the images. A personal computer used the signals to calculate the forces

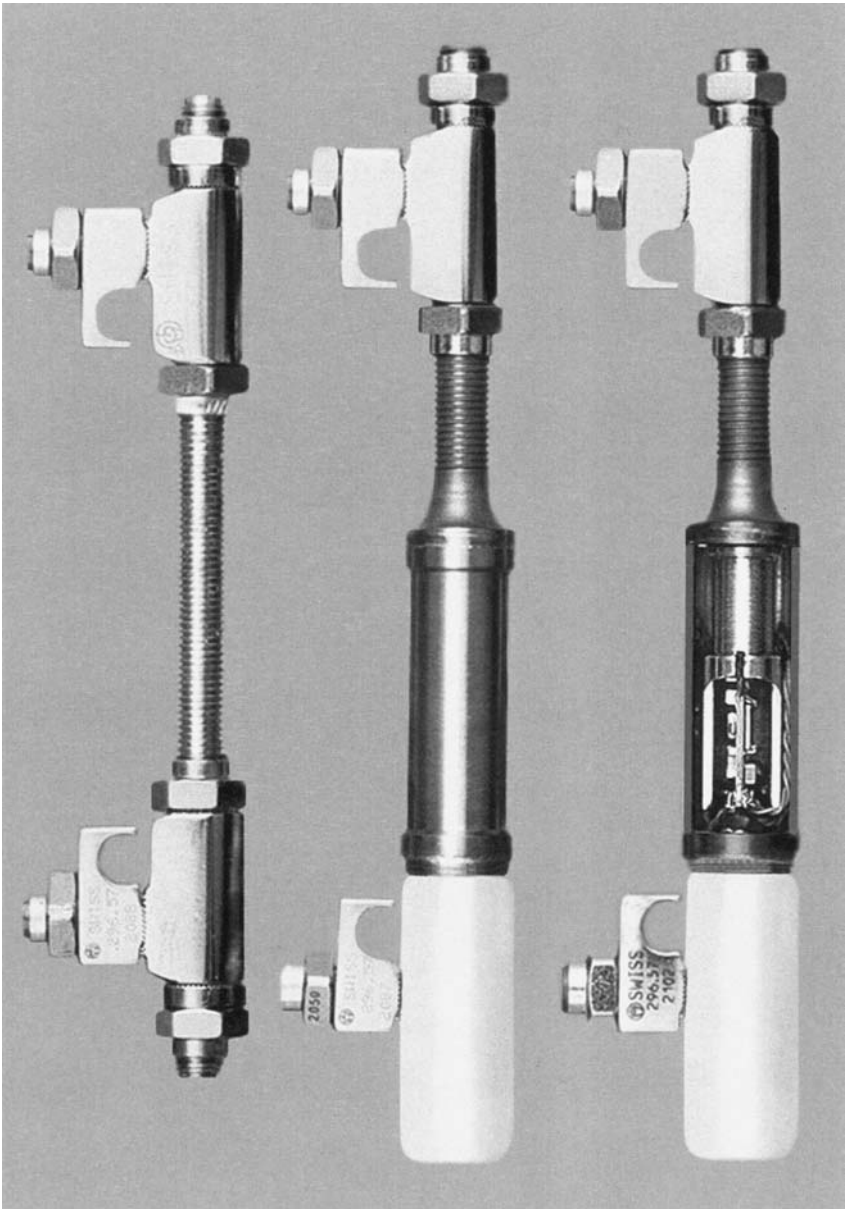

Figure 1 Original implant (left), instrumented fixator for in vivo load measurement (middle), and cross-sectional model of instrumented fixator (right). (Adapted from Journal of Biomechanics, Vol 27(7), Rohlmann, A., Bergmann, G., and Graichen, F. Copyright, 1994, with permission from Elseview Science.)

and moments acting on the implants, and a computer monitor displayed the loading curves on- and off-line. The instrumented implant, the telemetric system, the external equipment, and the accuracy of the device have been described in detail elsewhere [10,11]. Calibration constants were checked in the laboratory after implant removal. They had not changed significantly while the fixators were in place.

III. PATIENTS

Instrumented internal spinal fixation devices were implanted in 10 patients: 3 with degenerative instability and 7 with a vertebral compression fracture. Table 1 provides data on patients and surgical procedures. The bridged vertebral bodies comprised three at L4, two each at L3, L1, and T12, and one at T11. Bisegmental fixators bridging two discs and one vertebra were used in all cases. Anterior interbody fusion with one or two iliac crest bone grafts was performed in a second session. Five patients (No. 3, 5, 7, 9, and 10) had only the upper bridged intervertebral disc removed and the lower one left intact. A Zielke fixator was additionally implanted ventrally during anterior interbody fusion in patient No. 8. The fixators were implanted without direct bone contact so that only loads from the Schanz screws could be transferred to the longitudinal rod and measuring cartridge. Instrumented fixators were removed 12 months after implantation (range 3–21 months) on the average.

The Ethics Committee of the authors' university approved clinical implantation of the telemeterized fixators. Prior to surgery, the procedure was explained to the patients, and they gave their written consent to implantation of instrumented internal spinal fixators and subsequent implant load measurement.

IV. MEASUREMENTS

Implant loads were measured once or twice a week during hospitalization and then about once a month until implant removal. The number of measuring sessions varied between 13 and 25 per patient. Fixator loads were recorded for more than 100 hours. About 200 different activities were studied, and some 14,000 data sets of implant loads were stored in a data bank. When possible, implant loads (forces and moments) were determined for several common body positions and activities at all measuring sessions. These included sitting, standing, walking, lying in different body positions (i.e., supine, prone, and lateral), lifting an extended leg and lifting the pelvis in a supine position, abducting a leg, lifting only the knees and only the feet while lying in a lateral position, bending the upper part of the body in different directions, and rotating the upper body while standing and sitting. Implant loads were measured less frequently for some other activities such as jumping on a trampoline, skipping, bouncing on a physiotherapy ball, jogging on a treadmill, walking with a crutch, and flexing or extending the back while on hands and knees. We did not specify how to perform the exercises because of our interest in the interindividual variation of fixator loads.

V. EVALUATION

The force components perpendicular to the longitudinal axis of the fixator rod and the torsional moments were small for nearly all activities. The axial force component and the bending moment in the sagittal plane (Mb,sag) are the most important load components. The bending moment Mb,sag was calculated from the two moment components acting around axes perpendicular to the longitudinal implant axis. A negative bending moment Mb,sag indicated a flexion moment, and a negative axial force component signified compression. The measured load components were used to calculate the resultant peak force and the resultant peak bending moment for each fixator during the different activities. To compare results from different patients, these peak loads were normalized to those measured with the same patient standing upright. Some patients had markedly different implant loads in consecutive sessions. Thus, median implant load values were also determined for the body position or activity studied.

Table 1 Data on Patients and Surgical Procedures

	Patient no.									
	1	2	3	4	5	6	7	8	9	10
Gender (M/F)	F	M	F	M	M	M	F	F	F	F
Age (yr)	59	34	54	72	36	42	46	62	47	54
Weight (kg)	75	90	66	80	75	81	53	85	48	68
Height (cm)	170	185	162	171	173	164	165	157	160	171
Indication	Degenerative instability	Compression fracture (old)	Compression fracture	Degenerative instability	Compression fracture	Degenerative instability	Compression fracture (old)	Compression fracture (old)	Compression fracture	Compression fracture
Bridged vertebra	L3	L4	L3	L4	T11	L4	T12	L1	L1	T12
Implant levels	L2-L4	L3-L5	L2-L4	L3-L5	T10-T12	L3-L5	T11-L1	T12-L2	T12-L2	T11-L1
Bone grafts	L2/3 & L3/4	L3–L5	L2/L3	L3/4 & L4/5	T10/T11	L3/4 & L4/5	T11/T12	T12-L2	T12/L1	T11/T12
Implantation date (month/year)	4/94	6/94	8/95	8/96	7/97	8/97	9/97	5/98	6/98	6/98
Time between implantation and removal (months)	10	21	8	3	7	20	12	15	8	14
Time between 1st and 2nd operation (days)	28	108	21	21	24	30	–25[a]	28	16	18
Number of measuring sessions after 2nd operation	13	20	10	14	8	18	13	14	11	13
Distraction	Yes	—	Yes	Yes	Yes	Yes	—	Yes[b]	—	—
Compression	—	Yes	—	—	—	—	Yes	—	—	—
Lordosis increased	—	—	Yes	—	Yes	—	Yes	—	Yes	Yes

[a]First stage anterior interbody fusion, second stage implantation of fixators.
[b]Plus anterior Zielke fixator.
Source: Ref. 13.

VI. FIXATOR LOAD CHANGES AFTER ILIAC CREST AUTOGRAFT

To determine the effect of an autologous iliac crest graft on fixator loads, the forces and moments acting on the implant were measured for several body positions and activities before and after anterior interbody fusion. Nine patients were compared for implant loads measured a few days before anterior interbody fusion and up to 130 days thereafter when lying in supine position, standing, and walking. The median values from several measuring sessions before and after anterior interbody fusion were chosen for comparison. Only sessions with mild wound pain were included. Figure 2 shows loads measured in the left and right fixator of the nine patients when walking. Ten of the 18 fixators had a higher flexion bending moment and 11 a higher axial compression force after than before anterior interbody fusion. Similar results were found for standing. The maximum values and load changes were much smaller when lying supine than when walking or standing [12]. Leaving the lower of the bridged intervertebral discs intact led to only small changes in fixator loads after anterior interbody fusion. These data suggest that a bone graft alone does not guarantee a reduction of implant loads.

VII. POSTOPERATIVE TEMPORAL COURSE OF IMPLANT LOADS

The axial compression force and flexion bending moment in the sagittal plane were determined for different activities in up to 20 measuring sessions after anterior interbody fusion. The activities included walking, standing, sitting, lying in a supine position, and lifting an extended leg while in a supine position. The median value was calculated for exercises performed several times during a measuring session. Average maximum loads were determined for the left and right fixators. Figure 3 shows the postoperative temporal course of the axial compression force

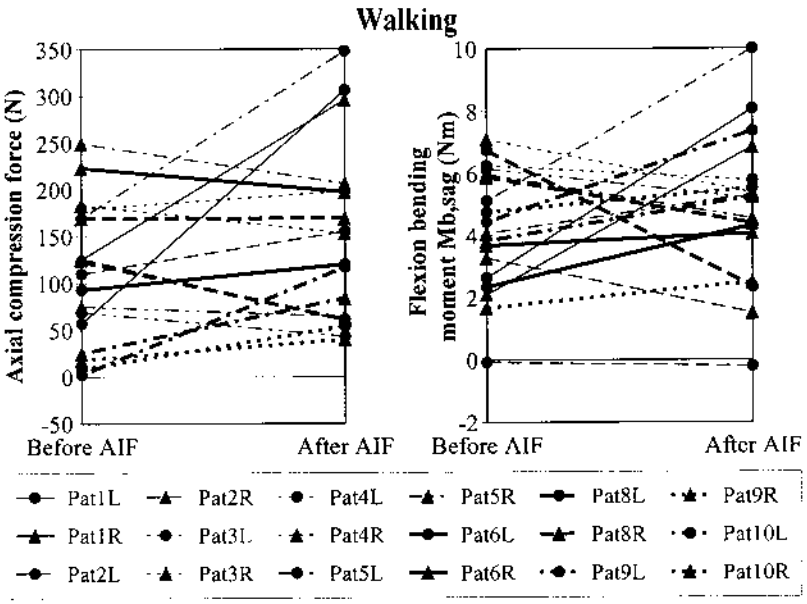

Figure 2 Axial compression force (left) and flexion bending moments in the sagittal plane (right) measured before and after anterior interbody fusion (AIF). The loads are given for the left and right fixators of nine patients measured for walking. (Adapted from Ref. 12.)

and flexion bending moment in the sagittal plane for the 10 patients while standing. The main component was compression for the axial forces and flexion for the bending moments. There were marked interindividual differences in the fixator loads. Implant loads often increased in the early phase after anterior interbody fusion. They decreased after approximately 180 days in patient 6 and were very low after one year. They decreased much less in other patients or even remained at nearly the same level until implant removal. The temporal course of loading curves was similar during sitting and walking. Most absolute values were slightly lower for sitting and slightly higher for walking. Implant loads also followed a similar postoperative temporal course for lying in a supine position, but most of them were considerably lower than those measured in an erect position [13]. In addition, most patients had an increased bending moment over a longer period immediately after the second operation. Fusion had no marked influence on the

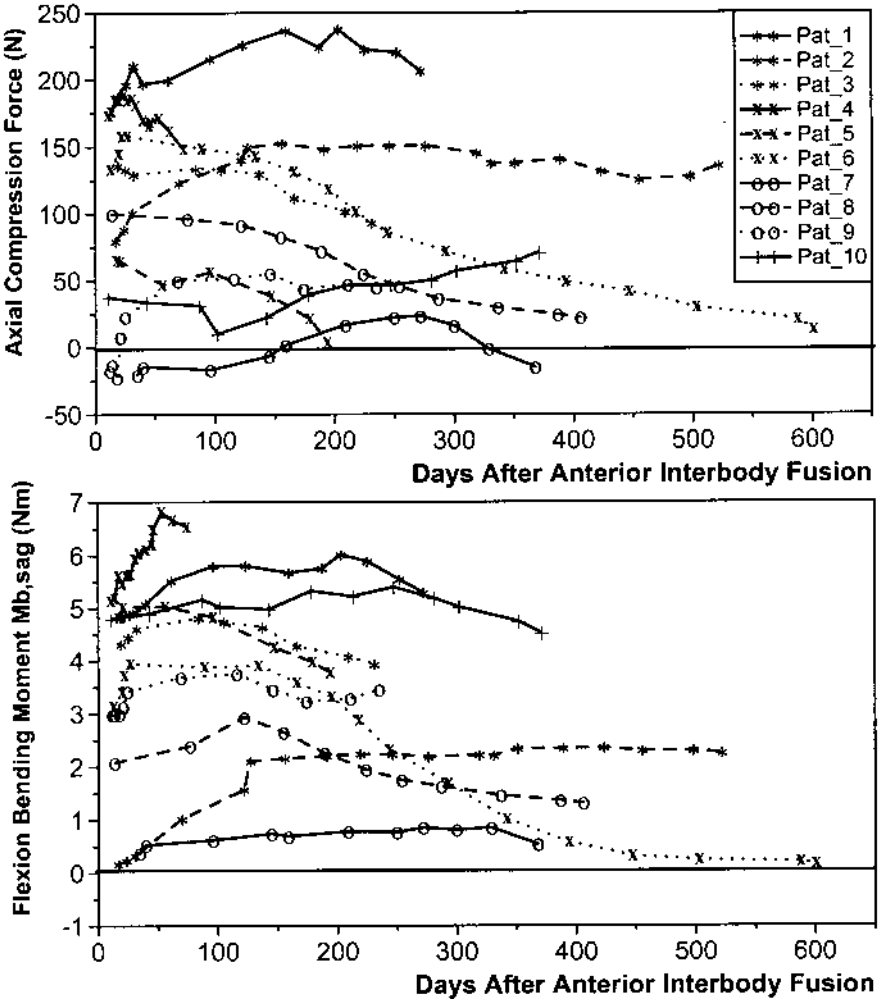

Figure 3 Implant loads for standing as a function of the time after anterior interbody fusion. The average axial compression force (top) and flexion bending moments in the sagittal plane (bottom) are shown in the left and right fixators of the 10 patients. The curves were slightly smoothed. (From Ref. 13.)

maximum implant loads. The loading curves of the fixators could not be used in this study to pinpoint the time of solid fusion. After solid fusion had occurred, some implants were still loaded with high flexion moments even in recumbent patients.

Implant loads were also measured with a patient under anesthesia, when no muscle forces are involved, and a long time after solid fusion had occurred [14]. The measured flexion bending moments were very similar to those measured in a conscious state. This means that, long after anterior interbody fusion, the pedicle screws fixed to the bone are elastically deformed even in the unloaded spine and thus cause a flexion bending moment in the longitudinal rod of the fixator. This also explains the correction loss often found after short-segment fusion of the thoracolumbar spine. The fact that implant loads often remained at nearly the same high level after solid fusion explains why pedicle screws sometimes break more than half a year after implantation. Thus, pedicle screw breakage does not prove that anterior interbody fusion has not occurred.

Patient 6 had very strongly decreased loads in the left and right fixator between 180 and 390 days after anterior interbody fusion [13]. On removing the implant, the surgeon discovered that both pedicle screws were loose on the left side, while the right implant screws were firmly fixed to the vertebral body, as were the pedicle screws in all the other patients. The loads in the two fixators of patient 6 differed only slightly during the postoperative temporal course. Therefore, the loose pedicle screws on the left side are probably not the main cause of the decreased fixator loads. Hip problems had developed in this patient approximately 9 months after surgery, and he often walked with a crutch afterwards. Though only 43 years old, patient 6 was much less active than the other nine patients. Most of the time he was sitting relaxed or lying down, which may explain why he had solid bone fusion with the fixators nearly unloaded.

In an upright body position, the spine is compressed at a given level by the body mass above it. This is not the case with the patient in a lying position. Therefore, the load on the spine is lower in a recumbent than in an erect position. The difference between implant bending moments in an erect and in a relaxed supine position reflects the stiffness of the bridged region. Figure 4 shows the temporal course of average fixator load differences between an erect and a lying position in 10 patients (standing – supine position). Three patients (No. 5, 7, and 10) showed negative differences in the mean axial compression force, which means that they had a higher axial compression force on their implant in a lying than in a standing position. Bridging involved the T11 or T12 vertebra in these cases but a lumbar vertebra in all others. The difference became negative 220 days after anterior interbody fusion in patient 8. The L1 vertebra was bridged in this patient, and she had an anterior Zielke fixator.

The axial fixator load in an erect position depends on several factors, including the body weight, the surgical procedure (compression, distraction of the bridged region), and the fusion level. Fixator positioning is concave in the lumbar and convex in the thoracic spine. In an upright body position, the natural curvature is slightly increased by gravitational force. Therefore, as a subject moves from a lying to an upright body position, axial fixator loads are increased by concave (lumbar spine) and decreased by convex (thoracic spine) implant fixation. This explains the lower axial compression forces for erect body positions as well as the decreased axial compression force measured when patients with a bridged thoracic vertebra carry a weight in their hands [15].

Differences in the flexion bending moment (Fig. 4, bottom) decreased strongly during the temporal course in four patients (No. 5, 6, 8, and 9). These differences were low at all times in two patients (No. 2 and 7), whose bridged region was compressed during fixator implantation. The flexion bending moments in the fixators are affected mainly by the indication for surgery [16] and the surgical procedure. Flexion bending moments are high in the implants if the bridged

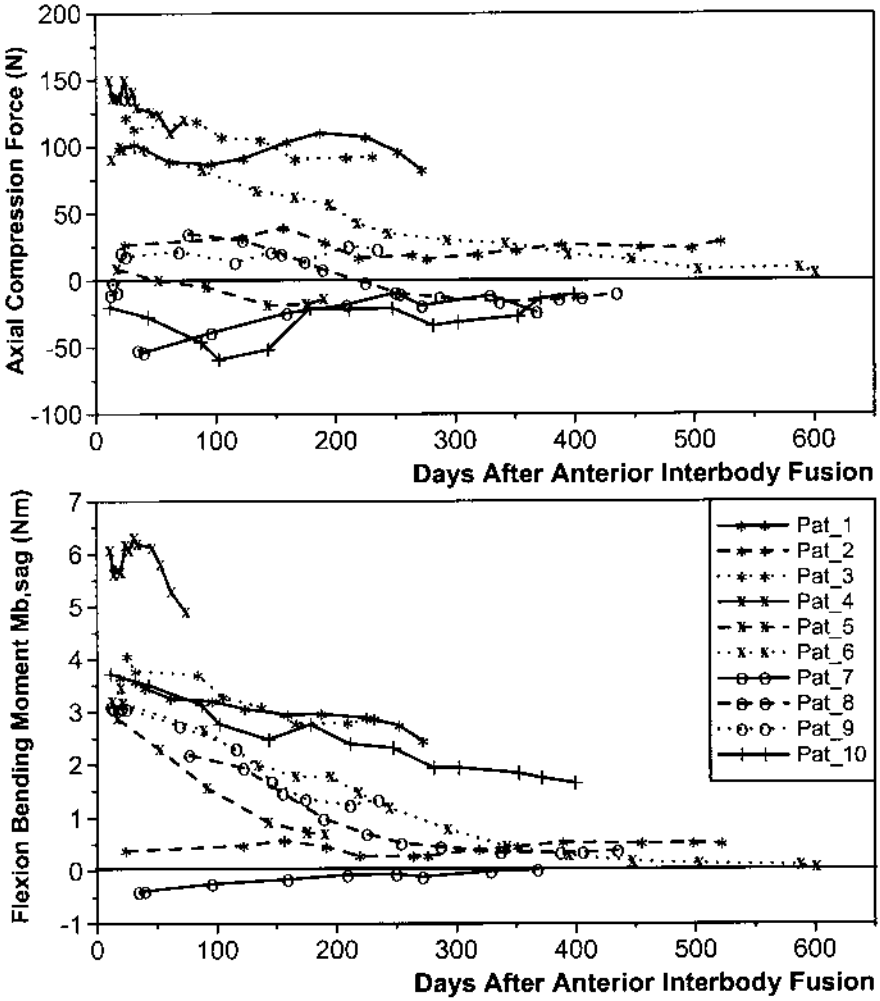

Figure 4 Load differences between a standing and lying position as a function of time after the anterior procedure. The figure shows average differences in load on the left and right fixators measured in the implants of the 10 patients. The curves were slightly smoothed. (From Ref. 13.)

region is distracted during fixator placement and low in the fixators if spinal stiffness in that region is increased by compression.

VIII. EFFECT OF A BRACE

Some surgeons try to avoid implant breakage and loosening of pedicle screws by supplying their patients with a brace. Support and/or immobilization are the main purposes of a brace after stabilization of the lumbar spine [17]. In order to determine the effect of a brace, implant loads were measured in six patients for several positions and activities, including sitting, standing, walking, bending forward, and lifting an extended leg in a supine position. The patients were

wearing no brace, a Boston overlap brace, or a Lumbotrain harness. There was also one patient wearing a reclination brace. None of the braces studied were able to markedly reduce loads on the fixators [18]. Very often, implant loads were even slightly higher when wearing a brace or harness. A brace did not significantly reduce implant loads even when bending forward in an upright position. Thus a brace does not seem helpful after mono- or bisegmental stabilization of the lumbar spine.

IX. COMPARISON OF INTRADISCAL PRESSURES AND FIXATOR LOADS

Little information exists about the loads acting on the spine during different activities of daily life. Direct in vivo measurement of complete spinal loading is not yet possible. Nachemson [4,5], Wilke et al. [3], and others have measured the intradiscal pressure for several activities. Wilke et al. [3] used a flexible pressure transducer to measure the intradiscal pressure in one volunteer. Their results for several body positions and activities were compared with the average bending moments found to act on the fixator in our 10 patients. Axial loading of the spine bends the pedicle screws and longitudinal rods of the fixators. Thus, the bending moments in the implants best reflect the spinal load. To compare intradiscal pressure and bending moments in the fixators, both were normalized to the values measured with the same patients standing upright. The value for standing was set at 100%. Figure 5 compares normalized intradiscal pressures and flexion bending moments for several standard body positions and activities. The relative values for intradiscal pressure and flexion bending moments in the fixators corresponded in most cases. Both independent studies showed comparatively low loads in all lying positions. The loads were slightly lower for sitting relaxed than for standing. Nachemson [4,5] reported 40% higher intradiscal pressure values for sitting. Our results contradict this but are in agreement with those obtained by another indirect load-measuring method using stadiometry. Althoff et al. [19] found an increase in body height when the subjects were sitting after standing for a while. This also indicates that the spinal load is lower for sitting than for standing. The differences between the results of Wilke et al. [3] and Nachemson [4,5] may be due to the different types of pressure transducers they used. Sitting consciously erect, actively straightening and extending the back, increased pressure in the disc and flexion bending moments in the fixators [20]. Higher muscle forces were needed for sitting straight than for sitting relaxed. Higher muscle forces in turn led to higher spinal loads. However, the load differences were small, and the slightly higher pressure is no argument against sitting erect. Intradiscal pressure and flexion bending moments in the fixators tended to differ when loading mainly the anterior column, as during flexion of the upper body or when lifting or carrying weights [21].

X. CONCLUSIONS

The forces and moments acting on internal spinal fixators were measured in 10 patients for various body positions and activities before and after anterior interbody fusion. Despite the different indications and bridged levels, there were some common implant load findings:

- The force components perpendicular to the longitudinal implant axis and the torsional moment are small for most exercises [22,23].
- The axial forces in the implant are predominantly compression forces [13] and depend mainly on the spinal level of fixator attachment. Axial forces are high for concave (lumbar region) and low for convex fixator positioning (thoracic region) [13,15,16].
- The bending moments in the sagittal plane are mainly flexion bending moments [13].

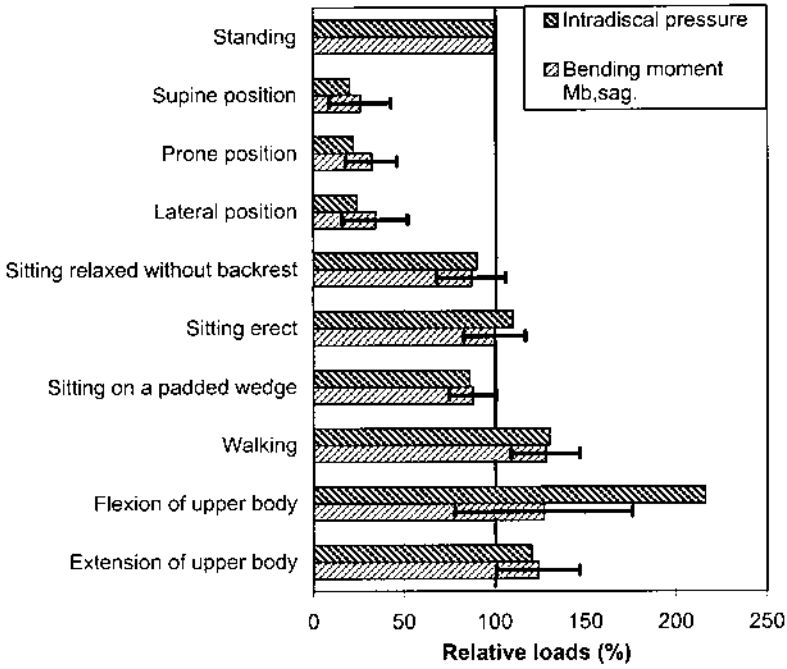

Figure 5 Peak intradiscal pressures (measured in one volunteer) and peak flexion bending moments (mean and SD) in the fixators (measured in 10 patients) for standard body positions and exercises. The values are given as a percentage of those for standing. (From Ref. 21.)

The bending moment in the fixation device depends primarily on the surgical procedure. Bending moments are high with distraction and low with compression of the bridged region [13,15,16].

Implant loads are altered but not necessarily reduced by insertion of a bone graft [12].

In most cases, implant loads increased in the period immediately after the second operation, especially with the patient in a lying position [13].

Most patients still had nearly constant implant loads more than 150 days after the anterior procedure [13]. Thus, pedicle screw breakage more than half a year after insertion does not prove that anterior interbody fusion has not occurred.

The time of solid fusion could not be determined from implant loads [13].

Fixator loads are small with the patients in a lying position [16,21].

Bending moments in the fixation devices when sitting relaxed were, on the average, only 87% of those for standing [16,21].

Sitting erect with an actively straightened back, as taught in some back schools, results in bending moments about as high as those caused by standing [21].

The type of seat (stool, physical therapy ball, knee stool) has a negligible effect on the fixator loads [21].

Of all activities performed regularly, walking causes the highest bending moments in the fixation devices with average values ranging around 128% of those for standing [21,22].

Implant loads are lower during physiotherapy than during walking [24].

Carrying a load in one or both hands has little effect on the bending moments in the fixators [15].

A brace or harness does not reduce implant loads [18].

Relative to the values for standing, the intradiscal pressure corresponds to the bending moments in the internal fixators for most activities [21].

ACKNOWLEDGMENTS

The authors greatly appreciate the cooperation of their patients. They thank Dr. J. Weirowski for editorial assistance. The work was supported by a grant from the Deutsche Forschungsgemeinschaft, Bonn, Germany (Ro 581/7-2).

REFERENCES

1. Yahiro MA. Comprehensive literature review. Pedicle screw fixation devices. Spine 1994; 19: 2274S–2278S.
2. Yuan HA, Garfin SR, Dickman CA, Mardjetko SM. A historical cohort study of pedicle screw fixation in thoracic, lumbar, and sacral spinal fusions. Spine 1994; 19:2279S–2296S.
3. Wilke HJ, Neef P, Caimi M, Hoogland T, Claes LE. New in vivo measurements of pressures in the intervertebral disc in daily life. Spine 1999; 24:755–762.
4. Nachemson A. The load on lumbar disks in different positions of the body. Clin. Orthop 1966; 45: 107–122.
5. Nachemson AL. Disc pressure measurements. Spine 1981; 6:93–97.
6. Schläpfer F, Magerl F, Jacobs R, Perren SM, Weber BG. In vivo measurements of loads on an external fixation device for human lumbar spine fractures. The Institution of Mechanical Engineers C131/80, 1980:59–64.
7. Wilke HJ, Dürselen L, Claes L, Wörsdörfer O. Messmethode für In-vivo-Messungen an Implantaten zur Wiederherstellung von Wirbelsäulenfrakturen. Biomed. Tech 1992; 37:78–85.
8. Wörsdörfer O. Operative Stabilisierung der thorakolumbalen und lumbalen Wirbelsäule: Vergleichende biomechanische Untersuchungen zur Stabilität und Steifigkeit verschiedener dorsaler Fixationssysteme, Thesis. Ulm, Germany: University of Ulm, 1981.
9. Dick W. Internal fixation of thoracic and lumbar spine fractures. Berne. Switzerland: H. Huber Publisher, 1989.
10. Graichen F, Bergmann G, Rohlmann A. Patient monitoring system for load measurement with spinal fixation devices. Med. Eng. Phys 1996; 18:167–174.
11. Rohlmann A, Bergmann G, Graichen F. A spinal fixation device for in vivo load measurement. J. Biomech 1994; 27:961–967.
12. Rohlmann A, Bergmann G, Graichen F, Weber U. Changes in the loads on an internal spinal fixator after iliac-crest autograft. J. Bone Joint Surg. Br 2000; 82:445–449.
13. Rohlmann A, Graichen F, Weber U, Bergmann G. 2000 Volvo Award winner in biomechanical studies: monitoring in vivo implant loads with a telemeterized internal spinal fixation device. Spine 2000; 25:2981–2986.
14. Rohlmann A, Bergmann G, Graichen F, Mayer HM. Influence of muscle forces on loads in internal spinal fixation devices. Spine 1998; 23:537–542.
15. Rohlmann A, Graichen F, Bergmann G. Influence of load carrying on loads in internal spinal fixators. J. Biomech 2000; 33:1099–1104.
16. Rohlmann A, Bergmann G, Graichen F. Loads on internal spinal fixators measured in different body positions. Eur. Spine J 1999; 8:354–359.
17. White AA, 3rd, Panjabi MM. Clinical Biomechanics of the Spine. Philadelphia: J.B. Lippincott Company, 1990.

18. Rohlmann A, Bergmann G, Graichen F, Neff G. Braces do not reduce loads on internal spinal fixation devices. Clin. Biomech 1999; 14:97–102.
19. Althoff I, Brinckmann P, Frobin W, Sandover J, Burton K. An improved method of stature measurement for quantitative determination of spinal loading. Application to sitting postures and whole body vibration. Spine 1992; 17:682–693.
20. Rohlmann A, Arntz U, Graichen F, Bergmann G. Loads on an internal spinal fixation device during sitting. J. Biomech 2001; 34:989–993.
21. Rohlmann A, Claes L, Bergmann G, Graichen F, Neef P, Wilke H-J. Comparison of intradiscal pressures and spinal fixator loads for different body positions and exercises. Ergonomics 2001; 44: 781–794.
22. Rohlmann A, Bergmann G, Graichen F. Loads on an internal spinal fixation device during walking. J. Biomech 1997; 30:41–47.
23. Rohlmann A, Bergmann G, Graichen F, Mayer HM. Telemeterized load measurement using instrumented spinal internal fixators in a patient with degenerative instability. Spine 1995; 20:2683–2689.
24. Rohlmann A, Graichen F, Bergmann G. Loads on an internal spinal fixation device during physical therapy. Phys. Ther 2002; 82:44–52.

47

New Anterior Cervical Instrumentation Systems Combining Intradiscal Cage with Integrated Plate: Biomechanics and Clinical Applications

George Samandouras
The Radcliffe Infirmary
Oxford, England

Peter John Hamlyn
The Royal London Hospital
London, England

I. INTRODUCTION

The controversy over the need for fusion, with or without instrumentation, in surgery for degenerative cervical disc disease is principally fuelled by the absence of an ideal technique. All modern techniques aimed at achieving a rapid and solid fusion originated in the 1950s, when Smith and Robinson [1] followed by Cloward [2] and Bailey [3] demonstrated the feasibility of interbody fusion following an anterior cervical approach to the spine. Autologous bone graft was successfully used by early surgeons and rapidly became the standard graft substrate. Its clinical success is attributable to its osteoinductive, osteoconductive, and structural properties [4,5].

Although some authors find the results of surgery after anterior interbody fusion no different from discectomy alone [6], the use of autologous tricortical iliac bone graft in addition to anterior cervical discectomy is currently the most commonly used technique for one-level cervical disc disease. The placement of appropriately shaped iliac bone grafts restores the disc space height, vertebral alignment, and lost cervical lordosis, avoiding the risk of postoperative kyphotic deformity. Moreover, by distracting the disc space, the foraminal size is increased, relieving nerve root compression without manipulation.

Numerous graft substrates have been used in both instrumented and noninstrumented procedures. Graft options include autologous iliac bone graft or, less commonly, fibula, either autologous or banked cadaveric. The patient's own bone provides the best fusion rates [7–9]; indeed this is the graft material most often chosen [8,10–13]. However, harvesting autologous iliac bone graft is associated with significant postoperative donor site pain, with reported frequency ranging from 2.8 to 49% [12,14–16]. Although the pain usually resolves within a period of weeks, a significant percentage of patients, reported as high as 17%, require narcotic pain relief [12,17].

Fusion of the cervical spine can be accomplished with bone graft only, obviating the need for additional instrumentation. However, fusion techniques relying on bone grafts alone tend to require prolonged external immobilization postoperatively, adding to discomfort and lengthening recovery. In addition, uninstrumented fusion methods have been reported as having high rates of fusion failure. Depending on the patient's age, number of levels involved, and underlying pathology, this rate has ranged, on average, from 2 to 10% but has been documented to be as high as 50% [18–24]. Other mechanisms of graft failure, relating to graft type, have included collapse, resorption resulting in postoperative kyphosis, anterior extrusion sometimes causing dysphasia or esophageal perforation, and posterior extrusion with compromise of the spinal canal or related foramina [6,24–30].

Anterior cervical instrumentation systems were developed in an attempt to address some of these complications. Bohler in 1964 [31] and Orozco in 1970 [32] reported the use of anterior cervical plating systems with screws. Until recently the main indication for anterior cervical plating was trauma since the requirement of bicortical screw purchase was associated with neurological and soft-tissue injuries [5,33]. The introduction of a locking screw mechanism by Morscher et al., perhaps obviating the need for bicortical purchase, decreased the risk of hardware-related complications [5,34].

Anterior cervical instrumentation devices have the theoretical advantage of limiting some graft-related problems and maintaining cervical lordosis. Although the surgical procedure becomes longer, more demanding technically, as well as more expensive, complication rates are minimal and patient comfort, recovery, and fusion rates are improved. In a large retrospective review, 233 patients who underwent one- or two-level anterior cervical discectomy with cortical allograft and plate stabilization were compared with a historical series of 289 patients treated at the same institution who underwent identical procedures without plating [5]. The fusion rate for one-level discectomy was 96% with plating compared to 90% without plating. The improved fusion rates (91% and 72%, respectively) was more clear in the two-level discectomies.

Although the precise indications for the use of anterior instrumentation in the treatment of cervical spondylosis remain to be defined [35], many plating devices are currently available. The efficacy and stability of most of these plating systems have been assessed by numerous clinical and biomechanical studies, and continuous modification of the systems has been a feature of the last decade [36–42]. However, no current device meets all the qualities described as desirable [18].

Designed by Professor Benezech of Montpellier, the recently developed PCB cervical plating device (SCIENT'X, Paris, France), offers a number of theoretical advantages over existing systems. The technical aspects and early clinical results have been reported by our institution [43].

II. INSTRUMENTATION

The hardware of the PCB plating system consists of a set of implants and instruments for insertion and filling of the device with bone chips. The titanium manufactured one-piece PCB cervical system consists of a hollow intradiscal spacer with an integrated plate (Fig. 1). Convergent screw design allows rostro-caudal screw positioning. The fixed screw trajectory requires unicortical screw purchase with no screw locking mechanism since the physiological forces are transmitted mainly to the cage.

The plate is gently prelordosed on the sagittal plane (Fig. 1) to maintain optimal contact with the vertebral body and to restore lost cervical alignment. The plate's wings are arranged obliquely to permit application to adjacent levels in multilevel fusion (Fig. 1). The PCB system has been used in anterior fixation of up to three consecutive levels in our institution.

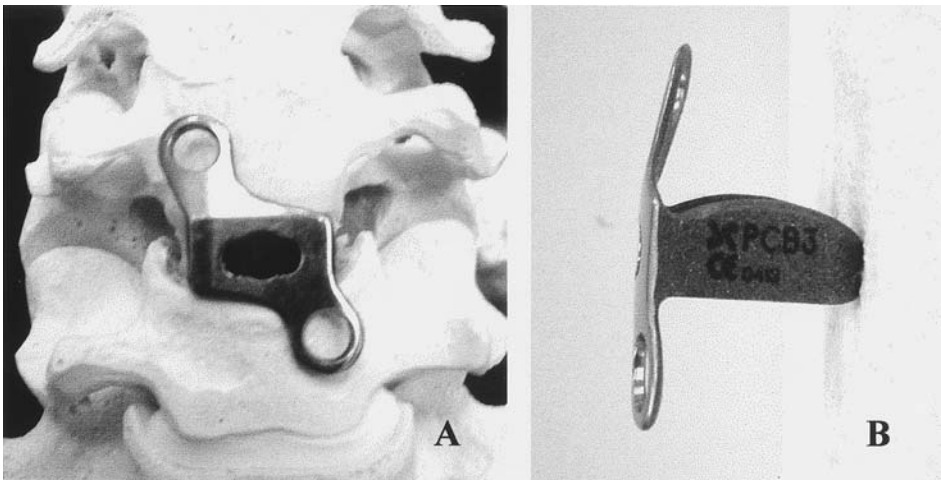

Figure 1 (A) Anterior aspect of the PCB device. An ovoid port at the center of the anterior surface provides access to the interior of the spacer. The end plates can clearly be seen through the port and guide screw positioning without the use of image intensifier. The plate's wings are arranged obliquely to permit application in multilevel fusion. (B) Lateral aspect of the PCB device. The shape of the spacer corresponds to the anatomical configuration of the disc space. The plate is prelordosed in the sagittal plate for optimal contact with the vertebral surfaces aiming to restore lost cervical lordosis.

The hollow intradiscal spacer acts as a cage retaining bone shavings, being closed from anterior, posterior, and lateral surfaces. In the center of the anterior surface, a small, roughly ovoid port provides access to the interior of the spacer (Fig. 1). Therefore, when cancelous bone chips are inserted via the port, the dowel cannot impact them into the spinal canal and related foramina, nor can they extrude anteriorly.

The spacer's configuration reproduces the anatomy of the disc space. The upper borders of its lateral surfaces have a convex configuration for optimal contact with the concave lower surface of the vertebra above (Fig. 1). The device is thereby spontaneously retained within the disc space, avoiding the risk of anterior or posterior migration. Axial and rotational forces are supported by the spacer transmitting minimal loads to the fixation screws. The surfaces of the facet joints remain parallel as in the intact healthy cervical spine. The device provides immediate stability postoperatively, obviating the need for external orthotic devices.

Three sizes of the PCB cage system are currently available, accompanied by three sizes of self-tapping screws (Table 1). However, in the vast majority of cases, a cage with height of 5.5 mm (corresponding to PCB 1) is used. The instrument system is compact; the entire set may readily be held on the palm of the hand (Fig. 2). Usual instruments for insertion of the PCB device and filling of the spacer include a snap-on handle, screw tap, square end, screwdriver, PCB holder, and graft compactor. The device has European approval for human use (Current European Community Medical Engineering and Physics Department Certificate number 41310276).

III. BIOMECHANICS

The biomechanical behavior of the PCB system was tested on various models of loading, including flexion, extension, axial rotation, and lateral bending. The mechanical tests were performed

Table 1 PCB Implant Sizes

PCB System			
PCB 1	H. 5.5	I. 12	L. 16
PCB 2	H. 7	I. 12	L. 16
PCB 3	H. 7	I. 15	L. 16
PCB Screw			
VC14		Length 14 mm	
VC16		Length 16 mm	
VC18		Length 18 mm	

H = cage height; 1 = width; L = length of the intradiscal cage (in mm).

at an independed laboratory certified ISO 9002 and approved by the French committee for accreditation (COFRAC) for program 136 concerning the ''tests on orthopaedic implants'' [44].

The test apparatus consisted of the PCB device inserted between two metallic blocks stimulating the cervical vertebra. The metallic blocks were made of steel to measure the actual biomechanical properties of the PCB device, avoiding any interference from the blocks or screws. An angular defect of 10° was given to the superior metallic block to copy the prelordosed shape of the upper wing of the plate. The insertion torque of the screws had a mean of 4 Nm. A ball-and-socket joint was used to apply the loads in flexion and extension. For the rotation tests an additional compression load of 3 dan was applied. For each of four movement types, three samples of PCB 1 were used.

The results are unpublished, though the data provided by the manufacturer is summarized in Table 2. Tests demonstrate displacement values of the PCB in flexion and extension of 0.18 ± 0.05 mm and 0.4 ± 0.2 mm, respectively. Recorded values were lower than those from

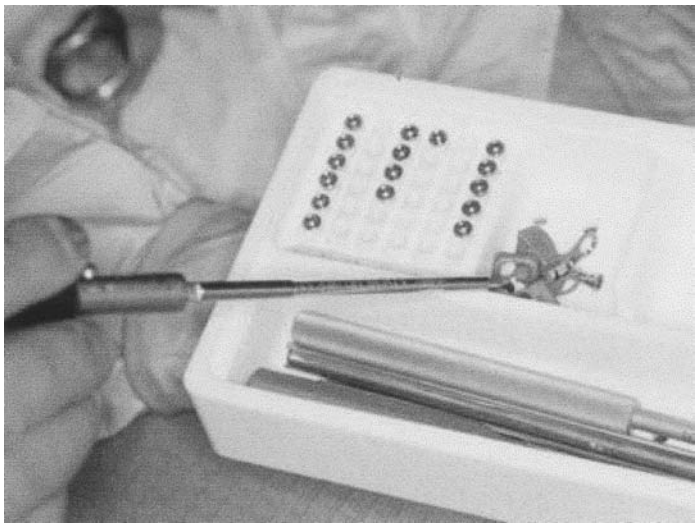

Figure 2 The set of implants and instruments is compact. A selection of PCB cages, screws, and all instruments for inserting and handling the device is displayed. The entire set can be held on the palm of the hand.

Table 2 Load Displacement Curve Results for Four Types of Loading

Type of load	Limit of elasticity	Displacement at the limit of elasticity	Limit at rupture	Displacement at the limit at rupture
Flexion	21 daN	0.75 ± 0.1 mm	145 daN	5.3 mm
Extension	4600 daN	2.45 ± 0.5 mm	5660 daN	3.2 mm
Right rotation	9.7 Nm	33° ± 2	10.1 Nm	34° ± 4
Left rotation	3.9 Nm	27° ± 9	6 Nm	70° ± 12

healthy cervical units under the load of 50 N (0.7 ± 0.3 mm in flexion and 1.1 ± 0.5 mm in extension) [45]. Under physiological conditions a plastic deformation of the PCB is not possible. In addition, rupture of the device is impossible to reach physiologically.

The angle value obtained in axial rotation for the elastic limit was 27°; up to this limit of axial rotation the deformation is reversible and the implant does not fail. Between 27° and 70° the PCB undergoes permanent deformation but with no risk of rupture. Angle values greater than 70° are required in axial rotation to cause the implant to break [44] (Fig. 3). These values exceed the angular limit (18°) thought to represent the limit of rupture of a healthy cervical unit [46].

IV. OPERATIVE TECHNIQUE

The patient is positioned supine on a padded operating table with his head resting in a neutral position on a horseshoe. Soft rolls are placed underneath the shoulder blades to create a moderate neck hyperextension and underneath the right hip to facilitate exposure of the donor site. A curvilinear skin incision is centered over the anterior border of the sternomastoid and curried

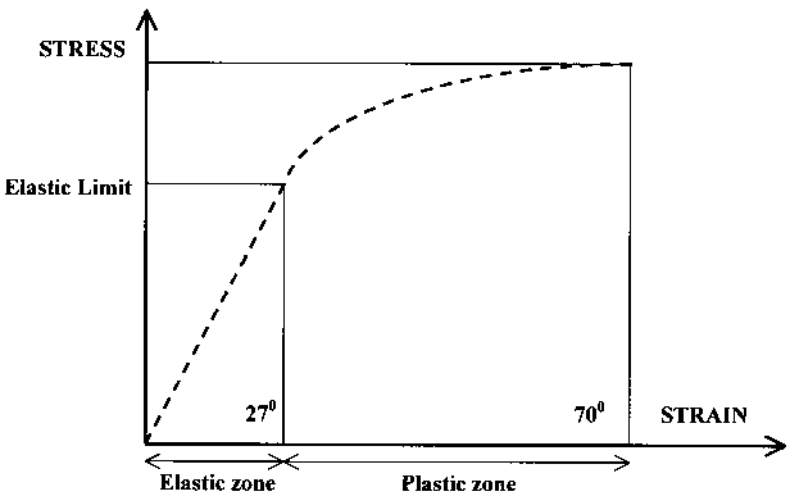

Figure 3 The stress/strain curve of the PCB system. When the elastic limit is reached (27°), permanent deformation occurs. This exceeds the angular limit at rupture (18°) of a healthy cervical spine.

through skin, subcutaneous tissue, and platysma. Using blunt dissection the standard plane between the carotid sheath laterally and the trachea and esophagus medially is developed.

The correct level is confirmed with image intensifier and the medial aspects of the longus coli muscles are diathermized to facilitate insertion of the self-retaining retractor blades. Care must be taken to remove the anterior osteophytes lest they obstruct subsequent settlement of the PCB device. Interbody distraction is applied by means of a standard spreader (Fig. 4). A Caspar retractor is usually avoided since its screw sites may later interfere with those of the PCB plate.

When most of the disc material is removed, the operating microscope is introduced and the end plates are cleared of cartilage with a curette and high-speed air drill. The preparation of the end plates is an important step in the settlement of the PCB device. The posterior osteophytes are drilled, and the posterior longitudinal ligament along with any retained disk fragments are cleared to reveal the dura and root. Although placement of the PCB system distracts the disc space opening the neural foramina, it is preferable to decompress the nerve roots prior to insertion of the device.

A set of trial implants is available to determine the correct size. This is not an entirely necessary step, since with experience it is easy to evaluate the disc space size. The spacer-holder is mounted in the slots on each side of the ovoid post on the anterior surface of the device. The small size of the holder preserves good operative field and enables easy manipulation. The depth of the disc is then measured to allow for the subsequent selection of screw length. The implant should fit snugly into the disc space. Usually simple pressure applied to the spacer holder is sufficient to locate the device, although occasionally it has to be tapped into place. Care should be taken not to overdistract the disc space, as this may add strain to adjacent levels.

The screws are self-tapping and are usually inserted after the cortex has been pierced by a sharp awl, although a tap can facilitate their run. The tap has a fixed stop at 14 mm. The correct screw length is selected using a depth gauge inserted within the disc space. The screws

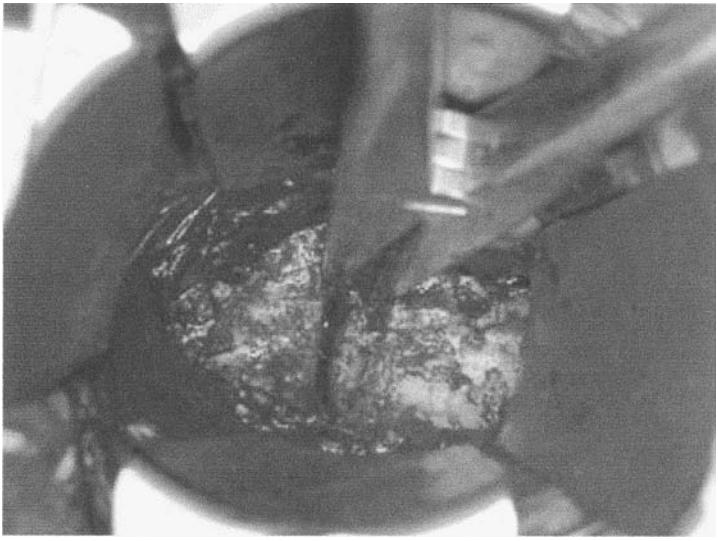

Figure 4 Following superficial discectomy, interbody distraction is applied using a standard spreader. A Caspar distactor can also be used, but its screw sites may later interfere with those of the PCB system. Rostral is left, caudal is right.

are available at lengths ranging from 14 to 18 mm and in diameters of 4 and 4.5 mm. Other screw sizes are available on request. They are positioned using a screwdriver with a conical hexagonal end for secure attachment during insertion.

The screws purchase the superficial anterior cortex and body only. This appears sufficient since the spacer is spontaneously retained in the disc space by virtue of its curved upper surface corresponding to the shape of the end plates. The end plates can clearly be seen via the port and guide the rostro-caudal positioning of the screw. Thus, the screws maybe placed safely without image intensification.

Following location of the device in the involved interspace, a 1 cm incision over the iliac crest is made (Fig. 5). The iliac cortex is pierced using a 0.5 cm osteotome (Fig. 6) and cancelous bone chips are harvested using a curette (Fig. 7). As an alternative bone syringe may be used. These are inserted into the PCB device via the port so as to firmly fill the space. They can be gently impacted using a graft compactor (Fig. 8). The amount of impacted bone shavings must be sufficient to allow optimal contact with the end plates.

Closure and postoperative care are standard. However, no collar is required. The authors have no experience of removing the device. However, it is believed that this would be possible by using a fine osteotome to separate it from the cortical layers.

V. CLINICAL RESULTS

In a French series from Lyon, 34 patients underwent anterior cervical discectomy and fusion with PCB device [47]. Thirty-two patients presented with radiculopathy and 2 with myelopathy. Five patients had fixation at two adjacent levels. All patients were followed up clinically and radiologically for a minimum period of 2 years and assessed by an independed observer. Ninety-five percent of patients had significant clinical improvement. Eighty-eight percent of patients had disappearance of radicular pain and 80% of axial pain.

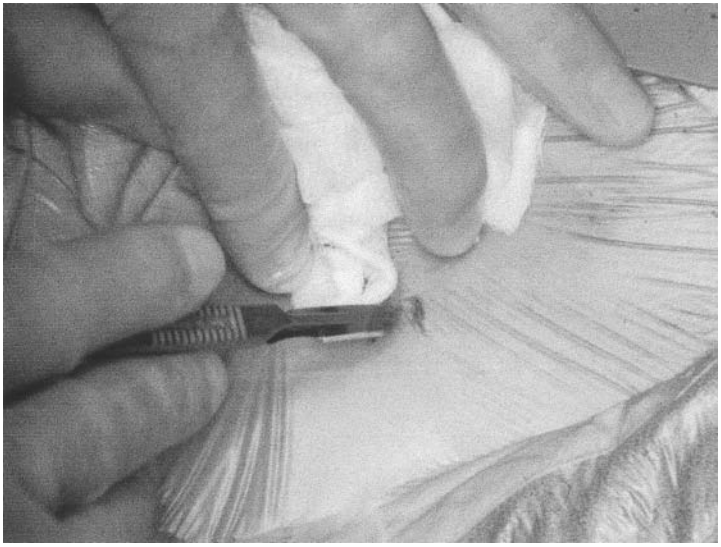

Figure 5 A <1 cm skin incision over the right iliac crest is required. Rostral is left, caudal is right.

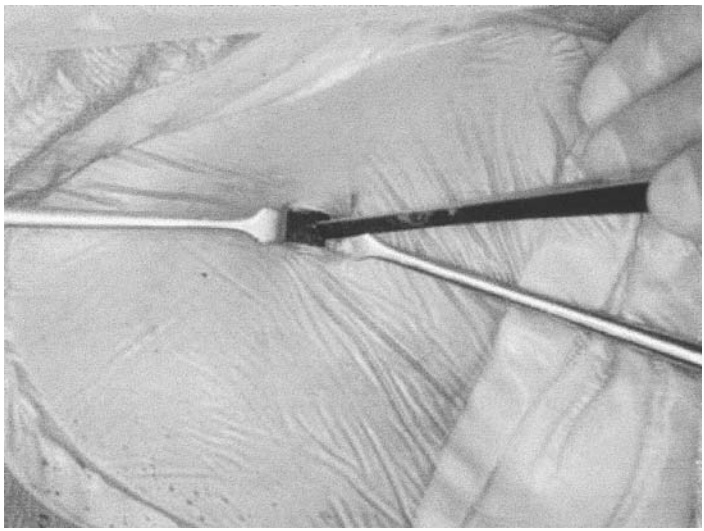

Figure 6 Following exposure, the cortex of the iliac bone is pierced using a 0.5 cm osteotome. Orientation is the same as in Figure 5.

There was no case with screw loosening or implant migration. No postoperative angular kyphosis was recorded on x-rays, and more than 80% had normal spinal stability. There were six complications related to the anterior approach to the cervical spine (three cases of transient dysphagia, two cases of transient hoarseness, and one case of a retropharengeal heamatoma that had to be drained). However, there were no hardware-related complications.

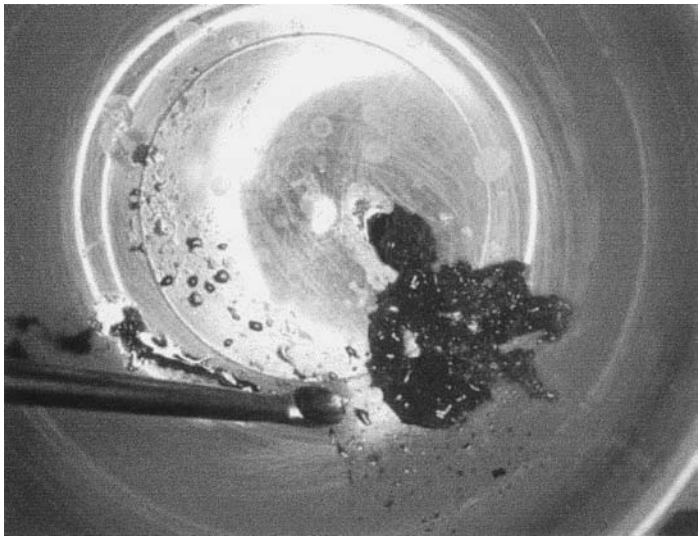

Figure 7 Using a curette, bone shavings are harvested from the iliac bone and collected in a plastic container. They are later inserted into the spacer through its ovoid port.

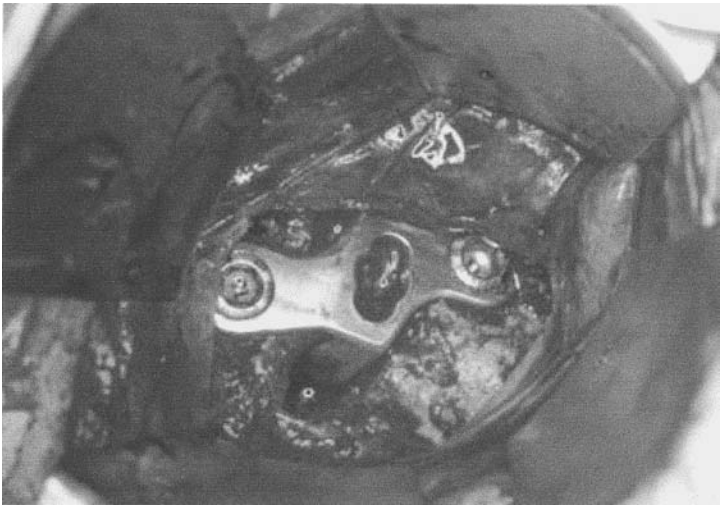

Figure 8 The PCB device is situ. The screws have been inserted and the spacer has been filled with bone shavings. Orientation is the same as in Figure 4.

Additional patients were included later in the study with increased range of follow-up (12–36 months; mean 20.7 months) [48]. Seventy-three patients presented with radiculopathy and 9 cases with myelopathy underwent anterior cervical discectomy and interbody fusion with the PCB implant. In this consecutive 82-patient series, 60 patients underwent fixation in one level, 19 patients in two levels, and 3 patients in three levels. The cage was filled with either autologous cancelous iliac bone or synthetic hydroxyapatite.

Flexion-extension x-rays obtained in 79 cases (96.4%). These revealed 2 cases of bone subsidence of the cortical endplates and 1 case of screw breakage and pseudoarthorosis requiring reoperation. The clinical outcome was excellent in 67%, satisfactory in 28%, and poor in 5%. However, no details on hardware failure cases or analytical data on clinical assessment were provided.

In a prospective German study, the PCP cage was implanted in 42 patients [49]. The cages were filled with autologous bone in 6 patients. A bone substitute (P-tricalcium-phospate) was used in the remaining 36 patients. Clinical improvement was achieved in 88% and 83% of patients with radiculopathy and myelopathy, respectively. Two patients had neurological deterioration. The surgeons found the intraoperative handling of the device safe and easy and, compared to autologous bone and anterior plate fixation, less time consuming.

The early clinical experience of our institution included 29 patients that underwent anterior cervical discectomy and instrumented fusion with the PCB device was reported [43]. Twenty-three patients were operated on for radiculopathy and 6 for myelopathy. Twenty patients underwent fixation at one level, 7 patients at two levels, and 2 patients at three levels. Single- and multiple-level symptomatic cervical spondylosis was the main indication for use of the device. It was not used in young adults with acute disc prolapse, in cases with gross instability and in patients with dystonia. Indications may be expanded as further data emerge. The patients were followed up from 5 to 24 months with a median of 8 months.

Our series was free from intraoperative complications. Graft recipient–site related complications including graft collapse, graft extrusion or impaction on the spinal canal, or related foramina did not occur. Hematoma or infection did not occur in the donor site of patients. Neck

or donor site pain requiring analgesia stronger than paracetamol did not occur. Operative blood loss did not exceed 100 mL. No collars were applied postoperatively. The early results showed disc height and normal cervical lordosis to have been restored. No screw backout, device failure, instability, or pseudoarthrosis was identified. The radioopaque titanium device obscures ready radiological evaluation of fusion, though it was possible with computed tomography (CT) scanning. The preliminary clinical outcome was marked by improvement in 27 cases, while deterioration and no change were recorded in one case each.

Since then the authors have inserted the PCB device in over 100 cases. The data are currently being analyzed, and the results so far are encouraging, tending to support our initial expectations. Sales data suggest that a PCB system has been used in over 20,000 fusions worldwide, and hopefully longer and more extensive studies will emerge.

VI. DISCUSSION

The standard surgical management of degenerative cervical spine disease is currently anterior decompression with fusion usually with autologous iliac bone graft. [6,26–29,50]. A significant number of spinal surgeons use anterior cervical plating systems.

Although initially anterior cervical plating systems were used in acute cervical injuries [5,51], the indications have expanded to include treatment of the degenerative cervical spine. Despite the lack of definitive clinical evidence, it was thought that some of the aforementioned graft-related complications could be addressed with the use of plating systems. The lack of motion across the fused spinal segment and the prevention of graft extrusion and possible postoperative kyphosis were among the theoretical advantages of numerous instrumentation systems that became available.

The majority of the anterior cervical plating systems consist of rigid titanium plates or its alloys, which provides almost 90% of the strength of steel but without causing significant artefacts when magnetic resonance (MR) imaging is required [23,32,41,52,53]. Different systems require unicortical or bicortical screw purchase, have variable or fixed screw trajectory, and may have a screw-locking mechanism. Spinal fusion and clinical improvement has been achieved with most of these systems.

The ideal anterior cervical instrumentation system provides immediate spine stabilization correcting underlying deformities, enhances fusion regardless of graft substrate without stress shielding the implanted graft, and is applied easily with minimal risk to the surrounding tissues. In addition, it adequately decompresses the spinal cord and related foramina with minimal hardware-related failures and allows postoperative imaging studies since it is radiolucent and does not obscure assessment of fusion [18]. Loss of spinal mobility and altered biomechanics causing facet hypertrophy, spinal stenosis, and disc degeneration at adjacent levels should not be caused by the ideal plating system.

No existing system meets all of these criteria. Numerous complications in the use of current systems have been reported, including screw failure or breakage, often necessitating reoperation. The increased cost and complexity of the operation has led to scepticism about the use of these systems [6,42,54–56].

The PCB device was developed as a simple one-piece design integrating a discal cage and plate permitting rapid realignment and fixation. The cage corresponding to the anatomical features of the intervertebral disc space is spontaneously retained. This minimizes the possibility of screw backout or breakage as the axial forces do not spread upon the screws but apply axially onto the spacer.

Donor site pain following graft harvesting remains a major concern for both surgeons and patients. This remains the major criticism against the use of autologous bone, although it is well

reported that autologous bone provides the highest fusion rates. The use of the PCB device requires bone shavings only, which can be harvested through a small skin incision and 5 mm iliac bone corticotomy. Our experience so far has shown that donor site morbidity is virtually eliminated.

Limitations of the PCB device include the inability to assess radiological evidence of fusion without CT scanning since the device is radiopaque. Newer radiolucent versions, bearing two small radiopaque dots located on the spacer permitting postoperative evaluation and monitoring of proper positioning, have been tested. However, further biomechanical tests are being performed at present and hybrids consisting of titanium and polyetherketone are being currently evaluated. Restoration of spinal mobility and avoidance of degenerative effects occurring at levels adjacent to a fusion are unlikely to be achieved with the PCB or, perhaps, with any other cervical instrumentation system.

The challenge of replicating normal range of motion in addition to producing immediate fixation and accurate transmission of physiological forces is more likely to be met by future technologies of disc replacement. There have been several reports on early clinical experience from the Bristol cervical disc prosthesis, originally designed by Cummins [57]. Another prosthesis, the Bryan cervical disc, is based on an elastic nucleus located between anatomically shaped titanium plates. It allows normal range of motion in flexion/extension, lateral bending, axial rotation, and translation. Early results are encouraging, but the device is currently being evaluated in clinical studies.

VII. CONCLUSION

The current generation of plating systems has improved our ability to reconstruct the spine in a variety of disease processes. The addition of the PCB plating system to a standard anterior discectomy and fusion is associated with minimal complications. It displays biomechanical and clinical qualities that have to be measured against other anterior cervical plating systems in prospective, randomized studies.

REFERENCES

1. Smith GW, Robinson RA. The treatment of certain cervical-spine disorders by anterior removal of the intervertebral disc and interbody fusion. J Bone Joint Surg Am 1958; 40-A:607–624.
2. Cloward RB. The anterior approach for removal of ruptured disks. J Neurosurg 1958; 15:602–614.
3. Bailey RW, Badgley CE. Stabilization of the cervical spine by anterior fusion. J Bone Joint Surg Am 1960; 42-A:565–594.
4. Boden SD, Schimandle JH. Biological enhancement of spinal fusion. Spine 1995; 20(suppl 24): 113S–123S.
5. Kaiser MG, Haid RW, Subach BR, Barnes B, Rodts GE, Jr. Anterior cervical plating enhances arthrodesis after discectomy and fusion with cortical allograft. Neurosurgery 2002; 50:229–238.
6. Lunsford LD, Bissonette DJ, Jannetta PJ, Sheptack PE, Zorub DS. Anterior surgery for cervical disc disease. Part 1: Treatment of lateral cervical disc herniation in 253 cases. J Neurosurg 1980; 53: 1–11.
7. Bishop RC, Moore KA, Hadley MN. Anterior cervical interbody fusion using autogenic and allogenic bone graft substrate: a prospective comparative analysis. J Neurosurg 1996; 85:206–210.
8. Shapiro S. Banked fibula and the locking anterior cervical fusions following cervical discectomy. J Neurosurg 1996; 85:736–737.

9. Wood EG, 3rd, Hanley EN, Jr. Types of anterior cervical grafts. Orthop Clin North Am 1992; 23(3): 475–486.
10. Arrington ED, Smith WJ, Chambers HG, Bucknell AL, Davino NA. Complications of iliac crest bone harvesting. Clin Orthop 1996; 329:300–309.
11. Macdonald RL, Fehlings MG, Tator GH. Multilevel anterior cervical corpectomy and fibular allograft fusion for cervical myelopathy. J Neurosurg 1997; 86:990–997.
12. Heary RF, Schlenk RP, Sacchieri TA, Barone D, Brotea CBE. Persistent iliac crest donor site pain: independent outcome assesment. Neurosurgery 2002; 50:510–517.
13. Zdeblick TA, Ducker TB. The use of freeze-dried allograft bone for anterior cervical fusions. Spine 1991; 16:726–729.
14. Fernyhough JC, Schimandle JJ, Weigel MC, Edwards CC, Levine AM. Chronic donor site pain complicating bone graft harvesting from the posterior iliac crest for spinal fusion. Spine 1992; 17: 1474–1480.
15. Gulet JA, Senunas LE, DeSilva GL, Greenfield MLVH. Autogenous iliac crest bone graft: complications and functional assessment. Clin Orthop 1997; 339:76–81.
16. Kurz LT, Garfin SR, Booth RE. Harvesting autigenous iliac bone grafts: a review of complications and techniques. Spine 1989; 12:1324–1331.
17. Sawin PD, Traynelis VC, Menezes AH. A comparative analysis of fusion rates and donor site morbidity for autogenic rib and iliac crest bone grafts in posterior cervical fusion. J Neurosurg 1998; 88: 255–265.
18. Cahil DW, Sonstein WS. Anterior cervical instrumentation. Tech Neurosurg 1999; 5:133–145.
19. Cloward RB. Treatment of acute fractures and fracture-dislocations of the cervical spine by vertebral-body fusion: a report of eleven cases. J Neurosurg 1960; 18:201–209.
20. Connolly ES, Seymour RJ, Adams JE. Clinical evaluation of anterior cervical fusion for degenerative cervical disc disease. J Neurosurg 1965; 23:431–437.
21. Goffin J, Plets C, Van den Bergh R. Anterior cervical fusion and osteosynthetic stabilisation according to Caspar: a prospective study of 41 patients with fractures and/or dislocations of the cervical spine. Neurosurgery 1989; 25:865–871.
22. Kewalrami L, Riggins R. Complications of anterior spondylosis for traumatic lesions of the cervical spine. Spine 1977; 2:25–38.
23. Raveh J, Stesh M, Sutter E, Greiner R. Use of titanium coated hollow screw and reconstruction plate system in bridging of lower jaw defects. J Oral Maxillofac Surg 1984; 42:281–294.
24. Robinson RA. Anterior and posterior cervical spine fusions. Clin Orthp 1964; 35:34–62.
25. Clements DH, O'Leary PF. Anterior cervical diskectomy and fusion. Spine 1990; 15:1023–1025.
26. DePalma AF, Cooke AJ. Results of anterior interbody fusion of the cervical spine. Clin Orthop 1968; 60:169–185.
27. Dohn DF. Anterior interbody fusion for treatment of cervical disc disease. JAMA 1966; 197:897–900.
28. Gore DR, Sepic SB. Anterior cervical fusion for degenerative or protruded discs: a review of one hundred forty six patients. Spine 1984; 9:667–671.
29. Rosenorn J, Hansen EB, Rosenorn MA. Anterior cervical discectomy with and without fusion: prospective study. J Neurosurg 1983; 59:252–255.
30. Saunders RL, Wilson DH. The surgery of cervical disc disease: new perspectives. Clin Orthop 1980; 146:119–127.
31. Bohler VJ. Sofort- und Frühbehandlung traumatisher Querschnittlahmungen. Z Orthop 1967; 103: 512–529.
32. Orozco CR, Tapies J. Osteointesis en las fraturas de raquis cervical: nota de technica. Rev Orthop Traum 1970; 14:285–288.
33. Smith MD, Bolesta MJ. Esophageal perforation after anterior cervical plate fixation: a report of two cases. J Spinal Disord 1992; 5:357–362.
34. Morscher E, Sutter F, Jenny H, Olerud S. Anterior plating of the cervical spine with the hollow screw-plate system of titanioum. Chirurg 1993; 18:702–707.
35. Connolly PJ, Esses SI, Kostuik JP. Anterior cervical fusion: outcome analysis of patients fused with and without anterior cervical plates. J Spinal Disord 1996; 9:202–206.

36. Aebi M, Zuber K, Marchesi D. Treatment of cervical spine injuries with anterior plating. Spine 1991; 16(3S):38–45.
37. An HS, Coppes M. Cervical spine instrumentation. In: Clark CR, ed. The Cervical Spine. 3rd ed.. Philadelphia: Lippincott-Raven, 1998:653–658.
38. Caspar W, Baebier DD, Klara PM. Anterior cervical fusion and Caspar plate stabilization for cervical trauma. Neurosurgery 1989; 25:491–502.
39. Gallagher MR, Maiman DJ, Reinartz J, Pintar F, Yoganandan N. Biomechanical evaluation of Caspar cervical screws: comparative stability under cyclical loading. Neurosurgery 1993; 33:1045–1050.
40. Grubb MR, Currier BL, Shih JS, Bonin V, Grabowski JJ, Chao EY. Biomechanical evaluation of anterior cervical spine stabilization. Spine 1998; 23:886–892.
41. Kostuik JP, Connolly Pj, Esses SI, Suh P. Anterior cervical plate fixation with titanium hollow screw plate system. Spine 1993; 18:1273–1278.
42. Lowery GL, McDonough RF. The significance of hardware failure in anterior cervical plate fixation. Patients with 2- to 7-year follow-up. Spine 1998; 23:181–186.
43. Samandouras G, Shafafy M, Hamlyn PJ. A new anterior cervical instrumentation system combining an intradiscal cage with an integrated plate. An early technical report. Spine 2001; 26:1188–1192.
44. Unpublished. Mechanical tests performed at the independent laboratory CRITT MDTS from Charleville-Mezieres. The results were recorded by Dr. Sandrine Moirez.
45. Panjabi M, Summers D, Pelker R, Videman T, Friedlaender G, Southwick W. Three dimentional load displacement curves due to forces on the cervical spine. J Ortho Res 1986; 4:152–161.
46. Shea M, Edwards W, White A, Hayes W. Variations of stiffness and strength along the human cervical spine. J Biomech 1991; 24:95–107.
47. Benezech J. Cervical fusion with monocomponent PCB plate. In: Szpalski M, Gunzburg R, eds. The Degenerative Cervical Spine. Philadelphia: Lippincot Williams and Wilkins, 2001:265–273.
48. Unpublished. Combined Plate-Cage Implant. Presentation in ''Disc Herniation in the Third Millenium'', Brussels, November 17–18, 2000.
49. Unpublished. Clinical Series from Schonmayer R, Ant M, Mokhtares S and Melzer M. Klinik für Neurochirurgie, Dr.-Horst-Schmidt-Kliniken GmbH, Wiesbaden, Germany.
50. Robinson R, Walker AE, Ferlic D. The results of anterior interbody fusion of the cervical spine. J Bone Joint Surg 1962; 44-A:1569–1587.
51. Randle MJ, Wolf A, Levi L, Rigamonti D, Mirvis S, Robinson W, Bellis E, Greenberg J, Salcman M. The use of anterior Caspar plate fixation in acute spine injury. Surg Neurol 1991; 36:181–189.
52. Hermann HD. Metal plate fixation after anterior fusion of unstable fracture dislocation of the cervical spine. Laryngoscope 1973; 83:17–21.
53. Orozco C, Tapies J. Osteosintesis en las lesions traumaticas y degenerativas de la columna cervical. Revista Traumatol Cirurg Rehabil 1971; 1:45–52.
54. Lowery GL, Reuter MW, Sutterlin C. Anterior cervical interbody arthrodesis with plate stabilization for degenerative disc disease. Orthop Trans 1994; 18:1273–1278.
55. Paramore CG, Dickman CA, Sonntag VKH. Radiographic and clinical follow-up review of Caspar plates in 49 patients. J Neurosurg 1996; 84:957–961.
56. Ryken TC, Clausen JD, Traynelis VC, Goel VK. Biomechanical analysis of bone mineral density, insertion technique, screw torque, and holding strength of anterior cervical plate screws. J Neurosurg 1995; 83:325–329.
57. Cummins BH, Robertson JT, Gill SG. Surgical experience with an implanted artificial cervical joint. J Neurosurg 1998; 88:943–948.

48

Improvement of Pedicle Screw Fixation with Hydroxyapatite Coating

Bengt Sandén
Uppsala University Hospital
Uppsala, Sweden

I. FIXATION AND LOOSENING OF PEDICLE SCREWS

The aim of spinal instrumentation is to maintain stability until fusion or fracture healing has occurred. When pedicle screws are used, the stability of the system is depending on the ability of the screws to maintain their purchase in the pedicle and the vertebral body. Loosening of the screws results in a loss of stability that might lead to nonunion or loss of reduction. Many reports have focused on the complications of pedicle screw fixation, including the frequency of screw loosening. McAfee et al. reported on 526 pedicle screws, of which 3% were broken, but none were loose [1]. In a survey analysis by Esses et al. of 617 cases treated by members of the American Back Society, the rate of screw loosening was 0.81%, and screw breakage 2.9% [2]. The study by Esses et al. included an extensive literature review, with a frequency of screw loosening varying from 0.6 to 11%. In a historical cohort study by Yuan et al., screw loosening was observed in 2.8% and screw breakage in 2.6% of 2153 patients treated for degenerative spondylolisthesis [3]. These studies with low rates of loosening and breakage of the screws do not comment on radiological methods or the criteria for screw loosening. In three studies with thorough descriptions of the radiological examinations and including in two of them strict criteria for screw loosening, the loosening rates were 18, 21, and 27%, respectively [4–6]. The frequencies of screw breakage were 21, 6, and 16%, respectively. In all these studies with very varying rates of screw loosening, stainless steel screws were used, with very few exceptions. In most studies screws of different designs and from different vendors were used. Therefore, it seems unlikely that the varying results could be explained by differences in materials and screw designs. The varying frequencies of radiological screw loosening in these studies could rather be explained by the differences in study design, with different definitions of screw loosening, and great variation in the follow-up of the patients. It seems likely that the frequency of loosening has been underestimated in several of these studies.

The fixation of pedicle screws depends on several factors. The major factors are the quality of the bone and the design and size of the screws [7–9]. The mechanism of failure of pedicle screw systems has been controversial. According to Spivak, the main failure mode is by pull-out, while unscrewing is not a failure mode seen clinically [10]. The ability to resist pull-out is dependent on the outer thread diameter of the screw, the shear strength of the bone at the outer thread margin, and to a lesser degree on the thread pitch and angle [11,12]. On the other

hand, some authors claim that axial pull-out represents bone strength and does not reflect screw failure in the clinical situation [13]. According to Christensen, the rotational stability of the screw is essential to maintain the stability of the whole construction, and the rotational stability is best reflected by the extraction torque of the screw. The insertion torque is generated primarily by the shearing force and friction in the bone-screw interface [14] and is dependent on the size of the screw and the quality of the bone in the interface. Some authors describe the mechanism of loosening of pedicle screws as a cyclic toggling under caudocephalad loads [14–16]. Also with this proposed mechanism, the bone quality and the size of the screw are important factors. The diameter of the screw is limited by the size of the pedicle and could not be further increased. Thus, the most effective way to improve the purchase of pedicle screws is to improve the bone quality and increase the amount of bone surrounding the screws.

II. BONE AND CAP MATERIALS

Bone is composed of an organic collagenous tissue, mainly type I collagen, and an inorganic mineral phase, together forming a composite structure. The composition of the mineral phase varies between different parts of the bone and over time, but the main constituent of bone mineral is hydroxyapatite [$Ca_{10}(PO_4)_6(OH)_2$] [17]. Hydroxyapatite (HA) is a calcium phosphate ceramic. Ceramics are solid compounds of metals with nonmetals. When ceramic compounds are formed, generally a large amount of energy is released. These compounds are in a low energy state, meaning that further spontaneous reactions are unlikely to occur. Due to this, ceramics are the most chemically and biologically inert of all materials [18]. HA and tricalcium phosphate are not as inert as most other ceramics and tend to be less strong and more chemically reactive [18]. Calcium phosphate ceramics are highly biocompatible, and due to the chemical similarity to the natural bone mineral they are capable of forming a direct biochemical bond with bone [17]. The calcium phosphates of biological interest are calcium salts of ortophosphoric acid [19]. There are six principal calcium ortophosphates; dicalcium phosphate dihydrate, dicalcium phosphate anhydrous, octacalcium phosphate, β-tricalcium phosphate, hydroxyapatite, and tetracalcium phosphate monoxide. Out of these six compounds, the first three are too soluble to be used for biomaterials [19]. Many ionic substitutions may occur in HA, for example, the hydroxyl group may be replaced by fluoride, and the compound is then named fluorapatite. β-Tricalcium phosphate and HA are the most commonly investigated calcium phosphates. The term tricalcium phosphate is used for any pure calcium phosphate with a Ca/P atomic ratio of 1.50 [19]. The term does not imply either a composition or a structure. Tricalcium phosphate is a naturally occurring component of mineralized tissues. It is resorbed to a greater extent and more rapidly than HA [20]. In contrast to tricalcium phosphate, synthetic HA is not readily bioresorbable in appropriate forms, and it is therefore suitable for long-term clinical applications [17]. Due to these properties, HA has been more thoroughly investigated than other calcium phosphate materials. HA materials have been used in particulate forms, as pastes mixed with collagen or other materials, and also in dense solid or composite forms. The Ca/P atomic ratio of pure HA is 1.67. Several characteristics differ between bone apatite and the apatite of HA coatings. The HA in bone is more inhomogeneous with lack of crystal and chemical perfection, and it is also more reactive than HA coatings due to the large surface area of trabecular bone [21].

Like other ceramics, HA is a brittle material with low tensile strength, while the compressive strength is high. In order to combine the mechanical properties of metals with the biocompatibility of ceramics, coatings of calcium phosphate ceramics have been developed. The coated implants have the advantages of the metallic material in terms of mechanical strength and other physical properties, along with the biological benefits of the coating [17]. Many different

techniques have been used to apply the coating to the substrate metals, like electrophoresis, dipping, and mechanical methods. The most commonly used technique is plasma spraying, introduced in the early 1980s (Fig. 1) [22]. An electric arc is struck between the cathode and the anode, while a stream of gases passes through the arc. This results in a ionized gas with a temperature up to 30,000°C. The temperature increase gives a large expansion and a velocity of the plasma stream approaching the speed of sound. The coating powder is introduced into the plasma stream, usually in a carrier gas, and then melted and propelled onto the substrate with a speed of at least 200 m/s. Solidification then occurs very rapidly, and the coating is formed. Because of the high plasma temperature, the coating material may be altered during the process, resulting in a chemically or structurally different material as the final product. According to some authors, all plasma-sprayed commercially available HA coats have undergone phase change [23]. The properties of the HA coating are also affected by the composition and purity of the starting powder material. Due to these factors, HA coatings from different manufacturers may vary significantly in structure, purity, composition, and crystallinity. HA coatings from different manufacturers demonstrate varying histological and mechanical characteristics [24]. A variability in coatings from a manufacturer may also be expected, and it has been recommended that surgeons using HA-coated prosthetic devices request a quality report for each batch delivered before inserting the prosthesis [25]. The optimal properties of HA coatings, such as thickness, have been debated. The mechanical properties of the coating are improved with decreasing thickness of the coat [26]. On the other hand, a thicker coat is more stable as it is less sensitive to dissolution, and a compromise between these factors must be made [27]. For other properties, such as purity, chemical composition, Ca/P ratio, trace element content, crystallinity, density, porosity, solubility, and mechanical properties, several standards have been proposed and published [28–30].

III. THE METAL SUBSTRATE

For most HA-coated implants bearing significant loads, titanium alloys, cobalt-chrome alloys, or stainless steel are used. The mechanical properties differ between these different materials; for example, the elastic modulus of cobalt-chrome is higher than the elastic modulus of titanium alloy (Ti-6Al-4V). The biocompatibility of both titanium alloy implants and cobalt-chrome

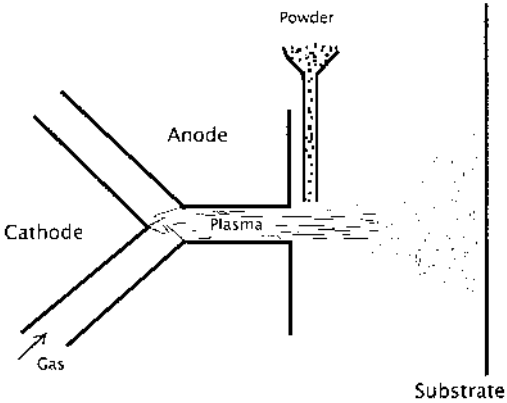

Figure 1 Schematic drawing of the plasma-spraying process.

implants are favorable [21]. In vitro, osteoblasts have been demonstrated to grow faster on titanium alloy (Ti-6Al-4V) than on cobalt-chrome alloy or stainless steel [31], and the biocompatibility of titanium has been described as superior to that of cobalt-chrome and stainless steel [32]. However, in most studies of the biocompatibility of titanium, commercially pure (c.p.) titanium has been used. C.p. titanium is routinely used for oral implants and show clearly better results in the long-term perspective than HA-coated implants [33]. Due to the limited strength of c.p. titanium, it is not used for pedicle screw instrumentations. Instead, titanium alloys are used, mostly Ti-6A1-4V. There is no data backing up the concept that titanium alloy is as well accepted in bone as is c.p. titanium [34]. HA coating adheres stronger to a titanium than to a cobalt-chrome substrate [35]. However, HA coatings of titanium and cobalt-chrome implants have been examined in an experimental study. Both mechanically and histologically, the HA-coated cobalt-chrome implants performed in a similar manner to the HA-coated titanium implants [36].

IV. EXPERIMENTAL STUDIES

Numerous studies of implants in unloaded animal models have indicated a more rapid bone response to HA-coated implants when compared to uncoated implants [37–42]. A review of these and other short-term studies implies a maximum for the bone-to-implant attachment after 6–12 weeks for HA-coated implants. The long-term effects of HA-coated implants in unloaded experimental studies have been uncertain. At one year after insertion there seems to be no evidence of any difference in fixation strength between HA-coated implants and uncoated controls. The percentages of bone-to-implant contact have varied between different studies, and higher, similar, and lower contact percentages have been reported [33].

HA coating of unloaded spinal implants has been investigated in two experimental studies. Augmentation of fixation of pedicle screws and iliac rods with plasma-sprayed coating of HA has been examined in dogs. The HA-coated screws were somewhat less resistant to pull-out than the standard screws 6 weeks after implantation, even though the difference was not significant. Microscopy revealed a section of shear failure through the HA coating at each thread, lowering the shear strength at the outer margin of the thread. Coating of the iliac rods gave a significant increase of pull-out strength at 6 weeks, whereas the uncoated rods showed a significant decrease in holding power at 6 weeks, when compared to the pull-out strength directly after insertion [10]. In a study using an unloaded sheep model, HA-coated titanium pedicle screws were compared to stainless steel screws and uncoated titanium (Ti-6Al-4V) screws. After 4 months of implantation, the extraction torque and the percentage of bone-to-implant contact were higher for the HA-coated screws than for the stainless and uncoated screws, respectively [43].

HA coating of loaded pedicle screws has been evaluated in two experimental studies. In a study focusing on the mechanical effects, 13 sheep were operated on with destabilizing laminectomies at two levels, L2–L3 and L4–L5 [44]. Two instrumentations with four pedicle screws in each were used for stabilization. Uncoated screws (stainless steel SAF 2507) or the same type of screws coated with plasma-sprayed HA were used in either the upper or the lower instrumentation in a randomized fashion. Four sheep were examined immediately after the application of the screws, three sheep at 6 weeks, and four sheep at 12 weeks. Two sheep were euthanized early due to complications. The pull-out resistance was recorded in two HA-coated and two standard screws in each animal. The maximum pull-out resistance was higher for the HA-coated screws at 0 ($p < 0.02$) and at 12 weeks ($p < 0.01$) when compared to the uncoated screws, while there was no significant difference between the groups at 6 weeks. The authors concluded that the higher pull-out resistance for HA-coated screws at 0 weeks was caused mainly

by differences in surface roughness, while the difference at 12 weeks was due to a favorable bone reaction around the HA-coated screws. Energy to failure was significantly higher for coated screws when compared to the uncoated screws at all three time points [44].

The histological effects of HA coating have been studied in a study using the same experimental model [45]. HA-coated and uncoated pedicle screws were used (Figs. 2,3). After 6 and 12 weeks, respectively, the sheep were killed and the specimens were prepared. The specimens were embedded in resin, ground to approximately 10 μm and stained with toluidine blue. Histological and histomorphometric evaluation was carried out in a Leitz Aristoplan light microscope equipped with a Leitz Microvid unit. The average percentage of bone-to-implant contact after 6 weeks was 69 ± 10 for the HA-coated screws and 18 ± 11 for the uncoated screws ($p < 0.03$), and after 12 weeks 64 ± 31 (HA-coated) and 9 ± 13 (uncoated; $p < 0.02$). The average bone volume in the area close to the screw was significantly higher for the HA-coated screws at both 6 and 12 weeks [45].

V. CLINICAL STUDIES

The clinical use of HA-coated pedicle screws was first reported by Lapresle and Missenard. They described the clinical results of 27 patients. However, the authors did not comment on the purchase of the screws or the frequency of radiological signs of screw loosening [46].

The mechanical consequences of HA coating have been described in two clinical studies [47,48]. In both studies, the Posterior Fixator System (Nordopedic, Gothenburg, Sweden) with stainless steel (SAF 2507) screws (Fig. 4) was used for the instrumentations. In the first study, the diameters of the screws were 5 or 6 mm, and the lengths 55–70 mm. All HA-coated screws in that study were fully HA coated. In the second study, only 6 mm screws with lengths 55–75 mm were used. Both fully and partly HA coated screws were used. The HA coating was applied with plasma-spraying technique by CAM Implants B.V., Leiden, Netherlands. The coating thickness was, as controlled by the manufacturer, approximately 45 μm, the density >95%, and the crystallinity 55% for all three batches used.

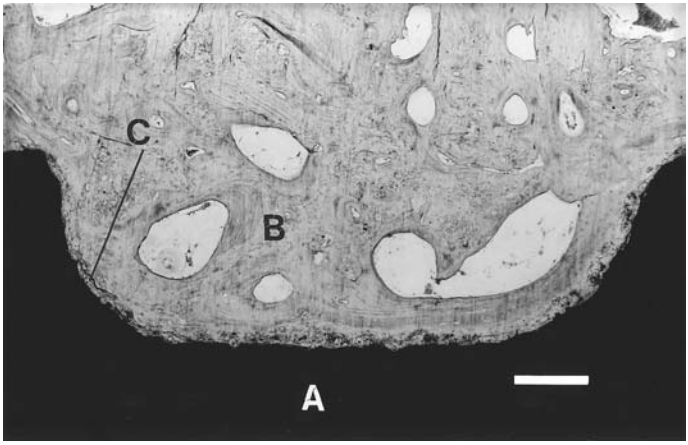

Figure 2 One thread from hydroxyapatite (HA)-coated pedicle screw after 12 weeks of implantation in a sheep model. The screw is outlined by bone. A of Screw; B = bone; C = HA coat. White line = 200 μm.

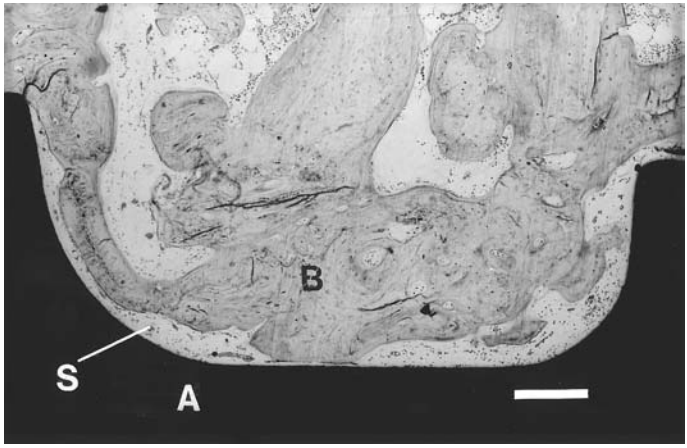

Figure 3 One thread from uncoated pedicle screw after 12 weeks of implantation in a sheep model, demonstrating minimal bone-to-implant contact. A = Screw; B = bone; S = soft tissue. White line = 200 μm.

Both these studies were prospective studies where HA-coated pedicle screws were compared to uncoated controls. In both studies, randomization occurred by using closed envelope technique immediately before surgery. Insertion and extraction torques were recorded using a torque gauge manometer. All the instrumentations were four-screw constructions, and all fusions were one-level or two-level fusions.

In the first study, seven patients were operated on [47]. In each patient, two HA-coated pedicle screws and two uncoated screws were used. The HA-coated screws were applied in either the upper or the lower of the instrumented levels in a randomized fashion. The screws

Figure 4 Stainless steel pedicle screws, 6 × 70 mm. Uncoated (upper), partly HA coated (middle), and fully HA coated (bottom). (From Ref. 48.)

were removed after 10–22 months in four patients. The fusions were healed by the time of extraction.

Two screws that had been removed with bone still attached made it possible to analyze the bone-implant interface histologically. The methods described for the experimental studies were used for the preparation. The histological examination demonstrated an irregular HA coating intermingled with bone-stained acellular tissue, reaching out at some distance from the coating layer. The acellular tissue did not polarize. There was a clear demarcation between this tissue and the normally polarizing bone structure. The implants were surrounded by a more lamellar bone tissue in the outer portions, whereas in the vicinity of the implants the tissue was more woven.

For most of the HA-coated screws, the extraction torque exceeded the upper limit for the manometer (600 Ncm), and the HA-coated screws demonstrated a higher extraction torque ($p < 0.01$).

This study [47] demonstrated a very good fixation of the HA-coated screws when used in only one of the two instrumented levels in a four-screw construction. The loosening mechanism of pedicle screws has been described as a cyclic caudocephalad toggling [14,15]. If loosening of the uncoated screws occurred while the HA-coated screws still had a sufficient anchorage, this could perhaps concentrate the toggling to the uncoated screws, thus protecting the HA-coated screws from loosening. To be clinically more relevant, an increased purchase of pedicle screws should comprise all screws in the instrumentation. For this reason, another study was designed where four screws of the same type were used in each instrumentation. As there were some problems with extraction of the fully HA-coated screws in the first clinical series, a screw that was partly coated with HA was included in the second series.

In the second study, 23 consecutive patients who planned to undergo instrumented lumbar or lumbosacral fusions for degenerative disorders were included [48]. The mean age was 56 ± 12 years. The patients were assigned to one of three treatment groups: uncoated pedicle screws, screws where the distal 50% of the threads was coated with HA (partly HA-coated group), and screws where the entire implanted portion of the screw was coated (fully HA-coated group). The insertion torques for the screws were recorded. After 11–16 months, the instruments were removed in 21 of the 23 patients. Radiographs were taken preoperatively, postoperatively, and 3 and 6 months after surgery and before extraction of the instruments.

The mean insertion torque was 76 ± 41 Ncm for the uncoated screws, 56 ± 22 Ncm for the partly HA-coated screws, and 122 ± 74 Ncm for the fully HA-coated screws. The insertion torque for the fully HA-coated screws was significantly higher than the torques for the uncoated screws and the partly HA-coated screws, respectively. There was no significant difference between the uncoated and the partly HA-coated screws.

The calculated values of mean extraction torque were 29 ± 36 Ncm for the uncoated group, 447 ± 114 Ncm for the partly HA-coated group, and 574 ± 52 Ncm for the fully HA-coated group (Fig. 5). There were significant differences between all three groups ($p < 0.001$). These differences were also significant when the average extraction torques for all four screws in each patient were analyzed.

The purchase of the screw expressed as the maximum torque increased from insertion to extraction for 0/32 screws in the uncoated group, 18/19 screws in the partly HA-coated group, and 19/19 screws in the fully HA-coated group. The maximum torque decreased from insertion to extraction for 31/32 screws in the uncoated group, while the torque was unchanged for one screw. There was no difference in extraction torque when analyzed by age or by level. Some of the fully HA-coated screws were difficult to extract with a screwdriver, while there were no problems with the extraction of uncoated and partly HA-coated screws.

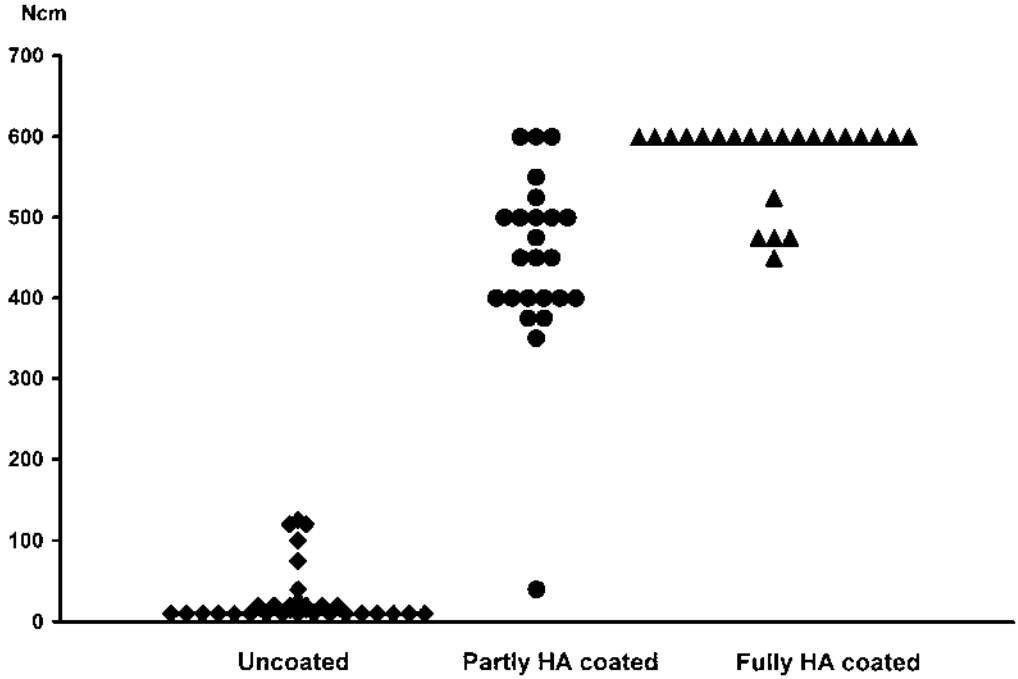

Figure 5 The maximum extraction torque for three types of screw. Each symbol indicates one screw. The upper limit of the torque gauge manometer used is 600 Ncm. (From Ref. 48.)

At the radiological evaluation, radiolucent zones surrounded 17/32 uncoated screws (in 7/8 patients) and 1/28 partly HA-coated screws. No radiolucent zones were seen in the fully HA-coated group [48].

VI. DISCUSSION

In most studies of pedicle screw fixation, the frequency of screw loosening is low. When special views were included in the radiographic examination in a clinical study, 17/32 uncoated stainless steel screws demonstrated radiolucent zones [48]. The very low frequency of screw loosening in several other studies could probably be explained by the use of other criteria for screw loosening, such as dislocations of the screws, or by the fact that most of these studies were retrospective, with varying standards for the radiographic examinations.

Due to the problems with loosening of pedicle screws, HA-coated screws have been compared to uncoated screws in controlled studies [44,45,47,48]. For almost all of the studied variables, HA-coated screws demonstrated superior results. The mechanism of the improved fixation and better bone apposition, however, is not clear. It could be caused by a direct chemical bond between bone and the plasma-sprayed HA of the implant. The close contact between bone and implant could also cause a mechanical bonding. Some authors have proposed that the fixation of HA-coated implants is caused by a chemical bond [49]. In other studies, dissolution of individual grains of the implant surface gave a rougher surface than originally implanted, and mechanical interlocking could not be eliminated as a contribution to bone-HA bonding [50,51].

Several mechanisms other than a chemical or mechanical bonding could be considered. There are considerable differences in surface roughness between HA-coated and uncoated screws. A fourfold increase in surface roughness of plasma-sprayed HA-coated implants when compared to machined titanium implants has been described [52], and the surface roughness of stainless steel is less than that of machined titanium. Surface roughness can influence the tissue response to an implant, such as the orientation of fibrous tissue and bone ongrowth [21], and therefore yield long-term effects on fixation. Regarding the mechanical effect of surface roughness only, it could cause the higher insertion torque for HA-coated screws. At follow-up, however, there was a marked increase in purchase over time for the HA-coated screws, compared to the decrease over time for the uncoated screws [47,48]. Therefore, the higher surface roughness of the HA-coated screws is unlikely as a direct mechanical cause for the better results at follow-up.

The plasma-sprayed HA coating increases the diameter of the coated screws with an average 80–90 μm when compared to the uncoated screws. This means a relative ''oversizing'' of approximately 2% of the HA-coated implants that could contribute to the higher insertion torque. For the same reasons as for surface roughness, oversizing is not likely to have caused the better purchase and bone apposition at follow-up.

In most studies of HA-coated pedicle screws, stainless steel screws have been used. In a study of unloaded pedicle screws, HA-coated screws were superior to stainless steel screws and titanium screws, while there was no significant difference between titanium and stainless steel [43]. Titanium and stainless steel pedicle screws have been compared in an experimental study with loaded instrumentations. There were no significant differences in pull-out resistance or bone volumes surrounding the screws, while the extraction torque and bone-to-implant contact was significantly higher for the titanium screws [13]. The differences between the two screw types were not so obvious as the differences between uncoated and HA-coated screws in other studies [44,45]. The favorable biocompatibility of titanium has been demonstrated for commercially pure titanium, and it has not been shown that titanium alloy, used for pedicle screw instrumentations, is as well accepted in bone as is commercially pure titanium [34]. It seems likely that HA coating is more effective for improvement of pedicle screw fixation than is the use of titanium alloy screws.

The use of HA coating can result in a very strong anchorage of the screws, and extraction could be troublesome in some cases [47]. This could be managed by varying the extent of the HA coat [48]. The further increase in purchase with fully coated screws may be useful for certain indications, such as surgery for tumors of the spine or in patients with osteoporosis. The HA coating used in the present studies appears to be effective for improving the anchorage of pedicle screws also in older patients. In a clinical study, there was no difference in the purchase of HA-coated screws between older and younger patients, with a very good purchase even in the oldest patients [48]. This is consistent with the results of experimental studies [53,54].

HA coatings from different manufacturers demonstrate varying histological and mechanical characteristics [24]. All the HA coats in the present studies came from the same manufacturer. Several batches were used, but the specifications from the supplier were similar, as were the processes. The type of coat used could be an important factor in the results of the present studies, and pedicle screws with HA coats from other manufacturers may give different results with respect to fixation and bone-to-implant contact.

REFERENCES

1. McAfee PC, Weiland DJ, Carlow JJ. Survivorship analysis of pedicle spinal instrumentation. Spine 1991; 16:S422–S427.

2. Esses SI, Sachs BL, Dreyzin V. Complications associated with the technique of pedicle screw fixation. A selected survey of ABS members. Spine 1993; 18:2231–2238.
3. Yuan HA, Garfin SR, Dickman CA, Mardjetko SM. A historical cohort study of pedicle screw fixation in thoracic, lumbar, and sacral spinal fusions. Spine 1994; 19:2279S–2296S.
4. Pihlajamaki H, Myllynen P, Bostman O. Complications of transpedicular lumbosacral fixation for non-traumatic disorders. J. Bone Joint Surg. Br 1997; 79:183–189.
5. Ohlin A, Karlsson M, Duppe H, Hasserius R, Redlund-Johnell I. Complications after transpedicular stabilization of the spine. A survivorship analysis of 163 cases. Spine 1994; 19:2774–2779.
6. Soini J, Laine T, Pohjolainen T, Hurri H, Alaranta H. Spondylodesis augmented by transpedicular fixation in the treatment of olisthetic and degenerative conditions of the lumbar spine. Clin. Orthop 1993; 297:111–116.
7. Krag MH, Beynnon BD, Pope MH, Frymoyer JW, Haugh LD, Weaver DL. An internal fixator for posterior application to short segments of the thoracic, lumbar, or lumbosacral spine. Design and testing. Clin. Orthop 1986; 203:75–98.
8. Coe JD, Warden KE, Herzig MA, McAfee PC. Influence of bone mineral density on the fixation of thoracolumbar implants. A comparative study of transpedicular screws, laminar hooks, and spinous process wires. Spine 1990; 15:902–907.
9. Soshi S, Shiba R, Kondo H, Murota K. An experimental study on transpedicular screw fixation in relation to osteoporosis of the lumbar spine. Spine 1991; 16:1335–1341.
10. Spivak JM, Neuwirth MG, Labiak JJ, Kummer FJ, Ricci JL. Hydroxyapatite enhancement of posterior spinal instrumentation fixation. Spine 1994; 19:955–964.
11. Ansell RH, Scales JT. A study of some factors which affect the strength of screws and their insertion and holding power in bone. J. Biomech 1968; 1:279–302.
12. Firoozbakhsh KK, DeCoster TA, Moneim MS. Effect of cyclical loading on the holding power of surgical screws. Orthopedics 1994; 17:607–611.
13. Christensen FB, Dalstra M, Sejling F, Overgaard S, Bunger C. Titanium-alloy enhances bone-pedicle screw fixation: mechanical and histomorphometrical results of titanium-alloy versus stainless steel. Eur Spine J 2000; 9:97–103.
14. Okuyama K, Abe E, Suzuki T, Tamura Y, Chiba M, Sato K. Can insertional torque predict screw loosening and related failures? An in vivo study of pedicle screw fixation augmenting posterior lumbar interbody fusion. Spine 2000; 25:858–864.
15. Zindrick MR, Wiltse LL, Widell EH, Thomas JC, Holland WR, Field BT, Spencer CW. A biomechanical study of intrapeduncular screw fixation in the lumbosacral spine. Clin. Orthop 1986; 203:99–112.
16. Law M, Tencer AF, Anderson PA. Caudo-cephalad loading of pedicle screws: mechanisms of loosening and methods of augmentation. Spine 1993; 18:2438–2443.
17. Thomas KA. Hydroxyapatite coatings. Orthopedics 1994; 17:267–278.
18. Cooke FW. Ceramics in orthopedic surgery. Clin. Orthop 1992; 276:135–146.
19. Heughebaert JC, Bonel G. Composition, stuctures and properties of calcium phosphates of biological interest. In: Christel P, Meunier A, Lee AJC, eds. Biological and Biomechanical Performance of Biomaterials. Amsterdam: Elsevier Science Publishers, 1986:9–14.
20. Jarcho M. Calcium phosphate ceramics as hard tissue prosthetics. Clin. Orthop 1981; 157:259–278.
21. Overgaard S. Calcium phosphate coatings for fixation of bone implants. Acta Orthop. Scand 2000; 71(suppl 297):1–74.
22. Gottlander M. On hard tissue reactions to hydroxyapatite-coated titanium implants. Thesis. Biomaterials group, University of Gothenburg. 1994.
23. Ducheyne P, Cuckler JM. Bioactive ceramic prosthetic coatings. Clin. Orthop 1992; 276:102–114.
24. Dalton JE, Cook SD. In vivo mechanical and histological characteristics of HA-coated implants vary with coating vendor. J. Biomed. Mater. Res 1995; 29:239–245.
25. Soballe K, Hansen ES, Brockstedt-Rasmussen H, Bunger C. Hydroxyapatite coating converts fibrous tissue to bone around loaded implants. J. Bone Joint Surg. Br 1993; 75:270–278.
26. Wang BC, Lee TM, Chang E, Yang CY. The shear strength and the failure mode of plasma-sprayed hydroxyapatite coating to bone: the effect of coating thickness. J.Biomed. Mater. Res 1993; 27: 1315–1327.

27. Koeneman J, Lemons J, Ducheyne P, Lacefield W, Magee F, Calahan T, Kay J. Workshop on characterization of calcium phosphate materials. J. Appl. Biomaterials 1990; 1:79–90.
28. ASTM, 1988. Standard specification for composition of ceramic hydroxylapatite for surgical implants. ASTM Special Technical Publication, F. Vol. 1185–88:514–515.
29. FDA Draft. Calcium phosphate (Ca-P) coating draft guidance for preparation of FDA submissions for orthopedic and dental endoosseous implants: Food and Drug Administration, 1997:1–14.
30. Draft International Standards, 1999. Implants for surgery—hydroxyapatite ceramics. Part 1 and 2. ISO/DIS, 13779.
31. Puleo DA, Holleran LA, Doremus RH, Bizios R. Osteoblast responses to orthopedic implant materials in vitro. J. Biomed. Mater. Res 1991; 25:711–723.
32. Head WC, Bauk DJ, Emerson RH, Jr. Titanium as the material of choice for cementless femoral components in total hip arthroplasty. Clin. Orthop 1995; 311:85–90.
33. Albrektsson T. Hydroxyapatite-coated implants: a case against their use. J. Oral Maxillofac. Surg 1998; 56:1312–1326.
34. Johansson C. On tissue reactions to metal implants. Thesis. Biomaterials group. Gothenburg, Sweden: University of Gothenburg, 1991.
35. Ducheyne P, Van Raemdonck W, Heughebaert JC, Heughebaert M. Structural analysis of hydroxyapatite coatings on titanium. Biomaterials 1986; 7:97–103.
36. Friedman RJ, Bauer TW, Garg K, Jiang M, An YH, Draughn RA. Histological and mechanical comparison of hydroxyapatite-coated cobalt-chrome and titanium implants in the rabbit femur. J. Appl. Biomaterials 1995; 6:231–235.
37. Gottlander M, Albrektsson T. Histomorphometric analyses of hydroxyapatite-coated and uncoated titanium implants. The importance of the implant design. Clin. Oral Impl. Res 1992; 3:71–76.
38. Gottlander M, Albrektsson T, Carlsson LV. A histomorphometric study of unthreaded hydroxyapatite-coated and titaniumcoated implants in rabbit bone. Int. J. Oral Maxillofac. Impl 1992; 7:485–490.
39. Hayashi K, Matsuguchi N, Uenoyama K, Kanemaru T, Sugioka Y. Evaluation of metal implants coated with several types of ceramics as biomaterials. J. Biomed. Mater. Res 1989; 23:1247–1259.
40. Oonishi H, Yamamoto M, Ishimaru H, Tsuji E, Kushitani S, Aono M, Ukon Y. The effect of hydroxyapatite coating on bone growth into porous titanium alloy implants. J. Bone Joint Surg. Br 1989; 71: 213–216.
41. Soballe K, Hansen ES, Brockstedt-Rasmussen H, Pedersen CM, Bunger C. Hydroxyapatite coating enhances fixation of porous coated implants. A comparison in dogs between press fit and noninterference fit. Acta Orthop. Scand 1990; 61:299–306.
42. Thomas KA, Kay JF, Cook SD, Jarcho M. The effect of surface macrotexture and hydroxylapatite coating on the mechanical strengths and histologic profiles of titanium implant materials. J. Biomed. Mater. Res 1987; 21:1395–1414.
43. Rocca M, Fini M, Greggi T, Parisini P, Carpi A, Giardino R. Biomaterials in spinal fixation. An experimental animal study to improve the performance. Int. J. Artif. Organs 2000; 23:824–830.
44. Sandén B, Larsson S, Olerud C. Hydroxyapatite coating enhances fixation of loaded pedicle screws: a mechanical in vivo study in sheep. Eur. Spine J 2001; 10:334–339.
45. Sandén B, Johansson C, Olerud C, Larsson S. Improved bone-screw interface with hydroxyapatite coating. An *in vivo* study of loaded pedicle screws in sheep. Spine 2001; 26:2673–2678.
46. Lapresle P, Missenard G. Hydroxylapatite-coated Diapason screws: first clinical report. J. Spinal Disord 1995; 8(suppl 1):S31–S39.
47. Sandén B, Larsson S, Olerud C, Johansson C. Improved extraction torque of hydroxyapatite-coated pedicle screws. Eur. Spine J 2000; 9:534–537.
48. Sandén B, Olerud C, Petren-Mallmin M, Larsson S. Hydroxyapatite coating improves fixation of pedicle screws. A clinical study. J. Bone Joint Surg. Br 2001; 84-B:387–391.
49. Geesink RG, Groot K, Klein CP. Bonding of bone to apatite-coated implants. J. Bone Joint Surg. Br 1988; 70:17–22.
50. Davies JE, Baldan N. Scanning electron microscopy of the bone-bioactive implant interface. J. Biomed. Mater. Res 1997; 36:429–440.
51. Edwards JT, Brunski JB, Higuchi HW. Mechanical and morphologic investigation of the tensile strength of a bone-hydroxyapatite interface. J. Biomed. Mater. Res 1997; 36:454–468.

52. Wennerberg A, Albrektsson T, Andersson B, Krol JJ. A histomorphometric and removal torque study of screw-shaped titanium implants with three different surface topographies. Clin. Oral Impl. Res 1995; 6:24–30.
53. Shirota T, Donath K, Matsui Y, Ohno K, Michi K. Reactions of bone tissue in old rats to three different implant materials. J. Oral Implantol 1994; 20:307–314.
54. Eckhoff DG, Turner AS, Aberman HM. Effect of age on bone formation around orthopaedic implants. Clin. Orthop 1995; 312:253–260.

49

Multilevel Cervical Decompression and Reconstruction

Michael L. Swank
Cincinnati Orthopaedic Research Institute
Cincinnati, Ohio, U.S.A.

I. INTRODUCTION

Cervical reconstruction after multilevel decompression of the cervical spine presents many technical challenges and consequently has provided for tremendous variability in treatment approaches and controversy in the literature. With the advent of new biomaterials, new fixation methods, and more experienced surgeons, the field of reconstruction, especially for multilevel reconstruction, is rapidly changing. This chapter will present a philosophy of treatment for surgical decompression and reconstruction as it has evolved in the author's practice and how it may evolve in the future. The initial overview will discuss the problems inherent with the currently accepted surgical reconstruction methods, briefly summarize the literature for each area, and then present the author's preferred treatment method for these conditions as well as early experience with these treatment methods including technical pitfalls and clinical results. Many of the treatment methods are just being published in the literature now, and others are not even currently available in the literature. Rationale for these reconstruction methods will be presented. The purpose of this chapter is to present an argument for moving surgery into the next century. Rather than being a comprehensive review of the literature, this is really designed to stimulate thought and provoke argument.

II. PROBLEMS WITH THE CURRENT RECONSTRUCTION METHODS

A. Nonunion

All multilevel reconstructions have a certain incidence of nonunion varying from the highest with multilevel interbody allograft reconstruction without plating to autologous iliac corpectomy with anterior plating. Increased risk factors for nonunion include number of levels, smoking, allograft use, multilevel discectomy vs. corpectomy, and instrumentation [1–4]. Figure 1 reveals a typical example of a three-level un-instrumented autograft reconstruction with a pseudarthrosis and persistent neck pain requiring narcotic medications. Figure 2 shows the same patient 2 years after rigid arthrodesis with lateral mass fixation resulting in union of the previous anterior pseudarthrosis even though the patient only underwent a posterior fusion during the second operation. Although he still had occasional neck pain, he was able to be withdrawn from narcotic

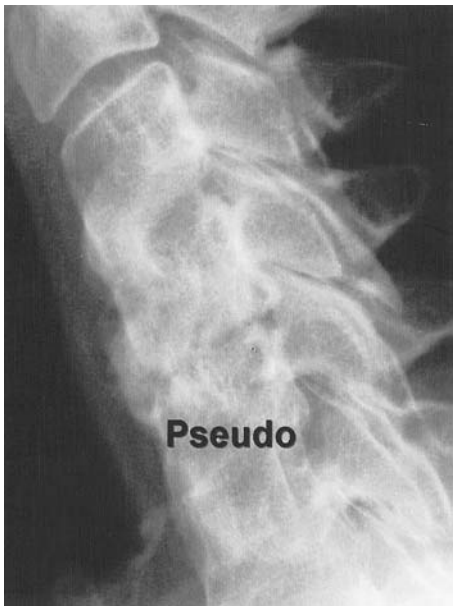

Figure 1 Pseudoarthrosis after three level uninstrumented allograft wedge reconstruction.

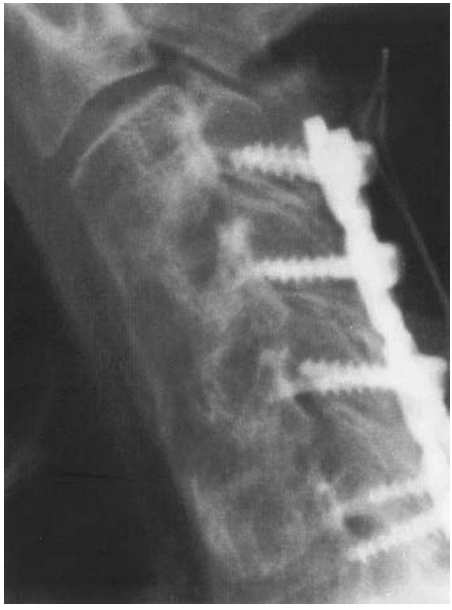

Figure 2 The same patient as in Fig. 1, 2 years after rigid fixation with lateral mass plating resulting in solid arthrodesis.

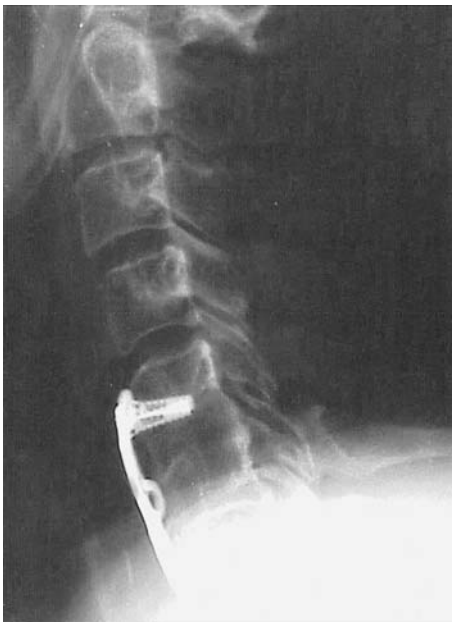

Figure 3 One year after two level allograft interbody reconstruction with one level delayed union.

medication completely. The patient in Figure 3 underwent an allograft interbody reconstruction with an anterior plate. At one year postoperatively, the patient had mild daily neck pain and an obvious delayed union at the lowest grafted level with intact hardware (Fig. 4). At 2 years, the patient's symptoms had resolved, and he had an apparent arthrodesis at both levels and the hardware remained intact (Fig. 5). An example of a patient who underwent a two-level interbody reconstruction with autograft and even at 2 years had a radiographic pseudarthrosis without evidence of hardware failure, but who was completely asymptomatic, can be seen in Figures 6 and 7.

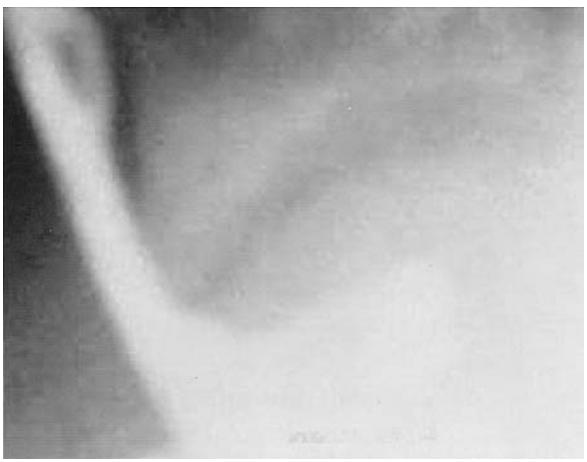

Figure 4 Close-up of delayed union at the lower level with intact hardware one year postoperatively.

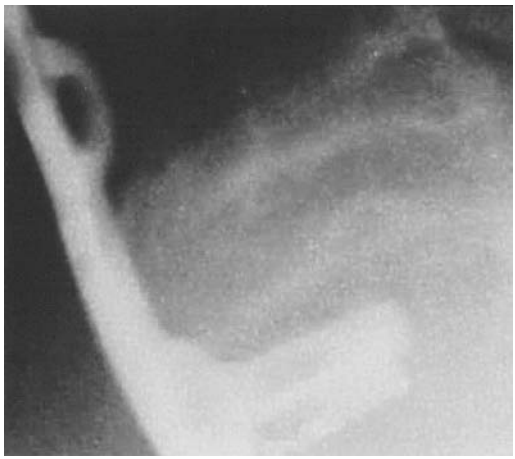

Figure 5 The same patient as in Fig. 4, 2 years postoperatively with apparent radiographic union.

B. Graft Material (Interbody Reconstruction) Complications

Allograft as a source of graft material has extensive historical use. Traditionally, the advantages of allograft include ease of use, availability, adaptability, defects of any size, low but still possible risk for infection, and risk of material supply. The major disadvantage has been lower incidence of union compared to autograft [1,2,5,6]. Consequently, machined allografts have recently been advocated as a more rigid implant fixation with presumed better unions. Although few data

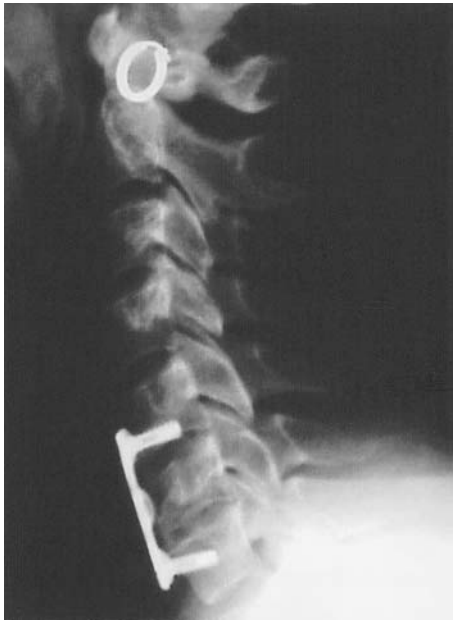

Figure 6 Three months postoperative radiograph of patient reconstructed with autograft and anterior plate.

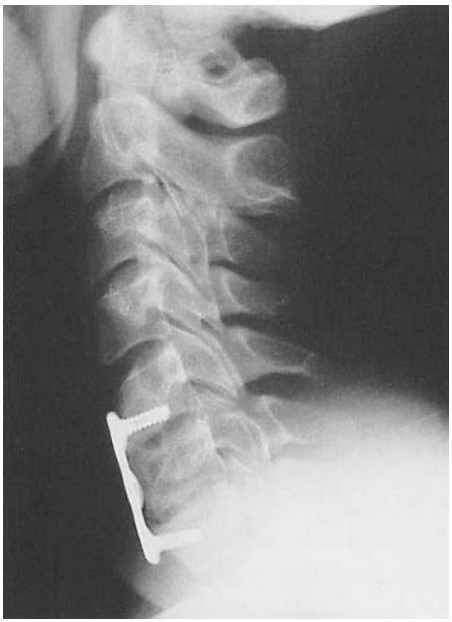

Figure 7 The same patient as in Fig. 6, 2 years postoperatively with asymptomatic radiographic nonunion.

have been available, at least one report [6] suggests that these will be better than the traditional iliac crest wedges or dowel grafts. Allograft with anterior plates has been advocated as a reconstruction method in multilevel discectomy and corpectomy models. When combined with rigid fixation, allograft reconstructions have been reported to have both an acceptable and unacceptable union rate in multilevel cases [5,6]. Cortical allografts, such as fibular struts, radiographically appear to incorporate at the ends of the graft host junction and side to side and do not appear to undergo complete resorption by creeping substitution. Figure 8 is an example of a fibular allograft for a multilevel corpectomy. The 6-week radiograph demonstrates the early postoperative appearance of the clearly demarcated hostgraft interface. Figure 9 shows how this demarcation disappears by 2 years postoperatively, and it appears to have incorporated into a host-graft composite. A CT scan at 2 years (Fig. 10) reveals the fibular graft host interface with evidence of complete onlay of host bone to the fibular strut, but with maintenance of the structural integrity of the strut itself without creeping substitution.

As an interbody graft, there have been an increasing number of choices from freeze-dried iliac crest, which is machined by the surgeon in the operating room, to machined corticocancellous wedge or sandwich grafts. While the data do not exist to strongly support one type of graft versus another, it has been my experience that the more rigid corticocancellous constructs take much longer to undergo creeping substitution and clear graft incorporation than the more cancellous grafts. Figures 11 and 12 show a cortico-cancellous machined wedge in the immediate postoperative appearance and at 1 year postoperatively. There has been minimal remodeling at the hostgraft interface, but the spinal alignment is excellent and the patient is doing well. On the other hand, Figure 13 demonstrates a less dense, predominantly cancellous graft which has undergone obvious creeping substitution and incorporation into the host bone at final follow up (Fig. 14). Autograft is considered the gold standard for single-level fusions. However, when used in a multilevel discectomy or corpectomy model and harvested from the iliac crest, it has

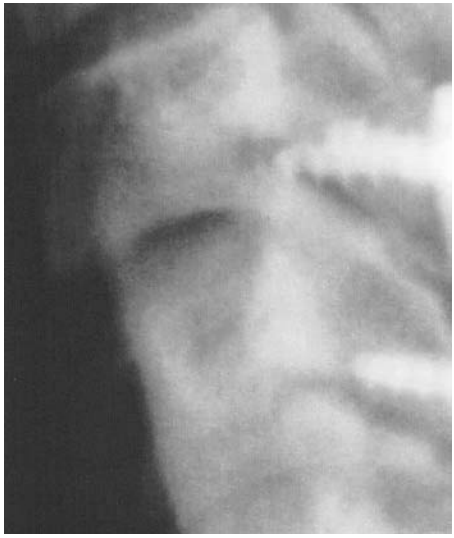

Figure 8 Six weeks postoperative film of fibular allograft strut reconstruction demonstrating the host graft interface.

been associated with major morbidity: donor site pain, paresthesias, and cosmetic defects as well as and occasionally limited supply in patients who have had multiple previous surgeries [7].

C. Kyphosis

While the exact role of localized kyphosis and development of axial neck pain or adjacent segment degeneration is not exactly known, several articles have implicated kyphosis as both

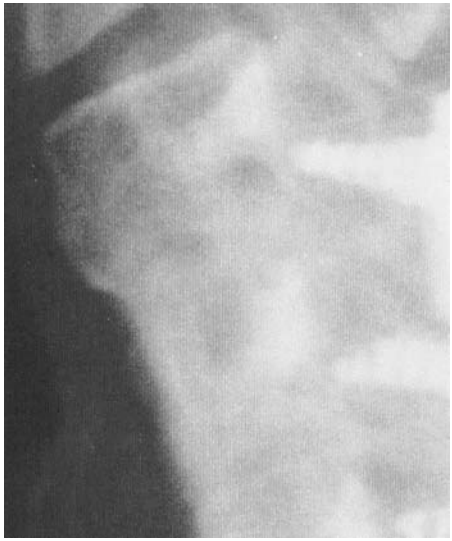

Figure 9 The same patient as in Fig. 8, 2 years postoperatively revealing maturation of host graft interface.

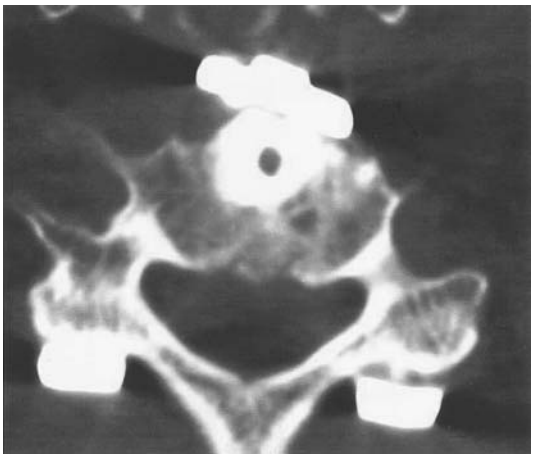

Figure 10 The same patient as in Fig. 8, 2 years postoperative CT scan demonstrating incorporation of fibular graft without creeping substitution.

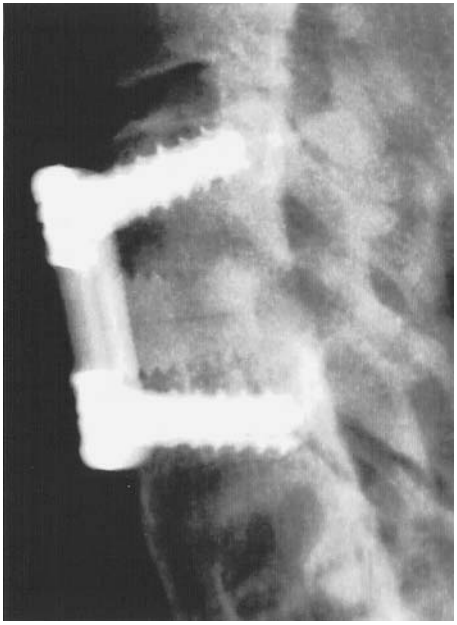

Figure 11 Six weeks postoperative appearance of machined dense cortico-cancellous wedge allograft and plate reconstruction.

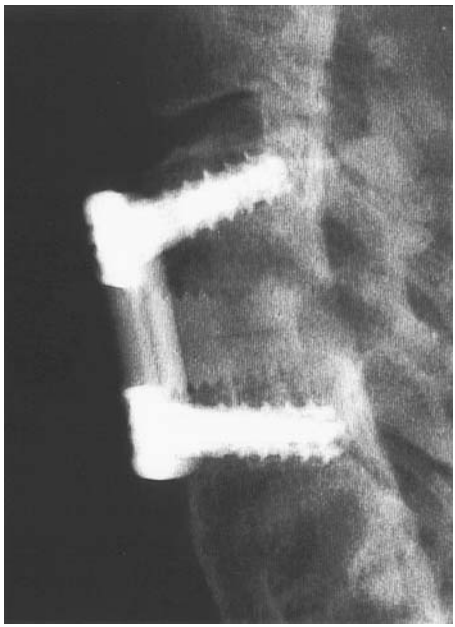

Figure 12 The same patient as in Fig. 11, one year postoperatively, with no obvious creeping substitution, but maintenance of spinal alignment.

a cause for initial surgery and as a potential source of rapid transition zone degenerative changes postoperatively [7,8]. Given these issues, at least theoretically restoring and maintaining sagittal alignment of the cervical spine after reconstrution appears to be a legitimate goal. Typically, kyphosis has been associated with un-instrumented allograft and autograft reconstructions, whether in multilevel discectomy or corpectomy models. Figure 15 shows an example of a

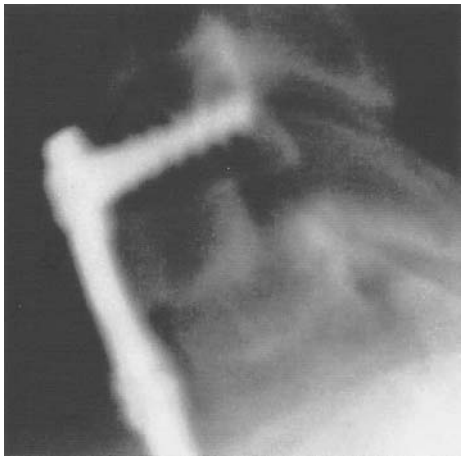

Figure 13 Six weeks postoperatively allograft reconstruction with dense cancellous graft.

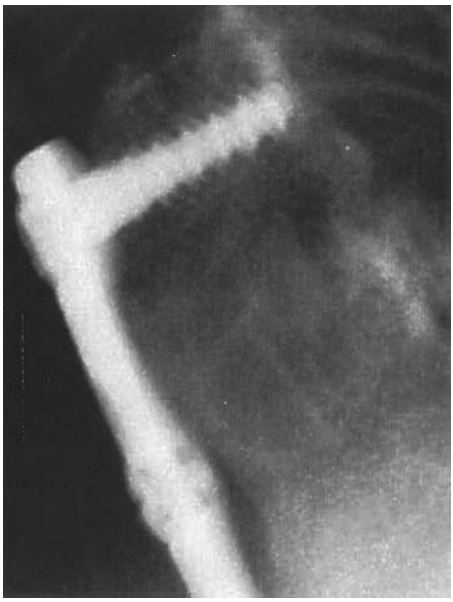

Figure 14 The same patient as Fig. 13, showing creeping substitution and solid arthrodesis.

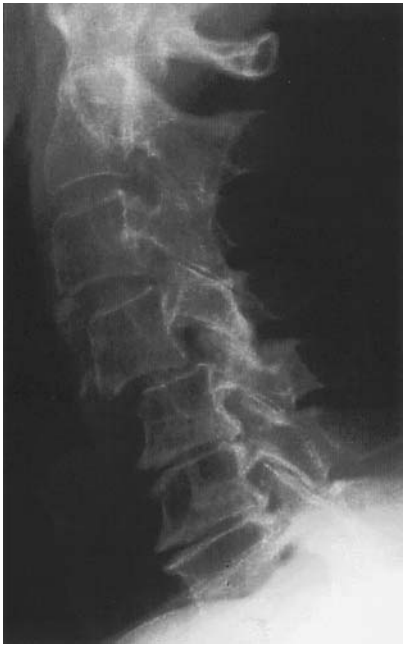

Figure 15 Patient with cervical spondylosis, spondylolisthesis causing myeloradiculopathy.

typical patient who has developed degenerative disc disease and spondylosis at two levels who then developed a spondylolisthesis at 4/5 which caused severe cord compression and necessitated the need for surgical intervention. This MRI (Fig. 16) clearly demonstrates the most significant compression at the level of the spondylolisthesis. Yet another example of the potential for kyphosis to result in severe cord compression and need for surgical intervention can be seen in Figure 17. This patient had an uninstrumented anterior arthrodesis 6 years previously and developed kyphosis with severe cord compression as seen on the sagittal MRI.

D. Instrumentation

Instrumentation, primarily anterior plates, has been developed to try to increase the union and prevent kyphotic angulation in multilevel reconstructions [1,3–5]. Obviously, adding a level of complexity to the surgery creates new potentials for complications related to misapplication and mechanical failure of the devices. I will discuss three basic modes of fixation that are commonly used and currently available.

1. Anterior Plates

Anterior plates were first developed as a modification of a small fragment bone plate and were useful in adding fixation to prevent graft extrusion (Figs. 18, 19) and were used to provide mechanical stability in indications such as spinal trauma. The initial plates, such as the AO H plate, were nonconstrained relatively flexible plates. They failed by either screw back-out or plate breakage. The second-generation plates, such as the Synthes CSLP or the Medtronic Orion, were designed to overcome these issues, and the plates were stronger and had mechanisms to ''constrain'' the screws to the plate. These failed early by screw breakage at the plate screw thread junction. Since the screw designs were improved, most of these plates now fail by cutting

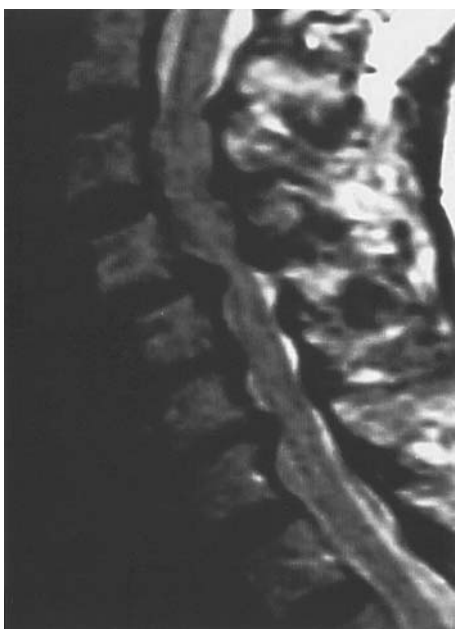

Figure 16 Sagittal MRI of same patient revealing severe cord compression.

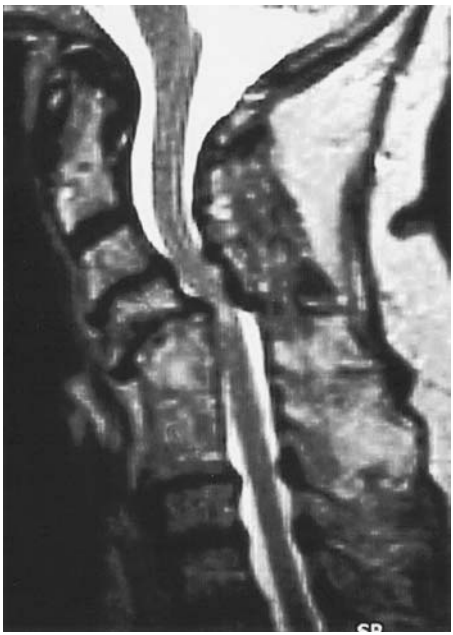

Figure 17 Patient 6 years after uninstrumented anterior cervical arthrodesis demonstrating proximal khyphosis and spondylolisthesis resulting in severe spinal cord compression.

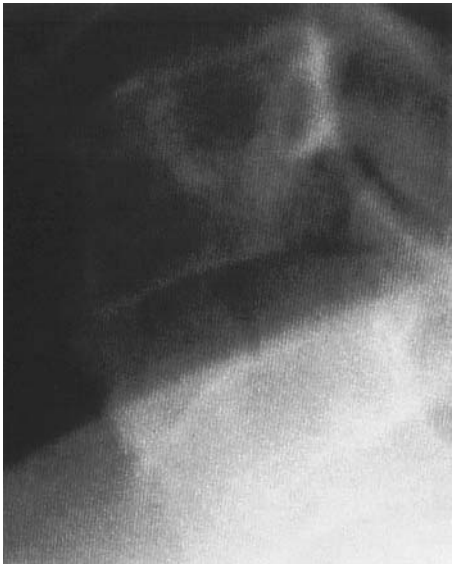

Figure 18 Initial postoperative appearances of uninstrumented autograft wedge reconstruction.

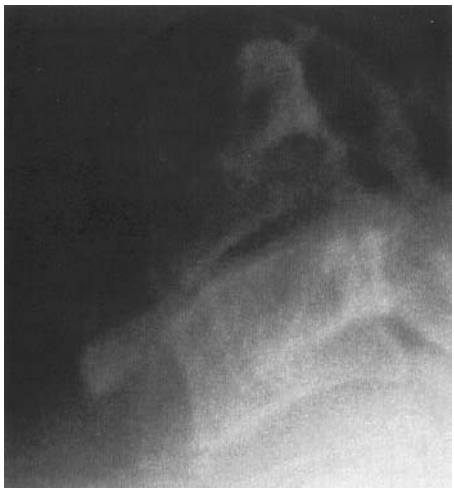

Figure 19 Postoperative appearance of the same patient as in Fig. 18, showing graft extrusion.

out through the vertebral body, usually at the caudad level. Biomechanical studies have revealed that these rigid plates create abnormal loading conditions for the interbody graft material, and third-generation plates have been designed to be ''load sharing'' or dynamic. Theoretically, these plates restore more normal load conditions to the host graft interface and can lead to a higher union rate. It remains to be seen whether these devices also lead to a greater incidence of kyphosis, however. The DOC system (Figs. 20, 21) was one of the first generation of ''dynamic'' plates.

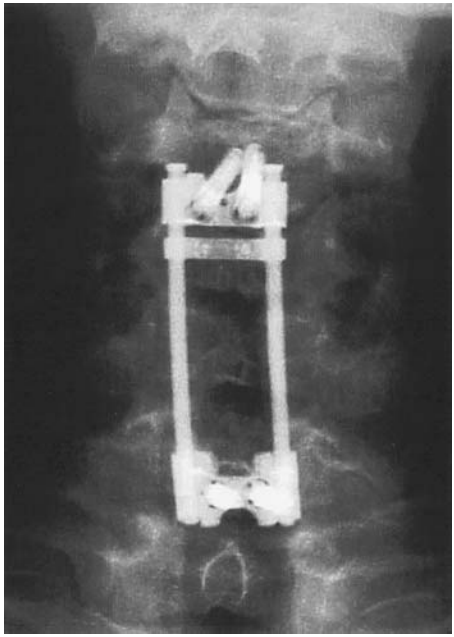

Figure 20 AP radiograph of first generation dynamic fixation with DOC rod system.

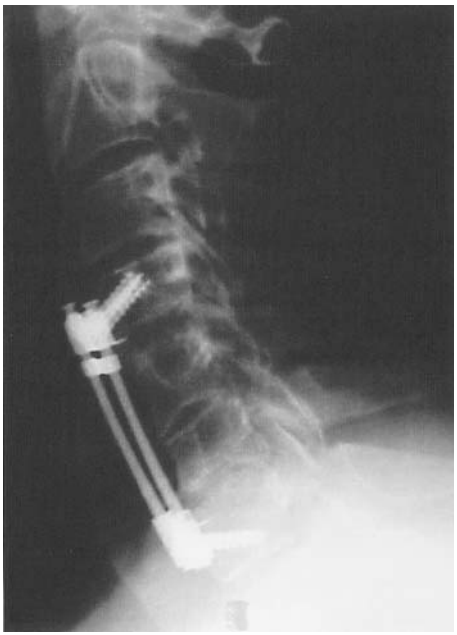

Figure 21 Lateral radiograph showing the DOC dynamic fixation system.

2. Posterior Wiring Techniques

For multilevel fixation, wiring techniques can be performed utilizing the spinous processes, the lamina or the facets. Biomechanically, none of these techniques provide rigid fixation over multiple levels, but they can be useful and safe if posterior elements are intact and available. Various techniques have been described by many authors. However, in most cases where spinous processes are available, simple wiring techniques are effective. Figure 22 demonstrates a spinous process wiring technique applied to an anterior pseudarthrosis, and Figure 23 clearly demonstrates osseous union of the anterior pseudarthrosis. Likewise, wiring techniques can be used to stabilize multilevel anterior reconstructions as seen in Figures 24 and 25.

3. Posterior Plating Techniques

While lateral mass fixation with screws and either plates or rods has not been approved by the FDA, several systems have been made available to perform these techniques. The need for rigid segmental fixation in multilevel reconstructions cannot be overemphasized. Lateral mass fixation has been demonstrated to be biomechanically superior to other forms of fixation in the posterior spine, especially in the absence of spinous processes and over more than one level. These systems represent a major advance in technology and have obviated the need for halo fixation in almost all cases of multilevel reconstruction. These devices can be used alone in cases in which the disease process is primarily spondylosis and facet arthropathy, as seen in Figure 26, or they can be used as adjunctive fixation in patients with multilevel anterior and posterior reconstructions (Fig. 27.)

E. Transition Zone Degeneration

All current reconstruction methods which involve multiple levels involve an arthrodesis of some type. The radiographs seen in Figure 28 demonstrate the effect of a long fusion construct with

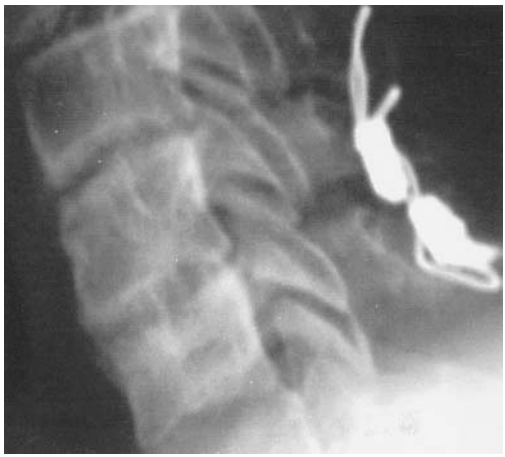

Figure 22 Six weeks postoperative radiograph showing spinous process wiring for anterior pseudoarthrosis.

degeneration of the proximal disc space requiring surgical decompression and reconstruction, in this case with an allograft and plate in an attempt to restore at least segmental lordosis (Fig. 29). Figures 30 and 31 reveal the development of disc space collapse and anterior osteophyte formation at the C7-T1 level below an instrumented C3-C7 arthrodesis within a 2-year follow-up period. Fortunately this patient is asymptomatic, and no further surgery has been required to date.

III. CONCLUSIONS: AUTHOR'S CURRENT TREATMENT FOR MULTILEVEL DISEASE AND THE RATIONALE FOR TREATMENT

A. Basic Principles

1. Perform an adequate decompression.
2. The decompression dictates the reconstruction required.

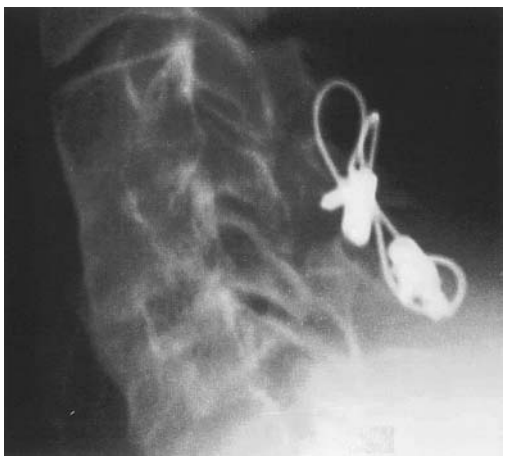

Figure 23 The same patient as Fig. 22, 2 years postoperatively revealing solid arthrodesis.

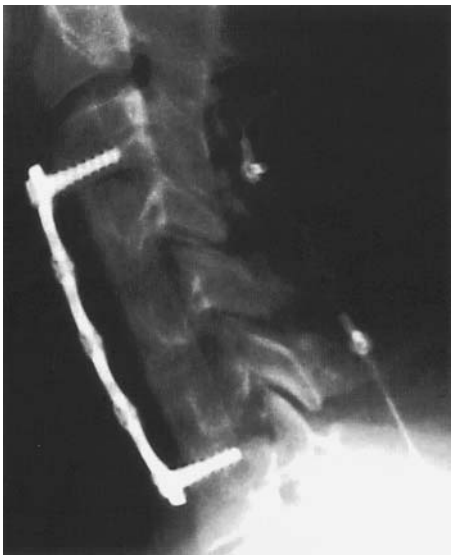

Figure 24 Six weeks postoperative radiograph of multilevel anterior reconstruction with supplemental posterior spinous wiring technique.

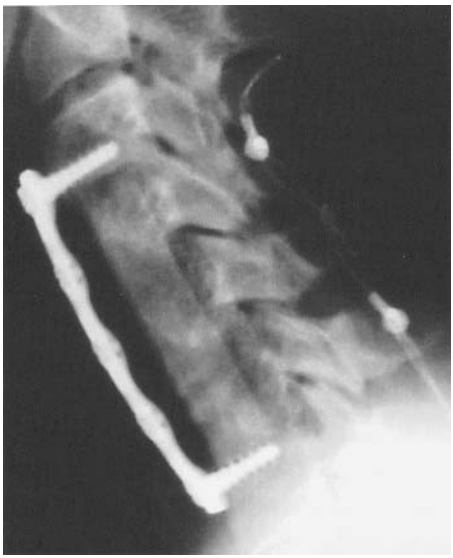

Figure 25 Two years postoperative radiograph of patient from Fig. 24, demonstrating solid arthrodesis.

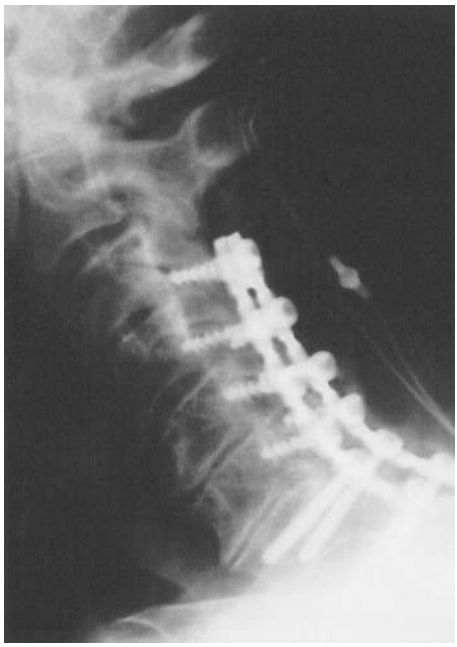

Figure 26 Postoperative radiograph of patient with posterior element (lateral mass and pedicle screw) fixation after multilevel laminectomy for cervical spondylosis with meylopathy.

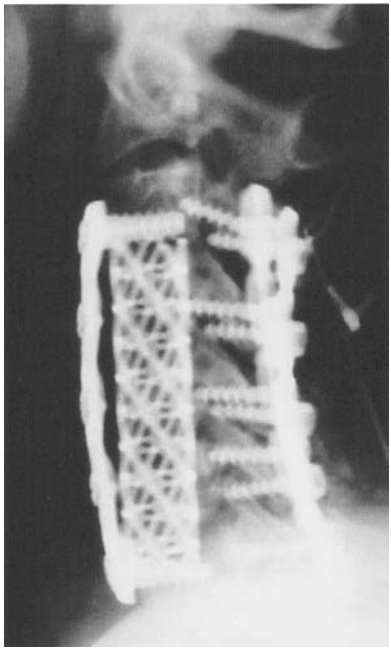

Figure 27 Anterior and posterior cervical decompression and reconstruction stabilized with lateral mass fixation.

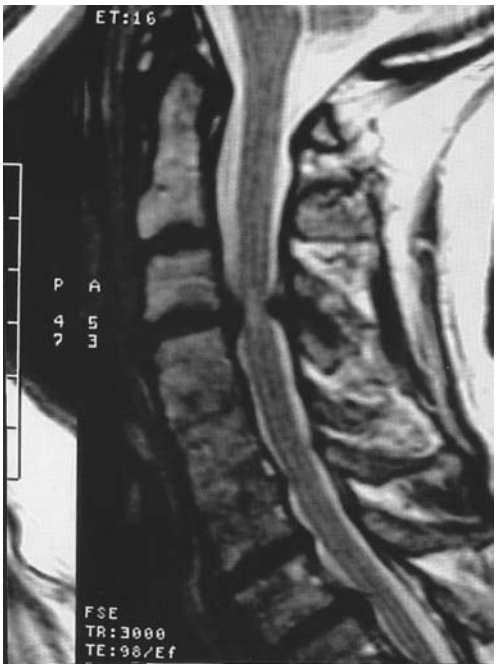

Figure 28 Severe stenosis with myelomalacia secondary to transition zone degeneration above previous arthrodesis.

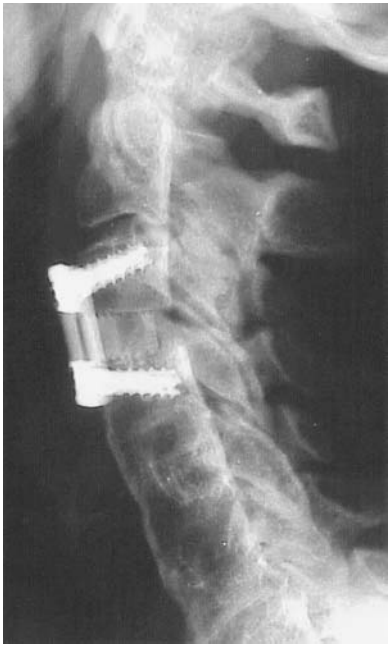

Figure 29 Reconstruction of patient in Fig. 28, with interbody allograft wedge and anterior plate.

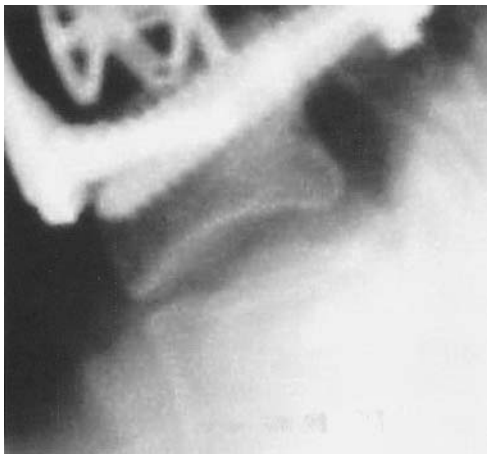

Figure 30 Six weeks postoperative appearance of patient's C7-T1 disc space after C3-7 anterior posterior fusion showing normal disc space height.

3. Perform the minimal reconstruction necessary to do the following:
    a. Obtain rigid fixation
    b. Restore lordosis
    c. Maintain lordosis
    d. Obtain union

4. Use synthetic or locally available autograft materials in an attempt to:
    a. Avoid allograft products of any type, including mineralized bone products
    b. Avoid any antigenic tissues or materials
    c. Avoid donor site complications and remote graft harvest

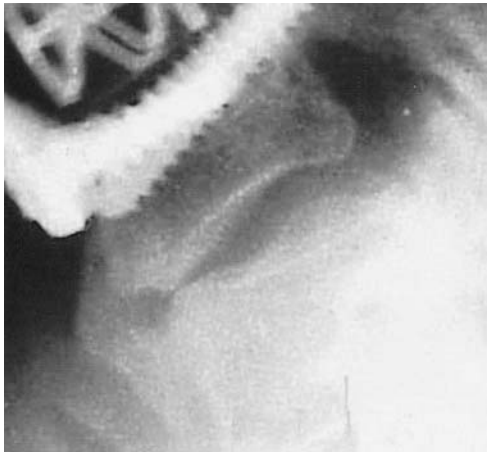

Figure 31 Two years postoperatively, patient has developed transition zone degeneration with disc space collapse and anterior osteophyte formation.

B. Two-Level Discectomy

Rather than perform a two-level discectomy, I perform a single-level corpectomy and use locally harvested corpectomy bone inside a mesh cage for graft material. The vertebral corpectomy bone is high-quality cancellous bone in almost all instances. I usually mix this with an autologous platelet-derived plasma product, which is harvested from the patient at the time of surgery, usually Symphony or AGF (Fig. 32). This supplements the corpectomy bone and makes it easier to pack the cages. After the interbody cage is placed, I will apply an anterior plate which has a screw locking mechanism and is typically constrained or semi-constrained.

C. Three or More Levels

Because of what I consider to be an unacceptable union rate in fusions involving three or more levels, I have approached these multilevel reconstructions with a combined anterior and posterior approach in most instances. The rationale for this is based on the nonunion rates noted in the literature on three or more disc levels in addition to the underlying principle that operating on osteoporotic bone, which many of these multilevel patients have, is somewhat akin to building a house in the sand. The more points of fixation that are available, the less likely construct failure will ensue, and a single point of fixation failure does not jeopardize the entire reconstruction. In my entire series of anterior and posterior instrumentation, which has included over 508 screws in 162 anterior plates, 592 lateral mass screws, and 169 cervical pedicle screws, I have not experienced a single screw or plate breakage. All my failures have been at the bone implant interface, and most are related to screw pullout failure of the bone (Figs. 36 and 37).

My bias towards circumferential arthrodesis, especially in degenerative spondylosis with stenosis, is based on a few patients in whom posterior-only constructs failed (Figs. 38, 39). I'm inclined to perform anterior-posterior stabilization in multilevel reconstruction (greater than 3 levels). Exceptions to this are posterior-only decompressions for spondylytic arthropathy with anterior osteophytosis, which is already stable, such as seen in Figure 40.

D. Posterior Reconstruction Methods

I perform anterior reconstruction with posterior stabilization with intraspinous wearing. Almost all patients in my series have severe spinal cord compression, so I typically have performed at

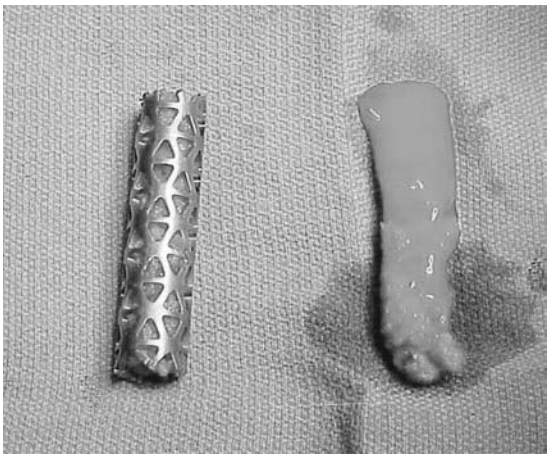

Figure 32 Titanium mesh cage with locally harvested bone graft and platelet gel.

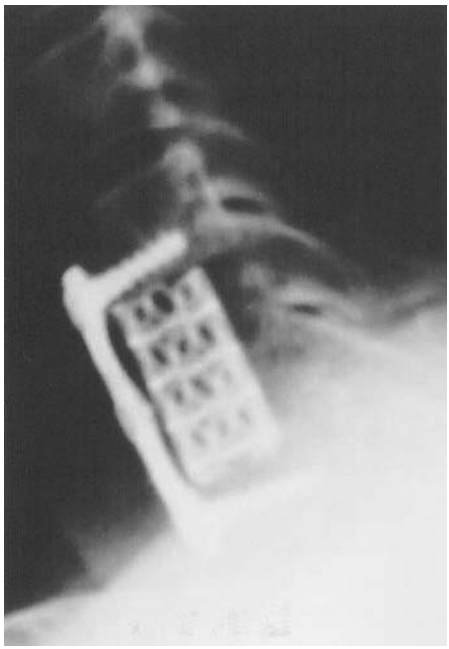

Figure 33 Single level corpectomy with titanium mesh cage local bone graft and anterior plate reconstruction.

Figure 34 Close-up of the same patient as in Fig. 33, revealing the host implant interface 6 weeks postoperatively.

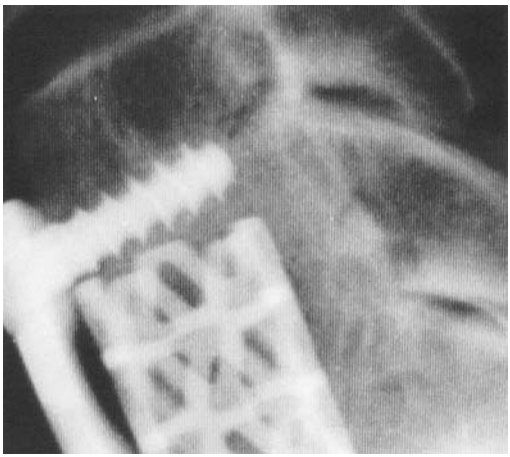

Figure 35 Two year postoperatively radiography of the same patient as in Fig. 34, revealing remodeling of host implant interface and apparent arthrodesis.

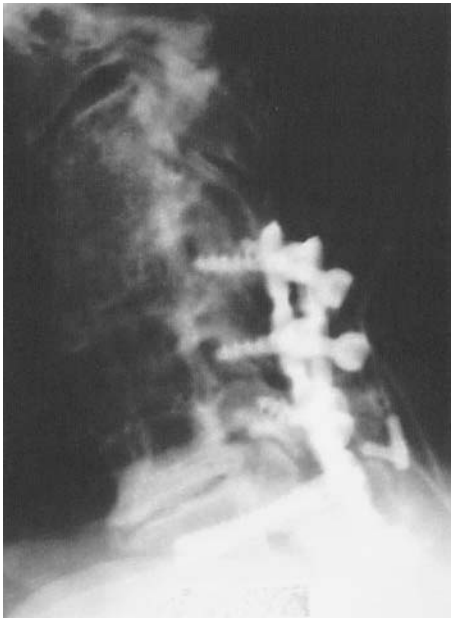

Figure 36 Patient who developed screw backout secondary to osteoporotic bone with gross fixation failure.

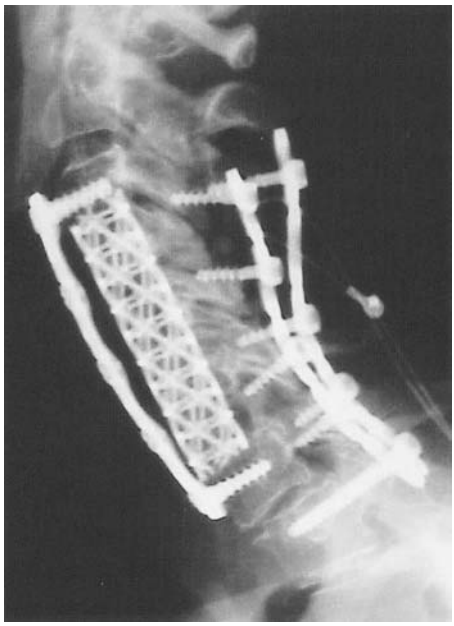

Figure 37 Lateral mass plate and screw failure after combines anterior and posterior decompression and reconstruction.

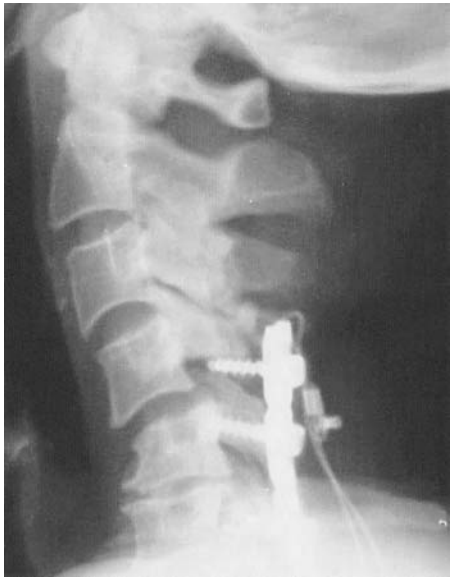

Figure 38 Six weeks postoperatively radiograph revealing inadequate placement of screws in the inferior quadrant of lateral masses of C4.

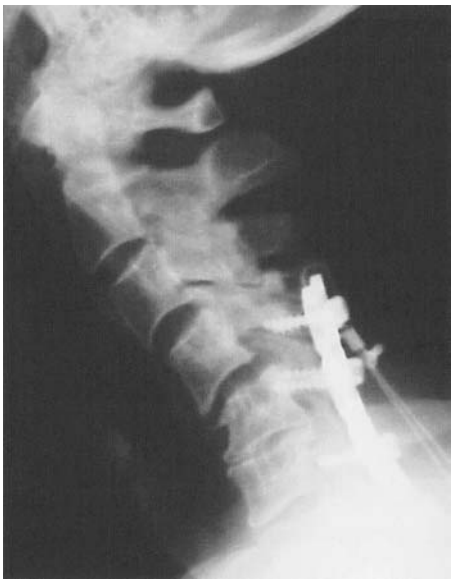

Figure 39 The same patient as Fig. 38, demonstrating localized khyphosis and gross mechanical failure of plate screw construct.

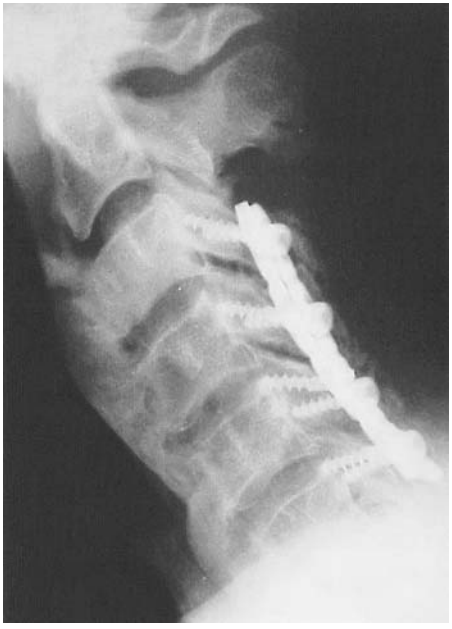

Figure 40 Multilevel posterior decompression and reconstruction in patient with stable anterior spine secondary to osteophyte formation.

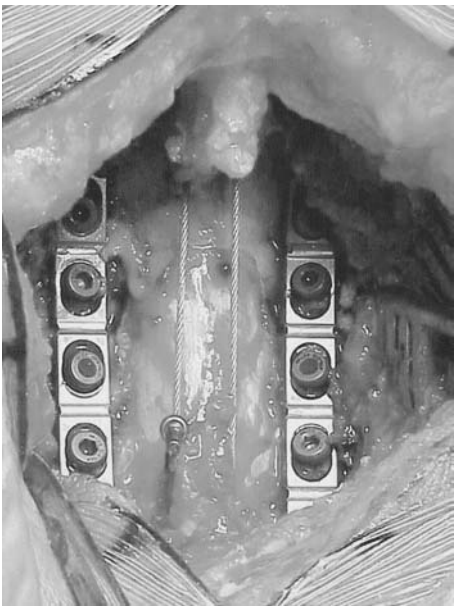

Figure 41 Intraoperative appearance of lateral mass screw and plate construct with interspinous wire.

least singular or multilevel laminectomies over the areas of most cord compression. Removal of the posterior elements makes intraspinous wearing on a segmental basis impossible and leaves only the options of facet and also makes hook placement impossible, at least in a segmental basis, and leaves only facet wiring and lateral mass or pedicle instrumentation as surgical treatment options.

Once lateral mass plate and rod systems became available, facet wiring techniques, in my opinion, became obsolete, as they have never been shown to have mechanically provided any substantial rigid fixation. Therefore, compared to the rotational and extension stability noted in lateral mass reconstructions, facet wiring does not tend to provide rigid internal fixation. Because of this, I have little or no experience with facet wiring, except in a consultatory fashion.

To add resistance to flexion, if there are spinous processes available at the top or bottom of the construct, I will add an intraspinous wire to the cephalad and caudad-most spinous process. I use this wire to do two things: first, to help restore lordosis prior to placement of lateral mass fixation, and second, to protect the spinal cord from the drill while I place lateral mass screws. Since I believe the most important part of this operation is decompression, I perform the decompression prior to placement of the screws, and the intraspinous wire helps provide a guide for the drill to prevent placement of the instruments on the spinal cord (Fig. 41). Third, intraspinous wires help to provide resistance to flexion and supplement the fixation of the lateral mass screws. Obviously, when going through the spinous process in osteoporotic bone, there is a limited amount of force that can be applied. Initially, 20 pounds per square inch was used. At this force, we had several cables pull out of the cephalad spinous process both intraoperatively and postoperatively. Therefore, depending on the bone quality, we apply somewhere between 10 and 20 pounds per square inch of force.

Lateral mass screws are used for C3–C6 and placed in a standard fashion as described by various authors. I will typically employ any technique necessary to make the plate or rod system align, and in my experience this requires variable placement of the lateral mass screws,

depending on the patient's anatomy, the spacing of the facet joints, and the specifics of the instrumentation system. At C7, T1, and below, I routinely place pedicle screws. Typically, I first started using pedicle screws at the lower levels because of the difficulty and inconsistency in size and shape of the C7 lateral mass and the need to angle screws differently, even into the rib heads. Since in most of these cases a foramenotomy or laminectomy is required for neural decompression, direct palpation of the pedicle wall is possible in order to direct screw placement. Typically a 3.5 or 4.0 cancellus or corticle screw will be placed. C-arm fluoroscopy can be used to check the screw position, and reasonable films can be obtained in almost all cases. Image guidance can be used to assist, but because the pedicles often do not allow for more than a millimeter margin of error, care must be used when using image-guided systems. The fixation obtained with pedicle screws, the availability of the pedicle as a consistent bone to fixate to, and the relatively small lateral mass at C7, in my opinion, make pedicle fixation preferable. In my series, I have placed 169 C7 or T1 pedicle screws with no adverse sequellae from either to date. On postoperative CT scanning, I certainly have had screws that have encroached upon the spinal canal (Fig. 42) or extended lateral to the vertebral body foramen (Fig. 43.) However, we have not removed a screw to date and have not had a radiculopathy that was felt to be secondary to screw placement per se.

E. Anterior Instrumentation

In multilevel corpectomy, I harvest local bone from the vertebral body and often mix it with a platelet-derived product to place the composite graft inside a titanium mesh cage. I have used fibular allograft with good success in anterior-posterior reconstructions (Figs. 44, 45 .) However, I feel that local bone and a cage diminishes any risk of disease transmission and is preferable. Furthermore, almost all strut grafts undergo at least some remodeling by creeping substitution, and there is concern in the fixation interface at that point during remodeling. Theoretically, the cages, like the graft material inside the cages, undergoes creeping substitution, provide mechanical strut with no potential loss of lordosis, and relatively protect the anterior plate. The cage is fashioned to fit the cephalad and caudad vertebral end plates, which are sloped, and some

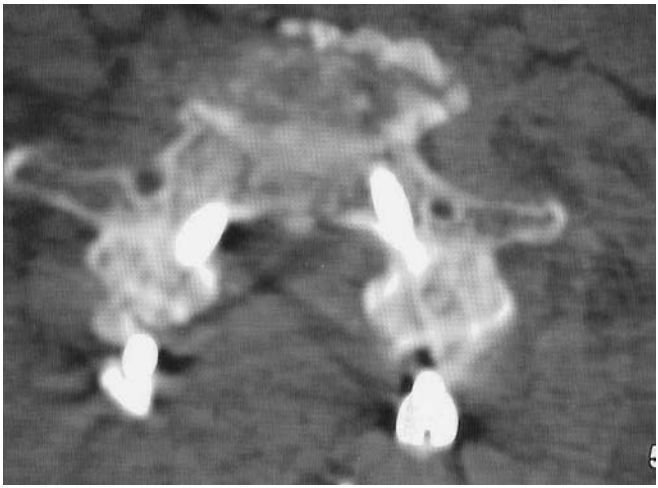

Figure 42 Postoperative CT scan appearance of C7 pedicle screw encroaching on right lateral recess.

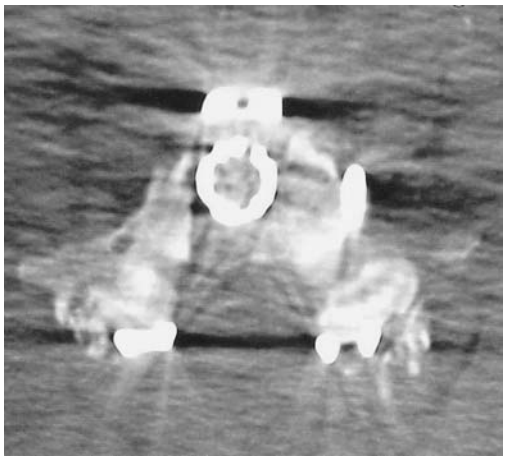

Figure 43 Postoperative CT scan of left C7 pedicle screw which protrudes laterally from vertebral body.

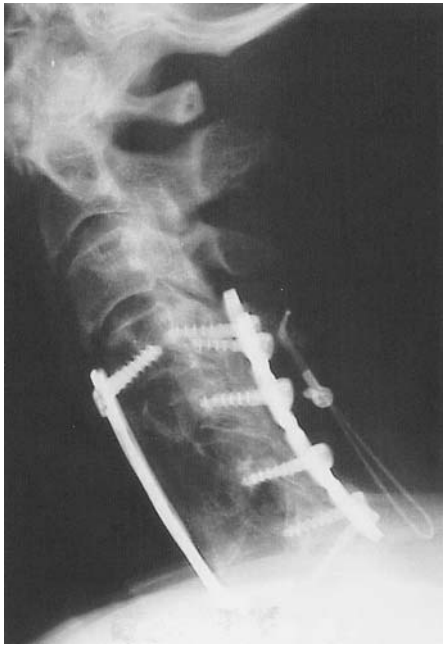

Figure 44 Postoperative appearance of C3-7 anterior allograft interbody strut with supplemental anterior and posterior plate reconstruction.

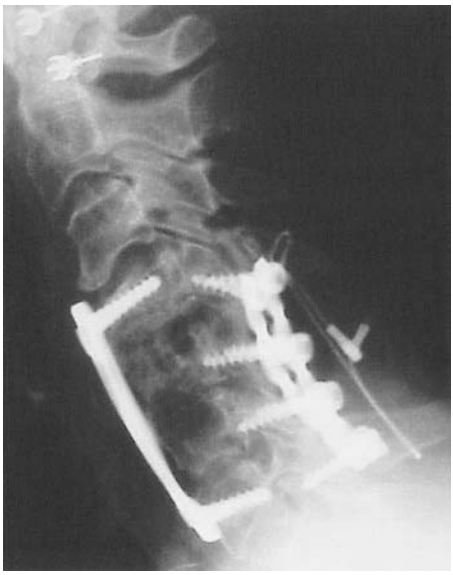

Figure 45 Postoperative radiograph of C3-6 anterior allograft interbody strut reconstruction with supplemental anterior and lateral mass plate reconstruction.

preparation of the vertebral end plates to allow insertion of the cage is necessary. However, I do not spare subchondral bone and do not try to remove subchondral bone and place titanium mesh cage in soft cancellous bone. After the cage is impacted and tested for stability, an anterior plate is applied. I use a plate with locking screws, which captures the screws to prevent screw back-out.

I have only had two patients in my entire series who had backout requiring screw and plate removal. One patient had a C2–C4 fusion, and because of the angle of the jaw with the early version of the instrumentation system, there was no instrument to place the upper locking screw and one of the upper screws backed out, necessitating hardware removal. The second one was a C3–C7 multilevel anterior-posterior reconstruction, which was a second-generation locking screw plate system. This was an early model that had screw locking failure. The screw locking mechanism failed and the screw backed out. Both these patients went on to union and required no other treatment.

F. Single-Level Anterior Corpectomy with Titanium Interbody Cage and Anterior Plate

To date I have performed 21 cases with minimum 6-month follow-up. While radiographic union is difficult to assess, there has been no hardware failure, no screw breakage, and no significant cage subsidence to date. Figure 33 shows the typical appearance of one of these reconstructions at the first postoperative visit at 2 weeks. The close-ups of the host-cage interface seen in the immediate postoperative period (Fig. 34) and at 2 years (Fig. 35) appear to demonstrate a solid arthrodesis. This method of filling the cage with locally harvested bone, usually augmented with an autologous platelet gel harvested at the time of surgery, has yielded excellent clinical results, completely avoids the risk of disease transmission and donor site morbidity, and shortens operating room time while providing a superior biomechanical construct for arthrodesis.

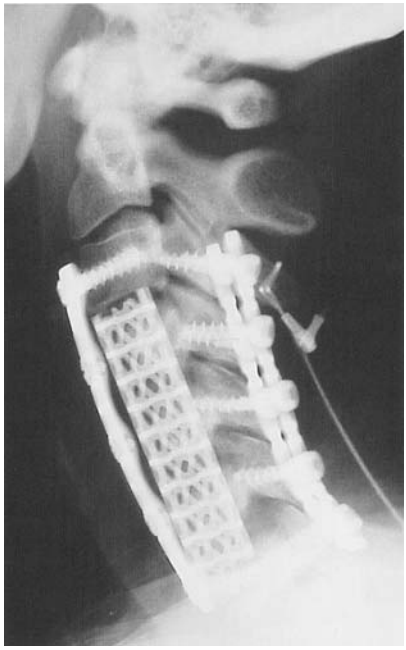

Figure 46 Postoperative lateral radiograph of multilevel anterior posterior decompression and reconstruction with titanium interbody cage, anterior plate and lateral mass reconstruction.

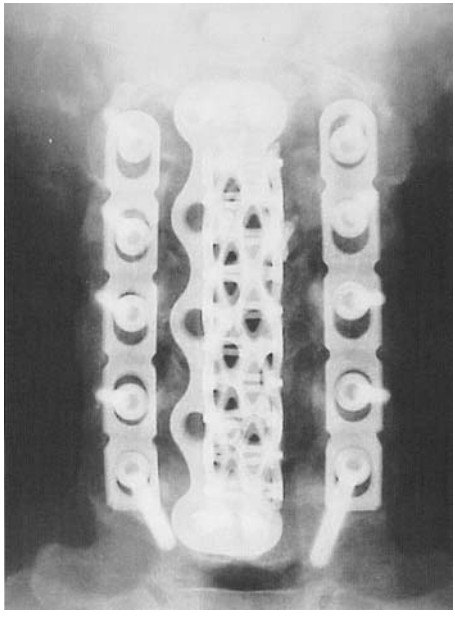

Figure 47 Postoperative AP radiograph demonstrating multilevel decompression and reconstruction with titanium mesh, anterior plate, and lateral mass and pedicle plates and screws.

G. Two- and Three-Level Anterior Corpectomy with Titanium Interbody Cage, Anterior Plate, and Lateral Mass Plates

When titanium cages (Figs. 46 and 47) became available, I began using these devices in all multilevel corpectomies. At the time of this writing, I have performed surgery with this particular construct in 53 patients. These surgeries were performed as staged same-day procedures in all cases. In spite of this rigid fixation, I have had 12 lateral mass screws in 9 patients develop asymptomatic screw back-out. However, no patient has required a reoperation to date for loss of fixation, malposition of hardware, or implant migration. No patient has radiographic evidence of pseudarthrosis. As with the single-level corpectomies, no patient received any risk of disease transmission and no patient had any graft donor site morbidity.

H. Three or More Level Posterior Decompressions and Reconstruction with Lateral Mass Plates

Generally, I have performed posterior-only constructs in patients who are very elderly (>75 years old), patients who have significant anterior osteophytes and apparent mechanical stability of the anterior column, patients who have primarily facet arthropathy as the cause of their spinal cord compression, and patients who have normal lordotic alignment in the sagittal plane. This obviously represents a fragile group of osteoporotic patients who push the limits of screw fixation. I have performed 14 multilevel constructs in this group of patients and have experienced 1 patient with gross hardware failure who still went on to arthrodesis, 1 patient who developed a fracture at T1/T2 9 weeks after a C3–T1 laminectomy and fusion, 2 patients who developed proximal kyphosis and pull-out of the superior lateral mass screws. No patient has been revised over the levels of instrumentation, and all patients improved neurologically from their decompression, but these patients remain a challenge to reconstruct biomechanically.

I. In Search of the Ideal Implant

While the methods I have outlined certainly improve upon the standard treatment methods for multilevel reconstruction by avoiding donor site morbidity, avoiding the risk of disease transmission, and lowering the risk of nonunion to essentially zero, these are difficult and technically demanding operations. The risk of iatrogenic injury to neurovascular structures associated with the placement of these devices is very real. The medical complications associated with performing these complex surgeries, especially in elderly patients, are significant and potentially life-threatening.

Consequently, newer implants and devices are constantly being sought to improve on the current methods and overcome the problems associated with rigid arthrodesis, especially transition zone changes that may require future interventions. The first three of the five major problems associated with multilevel reconstruction have been addressed. These methods have significantly advanced the problems associated with nonunion, graft material complications, and kyphotic angulation. Unfortunately, however, the use of these advanced techniques has increased the potential for instrumentation complications and, other than restoring lordosis, have not addressed the issue of transition zone degeneration. All of the methods I have discussed involve an arthrodesis which significantly alters spinal biomechanics. While these methods are a vast improvement on past methods of achieving arthrodesis, they do not restore normal spinal function. The ideal implants of the future will provide not only a reconstruction of spinal alignment, but also a reproduction of spinal mechanics. In the meantime, the current advances in materials and fixation devices has substantially lowered the morbidity associated with these complex reconstructions after multilevel spinal decompression.

REFERENCES

1. Bolesta MJ, Rechtine GR, Chrin AM. Three- and four-level anterior cervical discetomy and fusion with plate fixation: a prospective study. Spine 2000; 25(16):2040–2044.
2. An HS, Simpson JM, Glover JM, Stephany J. Comparison between allograft plus demineralized bone matrix versus autograft in anterior cervical fusion. A prospective multicenter study. Spine 1995; 20(20):2211–2216.
3. Connolly PJ, Esses SI, Kostuik JP. Anterior cervical fusion: outcome analysis of patients fused with and without anterior cervical plates. J Spinal Disord 1996; 9(3):202–206.
4. Wang JC, McDonough PW, Kanim LE, Endow KK, Delamarter RB. Increase fusion rates with cervical plating for three level anterior cervical discectomy and fusion. Spine 2001; 26(6):643–646.
5. Shapiro S. Banked fibula and the locking anterior cervical plate in anterior cervical fusions following cervical discectomy. J Neurosurg 1996; 84(2):161–165.
6. Shapiro S, Connolly P, Donnaldson J, Abel T. Cadaveric fibula, locking plate, and allogenic bone matrix for anterior cervical fusion after cervical discectomy for radiculopathy or myelopathy. J Neurosurg 2001; 95(1 suppl):43–50.
7. Ebraheim NA, Elgafy H, Xu R. Bone-graft harvesting from iliac and fibular donor sites: techniques and complications. J Am Acad Orthop Surg 2001; 9:210–218.
8. Katsuura A, Hukuda S, Saruhashi Y, Mori K. Kyphotic malalignment after anterior cervical fusion is one of the factors promoting the degenerative process in adjacent intervertebral levels. Eur Spine 2001; 10(4):320–324.

50

Decision Support Tools in Spinal Surgery: Artificial Neural Networks and Predictive Modeling

Scott G. Tromanhauser
The Boston Spine Group, LLC, and New England Baptist Hospital
Boston, Massachusetts, U.S.A.

Marc E. Parham
Interactive Analysis
Bedford, Massachusetts, U.S.A.

I. INTRODUCTION

The practice of medicine is essentially a process of interconnected decisions, where one decision leads us to take specific action that usually always results in the need for another decision. We *decide* what questions to ask of our patients, and based on their responses we *decide* to ask more questions, until we *decide* that we have a working diagnosis. We then, based on that presumptive diagnosis, perform a physical examination, which includes certain tests that we *decide* might support our initial impression. The results of those tests may lead us to *decide* to perform laboratory or imaging tests that, in the end, either support or refute our impression. If we find evidence from this exam that indeed the patient has the presumptive medical problem, we *decide* upon a treatment strategy.

Each of these decisions is subject to the limitations of our experience; time allotted for the patient's visit, communication skills of the patient and, most importantly, the memory and processing capacity of our own minds. That we have memory and processing limitations is a given [1]. As Dr. Lawrence Weed writes [2], ''Medical decisions are still based largely on the recall and processing of complex information by highly trained physicians. Yet, their cognitive inputs fall short of what medicine requires, too often producing decisions that are deficient in quality and resistant to organized improvement.'' How we choose to overcome these deficiencies is critical. This is not to suggest that all medical problems require significant time, testing, and thought to manage, but that some problems are overwhelmingly complex and our decision-making process could benefit from some additional ''support.'' Furthermore, if a flawed decision is made early in this process, then any subsequent decisions could be adversely affected as well, since our decision making is often sequentially dependent.

II. WHAT IS A DECISION SUPPORT TOOL?

As the world progressively and inevitably becomes more computerized, we as providers have the opportunity to apply some new and developing technologies into our practice of medicine.

With each passing year the percentage of healthcare providers using computers in their office increases. For some it may only be for administrative and business functions, but for others, increasing computer functionality has brought support tools right into the exam room. The computer itself, or hardware, may be a desktop, laptop, personal digital assistant (PDA), or tablet. It could have touchscreen capability and voice or handwriting recognition. As these devices become smaller and faster with better user interfaces, properties absolutely critical for widespread adaptation, and as more decision support software programs are developed, we as healthcare providers have the opportunity to change the way decisions are made. The result will certainly be improved accuracy of diagnosis and more effective and less variable treatment recommendations.

Decision support tools can take on various forms, but are generally considered to be either a computer software program or a process, e.g., a best practices guideline or problem-specific treatment algorithm. The former has the potential for more sophistication, whereas the latter two are often the distillation of ''expert'' opinions. What a decision support tool is not is a computer or PDA alone. Tools they are, but they do not support our decision making. Textbook or journal articles are only repositories of knowledge reflecting population specific experience but don't provide any patient-specific recommendations. The decision support tool must ''support'' the healthcare provider in decision making; it does not and should not make the decision directly. These tools should be based on real world experience and patient outcomes for the particular problem at hand. These tools have the potential to bring much needed consistency to medical practice at the same time improving quality of care. Having said this, it should be made clear that ''cookbook'' medicine is not the desired result. If the basic tenet of decision support is indeed support, then mindless adherence to machine-based recommendations is to be loathed and avoided. Just as the scalpel requires the surgeon's hand to be effective, so does the decision support tool need the surgeon's mind.

III. WHY DECISION SUPPORT?

The medical literature is replete with examples of regional variation in type and frequency of medical treatments for the same medical diagnosis. The work of Wennberg [3], using small area analysis, demonstrated the differences in rates of laminectomy in New England. We submit that, with accurate decision support tools, these variations could be reduced. The outcomes of lumbar spinal fusion for chronic pain of discal origin are markedly variable [9] mostly because this diagnosis is difficult to make and confirm, since the exact physiological mechanism of pain production is unknown. Furthermore, it is complicated by the fact that chronic pain can be a diagnosis, rather than simply a symptom caused by deranged anatomy. That some patients have remarkable results with spinal fusion while others fail miserably tells us that this problem is very complex, and decision making during patient workup and treatment is probably beyond our minds' processing power. There are too many variables and combinations of variables that influence the outcome. We know that psychosocioeconomic as well as physical factors play a role in outcomes of this surgery. Most spine surgeons believe and indeed the literature supports the notion that patients receiving worker's compensation or disability benefits have less predictable outcomes from lumbar fusion. How does having retained a worker's compensation attorney affect the outcome? Or a limited education? Does having a supportive family or high job satisfaction improve outcomes? What if the patient is 25 years old? Or 52? Furthermore, how do all of these factors interact and affect the outcome? We do not think that the human mind has the processing power to consider all of these factors and more and make reasonably accurate treatment recommendations in the case of chronic low back pain. Until we discover the physiological

cause or pain generator in these patients, we will be doomed to surgical outcomes that are mediocre at best and dismal at worse.

IV. ARTIFICIAL NEURAL NETWORKS

We have developed a process using an artificial neural network (ANN) that can serve as a decision support tool for surgeons when faced with just such a scenario outlined above. ANNs are modeled on the neural architecture of the human brain, hence the name. Figure 1 schematically depicts this process, where hidden neurons represent the interrelating of variables. ANNs are capable of processing large amounts of data involving multiple variables that, most importantly, may not be linearly related (as one variable changes, a second does so in a direct or linear fashion, either up or down). Most statistical methods used in medicine today assume that the relationship between variables is linear—witness the common use of linear and multiple regression modeling. Even the nonlinear extension of linear regression, i.e., logistic regression, is limited by preconceived assumptions about the data (Table 1). Unfortunately, linearity is not the norm in biological systems. ANNs make no assumptions about the interaction of the variables. Furthermore, this process allows the data to determine the mathematical algorithm that best describes it, rather than forcing the data to fit into a predetermined formula that may or may not reflect the true relationships of the variables.

ANNs are also considered ''intelligent,'' i.e., capable of learning, as long as new data are added back to the analysis over time. This form of ''artificial intelligence'' is very good at analyzing complex patterns in data that often elude the human thought process. For example, ANNs have been applied to Pap smear analysis [4] where data, in this case, visual, converted to digital, can be analyzed with more consistent outcomes than the human eye through a microscope. They have also been applied to the evaluation of electrocardiograms [5], where the digital

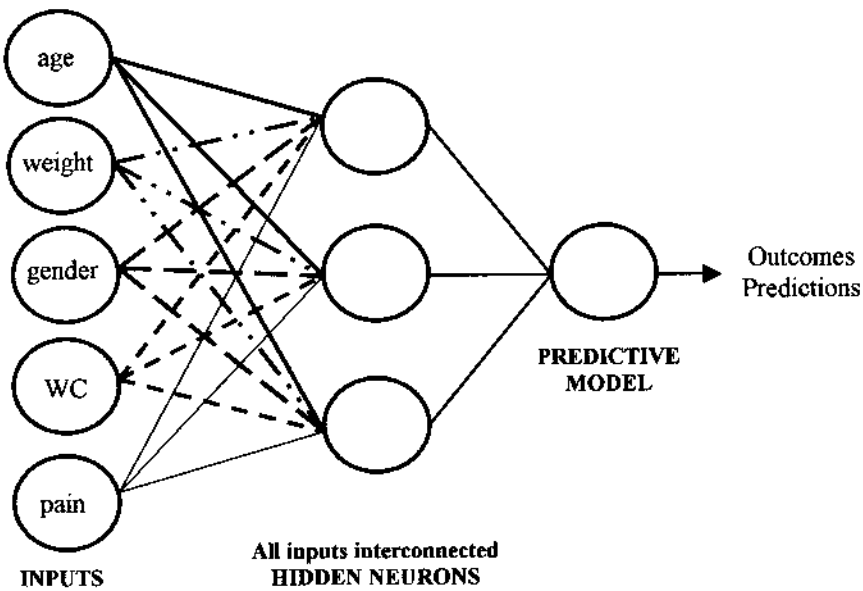

Figure 1 Schematic depiction of an artificial neural network.

Table 1 Comparison of Statistical Methods

Linear regression	Logistic regression	Neural networks
Assumes linear relationship between variables		Assumes no relationships (nonlinear) between variables
All data used to create model	Able to determine predictor variables	Chooses critical variables
No estimate of predictive accuracy	Used for dichotomous (binary) outcomes only	Maximizes predictive accuracy
No internal cross-checking of data	No internal cross-checking	Cross-checking constantly to obtain best fit and predictive power
Limited to two variables at a time	Compares one variable to limited number of others	Virtually unlimited number of variables

data is pushed directly into an ANN to interpret patterns for abnormalities. Indeed, applications of ANNs in medicine are growing and have found success in nearly all specialties [6].

We set out to determine if patient-specific (as opposed to population-specific) outcomes of lumbar fusion could be predicted in advance of treatment [7,8]. We were most interested in patients with chronic low back pain of at least one year duration, who had failed all manner of conservative care. These patients are generally believed to have pain of discogenic origin, be it from annular tears or some other degenerative process. That this diagnosis is difficult to make is understood and that the treatment is controversial is given, but, alas, this is outside the scope of this discussion. Nevertheless, billions of dollars are spent every year in the United States treating this problem, with questionable results. We wanted to find a way to improve outcomes and help patients and surgeons avoid poor outcomes from what is essentially an unpredictable operative procedure. Artificial neural networks were chosen because it was felt they could integrate all the potential variables and do so in a nonlinear manner, free of all operator bias beyond determining the influencing variables.

The process involves five steps in order to have a fully functional predictive model that can be used as a decision support tool (Fig. 2). In order for this support tool to be useful, it must have accuracy in predicting outcomes that exceeds that of the average spine surgeon. Since the outcomes of lumbar fusion for chronic back pain suggest that we achieve an acceptable outcome ~70% of the time, then that becomes our benchmark [9]. It could be argued that in which patient an acceptable outcome can be achieved is entirely unpredictable, suggesting that we are not at all accurate in predicting outcomes.

Step 1

We must first determine all the variables that might influence the outcome, leaving no reasonable factor off the list. Ideally, all of this information was collected prospectively and includes demographic, socioeconomic, and pertinent clinical data. We included the Visual Analog Scores (VAS) for pain and Oswestry Disability Indices, both collected pre- and postoperatively. Our usual outcomes efforts include the collection of educational, financial, and demographic data, which was included along with clinical, diagnostic, and imaging determinations. This left us with an exhaustive list of factors that we considered important to the outcome of lumbar fusion.

Next we decided upon the outcome that we were trying to predict. In this case, the most important outcome to our patients is pain level or VAS score. We felt that nearly all patients

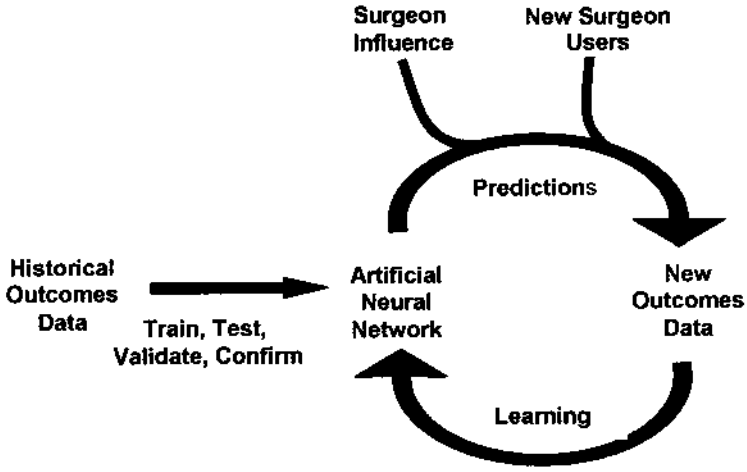

Figure 2 Development and learning cycle for ANN-based predictive model.

were at maximum medical improvement at one year. It could be argued that 2 years might be more appropriate, but in our experience very little additional benefit is achieved beyond one year and any problems usually surface within one year. Our predicted outcome was pain level at one year after undergoing a successful lumbar fusion. We made a point of including all outcomes, good and bad, with and without complications, an essential requirement if our predictions were to be useful. The best use for this tool is to identify those patients for whom there was little or no hope for improvement. These patients could then be considered for other less invasive and, hopefully, less expensive treatments. Ideally, in the future these alternate treatments would also have an ANN-based predictive model to which the patient's profile could be applied.

Step 2

With the database now complete with data on a large number of patients, including both pre- and posttreatment information, we can start to apply it to the neural network process. The first level of robustness in our analysis is achieved with the *training set*. In this step the data set are randomly ''split'' so that approximately 75% is first evaluated in an iterative process that results in many algorithms or mathematical formulas that describe the data. Some of these models will be more optimal descriptions of the data than others. The point of this training step is to find those models that optimize the actual vs. predicted outcomes error rate, in other words, the models that best predict the actual outcome.

Step 3

The next level of robustness involves applying another split of the data, say 15%, to the formulas generated by the training set. Again, both pre- and posttreatment data were included. This *test set* allows us to choose the model with the ''best fit,'' actually with the best R^2, or correlation coefficient (the closer to 1.0 the better). Roughly speaking, 1.0 represents 100% accuracy.

Step 4

The next step or, *validate set*, differs in that the remaining split of the data is applied to the best-fit model generated by the test set without the outcome data included. If the data can be used to create a useful predictive model, then this step should validate the model by producing an R^2 of at least 0.85. This would mean that 85% of the time the model predicts the actual outcome. Theoretically this should be the last step since the model was not given the outcomes in the validation set and accurately predicted the outcomes. One could start applying the model at this point and expect to predict the outcome correctly most of the time or, in the case of lumbar fusion, more often than one would expect from most surgeons.

Step 5

The highest level of robustness for this predictive model involves applying the use of the model in blinded fashion to new patients in a prospective manner. For example, the surgeon would make treatment decisions in the usual fashion but also apply the patient's profile to the predictive model, blinding himself and the patient to the predicted outcome. Then at one year, the patient's actual outcome can be compared with ANN predicted outcome. This last step serves as final confirmation. The validate step outlined above theoretically mirrors the accuracy of the confirmation step except in the case where a surgeon has not contributed data to the analysis. The ''intelligent'' aspect of the method would take this surgeon's outcomes data and apply them to the aggregate, making it equally accurate for him or her. Data collected after the model is in use, from existing or new users, are aggregated and serve to further improve the accuracy by ''learning'' (Fig. 3).

Our experience [7,8] has produced a working prototype, predictive model that achieved an R^2 for the training and test set of 0.99 and 0.89, respectively. The validate set requires more data that are presently being collected. We are also simultaneously conducting a confirmation test where the patients and surgeons are blinded to the predicted outcome. We expect to have a predictive model that will support our decisions to perform elective lumbar fusion for chronic low back pain whose predictive accuracy outperforms our own by 15–20%. This model will begin to address the shortcomings of our own judgment and the issue of ''patient selection'' that we hear so much about in the specialty of spinal surgery.

V. CONCLUSION

That computers and their processing advantages will inevitably pervade all of medicine and surgery is a given. The time frame for that to occur will no doubt be spread over a generation of physicians. Healthcare has been under the microscope of business and government for close to two decades with the goal of squeezing out inefficiencies and improving quality of care. The managed care decade has come for most of us and will for all in due time. Most of the egregious wastefulness and inefficiencies have been wrung out, picked like so much low hanging fruit. The cost pressures from industry and government, however, have not slowed. Decision support technology may lead the way to further improvements in quality and consistency of care and avoidance of unneeded and potentially costly interventions.

Artificial neural networks applied with the goal of predicting outcomes are a new approach to problem solving in medicine. This technology is applicable to virtually all medical treatments. The most gains will be seen when it is applied to treatments that are controversial, unpredictable, or expensive and are frequently performed. The modeling is data driven, not a trivial obstacle given the demands on physician time and resources. However, once a highly accurate predictive

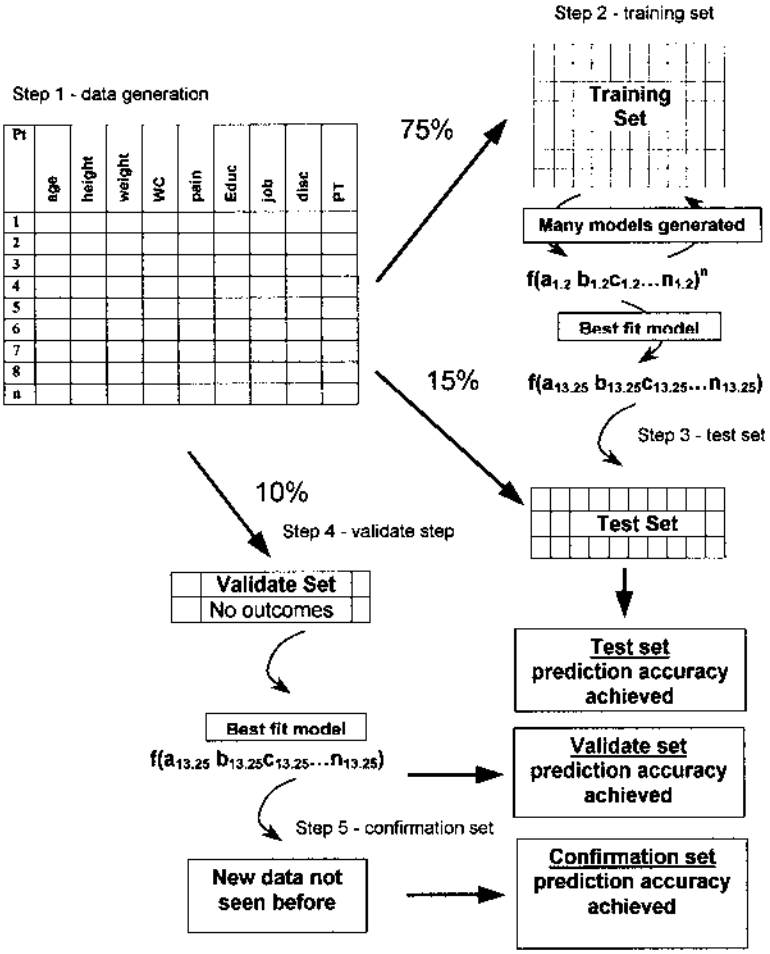

Figure 3 Data organization and testing.

model is created from data from a limited number of centers, it can ''learn'' and improve accuracy from the use by many.

REFERENCES

1. Grove W, Meehl P. Comparative efficiency of informal (subjective, impressionistic) and formal (mechanical, algorithmic) prediction procedures: the clinical-statistical controversy. Psychology, Public Policy and Law 1996; 2:293–323.
2. Weed LL, Weed L. Opening the black box of clinical judgment. Br. Med. J., electronic edition, eBMJ 1999; 319(7220) Part I):1–32.
3. Keller RB, Soule DN, Wennberg JE, Hanley JF. Dealing with geographic variations in the use of hospitals: The experience of the Maine medical assessment foundation orthopaedic study group. J. Bone. Joint. Surg 1990; 72A(9):1286–1293.

4. Mango L, Tjon R, Herriman J. Computer-assisted Pap smear screening using neural networks. Vol. I. San Diego. CA: World Congress on Neural Networks. (WCNN'94), 1994:84–89.
5. Bortolan G, Brohet C, Fusaro S. Possibilities of using neural networks for ECG classification. J. Electrocardiol 1996; 29(suppl):10–16.
6. www.emsl.pnl.gov:2080/proj/neuron/neural/bib/medicine.html.
7. LaRocca S, Tromanhauser S, Parham M. Predicting outcomes of lumbar spinal fusion surgery using a neural network. Presentation, North American Spine Society 16th Annual Meeting, Seattle, WA, 2001.
8. Tromanhauser S, Parham M. A neural network predictor of lumbar fusion surgery outcomes. Presentation, American Medical Informatics Association, Annual Meeting, Washington, DC, 2001.
9. Bono CM, Lee CK. Critical analysis of trends in fusion for degenerative disc disease over the last twenty years: influence of technique on fusion rate and clinical outcome. Presentation, North American Spine Society 17th Annual Meeting, Montreal, Canada. 2002.

51
Porous Tantalum for Spinal Interbody Fusion

Crispin C. Wigfield
Derriford Hospital
Plymouth, England

Bruce H. Robie
Implex Corporation
New Jersey, U.S.A.

I. BACKGROUND

Autologous bone grafting remains the gold standard against which other fusion techniques are judged. Forty years of experience have highlighted the shortcomings and complications of autograft.

Harvest of bone graft from the iliac crest is associated with significant short- and long-term morbidity. Infection, pelvic fracture, meralgia parasthetica, and chronic pain in up to 20% of cases may follow initial pain, bruising, and hematomas [1,2]. Those surgeons who advocate primary fusion have sought alternatives to the patient's own tricorticate bone. Experience with allograft has been mixed. It compares favorably with autograft for single-level fusions, especially in nonsmokers, although success rates diminish with multiple fusions. The use of allograft must take into account the costs of a bone bank, including a strict program of quality control. Concerns regarding the risks of transmissible agents such as human immunodeficiency virus (HIV) further restrict the use of allograft bone.

During the past two decades it has emerged that materials with a porous surface or structure can support tissue ingrowth, and the stability of orthopedic implants is supplemented by such ingrowth, resulting in a superior biological fixation. A variety of porous surfaces and materials have been used to obtain bony ingrowth and fixation. Developments have largely been in the field of orthopedic large joint replacement.

For spinal surgery the ideal device or bone substitute would provide immediate stability in compression and resist axial displacement, minimizing pain and maintaining spinal alignment and foraminal height. It would be entirely biocompatible, prompting rapid, pain-free fusion without adverse tissue reactions, and would not degrade subsequent radiological investigations. Autologous bone graft meets only some of these requirements.

The evaluation of fusion devices in spinal surgery is a complex process, which must take into account spinal pathophysiology and the biomechanical properties of materials [3]. Not all implants meet the mechanical requirements for promoting fusion and preventing collapse. Fewer still come with convincing evidence of osteointegration or osteoconduction. Early enthusiasm for some implants has been overshadowed by unacceptably high complication rates that could have been limited by paying closer attention to their testing and long-term surveillance [4].

II. POROUS TANTALUM

Tantalum is a highly biocompatible, corrosion-resistant, strong, and ductile metallic element with an atomic number of 73. Its potential as a biomaterial with applications in medicine were investigated over 50 years ago, and it is currently used in a variety of implants including pacemaker electrodes, cranioplasty plates, ligation clips, femoral endoprostheses and as a radiopaque marker for following bone ingrowth or implant migration. Because of its biocompatibility, it is accepted as a standard surgical implant material.

Porous tantalum is a new biomaterial that has been developed for application in reconstructive orthopedics and other surgical specialties such as maxillofacial and dental surgery and neurosurgery. The material is of particular interest since it has an unusually high porosity, which is interconnecting, and the pore size demonstrates considerable regularity and uniformity of shape.

The manufacture of porous tantalum originates with the pyrolysis of a thermosetting polymer foam precursor to obtain a low-density vitreous carbon skeleton, which has a repeating dodecahedron array of pores interconnected by smaller openings. Commercially pure tantalum is deposited onto the the carbon skeleton using a chemical vapor deposition/infiltration to create a porous metal construct (Fig. 1). The typical thickness of the tantalum coating is 50 μm. An increase in thickness of the tantalum deposition can affect the pore size and mechanical properties. Typically the strength and stiffness of porous tantalum increases with decreasing porosity.

Porous tantalum is of particular interest as an orthopedic and spinal implant material for several reasons. Macroscopically it has a fully interconnecting porous structure similar to cancellous bone. Its mechanical properties lie between those of cortical bone and cancellous bone for both its modulus of elasticity and its compressive strength, thus making it an ideal transitional material for bony interfaces (see Tables 1 and 2). It also has a high coefficient of friction against cortical and cancellous bone, which should reduce the possibility of implant displacement. Having a relatively low modulus of elasticity similar to cancellous bone should be favorable in reducing stress shielding and encouraging appropriate bone remodeling.

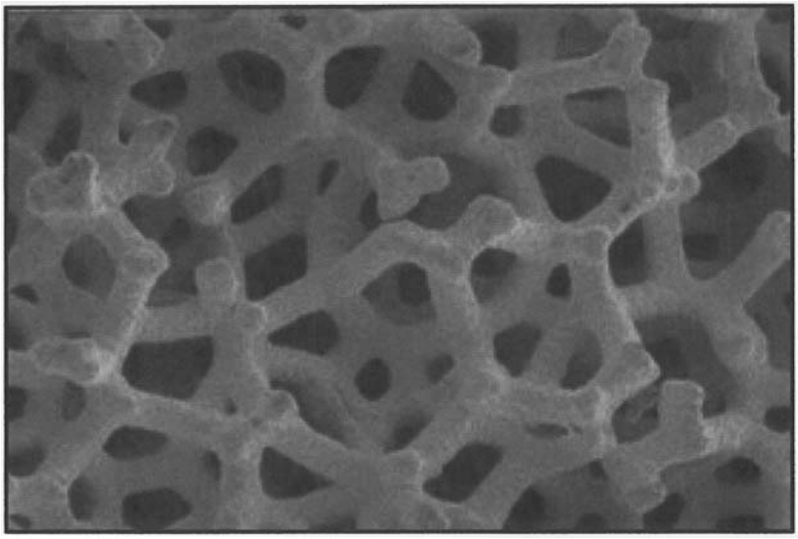

Figure 1 Scanning electron microscope image of the tantalum interconnecting porous structure.

Table 1 Elastic Modulus of Porous Tantalum in Relation to Other Materials

Material	Elastic modulus (GPa)
Cobalt chrome	210
Titanium	110
Cortical bone	15
Porous tantalum	3
Subchondral bone	2
Trabecular bone	0.1

III. EVIDENCE SUPPORTING THE USE OF POROUS TANTALUM

Several laboratory and clinical studies have highlighted the potential uses of porous tantalum as an orthopedic and spinal fusion material. Researchers at McGill University in Montreal have closely evaluated the biomechanical properties of porous tantalum implants. Tissue ingrowth with blood vessels seen at the tissue/implant interface suggestive of neovascularization has been demonstrated in porous tantalum implants placed adjacent to muscle fascia in mongrel dogs. Ingrowth into the implants formed rapidly over a 4-week period and resistance to pullout was demonstrated. Hacking et al. concluded that porous tantalum reproducibly supports soft tissue ingrowth and develops substantially faster and greater tissue attachment than conventional beaded surfaces [5]. Further canine studies have investigated the bone ingrowth and interface mechanics of porous tantalum implanted into femoral shafts. Bobyn et al. showed that at one year the average extent of bone ingrowth ranged from 63 to 80%. A pore size of 430 μm was associated with a statistically significantly greater percentage of bone ingrowth than larger pore sizes of 650 μm [6]. Bone ingrowth across the full diameter of the implant was commonly seen (Fig. 2).

Evidence to support the role of porous tantalum as a spinal fusion material has emerged within the past 5 years. Bosita et al. showed slightly greater histological fusion rates with porous tantalum compared to autologous iliac crest bone in a goat model, though the results were not statistically significant [7]. In Denmark, Zou et al. demonstrated a porous tantalum ring performed equivalently to a carbon fiber cage as an ALIF implant in a porcine lumber interbody fusion study [8]. Interbody fusion cages for the cervical and lumbar spine in a sheep model have demonstrated advanced rates of fusion when combined with bone morphogenic protein

Table 2 Compressive Strength of Porous Tantalum in Relation to Other Porous Materials

Material	Compressive strength (MPa)
Cortical bone	130–150
Other porous metals	20–150
Porous tantalum	50–80
Trabecular bone	10–50
Porous ceramics	3–30
Porous polyethylene	3–5

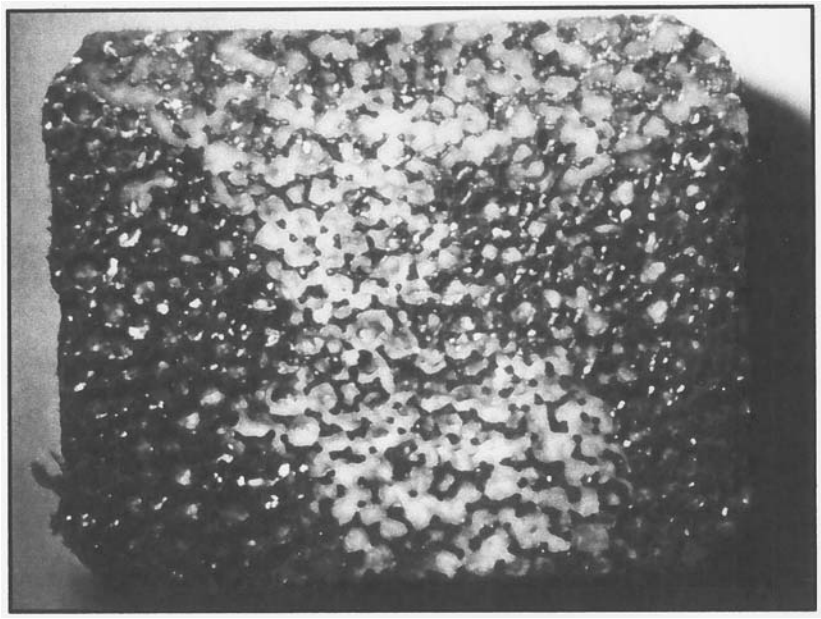

Figure 2 An explanted tantalum block showing bone growth (in white) through the block.

rhBMP-2. The interconnecting porous nature of the tantalum implants may make them ideal as a carrier matrix for compounds that can promote and accelerate spinal fusion [9].

In the United Kingdom a prospective clinical study was conducted of Hedrocel™, a porous tantalum implant, used in the cervical spine to achieve interbody fusion compared with autologous bone graft (Fig. 3). The porous tantalum implants achieved 100% fusion as assessed radiologically at one year postoperatively. In addition, neck disability index outcome scores were superior for the patients with tantalum implants. SF-36 assessment scores were equivalent for the two groups of patients at 2-year follow-up [10].

IV. IMAGING CHARACTERISTICS OF TANTALUM

The assessment of fusion is of interest to spinal surgeons and principally has to rely on the appearances of bone and implant using plain radiographs or computerized tomography. Assessing bony fusion in the spine can be difficult even for experienced spinal surgeons and musculoskeletal radiologists, particularly when there is no agreement on the optimum technique for evaluating the progress of fusion in the spine.

Tantalum being radiopaque permits easy assessment of the position of implants and facilitates evaluation of any degree of displacement or subsidence of an implant into surrounding bone (Fig. 4). In clinical practice porous tantalum does not permit visualization of the formation of bridging trabeculae due to its dense radio-opaque nature. Compared to titanium implants, porous tantalum has been shown to demonstrate greater streak artefact on computerized tomography [11]. Thus, computerized tomography is not the imaging modality of choice for porous tantalum. However, porous tantalum implants demonstrate reduced artefact on some magnetic resonance imaging sequences when compared to titanium implants [12]. This may be of considerable advantage to those surgeons wishing to visualize neural structures adjacent to an interbody implant.

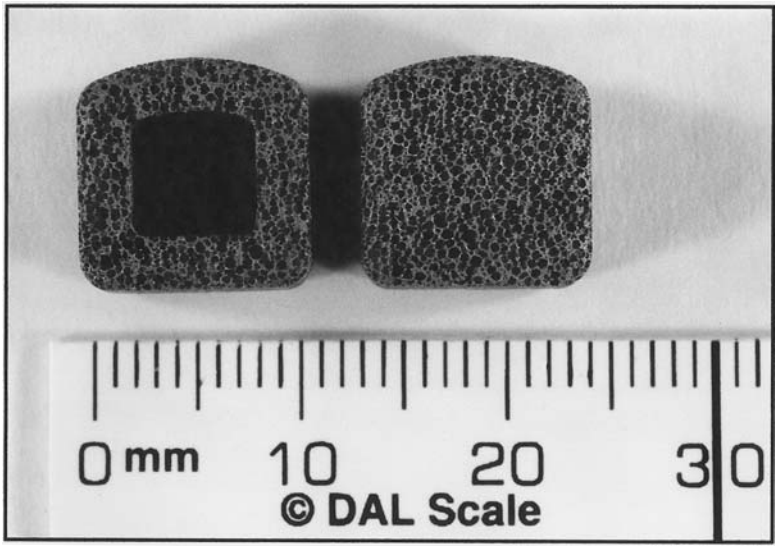

Figure 3 A porous tantalum ring and block used for cervical interbody fusion shown against a millimeter scale.

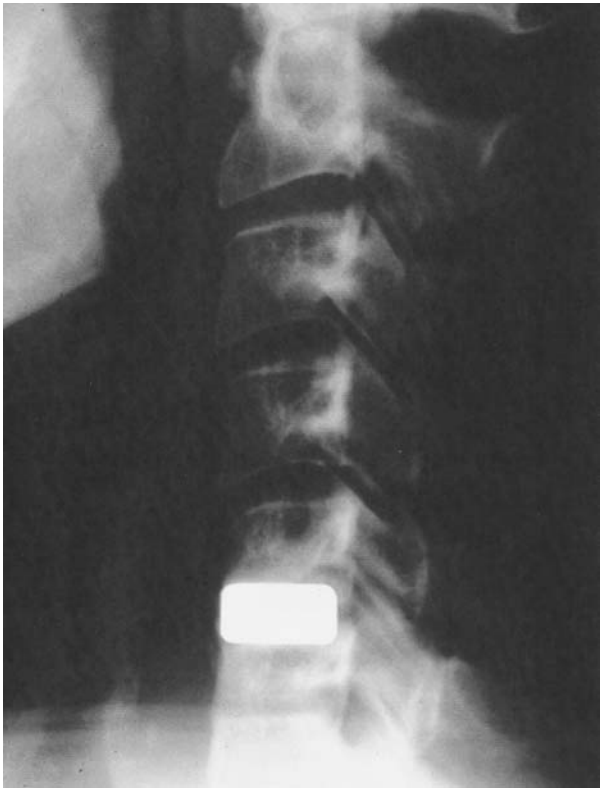

Figure 4 Bony fusion around a porous tantalum device at 12 months.

V. CONCLUSIONS

Presently there is little evidence that alternatives to autologous tri-cortical bone graft harvested from the iliac crest result in improved long-term clinical outcome [13–17]. Previous studies have suggested that many synthetic interbody devices and materials act as spacers only. Recent developments with bone morphogenic proteins (BMP) appear to be associated with improved prospects of osteointegration. The biomechanics of porous tantalum, in particular its biocompatibility with cancellous bone, suggests that it may have a place in interbody fusion and that this role could be enhanced with BMP.

REFERENCES

1. Brown C, Eismont F. Complications in spinal fusion. Orthopaed Clin North Am 1998; 29(4):679–699.
2. Zeidman S, Ducker T, Raycroft J. Trends and complications in cervical spinal surgery: 1989–1993. J Spinal Disord 1997; 10(6):523–526.
3. White AA. Clinical biomechanics of cervical spine implants. Spine 1989; 14(10):1040–1045.
4. Wigfield C, Nelson R. Interbody fusion devices in cervical spinal surgery: How strong is the evidence to justify their use. Spine 2001; 26(6):687–694.
5. Hacking SA, Toh K-K, Bobyn JD, Tanzer M, Krygier JJ. The strength of soft tissue attachment to porous tantalum. Presented at the 24th Annual meeting of the Society for Biomaterials. April 22–26, 1998, San Diego, California.
6. Bobyn J, Stackpool G, Hacking S, Tanzer M, Krygier J. Characteristics of bone ingrowth and interface mechanics of a new porous tantalum biomaterial. J Bone Joint Surg (Br) 1999; 81-B(5):907–914.
7. Bosita R, Yee A, Birkedal J, Emery S. Radiographic and histologic analysis of cervical spine fusion in Nubian goats: porous tantalum with plate vs. iliac crest bone autograft with plate. Personal communication.
8. Zou X, Li H, Bunger M, Xue Q, Egund N, Lind M, Bunger C. Characteristics of bone ingrowth on porous tantalum implants versus carbon fibre cages in porcine lumbar interbody fusion model. Personal communication.
9. Sandhu H, Kabo J, Turner S, Kanim L, Toth J. Porous tantalum metal as a biologically advantageous spinal fixation material; and rhBMP-2 augmentation of titanium fusion cages for experimental anterior lumbar fusion. American Acadamy of Orthopaedic Surgeons Annual Meeting, San Fransisco, 1997.
10. Wigfield C, Robertson J, Metcalf N, Nelson R. Problems associated with the radiologicalm assessment of porous tantalum for cervical interbody fusion. Presented at The European Cervical Spine Research Society, London, UK, June 2000.
11. Levi ADO, Choi WG, Keller PJ, Heiserman JE, Sonntag VKH, Dickman CA. The radiographic and imaging characteristics of porous tantalum implants within the human cervical spine. Spine 23(11): 1245–1251.
12. Wang JC, Yu WD, Sandhu HS, Tam V, Delamarter RB. A comparison of magnetic resonance and computed tomographic image quality after the implantation of tantalum and titanium spinal instrumentation. Spine 23(15):1684–1688.
13. Yu Y, Woo E, Huang C. Cervical spondylotic myelopathy and radiculopathy. Acta Neurol Scand 1987; 75(6):367–73.
14. Hayashi H, Okada Z, Hashimoto J, Tada K, Ueno R. Cervical spondylotic myelopathy in the aged patient. Spine 1988; 13(6):618–625.
15. Cusick J. Neurosurgical considerations of cervical myelopathy. Semin Neurol 1989; 9(3):193–9.
16. Bohlman H, Emery S. The pathophysiology of cervical spondylosis and myelopathy. Spine 1988; 13(7):843–846.
17. Lees F, Aldren Turner JW. Natural history and prognosis of cervical spondylosis. Br Med J 1963: 1607–1610.

52
Advances in Spinal Fusion

Sami Zeineddine and Reginald Q. Knight
Creighton University
Omaha, Nebraska, U.S.A.

Experienced spinal surgeons continue to refine the indications for spinal fusion. Studies related to successful outcomes strongly suggest that patient selection remains the most important variable in this equation. As demonstrated by advances in biomedical engineering, the 1990s could be defined as the decade of the spinal implant. In keeping with recent developments, the first 10 years of the new millennium may well become the decade of cell augmentation.

Multiple modalities which stimulate the host cell to function at heightened levels are now part of the surgeon's armamentarium. Basic scientists have demonstrated that endogenously occurring proteins (BMP, IGF, TGF-β) or exogenously applied electrical currents [direct currents or pulsed electromagnetic fields (PEMFs)] and ultrasound can stimulate the cells involved in the fusion process. Multiple modalities have been touted as adjuncts to the fusion process. However, only bone morphogenic protein (BMP) in a subcutaneous pouch model has been shown to truly stimulate bone formation. This process, de novo bone formation in a subcutaneous pouch, may well be the litmus test for all adjunctive agents.

Patient selection remains the key to surgical success. However, the technical task of obtaining a solid motion segment fusion in and of itself has often proven difficult. The patient's own physiology—diabetes, smoking, obesity, or chronic steroid use—may deter successful fusion. In addition, the surgical procedure performed (single-level fusion versus multilevel fusion) add increasing degrees of difficulty in obtaining a solid fusion. Cell augmentation will prove to be a valuable tool in altering surgical outcome in such difficult patient populations. Information contained in this chapter may aid the surgeon in selecting the most appropriate cell augmentation modality for the patient and procedure performed. Spine surgery ranks as one of the most common inpatient surgical procedures in the United States. Graves [1], using data from the National Hospital Discharge Survey (NHDS), studied the rates of spine surgery in the United States between 1979 and 1990. He noted that from the period of 1979–1981 compared with 1988–1990, each state had an increasing rate of hospitalization. Overall, spinal surgeries increased tremendously, with fusion surgeries increasing the most.

I. HISTORICAL PERSPECTIVES

Albee [2], who sought to inhibit tuberculous spread in patients with Pott's disease, first reported the concept of spinal fusion surgery in 1911. His goal was to provide mechanical support and stability to involved vertebrae. Another early pioneer, Hibbs [3], used fusion surgery to halt the progression of scoliotic deformity. Pioneering work by Urist [4] demonstrated the presence of

agents capable of producing bone in a subcutaneous pouch. These agents were later characterized as bone morphogenetic proteins within the matrix of demineralized bone.

Rates of spinal fusion procedures have continued to increase dramatically since the 1980s. Advances in technology have contributed to the growth in knowledge involving new spinal implants, including screws, rods, plates, cages, and biological grafting materials as well as electric stimulation. These technologies have expanded the indications for fusion considered by some surgeons and have allowed better surgical management of certain conditions, such as degenerative disc disease, tumor, and trauma. Varied fusion rate with an intervertebral cage and bone graft compared to autogenous intervertebral bone grafts alone has stimulated the concept of augmenting spinal fusion with endogenously occurring biological materials. Adjuncts presently under consideration are materials such as BMP, IGF, TGF-β, or gene therapy and exogenously applied electrical currents such as direct current or PEMF.

II. APPROACHES AND INSTRUMENTATION

The surgical techniques and instrumentation available for spinal fixation have advanced greatly in recent years. Spinal surgeons are exposed to an increasing assortment of specialized devices. Techniques can be divided on the basis of perceived patient morbidity into minimally invasive or traditional open procedures performed via either an anterior, lateral, or posterior approach. In addition, the fusion may occur in different anatomical locations: interbody fusion or intertransverse process fusion. Biomechanicaly, the interbody space tends to place the fusion material (bone or synthetic) under compression. The use of spinal instrumentation is intended to improve the local environment for fusion, i.e., reduced motion and increased motion segment rigidity. This increased rigidity promotes increased selection of osteoblast cell development as opposed to chondroblast or fibroblast. With interbody fusion, variable cage or interbody spacer design protects the graft material from excessive load and positions that material in the most advantageous location. In the case of intertransverse process fusion, bulky high profile implants may obliterate the space available for biological material (bone or synthetic) necessary for a healthy fusion. Experiments designed to test synthetic bone growth stimulators in the intertransverse process location have implied that the ''carrier'' of these agents is critical to the success of fusion. Unfortunately, the paraspinal muscle, which provides an excellent vascular fusion bed in primary surgical cases, can compress and flatten soft ''carriers'' (collagen sponges), producing a thin mechanically weak fusion mass.

III. GRAFT CHARACTERISTICS

Bone grafting is an integral part of spinal surgeries. The two choices for bone grafts are autograft and allograft. Each source has advantages or disadvantages. Allograft bone is available in greater quantity than autograft due to the possibility of using multiple donors and storing this bone for future use. With standard protocols of harvesting, the risk of disease transfer is negligible with allograft. However, the bone-forming properties of allograft are not comparable to autograft in most situations. Only fresh-frozen and freeze-dried products are presently used.

Currently, no bone graft substitutes are available that are equal to autografts in terms of their universal success of incorporation under similar physiological or biomechanical situations. The harvesting of an autograft bone is associated with certain morbidities, namely infection, donor site pain, and possible late fracture at the donor site. In addition, the use of autograft bone increases both operating time and blood loss. Therefore, spine surgeons are actively seeking alternatives to autologous bone grafts for spinal fusion. Autograft combines the dual properties

of osteoconduction and osteoinduction. Allograft is primarily an osteoconductive material. In addition, structural grafts of either type may provide a space-occupying property that morcellized grafts cannot.

To illustrate the biological principles of fusion, an interbody grafting procedure of either the anterior cervical or lumbar spine describes the steps of bone incorporation and maturation. Prior to bone graft placement, the superior and inferior surfaces of the adjacent vertebrae are decorticated to theoretically provide the osteoprogenitor cells necessary for bone production. As previously stated, patient's autogenous bone is both osteoconductive and osteoinductive; the osteoconductive property allows neovascularization and subsequent cell migration along the lattice of the trabecular bone, while the osteoinductive property is produced by a broad spectrum of biological materials within the bone, including BMP. The grafting structure may be in the form of a trapezoidal wedge or a cylindrical dowel depending on clinical need and surgeon preference.

For proper bone fusion to occur, there are four essential requirements of the bone graft substitute [5]. First, there should be a source of osteoprogenitor cells available that will allow for new bone formation. Second, there must be an agent available that will induce the differentiation of these progenitor cells into an osteoblast lineage so that bone will be formed. Third, there must be an osteoconductive surface available over which bone can be formed. Finally, proper stability must be obtained to allow proper bony remodeling and consolidation. The challenge now is to discover alternative bone graft substitutes that also can achieve satisfactory goals.

IV. ADJUNCTS TO SPINAL FUSION

A. Use of Biological Materials

Currently, the most popular adjuncts to or alternatives for autograft bone are bone morphogenetic proteins (BMP) absorbed on to a collagen sponge, demineralized bone matrix, autologous growth factors (TGF-β, IGF), gene therapy, and femoral cortical allograft rings and dowels.

1. Bone Morphogenetic Proteins

Through a series of investigations, researchers have shown that bone morphogenetic proteins are expressed at various points throughout the differentiation process of an osteoblast. Using this knowledge, bone morphogenetic proteins are now being used in various types of orthopedic fusion applications, particularly in spinal fusion. In 1986, Lovell et al. [6] published the first report of the use of bone morphogenetic protein in spinal fusion in dogs. Using demineralized matrix, they showed there was more vigorous bone growth when these growth factors were combined with autologous bone versus autologous bone alone. In 1995, Boden et al. [7] used bovine demineralized matrix to achieve spinal fusion in a rabbit posterior intertransverse process spinal fusion model. Schimandle et al. [8] used the bone morphogenetic protein-2 in achieving 100% fusion in both the rabbit and nonhuman primates. They examined spinal fusion in 48 New Zealand white rabbits that underwent a decompressive laminectomy and posterolateral intertransverse process fusion using hydroxyapatite as a carrier loaded with various amount of recombinant human bone morphogenetic protein-2 (rhBMP-2) compared to autologous bone alone. Several different BMP have now been isolated; presently BMP-2 and BMP-7 have enjoyed the largest clinical and experimental utility. Fusion was assessed by manual palpation, radiograph, and histology. Results showed that the best fusion was achieved when a carrier was loaded with the maximum amount of rhBMP-2 compared to autograft alone. Since then, various investigators have conclusively shown that the use of bone morphogenetic protein with autograft

can achieve a higher fusion rate than autograft alone [9–11]. Additional research has focused on using hydroxyapatite or tricalcium phosphate as potential carriers. Both are minerals found in normal bone matrix. Hydroxyapatite has been found to provide adequate structural support but is not readily reabsorbed during the healing of the spinal fusion. Conversely, tricalcium phosphate, while not having the structural stability of hydroxyapatite, is more easily resorbed during the healing phase [12]. Both of these materials have been shown to withstand the compression forces of the paraspinal muscles in the intertransverse process location. This has not been the case with collagen sponges. The collagen sponge has proved to be the carrier of choice with protective cages or interbody devices for anterior or lateral interbody fusion. The potential for exogenous bone formation following application for BMP to collagen sponges has precluded the use of this preparation via posterior or transforamenal interbody approaches.

2. *Demineralized Bone Matrix*

Demineralized bone matrix (DBM) is a composite of collagenous and noncollagenous proteins that contain bone growth factors. These factors present following mineral extraction of bone by biochemical processes. DBM may serve as both a bone graft enhancer and expander in spinal fusions. The osteoinductive potential of DBM is related to the presence of several osteoinductive proteins and growth factors, such as bone morphogenetic protein and transforming growth factor (TGF-β). TGF-β has a similar, yet less intense, physiological activity compared to BMP. Bone morphogenetic protein activity promotes bone formation via proliferative, angiogenic, and matrix-forming stimulation of osteoblastic cell lines [1]. The bone-forming cascade triggered by osteoinductive demineralized bone matrix was observed histologically [1]; this osteoinductive response was evident by day 14, when host mesenchymal cells are converted to chondroblasts and cartilage is formed within the implanted demineralized bone matrix. By day 28, bone formation begins as vascularization increases. At this time osteoblasts are clearly visible histologically within the regions of new bone formation. New woven bone is formed on the surface of mineralized cartilage. Demineralized bone matrix is currently available in four preparations [13]: powder, gel, putty, and flexible sheets. While demineralized bone matrix demonstrates bone-forming properties, the concentration of osteoinductive material is far less than that available with recombinant h-BMP. In addition, the concentration of BMP within each commercially available preparation of DBM varies considerably, as does the carrier (glycerol) and its retention at the fusion site (water solubility).

3. *Autologous Growth Factors (TGF-β, IGF)*

Within platelets are a variety of bone growth factors: TGF-β, platelet-derived growth factors (PDGF), IGF, and vascular endothelial growth factors (VEGF). Scientists have discovered that with a concentration of 1 million platelets/μL, enough growth factors can be isolated to enhance bone growth [14]. In addition, fibrinogen, which is found within the plasma containing the platelets, is used in this solution to aid in homeostasis. The formation of such solution is a multistep process [1,14]: To begin with, one unit of blood is drawn from the patient before surgery. Using a cell saver, this blood is separated into three parts: red cells, plasma, and a buffy coat. The buffy coat is taken and ultra-concentrated to a density of 1 million platelets/μL. This concentrate is then added to thrombin to make it into a soft or hard gel, depending on the concentration of thrombin added. The gel is then cut into strips and added to the fusion site as needed.

The advantages of using growth factor are that it is autologous and hence there is no risk for disease transmission or an adverse immune response. Second, because it comes in a gel form, it can be placed conveniently in any desired region and not be washed away. The disadvantage of

this substance is the limited number of clinical trials comparing the efficacy of this substance to autograft alone. In addition, Urist experiment of bone formation in a subcutaneous pouch has not been successfully carried out with isolates of TGF-β, IGF, or PDGF.

4. Gene Therapy

Another novel therapeutic modality that may improve fusion rates is gene therapy. Gene therapy is a technique in which nucleic acid, usually DNA, is transferred to target cells for a therapeutic effect. Although originally conceived as a modality for treatment of genetic diseases, gene therapy has begun to show promise for repair and regeneration of musculoskeletal tissues, including the spine. To date [15], much of the work in gene therapy for the enhancement of spine fusion has centered on the transfer of genes encoding BMP and related proteins. Potentially, genes encoding osteoinductive growth factors may be transferred to target cells, inducing the production of large amounts of the growth factor in a controlled and sustained fashion for a predictable period of time. Riew et al. [16] attempted to prolong the bone-inducing effect of BMP-2 using an adenoviral receptor carrying the human BMP-2 gene to transduce marrow-derived mesenchymal stem cells in New Zealand white rabbits. In their model, they isolated and expanded bone marrow mesenchymal cells from the resected ribs. Immunocytochemistry was used to show that approximately 80% of mesenchymal cells could be modified genetically to overexpress BMP-2 protein by treatment with an adenoviral vector encoding human BMP-2 (Adv-BMP-2). Four weeks after rib harvest, the rabbits underwent spinal fusion at L5-6. Genetically modified mesenchymal stem cells loaded onto collagen sponges were placed between the transverse processes of L-5 and L-6. Adv-BMP-2–transduced mesenchymal stem cells were placed on the left side and the Adv-gal cells on the right. On the five study rabbits, radiographic evidence of new bone formation on the side implanted with Adv-BMP-2 was seen 5 weeks after surgery. No new bone formation was observed on the control Adv-gal side. Rabbits were sacrificed 7 weeks after the operation, and histological examination of the rabbit with new bone revealed mature bone with a trabecular structure. Histology was unremarkable in the control side. Other related studies done by Boden et al., Alden et al., and Wang et al. [15] showed the possibility of using plasmid and/or adenovirus-mediated gene transfer of BMP and related genes in animal models. The transformed cells could produce BMP-2 in vivo that would exert an osteoinductive effect. Such studies warrant further work on the longevity, efficiency, and vector development of the gene transfer.

B. Electrical Stimulation (Pulse and Direct Electrical Stimulation)

It has been known since the 1950s that stressed bones develop negative potentials relative to other areas of the bone [17,18]. Bassett et al. [19] measured negative potentials in compressed areas of long bone and found new growth preferentially in areas where an electrical current had been supplied to dog femurs. Since then many investigators have confirmed the use of electrical stimulation as an adjunct to bone growth and remodeling including promotion of fracture union and spinal pseudarthrosis repair. Electrical stimulation for clinical use has three distinct forms [20]. One form uses direct current electric stimulation (DCES) produced by a generator to deliver electric energy via surgically implanted electrodes into the fusion bed. The alternative methods apply electric stimulation in the form of either pulsing electromagnetic fields (PEMF) or capacitively coupled electric energy. PEMFs and capacitively coupled electric fields may be delivered through external electrodes or corset-like apparatus [20].

1. Direct Current Electric Stimulation

The precise mechanisms by which electricity induces bone formation and healing are largely unknown. It has been established that the cathode consumes oxygen and produces hydroxyl

radicals [21]. The local tissue oxygen tension is thereby decreased, and local tissue PH is raised in proximity to the active cathode. Lower tissue oxygen tension has been demonstrated to be a favorable environmental factor for the promotion of osteogenesis. Experimental studies have demonstrated low PO_2 values at the bone-cartilage junction in the growth plate [22] and in newly formed bone and fracture calluses. Furthermore, optimum in vitro bone growth is know to occur in a low-oxygen tension environment, as growth plate cartilage and bone cells use a predominantly anaerobic metabolic pathway [23,24]. Howell et al. [25] demonstrated that an alkaline environment is found at the calcification front of the growth plate, which is thought to be optimal for calcification. Electric energy may also directly affect the activity of bone and cartilage. One possible mechanism for direct induction involves the activation of adenosine monophosphate (AMP) within the stimulated cell, triggering an intracellular second messenger system [26].

After the initial clinical study of Dwyer and Wickham [27], which demonstrated the efficacy of direct current electric stimulation (DCES) in healing spinal fusion, subsequent studies demonstrated that implantable DCES devices augment anterior and posterior spinal fusions and can be used successfully in the treatment of spinal pseudarthrosis and nonunion. In 1988, the results of a large multicenter clinical trial were examined. Groups of stimulated and control patients were comparable for age and sex. The stimulated group had a much higher incidence of previous surgery and pseudarthrosis when compared with controls. Despite this significant bias in patient history, which would seem to favor a better outcome among the control patients, a significant increase in successful fusion rates was found for stimulated patients compared with controls. An astonishing 91% of patients with pseudarthrosis achieved successful fusion when treated with DCES. The results for the control group were consistent with those previously published, with an overall success rate of 81%. Clinical studies by Kane [28] in 1988, Mooney [29] 1990, Rogozinski and Rogozinski [30] in 1996, and Kucharzyk [31] in 1999, among others, showed that DCES is a legitimate adjunct to spinal fusion surgery when it is applied to lumbosacral fusion or pseudarthrosis repair.

2. *Electromagnetic Fields and Capacitive Coupling*

The application of specifically configured electric fields or pulsing electromagnetic fields to living cells and tissues has been demonstrated to enable the selective control of various cellular functions. The range of conditions treatable by PEMF continues to expand and now includes musculoskeletal disorders (ununited fractures), nerve regeneration, wound healing, graft incorporation, diabetes, myocardial and cerebral ischemia [32]. More recently, capacitive coupling-induced, time-varying electric fields also have been demonstrated to be an effective, surgically noninvasive method for the treatment of nonunited fractures [33]. Bassett [34] and Bassett et al. [35] suggested that PEMF might cause increased calcification in bone-associated fibrocartilage, which in turn may prime such tissues for vascularization. In contrast to the effects of direct electrical stimulation, PEMF seem to affect differentiated bone cells instead of precursor cells [36]. The observed effects include increased vascularization of the fracture site, accelerated bone formation by osteoblasts, and inhibition of osteoclastic bone resorption. Despite numerous investigative efforts into the cellular response of bone to electromagnetic fields, conflicting theories persist regarding the precise mechanism of stimulation. Randomized double-blind prospective clinical trials of PEMF and capacitively coupled electrical stimulation, reported by Mooney [29] and Goodwin et al. [37], respectively, as well as single coil electromagnetic stimulation results reported by Linovitz et al. [38], have demonstrated a significant beneficial effect of nonunion fractures and lumbar fusion procedures. In 1989, Lee [39] reported the results of a clinical study using PEMF stimulation in patients with spinal pseudarthrosis. Of patients who

used PEMF stimulation consistently, 67% achieved bony fusion versus 19.2% of patients who used PEMF inconsistently or not at all. In the same year, Simmons et al. [40] presented findings from a multicenter study examining the effects of PEMF stimulation in patients with diagnosed spinal nonunions. Patients who used PEMF stimulation consistently were found to have a 76.7% successful fusion rate, whereas those who did not use PEMFs consistently had a 44.4% rate of solid fusion.

C. Ultrasound

The principle of resonant sonic and ultrasonic tools has long been known and used for cell destruction, cleaning, drilling, mixing, and welding [41]. Fundamentally the tools involve a conversion of electrical to mechanical energy (at higher efficiency than nearly any other such conversion). It is accomplished by exciting a dynamic stress wave in the tool structure at a repetition rate such as to find the length of the tool equal to a multiple of half wavelengths of the stress wave [41]. Polakov and Chemianov introduced ultrasonic surgery in 1964 in Moscow in collaboration with engineers of the Moscow Institute of Technology [42]. They discovered that ultrasonic vibrations have the property of fusing (welding) living bone and soft tissues based on a specific action of mechanical vibrations. The ultrasonic generator serves as a source of electric waves, which are transformed by acoustic nodes into mechanical vibrations. Acoustic transformers made of various magnetostrictive materials transmit mechanical vibration to special relays, corresponding to their own frequency of vibrations and the frequency of the electric vibrations. The terminals of the ultrasonic relays are equipped with exchangeable tips for fusing or cutting bone and soft tissues.

Introduction of ultrasonic methods in surgery and clinical practice was preceded by extensive and long-term experiments with animals. Polakov et al. [42] studied more than 1000 animals at their ultrasonic laboratory. Various methods of fusing and cutting bone and soft tissues were studied. Direct osteosynthesis of fractured fragments, fusion of relatively small bone fragments accompanying multiple fractures, fusion of bone grafts with their substrate, and formation of artificially fused bone conglomerates used to fill defects in the shaft or epiphysis of long bones have been studied. The experiments showed that ultrasonic fusion is not injurious to bone. ''The ultrasonically fused suture'' is followed by callous formation within a normal interval of time. Glazer et al. in 1998 [43] studied the effect of ultrasound in spinal arthrodesis in 28 rabbits. The animals were assigned to one of two groups to undergo spinal fusion using autologous bone with ultrasound or autologous bone without ultrasound. A specially designed plastic constraint was used to focus the ultrasound over the rabbits' lumbar spines 20 minutes per day. After 6 weeks, results showed that the rate of pseudarthrosis, evaluated radiographically and manually, decreased at a statistically significant rate (from 35% to 7%) with ultrasound. Biomechanical analysis of the fusion also showed that ultrasound resulted in statistically significant increases in stiffness (33%; $p = 0.03$). Qualitative histological assessment showed increased bone formation in those fusion exposed to ultrasound. Similarly, Anyaci et al. [44] studied the fusion rate of muscle-pediculated bone graft in spinal fusion. The 20 rabbits studied were assigned to one of two groups to undergo spinal arthrodesis using muscle-pedicle bone graft with ultrasound or muscle-pedicle bone graft without ultrasound. By macroscopic and radiological findings, fusion was detected in 11 control group rabbit (55%) and in 17 ultrasound group rabbits (85%). Histological specimens showed increased bone formation in the fusion exposed to ultrasound. Several other in vivo animal studies were done to study the spinal fusion rates using low-intensity ultrasound [45,46]; they all showed that low-intensity ultrasound accelerate bone fusion and fracture repair.

On the basis of the experimental studies mentioned above, it is unknown whether fusion achieved with the use of ultrasound will remain stronger with passing time than those achieved without ultrasound application, or whether both types will remodel to a similar endpoint. On the cellular level, ultrasound may affect protein synthesis, vascularization, synthesis, and calcification of a bony matrix. However, the effect of low-intensity ultrasound on spinal bone fusion may be substantially weaker due to the much greater distance between the skin and the fused bony structures in patients as compared to the animal model. Therefore, clinical trials are needed to demonstrate whether these results can be replicated in humans.

V. SUMMARY

The continued development of adjuncts to spinal fusion is not static. Even as we complete this writing, new and innovative ideas are being studied in the laboratory. Surgeons need to have the information to critically evaluate new science. At the present time, patient selection remains the key to success. No technology can displace clinical judgment. Once the decision is made as to which patients need surgery, the surgery needs to be planned in a manner improving the rate of technical success.

Presently, interbody fusion with cage technology lends itself to augmentation with growth factors. Of all the growth factors presently available, rh-BMP-2 has been tested in the laboratory and proven in clinical trial to improve fusion rate without significant risk of complication. Patient complaints of bone graft site pain have changed our practice patterns significantly. It is the author's opinion that most if not all patients can benefit from the use of BMP in an anterior or lateral application with cage support. We have not used BMP in a posterior application, interbody or intertransverse process location, for the reasons mentioned above.

Electrical stimulation has been an effective adjunct to our practice. We reserve the use of these modalities for patients who have demonstrated slow healing in a posterolateral lumbar fusion case. Prior to the advent of improved instrumentation choices, implanted electrical stimulation devices were more often used in long fusion constructs. In patients who show signs of poor compliance, implantable devices continue to hold favor over the external applications. However, technologies continue to take down barriers. Research into PEMF has reduced the time required for reported effect. While ultrasound has shown impressive laboratory results, clinically it has not been embraced at this point. Future clinical trials and widespread use of the techniques listed above will serve to more clearly define their clinical role.

REFERENCES

1. Graves EJ. National Hospital Discharge Survey: Animal Summary, 1987, 1988, 1990. National Center for Health Statistics. Vital Health Stat Series 13, 99, 106, 112, 1989; 1, 40–41, 1991; 1, 38–39, 44; 1992:1, 8, 44–45, 51.
2. Albee FH. Transplantation of a portion of the tibia into the spine for Pott's disease. JAMA 1911; 57:885–886.
3. Hibbs RA. An operation for progressive spinal deformities. A preliminary report of three cases from the service of the orthopaedic hospital. NY State J Med 1911; 93:1013–1016.
4. Urist MR. Bone; formation by autoinduction. Science 1965; 150(698):893–899.
5. Vaccaro AR, Sharan AD, Tuan RS, Kang JD, An HS, Morone MA, Savas PE, Hilibrand AS, Abitbol JJ. The use of biologic materials in spinal fusion. Orthopedics 2001; 24(2):191–197.
6. Lovell TP, Dawson EG, Nilsson OS, Urist MR. Augmentation of spinal fusion with bone morphogenetic protein in dogs. Clin Orthop 1989; 243:266–274.

7. Boden SD, Shimandle JH, Hutton WC. Lumbar intertransverse-process spinal arthrodesis with use of a bovine bone-derived osteoinductive protein. A preliminary report. J Bone Joint Surg Am 1995; 77:1404–1417.
8. Schimandle JH, Boden SD, Hutton WC. Experimental spinal fusion with recombinant human bone morphogenetic protein-2. Spine 1995; 20:1326–1337.
9. Chabot MC. Augmentation of autograft using rhBMP-2 and different carrier media in the canine spinal fusion model, Presented in 1994 at the Cervical Spine Research Society Meeting.
10. Takahashi T, Tominaga T, Watabe N, Yokohori AT, Sasada H, Yoshimoto T. Use of porous hydroxyapatite graft containing recombinant human bone morphogenetic protein-2 for cervical fusion in a caprine model. J Neurosurg 1999; 90(suppl):224–230.
11. Riew KD, Wright NM, Cheng S, Avioli LV, Lou J. Induction of bone formation using a recombinant adenoviral vector carrying the human BMP-2 gene in rabbit spinal fusion model. Calcif. Tissue Int 1998; 63:357–360.
12. Shirota T, Donath K, Matsui Y, Ohno K, Michi K. Reactions of bone tissue in old rats to three different implant materials. J Oral Implantol 1994; 20:307–314.
13. Martin GJ, Boden SD, Titus L, Scarborough NL. New formulations of demineralized bone matrix as a more effective graft alternative in experimental posterolateral lumbar spine arthrodesis. Spine 1999; 24:637–645.
14. Lowery GL, Kulkarni S, Pennisi AE. Use of autologous growth factors in lumbar spinal fusion. Bone 1999; 25:47S–50S.
15. Khan SN, Hidaka C, Sandhu HS, Girardi FP, Cammisa FP, Diwan AD. Gene therapy for spine fusion. Orthop Clin North Am 2000; 31(3):473–484.
16. Riew K, Wright N, Cheng S. Induction of bone formation using a recombinant adenoviral vector carrying the human BMP-2 gene in a rabbit spinal fusion model. Calcif Tissue Int 1998; 63:357–360.
17. Yasuda I, Noguchi K, Sata T. Dynamic callus and electrical callus. J Bone Joint Surg Am 1955; 37: 1292–1293.
18. Bassett CAL, Becker RO. Generation of electric potentials by bone in response to mechanical stress. Science 1962; 137:1063–1064.
19. Bassett CAL, Pawluk RJ, Becker RO. Effects of electric current on bone in vivo. Nature 1964; 204: 652–654.
20. Oishi M, Onesti S. Electrical bone graft stimulation for spinal fusion: a review. Neurosurgey 2000; 47(5):1041–1056.
21. Brighton CT, Friedenberg ZB. Electrical stimulation and oxygen tension. Ann NY Acad Sci 1974; 238:314–319.
22. Brighton CT, Heppenstall RB. Oxygen tension in zones of the epiphyseal plate, the metaphysis and diaphysis: an in vitro and in vivo study in rats and rabbits. J Bone Surg Am 1971; 53A:719–728.
23. Deiss WP, Holmes LB, Johnson CC. Bone matrix biosynthesis in vitro: labeling of hexosamine and collagen of normal bone. J Biol Chem 1962; 247:3555–3559.
24. Vases BM, Nichols G. Oxygen tension and the control of bone cell metabolism. Nature 1962; 193: 379–380.
25. Howell DS, Pita JC, Marquez JF, Madruga JE. Partition of calcium, phosphate, and protein in the fluid phase aspirated at calcifying sites in the epiphyseal cartilage. J Clin Invest 1968; 47:1121–1132.
26. Norton LA, Rodan GA, Bourret LA. Epiphyseal cartilage camp changes produced by electrical and mechanical perturbations. Clin Orthop 1977; 124:59–68.
27. Dwyer AF, Wickham CG. Direct current stimulation in spinal fusion. Med J Aust 1975; 6:265–279.
28. Kane WJ. Direct current electrical bone growth stimulation for spinal fusion. Spine 1988; 13:363–365.
29. Mooney V. A randomized double blind prospective study of the efficacy of pulsed electromagnetic fields for interbody lumbar fusions. Spine 1990; 15:708–712.
30. Rogozinski A, Rogozinski C. Efficacy of implanted bone growth stimulation in instrumented lumbosacral spinal fusion. 1996; 21:2479–2483.
31. Kucharzyk DW. A controlled prospective outcome study of implantable electrical stimulation with spinal instrumentation in a high-risk spinal fusion population. Spine 1999; 24:465–469.
32. Bassett CAL. Beneficial effects of electromagnetic fields. J Cell Biochem 1993; 51:387–393.

33. Brighton CT, Pollack SR. Treatment of recalcitrant non-union with a capacitively couple electrical field. J Bone Joint Surg Am 1985; 67A:577–585.
34. Bassett CAL. Pulsing electromagnetic fields: a new method to modify cell behavior in calcified and noncalcified tissues. Calcif Tissue Int 1982; 34:1–8.
35. Bassett CAL, Valdes MG, Hernandez F. Modification of fracture repair with selected pulsing electromagnetic fields. J Bone Joint Surg Am 1982; 64A:888–895.
36. Luben RA. Effects of low-energy electromagnetic fields (pulsed and DC) on membrane signal transduction processes in biological systems. Health Phys 1991; 61:15–28.
37. Goodwin CB, Brighton CT, Guyer RD, Johnson JR, Light KI, Yuan JH. A double-blind study of capacitively coupled electrical stimulation as an adjunct to lumbar spinal fusions. 1999; 24: 1349–1357.
38. Linovitz RJ, Ryaby JT, Magee FP, Faden JS, Ponder R, Muenz LR. Combined magnetic fields accelerate primary spine fusion: a double-blind, randomized, placebo controlled study. Presented at the 67th Annual Meeting of the American Association of Orthopaedic Surgeons, Orlando, FL, March 15–19, 2000.
39. Lee CK. Clinical investigation of the spinal stim system. Presented at the 56th Annual Meeting of the American Association of Orthopaedic Surgeons, Las Vegas, NV, February 9–14, 1989.
40. Simmons JW, Hayes MA, Cristensen KD. The effect of postoperative pulsing on lumbar fusion: an open trail phase study. Presented at the 4th Annual Meeting of the North American Spine Society, Quebec, Canada, June 29–July 2, 1989.
41. Poliakov VA, Chemianov GG. Ultrasonic osteosynthesis in open infected bone fractures (an experimental study.). Eksp Khia Anesteziol Jul–Aug 1974; 0(4):35–8. In Russian.
42. Poliakov VA. Osteosynthesis and repoir of bone tissue by ultrasonic fusion (''wedding''). Mater Med Pol Oct–Dec 1974; 6(4):291–3.
43. Glazer PA, Heilmann MR, Lotz JC, Bradford DS. Use of ultrasonic in spinal Arthrodesis. A rabbit model. Spine May 15, 1998; 23(10):1142–8.
44. Aynaci O, Onder C, Piskin A, Ozoran Y. The effect of ultrasound on the healing of muscle-peduculated bone graft in spinal fusion. Spine Jul 15, 2002; 27(14):1531–5.
45. Mohtadi N. Low intensity pulsed ultrasound therapy for fracture healing: a Meta analysis. Clin J. Sport Med Mar 2003; 13(2):127.
46. Heybeli N, Yesildag A, Oyar O, Bulsoy UK, Terikonsory MA, Mumcu EF. Diagnostic ultrasound treatment increases the bone fracture-healing rate in an internally fixed rat femoral osteotomy model. Ultrasound Med Dec 2002; 21(12):1357–63.